SHOUT
SHARE
IT

MBL

Volume 181 Number 1

THE BIOLOGICAL BULLETIN

Marine Biological Lab
LIBRARY
AUG 22 1991
Woods Hole, Mass.

AUGUST, 1991

Published by the Marine Biological Laboratory

Marine Biological Laborat
LIBRARY
AUG 22 1991
Woods Hole, Mass.

THE
BIOLOGICAL BULLETIN

PUBLISHED BY
THE MARINE BIOLOGICAL LABORATORY

Associate Editors

PETER A. V. ANDERSON, The Whitney Laboratory, University of Florida
DAVID EPEL, Hopkins Marine Station, Stanford University
J. MALCOLM SHICK, University of Maine, Orono

Editorial Board

GEORGE J. AUGUSTINE, University of Southern California
LOUIS LEIBOVITZ, Marine Biological Laboratory
RUDOLF A. RAFF, Indiana University
KENSAL VAN HOLDE, Oregon State University
STEVEN VOGEL, Duke University

Editor: MICHAEL J. GREENBERG, The Whitney Laboratory, University of Florida
Managing Editor: PAMELA L. CLAPP, Marine Biological Laboratory

AUGUST, 1991

Printed and Issued by
LANCASTER PRESS, Inc.
PRINCE & LEMON STS.
LANCASTER, PA

THE BIOLOGICAL BULLETIN

THE BIOLOGICAL BULLETIN is published six times a year by the Marine Biological Laboratory, MBL Street, Woods Hole, Massachusetts 02543.

Subscriptions and similar matter should be addressed to Subscription Manager, THE BIOLOGICAL BULLETIN, Marine Biological Laboratory, Woods Hole, Massachusetts 02543. Single numbers, $25.00. Subscription per volume (three issues), $72.50 ($145.00 per year for six issues).

Communications relative to manuscripts should be sent to Michael J. Greenberg, Editor-in-Chief, or Pamela L. Clapp, Managing Editor, at the Marine Biological Laboratory, Woods Hole, Massachusetts 02543. Telephone: (508) 548-3705, ext. 428. FAX: 508-540-6902.

POSTMASTER: Send address changes to THE BIOLOGICAL BULLETIN, Marine Biological Laboratory,
Woods Hole, MA 02543.

Copyright © 1991, by the Marine Biological Laboratory

Second-class postage paid at Woods Hole, MA, and additional mailing offices.
ISSN 0006-3185

INSTRUCTIONS TO AUTHORS

The Biological Bulletin accepts outstanding original research reports of general interest to biologists throughout the world. Papers are usually of intermediate length (10–40 manuscript pages). A limited number of solicited review papers may be accepted after formal review. A paper will usually appear within four months after its acceptance.

Very short, especially topical papers (less than 9 manuscript pages including tables, figures, and bibliography) will be published in a separate section entitled "Research Notes." A Research Note in *The Biological Bulletin* follows the format of similar notes in *Nature*. It should open with a summary paragraph of 150 to 200 words comprising the introduction and the conclusions. The rest of the text should continue on without subheadings, and there should be no more than 30 references. References should be referred to in the text by number, and listed in the Literature Cited section in the order that they appear in the text. Unlike references in *Nature*, references in the Research Notes section should conform in punctuation and arrangement to the style of recent issues of *The Biological Bulletin*. Materials and Methods should be incorporated into appropriate figure legends. See the article by Lohmann *et al.* (October 1990, Vol. **179:** 214–218) for sample style. A Research Note will usually appear within two months after its acceptance.

The Editorial Board requests that regular manuscripts conform to the requirements set below; those manuscripts that do not conform will be returned to authors for correction before review.

1. ***Manuscripts.*** Manuscripts, including figures, should be submitted in triplicate. (Xerox copies of photographs are not acceptable for review purposes.) The original manuscript must be typed in no smaller than 12 pitch, using double spacing (*including* figure legends, footnotes, bibliography, etc.) on one side of 16- or 20-lb. bond paper, 8½ by 11 inches. Please, no right justification. Manuscripts should be proofread carefully and errors corrected legibly in black ink. Pages should be numbered consecutively. Margins on all sides should be at least 1 inch (2.5 cm). Manuscripts should conform to the *Council of Biology Editors Style Manual*, 4th Edition (Council of Biology Editors, 1978) and to American spelling. Unusual abbreviations should be kept to a minimum and should be spelled out on first reference as well as defined in a footnote on the title page. Manuscripts should be divided into the following components: Title page, Abstract (of no more than 200 words), Introduction, Materials and Methods, Results, Discussion, Acknowledgments, Literature Cited, Tables, and Figure Legends. In addition, authors should supply a list of words and phrases under which the article should be indexed.

2. ***Title page.*** The title page consists of: a condensed title or running head of no more than 35 letters and spaces, the manuscript title, authors' names and appropriate addresses, and footnotes listing present addresses, acknowledgments or contribution numbers, and explanation of unusual abbreviations.

3. ***Figures.*** The dimensions of the printed page, 7 by 9 inches, should be kept in mind in preparing figures for publication. We recommend that figures be about 1½ times the linear dimensions of the final printing desired, and that the ratio of the largest to the smallest letter or number and of the thickest to the thinnest line not exceed 1:1.5. Explanatory matter generally should be included in legends, although axes should always be identified on the illustration itself. Figures should be prepared for reproduction as either line cuts or halftones. Figures to be reproduced as line cuts should be unmounted glossy photographic reproductions or drawn in black ink on white paper, good-quality tracing cloth or plastic, or blue-lined coordinate paper. Those to be reproduced as halftones should be mounted on board, with both designating numbers or letters and scale bars affixed directly to the figures. All figures should be numbered in consecutive order, with no distinction between text and plate figures. The author's name and an arrow indicating orientation should appear on the reverse side of all figures.

4. ***Tables, footnotes, figure legends, etc.*** Authors should follow the style in a recent issue of *The Biological Bulletin* in preparing table headings, figure legends, and the like. Because of the high cost of setting tabular material in type, authors are asked to limit such material as much as possible. Tables, with their headings and footnotes, should be typed on separate sheets, numbered with consecutive Roman numerals, and placed after

the Literature Cited. Figure legends should contain enough information to make the figure intelligible separate from the text. Legends should be typed double spaced, with consecutive Arabic numbers, on a separate sheet at the end of the paper. Footnotes should be limited to authors' current addresses, acknowledgments or contribution numbers, and explanation of unusual abbreviations. All such footnotes should appear on the title page. Footnotes are not normally permitted in the body of the text.

5. ***Literature cited.*** In the text, literature should be cited by the Harvard system, with papers by more than two authors cited as Jones *et al.*, 1980. Personal communications and material in preparation or in press should be cited in the text only, with author's initials and institutions, unless the material has been formally accepted and a volume number can be supplied. The list of references following the text should be headed Literature Cited, and must be typed double spaced on separate pages, conforming in punctuation and arrangement to the style of recent issues of *The Biological Bulletin*. Citations should include complete titles and inclusive pagination. Journal abbreviations should normally follow those of the U. S. A. Standards Institute (USASI), as adopted by BIOLOGICAL ABSTRACTS and CHEMICAL ABSTRACTS, with the minor differences set out below. The most generally useful list of biological journal titles is that published each year by BIOLOGICAL ABSTRACTS (BIOSIS List of Serials; the most recent issue). Foreign authors, and others who are accustomed to using THE WORLD LIST OF SCIENTIFIC PERIODICALS, may find a booklet published by the Biological Council of the U.K. (obtainable from the Institute of Biology, 41 Queen's Gate, London, S.W.7, England, U.K.) useful, since it sets out the WORLD LIST abbreviations for most biological journals with notes of the USASI abbreviations where these differ. CHEMICAL ABSTRACTS publishes quarterly supplements of additional abbreviations. The following points of reference style for THE BIOLOGICAL BULLETIN differ from USASI (or modified WORLD LIST) usage:

A. Journal abbreviations, and book titles, all underlined (for *italics*)

B. All components of abbreviations with initial capitals (not as European usage in WORLD LIST *e.g. J. Cell. Comp. Physiol.* NOT *J. cell. comp. Physiol.*)

C. *All* abbreviated components must be followed by a period, whole word components *must not* (*i.e. J. Cancer Res.*)

D. Space between all components (*e.g. J. Cell. Comp. Physiol.*, not *J.Cell.Comp.Physiol.*)

E. Unusual words in journal titles should be spelled out in full, rather than employing new abbreviations invented by the author. For example, use *Rit Vísindafjélags Islendinga* without abbreviation.

F. All single word journal titles in full (*e.g. Veliger, Ecology, Brain*).

G. The order of abbreviated components should be the same as the word order of the complete title (*i.e. Proc.* and *Trans.* placed where they appear, not transposed as in some BIOLOGICAL ABSTRACTS listings).

H. A few well-known international journals in their preferred forms rather than WORLD LIST or USASI usage (*e.g. Nature, Science, Evolution* NOT *Nature, Lond., Science, N.Y.; Evolution, Lancaster, Pa.*)

6. ***Reprints, page proofs, and charges.*** Authors receive their first 100 reprints (without covers) free of charge. Additional reprints may be ordered at time of publication and normally will be delivered about two to three months after the issue date. Authors (or delegates for foreign authors) will receive page proofs of articles shortly before publication. They will be charged the current cost of printers' time for corrections to these (other than corrections of printers' or editors' errors). Other than these charges for authors' alterations, *The Biological Bulletin* does not have page charges.

The Marine Biological Laboratory

Ninety-Third Report for the Year 1990 One-Hundred and Third Year

Officers of the Corporation

Denis M. Robinson, *Honorary Chairman of the Board of Trustees*
Prosser Gifford, *Chairman of the Board of Trustees*
Harlyn O. Halvorson, *President of the Corporation and Director*
Robert D. Manz, *Treasurer*
Kathleen Dunlap, *Clerk of the Corporation*

Contents

Report of the President and Director 1
Report of the Treasurer 5
Financial Statements 7
Report of the Librarian 17
Educational Programs
    Summer Courses 19
    Short Courses 23
Summer Research Programs
    Principal Investigators 28
    Other Research Personnel 30
    Library Readers 33
    Institutions Represented 34
Year-Round Research Programs 38
Honors 45
Board of Trustees and Committees 48
Laboratory Support Staff 51
Members of the Corporation
    Life Members 53
    Regular Members 54
    Associate Members 64
Certificate of Organization 68
Articles of Amendment 68
Bylaws 68

Report of the President and Director

I began last year's report by discussing the Laboratory's needs and reminding the Corporation of the pressing need for a new Marine Resources Center capable of providing a reliable, healthy, and genetically defined supply of marine organisms. I closed that discussion of the long-awaited, many-times-planned MRC with the hope that this important facility would become a reality "before too many more director's reports are filed."

I begin this director's report, my fourth, the Laboratory's ninety-third (covering its one-hundred third year) with the very good news that the new MRC will indeed be a reality—very soon. As I write this report (in the spring of 1991), the building is going up outside my window. Where we used to have a carpenters' shop and a parking lot, we now have pilings on top of which the walls of a state-of-the-art facility for holding marine animals are rising. The key step toward the MRC in 1990 was the passage, in October, of a Federal appropriation bill that included $4.75 million toward the MRC. Coupled with earlier Federal support, this brought funding for the MRC and related projects to a total of $8.95 million.

Part of the planning for the new MRC involved making alternate plans for parking and a re-location of the carpenters' shop. The plan at the close of 1990 is to build a new carpenters' shop on the MBL campus next to the Broderick House and to put a new, off-site parking lot in the MBL Woods off Oyster Pond Road near Memorial Circle. In the next director's report, I fully expect to be able to report that these auxiliary projects are completed and that the new MRC is up and very close to going on-line.

While preparations for construction of the MRC occupied much of our attention in 1990, we simultaneously continued to plan for an Advanced Studies Laboratory (ASL), which together with the MRC will constitute the Marine Biomedical Institute for Advanced Studies. At the close of 1990, the new ASL was in the second of three design phases.

The construction of the new Marine Resources Center and the progress toward a new Advanced Studies Laboratory are important steps toward ensuring a bright future for the Laboratory, but other long-standing and well-documented needs remain. To address these additional needs, the Trustees at their June 22 meeting initiated a long-range development program. The Executive Committee approved the use of a development consultant to help us review our readiness for mounting a major fund raising campaign. The consultant, Browning Associates, presented a cogent analysis of the Laboratory, which will help us greatly expand our development operation in 1991 and beyond.

Research

At the urging of the External Scientific Advisory Committee, we established in 1990 a Scientific Council to function in an advisory capacity to the Executive Committee. The Council is charged with guiding the Laboratory in:

- the development of scientific and educational programs
- the use of scientific resources
- the evaluation and promotion of scientific staff
- the recruitment of new scientific positions
- the initiation of institutional grant proposals.

The council is to work in conjunction with existing committees, such as the Research Space Committee and the Instruction Committee.

Council members are appointed by the director, with the approval of the Executive Committee. The council is to include up to three members of the year-round

Aerial view of the MBL's Marine Resources Center. Photo by Robert Golder.

scientific community, up to three members of the summer community, two non-MBL scientists, the MBL director who serves *ex officio,* and an *ex officio* executive secretary. The first council is composed of: year-round MBL scientists Drs. John Hobbie (vice-chairman), Mitchell Sogin, and Felix Strumwasser; summer MBL scientists Drs. Barbara Ehrlich, Gerald Fischbach, and Joseph Sanger; Dr. Holger Jannasch, Woods Hole Oceanographic Institution, and Dr. Howard Hiatt, Brigham and Women's Hospital. Dr. Leslie Garrick serves as *ex officio* executive secretary, and, as director of the MBL, I serve as *ex officio* chairman of the council.

The council met throughout 1990 to evaluate scientists for appointment and promotion and to set directions for future scientific development and expansion. They completed a draft of one position paper on Laboratory directions in cellular and developmental biology. The council plans to prepare additional position papers on environmental sciences/ecology, microbiology, molecular evolution, neurobiology, and plant sciences. These documents are targeted for completion in 1991 and 1992.

Instruction

The instruction program continued in 1990 with its unanimously acclaimed courses. One new short course was added: Pathogenesis of Neuroimmunologic Diseases, co-directed by J. Murdoch Ritchie, Yale University, and Byron H. Waksman, Harvard University and New York University.

At the urging of the External Scientific Advisory Committee, we have been taking a careful look at the cost of the courses. The Instruction Committee looked at cost containment in 1990, and, while there is as yet no consensus on how to proceed, it is clear that we will have to do something about spiraling cost increases in this age of decreasing federal support for advanced training.

New fellowships in 1990 included the Nikon Fellowship; a Bernard Davis Fellowship for studies in microbiology or molecular evolution; the Daniel S. Grosch Scholarship Fund for studies in environmental toxicology; and the Porter Fellowships for Minority Students/Investigators for work in physiology. A list of fellowship recipients appears later in this issue.

Library

The Library made continued progress toward applying computing technology to library services. As described in the Report of the Librarian, Jane Fessenden, the MBL Librarian of 29 years, retired in 1990. In December, Dr. David Stonehill accepted the position of Director of the MBL/WHOI Library and Scientific Information Research Center. Dr. Stonehill has been a national leader in the development of modern information services, having worked for

Jelle Atema, the new director of the Boston University Marine Program. Photo by Judith Anderson.

NASA, a number of leading universities, and—most recently—the President of the United States.

Governance

In August, Dr. Prosser Gifford announced his intention to step down from the chairmanship of the MBL Board of Trustees. Dr. Gifford led the MBL for 14 years, through a period of unprecedented change and growth. In a little short of a decade and a half, he worked with 4 of the 11 directors the Laboratory has had in its 103 year existence. Under his leadership, the Laboratory's facilities were significantly upgraded, the year-round science program grew substantially, the educational program maintained its character, the library prospered and began an exciting modernization program, and the administrative and development staffs were strengthened.

Neurobiologist Dr. Jelle Atema assumed the directorship of the Boston University Marine Program in August. He replaces Dr. Rudi Strickler, who had directed BUMP since 1987. Dr. Atema has energetic plans for BUMP's graduate and undergraduate programs, and his long acquaintance with the MBL bodes well for our partnership with Boston University.

In their February meeting, the Trustees approved a new Long Range Financial Planning Committee charged with reporting to the Trustees and/or the Executive Committee on the existence and appropriateness of long-range financial planning mechanisms of the laboratory. Responsibility for planning remains with the administration of the laboratory, while the new committee is to assure that the financial risks of growth have been properly anticipated and planned for. The committee is to include two at-large trustees, two corporate trustees, and the treasurer, *ex officio*. Treasurer Robert Manz chaired the new committee, which began by making a comprehensive review of the new MRC. In August, the Long Range Financial Planning Committee gave the Trustees a favorable report on the financial planning for the MRC. That favorable report was an important part of the briefing that led to the Trustees' decision to proceed toward construction of the new MRC.

Personnel

A group of MBL employees, including service, maintenance, and clerical workers, voted in February to affiliate with the Hospital Workers Union, Local 767. Collective bargaining negotiations began almost immediately after the election, and with the union and management both negotiating in a spirit of cooperation and mutual respect, we were able to negotiate our first contract in an impressively short time. A fair, reasonable, and workable contract was signed in July, and the work of the Laboratory proceeded without disruption.

Long-time manager of marine resources John Valois retired in November after 40 years at the MBL. In addition to running the collecting operation, Mr. Valois has served for years as a spokesman for marine biology and has appeared regularly in newspapers and on television extolling the virtues of marine animals as models for research. On his departure, Edward Enos was promoted to Superintendent of Marine Resources. Mr. Enos has been a collector for many years and was eminently well-prepared to take the reins of the department.

MBL Science Writing Fellows in the Hands-On Laboratory Course. Photo by James Hrynyshyn.

The Biological Bulletin

Under the editorship of Michael J. Greenberg, *The Biological Bulletin* continued to publish well-presented reports of outstanding research that is of general interest to biologists throughout the world. In 1990, Dr. Greenberg announced that all page charges would be dropped, and that authors would be offered 100 free reprints for publishing in the journal. Most importantly, he noted in his 1990 report to the corporation, a *carefully prepared* manuscript can now appear in print as soon as 3.6 months after its submission. In fact, some manuscripts meeting the criteria of the new Research Notes section—which features brief communications of high quality and currency—may appear in print even sooner. All of these initiatives have been highlighted in the journal's newsletter, *The Biological Board.* The newsletter, which is published "occasionally" by the editorial staff, was created to highlight and promote the articles appearing in, and the policies of, the journal.

Dr. Greenberg has also been attempting to adjust the mix of papers appearing in the *Bulletin* so that the journal more closely reflects research here at the MBL. To assist in this effort, Dr. Greenberg has recruited three Associate Editors to aid in the review and solicitation of manuscripts. Drs. J. Malcolm Shick (University of Maine, Orono), Peter A. V. Anderson (The Whitney Laboratory), and David Epel (Hopkins Marine Station) will serve four-year terms as Associate Editors in their respective fields of physiology and metabolism, neurobiology, and developmental biology.

Science Writing Fellowships

In its fifth year, the MBL Science Writing Fellowships Program evolved a one-week, hands-on course in cellular and molecular biology for science writers. Co-directed by Dr. Robert Goldman, Northwestern University Medical School, and Boyce Rensberger, *The Washington Post,* the course began with an introduction to cells and a microscopy demonstration, and ended five days later with the writers cloning and sequencing DNA. The course, which will be expanded to include a neurobiology component in 1991, is open to all science writers and serves as an orientation for the MBL Science Writing Fellows.

Directorship of the Science Writing Program has passed from founding director James Shreeve to Dr. Byron Waksman. Mr. Shreeve will continue to serve on the program's advisory board.

The Tokyo String Quartet. Photo by Christian Steiner.

Public programs

We continued to offer a few modest programs for our non-scientist neighbors on the Upper Cape. In July we held a public symposium on Science and Public Policy. The keynote address was delivered by Massachusetts Senator John Kerry, who urged the science community to become more involved in the very political process of forging a coherent national science policy. The symposium was followed by the second annual MBL Chamber Music Concert, featuring the Tokyo String Quartet.

The first annual Falmouth Forum concluded in early 1990 with presentations by Dr. Allen Counter on Black Arctic explorer Matthew Henson, Anne Hawley on the government as patron of the arts, a musical portrait of Harry Truman by David McCullough, and a panel discussion on energy and the environment. The series was well enough received by local audiences that the MBL Associates brought it back for the winter of 1990–91. Marshall Goldman began the second Falmouth Forum series in November with a presentation on Perestroika, and in December actress Julie Harris read from *Lucifer's Child,* her new one-woman play.

—Harlyn O. Halvorson

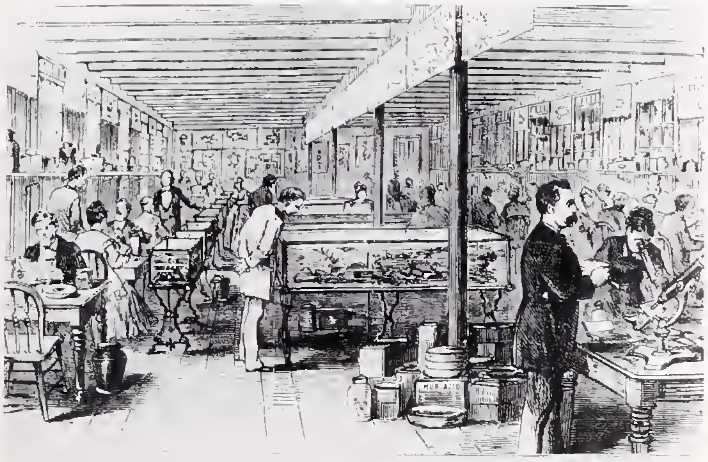

THE LABORATORY

Report of the Treasurer

The year 1990 was one of building for the Laboratory. Total support and revenues increased from $16.2 to $17.1 million due primarily to the initiation of construction of the Marine Resources Center, supported by a grant from the federal government; $1.4 million was received and expended on this project in 1990. Gifts received decreased approximately $1.6 million; 1989 was the last year of the receipt of significant funds from the Howard Hughes Foundation multi-year grant for the Library and the Education programs. Dining hall revenues rose $170,000 due to increases in food service functions, attendees, and meal card prices. Investment income grew $200,000 from 1989 to 1990 due to increases of long- and short-term investments and the length of time that they were available to the Laboratory during the respective years. Recovery of indirect costs related to research and instruction grew by approximately $150,000, all of which was attributable to the growth of MBL sponsored research. Other operating revenues were essentially unchanged from 1989.

Total expenses grew approximately $700,000, from $15 million in 1989 to $15.7 million in 1990. The most significant increases were in Research Services and Plant Operations; the former is due primarily to the expansion of the operations of the Mass Spectrometry Laboratory, the Instrument Development Laboratory, and the Protein and Nucleic Acid Chemistry Center operated jointly with the Woods Hole Oceanographic Institution; the latter is due primarily to increased utility, insurance, and labor costs, as well as significant expenses involving the removal of asbestos and other repairs and renovations of our housing. It is also worth noting that the Laboratory was able to offer approximately $100,000 more scholarships, fellowships, and stipends in 1990 than in 1989, a 35% increase. While our aim is to provide much more, the trend is very heartening, as we have almost doubled the amount of scholarships, fellowships, and stipends from 1988.

The Current Unrestricted Fund ended the year with an excess of support and revenues over expenses of $93,407. This combines the results of the Housing and Dining Auxiliary with all other Operations. The Housing and Dining Auxiliary had an excess of support and revenues over expenses of $267,761, of which $65,000 was used for scheduled repayment of debt owed on the Memorial Circle cottages and $199,863 was transferred to the Repairs and Replacements Reserve for housing. More sobering and troublesome, however, is that the operations of the Laboratory without the Housing and Dining operation experienced a deficiency of revenues to expenses of $174,354. The single greatest reason for this was our inability to meet budgeted goals for unrestricted current gifts.

The balance sheet shows that we ended 1990 with a significant degree of liquidity as cash and short-term investments accounted for approximately two-thirds of current assets. Investments at market grew by approximately $400,000. Essentially all of that was attributable to gifts for endowment, as the net impact of the market on the valuation of our investments was a decline of less than $100,000.

Land, buildings and equipment, net of accumulated depreciation, grew by almost $1 million due primarily to the beginning of construction of the Marine Resources Center. When completed, the cost of this project is expected to total $9 million.

The operating budget for 1991 reflects a determination to maintain the current level of services at the Laboratory in the most cost-effective manner possible, while we redouble our efforts to generate more funds to support operations.

Our greatest single challenge is still the need to find a cost-effective way to provide services that are primarily used during the summer months. The strategy of the Laboratory for the last 20 years has been to increase the size of the year-round program to provide a more stable financial base for the Laboratory. The Ecosystems Center has been the most notable success to date, and we trust that this will be a model for other MBL sponsored programs. The principal financial benefit of this strategy is the potential to achieve efficiencies in the cost of administration and services by spreading them across a broader base. We recognize that these will only be achieved by focusing on ways to be as efficient as possible.

The principal financial cost of this strategy is the capital cost of the laboratory building and equipment to house the scientists and their science, as well as the reserve or endowment funds necessary to attract scientists. Through the federal funding to date of the MBIAS project, we are well on our way towards funding the necessary buildings. The next significant challenge will be generating the necessary program support funds.

This strategy presumes the continued excellence of the summer research and education programs. Our education program shows many signs of health and vitality. Courses are oversubscribed; we have had renewed success in obtaining grants, and funding remains in place to support the overhead costs of the program for the next few years. Our single greatest challenge at the moment is the renewal of this support either through endowment or renewed medium-term funding.

Our summer research program shows signs of financial stress. Applications, occupancy, and revenues have been flat to marginally declining for the last couple of years. It is clear that reductions in federal funding have placed a greater budgetary burden on scientists seeking to come to the MBL in the summer, and some have had to withdraw.

The Laboratory has long subsidized the cost of a summer stay for all scientists from its discretionary resources—the summer laboratory fee falls significantly short of the fully allocated cost of the space—but our ability to do so is limited. We can selectively support a few scientists, principally young investigators, and we have had some success recently with the establishment of two Nikon fellowships for young summer scientists, but we need to do much more.

It is clear that increased attention needs to be paid to the summer research program to continue its financial vitality. We need to attract more applicants; we need to find more funds to allow young scientists to become familiar with the MBL; and we need to be as efficient as possible in offering and delivering the services that make a stay at the MBL the most productive scientific experience possible.

Financially, your Laboratory lives on the edge. On the positive side, we have continued to demonstrate our ability to attract funds from the federal government, from foundations, and from individuals. We are in the process of significantly upgrading our physical plant, to make the Laboratory an even more attractive place to do science. Our housing budget is currently generating the funds necessary to assure that we will be able to continue to maintain and upgrade those facilities. Our endowment has continued to grow. On the negative side, our endowment is not large enough to provide a financial cushion for any of our major programs with the significant exception of the Ecosystems Center. We have limited funds to recruit scientists whether for summer or year-round programs. Our support services do not cover their costs through charges for their services, and operations aside from Housing and Dining are in deficit.

To move off the edge we will need to do three things:

- More clearly define, articulate, and communicate the MBL's special contribution to science and society
- Significantly improve our generation of capital and operating support through fund raising
- Redefine for ourselves what constitutes the most effective delivery of services in the most efficient manner.

—Robert D. Manz

Coopers
&Lybrand

certified public accountants

REPORT OF INDEPENDENT ACCOUNTANTS

To the Trustees of
Marine Biological Laboratory
Woods Hole, Massachusetts

We have audited the accompanying balance sheet of Marine Biological Laboratory as of December 31, 1990 and the related statement of support, revenues, expenses and changes in fund balances for the year then ended. We previously examined and reported upon the financial statements of the Laboratory for the year ended December 31, 1989, which condensed statements are presented for comparative purposes only. These financial statements are the responsibility of the Laboratory's management. Our responsibility is to express an opinion on these financial statements based on our audit.

We conducted our audit in accordance with generally accepted auditing standards. Those standards require that we plan and perform the audit to obtain reasonable assurance about whether the financial statements are free of material misstatement. An audit includes examining, on a test basis, evidence supporting the amounts and disclosures in the financial statements. An audit also includes assessing the accounting principles used and significant estimates made by management, as well as evaluating the overall financial statement presentation. We believe that our audit provides a reasonable basis for our opinion.

In our opinion, the financial statements referred to above present fairly, in all material respects, the financial position of Marine Biological Laboratory at December 31, 1990, and its support, revenues, expenses and changes in fund balances for the year then ended in conformity with generally accepted accounting principles.

Our audit was conducted for the purpose of forming an opinion on the basic financial statements taken as a whole. The supplemental schedules of support, revenues, expense and changes in fund balances for current funds (Schedule I), endowment funds (Schedule II) and plant funds (Schedule III) as of December 31, 1990 are presented for purposes of additional analysis and are not a required part of the basic financial statements. Such information has been subjected to the auditing procedures applied in the audit of the basic financial statements and, in our opinion, is fairly stated, in all material respects, in relation to the basic financial statements taken as a whole.

Coopers & Lybrand

Boston, Massachusetts
April 19, 1991

MARINE BIOLOGICAL LABORATORY

BALANCE SHEETS

December 31, 1990
(with comparative totals for 1989)

ASSETS	*1990*	*1989*
Cash and savings deposits	$ 304,980	$ 496,014
Restricted cash	545,796	—
Short-term investments (Notes B and H)	1,654,044	965,000
Accounts receivable, net of allowance for uncollectible accounts	540,983	500,644
Receivables due for costs incurred on grants and contracts	581,880	1,200,558
Other assets	35,679	35,098
Total current assets	3,663,362	3,197,314
Investments, at market (Notes B and H)	16,395,852	15,971,459
Deposits with trustees (Note G)	143,006	133,000
Land, buildings and equipment (Notes B and C)	22,433,590	20,869,811
Less accumulated depreciation	(9,459,548)	(8,858,047)
	12,974,042	12,011,764
Total assets	$33,176,262	$31,313,537

LIABILITIES AND FUND BALANCES	*1990*	*1989*
Current portion of long-term debt	$ 65,000	$ 65,000
Accounts payable and accrued expenses	774,139	1,127,944
Deferred income	679,849	120,137
Total current liabilities	1,518,988	1,313,081
Mortgage and notes payable (Note G)	1,200,000	1,265,000
Deferred support (Note K)	4,774,618	4,450,222
Annuities payable (Note B)	117,381	105,355
Total long-term liabilities	6,091,999	5,820,577
Total liabilities	7,610,987	7,133,658
Current unrestricted fund balances	19,518	21,030
Endowment funds:		
Quasi-endowment unrestricted	237,279	426,982
Endowment, income for unrestricted purposes	3,291,503	3,234,878
Endowment, income for restricted purposes	5,122,448	4,804,006
Quasi-endowment restricted	4,565,674	4,480,887
	12,979,625	12,519,771
	13,216,904	12,946,753
Plant fund balances:		
Unrestricted	9,908,615	10,272,954
Repairs and replacement reserve	450,525	148,820
Restricted	1,969,713	790,322
Total plant funds	12,328,853	11,212,096
Total liabilities and fund balances	$33,176,262	$31,313,537

The accompanying notes are an integral part of the financial statements.

MARINE BIOLOGICAL LABORATORY

Statement of Support, Revenues, Expenses and Changes in Fund Balances

for the year ended December 31, 1990
(with comparative totals for 1989)

	Current Funds		Endowment Funds		Plant Funds		1990 Total All Funds	1989 Total All Funds
	Unrestricted	Restricted	Unrestricted	Restricted	Unrestricted	Restricted		
SUPPORT AND REVENUES:								
Grant reimbursement of direct cost		$4,872,529					$ 4,872,529	$ 5,090,117
Grant for capital additions						$1,429,322	1,429,322	574,821
Recovery of indirect costs related to research and instruction programs	$3,136,240						3,136,240	2,948,406
Tuition		484,749					484,749	440,562
Support activities:								
Dormitories	906,292						906,292	869,768
Dining hall	802,447						802,447	632,463
Library	273,475						273,475	249,128
Biological Bulletin	172,085						172,085	188,681
Research services	491,642	236,366					728,008	708,368
Marine resources	149,555						149,555	141,143
Investment income	466,931	674,423					1,141,354	942,951
	6,398,667	6,268,067				1,429,322	14,096,056	12,786,408
Gifts (Note I)	634,428	1,979,547		$ 314,972			2,928,947	4,597,591
Change in deferred support (Note K)	—	(324,396)		—			(324,396)	(1,498,560)
	634,428	1,655,151		314,972			2,604,551	3,099,031
Miscellaneous revenue	114,516	224,740					339,256	269,657
Total support and revenues	7,147,611	8,147,958		314,972		1,429,322	17,039,863	16,155,096

MARINE BIOLOGICAL LABORATORY

STATEMENT OF SUPPORT, REVENUES, EXPENSES AND CHANGES IN FUND BALANCES

for the year ended December 31, 1990
(with comparative totals for 1989)
(*continued*)

	Current Funds		Endowment Funds		Plant Funds		1990 Total	1989 Total
	Unrestricted	Restricted	Unrestricted	Restricted	Unrestricted	Restricted	All Funds	All Funds
EXPENSES:								
Instruction		1,370,282					1,370,282	1,328,404
Research		5,228,030					5,228,030	5,070,730
Scholarships, fellowships, and stipends		356,253					356,253	264,699
Support activities:								
Dormitories	638,531						638,531	736,272
Dining hall	690,644						690,644	543,797
Library	579,898	172,398					752,296	761,654
Biological Bulletin	141,118						141,118	192,741
Research services	658,115	347,996					1,006,111	843,511
Marine resources	443,676	6,791					450,467	373,571
Administration	1,979,541	35,014					2,014,555	1,897,994
Sponsored projects administration	278,221						278,221	316,501
Plant operations	1,644,460	1,009			$ 111,922		1,757,391	1,481,382
Depreciation					601,501		601,501	589,120
Other		432,408			8,500		440,908	574,696
Total expenses	7,054,204	7,950,181		—	721,923		15,726,308	14,975,072
Excess (deficit) of support and revenues over expenses	93,407	197,777		314,972	(721,923)	1,429,322	1,313,555	1,180,024
Realized gain on investments		1,649	$ 9,488	481,361			492,498	560,853
Unrealized gain (loss) on investments		19,868	(11,451)	(429,074)			(420,657)	994,541
Total gain (loss) on investments	—	21,517	(1,963)	52,287		—	71,841	1,555,394
Transfers	(94,919)	(219,294)	(187,740)	92,595	659,289	(249,931)	—	—
Net change in fund balances	(1,512)	—	(189,703)	459,854	(62,634)	1,179,391	1,385,396	2,735,418
Fund balances, beginning of year	21,030	—	426,982	12,519,771	10,421,774	790,322	24,179,879	21,444,461
Fund balances, end of year	$ 19,518	—	$237,279	$12,979,625	$10,359,140	$1,969,713	$25,565,275	$24,179,879

The accompanying notes are an integral part of the financial statements.

Marine Biological Laboratory

Notes to Financial Statements

A. *Purpose of the Laboratory:*

The purpose of Marine Biological Laboratory (the "Laboratory") is to establish and maintain a laboratory or station for scientific study and investigations, and a school for instruction in biology and natural history.

B. *Significant accounting policies:*

Basis of presentation—fund accounting

In order to ensure observance of limitations and restrictions placed on the use of resources available to the Laboratory, the accounts of the Laboratory are maintained in accordance with the principles of fund accounting. This is the procedure by which resources are classified into separate funds in accordance with specified activities or objectives. Separate accounts are maintained for each fund; however, in the accompanying financial statements, funds that have similar characteristics have been combined into fund groups. Accordingly, all financial transactions have been recorded and reported by fund group.

Externally restricted funds may only be utilized in accordance with the purposes established by the donor or grantor of such funds. However, the Laboratory retains full control over the utilization of unrestricted funds. Restricted gifts, grants, and other restricted resources are accounted for in the appropriate restricted funds. Restricted current funds are reported as revenue as the related costs are incurred (see Note K).

Endowment funds are subject to restrictions requiring that the principal be invested in perpetuity with income available for use for restricted or unrestricted purposes by the Laboratory. Quasi-endowment funds have been established by the Laboratory for the same purposes as endowment funds; however, the principal of these funds may be expended for various restricted and unrestricted purposes.

Fixed assets

Fixed assets are recorded at cost. Depreciation is computed using the straight-line method over estimated useful lives of fixed assets.

Contracts and grants

Revenues associated with contracts and grants are recognized in the statement of support, revenues, expenses and changes in fund balances as the related costs are incurred (see Note K). The Laboratory reimbursement of indirect costs relating to government contracts and grants is based on negotiated indirect cost rates with adjustments for actual indirect costs in future years. Any over or underrecovery of indirect costs is recognized through future adjustments of indirect cost rates.

Investments

Investments purchased by the Laboratory are carried at market value. Money market securities are carried at cost which approximates market value. Investments donated to the Laboratory are carried at fair market value at the date of the gift. For determination of gain or loss upon disposal of investments, cost is determined based on the average cost method.

The Laboratory is the beneficiary of certain endowment investments reported in the financial statements which are held in trust by others. Every ten years the Laboratory's status as beneficiary of these funds is reviewed to determine that the Laboratory's use of these funds is in accordance with the intent of the funds. The market values of these investments are $4,125,093 and $4,039,803 at December 31, 1990, and 1989, respectively.

Investment income and distribution

The Laboratory follows the accrual basis of accounting except that investment income is recorded on a cash basis. The difference between such basis and the accrual basis does not have a material effect on the determination of investment income earned on a year-to-year basis.

Investment income includes income from the investments of specific funds and from the pooled investment account. Income from the pooled investment account is distributed to the participating funds on the market value unit basis (Note L).

Annuities payable

Amounts due to donors in connection with gift annuities is determined based on remainder value calculations which generally assure a rate of return at 10%, maximum payout terms of eighteen years, and interest payout rate of 8%.

C. *Land, buildings and equipment:*

The following is a summary of the unrestricted plant fund assets:

	1990	*1989*
Land	$ 689,660	$ 689,660
Buildings	16,955,015	16,926,715
Equipment	2,819,202	2,672,838
Construction in progress	1,969,713	580,598
	22,433,590	20,869,811
Less accumulated depreciation	(9,459,548)	(8,858,047)
	$12,974,042	$12,011,764

D. *Retirement plan:*

The Laboratory participates in the defined contribution pension program of the Teachers Insurance and Annuity Association College Retirement Equities Fund. Contributions amounted to $451,665 in 1990 and $393,422 in 1989.

E. *Restricted pledges and grants:*

As of December 31, 1990, the Laboratory reported active pledge and grant commitments outstanding of $492,939 (unaudited) to be received. The restricted pledges are not included in the financial statements since it is not practicable to estimate the net realizable value of such pledges. Restricted pledges of $467,337, and $14,151 and $11,451 are scheduled to be paid in 1991, 1992, and 1993, respectively.

F. *Interfund borrowings:*

Current fund interfund balances at December 31 are as follows:

	1990	*1989*
Due to restricted endowment fund	$(4,750)	$(2,190)
Due to restricted quasi-endowment funds	(1,650)	(200)
	$(6,400)	$(2,390)

G. *Mortgage and notes payable:*

Long-term debt at December 31, 1990 amounted to $1,265,000. The aggregate amount of redemption due for each of the next five fiscal years is as follows:

	Amount
1991	$ 65,000
1992	60,000
1993	60,000
1994	60,000
1995	60,000
Thereafter	960,000
	1,265,000
Less current portion	65,000
	$1,200,000

In 1989, the Laboratory issued $1,330,000 Massachusetts Industrial Finance Authority (MIFA) Series 1989 Bonds, which pay varying annual interest rates and mature on October 31, 2011. The Series 1989 bonds are collateralized by a first mortgage on certain Laboratory property.

The interest rate is adjustable and was 7.25% and 6.5% at December 31, 1990 and 1989. In compliance with the Laboratory's MIFA bond indenture, deposits with Shawmut Bank N.A., as trustee, represent investments in the debt service reserve fund of $143,006 in 1990 and $133,000 in 1989.

H. *Investments:*

The following is a summary of the cost and market value of investments at December 31, 1990 and 1989 and the related investment income and distribution of investment income for the years ended December 31, 1990 and 1989.

	Cost		*Market*		*Investment Income*	
	1990	*1989*	*1990*	*1989*	*1990*	*1989*
Endowment and Quasi-Endowment						
U.S. Government securities	$ 1,934,834	$ 2,595,407	$ 1,957,512	$ 2,607,537	$ 214,300	$134,394
Corporate fixed income	6,663,376	5,900,736	6,809,264	6,032,642	506,490	363,439
Common stocks	4,284,165	3,392,001	6,346,778	5,901,724	234,690	196,452
Money market securities	590,735	595,467	590,735	593,544	121,787	87,994
Real estate	343,247	345,749	343,247	345,749	—	—
Total	13,816,357	12,829,360	16,047,536	15,481,196	1,077,267	782,279
Less custodian and management fees					(55,592)	(49,318)
Total	13,816,357	12,829,360	16,047,536	15,481,196	1,021,675	732,961
Restricted Current Fund						
Certificates of deposits	502,360	490,263	502,360	490,263	20,312	34,785
Money market securities	1,500,000	965,000	1,500,000	965,000	99,367	175,205
Total	2,002,360	1,455,263	2,002,360	1,455,263	119,679	209,990
Total investments	$15,818,717	$14,284,623	$18,049,896	$16,936,459	$1,141,354	$942,951

I. *Gift support for instruction:*

Current year unrestricted gifts includes $500,000 of gifts for the support of the Laboratory's instruction program available for indirect costs attributable to the instruction program.

J. *Tax-exempt status:*

The Laboratory is exempt from federal income tax under Section 501(c)3 of the Internal Revenue Code.

K. *Restricted current funds deferred support:*

The Laboratory defers recognition of revenue on current restricted funds until the related costs are incurred. Amounts received in excess of expenses are recorded as deferred support. The following summarizes the activity in the deferred support account for 1990 and 1989, respectively:

	1990	*1989*
Balance at beginning of year	$4,450,222	$2,951,662
Additions:		
Gifts, endowment income and grants received	8,499,360	9,382,212
Unrealized gains	19,868	30,672
Realized gain	1,649	—
Deductions:		
Funds expended under gifts and grants	7,977,187	7,542,909
Transfers	219,294	371,415
Balance at end of year	$4,774,618	$4,450,222

L. *Accounting for pooled investments:*

The major portion of investment assets is pooled for investment purposes with each participating fund subscribing to, or disposing of, units at market value at the beginning of the current quarter. The unit participation of the funds at December 31, 1990 and 1989, respectively, is as follows:

	1990	*1989*
Endowment and similar funds:		
Quasi-unrestricted	3,909	3,887
Quasi-restricted	7,436	7,416
Restricted endowment	39,401	36,488
	50,746	47,791

Pooled investment activity on a per-unit basis was as follows:

	1990	1989
Unit value at beginning of year	$109.57	$100.00
Unit value at end of year	108.90	109.57
Increase (decrease) in realized and unrealized appreciation	(.67)	9.57
Net income earned on pooled investments	5.99	5.73
Total return on pooled investments	$ 5.32	$ 15.30

Investment income is distributed to individual funds as earned.

SCHEDULE I

MARINE BIOLOGICAL LABORATORY

STATEMENT OF SUPPORT, REVENUES, EXPENSES AND CHANGES IN FUND BALANCES

CURRENT FUNDS

for the year ended December 31, 1990

	Operating Fund	*Auxiliary Enterprises Fund*	*Total Current Unrestricted Fund*	*Current Restricted Fund*	*Total*
SUPPORT AND REVENUES:					
Grant reimbursement of direct costs				$4,872,529	$4,872,529
Recovery of indirect costs related to research and instruction programs	$3,136,240		$3,136,240		3,136,240
Tuition				484,749	484,749
Support activities:					
Dormitories		$ 906,292	906,292		906,292
Dining hall		802,447	802,447		802,447
Library	273,475		273,475		273,475
Biological Bulletin	172,085		172,085		172,085
Research services	491,642		491,642	236,366	728,008
Marine resources	149,555		149,555		149,555
Investment income	466,931		466,931	674,423	1,141,354
	4,689,928	1,708,739	6,398,667	6,268,067	12,666,734
Gifts	634,428		634,428	1,979,547	2,613,975
Change in deferred support	—		—	(324,396)	(324,396)
	634,428		634,428	1,655,151	2,289,579
Miscellaneous revenue	114,516		114,516	224,740	339,256
Total support and revenues	5,438,872	1,708,739	7,147,611	8,147,958	15,295,569
EXPENSES:					
Instruction				1,370,282	1,370,282
Research				5,228,030	5,228,030
Scholarships, fellowships, and stipends				356,253	356,253
Support activities:					
Dormitories		638,531	638,531		638,531
Dining hall		690,644	690,644		690,644
Library	579,898		579,898	172,398	752,296
Biological Bulletin	141,118		141,118		141,118
Research services	658,115		658,115	347,996	1,006,111
Marine resources	443,676		443,676	6,791	450,467
Administration	1,867,738	111,803	1,979,541	35,014	2,014,555
Sponsored projects administration	278,221		278,221		278,221
Plant operations	1,644,460		1,644,460	1,009	1,645,469
Other	—		—	432,408	432,408
Total expenses	5,613,226	1,440,978	7,054,204	7,950,181	15,004,385
Excess (deficit) of support and revenues over expenses	(174,354)	267,761	93,407	197,777	291,184
Unrealized gain on investments				19,868	19,868
Realized gain on investments				1,649	1,649
Total gain on investments				21,517	21,517
TRANSFERS AMONG FUNDS:					
Debt service		(65,000)	(65,000)		(65,000)
Acquisition of fixed assets				(144,881)	(144,881)
To unrestricted plant fund	(21,653)		(21,653)		(21,653)
Housing transfer	2,898	(199,863)	(196,965)		(196,965)
To support operations	190,000		190,000	135,209	325,209
Instruction	(5,045)		(5,045)	5,045	—
Capitalize ecosystems income				(215,764)	(215,764)
Other	6,642	(2,898)	3,744	1,097	4,841
Total transfers among funds	172,842	(267,761)	(94,919)	(219,294)	(314,213)
Net change in fund balance	(1,512)	—	(1,512)	—	(1,512)
Fund balances, beginning of year	21,030	—	21,030	—	21,030
Fund balances, end of year	$ 19,518	—	$ 19,518	—	$ 19,518

SCHEDULE II

MARINE BIOLOGICAL LABORATORY

STATEMENT OF SUPPORT, REVENUES, EXPENSES AND CHANGES IN FUND BALANCES

ENDOWMENT FUNDS

for the year ended December 31, 1990

	Unrestricted	Restricted				
	Quasi-Endowment	*Endowment, Income for Unrestricted Purposes*	*Endowment, Income for Restricted Purposes*	*Quasi-Endowment*	*Total Restricted*	*Total*
SUPPORT AND REVENUES:						
Gifts			$ 312,522	$ 2,450	$ 314,972	$ 314,972
Total support and revenues			312,522	2,450	314,972	314,972
Excess of support and revenues over expenses			312,522	2,450	314,972	314,972
Realized gains on investments	$ 9,488	$ 165,441	121,543	194,377	481,361	490,849
Unrealized gain (loss) on investments	(11,451)	(110,737)	(113,465)	(204,872)	(429,074)	(440,525)
Total gain (loss) on investments	(1,963)	54,704	8,078	(10,495)	52,287	50,324
TRANSFERS AMONG FUNDS:						
Capitalize ecosystems income				215,764	215,764	215,764
Endowment transfers	(190,000)			(135,209)	(135,209)	(325,209)
Other transfers	2,260	1,921	(2,158)	12,277	12,040	14,300
Total transfers among funds	(187,740)	1,921	(2,158)	92,832	92,595	(95,145)
Net change in fund balances	(189,703)	56,625	318,442	84,787	459,854	270,151
Fund balances, beginning of year	426,982	3,234,878	4,804,006	4,480,887	12,519,771	12,946,753
Fund balances, end of year	$237,279	$3,291,503	$5,122,448	$4,565,674	$12,979,625	$13,216,904

Schedule III

MARINE BIOLOGICAL LABORATORY

Statement of Support, Revenues, Expenses and Changes in Fund Balances

Plant Funds

for the year ended December 31, 1990

	Unrestricted				
	Unrestricted	*Repairs and Replacement Reserve*	*Total Unrestricted*	*Restricted*	*Total*
SUPPORT AND REVENUES:					
Grant for capital additions				$1,429,322	$ 1,429,322
Total support and revenues				1,429,322	1,429,322
EXPENSES:					
Depreciation	$ 601,501		$ 601,501		601,501
Plant operations		$111,922	111,922		111,922
Other	8,500		8,500		8,500
Total expenses	610,001	111,922	721,923	—	721,923
Excess (deficit) of support and revenues over expenses	(610,001)	(111,922)	(721,923)	1,429,322	707,399
TRANSFERS AMONG FUNDS:					
Debt service	65,000		65,000		65,000
Acquisition of fixed assets	180,662		180,662		180,662
Transfers to unrestricted plant fund		(14,128)	(14,128)		(14,128)
Housing transfers		199,863	199,863		199,863
Other transfers		227,892	227,892	(249,931)	(22,039)
Total transfers among funds	245,662	413,627	659,289	(249,931)	409,358
Net change in fund balances	(364,339)	301,705	(62,634)	1,179,391	1,116,757
Fund balances, beginning of year	10,272,954	148,820	10,421,774	790,322	11,212,096
Fund balances, end of year	$ 9,908,615	$450,525	$10,359,140	$1,969,713	$12,328,853

Report of the Librarian

Library directors

In 1990, Jane Fessenden, who had been the librarian and worked at the MBL for 29 years, retired. Jane made the Library a productive home for its users, improved the collection whenever financially possible, and lead the Library through innumerable changes. During her tenure, the Library was converted from the Dewey Decimal System to Library of Congress, the first "stack move" took place (after three years of planning), the reading rooms were redone, the Rare Books Room was created, the Copy Service Center was developed in its present location, staff was increased, and new technology was initiated. She will be best remembered, however, for her unique ability to provide the services and support most desired by our users.

In December, Dr. David Stonehill accepted the position of Director of the MBL/WHOI Library and Scientific Information Research Center. Dr. Stonehill managed computer facilities on various NASA projects and directed computing services at academic institutions. From 1988 until his move to MBL, he was Director of Information Resources Managements for the Executive offices of the President of the United States. Under Dr. Stonehill, the Library plans to launch a Scientific Information Research Center, and we look forward to his leadership as we meld the traditional with the new methods of scientific information management.

New age information delivery

Using the report created by the Hughes Committee, the Library immediately began to implement some of its recommendations. A network manager was hired, and the network design was completed. What followed was a frenzy of equipment ordering and the installation of cable and wires to extend the network out of the library and into classrooms and labs in the Lillie and Loeb buildings and the Ecosystems Center. Because of the ease of communicating over the network, some of the traditional methods of the reference librarians moved into a new era during 1990. One advance, Current Contents loaded onto the librarians' computers, allowed us to send weekly up-dated bibliographies to requesters over the MBLnet.

The Library's catalog has been converted to electronic records, and all the books in the library were barcoded as part of the automation of library systems. The CLAMS network of libraries came on-line in 1990, and scientists in their laboratories, who are on the Woods Hole network, can connect to the catalog and see whether the library holds the book they are seeking.

Journal rates increase

Our Library has studied the effect of rising book and subscriptions costs beginning with the comprehensive Rockefeller Journal Use study. In 1990, the close to 30% projected journal price increase reduced our options and resulted in the cancellation of 338 current subscriptions. Our User Panel worked throughout the summer with lists of journals targeted for cancellation, using criteria established by the Joint Users Committee, to insure the best possible preservation of our collection and services.

This was not the only journal crisis of 1990—the space allocation for housing the journals had reached saturation. For over a year, the creation of a design to preserve our stack space has been developed and refined and the periodical collection will be moved during the beginning of 1991. The logical placement of the

collections according to the alphabet will be maintained, albeit into two places. The A–Z arrangement will be in the front part of the stacks for currently received journals and also in the back wing for the pre-1976 journals.

In an attempt to recover some of the escalating costs incurred in the Library, we have tried to create a model for users who are not directly associated with the contributing Woods Hole institutions. We have also changed our interlibrary loan policies and have increased resource sharing with a number of institutions, *i.e.,* Brandeis, University of Massachusetts Medical School, Wesleyan, University of Rhode Island and the Pell Laboratory. Escalating costs and U. S. postage rates drove the increase in interlibrary loan charges, and at the International Association of Marine Science Libraries and Information Centers' conference in Seattle, Washington, we were challenged, without ill will, but with some concern from the international community, about our rate increases. A solution to this problem may involve sharing the responsibility for serials collection development at the national and international level during the 1990s.

Preservation

Two documents that have been of historic and sentimental value to the scientists, staff, and visitors of the MBL were appraised and declared endangered. **Study Nature Not Books**—the black charcoal, handwritten sign of Louis Agassiz—had adhered to its backing and tears, holes, stains, rust, scratches, and smudges were evident everywhere. The same was true of the two-page **Last one to Go** message to American soldiers by Katsuma Dan. Both of these documents were sent to the Northeast Document Conservation Center for treatment and have been returned to the library for display.

—Cathy Norton
Acting Librarian

Educational Programs

Summer Courses

Biology of Parasitism (June 10 to August 10)

Co-Directors

John Donelson, University of Iowa College of Medicine
Carole Long, Hahnemann Medical College

Faculty

Steven Anderson, University of Iowa
John Boothroyd, Stanford University
Ted Bianco, Imperial College of Science & Technology, UK
Patrick Farley, Hahnemann Medical College
Steven Hajduk, University of Alabama, Birmingham
Peter Ham, Liverpool School of Tropical Medicine, UK
Michael E. Harris, University of Alabama, Birmingham
Mary Alice Hartman, University of Kentucky
Kwang S. Kim, University of Iowa
Peter Kima, Hahnemann Medical College
Yien Ming Kuo, Imperial College, UK
Rick Martin, University of Iowa
David Moser, University of Iowa
Elonne Petrin, University of Cincinnati
David Russell, New York University
David Sachs, NIH
Judy Sakanari, University of California, San Francisco
Sam Turco, University of Kentucky

Lecturers

Nina Agabian, University of California, San Francisco
Steven Beverley, Harvard Medical School
Kent Campbell, Centers for Disease Control
Dickson Despommier, Columbia University
Paul Englund, Johns Hopkins School of Medicine
Don Harn, Harvard University
Stephanie James, NIH
Keith Joiner, Yale University School of Medicine
Patricia J. Johnson, UCLA
Don Krogstad, Washington University, St. Louis
Ira Mellman, Yale University School of Medicine
George Nelson, Liverpool School, UK
Ruth Nussenzweig, New York University
Victor Nussenzweig, New York University
Richard Olds, Brown University
Bill Petri, University of Virginia
Robert Sauer, Massachusetts Institute of Technology
Alan Sher, NIH
Irwin Sherman, University of California, Riverside
Larry Simpson, UCLA
Mitch Sogin, MBL
Rick Tarleton, University of Georgia
Merv Turner, Merck Sharp & Dohme Research Laboratory
C. C. Wang, University of California, San Francisco
Leon Weiss, University of Pennsylvania
Don Wiley, Harvard University
Dyann Wirth, Harvard University

Students

Wanida Asawanahasakda, Mahidol University, Thailand
Fernanda R. Gadelha, University of Illinois
Eileen S. Gruszynski, University of California, Los Angeles
Michael J. Howard, Vanderbilt University
Christopher A. Hunter, University of Glasgow, Scotland
Gregory J. Jennings, Tulane University
Christopher L. Leptak, Yale University
Congjun Li, Worcester Foundation for Experimental Biology

Leo X. Liu, Beth Israel Hospital/Harvard University
James J. McCoy, University of Virginia
Gloria I. Palma, Univ. del Valle, Colombia
Laura J. Rocco, Johns Hopkins University
Nicola N. Schweitzer, Imperial College of Science, UK
Frank Seeber, Institüt für Tropenhygeine, Germany
Philippe G. Vandekerckhove, University of Leuven, Belgium
Gayl Wall, University of Dundee, Scotland

Embryology: Cell Differentiation and Gene Expression in Early Development

(June 21 to July 30)

Directors

Eric Davidson, California Institute of Technology
J. Richard Whitaker, MBL (Assistant Director)

Faculty

Michael Akam, University of Cambridge, UK
Amy Bejsovic, University of Cambridge, UK
Marianne Bronner-Fraser, University of California, Irvine
Scott Fraser, University of California, Irvine
Katherine Harding, Columbia University
Janet Heasman, University of Cambridge, UK
Linda Huffer, MBL
Wendy Katz, California Institute of Technology
Robert Kingsbury, Carnegie Institution, Baltimore
Thomas Lallier, University of California, Irvine
Robert Leclerc, University of Maryland
Michael Levine, Columbia University
David McClay, Duke University
Steven McKnight, Carnegie Institution of Washington
Robert Nickells, California Institute of Technology
Jerome Regier, University of Maryland
John Shuman, Carnegie Institution, Baltimore
Paul Sternberg, California Institute of Technology
Nicholas Torpey, University of Cambridge, UK
Kellie Whittaker, California Institute of Technology
Christopher Wylie, University of Cambridge, UK

Students

Kamran Ahmad, University of Utah
Michael J. Bank, Columbia University
Peter B. Bokor, Rockefeller University
James B. Castelli-Gair, University of Madrid, Spain
Robert A. Cornell, University of Washington
Maria G. Di Bernardo, Italian National Research Council, Italy
Win J. Dictus, University of Utrecht, The Netherlands
Anne D. Donaldson, MRC Laboratory, UK
Bruce W. Draper, University of Washington
Silvia B. Frenk, King's College, Cambridge, UK
Kareen M. Guida, University of Paris, France
Nan Ho, University of California, Berkeley
Jon F. Kayyem, California Institute of Technology
Dangeruta Kersulyte, Acadamy of Sciences of Lithuania, USSR
Daniel S. Kessler, Rockefeller University
Mary Ellen Lane, Columbia University
Thierry Lepage, University of Nice, France
Donal T. Manahan, University of Southern California, Los Angeles
Jeffrey R. Miller, Duke University
Anne Marie Murphy, Johns Hopkins University
Christof Niehrs, European Molecular Biology Lab., Germany
Mary E. Pownall, University of Virginia
Inge J. Van Wijk, Max-Planck Institute, Germany
Tongweng Wang, University of Florida

Marine Ecology: Concepts, Techniques and Applications of Molecular Probes

(June 17 to July 28)

Director

J. Woodland Hastings, Harvard University

Faculty

Cheryl Booth, Falmouth, MA
Ann Bucklin, Marine Biological Laboratory
Thomas T. Chen, Center of Marine Biotechnology, University of Maryland
Clara Cheng, University of Maryland
Toby Cole, Hopkins Marine Station, Stanford University
Lynna Hereford, Hopkins Marine Station, Stanford University
Chun-Mean Lin, University of Maryland
Kenneth Nealson, Great Lakes Research Center, University of Wisconsin, Milwaukee
Dennis Powers, Hopkins Marine Station, Stanford University
T. Roenneberg, University of Munich, Germany
Simona Sorger, Hopkins Marine Station, Stanford University
Keno Truper, Bonn, Germany
Barbara Wimpee, Great Lakes Research Center, University of Wisconsin, Milwaukee
Charles Wimpee, University of Wisconsin, Milwaukee

Lecturers

David Caron
Colleen Cavanaugh
Penny Chisholm
Ed De Long
Paul Dunlap
Brian Fry
Linda Goff
John Kessler
Lynn Margulis
James McCarthy
Dan Morse
Rob Olsen
Hans Paerl
Jack Palmer
Ned Ruby
G. Saylor
Ann Sesholz
Bob Simon
Mitch Sogin
Felix Strumwasser
John Waterbury

Students

Abdiel J. Alvarez, University of Puerto Rico
Brian J. Binder, Massachusetts Institute of Technology
Alice F. Brown, Brown University
Ka Hou Chu, Chinese University of Hong Kong, Hong Kong
Peter J. Edmunds, Northeastern University
Oivind Enger, University of Bergen, Norway
Jonathan B. Geller, University of Oregon
Gregory J. Hinkle, University of Massachusetts, Amherst
Robert E. Hodson, University of Georgia
Eric R. Holm, Duke University
Jerilyn Jewett-Smith, Whitman College
Lisa M. Kann, University of Rhode Island
James S. Maki, Harvard University
Kirk D. Malloy, University of Delaware
Adam G. Marsh, University of New Hampshire
Tracie-Lynn Nadeau, University of Wisconsin
Martin Polz, University of Vienna, Austria
Michael C. Schmale, University of Miami
Robin M. Schneider, University of Southern Louisiana
Lynda P. Shapiro, Bigelow Laboratory for Ocean Sciences
Robert L. Sinsabaugh, Clarkson University
Erika Stephens, Harvard University
Stephen C. Tsoi, University of Hong Kong, Hong Kong
Karl E. Wommack, University of Maryland

Microbiology: Molecular Aspects of Cellular Diversity **(*June 10 to July 26*)**

Co-Directors

Martin Dworkin, University of Minnesota
John Breznak, Michigan State University

Faculty

Richard Behmlander, University of Minnesota
Pamela Contag, University of Minnesota
Christiane Dahl, University of Bonn, Germany
Deborah Eastman, University of Minnesota
Andrew M. Kropinski, Queen's University, Canada
Hans Truper, University of Bonn, Germany
Stefan Wagener, Michigan State University

Lecturers

Paul Dunlap, Woods Hole Oceanographic Institution
Holger Jannasch, Woods Hole Oceanographic Institution
J. Waterbury, Woods Hole Oceanographic Institution

Students

Diane K. Arwood, University of Southern Mississippi
Joanna S. Brooke, University of Western Ontario, Canada
Joseph P. Calabrese, West Virginia University
Neena Din, University of British Columbia, Canada
Arnis Druka, Latvian State University, USSR
Olivia T. Harriott, University of Connecticut
Robert Huber, University of Regensburg, Germany
Jennifer B. Klenz, University of Saskatchewan, Canada
Judith A. Koskella, New York University
Bridget E. Laue, University of Colorado
Jared R. Leadbetter, Goucher College
Timothy C. Lilburn, University of British Columbia, Canada
Shi Liu, University of Oklahoma
Lynn V. Mendelman, Harvard Medical School
Elizabeth J. Orle, Colorado State University
Mechthild Pohlschroder, University of Massachusetts, Amherst
Frank J. Slack, Tufts University
Barth F. Smets, University of Illinois
Claire S. Ting, Cornell University
Mary A. Wyka, Merck & Co., Inc.

Neural Systems & Behavior **(*June 10 to August 1*)**

Co-Directors

Ronald Calabrese, Emory University
Martha Constantine-Paton, Yale University

Faculty

Arthur Arnold, University of California, Los Angeles
Alexander Borst, Max-Planck-Institüt für Biologisch Kybernetick, Germany
John Byrne, University of Texas Medical School
Thomas Carew, Yale University
Leonard Cleary, University of Texas Medical School at Houston
Robin Cloues, Harvard University
Michael Davis, Yale University
Robert M. Douglas, University of British Columbia, Canada
Lise Eliot, Center for Neurobiology & Behavior
Russell Fernald, University of Oregon
Leslie Fischer, Columbia University
William Frost, University of Texas Medical School
Cole Gilbert, University of Arizona
Dennis Gorlick, Columbia University
Jon Hayashi, Arizona Research Laboratory
Sally Hoskins, City College of CUNY
John Koester, New York State Psychiatric Institute
Richard B. Levine, University of Arizona
Yurin Levy, Brandeis University
Margaret Livingstone, Harvard Medical School
Anne Lohoff, Columbia University
Eduardo R. Macagno, Columbia University
Emilie Marcus, Yale University
Eve Marder, Brandeis University
Michael P. Nusbaum, University of Alabama, Birmingham
Mu-Ming Poo, Columbia University
David J. Sandstrom, University of California
Patricia Steen, Yale University
Nacita Tabti, Columbia University
Janis C. Weeks, University of Oregon
Angela Wenning, Universitat Konstanz, Germany
Michael Nitabach, Columbia University

Lecturers

Catherine Carr, University of Rochester
Joe Martinez, Jr., University of California

Students

Robert A. Berkowitz, Washington University
James P. Burke, University of Alabama, Birmingham
Belinda S. Chang, Harvard University
Miles G. Cunningham, Massachusetts Institute of Technology
Graeme W. Davis, University of Massachusetts, Amherst
Mayra Garcia-Ruiz, University of Nat. Autonoma, Mexico
John F. Hamilton, Meharry Medical College, Nashville
Tamara L. Harris, University of Ottawa, Canada
Valerie L. Kilman, University of Illinois
Barlett W. Mel, California Institute of Technology
Brett D. Mensch, Baylor College of Medicine
Alison R. Mercer, University of Otago, New Zealand
Edward P. Monaghan, University of California, Berkeley
Tanja Quenzer, Max-Planck-Institüt, Germany
Adina L. Roskies, University of California, San Diego
Hyunjune S. Seung, Harvard University
Deana L. Shackelford, University of Oklahoma
Petra Skiebe, Universitat Hamburg, Germany
John E. Spiro, University of California, San Diego
Douglas Syme, University of California, Irvine

Neurobiology (June 10 to August 11)

Co-Directors

Leonard Kaczmarek, Yale University
Irwin Levitan, Brandeis University
Christopher Miller, Brandeis University

Faculty

Cecilia Armstrong, University of Pennsylvania
Gary Banker, University of Virginia
Synnove Beckh, Max-Planck-Institüt für Biophysikalische Chemie, Germany
Andrew Czernik, Rockefeller University
Jan De Weer, Duke University
Judith Drazba, NINDS/NIH
Keith Elmslie, Case Western Reserve University
Stuart Firestein, Yale University School of Medicine
Paul Forscher, Yale University
Robert French, University of Calgary, Canada
Sara Garber, University of Alabama, Birmingham
Allison Hall, Case Western Reserve University
Richard Horn, Roche Institute for Molecular Biology
Richard Huganir, HHMI, Johns Hopkins Medical School
Stephen Jones, Case Western Reserve University
Richard Kramer, Columbia University
Kyu-Ho Lee, Johns Hopkins Medical School
Andrew Matus, Friedrich Meischer Institute, Switzerland
Robert Miller, Case Western Reserve University
Angus Nairn, Rockefeller University
Randall Reed, HHMI, Johns Hopkins Medical School
Thomas Reese, NINDS/NIH
Talvinder Sihra, Rockefeller University
Carolyn Smith, NINDS/NIH
Walter Stuhmer, Max-Planck-Institüt für Biophysikolische Chemie, Germany

Students

Ricardo C. Araneda, Albert Einstein Medical School
Sylwester Chyb, Wesleyan University
Dan H. Cox, Tufts University
Stuart D. Critz, University of Texas Medical School
Peter F. Drain, MIT
Kathryn J. Edson, University of Minnesota
Julie A. Haack, University of Utah
Lise R. Heginbotham, Harvard University
Marc A. Post, University of Michigan
Haohua Qian, University of Illinois
Hanno M. Roder, Massachusetts Institute of Technology
Maria A. Sosa, University of Florida

Physiology: Cell and Molecular Biology

(June 10 to July 21)

Director

Thomas D. Pollard, Johns Hopkins University

Faculty

Steven Almo, Johns Hopkins Medical School
Kerry Bloom, University of North Carolina
William Busa, Johns Hopkins University
Antony Galione, Johns Hopkins University
Neal R. Gliksman, University of North Carolina
Robert Jensen, Johns Hopkins School of Medicine
Margaret Kenna, University of North Carolina
John Maslanski, Johns Hopkins University
Jonathan McMenamin-Balano, University of Massachusetts, Boston
Robert Palazzo, Marine Biological Laboratory
Katherine Pollard, Johns Hopkins Medical School
Ted Salmon, University of North Carolina
Sue Schmidt, Glyndon, MD
John Simon, University of North Carolina
John Sinard, Johns Hopkins Medical School
Tammy Smith, University of North Carolina
Cynthia V. Stauffacher, Purdue University
Murray Stewart, Medical Research Council, UK
Elaine Yeh, University of North Carolina

Students

Robert L. Bacallao, University of California, Los Angeles
Sandra A. Brockman, Carnegie Mellon University
Thomas O. Carpenter, Yale University
Isabelle A. Carre, SUNY, Stony Brook
Joseph A. Cerro, Columbia University
Marc D. Coltrera, University of Washington
Tod A. Critchlow, Scripps Institute of Oceanography
Spencer J. Danto, Cornell Medical College
Michele I. Flatters, Tufts University
Holly V. Goodson, Stanford University
Supriya Jayadev, Duke University
John R. Jordan, University of Utah
David L. Keefe, Yale University
Karen L. King, Florida State University
Qingwen Li, University of Kansas
Helen McNeill, University of Pennsylvania
Michael E. Mendelsohn, Harvard/Brigham & Women's Hospital
Christa S. Merzdorf, Harvard University
Robert Mirro, University of Tennessee
Karen M. Page, Dartmouth College
Alice P. Pentland, Washington University, St. Louis
Zhican Qu, Johns Hopkins University
Joe W. Ramos, University of Virginia
Jean F. Regal, University of Minnesota
Eric A. Shelden, University of Massachusetts, Amherst
Charles B. Shuster, Tufts University
Thomas W. Smith, Brigham & Women's/Harvard Medical School
Robin L. Stears, SUNY, Stony Brook
Salme Taagepera, University of Virginia
Charlotte M. Vines, Harvard Medical School
Yingjian Wang, University of Miami
Christiane Wiese, Johns Hopkins Medical School
Elizabeth L. Winter, City College of New York
Vicki L. Wolff, Brandeis University
Qi Yang, University of Connecticut
Guangwen Zhou, Oregon State University

Short Courses

Analytical and Quantitative Light Microscopy in Biology, Medicine, and Materials Science

(May 10 to 18)

Co-Directors

Edward D. Salmon, University of North Carolina
Greenfield Sluder, Worcester Foundation for Experimental Biology
David E. Wolf, Worcester Foundation for Experimental Biology

Faculty and Course Assistants

Brad Amos, MRC, Cambridge, UK
Orit Baha, Worcester Foundation for Experimental Biology
Steven M. Block, Rowland Institute for Science
Richard Cardullo, Worcester Foundation for Experimental Biology
Walter Carrington, University of Massachusetts Medical School

Gordon Ellis, University of Pennsylvania
Fred Fay, University of Massachusetts Medical School
Jeff Gelles, Brandeis University
Richard Haugland, Molecular Probes, Eugene, OR
Linda Huffer, MBL
Shinya Inoué, MBL
Anthony Moss, Worcester Foundation for Experimental Biology
Rudolf Oldenbourg, MBL
Stephen Parsons, University of North Carolina
Robert V. Skibbens, University of North Carolina
Kenneth R. Spring, NIH
D. Lansing Taylor, Carnegie-Mellon University
Richard Walker, University of North Carolina

Students
Julia Barsony, NIDDK/NIH
Harold G. Bohlen, Indiana University Medical School
Daniel J. Brat, Mayo Graduate School
Barry J. Burbach, SUNY, Stony Brook
John P. Caufield, Harvard Medical School
Wendy Cheng, International Paper Company, Tuxedo, NY
Matthew H. Chestnut, The Procter and Gamble Co., Cincinnati, OH
Diana M. Cordova, Alcon Laboratories, Inc., Ft. Worth, TX
Sascha Dho, The Hospital for Sick Children, Toronto, Canada
Ulrich Dirnagl, Forschungslabor, Germany
Cynthia J. Forehand, University of Vermont
John J. Freeman, Monsanto Co., St. Louis, MO
Jill Gemmill, University of Alabama, Birmingham
John A. Hammer, III, NHLBI/NIH
Ray S. Hartman, Children's Hospital of Los Angeles
Donald T. Haynie, The Johns Hopkins University
Walter J. Koroshetz, Massachusetts General Hospital
Julia M. Lash, Indiana University School of Medicine
Michael I. Lethem, University of North Carolina
Steve Paddock, University of Wisconsin
Shoshana Paglin, Boston University School of Medicine
James R. Sellers, NHLBI/NIH
Anna Spudich, Stanford University
Fei Wang, Syracuse University

Dan Green (left) demonstrates a ratio imaging package from Universal Imaging during an AQLM course session.

Measurement and Control of Chemical Stimuli (April 25 to 30)

Director
Greg A. Gerhardt, University of Colorado

Faculty and Course Assistants
Barry W. Ache, C.V. Whitney Laboratory, University of Florida
Jelle Atema, Boston University Marine Program, MBL
Scott Brock, University of Colorado
Marilyne Friedemann, University of Colorado
John S. Kauer, Tufts—New England Medical Center
Stuart Firestein, Yale University School of Medicine
Paul Moore, Boston University Marine Program, MBL
Mike Palmer, University of Colorado
Michael Parrish, University of Colorado
Wayne L. Silver, Wake Forest University

Students
Carol E. Diebel, SUNY Health Science Center
Richard L. Doty, Hospital of the University of Pennsylvania
Heather L. Eisthen, Indiana University
Tim Granata, Southeastern Massachusetts University
Kristina-Viveka Hillegaart, Astra Research Centre, Sweden
Herman K. Lehman, University of Arizona
Celia Marrase, Boston University Marine Program, MBL
Pricilla E. Purnick, Columbia University
John R. Welborn, University of Southern California

Methods in Computational Neuroscience (August 5 to September 1)

Co-Directors
James M. Bower, California Institute of Technology
Christof Koch, California Institute of Technology

Lecturers and Instructors

Paul Adams, SUNY, Stony Brook
Edward Adelson, Massachusetts Institute of Technology
Daniel Alkon, NIH
Richard Anderson, Massachusetts Institute of Technology
David Beeman, University of Colorado, Boulder
Avis H. Cohen, Cornell University
Norberto Grzywacz, Massachusetts Institute of Technology
Nancy Kopell, Boston University
Rudolfo Llinas, NYU Medical Center
Kevan Martin, MRC, Oxford, UK
Michael Mascagni, Washington, DC
Kenneth Miller, University of California, San Francisco
Mark Nelson, California Institute of Technology
John Rinzel, NIH
David Rumelhart, Stanford University
Sylvia Ryckebusch, California Institute of Technology
Terrence Sejnowski, Salk Institute
Allen I. Selverston, University of California, San Diego
John Uhley, California Institute of Technology
David Van Essen, California Institute of Technology
Lucia Vaina, Boston University
Matthew Wilson, California Institute of Technology

Students

Aric Agmon, University of California, Irvine
Hagai Agmon, Hebrew University of Jerusalem, Israel
Dale Anders, University of California, San Diego
Evyatar Av-Ron, The Weizmann Institute of Science, Israel
Ellen Barton, University of Pennsylvania
Eyal Bartfeld, Rockefeller University
David Berkowicz, Yale University School of Medicine
Neil J. Berman, Oxford University, UK
Peter J. Braam, University of Utah
Dennis Bray, Colorado State University
Trevor Darrell, Massachusetts Institute of Technology
Gyongyi Gaal, University of Pennsylvania
Kurt Haas, Albert Einstein College of Medicine
Dirk Kautz, University of Oregon
Markus Lappe, NIH
Sean Marrett, Montreal Neurological Institute, Canada
Douglas Morton, Case Western Reserve University
Dietmar Rapf, MPI für biologische Kybernetik, Germany
Walter Schneider, University of Pittsburgh
Nelson Spruston, Baylor College of Medicine
Christoph Staub, Brain Research Institute, Switzerland
Fan-Gang Zeng, Syracuse University

Molecular Evolution (August 19 to 31)

Director

Mitchell L. Sogin, MBL

Faculty

Michael Clegg, University of California, Riverside
Daniel B. Davison, University of Houston
W. Ford Doolittle, Dalhousie University, Canada
Robert Dorit, Harvard University
John W. Drake, National Institute of Environmental Health Sciences
Joseph Felsenstein, University of Washington
Walter M. Fitch, University of California, Irvine
Barry G. Hall, University of Rochester
Andrew Knoll, Botanical Museum of Harvard University
David R. Maddison, Harvard University
Peter Maloney, The Johns Hopkins Medical School
Roger Milkman, The University of Iowa
Gary Olsen, University of Illinois
Norman R. Pace, Indiana University
David Joseph Patterson, University of Bristol, UK
Margaret Riley, University of Massachusetts, Amherst
David A. Shub, SUNY, Albany
Steve Smith, Harvard University
Temple F. Smith, Dana Farber Cancer Institute
Mark Wheelis, University of California, Davis
Allan C. Wilson, University of California, Berkeley
Elizabeth A. Zimmer, Smithsonian Institution

Students

Alexandra L. Basolo, University of Texas, Austin
Heidi G. Blair, SUNY, Albany
Judith Anne Blake, Smithsonian Institution
Laura Blinderman, San Diego State University
David J. Bogler, University of Texas, Austin
Diane M. Bridge, Yale University
Henner Brinkmann, Technische Universitat, Germany
James R. Brown, Simon Fraser University, Canada
Bruce E. Byers, University of Massachusetts, Amherst
Robert E. Calhoon, Queens College

Bruce J. Cochrane, University of South Florida
Rafael O. De Sa, University of Texas, Austin
Marcela Descalzi, University of Houston
Philippe Djian, Harvard Medical School
James W. Edwards, Salem College
Bruce A. Eichhorst, University of North Dakota
William Fischer, Los Alamos National Laboratory
Dean A. Glawe, University of Illinois
Robert M. Gould, New York State Institute for Basic Research
Sharon P. Gowan, Harvard University Herbaria
Lawrence I. Grossman, Wayne State University
Radhey S. Gupta, McMaster University, Canada
Raymond W. Holton, University of Tennessee
Bradford E. James, Dartmouth College
Matthew D. Kane, University of Illinois
Jessica C. Kissinger, Indiana University
Paul J. Kores, Tulane University
Maja Kricker, National Institute of Environmental Health Sciences
Uri Ladror, Chicago Medical School
Laura Landweber, Harvard University
Bang-Ning Lee, University of Texas, Houston
Heikki Lehvaslaiho, University of Helsinki, Finland
Wayne S. Leibel, Lafayette College
Enrique P. Lessa, University of California, Berkeley
Louise Ann Lewis, Ohio State University
Paul O. Lewis, Ohio State University
John M. Logsdon, Jr., Indiana University
Kenneth L. McNally, University of California
Linda K. Medlin, University of Bristol, UK
Thomas Mills, University of Houston
Judith Mongold, University of Massachusetts, Amherst
Barbara Moore, Massachusetts Institute of Technology
Rana Muzaffar, Florida State University
Lena M. Nielsen, University of Lund, Sweden
Elizabeth A. Oakenfull, MRC Haematology Unit, Oxford, UK
Yves P. Quentin, Los Alamos National Laboratory
James Ramsay, University of Utah
Judith M. Rhymer, Smithsonian Institution
Kenneth A. Rice, Harvard University
Bernardo Rudy, NYU Medical Center
Frank G. Salinas, University of Houston
Leo C. Schalkwyk, Dalhousie University, Canada
Michael Schloemann, Yale University
Jeffrey D. Silberman, University of Miami
Rama S. Singh, McMaster University, Canada
Elizabeth M. Snella, Indiana University
Elizabeth T. Snow, NYU Medical Center
Peter L. Starkweather, University of Nevada
Jeffrey L. Stein, University of California, San Diego
Youngbae Suh, Louisiana State University
Thomas R. Sutter, CIIT, Research Triangle Park, NC
Cheryl L. Tarr, University of North Dakota
Richard N. Williams, Boise State University
Charles G. Wray, Yale University

Optical Microscopy & Imaging in the Biomedical Sciences (October 6 to 12)

Co-Directors
Nina Strömgren Allen, Wake Forest University
Colin S. Izzard, SUNY, Albany

Faculty and Course Associates
Steven M. Block, Rowland Institute for Science
Joseph De Pasquale, SUNY, Albany
Alec Harootunian, HHMI, University of California, San Diego
Fredric S. Fay, University of Massachusetts Medical Center
Kenneth A. Jacobson, University of North Carolina
John M. Murray, University of Pennsylvania
Kenneth Orndorff, Dartmouth College
Julia S. Sizemore, Wake Forest University
Stephen J. Smith, Stanford University School of Medicine
Kenneth R. Spring, NHLBI/NIH
Anna Spudich, Stanford University School of Medicine
Roger Tsien, HHMI, University of California, San Diego

Lecturers
Jan Hinsch, Leica, Inc., Rockleigh, NJ
Shinya Inoué, MBL
Ernst Keller, Carl Zeiss, Inc., Thornwood, NY
Rudolf Oldenbourg, MBL

Students
Lawrence W. Argenbright, Boehringer Ingelheim Pharmaceuticals, Inc., Ridgefield, CT
Elikplimi K. Asem, Purdue University
Thomas G. Burke, City of Hope National Medical Center
Dean Cole, Los Alamos National Laboratory
R. Ford Denison, USDA
Camille DiLullo, University of Pennsylvania
Harold F. Dvorak, Beth Israel Hospital
David H. Eidelman, McGill University, Canada
T. R. Gowrishankar, University of Chicago
John W. Hanrahan, McGill University, Canada
Christopher M. Kenyon, Centre Hospitalier Thoracique de Montreal, Canada

Jeff Lansman, University of California, San Francisco
Stephen Lin, Harvard Medical School
William W. Mantulin, University of Illinois, Urbana—Champaign
Jose A. Mari Mutt, University of Puerto Rico
Jane E. Minturn, Yale University School of Medicine
Spering A. Scott, Purdue University
Jacqueline Sterner, University of Rochester
Scott J. Sternberg, Colorado State University
Xiao-Ying Tien, Case Western Reserve University
Susan M. Wall, NIH
David C. Zawieja, Texas A&M University

Pathogenesis of Neuroimmunologic Diseases
(August 19 to 31)

Co-Directors

J. Murdoch Ritchie, Yale University School of Medicine
Byron H. Waksman, Foundation for Microbiology

Faculty

Vahi E. Amassian, SUNY Health Science Center
Barry G. W. Arnason, University of Chicago
Joel A. Black, Yale University
Pietro DeCamilli, Yale University Medical School
Judah A. Denburg, McMaster Medical Center, Canada
Marc A. Dichter, University of Pennsylvania
Charles A. Dinarello, Tufts University Medical School
Diane Griffin, The Johns Hopkins University
Stephen L. Hauser, Massachusetts General Hospital
Henry Khachaturian, NIMH/NIH
Norman Latov, College of Physicians and Surgeons of Columbia University
Carl M. Leventhal, NINDS/NIH
W. Ian Lipkin, University of California, Irvine
Cathy G. McAllister, University of Pittsburgh
Dale E. McFarlin, NINDS/NIH
John Newsom-Davis, Oxford University, UK
Robert B. Nussenblatt, NEI/NIH
Nathanial G. Pitts, National Science Foundation
Jerome B. Posner, Memorial Sloan-Kettering Cancer Center
Donald L. Price, Johns Hopkins Hospital
Richard W. Price, University of Minnesota Health Center
James W. Prichard, Yale University Medical School
Cedric S. Raine, Albert Einstein College of Medicine
Anthony T. Reder, University of Chicago
David M. Regan, York University, Canada
Stephen C. Reingold, National Multiple Sclerosis Society
Benjamin F. Roy, Georgetown University School of Medicine
Clifford B. Saper, University of Chicago
Randolph B. Schiffer, Strong Memorial Hospital
Eli E. Sercarz, University of California, Los Angeles
Moon L. Shin, University of Maryland, Baltimore
Michael E. Shy, Thomas Jefferson University Hospital
Lawrence Steinman, Stanford Medical Center
Stephen G. Waxman, Yale University Medical School
Howard L. Weiner, Brigham and Women's Hospital
Jerry Wolinsky, University of Texas Health Science Center at Houston

Students

Anat Achiron, Beilinson Medical Center, Israel
Peter-Brian Andersson, Sir William Dunn School of Pathology, UK
Jody L. Baron, Yale University School of Medicine
Bruce F. Bebo, Jr., Texas A&M University
John R. Bethea, University of Alabama, Birmingham
Helen Clare Bodmer, Institut de Chimie Biologique, France
Arlene R. Collins, SUNY, Buffalo
Steven W. Dow, Colorado State University
Lorise C. Gahring, Research Institute of Scripps Clinic
Maureen N. Gannon, Rockefeller University
Claude Paul Genain, University of Kentucky
Koenraad Gijbels, University of Leuven, Belgium
Jonathan D. Glass, Johns Hopkins Hospital
John J. Hemperly, Becton Dickinson Research Center
Nancy A. Johnson, Washington University Medical School
Abraham Kessler, Weizmann Institute of Science, Israel
Judith Luber-Narod, University of Massachusetts Medical School
Mary Ann McKee, Columbia Presbyterian Hospital
Rune Midgard, Molde County Hospital, Norway
Nicholas T. Potter, University of Connecticut School of Medicine
Reijo Salonen, University of Turku, Finland
Jun-ichi Satoh, University of British Columbia, Canada
Tiziana Savio, Instituto Superiore di Sanita, Italy
Daryth D. Stallone, University of Pennsylvania School of Medicine
Sharon A. Stranford, Hahnemann University
Ursula I. Wesselmann, Northwestern University
Jurgen Zielasek, Diabetes Research Institute, Germany

Summer Research Programs

Principal Investigators

Alkon, Daniel, NIH, LMCN
Armstrong, Clay M., University of Pennsylvania
Armstrong, Peter, University of California
Augustine, George J., University of Southern California

Baker, Robert, New York University Medical Center
Barlow, Robert, Syracuse University
Barry, Daniel, University of Michigan Medical Center
Barry, Susan R., University of Michigan
Bass, Andrew H., Cornell University
Bates, William R., Carleton University, Canada
Bearer, Elaine L., University of California
Beauge, Luis, Instituto M. y M. Ferreyra, Argentina
Begenisich, Ted, University of Rochester Medical Center
Bennett, Michael V. L., Albert Einstein College of Medicine
Bezanilla, Francisco, University of California, Los Angeles
Bloom, George S., University of Texas Southwestern Medical Center
Bodznick, David, Wesleyan University
Borgese, Thomas A., Lehman College, CUNY
Boron, Walter F., Yale University School of Medicine
Borst, David W., Illinois State University
Boyer, Barbara C., Union College
Brady, Scott, University of Texas Southwestern Medical Center
Brehm, Paul, SUNY, Stony Brook
Brown, Joel E., Washington University School of Medicine
Bryant, Shirley, University of Cincinnati
Bug, William J., Columbia University
Burdick, Carolyn J., Brooklyn College
Burger, Max M., Friedrich Miescher-Institute, Switzerland

Callaway, Joseph C., University of North Carolina
Cariello, Lucio, Stazione Zoologica, Italy
Chang, Donald C., Baylor College of Medicine
Chappell, Richard L., Hunter College, CUNY
Charlton, Milton, University of Toronto, Canada
Charmantier, Guy, Université des Sciences et Techniq. du Languedoc, France
Charmantier-Daures, Mireille, Université des Sciences et Techniq. du Languedoc, France
Clay, John, NIH, NINDS
Cohen, Lawrence B., Yale University School of Medicine
Cohen, William D., Hunter College, CUNY
Collin, Shaun P., University of California, San Diego
Cooperstein, Sherwin J., University of Connecticut Health Center
Cuppoletti, John, University of Cincinnati

D'Alessio, Giuseppe, University of Naples, Italy
D'Avanzo, Charlotte, Hampshire College
De Weer, Paul, Washington University School of Medicine
Deitmer, Joachim W., University of Kaiserslautern, Germany
Dunlap, Kathleen, Tufts Medical School

Eckberg, William R., Howard University
Ehrlich, Barbara E., University of Connecticut Health Center

Feinman, Richard, SUNY Health Science Center
Ferguson, Donald, University of Cincinnati
Fieber, Lynne A., University of Miami
Fink, Rachel, Mount Holyoke College
Fishman, Harvey M., University of Texas Medical Branch

Gadsby, David C., Rockefeller University
Gainer, Harold, NIH, NINDS
Garrick, Rita Anne, New Jersey Medical School and Fordham University
Giuditta, Antonio, University of Naples, Italy

Glynn, Paul, Hunter College
Goldman, Robert D., Northwestern University Medical School
Gonzalez-Serratos, Hugo, University of Maryland School of Medicine
Griff, Edwin, University of Cincinnati

Haimo, Leah T., University of California
Hardin, John A., Yale University
Heiny, Judith, University of Cincinnati
Hernandez-Cruz, Arturo, Roche Institute of Molecular Biology
Highstein, Stephen M., Washington University
Holman, Molly A., The Whitney Laboratory, University of Florida
Hoskin, Francis C.G., Illinois Institute of Technology
Hoy, Ronald R., Cornell University
Hummon, William, Ohio University

Ilan, Joseph, Case Western Reserve University
Ilan, Judith, Case Western Reserve University
Ip, Wallace, University of Cincinnati

Johnston, Daniel, Baylor College of Medicine
Josephson, Robert K., University of California

Kaminer, Benjamin, Boston University School of Medicine
Kaneshiro, Edna S., University of Cincinnati
Kaplan, Ehud, Rockefeller University
Kaplan, Ilene M., Union College
Karp, Richard, University of Cincinnati
Kremer, James N., University of Southern California
Kriebel, Mahlon, SUNY Health Science Center, Syracuse

Langford, George, University of North Carolina, Chapel Hill
Laufer, Hans, University of Connecticut
Lee, Youngsook, Harvard University
Lehman, Michael, University of Cincinnati
Levin, Jack, University of California School of Medicine, San Francisco
Levine, Robert Paul, Washington University School of Medicine
Lian, Jane, University of Massachusetts Medical School
Linck, Richard W., University of Minnesota
Lipicky, Raymond John, U. S. Food and Drug Administration
Lisman, John, Brandeis University
Llinas, Rodolfo R., New York University Medical Center
Loewenstein, Werner R., University of Miami School of Medicine
Lohmann, Kenneth J., University of Washington

Malchow, Robert Paul, University of Illinois College of Medicine
Malinowska, D. H., University of Cincinnati
Martinez, Joe L., Jr., University of California
Matteson, Donald R., University of Maryland
Meinertzhagen, Ian A., Dalhousie University, Canada
Metuzals, Janis, University of Ottawa, Canada
Mitchison, Timothy, University of California, San Francisco
Moreno, Alonso P., Albert Einstein College of Medicine

Nasi, Enrico, Boston University School of Medicine
Nelson, Leonard, Medical College of Ohio
Noe, Bryan D., Emory University School of Medicine
Northcutt, R. Glenn, University of California, San Diego

Obaid, Ana Lia, University of Pennsylvania School of Medicine

Pant, Harish, NIH, NINDS
Pappas, George D., University of Illinois, Chicago
Parysek, Linda, University of Cincinnati
Peckol, Paulette, Smith College
Pierce, Sidney K., University of Maryland, College Park
Pierson, Beverly K., University of Puget Sound

Rafferty, Nancy S., Northwestern University
Rakowski, Robert F., UHS/The Chicago Medical School
Render, JoAnn, Hamilton College
Ripps, Harris, University of Illinois College of Medicine
Rose, Birgit, University of Miami School of Medicine
Ross, William N., New York Medical College
Ruderman, Joan V., Harvard Medical School
Russell, John M., University of Texas Medical Branch, Galveston
Ryan, Una S., Washington University

Salzberg, Brian M., University of Pennsylvania School of Medicine
Segal, Sheldon, Rockefeller Foundation

Sheetz, Michael P., Washington University Medical School
Silver, Robert B., Cornell University
Sloboda, Roger D., Dartmouth College
Speksnijder, Johanna E., Utrecht University, The Netherlands
Sperelakis, Nicholas, University of Cincinnati
Spiegel, Evelyn, Dartmouth College
Spiegel, Melvin, Dartmouth College
Spray, David C., Albert Einstein College of Medicine
Stein, Gary, University of Massachusetts Medical School
Steinacker, Antoinette, Washington University
Stracher, Alfred, SUNY Health Science Center, Brooklyn
Stuart, Ann E., University of North Carolina
Swandulla, Dieter, Max-Planck-Institüt, Germany
Swenson, Katherine I., Harvard Medical School

Tanguy, Joelle, Northwestern University
Telzer, Bruce R., Pomona College
Terada, Hirotoshi, Hamamatsu Photonics, K. K., Japan
Treistman, Steven N., Worcester Foundation for Experimental Biology
Trinkaus, John Philip, Yale University
Troll, Walter, New York University Medical Center
Tucker, Edward B., Baruch College
Tykocinski, Mark L., Case Western Reserve University
Tytell, Michael, Bowman Gray School of Medicine of Wake Forest University

Vaisberg, Eugeni A., Protein Research Institute, USSR
Vallee, Richard, Worcester Foundation for Experimental Biology
Van Egeraat, Jan M., Vanderbilt University
Vogel, Steven S., NIH, NIDDK

Weiss, Dieter G., Zoology Institute, Germany
Welsford, Jan G., University of Pennsylvania School of Medicine
Wolszon, Laura R., Columbia University
Worden, Mary Kate, Harvard Medical School

Yeh, Jay Z., Northwestern University

Zigman, Seymour, University of Rochester School of Medicine and Dentistry
Zottoli, Steven J., Williams College
Zukin, R. Suzanne, Albert Einstein College of Medicine

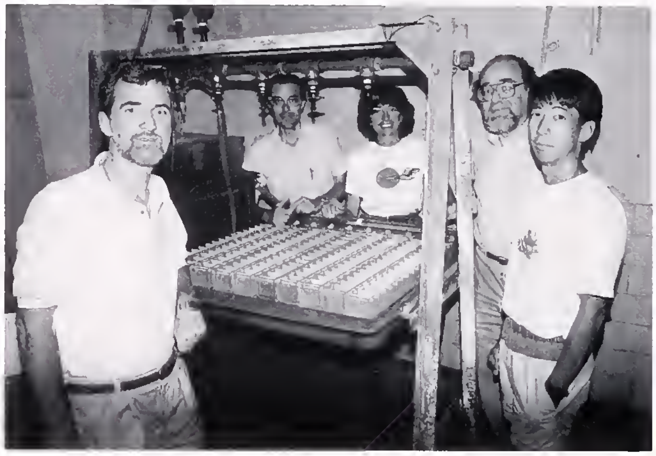

Summer investigators (left to right) David Borst, Guy Charmantier, Mireille Charmantier-Daures, Hans Laufer, and Brian Tsukimura

Other Research Personnel

Akeson, R. A., University of Cincinnati
Altamirano, Anibal A., University of Texas Medical Branch
Andrews, S. Brian, NIH, NINDS
Arnold, John, University of Hawaii

Bamrungphol, Wattana, University of Pennsylvania
Bargeron, Mary, Syracuse University
Batten, Bruce E., Dublin, OH
Bechtold-Imhof, Ruth, Boston University Medical Center
Belmont, Lisa, University of California, San Francisco
Bernal-Martinez, Juan, University of Connecticut Health Center
Bersoff, Rochelle, Washington University School of Medicine
Bezprozvanny, Ilya, University of Connecticut Health Center
Blanchard, Charles, Cambridge, MA
Bloom, Jonathan, Northwestern University
Bloom, Theodora, Harvard Medical School
Blubaugh, Diane, University of Puget Sound
Bollner, Tomas, Dalhousie University, Canada
Braithwaite, Scott, SUNY, Stony Brook
Breitweiser, Gerda E., Johns Hopkins University School of Medicine
Brezina, Vladimir, University of Connecticut Health Center
Brient, Heather L., Ohio University
Brodwick, M., University of Texas Medical Branch
Brooks, Brian P., University of Pennsylvania

Buelow, Neal, Syracuse University
Buerkett, Christopher G., Illinois State University
Burkart, Werner, Paul Scherrer Institut, Switzerland

Campos de Carvalho, Antonio, Federal University of Rio De Janeiro, Brazil
Capano, Carla Perrone, Stazione Zoologica, Italy
Caputo, Carlo, IVIC-Inst. Venezolano de Inv. Ciento, Venezuela
Carey, John P., University of Washington
Caviedes, Pablo, NIH, NIDDK
Chow, Robert H., University of Pennsylvania
Cohen, Avrum, Yale University School of Medicine
Collin, Carlos, NIH, LMCN
Correa, Ana Maria, University of California, Los Angeles
Cota, Gabriel, Centro de Investigacion del IPN, Mexico
Couch, Ernest, Texas Christian University

Davis, Marion, Yale University School of Medicine
Demers, David, University of California, Riverside
Dermietzel, Rolf, University of Regensburg, Germany
Derrick, Brian, University of California, Berkeley
Dessev, George N., Northwestern University Medical School
DiPolo, Reinaldo, IVIC, Venezuela
Diebel, Carol, SUNY Health Science Center at Brooklyn
Dohrmann, Cord, Harvard Medical School
Drazba, Judith, NIH, NINDS

Evans, Wayne A., Ohio University

Faeta, Hillary H., Ohio University
Falk, Chun Xiao, Yale University Medical School
Floyd, Carl C., NIH, NINDS
Flucher, Bernhard E., NIH, NINDS
Forman, Robin, Medical College of Virginia
Franzini-Armstrong, Clara, University of Pennsylvania
Fujiki, Hirota, National Cancer Center Research Institute, Japan

Gao, Qian, University of Pennsylvania School of Medicine
Gavi, Benny, SUNY, Binghamton
Genao, Ivan, Lehman College
Gerosa, Daniela, Friedrich Miescher Institut, Switzerland
Gill-Kumar, Pritam, U. S. Food and Drug Administration
Goldman, Anne E., Northwestern University Medical School
Gomez, Maria, Boston University
Gomez-Laganas, Froylan M., Centro de Investigacion del IPN, Mexico
Goodwill, Ken
Gould, Robert, New York State Institute for Basic Research
Grant, Philip, NIH, NINDS
Grassi, Daniel, Ft. Lauderdale, FL

Hammar, Kasia, NIH
Hamosh, Leora Y., Johns Hopkins School of Medicine
Haneji, Tatsuji, Chiba University School of Medicine, Japan
Hernandez, Michael R., University of Texas Medical Branch
Herzog, Eric, Syracuse University
Hessinger, David, Loma Linda University
Hogan, Emilia, Yale University School of Medicine
Homola, Ellen, University of Connecticut
Huang, Jack, NIH, NIDDK
Huddie, Patrick L., NIH, NINDS
Huerta, Patricio, Brandeis University

Jaffe, David, Baylor College of Medicine
Johnston, Jennifer, Dartmouth College
Jordan, John R., University of Utah

Kadam, P. A., The Population Council
Kahana, Alon, Brandeis University
Kenner, Glenda S., Ohio University
Key, Brian, Children's Hospital Medical Center, Cincinnati
Khanna, Anu, Lehman College
Kim, Nam Hew, Albert Einstein College of Medicine
Kingston, Samuel, New York
Klein, Kathryn, Emory University School of Medicine
Knudsen, Knud D., U. S. Food and Drug Administration
Koide, Samuel S., Population Council
Komura, Hitoshi, University of Pennsylvania School of Medicine
Konnerth, Arthur, Max-Planck-Institüt für Biophysikalische Chemie, Germany
Kowtha, Vijayanand C., NIH
Kozlowski, David, University of Connecticut
Krishna, Gobal, NIH
Kronidou, Nafsika, Dartmouth College
Kuhns, William, Hospital for Sick Children, Canada
Kumar, Sanjay S., University of Pennsylvania

Landau, Matthew, Stockton State College
Larsen, Mark, University of Puget Sound
Lasser-Ross, Nechama, New York Medical College
Latorre, Ramon, Universidad de Chile, Chile
Lederhendler, I. Izja, NIH, NINDS

Leidigh, Christopher, Brown University
Leonard II, Edward E., University of Pittsburgh
Levitan, Herbert, University of Maryland
Lin, Jen-Wei, New York University Medical Center
Locke, Rachel, Washington University
Lowe, Kris, New College
Luca, Frank, Harvard Medical School

Martin, Melissa, Illinois State University
McDonald, John K., Emory University School of Medicine
Menichini, Enrico, University of Naples, Italy
Miledi, Ricardo, University of California
Milgram, Sharon L., Emory University School of Medicine
Mimori, Tsuneyo, Keio University, Japan
Misevic, Gradimir, University Hospital of Basel, Switzerland
Moogan, Teresa, Hunter College
Moreira, Jorge E., NIH, NINDS
Moshiach, Simon, NIH
Murray, Sandra A., University of Pittsburgh

Niclas, Joshua, University of California, San Francisco
Nitabach, Michael, Massachusetts Institute of Technology
Norgren, Robert, University of Cincinnati

Olds, James, NIH, LMCN

Papaconstandinov, Eleni, University and Cantonal Hospital, Switzerland
Pardo, Alex, Hampshire College
Parsey, Ramin, University of Maryland
Parsons, Stephen, University of North Carolina, Chapel Hill
Perozo, Eduardo, University of California, Los Angeles
Piccoli, Renata, University of Naples, Italy
Plant, Charles P., Tufts University
Powers, Maureen K., Vanderbilt University
Pumplin, David W., University of Maryland, Baltimore

Quigley, James P., SUNY, Stony Brook

Rafferty, Keen A., University of Illinois
Rasgado-Flores, Hector, University of Health Sciences/Chicago Medical School
Reese, Thomas, NIH, NINDS
Rodriguez, Katrin, University of Illinois
Romero, Adarli, Washington University
Roth, William W., Emory University School of Medicine
Russell, Joshua C., University of Texas Medical Branch

Sagi, Amir, Hebrew University, Israel
Sakakibara, Manabu, Toyohashi, Japan
Sala, Salvador, University of Maryland, Baltimore
Sanchez, Ivelisse, Hunter College
Sanchez-Andres, Juan V., NIH
Sato, Eimei, Kyoto University, Japan
Schiminovich, Samuel, Englewood, NJ
Seemes, Eliana, University of Sao Paulo, Brazil
Sheetz, Jennifer, Woods Hole, MA
Sheller, Rebecca, University of Texas, Austin
Shibuya, Ellen, Harvard Medical School
Sivaramakrishnan, Shobhana, University of Southern California
Sosnicki, Andrzej A., University of Pennsylvania
Spires, Sherrill, University of Rochester
Steffen, Walter, University of Minnesota
Stewart, Patricia, University of Rochester
Stokes, Darrell R., Emory University
Stout, Matthew P., SUNY, Buffalo
Sugimori, Mutsuyuki, New York University Medical Center
Sweet, Hyla C., Union College
Syme, Douglas, University of California

Tewari, Kirti, University of Texas Medical Branch
Todaro, M. Antonio D., University of Modena, Italy
Tsukimura, Brian, Illinois State University
Turner, Robert, Lehman College

Ueno, Hiroshi, Rockefeller University

Vargas, Fernando, U. S. Food and Drug Administration
Vogel, Jackie M., Illinois State University

Wache, Susanne C., University of Connecticut
Wadsworth, Patricia, University of Massachusetts
Watson, Win, University of New Hampshire
Wells, Dan, Lexington, MA
Wiercinski, Floyd J., Northeastern Illinois University
Wu, Jian-Young, Yale University School of Medicine

Zakevicius, Jane M., University of Illinois College of Medicine
Zecevic, Dejan, University of Belgrade, Yugoslavia
Zheng, Qiang, Baylor College of Medicine
Zhi-quo, Liang, Population Council
Zigman, Bunnie Rose, University of Rochester School of Medicine and Dentistry
Zipser, David, E. Lansing, MI

Library Readers: General

Adler, Elizabeth, MBL
Apter, Nathanial, Nova University

Baccetti, Baccio, University of Siena, Italy
Barrett, Dennis, University of Denver
Bartolucci, Simonetta, Naples, Italy
Burdick, Jonathan, MBL
Bursztajn, S., Baylor College of Medicine

Carriere, Rita M., Downstate Medical Center
Child, Frank M., Trinity College
Chinard, Francis P., New Jersey Medical School
Cobb, Jewel Plummer, California State University, Fullerton
Cohen, Leonard, American Health Foundation

DeSimone, Douglas W., University of Virginia Health Science Center
DeToledo-Morrell, Leyla, Rush Medical Center
Dowling, John, Harvard University
Duncan, Thomas K., Nichols College

Edds, Kenneth T., SUNY, Buffalo
Eisen, Herman, Massachusetts Institute of Technology

Farmanfarmaian, A., Rutgers University
Fox, Tom, Harvard Medical School
Frenkel, Krystyna, NYU Medical Center
Friedler, Gladys, Boston University School of Medicine

German, James L., The New York Blood Center
Gilbert, Daniel L., NIH
Goldstein, Moise H., John Hopkins University
Goodman, Dewitt S., Columbia University
Gormley, Gerard, MBL
Guttenplan, Joseph, NYU Dental Center

Hill, Richard, Michigan State University
Humphreys, Tom, University of Hawaii

International Wildlife, MBL

Kaltenbach, Jane, Mount Holyoke College
Karlin, Arthur, Columbia University
Kelly, Robert, U.I.C. College of Medicine
Kisten & Babitsky, MBL
Klemow, Kenneth M., Wilkes University
Kremer, James N., University of South California

Laderman, Aimlee D., Yale University
Lee, John J., City College of CUNY
Levitz, Mortimer, NYU Medical Center

Marine Research, MBL
May, Ronald, MBL
Mitchell, Ralph, Harvard University
Mooseker, Mark S., Yale University
Musacchia, X. J., University of Louisville

Olins, Ada L., University of Tennessee, Oak Ridge
Olins, Donald, University of Tennessee, Oak Ridge
Oschman, James L., MBL

Passano, Leonard, University of Wisconsin
Peisach, Jack, Albert Einstein College of Medicine
Pollen, Daniel, University of Massachusetts Medical School
Prosser, C. Ladd, University of Illinois
Prusch, Robert, Gonzaga University

Robinson, Denis, MBL
Romagnani, Sergio, Università di Firenze, Italy
Rossi, Mose, Naples, Italy
Rourke, John, MBL
Russell-Hunter, W. D., Syracuse University

Sanger, Jean, University of Pennsylvania
Sanger, Joseph W., University of Pennsylvania
Schippers, Jay M., WAFRA, New York, NY
Shriftman, Mollie-Starr, North Nassau Health Center
Singh, Ajai Pratap, Bareilly College
Solomon, Dennis, MBL
Stein, Leonard, Health Sciences Center SUNY
Stephens, Philip J., Villanova University
Stephenson, William K., Earlham College
Sweet, Frederick, Washington University School of Medicine
Szent-Gyorgyi, Andrew, Brandeis University
Szulman, Aron, MaGee Womens Hospital

Trager, William, The Rockefeller University

Van Holde, Kensal E., Oregon State University
Vaina, Lucia, Boston University

Wagner, Robert R., University of Virginia
Wallace, Robert W., MBL
Warren, Leonard, Wistar Institute
Wilber, Charles G., Colorado State University
Wimpee, Charles, MBL
Wittenberg, Jonathan, Albert Einstein College of Medicine
Wolken, Jerome, Carnegie Mellon University
Worgul, Basil, Columbia University
Worgul, Kathleen, MBL

Young, Wise, NYU Medical Center
Young, Lily, NYU Medical Center

Library Readers: Desks

Anderson, Everett, Harvard Medical School
Avioli, Louis V., Jewish Hospital, St. Louis

Boyer, John F., Union College

Candelas, Graciela C., University of Puerto Rico
Chaet, Alfred B., University of W. Florida
Clark, Arnold, MBL
Cohen, Seymour, MBL
Collier, Marjorie M., St. Peters College
Copeland, Eugene, MBL
Corliss, Bruce, Duke University
Crews, David, University of Texas, Austin
Czinn, Steven J., RB&C Hospital, Cleveland

Festoff, Barry, VA Medical Center, Kansas City
Fussell, Catherine, University of Pennsylvania

Gibson, Kevin, University of Pittsburgh
Gross, Paul R., University of Virginia
Grossman, Albert, NYU
Gruner, John, NYU Medical Center

Haubrich, Robert, Denison University
Herskovitz, Theodore, Fordham University

Inoue, Sadayuki, McGill University, Canada

Katz, George M., Merck, Sharp & Dohme
King, Kenneth, Childrens Hospital
Krane, Stephen, Mass. General
Kravitz, Edward, Harvard Medical School

Leighton, Joseph, Peralta Cancer Research
Lorand, Laszlo, Northwestern University

Malbon, Craig C., SUNY
Mauzarall, David, Rockefeller University
Mizell, Merle, Tulane University
Morrell, Frank, St. Lukes Medical Center, Chicago

Narahashi, Toshio, Northwestern University Medical School
Nickerson, Peter A., SUNY, Buffalo

Paton, David, MBL
Person, Philip, VA Medical Center, Brooklyn

Robinson, Denis, MBL
Roth, Jay, University of Connecticut
Roth, Lorraine, MBL

Shanklin, Douglas, University of Tennessee
Shepard, Frank, Woods Hole Database
Shepro, David, Boston University
Sonnenblick, B. P., Rutgers University
Spector, Abraham, Columbia University
Speck, William, Case Western Reserve
Stuart, Ann, University of North Carolina
Sundquist, Eric, USGS, Woods Hole
Sydlik, Mary Anne, Eastern Michigan University

Tweedel, Kenyon, University of Notre Dame

Webb, Marguerite, MBL
Wittenberg, Beatrice, Albert Einstein College of Medicine

Yow, Frank, Kenyon College

Library Readers: Rooms

Hines, Michael, Duke University Medical School
Moore, John W., Duke University Medical School
Rabinowitz, Michael, Harvard Medical School
Reynolds, George, Princeton University
Weidner, Earl, Louisiana State University
Weissman, Gerald, NYU Medical Center
Zweig, Ronald, MBL

Domestic Institutions Represented

Alabama, University of Birmingham
Albert Einstein College of Medicine
American Bionetics, Inc.
American Psychological Association
Ames Laboratory
Analytical Luminescence Laboratory
Applied Biosystems
Arizona Research Laboratory
Arizona, University of
Arizona, University of, School of Medicine
Aspen Research Institute
Atlantex & Zieler Instrument Corporation
Axon Instruments, Inc.

Bareilly College
Baruch College of CUNY
Baylor College of Medicine
Beckman Instruments, Inc.
Bethesda Research Labs
Bio-Rad Laboratories
Bodega Marine Station
Boston University
Boston University School of Medicine
Bowling Green State University
Bowman Gray School of Medicine
Brandeis University
Brigham & Women's Hospital
Brinkmann Instruments, Inc..
Brooklyn College of CUNY
Brown University

Bryn Mawr College
Bunton Instrument Company, Inc.

California Institute of Technology
California, University of, Berkeley
California, University of, Davis
California, University of, Irvine
California, University of, Los Angeles
California, University of, Riverside
California, University of, San Diego
California, University of, San Francisco
California, University of, Santa Cruz
Cambridge Instruments
Cambridge Technology
Carnegie Institute of Washington
Carnegie-Mellon University
Case Western Reserve University
Center for Agricultural Biotechnology
Center for Marine Biotechnology
Center for Microbial Ecology, Michigan State University
Chicago, University of
Children's Hospital Medical Center
Ciba Corning Diagnostics Corp.
Cincinnati, University of
City College of New York
City University of New York (CUNY)
Clark University
Colgate University
Colorado College
Colorado, University of, Boulder
Columbia University
Columbia University College of Physicians and Surgeons
Connecticut, University of
Connecticut, University of, Health Center
Cornell University
Coy Laboratory Products
Crimson Camera Technical Sales
CSPI, Inc.

Dage MTI, Inc.
Dana-Farber Cancer Institute
Dartmouth College
Dawson Company
Delaware, University of
Diamond General Corporation
Digital Equipment Corporation
Donsanto Corporation
Duke University
Duke University Medical School

E. I. duPont de Nemours & Co., Inc.
Eastern Michigan University
East Tennessee State University
Eastman Kodak Company
E.G. & G., Inc.
Emory University
Emory University School of Medicine
Eppendorf, Inc.

Fisher Scientific
Florida State University
Florida, University of
Flow Laboratories
Fotodyne, Inc.

General Scanning, Inc.
Georgetown University Medical School
Georgia, University of
Gilson Medical Electronics, Inc.
Gonzaga University
Goucher College
Grass Instrument Company
Great Lakes Research Center

Hacker Instruments, Inc.
Frederick Haer & Company
Hahnemann Medical College
Hamilton College
Hampshire College
Harvard Medical School
Harvard University
Hawaii, University of
Health Sciences, University of
Holy Cross College
Honeywell Corporation
Howard Hughes Medical Institute
Howard University
Hunter College
Hunter College and CUNY Graduate Center

I.B.M.-T. J. Watson Research Center
ICN Radiochemicals
Illinois Institute of Technology
Illinois Natural History Survey
Illinois State University
Illinois, University of
Indec Systems, Inc.
Indiana University
International Biotechnologies, Inc.
Iowa, University of
Iowa, University of, College of Medicine
Institute for Basic Research in Developmental Disabilities
Institute of Neuroscience
ISCO, Inc.

JEOL
Jewish Hospital, St. Louis
Johns Hopkins University School of Medicine

Kansas, University of
Kentucky, University of
Kentucky, University of, Medical School
Kenyon College
Kinetic Systems
Kipp & Zonen
David Kopf Instruments

Lab Line Instruments, Inc.
Laser Science
Lehman College of CUNY
Lindberg Enterprises
Loma Linda University
Los Alamos National Laboratories
Loyola University
Ludlum Measurements, Inc.

MaGee Womens Hospital
Maryland, University of
Maryland, University of, School of Medicine
Massachusetts Institute of Technology
Massachusetts, University of, Amherst
Massachusetts, University of, Boston
Massachusetts, University of, Medical Center
Massachusetts, University of, Medical School
Medical College of Ohio
Medical College of Virginia
Medical Systems Corporation
Merck & Company, Inc.
Merck Sharp & Dohme Research Laboratory, New Jersey
Miami, University of
Miami, University of, School of Medicine
Michigan State University
Michigan, University of, Ann Arbor
Minnesota, University of
Molecular Probes
Monsanto Company
Mount Holyoke College
Murray State University

National Institutes of Health/NINDS
National Institutes of Health/NIEHS
National Institutes of Health/NIDDK
National Jewish Center for Immunology & Respiratory Medicine
National Science Foundation
Naval Medical Research Institute
Neslab Instruments, Inc.
New Brunswick Scientific Company, Inc.
New College of the University of South Florida
New England Medical Center
New Hampshire, University of
New Jersey Medical School
New York Medical College
New York University Medical Center

Nikon, Inc.
North Carolina, University of, Chapel Hill
North Dakota University
Northeastern University
North Nassau Health Center
Northwestern University Medical School
Notre Dame, University of

Ohio University
Oklahoma, University of
Olympus Corporation
Oregon State University
Oregon, University of

Pennsylvania State University
Pennsylvania, University of
Pennsylvania, University of, School of Medicine
Perceptics Corporation
Perkin-Elmer Corporation
Pharmacia, Inc.
Pharmacia LKB Nuclear, Inc.
Photometrics, Ltd.
Photonic Microscopy, Inc.
Photon Technology International
Pittsburgh, University of
Pittsburgh, University of, Medical School
Polaroid Corporation
Pomona College
Ponce School of Medicine
Population Council-CBR, The
Portland State University
Princeton University
Puerto Rico, University of
Puget Sound, University of
Purdue University

Quantex Corporation

Radiomatic Instruments & Chemical Company, Inc.
Reed College
Roche Institute of Molecular Biology
Rochester, University of
Rochester, University of, School of Medicine & Denistry
Rockefeller University, The

Salk Institute
San Francisco State University
Sarastro, Inc.
Savant Instruments, Inc.
Scanalytics
Scripps Clinic and Research Foundation
Scripps Institute of Oceanography
Sequoia Turner
Smith College
Sony Medical Electronics
Southern California, University of
Stanford University
Stanford University Medical Center
State University of New York
State University of New York, Albany
State University of New York, Buffalo
State University of New York, Purchase
State University of New York, Stony Brook
State University of New York, Syracuse
Stockton State College
Stratagene
Sutter Instrument Company
Swarthmore College
Swift Instruments, Inc.
Syracuse University

Technical Manufacturing Corporation
Technical Products International, Inc.
Technical Video, Ltd.
Temple University
Tennessee, University of
Texas Christian University
Texas Tech. University
Texas, University of, Austin
Texas, University of, Medical Branch
Texas, University of, Medical School
Texas, University of, Southwestern Medical Center
Tufts University School of Medicine
Tufts University School of Veterinary Medicine
Tulane University
Turner Designs

UHS/Chicago Medical School
Union College
United States Food & Drug Administration
Universal Imaging Corporation
Utah, University of

Vanderbilt University
Vassar College
Veterans Administration Medical Center
Videoscope International, Ltd.
Virginia, University of
Vital Images

Wake Forest University
Wake Forest University/Bowman Gray Medical School
Washington, University of
Washington University
Washington University School of Medicine
Wesleyan University
West Florida, University of
Wheaton College
Whitman College
Wild Leitz USA, Inc.
Williams College
Wisconsin, University of
Wistar Institute
Woods Hole Oceanographic Institution
Worcester Foundation for Experimental Biology

Yale University
Yale University School of Medicine

Zeiss, Carl, Inc.

Foreign Institutions Represented

Academy of Sciences, USSR

Basel, University of, Switzerland
Belgrade, University of, Yugoslavia
Bergen, University of, Norway
Bielefeld, University of, Germany
Biozentrum, Basel, Switzerland
Bonn, University of, Germany
British Museum of Natural History, UK

Calgary, University of, Canada
Cambridge, University of, UK
Carlton University, Canada
Catania, University of, Italy
Centro de Investigacion del IPN, Mexico
Chiba University, Japan
Chiba University School of Medicine, Japan
Chile, University of, C.E.C.S., Chile

CINEVESTAV-IPN, Mexico
Cologne, University of, Germany

Dalhousie University, Canada
Dalhousie University Medical School, Canada

Ecole normale supérieure, France

Federal University of Rio de Janeiro, Brazil
Freie Universität Berlin, Germany
Friedrich Miesener Institut, Switzerland

Göttingen, University of, Germany

Hamamatsu Photonics, K. K., Japan
Hebrew University, Israel
Hong Kong, University of, Hong Kong

Imperial College of Science & Technology, UK
Institute for Biological Research, Yugoslavia
Instituto di Biologia dello Sviluppo, CNS, Italy
Instituto M. y. M. Ferreyra, Argentina
I.V.I.C., Venezuela

Kaiserslautern, University of, Germany
Katholieke Universiteit Leuven, Belgium
Keio University, Japan
Kobe University, Japan
Köln, University of, Germany

Konstanz, University of, Germany
Kyoto University, Japan

Life Sciences Institute, Israel
London School of Hygiene & Tropical Medicine, UK
London, University of, Egham, UK

Max-Planck-Institüt für Biophysikalische Chemie, Germany
Max-Planck-Institüt, Göttingen, Germany
McGill University, Canada
Medical Research Council, UK
Milan, University of, Italy
Modena, University of, Italy
Montreal, University of, Canada

Naples, University of, Italy
Nice, University of, France
Nottingham, University of, UK

Osnabrück, University of, Germany
Ottawa, University of, Canada

Paris, University of, France
Paul Scherrer Institute, Switzerland
Philipps-Universität, Marburg, Germany
Philipps-Universität, Germany
Protein Research Institute, USSR

Queens College, UK
Queens University, Canada
Queensland, University of, Australia

Regensburg, University of, Germany

Sao Paulo, University of, Brazil
Saskatchewan, University of, Canada
St. Andrews University, Scotland, UK
Seoul National University, Korea
Siena, University of, Italy
Simon Bolivar, University of, Venezuela
State University of Utrecht, The Netherlands
Stazione Zoologica, Italy
Stockholm, University of, Sweden
Swiss Federal Institute, Switzerland
Swiss Federal Institute of Technology, Switzerland

Toronto, University of, Canada
Tubingen, University of, Germany

Università di Firenze, Italy
Università di Palermo, Italy
Université des Sciences et Techniq. du Languedoc, France
University College, UK
University Hospital of Basel, Switzerland
Utrecht University, The Netherlands

Vienna, University of, Austria
Vrije Universiteit Brussel, Belgium

Wolfson College, UK

Z.L.F. Kantonsspital, Basel, Switzerland
Zoologie Institut, Germany

Year-Round Research Programs

Boston University Marine Program

Faculty

Atema, Jelle (Professor of Biology, Program Director)
Humes, Arthur G. (Professor of Biology Emeritus)
Strickler, J. Rudi (Professor of Biology, Program Director)
Tamm, Sidney L. (Professor of Biology)
Valiela, Ivan (Professor of Biology)

Visiting faculty and investigators

Ache, Barry (C. V. Whitney Lab, St. Augustine, Florida)
Bambach, Richard (Virginia Polytech and State University)
Bloomer, Sherman (Boston University)
Borisy, Gary (University of Wisconsin, Madison)
Caballero, Pascual (University of Las Palmas, Gran Canaria)
Chang, Donald (Baylor College of Medicine, Texas)
D'Avanzo, Charlene (Hampshire College)
Dionne, Vincent (University of California)
Gerhardt, Greg (University of Colorado)
Good, Michael (Utrecht University, The Netherlands)
Hinga, Kenneth (University of Rhode Island)
Josephson, Robert (University of California, Irvine)
Kauer, John (Tufts University)
Kaufman, Les (New England Aquarium)
Kremer, James (University of Southern California)
Linck, Richard W. (University of Minnesota, St. Paul)
Marrase, Celia (University of Barcelona, Spain)
Meinertzhagen, Ian (Dalhousie University, Canada)
Nakamura, Shogo (Toyama University, Japan)
Patterson, David (University of Bristol, UK)
Peckol, Paulette (Smith College)
Perez Castillo, Fernando (CIQRO, Mexico)
Rhoads, Donald (Adjunct Professor of Geology)
Rietsma, Carol (SUNY, New Paltz)
Rosenbaum, Joel (Yale University)
Sardet, Christian (Villefranche-sur-Mer, France)
Sarda, Rafael (Centre d'Estudio Avancats de Blancs, Spain)
Singarajah, K. V. (University of Brazil, Brazil)
Steffan, Walter (University of Minnesota, St. Paul)
Speksnijder, Annelies (Utrecht University, The Netherlands)
Sulak, Ken (Huntsman Marine Science Centre, Canada)
Terasaki, Mark (NIH)

Research staff

Foreman, Kenneth (Research Associate)
Gerardo, Hortense (Research Associate)
Tamm, Signhild (Senior Research Associate)
Voigt, Rainer (Research Associate)

Teaching assistants and staff

Alber, Merryl (Course Assistant)
Coughlin, David (Course Assistant)
Cowan, Diane (Course Assistant)
Gomez, George (Course Coordinator)
Hahn, Dorothy (Senior Administrative Secretary)
Hersh, Douglas (Course Assistant)
LaMontagne, Michael (Course Assistant)
Mosiach, Simon (Course Assistant)
Mulsow, Sandor (Course Assistant)
Paullin, Susanne (Assistant to the Director)
Scholz, Nathaniel (Course Assistant)
Sunley, Madeline (Administrative Manager)
Varela, Diana (Course Assistant)

Graduate students

Alber, Merryl
Banta, Gary
Brewer, Matthew
Bohachevsky, Boris
Bryden, Cynthia
Coughlin, David
Cowan, Diane
Elskus, Adria
Gallager, Scott
Gomez, George
Hersh, Douglas
Hwang, Jiang-shiou
Karavanich, Christy
Katz, Andrea

Kennedy, Blain
LaMontagne, Michael
Lavalli, Kari
Lindstrom, Daniel
Mazel, Charles
Merrill, Carl
Moore, Paul
Mosiach, Simon
Mulsow, Sandor
Portnoy, John
Scholz, Nathaniel
Strubel, Ilana
Tamse Armando
Trager, Geoffrey
Usup, Gires
Varela, Diana
Weinstein, Diana
White, David

Undergraduate students Fall 1990

Annis, Eric
Boulanger, Lisa
Brand, Michelle (University of California, San Diego)
Carrama, Carolyn
Christine, Stephanie
Collumb, Chris (Trinity University)
Christman, Laurie
Cruse, Jennifer
Deiner, Michael (Tulane)
DeSantis, Michael
Dougall, David (University of Pittsburg, Johnstown)
Fernandez, Cecilia
Forrest, Davina
Fox, Pamela
Gibson, Mark (Wesleyan)
Goodbred, Steven
Guertin, Laura (Bucknell)
Harris, Matthew
Havert, Michael
Hoyer, Eric (Lawrence University)
Kinkade, Christopher
Kozlowski, Wendy
MacDonald, Robin
McKee, Nancy (Middlebury)
McNeil, Sean
Polsky, Matthew
Russell, John (Franklin & Marshall)
Seton-Haris, Genevieve
Shaz, David
Smith, Douglas
Smith, Kirsten
Spradlin, Trevor
Staunton, Edward
Steenburgh, Eric
Stousland, Brett (Lawrence University)
Tello, Christine
Valdes, Hugo
Warner, Jacqueline

BUMP graduate student Diane Cowan explains the finer points of the lobster to BUMP undergrads.

Youngberg, Jill
Ziemba, Robert

Visiting graduate students Fall 1990 WHMS

Burner Michael (Lawrence University)
Jones, Fynn (Vanderbilt)
Klaper, Rebecca (University of Illinois)
Maselli, Andrew (Knox College)
Naessig, Tricia (Augusta College)
Theis, Lisa (Lawrence University)

Summer undergraduate interns

Altes, Hester
Bergles, Dwight
Butler, Nina (Westown School, PA)
Casterline, Jennifer
Call, Christopher
Hoagland, Todd (Bucknell)
Lacomis, Lynne (SUNY, Binghamton)
Pfeifer, Shaili
Pardo, Alex (Five Colleges)
Reischauer, Alyssa (USC)
Sanders, Sophie (Dalton School)
Short, Graham
Szulgit, Greg

Fall undergraduate intern

Waggett, Caryl (Brown)

Laboratory of Jelle Atema

Organisms use chemical signals as their main channel of information about the environment. These signals are transported in the marine environment by turbulent currents, viscous flow, and molecular diffusion. Receptor cells extract signals through various filtering processes. Currently, the lobster with its exquisite sense of taste and smell, is our major model to study the signal filtering capabilities of the whole animal and its narrowly tuned receptor cells. Research focuses on amino acids (food signals) and pheromones (courtship and dominance) neurophysiology of receptor cells, behavior guided or modulated by chemical signals, and computational models of odor plumes and neural filters.

Laboratory of Arthur G. Humes

Research interests include systematics, development, host specificity, and geographical distribution of copepods associated with marine invertebrates. Current research is on taxonomic studies of copepods from invertebrates in the tropical Indo-Pacific area, and poecilostomatoid and siphonostomatoid copepods from deep-sea hydrothermal vents and cold seeps.

Laboratory of Ivan Valiela

Our major research activity involves the Waquoit Bay Land Margin Ecosystems Research Project. This work examines how human activity in coastal watersheds (including landscape use and urbanization) increases nutrient loading to groundwater and streams. Nutrients in groundwater are transported to the sea, and, after biogeochemical transformation, enter coastal waters. There, increased nutrients bring about a series of changes. The Waquoit Bay LMER is designed to help us to understand and model the coupling of land use and consequences to receiving waters, and to study the processes involved.

A second long-term research topic is the structure and function of salt marsh ecosystems, including the processes of predation, herbivory, decomposition, and nutrient cycles.

The Ecosystems Center

The Center was established in 1975 to promote research and education in ecosystems ecology. Eleven senior scientific staff and forty research assistants and support staff study the terrestrial and aquatic ecology of a wide variety of ecosystems ranging from northern Europe (trace gas emission from acid-rain affected forests) to the Alaskan Arctic (long-term studies of the controls of tundra, lake, and stream biota) to the Harvard Forest (long-term studies of the effects of disturbance in forest ecosystems) to Buzzards Bay (controls of anaerobic decomposition). Many projects, such as those dealing with sulfur transformations in lakes and nitrogen cycling in the forest floor, investigate the movements of nutrients and make use of the Center's mass spectrometry laboratory (directed by Brian Fry) to measure the stable isotopes of carbon, nitrogen, and sulfur. The research results are applied wherever possible to questions of the successful management of the natural resources of the earth. In addition, the ecological expertise of the staff is made available to public affairs groups and government agencies who deal with such problems as acid rain, ground water contamination, and possible carbon dioxide-caused climate change. Opportunities are available for postdoctoral fellows.

Staff and consultants

Hobbie, John E., Co-Director
Melillo, Jerry M., Co-Director
Banta, Gary
Bauman, Carolyn
Berger, Laurel
Bowles, Francis
Bowles, Margaret
Castro, Nancy
Cochran, Wendy
Davis, Sarah
Deegan, Linda
Dornblaser, Mark
Downs, Martha
Fafinski, Stephen
Fry, Brian
Garritt, Robert
Giblin, Anne
Gregg, Tim
Griffin, Elisabeth
Helfrich, John
Hopkinson, Charles
Hullar, Meredith
Jesse, Martha
Jordan, Marilyn
Kicklighter, David
Kracko, Karen
Laundre, James
Michmerhuizen, Catherine
Miliefsky, Michelle
Moller, Bernard
Nadelhoffer, Knute
Padien, Daniel
Pallant, Julie
Parmentier, Nancy
Peterson, Bruce
Raich, James
Rastetter, Edward
Regan, Kathleen
Ricca, Andrea
Russell, Ann
Saupe, Susan
Schwamb, Carol
Schwarzman, Elisabeth
Semino, Suzanne
Shaver, Gaius
Shulman, Laura
Steudler, Paul
Tholke, Kristin
Tucker, Jane

Postdoctorals

Bowden, Richard
Castro, Mark
Kling, George
McKane, Robert
Peterjohn, William
Ryan, Michael
Wainright, Sam

Visiting scholars

Joyce, Linda, U.S.D.A. Forest Service
McGuire, David, U.S.D.A. Forest Service
Neill, Christopher, University of Massachusetts, Amherst

Laboratory for Marine Animal Health

The laboratory provides diagnostic, consultative research, and educational services to the institutions and scientists of the Woods Hole community concerned with marine animal health. Diseases of wild, captive, and cultured animals are investigated.

Staff

Abt, Donald A., Director and The Robert R. Marshak Term Professor of Aquatic Animal Medicine and Pathology, School of Veterinary Medicine, University of Pennsylvania

A view of Alaska's Brooks Range form the Ecosystems Center's Toolik Lake research station. Photo by Mark Dornblaser.

Bullis, Robert A., Research Associate in Microbiology, University of Pennsylvania
Leibovitz, Louis, Director Emeritus
McCafferty, Michelle, Histology Technician, University of Pennsylvania
Moniz, Priscilla C., Secretary
Smolowitz, Roxanna, Research Associate in Pathology, University of Pennsylvania
Wadman, Elizabeth A., Microbiology Technician, University of Pennsylvania

Laboratory of Aquatic Biomedicine

This laboratory investigates leukemias of soft shell clams. Monoclonal antibodies developed by this laboratory and techniques in molecular biology are used to investigate the differences between normal and leukemic cells and their ontogeny. The impact of pollutants on leukemogenesis is currently being studied with an emphasis on regional superfund sites.

Staff

Reinisch, Carol L., Investigator, MBL, and Chairperson Department of Comparative Medicine, Tufts University School of Veterinary Medicine
Miosky, Donna, Laboratory Technician
White, Marja, Postdoctoral Fellow

Laboratory of Cell Biochemistry

This laboratory studies developmental, metabolic, and environmental influences on the genetic regulation of cellular enzymes. Current emphasis is on the gene products involved in hepatic heme biosynthesis and utilization in marine fish. These processes are responsive to hormonal and nutritional signals as well as to environmental pollutants and carcinogens. This work is being conducted with fish liver *in vivo*, with primary cultures of normal hepatocytes, and with cultured hepatoma cells isolated from a fish tumor. Gene activity is quantitated with cDNA probes, and the relevant genes are being cloned in bacteria to define better the actions of chemical inducers. Other research is concerned with translocation of proteins between various subcellular compartments both in fish hepatocytes and in invertebrate eggs before and after fertilization.

Staff

Cornell, Neal W., Senior Scientist
Bruning, Grace, Research Assistant
Foley, Kathleen, Research Assistant

Visiting scientist

Fox, T. O., Harvard Medical Center

Laboratory of Developmental Genetics

This research group studies the early gene control of cellular differentiation pathways (cell lineage determination) in the embryos of tunicates and other marine invertebrate species.

Staff

Whittaker, J. Richard, Senior Scientist
Crowther, Robert, Research Assistant
Loescher, Jane L., Research Assistant
Meedel, Thomas H., Assistant Scientist

Visiting investigators

Collier, J. R., Brooklyn College
Lee, James J., Columbia University, College of Physicians & Surgeons

Laboratory of Judith P. Grassle

Studies on the population genetics and ecology of marine invertebrates living in disturbed environments, especially of sibling species in the genus *Capitella* (Polychaeta).

Staff

Grassle, Judith P., Senior Scientist
Feinsilber, Sigalit, Research Assistant
Mills, Susan W., Research Assistant

Laboratory of Haryln O. Halvorson

This laboratory is interested in the molecular process of sporulation and germination in members of the genus *Bacillus*. Our earlier work has involved characterization of the *gerJ* gene in *Bacillus subtilis*, and determination of the germination requirements of marine endospore-forming bacteria.

Over the past year, we have isolated a large number of sporeformers from various marine environments like deep sea cores and sediments. Our intention is to characterize these bacteria at the molecular level, with emphasis on genes associated with sporulation and germination. Protocols based on DNA fingerprinting and quantitative hybridizations have been developed to differentiate these bacteria from one another, as well from terrestrial sporeformers. The hybridization data has shown that the bacterial isolates are not closely related to one another.

Numerical taxonomic methods are also being used to cluster the various isolates. The physiologically interesting sporeformers will also be characterized by physical mapping using rare-cutting restriction endonucleases.

Staff

Halvorson, Harlyn O., Principal Investigator
Chikarmane, Hemant, Assistant Scientist
Glick, Beatriz, Research Assistant
Pratt, Sara, Research Assistant
VanLooy, Lori, Research Assistant

Visiting investigators

Anderson, Porter, University of Rochester
Keynan, Alex, Hebrew University, Jerusalem, Israel
Kornberg, Hans, Christ's College, Cambridge, UK
Vincent, Walter, University of Delaware
Yashphe, Jacob, Hebrew University, Jerusalem, Israel

Laboratory of Shinya Inoué

Mechanism of mitosis and related motility. Development of high resolution 3-D video microscope systems. High resolution polarized light microscopy of muscle fibrils. Physical origin of edge birefringence and image formation in the polarized light microscope.

Staff

Inoué, Shinya, Distinguished Scientist
Knudson, Robert, Instrument Development Engineer
Oldenbourg, Rudolf, Visiting Assistant Scientist
Stukey, Jetly, Research Assistant
Szent-Gyorgyi, David, Research Assistant
Taracka, Richard, Instrument Maker
Woodward, Bertha M., Laboratory Manager

Visiting investigators

Inoué, Theodore, Universal Imaging Corporation, West Chester, Pennsylvania
Silver, Robert B., Cornell University, Ithaca, New York
Stemmer, Andreas, University of Basel, Switzerland

Laboratory of Alan M. Kuzirian

The research explores the functional morphology and ultrastructure of various organ systems in opisthobranch mollusks. The program includes mariculture of the nudibranch, *Hermissenda crassicornis*, with emphasis on developing reliable culture methods for rearing and maintaining the animal as a research resource. Studies include optimization of adult and larval nutrition, control of facultative pathogens and disease, and development of morphologic criteria for staging larvae and juveniles. These morphologic studies stress the ontogeny of neural and sensory structures. Concurrent with these studies is the development of a new technique to obtain and reconstruct serial block face images (SBFI) of epoxy embedded tissue actually sectioned inside an SEM by an *in situ* miniature ultramicrotome. Additional collaborative research includes histochemical investigations on strontium's role in initiating calcification in molluscan embryos (shell and statoliths), as well as immunocytochemical labelling of cell-surface and secretory product antigens of neurosecretory neurons in the eye of *Aplysia*.

Staff

Alan M. Kuzirian, Assistant Scientist
Catherine T. Tamse, Research Assistant

Dr. Alan Kuzirian and Catherine Tamse in the laboratory. Photo by George Liles.

Laboratory of Molecular Evolution

The major research effort of this laboratory is the structure analysis of ribosomal RNA. Similarities between small subunit ribosomal RNA sequences are used to infer the evolutionary history of eukaryotic microorganisms and to design molecular probes for studies in marine ecology.

Staff

Sogin, Mitchell L., Director
Bhattacharya, Debashish, Postdoctoral Fellow
Bibeau, Claude, Research Technician
Bucklin, Ann, Visiting Scientist
Stickel, Shawn, Research Technician
Wainwright, Patricia, Postdoctoral Fellow

Laboratory of Neuroendocrinology

This laboratory studies the molecular and cellular bases of two neural programs that regulate different important behaviors in the model mollusk *Aplysia*. Research is conducted on the mechanisms of the neuronal circadian oscillators located in the eyes. These circadian oscillators drive the circadian activity rhythm of the animal, which is concerned with the daily timing of food gathering and of prolonged rest. Additional research is conducted on a group of neuroendocrine cells that produce a peptide, "egg-laying hormone," that initiates egg laying and associated behaviors. The laboratory is interested in how the three-dimensional shape of this peptide hormone allows a highly specific interaction with its receptor and the intracellular processes that are triggered by it. In another project, the laboratory has discovered and is continuing research on a novel second messenger enzyme, an NADase, in the oocytes of *Aplysia*, that generates cyclic ADPR, a Ca^{2+}-mobilizing product.

Staff

Strumwasser, Felix, Director
Cox, Rachel L., Senior Research Assistant
Glick, David, Senior Postdoctoral Fellow
Hellmich, Mark, Postdoctoral Fellow
Rainville, Carol, Laboratory Assistant
Vogel, Jackie, Research Assistant

Laboratory of Robert E. Palazzo

This laboratory studies the biochemical regulation of cellular events during meiosis and mitosis. An integral part of the research effort is the design of reconstitution systems that faithfully execute cell cycle dependent events under defined conditions. Current cell biological, immunochemical, biochemical, and microscopic methodologies are employed. Using marine eggs as a material source, assays have been developed that allow the study of germinal vesicle breakdown (GVBD), aster formation, and reactivation of isolated mitotic apparatus *in vitro*. Current focus of the laboratory is on the identification of cell cycle dependent regulatory events with major emphasis on protein phosphorylation and other post-translational modifications. The ultimate goal is the identification of key enzymes and target substrates that are involved in the regulation of cell division and are highly conserved during evolution.

Laboratory of Monica Riley

Research in this laboratory focuses on the molecular evolution and gene expression in the bacterium *Escherichia coli*. In a collaborative effort, a database containing information on the intermediary metabolism and biochemical pathways of *E. coli* is being developed. When completed, this database is expected to contain information on each metabolic reaction, the enzyme, the reactants, products, cofactors, activators, inhibitors, kinetics, equilibrium constants, binding constants, etc.

Related research is on the evolution of the *E. coli* DNA and organization of the genes in the chromosome. Comparative nucleotide and amino acid sequence data provide information on the evolutionary relationships of *E. coli* genes to homologous genes in related bacteria.

Laboratory of Sensory Physiology

Since 1973, the laboratory has conducted research on various aspects of vision. Current studies focus on photoreceptor cells, on their light-absorbing pigments, and on their biochemical reactions initiated by light stimulation. Microspectrophotometric and biochemical techniques are used to study the receptors of both vertebrates (amphibia, fish, and mammals) and invertebrates (horseshoe crab and squid).

Staff

Harosi, Ferenc, Director, Associate Scientist, MBL, and Boston University School of Medicine
Szuts, Ete, Associate Scientist, MBL, and Boston University School of Medicine

Visiting investigators

Evans, Barbara I., University of Oregon, Eugene
Hawryshyn, Craig W., University of Victoria, Canada
Lall, Abner B., Johns Hopkins University

Laboratory of Osamu Shimomura

Biochemical studies of the various types of bioluminescent systems. Preparation of the improved forms of aequorin for measuring intracellular free calcium.

Staff

Shimomura, Osamu, Senior Scientist, MBL, and Boston University School of Medicine
Shimomura, Akemi, Research Assistant

Visiting investigator

Nakamura, Hideshi, Harvard University

Laboratory of Raquel Sussman

We investigate the molecular mechanism of DNA damage-inducible functions in *E. coli*. Present studies deal with novel genes that affect radiation-induced mutagenesis and analysis of RecA functions.

Staff

Sussman, Raquel, Associate Scientist
Hemant Chikarmane, Postdoctoral Research Associate
Dudley, Karen, Research Assistant

National Vibrating Probe Facility

We are exploring the roles of ionic currents, gradients, and waves in controlling development. We focus on controls of pattern and controls by calcium ions.

Staff

Jaffe, Lionel, Senior Scientist and Facility Director
Kuhtreiber, Willem, Physiologist
McLaughlin, Jane, Research Assistant
Miller, Andrew, Research Associate
Sanger, Richard, Technician
Shipley, Alan, Technician

Visiting investigators

Allen, Nina, Wake Forest College
Bates, William, Carleton University, Canada
Buonano, Mark, Massachusetts Institute of Technology
Chrystal, Jane, University of Sidney, Australia
Cornwall, Carter, Boston University
Danilchik, Michael, Wesleyan University
Gillot, Isabelle, Station Zoologique, Villefranche-sur-mer, France
Isaacs, Hugh, Brookhaven National Laboratories
Kinnamon, Sue, Colorado State University
Koshian, Leon, Cornell University
Lucas, William, University of California, Davis
McConnaughey, Ted, Marine Biological Laboratory
O'Donnell, Michael, McMaster University, Canada
Ripps, Harris, University of Illinois College of Medicine
Rubinacci, Allessandro, University of Milan, Italy
Sardet, Christian, Station Zoologique, Villefranche-sur-mer, France
Saunders, Mary Jane, University of South Florida, Tampa
Schiefelbein, John, University of Michigan
Shapiro, James, University of Chicago
Smith, Peter, Cambridge University, UK
Speksnijder, Johanna, University of Utrecht, The Netherlands

Other Year-Round Investigators and Staff

Stephens, Raymond E., Principal Investigator
Szent-Gyorgy, Gwen, Research Assistant
Warren, Lisa, Research Assistant

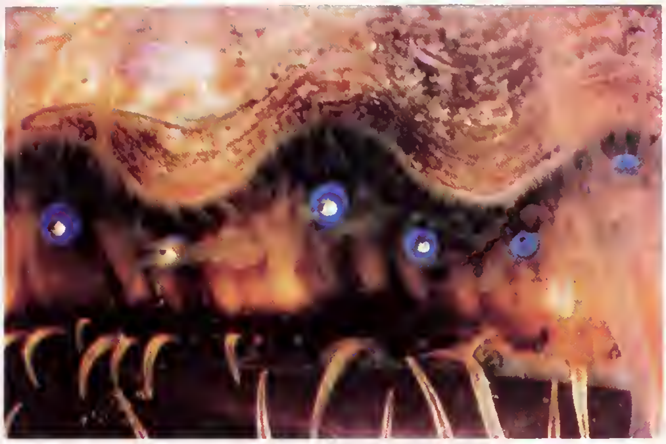

Honors

Friday Evening Lectures

Dennis Powers, Stanford University, Hopkins Marine Station, 29 June *"Adapting to a Changing Environment: Genetic and Physiological Mechanisms"*

Joan Ruderman, Harvard Medical School, 6 July *"Controlling Cell Division"*

James Spudich, Stanford University School of Medicine, 13 July *"Manifestation of a Molecular Motor: From Muscle to Amoebae"*

Ricardo Miledi, University of California, 19, 20 August (Forbes Lectures) *"How to Study the Brain Using Frog Oocytes"*

James Tiedje, Michigan State University, 27 July *"Destruction of PCBs and Other Pollutants by a New Class of Anaerobic Sediment Microorganisms"*

Ruth Sager, Dana-Farber Cancer Institute, 3 August *"Tumor Repressor Genes"*

A. James Hudspeth, University of Texas Southwestern Medical Center, 10 August *"How the Ear's Works Work: Mechanoelectrical Transduction, Frequency Tuning, and Synaptic Transmission by Hair Cells of the Internal Ear"*

Phil Leder, Harvard Medical School, 17 August *"Limb Deformity: A Pleiotropic Mutation Governing Embryonic Pattern Formation in the Mouse"*

Brian Fry, MBL Ecosystems Center, 24 August *"Consumers and Carbon Isotopes: Good Chemistry in the Sea"*

Thoru Pederson, Worcester Foundation for Experimental Biology, 31 August *"Between Nucleus and Cytoplasm: The Baroque Process of Making mRNA as Studied from the Perspective of Cell Biology"*

Fellowships

Robert Day Allen Fellowship

Eugeni A. Vaisberg, Protein Research Institute, USSR

Frederick B. Bang Fellowship Fund

Elaine Bearer, University of California, San Francisco

Jean and Katsuma Dan Fellowship

Douglas E. Koshland (financial support by Japanese Dan Fellowship), Carnegie Institution of Washington

M. G. F. Fuortes Fellowship

Joseph Charles Callaway, University of North Carolina, Chapel Hill

Stephen W. Kuffler Fellowship

Joachim W. Deitmer, University of Kaiserslauten, Zoologie, Germany

Dieter Swandulla, Max-Planck-Institüt, Germany

Hayden-Baille Fellowship

Neena Din, University of British Columbia, Canada

Anne Donaldson, MRC Laboratory of Molecular Biology, UK

Faith Miller Fellowship

Elaine L. Bearer, University of California, San Francisco

Youngsook Lee, Harvard University

Nikon Fellowship

Timothy Mitchison, University of California, San Francisco

Science Writing Fellowships

Robin Henig, Freelance
Bruce Jacobs, Freelance
Bill Krasean, *Kalamazoo Gazette*
June Kinoshita, Freelance
Keming Kuo, Voice of America
Beth Livermore, Freelance
Michael Skoler, National Public Radio
Pamela Weintraub, *Omni*
Rick Weiss, *Science News*

H. Burr Steinbach Memorial Fellowship

Youngsook Lee, Harvard University

Steps Toward Independence—MBL Summer Fellowship

Elaine Bearer, University of California, San Francisco
Robert Paul Malchow, University of Illinois
JoAnn Render, Hamilton College
Katherine Swenson, Harvard Medical School
Johanna E. Speksnijder, Utrecht University, The Netherlands
Eugeni Vaisberg, Protein Research Institute, USSR

Scholarships

APA Fellow

Maria A. Sosa, University of Florida
John F. Hamilton, Meharry Medical College

ARCS Foundation Fellow

Daniel S. Kessler, Rockefeller University

ASCB Fellows

Abdiel J. Alvarez, University of Puerto Rico
Robert L. Bacallao, University of California, Los Angeles
Miles G. Cunningham, Massachusetts Institute of Technology
Charlotte M. Vines, Harvard Medical School

Biology Club of CUNY

Elizabeth L. Winter, City College of New York

Father Arsenius Boyer Scholarship Fund

Haohua Qian, University of Illinois

C. Lalor Burdick Scholarship

Ann Marie Murphy, Johns Hopkins University

Gary N. Calkins Memorial Scholarship

Hanno M. Roder, Massachusetts Institute of Technology

Frances S. Claff Memorial Scholarship

Ka Hou Chu, Chinese University of Hong Kong, Hong Kong

Edwin Grant Conklin Memorial Scholarship

Sylwester Chyb, Wesleyan University

Lucretia Crocker Endowment Fund

Silvia E. Frenk, King's College, Cambridge, UK

Bernard Davis Scholarship

Diane K. Arwood, University of Southern Mississippi
Joanna S. Brooke, University of Western Ontario, Canada
Joseph P. Calabrese, West Virginia University
Judith A. Koskella, New York University
Bridget E. Laue, University of Colorado
Jared R. Leadbetter, Goucher College
Shi Liu, University of Oklahoma
Lynn V. Mendelman, Harvard Medical School
Elizabeth J. Orle, Colorado State University
Mechthild Pohlschroder, University of Massachusetts, Amherst

William F. and Irene Diller Scholarship Fund

Sylwester Chyb, Wesleyan University

Caswell Grave Scholarship

Ricardo Araneda, Albert Einstein College of Medicine
Sylwester Chyb, Wesleyan University
Kareen M. Guida, University of Paris, France

Aline D. Gross Scholarship

Anne Marie Murphy, Johns Hopkins University

Arthur Klorfein Fund Scholarship

Dangeruta Kersulyte, Academy of Science, Lithuania, USSR

Thierry Lepage, University of Nice, France
Kareen M. Guida, University of Paris, France

Edwin S. Linton Memorial Scholarship

Michael C. Schmale, University of Miami

S. O. Mast Founders Scholarship

Peter J. Edmunds, Northeastern University
Ka Hou Chu, Chinese University of Hong Kong, Hong Kong

Center for Microbial Ecology, Michigan State Scholarship

Olivia T. Harriott, University of Connecticut

Alberto Monroy Fellow

Maria G. DiBernardo, Instituto di Biologia dello Sviluppo, CNS, Italy

James S. Mountain Memorial Fund Scholarship

Karen M. Page, Dartmouth College
Eric A. Shelden, University of Massachusetts, Amherst
Salme Taagepera, University of Virginia
Sandra A. Brockman, Carnegie-Mellon University
Tod A. Critchlow, Scripps Institute of Oceanography

Planetary Biology Internship

Jennifer E. Klenz, University of Saskatchewan, Canada

William Townsend Porter Foundation Fellowship

Abdiel J. Alvarez, University of Puerto Rico
Robert L. Bacallao, University of California, Los Angeles
Miles G. Cunningham, Massachusetts Institute of Technology
Domingo T. Rivera, Worcester Foundation for Experimental Biology
Charlotte M. Vines, Harvard Medical School
Ebenezer Yamoah, University of Alberta, Canada

Herbert W. Rand Scholarship

Brian J. Binder, Massachusetts Institute of Technology
Sandra A. Brockman, Carnegie-Mellon University
Isabelle Carre, SUNY, Stony Brook
Joseph Cerro, Columbia University
Ka Hou Chu, Chinese University of Hong Kong, Hong Kong
Tod A. Critchlow, Scripps Institute of Oceanography
Michele I. Flatters, Tufts University
Holly Y. Goodson, Stanford University
Jerilyn Jewett-Smith, Whitman College
John R. Jordan, University of Utah
David L. Keefe, Yale University
Karen L. King, Florida State University
Qingwen Li, University of Kansas
Helen McNeill, University of Pennsylvania
Christa S. Merzdorf, Harvard University
Robert Mirro, University of Tennessee
Qi Yang, University of Connecticut

Society for General Physiologists Scholarships

Robert A. Berkowitz, Washington University
Daniel H. Cox, Tufts University
Holly Y. Goodson, Stanford University
Daniel S. Kessler, Rockefeller University

Marjorie W. Stetten Fund

Haohua Qian, University of Illinois

Surdna Foundation Scholarship

Peter J. Edmunds, Northeastern University
Oivind Enger, University of Bergen, Norway
Robert E. Hodson, University of Georgia
James S. Maki, Harvard University
Martin Polz, University of Vienna, Austria
Stephen C. Tsoi, University of Hong Kong, Hong Kong

William Morton Wheeler Family Founders' Scholarship

Hanno M. Roder, Massachusetts Institute of Technology

Awards

Lewis Thomas Award

Natalie Angier, *The New York Times*

MBL Tour Guides Award for Outstanding Science Presentation to the General Public

Nancy Rafferty, Northwestern University
Seymour Zigman, University of Rochester School of Medicine

Board of Trustees and Committees

Corporation Officers and Trustees

Ex officio

Honorary Chairman of the Board of Trustees, Denis M. Robinson, Key Biscayne, FL
Chairman of the Board of Trustees, Prosser Gifford, Washington, DC
President of the Corporation and Director, Harlyn O. Halvorson, Marine Biological Laboratory, Woods Hole, MA
Treasurer, Robert D. Manz, Helmer & Associates, Waltham, MA
Clerk of the Corporation, Kathleen Dunlap, Tufts University School of Medicine, Boston, MA

Class of 1994—Trustees

Robert D. Goldman, Northwestern University, Chicago, IL
Rodolfo R. Llinas, New York University Medical Center, New York, NY
Thomas D. Pollard, Johns Hopkins University, Baltimore, MD
Joan V. Ruderman, Harvard University School of Medicine, Boston, MA
Joseph Sanger, University of Pennsylvania School of Medicine, Philadelphia, PA
Ann Stuart, Marine Biological Laboratory, Woods Hole, MA

Class of 1994—Trustees-at-Large

Frederick Bay, Gaston Snow Beekman & Bogue, New York, NY
Mary-Ellen Cunningham, Grosse Pointe Farms, MI
Robert W. Pierce, Boca Grande, FL
Irving Rabb, University Place at Harvard Square, Cambridge, MA

Class of 1993

Garland E. Allen, Washington University, St. Louis, MO
Jelle Atema, Marine Biological Laboratory, Woods Hole, MA
William L. Brown, Weston, MA
Alexander W. Clowes, University of Washington School of Medicine, Seattle, WA
Barbara Ehrlich, University of Connecticut, Farmington, CT
Edward A. Kravitz, Harvard Medical School, Boston, MA
Robert E. Mainer, The Boston Company, Boston, MA
Jerry M. Melillo, Marine Biological Laboratory, Woods Hole, MA
Roger D. Sloboda, Dartmouth College, Hanover, NH

Class of 1992

Norman Bernstein, Bernstein Management, Inc., Washington, DC
Ellen R. Grass, Grass Foundation, Quincy, MA
Neil Jacobs, Hale & Dorr, Boston, MA
Sir Hans Kornberg, Christ's College, Cambridge, UK
George Langford, University of North Carolina, Chapel Hill, NC
Jack Levin, V.A. Medical Center, San Francisco, CA
Evelyn Spiegel, Dartmouth College, Hanover, NH
Andrew G. Szent-Györgyi, Brandeis University, Waltham, MA
Kensal E. VanHolde, Oregon State University, Corvallis, OR
Stanley W. Watson, Associates of Cape Cod, Inc., Falmouth, MA

Class of 1991

Robert B. Barlow Jr., Syracuse University, Syracuse, NY
Dieter Blennemann, Carl Zeiss, Inc., Thornwood, NY
James M. Clark, Palm Beach, FL
Wensley G. Haydon-Baillie, Porton, Int., London, UK
Laszlo Lorand, Northwestern University, Evanston, IL
Lionel I. Rebhun, University of Virginia, Charlottesville, VA
Carol L. Reinisch, Tufts University School of Veterinary Medicine, Boston, MA
Brian M. Salzberg, University of Pennsylvania, Philadelphia, PA
Sheldon J. Segal, The Rockefeller Foundation, New York, NY

Emeriti

John B. Buck, NIH, Bethesda, MD
Seymour S. Cohen, Woods Hole, MA
Arthur L. Colwin, Key Biscayne, FL
Laura Hunter Colwin, Key Biscayne, FL
D. Eugene Copeland, MBL, Woods Hole, MA
Sears Crowell, Indiana University, Bloomington, IN
Alexander T. Daignault, Boston, MA
William T. Golden, New York, NY
Teru Hayashi, Woods Hole, MA
Ruth Hubbard, Cambridge, MA
Lewis Kleinholz, Reed College, Portland, OR
Maurice E. Krahl, Tucson, AZ
Charles B. Metz, Miami, FL
Keith R. Porter, University of Pennsylvania, Philadelphia, PA
C. Ladd Prosser, University of Illinois, Urbana, IL
S. Meryl Rose, E. Falmouth, MA
W. D. Russell-Hunter, Syracuse University, Syracuse, NY
John Saunders, Jr., Waquoit, MA
Mary Sears, Woods Hole, MA
Homer P. Smith, Woods Hole, MA
W. Randolph Taylor, Ann Arbor, MI
D. Thomas Trigg, Wellesley, MA
Walter S. Vincent, Woods Hole, MA
George Wald, Cambridge, MA

Executive Committee of the Board of Trustees

Prosser Gifford*, Chairman
Robert B. Barlow Jr., 1991
Ray L. Epstein*
Robert D. Goldman, 1994
Harlyn O. Halvorson*
Robert E. Mainer, 1993
Robert D. Manz*
Jerry M. Melillo, 1992
Irving W. Rabb, 1991
Sheldon J. Segal, 1992
D. Thomas Trigg, 1990

Trustee Committees 1990

Audit

Robert Mainer, Chairman
Ray L. Epstein*
Robert D. Manz*
Sheldon J. Segal
Andrew G. Szent-Györgyi
D. Thomas Trigg
Kensal E. Van Holde
Stanley W. Watson

Compensation

Prosser Gifford, Chairman
Robert E. Mainer
Robert D. Manz
Irving W. Rabb
D. Thomas Trigg

Investment

D. Thomas Trigg, Chairman
William L. Brown
Ray L. Epstein*
William T. Golden
Maurice Lazarus
Werner R. Loewenstein
Robert D. Manz*
Irving W. Rabb
W. Nicholas Thorndike

Standing Committees for the Year 1990

Buildings & Grounds

Kenyon Tweedell, Chairman
Alfred Chaet
Lawrence B. Cohen
Richard Cutler*
Alan Fein
Ferenc Harosi
Donald B. Lehy*
Thomas Meedel
Philip Person
Evelyn Spiegel

Fellowships

Thoru Pederson, Chairman
Martha Constantine-Paton
Ray L. Epstein*
Leslie D. Garrick*
Ann Giblin
George M. Langford
Eduardo Macagno
Carol L. Reinisch
J. Richard Whittaker

Housing, Food Service, and Child Care

Thomas Reese, Chairman
Jelle Atema
Andrew Bass
Susan Barry
Donald Chang
Richard Cutler*
Stephen Highstein
LouAnn King*

Institutional Animal Care and Use

Leslie D. Garrick*, Chairman
Robert B. Bullis
Alfred Chaet
Ray L. Epstein*
Edward Jaskun
Andrew Mattox*

Institutional Biosafety

Raquel Sussman, Chairman
Paul De Weer
Paul Englund
Harlyn O. Halvorson*
Paul Lee
Donald B. Lehy*
Joseph Martyna
Andrew Mattox*
Alfred W. Senft

Instruction

Roger Sloboda, Chairman
Ray L. Epstein*
Rachel Fink
Leslie D. Garrick*
Leah Haimo
Ron Hoy
Hans Laufer
Joan Ruderman
Robert Silver
Ray Stephens

Library Joint Management

Harlyn O. Halvorson*, Chairman
Garland Allen
Craig Dorman, WHOI
Ray Epstein
George Grice, WHOI
John W. Speer*
Gary Walker, WHOI

Library Joint Users

Garland Allen, Chairman
Henry J. B. Dick, WHOI
A. Farmanfarmaian
Lionel Jaffe
Catherine Norton*
John Teal, WHOI
Geoff Thomson, WHOI
Page Valentine, USGS
Carole Winn*, WHOI

Marine Resources

Robert Goldman, Chairman
Donald Abt
William Cohen
Richard Cutler*
Toshio Narahashi
George Pappas
Roger Sloboda
Melvin Spiegel
Antoinette Steinacher
John Valois*

Radiation Safety

Ete Z. Szutz, Chairman
David W. Borst
Richard L. Chappell
Sherwin J. Cooperstein
Louis M. Kerr
Andrew Mattox*
Robert Rakowski
Walter Vincent

---

ex officio

Research Services

Brian Noe, Chairman
Peter Armstrong
Robert B. Barlow Jr.
Richard Cutler*
Barbara Ehrlich
Ken Forman
Ehud Kaplan
Samuel S. Koide
Aimlee Laderman
Jack Levin
Andrew Mattox*
Robert Palazzo
Paul Steudler

Research Space

Joseph Sanger, Chairman
Paul De Weer
Ray L. Epstein*
Leslie D. Garrick*
John Hildebrand
David Landowne
Hans Laufer
Eduardo Macagno
Jerry M. Melillo
Joan V. Ruderman
Robert Silver
Steven Treistman
Ivan Valiela
Richard Vallee

Safety

John Hobbie, Chairman
D. Eugene Copeland
Richard Cutler*
Edward Enos*
Louis Kerr
Alan Kuzirian
Donald B. Lehy*
Andrew Mattox*
Paul Steudler

**ex officio*

Laboratory Support Staff*

Biological Bulletin

Clapp, Pamela L., Managing Editor
Puckett, Kathryn
Stone, Beth Ready

Computer Services

Tollios, Constantine D., Manager
Schmidt, Valerie

Controller's Office

Speer, John W., Controller

Accounting Services

Binda, Ellen F.
Campbell, Ruth B.
Davis, Doris C.
Ghetti, Pamela M.
Gilmore, Mary F.
Hobbs, Roger W., Jr.
Hough, Rose A.
Oliver, Elizabeth
Poravas, Maria
Riley, Janis E.

Chem Room

Chisholm, Caroline G.
Miller, Lisa A.
Sadowski, Edward A.

Purchasing

Hall, Lionel E., Jr.
Schorer, Timothy M.

Copy Service Center

Mountford, Rebecca J., Supervisor
Jackson, Jacquelyn F.
Ridley, Sherie

Development Office

Ayers, Donald E., Director
Berthel, Dorothy
Lessard, Kelley J.
Thimas, Lisa M.

Director's Office

Halvorson, Harlyn O., President and Director
Burrhus, I. Elaine
Catania, Didia
Epstein, Ray L.
Kinneally, Kathleen R.
Power, Linda M.
Watkins, Joan E.

Gray Museum

Backus, Richard H., Curator
Armstrong, Ellen P.
Montiero, Eva

Housing

King, LouAnn D., Conference Center and Housing Manager
Barnes, Susan M.
Farrell, Bernice R.
Johnson, Frances N.
Krajewski, Viola I.
Kuil, Elisabeth
Mancevice, Denise M.
McNamara, Noreen
Sadovsky, Sebastian

Telephone Office

Baker, Ida M.
Geggatt, Agnes L.
Ridley, Alberta W.

Human Resources

Goux, Susan P., Manager
Donovan, Marcia H.

Library

Norton, Catherine N., Acting Librarian
Ashmore, Judith A.
Costa, Marguerite E.
Fessenden, Jane
Fisher, Susan
Goux, Randal
Huguenin, Sanders
Keenan, Patrick M.
Mirra, Anthony J.
Mountford, Rebecca J.
Nelson, Heidi
Pratson, Patricia G.
Showalter, Christine M.
Tamm, Ingrid
deVeer, Joseph M.
Wright, Rosemary

MBL Associates Liaison

Scanlon, Deborah

Public Information Office

Liles, George W., Jr., Director
Anderson, Judith L.
Kaye-Peterson, Amy
Stone, Beth Ready

Safety Services

Mattox, Andrew H., Safety Officer

Apparatus

Barnes, Franklin D.
Haskins, William A.
Martin, Lowell V.
Nichols, Francis H., Jr.

Shipping and Receiving

Geggatt, Richard E.
Illgen, Robert F.
Monteiro, Dana

* *Including persons who joined or left the staff during 1990.*

Services, Projects, and Facilities

Cutler, Richard D., Manager
  Enos, Joyce B.
  Kurland, Charles J.

Buildings and Grounds

Lehy, Donald B., Superintendent
  Baldic, David P.
  Blumsack, Jeffrey J.
  Blunt, Hugh F.
  Bourgoin, Lee E.
  Carini, Robert J.
  Fish, David L., Jr.
  Fuglister, Charles K.
  Gonsalves, Walter W., Jr.
  Hathaway, Peter
  Jones, Leeland
  Justason, C. Scott
  Lochhead, William M.
  Lunn, Alan G.
  MacLeod, John B.
  McAdams, Herbert M., III
  Mills, Stephen A.
  Olive, Charles W., Jr.
  Rattacasa, Frank D.
  Schoepf, Claude
  deVeer, Robert L.
  Weeks, Gordon W.

Electron Microscopy Lab

Kerr, Louis M.

Housekeeping Services

Jerry Phillabaum, General Supervisor
  Allen, Wayne D.
  Anderson, Lewis B.
  Boucher, Richard L.
  Collins, Paul J.
  Conlin, Henry P.
  Gibbons, Roberto G.
  Krajewski, Chester J.
  Lynch, Henry L.

Instrument Development Lab

Robert Knudson

Machine Shop

Sylvia, Frank E.

Marine Resources Center

Valois, John J., Manager
Enos, Edward G., Jr., Superintendent
  Fisher, Harry T., Jr.
  Hanley, Janice S.
  Moniz, Priscilla C.
  Monteiro, Dana
  Revellese, Christopher
  Sullivan, Daniel A.
  Tassinari, Eugene
  Torres, Sophie J.

Photolab

Golder, Linda M.
Golder, Robert J.
Rugh, Douglas E.

Sponsored Programs

Garrick, Leslie D., Administrator
  Dwane, Florence
  Huffer, Linda
  Lynch, Kathleen F.

Animal Care Facility

Hanley, Janice S.
Shephard, Jennifer

Summer Support Staff

Albrecht, Helen
Amon, Tyler C.
Anderson, Penny
Ashmore, Lynne E.
Ayers, Andrew D.
Bolton, Hugh
Burke, Sean
Cadwalader, George, Jr.
Campbell, Robert E.
Capobianco, James A.
Child, Malcolm S.
Cishek, Dawn
Clinard, Nathan
Cullen, Timothy
Cutler, Laura
Demir, Oktay
Dias, John, III
Donovan, Erin
Donovan, Jason P.
Ford, John, III
Grassle, J. Thomas
Halpin, Michelle
Hamilton, Elizabeth R.
Hibbitt, Catherine
Hrynyshyn, James
Hullum, Rebekah
Illgen, Robert C.
Kaplan, Liat
Kinneally, Kara J.
Langton, Lori
Leatherbee, Amy
Marini, Michael F.
Montroll, Charles
Northern, Marc D.
Peal, Jennifer
Peal, Richard W.
Philbin, Linda M
Phillips, Daniel
Piazza, Lucia
Remsen, Andrew S.
Roderick, Paul
Rosenkranz, Margalit
St. Jean, Jeannette
Scherer, Aimee
Sheetz, Jonathan
Sheffield, James
Shepherd, Jennifer
Shock, Duane
Snyder, Matthew
Snyder, Rebecca
Sofferman, Rebecca
Swope, John G.
Tilghman, Alison
Varao, John
Vardac, Michael
Wetzel, Ernest D.
Wilkes, Jennifer

Members of the Corporation*

Life Members

Abbott, Marie, c/o Vaughn Abbott, Flyer Rd., East Hartland, CT 06027

Beams, Harold W., Department of Biology, University of Iowa, Iowa City, IA 52242
Bernheimer, Alan W., Department of Microbiology, New York University Medical Center, 550 First Ave., New York, NY 10016
Bertholf, Lloyd M., Westminster Village #2114, 2025 E. Lincoln St., Bloomington, IL 61701
Bodian, David, 4100 North Charles St., #913, Baltimore, MD 21218
Bridgman, A. Josephine, 715 Kirk Rd., Decatur, GA 30030
Buck, John B., NIH, Laboratory of Physical Biology, Room 112, Building 6 Bethesda, MD 20892
Burbanck, Madeline P., Box 15134, Atlanta, GA 30333
Burbanck, William D., Box 15134, Atlanta, GA 30333

Carpenter, Russell L., 60-H Lake St., Winchester, MA 01890
Chase, Aurin, Department of Biology, Guyot Hall, Princeton University, Princeton, NJ 08544 (resigned)
Clark, Arnold M., 53 Wilson Rd., Woods Hole, MA 02543
Cohen, Seymour S., 10 Carrot Hill Rd., Woods Hole, MA 02543-1206
Colwin, Arthur, 320 Woodcrest Rd., Key Biscayne, FL 33149
Colwin, Laura Hunter, 320 Woodcrest, Key Biscayne, FL 33149
Copeland, D. E., 41 Fern Lane, Woods Hole, MA 02543
Costello, Helen M., Carolina Meadows, Villa 137, Chapel Hill, NC 27514
Crouse, Helen, Address unknown

Failla, Patricia M., 2149 Loblolly Lane, Johns Island, SC 29455
Ferguson, James K. W., 56 Clarkehaven St., Thornhill, Ontario L4J 2B4 Canada
Fries, Erik F., 41 High Street, Woods Hole, MA 02543 (deceased)

Goldman, David, 63 Loop Rd., Falmouth, MA 02540
Graham, Herbert, 36 Wilson Rd., Woods Hole, MA 02543
Green, James W., 409 Grant Ave., Highland Park, NJ 08904
Grosch, Daniel S., 1222 Duplin Road, Raleigh, NC 27607

Hamburger, Viktor, Department of Biology, Washington University, St. Louis, MO 63130
Hamilton, Howard L., Department of Biology, University of Virginia, 238 Gilmer Hall, Charlottesville, VA 22901
Harding, Clifford V., Jr., Wayne State University School of Medicine, Department of Ophthalmology, Detroit, MI 48201
Haschemeyer, Audrey E. V., 21 Glendon Road, Woods Hole, MA 02543
Hauschka, Theodore S., FD1, Box 781, Damariscotta, ME 04543
Hisaw, F. L., 5925 SW Plymouth Drive, Corvallis, OR 97330
Hollaender, Alexander, Council for Research Planning, 1717 Massachusetts Ave. NW, Washington, DC 20036 (deceased)
Hubbard, Ruth, 21 Lakeview Avenue, Cambridge, MA 02138
Humes, Arthur G., Marine Biological Laboratory, Woods Hole, MA 02543

Johnson, Frank H., Department of Biology, Princeton University, Princeton, NJ 08540

Kaan, Helen W., Royal Megansett Nursing Home, Room 205, P. O. Box 408, N. Falmouth, MA 02556
Karush, Fred, Department of Microbiology, University of Pennsylvania School of Medicine, Philadelphia, PA 19104-6076
Kille, Frank R., 1111 S. Lakemont Ave. #444, Winter Park, FL 32782
Kingsbury, John M., Department of Plant Biology, Cornell University, Ithaca, NY 14853
Kleinholz, Lewis, Department of Biology, Reed College, 3203 SE Woodstock Blvd., Portland, OR 97202

Laderman, Ezra, Yale University, School of Music, New Haven, CT 06520
Lauffer, Max A., Address unknown
LeFevre, Paul G., 15 Agassiz Road, Woods Hole, MA 02543
Levine, Rachmiel, 2024 Canyon Rd., Arcadia, CA 91006
Lochhead, John H., 49 Woodlawn Rd., London SW6 6PS, England, UK
Loewus, Frank A., Washington State University, Institute of Biological Chemistry, Pullman, WA 99164
Loftfield, Robert B., Department of Chemistry, University of New Mexico School of Medicine, Albuquerque, NM 87131
Lynn, W. Gardner, Department of Biology, Catholic University of America, Washington, DC 20017 (deceased)

Magruder, Samuel R., 270 Cedar Lane, Paducah, KY 42001
Malkiel, Saul, Allergic Diseases, Inc., 130 Lincoln St., Worcester, MA 01609
Mathews, Rita W., Box 131, Southfield, MA 01259
Miller, James A., 307 Shorewood Drive, E. Falmouth, MA 02536
Moore, John A., Department of Biology, University of California, Riverside, CA 92521
Moscona, Arthur A., University of Chicago, Department of Molecular Genetics and Cell Biology, 920 East 58th Street, Chicago, IL 60637
Mullins, Lorin J., University of Maryland School of Medicine, Department of Biophysics, Baltimore, MD 21201

Nace, Paul F., P. O. Box 529, Cutchogue, NY 11935 (deceased)

Page, Irving H., Box 516, Hyannisport, MA 02647
Pollister, A. W., 8 Euclid Ave., Belle Mead, NJ 08502
Prosser, C. Ladd, Department of Physiology and Biophysics, Burrill Hall 524, University of Illinois, Urbana, IL 61801

---

* Including action of the 1990 Annual Meeting.

Provasoli, Luigi, Via Stazione 43, 21025 Comerio (VA), Italy
Prytz, Margaret McDonald, Address unknown

Renn, Charles E., Address unknown
Richards, A. Glenn, 942 Cromwell Ave., St. Paul, MN 55114
Rice, Robert V., 30 Burnham Dr., Falmouth, MA 02540
Rockstein, Morris, 600 Biltmore Way, Apt. 805, Coral Gables, FL 33134
Ronkin, Raphael R., 3212 McKinley St., NW, Washington, DC 20015
Rose, S. Meryl, 32 Crosby Ln., E. Falmouth, MA 02536

Sanders, Howard, Woods Hole Oceanographic Institution, Woods Hole, MA 02543
Scharrer, Berta, Department of Anatomy, Albert Einstein College of Medicine, 1300 Morris Park Avenue, Bronx, NY 10461
Schlesinger, R. Walter, University of Medicine and Dentistry of New Jersey, Department of Molecular Genetics and Microbiology, Robert Wood Johnson Medical School, Piscataway, NJ 08854-5635
Schmitt, F. O., Room 16-512, Massachusetts Institute of Technology, Cambridge, MA 02139
Scott, Allan C., 1 Nudd St., Waterville, ME 04901
Shemin, David, 33 Lawrence Farm Rd., Woods Hole, MA 02543
Silverstein, Arthur M., The Johns Hopkins Hospital Wilmer Institute, Baltimore, MD 21205
Smith, Homer P., 8 Quissett Ave., Woods Hole, MA 02543
Smith, Paul F., P. O. Box 264, Woods Hole, MA 02543
Sonnenblick, B. P., 515A Heritage Hill, Southbury, CT 06488
Steinhardt, Jacinto, 1508 Spruce St., Berkeley, CA 94709

Taylor, Robert E., 20 Harbor Hill Rd., Woods Hole, MA 02543
Taylor, W. Randolph, The Herbarium, North University Bldg., University of Michigan, Ann Arbor, MI 48109 (deceased)
TeWinkel, Lois E., Rockridge, 25 Coles Meadow Road, Northampton, MA 01060
Trager, William, The Rockefeller University, 1230 York Ave., New York, NY 10021

Villee, Claude A., Harvard Medical School, Parcel B/Room 122, 25 Shattuck Street, Boston, MA 02115

Wald, George, 21 Lakeview Ave., Cambridge, MA 02138
Waterman, T. H., Yale University, Biology Department, Box 6666, New Haven, CT 06511
Weiss, Paul A., Address unknown
Wichterman, Ralph, 31 Buzzards Bay Ave., Woods Hole, MA 02543
Wiercinski, Floyd J., 36 James St., Woods Hole, MA 02543
Wilber, Charles G., Department of Biology, Colorado State University, Fort Collins, CO 80523

Zinn, Donald J., Department of Zoology, University of Rhode Island, Kingston, RI 02881
Zorzoli, Anita, 18 Wilbur Blvd., Poughkeepsie, NY 12603
Zweifach, Benjamin W., 8811 Nottingham Place, La Jolla, CA 92037

Regular Members

Abt, Donald A., Marine Biological Laboratory, Woods Hole, MA 02543
Acheson, George H., 25 Quissett Ave., Woods Hole, MA 02543
Adams, James A., Department of Natural Sciences, University of Maryland, Princess Anne, MD 21853
Adelberg, Edward A., Provost's Office, 115 Hall of Graduate Studies, Yale University, New Haven, CT 06520
Adelman, William J., Jr., 160 Locust St., Falmouth, MA 02540
Afzelius, Bjorn, Wenner-Gren Institute, University of Stockholm, Stockholm, Sweden
Alberte, Randall S., Department of Molecular Genetics and Cell Biology, University of Chicago, 1103 E. 57th Street, Chicago, IL 60637
Alkon, Daniel, NINCDS/NIH, Dept. LMNC, Bldg. Park, Rm. 431, Bethesda, MD 20852
Allen, Garland E., Department of Biology, Washington University, St. Louis, MO 63130
Allen, Nina S., Department of Biology, Wake Forest University, Box 7325, Winston-Salem, NC 27109
Allen, Suzanne T., 155 Webster St., W. Newton, MA 02165
Amatniek, Ernest, 4797 Boston Post Rd., Pelham Manor, NY 10803
Anderson, Everett, Department of Anatomy & Cell Biology, LHRBB, Harvard Medical School, 45 Shattuck St., Boston, MA 02115
Anderson, J. M., 110 Roat St., Ithaca, NY 14850
Armett-Kibel, Christine, Department of Biology, University of Massachusetts, Boston, MA 02125
Armstrong, Clay M., Department of Physiology, University of Pennsylvania Medical School, Philadelphia, PA 19104
Armstrong, Peter B., Department of Zoology, University of California, Davis, CA 95616
Arnold, John M., Pacific Biomedical Research Center, 209 Snyder Hall, University of Hawaii, Honolulu, HI 96822
Arnold, William A., 102 Balsam Rd., Oak Ridge, TN 37830
Ashton, Robert W., Gaston Snow Beekman and Bogue, 666 5th Avenue, 31st Floor, New York, NY 10103
Atema, Jelle, Boston University Marine Program, Marine Biological Laboratory, Woods Hole, MA 02543
Atwood, Kimball C., III, P. O. Box 673, Woods Hole, MA 02543
Augustine, George J., Section of Neurobiology, Department of Biological Sciences, University of Southern California, Los Angeles, CA 90089-0371
Ayers, Donald E., Marine Biological Laboratory, Woods Hole, MA 02543

Baccetti, Baccio, Institute of General Biology, 53100 Siena, Italy
Baker, Robert G., Department of Physiology and Biophysics, New York University Medical Center, 550 First Ave., New York, NY 10016
Baldwin, Thomas O., Department of Biochemistry and Biophysics, Texas A&M University, College Station, TX 77843
Bang, Betsy, 76 F. R. Lillie Rd., Woods Hole, MA 02543
Barlow, Robert B., Jr., Institute for Sensory Research, Syracuse University, Merrill Lane, Syracuse, NY 13244-5290
Barry, Daniel T., Department of Physical Medicine and Rehabilitation, ID204, University of Michigan Hospital, Ann Arbor, MI 48109-0042
Barry, Susan R., Department of Physical Medicine and Rehabilitation, ID204, University of Michigan Hospital, Ann Arbor, MI 48109-0042
Bartell, Clelmer K., 2000 Lake Shore Drive, New Orleans, LA 70122
Bartlett, James H., Department of Physics, Box 870324, University of Alabama, Tuscaloosa, AL 35487-0324
Bass, Andrew H., Seely Mudd Hall, Department of Neurobiology, Cornell University, Ithaca, NY 14853
Battelle, Barbara-Anne, Whitney Laboratory, 9505 Ocean Shore Blvd., St. Augustine, FL 32086
Bauer, G. Eric, Department of Anatomy, University of Minnesota, Minneapolis, MN 55455
Bay, Frederick, Bay Foundation, Gaston Snow Beckman & Bogue, 666 5th Ave., 31st Floor, New York, NY 10103
Beauge, Luis Alberto, Department of Biophysics, Instituto M.y.M. Ferreyra, Casilla de Correo 389, 5000 Cordoba, Argentina

Beck, L. V., School of Experimental Medicine, Department of Pharmacology, Indiana University, Bloomington, IN 47401
Begenisich, Ted, Department of Physiology, University of Rochester, Medical Center, Box 642, 601 Elmwood Ave., Rochester, NY 14642
Begg, David A., LHRRB, Harvard Medical School, 45 Shattuck St., Boston, MA 02115
Bell, Eugene, Organogenesis, Inc., 83 Rogers St., Cambridge, MA 02142
Benacerraf, Baruj, Dana-Farber Cancer Institute, 44 Binney Street, Boston, MA 02115
Benjamin, Thomas L., Department of Pathology, Harvard Medical School, 25 Shattuck St., Boston, MA 02115
Bennett, M. V. L., Albert Einstein College of Medicine, Department of Neuroscience, 1410 Pelham Pkwy. S., Bronx, NY 10461
Bennett, Miriam F., Department of Biology, Colby College, Waterville, ME 04901
Berg, Carl J., Jr., P. O. Box 769, Kilauea, Kauai, HI 96754-0769
Berne, Robert M., Department of Physiology, University of Virginia, School of Medicine, Charlottesville, VA 22908
Bernstein, Norman, Diane and Norman Bernstein Foundation, Inc., 2025 Eye St., N.W., #400, Washington, DC 20009
Bezanilla, Francisco, Department of Physiology, University of California, Los Angeles, CA 90024
Biggers, John D., Department of Physiology, Harvard Medical School, Boston, MA 02115
Bishop, Stephen H., Department of Zoology, Iowa State University, Ames, IA 50010
Blaustein, Mordecai P., Department of Physiology, School of Medicine, University of Maryland, 655 W. Baltimore Street, Baltimore, MD 21201
Blennemann, Dieter, Carl Zeiss, Inc., One Zeiss Drive, Thornwood, NY 10594
Bloom, George S., Department of Cell Biology and Neuroscience, The University of Texas Southwestern Medical Center, 5223 Harry Hines Blvd., Dallas, TX 75235-9039
Bloom, Kerry S., Department of Biology, University of North Carolina, Wilson Hall, CB#3280, Chapel Hill, NC 27599-3280
Bodznick, David A., Department of Biology, Wesleyan University, Lawn Avenue, Middletown, CT 06457
Boettiger, Edward G., 29 Juniper Point, Woods Hole, MA 02543
Boolootian, Richard A., Science Software Systems, Inc., 3576 Woodcliff Rd., Sherman Oaks, CA 91403
Borgese, Thomas A., Department of Biology, Lehman College, CUNY, Bronx, NY 10468
Borisy, Gary G., Laboratory of Molecular Biology, University of Wisconsin, Madison, WI 53706
Borst, David W., Jr., Department of Biological Sciences, Illinois State University, Normal, IL 61761-6901
Bosch, Herman F., Box 617, Woods Hole, MA 02543
Bowles, Francis P., P. O. Box 674, Woods Hole, MA 02543
Boyer, Barbara C., Department of Biology, Union College, Schenectady, NY 12308
Brandhorst, Bruce P., Department of Biological Sciences, Simon Fraser University, Barnaby, BC V5A 156 Canada
Brehm, Paul, Department of Neurobiology and Behavior, SUNY at Stony Brook, Stony Brook, NY 11794
Brinley, F. J., Neurological Disorders Program, NINCDS, 812 Federal Building, Bethesda, MD 20892
Brown, Joel E., Department of Ophthalmology, Box 8096 Sciences Center, Washington University, 660 S. Euclid Ave., St. Louis, MO 63110
Brown, Stephen C., Department of Biological Sciences, SUNY, Albany, NY 12222
Brown, William L., Bank of Boston (01-23-11), 100 Federal St., Boston, MA 02106-2016
Bryant, Shirley H., Department of Pharmacology and Cell Biophysics, University of Cincinnati, Cincinnati, OH 45267
Bullis, Robert A., Marine Biological Laboratory, Woods Hole, MA 02543
Burd, Gail Deerin, Department of Molecular and Cell Biology, University of Arizona, Tucson, AZ 85721
Burdick, Carolyn J., Department of Biology, Brooklyn College, Bedford Avenue & Avenue H, Brooklyn, NY 11210
Burger, Max, Freidrich Miesner Institut Bau 1060 Postfach 2543, Basel 4002, Switzerland
Burgos, Mario, IHEM Medical School, UNC 5500 Mendoza, Argentina
Burky, Albert, Department of Biology, University of Dayton, Dayton, OH 45469
Burstyn, Harold Lewis, Melvin and Melvin, 700 Merchants Bank Bldg., Syracuse, NY 13202-1686
Bursztajn, Sherry, Harvard Medical School, Mailman Research Center, 115 Mill St., Belmont, MA 02178
Bush, Louise, 7 Snapper Lane, Falmouth, MA 02540

Calabrese, Ronald L., Department of Biology, Emory University, 1555 Pierce Drive, Atlanta, GA 30322
Candelas, Graciela C., Department of Biology, University of Puerto Rico, Rio Piedras, PR 00931
Carew, Thomas J., Department of Psychology, Yale University, P. O. Box 11A, Yale Station, New Haven, CT 06520
Cariello, Lucio, Biochemistry Department, Stazione Zoologica, Villa Comunale, 80121 Naples, Italy
Carlson, Francis D., 2302 W. Rogers Avenue, Baltimore, MD 21209
Carriere, Rita M., Department of Anatomy and Cell Biology, Box 5, SUNY Health Science Center, 450 Clarkson Ave., Brooklyn, NY 11203
Case, James, Office of Research Development, Cheadle Hall, University of California, Santa Barbara, CA 93111
Cassidy, Rev. J. D., St. Stephen Priory, Spiritual Life Center, 20 Glen St., Box 370, Dover, MA 02030-0370
Cebra, John J., Department of Biology, Leidy Labs, G-6, University of Pennsylvania, Philadelphia, PA 19174
Chaet, Alfred B., University of West Florida, Pensacola, FL 32504
Chambers, Edward L., Department of Physiology and Biophysics, University of Miami, School of Medicine, P. O. Box 016430, Miami, FL 33101
Chang, Donald C., Department of Physiology, Baylor College of Medicine, One Baylor Plaza, Houston, TX 77030
Chappell, Richard L., Department of Biological Sciences, Hunter College, Box 210, 695 Park Ave., New York, NY 10021
Chauncey, Howard H., 30 Falmouth St., Wellesley Hills, MA 02181
Child, Frank M., III, Department of Biology, Trinity College, Hartford, CT 06106
Chisholm, Rex L., Department of Cell Biology and Anatomy, Northwestern University Medical School, 303 E. Chicago Avenue, Chicago, IL 60611
Citkowitz, Elena, 410 Livingston St., New Haven, CT 06511
Clark, Eloise E., Academic Affairs, Bowling Green State University, Bowling Green, OH 43403
Clark, Hays, 26 Deer Park Drive, Greenwich, CT 06830
Clark, James M., 210 Emerald Lane, Palm Beach, FL 33480
Clark, Wallis H., Jr., Bodega Marine Laboratory, P. O. Box 247, Bodega Bay, CA 94923
Claude, Philippa, Primate Center, Capitol Court, Madison, WI 53706
Clay, John R., Laboratory of Biophysics, NIH, Building 9, Room 1E-124, Bethesda, MD 20892

Clowes, Alexander W., Department of Surgery RF-25, University of Washington School of Medicine, Seattle, WA 98195
Clutter, Mary, Office of the Director, Room 518, National Science Foundation, Washington, DC 20550
Cobb, Jewel Plummer, California State University, 800 State College Boulevard, Fullerton, CA 92634
Cohen, Adolph I., Department of Ophthalmology, School of Medicine, Washington University, 660 S. Euclid Ave., St. Louis, MO 63110
Cohen, Avis H., Section of Neurobiology and Behavior, Mudd Hall, Cornell University, Ithaca, NY 14853-2702
Cohen, Carolyn, Rosenstiel Basic Medical Sciences Research Center, Brandeis University, Waltham, MA 02254
Cohen, Lawrence B., Department of Physiology, Yale University School of Medicine, 333 Cedar Street, New Haven, CT 06510-8026
Cohen, Maynard, Department of Neurological Sciences, Rush Medical College, 600 South Paulina, Chicago, IL 60612
Cohen, Rochelle S., Department of Anatomy, University of Illinois, 808 W. Wood Street, Chicago, IL 60612
Cohen, William D., Department of Biological Sciences, Hunter College, 695 Park Ave., Box 79, New York, NY 10021
Coleman, Annette W., Division of Biology and Medicine, Brown University, Providence, RI 01912
Collier, Jack R., Department of Biology, Brooklyn College, Bedford & Avenue H, Brooklyn, NY 11210
Collier, Marjorie McCann, Biology Department, Saint Peter's College, 2641 Kennedy Boulevard, Jersey City, NJ 07306
Cook, Joseph A., The Edna McConnell Clark Foundation, 250 Park Ave., New York, NY 10017
Cooperstein, S. J., University of Connecticut Health Center, Department of Anatomy, Farmington Ave., Farmington, CT 06032
Corliss, John O., P. O. Box 53008, Albuquerque, NM 87153
Cornell, Neal W., Marine Biological Laboratory, Woods Hole, MA 02543
Cornwall, Melvin C., Jr., Department of Physiology L714, Boston University School of Medicine, 80 E. Concord St., Boston, MA 02118
Corson, David Wesley, Jr., 1034 Plantation Lane, Mt. Pleasant, SC 29464
Corwin, Jeffrey T., Department of Otolaryngology, University of Virginia Medical Center, Box 430, Charlottesville, VA 22908
Costello, Walter J., Department of Zoology, College of Medicine, Ohio University, Athens, OH 45701
Couch, Ernest F., Department of Biology, Texas Christian University, Fort Worth, TX 76129
Cremer-Bartels, Gertrud, Universitats Augenklinik, 44 Munster, Germany
Crow, Terry J., Department of Neurobiology and Anatomy, University of Texas Medical School, Houston, TX 77225
Crowell, Sears, Department of Biology, Indiana University, Bloomington, IN 47405
Crowther, Robert, Marine Biological Laboratory, Woods Hole, MA 02543
Cunningham, Mary-Ellen, 62 Cloverly Road, Grosse Pointe Farms, MI 48236
Currier, David L., P. O. Box 2476, Vineyard Haven, MA 02568
Cutler, Richard, Marine Biological Laboratory, Woods Hole, MA 02543

Daignault, Alexander T., 280 Beacon St., Boston, MA 02116
Dan, Katsuma, Tokyo Metropolitan Union, Meguro-ku, Tokyo, Japan
D'Avanzo, Charlene, School of Natural Science, Hampshire College, Amherst, MA 01002
David, John R., Seeley G. Mudd Building, Room 504, Harvard Medical School, 250 Longwood Ave., Boston, MA 02115
Davidson, Eric H., Division of Biology, 156-29, California Institute of Technology, Pasadena, CA 91125
Davis, Bernard D., Bacterial Physiology Unit, Harvard Medical School, Boston, MA 02115
Davis, Joel P., Seapuit, Inc., P. O. Box G, Osterville, MA 02655
Daw, Nigel W., 78 Aberdeen Place, Clayton, MO 63105
DeGroof, Robert C., 145 Water Crest Dr., Doylestown, PA 18901
DeHaan, Robert L., Department of Anatomy and Cell Biology, Emory University School of Medicine, Atlanta, GA 30322
DeLanney, Louis E., Institute for Medical Research, 2260 Clove Drive, San Jose, CA 95128
DePhillips, Henry A., Jr., Department of Chemistry, Trinity College, 300 Summit Street, Hartford, CT 06106
DeSimone, Douglas W., Department of Anatomy and Cell Biology, Box 439, Health Sciences Center, University of Virginia, Charlottesville, VA 22908
DeToledo-Morrell, Leyla, Department of Neurological Sciences, Rush Medical College, Chicago, IL 60614
Dettbarn, Wolf-Dietrich, Department of Pharmacology, School of Medicine, Vanderbilt University, Nashville, TN 37127
De Weer, Paul J., Department of Physiology, University of Pennsylvania School of Medicine, Philadelphia, PA 19104-6085
Dixon, Keith E., School of Biological Sciences, Flinders University, Bedford Park, 5042, South Australia, Australia
Dowdall, Michael J., Department of Zoology, School of Biological Sciences, University of Nottingham, University Park, Nottingham NG7 2RD, England, UK
Dowling, John E., The Biological Laboratories, Harvard University, 16 Divinity St., Cambridge, MA 02138
DuBois, Arthur Brooks, John B. Pierce Foundation Laboratory, 290 Congress Ave., New Haven, CT 06519
Dudley, Patricia L., Department of Biological Sciences, Barnard College, Columbia University, 3009 Broadway, New York, NY 10027
Duncan, Thomas K., Department of Environmental Sciences, Nichols College, Dudley, MA 01570
Dunham, Philip B., Department of Biology, Syracuse University, Syracuse, NY 13244
Dunlap, Kathleen, Department of Physiology, Tufts University Medical School, Boston, MA 02111

Ebert, James D., Office of the Director, Chesapeake Bay Institute, The Johns Hopkins University, Suite 340, The Rotunda, 771 West 40th St., Baltimore, MD 21211
Eckberg, William R., Department of Zoology, Howard University, Washington, DC 20059
Edds, Kenneth T., Department of Anatomical Sciences, SUNY, Buffalo, NY 14214
Eder, Howard A., Albert Einstein College of Medicine, 1300 Morris Park Ave., Bronx, NY 10461
Edstrom, Joan, 2515 Milton Hills Dr., Charlottesville, VA 22901
Edwards, Charles, University of Southern Florida College of Medicine, MDC Box 40, 12901 Bruce B. Downs Blvd., Tampa, FL 33612
Egyud, Laszlo G., 18 Skyview, Newton, MA 02150
Ehrlich, Barbara E., Division of Cardiology, University of Connecticut Health Center, 263 Farmington Avenue, Farmington, CT 06032
Eisen, Arthur Z., Division of Dermatology, Washington University, St. Louis, MO 63110
Eisenman, George, Department of Physiology, University of California Medical School, Los Angeles, CA 90024

Elder, Hugh Young, Institute of Physiology, University of Glasgow, Glasgow, Scotland G12 8QQ
Elliott, Gerald F., The Open University Research Unit, Foxcombe Hall, Berkeley Rd., Boars Hill, Oxford, England OX1 5HR
Englund, Paul T., Department of Biological Chemistry, Johns Hopkins School of Medicine, Baltimore, MD 21205
Epel, David, Hopkins Marine Station, Pacific Grove, CA 93950
Epstein, Herman T., 18 Lawrence Farm Road, Woods Hole, MA 02543
Epstein, Ray L., Marine Biological Laboratory, Woods Hole, MA 02543
Erulkar, Solomon D., 318 Kent Rd., Bala Cynwyd, PA 19004
Essner, Edward S., Kresge Eye Institute, Wayne State University, 540 E. Canfield Ave., Detroit, MI 48201

Farb, David H., Department of Pharmacology L603, Boston University School of Medicine, Boston, MA 02118
Farmanfarmaian, A., Department of Biological Sciences, Nelson Biological Laboratory, Rutgers University, Piscataway, NJ 08855
Fein, Alan, Department of Physiology, University of Connecticut Health Center, Farmington, CT 06032
Feinman, Richard D., Box 8, Department of Biochemistry, SUNY Health Science Center, 450 Clarkson Avenue, Brooklyn, NY 11203
Feldman, Susan C., Department of Anatomy, University of Medicine and Dentistry of New Jersey, New Jersey Medical School, 100 Bergen St., Newark, NJ 07103
Fessenden, Jane, Marine Biological Laboratory, Woods Hole, MA 02543
Festoff, Barry W., Neurology Service (127), Veterans Administration Medical Center, 4801 Linwood Blvd., Kansas City, MO 64128
Fink, Rachel D., Department of Biological Sciences, Clapp Laboratory, Mount Holyoke College, South Hadley, MA 01075
Finkelstein, Alan, Albert Einstein College of Medicine, 1300 Morris Park Ave., Bronx, NY 10461
Fischbach, Gerald, Department of Neurobiology, Harvard Medical School, 220 Longwood Ave., Boston, MA 02115
Fishman, Harvey M., Department of Physiology and Biophysics, University of Texas Medical Branch, Galveston, TX 77550
Flanagan, Denis, 12 Gay St., New York, NY 10014
Franzini-Armstrong, Clara, Department of Biology G-3, School of Medicine, University of Pennsylvania, Philadelphia, PA 19143
Frazier, Donald T., Department of Physiology, University of Kentucky Medical Center, Lexington, KY 40536
Friedler, Gladys, Boston University School of Medicine, 80 East Concord Street, Boston, MA 02118
French, Robert J., Health Sciences Center, University of Calgary, Calgary, Alberta, T2N 4N1, Canada
Freygang, Walter J., Jr., 6247 29th St., NW, Washington, DC 20015
Fry, Brian, Marine Biological Laboratory, Woods Hole, MA 02543
Fukui, Yoshio, Department of Cell Biology and Anatomy, Northwestern University Medical School, Chicago, IL 60201
Fulton, Chandler M., Department of Biology, Brandeis University, Waltham, MA 02254
Furshpan, Edwin J., Department of Neurophysiology, Harvard Medical School, Boston, MA 02115
Futrelle, Robert P., College of Computer Science, Northeastern University, 360 Huntington Avenue, Boston, MA 02115

Gabriel, Mordecai, Department of Biology, Brooklyn College, Brooklyn, NY 11210
Gadsby, David C., Laboratory of Cardiac Physiology, The Rockefeller University, 1230 York Avenue, New York, NY 10021
Gainer, Harold, Section of Functional Neurochemistry, NIH, Bldg. 36, Room 4D-20, Bethesda, MD 20892
Galatzer-Levy, Robert M., 180 N. Michigan Avenue, Chicago, IL 60601
Gall, Joseph G., Carnegie Institution, 115 West University Parkway, Baltimore, MD 21210
Gallant, Paul E., NIH, Bldg. 36, Rm. 2A-29, Bethesda, MD 20892
Gascoyne, Peter, Department of Experimental Pathology, Box 85E, University of Texas System Cancer Center, M. D. Anderson Hospital and Tumor Institute, Texas Medical Center, 6723 Bertner Avenue, Houston, TX 77030
Gelperin, Alan, Department of Biophysics, AT&T Bell Labs, Room 1C464, 600 Mountain Avenue, Murray Hill, NJ 07974
German, James L., III, Lab of Human Genetics, The New York Blood Center, 310 East 67th St., New York, NY 10021
Gibbs, Martin, Institute for Photobiology of Cells and Organelles, Brandeis University, Waltham, MA 02254
Giblin, Anne E., Ecosystems Center, Marine Biological Laboratory, Woods Hole, MA 02543
Gibson, A. Jane, Wing Hall, Cornell University, Ithaca, NY 14850
Gifford, Prosser, 540 N Street, SW, S-903, Washington, DC 20024
Gilbert, Daniel L., Laboratory of Biophysics, NIH/NINDS, Bldg. 9, Room IE-124, Bethesda, MD 20892
Giudice, Giovanni, Dipartimento di Biologia Cellulare e Dello Sviluppo, I-90123, Via Archirafi 22, Universita di Palermo, Palermo, Italy
Glusman, Murray, 50 East 72nd Street, New York, NY 10021
Glynn, Paul, Hunter College of CUNY, Department of Biological Sciences, 695 Park Avenue, New York, NY 10021
Golden, William T., Golden Family Foundation, 40 Wall St., Room 4201, New York, NY 10005
Goldman, Robert D., Department of Cell, Molecular and Structural Biology, Northwestern University, 303 E. Chicago Ave., Chicago, IL 60611
Goldsmith, Paul K., NIH, Bldg. 10, Room 9C-101, Bethesda, MD 20892
Goldsmith, Timothy H., Department of Biology, Yale University, New Haven, CT 06510
Goldstein, Moise H., Jr., ECE Department, Barton Hall, Johns Hopkins University, Baltimore, MD 21218
Goodman, Lesley Jean, Department of Biological Sciences, Queen Mary College, Mile End Road, London, E1 4NS, England, UK
Goudsmit, Esther M., Department of Biology, Oakland University, Rochester, MI 48309
Gould, Robert Michael, Institute for Basic Research in Developmental Disabilities, 1050 Forest Hill Rd., Staten Island, NY 10314
Gould, Stephen J., Museum of Comparative Zoology, Harvard University, Cambridge, MA 02138
Govind, C. K., Life Sciences Division, University of Toronto, 1265 Military Trail, West Hill, Ontario, M1C 1A4, Canada
Graf, Werner, Rockefeller University, 1230 York Ave., New York, NY 10021
Grant, Philip, 2939 Van Ness Street, N.W., Apt. 302, Washington, DC 20008
Grass, Albert M., The Grass Foundation, 77 Reservoir Rd., Quincy, MA 02170
Grass, Ellen R., The Grass Foundation, 77 Reservoir Rd., Quincy, MA 02170
Grassle, Judith, Marine Biological Laboratory, Woods Hole, MA 02543
Graubard, Katherine, Department of Zoology, NJ-15, University of Washington, Seattle, WA 98195
Greenberg, Everett Peter, Department of Microbiology, College of Medicine, Iowa City, IA 52242
Greenberg, Michael J., Whitney Laboratory, 9505 Ocean Shore Blvd., St. Augustine, FL 32086

Griffin, Donald R., Concord Field Station, Harvard University, Old Causeway Road, Bedford, MA 01730
Gross, Paul R., Center for Advanced Studies, University of Virginia, 444 Cabell Hall, Charlottesville, VA 22903
Grossman, Albert, New York University Medical Center, 550 First Ave., New York, NY 10016
Grossman, Lawrence, Department of Biochemistry, Johns Hopkins University, 615 North Wolfe Street, Baltimore, MD 21205
Gruner, John, Department of Neurosurgery, New York University Medical Center, 550 First Ave., New York, NY 10016
Gunning, A. Robert, P. O. Box 165, Falmouth, MA 02541
Gwilliam, G. P., Department of Biology, Reed College, Portland, OR 97202

Haimo, Leah, Department of Biology, University of California, Riverside, CA 92521
Hall, Linda M., Department of Biochemistry and Pharmacology, SUNY, 317 Hochstetter, Buffalo, NY 14260
Hall, Zack W., Department of Physiology, University of California, San Francisco, CA 94143
Halvorson, Harlyn O., Marine Biological Laboratory, Woods Hole, MA 02543
Hamlett, Nancy Virginia, Department of Biology, Swarthmore College, Swarthmore, PA 19081
Hanna, Robert B., College of Environmental Science and Forestry, SUNY, Syracuse, NY 13210
Harosi, Ferenc I., Laboratory of Sensory Physiology, Marine Biological Laboratory, Woods Hole, MA 02543
Harrigan, June F., 7415 Makaa Place, Honolulu, HI 96825
Harrington, Glenn W., Division of Cell Biology and Biophysics, 403 Biological Sciences Building, University of Missouri, Kansas City, MO 64110
Harris, Andrew L., Department of Biophysics, Johns Hopkins University, 34th & Charles Sts., Baltimore, MD 21218
Hastings, J. W., The Biological Laboratories, Harvard University, 16 Divinity Street, Cambridge, MA 02138
Hayashi, Teru, 7105 SW 112 Place, Miami, FL 33173
Haydon-Baillie, Wensley G., Porton Int., 2 Lowndes Place, London, SW1X 8DD, England, UK
Hayes, Raymond L., Jr., Department of Anatomy, Howard University, College of Medicine, 520 W St., NW, Washington, DC 20059
Hepler, Peter K., Department of Botany, University of Massachusetts, Amherst, MA 01003
Herndon, Walter R., University of Tennessee, Department of Botany, Knoxville, TN 37996-1100
Hiatt, Howard H., Department of Medicine, Brigham and Women's Hospital, 75 Francis Street, Boston, MA 02115
Highstein, Stephen M., Department of Otolaryngology, Washington University School of Medicine, St. Louis, MO 63110
Hildebrand, John G., Arizona Research Laboratories, Division of Neurobiology, 603 Gould-Simpson Science Building, University of Arizona, Tucson, AZ 85721
Hill, Richard W., Department of Zoology, Michigan State University, E. Lansing, MI 48824
Hill, Susan D., Department of Zoology, Michigan State University, E. Lansing, MI 48824
Hillis-Colinvaux, Llewellya, Department of Zoology, Ohio State University, 1735 Neil Ave., Columbus, OH 43210
Hillman, Peter, Department of Biology, Life Sciences & Neurobiology, Hebrew University, Jerusalem 91904, Israel
Hinegardner, Ralph T., Division of Natural Sciences, University of California, Santa Cruz, CA 95064
Hinsch, Gertrude, W., Department of Biology, University of South Florida, Tampa, FL 33620
Hobbie, John E., Ecosystems Center, Marine Biological Laboratory, Woods Hole, MA 02543
Hodge, Alan J., 3843 Mt. Blackburn Ave., San Diego, CA 92111
Hoffman, Joseph, Department of Physiology, School of Medicine, Yale University, New Haven, CT 06515
Hollyfield, Joe G., Baylor School of Medicine, Texas Medical Center, Houston, TX 77030
Holtzman, Eric, Department of Biological Sciences, Columbia University, New York, NY 10017
Hoskin, Francis C. G., Department of Biology, Illinois Institute of Technology, Chicago, IL 60616
Houghton, Richard A., III, Woods Hole Research Center, P. O. Box 296, Woods Hole, MA 02543
Hoy, Ronald R., Section of Neurobiology and Behavior, Cornell University, Ithaca, NY 14853
Hufnagel, Linda A., Department of Microbiology, University of Rhode Island, Kingston, RI 02881
Hummon, William D., Department of Zoology, Ohio University, Athens, OH 45701
Humphreys, Susie H., Research & Development, Kraft, Inc., 801 Waukegan Rd., Glenview, IL 60025
Humphreys, Tom D., University of Hawaii, PBRC, 41 Ahui St., Honolulu, HI 96813
Hunter, Robert D., Department of Biological Sciences, Oakland University, Rochester, MI 48309-4401
Hunter, W. Bruce, Box 321, Lincoln Center, MA 01773
Hurwitz, Charles, Basic Science Research Lab, Veterans Administration Hospital, Albany, NY 12208
Hurwitz, Jerard, Sloan Kettering Institute for Cancer Research, 1275 York Avenue, New York, NY 11021
Huxley, Hugh E., Department of Biology, Rosenstiel Center, Brandeis University, Waltham, MA 02154
Hynes, Thomas J., Jr., Meredith and Grew, Inc., 160 Federal Street, Boston, MA 02110-1701

Ilan, Joseph, Department of Developmental Genetics and Anatomy, Case Western Reserve University School of Medicine, Cleveland, OH 44106
Ingoglia, Nicholas, Department of Physiology, New Jersey Medical School, 100 Bergen St., Newark, NJ 07103
Inoué, Saduyki, Department of Anatomy, McGill University Cancer Centre, 3640 University St., Montreal, PQ, H3A 2B2, Canada
Inoué, Shinya, Marine Biological Laboratory, Woods Hole, MA 02543
Isselbacher, Kurt J., Massachusetts General Hospital, 32 Fruit Street, Boston, MA 02114
Issidorides, Marietta, R., Department of Psychiatry, University of Athens, Monis Petraki 8, Athens, 140 Greece
Izzard, Colin S., Department of Biological Sciences, SUNY, 1400 Washington Ave., Albany, NY 12222

Jacobs, Neil, Hale & Dorr, 60 State St., Boston, MA 02019
Jacobson, Antone G., Department of Zoology, University of Texas, Austin, TX 78712
Jaffe, Lionel, Marine Biological Laboratory, Woods Hole, MA 02543
Jannasch, Holger W., Department of Biology, Woods Hole Oceanographic Institution, Woods Hole, MA 02543
Jeffery, William R., Bodega Marine Laboratory, Box 247, Bodega Bay, CA 94923
Jones, Meredith L., Division of Worms, Museum of Natural History, Smithsonian Institution, Washington, DC 20560
Josephson, Robert K., Department of Biological Sciences, University of California, Irvine, CA 92717

Kabat, E. A., Department of Microbiology, College of Physicians and Surgeons, Columbia University, 630 West 168th St., New York, NY 10032
Kaley, Gabor, Department of Physiology, Basic Sciences Building, New York Medical College, Valhalla, NY 10595
Kaltenbach, Jane, Department of Biological Sciences, Mount Holyoke College, South Hadley, MA 01075
Kaminer, Benjamin, Department of Physiology, School of Medicine, Boston University, 80 East Concord St., Boston, MA 02118
Kane, Robert E., PBRC, University of Hawaii, 41 Ahui St., Honolulu, HI 96813
Kaneshiro, Edna S., Department of Biological Sciences, University of Cincinnati, Cincinnati, OH 45221
Kao, Chien-yuan, Department of Pharmacology, Box 29, SUNY, Downstate Medical Center, 450 Clarkson Avenue, Brooklyn, NY 11203
Kaplan, Ehud, Department of Biophysics, The Rockefeller University, 1230 York Ave., New York, NY 10024
Karakashian, Stephen J., Apt. 16-F, 165 West 91st St., New York, NY 10024
Karlin, Arthur, Department of Biochemistry and Neurology, Columbia University, 630 West 168th St., New York, NY 10032
Katz, George M., Fundamental and Experimental Research Labs, Merck Sharp and Dohme, P. O. Box 2000, Rahway, NJ 07065
Kelly, Robert E., Department of Anatomy, College of Medicine, University of Illinois, P. O. Box 6998, Chicago, IL 60680
Kemp, Norman E., Department of Biology, University of Michigan, Ann Arbor, MI 48109
Kendall, John P., Faneuil Hall Associates, 176 Federal Street, 2nd Floor, Boston, MA 02110
Kendall, Richard E., Commissioner of Environmental Management, 100 Cambridge Street, Room 1905, Boston, MA 02202
Kerr, Louis M., Marine Biological Laboratory, Woods Hole, MA 02543
Keynan, Alexander, Hebrew University, Jerusalem, Israel
Kiehart, Daniel P., Department of Cellular and Developmental Biology, Harvard University, 16 Divinity Street, Cambridge, MA 02138
Kirk, Mark D., Division of Biological Sciences, University of Missouri, Columbia, MO 65211
Klein, Morton, Department of Microbiology, Temple University Medical School, Philadelphia, PA 19103
Klotz, Irving M., Department of Chemistry, Northwestern University, Evanston, IL 60201
Knudson, Robert A., Marine Biological Laboratory, Woods Hole, MA 02543
Koide, Samuel S., Population Council, The Rockefeller University, 1230 York Avenue, New York, NY 10021
Kornberg, Sir Hans, The Master's Lodge, Christ's College, Cambridge CB2 3BU, England, UK
Kosower, Edward M., Ramat-Aviv, Tel Aviv, 69978 Israel
Krahl, M. E., 2783 W. Casas Circle, Tucson, AZ 85741
Krane, Stephen M., Arthritis Unit, Massachusetts General Hospital, Fruit Street, Boston, MA 02114
Krauss, Robert, FASEB, 9650 Rockville Pike, Bethesda, MD 20814
Kravitz, Edward A., Department of Neurobiology, Harvard Medical School, 220 Longwood Ave., Boston, MA 02115
Kriebel, Mahlon E., Department of Physiology, SUNY Health Science Center, Syracuse, NY 13210
Kristan, William B., Jr., Department of Biology B-022, University of California San Diego, La Jolla, CA 92093
Kropinski, Andrew M. B., Department of Microbiology/Immunology, Queen's University, Kingston, Ontario K7L 3N6, Canada
Kuhns, William J., Hospital for Sick Children, Department of Biochemistry Research, Toronto, Ontario M5G 1X8, Canada
Kuhtreiber, Willem M., Marine Biological Laboratory, Woods Hole, MA 02543
Kusano, Kiyoshi, NIH, Bldg. 36, Room 4D-20, Bethesda, MD 20892
Kuzirian, Alan M., Marine Biological Laboratory, Woods Hole, MA 02543

Laderman, Aimlee, Yale University, New Haven, CT 06520
LaMarche, Paul H., Eastern Maine Medical Center, 489 State St., Bangor, ME 04401
Landis, Dennis M. D., Department of Developmental Genetics and Anatomy, Case Western Reserve University School of Medicine, Cleveland, OH 44106
Landowne, David, Department of Physiology, P. O. Box 016430, University of Miami School of Medicine, Miami, FL 33101
Langford, George M., Department of Physiology, CB7545 University of North Carolina School of Medicine, Chapel Hill, NC 27599-7545
Laster, Leonard, University of Massachusetts Medical School, 55 Lake Avenue, North, Worcester, MA 01655
Laufer, Hans, Department of Biological Science, Molecular and Cell Biology, Group U-125, University of Connecticut, Storrs, CT 06268
Lazarow, Paul B., Department of Cell Biology and Anatomy, Mount Sinai Medical School, Box 1007, 5th Avenue & 100th Street, New York, NY 10021
Lazarus, Maurice, Federated Department Stores, Inc., Sears Cresent, City Hall Plaza, Boston, MA 02108
Leadbetter, Edward R., Department of Molecular and Cell Biology, U-131, University of Connecticut, Storrs, CT 06268
Lederberg, Joshua, The Rockefeller University, 1230 York Ave., New York, NY 10021
Lee, John J., Department of Biology, City College of CUNY, Convent Ave. and 138th St., New York, NY 10031
Lehy, Donald B., Marine Biological Laboratory, Woods Hole, MA 02543
Leibovitz, Louis, 3 Kettle Hole Road, Woods Hole, MA 02543
Leighton, Joseph, 2324 Lakeshore Avenue, #2, Oakland, CA 94606
Leighton, Stephen, NIH, Bldg. 13 3W13, Bethesda, MD 20892
Leinwand, Leslie Ann, Department of Microbiology and Immunology, Albert Einstein College of Medicine, 1300 Morris Park Ave., Bronx, NY 10461
Lerman, Sidney, Eye Research Lab, Room 41, New York Medical College, 100 Grasslands Ave., Valhalla, NY 10595
Lerner, Aaron B., Yale University, School of Medicine, New Haven, CT 06510
Lester, Henry A., 156-29 California Institute of Technology, 156-29, Pasadena, CA 91125
Levin, Jack, Veterans Administration Medical Center, 113A, 4150 Clement St., San Francisco, CA 94121
Levinthal, Cyrus, Department of Biological Sciences, Columbia University, Broadway and 116th Street, New York, NY 10026 (deceased)
Levitan, Herbert, Department of Zoology, University of Maryland, College Park, MD 20742
Levitan, Irwin B., Department of Biochemistry, Brandeis University, Waltham, MA 02254
Linck, Richard W., Department of Anatomy, Jackson Hall, University of Minnesota, 321 Church Street, S. E., Minneapolis, MN 55455
Lipicky, Raymond J., Department of Cardio-Renal/Drug Prod. Div., FDA, Rm. 16B-45, 5600 Fishers Lane, Rockville, MD 20857
Lisman, John E., Department of Biology, Brandeis University, Waltham, MA 02254
Liuzzi, Anthony, 55 Fay Rd., Box 184, Woods Hole, MA 02543

Llinas, Rodolfo R., Department of Physiology and Biophysics, New York University Medical Center, 550 First Ave., New York, NY 10016
Loew, Franklin M., Tufts University School of Veterinary Medicine, 200 Westboro Rd., N. Grafton, MA 01536
Loewenstein, Birgit R., Department of Physiology and Biophysics, R-430, University of Miami School of Medicine, Miami, FL 33101
Loewenstein, Werner R., Department of Physiology and Biophysics, University of Miami, P. O. Box 016430, Miami, FL 33101
London, Irving M., Massachusetts Institute of Technology, E-25-551, Cambridge, MA 02139
Longo, Frank J., Department of Anatomy, University of Iowa, Iowa City, IA 52442
Lorand, Laszlo, Department of Biochemistry and Molecular Biology, Northwestern University, 2153 Sheridan Road, Evanston, IL 60208
Luckenbill-Edds, Louise, 155 Columbia Ave., Athens, OH 45701
Luria, Salvador E., 48 Peacock Farm Rd., Lexington, MA 02173 (deceased)

Macagno, Eduardo R., 1003B Fairchild, Department of Biosciences, Columbia University, New York, NY 10027
MacNichol, E. F., Jr., Department of Physiology, Boston University School of Medicine, 80 E. Concord St., Boston, MA 02118
Maglott-Duffield, Donna R., American Type Culture Collection, 12301 Parklawn Drive, Rockville, MD 20852-1776
Maienschein, Jane Ann, Department of Philosophy, Arizona State University, Tempe, AZ 85287-2004
Mainer, Robert, The Boston Company, One Boston Place, OBP-15-D, Boston, MA 02168
Malbon, Craig Curtis, Department of Pharmacology, Health Sciences Center, SUNY, Stony Brook, NY 11794-8651
Manalis, Richard S., Department of Biological Sciences, Indiana University—Purdue University at Fort Wayne, 2101 Coliseum Blvd., E. Fort Wayne, IN 46805
Mangum, Charlotte P., Department of Biology, College of William and Mary, Williamsburg, VA 23185
Manz, Robert D., Helmer and Associates, Suite 1310, 950 Winter St., Walthan, MA 02154
Margulis, Lynn, Botany Department, University of Massachusetts, Morrill Science Center, Amherst, MA 01003
Marinucci, Andrew C., 102 Nancy Drive, Mercerville, NJ 08619
Marsh, Julian B., Department of Biochemistry and Physiology, Medical College of Pennsylvania, 3300 Henry Ave., Philadelphia, PA 19129
Martin, Lowell V., Marine Biological Laboratory, Woods Hole, MA 02543
Martinez-Palomo, Adolfo, Seccion de Patologia Experimental, Cinvesav-ipn, 07000 Mexico, D.F. A.P., 140740, Mexico
Maser, Morton, Woods Hole Education Assoc., P. O. Box EM, Woods Hole, MA 02543
Mastroianni, Luigi, Jr., Department of Obstetrics and Gynecology, Hospital of the University of Pennsylvania, 106 Dulles, 3400 Spruce Street, Philadelphia, PA 19104-4283
Matteson, Donald R., Department of Biophysics, University of Maryland School of Medicine, 660 Redwood Street, Baltimore, MD 21201
Mautner, Henry G., Department of Biochemistry, Tufts University School of Medicine, 136 Harrison Ave., Boston, MA 02111
Mauzerall, David, The Rockefeller University, 1230 York Ave., New York, NY 10021
McCann, Frances, Department of Physiology, Dartmouth Medical School, Hanover, NH 03755
McLaughlin, Jane A., Marine Biological Laboratory, Woods Hole, MA 02543
McMahon, Robert F., Department of Biology, Box 19498, University of Texas, Arlington, TX 76019
Meedel, Thomas, Marine Biological Laboratory, Woods Hole, MA 02543
Meinertzhagen, Ian A., Department of Psychology, Life Sciences Center, Dalhousie University, Halifax, Nova Scotia B3H 4J1, Canada
Meiss, Dennis E., 462 Soland Avenue, Hayward, CA 94541
Melillo, Jerry A., Ecosystems Center, Marine Biological Laboratory, Woods Hole, MA 02543
Mellon, DeForest, Jr., Department of Biology, Gilmer Hall, University of Virginia, Charlottesville, VA 22903
Mellon, Richard P., P. O. Box 187, Laughlintown, PA 15655
Metuzals, Janis, Department of Pathology, University of Ottawa, Ottawa, Ontario, K1H 8M5 Canada
Metz, Charles B., 7220 SW 124th St., Miami, FL 33156
Milkman, Roger, Department of Biology, University of Iowa, Iowa City, IA 52242
Mills, Robert, 10315 44th Avenue, W 12 H Street, Bradenton, FL 33507-1535
Mitchell, Ralph, DAS, Harvard University, 29 Oxford Street, Cambridge, MA 02138
Miyamoto, David M., Department of Biology, Drew University, Madison, NJ 07940
Mizell, Merle, Laboratory of Tumor Cell Biology, Tulane University, New Orleans, LA 70118
Moore, John W., Department of Neurobiology, Box 3209, Duke University Medical Center, Durham, NC 27710
Moore, Lee E., Department of Physiology and Biophysics, University of Texas Medical Branch, Galveston, TX 77550
Morin, James G., Department of Biology, University of California, Los Angeles, CA 90024
Morrell, Frank, Department of Neurological Science, Rush Medical Center, 1753 W. Congress Parkway, Chicago, IL 60612
Morse, M. Patricia, Marine Science Center, Northeastern University, Nahant, MA 01908
Morse, Robert W., Box 574, N. Falmouth, MA 02556
Morse, Stephen Scott, The Rockefeller University, 1230 York Ave., Box 2, New York, NY 10021-6399
Mote, Michael I., Department of Biology, Temple University, Philadelphia, PA 19122
Mountain, Isabel, Vinson Hall #112, 6251 Old Dominion Drive, McLean, VA 22101
Muller, Kenneth J., Department of Physiology and Biophysics, University of Miami School of Medicine, Miami, FL 33101
Murray, Sandra Ann, Department of Neurology, Anatomy and Cell Science, University of Pittsburgh School of Medicine, Pittsburgh, PA 15261
Musacchia, Xavier J., Department of Physiology and Biophysics, University of Louisville School of Medicine, Louisville, KY 40292

Nabrit, S. M., 686 Beckwith St., SW, Atlanta, GA 30314
Nadelhoffer, Knute, Marine Biological Laboratory, Woods Hole, MA 02543
Naka, Ken-ichi, 2-9-2 Tatsumi Higashi, Okazaki, Japan 444
Nakajima, Shigehiro, Department of Pharmacology and Cell Biology, University of Illinois College of Medicine at Chicago, 808 S. Wolcott Street, Chicago, IL 60612
Nakajima, Yasuko, Department of Anatomy and Cell Biology, University of Illinois College of Medicine at Chicago, M/C 512, Chicago, IL 60612
Narahashi, Toshio, Department of Pharmacology, Northwestern University Medical School, 303 East Chicago Ave., Chicago, IL 60611

Nasatir, Maimon, Department of Biology, University of Toledo, Toledo, OH 43606

Nelson, Leonard, Department of Physiology, CS10008, Medical College of Ohio, Toledo, OH 43699

Nelson, Margaret C., Section of Neurobiology and Behavior, Cornell University, Ithaca, NY 14850

Nicholls, John G., Biocenter, Klingelbergstrasse 70, Basel 4056, Switzerland

Nickerson, Peter A., Department of Pathology, SUNY, Buffalo, NY 14214

Nicosia, Santo V., Department of Pathology, University of South Florida, College of Medicine, Box 11, 12901 North 30th St., Tampa, FL 33612

Noe, Bryan D., Department of Anatomy and Cell Biology, Emory University School of Medicine, Atlanta, GA 30322

Northcutt, R. Glenn, Department of Neuroscience, A-001, Scripps Institution of Oceanography, La Jolla, CA 92093-0201

Norton, Catherine N., Marine Biological Laboratory, Woods Hole, MA 02543

Obaid, Ana Lia, Department of Physiology and Pharmacy, University of Pennsylvania School of Medicine, B-400 Richards Bldg., Philadelphia, PA 19104-6085

Oertel, Donata, Department of Neurophysiology, University of Wisconsin, 281 Medical Science Bldg., Madison, WI 53706

O'Herron, Jonathan, 45 Swifts Lane, Darien, CT 06820

Ohki, Shinpei, Department of Biophysical Sciences, SUNY at Buffalo, 224 Cary Hall, Buffalo, NY 14214

Olins, Ada L., University of Tennessee-Oak Ridge, Graduate School of Biomedical Sciences, Biology Division ORNL, P. O. Box 2009, Oak Ridge, TN 37831-8077

Olins, Donald E., University of Tennessee-Oak Ridge, Graduate School of Biomedical Sciences, Biology Division ORNL, P. O. Box 2009, Oak Ridge, TN 37831-8077

O'Melia, Anne F., 16 Evergreen Lane, Chappaqua, New York 10514

Oschman, James L., 31 Whittier Street, Dover, NH 03820

Palazzo, Robert E., Marine Biological Laboratory, Woods Hole, MA 02543

Palmer, John D., Department of Zoology, University of Massachusetts, Amherst, MA 01002

Palti, Yoram, Rappaport Institution, Technion, POB 9697, Haifa, 31096 Israel

Pant, Harish C., NINCDS/NIH, Laboratory of Neurochemistry, Bldg. 36, Room 4D-20, Bethesda, MD 20892

Pappas, George D., Department of Anatomy, College of Medicine, University of Illinois, 808 South Wolcott St., Chicago, IL 60612

Pardee, Arthur B., Department of Pharmacology, Harvard Medical School, Boston, MA 02115

Pardy, Roosevelt L., School of Life Sciences, University of Nebraska, Lincoln, NE 68588

Parmentier, James L., Becton Dickinson Research Center, P. O. Box 12016, Research Triangle Park, NC 27709

Passano, Leonard M., Department of Zoology, Birge Hall, University of Wisconsin, Madison, WI 53706

Pearlman, Alan L., Department of Physiology, School of Medicine, Washington University, St. Louis, MO 63110

Pederson, Thoru, Worcester Foundation for Experimental Biology, Shrewsbury, MA 01545

Perkins, C. D., 400 Hilltop Terrace, Alexandria, VA 22301

Person, Philip, Research Testing Labs, Inc., 167 E. 2nd St., Huntington Station, NY 11746

Peterson, Bruce J., Ecosystems Center, Marine Biological Laboratory, Woods Hole, MA 02543

Pethig, Ronald, School of Electronic Engineering Science, University College of N. Wales, Dean St., Bangor, Gwynedd, LL57 1UT, UK

Pfohl, Ronald J., Department of Zoology, Miami University, Oxford, OH 45056

Pierce, Robert W., 4851 Shore Lane, P. O. Box 1404, Boca Grande, FL 33921

Pierce, Sidney K., Jr., Department of Zoology, University of Maryland, College Park, MD 20742

Poindexter, Jeanne S., Science Division, Long Island University, Brooklyn Campus, Brooklyn, NY 11201

Pollard, Harvey B., NIH, NIDDKD, Bldg. 8, Rm. 401, Bethesda, MD 20892

Pollard, Thomas D., Department of Cell Biology and Anatomy, Johns Hopkins University, 725 North Wolfe St., Baltimore, MD 21205

Poole, Alan F., P. O. Box 533, Woods Hole, MA 02543

Porter, Beverly H., 13617 Glenoble Drive, Rockville, MD 20853

Porter, Keith R., Department of Biology, Leidy Laboratories, Rm. 303, University of Pennsylvania, Philadelphia, PA 19104-6018

Porter, Mary E., Department of Cell Biology and Neurology, University of Minnesota, 4-147 Jackson Hall, Minneapolis, MN 55455

Potter, David, Department of Neurobiology, Harvard Medical School, Longwood Avenue, Boston, MA 02115

Potts, William T., Department of Biology, University of Lancaster, Lancaster, England, UK

Powers, Maureen K., Department of Psychology, Vanderbilt University, Nashville, TN 37240

Pratt, Melanie M., Department of Anatomy and Cell Biology, University of Miami School of Medicine (R124), P. O. Box 016960, Miami, FL 33101

Prendergast, Robert A., Wilmer Institute, Johns Hopkins Hospital, 601 N. Broadway, Baltimore, MD 21205

Presley, Phillip H., Carl Zeiss, Inc., 1 Zeiss Drive, Thornwood, NY 10594

Price, Carl A., Waksman Institute of Microbiology, Rutgers University, P. O. Box 759, Piscataway, NJ 08854

Prior, David J., Department of Biological Sciences, NAU Box 5640, Northern Arizona University, Flagstaff, AZ 86011

Prusch, Robert D., Department of Life Sciences, Gonzaga University, Spokane, WA 99258

Purves, Dale, Department of Neurobiology, Duke University Medical School, Box 3209, Durham, NC 27710

Quigley, James, Department of Pathology, SUNY Health Science Center, BHS Tower 9, Rm. 140, Stony Brook, NY 11794

Rabb, Irving W., 1010 Memorial Drive, Cambridge, MA 02138

Rabin, Harvey, DuPont Co., CRD, Exp. Station 328/358, Wilmington, DE 19880

Rabinowitz, Michael B., Marine Biological Laboratory, Woods Hole, MA 02543

Rafferty, Nancy S., Department of Anatomy, Northwestern University Medical School, 303 E. Chicago Avenue, Chicago, IL 60611

Rakowski, Robert F., Department of Physiology and Biophysics, UHS/The Chicago Medical School, 3333 Greenbay Rd., N. Chicago, IL 60064

Ramon, Fidel, Dept. de Fisiologia y Biofisca, Centro de Investigacion y de Estudius Avanzados del ipn, Apurtado Postal 14-740, D.F. 07000, Mexico

Rabh, Irving W., 1010 Memorial Drive, Cambridge, MA 02138

Rabin, Harvey, DuPont Co., CRD, Exp. Station 328/358, Wilmington, DE 19880

Rabinowitz, Michael B., Marine Biological Laboratory, Woods Hole, MA 02543

Rafferty, Nancy S., Department of Anatomy, Northwestern University Medical School, 303 E. Chicago Avenue, Chicago, IL 60611

Rakowski, Robert F., Department of Physiology and Biophysics, UHS/The Chicago Medical School, 3333 Greenbay Rd., N. Chicago, IL 60064

Ramon, Fidel, Dept. de Fisiologia y Biofisca, Centro de Investigacion y de Estudius Avanzados del ipn, Apurtado Postal 14-740, D.F. 07000, Mexico

Ranzi, Silvio, Sez Zoologia Sc Nat, Via Coloria 26, 120133, Milano, Italy

Rastetter, Edward B., Ecosystems Center, Marine Biological Laboratory, Woods Hole, MA 02543

Ratner, Sarah, Department of Biochemistry, Public Health Research Institute, 455 First Ave., New York, NY 10016

Rebhun, Lionel I., Department of Biology, Gilmer Hall, University of Virginia, Charlottesville, VA 22901

Reddan, John R., Department of Biological Sciences, Oakland University, Rochester, MI 48309-4401

Reese, Barbara F., NINCDS/NIH, Bldg. 36, Room 3B26, 9000 Rockville Pike, Bethesda, MD 20892

Reese, Thomas S., NINCDS/NIH, Bldg. 36, Room 2A27, 9000 Rockville Pike, Bethesda, MD 20892

Reiner, John M., 111 Emerson St., Apt. 623, Denver, CO 80218

Reinisch, Carol L., Tufts University School of Veterinary Medicine, 136 Harrison Avenue, Boston, MA 02111

Reynolds, George T., Department of Physics, Jadwin Hall, Princeton University, Princeton, NJ 08544

Rice, Robert V., 30 Burnham Dr., Falmouth, MA 02540

Rich, Alexander, Department of Biology, Massachusetts Institute of Technology, Cambridge, MA 02139

Rickles, Frederick R., Department of Medicine, Division of Hematology-Oncology, University of Connecticut Health Center, Farmington, CT 06032

Ripps, Harris, Department of Ophthalmology, University of Illinois College of Medicine, 1855 W. Taylor Street, Chicago, IL 60611

Robinson, Denis M., 200 Ocean Lane Drive #908, Key Biscayne, FL 33149

Rosenbaum, Joel L., Department of Biology, Kline Biology Tower, Yale University, New Haven, CT 06520

Rosenberg, Philip, School of Pharmacy, Division of Pharmacology, University of Connecticut, Storrs, CT 06268

Rosenbluth, Jack, Department of Physiology, New York University School of Medicine, 550 First Ave., New York, NY 10016

Rosenbluth, Raja, Department of Biological Sciences, Simon Fraser University, Burnaby, BC, V5A 1S6, Canada

Roslansky, John, Box 208, Woods Hole, MA 02543

Roslansky, Priscilla F., Box 208, Woods Hole, MA 02543

Ross, William N., Department of Physiology, New York Medical College, Valhalla, NY 10595

Roth, Jay S., 18 Millfield Street, P. O. Box 285, Woods Hole, MA 02543

Rowland, Lewis P., Neurological Institute, 710 West 168th St., New York, NY 10032

Ruderman, Joan V., Department of Anatomy and Cell Biology, Harvard University School of Medicine, Boston, MA 02115

Rushforth, Norman B., Department of Biology, Case Western Reserve University, Cleveland, OH 44106

Russell-Hunter, W. D., Department of Biology, Lyman Hall 012, Syracuse University, Syracuse, NY 13244

Saffo, Mary Beth, Institute of Marine Sciences, 272 Applied Sciences, University of California, Santa Cruz, CA 95064

Sager, Ruth, Dana Farber Cancer Institute, 44 Binney St., Boston, MA 02115

Salama, Guy, Department of Physiology, University of Pittsburgh, Pittsburgh, PA 15261

Salmon, Edward D., Department of Biology, Wilson Hall, CB3280, University of North Carolina, Chapel Hill, NC 27599

Salzberg, Brian M., Department of Physiology, University of Pennsylvania, B-400 Richards Bldg., Philadelphia, PA 19104-6085

Sanborn, Richard C., 11 Oak Ridge Road, Teaticket, MA 02536

Sanger, Jean M., Department of Anatomy, School of Medicine, University of Pennsylvania, 36th and Hamilton Walk, Philadelphia, PA 19174

Sanger, Joseph, Department of Anatomy, School of Medicine, University of Pennsylvania, 36th and Hamilton Walk, Philadelphia, PA 19174

Sato, Hidemi, Faculty of Social Science, Nagano University, Shiminogo, Ueda, Nagano 386-12, Japan

Sattelle, David B., AFRC Unit-Department of Zoology, University of Cambridge, Downing St., Cambridge CB2 3EJ, England, UK

Saunders, John W., Jr., P. O. Box 381, Waquoit Station, Waquoit, MA 02536

Saz, Arthur K., Department of Immunology, Georgetown University Medical School, Washington, DC 20007

Schachman, Howard K., Department of Molecular Biology, University of California, Berkeley, CA 94720

Schatten, Gerald P., Integrated Microscopy Facility for Biomedical Research, University of Wisconsin, 1117 W. Johnson St., Madison, WI 53706

Schatten, Heide, Department of Zoology, University of Wisconsin, Madison, WI 53706

Schiff, Jerome A., Institute for Photobiology of Cells and Organelles, Brandeis University, Waltham, MA 02254

Schmeer, Arline C., Mercenene Cancer Research Institute, Hospital of Saint Raphael, New Haven, CT 06511

Schmidek, Henry H., Henry Ford Neurosurgical Institute, Henry Ford Hospital, Detroit, MI 48202

Schnapp, Bruce J., Department of Physiology, Boston University Medical School, 80 East Concord Street, Boston, MA 02118

Schneider, E. Gayle, Department of Obstetrics and Gynecology, Yale University School of Medicine, 333 Cedar St., New Haven, CT 06510

Schneiderman, Howard A., Monsanto Company, 800 North Lindbergh Blvd., D1W, St. Louis, MO 63166 (deceased)

Schuel, Herbert, Department of Anatomical Sciences, SUNY, Buffalo, Buffalo, NY 14214

Schuetz, Allen W., School of Hygiene and Public Health, Johns Hopkins University, Baltimore, MD 21205

Schwartz, James H., Center for Neurobiology and Behavior, New York State Psychiatric Institute—Research Annex, 722 W. 168th St., 7th Floor, New York, NY 10032

Scofield, Virginia Lee, Department of Microbiology and Immunology, UCLA School of Medicine, Los Angeles, CA 90024

Scott, Allan C., 1 Nudd St., Waterville, ME 04901

Sears, Mary, P. O. Box 152, Woods Hole, MA 02543

Segal, Sheldon J., Population Division, The Rockefeller Foundation, 1133 Avenue of the Americas, New York, NY 10036

Selman, Kelly, Department of Anatomy, College of Medicine, University of Florida, Gainesville, FL 32601

Shanklin, Douglas R., Department of Pathology, Room 584, University of Tennessee College of Medicine, 800 Madison Avenue, Memphis, TN 38163

Shapiro, Herbert, 6025 North 13th St., Philadelphia, PA 19141

Shaver, Gaius R., Ecosystems Center, Marine Biological Laboratory, Woods Hole, MA 02543

Shaver, John R., 18 Las Parras, Cayey, PR 00633

Sheetz, Michael P., Department of Cell Biology and Physiology, Washington University Medical School, 606 S. Euclid Ave., St. Louis, MO 63110

Shepard, David C., P. O. Box 44, Woods Hole, MA 02543

Shepro, David, Department of Microvascular Research, Boston University, 5 Cummington St., Boston, MA 02215

Sher, F. Alan, Immunology and Cell Biology Section, NIAID/NIH, Laboratory of Parasitic Disease, Building 5, Room 114, Bethesda, MD 20892

Sheridan, William F., Biology Department, University of North Dakota, Box 8238, University Station, Grand Forks, ND 58202-8238

Sherman, I. W., Department of Biology, University of California, Riverside, CA 92521

Shimomura, Osamu, Marine Biological Laboratory, Woods Hole, MA 02543

Siegel, Irwin M., Department of Ophthalmology, New York University Medical Center, 550 First Avenue, New York, NY 10016

Siegelman, Harold W., Department of Biology, Brookhaven National Laboratory, Upton, NY 11973

Silver, Robert B., Department of Physiology, Cornell University, 822 Veterinary Research Tower, Ithaca, NY 14853-6401

Sjodin, Raymond A., Department of Biophysics, University of Maryland, Baltimore, MD 21201

Skinner, Dorothy M., Oak Ridge National Laboratory, P. O. Box 2009, Biology Division, Oak Ridge, TN 37831

Sloboda, Roger D., Department of Biological Sciences, Dartmouth College, Hanover, NH 03755

Sluder, Greenfield, Worcester Foundation for Experimental Biology, 222 Maple Ave., Shrewsbury, MA 01545

Smith, Michael A., Jl Sinabung, Buntu #7, Semarang, Java, Indonesia

Smith, Ralph I., Department of Zoology, University of California, Berkeley, CA 94720

Sogin, Mitchell, Marine Biological Laboratory, Woods Hole, MA 02543

Sorenson, Martha M., Depto de Bioquimica-RFRJ, Centro de Ciencias da Saude-I. C. B., Cidade Universitaria-Fundad, Rio de Janeiro, Brasil 21.910

Speck, William T., Department of Pediatrics, Case Western Reserve University, Cleveland, OH 44106

Spector, Abraham, College of Physicians and Surgeons, Columbia University, 630 West 168th Street, New York, NY 10032

Speer, John W., Marine Biological Laboratory, Woods Hole, MA 02543

Sperelakis, Nicholas, Department of Physiology & Biophysics, University of Cincinnati, Cincinnati, OH 45267-0576

Spiegel, Evelyn, Department of Biological Sciences, Dartmouth College, Hanover, NH 03755

Spiegel, Melvin, Department of Biological Sciences, Dartmouth College, Hanover, NH 03755

Spray, David C., Albert Einstein College of Medicine, Department of Neurosciences, 1300 Morris Park Avenue, Bronx, NY 10461

Steele, John Hyslop, Woods Hole Oceanographic Institution, Woods Hole, MA 02543

Steinacker, Antoinette, Dept. of Otolaryngology, Washington University, School of Medicine, Box 8115, 4566 Scott Avenue, St. Louis, MO 63110

Steinberg, Malcolm, Department of Biology, Princeton University, Princeton, NJ 08540

Stephens, Grover C., Department of Ecol. and Evol. Biology, School of Biological Sciences, University of California, Irvine, CA 92717

Stephens, Raymond E., Marine Biological Laboratory, Woods Hole, MA 02543

Stetten, DeWitt, Jr., NIH, Bldg. 16, Room 118, Bethesda, MD 20892 (deceased)

Stetten, Jane Lazarow, 4701 Willard Ave., Chevy Chase, MD 20815

Steudler, Paul A., Ecosystems Center, Marine Biological Laboratory, Woods Hole, MA 02543

Stokes, Darrell R., Department of Biology, Emory University, Atlanta, GA 30322

Stommel, Elijah W., Marine Biological Laboratory, Woods Hole, MA 02543

Stracher, Alfred, Department of Biochemistry, SUNY Health Science Center, 450 Clarkson Ave., Brooklyn, NY 11203

Strehler, Bernard L., 2235 25th St., #217, San Pedro, CA 90732

Strickler, J. Rudi, Center for Great Lakes Studies, 600 East Greenfield Ave., Milwaukee, WI 53204

Strumwasser, Felix, Marine Biological Laboratory, Woods Hole, MA 02543

Stuart, Ann E., Department of Physiology, Medical Sciences Research Wing 206H, University of North Carolina, Chapel Hill, NC 27599-7545

Sugimori, Mutsuyuki, Department of Physiology and Biophysics, New York University Medical Center, 550 First Avenue, New York, NY 10016

Summers, William C., Huxley College of Environmental Studies, Western Washington University, Bellingham, WA 98225

Suprenant, Kathy A., Department of Physiology and Cell Biology, 4010 Haworth Hall, University of Kansas, Lawrence, KS 66045

Sussman, Maurice, 72 Carey Lane, Falmouth, MA 02540

Sussman, Raquel B., Marine Biological Laboratory, Woods Hole, MA 02543

Sweet, Frederick, Box 8064, Washington University School of Medicine, 499 South Euclid, St. Louis, MO 63110

Sydlik, Mary Anne, Department of Biology, Eastern Michigan University, Ypsilanti, MI 48197

Szent-Gyorgyi, Andrew, Department of Biology, Brandeis University, Bassine 244, 415 South Street, Waltham, MA 02254

Szuts, Ete Z., Laboratory of Sensory Physiology, Marine Biological Laboratory, Woods Hole, MA 02543

Tabares, Lucia, AVDA, Department of Physiology, Sanchez, Pizjuan 4, 411009 Seville, Spain

Tamm, Sidney L., Boston University Marine Program, Marine Biological Laboratory, Woods Hole, MA 02543

Tanzer, Marvin L., Department of Oral Biology, Medical School, University of Connecticut, Farmington, CT 06032

Tasaki, Ichiji, Laboratory of Neurobiology, NIMH/NIH, Bldg. 36, Rm. 2B-16, Bethesda, MD 20892

Taylor, Douglass L., Center for Fluorescence Research, Carnegie Mellon University, 440 Fifth Avenue, Pittsburgh, PA 15213

Teal, John M., Department of Biology, Woods Hole Oceanographic Institution, Woods Hole, MA 02543

Telfer, William H., Department of Biology, University of Pennsylvania, Philadelphia, PA 19104

Telzer, Bruce, Department of Biology, Pomona College, Claremont, CA 91711

Thorndike, W. Nicholas, Wellington Management Company, 28 State St., Boston, MA 02109

Trager, William, Rockefeller University, 1230 York Ave., New York, NY 10021

Travis, D. M., Veterans Administration Medical Center, 2101 Elm Street, Fargo, ND 58102

Treistman, Steven N., Worcester Foundation for Experimental Biology, 222 Maple Avenue, Shrewsbury, MA 01545

Trigg, D. Thomas, 125 Grove St., Wellesley, MA 02181

Trinkaus, J. Philip, Department of Biology, Box 6666, Yale University, New Haven, CT 06511

Troll, Walter, Department of Environmental Medicine, College of Medicine, New York University, New York, NY 10016

Troxler, Robert F., Department of Biochemistry, School of Medicine, Boston University, 80 East Concord St., Boston, MA 02118

Tucker, Edward B., Department of Natural Sciences, Baruch College, CUNY, 17 Lexington Ave., New York, NY 10010

Turner, Ruth D., Mollusk Department, Museum of Comparative Zoology, Harvard University, Cambridge, MA 02138

Tweedell, Kenyon S., Department of Biological Sciences, University of Notre Dame, Notre Dame, IN 46656

Tytell, Michael, Department of Anatomy, Bowman Gray School of Medicine, Wake Forest University, Winston-Salem, NC 27103

Ueno, Hiroshi, Department of Biochemistry, The Rockefeller University, 1230 York Ave., New York, NY 10021

Valiela, Ivan, Boston University Marine Program, Marine Biological Laboratory, Woods Hole, MA 02543

Vallee, Richard, Cell Biology Group, Worcester Foundation for Experimental Biology, Shrewsbury, MA 01545

Valois, John, Marine Biological Laboratory, Woods Hole, MA 02543

Van Holde, Kensal, Department of Biochemistry and Biophysics, Oregon State University, Corvallis, OR 97331-6503

Vincent, Walter S., 16 F. R. Lillie Road, Woods Hole, MA 02543

Vogel, Steven S., LBM, NIDDK/NIH, Bldg. 10, Rm. 9B04, Bethesda, MD 20894

Waksman, Byron, Foundation for Microbiology, 300 East 54th St., New York, NY 10022

Wall, Betty, 9 George St., Woods Hole, MA 02543

Wallace, Robin A., Whitney Laboratory, 9505 Ocean Shore Blvd., St. Augustine, FL 32086

Wang, Ching Chung, Department of Pharmaceutical Chemistry, University of California, San Francisco, CA 94143

Warner, Robert C., Department of Molecular Biology and Biochemistry, University of California, Irvine, CA 92717

Warren, Kenneth S., Maxwell Communications Corp., 866 Third Avenue, New York, NY 10022

Warren, Leonard, Wistar Institute, 36th and Spruce Streets, Philadelphia, PA 19104

Waterbury, John B., Department of Biology, Woods Hole Oceanographic Institution, Woods Hole, MA 02543

Watson, Stanley, Associates of Cape Cod, Inc., P. O. Box 224, Woods Hole, MA 02543

Waxman, Stephen G., Department of Neurology, LCI 708, Yale School of Medicine, 333 Cedar Street, New Haven, CT 06510

Webb, H. Marguerite, Marine Biological Laboratory, Woods Hole, MA 02543

Weber, Annemarie, Department of Biochemistry and Biophysics, School of Medicine, University of Pennsylvania, Philadelphia, PA 19066

Weidner, Earl, Department of Zoology and Physiology, Louisiana State University, Baton Rouge, LA 70803

Weiss, Dieter G., Institut fur Zoologie, Technische Universitat Munchen, 8046 Garching, FRG

Weiss, Leon P., Department of Animal Biology, School of Veterinary Medicine, University of Pennsylvania, Philadelphia, PA 19104

Weiss, Paul A., Address unknown

Weissmann, Gerald, New York University Medical Center, 550 First Avenue, New York, NY 10016

Werman, Robert, Neurobiology Unit, The Hebrew University, Jerusalem, Israel

Westerfield, R. Monte, The Institute of Neuroscience, University of Oregon, Eugene, OR 97403

Whittaker, J. Richard, Marine Biological Laboratory, Woods Hole, MA 02543

Wigley, Roland L., 35 Wilson Road, Woods Hole, MA 02543

Wilson, Darcy B., Medical Biology Institute, 11077 North Torrey Pines Road, La Jolla, CA 92037

Wilson, T. Hastings, Department of Physiology, Harvard Medical School, Boston, MA 02115

Witkovsky, Paul, Department of Ophthalmology, New York University Medical Center, 550 First Ave., New York, NY 10016

Wittenberg, Jonathan B., Department of Physiology and Biophysics, Albert Einstein College, 1300 Morris Park Ave., Bronx, NY 01461

Wolfe, Ralph, Department of Microbiology, 131 Burrill Hall, University of Illinois, Urbana, IL 61801

Wolken, Jerome J., Department of Biological Sciences, Carnegie Mellon University, 440 Fifth Ave., Pittsburgh, PA 15213

Worgul, Basil V., Department of Ophthalmology, Columbia University, 630 West 168th St., New York, NY 10032

Wu, Chau Hsiung, Department of Pharmacology, Northwestern University Medical School, Chicago, IL 60611

Wyttenbach, Charles R., Department of Physiology and Cell Biology, University of Kansas, Lawrence, KS 66045

Yeh, Jay Z., Department of Pharmacology, Northwestern University Medical School, Chicago, IL 60611

Zigman, Seymour, School of Medicine and Dentistry, University of Rochester, 260 Crittenden Blvd., Rochester, NY 14620

Zigmond, Richard E., Center for Neurosciences, School of Medicine, Case Western Reserve University, Cleveland, OH 44106

Zimmerberg, Joshua J., NIH, Bldg. 12A, Room 2007, Bethesda, MD 20892

Zottoli, Steven J., Department of Biology, Williams College, Williamstown, MA 01267

Zucker, Robert S., Neurobiology Division, Department of Molecular and Cellular Biology, University of California, Berkeley, CA 94720

Zukin, Ruth Suzanne, Department of Neuroscience, Albert Einstein College of Medicine, 1300 Morris Park Ave., Bronx, NY 10461

Associate Members

Ackroyd, Dr. Frederick W.
Adams, Dr. Paul
Adelberg, Mrs. Edward A.
Ahearn, Mr. and Mrs. David
Alden, Mr. John M.
Allard, Dr. Dean C., Jr.
Allen, Miss Camilla K.
Allen, Dr. Nina S.
Allison, Mr. and Mrs. Douglas F.
Amon, Mr. Carl H. Jr.
Anderson, Mr. J. Gregory
Anderson, Drs. James L. and Helene M.
Anderson, Mr. and Mrs. Seneca
Andrews, Dr. Edwin J.
Antonucci, Dr. Robert V.
Armstrong, Dr. and Mrs. Samuel C.
Arnold, Mrs. Lois
Arvin, Ms. Kara L.

Ashworth, Mr. and Mrs. Henry
Aspinwall, Mr. and Mrs. Duncan
Atwood, Dr. and Mrs. Kimball C., III
Ayers, Mrs. Donald
Backus, Mrs. Nell
Bagley, Mr. Everett E.
Baker, Mrs. C. L.
Ball, Mrs. Eric G.
Ballantine, Dr. and Mrs. H. T., Jr.
Bang, Mrs. Frederik B.
Bang, Miss Molly
Banks, Ms. Jamie
Banks, Mr. and Mrs. William L.
Barlow, Dr. and Mrs. Robert B. Jr.
Barrows, Mrs. Albert W.
Bator, Mrs. Frances B.
Baum, Mr. Richard T.
Baylor, Drs. Edward and Martha
Beckman, Mrs. Barbara
Beers, Mrs. Yardley
Belesir, Mr. Tasos
Bennett, Drs. Michael and Ruth
Berg, Mr. and Mrs. C. John
Bernheimer, Drs. Alan W. and Harriet P.
Bernstein, Mr. and Mrs. Norman
Bicker, Mr. Alvin
Bigelow, Mr. and Mrs. Robert O.
Bihrle, Dr. William
Bird, Mr. William R.
Bishop, Mrs. John
Bleck, Dr. Thomas B.
Blumefeld, Ms. Olga
Boche, Mr. Robert
Bodeen, Mr. and Mrs. George H.
Boettiger, Dr. and Mrs. Edward G.
Boettiger, Mrs. Julie
Bolton, Mr. and Mrs. Thomas C.
Bonn, Mr. Theodore H.
Borg, Dr. and Mrs. Alfred F.
Borgese, Dr. and Mrs. Thomas
Bowles, Dr. and Mrs. Francis P.
Bradley, Dr. and Mrs. Charles C.
Bradley, Mr. Richard
Brown, Ms. Cornelia
Brown, Mrs. Frank A., Jr.
Brown, Mr. James
Brown, Mrs. Neil
Brown, Mr. and Mrs. T. A.
Brown, Dr. and Mrs. Thornton
Browne, Dr. John M.
Broyles, Dr. Robert H.
Buck, Dr. and Mrs. John B.
Buckely, Mr. George D.
Bunts, Mr. and Mrs. Frank E.
Burt, Mrs. Charles E.
Burwell, Dr. and Mrs. E. Langdon
Bush, Dr. Louise
Butler, Dr. Dore
Buxton, Mr. and Mrs. Bruce E.
Buxton, Mr. E. Brewster
Cadwalader, Mr. George
Calkins, Mr. G. N., Jr.
Campbell, Mrs. David G.
Carlson, Dr. and Mrs. Francis
Carlton, Mr. and Mrs. Winslow G.
Case, Mrs. Barbara L.
Case, Mrs. James
Chaet, Mrs. Alfred
Chandler, Mr. Robert
Chase, Mr. Thomas H.
Chevalier, Mr. Randall H.
Child, Dr. and Mrs. Frank M., III
Chisholm, Dr. Sallie W.
Church, Dr. Wesley
Claff, Mr. and Mrs. Mark
Clark, Dr. and Mrs. Arnold M.
Clark, Mr. and Mrs. Hays
Clark, Mr. James McC.
Clark, Mr. and Mrs. John
Clark, Mr. and Mrs. Leroy, Jr.
Clark, Dr. Peter L.
Clarke, Dr. Barbara J.
Clement, Mrs. Anthony C.
Cloud, Dr. Laurence P.
Clowes Fund, Inc.
Clowes, Dr. and Mrs. Alexander W.
Clowes, Mr. Allen W.
Clowes, Mrs. G. H. A., Jr.
Cobb, Dr. Jewel P.
Coburn, Mr. and Mrs. Lawrence
Cohen, Mrs. Seymour S.
Coleman, Drs. John and Annette
Collum, Mrs. Peter
Colt, Dr. LeBaron C., Jr.
Connell, Mr. and Mrs. W. J.
Cook, Dr. and Mrs. Joseph
Cook, Dr. and Mrs. Paul W., Jr.
Copel, Mrs. Marcia N.
Copeland, Dr. and Mrs. D. Eugene
Copeland, Mr. Frederick C.
Copeland, Mr. and Mrs. Preston S.
Costello, Mrs. Donald P.
Cowan, Mr. and Mrs. James F., III
Cowan, Ms. Stacy
Cowling, Mr. John
Cowling, Dr. Vincent
Crabb, Mr. and Mrs. David L.
Crain, Mr. and Mrs. Melvin C.
Cramer, Mr. and Mrs. Ian D. W.
Crane, Mrs. John O.
Crane, Josephine B., Foundation
Crane, Mr. Thomas S.
Crosby, Miss Carol
Cross, Mr. and Mrs. Norman C.
Crossley, Miss Dorothy
Crossley, Miss Helen
Crowell, Dr. and Mrs. Sears
Currier, Mr. and Mrs. David L.
Daignault, Mr. and Mrs. Alexander T.
Daniels, Mr. and Mrs. Bruce G.
Davidson, Dr. Morton
Davis, Mr. and Mrs. Joel P.
Day, Mr. and Mrs. Pomeroy
Decker, Dr. Raymond F.
DeMello, Mr. John
DiBerardino, Dr. Marie A.
DiCecca, Dr. and Mrs. Charles
Dickson, Dr. William A.
Dierolf, Dr. Shirley H.
Donnette, Mr. and Mrs. Joseph
Donovan, Mr. David L.
Dorman, Dr. and Mrs. Craig
Dreyer, Mrs. Frank
Drummey, Mr. and Mrs. Charles E.
Drummey, Mr. Todd A.
DuBois, Dr. and Mrs. Arthur B.
Dudley, Dr. Patricia
Dugan, Mr. and Mrs. William P.
DuPont, Mr. A. Felix, Jr.
Dutton, Mr. and Mrs. Roderick L.
Ebert, Dr. and Mrs. James D.
Egloff, Dr. and Mrs. F. R. L.
Engles, Mr. and Mrs. George
Enos, Mr. Edward, Jr.
Eppel, Mr. and Mrs. Dudley
Epstein, Mr. and Mrs. Ray L.
Estabrooks, Mr. Gordon C.
Evans, Mr. and Mrs. Dudley
Farley, Miss Joan
Farmer, Miss Mary
Faull, Mr. J. Horace, Jr.
Fausch, Mr. David
Ferguson, Dr. and Mrs. James J., Jr.
Fisher, Mrs. B. C.
Fisher, Mr. Frederick S., III
Fisher, Dr. and Mrs. Saul H.
Fluck, Mr. Richard A.
Folino, Mr. John W., Jr.
Forbes, Mr. John M.
Ford, Mr. John H.
Fowlkes, Mr. Aaron
Francis, Mr. Lewis W., Jr.
Frenkel, Dr. Krystyna
Fribourgh, Dr. James H.
Friendship Fund
Fries, Dr. and Mrs. E. F. B.
Frosch, Dr. and Mrs. Robert A.
Funkhouser, Dr. John J.
Fye, Mrs. Paul M.
Gabriel, Dr. and Mrs. Mordecai L.
Gagnon, Mr. Michael
Gaiser, Mrs. David W.
Gallagher, Mr. Robert O.
Garcia, Dr. Ignacio
Garfield, Miss Eleanor
Gault, Ms. Christine
Gellis, Dr. and Mrs. Sydney
Gephard, Mr. Stephen
Gerhard, Mrs. Sylvia K.
German, Dr. and Mrs. James L., III
Gewecke, Mr. and Mrs. Thomas H.
Gifford, Mr. and Mrs. Cameron
Gifford, Dr. and Mrs. Prosser
Gilbert, Drs. Daniel L. and Claire
Gildea, Dr. Margaret C. L.
Gillette, Mr. and Mrs. Robert S.
Glad, Mr. Robert
Glass, Dr. and Mrs. H. Bentley
Glazebrook, Mr. James G.
Glazebrook, Mrs. James R.
Glenn, Mr. Gary
Gmeiner, Mr. and Mrs. John
Goldman, Mrs. Mary
Goldring, Mr. Michael
Goldstein, Dr. and Mrs. Moise H., Jr.
Goodgal, Dr. Sol H.
Goodwin, Mr. and Mrs. Charles
Gould, Miss Edith
Grace, Miss Priscilla B.
Grant, Mrs. Philip
Grassle, Mrs. J. K.
Greene, Mrs. Davis Crane
Greenberg, Noah and Mosher, Diane
Greer, Mr. and Mrs. W. H., Jr.
Griffin, Mrs. Robert W.
Griffith, Dr. and Mrs. B. Herold
Grosch, Dr. and Mrs. Daniel S.
Gross, Mrs. Mona
Gunning, Mr. and Mrs. Robert
Haakonsen, Dr. Harry O.
Hadamard, Dr. Antoine F.
Haigh, Mr. and Mrs. Richard H.
Hall, Mr. Peter A.
Hall, Mr. Warren C.
Halvorson, Dr. and Mrs. Harlyn O.
Hamstrom, Miss Mary Elizabeth
Harrington, Mr. Robert D., Jr.
Harrington, Mr. Robert B.
Harvey, Dr. and Mrs. Richard B.
Hassett, Mr. and Mrs. Charles
Hastings, Dr. and Mrs. J. Woodland
Hathaway, Ms. Elizabeth E.
Haubrich, Mr. Robert R.
Hay, Mr. John
Hays, Dr. David S.
Heaney, Mr. John D.
Hedberg, Mrs. Frances
Hedberg, Dr. Mary
Hersey, Mrs. George L.
Hiatt, Dr. and Mrs. Howard
Hichar, Dr. Barbara

Hill, Mrs. Samuel E.
Hirschfeld, Mrs. Nathan B.
Hobbie, Dr. and Mrs. John
Hocker, Mr. and Mrs. Lon
Hodge, Dr. and Mrs. Stuart
Hodosh, Mrs. Helen
Hokin, Mr. Richard
Holmes, Mrs. George
Hornor, Mr. Townsend
Horwitz, Dr. and Mrs. Norman H.
Hoskin, Dr. and Mrs. Francis C. G.
Hough, Mr. John T.
Houston, Mr. and Mrs. Howard E.
Howard, Mrs. L. L.
Hoyle, Dr. Merrill C.
Huckle, Mrs. Eleanor L.
Huettner, Ms. Susan A.
Huettner, Dr. and Mrs. Robert J.
Hutchinson, Mr. Alan D.
Hyde, Mr. and Mrs. Robinson
Hynes, Mr. and Mrs. Thomas J., Jr.
Inouë, Dr. and Mrs. Shinya
Issokson, Mr. and Mrs. Israel
Jackson, Miss Elizabeth B.
Jaffe, Dr. and Mrs. Ernst R.
Janney, Mrs. F. Wistar
Jewett, G. F., Foundation
Jewett, Mr. and Mrs. G. F., Jr.
Jewett, Mr. and Mrs. Raymond L.
Jones, Mrs. Barbara W.
Jones, Mr. and Mrs. DeWitt C., III
Jones, Mr. and Mrs. Frederick, II
Jones, Mr. Frederick S., III
Jordan, Dr. and Mrs. Edwin P.
Juterbock, Mrs. Barbara J.
Kaan, Dr. Helen W.
Kahn, Dr. Harry S.
Kahler, Mrs. Robert W.
Kaminer, Dr. and Mrs. Benjamin
Kanellopoulos, Mrs. Barbara
Karplus, Mrs. Alan K.
Karush, Dr. and Mrs. Fred
Kavaru, Dr. Madhav
Kelleher, Mr. and Mrs. Paul R.
Kendall, Mr. and Mrs. Richard E.
Keosian, Mrs. Jessie
Keoughan, Miss Patricia
Ketchum, Mrs. Paul
Kinnard, Mrs. L. Richard
Kirschenbaum, Mrs. Donald
Kissam, Mr. and Mrs. William M.
Kivy, Dr. and Mrs. Peter
Koller, Dr. Lewis R.
Korgen, Dr. Ben J.
Kraco, Ms. Karen
Kravitz, Dr. and Mrs. Edward
Kroll, Dr. Peter
Kuffler, Mrs. Stephen W.
Kutner, Dr. Lawrence
Laderman, Mr. and Mrs. Ezra
Lafferty, Miss Nancy
Lahner, Mrs. Alta S.
Lakian, Mr. and Mrs. John
Larmon, Mr. Jay
Lash, Ms. Rebecca
Laster, Dr. and Mrs. Leonard
Latham, Mrs. Eunice
Laufer, Dr. and Mrs. Hans
Laufer, Jessica, and Weiss, Malcolm
Laufer, Dr. Marc R.
La Vigne, Mrs. Richard J.
Lawrence, Mr. Frederick V.
Lawrence, Mr. William
Leach, Dr. and Mrs. Berton J.
Leatherbee, Mrs. John H.
LeBlond, Mr. and Mrs. Arthur
Leeson, Mr. and Mrs. A. Dix
LeFevre, Dr. Marian E.
Leffler, Dr. Charles W.
Lehman, Miss Robin
Lenher, Dr. and Mrs. Samuel
Leprohon, Mr. Joseph
Levine, Mr. Joseph
Levine, Dr. and Mrs. Rachmiel
Levitz, Dr. Mortimer
Levy, Mr. and Mrs. Stephen R.
Libbin, Mr. Edwin M.
Light, Mr. and Mrs. Donald W.
Lindner, Mr. Timothy P.
Little, Mrs. Elbert
Livingstone, Mr. and Mrs. Robert
Lloyd, Mr. and Mrs. James
Loeb, Mrs. Robert F.
Loessel, Mrs. Edward
Londergan, Mr. Bob
Lovell, Mr. and Mrs. Hollis R.
Lovering, Mr. Richard C.
Low, Miss Doris
Lowe, Dr. and Mrs. Charles U.
Lowengard, Mrs. Joseph
Mackey, Mr. and Mrs. William K.
MacLeish, Mrs. Margaret
MacNary, Mr. B. Glenn
MacNichol, Dr. and Mrs. Edward F., Jr.
Maddigan, Mrs. Thomas
Magee, Ms. Chris
Maher, Miss Anne Camille
Mahler, Mrs. Henry
Mahler, Mrs. Suzanne
Mansworth, Miss Marie
Manual, Dr. Isabelle
Maples, Dr. Philip B.
Marken, Mrs. Madeline
Marsh, Dr. and Mrs. Julian
Martyna, Mr. and Mrs. Joseph C.
Mason, Mr. and Mrs. Appleton
Mastroianni, Dr. and Mrs. Luigi, Jr.
Mather, Mr. and Mrs. Frank J., III
Matherly, Mr. and Mrs. Walter
Matthiessen, Dr. and Mrs. G. C.
Mauzerall, Mrs. Miriam J.
McClane, Mrs. Louise
McCusker, Mr. and Mrs. Paul T.
McElroy, Mrs. Nella W.
McIlwain, Dr. Susan G.
McMurtrie, Mrs. Cornelia Hanna
Meigs, Mr. and Mrs. Arthur
Meigs, Dr. and Mrs. J. Wister
Melillo, Dr. and Mrs. Jerry M.
Mellon, Richard King, Trust
Mellon, Mr. and Mrs. Richard P.
Mendelson, Dr. Martin
Metz, Dr. and Mrs. Charles B.
Meyers, Mr. and Mrs. Richard
Miller, Dr. Daniel A.
Miller, Mr. and Mrs. Paul
Mills, Mrs. Margaret A.
Mirro, Dr. Robert
Mixer, Mrs. Florence E.
Mizell, Dr. and Mrs. Merle
Monroy, Mrs. Alberto
Montgomery, Dr. and Mrs. Charles H.
Montgomery, Mrs. Raymond B.
Moore, Drs. John and Betty
Morgan, Miss Amy
Morse, Mrs. Charles L., Jr.
Morse, Dr. M. Patricia
Moul, Mrs. Edwin T.
Munson, Mr. William
Murchelano, Dr. Robert
Murray, Mr. David M.
Myles-Tochko, Drs. Christina J. and John
Nace, Dr. and Mrs. Paul
Nace, Mr. Paul F., Jr.
Naugle, Mr. John E.
Neall, Mr. William G.
Nelson, Dr. and Mrs. Leonard
Nelson, Dr. Pamela
Newton, Mr. William E.
Nickerson, Mr. and Mrs. Frank L.
Norman, Mr. and Mrs. Andrew E.
Norman Foundation
Norris, Mr. and Mrs. Barry
Norris, Mr. and Mrs. John A.
Norris, Mr. William
Norton, Mrs. Thomas J.
O'Connell, Dr. and Mrs. Clifford
Offenback, Dr. Jack A.
O'Herron, Mr. and Mrs. Jonathan
Olszowka, Dr. Janice S.
O'Neil, Mr. and Mrs. Barry T.
O'Rand, Mr. and Mrs. Michael
O'Sullivan, Dr. Renee Bennett
Ott, Drs. Philip and Karen
Palmer, Mr. and Mrs. David
Pappas, Dr. and Mrs. George D.
Park, Mr. and Mrs. Malcolm S.
Parmenter, Dr. Charles
Parmenter, Miss Carolyn L.
Pearce, Dr. John B.
Pearson, Mrs. Oscar H.
Peltz, Mr. and Mrs. William L.
Pendergast, Mrs. Claudia
Pendleton, Dr. and Mrs. Murray E.
Peri, Mr. and Mrs. John B.
Perkins, Mr. and Mrs. Courtland D.
Person, Dr. and Mrs. Philip
Peters, Mr. and Mrs. Frederick S.
Peterson, Mr. and Mrs. E. Gunnar
Peterson, Mr. and Mrs. E. Joel
Peterson, Mr. Raymond W.
Petty, Mr. Richard F.
Pfeiffer, Mr. and Mrs. John
Plough, Ms. Frances
Plough, Mr. and Mrs. George H.
Plough, Mrs. Harold H.
Pointe, Mr. Albert
Pointe, Mr. Charles
Porter, Dr. and Mrs. Keith R.
Pothier, Dr. and Mrs. Aubrey
Press, Dr. Frank
Proskauer, Mr. Joseph H.
Proskauer, Mr. Richard
Prosser, Dr. and Mrs. C. Ladd
Psaledakis, Mr. Nicholas
Psychoyos, Dr. Alexandre
Putnam, Mr. and Mrs. Allan Ray
Putnam, Mr. and Mrs. William A., III
Rankin, Mrs. John
Raphael, Ms. Ellen S.
Raymond, Dr. Samuel
Reese, Miss Bonnie
Regis, Ms. A. Kathy
Reingold, Mr. Stephen C.
Reynolds, Mrs. George
Reynolds, Dr. John L.
Reynolds, Mr. and Mrs. Robert M.
Reznikoff, Mrs. Paul
Ricca, Dr. and Mrs. Renato A.
Righter, Mr. and Mrs. Harold
Riina, Mr. John R.
Riley, Dr. Monica
Robb, Mrs. Alison A.
Roberts, Miss Jean
Roberts, Mr. Mervin F.
Robertson, Mrs. C. W.
Robinson, Dr. Denis M.
Robinson, Mr. John G.
Robinson, Mr. and Mrs. Marius A.
Root, Mrs. Walter S.
Rosenthal, Miss Hilde

Roslansky, Drs. John and Priscilla
Ross, Dr. and Mrs. Donald
Ross, Dr. Robert
Ross, Dr. Virginia
Roth, Dr. Stephen
Rowan, Mr. Edward
Rowe, Dr. Don
Rowe, Mrs. William S.
Rugh, Mrs. Roberts
Ryder, Mr. Francis C.
Sager, Dr. Ruth
Sanidas, Dr. and Mrs. Dennis J.
Sardinha, Mr. George J.
Saunders, Dr. and Mrs. John W.
Saunders, Mrs. Lawrence
Saunders, Lawrence, Fund
Sawyer, Mr. and Mrs. John E.
Saz, Mrs. Ruth L.
Schlesinger, Dr. and Mrs. R. Walter
Schwamb, Mr. and Mrs. Peter
Schwartz, Dr. Lawrence
Scott, Mrs. George T.
Scott, Mr. and Mrs. Norman E.
Sears, Mr. Clayton C.
Sears, Mr. and Mrs. Harold B.
Sears, Mr. Harold H.
Seaver, Mr. George
Seder, Mr. John
Segal, Dr. and Mrs. Sheldon J.
Selby, Dr. Cecily
Senft, Dr. and Mrs. Alfred
Shanklin, Dr. D. R.
Shapiro, Mr. and Mrs. Howard
Shapley, Dr. Robert
Sharp, Mr. and Mrs. Robert W.
Shemin, Dr. and Mrs. David
Shepro, Dr. and Mrs. David
Sherblom, Dr. James P.
Sichel, Dr. Enid
Siegel, Mr. and Mrs. Alvin
Simmons, Mr. Tim
Simon, Mr. and Mrs. Stephen
Singer, Mr. and Mrs. Daniel M.
Smith, Drs. Frederick E. and Marguerite A.
Smith, Mr. and Mrs. Homer P.
Smith, Mr. Van Dorn C.
Snyder, Mr. Robert M.
Solomon, Dr. and Mrs. A. K.
Sonnenblick, Mrs. Perle
Specht, Mr. and Mrs. Heinz
Speck, Dr. William T.
Spiegel, Drs. and Mrs. Melvin and Evelyn
Spotte, Mr. Stephen
Steele, Mrs. John H.
Steele, Dr. Robert E.
Stein, Mr. Ronald
Steinbach, Mrs. H. Burr
Stetson, Mrs. Thomas J.
Stetten, Dr. Gail
Stetten, Dr. and Mrs. H. DeWitt, Jr.
Stracher, Dr. Dorothy
Sudduth, Dr. William
Swain, Mr. Albert H.
Sussman, Dr. and Mrs. Maurice
Swanson, Mrs. Carl P.
Swift, Mr. and Mrs. E. Kent
Swope, Mrs. Gerard, Jr.
Swope, Mr. and Mrs. Gerard L.
Szent-Györgyi, Dr. Andrew
Taber, Mr. George H.
Talamas-Rohana, Dr. Eduardo
Taylor, Mr. James K.
Taylor, Dr. and Mrs. W. Randolph
Tietje, Mr. Emil D., Jr.
Timmins, Mrs. William
Tochko, Dr. John S.
Todd, Mr. and Mrs. Gordon F.
Tolkan, Mr. and Mrs. Norman N.
Trager, Mrs. William
Trigg, Mr. and Mrs. D. Thomas
Troll, Dr. and Mrs. Walter
Trousof, Miss Natalie
Tucker, Miss Ruth
Tully, Mr. and Mrs. Gordon F.
Ulbrich, Mr. and Mrs. Volker
Valois, Mr. and Mrs. John
Vancouver Public Aquarium
Van Buren, Mrs. Harold
Van Holde, Mrs. Kensal E.
Veeder, Mrs. Ronald A.
Veeder, Ms. Susan
Vincent, Mr. and Mrs. Samuel W.
Vincent, Dr. Walter S.
Vonderhaar, Dr. William
Wagner, Mr. Mark
Waksman, Dr. and Mrs. Byron H.
Ward, Dr. Robert T.
Ware, Mr. and Mrs. J. Lindsay
Warren, Dr. Henry B.
Warren, Dr. and Mrs. Leonard
Watt, Mr. and Mrs. John B.
Weeks, Mr. and Mrs. John T.
Weiffenbach, Dr. and Mrs. George
Weinstein, Miss Nancy B.
Weisberg, Mr. and Mrs. Alfred M.
Weissmann, Dr. and Mrs. Gerald
Wheeler, Dr. and Mrs. Paul S.
Wheeler, Dr. William M.
Whitehead, Mrs. Fred
Whitney, Mr. and Mrs. Geoffrey G., Jr.
Wichterman, Dr. and Mrs. Ralph
Wickersham, Mr. and Mrs. A. A. Tilney
Wiese, Dr. Konrad
Wilber, Mrs. Clare M.
Wilhelm, Dr. Hazel S.
Willis, Mr. Herbert F.
Wilson, Mr. and Mrs. Leslie J.
Wilson, Mr. and Mrs. T. Hastings
Winn, Dr. William M.
Winsten, Dr. Jay A.
Witting, Miss Joyce
Woitkoski, Miss Nancy
Wolfinsohn, Mrs. Wolfe
Woodwell, Dr. and Mrs. George M.
Wrigley, Mrs. Roland
Yntema, Mrs. Chester L.
Young, Miss Nina L.
Zinn, Dr. and Mrs. Donald J.
Zipf, Dr. Elizabeth

Gift Shop Volunteers

Marian Adelberg
Louise Atkins
Barbara Atwood
Gloria Borgese
Jennie Brown
Elisabeth Buck
Patricia Case
Summers Case
Shirley Chaet
Julia Child
Vera Clark
Margaret Clowes
Villa Crowell
Elizabeth Daignault
Janet Daniels
Alma Ebert
Margaret German
Rebeckah Glazebrook
Michael Goldring
Rose Grant
Martha Griffin
Edith Grosch
Jean Halvorson
Helen Hodosh
Adele Hoskins
Pauline Hyde
Sona Jones
Sally Karush
Ruth Ann Laster
Barbara Little
Sarah Loessel
Winnie Mackey
Constance Martyna
Florence Mixer
Lorraine Mizell
Phyllis Meyers
Bertha Person
Julia Rankin
Virginia Reynolds
Lilyan Saunders
Elsie Scott
Deborah Senft
Charlotte Shemin
Marilyn Shepro
Cynthia Smith
Marguerite Smith
Louise Specht
Judith Stetson
Dorothy Stracher
Mary Ulbrich
Barbara van Holde
Barbara Whitehead
Clare Wilber

MBL Tour Guides

Betsy Bang
John Buck
Sears Crowell
Teru Hayashi
Sally Loessel
Isabel Mountain
Julie Rankin
Lola Robinson
Donald Zinn
Margery Zinn

Certificate of Organization
Articles of Amendment
Bylaws of the MBL

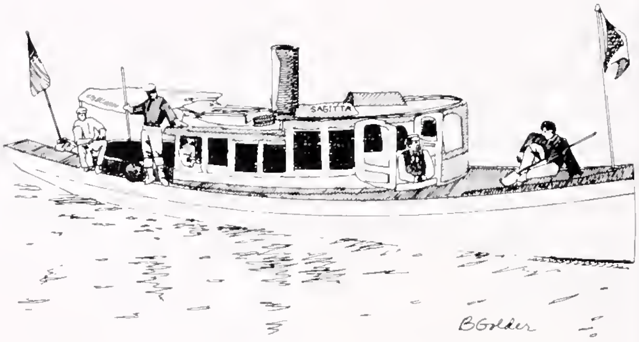

Certificate of Organization

(On File in the Office of the Secretary of the Commonwealth)

No. 3170

We, Alpheus Hyatt, President, William Stanford Stevens, Treasurer, and William T. Sedgwick, Edward G. Gardiner, Susan Mims and Charles Sedgwick Minot being a majority of the Trustees of the Marine Biological Laboratory in compliance with the requirements of the fourth section of chapter one hundred and fifteen of the Public Statutes do hereby certify that the following is a true copy of the agreement of association to constitute said Corporation, with the names of the subscribers thereto:

We, whose names are hereto subscribed, do, by this agreement, associate ourselves with the intention to constitute a Corporation according to the provisions of the one hundred and fifteenth chapter of the Public Statutes of the Commonwealth of Massachusetts, and the Acts in amendment thereof and in addition thereto.

The name by which the Corporation shall be known is
THE MARINE BIOLOGICAL LABORATORY.

The purpose for which the Corporation is constituted is to establish and maintain a laboratory or station for scientific study and investigations, and a school for instruction in biology and natural history.
The place within which the Corporation is established or located is the city of Boston within said Commonwealth.
The amount of its capital stock is none.
In Witness Whereof, we have hereunto set our hands, this twenty seventh day of February in the year eighteen hundred and eighty-eight, Alpheus Hyatt, Samuel Mills, William T. Sedgwick, Edward G Gardiner, Charles Sedgwick Minot, William G. Farlow, William Stanford Stevens, Anna D. Phillips, Susan Mims, B. H. Van Vleck.
That the first meeting of the subscribers to said agreement was held on the thirteenth day of March in the year eighteen hundred and eighty-eight.
In Witness Whereof, we have hereunto signed our names, this thirteenth day of March in the year eighteen hundred and eighty-eight, Alpheus Hyatt, President, William Stanford Stevens, Treasurer, Edward G. Gardiner, William T. Sedgwick, Susan Mims, Charles Sedgwick Minot.
(Approved on March 20, 1888 as follows:
I hereby certify that it appears upon an examination of the within written certificate and the records of the corporation duly submitted to my inspection, that the requirements of sections one, two and three of chapter one hundred and fifteen, and sections eighteen, twenty and twenty-one of chapter one hundred and six, of the Public Statutes, have been complied with and I hereby approve said certificate this twentieth day of March A.D. eighteen hundred and eighty-eight.

Charles Endicott
Commissioner of Corporations)

Articles of Amendment

(On File in the Office of the Secretary of the Commonwealth)

We, James D. Ebert, President, and David Shepro, Clerk of the Marine Biological Laboratory, located at Woods Hole, Massachusetts 02543, do hereby certify that the following amendment to the Articles of Organization of the Corporation was duly adopted at a meeting held on August 15, 1975, as adjourned to August 29, 1975, by vote of 444 members, being at least two-thirds of its members legally qualified to vote in the meeting of the corporation:

Voted: That the Certificate of Organization of this corporation be and it hereby is amended by the addition of the following provisions:
"No Officer, Trustee or Corporate Member of the corporation shall be personally liable for the payment or satisfaction of any obligation or liabilities incurred as a result of, or otherwise in connection with, any commitments, agreements, activities or affairs of the corporation.
"Except as otherwise specifically provided by the Bylaws of the corporation, meetings of the Corporate Members of the corporation may be held anywhere in the United States.
"The Trustees of the corporation may make, amend or repeal the Bylaws of the corporation in whole or in part, except with respect to any provisions thereof which shall by law, this Certificate or the bylaws of the corporation, require action by the Corporate Members."

The foregoing amendment will become effective when these articles of amendment are filed in accordance with Chapter 180, Section 7 of the General Laws unless these articles specify, in accordance with the vote adopting the amendment, a later effective date not more than thirty days after such filing, in which event the amendment will become effective on such later date.

In Witness whereof and Under the Penalties of Perjury, we have hereto signed our names this 2nd day of September, in the year 1975, James D. Ebert, President; David Shepro, Clerk.
(Approved on October 24, 1975, as follows:
I hereby approve the within articles of amendment and, the filing fee in the amount of $10 having been paid, said articles are deemed to have been filed with me this 24th day of October, 1975.

Paul Guzzi
Secretary of the Commonwealth)

Bylaws of the Corporation of the Marine Biological Laboratory

(Revised August 17, 1990)

(These Bylaws have been extensively amended by the Board of Trustees and are subject to approval by the Corporation. If these amendments are not approved by the Corporation, the existing Bylaws will then remain in place.)

ARTICLE I—THE CORPORATION

A. Name and Purpose. The name of the Corporation shall be The Marine Biological Laboratory. The Corporation's purpose shall be to establish and maintain a laboratory or station for scientific study and investigation and a school for instruction in biology and natural history.

B. Nondiscrimination. The Corporation shall not discriminate on the basis of age, religion, color, race, national or ethnic origin, sex or sexual preference in its policies on employment and administration or in its educational and other programs.

ARTICLE II—MEMBERSHIP

A. Members. The Members of the Corporation ("Members") shall consist of persons elected by the Board of Trustees (the "Board"), upon such terms and conditions and in accordance with such procedures, not inconsistent with law or these Bylaws, as may be determined by the Board. At any regular or special meeting of the Board, the Board may elect new Members. Any Member may vote at any meeting of the Members either in person or by proxy executed no more than three months prior to the date of such meeting. Except as otherwise limited therein, proxies shall entitle the persons named therein to vote at any adjournment of such meeting, but shall not be valid after final adjournment of such meeting. Proxies need not be sealed or attested and proxy purported to be executed by or on behalf of a Member entitled to vote shall be deemed valid unless challenged at or prior to its exercise. Members shall serve until their death or resignation unless earlier removed with or without cause by the affirmative vote of two-thirds of the Trustees then in office. Any Member who has retired from his or her home institution may, on written request to the Corporation, be designated a Life Member. Life Members shall not have the right to vote and shall not be assessed for dues.

B. Meetings. The annual meeting of the Members shall be held on the Friday following the second Tuesday in August of each year, at the Laboratory of the Corporation in Woods Hole, Massachusetts, at 9:30 a.m. If no annual meeting is held in accordance with the foregoing provision, a special meeting may be held in lieu thereof with the same effect as the annual meeting, and in such case all references in these Bylaws, except in this Article II.B., to the annual meeting of the Members shall be deemed to refer to such special meeting. Members shall transact business as may properly come before the meeting. Special meetings of the Members may be called by the Chairman or the Trustees, and shall be called by the Clerk, or in the case of the death, absence, incapacity or refusal by the Clerk, by any other officer, upon written application of Members representing at least ten percent of the smallest quorum of Members required for a vote upon any matter at the annual meeting of the Members, to be held at such time and place as may be designated. The Chairman of the Board shall preside at all meetings of the Corporation.

C. Notice of Meetings. Notice of any annual meeting or special meeting of Members, if necessary, shall be given by the Clerk by mailing notice of the time and place and purpose of such meeting at least 15 days before such meeting to each Member at his or her address as shown on the records of the Corporation.

D. Waiver of Notice. Whenever notice of a meeting is required to be given a Member under any provision of the Articles or Organization or Bylaws of the Corporation, a written waiver thereof, executed before of after the Meeting by such Member, or his or her duly authorized attorney, shall be deemed equivalent to such notice.

E. Adjournments. Any meeting of the Members may be adjourned to any other time and place by the vote of a majority of those Members present or represented at the meeting, whether or not such Members constitute a quorum, or by any officer entitled to preside at or to act as Clerk of such meeting, if no Member is present or represented. It shall not be necessary to notify any Members of any adjournment unless no Member is present or represented at the meeting which is adjourned, in which case, notice of the adjournment shall be given in accordance with Article II.E. Any business which could have been transacted at any meeting of the Members as originally called may be transacted at an adjournment thereof.

ARTICLE III—ASSOCIATES OF THE CORPORATION

Associates of the Corporation. The Associates of the Marine Biological Laboratory shall be an unincorporated group of persons (including associations and corporations) interested in the Laboratory and shall be organized and operated under the general supervision and authority of the Trustees. The Associates of the Marine Biological Laboratory shall have no voting rights.

ARTICLE IV—BOARD OF TRUSTEES

A. Powers. The Board of Trustees shall have the control and management of the affairs of the Corporation. The Trustees shall annually elect a Chairman of the Board who shall serve until his or her successor is selected and qualified. They shall annually elect a President of the Corporation who shall also be the Vice Chairman of the Board and Vice Chairman of meetings of the Corporation. They shall annually elect a Treasurer. They shall elect a Clerk, who shall be a resident of Massachusetts and shall serve a term of four years. Eligibility for re-election of the Clerk shall be in accordance with the content of this Article IV as applied to Corporate or Board Trustees. They shall elect Trustees-at-Large as specified in this Article IV. They shall appoint a Director of the Laboratory for a term not to exceed five years, provided the term shall not exceed one year, if the candidate has attained the age of 65 years prior to the date of the appointment. They may choose such other officers and agents as they shall think best. They may fix the compensation of all officers and agents of the Corporation and may remove them at any time. They may fill vacancies occurring in any of the offices. The Board shall have the power to choose an Executive Committee from their own number as provided in Article V, and to delegate to such Committee such of their own powers as they may deem expedient in addition to those powers conferred by Article V. They shall, from time to time, elect Members to the Corporation upon such terms and conditions as they shall have determined, not inconsistent with law or these Bylaws.

B. Composition and Election. There shall be four groups of Trustees:

(1) Trustees (the "Corporate Trustees") elected by the Members according to such procedures, not inconsistent with these Bylaws, as the Trustees shall have determined. Except as provided below, such Trustees shall be divided into four classes of six, one class to be elected each year to serve for a term of four years. Such classes shall be designated by the year of expiration of their respective terms.

(2) Trustees ("Trustees-at-Large"). Nominees for Trustees-at-Large shall be introduced at the annual meeting of the Corporation for subsequent election by the Board according to such procedures, not inconsistent with these Bylaws, as the Trustees shall have determined. Such Trustees-at-Large shall be divided into four classes of four Trustees, one class to be elected each year to serve for a term of four years. Such classes shall be designated by the year of expiration of their respective terms. It is contemplated that, unless otherwise determined by the Trustees for good reason, Trustees-at-Large, shall be individuals who have not been considered for elections as Corporate Trustees.

(3) Trustees *ex officio* shall be the Chairman, the President, the Treasurer, the Clerk and the Director of the Laboratory.

(4) Trustees emeriti shall include any Member who has retired from his or her home institution and has requested to serve as a Trustee emeritus provided he or she has served at least two terms as a Trustee. A Trustee ex officio is eligible to serve as a Trustee emeritus provided he or she has served as Trustee *ex officio* for at least eight years. Trustees *ex officio* and emeriti shall have all the rights of the Trustees, except that Trustees emeriti shall not have the right to vote.

(5) The total number of Corporate Trustees and Trustees-at-Large elected in any year (excluding Trustees elected to fill vacancies which do not result from expiration of a term) shall not exceed ten. The number of Trustees-at-Large so elected shall not exceed four and, unless otherwise determined by vote of the Trustees, the number of Corporate Trustees so elected shall not exceed six. Corporate Trustees shall always constitute a majority on the Board of those elected or approved by the Members.

(6) Newly elected Trustees shall take office at the February meeting of the Board, but may participate in discussions at intervening meetings following their election, without voting rights.

(7) The Trustees and officers shall hold their respective offices until their successors are chosen and qualified.

C. Eligibility. A Corporate Trustee or a Trustee-at-Large who has served an initial term of at least two years' duration shall be eligible for re-election to a second term, but shall be ineligible for re-election to any subsequent term until two years have elapsed after he/she has last served as a Trustee.

D. Removal. Any Trustee may be removed from office at any time without cause, by vote of a majority of the Members entitled to vote in the election of Trustees; or for cause, by vote of two-thirds of the Trustees then in office. A Trustee may be removed for cause only if notice of such action shall have been given to all of the Trustees or Members entitled to vote, as the case may be, prior to the meeting at which such action is to be taken and if the Trustee to be so removed shall have been given reasonable notice and opportunity to be heard before the body proposing to remove him or her.

E. Vacancies. Any vacancy in the Board, unless and until filled by the Members at any annual or special meeting of the Members, may be filled by vote of a majority of the remaining Trustees present at a meeting of Trustees at which a quorum is present or by appointment of all of the Trustees if less than a quorum shall remain in office.

F. Meetings. The annual meeting of the Trustees shall be held promptly after the annual meeting of the Members at the Laboratory in Woods Hole, Massachusetts. Special meetings of the Trustees may be called by the Chairman, the President or by any seven Trustees to be held at such time and place as may be designated. The Chairman of the Board, when present, shall preside over all meetings of the Trustees. Written notice shall be sent to a Trustee's usual or last known place of residence at least two weeks before the meeting. Notice of a meeting need not be given to any Trustee if a written waiver of notice executed by such Trustee before or after the meeting is filed with the records of the meeting, or if such Trustee shall attend the meeting without protesting prior thereto or at its commencement the lack of notice given to him or her.

G Quorum Twenty-five Members shall constitute a quorum at any meeting. Except as otherwise required by law or these Bylaws, the affirmative vote of a majority of the Members voting in person or by proxy at a meeting attended by a quorum (present in person or by proxy) shall consitute action on behalf of the Members.

H Transfers of Interests in Land There shall be no transfer of title or long-term lease of real property held by the Corporation without prior approval of not less than two-thirds of the Trustees. Such real property transactions shall be finally acted upon at a meeting of the Board only if presented and discussed at a prior meeting of the Board. Either meeting may be a special meeting and no less than four weeks shall elapse between the two meetings. Any property acquired by the Corporation after December 1, 1989 may be sold with the prior approval of not less than two-thirds of the Trustees (other than any Trustee or Trustees with a direct or indirect financial interest in the transaction being considered for approval) who are present at a regular or special meeting of the Board at which there is a quorum.

ARTICLE V—COMMITTEES

A Executive Committee The Executive Committee is hereby designated to consist of not more than ten Trustees, including the *ex officio* Trustees (Chairman of the Board, President, Treasurer, and Director of the Laboratory); and six additional Trustees, two of whom shall be elected by the Board each year, to serve for a three-year term.

Beginning with the Members elected for terms ending in 1990, one of the Trustees elected to serve on the Executive Committee shall be a Trustee-at-Large. Beginning with the Members elected for terms ending in 1991, the Trustees will elect, to the Executive Committee, Trustees to ensure that the Committee includes four Corporate Trustees and two Trustees-at-Large.

The Chairman of the Board shall act as Chairman of the Executive Committee and the President as Vice Chairman. The Executive Committee shall meet at such times and places and upon such notice and appoint such subcommittees as the Committee shall determine.

The Executive Committee shall have and may exercise all the powers of the Board during the intervals between meetings of the Board except those powers specifically withheld, from time to time, by vote of the Board or by law. The Executive Committee may also appoint such committees, including persons who are not Trustees, as it may, from time to time, approve to make recommendations with respect to matters to be acted upon by the Executive Committee or the Board.

The Executive Committee shall keep appropriate minutes of its meetings, which shall be reported to the Board. Any actions taken by the Executive Committee shall also be reported to the Board.

The elected Members of the Executive Committee shall constitute a Standing Committee for the Nomination of Officers, responsible for making nominations at each annual meeting of the Members and of the Board for candidates to fill each office as the respective terms of office expire (Chairman of the Board, President, Treasurer, Clerk and Director of the Laboratory).

B Board Committees Generally The Board shall have the power, by vote of a majority of the Trustees then in office, to elect an Investment Committee, a Nominating Committee and any other committee and, by like vote, to delegate thereto some or all of the powers of the Board except those which by law, the Articles of Organization or these Bylaws they are prohibited from delegating. The members of any such committee shall have such tenure and duties as the Trustees shall determine. The Investment Committee, which shall oversee the management of the Corporation's endowment funds and marketable securities shall include as *ex officio* members, the Chairman of the Board, the Treasurer and the Chairman of the Audit Committee, together with such Trustees as may be required for not less than two-thirds of the Investment Committee to consist of Trustees. Except as otherwise provided by these Bylaws or determined by the Trustees, any such committee may make rules for the conduct of its business, but, unless otherwise provided by the Trustees or in such rules, its business shall be conducted as nearly as possible in the same manner as is provided by these Bylaws for the Trustees.

C Actions Without a Meeting Any action required or permitted to be taken at any meeting of the Executive Committee or any other committee elected by the Trustees may be taken without a meeting if all Members of such committees consent to the action in writing and such written consents are filed with the records of meetings. Members of the Executive Committee or any other committee elected by the Trustees may also participate in any meeting by means of a telephone conference call, or otherwise take action in such a manner as may, from time to time, be permitted by law.

ARTICLE VI—OFFICERS

A Enumeration The officers of the Corporation shall consist of a President, a Treasurer and a Clerk, and such other officers having the powers of President, Treasurer and Clerk as the Board may determine, and a Director of the Laboratory. The Corporation may have such other officers and assistant officers as the Board may determine, including (without limitation) a Chairman of the Board, and one or more Vice-Presidents, Assistant Treasurers or Assistant Clerks. Any two or more offices may be held by the same person. An officer need not be a Member or Trustee of the Corporation. If required by the Trustees, any officer shall give the Corporation a bond for the faithful performance of his or her duties in such amount and with such surety or sureties as shall be satisfactory to the Trustees.

B Tenure Except as otherwise provided by law, by the Articles of Organization or by these Bylaws, the President, Treasurer, and all other officers shall hold office until the first meeting of the Board following the annual meeting of Members and thereafter, until his or her successor is chosen and qualified.

C Resignation Any officer may resign by delivering his or her written resignation to the Corporation at its principal office or to the President or Clerk and such resignation shall be effective upon receipt unless it is specified to be effective at some other time or upon the happening of some other event.

D Removal The Board may remove any officer with or without cause by a vote of a majority of the entire number of Trustees then in office, at a meeting of the Board called for that purpose and for which notice of the purpose thereof has been given, provided that an officer may be removed for cause only after having an opportunity to be heard by the Board at a meeting of the Board at which a quorum is personally present and voting.

E Vacancy. A vacancy in any office may be filled for the unexpired balance of the term by vote of a majority of the Trustees present at any meeting of Trustees at which a quorum is present or by written consent of all of the Trustees if less than a quorum of Trustees shall remain in office.

F Director. The Director shall be the chief operating officer and, unless otherwise voted by the Trustees, the chief executive officer of the Corporation. The Director shall, subject to the direction of the Trustees, have general supervision of the Laboratory and control of the business of the Corporation. At the annual meeting, the Director shall submit a report of the operations of the Corporation for such year and a statement of its affairs, and shall, from time to time, report to the Board all matters within his or her knowledge which the interests of the Corporation may require to be brought to its notice.

G Deputy Director The Deputy Director, if any, or if there shall be more than one, the Deputy Directors in the order determined by the Trustees, shall, in the absence or disability of the Director, perform the duties and exercise the powers of the Director and shall perform such other duties and shall have such other powers as the Trustees may, from time to time, prescribe.

H President The President shall have the powers and duties as may be vested in him or her by the Board.

I Treasurer and Assistant Treasurer The Treasurer shall, subject to the direction of the Trustees, have general charge of the financial affairs of the Corporation, including its long-range financial planning, and shall cause to be kept accurate books of account. The Treasurer shall prepare a yearly report on the financial status of the Corporation to be delivered at the annual meeting. The Treasurer shall also prepare or oversee all filings required by the Commonwealth of Massachusetts, the Internal Revenue Service, or other Federal and State Agencies. The account of the Treasurer shall be audited annually by a certified public accountant.

The Assistant Treasurer, if any, or if there shall be more than one, the Assistant Treasurers in the order determined by the Trustees, shall, in the absence or disability of the Treasurer, perform the duties and exercise the powers of the Treasurer, shall perform such other duties and shall have such other powers as the Trustees may, from time to time, prescribe.

J Clerk and Assistant Clerk The Clerk shall be a resident of the Commonwealth of Massachusetts, unless the Corporation has designated a resident agent in the manner provided by law. The minutes or records of all meetings of the Trustees and Members shall be kept by the Clerk who shall record upon the record book of the Corporation minutes of the proceedings at such meetings. He or she shall have custody of the record books of the Corporation and shall have such other powers and shall perform such other duties as the Trustees may, from time to time, prescribe.

The Assistant Clerk, if any, or if there shall be more than one, the Assistant Clerks in the order determined by the Trustees, shall, in the absence or disability of the Clerk, perform the duties and exercise the powers of the Clerk and shall perform such other duties and shall have such other powers as the Trustees may, from time to time, prescribe.

In the absence of the Clerk and an Assistant Clerk from any meeting, a temporary clerk shall be appointed at the meeting.

K. Other Powers and Duties. Each officer shall have in addition to the duties and powers specifically set forth in these Bylaws, such duties and powers as are customarily incident to his or her office, and such duties and powers as the Trustees may, from time to time, designate.

ARTICLE VII—AMENDMENTS

These Bylaws may be amended by the affirmative vote of the Members at any meeting, provided that notice of the substance of the proposed amendment is stated in the notice of such meeting. As authorized by the Articles of Organization, the Trustees, by a majority of their number then in office, may also make, amend or repeal these Bylaws, in whole or in part, except with respect to the (a) the provisions of these Bylaws governing (i) the removal of Trustees and (ii) the amendment of these Bylaws and (b) any provisions of these Bylaws which by law, the Articles of Organization or these Bylaws, requires action by the Members.

No later than the time of giving notice of meeting of Members next following the making, amending or repealing by the Trustees of any Bylaw, notice thereof stating the substance of such change shall be given to all Members entitled to vote on amending the Bylaws.

Any Bylaw adopted by the Trustees may be amended or repealed by the members entitled to vote on amending the Bylaws.

ARTICLE VIII—INDEMNITY

Except as otherwise provided below, the Corporation shall, to the extent legally permissible, indemnify each person who is, or shall have been, a Trustee, director or officer of the Corporation or who is serving, or shall have served at the request of the Corporation as a Trustee, director or officer of another organization in which the Corporation directly or indirectly has any interest as a shareholder, creditor or otherwise, against all liabilities and expenses (including judgments, fines, penalties, and reasonable attorneys' fees and all amounts paid, other than to the Corporation or such other organization, in compromise or settlement) imposed upon or incurred by any such person in connection with, or arising out of, the defense or disposition of any action, suit or other proceeding, whether civil or criminal, in which he or she may be a defendant or with which he or she may be threatened or otherwise involved, directly or indirectly, by reason of his or her being or having been such a Trustee, director or officer.

The Corporation shall provide no indemnification with respect to any matter as to which any such Trustee, director or officer shall be finally adjudicated in such action, suit or proceeding not to have acted in good faith in the reasonable belief that his or her action was in the best interests of the Corporation. The Corporation shall provide no indemnification with respect to any matter settled or comprised unless such matter shall have been approved as in the best interests of the Corporation, after notice that indemnification is involved, by (i) a disinterested majority of the Board of the Executive Committee, or (ii) a majority of the Members.

Indemnification may include payment by the Corporation of expenses in defending a civil or criminal action or proceeding in advance of the final disposition of such action or proceeding upon receipt of an undertaking by the person indemnified to repay such payment if it is ultimately determined that such person is not entitled to indemnification under the provisions of this Article VIII, or under any applicable law.

As used in the Article VIII, the terms "Trustee," "director" and "officer" include their respective heirs, executors, administrators and legal representatives, and an "interested" Trustee, director or officer is one against whom in such capacity the proceeding in question or another proceeding on the same or similar grounds is then pending.

To assure indemnification under this Article VIII of all persons who are determined by the Corporation or otherwise to be or to have been "fiduciaries" of any employee benefits plan of the Corporation which may exist, from time to time, this Article VIII shall be interpreted as follows: (i) "another organization" shall be deemed to include such an employee benefit plan, including without limitation, any plan of the Corporation which is governed by the Act of Congress entitled "Employee Retirement Income Security Act of 1974," as amended, from time to time, ("ERISA"); (ii) "Trustee" shall be deemed to include any person requested by the Corporation to serve as such for an employee benefit plan where the performance by such person of his or her duties to the Corporation also imposes duties on or otherwise involves services by, such person to the plan or participants or beneficiaries of the plan; (iii) "fines" shall be deemed to include any excise tax plan pursuant to ERISA; and (iv) actions taken or omitted by a person with respect to an employee benefit plan in the performance of such person's duties for a purpose reasonably believed by such person to be in the interest of the participants and beneficiaries of the plan shall be deemed to be for a purpose which is in the best interests of the Corporation.

The right of indemnification provided in this Article VIII shall not be exclusive of or affect any other rights to which any Trustee, director or officer may be entitled under any agreement, statute, vote of Members or otherwise. The Corporation's obligation to provide indemnification under this Article VIII shall be offset to the extent of any other source of indemnification of any otherwise applicable insurance coverage under a policy maintained by the Corporation or any other person. Nothing contained in the Article shall affect any rights to which employees and corporate personnel other than Trustees, directors or officers may be entitled by contract, by vote of the Board or of the Executive Committee or otherwise.

ARTICLE IX—DISSOLUTION

The consent of every Trustee shall be necessary to effect a dissolution of the Marine Biological Laboratory. In case of dissolution, the property shall be disposed of in such a manner and upon such terms as shall be determined by the affirmative vote of two-thirds of the Trustees then in office in accordance with the laws of the Commonwealth of Massachusetts.

ARTICLE X—MISCELLANEOUS PROVISIONS

A. Fiscal Year. Except as otherwise determined by the Trustees, the fiscal year of the Corporation shall end on December 31st of each year.

B. Seal. Unless otherwise determined by the Trustees, the Corporation may have a seal in such form as the Trustees may determine, from time to time.

C. Execution of Instruments. All checks, deed, leases, transfers, contracts, bonds, notes and other obligations authorized to be executed by an officer of the Corporation in its behalf shall be signed by the Director or the Treasurer except as the Trustees may generally or in particular cases otherwise determine. A certificate by the Clerk or an Assistant Clerk, or a temporary Clerk, as to any action taken by the Members, Board of Trustees or any officer or representative of the Corporation shall as to all persons who rely thereon in good faith be conclusive evidence of such action.

D. Corporate Records. The original, or attested copies, of the Articles of Organization, Bylaws and records of all meetings of the Members shall be kept in Massachusetts at the principal office of the Corporation, or at an office of the Corporation's Clerk or resident agent. Said copies and records need not all be kept in the same office. They shall be available at all reasonable times for inspection by any Member for any proper purpose, but not to secure a list of Members for a purpose other than in the interest of the applicant, as a Member, relative to the affairs of the Corporation.

E. Articles of Organization. All references in these Bylaws to the Articles of Organization shall be deemed to refer to the Articles of Organization of the Corporation, as amended and in effect, from time to time.

F. Transactions with Interested Parties. In the absence of fraud, no contract or other transaction between this Corporation and any other corporation or any firm, association, partnership or person shall be affected or invalidated by the fact that any Trustee or officer of this Corporation is pecuniarily or otherwise interested in or is a director, member or officer of such other corporation or of such firm, association or partnership or is a party to or is pecuniarily or otherwise interested in such contract or other transaction or is in any way connected with any person or persons, firm, association, partnership, or corporation pecuniarily or otherwise interested therein; provided that the fact that he or she individually or as a director, member or officer of such corporation, firm, association or partnership is such a party or is so interested shall be disclosed to or shall have been known by the Board of Trustees or a majority of such Members thereof as shall be present at a meeting of the Board of Trustees at which action upon any such contract or transaction shall be taken; any Trustee may be counted in determining the existence of a quorum and may vote at any meeting of the Board of Trustees for the purpose of authorizing any such contract or transaction with like force and effect as if he/she were not so interested, or were not a director, member or officer of such other corporation, firm, association or partnership, provided that any vote with respect to such contract or transaction must be adopted by a majority of the Trustees then in office who have no interest in such contract or transaction.

Reference: *Biol. Bull.* **181:** 72–80. (August, 1991)

Ethel Browne, Hans Spemann, and the Discovery of the Organizer Phenomenon

HOWARD M. LENHOFF

Department of Developmental and Cell Biology, University of California, Irvine, California 92717

Abstract. Ethel Browne Harvey (1885–1965) will be familiar to some as a researcher on the embryology of sea urchins. Few, however, know her as Ethel Browne who, as a graduate student, published, in 1909, a remarkable paper demonstrating for the first time the induction by a transplant of a secondary axis of polarity in the host. This process was later named "organization" by Spemann and Mangold (1924) in a paper that led to Spemann's being awarded the Nobel Prize. Why did the Nobel Committee, or other embryologists for that matter, not connect Browne's discovery with that of Spemann and Mangold? Did they consider the development of hydra as being too remote from that occurring in embryos of vertebrates? Did the 1909 paper of Ethel Browne in any way influence the thinking of Spemann or Mangold, although it was never referred to in any of Spemann's papers? In light of new information about Spemann's knowledge of Browne's work, we also can ask a number of questions about the interplay of basic prejudices in the reception accorded Browne's work.

Introduction

Ethel Browne Harvey (1885–1965) (Fig. 1) is perhaps best known to biologists for her research on sea urchin eggs, and especially for her use of the centrifuge to separate the egg into nucleated and enucleated parts. These and many of her other contributions are summarized in her classic volume, *The American* Arbacia *and Other Sea Urchins* (1956).

Long-time associates of the Marine Biological Laboratory (MBL) at Woods Hole, Massachusetts, may remember her as a summer researcher on sea urchins, as a trustee of the Laboratory, and as only the third woman to deliver a prestigious Friday Evening Lecture at the MBL, in 1944. Her husband was the Princeton physiologist, E. Newton Harvey, known for his pioneering work on bioluminescence.

Ethel Browne received her graduate training at Columbia University (1906–1913). While there, she was very productive, having published six papers, and was greatly influenced by T. H. Morgan and E. B. Wilson. Her dissertation, under Wilson's guidance, was a cytological study of the male gametes of the aquatic hemipteran, *Noctonecta*. She participated in and initiated a number of other studies, and was a junior author on a short note about selective fertilization with T. H. Morgan (Morgan *et al.*, 1910).

Students of the biology of hydra, however, will think of Ethel Browne as the first person to demonstrate that a transplant could induce a secondary axis of polarity in a host (Browne, 1909). A similar process in amphibian embryos was later named "organization" by Spemann and Mangold (1924). The story of that work by Ethel Browne, and some unanswered questions about how her findings were received, are the subject of this paper.

The experiments reported in her remarkable 1909 paper were carried out during "the winters of 1906–1908," and in the first paragraph of that paper she acknowledges T. H. Morgan for his "kind interest and help." She then describes a series of carefully planned and executed experiments on hydra. These experiments appear homologous to the Nobel Prize experiments of Spemann and Mangold (1924), if we consider the mouth tissue of the diploblastic hydra to be developmentally like that of the lip of the blastopore of the amphibian embryo. Why did the Nobel Committee not recognize her discovery? Did it consider the hydra's development too remote from that occurring in embryos of vertebrates? Although it was never referred to in any of Spemann's papers, did the 1909 paper of

Received 9 October 1990; accepted 30 April 1991.

Figure 1. Ethel Browne Harvey (1885–1965). Taken in 1928; from the Archives of the Library, Marine Biological Laboratory, Woods Hole, Massachusetts.

Ethel Browne in any way influence the thinking of Spemann or Mangold? These and related questions are quite provocative in light of new information about Spemann's knowledge of Browne's work.

I will first discuss the similarities between the Nobel Prize experiments of Spemann and Mangold (1924) in which the process of embryonic induction (*i.e.* the organizer phenomenon) was demonstrated, and the 1909 work of Ethel Browne, in which she showed that a piece of hydra mouth tissue grafted to another hydra would induce the formation of a secondary axis of polarity in the recipient.

Second, I will consider newly discovered evidence showing that Spemann was aware of Browne's work long before Hilde Mangold (nee Proescholdt) began her famous organizer experiments. In addition, there is the provocative information that Mangold had worked on hydra immediately before initiating her work on amphibian embryos.

Finally, this case study raises questions about the possible interplay of basic prejudices: (1) those of medical scientists in general, and the Nobel Committee in particular, in using anthropocentric criteria when evaluating research in the biological sciences; and (2) those of male scientists in evaluating the research of female scientists, especially the work of female graduate students or of females who have no significant academic rank.

The Nobel Prize Experiment of Spemann and Mangold

Mangold's experiment involved taking a piece of the lip of the blastopore of the gastrula stage of the amphibian embryo and grafting it to the wall (flank) of another gastrula at a site distant from the host blastopore (Fig. 2). In some cases, she actually grafted the lip tissue, and in other cases simply slipped the lip tissue into the host's blastocoel. Further, to prove that the transplanted tissue actually induced changes in those of the host, Mangold took the transplant from a pigmented embryo of one species and grafted it to an unpigmented embryo of another species.

The results, of course, were remarkable and unexpected. The small piece of grafted tissue "*organized*" the tissue next to it in the host, "*inducing*" it to develop a secondary axis of polarity so that the original tissue of the host developed into two embryos rather than one (Fig. 2).

This discovery rocked the world of embryology. Hilde Mangold, in the laboratory of Hans Spemann, had shown that a piece of embryonic tissue was capable of inducing adjacent tissue to develop in a specific manner. From that moment, the search for the nature of "the organizer" was on, and for years biologists would carry out a variety of imaginative experiments, hoping to identify the organizing principle (see Hamburger, 1988). None succeeded until recently. It now appears that Melton and his associates (*e.g.,* see Ruiz i Altaba and Melton, 1989) have shown that peptide growth factors affect homeobox genes. Their findings may provide a key to understanding the elusive "organizer" in frogs.

What, then, were the experiments of Ethel Browne (1909), and how similar were they to those of Spemann and Mangold (1924)?

Key Discovery of Ethel Browne on Induction in Hydra

Ethel Browne (1909) described how the hypostomal tissue (*i.e.,* the tissue making up the mouth area of a hydra), when grafted at a certain site in the body wall of another hydra, gave "the necessary stimulus to call forth the development of a new hydranth" at that site (Fig. 3).

Although she did not use the word "organizer" in reporting her findings, her experiments describe, for the first time, the induction or "organization" of a secondary axis of polarity. Furthermore, if we consider the diploblastic,

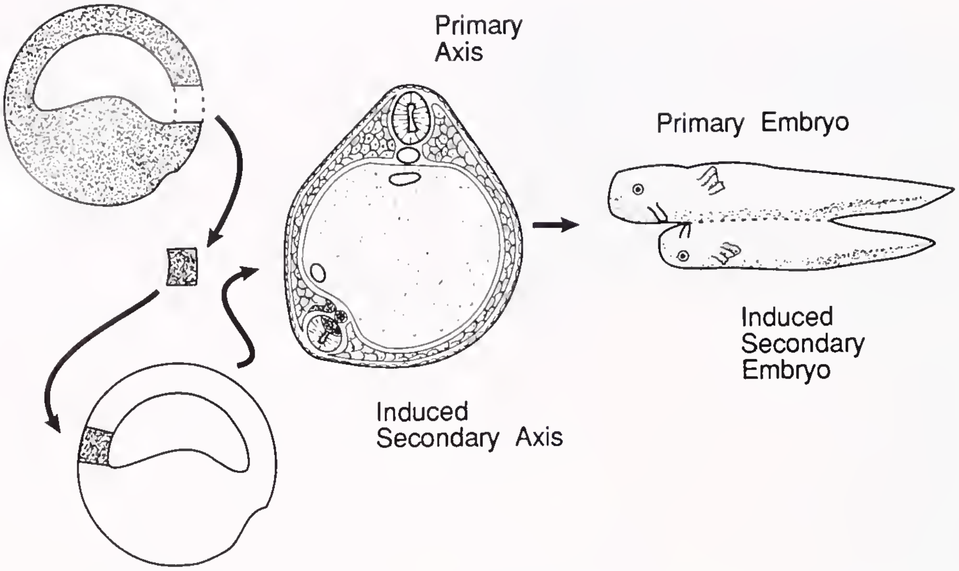

Figure 2. Mangold-Spemann transplantation experiment. Mangold removed the dorsal lip of the blastopore from a donor amphibian embryo (stippled), grafted it to the flank of a host embryo, and thereby induced a secondary axis of polarity in the host that eventually developed into a secondary embryo.

sac-like hydra as a diploblastic gastrula with a ringlet of tentacles emanating from the lips surrounding the "blastopore," her results bear a remarkable resemblance to those of the organizer experiments that Spemann and Mangold (1924) reported 15 years later using amphibian embryos.

Structure and Development of the Diploblastic Hydras

Before reviewing Browne's key experiments in detail, it is important to understand the basic structure and development of hydras. The hydra is a simple diploblastic epithelial animal made up of two cell layers—the ectoderm and endoderm—separated by a thin basal membrane called the mesoglea (Fig. 4). At one end of the animal is the "hydranth," the part involved in feeding (the capture and ingestion of prey). Between the ringlet of tentacles on the hydranth is the mouth, an opening made up of tissue called the hypostome (Fig. 4).

The hydra can reproduce asexually, by producing a bud at about the middle of its tubular body (Fig. 5A). Once

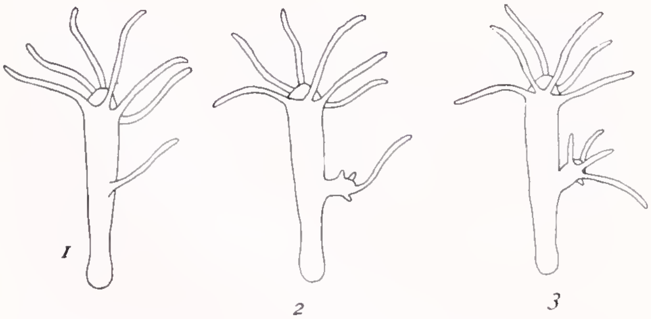

Figure 3. Browne transplantation experiment with hydra. Browne removed a piece of the hypostome (see Fig. 4) with a single tentacle (as a label) from a donor hydra, grafted it to the flank of a host hydra (#1), and thereby induced a secondary axis of polarity in the host (#2) which eventually developed into a secondary hydranth (see Fig. 4). The figures are those of Browne (1909).

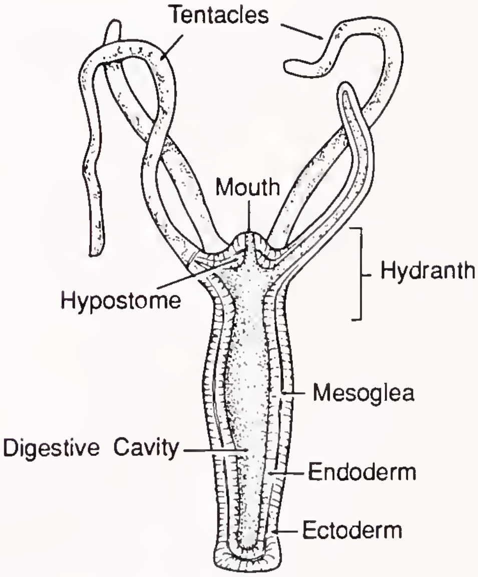

Figure 4. Diagram of a hydra illustrating its major structures.

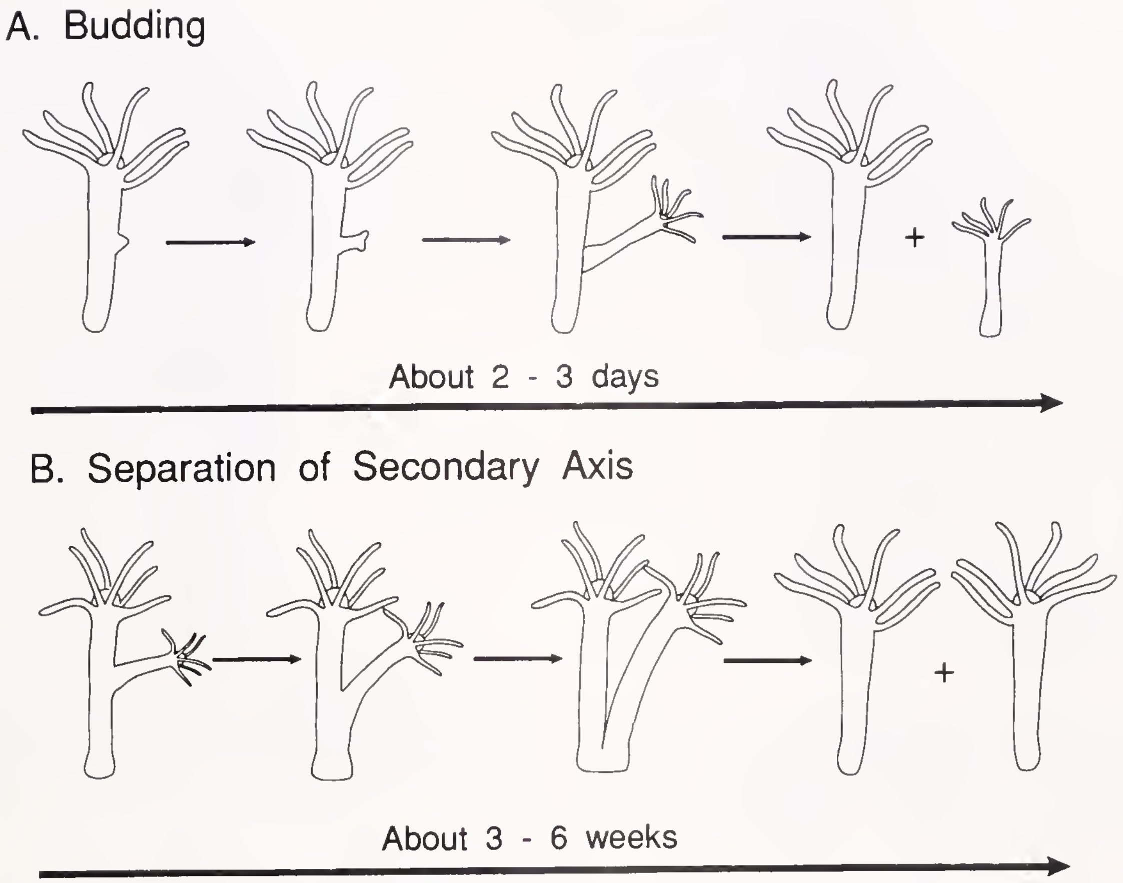

Figure 5. Difference between budding (A) and separation of a secondary axis of polarity (B) in hydra. The secondary axis of polarity can be established by the induction method of Browne described in the text, or by a kind of longitudinal fission, which can occur naturally or be initiated by cutting the upper half a hydra partway down the middle of the body column.

this bud starts to form, it will normally develop a basal disc at the point of junction between the bud and parental body tube and will detach from the parental body tube as a small, fully developed hydra within 2–3 days.

Some species of hydra are diecious; others are monecious. The gonads are usually not present when the animal is reproducing asexually by budding, and they appear at different times in different species. The zygote then develops into a miniature diploblastic hydra that is structurally homologous to a diploblastic gastrula of a number of invertebrates (Fig. 6; Brien, 1965). Note, however, that the embryo of hydra does not develop by the classically described process of the invagination of a blastula, but rather by a process similar to a delamination of cell layers (Brien, 1965).

Ethel Browne's Basic Experiments

In her first induction experiments, Browne removed a piece of the hypostome with a tentacle attached to it to serve as a marker, and grafted that tissue to various sites along the body wall of another hydra of the same species. She found that only when the hypostomal tissue (with the tentacle) was grafted to about the center of the body tube, a "new hydranth regenerated there." That new hydranth initially had one long tentacle, the one from the grafted tissue (Fig. 3).

Within a few days, this second hydranth developed a mouth and tentacles and became a secondary axis of polarity to the body of the host hydra. This new hydranth, with its accompanying body, was not a bud. Recall that a new bud develops a basal disc ("foot") and detaches from the parent stalk within 2–3 days after developing (Fig. 5A). The secondary hydranth induced in Ethel Browne's experiment, to the contrary, remained on the parental body tube for weeks before it eventually separated by a sort of longitudinal fission (*e.g.*, Fig. 5B). Browne's experiment is simple to perform; I have repeated it several times with very little difficulty.

Figure 3 shows clearly that a new hydranth was induced and that it developed a secondary axis of polarity by drawing out with it some more parental tissue. Browne asked the key question as to whether the transplanted tissue actually induced the formation of a new hydranth, or whether the cells of the transplanted tissue multiplied and then, themselves, formed the new hydranth.

To test these two possibilities, Browne devised an elegant but simple experiment involving pigmented and nonpigmented tissues. As a transplant, she used tissue taken from a green hydra the intracellular algae of which had been removed by a process described two years earlier by Whitney (1907). Normally the endodermal cells of the green *Hydra viridissima* are laden with symbiotic green algae. The host tissue in Browne's experiment was such a green hydra of the same species. Through this experiment involving the use of a piece of nonpigmented tissue transplanted to a pigmented host of the same species, Browne showed conclusively that the pigmented host tissue was organized by the nonpigmented transplant to develop into a hydranth and a secondary axis of polarity (Fig. 7).

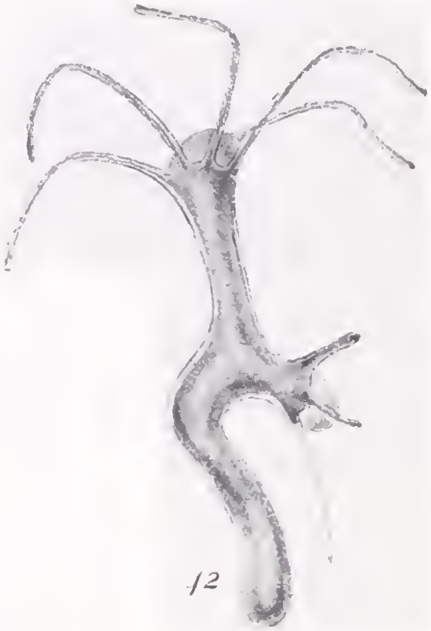

Figure 7. Result of Browne's experiment in which she grafted, as donor, a piece of the hypostome and a tentacle taken from a "green" hydra whose algae had been removed, to the flank of a green hydra that still contained its endosymbiotic algae. The transplant induced a pigmented secondary axis of polarity in the host. The figure is that of Browne, 1909.

Browne did numerous other experiments proving that it was only the hypostomal tissue (analogous to the lip of the blastopore of a gastrula) that would induce the formation of both a hydranth and a secondary axis of polarity. As she said, "it depends . . . entirely on the differentiation of the grafted material." That is to say, only the hypostomal tissue had this organizing capacity, not other tissues of hydra, such as a tentacle. Since the publication of Browne's paper (1909), a number of other investigators have used her findings in their experiments describing the developmental capacities of hydra tissues (*e.g.*, Yao, 1945; Webster and Wolpert, 1966).

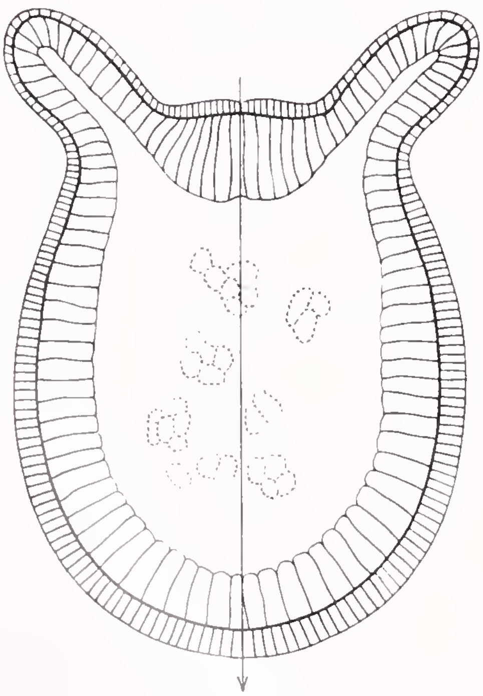

Figure 6. A young hydra just as it emerged from the embryo (Brien, 1965).

Was Either Spemann or Mangold Aware of Browne's Experiments Before Beginning Theirs?

The close analogies between the experiments of Browne (1909) and the Nobel Prize experiments of Spemann and Mangold (1924) are manifest. Both papers showed that tissue taken from specific regions of an organism or embryo, when transplanted, could organize the adjoining host tissue and induce it to form a secondary axis of polarity that is similar, in most respects, to the primary axis of polarity. But more importantly, through the use of pigmented and nonpigmented tissues, both sets of experiments proved conclusively that a true organization occurred, and not a growth and reorganization of the transplanted tissues. Browne's experiment was even more conclusive because she used pigmented and nonpigmented tissues from organisms of the same species,

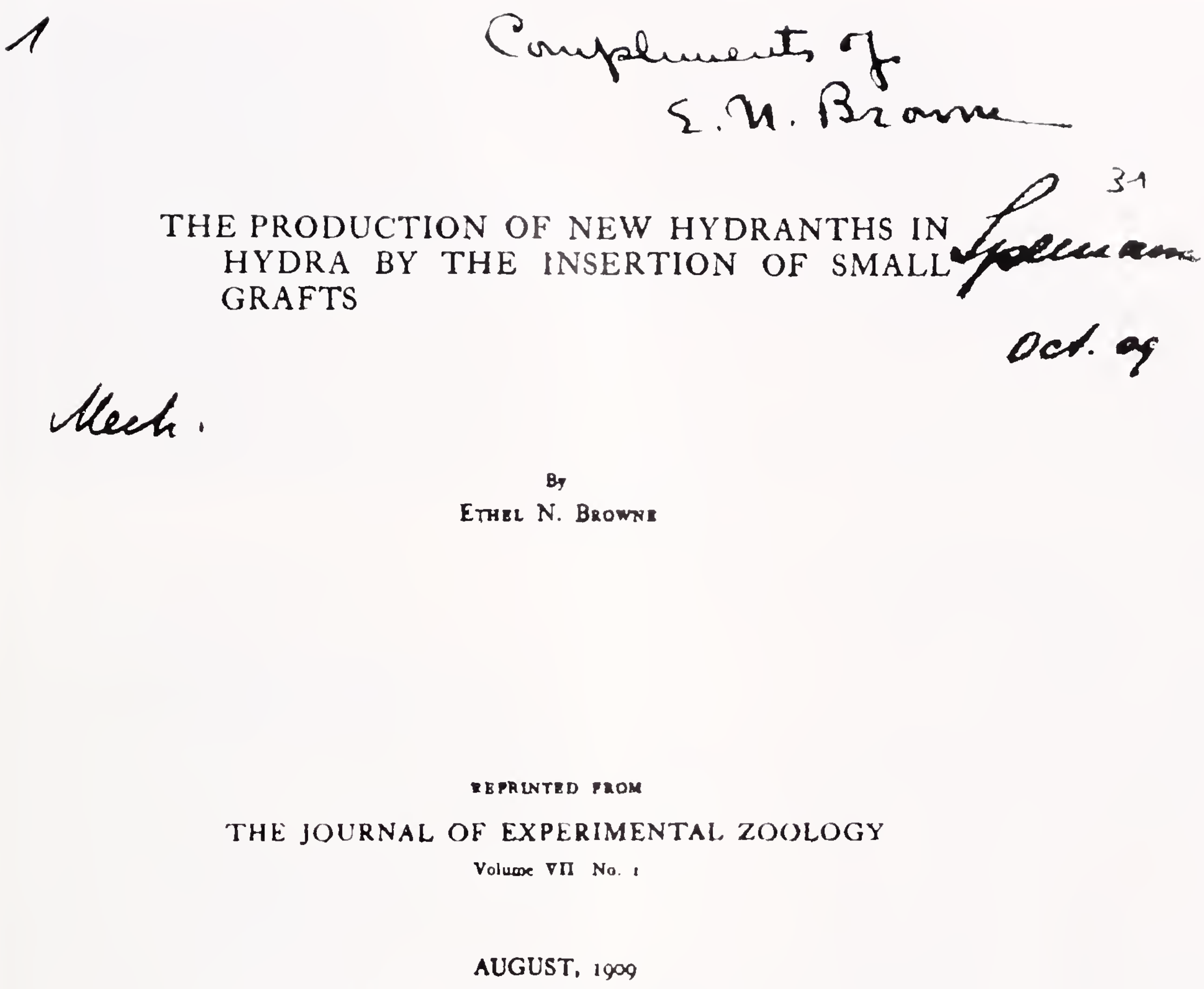

1

Compliments of
E. N. Browne

31

THE PRODUCTION OF NEW HYDRANTHS IN HYDRA BY THE INSERTION OF SMALL GRAFTS

Spemann

Oct. 09

Mech.

By
Ethel N. Browne

REPRINTED FROM
THE JOURNAL OF EXPERIMENTAL ZOOLOGY
Volume VII No. 1

AUGUST, 1909

Figure 8. Cover page of reprint of Browne's 1909 paper found in Spemann's reprint collection.

whereas Spemann and Mangold (1924) used tissues taken from two different species.

Recently, in a roundabout way, I received conclusive evidence that Hans Spemann was aware of Browne's paper as early as a few months after its publication. The information came to my attention as a result of a paper on Abraham Trembley published in *Scientific American* (Lenhoff and Lenhoff, 1988). In response to that paper, we received kind letters from a number of scholars, among them Professor K. Sander of the Albert-Ludwigs-Universität in Freiberg. Professor Sander is the current Director of the University's Institute for Biology (Zoology), once directed by Spemann. In his letter (30 May 1988), Professor Sander stated that, at Spemann's suggestion, Hilde Mangold's original thesis topic was to repeat Trembley's experiment of turning hydra inside out, then following the fate of the ectoderm and endoderm in the inverted animals. Spemann, we know, was a biologist of great breadth, and, as Viktor Hamburger (1988) has noted, Spemann was aware of Trembley's famous inversion experiment and wanted to see if, after a hydra was inverted, its ectoderm would be converted to endoderm, and vice versa. Spemann apparently had no trouble in considering hydra's two cell layers as analogous to the ectoderm and endoderm of embryos. It was only after Mangold's attempts to invert hydra failed that, according to Hamburger (1988), Spemann suggested that she transplant the dorsal lip of one newt gastrula to the flank of another newt gastrula.

Responding to Sander's letter, I asked if he could find any evidence that Spemann had been aware of Browne's experiments on hydra (*i.e.*, those published in 1909). Professor Sander replied (11 July 1988) with two pages of photocopied material. The first shows the cover page of Browne's reprint found in Spemann's collection (Fig. 8). Note that the paper by Browne had a published date of

August 1909 and that Spemann, under his signed name, wrote the date "October, '09." In the upper right corner is Ethel Browne's signature after the courteous, sometimes routine, "Compliments of." Thus we know that a reprint of Ethel Browne's paper was in Spemann's possession soon after her paper was published, and that it was in his reprint collection.

From this single piece of evidence, we cannot say conclusively that Spemann read the paper first in the journal, was interested in it, and wrote (or had someone write) for a reprint. Although I find it hard to believe that, in 1909, a graduate student, on her own, would send her reprint unsolicited to a distinguished professor, that may have been the case. Perhaps because her paper dealt with the induction phenomenon, Browne may have sent the paper to Spemann unsolicited because he had published in that field earlier (Spemann, 1901). Or, because T. H. Morgan was acquainted with many European embryologists, she may have sent the paper to Spemann at Morgan's suggestion. Another scenario would be more typical: Spemann saw the paper, read it (or parts of it), and wrote to Browne for a reprint.

The other photocopied item sent to me by Professor Sander is the only page of the article having any markings (Fig. 9). Only one phrase is underlined—one containing the word "induced"—and it is accompanied by an exclamation mark in the margin. This is the only place in Browne's entire paper where she used the word "induced;" elsewhere she used such expressions as "stimulated to form." (Interestingly, she used the word "induced" regarding a case in which induction did not, and, as she proved, could not occur.) Nonetheless, even the presence of this underlining is not absolute proof that Spemann got some ideas from Browne, for we have no way of knowing with certainty whether it was Spemann himself who entered the underlining, nor when the underlining was done. But would a graduate student, postdoctoral fellow, or a visiting scholar have marked the Professor's reprint? More likely Spemann himself underlined the word "induced," for he had been working on lens induction since the turn of the century (Spemann, 1901).

As a related interpretation, one critic has suggested that Spemann may have underlined the phrase "induced to form" and entered the exclamation mark because he was peeved that Browne did not refer to his earlier work on lens induction (1901). If we accept that interpretation, then we also would have to accept that Spemann had read her paper and must have believed that Browne had truly observed a case of induction, albeit a remarkable one in which a secondary axis of polarity was induced.

From the evidence on hand, however, we can only conclude that: (1) Spemann was a man of some breadth who was familiar with the zoological, as well as the embryological literature; (2) he possessed a signed reprint of Browne's paper and received it soon after it was published; (3) someone underlined the only phrase in the paper that contained the word "induced"; (4) Spemann considered the freshwater hydra a suitable experimental system for the study of development; and (5) at his suggestion, Hilde Proescholdt (Mangold) had been working on hydra immediately before she began her research on the newt. All else remains speculation.

Was Spemann Influenced in any way by Browne's Findings?

We cannot be sure. For the sake of argument, however, let us assume that Spemann was influenced by Browne's work, and that he saw the direct link between Browne's findings and his own. If such was the case, was Spemann the sort of person who would acknowledge such a debt?

Horder and Weindling (1985, p. 204), in their article titled "Hans Spemann and the Organiser," attempt to analyze the complex nature of the man as a scientist and as an individual who had "a strong sense of nationalism." They write, "Spemann confessed in moments of humility that he was often prone to forget relevant literature which had earlier impressed him. . . ." From my limited search of the literature, I can find no reference to Ethel Browne in any of Spemann's publications (*e.g.*, Spemann, 1938).

We can get a little more insight into Spemann's personality from an interesting anecdote revealed by Viktor Hamburger in his book on *The Heritage of Experimental Embryology: Hans Spemann and the Organizer* (1988). Hamburger notes that Spemann did not put his name on papers originating from the thesis research of his graduate students, at least he did not in the cases of Hamburger and Holtfreter. With Mangold, however, Spemann not only put his name on the publication that reported the results of her thesis research, but, despite her protests (ac-

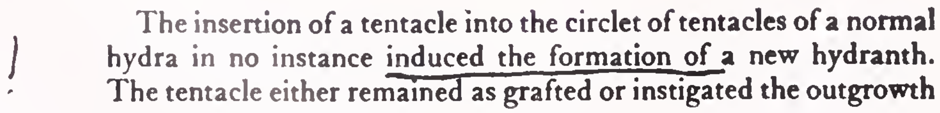

!

The insertion of a tentacle into the circlet of tentacles of a normal hydra in no instance induced the formation of a new hydranth. The tentacle either remained as grafted or instigated the outgrowth

Figure 9. Only excerpt showing underlining in reprint of Browne's 1909 paper found in Spemann's reprint collection.

cording to Hamburger), he even insisted on putting his name first. Some think he did the correct thing; Hamburger (1988) writes that "Spemann was perfectly right in claiming precedence . . . [because] she apparently did not fully realize the significance of her results." I could argue, however, that Mangold, who had been working on hydra just a few years earlier (Hamburger, 1988), was aware of the literature on hydra including Browne's 1909 paper, recognized the significance of Browne's experiment using pigmented and nonpigmented tissues, and, independently of Spemann, decided to conduct a similar experiment using her amphibian embryos. Mangold died in an explosion of a gasoline heater in her kitchen in 1924, the same year that her classic paper was published. She never lived to learn that her thesis work had led to a Nobel Prize.

The Nobel Prize

Mangold did not share the Nobel Prize with Spemann because the Prize is never awarded posthumously. But should not Ethel Browne have shared in the prize? I believe so; her results were essentially the same as those of Spemann and Mangold, and her published work preceded theirs by 15 years. How could the Nobel Committee have known about Ethel Browne's work if Spemann never referred to it? The usual way—by reading the literature, or by having as advisors scholars who knew the literature. But if they had read her paper, would they have recognized its significance? Probably not; most biologists of the time (and thereafter) failed to recognize the significance of Ethel Browne's extraordinary findings.

Are there other reasons why Ethel Browne's discovery was little heralded? Did the members of the Nobel Committee selecting the awardee for the prize in physiology and medicine at that time recognize primarily those discoveries that had obvious connections with human health and development? As such, was research that had some conspicuous anthropocentric connection more often recognized? Did this oversight reflect the regressive aspects of overspecialization, in that a developmental finding in an organism past the embryonic state was not considered important to embryology? (Only in recent times have we seen graduate programs and books categorized as "developmental biology," rather than as embryology alone.) Was Ethel Browne's work ignored because she was a woman with no significant station in academe?

I have presented this story to one national meeting[1] in the United States and to one international congress[2] in Great Britain. In both instances the paper polarized the audiences, even though most agreed that the experiments of Ethel Browne, like those of Hilde Proescholdt Mangold, demonstrated the phenomenon of induction of a secondary axis of polarity. Some felt that Ethel Browne's discovery was neglected, either because she was a woman graduate student, or because it was not made on a vertebrate embryo.

Opposing arguments went as follows. (1) Her work was ground-breaking, but she really did not understand the significance of her findings. (2) If she did not use the word "organizer," then she did not discover the phenomenon. (3) She was a graduate student and did what a graduate student is supposed to do: the work suggested by her mentor. (4) "I knew her for years at Woods Hole, and not once did she ever mention to me her experiments on hydra."

From reading Browne's paper closely, it seems abundantly clear that she understood the significance of her findings. In fact, if we accept the possibility that she sent her paper to Spemann unsolicited, then this would be evidence that she did understand that her findings dealt with induction. When I presented this paper in Southampton, England, Dr. Sears Crowell, a long-time researcher on hydroids at the MBL, made a comment regarding Ethel Browne Harvey that he subsequently repeated in a letter dated 3 August 1989:

> We happened to meet as she was leaving the MBL [Marine Biological Laboratory] building where she had a lab. Somewhat out of the blue she said: "You know that it was I who first discovered the organizer." Not an exact quotation. I replied that I did recognize that this was indeed the case. . . .

Ethel Browne Harvey died 2 September 1965. There is an obituary in *The Biological Bulletin* (Vol. **133:** 11). It does not mention her transplants with hydra.[3]

Acknowledgments

I thank Dr. Richard Campbell for pointing out the paper by Paul Brien to me, Dr. Klaus Sander for uncovering the reprint of Ethel Browne's paper in the collection of the late Hans Spemann, and Dr. Sears Crowell for his letter recalling his conversation with Ethel Browne Harvey. For editorial comments, I thank my colleagues at the Developmental Biology Center at the University of California, Irvine, and especially my wife and colleague,

---

[1] Historical Session of the American Society of Zoologists, San Francisco, California, December 1988.

[2] Historical Session of the Fifth International Congress of Coelenterate Biology, Southampton, England, July 1989.

[3] Crowell noted that the last year that Ethel Browne Harvey was listed as an investigator at the Marine Biological Laboratory was 1962. He guessed that the date of his conversation with her was in the "late summer of 1961 or 1962."

Sylvia G. Lenhoff who, like Ethel Browne, was a graduate of Goucher College of Maryland.

Literature Cited

Browne, E. 1909. The production of new hydranths in hydra by the insertion of small grafts. *J. Exp. Zool.* **7:** 1–37.

Brien, P. 1965. L'Embryogenèse et la sénescence de l'Hydre d'eau douce. *Mémoires, Académie royale Belgique, Classe des Sciences,* Tome XXXVI, Fascicule 1. Pp. 7–113. [Fig. 54 D on p. 77]

Hamburger, V. 1988. Hilde Mangold, co-discoverer of the organizer. Appendix in *The Heritage of Experimental Biology: Hans Spemann and the Organizer.* Oxford University Press, New York. Pp. xii + 198.

Harvey, E. B. 1956. *The American* Arbacia *and Other Sea Urchins.* Princeton University Press, Princeton, New Jersey. Pp. viii + 298.

Horder, T. J., and P. J. Weindling. 1985. Hans Spemann and the Organiser. Pp. 183–242 in *A History of Embryology,* Horder, T. J., J. A. Witowski, and C. C. Wylie, eds. Cambridge University Press, Cambridge. Pp. xxiv + 477.

Lenhoff, H. M., and S. G. Lenhoff. 1988. Trembley's polyps. *Sci. Am.* **256:** 108–113.

Morgan, T. H., F. Payne, and E. N. Browne. 1910. A method to test the hypothesis of selective fertilization. *Biol. Bull.* **18:** 76–78.

Ruiz i Altaba, A., and D. A. Melton. 1989. Interaction between peptide growth factors and homeobox genes in the establishment of antero-posterior polarity in frog embryos. *Nature* **341:** 33–38.

Spemann, H. 1901. Über Korrelationen in der Entwicklung des Auges. *Verh. Anat. Ges.* 15 Vers. Bonn, Pp. 61–79. (from Spemann, 1938)

Spemann, H. 1938. *Embryonic Development and Induction.* Reprinted in 1967 by Hafner Publishing Co., New York. Pp. xii + 401.

Spemann, H., and H. Mangold. 1924. Über Induktion von Embryonanlagen durch Implantation artfremder Organisatoren. *Arch. Mikr. Anat. Entw. Mech.* **100:** 599–638.

Webster, G., and L. Wolpert. 1966. Studies on pattern regulation in hydra. I. Regional differences in time required for hypostome determination. *J. Embryol. Exp. Morphol.* **16:** 91–104.

Whitney, D. D. 1907. Artificial removal of green bodies of *Hydra viridis. Biol. Bull.* **13:** 291–299.

Yao, T. 1945. Studies on the organizer problem in *Pelmatohydra oligactis* I. The induction potency of the implants and the nature of the induced hydranth. *J. Exp. Zool.* **21:** 147–150.

Reference: *Biol. Bull.* **181:** 81–94. (August, 1991)

Relative Contributions of the Egg Layer and Egg Cordon to Pheromonal Attraction and the Induction of Mating and Egg-laying Behavior in *Aplysia*

SHERRY D. PAINTER, MARIA G. CHONG, MARY A. WONG, ANN GRAY,
JEFFRY G. CORMIER, AND GREGG T. NAGLE

*The Marine Biomedical Institute and the Department of Anatomy and Neurosciences,
University of Texas Medical Branch, Galveston, Texas 77550-2781*

Abstract. Many species of the opisthobranch mollusk *Aplysia* form breeding aggregations during the reproductive season. The aggregations contain both mating and egg-laying animals, and are associated with egg cordons. Although pheromones play a significant role in developing and maintaining the aggregations, little is known about the active factors. Behavioral studies have shown that egg-laying animals are more attractive than nonlaying animals, have shorter latencies to mating, and induce conspecifics to lay eggs. As a first step toward isolating and chemically characterizing the active factors, we examined the relative importance of the egg layer and egg cordon as sources of pheromonal activity in *Aplysia brasiliana*. T-maze experiments showed that both animal-derived and cordon-derived factors are attractive, and that the animal-derived factors are specifically associated with egg layers. Extracts of the atrial gland—an exocrine organ secreting into the oviduct—increased the attractiveness of nonlaying animals when placed in the surrounding seawater, suggesting that the "cordon-derived" aggregation pheromones may be products of the atrial gland. Mating studies showed that both animal-derived and cordon-derived factors induce mating, and that the animal-derived factors are associated with both egg layers and nonlayers. In contrast, neither animal-derived nor cordon-derived factors induced egg laying. Comparable results were obtained with either one or two animals in the chamber, suggesting that the accessibility of a potential mate did not influence the results. The lack of effect may result from the low-probability nature of egg-laying activity.

Introduction

Pheromones appear to play an important role in coordinating reproductive activities in the marine opisthobranch mollusk *Aplysia.* Field studies of both *A. californica* (Kupfermann and Carew, 1974; Audesirk, 1979) and *A. fasciata* (Susswein *et al.*, 1983, 1984) indicate that these simultaneous hermaphrodites are solitary animals during most of the year. During the summer reproductive season, however, they move into breeding aggregations or "brothels." The aggregations are typically associated with recently deposited egg cordons, often laid one on top of another, and contain both mating and egg-laying animals. Most of the egg-laying animals simultaneously mate as females, even though mating does not cause reflex ovulation (*A. brasiliana,* Blankenship *et al.*, 1983), suggesting that egg laying may precede mating in the aggregations rather than result from it.

This sequence of activities is important because of the reproductive physiology of *Aplysia.* Four characteristics of the system are worth noting. First, *Aplysia* are non-self-fertilizing hermaphrodites that store large amounts of exogenous sperm for future use (*A. californica,* MacGinitie, 1934). Second, many species of *Aplysia* lay egg cordons containing from one to several million fertilized eggs (*e.g., A. californica,* MacGinitie, 1934; *A. depilans* and *A. fasciata,* Thompson and Bebbington, 1969; *A. dactylomela* and *A. juliana,* Switzer-Dunlap and Hadfield, 1977). In these species, a single bout of egg laying significantly reduces the amount of exogenous sperm stored, although the stores are not depleted. Third, animals lay

Received 20 December 1990; accepted 16 April 1991.

Abbreviations: AGE, atrial gland extract; AG-LE, atrial gland-like epithelium; ASW, artificial seawater; BCP, bag-cell peptide; ELH, egg-laying hormone.

eggs regardless of whether sperm are available to fertilize them (*A. californica*, MacGinitie, 1934), suggesting that there is not a strong internal link between the amount of exogenous sperm stored and egg deposition. Finally, sperm are transferred between animals in an immature state, and cannot immediately fertilize the recipient's oocytes (*A. depilans, A. fasciata*, and *A. punctata*, Thompson and Bebbington, 1969). Mating as a female during, or shortly after, egg deposition thus ensures that mature and capacitated sperm will be available to fertilize oocytes during future egg-laying episodes.

Laboratory experiments suggest that the egg layer or its egg cordon are potential sources of pheromones that attract conspecifics and induce mating activity (*A. brasiliana*, Aspey and Blankenship, 1976; Jahan-Parwar, 1976; Painter *et al.*, 1989; *A. californica*, Jahan-Parwar, 1976; Audesirk, 1977); there is also evidence suggesting that they induce egg laying (*A. californica*, Audesirk, 1977) and may be responsible for the masses of egg cordons associated with the aggregations. Since mating animals are no more attractive than nonmating animals (*A. dactylomela*, Lederhendler *et al.*, 1977) and mating does not cause reflex ovulation (*A. brasiliana*, Blankenship *et al.*, 1983), the layer-derived or cordon-derived factors are likely to be responsible for developing and maintaining the breeding aggregations.

Although relatively little is known about pheromonal regulation of any component of *Aplysia* reproductive activity, a great deal is known about the neuroendocrine regulation of one component—egg laying. The bag cells, two clusters of neurosecretory cells located at the rostral margin of the abdominal ganglion (*A. californica*, Frazier *et al.*, 1967; *A. brasiliana*, Blankenship and Coggeshall, 1976) are part of the final common pathway leading to egg deposition. These normally quiescent cells periodically enter a prolonged phase of rapid and synchronous electrical activity (*A. californica*, Kupfermann and Kandel, 1970; *A. brasiliana*, Dudek and Blankenship, 1977) which releases several peptides into the connective tissue sheath surrounding the bag-cell clusters and abdominal ganglion (*A. californica*, Stuart *et al.*, 1980); this activity is consistently followed by egg laying (*A. brasiliana*, Dudek *et al.*, 1979). Most of the released peptides have been isolated and chemically characterized, including the ovulation-inducing egg-laying hormone (ELH) (*A. californica*, Chiu *et al.*, 1979; *A. brasiliana*, Nagle *et al.*, 1988a) and the autocrine alpha bag-cell peptide (αBCP) (*A. californica*, Rothman *et al.*, 1983).

The bag-cell products that have been characterized to date are all encoded by the ELH gene, one member of a small family of structurally related genes that are expressed in a tissue-specific manner in *Aplysia* (*A. californica*, Scheller *et al.*, 1983; Mahon *et al.*, 1985). Each gene encodes a precursor protein containing a sequence homologous to ELH and one or more sequences homologous to αBCP. Although the gene sequences are highly conserved (*ca.* 90% identity), the resulting precursor proteins are processed into homologous but nonidentical sets of peptides with similar pharmacological properties but different physiological functions.

Several ELH-related genes are expressed in the atrial gland (*A. californica*, Scheller *et al.*, 1983; Mahon *et al.*, 1985), an exocrine organ secreting into the oviduct of *Aplysia* (*A. californica*, Arch *et al.*, 1980; Beard *et al.*, 1982; Painter *et al.*, 1985). Although extracts of this organ induce egg laying when injected into receptive animals (*A. californica*, Arch *et al.*, 1978), the exocrine nature of its secretory activity indicates that the atrial gland products do not function as hormones to induce egg laying. Recent behavioral studies suggest that the atrial gland products may function as sexual pheromones instead (Painter *et al.*, 1989; also see Susswein and Benny, 1985). Peptide products of a small family of structurally related genes may thus act as nonsynaptic neurotransmitters, neurohormones, and pheromones to regulate and coordinate both male and female reproductive activities.

The studies presented in this paper examine the relative contributions of the egg layer and its cordon to pheromonal attraction and to the pheromonal induction of both mating and egg-laying activity. They demonstrate that the egg cordon plays an important role in both attraction and induction of mating, and suggest that products of the atrial gland may contribute to these activities.

Materials, Methods, and Results

Animals

Specimens of *Aplysia brasiliana* (Rang), weighing from 100 to 400 g, were collected from South Padre Island, Texas, and were used in experiments between June and August, the normal reproductive season for this species. *Aplysia brasiliana* was selected as the experimental animal because it lays eggs and mates more frequently than *A. californica* (Pinsker and Parsons, 1985), and can be collected in large numbers from the south Texas coast during the reproductive season. The animals were housed in individual cages in one of five large aquaria containing recirculating artificial seawater (ASW; Instant Ocean, Aquarium Systems, Mentor, Ohio) at room temperature (20 ± 2°C); the salinity ranged from 30 to 32 ppt. A 14:10 light:dark cycle was maintained, with the light period starting at 6 am; animals were fed dried laver in the late afternoon (4–6 pm) after experiments were completed.

Specimens of *Aplysia californica* (Cooper) were purchased from Alacrity Marine Biological Services (Redondo Beach, California) and were used as a source of atrial glands for extracts. They were maintained as described above for *A. brasiliana*, except that the ASW was cooled to 14 ± 2°C.

Atrial gland extracts

Sexually mature individuals of *Aplysia californica* were used as sources of tissue for extracts because the atrial gland in this species is large and well-defined; the homologous organ in *A. brasiliana* [the atrial gland-like epithelium (AG-LE)] is a thin band of secretory tissue that extends along the length of the oviduct and is difficult to recognize except in fixed or sectioned material (Painter *et al.*, 1985). Both organs secrete into the oviduct (Painter *et al.*, 1985), and there is evidence that their peptide products are highly conserved: (1) extracts of either organ induce egg laying when injected into receptive animals of either species (Painter *et al.*, 1985; also see Blankenship *et al.*, 1983); (2) secretory granules of either organ are specifically labeled by antisera raised against low molecular weight peptides isolated from the *A. californica* atrial gland (Painter *et al.*, 1985); and (3) restriction enzyme maps of the ELH-related genes in the two species suggest a high degree of sequence identity (Nambu and Scheller, 1986).

In most cases, the extracts were used as a tool to induce egg laying—0.1 ml of an ASW extract of the gland was injected through the foot into the hemocoel, and egg deposition began within approximately 30 min. Extracts were prepared by removing atrial glands (approximately 100 mg wet weight per gland) from 10 animals and homogenizing them in 10 ml of filtered ASW with a Brinkmann Polytron homogenizer (setting 4 for 1 min at 4°C). The homogenate was centrifuged at 1500 × *g* for 30 min at 4°C, the supernatant removed, and aliquots frozen at −20°C until use.

Since previous studies have shown that acidic extracts of the *A. californica* atrial gland induce *A. brasiliana* to mate (Painter *et al.*, 1989), acidic extracts of the *A. californica* atrial gland were directly assayed for pheromonal attractiveness in *A. brasiliana*. In this case, atrial glands were removed from 10 animals and homogenized in 15 ml of 1 *M* acetic acid containing 20 m*M* HCl with a Brinkmann Polytron homogenizer (setting 4 for 1 min at 4°C). The homogenate was centrifuged at 48,000 × *g* for 20 min at 4°C, the supernatant removed, and the pellet rehomogenized in 5 ml of the acidic medium. After centrifugation, the supernatants were combined, distributed into 20 aliquots, lyophilized, and stored at −20°C until use. Each lyophilized aliquot was resuspended in 1 ml of ASW immediately before addition to the maze, and was equivalent to approximately 50% of the material in one gland.

Pheromonal attraction

Apparatus. A T-maze (Fig. 1A) was constructed of clear Plexiglas (0.62 cm thick) and sealed with clear aquarium cement; it was cured for several days in ASW before use. Experiments were performed in a room adjacent to the aquarium facility with overhead fluorescent lighting; the maze was positioned so that the lighting was uniform throughout the apparatus.

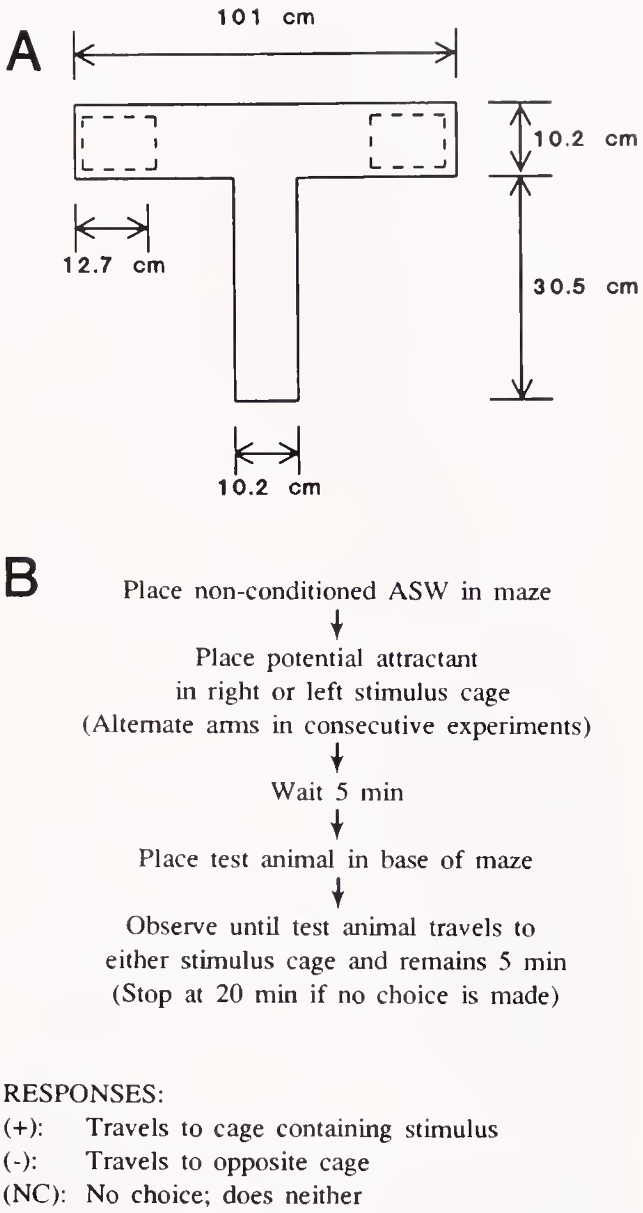
A
101 cm
10.2 cm
12.7 cm
30.5 cm
10.2 cm
B
Place non-conditioned ASW in maze
Place potential attractant
in right or left stimulus cage
(Alternate arms in consecutive experiments)
Wait 5 min
Place test animal in base of maze
Observe until test animal travels to
either stimulus cage and remains 5 min
(Stop at 20 min if no choice is made)
RESPONSES:
(+): Travels to cage containing stimulus
(-): Travels to opposite cage
(NC): No choice; does neither

Figure 1. (A) Schematic diagram of the T-maze with removable stimulus cages (dashed outlines) in place. T-maze depth: 10.2 cm. (B) Flow diagram of the experimental protocol.

Experimental protocol and statistical analyses. In a typical experiment (Fig. 1B), 6 l of aerated ASW that had not previously contacted an *Aplysia* ("non-conditioned ASW") was placed in a cleaned and air-dried maze. A potential attractant, usually consisting of a "stimulus" animal with or without an egg cordon or extract, was placed in a perforated plastic cage in one arm. A nontreated sexually mature "test" animal was placed in the base of the maze 5 min later. Both the stimulus and test animals were briefly rinsed in non-conditioned ASW before being introduced into the maze. A response was considered to be positive if the test animal travelled to the stimulus within 20 min and remained in contact with the stimulus cage for 5 min, negative if it travelled to the opposite arm and remained for 5 min, and no choice if it did neither. Animals were choosing between a stimulus and no stimulus in these experiments, rather than between two qualitatively or quantitatively different stimuli. Fifteen experiments were performed for each potential attractant, and the attractant was alternated between arms in consecutive experiments. Statistical significance was assessed by χ^2 analyses.

Animals. A total of 183 *Aplysia brasiliana* individuals were used in these studies. All were sexually mature—they laid eggs spontaneously or in response to injections of atrial gland extract—and all had been observed mating before they were separated into individual cages. Four criteria were used to select animals for each experiment: (1) the animal must not have laid eggs during the preceding 24 h; (2) the animal must not have participated in a behavioral experiment during the preceding 24 h; (3) the animal must not have been a test animal for the stimulus being studied; and (4) the test and stimulus animals must have been housed in the same aquarium. Egg layers were animals that had been injected with atrial gland extract to induce egg laying and, unless otherwise specified, had completed laying eggs within the preceding 30 min; nonlayers were animals that had not laid eggs during the preceding 24 h. Only nonlayers were used as test animals; both egg layers and nonlayers were used as stimulus animals.

Results. To assess directional bias and chance levels of attraction in the maze, 15 experiments were performed in which no stimulus was placed in either arm. Four of the animals (26.7%) moved to the left arm and remained, three (20%) moved to the right arm and remained, while eight (53.3%) did neither (Fig. 2), demonstrating that there is no directional bias in the maze and establishing chance levels of attraction at 3–4 animals (20–26.7%).

A similar level of attraction (3 animals; 20%) and pattern of responses was observed when a nonlaying conspecific without an egg cordon was the stimulus (Fig. 2). The two sets of responses were not significantly different [$\chi^2(2) = 0.14$; $0.90 < P < 0.95$], demonstrating that nonlayers without egg cordons are not attractive to *Aplysia brasiliana*. A higher level of attraction (12 animals; 80%) and lower level of no-choice responses (1 animal; 6.7%) was observed when the stimulus was a conspecific that was actively laying eggs (Fig. 2). This pattern of responses was significantly different from that to nonlaying animals without egg cordons [$\chi^2(2) = 34.12$; $P < 0.005$], demonstrating that egg-laying animals are attractive.

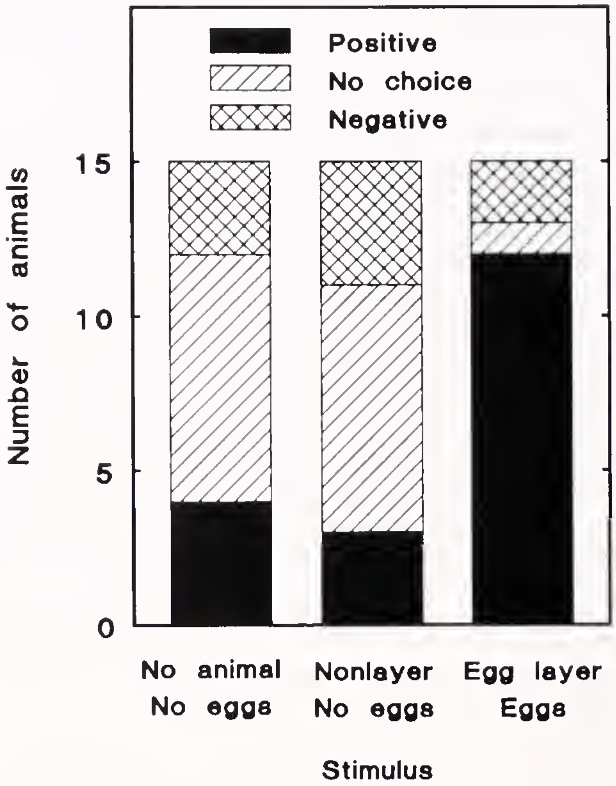

Figure 2. There is no directional bias in the T-maze, as indicated by the distribution of responses to the no-stimulus control (no animal, no eggs): approximately equal numbers of animals travelled to the left and right arms of the maze. (Note: for this quantification, movement to the left was defined as a positive response and movement to the right a negative response.) *Aplysia brasiliana* is not attracted to nonlaying animals without egg cordons: the response pattern did not differ significantly from that observed with the no-stimulus control [$\chi^2(2) = 0.14$; $0.90 < P < 0.95$]. *A. brasiliana* are attracted to egg-laying conspecifics with egg cordons, however: the level of attraction and pattern of responses differed significantly from those observed when a nonlayer without eggs was the stimulus [$\chi^2(2) = 34.12$; $P < 0.005$]. This bar graph is based on 15 no-stimulus control experiments and 30 single-arm experiments, 15 each for "nonlayer, no eggs" and "egg layer, eggs"; in the single-arm experiments, animals were choosing between a stimulus in one arm and no stimulus in the other.

Because the "egg-laying animal" stimulus has two components—the egg layer and its egg cordon—subsequent experiments focused on their relative contributions to pheromonal attraction. More animals were attracted to egg layers without egg cordons than had been attracted to nonlayers without egg cordons, and fewer made no choice (Fig. 3); the difference in response patterns was statistically significant [$\chi^2(2) = 15.38$; $P < 0.005$], demonstrating that the egg layer is a source of aggregation pheromones. Identical results were obtained when a nonlayer with a recently deposited egg cordon was used as the stimulus (Fig. 3), indicating that the egg cordon is also

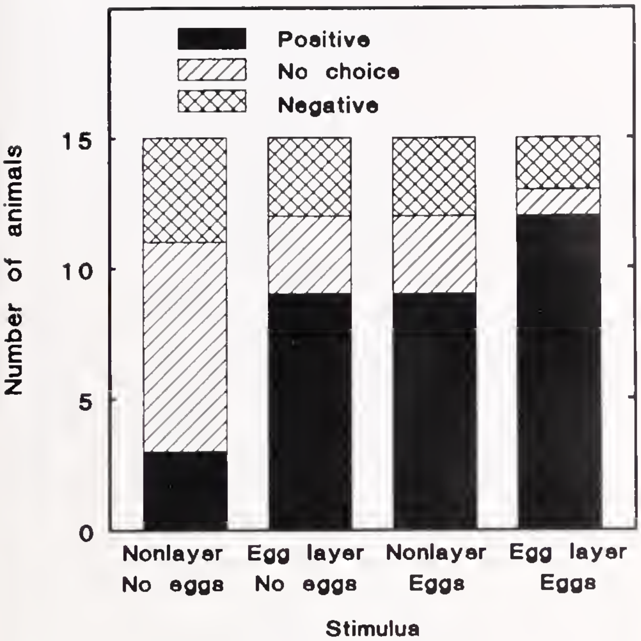

Figure 3. Egg layers are attractive to *Aplysia brasiliana:* a larger number of animals was attracted to an egg layer without eggs than was attracted to a nonlayer without eggs, and the patterns of responses to the two stimuli are significantly different [$\chi^2(2) = 15.38$; $P < 0.005$]. Egg cordons are also attractive to *A. brasiliana:* a larger number of animals was attracted to a nonlayer with eggs than was attracted to a nonlayer without eggs, and the response patterns are significantly different [$\chi^2(2) = 15.38$; $P < 0.005$]. The effects of egg layers and egg cordons are not additive at the concentrations tested: the response patterns for a nonlayer with eggs and an egg layer without eggs are identical, and do not differ significantly from the pattern obtained for an egg layer with eggs [$\chi^2(2) = 2.83$; $0.25 < P < 0.50$]. This bar graph is based on 60 single-arm experiments, 15 per stimulus; in each experiment, animals were choosing between a stimulus in one arm and no stimulus in the other.

a source of pheromonal activity. Neither pattern differed significantly from that obtained for an egg-laying animal with an egg cordon [$\chi^2(2) = 2.83$; $0.10 < P < 0.25$], demonstrating that the effects of the layer-derived and cordon-derived factors are not additive at the concentrations tested.

Subsequent experiments examined whether animal-derived factors are required for the attractiveness of the egg cordon and whether the attraction is visually mediated. Two series of experiments were performed. In the first, an egg cordon without any animal served as the stimulus. The level of attraction and pattern of responses were identical to those obtained using an egg layer and its cordon as the stimulus (Figs. 3, 4), demonstrating that egg cordons are sufficient to attract conspecifics. In the second series of experiments, a "sham" cordon (a tangled mass of silastic tubing; vol = 2 ml) served as the stimulus. The level of attraction and pattern of responses differed significantly from those observed with the egg cordon [$\chi^2(2) = 15.27$; $P < 0.005$], but did not differ from those observed in no-stimulus control experiments [Fig. 4; $\chi^2(2) = 1.70$; $0.25 < P < 0.50$]. The differential responses to egg cordons and sham cordons suggests that the attraction is chemically rather than visually mediated. The results of these two series of experiments, in conjunction with those reported above, demonstrate that both egg layers and egg cordons are sufficient to attract conspecifics, but that neither is uniquely required.

As a first step toward identifying tissue sources of the cordon-derived aggregation pheromones, acidic extracts of the atrial gland (equivalent to 50% of the material in one gland) were assayed for the ability to increase the attractiveness of a nonlaying animal when placed in the surrounding ASW. A higher level of attraction to nonlaying animals and lower level of no-choice responses was observed when the extract was present (Fig. 5); the dif-

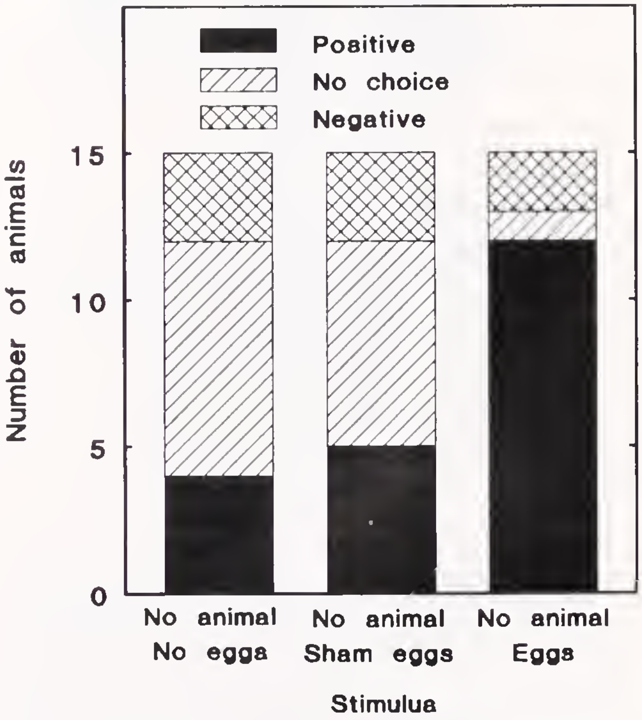

Figure 4. Animals are not required for an egg cordon to be attractive to *Aplysia brasiliana:* a larger number of animals was attracted to an egg cordon without an animal than was attracted to a sham cordon without an animal, and the response pattern was significantly different [$\chi^2(2) = 15.27$; $P < 0.005$]. The sham cordon was a tangled mass of silastic tubing, 2 ml in volume. The attractiveness of an egg cordon is not visually mediated: the pattern of responses to a sham cordon without an animal did not differ significantly from the no-stimulus control (no animals, no eggs) [$\chi^2(2) = 1.70$; $0.25 < P < 0.50$]. (Note: for the no-stimulus control, movement to the left was defined as a positive response and movement to the right a negative response.) This bar graph is based on 15 no-stimulus control experiments and 30 single-arm experiments, 15 each for "no animal, sham eggs" and "no animal, eggs"; in the single-arm experiments, animals were choosing between a stimulus in one arm and no stimulus in the other.

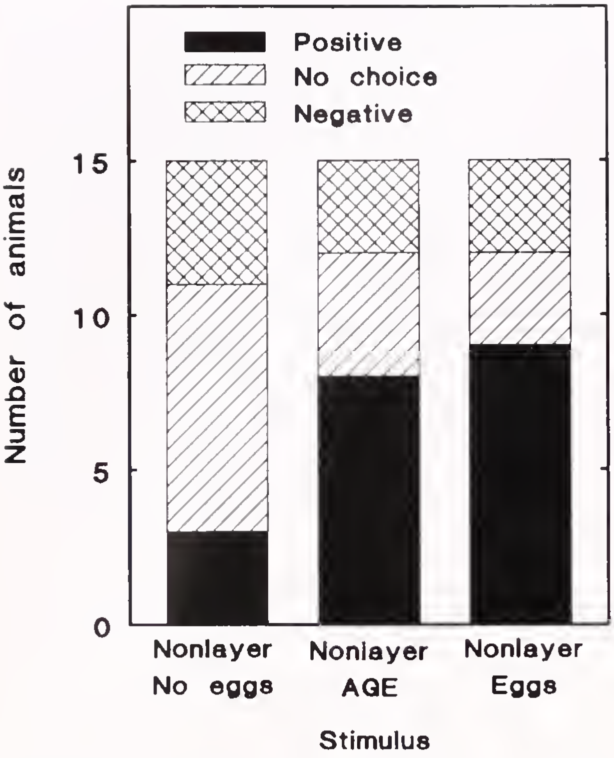

Figure 5. Secretory products of the *Aplysia californica* atrial gland (or *A. brasiliana* AG-LE) may contribute to the attractiveness of an egg cordon. The number of animals attracted to a nonlayer was increased when an extract of the *A. californica* atrial gland (AGE) was placed in the surrounding ASW. The pattern of responses differed significantly from that observed for a nonlaying animal without eggs [$\chi^2(2) = 10.58$; $P < 0.01$], but did not differ significantly from that for a nonlaying animal with eggs [$\chi^2(2) = 0.44$; $0.90 < P < 0.95$]. This bar graph is based on 45 single-arm experiments, 15 per stimulus; in each experiment, animals were choosing between a stimulus in one arm and no stimulus in the other.

ference in response patterns was significant [$\chi^2(2) = 10.58$; $P < 0.01$]. Interestingly, the level of attraction and pattern of responses did not differ significantly from those obtained when a recently deposited conspecific egg cordon was placed in the same location [Fig. 5; $\chi^2(2) = 0.44$; $0.75 < P < 0.90$], suggesting that products of the *A. californica* atrial gland (or *A. brasiliana* AG-LE) might significantly contribute to the attractiveness of an egg cordon.

Induction of mating activity

Animals. A pool of 205 sexually mature *Aplysia brasiliana* individuals was used in these studies. Small plastic fish tags (11 mm in diameter; Howitt Plastics, Molalla, Oregon) were sutured to the caudal region of the right parapodium so that individuals could be identified. Four criteria were used to select animals for each experiment: (1) the animal must not have laid eggs during the preceding 24 h; (2) the animal must not have participated in a behavioral experiment during the preceding 24 h; (3) the animal must not have been tested with the stimulus; and (4) all of the animals in an experiment must have been housed in the same aquarium. Once selected, the animals were randomly assigned to treatments. All experiments were begun between 9 and 10 am, because there is evidence of a circadian rhythm in *Aplysia* mating behavior (*A. fasciata*, Susswein *et al.*, 1983, 1984).

Relative contributions of the egg layer and egg cordon: experimental protocol and statistical analyses. Eight animals were used in each experiment (Fig. 6). One animal was injected with 0.1 ml of atrial gland extract and placed in a 4-l plastic beaker containing 3 l of aerated non-conditioned ASW; this treatment induced egg laying, usually within 30 min, and the egg layer conditioned the ASW in the beaker. A second animal was handled and placed in an identical beaker; this treatment did not induce egg laying, but the nonlayer conditioned the ASW. When the injected animal finished laying eggs (70.3 ± 4.1 min after injection; mean ± S.E.M.), it was removed, rinsed in fresh non-conditioned ASW and transferred to a third beaker; the handled animal was treated in the same way and transferred to a fourth beaker. Nontreated animals were then distributed among the four beakers so that each contained two animals. The resulting experimental conditions are: (1) two nonlayers in animal-conditioned ASW with an egg cordon; (2) two nonlayers in animal-conditioned ASW without an egg cordon; (3) one egg layer and one nonlayer in non-conditioned ASW without an egg cordon; and (4) two nonlayers in non-conditioned ASW without an egg cordon.

The reproductive activity of each individual was assessed at 10-min intervals for 270 min. Three categories of mating activity were recognized (male, female, and simultaneous hermaphrodite); egg-laying activity was also recorded, but courtship was not. For calculation purposes, animals that did not mate or lay eggs during the observation period were assigned a 280-min latency for that activity. Although this approach underestimates the difference in mean latency to mating between strongly positive and control conditions, the effect is relatively small because at least 85% of the animals mated in every experimental condition tested. Statistical significance was assessed by a one-way analysis of variance, followed by Duncan's multiple range test for pairwise comparisons. When time courses of mating activity were compared, statistical significance was assessed by χ^2 analysis of individual time points. Egg cordon volume was measured at the end of each experiment by ASW displacement in a graduated cylinder and averaged 1.7 ml (1.7 ± 0.2 ml; mean ± S.E.M.). Twenty experiments were performed in this series.

Results. Animal-conditioning the ASW with a nonlaying animal resulted in an increase in the percentage of

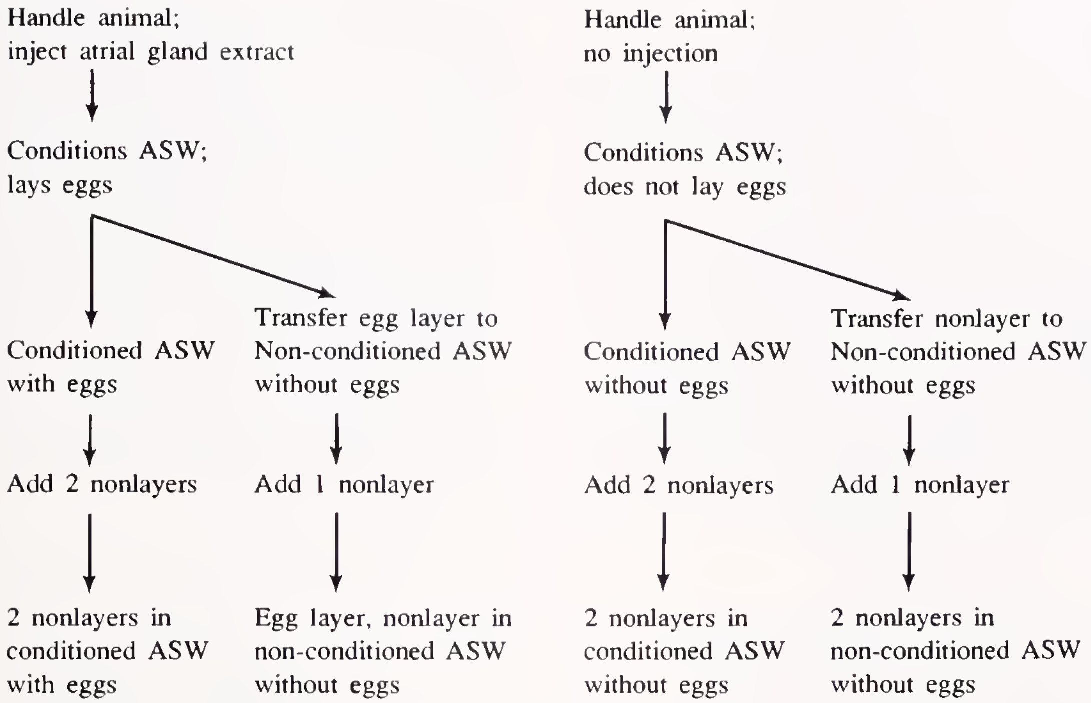
Handle animal; inject atrial gland extract
Conditions ASW; lays eggs
Conditioned ASW with eggs
Transfer egg layer to Non-conditioned ASW without eggs
Add 2 nonlayers
Add 1 nonlayer
2 nonlayers in conditioned ASW with eggs
Egg layer, nonlayer in non-conditioned ASW without eggs
Handle animal; no injection
Conditions ASW; does not lay eggs
Conditioned ASW without eggs
Transfer nonlayer to Non-conditioned ASW without eggs
Add 2 nonlayers
Add 1 nonlayer
2 nonlayers in conditioned ASW without eggs
2 nonlayers in non-conditioned ASW without eggs

Figure 6. Flow diagram of the protocol used in the first series of mating experiments. One animal was injected with an extract of the atrial gland to induce egg laying and placed in a beaker containing aerated non-conditioned ASW; a second animal was handled and placed in a second beaker containing aerated non-conditioned ASW. When egg deposition was complete, the egg layer was transferred to a third beaker and the handled nonlayer to a fourth beaker. Additional nontreated animals were then distributed among the four beakers so that each contained a pair of *Aplysia;* the resulting experimental conditions are indicated at the bottom of the diagram. Mating and egg-laying behaviors were scored at 10-min intervals for 270 min; animals failing to exhibit a behavior during the observation period were assigned a 280-min latency for calculations.

animals mating at early time periods relative to non-conditioned ASW controls (Fig. 7A); the difference was statistically significant at three time periods—40, 50, and 60 min [$\chi^2(1) > 3.84$ for each; $P < 0.05$]. The mean latency to mating was also reduced (Fig. 7B), but did not differ significantly from that of the non-conditioned ASW controls ($P = 0.29$; one-way analysis of variance). It is important to note that these effects, although small, were consistently observed when the ASW was animal-conditioned. Comparable results were obtained in an independent series of experiments performed in our laboratory (A. R. Gustavson, unpubl. data). The studies used a different pool of *A. brasiliana* and animal-conditioned the ASW for 60 rather than 70 min, but produced quantitatively similar responses. A higher percentage of animals mated at early time periods relative to the non-conditioned ASW controls [$\chi^2(1) \geq 3.84$ at 30, 40, 70, 80, 90, 100, and 110 min; $P \leq 0.05$ for each]; the mean latency to mating was reduced, but the change was not statistically significant ($P = 0.28$; one-way analysis of variance). The consistency of these two sets of results suggests that animal-derived factors induce mating, but that their activity or concentration is relatively low under the conditions tested. The idea that animal-derived factors induce mating in *Aplysia* is consistent with a recent report in the literature that the amount of time that *A. fasciata* spend mating is a function of the number of animals available as copulatory partners (Ziv *et al.,* 1989) and thus, presumably, a function of the concentration of animal-derived factors in the ASW.

Similar, but quantitatively larger, effects were observed when the ASW was animal-conditioned by an egg layer and contained an egg cordon (Fig. 7A, B). The percentage of animals mating at early time periods was increased relative to non-conditioned ASW controls, and the difference was statistically significant for every observation period from 10 through 110 min [$\chi^2(1) \geq 3.84$ for each; $P \leq 0.05$]. The mean latency to mating was significantly reduced ($P = 0.002$; one-way analysis of variance). Assuming that animal-conditioning the ASW with an egg layer is comparable to animal-conditioning with a nonlayer (see below), these results demonstrate that cordon-derived factors induce mating, and suggest that the effects of the animal-derived and cordon-derived factors may be additive.

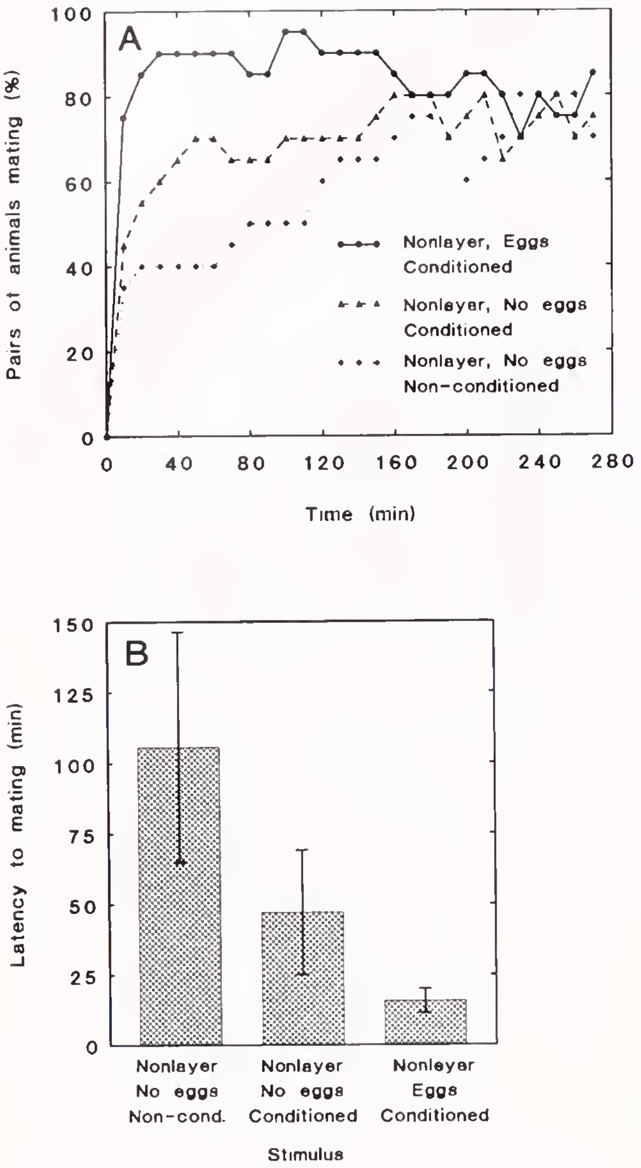

Figure 7. Both animal-derived and cordon-derived factors induce mating activity in *Aplysia brasiliana* (A) The percentage of animals mating at early time periods was increased by animal-conditioning the ASW with a nonlaying animal; the difference was significant at 40, 50, and 60 min [$\chi^2(1) > 3.84$; $P < 0.05$]. The percentage was further increased by animal-conditioning the ASW with an egg-laying animal and leaving the egg cordon in the ASW; the percentages were significantly higher than those obtained in non-conditioned ASW without an egg cordon at every observation period from 10 through 110 min [$\chi^2(1) > 3.84$ for each; $P < 0.05$]. The experimental protocol is shown in Figure 6 (n = 20 experiments). Because *Aplysia* tend to mate in bouts lasting approximately 60 min and the bouts are often separated by periods during which no mating occurs (Leonard and Lukowiak, 1987), it is not possible to read a mean latency to mating directly from this graph. (B) The latency to mating (mean ± S.E.M.) was reduced by animal-conditioning the ASW with a nonlaying animal, but the difference was not statistically significant ($P = 0.29$; one-way analysis of variance). The latency was further reduced in animal-conditioned ASW with an egg cordon, and differed significantly from that obtained for non-conditioned ASW without an egg cordon ($P < 0.002$; one-way analysis of variance).

Animals did not distinguish between recent egg layers and nonlayers in non-conditioned ASW without an egg cordon. There were no significant differences in the time courses of mating activity (Fig. 8A), in the latencies to mating (Fig. 8B), or in the sexual role first assumed by the animals (Table I). These results suggest that there is not a prolonged change in the motivational state of the egg layer (*i.e.*, an increase in receptivity to courtship) that persists in the absence of an egg cordon. More importantly, they suggest that the egg cordon, rather than the egg layer, may be primarily responsible for the relatively short latencies to mating observed when animals are actively laying eggs. The experiments did not address the question of whether specific layer-derived or animal-derived factors are required for the induction of mating by egg cordons, however, and this issue was examined in the next series of experiments.

Induction of mating by egg cordons in non-conditioned ASW: experimental protocol and statistical analyses. Five animals, selected as described above, were used in each experiment (Fig. 9). One was injected with atrial gland extract and placed in a beaker to lay eggs. When deposition was complete, the egg cordon was removed, quickly rinsed, and transferred to a second beaker containing non-conditioned ASW; a pair of animals was then placed in this beaker and another pair placed in a third beaker that contained only non-conditioned ASW. The resulting experimental conditions are: (1) two nonlayers in non-conditioned ASW with an egg cordon; and (2) two nonlayers in non-conditioned ASW without an egg cordon. Reproductive behavior was assessed for each animal at 10-min intervals for 270 min and analyzed as in the preceding experiments. Egg volume was measured after each experiment and averaged 2.0 ml (2.0 ± 0.3 ml; mean ± S.E.M.). Fifteen experiments were performed.

Results. Placing a recently deposited egg cordon in the non-conditioned ASW surrounding two nonlaying animals significantly increased the percentage of animals mating in 9 of the first 14 observation periods [Fig. 10A; $\chi^2(1) \geq 3.84$ at 20–40 min, 70 min, and 100–140 min; $P \leq 0.05$ for each], and significantly reduced their mean latency to mating relative to the control group (Fig. 10B; $P < 0.01$; one-way analysis of variance). These results demonstrate that cordon-derived factors alone are sufficient to induce mating.

Induction of egg-laying activity

Egg deposition was also monitored in the experiments described above. Neither animal-derived nor cordon-derived factors significantly affected the percentage of animals laying eggs (Table II), and the low percentages made calculations of mean latency to deposition meaningless. Because *Aplysia brasiliana* lays eggs more frequently when

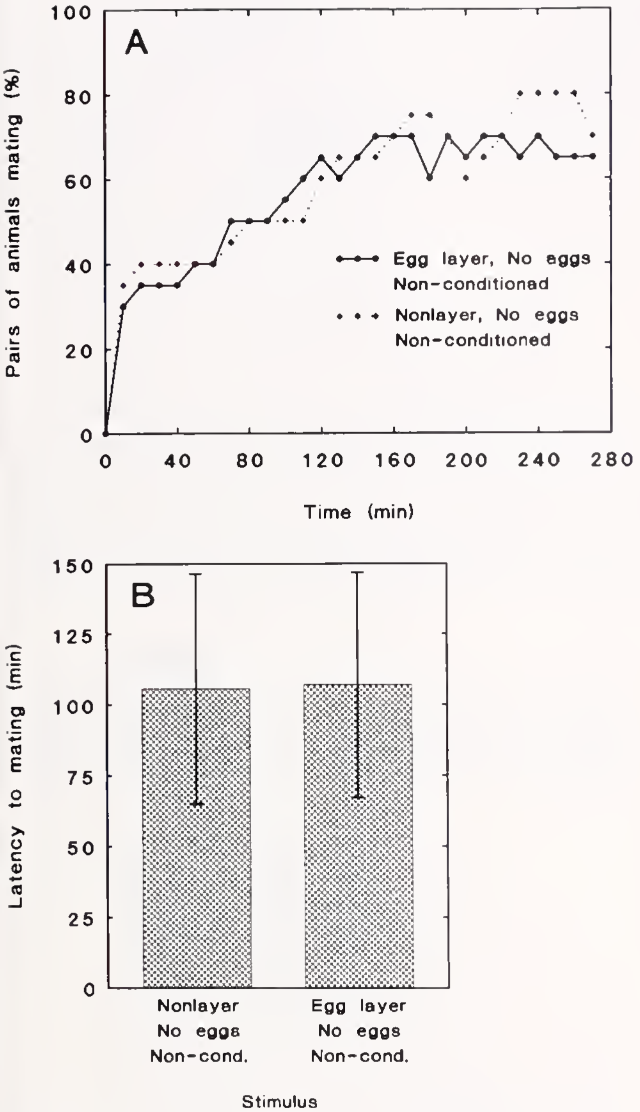

Figure 8. *Aplysia brasiliana* does not distinguish between recent egg layers and nonlayers in non-conditioned ASW without an egg cordon. (A) Recent egg layers and nonlayers mated at the same frequency in non-conditioned ASW without an egg cordon. The experimental protocol is shown in Figure 6 (n = 20 experiments). (B) There is no difference in mean latency to mating between recent egg layers and nonlayers in non-conditioned ASW without an egg cordon.

caged alone rather than in pairs (Blankenship *et al.*, 1983), the experiments were repeated with one animal in each beaker rather than two.

Single-animal experiments: protocol. Four test animals, selected as described in the mating studies, were used in each experiment. One was placed in each of four beakers and egg-laying activity assessed at 10-min intervals for 270 min. The ASW in each beaker contained a different combination of animal-derived and cordon-derived factors: (1) non-conditioned ASW without an egg cordon (negative control); (2) non-conditioned ASW with an egg cordon (cordon-derived factors only); (3) animal-conditioned ASW without an egg cordon (animal-derived factors only); and (4) animal-conditioned ASW with an egg cordon (both animal-derived and cordon-derived factors). The conditions in each beaker were established as described in the section on mating (see Figs. 6 and 9). The volumes of the stimulus egg cordons were measured at the end of every experiment and averaged 3.2 ml (3.2 ± 0.6 ml; mean ± S.E.M.). In five experiments, all animals that were not induced to lay eggs were injected with atrial gland extract to verify that they were physiologically competent to do so; all laid egg cordons in response to the injection, demonstrating that the experimental conditions were not interfering with the activity.

Results. Neither animal-derived nor cordon-derived factors had a significant effect on egg deposition (Table II).

Discussion

Pheromonal attraction

These studies have shown that *Aplysia brasiliana* is not attracted to nonlaying animals in the absence of an egg cordon. The results contrast with those of Lederhendler and colleagues (1977), which showed that *Aplysia dactylomela* is attracted to nonlaying conspecifics and that the magnitude of the attraction increases as the number of stimulus animals increases. We do not know whether the difference reflects species differences or whether it results from differences in experimental design (*e.g.*, from differences in concentration produced by using 5-min rather than 60-min conditioning periods), and we have not examined the possibility that a group of nonlaying *A. brasiliana* would be attractive. We have, however, tested *A. californica* in T-maze experiments and have found that *A. californica*, like *A. brasiliana*, is not attracted to nonlaying conspecifics under these conditions (S. D. Painter, unpubl. data). These results are consistent with earlier studies by Audesirk (1977), which showed that *A. californica* is not attracted to nonlaying animals in Y-maze experiments. Although there is electrophysiological evidence that *A. californica* detects the odors of nonlaying conspecifics (Audesirk and Audesirk, 1977; Chase, 1979), there is no evidence to date that the electrophysiological response is to species-specific odors (Chase, 1979) and no behavioral evidence that the odors are attractive.

Aplysia brasiliana is attracted to egg-laying animals with egg cordons. The ability to distinguish egg-laying animals with egg cordons from nonlaying animals without egg cordons was previously described in burrowing studies in this species (Aspey and Blankenship, 1976). In those studies, when a nonlaying animal was introduced into an aquarium containing a burrowed conspecific, the introduced animal burrowed; when an egg-laying animal was

Table I

The effects of recent egg deposition on sexual role in Aplysia brasiliana

Conditions	Animal	% of animals first mating as: Female	Male	Hermaphrodite	% Not mating
Conditioned ASW, egg cordon present[a]	Egg layer	90	10	0	0
Non-conditioned ASW, no egg cordon[b]	Egg layer	45	30	15	10
Non-conditioned ASW, no egg cordon[b]	Nonlayer	40	40	10	10

[a] From Painter *et al* (1989). Some egg layers were actively laying eggs when the second animal was introduced into the chamber. The ASW was animal-conditioned by the egg layer. n = 20.

[b] In each case, the experimental animal was introduced into a new chamber at the beginning of the observation period and the ASW was not animal-conditioned. Egg layers were animals that had just completed egg deposition; nonlayers were those that had not laid within the preceding 24 h. The activity pattern of an egg layer in non-conditioned ASW without an egg cordon differed significantly from that of an egg layer in animal-conditioned ASW with an egg cordon [$\chi^2(3) = 16.67$; $P < 0.005$], but did not differ from that of a nonlayer in non-conditioned ASW without an egg cordon ($\chi^2 = 1.11$; $0.75 < P < 0.90$). n = 20 for each.

introduced, however, the burrowed animal emerged to mate with it. The distinction is also evident in mating experiments (Painter *et al.*, 1989), which showed that egg-laying animals have significantly shorter latencies to mating than do sexually mature but nonlaying animals. Other species of *Aplysia* also make the distinction. Copulatory

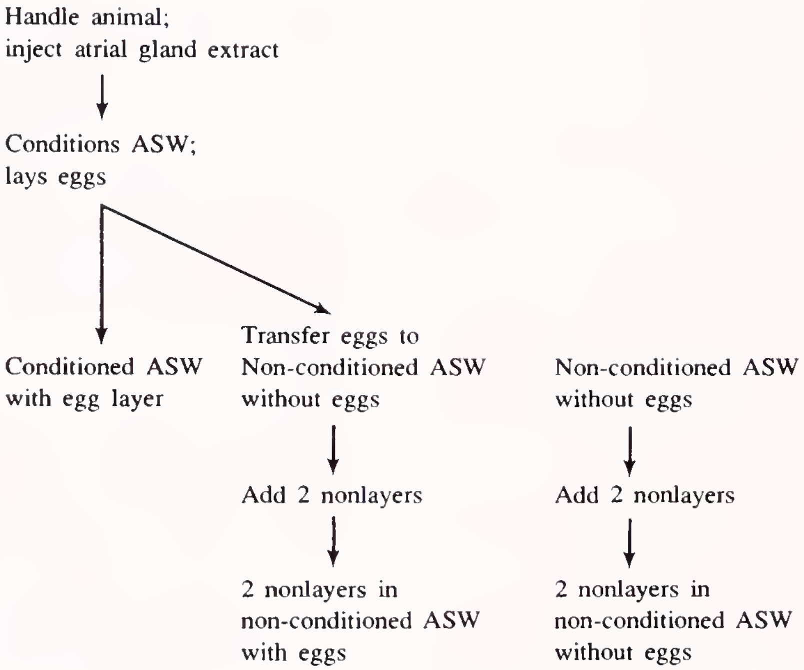
Handle animal;
inject atrial gland extract
Conditions ASW;
lays eggs
Conditioned ASW
with egg layer
Transfer eggs to
Non-conditioned ASW
without eggs
Non-conditioned ASW
without eggs
Add 2 nonlayers
Add 2 nonlayers
2 nonlayers in
non-conditioned ASW
with eggs
2 nonlayers in
non-conditioned ASW
without eggs

Figure 9. Flow diagram of the protocol followed in the second series of mating experiments. One animal was injected with an extract of the atrial gland to induce egg laying and placed in a beaker containing aerated non-conditioned ASW. When egg deposition was complete, the egg cordon was removed from the container, quickly rinsed, and transferred to a second beaker containing non-conditioned ASW. Two nontreated animals were then added to the beaker containing the egg cordon, and two others added to a third beaker containing only non-conditioned ASW. The resulting experimental conditions are indicated at the bottom of the diagram. Reproductive behaviors were scored at 10-min intervals for 270 min.

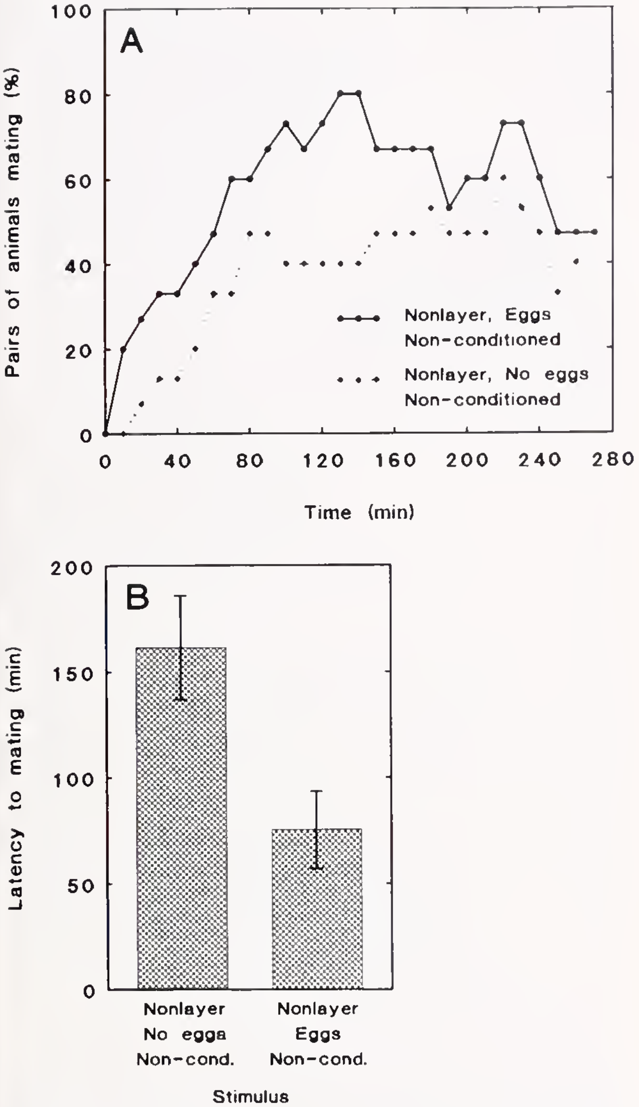

Figure 10. High concentrations of animal-derived factors are not required for the induction of mating activity by recently deposited egg cordons. (A) A higher percentage of nonlaying *Aplysia brasiliana* mated at early time periods when an egg cordon was placed in the surrounding non-conditioned ASW; the increase was statistically significant at 20, 30, 40, 70, and 100–140 min [$\chi^2(1) > 3.84$ in each case; $P < 0.05$]. The experimental protocol is shown in Figure 9 (n = 15 experiments). (B) Placing an egg cordon in the non-conditioned ASW surrounding two nonlaying animals significantly reduced their latency to mating relative to nonlaying animals without an egg cordon ($P < 0.01$; one-way analysis of variance). The experimental protocol is shown in Figure 9 (n = 15 experiments).

chains of *A. californica*, for example, are both more stable and more attractive when the first animal in the chain is laying eggs (Audesirk, 1977).

The present studies have shown that both egg-layer-derived and cordon-derived factors contribute to the attractiveness of an egg-laying animal. Although there are two apparent sources of this pheromonal activity, it remains to be demonstrated whether the two sets of factors differ biochemically. There is extensive and prolonged contact between the egg layer and its cordon, both during and following oviposition, which would facilitate a transfer of activity between the two.

The attractiveness of a nonlaying animal was increased by placing a recently deposited egg cordon in the same arm of the T-maze, providing the basis for a simple bioassay system in which to identify potential tissue sources of the "cordon-derived" pheromonal activity. Extracts of the *A. californica* atrial gland were assayed in this system and also increased the attractiveness of a nonlaying animal, suggesting that secretory products of the *A. californica* atrial gland (or *A. brasiliana* AG-LE) may contribute to the cordon-derived activity. The extracts each contained 50% of the material in a single atrial gland and were as attractive as *A. brasiliana* egg cordons, suggesting that the *A. brasiliana* and *A. californica* aggregation pheromones may be chemically similar or identical. This issue is currently being examined by HPLC analyses of egg cordon eluates, and by compositional and microsequence analyses of active fractions. It is worth noting that extracts of the *A. californica* atrial gland also induce copulatory activity in *A. brasiliana* (Painter *et al.*, 1989), and that field studies suggest that *Aplysia* aggregation pheromones may not be entirely species-specific (*A. vaccaria*, for example, has been observed in association with *A. californica* aggregations; Kupfermann and Carew, 1974).

Mating activity

The experiments showed that both animal-derived and cordon-derived factors reduce the latency to mating in

Table II

Neither animals nor egg cordons stimulated egg-laying activity in Aplysia brasiliana

Conditions	% Animals laying eggs 2 Animals in chamber	 1 Animal in chamber
Non-conditioned ASW		
No egg cordon	0^{a}	0^{b}
Egg cordon	6.7^{a}	6.7^{b}
Animal-conditioned ASW		
No egg cordon	7.5^{c}	0^{d}
Egg cordon	12.5^{c}	10^{d}

[a] n = 15; 30 possible egg-laying episodes. Not significantly different [$\chi^2(1) = 2.14$; $0.10 < P < 0.25$].

[b] n = 15; 15 possible egg-laying episodes. Not significantly different [$\chi^2(1) = 1.07$; $0.25 < P < 0.50$].

[c] n = 20; 40 possible egg-laying episodes. Not significantly different [$\chi^2(1) = 1.44$; $0.10 < P < 0.25$].

[d] n = 20; 20 possible egg-laying episodes. Not significantly different [$\chi^2(1) = 2.22$; $0.10 < P < 0.25$].

Aplysia, and suggest that their effects are additive. We did not record courtship behavior in any of these experiments, however, and do not know whether the effect results from a reduction in the latency to courtship (*i.e.*, an increase in male behaviors), a reduction in the duration of courtship (*i.e.*, an increase in female receptivity), or from some combination of the two.

The experiments also showed that the active animal-derived factors are not uniquely associated with the egg layer. Although the effect was small, animal-conditioning the ASW with a handled nonlayer consistently reduced the latency to mating, and animals did not distinguish between recent egg layers and handled nonlayers in non-conditioned ASW without an egg cordon. These results suggest that cordon-derived factors are primarily responsible for the relatively short latencies to mating observed with egg-laying animals.

Although previous studies reported that 90% of egg-laying animals initially mated as females (Painter *et al.*, 1989), only 45% did so in the present studies. The difference probably reflects differences in experimental protocol, two of which are particularly significant. First, the animals in the previous studies were tested in animal-conditioned ASW with an egg cordon rather than in non-conditioned ASW without an egg cordon. This suggests that the increase in receptivity might have been due to pheromonal factors rather than a persistent change in motivational state caused by bag-cell activity, ovulation, or movement of eggs through the reproductive tract. It is worth noting that bag-cell activity normally precedes ovulation *in vivo* (*A. brasiliana*, Dudek *et al.*, 1977), that bag-cell products affect neuronal activity (*A. californica*, Mayeri, 1979; Stuart and Strumwasser, 1980), and that certain aspects of egg-laying behavior depend upon movement of eggs through the reproductive tract (*A. brasiliana*, Cobbs and Pinsker, 1982). Second, the time period between injecting atrial gland extract and adding the second animal was held constant at 60 min in the previous studies (Painter *et al.*, 1989), but varied depending upon the time required to complete egg deposition in the present studies, averaging approximately 70 min. Although the egg cordons were smaller in the first study (0.8 compared to 1.7 ml), it is likely that some proportion of the animals were laying eggs when the second animal was introduced. Because egg-laying animals cannot simultaneously mate as males (Leonard and Lukowiak, 1987), these animals would skew the percentages toward mating as a female. In either case, the experiments suggest that, if the receptivity of the egg layer is increased by egg deposition, the effect is dependent on cordon-derived pheromones.

Egg-laying activity

Although both cordon-derived and animal-derived factors attracted animals and induced mating in our studies, they did not elicit egg deposition. Comparable results were obtained with either one or two animals in the test chamber, demonstrating that egg deposition was not being influenced to a significant degree by the accessibility of a potential mate. It is more likely that the lack of effect resulted from the small percentage of animals that are in the correct motivational state to respond to pheromonal stimulation. This suggestion is based on a comparison with earlier studies by Audesirk (1977), which indicated that egg-laying *Aplysia californica* induce egg laying in conspecifics. In contrast to the present studies, however, the *A. californica* experiments were designed to detect low-frequency events. An egg-laying animal was placed in one of two aquaria, each of which contained four to five individually caged animals, and activity was monitored until an animal in one of the two aquaria began to lay eggs; in 12 of the 15 trials, the first animal to lay eggs was in the aquarium containing the egg-laying animal stimulus, and egg deposition usually began within 3 h. Although the two series of experiments are not identical in design, egg-laying activity on a per-animal basis over a 3- to 3.5-h period is similar: 4–5% laid eggs in the negative control aquarium and 16–20% in the aquarium containing the egg-laying animal stimulus (Audesirk, 1977), compared to 0% in our negative control (non-conditioned ASW without an egg cordon) and 10–12.5% in the animal-conditioned ASW with an egg cordon. The low percentage of animals responding to this stimulus may have physiological significance, allowing some animals to mate as males and providing a mechanism by which the aggregation can be maintained over a relatively long period of time (see Audesirk, 1977).

A comparison of aggregation and mating pheromones

These studies demonstrate that both animal-derived and cordon-derived factors contribute to the development and maintenance of breeding aggregations, by attracting animals to the area and inducing them to mate. Animal-derived and cordon-derived factors appear to be equally attractive. There were no significant differences in levels of attraction or patterns of responses to: (1) an egg layer without eggs; (2) an egg layer with eggs; (3) a nonlayer with eggs; and (4) eggs without any animal. The animal-derived pheromones appear to be uniquely associated with the egg layer since nonlaying animals without egg cordons were not attractive.

Cordon-derived factors appear to be primarily responsible for the induction of mating by an animal that is actively laying eggs. This idea is supported by three sets of observations. First, animals do not distinguish between recent egg layers and nonlayers in non-conditioned ASW without an egg cordon; there were no significant differences in the time courses of mating activity or in the mean latencies to mating in our studies. Animals do distinguish between recent egg layers with egg cordons and nonlayers without egg cordons (Aspey and Blankenship, 1976; Painter *et al.*, 1989), however, suggesting that the distinction is based on cordon-derived, rather than animal-derived, factors. Second, placing a recently deposited egg cordon in the non-conditioned ASW surrounding two nonlaying animals significantly reduced their mean latency to mating relative to non-conditioned ASW controls. Animal-conditioning the ASW also reduced the mean latency to mating relative to the controls but, in this case, the reduction was not statistically significant. Thus, although cordon-derived and animal-derived factors are each sufficient to induce mating, the cordon-derived factors are likely to play the more significant role in eliciting the activity. Finally, the animal-derived factors that induce mating are associated with both egg layers and nonlayers, suggesting that they are not responsible for the differences in mating activity observed in the two groups (Painter *et al.*, 1989).

From a behavioral point of view, it is somewhat puzzling that an egg layer is more attractive than a nonlayer in nonconditioned ASW without an egg cordon, but does not have a shorter latency to mating. It should be kept in mind, however, that these conditions rarely, if ever, occur in the natural environment. Egg-laying animals maintain contact with their egg cordons for extended periods of time, and often begin mating before deposition is complete (*A. brasiliana*, Blankenship *et al.*, 1983).

Cordon-derived pheromones and the atrial gland

It has yet to be determined whether the cordon-derived factors that induce aggregation are identical to the ones that induce mating. However, it is important to note that the effects of recently deposited egg cordons can be quantitatively mimicked in both assay systems by placing an extract of the atrial gland into the surrounding ASW (aggregation, present studies; mating, Painter *et al.*, 1989); extracts containing approximately 50% of the material in a single gland (T-maze experiments; 67% was tested in mating experiments) are as active as one egg cordon, suggesting that these effects may be of physiological rather than purely pharmacological interest.

It is worth noting that the atrial gland is one of only five exocrine organs associated with the female reproductive tract, and that it is the last of the five to contact the egg cordon before deposition (*A. californica*, Coggeshall, 1972; Painter *et al.*, 1985). Moreover, the gland synthesizes large amounts of a few structurally related precursor proteins and processes them into small families of structurally related peptides with similar pharmacological properties. It stores milligram quantities of the products (*A. californica*, Heller *et al.*, 1980; Nagle *et al.*, 1986, 1988b; Rothman *et al.*, 1986), and releases them in response to depolarizing stimuli (*A. californica*, Arch *et al.*, 1980). These characteristics are consistent with the atrial gland being a tissue source of the "cordon-derived" pheromonal activity, but it remains to be determined whether the atrial gland serves this function in the animal and whether the "cordon-derived" pheromones are products of the ELH-related genes expressed in the gland.

Acknowledgments

The authors thank Mike Moore and Bret Clough for collecting and maintaining the animals and Debbie Pavlu for preparing the manuscript. This work was supported by NIH grants NS22079 (S.D.P.), NS23169 and NS11225; by NSF grants BNS 85 17575 (G.T.N.) and BBS 87 11368; and by the Marine Biomedical Institute Summer Student Program. The Florence and Marie Hall Endowment for Programs of Excellence in the Biomedical Sciences provided support for the computer facilities used in the project.

Literature Cited

Arch, S., J. Lupatkin, T. Smock, and M. Beard. 1980. Evidence for an exocrine function of the *Aplysia* atrial gland. *J. Comp. Physiol.* **151:** 131–137.

Arch, S., T. Smock, R. Gurvis, and C. McCarthy. 1978. Atrial gland induction of the egg-laying response in *Aplysia californica J. Comp. Physiol.* **128:** 67–70.

Aspey, W. P., and J. E. Blankenship. 1976. *Aplysia* behavioral biology. I. Induced burrowing in swimming *A. brasiliana* by a burrowed conspecific. *Behav. Biol.* **17:** 301–312.

Audesirk, T. E. 1977. Chemoreception in *Aplysia californica*. III. Evidence for pheromones influencing reproductive behavior. *Behav. Biol.* **20:** 235–243.

Audesirk, T. E. 1979. A field study of growth and reproduction in *Aplysia californica*. *Biol. Bull.* **157:** 407–421.

Audesirk, T. E., and G. J. Audesirk. 1977. Chemoreception in *Aplysia californica*. II. Electrophysiological evidence for detection of the odors of conspecifics. *Comp. Biochem. Physiol., pt. A* **56:** 267–270.

Beard, M., L. Millechia, C. Masuoka, and S. Arch. 1982. Ultrastructure of secretion in the atrial gland of a mollusc *(Aplysia)*. *Tissue and Cell* **14:** 297–308.

Blankenship, J. E., and R. E. Coggeshall. 1976. The abdominal ganglion of *Aplysia brasiliana:* a comparative morphological and electrophysiological study, with notes on *A. dactylomela*. *J. Neurobiol.* **7:** 383–405.

Blankenship, J. E., M. K. Rock, L. C. Robbins, C. A. Livingston, and H. K. Lehman. 1983. Aspects of copulatory behavior and peptide control of egg laying in *Aplysia*. *Fed. Proc.* **42:** 96–100.

Chase, R. 1979. An electrophysiological search for pheromones of *Aplysia californica*. *Can. J. Zool.* **57:** 781–784.

Chiu, A. Y., M. W. Hunkapiller, E. Heller, D. K. Stuart, L. E. Hood, and F. Strumwasser. 1979. Purification and primary structure of the neuropeptide egg-laying hormone of *Aplysia californica*. *Proc. Natl. Acad. Sci. USA* **76:** 6656–6660.

Cobbs, J. S., and H. M. Pinsker. 1982. Role of bag cells in egg deposition of *Aplysia brasiliana*. II. Contribution of egg movement to elicited behaviors. *J. Comp. Physiol., pt. A* **147:** 537–546.

Coggeshall, R. E. 1972. The structure of the accessory genital mass in *Aplysia californica. Tissue and Cell* **4:** 105–127.

Dudek, F. E., and J. E. Blankenship. 1977. Neuroendocrine cells of *Aplysia brasiliana.* I. Bag cell potentials and afterdischarge. *J. Neurophysiol.* **40:** 1301–1311.

Dudek, F. E., J. S. Cobbs, and H. M. Pinsker. 1979. Bag cell electrical activity underlying spontaneous egg laying in freely behaving *Aplysia brasiliana. J. Neurophysiol.* **42:** 804–817.

Frazier, W. T., E. R. Kandel, I. Kupfermann, R. Waziri, and R. E. Coggeshall. 1967. Morphological and functional properties of identified neurons in the abdominal ganglion of *Aplysia californica. J. Neurophysiol.* **30:** 1288–1351.

Heller, E., L. K. Kaczmarek, M. W. Hunkapiller, L. E. Hood, and F. Strumwasser. 1980. Purification and primary structure of two neuroactive peptides that cause bag cell afterdischarge and egg-laying in *Aplysia Proc. Natl. Acad. Sci. USA* **77:** 2328–2332.

Jahan-Parwar, B. 1976. Aggregation pheromone from the egg-mass of *Aplysia The Physiologist* **19:** 240.

Kupfermann, I., and T. Carew. 1974. Behavior patterns of *Aplysia californica* in its natural environment. *Behav. Biol.* **12:** 317–337.

Kupfermann, I., and E. R. Kandel. 1970. Electrophysiological properties and functional interconnections in two symmetrical neurosecretory clusters (bag cells) in abdominal ganglion of *Aplysia. J. Neurophysiol.* **33:** 865–876.

Lederhendler, I. I., K. Herriges, and E. Tobach. 1977. Taxis in *Aplysia dactylomela* (Rang, 1828) to water-borne stimuli from conspecifics. *Anim. Learning Behav.* **5:** 355–358.

Leonard, J. L., and K. Lukowiak. 1987. The behavior of *Aplysia californica* Cooper (Gastropoda: Opisthobranchia). *Behavior* **98:** 320–360.

MacGinitie, G. E. 1934. The egg-laying activities of the sea hare *Tethys californica* (Cooper). *Biol. Bull.* **62:** 300–303.

Mahon, A. C., J. R. Nambu, R. Taussig, M. Shyamala, A. Roach, and R. Scheller. 1985. Structure and expression of the egg-laying hormone gene family in *Aplysia. J Neurosci.* **5:** 1872–1880.

Mayeri, E. 1979. Local hormonal modulation of neural activity in *Aplysia. Fed. Proc.* **38:** 2103–2108.

Nagle, G. T., S. D. Painter, J. E. Blankenship, J. D. Dixon, and A. Kurosky. 1986. Evidence for the expression of three genes encoding homologous atrial gland peptides that cause egg laying in *Aplysia. J. Biol. Chem.* **261:** 7853–7859.

Nagle, G. T., S. D. Painter, J. E. Blankenship, J. V. A. Choate, and A. Kurosky. 1988a. The bag cell egg-laying hormones of *Aplysia brasiliana* and *Aplysia californica* are identical. *Peptides* **9:** 867–872.

Nagle, G. T., S. D. Painter, J. E. Blankenship, and A. Kurosky. 1988b. Proteolytic processing of egg-laying hormone-related precursors in *Aplysia.* identification of peptide regions critical for biological activity. *J Biol. Chem.* **263:** 9223–9237.

Nambu, J. R., and R. H. Scheller. 1986. Egg-laying hormone genes of *Aplysia:* evolution of the ELH gene family. *J. Neurosci.* **6:** 2026–2036.

Painter, S. D., A. R. Gustavson, V. K. Kalman, G. T. Nagle, and J. E. Blankenship. 1989. Induction of copulatory behavior in *Aplysia:* atrial gland factors mimic the excitatory effects of freshly deposited egg cordons. *Behav. Neural Biol.* **51:** 222–236.

Painter, S. D., V. K. Kalman, G. T. Nagle, R. A. Zuckerman, and J. E. Blankenship. 1985. The anatomy and functional morphology of the large hermaphroditic duct of three species of *Aplysia,* with special reference to the atrial gland. *J. Morphol.* **186:** 167–194.

Pinsker, H. M., and D. W. Parsons. 1985. Temperature dependence of egg laying in *Aplysia. J Comp. Physiol., pt. B* **56:** 21–27.

Rothman, B. S., D. H. Hawke, R. O. Brown, T. D. Lee, A. A. Dehghen, J. E. Shively, and E. Mayeri. 1986. Isolation and primary structure of the califins, three biologically active ELH-like peptides from the atrial gland of *Aplysia J Biol. Chem.* **261:** 1616–1623.

Rothman, B. S., E. Mayeri, R. O. Brown, P.-M. Yuan, and J. E. Shively. 1983. Primary structure and neuronal effects of α-bag cell peptide, a second candidate neurotransmitter encoded by a single gene in bag cell neurons of *Aplysia. Proc. Natl. Acad. Sci. USA* **80:** 5753–5757.

Scheller, R. H., J. F. Jackson, L. B. McAllister, B. S. Rothman, E. Mayeri, and R. Axel. 1983. A single gene encodes multiple neuropeptides mediating a stereotyped behavior. *Cell* **32:** 7–22.

Stuart, D. K., A. Y. Chiu, and F. Strumwasser. 1980. Neurosecretion of egg-laying hormone and other peptides from electrically active bag cell neurons of *Aplysia. J. Neurophysiol* **43:** 488–498.

Stuart, D. K., and F. E. Strumwasser. 1980. Neuronal sites of action of a neurosecretory peptide, egg-laying hormone, in *Aplysia californica. J. Neurophysiol.* **43:** 499–519.

Susswein, A. J., and M. Benny. 1985. Sexual behavior in *Aplysia fasciata* induced by homogenates of the large hermaphroditic duct. *Neurosci. Lett.* **59:** 325–330.

Susswein, A. J., S. Gev, Y. Achituv, and S. Markovitch. 1984. Behavioral patterns of *Aplysia fasciata* along the Mediterranean coast of Israel. *Behav. Neural Biol.* **41:** 7–22.

Susswein, A. J., S. Gev, E. Feldman, and S. Markovitch. 1983. Activity patterns and time budgeting of *Aplysia fasciata* under field and laboratory conditions. *Behav. Neural Biol.* **39:** 203–220.

Switzer-Dunlap, M., and M. G. Hadfield. 1977. Observations on development, larval growth and metamorphosis of four species of Aplysiidae (Gastropoda: Opisthobranchia) in laboratory culture. *J. Exp. Mar. Biol. Ecol.* **29:** 245–261.

Thompson, T. E., and A. Bebbington. 1969. Structure and function of the reproductive organs of three species of *Aplysia* (Gastropoda: Opisthobranchia). *Malacologia* **7:** 347–380.

Ziv, I., M. Benni, S. Markovich, and A. Susswein. 1989. Motivational control of sexual behavior in *Aplysia fasciata:* sequencing and modulation by sexual deprivation and by addition of partners. *Behav. Neural Biol.* **52:** 180–193.

Reference: *Biol. Bull.* **181**: 95–103. (August, 1991)

Immunological Survey of Planktonic Embryos and Larvae of the Starfish *Asterina pectinifera*, Obtained from the Sea, Using a Monoclonal Antibody Directed against Egg Polypeptides

SUSUMU IKEGAMI, TOMOKO MITSUNO, MASANORI KATAOKA,
SATOSHI YAJIMA, AND MIÉKO KOMATSU[1]

*Faculty of Applied Biological Sciences, Hiroshima University, Kagamiyama 1-Chome,
Higashihiroshima-shi, Hiroshima 724, Japan; and [1]Department of Biology,
Faculty of Science, Toyama University, Toyama 930, Japan*

Abstract. A monoclonal antibody, K1, specifically recognizes polypeptides with apparent molecular masses of 56 and 58 kDa, in the egg of the starfish *Asterina pectinifera*. The K1 antibody reacted with extracts prepared from ovaries, oocytes, morulae, blastulae, gastrulae, and bipinnariae. Brachiolariae, testes, pyloric ceca, body walls, and tubefeet did not contain K1-reactive antigenic molecules. Extracts of eggs of the starfish *Asterias amurensis* and several sea urchin species did not react with the K1 antibody. Among the members of the genus *Asterina*, extracts of brachiolariae of *A. batheri* and *A. minor* were not reactive, whereas blastulae and brachiolariae of *A. pseudoexigua pacifica* did contain an antigenic component. Unlike the antigenic peptides in *A. pectinifera* eggs, the apparent molecular mass of the antigen molecule in embryos and larvae of *A. pseudoexigua pacifica* was 41 kDa, which represents a remarkable phylogenetic variation of antigen molecules. Using the K1 antibody, we have developed an assay system that detects embryos and larvae of *A. pectinifera* in complex mixtures of biological specimens obtained from the sea.

Introduction

The development of a number of starfish species has been described (Oguro and Komatsu, 1988). Nevertheless, the embryos and larvae obtained from the sea have hitherto been unidentifiable, because the entire process of their development and metamorphosis is not sufficiently well known. Furthermore, the identification of individual species by examination of external morphological features alone tends to be equivocal. Therefore, specific methods for detecting chemical components present exclusively in embryos and larvae of one species are needed.

We report the discovery of specific antigenic polypeptides that are present in eggs, embryos, and larvae of *Asterina pectinifera*, but not in those of other species belonging to the same genus. A single embryo or larva in a complex plankton mixture can be detected by immunological analysis with an enzyme-linked immunosorbent assay (ELISA) or immunoblot procedure, using a monoclonal antibody that recognizes the unique antigen molecules present in embryos and larvae.

Materials and Methods

Animals

Adults of the following starfish and sea urchin species were collected, during their breeding seasons, along the coast of the Japan Islands. The starfish were collected from the following areas: *A. pectinifera*—off Asamushi in Aomori Prefecture, off Otsuchi in Iwate Prefecture, off Hashirimizu in Kanagawa Prefecture, off Sensui Island

Received 10 December 1990; accepted 1 April 1991.

Abbreviations: ASW, artificial seawater; BSA, bovine serum albumin; CaFSW, calcium-free seawater; D-MEM, Dulbecco's modification of Eagle medium; ELISA, enzyme-linked immunosorbent assay; FCS, fetal calf serum; FITC, fluorescein isothiocyanate; HAT, hypoxanthine-aminopterine-thymidine; IgG, immunoglobulin G; kDa, kilodaltons; NSW, normal seawater; PBS, phosphate buffered saline without divalent cations; PMSF, phenylmethylsulfonyl fluoride; SDS, sodium dodecyl sulfate; T·TBS, 0.5 M NaCl, 10 mM Tris-HCl (pH 7.8) and 0.05% Tween 20.

in Hiroshima Prefecture, and off Gogo Island in Ehime Prefecture; *Asterina pseudoexigua pacifica*—from the undersurface of stones at the intertidal zone of Kushimoto in Wakayama Prefecture; and *Asterina minor* and *Asterina batheri*—along the coast of the Noto Peninsula in Ishikawa Prefecture. The sea urchins, *Scaphechinus mirabilis, Hemicentrotus pulcherrimus,* and *Pseudocentrotus depressus,* were collected off Sensui Island in Hiroshima Prefecture, off Kiwado in Yamaguchi Prefecture, and off Sugashima Island in Mie Prefecture, respectively.

The plankton samples were collected by a diver equipped with SCUBA, who towed plankton nets (100 μm-mesh; open mouth, 40 cm in diameter) horizontally 50 m at discrete depths off Sensui Island in Hiroshima Prefecture.

Gametes, embryos, and larvae

Fertilizable eggs were induced to spawn from isolated ovaries of female *A. pectinifera* and *A. amurensis* by application of 1-methyladenine at a final concentration of 150 ng/ml (Kanatani, 1973). Spawned *A. pectinifera* eggs were washed several times with artificial seawater (ASW), Jamarin U (Jamarin Laboratory, Osaka), and inseminated at 40–60 min after the start of 1-methyladenine treatment. Formed embryos were cultured in ASW at 23° ± 2°C, and the early brachiolariae were reared in natural seawater (NSW), which was kept in the sun and changed every two or three days. Embryos of *A. batheri* were obtained similarly. Embryos and larvae of hermaphroditic *A. minor* were obtained from a container of adult colonies collected during the breeding season, during June at the Noto Peninsula in Ishikawa Prefecture. Embryos and larvae of *A. pseudoexigua pacifica* were collected from the body cavity of the adult during the breeding season, in July at Kushimoto in Wakayama Prefecture. Eggs of sea urchins were obtained by introducing 0.5 *M* KCl into the body cavity.

Eggs, embryos, and larvae were washed several times with ASW or NSW before being stored at −80°C until required.

Protein determination

Protein was determined by the protein-dye binding assay, with bovine serum albumin (BSA) as the standard (Bradford, 1976).

Sodium dodecyl sulfate-polyacrylamide gel electrophoresis

Discontinuous sodium dodecyl sulfate (SDS)-polyacrylamide gel electrophoresis was performed with 5% stacking gel, as described by Laemmli (1970). The gels were then stained with Coomassie brilliant blue R-250 or blotted onto nitrocellulose sheets (Bio-Rad), as described below.

Preparation of antigens

Mature eggs (3 ml packed volume) from *A. pectinifera,* shed from the isolated ovaries of adults by application of 1-methyladenine at a final concentration of 150 ng/ml, were collected 1 h after the hormone treatment had started. They were washed, by settling, in 5 vol of ASW and homogenized, in a Potter-Elvehjem glass homogenizer, at 0°C in 12 ml 20 m*M* Tris-HCl (pH 7.5) buffer with 0.1 m*M* phenylmethylsulfonyl fluoride (PMSF). The subsequent procedures were carried out at 4°C, unless otherwise stated. The homogenate was centrifuged at 18,000 × *g* for 20 min. The pellet was resuspended in 15 ml 20 m*M* Tris-HCl (pH 7.5) buffer with 0.1 m*M* PMSF, and the suspension was centrifuged again. The supernatants were combined, and solid ammonium sulfate was added to a final ammonium sulfate concentration of 20% (w/v). The mixture was stirred for 1 h, then centrifuged at 18,000 × *g* for 20 min. The supernatant was removed, the ammonium sulfate concentration was adjusted to 80% (w/v) by adding solid ammonium sulfate, and 1 h later, the mixture was centrifuged as before. The precipitate was removed and dissolved in 2 l loading buffer, composed of 50 m*M* Tris-HCl (pH 7.4) with 0.1 m*M* PMSF. The solution was then loaded onto a Whatman DE-52 ion-exchange resin column (2.5 × 3.3 cm), which had been equilibrated with loading buffer. Step-wise elution was performed with solutions of NaCl in loading buffer using 50 ml each of 20, 150, 200, and 500 m*M* concentrations. The fractions eluted with 150 and 200 m*M* NaCl were pooled and dialyzed against phosphate-buffered saline without divalent cations (PBS). The non-dialyzable fraction was frozen at −80°C for future use.

Preparation of nuclei

Two thousand, five hundred (2500) *A. pectinifera* embryos were washed twice with calcium-free seawater (CaFSW, Jamarin Laboratory, Osaka; 4°C) and once with buffer A (4°C), which consisted of 250 m*M* sucrose, 5 m*M* $MgCl_2$, 40 m*M* NaCl, and 50 m*M* Tris-HCl (pH 7.5). They were homogenized with a Dounce homogenizer at 4°C in 5 ml buffer A containing 1% (w/v) Triton X-100. The homogenate was passed through a 40-μm stainless steel filter by gravity. The filtrate was centrifuged at 1000 × *g* at 4°C for 5 min. The nuclear pellet was resuspended in 2.5 ml buffer A, followed by centrifugation at 1000 × *g* for 5 min. This process was repeated once. The washed nuclear preparations were frozen at −80°C for future use.

Monoclonal antibody production

A 7-week-old BALB/c female mouse was injected intraperitoneally with 100 μg protein in complete Freund's adjuvant. Four and then five weeks later, booster injections of 50 μg protein were administered. And three days after the second booster, the mouse was sacrificed, its spleen was removed, and the cells allowed to fuse, for 8 min, with myeloma cells (SP-2) (at a ratio of $1 \times 10^8/1 \times 10^7$ spleen cells/myeloma cells). The fusion was carried out in 1 ml Dulbecco's modification of Eagle medium (D-MEM), without serum, but containing 50% polyethylene glycol-6,000. To stop the fusion, 20 ml D-MEM was added drop-wise, and cell pellets were precipitated by centrifugation at 250 × *g* for 5 min. The cell pellets were resuspended in 5 ml D-MEM containing 5% fetal calf serum (FCS, Microbiological Associates), incubated for 12–18 h, then plated in 98-well microtiter dishes at 200 μl/well in HAT medium (complete D-MEM containing 1×10^{-4} *M* hypoxanthine, 4×10^{-7} *M* aminopterin, 1.6×10^{-5} *M* thymidine, and 10% FCS). Half of the medium was removed from each well and replaced with fresh HAT medium after 2, 4, 7, and 10 days. The supernatants were harvested when the clones began to exhaust their medium and were screened by protein blotting, as described below. Hybridomas that showed reactivity were expanded and subcloned by limited dilution.

Hybridomas (1×10^7 cells) were injected intraperitoneally into a BALB/c mouse which, 1–2 weeks previously, at 8 weeks old, had received an injection of 0.5 ml 2,6,10,14-tetramethylpentadecane. One to two weeks after the injection of hybridomas, the ascites were collected and centrifuged at 1500 × *g* for 30 min. The supernatant (1 ml) was dialyzed, at 4°C, against 50 m*M* Tris-HCl (pH 8.6) with 0.15 *M* NaCl. The non-dialyzable fraction was loaded onto a column (0.6 × 10 cm) of Protein-A cellulofine (Seikagaku Kogyo, Tokyo), which had been equilibrated with 50 m*M* Tris-HCl (pH 8.6) with 0.15 *M* NaCl. After washing with 30 ml 50 m*M* Tris-HCl (pH 8.6) with 0.15 *M* NaCl, the immunoglobulin G (IgG) fraction was eluted out by 0.05 *M* sodium acetate (pH 4.0) and 0.15 *M* NaCl. The pH of the IgG solution was adjusted to 7.2 by adding 1 *M* Tris-HCl (pH 9.0). The protein concentration was adjusted to 500 μg/ml, and then the IgG solution was frozen at −80°C for future use.

Immunoblotting

For screening hybridomas, nitrocellulose blots were prepared by electrophoretic transfer from preparative SDS-polyacrylamide gels of the 150 and 200 m*M* NaCl fractions obtained by Whatman DE-52 ion-exchange chromatography, performed as described above, followed by blocking in a solution of 10 m*M* Tris-HCl (pH 7.4), 0.5 *M* NaCl and 3% gelatin. Nitrocellulose strips (Bio-Rad) were incubated with undiluted culture supernatant at 37°C for 2 h with gentle stirring. After a brief wash with distilled water, they were then washed, for 10 min each, in two changes of excess 10 m*M* Tris-HCl (pH 7.4), 0.5 *M* NaCl and 0.05% Tween 20, and incubated for 2 h at 37°C with horseradish peroxidase-conjugated goat anti-mouse IgG (Bio-Rad) diluted 1:3000 in the same buffer that was used to block the nitrocellulose strips. After washing again, strips were assayed for peroxidase activity using H_2O_2 and 4-chloro-1-naphthol. The reaction was stopped by rinsing with water and strips were dried in air.

Protein blots of oocytes, eggs, embryos, and larvae were obtained by electrophoretic transfer from SDS-polyacrylamide gel to nitrocellulose sheets and then treated as specified above, except that the IgG solutions, diluted 1:100 to 1:1000 in PBS, were used for antibody incubations instead of hybridoma culture supernatant.

Immunofluorescence microscopy

Embryos were washed twice with ASW, fixed with 100% methanol for 10 min, immersed in 100% ethanol for 10 min and then embedded in polyester wax (BDH). Sections 7 μm thick were placed onto 0.1% (w/v) amylopectin-coated coverslips and incubated with IgG solution diluted 1:100 in PBS for 1 h, at room temperature, after which they were washed in PBS for 30 min. Fluorescein isothiocyanate (FITC)-conjugated goat anti-mouse IgG (Tago), diluted 1:200 in PBS containing 2% BSA was then added and the sections were incubated, in the dark, at room temperature, for 1 h, after which they were washed with PBS for 30 min. Coverslips were mounted in a solution of 20% glycerol in PBS, sealed, and viewed under a Nikon TMD-EP2 photomicroscope. Photographs were then taken using Kodak Tri-X pan ASA 400 film.

ELISA assay

Five thousand (5000) oocytes, eggs, or embryos were boiled for 2 min in 1 ml SDS sample buffer containing 62.5 m*M* Tris-HCl (pH 6.8), 2% SDS and 5% 2-mercaptoethanol (Laemmli, 1970). One hundred microliters of each of the extracts, at a dilution of 1:2000 in PBS, were added to a well of a microtiter plate for ELISA assay (Probind, Falcon), the content of the lysate in a well being equivalent to 0.25 oocytes, eggs, or embryos, and absorbed for 2 h at 37°C. The solution was removed, and the wells were treated at room temperature with 200 μl PBS with 1% BSA for 30 min. The IgG solution was diluted 1:1000 in PBS, a 100-μl aliquot was added to each well and incubated for 2 h at 37°C. The wells were washed twice with T · TBS buffer, composed of 0.5 *M* NaCl, 10 m*M* Tris-HCl (pH 7.4), and 0.05% (v/v) Tween 20, and then three times with distilled water. One hundred microliters of a solution of horseradish peroxidase linked to goat anti-

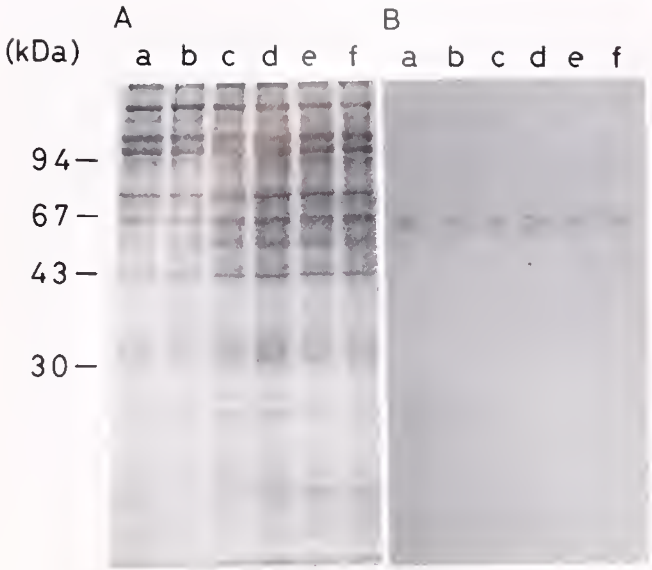

Figure 1. Immunoblots of *Asterina pectinifera* extracts. The extracts (5 μg protein each) were electrophoresed on SDS-12.5% polyacrylamide gels. Gels were either stained with Coomassie brilliant blue (A), or transblotted onto a nitrocellulose filter, which was probed with culture medium conditioned by a K1 antibody-producing hybridoma cell line (B). Lanes a, b, c, d, e, and f correspond to the extract of oocytes, eggs, 32-cell-stage morulae, 256-cell-stage blastulae, mid-blastulae (10 h after fertilization) and early gastrulae (24 h after fertilization), respectively.

mouse IgG, diluted 1:3000 in PBS with 0.05% Tween 20 and 1% gelatin, was added then incubated for 2 h at 37°C. The wells then were washed twice with T · TBS followed by three times with distilled water.

Two hundred microliters of substrate solutions containing H_2O_2 and *o*-phenylenediamine were added, left for 10–30 min, and then the reaction was stopped by the addition of 100 μl 4 N H_2SO_4. The absorbance at 492 nm was measured within 30 min of the sulfuric acid addition.

When the primary antibody was replaced with preimmune serum, or was omitted, the result was a completely negative one.

Results

Mice were immunized with the pooled 150 and 200 m*M* NaCl eluates obtained by Whatman DE-52 ion-exchange resin chromatography to produce monoclonal antibodies that would react with components present in *A. pectinifera* eggs, but not with any components of *A. amurensis* eggs. The spleen was dissociated from the immunized mice. The cells were fused to myeloma cells plated at a clonal dilution. From this fusion, 30 hybridoma clones grew. Hybridoma clones were selected by screening antibodies secreted in the media with the ELISA and immunoblot assays. Thirteen clones produced antibodies against *A. pectinifera* egg components with molecular masses of 188 or 133 kDa. All of these antibodies were found to bind to some components of *A. amurensis* eggs. One clone produced an antibody that recognized components of *A. pectinifera* eggs, but not those of *A. amurensis* eggs, in an ELISA assay. This specific antibody, K1, bound to *A. pectinifera* egg components with molecular masses of 58 and 56 kDa in an immunoblot assay (Fig. 1). The immunoreactive components were also present in extracts of *A. pectinifera* oocytes and embryos at the 32-cell morula, the 256-cell early blastula, mid-blastula (10 h after fertilization), and early gastrula (24 h after fertilization) stages. Protein A binding experiments indicated that the K1 antibody was of the IgG class.

The minimum number of eggs detectable by immunoblot analysis was then determined as follows. Graded amounts of egg lysate were loaded into slots of an SDS-polyacrylamide gel. After electrophoresis, the gel was blotted onto a nitrocellulose filter that was then probed with the K1 antibody. The lysate obtained from one sixteenth of an egg and loaded into a slot gave two bands at molecular masses of 58 and 56 kDa. The intensity of the bands was close to the limit of detection (data not shown).

To determine whether the antigenic molecules were polypeptides, we incubated 5 μg egg extract protein with 0.001 to 0.01 units of papain at 37°C for 30 min and subjected the reaction mixture to SDS-polyacrylamide gel electrophoresis. The gel was blotted onto a nitrocellulose filter, which was probed with the K1 antibody. The 58-

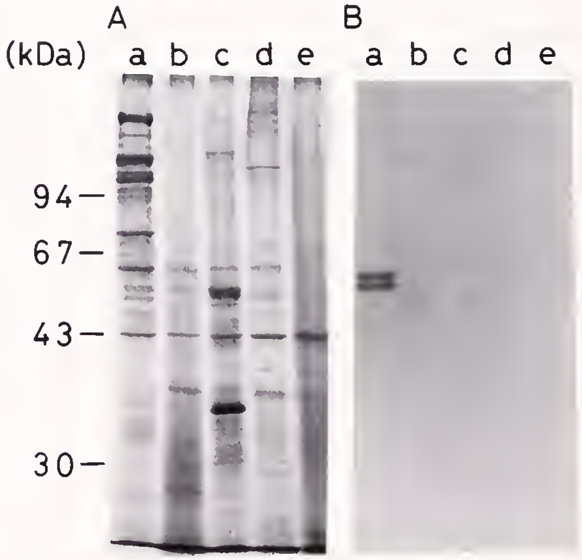

Figure 2. Immunoblots of tissues of adult *Asterina pectinifera*. The extracts (5 μg proteins each) were electrophoresed on SDS-10% acrylamide gels. Gels were either stained with Coomassie brilliant blue (A) or blotted onto nitrocellulose and probed with the K1 antibody (B), as described in Materials and Methods. Lanes a, b, c, d, and e correspond to extracts of ovary, pyloric cecum, testis, body-wall and tube-foot, respectively.

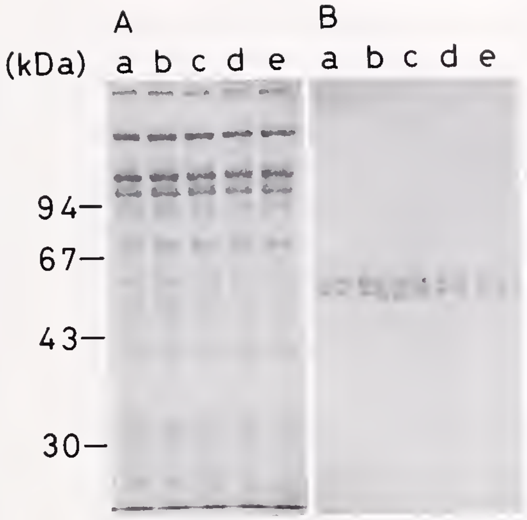

Figure 3. Immunoblots of extracts of *Asterina pectinifera* eggs and embryos. The extracts (5 μg protein each) were electrophoresed on SDS-10% polyacrylamide gels. Gels were either stained with Coomassie brilliant blue (A) or blotted onto nitrocellulose and probed with the K1 antibody (B) as described in Materials and Methods. Lanes a, b, c, d, and e correspond to the extract of eggs, 1-day-old early gastrulae, 2-day-old mid-gastrulae, 3-day-old late gastrulae and 4-day-old early bipinnariae, respectively.

and 56-kDa forms were no longer detectable on the immunoblot, and prominent degradation products with molecular masses of 49, 46, 43, and 40 kDa were observed (data not shown). Treatment of an identical amount of extract with a higher amount (0.1 unit) of papain resulted in total loss of immunoreactivity. These results demonstrate that the components recognized by the antibody were proteinaceous. The immunoreactive 58- and 56-kDa proteins were designated p58/56.

Distribution of the antigens in tissues, oocytes and embryos of A. pectinifera

Several tissues were excised from adult *A. pectinifera,* and their extracts were examined, by immunoblot analysis, to determine whether K1-reactive antigens were present. Antigenic p58/56 were found to be present in ovarian extracts of ovaries, whereas testes, pyloric ceca, and tube-feet contained no antigenic components (Fig. 2). Next, we surveyed extracts of hatched embryos and larvae by immunoblot analysis and found that p58/56 were present in all the samples examined; the amount of p58/56, on a protein weight basis, was almost constant throughout early embryonic development up to the early bipinnaria stage (Fig. 3).

Subcellular localization of the antigens in A. pectinifera *eggs and embryos*

Embryonic extracts were separated, by centrifugation, into nuclear and cytoplasmic fractions. Immunoblot analysis of these fractions showed that p58/56 were present in the cytoplasmic, but not in the nuclear fraction, as shown in Figure 4.

Embryos were fixed with methanol, embedded in polyester wax, sectioned, and the sections subjected to immunofluorescence staining. The K1 antibody stained the cytoplasm, but not the nucleus of an 8-cell-stage embryo (Fig. 5a). Figure 5b shows a section of a bipinnaria (4 days after fertilization) that was stained with the K1 antibody. Almost all of the embryonic cells contained some antigen molecules.

Occurrence of antigen molecules in other Asterina *species*

We attempted to survey the distribution of antigens in the eggs and embryos of some sea urchin and starfish species. Lysates were prepared from eggs of *S. mirabilis, P. depressus, H. pulcherrimus,* and *A. amurensis* and were subjected to immunoblot analysis; 10 μg of lysate were loaded into each slot. The analysis showed that no molecules reactive with the K1 antibody were present in these sea urchin and starfish eggs (Fig. 6).

Next, we examined embryos of species belonging to the genus *Asterina: A. minor, A. pseudoexigua pacifica,* and *A. batheri.* Development of these species is direct, with

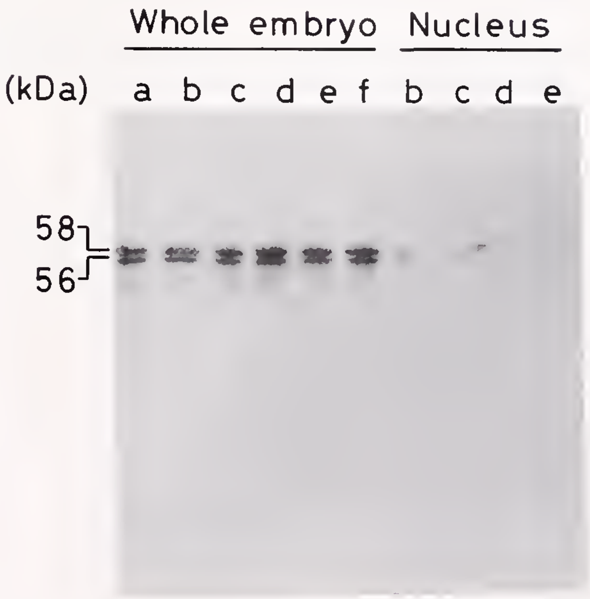

Figure 4. Immunoblots of whole and nuclear extracts of *Asterina pectinifera* embryos. The extracts (5 μg proteins each) were electrophoresed on an SDS-12.5% polyacrylamide gel. The gel was blotted onto nitrocellulose and probed with the K1 antibody, as described in Materials and Methods. Lanes a, b, c, d, e, and f correspond to the extracts at the 32-cell morulae, 256-cell early blastulae, 512-cell early blastulae, 1024-cell early blastulae, mid-blastulae (10 h after fertilization) and early gastrulae (24 h after fertilization), respectively.

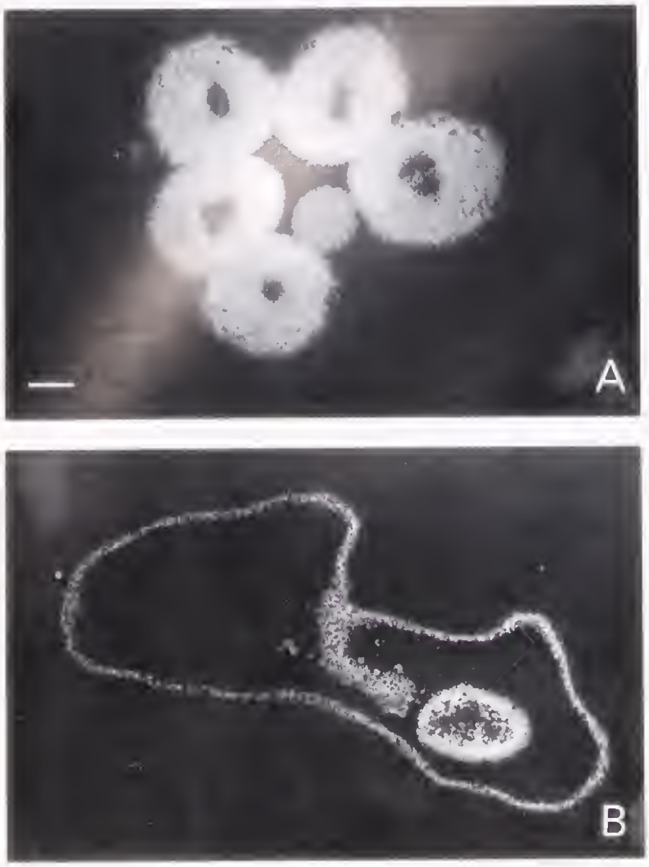

Figure 5. Immunofluorescence microscopy of sections of *Asterina pectinifera* embryos using the K1 antibody. A and B correspond to a 32-cell morula and an early bipinnaria, respectively. Bar indicates 100 μm. The magnification of B is the same as that of A.

no bipinnaria stage, unlike that of *A. pectinifera. A. minor* is hermaphroditic (Komatsu, 1976), and when spawning occurs, the animals cling to one another along the margins of their bodies, or they are imbricated with others (Komatsu *et al.*, 1979). Eggs that were spawned spontaneously and fertilized were cultured in the laboratory and allowed to develop into brachiolariae, which were then used for immunoblot analysis. *A. pseudoexigua pacifica* is ovoviviparous (Komatsu *et al.*, 1990), and we were able to collect early blastulae, wrinkled blastulae, and brachiolariae from the adult ovary. Brachiolariae of *A. batheri* (Kano and Komatsu, 1978) were obtained by rearing artificially inseminated, spontaneously spawned eggs. These embryos were boiled in SDS sample buffer and loaded onto a gel, which was electrophoresed and immunoblotted as described above. None of the peptides from the brachiolariae of *A. minor* or *A. batheri* reacted with the K1 antibody (Fig. 7). But when lysates of early blastulae, wrinkled blastulae, or brachiolariae of *A. pseudoexigua pacifica* were separated on a gel, a band at 41 kDa was detected on the blot (Fig. 8).

Detection of A. pectinifera *embryos in the ocean*

As *A. pseudoexigua pacifica* never swims or drifts at any stage of its life cycle (Komatsu *et al.*, 1990), its embryos and larvae should not be present in specimens collected from the sea with a plankton net. *A. pectinifera*, however, starts its planktonic life at the late blastula stage and then sinks to the bottom at the late brachiolaria stage. Therefore, we would expect that an ELISA system, with the K1 monoclonal antibody as the detecting antibody, could be used to quantify embryos and larvae of *A. pectinifera* in a complex planktonic sample.

We assessed the sensitivity of the assay system for embryos of *A. pectinifera* by testing graded quantities of embryos. Five thousand (5000) embryos, at each developmental stage, were boiled in 1 ml SDS sample buffer, the lysates were diluted 1:5000 to 1:40,000 in PBS, and a 100-μl aliquot was added to a well of a microtiter plate for ELISA. The absorbance decreased as development progressed, although on a per protein weight basis, the absorbance was nearly the same for all stages of the embryos examined. The protein content of a single oocyte, egg, or embryo at the mid-blastula stage (9 h after fertilization) was 0.30 μg; that of a single embryo at the mid-gastrula stage (24 h after fertilization) was 0.21 μg; and that of an early bipinnaria (72 h after fertilization) or mid-bipinnaria (96 h after fertilization) was 0.10 μg. The absorbance values changed linearly with concentration over the following

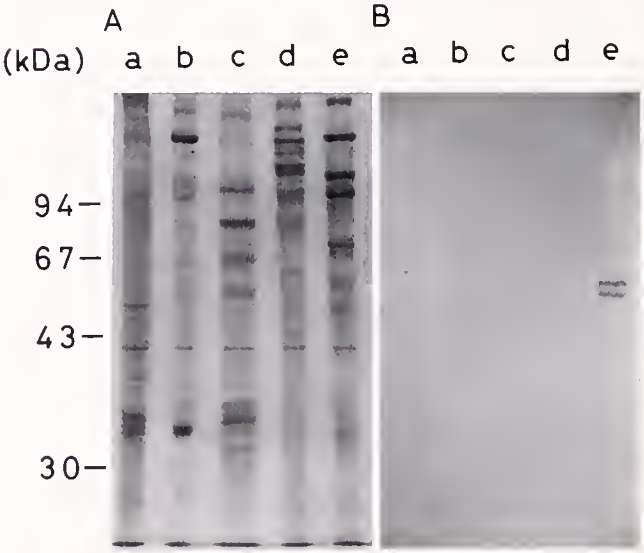

Figure 6. Immunoblots of eggs of *Scaphechinus mirabilis* (a), *Pseudocentrotus depressus* (b), *Hemicentrotus pulcherimus* (c), *Asterias amurensis* (d), and *Asterina pectinifera* (e). Eggs were solubilized in SDS sample buffer, and an aliquot of the sample solution equivalent to 10 μg protein was loaded onto each lane of SDS-10% polyacrylamide gel, electrophoresed, and then either stained with Coomassie brilliant blue (A) or blotted onto nitrocellulose and probed with the K1 antibody (B), as described in Materials and Methods.

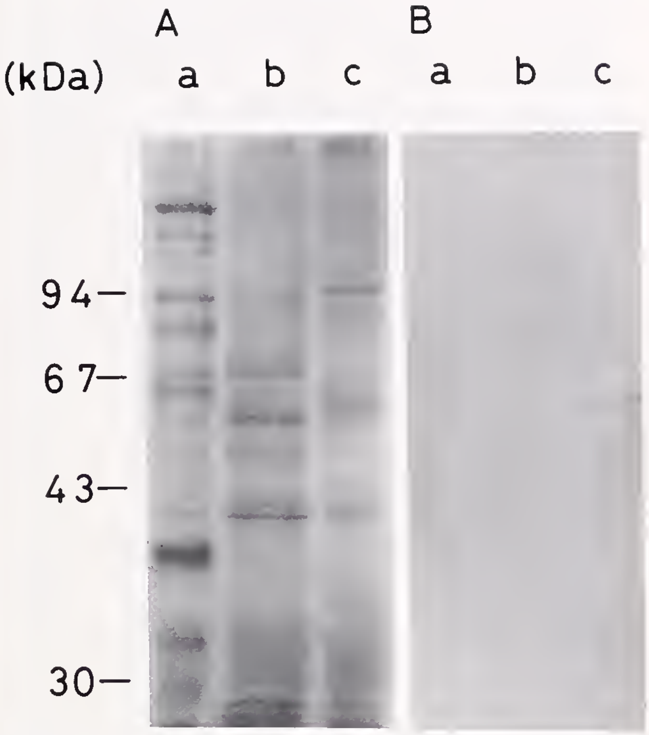

Figure 7. Immunoblots of *Asterina batheri* brachiolariae (a), *Asterina minor* brachiolariae (b), and *Asterina pectinifera* oocytes (c). Embryos and oocytes were solubilized in SDS sample buffer and an aliquot of the sample solution, equivalent to 5 μg protein, was loaded onto each lane of SDS-10% polyacrylamide gel, electrophoresed, and then stained with Coomassie brilliant blue (A) or blotted onto a nitrocellulose sheet (B). The sheet was probed with the K1 antibody, as described in Materials and Methods.

ranges: 0.0125 to 0.05 individuals per well for oocytes, eggs, and mid-gastrulae (24 h after fertilization); and 0.025 to 0.1 individuals per well for early bipinnariae (72 h after fertilization) and mid-bipinnariae (92 h after fertilization). It is not known at which stage of development the amount of the antigenic p58/56 in an embryo or larva becomes lower than the detection limit of the ELISA system with the K1 antibody. However, we succeeded in rearing five early brachiolaria of *A. pectinifera* (12 days after fertilization) by feeding bipinnariae in the laboratory. They were all loaded into a slot of an SDS-polyacrylamide gel, which was subjected, after electrophoresis, to immunoblot analysis. The sensitivity of the immunoblot analysis is approximately five times lower than that of the ELISA system used in this study. There were no immunoreactive bands on the slot (data not shown), suggesting that the amount of p58/56 present in a larva at the mid-bipinnaria stage decreased to less than 10% as development progressed to the early brachiolaria stage.

Although neither embryos nor larvae at various developmental stages could be quantified by the ELISA system, it could be used to estimate the minimum number of embryos or larvae present in a sample. We collected planktonic samples from 6 tons of water from the sublittoral zone of Hikonoura (1 or 3.5 m above the bottom of the sea, *ca.* 100 m off Sensui Island, *ca.* 34 23'N, 133 24'E) at high tide on November 22, 1987. The samples were spun down at 1000 × *g* for 10 min, and the precipitate was lysed in SDS sample buffer. Aliquots of the lysates were diluted 1:1000 in PBS, added to wells of a microtiter plate, and assayed by the ELISA system. The observed values were corrected with reference to a preparation containing a known number of *A. pectinifera* embryos at the mid-gastrula stage mixed with a standard amount of plankton lysate. The estimated numbers of *A. pectinifera* embryos or larvae in the three plankton samples collected separately from 6 tons each of water were 30, 130, and 130, assuming that the planktonic embryos were all mid-gastrulae. As described above, these figures are the minimum numbers of embryos and larvae present in the specimens, since the response of lysed larvae at later developmental stages was low compared with that of the mid-gastrulae, as shown in Figure 9.

Discussion

Mochizuki and Hori (1980) examined the phylogenetic relationship between five *Asterina* species by the enzyme

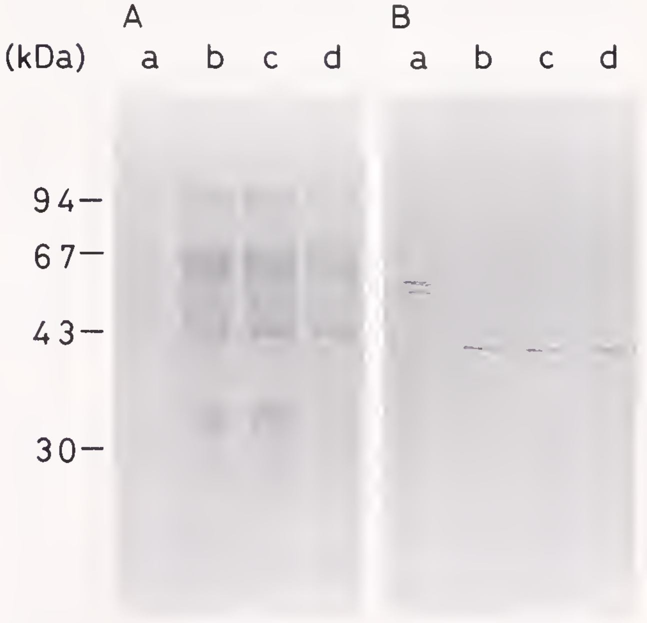

Figure 8. Immunoblots of *Asterina pectinifera* oocytes (a), and *Asterina pseudoexigua pacifica* early blastulae (b), wrinkled blastulae (c), and brachiolariae (d). Embryos and oocytes were solubilized in SDS sample buffer, and an aliquot of the sample solution, equivalent to five oocytes or embryos, was loaded onto each lane of SDS-10% polyacrylamide gel, electrophoresed, and then stained with Coomassie brilliant blue (A) or blotted onto a nitrocellulose sheet (B). The sheet was probed with the K1 antibody, as described in Materials and Methods.

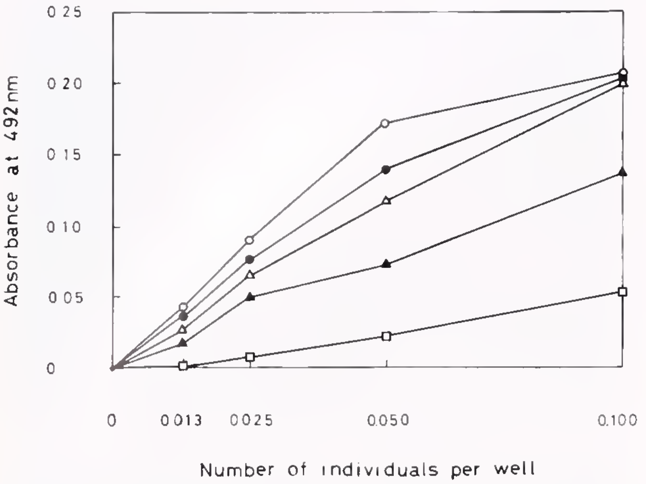

Figure 9. Measurement of antigen content in extracts of *Asterina pectinifera* oocytes (○), eggs (●), 1-day-old early gastrulae (△), 3-day-old late gastrulae (▲), and 4-day-old early bipinnariae (□) using an ELISA system with the K1 antibody. The method of measurement of antigen content is described in Materials and Methods.

inhibition test, using rabbit anti-*A. pectinifera* hexokinase antisera. The antisera inhibited the activity from hexokinase of *A. batheri, Asterina coronata japonica,* and *A. pseudoexigua pacifica* by 50–54% and that of *A. minor* by 30%. In light of these results, Mochizuki and Hori suggested that *A. pectinifera* and *A. minor,* but not the other *Astrina* species, belong to convergent lineages. Matsuoka (1981) arrived at a similar conclusion as a result of electrophoretic analysis of hexokinase and six other enzymes from five *Asterina* species. In our study, a peptide capable of recognizing the K1 monoclonal antibody, which is reactive to *A. pectinifera* p58/56, was found only in embryos and larvae of *A. pseudoexigua pacifica* among the *Asterina* species examined. Since little information is available regarding the function and structure of the peptides containing the K1 epitope, the reason for the phylogenetic variation of the peptides in these two species remains unclear.

So far, *A. pseudoexigua pacifica* has been found only in Sabiura, off Kushimoto in Wakayama Prefecture (Komatsu *et al.,* 1990). It is tiny (its body is only 5 mm long) and ovoviviparous. Development of this species, from fertilization to the completion of metamorphosis, occurs within the gonad. The juveniles, measuring approximately 0.5 mm in total length, crawl out of the gonad and pass through the gonoduct. According to the observation of Komatsu and Kano, made in July and August of 1972, the maximum number of juveniles released from a single adult was 1288 (Komatsu *et al.,* 1990). On the other hand, *A. pectinifera* is extremely abundant along the Japan Islands; an individual spawns more than 100,000 eggs, and it has embryonic and larval forms that live for a short time as members of the plankton community before moving into the benthic environment and undergoing metamorphosis. Therefore, the K1 antibody-reactive components detected by the ELISA assay in the plankton specimen were very unlikely to have been derived from embryos or larvae of *A. pseudoexigua pacifica.* Although we did not analyze the plankton specimens collected in the field by immunoblot assay, this assay can discriminate between embryos of *A. pseudoexigua pacifica* and those of *A. pectinifera,* according to the differences between molecular masses of the immunoreactive components. This enables *A. pectinifera* embryos and larvae in the mixed planktonic specimens to be identified unambiguously.

A. pectinifera differs from the other *Asterina* species in that the size and yolk content of its eggs are small, and that larval development, at both bipinnaria and brachiolaria stages, is indirect (Oguro and Komatsu, 1988). Therefore, this species can usually be identified accurately by microscopic examination of a larval specimen. However, there are huge numbers of diatoms in planktonic samples collected from water along the Japan Islands, and these make the detection of small numbers of starfish embryos and larvae almost impossible. Therefore, an immunological search for embryos and larvae in a complex plankton sample is particularly useful when their population is thin.

This study was aimed at determining the spawning season of *A. pectinifera* at specified regions along the coast of the Japan Islands. Ten percent of the total number of adult *A. pectinifera* caught on 29 October 1987, at Hikonoura off Sensui Island, contained ripe ovaries with full-grown oocytes. This fell to 3% on 15 November and to 1.7% on 19 December. These observations suggest that, at this sampling site, many adult *A. pectinifera* spawned at the beginning of November. For three years, spawning at this location has been observed to occur in November. Our results, obtained by immunological detection using an ELISA system, for *A. pectinifera* embryos or larvae in plankton samples collected at this location on 22 November 1987, agree well with these observations. However, inspection of the ovaries of adults collected from other areas along the coast of the Japan Islands revealed that the breeding season of this species is quite diverse, occurring in May in Tokyo Bay in Kanagawa Prefecture, June in Ago Bay in Mie Prefecture, July and August in the south-western part of the Inland Sea of Japan in Ehime Prefecture, September in Mutsu Bay in Aomori Prefecture, and November in the Sea of Yatsushiro in Kumamoto Prefecture. The spawning season in most other parts of Japan is, as yet, unknown. The spawning season in a specified region of the sea could be predicted by analyzing plankton specimens, sampled periodically, with the immunological assay method as described in this paper.

In summary, we have developed an assay system that detects embryos and larvae of *A. pectinifera* in complex biological specimens. The results of the this investigation suggest that immunological techniques are useful tools for taxonomic identification of eggs, embryos, or larvae in plankton populations.

Acknowledgments

This work was supported in part by a Grant-in-Aid for Cancer Research from the Japanese Ministry of Education, Science and Culture, and by grants from the Nissan Science Foundation and from the Japanese Fisheries Agency to S.I. We thank Professor C. Oguro, Toyama University, for his valuable suggestions and encouragement.

Literature Cited

Bradford, M. M. 1976. A rapid and sensitive method for the quantification of microgram quantities of protein using the principle of protein-dye binding. *Anal. Biochem.* **72:** 248–254.

Kanatani, H. 1973. Maturation-inducing substance in starfishes. *Int. Rev. Cytol.* **35:** 253–298.

Kano, Y. T., and M. Komatsu. 1978. Development of the sea-star, *Asterina batheri* Goto. *Dev. Growth Differ.* **20:** 107–114.

Komatsu, M. 1976. Wrinkled blastula of the sea-star, *Asterina minor* Hayashi. *Dev. Growth Differ.* **18:** 435–438.

Komatsu, M., Y. T. Kano, and C. Oguro. 1990. Development of a true ovoviviparous sea star, *Asterina pseudoexigua pacifica* Hayashi. *Biol. Bull.* **179:** 254–263.

Komatsu, M., Y. T. Kano, H. Yoshizawa, S. Akabane, and C. Oguro. 1979. Reproduction and development of the hermaphroditic sea-star, *Asterina minor* Hayashi. *Biol. Bull.* **157:** 258–274.

Laemmli, U. K. 1970. Cleavage of structural proteins during the assembly of the head of bacteriophage T4. *Nature* **227:** 680–685.

Matsuoka, N. 1981. Phylogenetic relationships among five species of starfish of the genus, *Asterina:* an electrophoretic study. *Comp. Biochem. Physiol.* **70B:** 739–743.

Mochizuki, Y., and S. Hori. 1980. Immunological relationships of starfish hexokinases: phylogenetic implication. *Comp. Biochem. Physiol.* **65B:** 119–125.

Oguro, C., and M. Komatsu. 1988. Asteroidea. Pp. 339–356 in *Development of Invertebrates,* K. Dan, K. Sekiguchi, H. Ando and H. Watanabe, eds. Baifukan, Tokyo. (in Japanese)

Reference: *Biol. Bull.* **181**: 104–122. (August, 1991)

Enzymatic Characterization of the Morphogen Recognized by *Agaricia humilis* (Scleractinian Coral) Larvae

DANIEL E. MORSE AND AILEEN N. C. MORSE

Department of Biological Sciences and the Marine Science Institute,
University of California, Santa Barbara, California 93106

Abstract. Larvae of the common Caribbean scleractinian coral, *Agaricia humilis,* are induced to settle and metamorphose by contact with specific crustose (nongeniculate) coralline red algae. This requirement for an exogenous trigger of settlement and metamorphosis has been shown to control the distribution of recruits of this coral in the natural environment. Results reported here demonstrate that the stringency and specificity of this larval requirement persist for at least 30 days following the planktonic release of the brooded larvae, thus enhancing both the capacity for dispersal of the larvae and the substratum specificity of their metamorphosis and recruitment.

The inducer of metamorphosis is shown to be associated with an insoluble macromolecular carbohydrate. This molecule is found with the partially purified cell walls obtained from a morphogenetic crustose red alga, *Hydrolithon boergesenii,* or its associated microflora. Because two non-inductive crustose red algal species also lack the cell wall-associated inducer, the substratum specificity of metamorphosis is probably the result of larval recognition of this molecule. In procedures that should prove widely applicable to other systems, purified and highly specific enzymes were used to cleave the inductive cell wall-associated polysaccharides and to solubilize the active morphogen. Enzymes were also used as probes with which to identify essential structural features required for the morphogenetic activity. These enzymatic and related biochemical studies show that the morphogen is associated with, and may itself contain, a sulfated glycosaminoglycan that includes multiple N-acetylglucosamine and galactose residues. The larval receptors that recognize this complex carbohydrate cue may thus be related to lectins. The solubilized morphogen induces normal settlement, attachment, and the metamorphosis of *A. humilis* and *A. tenuifolia* larvae on clean polystyrene surfaces, and the larvae seem to have no other requirement. This effect is apparently specific for larvae of species induced to settle by the intact alga; larvae of the sympatric coral *Tubastraea aurea* are not induced by this chemical, or by the intact algal surface. A wide variety of other natural and synthetic sulfated polysaccharides and related polymers have little or no inductive effect on the *A. humilis* larvae, suggesting that the larval receptors involved in substratum recognition are highly specific. A similar high specificity of lectin- and sulfated polysaccharide-mediated recognition, and the resulting control of differentiation, has been observed in a wide variety of biological systems.

Introduction

Agaricia humilis is a shallow-water scleractinian coral common throughout much of the central and southern Caribbean. *A. humilis* releases copious planula larvae throughout the year (van Moorsel, 1983). Recruitment of this and closely related congeneric species dominates patterns of scleractinian recruitment in many areas within their range (Dustan, 1977; Bak and Engel, 1979; Rylaarsdam, 1983; Rogers *et al.,* 1984; Hughes, 1985; Hughes and Jackson, 1985; van Moorsel, 1989).

The recruitment of *Agaricia humilis* is determined, in part, by larval selection of specific settlement sites, and is thus not a wholly stochastic or lottery-like process (Morse *et al.,* 1988; van Moorsel, 1989). The substratum-speci-

Received 18 January 1991; accepted 30 April 1991.

Abbreviations: Tris, tris-hydroxymethylaminomethane; DEAE, diethylaminoethyl; HPLC, high-pressure liquid chromatography; CCA, crustose (nongeniculate) coralline red alga/algae.

ficity of these larvae is governed by their recognition, upon contact, of particular nongeniculate encrusting coralline red algae; the principal factor controlling this recognition is a non-diffusing chemical cue associated with the algal surface (Morse *et al.*, 1988). The molecule responsible is insoluble and apparently associated with the cell walls of the recruiting algae or their microbial symbionts (Morse *et al.*, 1988). Instability of the molecule has further complicated efforts to characterize the inducer.

To overcome these difficulties, we have taken advantage of the specificities of purified enzymes in analyzing and solubilizing the morphogen recognized by *Agaricia humilis* larvae. The results reported here demonstrate that the molecule, which is biologically specific in its action as a morphogen, is a sulfated glycosaminoglycan. This result further suggests that the larval receptors involved in the recognition of this inducer may be related to lectins.

Materials and Methods

Larvae, and assays of metamorphosis

The procedures used are minor modifications of those described previously (Morse *et al.*, 1988). Adult colonies of *Agaricia humilis, A. tenuifolia,* and *A. agaricites agaricites* were identified by the taxonomic criteria of Wells (1973) and van Moorsel (1983, 1989). Colonies of these species and of the sympatric ahermatype, *Tubastraea aurea,* were collected from depths of 1–5 m in Bonaire, Netherlands Antilles, and incubated in the dark in 20–60 l of seawater at 28°C. Planula larvae (0.4–2 mm in length, depending on species; van Moorsel, 1983) were released copiously between 1800 and 2300 h, collected from the surface with a Pasteur pipet, and maintained at densities of ≤ 0.5 larva/ml in 600 ml polystyrene containers of 0.2 μm-filtered seawater containing 2 μg/ml of the antibacterial antibiotic, rifampicin, at 28°C, under continuous indirect illumination from a 40-W incandescent bulb at 3 m.

Assays for the induction of larval attachment and metamorphosis were (unless otherwise noted) performed in duplicate samples of 5 larvae/sample, in 10 ml of seawater (0.2 μm-filtered) containing 2 μg/ml rifampicin and other additions as noted, in 20 ml polystyrene disposable breakers incubated at 28°C with indirect illumination (as described above) for 24 h. Results (except those in Table V) are presented as the mean percentage ± S.D. of larvae metamorphosed; where no deviation is shown, there was no variation between duplicate assays. Metamorphosis, defined as the differentiation and calcification of the septal ridges following permanent attachment and cellular differentiation, was quantified by examination with a binocular microscope. This transition is thus an unequivocally recognized (and in these species, irreversible; *cf.* Morse *et al.*, 1988) developmental event, and not simply a behavioral change. Under the conditions of the assay employed, metamorphosis of the agariciid larvae is density-independent and unaffected by the presence or absence of newly metamorphosed conspecifics (Morse *et al.*, 1988).

For the analysis of DEAE binding of the inducer (presented in Table V), a scale for quantitation of units of inducer activity was employed. Units are defined in the section describing the DEAE binding experiments.

Coralline red algae, and preparation of cell wall-associated morphogen

Agaricia humilis larvae can be induced to metamorphose by only certain specific nongeniculate coralline red algae (Morse *et al.*, 1988; A. Morse and R. Steneck, in prep.). Where responsiveness to such algae was measured, small, repeatedly rinsed chips (approx. 50/assay, *ca.* 1 mm^3) of an inductive species, *Hydrolithon boergesenii,* or the non-inductive species *Neogoniolithon megacarpum* and *Porolithon pachydermum* (A. Morse and R. Steneck, in prep.), collected from the habitat of the adult *A. humilis,* were used. All crustose red algae were carefully cleaned of macroscopic epibionts before use in these and all other experiments.

Preparation of the decalcified, cell wall-associated morphogen from *Hydrolithon boergesenii* (and its associated microbial symbionts) was performed at 28°C as follows. The fresh coralline alga was cleaned of macroscopic epibionts, rinsed with distilled water, scraped from its substratum, blotted dry, and ground with a mortar and pestle to a viscous paste. For each 1 g of the resulting homogenate, 10 ml of 0.2 μm-filtered seawater containing 2 μg/ml rifampicin was added, and homogenization was continued with the mortar and pestle until an extremely viscous and very finely ground consistency was achieved. This material was forced by compressed air (10 p.s.i.) through a nitrocellulose filter (0.2 μm, 47 mm diam.) in a Nalgene filter apparatus. The resulting filter cake was washed successively with 5–7 portions (20 ml each) of rifampicin-containing seawater, the filtrand being resuspended as necessary, until the last filtrate was colorless (*i.e.*, all of the available red phycobiliproteins had been extracted). Chlorophyll and certain other organics then were extracted with 8–10 successive washes of the filtrand, as above, with 50 ml portions of 95% ethanol; these washes were continued until the filtrate was colorless. The remaining filter cake was light tan. The filtrand then was decalcified by uniform dispersion in 100 ml of 5% acetic acid. This slurry was incubated for 1 h with vigorous magnetic stirring, after which it was filtered through a nitrocellulose filter as described above. The resulting decalcified, insoluble crude cell wall preparation was washed extensively, on the filter, with 150 ml of distilled water, resuspended in 4 ml distilled water (using a Dounce homogenizer), adjusted on a pH meter to pH 8.2 (with about 3 drops of 0.1 *N* NaOH), assayed for morphogenic activity, and stored frozen. The activity of this material remained stable when frozen for at least several weeks.

Treatment with periodate and enzymes; assays for sulfate

Periodate oxidation was performed under standard conditions (Hassid and Abraham, 1957) as a test for the possible dependence of morphogenetic activity on *vic*-glycols typical of carbohydrates. Duplicate 1 ml aliquots of the decalcified cell wall-associated morphogen (see above) were incubated with an equal volume of 0.37 *M* sodium m-periodate for 1 h at 28°C. In one sample, the remaining periodate then was consumed by the addition of a 20-fold molar excess of glycerol; in the control sample, the periodate had been inactivated with this quantity of glycerol *prior* to its addition to the cell wall fraction. Both particulate samples then were washed free of the added chemicals by filtration on nitrocellulose filters (0.2 μm, 25 mm diam.), rinsed with rifampicin-containing filtered seawater, resuspended in this medium, and assayed in duplicate, in their entirety, for morphogenetic activity.

The following purified enzymes were used to analyze the structural determinants of morphogenetic activity, and to solubilize morphogens from the decalcified cell wall fraction. The quantities indicated in parentheses are the amounts used in each separate incubation: sulfatase purified from *Aerobacter aerogenes* (10 units), from *Patella vulgata* (200 units), and from *Haliotis cracherodii* (200 units, except where indicated otherwise in Fig. 5); trypsin (from bovine pancreas, 100 μg); papain (100 μg); β-galactosidase (from *Escherichia coli*, 1000 units); α-galactosidase (from *E. coli*, 10 units); β-glucuronidase (from *Helix aspersa*, 10,000 units); hyaluronidase (from bovine testes, 100 μg); agarase (from *Pseudomonas atlantica*, 1000 units); lysozyme (from chicken egg white, 10,000 units); and endo-β-galactosidase (from *Bacteroides fragilis*, 0.1 unit). Each of these enzymes was of the highest purity commercially available; all were obtained from Sigma (St. Louis), with the exception of endo-β-galactosidase, which was from Boehringer Mannheim (Mannheim). In addition to these highly purified enzymes, a crude preparation of digestive enzymes partially purified from *Haliotis cracherodii* was obtained from Sigma; this mixture, principally containing sulfatase, with lesser amounts of β-glucuronidase and other enzymes, was used in one experiment (Fig. 4) in amounts of 100 μg per incubation.

All enzyme incubations were carried out at 28°C for 1 h in 0.2 μm-filtered seawater containing 2 μg/ml rifampicin, with 0.5–1.0 ml of the final resuspended decalcified, cell wall-associated inducer (see above) used as substrate in each incubation, unless otherwise noted. Incubations of this particulate inducer (substrate) alone, with no added enzymes, were always conducted in parallel with the enzyme digestions.

Two methods were used to separate the enzymes and to solubilize the inducing molecules from the particulate cell wall fraction that was used as substrate. (1) In the first method, the samples were filtered (and washed) on nitrocellulose membrane filters; the remaining particulate cell wall fractions were then resuspended and assayed for retention of morphogenic activity. Assays with the chromogenic substrate, p-nitrophenylsulfate, showed that this method removed all detectable traces of sulfatase from the treated particulate fraction. This method has the further advantage that most of the enzyme proteins were adsorbed to the nitrocellulose filters, so that preliminary assays of soluble morphogen released into the filtrate could be performed (*cf.* Fig. 7). (2) In the second method, designed to ensure complete separation of the *solubilized* morphogens from any possible traces of the enzymes prior to assay, the enzyme digestions were performed inside closed dialysis tubing, and the small soluble morphogens were collected in the external dialysate (20 ml of 0.2 μm-filtered seawater containing 2 μg/ml rifampicin); the morphogens could then be assayed directly, in duplicate 10 ml portions. The use of dialysis membranes with calibrated retention limits of 2,000 Da, 6,000–8,000 Da, and 10,000–14,000 Da (Spectrapor, from Spectrum Medical Industries, Los Angeles) allowed us to estimate the molecular weights of the soluble morphogens thus obtained.

In one additional enzymatic technique, insoluble forms of trypsin and of papain (each covalently conjugated to agarose beads) were used to probe the structural determinants of a soluble, low molecular weight morphogen. This procedure, which affords rapid separation (by filtration) of the morphogen from the enzyme, was necessitated by the instability of the low molecular weight morphogen. The conjugated enzymes were from Sigma.

Sulfate was assayed turbidimetrically by precipitation with barium, after strong acid hydrolysis (Beeley, 1985).

Partial alkaline hydrolysis

The decalcified, cell-wall associated inducer from 100 mg of *Hydrolithon boergesenii* was incubated in 14 ml H_2O, after adjustment with NaOH to pH 12.0, in a sealed tube with vigorous magnetic stirring at 28°C. As a function of time, 1.5 ml aliquots were withdrawn, diluted with a 20-fold excess of 0.2 μm-filtered seawater containing 2 μg/ml rifampicin, and adjusted carefully with HCl to pH 8.2 (±.05). The neutralized samples then were filtered through nitrocellulose filters (0.2 μm, 47 mm diam.) and the soluble fraction assayed (in duplicate 10 ml samples) under the standard conditions.

Molecular weight estimation

The molecular weight of the small morphogen solubilized by partial alkaline hydrolysis was estimated by three independent methods: (1) *Gel-filtration through Sephadex G-10 (exclusion limit = ca. 2000 Da) in a column (0.9 cm diam × 14 cm length) calibrated with the excluded dye, Blue Dextran.* The sample was applied in 2 ml (10 mM Tris-Cl, 40 mM NaCl, pH 8.2), and eluted in 1 ml fractions of the same buffer. Each fraction was assayed in duplicate 0.5 ml aliquots in a final volume of 10 ml (0.2 μm-filtered seawater containing 2 μg/ml rifampicin) in the standard assay for morphogenic activity.

(2) *Ultrafiltration through Amicon YM-5 calibrated ultrafiltration membranes (retention limit = 5000 Da) in a low-volume Amicon pressure filtration cell.* Duplicate samples of 2 ml (in 0.2 μm-filtered seawater containing 2 μg/ml rifampicin) were filtered, and the resulting filtrates each analyzed in duplicate. Retained molecules were eluted from the upper face of the filters and assayed in duplicate. Molecules adsorbed or trapped on the filters also were assayed directly; finely cut fragments of the entire filters were immersed in the standard assay beakers.

(3) *Dialysis through Spectrapor calibrated dialysis tubing (retention limit = 2000 Da).* Duplicate 2 ml samples (in 0.2 μm-filtered seawater containing 2 μg/ml rifampicin) were dialyzed against 20 ml of the same medium outside the membrane. After the first dialysis for 5 h, the external dialysate was removed, and a second portion of 20 ml was placed outside the membrane for a further 5-h dialysis. At the end of the 10-h period, assays were performed on duplicate 10-ml aliquots of the two external dialysates from each sample and on the sample remaining inside the membrane (duplicate 1-ml aliquots assayed in a final volume of 10 ml). Assays performed on a sample incubated in parallel with no dialysis controlled for loss of activity resulting from inactivation during the 10-h experiment.

Binding to DEAE

Adsorption to the diethylaminoethyl (DEAE)-based anion exchanger was investigated with two different types of DEAE-substituted adsorbant, DEAE-Sephadex (A-50, from Pharmacia, Piscattaway) and DEAE-nitrocellulose filters (NA-45, from Schliecher and Schuell, Keene). For the purpose of these experiments, units of morphogenetic activity were defined as the mean percentage of larvae metamorphosed (in duplicate standard assays after 24 h) per ml of sample (in the linear, concentration-dependent range of the assay below saturation), multiplied by the number of ml in the sample ÷ 1%. When care has been taken to ensure that assays are performed in the linear range, results with the low molecular weight morphogen have proven quantitatively reliable for inventory purposes (*cf.* Table V).

A 3-ml bed-volume column of DEAE-Sephadex A-50 was loaded with 1000 units of the low molecular weight morphogen obtained by mild alkaline hydrolysis. The sample was applied in 18 ml of 1 mM Tris-Cl, pH 8.2; the column then was successively eluted with an additional 10 ml of this buffer, followed by 30 ml of the same buffer containing 0.4 M NaCl. Fractions of 5 ml were collected, and each was assayed in duplicate portions (of 0.2, 0.5, and 1.0 ml each), in a final volume of 10 ml, for morphogenetic activity. After chromatography, samples of the resin were assayed as well.

DEAE-nitrocellulose filters were pre-washed (with 1 mM Tris-Cl, pH 8.2), loaded with 640 units of the low molecular weight morphogen in 4 ml of the same buffer, and then eluted with a syringe. After application of the sample, the filters were washed successively with additional 4 ml portions of: (a) the same buffer; (b) the same buffer containing 0.4 M NaCl; and (c) cold 0.4 N HCl, at an apparent pH = 0.53. The acid eluate was immediately adjusted to 1 mM Tris-Cl and neutralized with NaOH to pH 8.2. Each eluate then was assayed in duplicate 0.5 ml aliquots for morphogenetic activity; the filters were cut into fine segments, rinsed in distilled water, and assayed directly as well.

Results

Persistence of larval competence, stringency and specificity

We had previously found that larvae of *Agaricia humilis* maintain their competence to undergo metamorphosis for at least 12 days following planulation (Morse *et al.*, 1988). The results shown in Figure 1 extend those observations, demonstrating that morphogenetic competence, and the stringency of the larval dependence on an exogenous morphogenetic inducer, are maintained for at least 30 days following larval release. The specificity of the larvae for only certain species of CCA as morphogenetic inducers also persists for this time. Surfaces of the alga *Hydrolithon boergesenii* are recognized as morphogenetic stimuli by larvae 30 days after release, as well as by larvae only hours after release, while surfaces of *Neogoniolithon megacarpum* are not inductive throughout this period (Fig. 1). However, the initial rate of response of the larvae to the *Hydrolithon* inducer declines after about 2 weeks following larval release (Morse and Morse, in prep.). For that reason, all subsequent experiments were performed with larvae within the first 5 days following release.

Morphogen is associated with alga-specific cell wall carbohydrate

The morphogen associated with surfaces of *Hydrolithon boergesenii* was found previously to be detectable in ho-

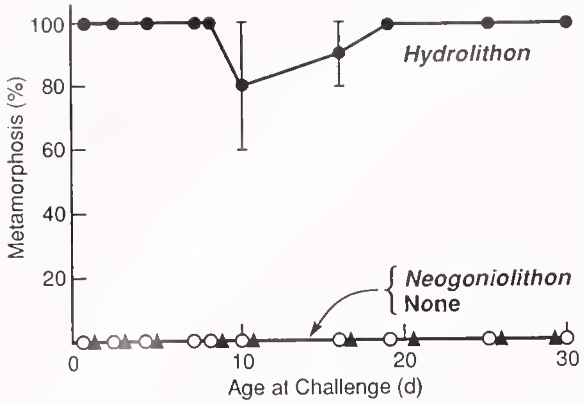

Figure 1. Persistence of stringency and specificity of the requirement of *Agaricia humilis* larvae for specific nongeniculate coralline red algae, *e.g.*, *Hydrolithon boergesenii* (●), to induce settlement and metamorphosis. Larvae exposed to non-inductive *Neogoniolithon megacarpum* (▲) or to no inducer (○) fail to metamorphose. (5 larvae/trial; n = 2–4 trials each; 36 h). Where no error bars are shown, variation = 0.

mogenates prepared from the intact alga in seawater, but little or no activity could be found in the soluble filtrates of such homogenates; activity remained associated with the washed, insoluble fraction (Morse *et al.*, 1988). The morphogen was insoluble in water (tested up to 60°C), organic solvents (ethanol, methanol, acetone, and ether), and 5% acetic acid. Preparation of a cell wall fraction from *Hydrolithon boergesenii* (and its associated microsymbionts) by sequential homogenization, extraction of the water-soluble cytoplasmic fraction, removal of chlorophyll and lipids by extraction with ethanol, and decalcification with dilute acetic acid, as described in Materials and Methods, yielded material containing the inducer. The acetic acid decalcification increased the morphogenetic activity of the preparation by about 60–100% relative to that in the seawater-extracted crude homogenate (data not shown). The resulting crude cell wall preparation shows strong morphogenetic activity that is both dose- and time-dependent (Fig. 2), with lower amounts of the material exhibiting a pronounced lag in the induction of larval metamorphosis. Two species of nongeniculate red algae (*Porolithon pachydermum* and *Neogoniolithon megacarpum*) that do not induce *A. humilis* larvae to settle or metamorphose lack the chemical inducer associated with the cell wall fraction (Table I). Thus the recognition of this chemical inducer is likely to be the basis for the observed algal substratum specificity.

The decalcified, cell wall-associated morphogen from *Hydrolithon boergesenii* was tested for its sensitivity to inactivation by exposure to the mild chemical oxidant, sodium-*m*-periodate. Exposure to periodate for 1 h at 28°C, followed by inactivation of the remaining periodate with glycerol, and washing of the treated sample by ultrafiltration, completely inactivated the morphogen (Fig. 3). Activity also could not be detected in the filtrate of the periodate-treated sample. As seen in Figure 3, a control sample treated in parallel, but receiving "periodate" only after the oxidant had first been inactivated with glycerol, retained full morphogenetic activity. The observed sensitivity of the morphogen, and the known specificity of the oxidant under the conditions used (Hassid and Abraham, 1957), suggest that the morphogen may contain a carbohydrate or other *vic*-glycol moiety essential for its activity.

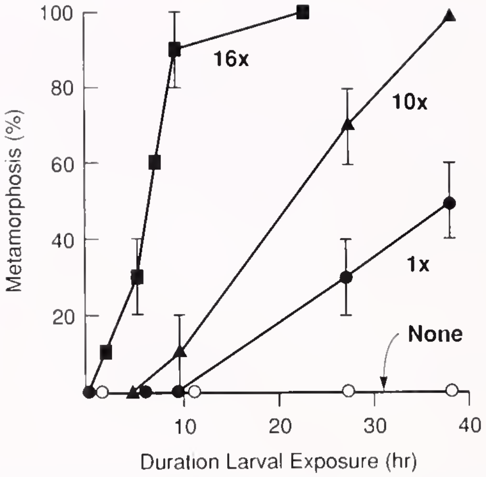

Figure 2. Inducer of larval attachment and metamorphosis is associated with cell wall fraction purified from *Hydrolithon boergesenii* (and associated microsymbionts). Results show time-dependent induction of metamorphosis by 1×, 10×, or 16× relative amounts of cell wall fraction; 1× = 0.02 ml of decalcified cell wall fraction. Standard assay conditions as described in Materials and Methods.

Enzyme probes reveal essential features of morphogen structure

The association of the morphogen with a decalcified crude cell wall preparation (Fig. 2) and its sensitivity to

Table I

Non-inductive algae lack the cell wall-associated chemical inducer

	Metamorphosis (%)		
Addition	*Hydrolithon boergesenii*	*Porolithon pachydermum*	*Neogoniolithon megacarpum*
Alga	100 ± 0	0 ± 0	0 ± 0
Homogenate	60 ± 0	0 ± 0	0 ± 0
Cell wall fraction	100 ± 0	0 ± 0	0 ± 0

Larvae of *Agaricia humilis* were assayed for metamorphic response to three species of nongeniculate coralline red algae, and in parallel, to the crude homogenates and decalcified cell wall fractions prepared from these algae. Metamorphosis scored at 48 h; other details as in Figure 1.

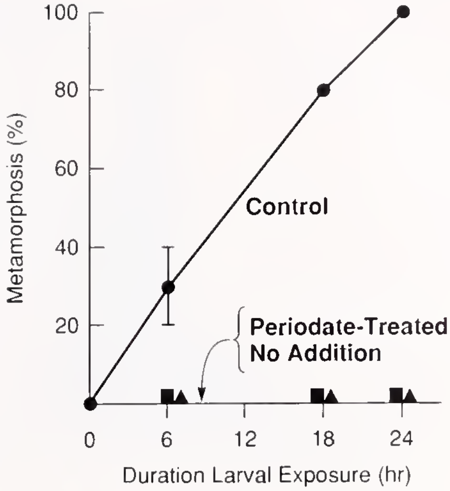

Figure 3. Inactivation of the cell wall-associated inducer of larval metamorphosis by oxidation with periodate. The control and periodate-treated samples of cell wall-associated inducer (equal amounts, incubated in parallel) differed only in the time at which the periodate was inactivated with glycerol. In the control sample, the periodate was inactivated prior to its addition to the inducer; in the treated sample, the periodate was inactivated 1 h after exposure to the inducer. Further details are in Materials and Methods. All assays in duplicate.

periodate (Fig. 3) strongly suggest the presence of a carbohydrate, and possibly a polysaccharide, component. This suggestion has been confirmed, and essential features of the morphogenic polysaccharide have been revealed, through the use of enzymes as structural probes.

The morphogenic activity of the cell wall preparation proved sensitive to a crude mixture of sulfatase and other digestive enzymes from the gut of the herbivorous gastropod, *Haliotis cracheroddi* (black abalone). Equivalent amounts of the inducer were incubated in the presence and absence of the abalone digestive enzymes for 1 h at 28°C; after this incubation, the enzymes were removed and the cell wall fractions washed by ultrafiltration. Equivalent portions then were assayed, in quadruplicate, with *Agaricia humilis* larvae (Fig. 4). This enzyme treatment completely inactivated the cell wall-associated morphogen. Assays of the filtrate (not shown) confirmed that the active moiety had been destroyed, and not simply solubilized. In the experiment illustrated in Figure 4, small samples of untreated *Hydrolithon boergesenii* were added to duplicate groups of larvae that had been incubated for 24 h in the presence of the treated or untreated inducer, or incubated for that period in the absence of inducer. All of these larvae (100% ± 0%) metamorphosed in response to the added coralline alga, indicating that the prior enzyme treatment had in no way affected the larvae; *i.e.*, the enzyme had inactivated the morphogen, and not the larvae.

Similar results were obtained when the morphogen was treated with the digestive sulfatase purified from the limpet, *Patella vulgata* (Table II). A significant reduction in the dose-dependent activity of the cell wall-associated morphogen resulted from this enzyme treatment. When

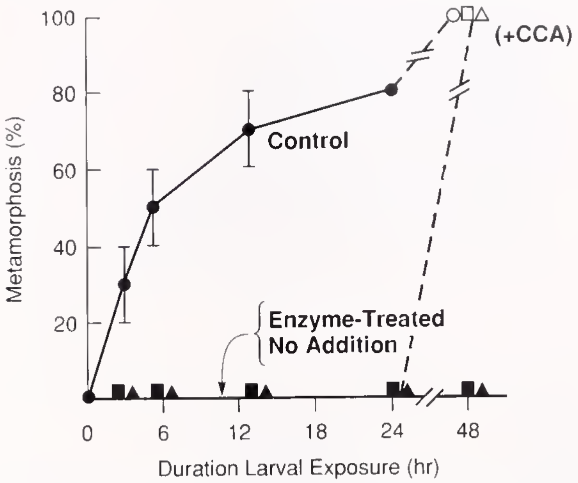

Figure 4. Inactivation of the cell wall-associated inducer by treatment with digestive enzymes from abalone. Equivalent amounts of inducer were incubated in parallel (1 h, 28°C) with or without exposure to enzymes. Samples then were washed by ultrafiltration. Assays with the chromogenic substrate for sulfatase, p-nitrophenylsulfate, confirmed that all of the enzyme was removed from the particulate samples by this washing procedure. The washed samples then were assayed in quadruplicate for remaining morphogenic activity (in parallel with assays with no addition). After 24 h of exposure of the larvae to each of the three assay conditions, fresh samples of the inductive crustose coralline red alga *Hydrolithon boergesenii* (CCA) were added to duplicate samples of each assay type (open symbols), to assess the remaining responsiveness of the larvae.

Table II

Effect of sulfatase purified from Patella vulgata *on cell wall-associated morphogen*

Inducer (equivalents)[1]		Metamorphosis[2]
Untreated	Enzyme-treated	(%)
0	0	0 ± 0
1	0	70 ± 10
6	0	100 ± 0
0	1	0 ± 0
0	6	20 ± 0
1	1	70 ± 10

[1] The decalcified morphogen was incubated with or without enzyme for 1 h at 28°C, and subsequently washed free of enzyme, as described in Materials and Methods. One equivalent corresponds to 0.25 ml of the original decalcified morphogen. Portions of the two samples then were assayed, either singly or in pre-mixed combination, in the relative amounts shown.

[2] Assays were conducted with 5 larvae/trial, and scored for metamorphosis after 24 h; results = mean ± S.D.; n = 2 trials for each condition.

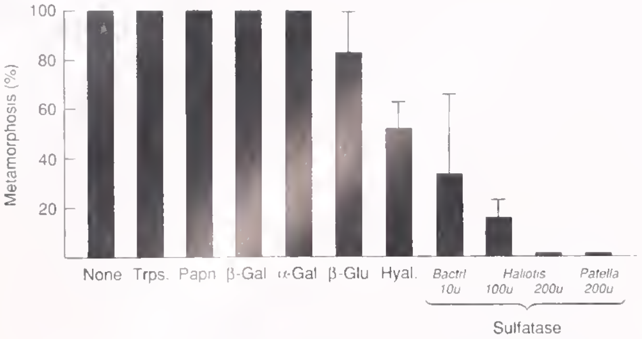

Figure 5. Effects of purified enzymes used as probes for structural determinants of the cell wall-associated inducer of larval metamorphosis. Trps. = trypsin; Papn. = papain; β-Gal. = β-galactosidase; α-Gal. = α-galactosidase; β-Glu. = β-glucuronidase; Hyal. = hyaluronidase; sulfatases purified from the bacterium *Aerobacter aerogenes*, the limpet *Patella vulgata*, and the abalone *Haliotis cracherodii*, were used in the amounts (enzyme units) indicated. Assays, after treatment and washing of the particulate samples, were performed in duplicate; all other details as in Figure 4 and Materials and Methods.

equivalent amounts of the enzyme-treated and the untreated morphogen were mixed and assayed together, no reduction in the activity of the untreated morphogen was observed, thus confirming the conclusion that the molluscan enzymes inactivated the inducer, and not the larvae. Larvae exposed to molluscan digestive enzyme-treated inducer, and either subsequently (Fig. 4) or simultaneously (Table II) exposed to untreated inducer, responded normally and completed metamorphosis.

The digestive enzyme preparation from *Haliotis* that inactivated the coral morphogen (Fig. 4) is a relatively crude mixture containing high quantities of a sulfatase (Spaulding and Morse, 1991) and lower quantities of β-glucuronidase and several other enzymes. When purified molluscan sulfatase and β-glucuronidase were tested separately, the sulfatase was a potent inactivator of the cell wall-associated morphogen, whereas β-glucuronidase had little if any significant activity (Fig. 5). The data show that sulfatases purified from *Haliotis*, *Patella*, and from a bacterium all inactivate the morphogen, and that the effect of the *Haliotis* sulfatase is concentration-dependent. (The slight inactivation caused by treatment with the β-glucuronidase preparation is likely to reflect the activity of the small amount of sulfatase known to still contaminate this preparation.)

In similar tests, five other purified enzymes were used to probe for essential features of the morphogen structure. Of these, only hyaluronidase, which cleaves sulfated polysaccharide chains, reduced the activity of the insoluble, cell wall-associated morphogen (Fig. 5). The proteolytic enzymes trypsin and papain, and the exosaccharidases α-galactosidase and β-galactosidase, were completely without effect. These results, and those presented above, strongly suggest that a sulfated polysaccharide is an essential component of the morphogen recognized by the *Agaricia humilis* larvae.

Enzymes release and degrade soluble morphogen

Four purified endopolysaccharidases, including agarase, endo-β-galactosidase, lysozyme, and hyaluronidase, released a soluble morphogen from the insoluble cell wall preparation (Fig. 6). The subsequent time-dependent decline in soluble morphogen activity seen with prolonged exposure to agarase suggests that this enzyme may continue to attack the solubilized inducer; this suggestion is confirmed by experiments presented below. None of the other enzymes tested in the experiment shown in Figure 5 released any detectable soluble activity.

The enzyme-solubilized morphogen was a potent inducer, causing the *Agaricia humilis* larvae to quickly attach either to the sides or bottoms of the clean polystyrene assay beakers, and to undergo rapid and normal metamorphosis and post-metamorphic growth (*cf.* Fig. 10). These results, and those with the alkali-solubilized material discussed below, prove that the larvae do not require any specific tactile stimulus from the morphogen, but respond solely to its chemical structure.

Experiments in which aliquots of the cell wall-associated morphogen were incubated in the presence and absence of purified enzymes, inside dialysis tubing, confirmed that agarase and other endosaccharidases continue to attack and subsequently degrade the soluble morphogenic molecules they first release (as suggested by the data in Fig.

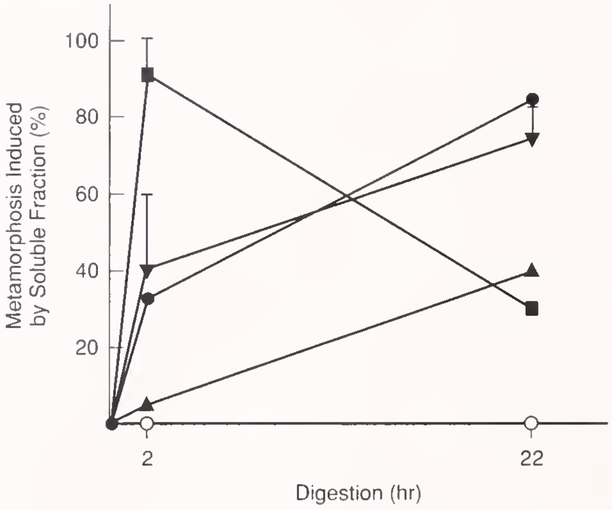

Figure 6. Solubilization of morphogen by treatment with purified endopolysaccharidases. Agarase (squares); endo-β-galactosidase (filled circles); hyaluronidase (upward triangles); lysozyme (downward triangles); no enzyme controls (open circles). Other procedures similar to experiment shown in Figure 5. Details are in Materials and Methods.

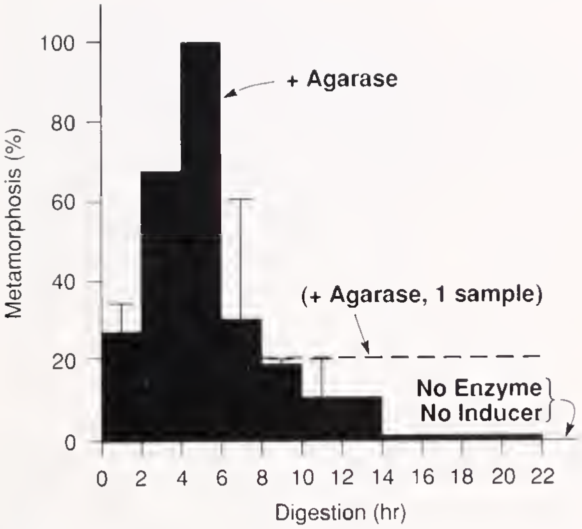

Figure 7. Enzymatic solubilization and further purification of small morphogen. The insoluble, cell wall-associated inducer of larval metamorphosis was digested inside a dialysis tubing (retention limit = 14,000 Da) with purified agarase. Small morphogens released from the insoluble inducer were allowed to accumulate in the external dialysate, which was removed and assayed, and replaced with fresh external medium, every two hours. An otherwise identical sample was digested in parallel with no change of dialysate for 22 h, after which the external medium was removed and assayed (dotted line). Other details as described in the text; all assays were performed in duplicate under standard conditions. Controls conducted in parallel included assays of dialysates changed every 2 h from a sample incubated with no enzyme, and larvae incubated with no additions; these gave 0 ± 0% metamorphosis. Results show metamorphosis induced by the dialysates.

6). The external dialysates (including the permeant small morphogens released) were allowed to diffuse and accumulate outside of the membranes for a fixed interval, after which they were removed for assay, and replaced with fresh external liquid for the next interval of incubation. With purified agarase, and 2-h intervals for accumulation, removal, and replacement of the external dialysates, we observed a time-dependent increase and subsequent decline in the rate of appearance of dialyzable morphogenic activity with $\bar{M} \leq 14{,}000$ Da (Fig. 7). However, far less of the total morphogenic activity could be detected in an otherwise identical incubation, in which only one sample of dialysate was collected and assayed after prolonged incubation (24 h). All of the dialysates were held at 28°C until the end of the experiment (24 h) and assayed simultaneously, to control for any time-dependent decay of activity. Because the difference between the two parallel incubations thus was in the limitation (2 h interval) or prolongation (24 h interval) of the opportunity for the small dialyzable morphogen to diffuse back and forth between the outside and inside of the dialysis tubing, we conclude that prolonged exposure of released, dialyzable morphogen to the agarase resulted in degradation of the active morphogen. We therefore conclude that agarase, which cleaves sulfated polysaccharides, particularly at β-1,4-linked galactose residues, not only releases the active morphogen from a sulfated polysaccharide parent molecule, but degrades the morphogen itself, as well. Therefore, the structure of the morphogen would seem to contain a sulfated polysaccharide with galactose residues.

In similar experiments, we compared dialysis membranes with calibrated porosites of *ca.* 10,000–14,000 Da and *ca.* 6,000–8,000 Da, and two other endosaccharidases in addition to agarase (Fig. 8). When lysozyme was used we again saw a time-dependent increase and subsequent decline in the rate of accumulation of dialyzable morphogen with $\bar{M} \leq 14{,}000$ Da. There was a similar, but displaced, rise and fall in the accumulation of smaller morphogen ($\bar{M} \leq 8000$ Da), suggesting that these smaller molecules may be derived, in part, by enzymatic cleavage of the larger dialyzable inducers. With the 8-h intervals

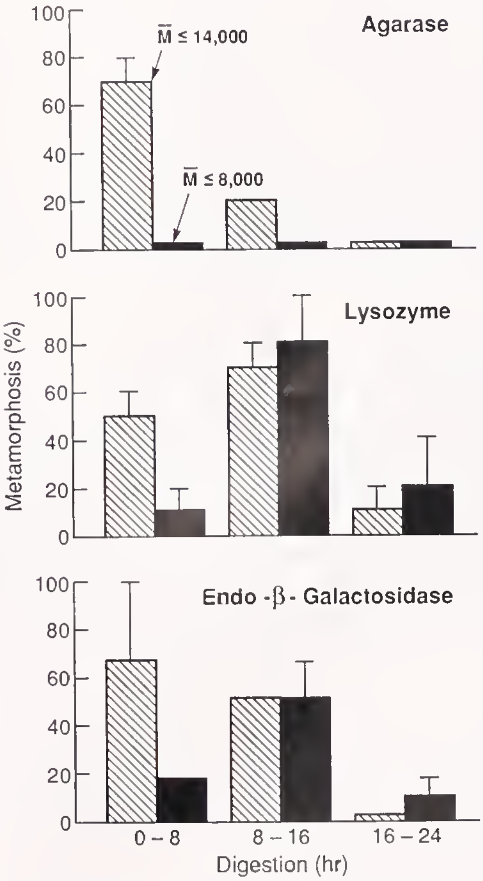

Figure 8. Enzymatic solubilization and further purification of small morphogen through dialysis membranes of two different porosities. Experiment performed as in Figure 7, except that: agarase, lysozyme and endo-β-galactosidase were compared; the digestions were performed in parallel in dialysis tubings with retention limits of 14,000 Da (hatched bars) and 8,000 Da (solid bars); the external dialysates were changed and saved for assays every 8 h.

Table III

Specificities and effects of enzyme probes used to solubilize and characterize the morphogen

		Effect of morphogen[3]			
Enzyme	Cleaves specifically[2]	Inactivates	Solubilizes	$\bar{M} \leq 14{,}000$	$\bar{M} \leq 8{,}000$
Proteases					
Papain	Peptides	No	No	—	—
Trypsin	Peptides at Lys, Arg	No	No	—	—
Exosaccharidases					
β-Glucuronidase	Terminal β-glucuronate glycosides	No	No	—	—
β-Galactosidase	Terminal β-galactosides	No	No	—	—
α-Galactosidase	Terminal α-galactosides	No	No	—	—
Sulfatases[1]					
Sulfatase-1	Organic sulfate esters	Yes	No	—	—
Sulfatase-2	Organic sulfate esters	Yes	No	—	—
Sulfatase-3	Organic sulfate esters	Yes	No	—	—
Endosaccharidases					
Hyaluronidase	Sulfated polysac. chains	(Yes)	(Yes)	No	No
Agarase	Galactans & sulfated galactan chains at β-1,4 linkages	(Yes)	Yes	Yes	No
Lysozyme	Polysac. chains at β-1,4 linkages to N-acetyl-glucosamine	(Yes)	Yes	Yes	Yes
Endo-β-galactosidase	Polysac. chains at internal β-1,4, linkages between galactose and N-acetyl-glucosamine or N-acetyl-glucosamine-sulfate	(Yes)	Yes	Yes	Yes

[1] Sulfatases -1, -2, and -3 = enzymes purified from *Haliotis, Patella,* and *Aerobacter,* respectively.

[2] Enzyme specificities: endo-β-galactosidase (Li *et al.*, 1982; Kitamikado *et al.*, 1982; Scudder *et al.*, 1983, 1984); β-agarase (Morrice *et al.*, 1983a, b; Usov and Ivanova, 1987); sulfatase (De *et al.*, 1978; Dodgson and Fitzgerald, 1982); others (Zubay, 1983; Freifelder, 1983).

[3] Solubilization refers to the release of active morphogen into a 0.2 μm ultrafiltrate; M values refer to release of small dialyzable morphogen with the indicated approximate molecular weight. Parentheses indicate that the effect is observed but slow.

for dialysate accumulation employed in the experiment shown in Figure 8 (compared to the 2-h intervals employed in Fig. 7), only a time-dependent decline in the rate of accumulation of morphogen ≤ 14,000 Da was observed when digestion was catalyzed by endo-β-galactosidase. A slower, time-dependent rise and subsequent fall in accumulation of smaller morphogenic molecules ($\bar{M} \leq$ 8,000 Da) is seen, however, again suggesting that some of these smaller molecules may be produced by cleavage of the larger but still dialyzable morphogens. The activity of the small dialyzable morphogen released by endo-β-galactosidase was unaffected by incubation for several hours in the presence or absence of trypsin or papain linked to insoluble matrices (data not shown), confirming the earlier finding (*cf.* Fig. 5) that the morphogen is resistant to these proteases.

With agarase catalyzing cleavage, the 8-h collection intervals permit only the observation of the time-dependent decline in the rate of accumulation of morphogen ≤ 14,000 Da (Fig. 8). Little or no active morphogen ≤ 8,000 Da was observed from the agarase digestion, suggesting perhaps that the smaller fragments produced by this enzyme either lack essential morphogenetic determinants, or may be particularly labile to subsequent inactivation (either spontaneous or enzymatic). Similar experiments with hyaluronidase produced no detectable morphogen in the dialysates from either porosity membrane (data not shown). This failure of hyaluronidase to yield dialyzable morphogen might reflect either the failure of cleavages catalyzed by this enzyme to yield molecules sufficiently small to leave the dialysis tubing, or the destruction by hyaluronidase of sites required for morphogenic activity.

The substrate specificities of the enzyme probes employed in these studies, and the results observed, are summarized in Table III. Reduction in the yield of the low molecular weight ($\bar{M} \leq$ 8,000 Da) morphogen when any two of the tested endopolysaccharidases are present (results not shown) suggests that this small molecule itself contains sites cleaved by agarase, lysozyme, and hyaluronidase (as does the cell wall-associated complex from which the morphogen can be released by these enzymes). A similar conclusion had been drawn independently from the experiments with agarase alone (Figs. 6, 7). The substrate specificities of these purified enzymes (Table III) thus suggest that the small morphogen contains a sulfated

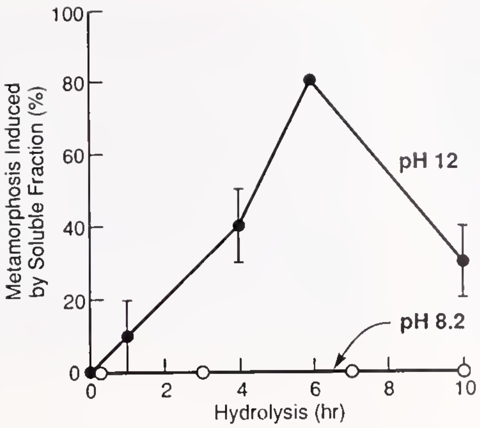

Figure 9. Time-course of solubilization of morphogen by mild alkaline hydrolysis. The decalcified, cell wall-associated inducer from *Hydrolithon boergesenii* was incubated with vigorous stirring at pH 12.0. At the times indicated, aliquots were withdrawn, neutralized to pH 8.2, filtered through nitrocellulose filters (0.2 μm, 47 mm diam.), and the soluble fractions assayed (in duplicate 10 ml samples) under the standard conditions. Details are in Materials and Methods. Results shown are the average percentages of larvae induced to attach and metamorphose by the soluble fractions, ±S.D. Results of a parallel and otherwise identical incubation held continuously at pH 8.2 are included for comparison.

polysaccharide (cleaved by hyaluronidase, agarase, and sulfatase), with multiple, substituted residues of N-acetylglucosamine (linkages cleaved by lysozyme and endo-β-galactosidase) and multiple residues of galactose (linkages cleaved by agarase and endo-β-galactosidase). Protein (or peptide) does not appear to be an essential component, nor do several specific free or terminal sugars or saccharide units.

Hydrolysis with dilute alkali releases small anionic morphogen containing sulfate

The finding that specific endopolysaccharidases can release a soluble morphogen from the insoluble cell wall-associated fraction suggested that non-enzymatic, partial hydrolysis under mild conditions might yield similar results. While some desulfation also would occur, hydrolysis with sufficiently dilute alkali would be expected to yield oligosaccharide fragments with retention of at least some of the original sulfate groups (Percival and McDowell, 1967). As predicted, exposure of the decalcified, particulate cell wall fraction to dilute alkali (pH 11–12) released a soluble, sulfate-containing morphogen. The increase in yield of soluble morphogenic activity as a function of the time of incubation at pH 12 is shown in Figure 9. The apparent decline in yield after 6 h suggests that the morphogen itself is slowly inactivated at pH 12. Exposure to strong acid (4 *N* HCl) or strong base (4 *N* NaOH) causes more rapid inactivation.

The morphogen released by mild alkaline hydrolysis is of relatively low molecular weight, strongly anionic, sulfate-containing, and unstable. Estimates of the apparent molecular weight were made by three independent methods: ultrafiltration through a calibrated membrane, dialysis through a calibrated dialysis membrane, and Sephadex gel filtration (Table IV). In ultrafiltration, all of the applied activity was recovered in the YM-5 membrane ultrafiltrates, consistent with $\bar{M} \leq 5000$ Da. In dialysis through a calibrated membrane, all of the recovered activity (equal to that in the non-dialyzed control) was found in the first external dialysate, (see Materials and Methods), consistent with $\bar{M} \leq 2000$ Da. These results were confirmed by gel-filtration through Sephadex G-10, in which all of the applied activity was eluted at the end of the included volume, indicating $\bar{M} \leq 2000$ Da. These findings all indicate, therefore, that the morphogen solubilized by alkaline hydrolysis may be as small as 2000 Da or less (Table IV).

This low molecular weight material is strongly anionic; it binds tightly to DEAE Sephadex and to DEAE-nitrocellulose (Table V). Because the material does not bind to Sephadex or nitrocellulose alone, without DEAE substitution, the binding is most likely dependent on ionic interaction. This binding proves to be very strong; little activity could be removed from the DEAE Sephadex by elution with 0.4 *M* NaCl, and 75% of the initially applied activity was found still adsorbed to the resin (Table V). Similarly, 63% ± 13% of the activity applied to a DEAE-nitrocellulose filter was found still adsorbed to the filter, even after elution with 0.4 *N* HCl. That the morphogen was not eluted from DEAE by 0.4 *N* HCl indicates that its ionic binding was dependent on more strongly anionic groups than uronic acids or other simple carboxylates (pK *ca.* 2). These results are consistent with the conclusion, based on sulfatase sensitivity (*cf.* Figs. 4, 5; Table II), that the morphogen contains sulfate groups (see Discussion).

The presence of sulfate esters in this solubilized morphogen was confirmed independently by turbidimetric analysis with barium after strong acid hydrolysis (method according to Beeley, 1985). The yields obtained indicate

Table IV

Estimation of molecular weight of the small morphogen solubilized by partial alkaline hydrolysis

Method	$\bar{M}$ Estimate (Da)
Ultrafiltration	≤5000
Dialysis	≤2000
Sephadex gel filtration	≤2000

Details are as described in Materials and Methods. Independent experiments verified that there was no significant adsorption of the morphogen to the gel-filtration matrix or to the ultrafiltration or dialysis membranes.

Table V

Adsorption of the small morphogen, solubilized by partial alkaline hydrolysis, to DEAE

Adsorbant	Eluant or fraction	Units	Recovery (%)
DEAE Sephadex	Application	1,000	—
	1 m*M* Tris	0	0
	1 m*M* Tris + 0.4 *M* NaCl	50	5
	Remaining on DEAE	753	75.3
	(Total)		(80.3)
DEAE Nitrocellulose	Application	640	—
	1 m*M* Tris	0	0
	1 m*M* Tris + 0.4 *M* NaCl	0	0
	0.4 *N* HCl	0	0
	Remaining on DEAE	400 ± 80	63 ± 13
	(Total)		(63 ± 13)

Details are as described in Materials and Methods. Morphogen recovered in the high-salt eluate, and that remaining on the DEAE, induced larvae to attach firmly to the polystyrene assay beakers and metamorphose normally. Control experiments demonstrated that the DEAE adsorbants without the applied morphogen had no such activity. Additional controls showed that there is no binding of the soluble morphogen either to Sephadex or nitrocellulose alone, without the DEAE ion-exchange groups present.

the presence of *ca.* 8–14% (w/w) sulfate in the alkali-solubilized morphogenic fraction.

Agaricia humilis larvae exposed to the alkali-solubilized low molecular weight morphogen, either free in solution or bound to DEAE (Sephadex or nitrocellulose) showed rapid, normal, and complete metamorphosis. The activity of both the soluble and DEAE-bound morphogen was concentration- or dose-dependent.

Activity, specificity, and stability of the small soluble morphogen

The small, dialyzable morphogens obtained in the experiments shown in Figures 6–9 induce rapid and normal larval settlement, attachment, complete metamorphosis, and normal post-metamorphic growth (Fig. 10). These processes induced by the small morphogenic molecules are indistinguishable from those induced by the native, intact nongeniculate coralline alga.

The low molecular weight morphogens produced by enzymatic or alkaline hydrolysis of the particulate cell wall fraction from *Hydrolithon boergesenii* (or associated microbial symbionts) induce metamorphosis of at least one other agariciid coral, in addition to *Agaricia humilis.* Larvae of the sympatric *A. tenuifolia,* which also are induced to settle and metamorphose by the intact *Hydrolithon boergesenii* (A. Morse *et al.,* in prep.), are induced to metamorphose by the dialyzable morphogen released by agarase digestion of the cell wall fraction from this alga, with an efficiency comparable to that exhibited for the *A. humilis* larvae (Table VI). In both of these species, the coral larvae are induced to attach to the walls or bottom of the polystyrene containers, metamorphose completely, and begin normal post-metamorphic growth in response only to the low molecular weight chemical morphogen. In contrast, larvae of the sympatric ahermatypic coral, *Tubastraea aurea,* which are not induced to metamorphose by *Hydrolithon boergesenii,* are not induced by the low molecular weight morphogen enzymatically released from the algal cell wall fraction (Table VI). This demonstrates that the morphogenic activity of this chemical is biologically specific for those larvae that respond to the intact alga.

Whereas the decalcified, cell wall-associated, insoluble morphogen is relatively stable when frozen at −10°C, the small, dialyzable morphogen ($\bar{M} \leq 8000$ Da) released from this parent material by endo-β-galactosidase is stable for only a few days at −10°C. The lower molecular weight morphogen released by mild alkaline hydrolysis ($\bar{M} \leq 2000$) proved to be even more unstable. Even when frozen at −10°C, this material lost activity with a half-life that varied in different preparations between 24 and 72 h.

Activities of known compounds

We have tested a wide variety of sulfated and non-sulfated polysaccharides and related polymers, including several substrates for the enzymes used in this study. These (all pre-adjusted to the pH of ambient seawater prior to testing) have included: agar; agarose; agaric acid; alginic acid; ascophyllan; λ-, ι-, and κ-carrageenans; fucoidan, furcellaran; laminarin; chitin; di-N-acetylchitobiose; tri-N-acetylchitotriose; keratan sulfate; chondroitin sulfates A, B, and C; heparin; heparan sulfate; hyaluronic acid; asialofetuin; dextran sulfate; pentosan sulfate; polyvinyl sulfate; polyanethol sulfate; pectin; amylopectin; cellulose; cellulose sulfate; sulfoethylcellulose; and sulfopropylsepharose. Most of these proved inactive with *Agaricia humilis* larvae. Only the κ-carrageenan (a sulfated polymer rich in galactose), fucoidan (a sulfated polymer rich in fucose), and keratan sulfate (a sulfated glycosaminoglycan) induced metamorphosis, although this activity was weak and evident only at very high concentrations (≥5 mg/ml).

Discussion

Recent field and laboratory studies have shown that recruitment of the shallow-water agariciid corals, *Agaricia humilis* and *A. tenuifolia,* is determined in part by larval recognition of a chemical inducer of substratum-specific settlement and metamorphosis (Morse *et al.,* 1988). This inducer is associated with specific nongeniculate coralline red algae. In the case of *A. humilis,* only certain coralline

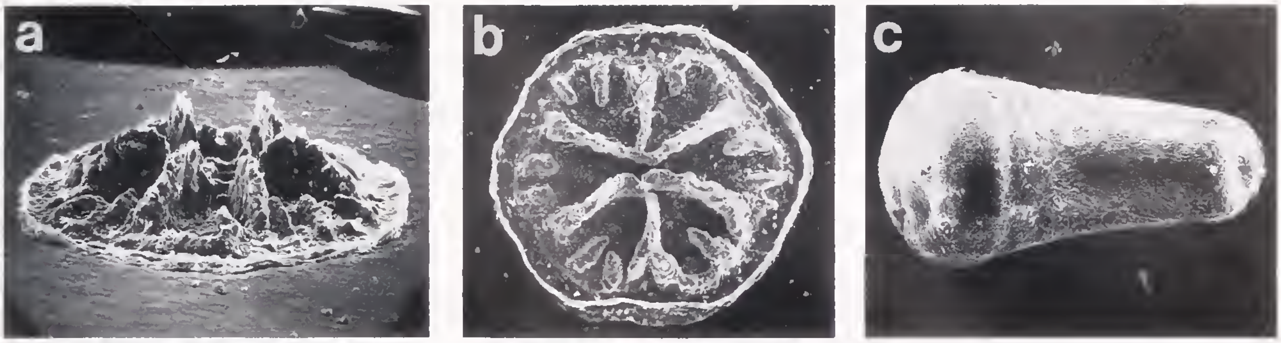

Figure 10. Normal attachment and metamorphosis of *Agaricia humilis* larva induced by the soluble morphogen. Scanning electron micrographs of the endoskeleton of a post-metamorphic corallite attached to polystyrene, dorsolateral (a) and dorsal (b) views, and for comparison, a pre-metamorphic planula larva (c). The pronounced calcified septa and the attachment plaque are clearly visible in the 2-day post-metamorphic corallite. Diameter of the corallite *ca.* 1.5 ± 0.1 mm; length of the planula *ca.* 0.7 ± 0.1 mm. The soluble morphogen was obtained by digestion with endo-β-galactosidase, followed by dialysis, as in Figure 8. Tissue-digestion, fixation, dehydration, critical-point drying, and electron microscopy were by standard procedures.

red algae contain the inducing morphogen (Fig. 1; Table I; *cf.* Morse *et al.*, 1988; A. Morse and R. Steneck, in prep.).

We have extended our previous finding that *Agaricia humilis* larvae maintain both the stringency of their dependence upon the alga-associated morphogen, and the specificity of this requirement, for at least 30 days following their release (Fig. 1). While most larvae probably settle and metamorphose in less than 30 days in the natural environment, this capacity to delay metamorphosis in the absence of the required morphogen can enhance both the dispersal of the larvae, and the substratum-specificity of the final distribution of recruits. Although much of scleractinian recruitment may be locally seeded (Bak and Engle, 1979; Rylaarsdam, 1983; Baggett and Bright, 1985; Sammarco and Andrews, 1988), the larvae of *A. humilis* (*cf.* Fig. 1; also Morse *et al.*, 1988) and certain other species (*cf.* Harrigan, 1972; Richmond, 1981, 1985, 1987; Harrison *et al.*, 1984; Scheltema, 1986; Morse *et al.*, 1988; Richmond and Hunter, 1990) are capable of distant dispersal as well. Indeed, temporal pulses of scleractinian recruitment at certain sites on the Great Barrier Reef are dependent on the settlement of larvae produced at distant locations (Wallace, 1985; Babcock, 1988). In addition to the importance of hydrodynamic, topographic, and geographic features for the control of larval dispersal and consequent recruitment (*e.g.*, Frith *et al.*, 1986; Roughgarden *et al.*, 1988; Sammarco and Andrews, 1988; Black, 1988), and the effects of predation, nutrition, competition, and other biotic factors, studies of *A. humilis* (Morse *et al.*, 1988; and those reported here) indicate that for some coral species, the stringency and specificity of the larval requirements for the induction of settlement and metamorphosis also can be important in controlling the spatial distribution of recruits. A similar larval requirement for a substratum-specific biochemical inducer of settlement

Table VI

Induction of metamorphosis of Agaricia humilis *and* A. tenuifolia *larvae, and absence of induction of* Tubastraea aurea, *by the low molecular weight (LMW) morphogen*

Treatment	Metamorphosis at 24 h ($\bar{X}$ ± S.D.)		
	Agaricia humilis	*Agaricia tenuifolia*	*Tubastraea aurea*
LMW morphogen	95% ± 10% (n = 4)	87% ± 23% (n = 3)	0% ± 0% (n = 3)
Seawater control	0% ± 0% (n = 5)	0% ± 0% (n = 5)	0% ± 0% (n = 3)

Soluble morphogen was prepared by agarase digestion of the particulate cell wall preparation of *Hydrolithon boergesenii* (agarase, 1 mg, 1000 units), and dialysis through a membrane retaining molecules with $\bar{M} \geq 14{,}000$ Da, as described in Materials and Methods. Larvae of each of the three coral species were assayed for metamorphosis in response to the dialyzable morphogen and seawater controls in parallel; 5 larvae/trial; n = number of trials.

and metamorphosis, and larval recognition of the chemical inducer in the ocean environment, recently were shown to determine the fine-scale spatial distribution of recruitment of the polychaete, *Phragmatopoma californica* (Jensen and Morse, 1990).

Chemical nature of the inducer

The inducer of *Agaricia humilis* settlement and metamorphosis that is associated with specific nongeniculate coralline red algae is chemical in nature (Table I; *cf.* Morse *et al.*, 1988). This morphogenic substance is insoluble in a wide range of solvents, apparently because it is associated with cell wall polysaccharides (with which the morphogen is partially purified; *cf.* Fig. 2). Solubilized fractions of the inducer can be generated, however, by hydrolysis with enzymes or mild alkali. The fact that these solubilized fractions are sufficient to trigger normal attachment and metamorphosis of *A. humilis* larvae on clean polystyrene surfaces (Fig. 10) proves that the requirement of the larvae for a morphogenetic inducer is satisfied by a chemical substance from the inductive algal substratum. Non-recruiting algal substrata do not yield this activity (Table I). These results thus confirm and extend the finding that larval recognition of the inductive but insoluble particulate fraction, partially purified from the settlement-inducing algal surface, is dependent upon the integrity of a periodate-sensitive (Fig. 3) and sulfatase-sensitive (Fig. 5; Table II) chemical structure. These sensitivities, the insolubility of the crude inducer, and its insensitivity to proteolytic enzymes, suggested that the inducer is associated with a sulfated polysaccharide.

Consistent with this suggestion, we have found that the inducer can be solubilized by cleavage with purified endoglycosidases that can act on sulfated polysaccharides (Figs. 6–8). As summarized in Table III, the cleavage by agarase and by endo-β-galactosidase indicates that the substrate polymer contains galactose units; cleavage by lysozyme and by endo-β-galactosidase indicates that this polymer also contains β-1,4 linked N-acetylglucosamine or N-acetylglucosamine sulfate units (*cf.* Li *et al.*, 1982; Kitamikado *et al.*, 1982; Scudder *et al.*, 1983, 1984; Morrice *et al.*, 1983a, b; Usov and Ivanova, 1987). Because continued hydrolysis by each of these enzymes leads first to solubilization, and then to progressive inactivation of the inducer, the inductive moiety itself probably contains the above-mentioned sites of hydrolysis. The morphogenetic inducer is thus associated with, and may itself contain, a sulfated glycosaminoglycan, *i.e.*, a sulfated polysaccharide that includes multiple N-acetylglucosamine and galactose units. The finding that partial alkaline hydrolysis liberates a sulfate-containing, strongly anionic, small morphogen is consistent with this conclusion. Recently, hydrolysis, ion-exchange HPLC, and sensitive detection of the resolved monosaccharides by pulsed amperometry have independently confirmed that glucosamine (derived from N-acetylglucosamine) and galactose are indeed principal components of this solubilized small morphogen (M. Hardy, Dionex Corp., pers. comm.). Sulfated polysaccharides that contain amino sugars and are rich in galactose, similar to those in foliose red algae (*cf.*, Percival and McDowell, 1967; Percival, 1978; McCandless, 1981; Yaphe, 1984), previously were found in other coralline red algae (Turvey and Simpson, 1965).

Keratan sulfate, which proved to be slightly active as a morphogen, has three characteristics that make it unique among the known sulfated glycosaminoglycans tested. In these same features, it also, to some degree, resembles the morphogen recognized by *Agaricia humilis* larvae: (1) it contains multiple galactose-β-1,4-N-acetylglucosamine units (whereas heparin, heparan sulfate, and the three different chondroitin sulfates all contain glucuronic acid or other uronic acid units in place of galactose); (2) it is readily cleaved by endo-β-galactosidase (Scudder *et al.*, 1983), whereas the other known compounds tested are not; and (3) the keratan sulfates from some sources cannot be eluted from anion exchangers at salt concentrations below 3–4 *M* (Rodén *et al.*, 1972; *cf.* our results with DEAE, Table V), whereas the other sulfated glycosaminoglycans are readily eluted at significantly lower concentrations (Rodén *et al.*, 1972). Very highly sulfated galactans from red algae also are not eluted from DEAE, or else are eluted only at high concentrations of urea or at high temperature (Yaphe, 1984). However, the weak morphogenetic activity evident at only high concentrations of keratan sulfate, carrageenan, and fucoidan indicates that although these substances may be somewhat similar to the natural inducer, they differ in structural features (possibly including positions of the sulfate groups or other linkages) from those of the natural morphogen.

The morphogenetic activity of the natural inducer solubilized from the cell wall fraction obtained from *Hydrolithon boergesenii* or its associated microflora is biologically specific (Table VI). This molecule induces normal attachment and metamorphosis in larvae of two species of *Agaricia* that are also induced by the intact alga from which the morphogen was obtained. However, the molecule fails to induce these reactions in larvae of the sympatric *Tubastraea aurea*, which are not induced by the intact alga.

The high specificity of the *Agaricia humilis* larvae for morphogens associated with only certain nongeniculate coralline red algae (Fig. 1; Table I; Morse *et al.*, 1988; A. Morse and R. Steneck, in prep.) is apparently a reflection of the chemical specificity of the larval receptors for only some unique sulfated glycosaminoglycans. This suggestion is supported by the finding that a wide variety of synthetic natural sulfated polysaccharides, glycosaminoglycans, and structurally related polymers have either little or no morphogenetic activity. A better understanding of the chemical basis for the high specificity of the larval receptors awaits further information about the stereochemistry and structure of the organic sulfate esters and other substituents in the natural morphogen.

Relation to other systems

Sulfated glycosaminoglycans and other sulfated polysaccharides have been widely implicated in other highly specific cell recognition phenomena that control differentiation, including inter-phyletic symbiosis, fertilization, aggregation of sponge cells, the "homing" of circulating mammalian lymphocytes into the lymph nodes, pattern formation in the developing nervous system, and the metastasis and invasiveness of tumors. The number of structural permutations of such molecules, and hence the complexity of coding of cell recognition ideotypes, far exceed those of the proteins, which are more fully understood (Drickamer, 1988; Sharon and Lis, 1989).

Recent evidence has shown that the host specificity for nodule induction in leguminous plants by the nitrogen-fixing symbiotic bacterium, *Rhizobium meliloti*, is determined by recognition of a unique sulfated glycosaminoglycan signal (a tetrasaccharide containing one sulfate and one acylamino group) produced by the bacterium (Lerouge *et al.*, 1990). Recognition, by the host plant, of this inducing bacterial signal, and the resulting specificity of the inter-phyletic symbiosis, has long been thought to be governed by a class of receptors known as lectins, present on the plant root hair surfaces (Kijne *et al.*, 1989). Recently, this suggestion was strongly confirmed when the intergeneric transfer between plants of the DNA coding for one such root lectin resulted in the transfer of host specificity for nodulation induced by the bacterium (Diaz *et al.*, 1989). Recognition of specific sulfated polysaccharides at the surface of *Strongylocentrotus purpuratus* sea urchin eggs by conspecific sperm has been demonstrated to be essential for fertilization (Rossignol *et al.*, 1984; DeAngelis and Glabe, 1987). In this reaction (DeAngelis and Glabe, 1987), and in the binding of heparin to antithrombin (Atha *et al.*, 1985), the locations of the sulfate esters on the sugars have been found to be of critical importance; in the latter case, removal of one specific sulfate reduced the affinity of specific binding by as much as 10,000-fold (Atha *et al.*, 1985). The lengths of the sulfated polysaccharides are also critical determinants of the strength (and hence, the specificity) of these binding reactions (Hoylaerts *et al.*, 1984; DeAngelis and Glabe, 1987). Evidence also suggests that lectin-like recognition of cell surface sulfated glycosaminoglycans controls an essential phase in the species-specific reaggregation and subsequent differentiation of sponge cells (Henkart *et al.*, 1973; Turner and Burger, 1973; Jumblatt *et al.*, 1980; Conrad *et al.*, 1984; Diehl-Seifert *et al.*, 1985, 1989; Margoliash *et al.*, 1965; Coombe *et al.*, 1987; Coombe and Parish, 1988; Schröder *et al.*, 1988; Gramzow *et al.*, 1989).

Recognition and binding of sulfated glycosaminoglycan moieties of cell surface proteoglycans also controls adhesion, tissue-specific differentiation and growth in a wide variety of mammalian and other higher systems (Edelman, 1985; Fransson, 1987; Ruoslahti, 1989). The structures and positions of the sulfate esters can be critically important in the control of these functions as well (Fransson, 1987). Sulfated glycosaminoglycans and other sulfated polysaccharides bind to lectin-like receptors on the surfaces of lymphocytes (Parish *et al.*, 1984; Parish and Snowden, 1985; Chong and Parish, 1985, 1986; Thurn and Underhill, 1986; Brenan and Parish, 1986; Brandley *et al.*, 1987). Recently, the genes coding for two distinct "homing receptors" from the surfaces of mammalian lymphocytes have been cloned and sequenced (Gallatin *et al.*, 1986; Yednock *et al.*, 1987a; Goldstein *et al.*, 1989; Holzmann *et al.*, 1989; Siegelman *et al.*, 1989; Stamenkovic *et al.*, 1989; Stoolman, 1989). Lectin-like recognition of specific sulfated or other anionic carbohydrates in the target lymphoid tissues, mediated by these receptors, is thought to direct the homing of specific subsets of lymphocytes from the circulation to adhere to the blood vessel endothelia of their target lymphoid organs (lymph nodes, Peyer's patches, etc.), where the recruited lymphocytes then differentiate to produce antibodies (Brenan and Parish, 1986; Gallatin *et al.*, 1986; Yednock *et al.*, 1987a, b; Jalkanen *et al.*, 1988; Stoolman, 1989; Coombe and Rider, 1989).

The parallels between this lymphocyte homing reaction and the settlement and metamorphosis of *Agaricia humilis* larvae are potentially interesting. In both, substratum-specific "recruitment," attachment, and differentiation are apparently induced by recognition of a non-diffusing, substratum-specific sulfated polysaccharide. Our further observation that the partially purified sulfated polysaccharide that induces *A. humilis* larvae to attach and metamorphose also induces murine lymphocytes to undergo mitosis (Morse and Eardley, unpub. obs.), may therefore be worth further investigation. The specificity of this latter reaction is unclear, however, as a wide variety of sulfated polysaccharides and related polymers, including several carrageenans, fucoidan, and ascophylan, induce lymphocyte mitosis. Whether the same subset of lymphocytes responds to each of these compounds has not yet been determined. In contrast, the *A. humilis* larvae respond only slightly and incompletely to carrageenan and fucoidan, and only at very high concentrations.

Cell-surface recognition of polysaccharides and other complex carbohydrates in such non-immune systems is generally considered to be mediated by lectins, a broad class of ubiquitous, carbohydrate-specific receptors that recently has been redefined (Barondes, 1988; Drickamer, 1988; Sharon and Lis, 1989). Mitchell and his colleagues first demonstrated that the settlement and metamorphosis of larvae of the polychaete, *Janua brasiliensis,* are mediated by a lectin-like recognition of inductive exopolysaccharides produced by specific bacteria (Kirchman *et al.*, 1982a, b; Mitchell and Kirchman, 1984; Maki and Mitchell, 1985, 1986). These authors first pointed out the similarities between this larval settlement reaction and other lectin-mediated recognition phenomena, including the root nodule-bacteria symbiosis discussed above. Weiner *et al.* (1985) and Bonar *et al.* (1986) also have shown that specific bacterial exopolysaccharides may play a role in the induction of settlement and metamorphosis of *Crassostrea virginica* and *C. gigas* oyster larvae, although induction in those systems is complex, and more than one class of compound is known to be involved (Coon *et al.*, 1985; Coon and Bonar, 1987; Fitt *et al.*, 1989; Bonar *et al.*, 1990).

The results reported here, demonstrating sensitivity of the *Agaricia humilis* morphogen to cleavage by endo-β-galactosidase and agarase, (and resistance to the exoglycosidic β-galactosidase), indicate that the morphogen contains essential internal β-galactoside units. This finding may be of particular interest in view of the suggested importance of β-galactoside-specific lectins in controlling differentiation in higher animal systems (Barondes *et al.*, 1988; Sharon and Lis, 1989).

Remaining problems

Two problems remaining are the determination of the complete chemical structure of the inducing molecule recognized by the *Agaricia humilis* larvae, and the unequivocal identification of the biological source of this inducer. A number of compounds that induce metamorphosis of various marine invertebrate larvae have been partially purified from the respective inductive substrata, and the structures of these compounds have been partially characterized. But we are aware of only two natural inductive molecules that have been completely characterized. These include the algal molecules that induce metamorphosis of the scallop, *Pecten maximus* (Yvin *et al.*, 1985), and the hydrozoan, *Coryne uchidai* (Kato *et al.*, 1975). Significantly, both of these are small molecules soluble in organic solvents, and thus amenable to gas-chromatography and mass spectroscopy. In a large number of the other cases investigated, however, the native inducers have proved to be either water soluble (*e.g.*, Highsmith, 1982; Hadfield and Scheuer, 1985; Burke, 1986; Hadfield and Pennington, 1990), or polymeric and insoluble (*e.g.*, Jensen and Morse, 1984, 1990; Morse *et al.*, 1988). [We are not including in this discussion such molecules as potassium or calcium salts, fatty acids, cyclic nucleotides, or other widely active effectors of depolarization, protein phosphorylation, or signal transduction pathways; these all have been shown to induce metamorphosis of larvae without species- or substratum-specificity (*e.g.*, Baloun and Morse, 1984; Morse, 1985, 1990; Yool *et al.*, 1986; Pechenik and Heyman, 1987; Jensen and Morse, 1990; Jensen *et al.*, 1990)]. The inducer of *Agaricia humilis* metamorphosis described here is in its native form associated with a substratum-specific insoluble polymer. Partial hydrolysis with either enzymes or dilute alkali releases a smaller, water-soluble and strongly anionic inducer which is markedly unstable. This instability has hindered analyses of the active morphogen. The use of highly purified enzymes, and employment of their specificities for selective cleavage, solubilization, and as probes of the structural determinants of morphogenetic activity, may prove widely useful in further studies of such otherwise intractable molecules.

The inductive molecule that we have described is obtained from homogenates of the nongeniculate coralline red alga, *Hydrolithon boergesenii.* Larvae of *Agaricia humilis* are induced to metamorphose by contact with intact specimens of that alga, and recruits of the coral are found preferentially on that alga in the field (Morse *et al.*, 1988; A. Morse and R. Steneck, in prep.). Three other species of anthozoan, including the scleractinian *Agaricia tenuifolia* (Morse *et al.*, 1988), the temperate octocoral *Alcyonium siderium* (Sebens, 1983a, b), and a tropical gorgonian, *Plexaura* sp. (Lasker, 1990), also have been found to settle and metamorphose in response to crustose red algal surfaces. But in each of these cases, the inductive molecule could have been produced by bacteria or other microorganisms associated with the algal surfaces. Bacteria or bacterial films have been implicated in the control of larval settlement and metamorphosis in a few other cnidarians in which these processes are chemically induced. Larvae of the hydroid, *Hydractinia echinata,* settle and metamorphose in response to films of the bacterium, *Alteromonas* sp., on shells inhabited by hermit crabs (Spindler and Müller, 1972). *Cassiopea andromeda* (scyphozoan) larvae also are induced to settle and metamorphose by bacteria, apparently in response to soluble peptides produced by the action of bacterial degradative enzymes (Fitt and Hofmann, 1985; Fitt *et al.*, 1987; Hofmann and Brand, 1987). Bacterial films have been widely implicated in the control of larval settlement and metamorphosis in many other kinds of invertebrates as well (Wilson, 1955; Cameron and Hinegardner, 1974; Brancato and Woolacott, 1982; Kirchman *et al.*, 1982; Mitchell and Kirchman, 1984; Bonar *et al.*, 1986; Maki and Mitchell, 1986; Fitt *et al.*, 1989; Maki *et al.*, 1990). Moreover, as Maki *et al.* (1990) have suggested in the case of barnacle larvae, the larval response may depend in a complex way on the interaction between bacteria and the surface on which they are attached.

The structure of the morphogen recognized by *Agaricia humilis* larvae, suggested by the results reported here to be a sulfated glycosaminoglycan, would be equally consistent with a molecule of the red algal cell wall and of a cell wall or other exopolymer produced by an associated bacterium (Percival and McDowell, 1967; Mackie and Preston, 1974; Sanford *et al.*, 1977; McCandless, 1981; Drews and Weckesser, 1982; Boyle and Reed, 1983). We have found, however, that the activity of crude homogenates appears markedly enhanced following decalcification, consistent with the unmasking of constituents of the algal cell wall. Attempts to culture the algal cells axenically from isolated protoplasts, by the methods of Polne-Fuller and Gibor (1984) and Kloareg *et al.* (1989), and attempts to culture the alga-associated microbial symbionts, may help further resolve the source of the inducer. Mass-cultivation of the producing cells would also help provide sufficient quantities of the inducer and thus facilitate its complete structural characterization.

Acknowledgments

This research has been supported by a grant (OCE87-22959) from the National Science Foundation, Biological Oceanography Program. We thank our colleagues R. Steneck, N. Hooker, R. Petty, and T. Clarke for their expert contributions and assistance; S. Roseman and M. Hardy for arranging and providing the confirmatory sugar analyses; and E. Newton, R. Hensen, and the government of Bonaire, Netherlands Antilles, for their generous hospitality and assistance.

Literature Cited

Atha, D. H., J. Lormeau, M. Petitou, R. D. Rosenberg, and J. Choay. 1985. Contribution of monosaccharide residues in heparin binding to antithrombin III. *Biochemistry* **24:** 6723–6729.

Babcock, R. C. 1988. Fine-scale spatial and temporal patterns in coral recruitment. *Proc. 6th Intl. Coral Reef Symp.* **2:** 635–639.

Baggett, L. S., and T. J. Bright. 1985. Coral recruitment at the East Flower Garden Reef. *Proc. 5th Intl. Coral Reef Cong.* **4:** 379–384.

Bak, R. P. M., and M. S. Engle. 1979. Distribution, abundance and survival of juvenile hermatypic corals (Scleractinia) and the importance of life history strategies in the parent coral community. *Mar Biol.* **59:** 341–352.

Baloun, A. J., and D. E. Morse. 1984. Ionic control of settlement and metamorphosis in larval *Haliotis rufescens* (gastropoda). *Biol. Bull.* **167:** 124–138.

Barondes, S. H. 1988. Bifunctional properties of lectins: Lectins redefined. *Trends Biochem. Sci.* **13:** 480–482.

Barondes, S. H., M. A. Gitt, H. Leffler, and D. N. Cooper. 1988. Multiple soluble vertebrate galactose-binding lectins. *Biochimie* **70:** 1627–1632.

Beeley, J. G. 1985. *Glycoprotein and Proteoglycan Techniques. Laboratory Techniques in Biochemistry and Molecular Biology*, vol. 16. Elsevier, Amsterdam, 462 pp.

Black, K. P. 1988. The relationship of reef hydrodynamics to variation in numbers of planktonic larvae on and around coral reefs. *Proc. 6th Intl. Coral Reef Symp.* **2:** 125–130.

Bonar, D. B., R. M. Weiner, and R. R. Colwell. 1986. Microbial-invertebrate interactions and potential for biotechnology. *Microb. Ecol.* **12:** 101–110.

Bonar, D. B., S. L. Coon, M. Walsh, R. M. Weiner, W. K. Fitt. 1990. Control of oyster settlement and metamorphosis by endogenous and exogenous chemical cues. *Bull. Mar. Sci.* **46:** 484–498.

Boyle, C. D., and A. E. Reade. 1983. Characterization of two extracellular polysaccharides from marine bacteria. *Appl. Env. Micro.* **46:** 392–399.

Brancato, M. S., and R. M. Woolacott. 1982. Effect of microbial films on settlement of bryozoan larvae (*Bugula simplex, B. stolinifera* and *B. turrita*). *Mar. Biol.* **71:** 51–56.

Brandley, B. K., T. S. Ross, and R. L. Schnaar. 1987. Multiple carbohydrate receptors on lymphocytes revealed by adhesion to immobilized polysaccharides. *J. Cell. Biol.* **105:** 991–997.

Brenan, M., and C. R. Parish. 1986. Modification of lymphocyte migration by sulfated polysaccharides. *Eur. J. Immunol.* **16:** 423–430.

Burke, R. D. 1986. Pheromones and the gregarious settlement of marine invertebrate larvae. *Bull. Mar. Sci.* **39:** 323–331.

Cameron, R. A., and R. T. Hinegardner. 1974. Initiation of metamorphosis in laboratory cultured sea urchins. *Biol. Bull.* **146:** 335–342.

Chong, A. S.-F., and C. R. Parish. 1985. Nonimmune lymphocyte-macrophage interaction. II. Evidence that the interaction involves sulfated polysaccharide recognition. *Cell. Immunol.* **92:** 277–289.

Chong, A. S.-F., and C. R. Parish. 1986. Cell surface receptors for sulfated polysaccharides: a potential marker for macrophage subsets. *Immunology* **58:** 277–284.

Conrad, J., G. Uhlenbruck, R. K. Zahn, B. Kurelec, B. Jericevic, and W. E. G. Müller. 1984. The role of lectin I and of glyconjugates in recognition of cells from the silicaceous sponge *Geodia cydonium*. *Biol. Cell.* **51:** 287–294.

Coombe, D. R., and C. R. Parish. 1988. Sulfated polysaccharide-mediated sponge cell aggregation: the clue to invertebrate self/nonself-recognition? Pp. 31–53 in *Invertebrate Historecognition*, R. K. Grosberg, D. Hedgecock and K. Nelson, eds. Plenum, New York.

Coombe, D. R., and C. C. Rider. 1989. Lymphocyte homing receptors cloned—a role for anionic polysaccharides in lymphocyte adhesion. *Immunol. Today* **10:** 289–291.

Coombe, D. R., K. B. Jakobsen, and C. R. Parish. 1987. A role for sulfated polysaccharide recognition in sponge cell aggregation. *Exp. Cell Res.* **170:** 381–401.

Coon, S. L., and D. B. Bonar. 1987. Pharmacological evidence that alpha$_1$-adrenoreceptors mediate metamorphosis of the pacific oyster, *Crassostrea gigas*. *Neuroscience* **23:** 1169–1174.

Coon, S. L., D. B. Bonar, and R. M. Weiner. 1985. Induction of settlement and metamorphosis of the pacific oyster, *Crassostrea gigas* (Thunberg) by L-DOPA and catecholamines. *J. Exp. Mar. Bio. Ecol.* **94:** 211–221.

De, K. K., K. Yamamoto, and R. L. Whistler. 1978. Enzymatic formation and hydrolysis of polysaccharide sulfates. Pp. 121–147 in *Carbohydrate Sulfates*, R. G. Schweiger, ed. Am. Chem. Soc., Washington.

DeAngelis, P. L., and C. G. Glabe. 1987. Polysaccharide structural features that are critical for the binding of sulfated fucans to bindin, the adhesive protein from sea urchin sperm. *J. Biol. Chem.* **262:** 13,946–13,952.

Diaz, C. L., L. S. Melchers, P. J. J. Hooykaas, B. J. J. Lugtenberg, and J. W. Kijne. 1989. Root lectin as a determinant of host-plant specificity in the *Rhizobium*-legume symbiosis. *Nature* **338:** 579–581.

Diehl-Seifert, B., G. Uhlenbruck, M. Geisert, R. K. Zahn, and W. E. G. Müller. 1985. Physicochemical and functional characterization of the polymerization process of the *Geodia cydonium* lectin. *Eur. J. Biochem.* **147:** 517–523.

Diehl-Seifert, B., V. Amberger, M. Gramzow, R. Batel, M. Bachmann, H. C. Schröder, and W. E. G. Müller. 1989. Directed migration of cells from the sponge *Geodia cydonium*. *Tissue Cell.* **21:** 25–36.

Dodgson, K. S., and J. W. Fitzgerald, eds. 1982. *Sulfatases of Microbial Origin*, Vol. 1. CRC Press, Boca Raton, FL. 199 pp.

Drews, G., and J. Weckesser. 1982. Function, structure and composition of cell walls and external layers. Pp. 333–357 in *The Biology of Cyanobacteria*, N. G. Carr and B. A. Whitton, eds. Blackwell, Oxford.

Drickamer, K. 1988. Two distinct classes of carbohydrate-recognition domains in animal lectins. *J. Biol. Chem.* **263:** 9557–9560.

Dustan, P. 1977. Vitality of reef coral populations off Key Largo, Florida: recruitment and mortality. *Environ. Geol.* **2:** 51–58.

Edelman, G. M. 1985. Cell adhesion and the molecular processes of morphogenesis. *Ann. Rev. Biochem.* **54:** 135–169.

Fitt, W. K., and D. K. Hofmann. 1985. Chemical induction of settlement and metamorphosis of the reef-dwelling coelenterate *Cassiopea andromeda*. *Proc. 5th Intl. Coral Reef Cong.* **5:** 239–244.

Fitt, W. K., D. K. Hofmann, M. Wolk, and M. Rahat. 1987. Requirements of exogenous inducers for the development of axenic larvae and buds of *Cassiopea andromeda* (Cnidaria: Scyphozoan). *Mar. Biol.* **94:** 415–422.

Fitt, W. K., M. P. LaBare, W. C. Fuqua, M. Walch, S. L. Coon, D. B. Bonar, R. R. Colwell, and R. M. Weiner. 1989. Factors influencing bacterial production of inducers of settlement behavior of larvae of the oyster *Crassostrea gigas*. *Microb. Ecol.* **17:** 287–298.

Fransson, L.-A. 1987. Structure and function of cell-associated proteoglycans. *Trends Biochem. Sci.* **12:** 406–411.

Freifelder, D. 1983. *Physical Biochemistry: Applications to Biochemistry and Molecular Biology*, 2nd ed. W. H. Freeman, San Francisco. 761 pp.

Frith, C. A., J. M. Leis, and B. Goldman. 1986. Currents in the Lizard Island region of the Great Barrier Reef Lagoon and their relevance to potential movements of larvae. *Coral Reefs* **5:** 81–92.

Gallatin, M., T. P. St. John, M. Siegelman, R. Reichert, E. C. Butcher, and I. L. Weissman. 1986. Lymphocyte homing receptors. *Cell* **44:** 673–680.

Goldstein, L. A., D. F. H. Zhou, L. J. Picker, C. N. Minty, R. F. Bargatze, J. F. Ding, and E. C. Butcher. 1989. A human lymphocyte homing receptor, the hermes antigen, is related to cartilage proteoglycan core and link proteins. *Cell* **56:** 1063–1072.

Gramzow, M., H. C. Schröder, U. Fritsche, B. Kurelec, A. Robitzki, H. Zimmermann, K. Friese, M. H. Kreuter, and W. G. Müller. 1989. Role of phospholipase A_2 in the stimulation of sponge cell proliferation by homologous lectin. *Cell* **59:** 939–948.

Hadfield, M. G., and D. Scheuer. 1985. Evidence for a soluble metamorphic inducer in *Phestilla*: ecological, chemical and biological data. *Bull. Mar. Sci.* **37:** 556–566.

Hadfield, M. G., and J. T. Pennington. 1990. Nature of the metamorphic signal and its internal transduction in larvae of the nudibranch *Phestilla sibogae*. *Bull. Mar. Sci.* **46:** 455–464.

Harrigan, J. S. 1972. The planula larvae of *Pocillopora damicornis*, lunar periodicity of swarming and substratum selection behavior. Ph.D. thesis, University of Hawaii. 319 pp.

Harrison, P. L., R. C. Babcock, G. D. Bull, J. K. Oliver, C. C. Wallace, and B. L. Willis. 1984. Mass spawning in tropical reef corals. *Science* **223:** 1186–1189.

Hassid, W. Z., and S. Abraham. 1957. Chemical procedures for analysis of polysaccharides. *Methods in Enzymol.* **3:** 34–50.

Henkart, P., S. Humphreys, and T. Humphreys. 1973. Characterization of sponge aggregation factor. A unique proteoglycan complex. *Biochemistry* **12:** 3045–3050.

Highsmith, R. C. 1982. Induced settlement and metamorphosis of sand dollar (*Dendraster excentricus*) larvae in predator-free sites: adult sand dollar beds. *Ecology* **63:** 329–337.

Hofmann, D. K., and U. Brand. 1987. Induction of metamorphosis in the symbiotic scyphozoan *Cassiopea andromeda*: role of marine bacteria and of biochemicals. *Symbiosis* **4:** 99–116.

Holzmann, B., B. W. McIntyre, and I. L. Weissman. 1989. Identification of a murine Peyer's patch-specific lymphocyte homing receptor as an integerin molecule with an α chain homologous to human VLA-4α. *Cell* **56:** 37–46.

Hoylaerts, M., W. G. Owen, and D. Collen. 1984. Involvement of heparin chain length in the heparin-catalyzed inhibition of thrombin by antithrombin III. *J. Biol. Chem.* **259:** 5670–5677.

Hughes, T. P. 1985. Life histories and population dynamics of early successional corals. *Proc. 5th Intl. Coral Reef Cong.* **4:** 101–106.

Hughes, T. P., and J. B. C. Jackson. 1985. Population dynamics and life histories of foliaceous corals. *Ecol. Monogr.* **55:** 141–166.

Jalkanen, S., M. Jalkanen, R. Bargatze, M. Tammi, and E. C. Butcher. 1988. Biochemical properties of glycoproteins involved in lymphocyte recognition of high endothelial venules in man. *J. Immunol.* **141:** 1615–1623.

Jensen, R., and D. E. Morse. 1984. Intraspecific facilitation of larval recruitment: gregarious settlement of the polychaete *Phragmatopoma californica*. *J. Exp. Mar. Biol. Ecol.* **83:** 107–126.

Jensen, R. A., and D. E. Morse. 1990. Chemically induced metamorphosis of polychaete larvae in both the laboratory and the ocean environment. *J. Chem. Ecol.* **16:** 911–930.

Jensen, R. A., D. E. Morse, N. Hooker, and R. Petty. 1990. Artificial induction of larval metamorphosis by free fatty acids. *Mar. Ecol. Prog. Ser.* **67:** 55–71.

Jumblatt, J., V. Schlup, and M. M. Burger. 1980. Cell-cell recognition: specific binding of *Microciona* sponge aggregation factor to homotypic cells and the role of calcium ions. *Biochemistry* **19:** 1038–1042.

Kato, T., A. S. Kumanireng, I. Ichinose, Y. Kitihara, Y. Kakinuma, M. Nishihira, and M. Kato. 1975. Active components of *Saragassum tortile* effecting settlement of swimming larvae of *Coryne uchidai*. *Experientia* **31:** 433.

Kijne, J. W., C. L. Diaz, and B. J. J. Lugtenberg. 1989. *Signal Molecules in Plant and Plant-Microbe Interactions.* B. J. J. Lugtenberg, ed. Springer, Berlin. Pp. 351–358.

Kirchman, D., S. Graham, D. Reish, and R. Mitchell. 1982a. Bacteria induce settlement and metamorphosis of *Janua* (*Dexiospira*) *brasiliensis* (Grube). *J. Exp. Mar. Biol. Ecol.* **56:** 153–163.

Kirchman, D., S. Graham, D. Reish, and R. Mitchell. 1982b. Lectins may mediate in the settlement and metamorphosis of *Janua* (*Dexiospira*) *brasiliensis* (Grube). *Mar. Biol. Lett.* **3:** 131–142.

Kitamikado, M., M. Ito, and Y.-T. Li. 1982. Endo-β-galactosidase from *Flavobacterium keratolyticus*. *Methods Enzymol.* **83:** 619–625.

Kloareg, B., M. Polne-Fuller, and A. Gibor. 1989. Mass production of viable protoplasts from *Macrocystis pyrifera* (L.) C.Ag. (Phaeophyta). *Plant Sci.* **62:** 105–112.

Lasker, H. R. 1990. Development and settlement behavior of plexaurid gorgonian planulae. *Benthic Ecol. Mtg. Abstr.* **1990:** 26.

Lerouge, P., P. Roche, C. Faucher, F. Maillet, G. Truchet, J. C. Prome, and J. Dénarié. 1990. Symbiotic host-specificity of *Rhizobium meliloti* is determined by a sulfated and acylated glucosamine oligosaccharide signal. *Nature* **344:** 781–784.

Li, Y.-T., H. Nakagawa, M. Kitamikado, and S.-C. Li. 1982. Endo-β-galactosidase from *Escherichia freundii*. *Methods Enzymol.* **83:** 610–619.

Mackie, M., and R. D. Preston. 1974. Cell wall and intracellular region polysaccharides. Pp. 40–85 in *Algal Physiology and Biochemistry*, W. D. P. Stewart, ed. Blackwell Scientific Publications, Oxford.

Maki, J. S., and R. Mitchell. 1985. Involvement of lectins in the settlement and metamorphosis of marine invertebrate larvae. *Bull. Mar. Sci.* **37:** 675–683.

Maki, J. S., and R. Mitchell. 1986. The function of lectins in interaction among marine bacteria, invertebrates and algae. Pp. 409–425 in *Microbial Lectins and Agglutinins. Properties and Biological Activity*, D. Mirelman, ed. John Wiley & Sons, New York.

Maki, J. S., D. Rittschof, M.-O. Samuelsson, U. Szewzyk, A. B. Yule, S. Kjelleberg, J. D. Costlow, and R. Mitchell. 1990. Effect of marine bacteria and their exopolymers on the attachment of barnacle cypris larvae. *Bull. Mar. Sci.* **46:** 599–511.

Margoliash, E., J. R. Schenk, M. P. Hargie, S. Burokas, W. R. Richter, G. H. Barlow, and A. Moscuna. 1965. Characterization of specific cell aggregating materials from sponge cells. *Biochem. Biophys. Res. Commun.* **20:** 383–388.

McCandless, E. 1981. Polysaccharides of the seaweeds. Pp. 559–588 in *The Biology of the Seaweeds*, C. S. Lobbar and M. J. Wynne, eds. Univ. of Calif. Press, Berkeley.

Mitchell, R., and D. Kirchman. 1984. The microbial ecology of marine surfaces. Pp. 49–56 in *Marine Biodeterioration*, J. D. Costlow and R. C. Tipper, eds. Naval Institute Press, Annapolis.

Morrice, L. M., M. W. McLean, W. F. Long, and F. B. Williamson. 1983a. β-agarases I and II from *Pseudomonas atlantica*: Substrate specificities. *Eur. J. Biochem.* **137:** 149–154.

Morrice, L. M., M. W. McLean, W. F. Long, and F. B. Williamson. 1983b. Porphyran primary structure: an investigation using β-agarase I from *Pseudomonas atlantica* and ^{13}C-NMR spectroscopy. *Eur. J. Biochem.* **133:** 673–684.

Morse, D. E. 1985. Neurotransmitter-mimetic inducers of settlement and metamorphosis of marine planktonic larvae. *Bull. Mar. Sci.* **37:** 697–706.

Morse, D. E. 1990. Recent progress in larval settlement and metamorphosis: closing the gaps between molecular biology and ecology. *Bull. Mar. Sci.* **46:** 465–483.

Morse, D. E., N. Hooker, A. N. C. Morse, and R. Jensen. 1988. Control of larval metamorphosis and recruitment in sympatric agariciid corals. *J. Exp. Mar. Biol. Ecol.* **116:** 193–217.

Parish, C. R., and J. M. Snowden. 1985. Lymphocytes express a diverse array of specific receptors for sulfated polysaccharides. *Cell. Immunol.* **91:** 201–214.

Parish, C. R., D. B. Rylatt, and J. M. Snowden. 1984. Demonstration of lymphocyte surface lectins that recognize sulfated polysaccharides. *J. Cell. Sci.* **67:** 145–158.

Pechenik, J. A., and W. D. Heyman. 1987. Using KCl to determine size at competence for larvae of the marine gastropod, *Crepidula fornicata* (L.). *J. Exp. Mar. Biol. Ecol.* **112:** 27–38.

Percival, E. 1978. Sulfated polysaccharides of the *Rhodophyceae*—a review. Pp. 213–224 in *Carbohydrate Sulfates*, R. G. Schweiger, ed. Amer. Chem. Soc., Washington.

Percival, E., and R. H. McDowell. 1967. *Chemistry and Enzymology of Marine Algal Polysaccharides*. Academic Press, London. 219 pp.

Polne-Fuller, M., and A. Gibor. 1984. Developmental studies in *Porphyra* I. Blade differentiation in *Porphyra perforata* as expressed by morphology, enzymatic digestion, and protoplast regeneration. *J. Phycol.* **20:** 609–616.

Richmond, R. H. 1981. Energetic consideration in the dispersal of *Pocillopora damicornis* (Linnaeus) planulae. *Proc. 4th Intl. Coral Reef Symp.* **2:** 153–156.

Richmond, R. H. 1985. Variations in the population biology of *Pocillopora damicornis* across the Pacific. *Proc. 5th Intl. Coral Reef Cong.* **6:** 101–106.

Richmond, R. H. 1987. Energetics, competency, and long-distance dispersal of planula larvae of the coral *Pocillopora damicornis*. *Mar. Biol.* **93:** 527–533.

Richmond, R. H., and C. L. Hunter. 1990. Reproduction and recruitment of corals: comparisons among the Caribbean, the tropical Pacific, and the Red Sea. *Mar. Ecol. Prog. Ser.* **60:** 185–203.

Rodén, L., J. R. Baker, J. A. Cifonelli, and M. B. Mathews. 1972. Isolation and characterization of connective tissue polysaccharides. *Methods Enzymol.* **28:** 73–140.

Rogers, C. S., H. C. Fitz III, M. Gilnack, J. Beets, and J. Hardin. 1984. Scleractinian coral recruitment patterns at Salt River submarine canyon, St. Croix, U. S. Virgin Islands. *Coral Reefs* **3:** 69–76.

Rossignol, D. P., B. J. Earles, G. L. Decker, and W. J. Lennarz. 1984. Characterization of the sperm receptor on the surface of eggs of *Strongylocentrotus purpuratus*. *Dev. Biol.* **104:** 308–321.

Roughgarden, J., S. Gaines, and H. Possingham. 1988. Recruitment dynamics in complex life cycles. *Science* **241:** 1460–1466.

Ruoslahti, E. 1989. Proteoglycans in cell regulation. *J. Biol. Chem.* **264:** 13369–13372.

Rylaardsdam, K. W. 1983. Life histories and abundance patterns of colonial corals on Jamaican reefs. *Mar. Ecol. Prog. Ser.* **13:** 249–260.

Sammarco, P. W., and J. C. Andrews. 1988. Localized dispersal and recruitment in Great Barrier Reef corals: The Helix experiment. *Science* **239:** 1422–1424.

Sanford, P. A., J. E. Pittsley, C. A. Knutson, P. R. Watson, M. C. Cadmus, and A. Jeanes. 1977. Variation in *Xanthomonas campestris* NRRL B 1459: characterization of xanthan products of differing pyruvic content. Pp. 192–210 in *Extracellular Microbial Polysaccharides*, P. A. Sanford and A. Laskin, eds. Am. Chem. Soc., Washington.

Scheltema, R. S. 1986. Long-distance dispersal by planktonic larvae of shoal-water benthic invertebrates among central Pacific islands. *Bull. Mar. Sci.* **39:** 241–256.

Schröder, H. C., Y. Kuchino, M. Gramzow, B. Kurelec, U. Friese, G. Uhlenbruck, and W. G. Müller. 1988. Induction of *ras* gene expression by homologous aggregation factor in cells from the sponge *Geodia cydonium*. *J. Biol. Chem.* **263:** 16334–16340.

Scudder, P., K.-I. Uemura, J. Dolby, M. N. Fukuda, and T. Feizi. 1983. Isolation and characterization of endo-β-galactosidase from *Bacteroides fragilis*. *Biochem. J.* **213:** 485–494.

Scudder, P., P. Hanfland, K.-I. Uemara, and T. Feizi. 1984. Endo-β-galactosidases of *Bacteroides fragilis* and *Escherichia freundii* hydrolyze linear but not branched oligosaccharide domains of glycolipids of the neolacto series. *J. Biol. Chem.* **259:** 6586–6592.

Sebens, K. P. 1983a. Settlement and metamorphosis of a temperate soft-coral larva (*Alcyonium siderium* Verill): induction by crustose algae. *Biol. Bull.* **165:** 286–304.

Sebens, K. P. 1983b. The larval and juvenile ecology of the temperate octocoral *Alcyonium siderium* Verrill. I. Substratum selection by benthic larvae. *J. Exp. Mar. Biol. Ecol.* **71:** 73–89.

Sharon, N., and H. Lis. 1989. Lectins as cell-recognition molecules. *Science* **246:** 227–234.

Siegelman, M., M. van de Rijn, and I. L. Weissman. 1989. Mouse lymph node homing receptor cDNA encodes a glycoprotein revealing tandem interaction domains. *Science* **243:** 1165–1172.

Spaulding, D., and D. E. Morse. 1991. Purification and characterization of sulfatases from *Haliotis rufescens*: evidence for changes in synthesis and heterogeneity during development. *J. Comp. Physiol. B* (in press).

Spindler, K.-D., and W. A. Müller. 1972. Induction of metamorphosis by bacteria and by a lithium-pulse in the larvae of *Hydractinia echinata* (Hydrozoa). *Wilhelm Roux's Arch.* **169:** 271–280.

Stamenkovic, I., M. Amiot, J. M. Pesandro, and B. Seed. 1989. A lymphocyte molecule implicated in lymph node homing is a member of the cartilage link protein family. *Cell* **56:** 1057–1062.

Stoolman, L. M. 1989. Adhesion molecules controlling lymphocyte migration. *Cell* **56:** 907–910.

Thurn, A. L., and C. B. Underhill. 1986. Heparin-induced aggregation of lymphoid cells. *J. Cell. Physiol.* **126:** 352–358.

Turner, R. S., and M. M. Burger. 1973. Involvement of a carbohydrate group in the active site for surface-guided reassociation of animal cells. *Nature* **244:** 509–510.

Turvey, J. R., and P. R. Simpson. 1965. Polysaccharides from *Corallina officianalis. Proc. Intl. Seaweed Symp.* **V:** 323–327.

Usov, A. I., and E. G. Ivanova. 1987. Polysaccharides of algae. XXXVII: characterization of hybrid structure of substituted agarose from *Polysiphonia morrowii* (Rhodophyta, Rhodomelaceae) using β-agarase and ^{13}C-NMR spectroscopy. *Bot. Mar.* **30:** 365–370.

van Moorsel, G. W. N. M. 1983. Reproductive strategies in two closely related stony corals (*Agaricia,* Scleractinia). *Mar. Ecol. Prog. Ser.* **13:** 273–283.

van Moorsel, G. W. N. M. 1989. Juvenile ecology and reproductive strategies of reef corals. Doctoral Dissertation, Rijksuniversiteit, Groningen. 103 pp.

Wallace, C. C. 1985. Four years of juvenile coral recruitment to five reef front sites. *Proc. 5th Intl. Coral Reef Cong.* **4:** 385–390.

Weiner, R. M., and R. R. Colwell. 1982. Induction of settlement and metamorphosis in *Crassostrea virginica* by a melanin-synthesizing bacterium. *Technical Report Maryland Sea Grant Program,* Publication No. UM-SG-TS-82-05, 44 pp.

Weiner, R. M., A. M. Segall, and R. R. Colwell. 1985. Characterization of a marine bacterium associated with *Crassostrea virginica* (the Eastern Oyster). *Appl. Environ. Microbiol.* **49:** 83–90.

Wells, J. W. 1973. New and old scleractinian corals from Jamaica. *Bull. Mar. Sci.* **23:** 16–58.

Wilson, D. P. 1955. The role of micro-organisms in the settlement of *Ophelia bicornis* Savigny. *J. Mar. Biol. Assoc. U.K.* **34:** 531–543.

Yaphe, W. 1984. Chemistry of agars and carrageenans. *Hydrobiol.* **116/117:** 171–186.

Yednock, T. A., E. C. Butcher, L. M. Stoolman, and S. D. Rosen. 1987a. Receptors involved in lymphocyte homing: relationship between a carbohydrate-binding receptor and the MEL-14 antigen. *J. Cell Biol.* **104:** 725–731.

Yednock, T. A., L. M. Stoolman, and S. D. Rosen. 1987b. Phosphomannosyl-derivitized beads detect a receptor involved in lymphocyte homing. *J. Cell. Biol.* **104:** 713–723.

Yool, A. J., S. M. Grau, M. G. Hadfield, R. A. Jensen, D. A. Markell, and D. E. Morse. 1986. Excess potassium induces larval metamorphosis in four marine invertebrate species. *Biol. Bull.* **170:** 255–266.

Yvin, J. C., L. Chevolot, A. M. Chevolot-Magueur, and J. C. Cochard. 1985. First isolation of jacaranone from an alga, *Delesseria sanguinea.* A metamorphosis inducer of *Pecten* larvae. *J. Nat. Prods.* **48:** 814–816.

Zubay, G. 1983. *Biochemistry.* Addison-Wesley, Reading. 1268 pp.

Reference: *Biol. Bull.* **181:** 123–126. (August, 1991)

Outbreeding Depression as a Cost of Dispersal in the Harpacticoid Copepod, *Tigriopus californicus*

ALICE F. BROWN

Graduate Program in Ecology and Evolutionary Biology, Brown University,
Providence, Rhode Island 02912

Abstract. The costs of dispersing can be evaluated in terms of genetic expenses. These costs are associated with outbreeding depression. In the supralittoral zone of the rocky shore, both outbreeding depression and inbreeding depression may be important in determining whether an organism should disperse. These genetic costs were investigated in the harpacticoid copepod, *Tigriopus californicus*, which inhabits supralittoral pools. Matings between individuals from different pools were performed in the lab. The results suggest high costs to dispersing.

Introduction

In dispersing, any organism will most likely experience some costs. Many of these costs, such as loss of energy while moving, production of dispersal mechanisms, or risk of not reaching a suitable habitat, are ecological in nature and have been fairly well examined (*e.g.*, Palmer and Strathmann, 1981; Strathmann *et al.*, 1981; Cohen and Motro, 1989). There are also genetic costs of dispersing that are associated with outbreeding depression. Individuals choosing mates from different populations may have lower fitness than individuals choosing mates from the same population (*e.g.*, Price and Waser, 1979; Shields, 1982; review by Waldman, 1988). Outbreeding depression will be strongest for individuals in populations that normally have limited gene flow and that live in a heterogeneous environment (*i.e.*, dramatically different selective pressures affect different populations).

In some circumstances, the costs of dispersing must be evaluated relative to the costs of not dispersing. In addition to losing the ecological benefits of dispersing (reviewed by Howe and Smallwood, 1982), individuals may experience genetic costs if they fail to disperse. If individuals within a population are closely related, inbreeding depression may be a cost of not dispersing (*e.g.*, Greenwood *et al.*, 1978; Packer, 1979; Hoogland, 1982; Holekamp and Sherman, 1989; reviewed by Johnson and Gaines, 1990). Inbreeding depression will be most significant in small, isolated populations; populations that were founded by only a few individuals; or populations that have suffered an extreme bottleneck in size.

Here, I examine a habitat in which both inbreeding depression and outbreeding depression may play important roles in determining dispersal. This habitat is that part of the rocky supralittoral zone that holds small pools of water. Because these pools are above the high tide line, introductions by marine organisms are probably rare. Colonizations occur during relatively uncommon events, such as extreme wave splash or exceptionally heavy rains, which may create channels among pools and access to the ocean. The pools are discrete microhabitats differing from one another in many potentially important characters. These differences are caused often by only small changes in pool shape, tidal height, orientation, or other factors and may generate considerable heterogeneity in selective pressures, such as temperature or salinity, among pools. For example, for 22 pools surveyed on the Oregon coast over 4 months, mean salinity varied from 0.8 to 17 ppt with a range from 0 to 45 ppt and mean temperature varied from 12 to 17°C with a range from 8 to 30°C.

The harpacticoid copepod *Tigriopus californicus* (hereafter called *Tigriopus*) is a common inhabitant of supralittoral pools of the eastern Pacific coast. This organism is ideal for testing hypotheses regarding outbreeding depression and inbreeding depression. There appears to be limited migration of *Tigriopus* among pools. Migration has been documented in streams of water (Cooper, unpub.), which are rare in the supralittoral zone except during storms. Migration has also been observed on the

Received 15 February 1991; accepted 29 April 1991.

legs of the shore crab *Pachygrapsus* sp. (Egloff, 1966), which are presumably uncommon on bare rock away from crevices (pers. obs). Limited migration, coupled with abiotic and biotic differences among pools, should promote adaptive differences among *Tigriopus* populations in different pools. Therefore, matings between individuals from different pools (hereafter called non-poolmates) may result in outbreeding depression. Because migrations are probably rare, any pool may be colonized by only a few gravid females, causing many close relatives to be in each pool. The consequences of this founder effect are intensified because of the copepod's breeding system. A female *Tigriopus* will mate only once and can potentially produce 12–14 broods, each with up to 150 eggs (Vittor, 1971; pers. obs.). Therefore, matings between individuals from the same pool (poolmates) may result in inbreeding depression. I investigated the genetic costs to *Tigriopus* of dispersing *versus* staying in one pool by assaying for outbreeding depression and inbreeding depression in laboratory populations.

Methods and Results

I collected *Tigriopus* 5 km north of Newport, Oregon, from a basalt outcrop near Yaquina Head. I chose six pools from which to collect populations for laboratory mating studies. In choosing pools, I tried to span the range of physical variation to maximize the potential for genetic differentiation among pools, if its exists. Therefore, the pools chosen were different from one another in a maximum number of physical and biotic parameters and should have rarely, if ever, had water flow among them. The pools spanned a horizontal range of >70 m and two distinct outcrops, separated by a rock gully. The characters by which pools differed were salinity, temperature, pool substratum, and pool size (Table I and Brown, 1985). In the lab, I isolated gravid females and their juveniles (as released) from each of the six populations to set up family lines and to assure virginity of the test individuals. The isolated copepods were maintained in 2 ml clear plastic culture chambers in an incubator at 20°C and at a 16:8 light:dark schedule. They were fed a mixture of Tetramin® flaked fish food and nutritional yeast.

I performed three types of crosses to estimate outbreeding depression and inbreeding depression. The crosses were female × non-poolmate, female × poolmate, and female × sibling. Poolmate matings represent the normal breeding situation for non-dispersing *Tigriopus*. Non-poolmate matings should represent the breeding situation for dispersing copepods; any reduction in fitness in the non-poolmate matings reflects outbreeding depression. Similarly, sibling matings should represent the worst-case result of not dispersing; any reduction in fitness in sibling matings reflects inbreeding depression. However, if pools are full of close relatives, and therefore close inbreeding represents the normal breeding situation, then sibling matings and poolmate matings should have similar results. Furthermore, inbreeding depression is expected to be minimized in this case because many of the deleterious alleles will have been eliminated from the pool population.

After mating occurred in the lab test pairs, I removed the males and placed each female in a large (50 ml) vial with excess food to minimize cannibalism following hatching of the juveniles. From the single mating, females then produced continuous broods. At the end of three weeks (approximately one generation), I counted the total number of individuals (nauplii, copepidites, and adults) in each vial and used this number as a measure of fitness. The rationale for using this number as an index of fitness is that *Tigriopus* probably maximize their fitness most effectively by producing the greatest possible number of offspring. The high fecundity of *Tigriopus* may support this hypothesis.

The number of offspring produced varies with type of cross (Fig. 1). Females mated with random poolmates produced significantly more offspring than did either females mated with non-poolmates or females mated with siblings ($\bar{E}_3^2 = 0.061$, $P = 0.02$). Number of offspring was compared by isotonic regression (see Gaines and Rice,

Table I

Characteristics of pools from which lab populations were taken

Pool	Salinity (ppt) mean (range)	Temperature (°C) mean (range)	Pool size (cm)	Substratum type
1	5.7 (0–15)	14.9 (9–25)	100 × 100 × 17	upright algae, sand
2	9.2 (0–20)	15.9 (9–24)	63 × 28 × 3	algal mat
3	10.0 (0–20)	13.9 (9–20)	45 × 25 × 3	rock, sand
4	17.1 (0–40)	15.6 (9–28)	100 × 50 × 4	algal mat
5	10.0 (0–20)	14.8 (8–27)	100 × 53 × 8	sand
6	9.2 (5–15)	15.2 (9–23)	100 × 100 × 28	upright algae, sand

Mean salinity and mean temperature over a four month sampling period are shown. Approximate pool size is given for maximum values of three dimensions: length × width × depth.

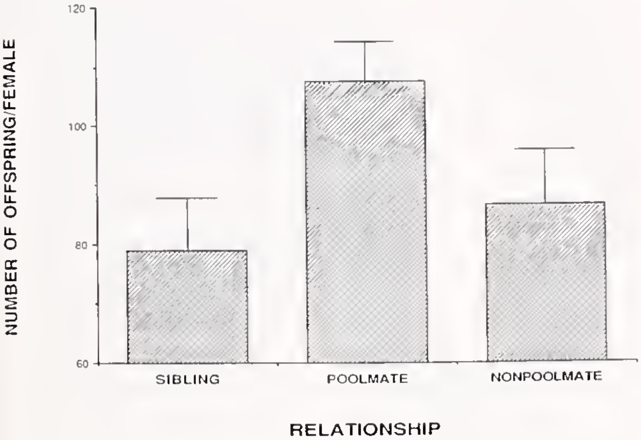

Figure 1. Effect of mate relationship on the number of offspring produced. Columns show the mean number of offspring produced in three weeks by females mated with siblings, poolmates, and non-poolmates. Sample sizes are 30, 37, and 35 females, respectively. Bars represent one standard error.

1990) because the direction of change was specified *a priori*.

Discussion

The results suggest that there are high costs to dispersal in *Tigriopus* associated with outbreeding depression. This result reflects the heterogeneous habitat in which *Tigriopus* live and supports the assumption of limited movement among pools. However, these results are somewhat different from the results of previous studies of *Tigriopus* (Burton and Feldman, 1981; Burton and Swisher, 1984), which demonstrated limited movement among rocky outcrops but high dispersal within any outcrop. The pools I studied are probably most similar to Burton's pools on different outcrops in that there was little or no potential for migration among the pools. Burton (1986, 1990) did find similar costs to outbreeding as evidenced by a decrease in F_2 survival and an increase in developmental time with crosses between populations. The costs of dispersal shown in my study are so great, indeed, that outbreeding depression, due to mating with a non-poolmate, is not significantly different from inbreeding depression due to mating with a sibling.

The results also suggest that a primary benefit of not dispersing is remaining in the proximity of poolmates, which are apparently better mates than non-poolmates. Traditional theory implies that in not dispersing, an individual may suffer inbreeding depression. However, inbreeding depression is not an important cost in the pools because matings between random poolmates result in significantly more offspring than matings between siblings. As previously discussed, if inbreeding were common in pools, then poolmate matings and sibling matings would result in similar numbers of offspring produced. The results suggest that the gene pool size in each pool population is fairly large.

Mate choice studies in the lab further support the hypothesis that inbreeding in pools is not an important selective pressure for *Tigriopus*. If inbreeding were a strong selective pressure, then identification and avoidance of close relatives as mates might be expected. However, when I presented virgin female *Tigriopus* with pairwise choices of males (sibling + poolmate, sibling + non-poolmate, or poolmate + non-poolmate), they never chose mates significantly different from random (Table II). Nonrandom mate choice probably hasn't evolved because there is no selective advantage to chosing mates in a pool nonrandomly. Pool populations appear to be large enough that siblings are rare as potential mates. A random mate chosen in the pool will most likely be a non-sib poolmate. Nonrandom mate choice or increased frequency of dispersal might evolve when inbreeding depression becomes significant.

In conclusion, dispersal in *Tigriopus* may be costly from a genetic perspective due to significant outbreeding depression. Lack of dispersal (staying in the native pool) does not seem to impose serious genetic costs. These re-

Table II

Results of mate choice tests

Female Choice				χ^2 Relation effect	χ^2 Stain effect
1. Sibling and Poolmate					
	S	P	Σ		
stained	13	13	26	0.40	3.60
unstained	9	5	14	$P > .50$	$P > .05$
Σ	22	18	40		
2. Sibling and Non-poolmate					
	S	P	Σ		
stained	15	18	33	0.02	1.41
unstained	13	11	24	$P > .90$	$P > .05$
Σ	28	29	57		
3. Poolmate and Non-poolmate					
	P	N	Σ		
stained	12	11	23	0.40	1.40
unstained	10	7	17	$P > .50$	$P > .05$
Σ	22	18	40		

In each test, the female was given a choice of two males—sibling + poolmate, sibling + non-poolmate, or poolmate + non-poolmate. Sample sizes were 40, 57, and 40, respectively. "Stained" males were dyed red with carmine powder to facilitate individual recognition for testing. S = sibling, P = poolmate, and N = non-poolmate.

sults suggest that frequent dispersal may not always be the most adaptive reproductive strategy.

Acknowledgments

I wish to thank T. Farrell, J. Lubchenco, B. Menge, and the rest of the Zoology gang for their advice and patience. C. King graciously provided the lab space. The manuscript was improved greatly due to comments from R. Burton, S. Gaines, P. Yund, an anonymous reviewer, and the attendees of the Brown Bag seminars. Support came through a ZoRF grant from Oregon State University.

Literature Cited

Brown, A. F. 1985. An experimental test of optimal outbreeding in the harpacticoid copepod *Tigriopus californicus*. MS Thesis, Oregon State University.

Burton, R. S. 1986. Evolutionary consequences of restricted gene flow among natural populations of the copepod *Tigriopus californicus*. *Bull. Mar. Sci.* **39:** 526–535.

Burton, R. S. 1990. Hybrid breakdown in developmental time in the copepod *Tigriopus californicus*. *Evolution* **44:** 1814–1822.

Burton, R. S., and M. W. Feldman. 1981. Population genetics of *Tigriopus californicus*. II. Differentiation among neighboring populations. *Evolution* **35:** 1192–1205.

Burton, R. S., and S. G. Swisher. 1984. Population structure of the intertidal copepod *Tigriopus californicus* as revealed by field manipulation of allele frequencies. *Oecologia* **65:** 108–111.

Cohen, D., and U. Motro. 1989. More on optimal rate of dispersal: taking into account the cost of dispersal mechanisms. *Am. Nat.* **134:** 659–663.

Egloff, D. A. 1966. Ecological aspects of sex ratio and reproduction in experimental and field populations of the marine copepod *Tigriopus californicus* (Baker). *J. Exp. Mar. Biol. Ecol.* **42:** 99–111.

Gaines, S. D., and W. R. Rice. 1990. Analysis of biological data when there are ordered expectations. *Am. Nat.* **135:** 310–317.

Greenwood, P. J., P. H. Harvey, and C. M. Perrins. 1978. Inbreeding and dispersal in the great tit. *Nature* **271:** 52–54.

Holekamp, K. E., and P. W. Sherman. 1989. Why male ground squirrels disperse. *Am. Sci.* **77:** 232–239.

Hoogland, J. L. 1982. Prairie dogs avoid extreme inbreeding. *Science* **215:** 1639–1641.

Howe, H. F., and J. Smallwood. 1982. Ecology of seed dispersal. *Annu. Rev. Ecol. Syst.* **13:** 201–228.

Johnson, M. L., and M. S. Gaines. 1990. Evolution of dispersal: theoretical models and empirical tests using birds and mammals. *Annu. Rev. Ecol. Syst.* **21:** 449–480.

Packer, C. 1979. Inter-troop transfer and inbreeding avoidance in *Papio anubis*. *Anim. Behav.* **27:** 1–36.

Palmer, A. R., and R. R. Strathmann. 1981. Scale of dispersal in varying environments and its implications for life histories of marine invertebrates. *Oecologia* **48:** 408–418.

Price, M. V., and N. M. Waser. 1979. Pollen dispersal and optimal outcrossing in *Delphinium nelsoni*. *Nature* **277:** 294–297.

Shields, W. M. 1982. *Philopatry, Inbreeding, and the Evolution of Sex.* SUNY Press, Albany.

Strathmann, R. R., E. S. Branscomb, and K. Vedder. 1981. Fatal errors as a cost of dispersal and the influence of intertidal flora on set of barnacles. *Oecologia* **48:** 13–18.

Vittor, B. A. 1971. Effects of the environment on fitness-related life history characters in *Tigriopus californicus*. Ph. D. Thesis, University of Oregon.

Waldman, B. 1988. The ecology of kin recognition. *Annu. Rev. Ecol. Syst.* **19:** 543–571.

Reference: *Biol. Bull.* **181:** 127–134. (August, 1991)

Alloimmunity in the Gorgonian Coral *Swiftia exserta*

LUISA SALTER-CID AND CHARLES H. BIGGER

Department of Biological Sciences, Florida International University, Miami, Florida 33199

Abstract. This study of histocompatibility demonstrates that the gorgonian *Swiftia exserta* (Coelenterata, Anthozoan) fulfills the minimal functional criteria of cytotoxicity, specificity, and altered secondary response (memory) that characterize an adaptive immune response. All autografts (self grafts) fused, and all allografts (intraspecific grafts) underwent rejection, which is characterized by rapid and progressive blanching, necrosis, and loss of tissue in the immediate contact area. Initial reactions required 7–9 days to produce 1 mm of necrosis, but after a resting period, a second contact at a new tissue area yielded the same reaction in 3–4 days. After primary sensitization, intervals of up to eight weeks still produced a significantly accelerated secondary response. Significant differences between the reaction times of second set and third party allografts demonstrated recognition specificity in these responses. Thus, this is the first report of an adaptive alloimmune response in gorgonians.

Introduction

Most immunologists would agree that specificity and memory are the hallmarks of adaptive immune reactivity. According to some authors (Hildemann *et al.*, 1979), only the following functional criteria are necessary to define such immunological competence: (1) antagonistic or cytotoxic reaction after sensitization; (2) selective or specific reactivity; and (3) inducible memory, *i.e.*, selectively altered (positive or negative) reactivity on secondary contact.

Possession of a specific adaptive immune system, including immunorecognition leading to selectively inducible responses with a memory component, was, until recently, considered to be restricted to vertebrates (Klein, 1989). Invertebrate defense mechanisms, often associated with phagocytosis and encapsulation, were thought to lack sharp specificity. We now know that at least some metazoan invertebrates, ranging from sponges to protochordates, possess a well-developed capacity for allogeneic recognition followed by incompatibility reactions (see Bigger, 1988).

Some definitive studies have been carried out on invertebrates. Relatively short-term memories were found in the sponge *Callyspongia diffusa* (4 weeks; Bigger *et al.*, 1982) and the coral *Montipora verrucosa* (8 weeks; Hildemann *et al.*, 1980a), but a longer term memory was reported for allograft rejection in the sea urchin, *Lytechinus pictus* (6 months; Coffaro, 1980). Specific immune memory, however, has not been found in all invertebrates even within the same class or phylum. For example, immune memory has been reported to be absent in some sponges (*e.g.*, Van de Vyver, 1980; Smith and Hildemann, 1984) and earthworms (Parry, 1978). Therefore, without testing, we cannot assume that the details of an immune response in one species are transferable to other members of the phylum.

The gorgonians (Anthozoa; Alcyonaria) are an Order of soft corals that includes sea fans and sea whips. Theodor's extensive studies (Theodor, 1966, 1969, 1970, 1976; Serre and Theodor, 1967; Theodor and Carriere, 1975; Theodor and Senelar, 1975) of *Eunicella stricta* and *Lophogorgia sarmentosa*, and the preliminary work of Bigger and Runyan (1979) on *Leptogorgia virgulata*, *Pseudopterogorgia elisabethae* and *Plexura flexulosa*, have identified some of the major characteristics of histocompatibility in the Order. Naturally occurring grafts within the same colony (autografts) occur in field, and all experimentally induced autografts rapidly fuse within 24 h. (Theodor, 1970; Bigger and Runyan, 1979). Rapid xenogeneic reactions (between two individuals of different species) were the focus of Theodor's study of gorgonian histocompatibility; he hypothesized a system of "induced suicide" underlying graft rejection. The delay in the cytotoxic responses of

Received 2 May 1990; accepted 1 April 1991.

Abbreviations: RT—reaction time, MRT—mean reaction time, 1°—first (primary) graft, 2°—secondary graft, 3P—third party graft.

allografts (between two individuals of the same species) suggested, to Theodor, fundamental differences in the mechanisms operative in xenogeneic *versus* allogeneic cytotoxic incompatibilities. Gorgonian histoincompatibility mechanisms have not been characterized at the cellular and molecular levels. As for immunocompetence, the gorgonians certainly fulfilled the first criterion of cytotoxic alloincompatibility; but prior to this study, the parameters of rejection and other aspects, such as those of memory and specificity, had not been tested or were not found.

The purpose of this project was to study tissue incompatibility reactions between different colonies of the gorgonian coral *Swiftia exserta* (Fig. 1). We asked whether the corals possess attributes of an adaptive immune system.

Materials and Methods

Animal collection and maintenance

Swiftia exserta individuals were purchased from various sources and were collected in the waters off Southeast Florida, at depths of approximately 30 m. The animals were transported to Florida International University, where they were maintained in 25 or 100 gallon seawater aquaria with sub-gravel filters, and fed newly hatched *Artemia.*

All aquaria were subjected to alternating periods of 12 hours of light and dark. The water temperature was generally maintained at 20–22°C with aquarium heaters, although during the summer, the temperatures occasionally rose to 25°C. Individual experiments were confined to a range of about 1°C or less. Salinity values ranged from 31 to 34 0/00. Because all treatments in an experiment were run concurrently in the same aquarium, all were subjected to the same general conditions. Although there were several colonies in each aquarium, they were not in contact. The animals were acclimated for at least 4 days before being placed in experimental contact. As opposed to many other gorgonians, *Swiftia exserta* lives well under laboratory conditions. Also, as we report in this study, its rapid allogenic reactions make it especially attractive for immunological studies.

Techniques of grafting and scoring

Small branches, 2–3 cm, were clipped from a gorgonian colony with surgical scissors and immediately placed in either allogeneic (intraspecific) or isogeneic (= autograft) combinations. To eliminate any influence of size on the reactions, all pairings involved tissue pieces of about the same size. The two pieces were gently placed in close contact without traumatizing the cell surfaces. We call this grafting. Unless otherwise stated, secondary grafts (2°) were performed after a sensitization period of three days; *i.e.*, the tissues were put in contact for three days and then separated for some given length of time before regrafting. A three-day period of sensitization was chosen to assure full maturation of the immune response; *i.e.*, at this time cytotoxic reactions were underway in all graft pairs but not completed.

A system of third-party grafting (3P) was used to test for specificity in the allograft response. It was performed like the secondary graft except that tissue from an allogeneic animal not used in the sensitization was separately grafted with each of the test tissues for the second interaction. A lack of specificity should result in all allogeneic tissue being treated the same, and that would be reflected in similar second set and third-party rejection times. Specificity would be demonstrated if the third party grafts were treated in a naive fashion.

The coral branches were immobilized in small holders, each consisting of a 4 mm diameter × 5–6 cm length of glass tube bent into a "v" shape. The ends of the glass tube were covered with Nalgene 8000 plastic tubing (1/8″ ID × 1/16″ wall) 1–1.5 cm long. Small cuts (2 mm) were made in the plastic into which the coral branches were inserted (Fig. 2). A 2–3 mm long section of tissue was removed from the axial skeleton at the cut end of the branch that was inserted into the tubing; this operation precluded the necrosis that is induced when the tissue is pinched. Contact was between intact surfaces rather than the cut-ends of the branch.

Tip to side, side to side, and tip to tip cytotoxic reactions were similar in direction and appearance, and paired *t*-tests between reaction times showed no significant differences between the rates (data not shown). Therefore, the reaction is independent of the site chosen for pairing. In tip to tip, and some tip to side grafts, the support was unstable, and the individual pieces separated before the reaction endpoint was reached. No response would occur in such cases, because rejection seems to depend on unbroken physical contact. Because no significant influence of tissue locality was observed, side to side grafting was used in all the subsequent experiments and technical problems were minimized.

After grafting, the individuals were examined daily under a dissecting microscope at 40× magnification. One of two responses occurred: either *fusion*—complete growing together of the tissues of the two branches (Fig. [illegible]), or *rejection*—tissue necrosis of one or both individuals at the contact zone between the two colonies (Fig. 4).

Cytoxic reactions were arbitrarily scored as definitive when soft tissue destruction extended 1.0 mm or more to either side of an interface. The time required, in days, to reach that point was called the reaction time (RT). The reaction is easy to score for this species because the white necrotic tissue stands out in marked contrast to the orange

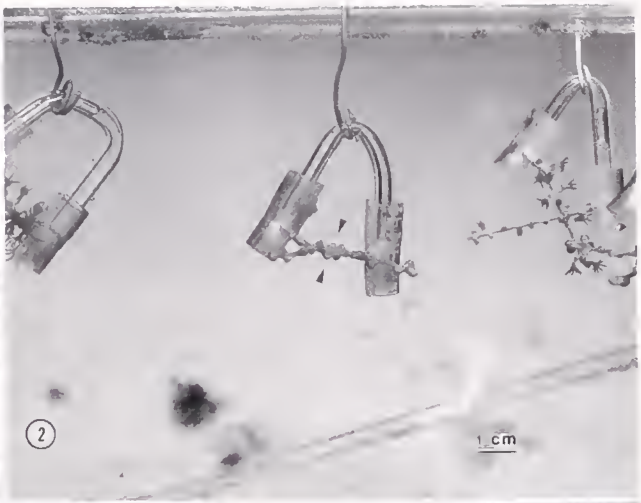

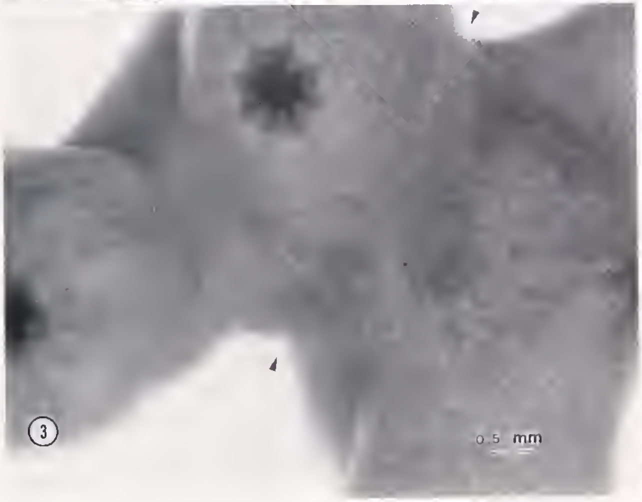

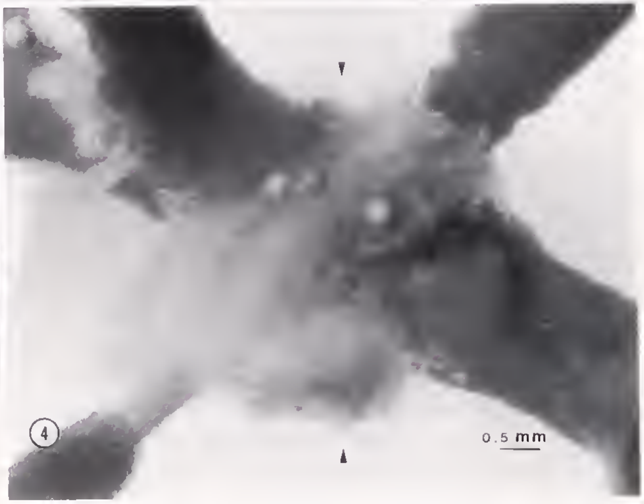

Figure 1. Colony of *Swiftia exserta.*

Figure 2. Technique of pair grafting. Coral pieces cut from the same or separate colonies of *S. exserta* are immobilized by the holders with their contact surfaces intimately opposed (between arrows).

Figure 3. Intracolony autografts of *S. exserta* showing compatible fusion at interface (arrows).

Figure 4. Intracolony allografts of *S. exserta* showing cytotoxic incompatibility restricted to the immediate contact zone. Note blanching and soft tissue death at interface (arrows) and exposed axial skeleton.

color of the living soft tissues. Because as little as 0.1 mm of necrosis can usually be discriminated, end points can be determined quantitatively.

Data analysis

Mean reaction times (MRT) and their standard deviations in days were determined. Paired *t*-tests were used to determine the significance of the differences between the experimental and control data because the animals, in both cases, were genetically identical.

Results

Pathology

Grafts between parts of the same colony were always compatible. Soft tissues fused in the area of contact as early as one day after grafting. Neither tissue bleaching nor necrosis accompanied fusion in any of the ten pairs tested (Fig. 3). Compatible fusion persisted indefinitely. The fused branches could not be pulled apart easily; the tissues always tore before separating.

Rejection of initial allografts was preceded by a lag of 3–5 days; during this time intimate tissue contact was required. Progressive allograft rejection occurred in the following sequence: (1) tissue blanching caused by the disappearance of pigmentation in the immediate contact zone; (2) loss of spicules from the tissues; and (3) tissue death eventually leading to exposure of the hard axial skeleton (Fig. 4). Intensified reactivity (more rapid and acute necrosis) was accompanied by secretion of mucus at the interface. On two occasions, overgrowth of one col-

Table I

Timing of initial allosensitization or immune induction in Swiftia exserta

Duration of initial allogeneic contact (a) (days)	No. of coral pairs tested (n)	Graft (b)	Mean reaction time (days) (c)	Range of indiv. react. times (days)	Difference between 1st and 2nd reaction times (d)
1	45	ctl.	8.3 ± 0.5	7–9	N.S.—$P \geq 0.4$
		test	8.2 ± 0.7	7–9	
2	45	ctl.	8.0 ± 0.4	7–9	SIG—$P \leq 0.001$
		test	3.3 ± 0.5	3–4	
3	45	ctl.	8.3 ± 0.6	7–9	SIG—$P \leq 0.001$
		test	3.7 ± 0.5	3–4	

(a) Sensitization by first-set allografting was allowed for 1, 2, or 3 days at 22–24°C; coral pairs were then each regrafted at a new interface 3 days later.

(b) Concurrent controls (primary grafts) were performed with the same combinations as the test grafts.

(c) Mean ± standard deviation of the mean.

(d) N.S.—not significant. SIG—significant at the 0.1% level. Significance was determined by the paired *t*-test.

ony by the other at one or both sides of the interface was observed; this overgrowth was concurrent with the usual necrosis.

Parameters of graft response

Reproducibility of reaction times. The first experimental set consisted of grafting 10 replicates of each of 10 allogeneic combinations and 8 replicates of each of 10 isogeneic combinations. The very similar reaction times (RTs), and standard deviations that were less than one day for each combination, justified our use of a single graft of each combination in all subsequent treatments (data not shown).

Alloimmune memory. In a series of 45 test pairs, control primary allografts yielded a mean reaction time of 8.3 ± 0.6 days. Secondary allograft tests, established by resetting the same coral pairs at new interfaces away from the original contact area following a three-day separation, showed accelerated and intensified cytotoxic reactions with a MRT of 3.7 ± 0.5 days (Table I). The MRT difference, with an interval of three days between first-set and second-set grafting, was highly significant ($P < 0.001$), indicative of immune memory. Intensified second-set reactivity was characterized by an earlier onset and stronger necrosis and secretion of mucus at the interfaces.

Three days of presensitization were successful in eliciting an accelerated second-set reaction. Possible earlier induction of memory was tested by disjoining initial allografts after one or two days of contact and regrafting the same pairs at new interfaces three days later (Table I).

Coral pairs regrafted after only 1 day of allogeneic contact yielded a MRT of 8.2 days with a range of individual cytotoxic reaction times of 7–9 days (Table I). Thus, no significant difference was observed between the RTs of the control and test pairs. As shown in Table I, after 2 days of presensitization, all second-set grafts already displayed accelerated activity with a MRT of 3.3 ± 0.5 days. Paired *t*-tests showed that the difference between the primary and secondary RTs was significant ($P < 0.001$).

Two days of tissue contact were sufficient to elicit accelerated allograft responses. Longer sensitization periods did not improve the response time, and the sensitization appeared to be "all or nothing" rather than a gradual transition.

To test for specificity, 90 pairs of third-party grafts were performed. The protocol is shown in Figure 5. Rather than responding in a purely naive or sensitized manner, these third-party grafts yielded a broad range of cytotoxic reaction times reflecting a distribution of accelerated to non-accelerated responses as is shown by the range of individual reaction times of 4–9 days (Table II). The reaction time of third-party grafts (mean 5.9 days) was significantly different from both first and second-set graft reaction times (8.2 days and 3.5 days respectively, Table II).

To test for long-term memory, groups of grafts were reset at new interfaces at 2, 4, 6, and 8 weeks after separation from primary contact. The resulting MRTs, standard deviations, and the range of individual cytotoxic reaction times, are given in Table III. Strong alloimmune memory was present in the second-set group grafted 2 weeks after first-set separation, as shown by an early MRT of 4.1 days ± 0.5 days and a significant difference ($P < 0.001$) between the primary and secondary RTs. This sensitized state was still present after 4 weeks, with an MRT of 3.6 ± 0.6 days. At 6 weeks after first-set separation, the accelerated reaction started to fade, as is shown by the MRT of 6.4 and the individual reaction times of 5–8 days, but is still significant ($P < 0.001$). This fading of alloimmune memory was still more accentuated at the 8-weeks period, with a MRT of 6.9 ± 0.9 and an individual range of 6–9 days. Although there is some degree of overlapping in the values of the control and test grafts from the 8-week group, the difference between the primary and secondary RTs is still significant ($P < 0.001$); the response gets progressively weaker in all combinations approaching the timing of a naive response.

Discussion

This study demonstrates that the anthozoan gorgonian *Swiftia exserta* displays: (a) cytotoxic reactivity accompanying allogeneic incompatibility, (b) early and vigorous primary allograft rejection, and (c) selective alloimmunity with a specific memory component. Thus, *S. exserta* fulfills the three criteria for an adaptive immunological response, described by Hildemann *et al.* (1979).

Among other coelenterates, allogeneic incompatibilities have been documented for hydrozoans (*e.g.*, Ivker, 1972; Buss *et al.*, 1984) and anthozoans, including gorgonians (*e.g.*, Theodor, 1970), sea anemones (*e.g.*, Bigger, 1980), and scleractinian corals (*e.g.*, Hildemann *et al.*, 1977). Except for the coral *Montipora verrucosa* (Hildemann *et al.*, 1980a), however, no substantial data bearing on the existence or persistence of immune memory in this phylum has heretofore been available.

In the gorgonian coral, *Swiftia exserta*, autografts fuse compatibly, but allografts were invariably incompatible. The pattern of necrosis (Fig. 4) suggests that the response is triggered by a cellular process rather than a diffusible factor; *i.e.*, because tissue destruction was limited to the graft interface, either cell contact or a very short-range cytotoxic molecule was responsible for the cytotoxic response. *Swiftia exserta* is an attractive model for tissue

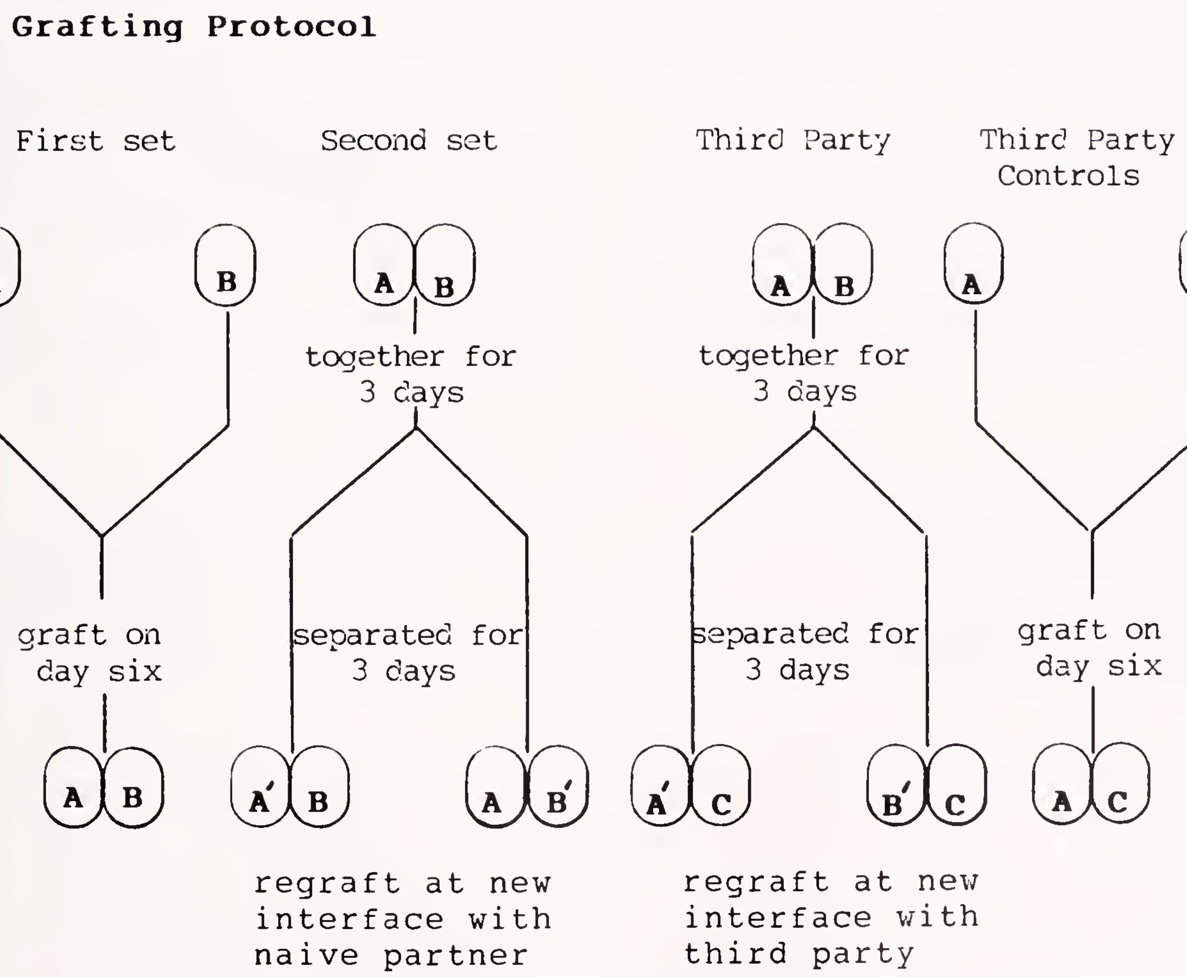
Grafting Protocol
First set
Second set
Third Party
Third Party Controls
A
B
A B
together for 3 days
A B
together for 3 days
A
C
graft on day six
separated for 3 days
separated for 3 days
graft on day six
A B
A′ B
A B′
A′ C
B′ C
A C
regraft at new interface with naive partner
regraft at new interface with third party

Figure 5. Experimental protocols used in the specificity study (Table II). A, B, and C stand for naive tissue from colonies (clones). A, B, and C. A′ and B′ denote presensitized individuals from the same respective colonies. 1°—first-set; 2°—second-set; 3P—third party; ctl—third-party controls.

Table II

Specificity of allograft reaction times in Swiftia exserta

Grafts (a)	No. of coral pairs tested (n)	Mean reaction time (b) (days)	Range of individual reaction times (days)
First set	45	8.2 ± 0.6	7–9 (c)
Second set	90	3.5 ± 0.4	3–4 (c)
Third party	90	5.9 ± 1.5	4–9 (c)
Control	90	8.3 ± 0.6	7–9 (c)

(a) Concurrent controls were performed with the same combinations as the third party grafts.

(b) Mean ± standard deviations of the mean.

(c) The difference between second-set and third-party (3P) graft responses and the difference between 3P and control graft responses are both highly significant ($P \leq 0.001$, paired t test).

Experimental temperature range: 21–24°C.

grafting, because the responses are easily scored and the rapid rates of rejection (primary MRTs of about 7 to 10 days) are closer to those observed in mammalian transplantation than in the coral *M. verrucosa* (MRTs of about 18 to 22 days, Hildemann *et al.*, 1980a).

As Burnet (1969) pointed out, recognition of self/not-self is the cornerstone of immunological recognition. It has been suggested that while vertebrates recognize not-self, invertebrate responses are based on recognition of self (*e.g.*, Burnet, 1971). Although *S. exserta* shows a range of reaction times and severity, the results from a given combination of colonies were highly reproducible. This pattern of differing responses between different allogeneic combinations and the specificity associated with memory, *i.e.*, that different allogeneic "not-self" elicits different responses, supports the opposite hypothesis, that allogeneic rejection is based on a recognition of "not-self" (see Bigger, 1988; Neigel, 1988). Among 1479 alloparabiotic combinations of the gorgonian *Eunicella stricta* collected in the Banyuls-sur-mer (France) area, Theodor (1976) observed only 11 or 0.7% compatible fusions, whereas the remaining 99.3% exhibited rejection reactions. Even the small number of compatible gorgonians could have originated from the same clone, because all the specimens were collected from the same area. That impressive variation of histocompatibility markers, as well as that found between the 10 colonies employed in the present study, suggest that each separate clone or colony has a unique array of alloimmunorecognition molecules, as predicted by the concept of the "uniqueness of the individual" developed by Medawar (*e.g.*, Jokiel *et al.*, 1983).

The early acquisition of immune memory in other corals (Hildemann *et al.*, 1980a) seemed to be a gradual or quantitative process, with accelerated reactivity present after 2 to 4 days of contact and maximal presensitization developed after 4 to 8 days; that activation or positive memory then persisted or diminished only slightly after prolonged primary contact. In *S. exserta*, because there is apparently no significant difference between the MRTs of the secondary responses elicited after 2 or 3 days of primary contact (3.3 and 3.7 d respectively, Table I), it seems to be an all or none process occurring at approximately 2 days.

The present study demonstrates that significant short-term alloimmune memory persists for at least 8 weeks,

Table III

Duration of Swiftia exserta *alloimmune memory*

Time interval between 1st sensitization and 2nd graft (weeks)	No. of coral pairs tested (n)	Graft (a)	Mean reaction time (b) (days)	Range of indiv. react. times (days)	Significance of the difference between the primary and secondary reaction times (c)
2	43	ctl.	8.1 ± 1.0	7–10	SIG
		test	4.1 ± 0.5	3–4	
4	45	ctl.	7.9 ± 0.8	7–9	SIG
		test	3.6 ± 0.6	3–5	
6	42	ctl.	7.8 ± 0.8	7–9	SIG
		test	6.4 ± 1.0	5–8	
8	39	ctl.	7.9 ± 0.8	7–9	SIG
		test	6.9 ± 0.9	6–9	

(a) Concurrent controls (primary grafts) were performed with the same combination as the test grafts.

(b) Mean ± standard deviation of the mean.

(c) Significance was determined by the paired t-test and in all cases represents $P \leq 0.001$.

but starts to fade at 6 weeks in the gorgonian coral *S. exserta* (Table III). As with similar short-term immune memory in the sponge *C. diffusa* (Bigger *et al.*, 1982), annelids (Dales, 1978), and echinoderms (Coffaro, 1980), this appears to constitute a major difference from the long-term alloimmune memory found in mammals (Hildemann, 1984). In mice and rats, immune memory demonstratable by accelerated rejection of test skin allografts resides in lymphocytes and persists more than one year after sensitization (Billingham *et al.*, 1963). It is important to note however, that in this study, no tests were performed after prolonged sensitization (> 3 days) and that there was no investigation of environmental factors such as temperature, light, and salinity, which may affect the effectiveness of sensitization and the cytotoxic reaction times (*e.g.*, Johnston *et al.*, 1981). Further investigation of conditions that might favor long-term memory is desirable, because the absence of this characteristic could be a major distinguishing feature of invertebrates. Memory that lasts only weeks (Bigger *et al.*, 1982), rather than months or years (Billingham *et al.*, 1963), could have several causes. This immunologic feature in sponges and corals may be the result of shorter-lived memory residing in immunocytes with commensurate life spans (Hildemann *et al.*, 1980b). For example, the sensitized immunocytes may be replaced by naive cells. Alternatively, the molecules in which memory is imprinted may become inactive with time or with immunocyte division. Killer cells or molecules involved with memory have yet to be identified as a special subset in any coelenterate (see Bigger and Hildemann, 1982). Thus, these studies of memory must await further progress.

Only 27% of the third-party individuals reacted as fast as the slowest of the second-set allografts, while the remainder responded in a similar fashion to primary grafts or at intermediate times, demonstrating a specificity involved in the secondary response. These results contrast with the ones obtained by Hildemann *et al.* (1980a) in *M. verrucosa*. A bimodal distribution of third-party reaction times such that approximately 66% of the third-party individuals reacted as fast as the second-sets led them to suggest the occurrence of cross reactivity. The present study presents a different situation; third-party reaction times were not bimodal and, while there is a demonstrable specificity, an allogeneicly non-specific effect appears to be manifested in the third-party allografts. Alternatively, another explanation is that the accelerated responses of some third-party individuals could be the result of the sharing of a limited repertoire at minor histocompatibility loci (locus), which might exist together with a not-shared, highly polymorphic MHC. However, there is no genetic data that pertains. Why third-party grafts reacted in a significantly different way from primary as well as secondary grafts must await further investigation.

This study supports the hypothesis (*e.g.*, Burnet, 1976) that invertebrates may be capable of anticipatory immune responses, as opposed to suggestions (Klein, 1989) that, whereas vertebrate immune responses are based on recognition of not-self, invertebrate responses are not anticipatory and are non-specific. Unfortunately, the study of immunity in invertebrates has been restricted so far to very few animals, and most of these have been investigated in little detail; therefore, many questions remain unanswered. *Swiftia exserta* provides a very good model in which to study these invertebrate defense mechanisms, which need clarification.

Acknowledgments

Thanks are due to Ms. Cecile Olano for providing photographic assistance, Ms. Lois Bigger for editorial assistance, and anonymous reviewers for their helpful comments. Support was provided by NIH grant RR08205.

Literature Cited

Bigger, C. H. 1980. Interspecific and intraspecific acrorhagial aggressive behavior among sea anemones, a recognition of self and not-self. *Biol. Bull.* **159:** 117–134.

Bigger, C. H. 1988. Historecognition and immunocompetence in selected marine invertebrates. Pp. 55–65 in *Invertebrate Historecognition*, R. Grosberg, D. Hedgecock, and K. Nelson, eds. Plenum Press, New York.

Bigger, C. H., and W. H. Hildemann. 1982. Cellular defense systems of the coelenterata. Pp. 59–87 in *The Reticuloendothelial System*, N. Cohen and M. M. Sigel, eds. Plenum Publishing Corp., New York.

Bigger, C. H., P. L. Jokiel, W. H. Hildemann, and I. S. Johnston. 1982. Characterization of alloimmune memory in a sponge. *J. Immunol.* **129:** 1570–1572.

Bigger, C. H., and R. Runyan. 1979. An *in situ* demonstration of self-recognition in gorgonians. *Dev. Comp. Immunol.* **3:** 591–594.

Billingham, R. E., W. K. Silvers, and D. B. Wilson. 1963. Further studies on adaptive transfer of sensitivity to skin homografts. *J. Exp. Med.* **118:** 397–401.

Burnet, F. M. 1969. *Self and Not-Self: Cellular Immunology, Book 1.* Melbourne and Cambridge University Presses, Carlton, Victoria, and London.

Burnet, F. M. 1971. "Self-recognition" in colonial marine forms and flowering plants in relation to the evolution of immunity. *Nature* **232:** 230–235.

Burnet, F. M. 1976. The evolution of receptors and recognition in the immune system. Pp. 35–58 in *Receptors and Recognition I*, P. Cuatrecasa and M. F. Greaves, eds. Chapman and Hall, London.

Buss, L. W., C. S. McFadden, and D. R. Keene. 1984. Biology of hydractinid hydroids. 2. Histocompatibility effector system/competitive mechanism mediated by nematocyst discharge. *Biol. Bull.* **157:** 139–158.

Coffaro, K. A. 1980. Memory and specificity in the sea urchin *Lytechinus pictus*. Pp. 77–88 in *Phylogeny of Immunological Memory*, M. J. Manning, ed. Elsevier/North Holland, New York.

Dales, R. P. 1978. The basis of graft rejection in the earthworms *Lumbricus terrestris* and *Eisenia foetida*. *J. Invertebr. Pathol.* **32:** 264–268.

Hildemann, W. H. 1984. A question of memory. *Dev. Comp. Immunol.* **8:** 747–756.

Hildemann, W. H., C. H. Bigger, and I. S. Johnston. 1979. Histoincompatibility reactions and allogeneic polymorphism among invertebrates. *Transplant Proc.* **11:** 1136–1141.

Hildemann, W. H., P. L. Jokiel, C. H. Bigger, and I. S. Johnston. 1980a. Allogeneic polymorphism and alloimmune memory in the coral *Montipora verrucosa. Transplantation* **30:** 277–301.

Hildemann, W. H., C. H. Bigger, P. L. Jokiel, and I. S. Johnston. 1980b. Characteristics of immune memory in invertebrates. Pp. 9–14 in *Phylogeny of Immunological Memory,* M. J. Manning, ed. Elsevier/North Holland, New York.

Hildemann, W. H., R. L. Raison, G. Cheung, C. J. Hull, C. Akabe, and J. Okanoto. 1977. Immunological specificity and memory in a scleractinian coral. *Nature* **270:** 219–223.

Ivker, F. B. 1972. A hierarchy of histoincompatibility in *Hydractinia echinata. Biol. Bull.* **143:** 162–174.

Johnston, I. S., P. L. Jokiel, C. H. Bigger, and W. H. Hildemann. 1981. The influence of temperature on the kinetics of allograft reactions in a tropical sponge and a reef coral. *Biol. Bull.* **160:** 280–291.

Jokiel, P. L., W. H. Hildemann, and C. H. Bigger. 1983. Clonal population structure of two sympatric species of the reef coral *Montipora Bull. Mar. Sci.* **33:** 181–187.

Klein, J. 1989. Are invertebrates capable of anticipatory immune responses? *Scand. J. Immunol.* **29:** 499–505.

Neigel, J. E. 1988. Recognition of self or non-self? Theoretical implications and an imperical test. Pp. 127–142 in *Invertebrate Historecognition,* R. Grosberg, D. Hedgecock, and K. Nelson, eds. Plenum Press, New York.

Parry, M. J. 1978. Survival of body wall autografts, allografts and xenografts in the earthworm *Eisenia foetida J. Invertebr. Pathol.* **31:** 383–392.

Serre, A., and J. Theodor. 1967. Mise en évidence d'une reconnaissence immunologique de tisus chez un invertébré. *G.R. Acad. Sc. Paris.* **264:** 513–514.

Smith, L. C., and W. H. Hildemann. 1984. Alloimmune memory is absent in *Hymeniacidon sinapium,* a marine sponge. *J. Immunol.* **133:** 2351–2355.

Theodor, J. 1966. Contribution à l'étude des Gorgones (V) les greffs chez les gorgones: étude d'un système de reconnaissence du tissus. *Bull. Inst. Oceanogr. Monaco.* **66:** 1–7.

Theodor, J. 1969. Histotoxicité *in vivo* et *in vitro* entre tissus xénogéniqus et entre tissus allogénipus chez un invertébré. *C. R. Acad. Sc. Paris.* **268:** 2534–2535.

Theodor, J. 1970. Distinction between "self" and "not-self" in lower invertebrates. *Nature.* **227:** 690–692.

Theodor, J. 1976. Histoincompatibility in a natural population of gorgonians. *Zool. J. Linnean Soc.* **58:** 173–176.

Theodor, J., and J. Carriere. 1975. Direct evidence of heterolysis of gorgonian target cells. Pp. 101–104 in *Immunologic Phylogeny,* W. H. Hildemann and A. A. Benedict, eds. Plenum Press, New York.

Theodor, J., and R. Senelar. 1975. Cytotoxic interaction between gorgonian explants: mode of action. *Cell. Immunol.* **19:** 194–200.

Van de Vyver, G. 1980. Second-set allograft rejection in two sponge species and the problem of an alloimmune memory. Pp. 15–25 in *Phylogeny of Immunological Memory,* M. J. Manning, ed. Elsevier/North Holland, New York.

Reference: *Biol. Bull.* **181:** 135–143. (August, 1991)

Restriction Fragment Length Polymorphism Analysis Reveals High Levels of Genetic Divergence Among the Light Organ Symbionts of Flashlight Fish

CONNIE J. WOLFE AND MARGO G. HAYGOOD

Scripps Institution of Oceanography, University of California, San Diego, California 92093

Abstract. Restriction fragment length polymorphisms within the *lux* and 16S ribosomal RNA gene regions were used to compare unculturable bacterial light organ symbionts of several anomalopid fish species. The method of Nei and Li (1979) was used to calculate phylogenetic distance from the patterns of restriction fragment lengths of the *lux*A and 16S rRNA regions. Phylogenetic trees constructed from each distance matrix (*lux*A and 16S rDNA data) have similar branching orders. The levels of divergence among the symbionts, relative to other culturable luminous bacteria, suggests that the symbionts differ at the level of species among host fish genera. Symbiont relatedness and host geographic location do not seem to be correlated, and the symbionts do not appear to be strains of common, free-living, luminous bacteria. In addition, the small number of hybridizing fragments within the 16S rRNA region of the symbionts, compared with that of the free-living species, suggests a decrease in copy number of rRNA operons relative to free-living species. At this level of investigation, the symbiont phylogeny is consistent with the proposed phylogeny of the host fish family and suggests that each symbiont strain coevolved with its host fish species.

Introduction

Members of the teleost fish family Anomalopidae harbor luminous bacterial symbionts in specialized light organs, located under each eye. Light is produced continuously by the bacteria through the action of bacterial luciferase; but depending on the species, the light may be occluded, either by rotation of the entire light organ, or by a shutter mechanism (Kessel, 1977; Leisman *et al.*, 1980; Johnson and Rosenblatt, 1988). The four genera of anomalopid fishes contain five species: *Anomalops katoptron, Photoblepharon palpebratus, Photoblepharon steinitzi, Kryptophanaron alfredi,* and *Phthanophaneron harveyi.* Evidence from comparative morphology and biogeography suggests the following familial phylogeny (Johnson and Rosenblatt, 1988). The anomalopids appear to have branched off of the Trachithyid lineage during the Cretaceous period. The genus *Anomalops* probably diverged later in the Cretaceous and is radically different from the other genera. *Phthanophaneron* diverged in the Miocene with *Kryptophanaron,* and *Photoblepharon* diverged most recently, in the Pliocene.

Luminous bacterial symbionts in several other families of fishes have been cultured. In these instances, a single species of symbiont is associated with an entire family of host fish. These bacteria belong to species that have also been isolated directly from seawater, and the juvenile host may acquire its symbionts from the surrounding water at each generation (Ruby and Nealson, 1976; Fitzgerald, 1977; Reichelt *et al.*, 1977; Leis and Bullock, 1986; Wei and Young, 1989). Other light organ symbioses, in ceratioid fishes and pyrosomes, contain unculturable symbionts, and the identity of the symbionts is unknown in those cases. The anomalopid symbionts have, as yet, defied all of our attempts to culture them in laboratory media. Our inability to culture the symbionts, combined with the extensive morphological adaptations of the host fish, suggest an obligate symbiosis in which the bacteria may have coevolved with the fish host.

We have compared the symbionts in four species of anomalopid fish by analyzing restriction fragment length polymorphisms (RFLPs) of fragments containing either the luciferase structural genes (*lux*AB), or the 16S ribosomal RNA genes. RFLPs of other structural genes have frequently been used to compare species and populations of bacteria (Stanley *et al.*, 1985; Franche and Cohen-Ba-

Received 20 November 1990; accepted 18 March 1991.

zire, 1987; Denny *et al.*, 1988; Lindblad *et al.*, 1989). Ribosomal RNA genes are very conserved, and comparisons of rRNA gene restriction patterns had previously been used to differentiate between species, as well as subspecies, of bacteria (Gottlieb and Rudner, 1985; Grimont and Grimont, 1986; Saunders *et al.*, 1988; Stull *et al.*, 1988; Buyser *et al.*, 1989). Our goal was to analyze both gene regions to determine: (1) whether the symbionts are the same species in all of the anomalopids or are specific to fish species, genus, or geographic location; (2) the interrelationships of the symbionts compared with the phylogeny of the host fish, to support or refute the coevolution hypothesis; and (3) the broader phylogenetic affiliations of the symbionts within the luminous bacteria.

Materials and Methods

Bacterial strains

Bacterial strains used in this study are described in Table I. The free-living luminescent strains were grown in complex seawater broth (SWC: Ruby and Nealson, 1978) at 25°C.

Fish collection

Fish were hand-collected by SCUBA divers in the locations shown in Table I. Samples of four species of fish were obtained, including two species (*A. katoptron* and *P. palpebratus*) from two genera collected at the same location in Papua New Guinea. Both specimens of *Photoblepharon* from Papua New Guinea would be identified as *P. palpebratus* on the criteria given by McCosker and Rosenblatt (1986). The two specimens are similar in meristics and overall morphology, but differ in coloration. *P. palpebratus* #1 is dark, has the white area on the opercle characteristic of the species, and the white reflecting scales and fin edgings shared with *P. steinitzi*. *P. palpebratus* #2 is grey, and lacks contrasted white areas on the body and fins (R. H. Rosenblatt, pers. comm.). The *P. steinitzi* specimen was obtained at Eilat, Israel, and is thus virtually certainly *P. steinitzi,* although the specimen is no longer available for positive identification.

DNA preparation

Samples of DNA were prepared from single, entire, fish light organs as in Haygood and Cohn (1986). Total DNA yield per light organ ranged from 5 to 63 μg of DNA. DNA from the other luminous bacterial strains was isolated by the method of Ditta *et al.* (1980). DNA concentration was determined spectrophotometrically by absorbance at 260 nm.

DNA digestion, electrophoresis, and hybridization

DNA samples were digested with the following enzymes: *Hpa*I, *Sca*I, *Bgl*II, *Kpn*I, *Pst*I, *Cla*I, *Hinc*II and *Sph*I for *lux* RFLP analysis; and *Eco*RI, *Bgl*II, *Hind*III and *Nci*I for the 16S rRNA gene comparison. Each digest consisted of about 200 ng of DNA. The digests were separated by 0.8% agarose gel electrophoresis in 40 m*M* Tris acetate/1 m*M* EDTA pH 8.0. The agarose gels were dried at 60°C, denatured, neutralized (Tsao *et al.*, 1983), and prehybridized at 60°C in 6 × SSC (sodium chloride/sodium citrate; Maniatis *et al.*, 1982), 2.5 m*M* EDTA, 200 μg/ml denatured salmon sperm DNA and 0.5 mg/ml dried milk. In previous work, the *K. alfredi* symbiont *lux* region was cloned into pDR720 (Haygood and Cohn, 1986). A 1.73 kb *Hpa*I/*Kpn*I fragment containing *lux*A and half of

Table I

Origins of DNA samples

Bacterial species	Strain	Host	Collection site	Source or reference
Vibrio harveyi	B392	NA	Unknown	Reichelt and Baumann, 1973
Vibrio harveyi	BB7	NA	Sargasso Sea	Belas *et al.*, 1984
Vibrio orientalis #1	ATCC #33933	NA	Yellow Sea	Yang *et al.*, 1983
Vibrio orientalis #2	ATCC #33934	NA	Yellow Sea	Yang *et al.*, 1983
Vibrio fischeri	B61	NA	20°30′ latitude, 157°30′ longitude	Baumann *et al.*, 1971
Vibrio fischeri	MJ1	*Monocentris japonicus*	50 miles southeast of Tokyo, Japan	Ruby and Nealson, 1976
Photobacterium phosphoreum	NZ11D	*Nezumia aequalis*	28°42′N, 13°8′W; 906 to 936 m depth	Ruby and Morin, 1978
NA	NA	*Kyptophanaron alfredi* #1	La Parguera, Puerto Rico	Haygood and Cohn, 1986
NA	NA	*Kryptophanaron alfredi* #16	Roatan, Honduras	This study
NA	NA	*Anomalops katoptron* #1	Port Moresby, Papua New Guinea	This study
NA	NA	*Anomalops kaptoptron* #2	Madang, Papua New Guinea	This study
NA	NA	*Photoblepharon palpebratus* #1	Port Moresby, Papua New Guinea	This study
NA	NA	*Photoblepharon palpebratus* #2	Port Moresby, Papua New Guinea	This study
NA	NA	*Photoblepharon steinitzi*	Eilat, Israel	This study

NA, not applicable.

Table II

Pairwise comparisons of the percentage conserved fragments and the genetic distances (see Materials and Methods) within the lux *gene regions of* Vibrio harveyi *and the anomalopid symbionts*

	Strain				
Strain	*V. harveyi* B392	*A. katoptron* #1	*K. alfredi* #1	*P. palpebratus* #2	*P. steinitzi*
Vibrio harveyi B392		16.0	>17.8	>16.0	>16.8
Anomalops katoptron #1	8.3		>16.8	>14.7	>15.7
Kyptophanaron alfredi #1	<6.5	<7.4		12.0	17.6
Photoblepharon palpebratus #2	<8.3	<10.0	14.8		10.9
P. steinitzi	<7.4	<8.7	6.7	17.4	

The lower values are the percentage of conserved fragments and the upper values the estimated genetic distances (multiplied by 100). In cases where no fragments were conserved, values are listed as being less than the minimum conservation which can be calculated from the total number of observed fragments or greater than the minimum calculable genetic distance.

*lux*B was isolated from the plasmid by 0.8% low melting point agarose electrophoresis. Plasmid pNO1301 (Gourse *et al.*, 1982; Jinks-Robertson *et al.*, 1983) carrying rRNA genes of *Escherichia coli* was digested with *Hind*III, and a 568 bp fragment within the 16S rRNA gene was isolated on a 0.8% low melting point agarose gel. The fragments were cut out of the gel, the gel slices were melted, and this material was used directly with the Pharmacia random priming kit to obtain [a-^{32}P]dCTP labeled probe. Probes were added to each prehybridized gel and incubated for 16 h at 60°C. After hybridization, the gels were washed in 1 × SSC, 0.1% SDS at 60°C, and exposed to X-ray film. Each gel was exposed for several different intervals to ensure the detection of all hybridization fragments. Control experiments indicated that there was no hybridization of the *lux* probe to *E. coli* genomic DNA, or of the *E. coli* 16S probe to flashlight fish genomic DNA under these conditions.

Estimation of sequence divergence

An estimation of sequence divergence (number of nucleotide substitutions per site) was calculated from the fraction of conserved hybridizing fragments for each pair of DNAs (Nei and Li, 1979; Nei, 1987). This estimation is applicable to closely related DNA sequences and is based on the assumption that fragment changes occur due to base substitutions within the restriction sites, rather than to major deletions or rearrangements. The sequence divergence within and surrounding the *lux*A gene was estimated for the four symbiont species and *Vibrio harveyi* by comparing the hybridization patterns obtained from restriction digests hybridized to the *K. alfredi* symbiont *lux* probe. All of the restriction enzymes used in the lux analysis recognized 6 bp; thus the data from all digests were additive and analyzed together (Nei and Li, 1979; Nei, 1987). Divergence within and around the 16S rRNA genes of the symbionts and several strains of free-living luminous bacteria was determined by analysis of common hybridizing fragments to the 568 bp probe. The 16S rRNA data from *Hind*III, *Bgl*II, and *EcoR*I enzyme digestions were additive and were analyzed together; the data from *Nci*I digestion were analyzed separately because *Nci*I recognizes 5 bp rather than 6 (Nei and Li, 1979; Nei, 1987). Data for each enzyme within both analyses were also analyzed individually and compared with the additive data set. When no common hybridizing fragments were observed between a pair, the fraction of conserved hybridizing fragments was given as less than the smallest calculable fraction, and the genetic distance between the pair was given as greater than the maximum calculable distance. All resulting distance matrices were analyzed using the Fitch-Margoliash method to form trees [program FITCH, from the Phylogenetic Inference Package (PHYLIP) version 3.2, by Dr. J. Felsenstein]. Each group of tree files was read by the CONSENSE program (also from PHYLIP), and consensus trees were generated and compared.

Results

Comparison of RFLPs within the luxAB gene region

The percentage of conserved fragments among *V. harveyi* and the various anomalopid symbionts was calculated from pair-wise comparisons of fractions of conserved hybridizing fragments (Table II, lower left). The *K. alfredi* symbiont *lux* probe hybridized to restriction fragments of each of the symbionts, but the hybridization patterns showed little conservation (Fig. 1). In fact, no enzyme of the eight tested produced a hybridization fragment conserved among all of the symbionts. Three of the enzymes (*Bgl*II, *Hinc*II and *Hpa*I) revealed no conserved hybridizing fragments between the symbionts, or between any symbiont and *V. harveyi* B392. The *Photoblepharon palpebratus* and *P. steinitzi* symbionts (P. p. #1 and P. s. #1)

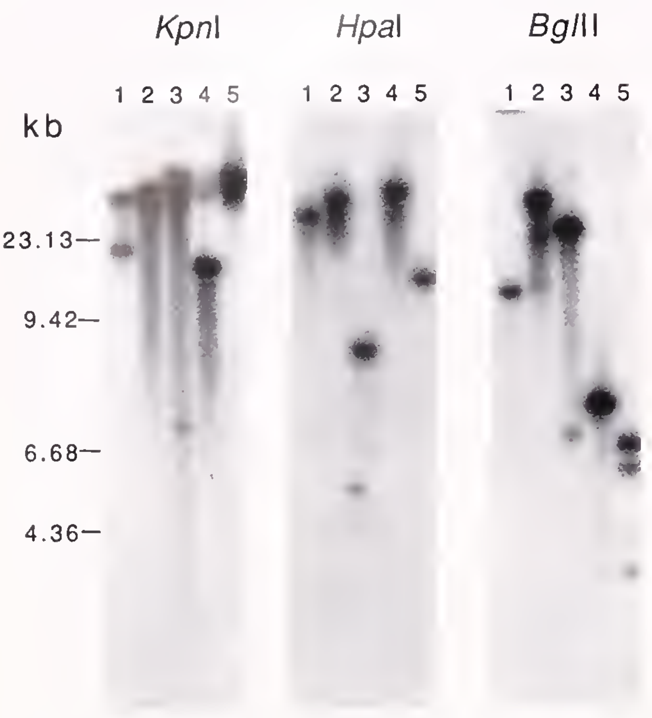

Figure 1. Autoradiogram obtained from hybridization of the ^{32}P-labeled 1.73 kb *lux* probe to DNA extracted from *Vibrio harveyi* B392 (1) and the light organs of *Anomalops katoptron* #1 (2), *Kryptophanaron alfredi* #1 (3), *Photoblepharon palpebratus* #2 (4), and *Photoblepharon steinitzi* (5). DNA was digested with *Kpn*I, *Hpa*I and *Bgl*II.

are most similar, with a distance of 0.109. The *A. katoptron* specimen has no conserved hybridizing fragments with any of the other anomalopid symbionts; thus the calculated distances are underestimates of an unknown distance. The divergence (d) among symbionts and between symbionts and *V. harveyi* ranges from 0.109 to >0.178 when calculated with Nei and Li's method (Table II, upper right). Values for *d* have been multiplied by 100 in Table II, to facilitate easy visual comparison. The consensus tree is shown in Figure 2.

Comparison of RFLPs detected by the 16S rRNA gene probe

In DNA digests of every bacterial strain tested, the 568 bp 16S rRNA gene probe hybridized with between 1 and 12 restriction fragments generated by enzymes with six-base-pair recognition sequences (Fig. 3). Digestion of the *V. harveyi* strains generated the highest number of hybridizing fragments (~9/digest), while digestion of the symbiont DNAs, particularly from *Anomalops* and *Kryptophanaron*, resulted in fewer hybridizing fragments (~2/digest). In both the *lux* and 16S comparisons, the number of hybridizing fragments indicates that a single symbiont inhabits each light organ or that any additional symbionts are present at undetectable levels. The number of hybridizing fragments in the *lux* comparisons are consistent with the presence of a single copy of the *lux* genes, in both the symbionts and the culturable strain. In the 16S comparisons, the low number of symbiont fragments indicates that a mixed symbiont culture is unlikely. As shown by the fractions of conserved hybridizing fragments (Table III, lower left), the 16S probe generally yielded a higher number of conserved fragments than the *lux* probe. Distances calculated from hybridization patterns among culturable species range from 0.062 to 0.216, with a mean of 0.113 ± 0.040 (the standard deviation was calculated from values in Table III). As in Table II, the *d* values shown in Table III have been multiplied by 100 to ease visual comparison. The symbionts differ from the culturable species with distances ranging from 0.099 to >0.180. Distances among symbionts from fish of different genera range from >0.117 to >0.151, contrasting strongly with the level of difference seen between strains of culturable species (0.029 ± 0.021). Thus, the symbionts in this family do not appear to be members of a single species.

In two instances, a strain-level relationship was seen between symbionts. The two specimens of *A. katoptron* were indistinguishable, and distance values for symbiont DNAs from *P. steinitzi* and *P. palpebratus* #1 are also close, with a calculated distance of 0.023. Thus, because these values are within the range that we have seen when comparing strains of the same species of *Vibrio* (Table III), these two symbiont strains should be considered as

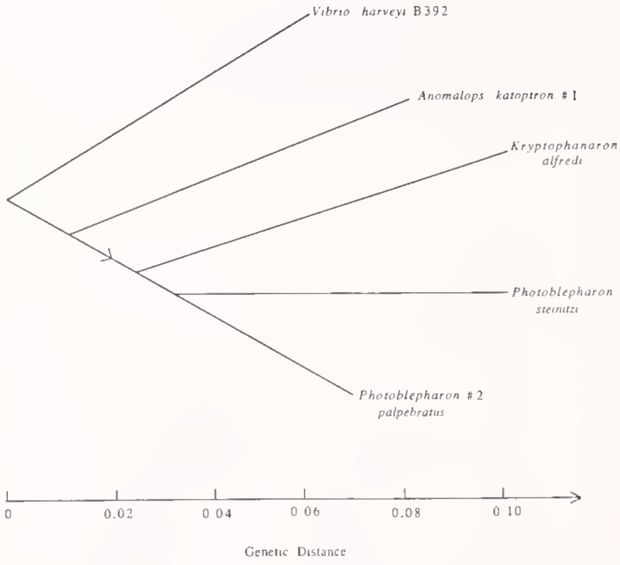

Figure 2. Phylogenetic tree for anomalopid symbiont strains and *Vibrio harveyi* constructed from the *lux* region genetic distance data in Table II. The tree is a majority rule consensus tree derived from the CONSENSE program of PHYLIP (see Materials and Methods). Branch lengths were obtained from the data in Table II using the FITCH program of PHYLIP. The arrow indicates that the following branch lengths are minimum estimates; there were few or no conserved hybridizing fragments between this group of strains and the others compared.

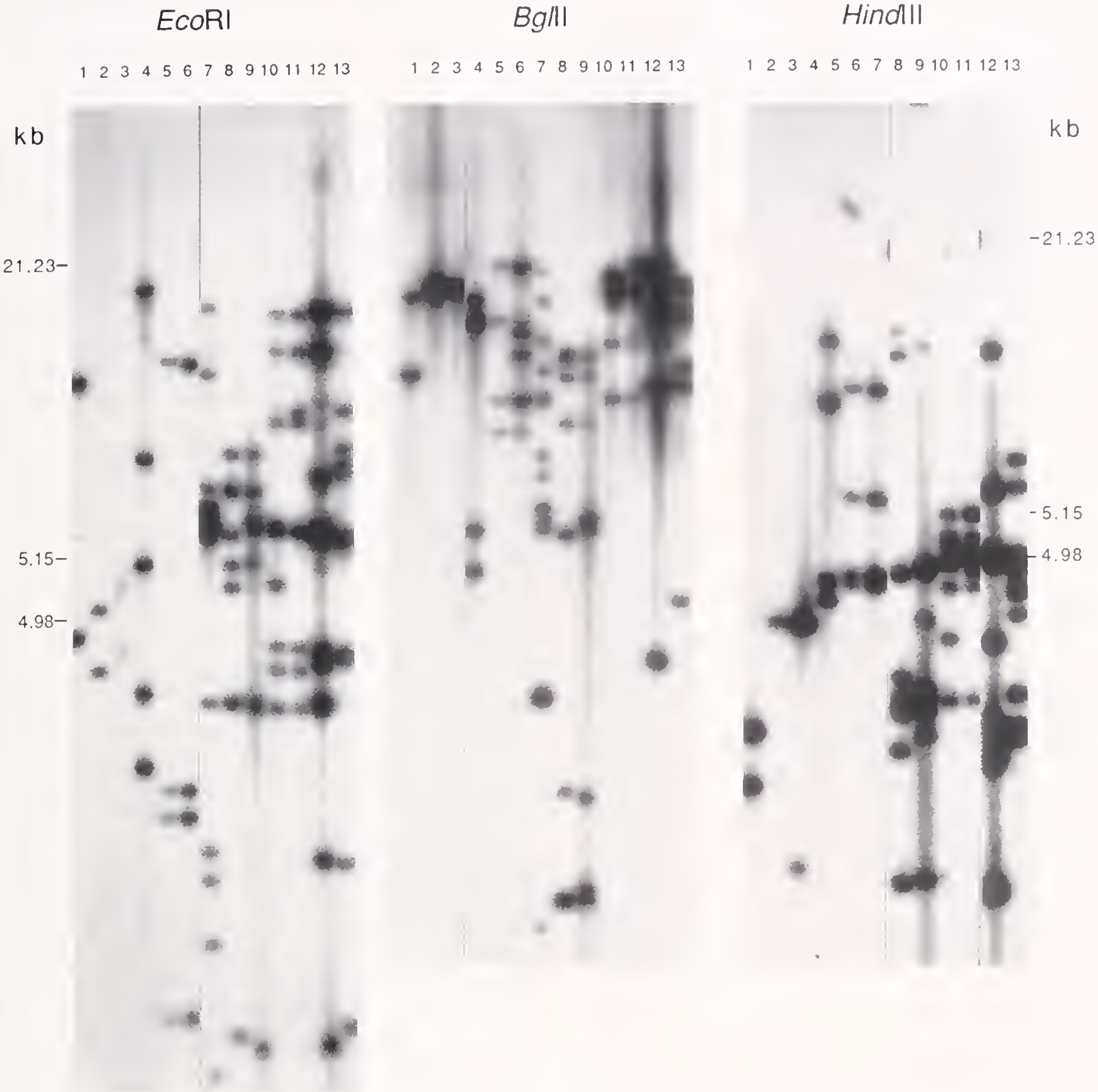

Figure 3. Autoradiogram obtained from hybridization of the ^{32}P-labeled 16S rRNA gene probe to DNA extracted from the light organs of *Kryptophanaron alfredi* #16 (1), *Anomalops katoptron* #2 (2), *Anomalops katoptron* #1 (3), *Photoblepharon palpebratus* #2 (4), *Photoblepharon palpebratus* #1 (5), *Photoblepharon steinitzi* (6), and from laboratory cultures of *Vibrio fischeri* B61 (7), *Vibrio fischeri* MJ1 (8), *Vibrio orientalis* #2 (9), *Vibrio orientalis* #1 (10), *Vibrio harveyi* BB7 (11), and *Vibrio harveyi* B392 (12). DNA was digested with *Eco*RI, *Bgl*II and *Hind*III. Molecular weight markers are the same for both *Eco*RI and *Bgl*II.

belonging to the same species. All of the *Photoblepharon* symbionts (P. p. #1, P. p. #2, and P. s. #1) are more similar to each other than to *K. alfredi* and *A. katoptron*. However, two samples from different individuals of *P. palpebratus* (P. p. #1 and P. p. #2) collected in the same geographic location showed considerable differences in their restriction patterns. Moreover, one *P. palpebratus* sample (P. p. #1) is more closely related to the sample of *P. steinitzi* than to the other *P. palpebratus* sample (P. p. #2). The degree of difference between the symbionts of the *P. palpebratus* specimens is even more anomalous when compared to the total conservation of restriction fragments from the DNA of two *Anomalops* specimens from different geographic locations. The possibility of inadvertent exchange of samples was investigated and it does not appear to have occurred; the experiments were repeated with

Table III

Pairwise comparisons of the percentage conservation and the genetic distances (see Materials and Methods) between the 16S rRNA gene regions of the anomalopid symbionts and several strains of free-living luminescent bacteria

Strain	Strains V. harveyi B392	V. harveyi BB7	V. orientalis #1	V. orientalis #2	V. fischeri MJ1	V. fischeri B61	P. steinitzi	P. palpebratus #1	P. palpebratus #2	A. katoptron #1 & #2	K. alfredi #16	P. phosphoreum NZ11D
Vibrio harveyi B392		4.5	7.5	7.6	10.5	21.6	15.2	15.1	15.4	14.2	18.9	13.6
V. harveyi BB7	46.4		6.9	6.2	11.5	16.0	11.7	14.3	19.7	18.3	>18.0	11.0
V. orientalis #1	29.2	31.8		0.5	12.2	11.9	10.2	9.9	13.1	11.5	16.0	8.3
V. orientalis #2	28.6	35.6	91.9		12.4	14.9	10.4	10.2	18.3	16.6	16.3	8.5
V. fischeri MJ1	18.5	16.0	14.3	14.0		3.8	19.1	18.9	14.3	17.8	12.7	8.0
V. fischeri B61	3.9	8.3	15.0	9.8	52.2		13.8	18.5	18.9	>17.3	12.2	15.2
Photoblepharon steinitzi	9.3	15.4	19.4	18.8	5.4	11.4		2.3	16.8	>14.7	>14.3	18.5
P. palpebratus #1	9.5	10.5	20.0	19.4	5.6	5.9	96.0		16.6	>14.3	>14.0	18.3
P. palpebratus #2	9.1	5.0	12.5	6.1	10.5	5.6	7.4	7.7		>15.1	14.7	13.8
Anomalops katoptron #1	10.8	6.1	16.0	7.7	6.5	<6.9	<10.0	<10.5	<9.5		>11.7	>17.1
A. katoptron #2	10.8	6.1	16.0	7.7	6.5	<6.9	<10.0	<10.5	<9.5		>11.7	>17.1
Kryptophanaron alfredi #16	5.6	<6.3	8.3	8.0	13.3	14.3	<10.5	<11.1	10.0	<15.4		16.8
P. phosphoreum	11.8	17.0	25.6	25.0	26.7	9.3	5.9	6.1	11.4	<7.1	7.4	

The lower values are the percentage conserved fragments and the upper the estimated genetic distances (multiplied by 100) from the combined data obtained from *Eco*RI, *Bgl*II and *Hind*III with the 16S rRNA gene probe. In cases where no fragments were conserved, values are listed as less than the minimum conservation which can be calculated from the total number of observed fragments or greater than the maximum calculable genetic distance.

identical results. The consensus tree generated is shown in Figure 4.

Discussion

Our data indicate that the bacterial symbionts differ dramatically within the family Anomalopidae. Based on RFLP analysis within the *lux* gene region, the symbionts from different genera are almost as different from one another as the *Kryptophanaron* symbiont is from *V. harveyi*. Comparison of the symbiont restriction patterns with those of known species of luminous bacteria within the 16S rRNA gene region strongly supports the conclusion, drawn from the *lux* data, that the symbionts differ at greater than strain level between genera within the family Anomalopidae.

In other light organ symbioses, in which the symbionts have been cultured, all members of the fish family contain the same bacterial species. RFLP analysis supports this assertion for *Photobacterium phosphoreum*, a bacterial species that inhabits light organs of several families of fishes. The genetic distances between three strains of *P. phosphoreum* from two species of opisthoproctid fishes (*Opisthoproctus grimaldii* and *Opisthoproctus soleatus*) and *P. phosphoreum* NZ11D, a symbiont from a macrourid fish, were determined using the same 16S RFLP analysis method, and ranged from 0.002 to 0.006 (data not shown). The small genetic distances observed for the opisthoproctid symbionts contrast greatly with the large differences observed among the anomalopid symbionts.

Clearly, the anomalopids do not appear to host a single species. Symbionts from different anomalopid genera differ at least as much as species of culturable luminous bacteria. In the 16S rRNA analysis, the observed distances between the anomalopid symbionts are considerably greater than the distance between *V. harveyi* and *V. orientalis*, approaching the distance between *V. harveyi* and *V. fischeri*, two highly divergent members of the genus *Vibrio* (Baumann *et al.*, 1980). In contrast, there is a high level of conservation among strains of characterized *Vibrio* species, even among the free-living and monocentrid symbiont strains of *V. fischeri* from different locations (strains B61 and MJ1, Table I and Fig. 4).

Within the anomalopid family, equivalent strain levels of similarity are found only within genera, in two of the three samples from the genus *Photoblepharon* (P. p. #1 and P. s. #1) and the samples from different specimens of *A. katoptron*. In addition, we recently collected several specimens of *Kryptophanaron alfredi* from Roatan, Honduras, and compared five light organ samples, using the 16S probe and the same restriction enzymes previously used in this study. The specimens were indistinguishable, with all fragments conserved. Thus, although we do not have additional samples of each fish species within the anomalopid family, it seems likely that symbionts within

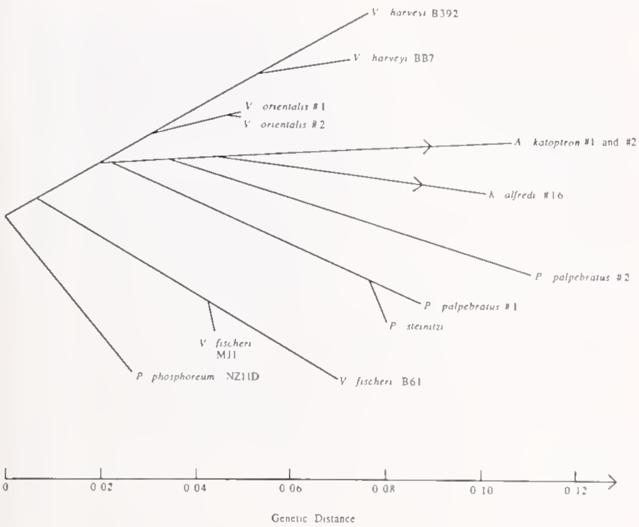

Figure 4. Phylogenetic tree for anomalopid symbionts and several free-living luminous bacteria constructed from the 16S rRNA gene region genetic distance data in Table III. The tree is a majority rule consensus tree derived from the CONSENSE program of PHYLIP. Branch lengths were obtained from the data in Table III using the FITCH program of PHYLIP. Arrows on two of the branches indicate that the branch lengths are minimum estimates; there were few or no conserved hybridizing fragments between these strains and the others compared.

each host species comprise a single species. The anomalous result with *P. palpebratus* #2 is discussed below.

The observed diversity among symbionts within the family Anomalopidae is not associated with geographical location, and this might be expected if the symbionts engage in genetic exchange with bacterial populations in the environment. DNA from specimens of *P. palpebratus* and *A. katoptron* collected from the same location in Papua New Guinea are no more similar to each other than each is to the *K. alfredi* symbiont from the Caribbean. In fact, they are considerably less similar than the symbionts from Photoblepharon specimens from the Red Sea and Papua New Guinea (P. p. #1 and P. s. #1). In addition, symbionts from two samples of *A. katoptron*, collected from different locations in Papua New Guinea (~800 miles apart) appear identical within the 16S rRNA gene region. Thus, the genetic similarity of symbionts seems to correlate more with host phylogeny than geographic location.

Precise comparisons of the symbiont branching order to the proposed evolutionary history of the host fish are difficult because the branch lengths are very rough estimates. However, the branching order, is similar in both analyses and is consistent with that of the fish host (Johnson and Rosenblatt, 1988). These highly conservative estimates of distance indicate that the *Anomalops* symbiont differs from the other symbionts at the specific, and possibly the generic, level. *Anomalops* is very different from the other genera in the family Anomalopidae and is thought to have diverged from the ancestral lineage at least 60 million years before the divergence of *Kryptophanaron* and *Photoblepharon* (<5 million years ago). The *Kryptophanaron* symbiont also differs from the *Photoblepharon* symbionts, but does share some conserved hybridizing fragments with *Photoblepharon* symbionts in both the *lux* and rRNA analyses. These data suggest that the symbionts may have coevolved with the host fish. However, the divergence between the two *P. palpebratus* samples raises the possibility that the apparent correspondence between symbiont and host trees could disappear when more samples are examined; *i.e.*, that extreme divergence may occur in symbionts within host species as well as between host genera. However, this hypothesis is not supported by the identity observed between the two *Anomalops* samples from different locations, the similarity of *P. palpebratus* #1 and *P. steinitzi*, and our comparison of five *K. alfredi* samples. Equally likely alternatives are that (1) the genus *Photoblepharon* is more complex than current systematics would suggest, and that more than one type of *Photoblepharon* may occur at our collection site (see Materials and Methods) or (2) a gene rearrangement in the *P. palpebratus* #2 symbiont relative to the other anomalopid symbionts could give an overestimate of genetic distance. Unfortunately, the additional specimens needed to resolve this anomaly are not currently available and will be difficult to obtain. Further study of both the systematics of *Photoblepharon* and the genetic relatedness of the symbionts is required.

Another interesting aspect of the 16S rRNA RFLP analysis is the variation in number of hybridizing restriction fragments between symbiont and free-living bacterial DNA. In all cases, the symbionts show fewer hybridizing fragments to the 16S probe than the free-living strains. The low number of hybridizing fragments revealed in this study suggests the presence of a bacterial monoculture in the light organ. In addition, these data could indicate a difference in copy number of the rRNA genes; *i.e.*, the symbionts have a lower number of operons than the free-living luminescent strains. Similar studies on pea-aphid endosymbionts revealed that the endosymbionts have only a single copy of the rRNA operon, while related free-living organisms have several (Unterman and Baumann, 1990). Restriction fragment analyses of mycobacteria 1 DNA have shown that the number of rRNA copies correlates with growth rate, *i.e.*, slow growing species have fewer copies of the rRNA operon than those growing more rapidly (Bercovier *et al.*, 1986; Suzuki *et al.*, 1987). Previous studies of anomalopids suggested that symbionts in the light organ have slow growth rates [doubling times of 8–23 hours; (Haygood *et al.*, 1984)]. A reduced rRNA operon copy number in the anomalopid symbionts may represent a permanent adaptation to light organ conditions, such that the growth rate is inherently low in the anomalopid symbionts.

The taxonomic identity of the anomalopid symbionts remains unknown. None of the luminous species included in the 16S rRNA region analysis appear to be the same species as the symbionts, which fall somewhere between *V. orientalis* and *V. fischeri*. The 16S rRNA region analysis suggests that the symbionts are more closely related to *V. orientalis* than to *V. harveyi*. *Lux*A nucleotide sequence data for *V. harveyi*, *V. fischeri*, and the *Kryptophanaron alfredi* symbiont reveal a closer relationship between *V. harveyi* and the *K. alfredi* symbiont (75% identity) than between the symbiont and *V. fischeri* [63% (Haygood, 1990)]. This relationship is not observed in the 16S data, which indicate that the symbionts are equally related to both *V. harveyi* and *V. fischeri*. This discrepancy could indicate that the similarity of the symbiont with *V. harveyi* is found only within the *lux* region and is not distinguishable at the rRNA level.

The RFLP approach has some limitations, due to errors in the estimation of distance. These errors result from small, undetected fragments, or fragments of slightly different lengths, that are indistinguishable at the level of gel electrophoresis. The major virtue of the RFLP approach is that many samples can be analyzed directly and simultaneously. The calculations of genetic distance are based on assumptions about the substitution rate and frequency of the four nucleotides within a sequence (Nei, 1987). The errors in these assumptions are negligible when the estimated nucleotide substitution (d) is small [>0.1; (Nei, 1987)], but have an increasingly large effect as d increases, resulting in an underestimation of the distances and a corresponding decrease in accuracy. The distances between the symbionts in this study are large, approaching, and in some cases exceeding, the upper limit of accuracy for this method.

Differences in copy number are also a problem in the 16S RFLP analysis, because these differences represent differences in genome organization rather than actual sequence divergence. Including all fragments in an analysis between two samples with different copy numbers will overestimate the calculated divergence by inflating the denominator in the fraction of conserved hybridizing fragments. There is no valid way to normalize the data, but to test the robustness of our conclusions, we attempted a conservative compensation for copy number discrepancies by recalculating divergence with the denominator normalized to the smallest number of fragments in each sample pair. The values obtained by these calculations should be the lowest possible estimates of divergence within each pair. Using this method of estimation, the intergeneric divergences among the symbionts are not significantly changed [ranging from 0.112 to >0.122 (corrected) *versus* >0.117 to >0.151 (presented in Table III)] and still correspond to species level differences among the characterized specimens.

The number of symbiont samples examined in this study is sub-optimal, due to the difficulty and expense involved in obtaining specimens, but we have attempted to compensate for the small sample size. The large intergeneric differences among the anomalopid symbionts is supported by 17 independent comparisons, *i.e.*, each symbiont sample compared to each sample from a different fish genus. Even if *P. palpebratus* #2 were excluded due to a possible gene rearrangement, there are still 15 independent comparisons in support of our conclusion.

Despite the limitations of the analysis, several conclusions can be drawn. First, the symbionts are obviously not the same species in all members of the family Anomalopidae. The differences are so extreme that even the largest possible estimates of variance cannot obscure them. This result stands in distinct contrast to all those symbioses in other fish light organs in which symbiont identity has been studied. In addition, no geographical connection between host location and symbiont species is apparent, implying that no significant genetic exchange occurs between symbionts from different hosts via free-living populations. Furthermore, the symbiont branching order is consistent with the proposed sequence of evolution within the family Anomalopidae. Thus, at this level of analysis, the symbionts appear to have coevolved with the host fish. The large difference between *P. palpebratus* #1 and #2 could be due to a rearrangement or unrecognized difference in the host fishes. Finally, the apparent low copy number of the 16S rRNA operon in the symbionts may represent genetic adaptation to the light organ environment. In any case, the symbiont divergence observed in the association between these luminescent bacteria and the anomalopid fishes appears to be novel among previously characterized light organ symbioses.

Acknowledgments

We thank A. C. Arneson and the Department of Marine Sciences of the University of Puerto Rico for assistance in collecting *K. alfredi*, A. C. Arneson and P. Colin for the *A. katoptron* and *P. palpebratus* specimens, and the staff of the H. Steinitz Marine Biological Laboratory, Eilat, Israel, for the *P. steinitzi* sample. We are grateful to Dr. G. Wilson for help in obtaining and running the computer programs, and Dr. R. Rosson and B. Tebo for their helpful suggestions. We also thank Dr. R. Rosenblatt for his identification of the *Photoblepharon* specimens and critical reading of the manuscript. Thanks are also due to M. P. Quaranta for help in writing the distance estimation program. This research was funded by the Office of Naval Research, grant no. N00014-89-J-1742.

Literature Cited

Baumann, P., L. Baumann, S. S. Bang, and M. J. Woolkalis. 1980. Reevaluation of the taxonomy of *Vibrio*, *Beneckea*, and photobacterium: abolition of the genus *Beneckea*. *Curr. Microbiol.* **4:** 127–132.

Baumann, P., L. Baumann, and M. Mandel. 1971. Taxonomy of marine bacteria: the genus *Benecka*. *J. Bacteriol.* **107**(1): 268–294.

Belas, R., A. Mileham, M. Simon, and M. Silverman, 1984. Transposon mutagenesis of Marine *Vibrio* spp. *J. Bacteriol.* **158**(3): 890–896.

Bercovier, H., O. Kafri, and S. Sela. 1986. Mycobacteria possess a surprisingly small number of ribosomal RNA genes in relation to the size of their genome. *Biochem. Biophys. Res. Comm.* **136**(3): 1136–1141.

De Buyser, M. L., A. Morvan, F. Grimont, and N. El Solh. 1989. Characterization of *Staphylococcus* species by ribosomal RNA gene restriction patterns. *J. Gen. Microbiol.* **135:** 989–999.

Denny T., M. N. Gilmour, and R. K. Selander. 1988. Genetic diversity and relationships of two pathovars of *Pseudomonas syringae*. *J. Gen. Microbiol.* **134:** 1949–1960.

Ditta, G., S. Stanfield, D. Corgin, and D. R. Helinski. 1980. Broad host-range DNA cloning system for Gram-negative bacteria: construction of a gene bank of *Rhizobium meliloti*. *Proc. Natl. Acad Sci. USA* **77:** 7347–7357.

Fitzgerald, J. M. 1977. Classification of luminous bacteria from the light organ of the Australian pinecone fish. *Cleidopus gloriamaris*. *Arch. Microbiol.* **112:** 153–156.

Franche, C., and G. Cohen-Bazire. 1987. Evolutionary divergence in the *nif* H.D.K. gene region among nine symbiotic *Anabaena azollae* and between *Anabaena azollae* and some free-living heterocystous cyanobacteria. *Symbiosis* **3:** 159–178.

Gottlieb, P., and R. Rudner. 1985. Restriction site polymorphism of ribosomal ribonucleic acid gene sets in members of the genus *Bacillus*. *Int. J. Sys. Bact.* **35**(3): 244–252.

Gourse, R. L., M. J. R. Stark, and A. E. Dalhberg. 1982. Site-directed mutagenesis of ribosomal RNA: construction and characterization of deletion mutants. *J. Mol. Biol.* **159:** 397–416.

Grimont, F., and P. A. D. Grimont. 1986. Ribosomal ribonucleic acid gene restriction patterns as potential taxonomic tools. *Ann. Inst. Pasteur/Microbiol.* **137 B:** 165–175.

Haygood, M. G. 1990. Relationship of the luminous bacterial symbiont of the Caribbean flashlight fish, *Kryptophanaron alfredi* (family Anomalopidae) to other luminous bacteria based on bacterial luciferase (luxA) genes. *Arch. Microbiol.* **154:** 496–503.

Haygood, M. G., and D. H. Cohn. 1986. Luciferase genes cloned from the unculturable luminous bacteriod symbiont of the Caribbean flashlight fish, *Kryptophanaron alfredi*. *Gene* **45:** 203–209.

Haygood, M. G., B. M. Tebo, and K. H. Nealson. 1984. Luminous bacteria of a monocentrid fish (*Monocentris japonicus*) and two anomalopid fishes (*Photoblepharon palpebratus* and *Kryptophanaron alfredi*): population sizes and growth within the light organs, and rates of release into the seawater. *Mar. Biol.* **78:** 249–254.

Jinks-Robertson, S., R. Gourse, and M. Nomura. 1983. Expression of rRNA and tRNA genes in *Escherichia coli:* evidence for feedback regulation by products of rRNA operons. *Cell* **33:** 865–876.

Johnson, G. D., and R. H. Rosenblatt. 1988. Mechanisms of light organ occlusion in flashlight fishes, family Anomalopidae (Teleotei: Beryciformes), and the evolution of the group. *Ann. Linnean Soc. Lond.* **94:** 65–96.

Kessel, M. 1977. The ultrastructure of the relationship between the luminous organ of the teleost fish *Photoblepharon palpebrartus* and its symbiotic bacteria. *Cytobiologie* **15:** 145–158.

Leis, J. M., and S. Bullock. 1986. The luminous cardinalfish *Siphamia* (Pisces, Apogonidae): Development of larvae and the luminous organ. Pp. 703–714 in *Indo-Pacific Fish Biology: Proceedings of the Second International Conference on Indo-Pacific Fishes*, R. A. T. Uyeno, T. Taniuchi, and K. Matsuura, eds. Ichthyological Society of Japan, Tokyo.

Leisman, G., D. H. Cohn, and K. H. Nealson. 1980. Bacterial origin of luminescence in marine animals. *Science* **208:** 1271–1273.

Lindblad, P., R. Haselkorn, B. Bergman, and S. A. Nierzwicki-Bauer. 1989. Comparison of DNA restriction fragment length polymorphisms of *Nostoc* strains in and from cycads. *Arch. Microbiol.* **152:** 20–24.

Maniatis, T., E. F. Fritsch, and J. Sambrook. 1982. *Molecular Cloning (A Laboratory Manual).* Cold Spring Harbor Laboratory, New York. P. 447.

McCosker, J. E., and R. H. Rosenblatt. 1986. Notes of the biology, taxonomy, and distribution of flashlight fishes (Beryciformes: Anomalopidae). *Japn. J. Ichthyol.* **34**(2): 157–163.

Nei, M. 1987. *Molecular Evolutionary Biology.* Columbia University Press, New York. Pp. 106–107.

Nei, M., and W. Li. 1979. Mathematical model for studying genetic variation in terms of restriction endonucleases. *Proc. Natl. Acad Sci. USA* **76**(10): 5269–5273.

Reichelt, J. L., and P. Baumann. 1973. Taxonomy of the marine, luminous bacteria. *Arch. Mikrobiol.* **94:** 283–330.

Reichelt, J. L., K. Nealson, and J. W. Hastings. 1977. The specificity of symbiosis: pony fish and luminescent bacteria. *Arch. Microbiol.* **112:** 157–161.

Ruby, E. G., and K. H. Nealson. 1976. Symbiotic association of *Photobacterium fischeri* with the marine luminous fish *Monocentris japonica:* a model of symbiosis based on bacterial studies. *Biol. Bull.* **151:** 574–586.

Ruby, E. G., and K. H. Nealson. 1978. Seasonal changes in the species composition of luminous bacteria in nearshore seawater. *Limnol. Oceanogr.* **23**(3): 530–533.

Ruby, E. G., and J. G. Morin. 1978. Specificity of symbiosis between deep-sea fishes and psychotrophic luminous bacteria. *Deep-Sea Res.* **25:** 161–167.

Saunders, N. A., T. G. Harrison, N. Kachwalla, and A. G. Taylor. 1988. Identification of species of the genus *Legionella* using a cloned rRNA gene from *Legionella pneumophila*. *J. Gen. Microbiol.* **134:** 2363–2374.

Stanley, J., G. G. Brown, and D. P. S. Verma. 1985. Slow-growing *Rhizobium japonicum* comprises two highly divergent symbiotic types. *J. Bacteriol.* **163**(1): 148–154.

Stull, T. L., J. J. LiPuma, and T. D. Edlind. 1988. A broad-spectrum probe for molecular epidemiology of bacteria: ribosomal RNA. *J. Infect. Dis.* **157**(2): 280–286.

Suzuki, Y., T. Mari, Y. Miyata, and T. Yamada. 1987. The number of ribosomal RNA genes in *Mycobacterium lepraemurium*. *FEBS Lett.* **44:** 73–76.

Tsao, S. G. S., C. F. Brunk, and R. E. Pearlman. 1983. Hybridization of nucleic acids directly in agarose gels. *Anal. Biochem.* **131:** 365–372.

Unterman, B. M., and P. Baumann. 1990. Partial characterization of the ribosomal RNA operons of the pea-aphid endosymbionts: evolutionary and physiological implications. Pp. 329–350 in *Aphid-Plant Genotype Interactions*, R. K. Campbell and R. D. Eikenbary, eds. Elsevier Press, New York.

Wei, S. L., and R. E. Young. 1989. Development of symbiotic bacterial bioluminescence in a nearshore cephalopod, *Euprymna scolopes*. *Mar. Biol.* **103:** 541–546.

Yang, Y., L. Yeh, Y. Cao, L. Baumann, P. Baumann, J. Sung-en Tang, and B. Beaman. 1983. Characterization of marine luminous bacteria isolated off the coast of China and description of *Vibrio orientalis* sp. nov. *Curr. Microbiol.* **8:** 95–100.

Reference: *Biol. Bull.* **181:** 144–157. (August, 1991)

Fine Structure of Photophores in *Gonostoma elongatum:* Detail of a Dual Gland Complex

D. EUGENE COPELAND

Marine Biological Laboratory, Woods Hole, Massachusetts 02543

Abstract. *Gonostoma elongatum* Gunther 1878 is a mesopelagic fish that has numerous light-bearing organs (the photophores). Some of the photophores are unusual in that they incorporate two different glands: glands D and V. These dual gland photophores are found: (1) in the upper serial row on the body, (2) among the suborbital photophores, and (3) in the caudal photophores. In a ventral serial row of photophores, each organ possesses one gland only: gland D. Glands D and V in the upper serial photophores have secretory ducts that fuse to form a common duct that empties to the surface. Gland D, which produces a bluish light, has dioptric material that could provide both spectral reflection and filter transmission. Gland V also has dioptric material associated with it. The entire glandular complex is covered by a shield of alternately layered collagen, which has a lens-like bulge over gland D. Immediately beneath the shield are slanted, overlapping rows of dioptric material. The detailed morphology of the dual gland photophore in the upper serial row is presented and briefly compared to some of the other photophores on the fish. Noteworthy are the various arrangements of materials that can efficiently guide the light from gland D and, possibly, from gland V. The result would be a diffuse glow suitable for counter illumination.

Introduction

Throughout the oceans there is a large population of mesopelagic fishes, the so-called midwater fishes. The term "midwater" is somewhat misleading in that, even in the deepest of oceans, the average habitat depth is within the range of 300 to 1500 meters, and at night some of the fish migrate to the surface. The primary concentration is usually associated with a thermocline marking the junction of warm, actively mixed surface water and the colder, less active deeper waters. The specific gravity difference at that interface permits trapping of material that provides an ecological niche.

One very interesting adaptation of mesopelagic fishes to the darkness of their habitat is the presence of photophores (bioluminescent organs). The photophores are usually distributed in a characteristic order over the body, so much so that the pattern can be used for taxonomic identification (Grey, 1964). The anatomical morphology of the photophores ranges from the huge, complex organs in *Argyropelecus* to the simple skin photophores of *Chauliodus* (Bassott, 1966; Herring and Morin, 1978).

Gonostoma elongatum is a relatively large mesopelagic fish that possesses many of the various types of photophores, such as lateral serial, orbital, opercular, branchiostegal, and caudal (sternchase). Representative photophores from the upper lateral serial row were chosen for study.

Attention was drawn to the upper serial photophores because each has two parts, a dorsal spherical unit and a closely associated ventral unit, plate-like, silvery, and reflective. The upper unit is accepted as a glandular photophore in the usual sense and used for taxonomic purposes (Grey, 1964; Badcock, 1984), but there is no general agreement as to the nature of the lower unit. One of the first to describe it was Brauer (1908) who called it a "sack formigen Organ." In the more recent literature, it is referred to as "glandular" (Grey, 1964, and Badcock, 1984). I find no cytological descriptions of the lower gland or estimates as to its function.

Buck (1978) and Young (1983) provide extensive discussion of bioluminescence as linked to counterillumination, species and sex recognition, searchlights, lures, flashes or clouds to distract predators, and so forth. Clarke (1963) observed that most photophores in fish provide a

Received 24 April 1990; accepted 8 April 1991.

light nearly matching the blue spectral value (478 nm) of residual down-dwelling light from the ocean surface. Thus, the light from the photophores could "camouflage" the fish from the sight of predators, and especially from below. This possibility is described in some detail by McAllister (1967), Herring (1982), and Denton *et al.* (1985). Details as to the spectral values of photophore light, as compared to those of the environment at oceanic depths, are provided by Denton and Herring (1978) and Herring (1984). Evidence that fish can adjust the strength of their photophore emissions to match the intensity of down-dwelling light is provided by Case *et al.* (1977), Lawry (1974), and Young and Roper (1977). As an additional comment about spectral values and their ecological import, it should be noted that the eyes of deep sea fishes have a chrysopin pigment that absorbs maximally at about 480 nm, virtually the same as the down-dwelling light and that of the photophores (see discussion by Nicol, 1989).

Gonostoma might be an exceptional fish, in that Swift *et al.* (1977) have reported a photophore spectral value of 503 nm for it, but this observation of *Gonostoma* was based on a single photophore on a single specimen that was so badly damaged the species could not be identified with certainty. More significantly, Swift *et al.* used an early spectrometric system requiring slow point by point measurement, which could lead to uncertainty. The observation need not be discarded, but it should always be qualified. Widder *et al.* (1983) used the more sophisticated optical multichannel analyzer (OMA) and surveyed spectral values emitted by some 70 marine species; the values mostly ranged from 470 to 480 nm.

This article describes in detail the histological and cytological morphology of the two units in the upper serial row of photophores in *G. elongatum* and the connection between the two. Also of note is the associated array of dioptric tissues that may guide light emission. Brief comparisons are made between the upper serial photophore and three others in the same fish: lower serial, suborbital, and caudal photophores.

Materials and Methods

The largest collections of *Gonostoma elongatum* were made on two cruises: the Woods Hole Oceanographic Institute (WHOI) RV Knorr cruise #118-4 on a transect from San Juan, Puerto Rico, to Woods Hole, Massachusetts; and the WHOI RV Oceanus cruise #183. On both trips, a 10-ft.[2] MocNess midwater trawl was used, and the best collections were made near the outer edge of the continental shelf in the general area of the Hudson Canyon or slightly south thereof. On other trips, few random *G. elongatum* individuals were otherwise collected by using less efficient meter nets. Estimated collection depth ranged from 350 to 900 meters. The specimens were between 150 and 225 mm in length.

The retrieved fish were moribund by the time they reached the decks (hearts fibrillating and weak reflexes), but showed little trauma compared to others, such as *Benthosema*. Air emboli in the circulatory systems was a probable cause of morbidity. Whole fish were fixed immediately after retrieval by total immersion in cold 3% glutaraldehyde buffered to 7.4 pH with 0.1 *M* sodium cacodylate at refrigerator temperature (*ca.* 4.0°C). Specimens were stored in a refrigerator, and the fixative was replaced with fresh fixative after about 12 h. After 2–3 days, the fish were finally stored in 1% glutaraldehyde in 0.1 *M* cacodylate. Dissection of photophores, post osmication, and embedment in epoxy resin of tissues for future study were made shortly after returning to port.

Thick (1 micron) epoxy sections for light microscopy were stained with methylene blue-azure II. The light micrographs in Figures 3, 11, 15, and 17 were made with a Zeiss Axiophot microscope. Thin sections for electron microscopy were stained with uranyl acetate, followed by Reynolds lead citrate, and were studied with a Zeiss 10 electron microscope.

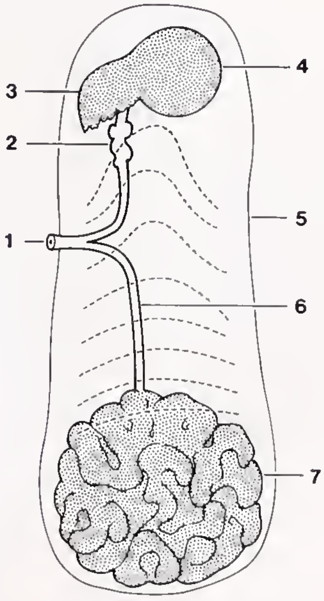

1

Figure 1. Diagram of an entire photophore complex [from the upper serial row (OA)] as viewed through the surface of the fish. (1) Joint secretory duct orifice to external surface. (2) Secretory duct of gland D with attached clusters of secretory cells. (3) Lateral hemispheric canopy of gland D. (4) Gland D. (5) Transparent collagen covering shield. (6) Secretory duct of gland V. (7) Gland V. Dashed lines indicate the pattern of overlapping rows of dioptric material (see Fig. 17) that lie immediately under the shield.

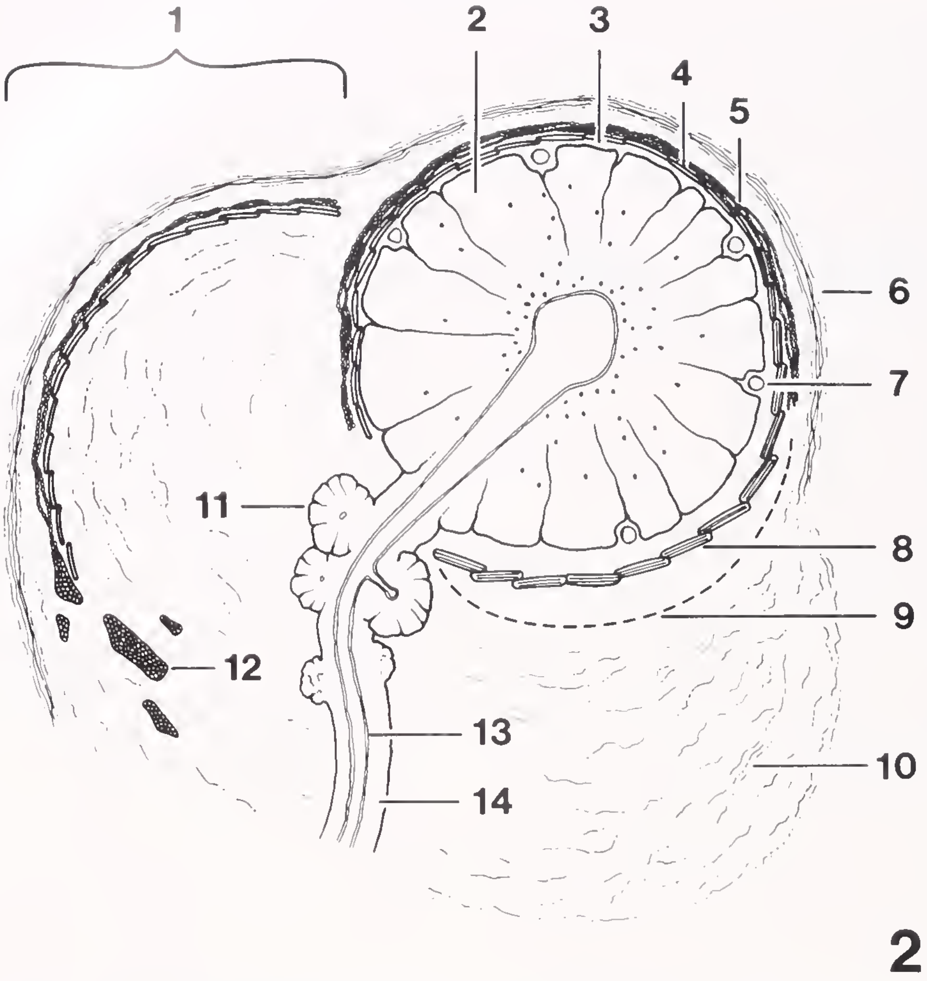

Figure 2. Diagram of gland D, same orientation as in Figure 1. (1) Canopy with outer connective tissue layer, a middle layer of iridosomes and an inner layer of thin platelets composed of laminations of dioptric material. (2) Radiating spindle shaped cluster of secretory cells arranged in packets of five or six cells. (3) Thin layer of connective tissue. (4) Layer of thin dioptric platelets similar to the layer in the canopy. (5) Beaded layers of oriented iridosomes (see Fig. 7a). (6) Layer of connective tissue that encompasses both gland D and its canopy. (7) Blood vessel. (8) Thick laminated dioptric facet (see Figs. 3, 10, 11). (9) Location of a continuation of the platelet layer that drops down in back of gland D forming a cup-like shelf that terminates near the plane of section, *i.e.*, the free edge faces the surface of the fish (see 4 in Fig. 3). (10) Oriented layers of sparse, flattened connective tissue cells (see Fig. 8) embedded in finely granular lucent material that extends from under the canopy to form a lenticular bulge. (11) Cluster of secretory cells similar to those within the gland proper but on a smaller scale. (12) Small clusters of cells containing irregularly arranged iridosomes. (13) Epithelial layer of secretory duct. (14) Connective tissue sheath of secretory duct.

Figure 3. Light micrograph of gland D. Plane of section is at right angle to the diagram in Figure 1, *i.e.*, at right angle to the surface of the fish. (1) Thin laminated dioptric platelets. (2) Sheets of beaded melanin-like iridosomes. (3) Thick dioptric plates or facets. (4) Shelf of thin dioptric platelets continuing from the posterior-ventral edge of layer 1; its out of plane position is indicated in Figure 2 by dashed line. (5) Overlapping dioptric material, closely packed. (6) Dioptric material, more dense, and oriented at right angle to the lens of the shield. (7) Lens-like thickening of the shield. (8) Cross section of overlapping dioptric ribbons that range on down to the level of gland V (see dashed lines in Fig. 1). (9) The main bulge of lenticular material. The curving layers of connective tissue help to maintain the symmetry of the bulge. Collecting channels of the secretory cell packets are indicated by arrows (also see Figs. 5, 6). Scale bar = 20 μm.

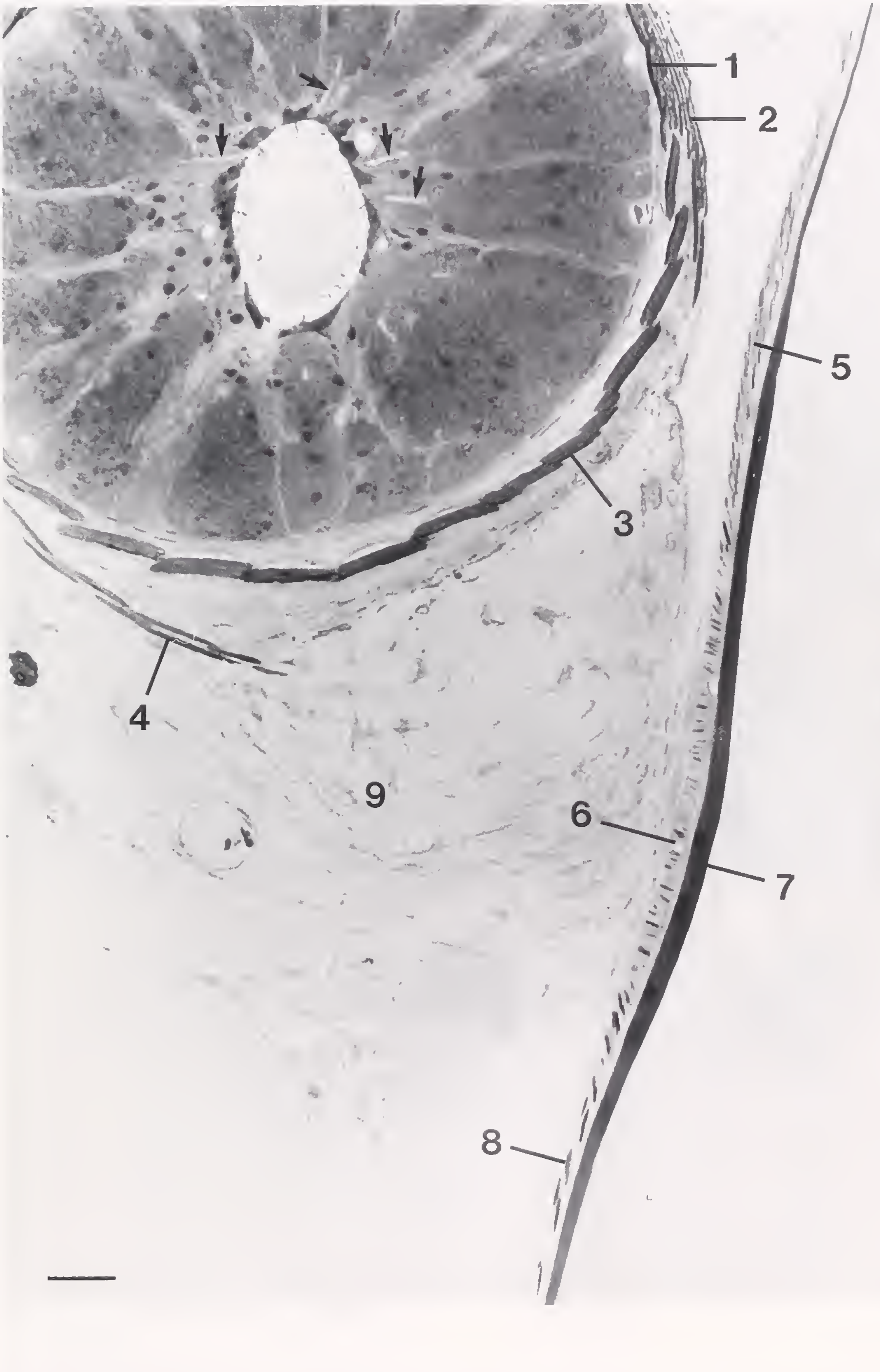

3

Light microscope studies of whole mounts were made by two methods. First, reasonable detail could be seen when the flat, embedded epoxy blocks were placed on a slide and observed through the upper (shiny) surface with the 10× and 40× objectives of a compound microscope. The osmium tetroxide in the post osmication process acted as a stain. However, the best whole mount preparations were obtained after the melanin pigment had been bleached away (1% chromic acid in 1% calcium chloride, 6 to 12 h at room temperature). The tissues were then stained in Lynch's precipitated borax carmine, followed by dehydration and mounting on slides with Permount.

An additional effort was made to reveal the internal fine structure of the iridosomes, which, although "melanin-like," resisted bleaching with chromic acid. Treatment with the more potent peracetic acid (Barka and Anderson, 1963) to the point of tissue maceration produced no marked bleaching. Some visualization of internal ultrastructure was obtained only by use of very thin (grey) sections. Several attempts were made to demonstrate nerves with Protargol (Winthrop Chemical Co.), but the efforts were not successful. Because silver stains for nerves are notoriously capricious, the failure does not indicate that nerves are absent.

Results

The serial photophores of *Gonostoma elongatum* are arranged in two rows on the ventro-lateral side of the body. The upper serial row (OA) runs from the operculum to the anal level, and each photophore includes two glandular structures. The lower row (IV, VAV, AC) runs the full length of the body and each has only one structure. (For diagrams and keys to the photophores of *Gonostoma* see pp. 284 and 300 in Badcock, 1984.) Each of the upper serial photophores has two distinct glands (Fig. 1). Each gland has a duct that joins the other, and the common duct exits by an orifice to the surface of the fish. The whole glandular complex is covered by a transparent shield of multilayered collagen. The common secretory duct empties to the external surface close to the posterior edge of the shield. For convenience, the dorsal gland is referred to as "gland D," and the ventral gland is called "gland V."

A faint, bluish light was observed along the ventrolateral aspects of several *G. elongatum* in a darkened room aboard ship, but I did not have equipment to localize or enhance the light source. Also, admittedly, my primary concern was to initiate fixation as quickly as possible.

Gland D

Gland D is spherical and composed of long secretory cells radiating from a central collecting cavity (Fig. 2). The cavity is lined with epithelial cells that continue on to form the lining of the secretory duct. The radiating cells are grouped in clusters of 5 or 6 in such a way that the central adjoining membranes of the cluster form a channel (Figs. 5, 6) that connects to the central collecting cavity. (The term "channel" is preferred over "duct" because there is no epithelial lining present.) The lateral surfaces of each spindle-like cluster of cells borders on areas filled with connective tissue and blood vessels (Fig. 4).

Each glandular cell is filled tightly, in an oriented fashion, with secretory granules and multiple layers of rough endoplasmic reticulum (RER). The RER is layered parallel to that part of the cell adjacent to the connective tissue space (Fig. 4) and fills the outer, more broad end of the cell. The secretory granules are found in that part of the cells adjacent to the common channels (Fig. 5), and that association persists to the point where the chan-

Figure 4. Longitudinal section along a radius of gland D, including the surfaces of two cells from adjoining packets of cells, and together with intervening connective tissue and vascular supply (C). Rough endoplasmic reticulum (R) lies parallel to the cell surfaces facing the connective tissue. Large secretory granules (S) are located away from the connective tissue layers and are found adjacent to the secretory channels in the middle of the packets (see Fig. 5). Scale bar = 1 μm

Figure 5. Cross section near the midpoint of a radiating packet of secretory cells in gland D. Secretory granules (S) are packed about a central collecting channel (C). There is no tubular epithelium but the glandular cells do have tight junctions (twin arrows) and desmosomes (single arrow). Scale bar = 1 μm

Figure 6. Section closely parallel to the central collecting cavity of gland D cutting through the epithelium lining which has dense nuclei (Nu) and dense cytoplasm. Each packet of radiating glandular cells (G) narrows and penetrates the epithelium so that the collecting channels (C) connect to the central cavity. At this level, secretory granules are predominant in the secretory cells. Scale bar = 1 μm

Figure 7a. Flattened, oval-shaped iridosomes held in orderly fashion by parallel membranes having cross bridges. They are quite dense, and both chromic acid and peracetic acid treatment failed to bleach the melanin-appearing granules. Scale bar = 0.27 μm.

Figure 7b. Higher magnification of Figure 7a (which is an extremely thin section) with enhanced contrast to reveal the faint laminations that are registered parallel to the bounding membranes of the iridosomes.

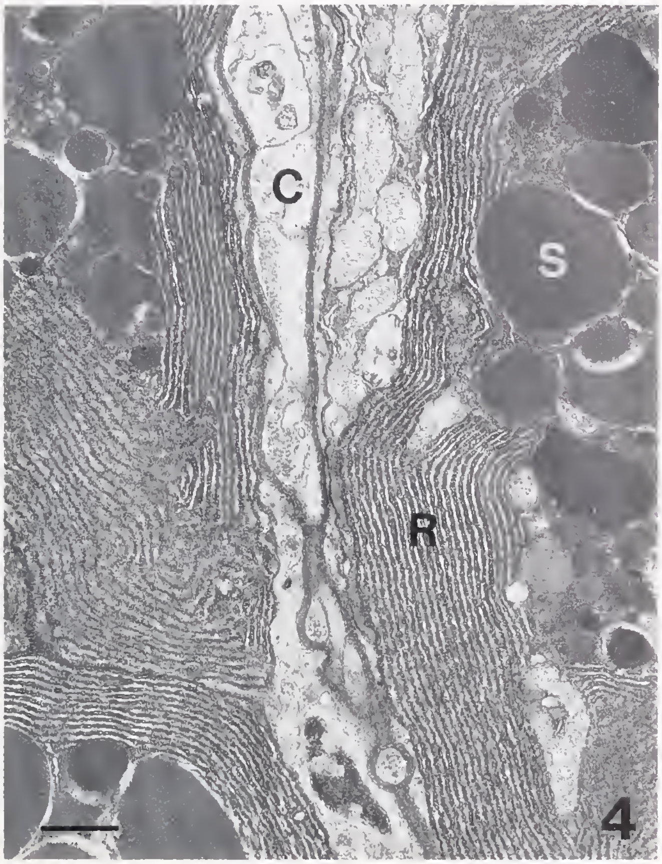
C
S
R
4

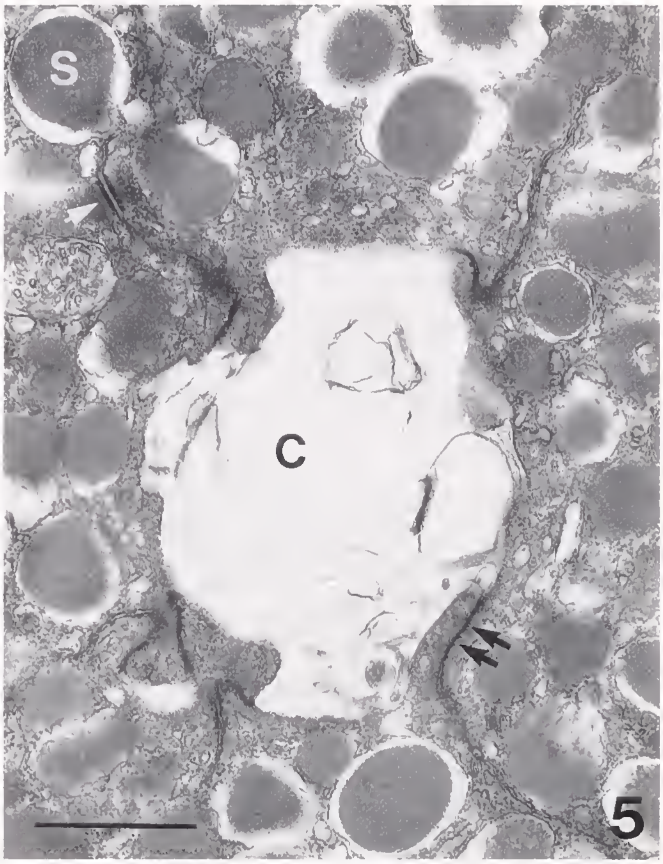
S
C
5

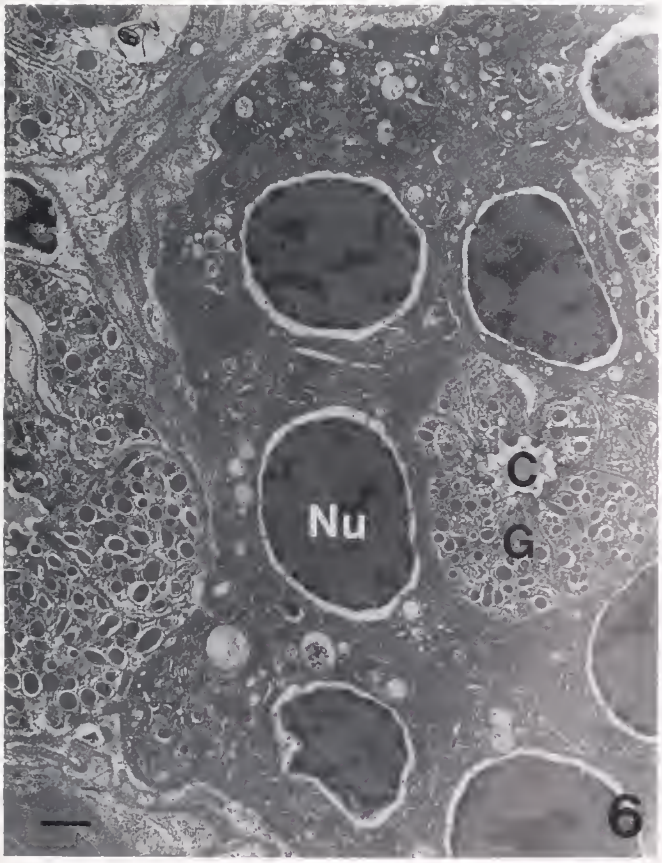
Nu
C
G
6

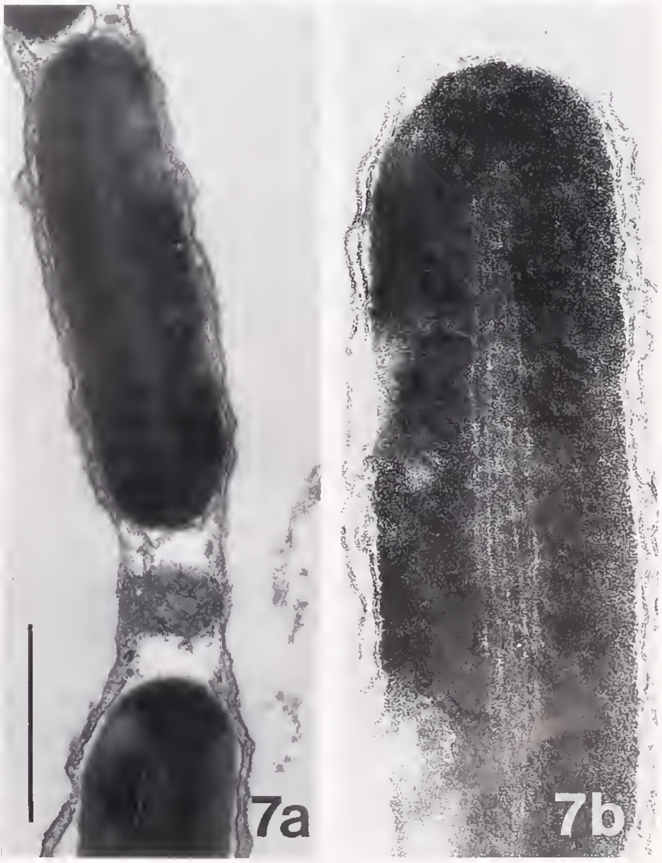
7a
7b

nels empty into the central secretory collecting cavity after penetrating the epithelial lining (Fig. 6).

The secretory duct immediately adjacent to gland D has small clusters of cells attached to it. The cells are secretory and similar to those in the main part of the gland in having plentiful RER and secretory granules. They differ only in being more rounded and having very short collecting channels (Fig. 2). The base of the secretory duct and its attached cluster cells is covered by a cup-like hemispheric "canopy" extending laterally from the spherical gland (Fig. 2). The dorsal three quarters of gland D is covered by a double layer, the innermost being composed of a thin layer of laminated, dioptric platelets (Figs. 2, 3); [structures in this article that respond to polarized light are called "dioptric" (see Fig. 12)]. The outer layer is composed of beaded rows of melanin-like iridosomes (Figs. 2, 3, 7). A similar double layer also extends over the inner surface of the canopy. Irregular cellular clusters of iridosomes are found at the free edge of the canopy (Fig. 2).

The dioptric platelet layer covering gland D extends down on all sides, slightly more so on the ventro-medial side where it forms a narrow shelf or band (out of plane of section in Fig. 2, but seen in Fig. 3). The lower surface of the gland D lacks iridosomes and has a circular pattern of dioptric material forming thickened, multilayered plates or facets. The facets slightly overlap each other inward to the central dorso-ventral axis of the gland (Figs. 2, 3). The facets, when viewed with transmitted light in epoxy embedded material, can be seen to form a brilliant blue pattern resembling that of mosaic tile. The facets are composed of orderly, multiple layers of membrane-bound material (Figs. 10, 11), which presumably accounts for the response to polarized light. All of the other dioptric materials mentioned in this article have similar layering.

The iridosomes are small, flattened, lozenge-shaped particles with their long axes held in register by membranes. The result is a sheet of iridosomes that in cross section looks like a beaded necklace (Fig. 7). The outer layer covering gland D is composed of many sheets of such material. The pigment of the bead-like iridosomes is quite resistant to chromatic acid digestion and responds only slightly to the more corrosive peracetic acid. It probably is not representative of the usual melanin. A multiple layering of material can be seen within the matrix of the ovoid iridosome particle. The layers are parallel to the free surface of the beaded sheets of iridosomes and can be visualized only in very thin (grey in color) ultratome sections.

The space covered by the canopy is filled with an orderly arrangement of loose connective tissue (Fig. 2). Sparse, oriented, flattened cells (Figs. 8, 9), supported by some random collagen, fill the cavity and extend ventrally. The ventral extension expands into a bulge underneath gland D (Figs. 2, 3). Because of its spherical shape, and because a better designation is lacking, I call it a "lenticula." It has a fine glandular matrix that is completely transparent in preserved material. Where the lenticula adjoins the covering shield the concentration of collagen in the matrix markedly increases (Fig. 9).

The secretory cavity of gland D is emptied by a duct that also connects to a similar duct from gland V (Fig. 1). The common duct then exits through the epithelial surface of the fish (Fig. 12). The cavity and the ducts are lined with a distinct epithelium characterized by dense nuclei (Fig. 6). A layer of connective tissue surrounds both ducts, and the lumen of each duct contains a glandular nondescript material.

Gland V

The plate-shaped gland V is anatomically and cytologically different from gland D. The secretory cells form a single layer adherent to a network of thin-walled interconnecting capillaries. The labyrinthic space between the capillaries (with their adherent cells) is packed with secretory material (Fig. 13). There is no collecting chamber, and the duct for gland V is attached directly to one of the upper (dorsal) arms of the sprawling labyrinth that contains secreted material. The cells of gland V have obvious

Figure 8. Cross section of flattened connective tissue cells in the transparent bulge (lenticula) located below gland D. Note oriented parallel array. Small clusters of collagen fibers (arrow) are barely visible at this magnification. Matrix is of fine amorphous material. Scale bar = 20 μm.

Figure 9. Higher magnification of the lenticula as it adjoins the covering shield. Collagen fibers (asterisk) are much more numerous and the connective tissue cells are larger and more irregular. Arrow points in the direction of the attachment to the covering shield. Scale bar = 5.0 μm.

Figure 10. Cross section of a multilayered dioptric facet of gland D. Note the regular periodicity of the layer being sequestered from a parent cell (arrow). Scale bar = 1 μm.

Figure 11. Multilayered dioptric facets of gland D illuminated by polarized light. Strong response is obtained. Also, note the overlapping arrangement of the plates (see Figs. 2, 3). Scale bar = 1 μm.

Figure 12. Longitudinal section of the lips of the common secretory duct as it exits to the externum of the fish. Scale bar = 10 μm.

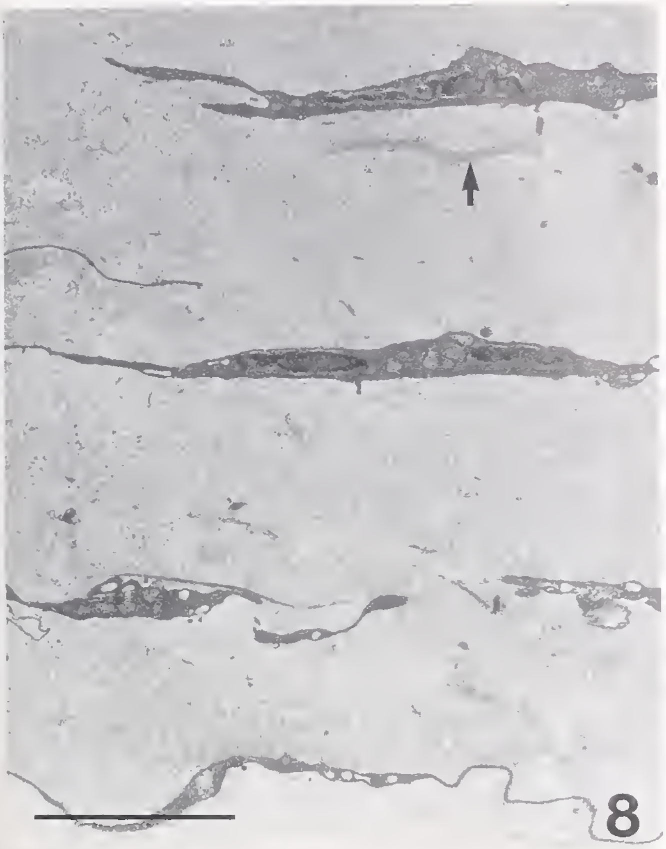
8

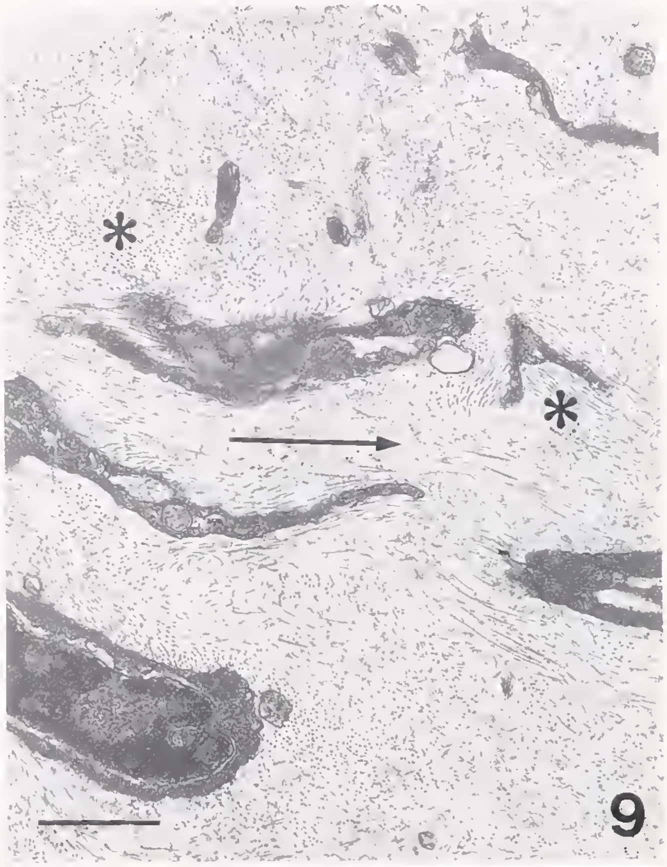
9

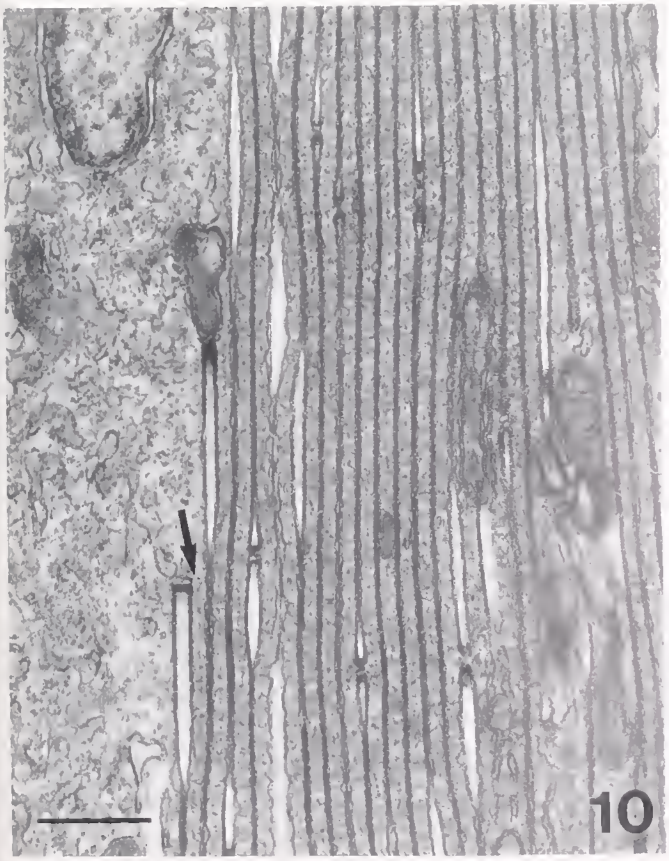
10

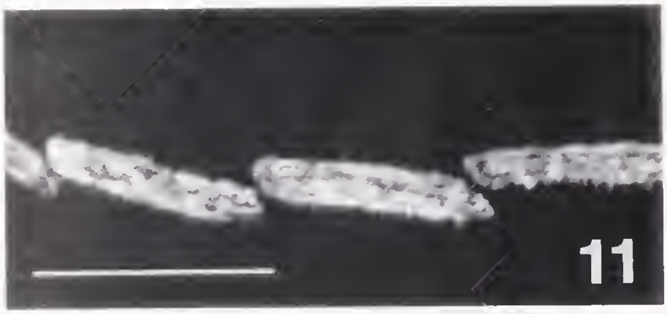
11

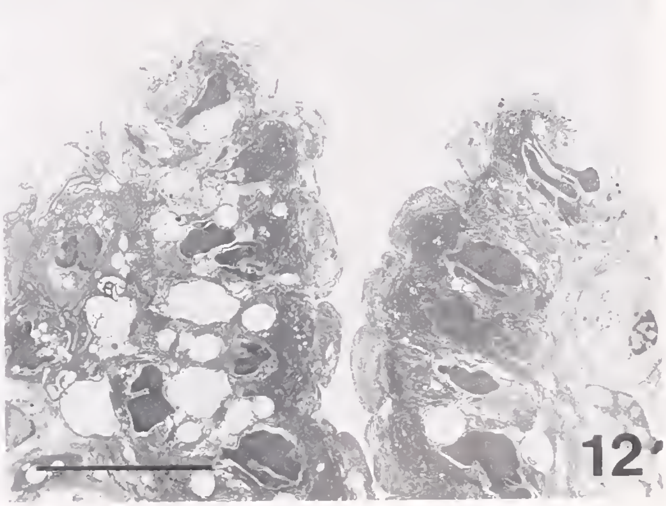
12

secretory elements such as granules and rough endoplasmic reticulum (Fig. 14). The number of secretory granules and the number of cells having the granules is quite variable. Cells possessing granules are usually distributed in a gradient, the cells having the highest concentration of granules being found at the upper (dorsal) end of the gland.

Gland V has dioptric material in a layer immediately under that organ (Fig. 15). It is in the form of thin rectangular ribbons overlapping and randomly disposed with no prevailing orientation when viewed in embedded material by light microscopy. Each ribbon is about 20 × 100 μm and has four or five layers of laminated material similar to that in Figure 10. The ribbons probably provide the whiteish, silvery reflection seen in the living, though moribund, animal. Sometimes the reflection has a faint yellow color in fixed material.

Shield

The entire dual gland complex is covered by a transparent shield (Fig. 1) of collagen orientated in alternating layers that are at right angles to each other (Fig. 16). Fifteen or so of the layers form a lens-like thickening at the level of gland D (Fig. 3). The number of layers drops off in all directions until there is only one layer of amorphous material at the edge of the shield. That periphery is embedded in a rod-like rim of cellular material (Fig. 18). The free surface of the shield is covered by a thin layer of epidermal epithelium that is frequently lost during collection and preparation.

Immediately beneath the shield is oriented dioptric material arranged in rows parallel to each other (dotted lines in Fig. 1). The rows of ribbons overlap in a steeply pitched, shingle-like fashion (Fig. 17). The angle of the pitch is downward, *i.e.*, laterally and ventrally to the body. The region of layered shingles reaches from about the median level of gland D (Fig. 3), down to the upper edge of gland V (*i.e.*, it does not cover gland V). The parallel rows of dioptric material extend straight across the shield just above gland V level, but as the gland D level is approached, the rows increasingly bulge upward (Fig. 1). There is a regional change in the orientation of the shingles where the connective tissue of the lenticula adheres to the shield. In that region, the dioptric material is more coarse and oriented at right angles to the shield (Fig. 3). The modified shingles lie between the lens of the shield and the lenticula of gland D. Above that region, the dioptric material again slants downward, is more compact, and ends. Although the light microscope cross sections of the shingles responded to polarized light, at no time was color or reflection evident in the intact animal, living or fixed. The dioptric material is transparent and can easily be overlooked at the light level unless differential interference contrast (DIC) lighting of embedded material is used.

Comparison with some other types of photophore in G. elongatum

The lower serial row, the suborbital, and the caudal photophores each have a gland that, in size and cytology, is similar to gland D. However, the lower serial photophores have no gland V; the singular gland D connects directly to the surface via a single duct. Both the suborbital and caudal photophores have gland V type tissue, but noteworthy in each case, the glands V and D are connected directly to each other by a duct that does *not* approach the surface.

Discussion

Gland D and its dioptric material

Herring and Morin (1978, p. 306) have provided (after Bassott) a line drawing of gland D in *Gonostoma* at the light histology level. They diagram the radiating arrangement of secretory cells focussed on a central collecting cavity and say that a duct connects to the surface of the fish, but do not show a clearly organized duct or associated cluster cells. Also, items such as canopy, facets, and lenticula are not depicted, and gland V is not mentioned. Gland D of *Gonostoma* is better illustrated in a micrograph by Nicol (1969, p. 365). The

---

Figure 13. Cross section of several thin-walled capillaries (arrows) in gland V. The capillaries form a flattened irregularly branching, network of vessels and are covered by a single layer of glandular cells (G). The labyrinthic space between the capillaries is filled with secretory material (S). The capillaries are distended, and the lumen (L) is empty of red blood corpuscles because of emboli located somewhere else in the system. Scale bar = 10 μm.

Figure 14. Detail of a secretory cell in gland V. Note usual glandular characteristics such as rough endoplasmic reticulum (R), Golgi apparatus (G), and secretory granules (S) and secreted material (asterisk). Also, note the irregular protrusions of the cell surface that may aid in secretory release. Scale bar = 1 μm.

Figure 15. Light micrograph of a section through the layer of dioptric ribbons that lay beneath gland V. The ribbons are thin (4 or 5 laminations), rectangular (about 20 × 100 μm), and randomly disposed within the layer. Cross section of a ribbon (single arrow) and longitudinal section (twin arrows). Scale bar = 20 μm.

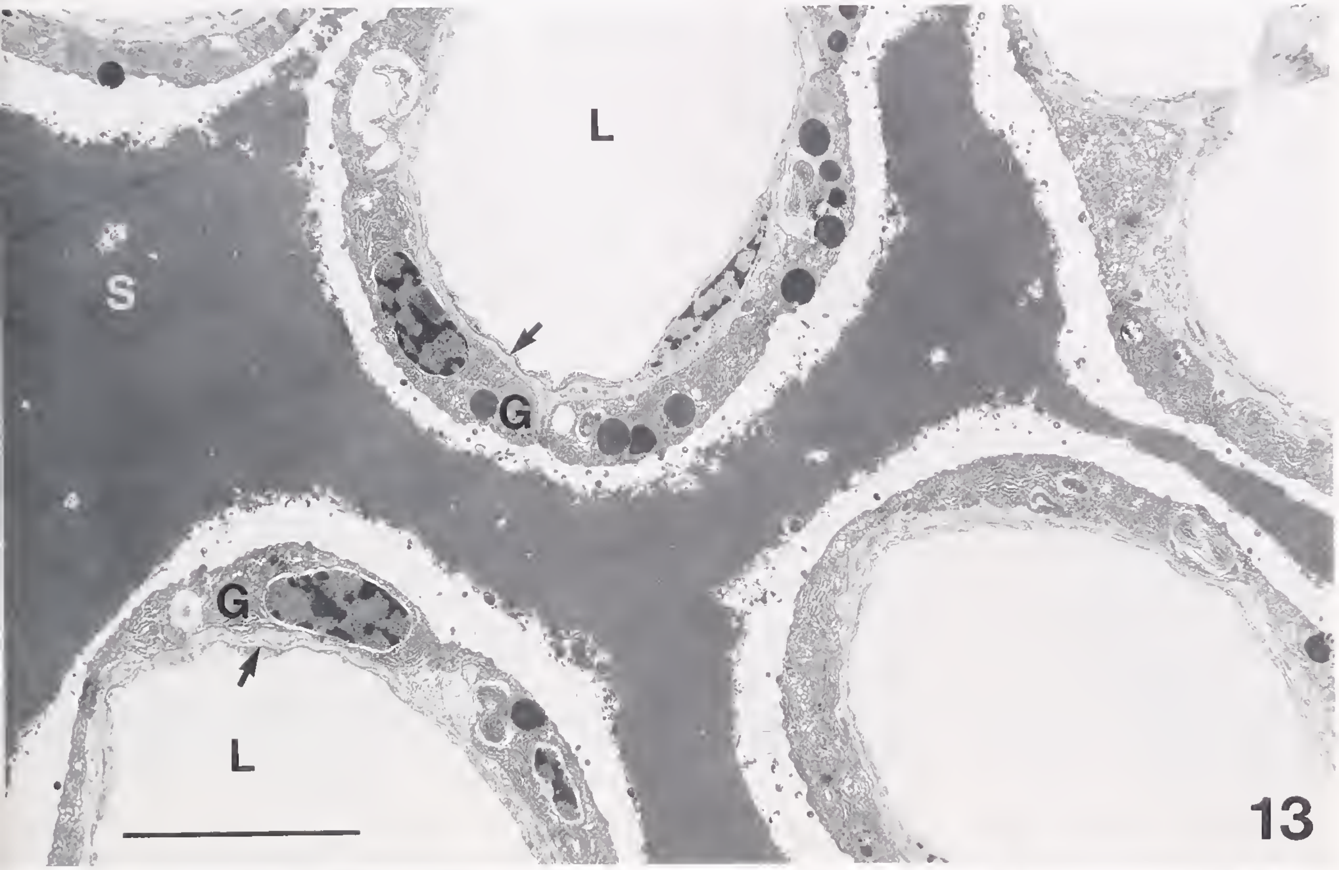
L
S
G
G
L
13

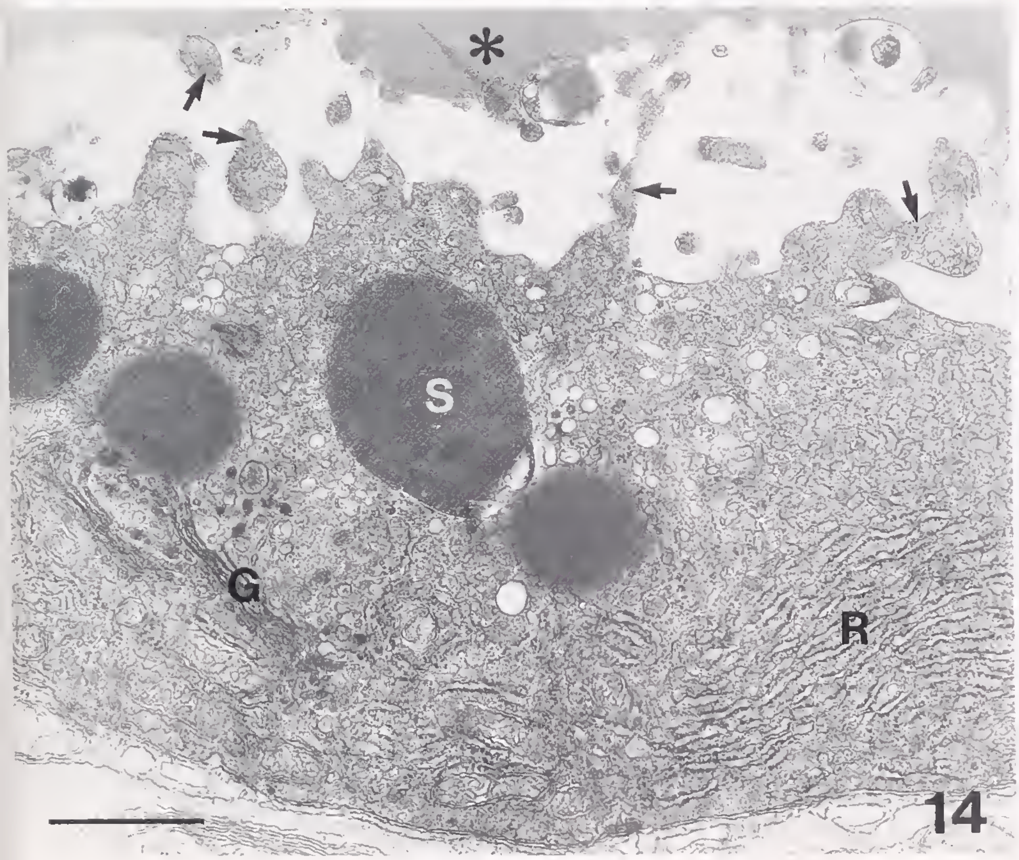
*
S
G
R
14

15

photophore is from the "lower trunk." If trunk is defined as post-anal, then the photophore is one of the lower serial row that has no gland V (the upper serial row of dual gland photophores is on the abdomen anterior to the anus). However, because gland D in the upper and lower serial rows are quite similar, the photograph by Nicol is comparable to the gland D described here (but not in as much detail). The secretory cells of gland D are equivalent in all respects to the A photocytes of Bassott (1966). However, I found no cells equivalent to his type B photocytes. The lack of type B cells in the photophores of gonostomids has been noted by Bassott (1966) and Nicol (1969).

Gland D is capped with a layer of dioptric platelets backed by a layer of iridosomes in such a manner that light can be reflected ventrally and laterally toward the external surface, a common phenomenon in photophores located laterally on the body. These layers may selectively reflect spectral light (Denton *et al.*, 1985). The canopy, as an auxiliary structure, may have a light concentrating role. The layer of dioptric platelets, plus iridosomes, could have a reflective and light concentrating effect. It is in a position suited to reflect some light from gland D and much of the light from the cluster cells at the base of the collecting duct. The slightly overlapping, concentric arrangement of the dioptric facets on the ventral side of the sphere could have a concentrating effect as well as a possible light filter effect similar to that described by Denton *et al.* (1985). Furthermore, the shelf of dioptric platelets (Figs. 2, 3) that slopes toward the shield could provide a deflecting effect, guiding more light through the lenticula into the lens.

Lenticula as a light collector and anchor

The lenticular tissue is in the shape of an inverted comma with the tail under the canopy and the spherical bulge positioned below the gland proper (Fig. 2). The highly oriented loose connective tissue and amorphous matrix could allow for an optically clear structure with an index of refraction suitable for concentrating light. The tissue might also act as a light filter (Denton *et al.*, 1985). Bassott (1960) describes a photophore in the closely related gonostomatid *Maurolicus* that has a body that is gelatinous, transparent, homogeneous, and refractive; and suggests that it may act as a lens. The oriented collagenous attachment of the lenticular apparatus to the shield could serve two purposes. The most obvious would be to pass light to the lens of the shield in a registered fashion. The other purpose, in lack of other connective tissue, would be to serve as an anchor for gland D, keeping it oriented and in place.

Gland V and its dioptric material

Although gland D in *Gonostoma* has been repeatedly identified in the literature as a photophore and considered as furnishing a taxonomic pattern (Grey, 1964), the associated gland V has received little attention. One of the first to identify it was Brauer (1908), who referred to it as a "sack formigen Organ." It has been referred to as being glandular and having a direct connection to gland D, but there is no description of the two secretory ducts fusing into a *common* duct to empty to the surface. Also, I find no cytological descriptions of the gland V.

The secretory cells of gland V have little or nothing in common with the secretory cells in gland D, either anatomically or cytologically. The type cell of gland V has a well-developed Golgi apparatus and associated granules that indicate the usual merocrine type of secretion. However, granules do not approach the dense population seen in gland D.

There is no evidence in the literature suggesting that gland V produces luminescence. Most certainly it has no category "A" photocytes as found by Bassott (1966) in a broad spectrum of photophore types in teleosts. The dioptric ribbon-like material beneath gland V must serve as a reflector, and account for the silvery appearance.

The shield and its dioptric material

The shield is composed of multiple layers of collagen, each arranged at right angles to the neighboring layers. Thus, maximum stiffening is obtained. The shield is further strengthened at the tapering circumferences by a rod-like rim of cells. The thin overlying cutaneous epithelium is easily displaced in dissection and probably does not contribute much strength to the system.

The shield may be involved in two aspects of light release. First, the shield itself is thickened to form a lens, albeit it may be weak. That lens is positioned directly opposite and attached to the lenticula of gland D, so that light passing from the lenticula may be collected by it. Second, the oriented rows of dioptric material associated with the shield may have indices of refraction that would help to guide light downward from gland D (with a possible exception at the level of the lenticula). The rather complicated orientation of the rows in relation to gland D, straight rows transitioning to curved, supports this interpretation. Moreover, there is no such dioptric material accompanying the shield over gland V. Whatever the function of the dioptric material associated with the shield, it must be in reference to gland D.

Iridosomes

Bassott (1966) describes the photophores found throughout the stomiatoidei (which includes *Gonostoma*)

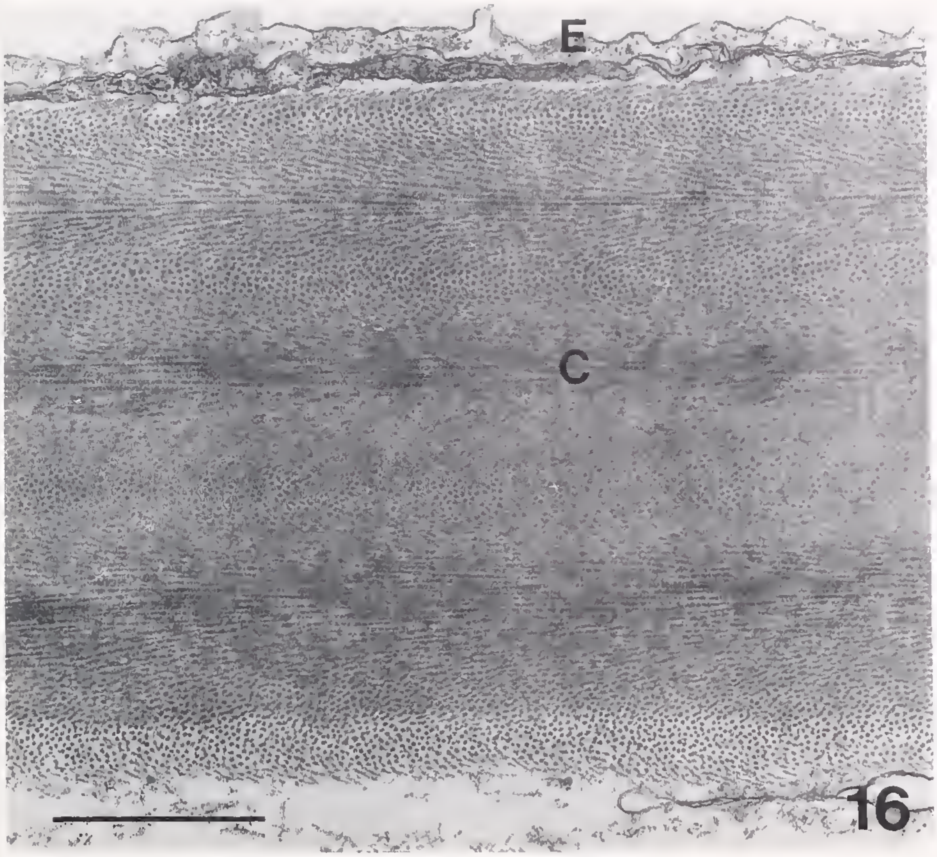

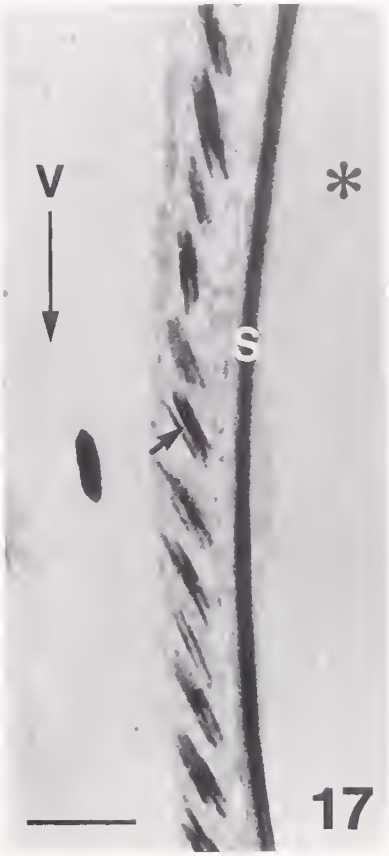

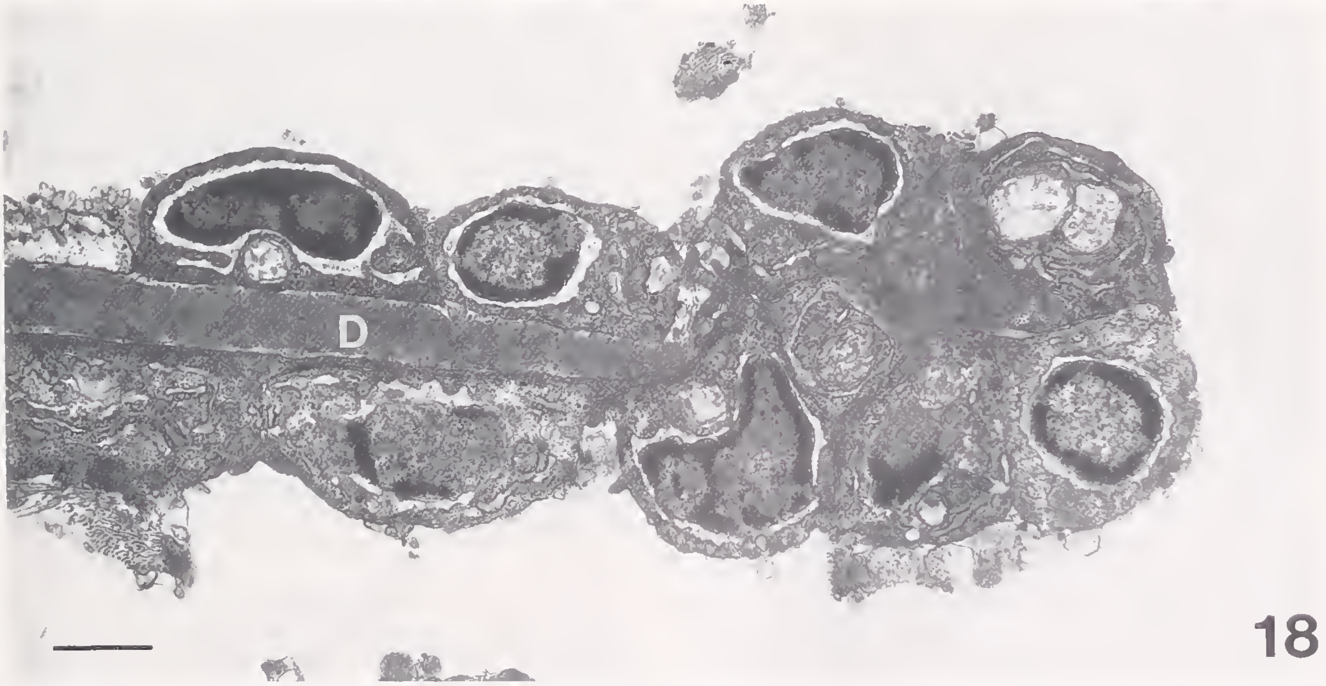

Figure 16. Cross section of the shield, median between its free edge and the lens thickening. Note that the alternating layers of parallel collagen fibers are at 90° angles to each other, thus adding strength to the shield. Collagen (C). Skin epithelium (E). Scale bar = 1 μm.

Figure 17. Light micrograph of a cross section of the dioptric ribbons that lay in overlapping fashion immediately under the shield. (See Fig. 1 for their distribution). Ventral direction (V). Collagen shield (S). Dioptric material (arrow). External medium (asterisk). Scale bar = 10 μm.

Figure 18. Cross section of the edge of the collagen shield. The shield proper tapers peripherally to a narrow flange of dense material (D), almost devoid of collagen fibers, and is finally bordered by a rod of supporting cells that may have participated in the growth of the shield. Scale bar = 1 μm.

as "urn, sphere or retort shaped." The wall of the sphere is always formed of reflector cells which, in turn, are coated with a "layer of iridocytes of melanine" (Bassott, 1966, p. 566). The particles in Figure 7 could be called "melanosomes" because they look melanin-like and have no proven iridescence. However, the particles, by reason of their laminated substructure, their rigid orientation within sheets, and their resistance to chromic acid and peracetic acid digestion, may not be usual melanin granules. For example, Nicol (1989) describes two kinds of "melanoid substances" to be found as chemical components in the reflectors of fishes. He uses the term "melanoid" because the two are chemically derived in part from tyrosine by tryosinase catalysis and exhibit certain parallels to melanin synthesis. By precedent, the term "iridosome" is chosen in this article as representing the particles within the "iridocyte" of Bassott.

The sheets of iridosomes are ideally located about gland D and under the ribbons of gland V for a possible light modifying function. The hitherto unreported laminations in the particle, plus their orientation to the long axis of the sheets, suggests that such could be true. (On the other hand, they may be exceptionally efficient light suppressors.)

Functional aspects

I approach the discussion of possible functions with trepidation, and I quote Buck (1978, p. 420): "At least 20 functions of bioluminescence in one animal or another have been proposed—Though often quite plausible, most of these proposals were originally more a reflection of the ingenuity of observers than of the solidity of the observations, and there has been an unfortunate tendency for later authors who are casting about for functions of luminescence in their own material simply to list possibilities without adducing any additional support." This comment is particularly appropriate when considering the mesopelagic fish, which are difficult to observe or to test in any way.

Doubtless, type D gland photophore luminesces. Swift *et al.* (1977) recorded luminescence in a *Gonostoma* photophore, "about 2/3 of the distance from the head to the tail." That distance would locate it in the area of the body that has only lower serial photophores with gland D (see illustration, Badcock, 1984, p. 300). Furthermore, Anctil (1972) has stimulated luminescence in the photophores of the closely related gonostomid, *Maurolicus.*

I find no record where gland V is given the status of a photophore. However, the enlarged type V gland tissue in the caudal gland of *G. elongatum* has been referred to as "luminous tissue" by Grey (1964), and it has associated with it, at a tangent and relatively inconspicuous, type D gland that is cytologically akin to the lower serial photophore that has been proven to luminesce (as stated above). Thus, both glands D and V may produce light. Keeping Buck's admonition in mind, one would add that proof for a luminescent function for gland V is faint.

The possibility that luminescence may occur other than in gland D or gland V (*i.e.,* in surface slime) cannot be discounted. Bassott (1966) says of *Gonostoma* that the absence of clearly characterized B cells in association with the A cells could be explained by the possibility that the A cell secretion is secreted to the outside and there mixed with other agents. Also, Swift *et al.* (1977, p. 822) quote Brauer (1908) and say "the light organs in *G. elongatum* have ducts leading externally which suggests along with the large value of FWHM (Table 1) that its spectra show little effect from the masking of overlying tissue." The implication is that the ducts bring the luminescence to the surface, where it is more easily seen. My own observations of the faint bluish luminescence in *G. elongatum* were not sufficient for a specific localization of source. I hazard no thoughts regarding the function of a direct ductal connection between glands D and V in the suborbital and caudal photophores. It is interesting that, at least in *G. elongatum,* gland V is always associated with a gland D. However, gland D is not necessarily associated with gland V.

One of the noteworthy features of this article is the detailed analysis of a whole array of dioptric materials that can efficiently handle the luminescent light in such a way as to produce a downward, evenly diffused lighting for the fish, that could function as counterillumination.

Acknowledgments

This work was supported by grant NSF-PCM-80-23166 to D.E.C. and grant NSF-OCE-84-16206 to Holger Jannasch. I am grateful to J.A.C. Nicol for his comments and encouragement and to Margaret McFall-Ngai for the loan of a midwater collecting net. Not least, the cooperative crews and excellent ship facilities of the RSV Oceanus and RSV Knorr (Woods Hole Oceanographic Institution) must be acknowledged.

Literature Cited

Anctil, M. 1972. Stimulation of bioluminescence in lantern-fishes (Mycotphidae). II. *Can. J. Zool.* **50:** 233–237.

Badcock, J. 1984. Gonostomatidae. Pp. 284–301 in *Fishes of Northeastern Atlantic and Mediterranean.,* Vol. 1, P. J. Whitehead, M.-L. Bauchot, J.-C. Hureau, J. Nielsen, and E. Tortonese, eds. Unesco Publishers, Paris.

Barka, T., and P. J. Anderson. 1963. *Histochemistry. Theory, Practice and Bibliography.* Harper and Row, New York, Evanston, and London.

Bassott, J.-M. 1960. Données histochimiques et cytologiques sur les phophores due téléostéen *Maurolicus pennanti. Arch. Anat. Morphol. Exp.* **49:** 23–71.

Bassott, J.-M. 1966. On the comparative morphology of some luminous organs. Pp. 557–610 in *Bioluminescence in Progress,* F. H. Johnson and Y. Haneda, eds. Princeton University Press, New Jersey.

Brauer, A. 1908. Die Tiefsee-Fische. *Wiss. Ergebn. deut Tiefsee-Exped., "Valdivia"* **15:** 1–432.

Buck, J. 1978. Functions and evolutions of bioluminescence. Pp. 419–460 in *Bioluminescence in Action,* P. J. Herring, ed. Academic Press, New York.

Case, J. F., J. Warner, A. T. Barnes, and M. Lowenstein. 1977. Bioluminescence of lantern fish *Myctophidae* in response to changes in light intensity. *Nature* **265:** 179–181.

Clarke, W. D. 1963. Function of bioluminescence in mesopelagic organisms. *Nature* **198:** 1244–1246.

Denton, E. J., and P. J. Herring. 1978. On the filters in the ventral photophores of mesopelagic animals. *J. Physiol. (Lond.)* **284:** 42 P.

Denton, E. J., P. J. Herring, E. A. Widder, M. A. Latz, and J. F. Case. 1985. The roles of filters in the photophores of oceanic animals and their relation to vision in the oceanic environment. *Proc. R. Soc. Lond. B* **225:** 63–97.

Grey, M. 1964. Genus *Gonostoma.* Pp. 163–180 in *Fishes of Western North Atlantic. Part 4,* H. B. Bigelow, ed. Sears Foundation for Marine Research, Yale University, New Haven, CT.

Herring, P. J. 1982. Aspects of bioluminescence of fishes. *Oceanogr. Mar Biol. Ann Rev.* **20:** 415–570.

Herring, P. J. 1984. The spectral characteristics of luminous marine organisms. *Proc. R. Soc. Lond. B.* **220:** 183–217.

Herring, P. J., and J. G. Morin. 1978. Bioluminescence in fishes. Pp. 273–329 in *Bioluminescence in Action,* P. J. Herring, ed. Academic Press.

Lawry, J. V. 1974. Lanternfish compare down dwelling light and bioluminescence. *Nature* **247:** 155–157.

McAllister, J. V. 1967. The significance of ventral bioluminescence in fishes. *J. Fish. Res. Bd. Can.* **24:** 537–554.

Nicol, J. A. C. 1969. Bioluminescence. Pp. 355–400 in *Fish Physiology, Vol. III,* W. S. Hoar and D. J. Randall, eds. Academic Press, New York.

Nicol, J. A. C. 1989. *Eyes of Fishes.* Clarendon Press of Oxford University, Oxford.

Swift, E., W. H. Biggley, and T. A. Napora. 1977. The bioluminescence emission spectra of *Pyrosoma atlanticum. P. spinosum (Tunicata), Euphausia tenera (Crustacea)* and *Gonostoma sp. (Pisces). J. Mar Biol. Assoc. U K.* **57:** 817–823.

Widder, E. A., M. L. Latz, and J. F. Case. 1983. Marine bioluminescence spectra measured with an optical multichannel detection system. *Biol. Bull.* **165:** 791–801.

Young, R. E. 1983. Oceanic bioluminescence: an overview of general functions. *Bull. Mar. Sci.* **33:** 829–845.

Young, R. E., and C. F. E. Roper. 1977. Intensity regulation of bioluminescence during countershading in living midwater animals. *Fish. Bull.* **75:** 239–252.

Reference: *Biol. Bull.* **181:** 158–168. (August, 1991)

Morphology and Behavior of an Unusually Flexible Thoracic Limb in the Snapping Shrimp, *Alpheus heterochelis*

A. T. READ, J. A. McTEAGUE, AND C. K. GOVIND

Life Sciences Division, Scarborough College, University of Toronto,
1265 Military Trail, Scarborough, Ontario M1C 1A4

Abstract. The second thoracic limb in the snapping shrimp, *Alpheus heterochelis*, is much thinner, more elongated and flexible, and has a larger ganglion than its serial homologs. The greater length and flexibility is largely due to one of the limb segments—viz., the carpus—which consists of five separate segments, rather than the single segment typical of the other limbs. Externally, the multisegmented carpus is relatively free of cuticular projections except for scattered simple setae. The adjoining segments—the merus and the propus—are also smooth except for clusters of long simple setae on the pollex and dactyl. Internally, each of the carpal segments has three muscles—a bender, stretcher and rotator—all restricted to the distal half of the segment. In keeping with the sensillum-free exterior of the multisegmented carpus, only about 1000 axon profiles originate in the carpus out of a total of 6000 counted at the base of the ganglion. This total number is roughly half that found in the first thoracic limbs. Conversely, the number of axon profiles in the longitudinal connectives to the second thoracic ganglion is about 25% greater than that to the first thoracic ganglion and may partly account for the size difference between these two ganglia.

In terms of their behavior, the second thoracic limbs are almost constantly active, mostly probing the substrate, and occasionally grooming various body parts. Part of the probing behavior consists of food foraging and retrieval, especially from concealed and hard-to-reach locations. Because of their flexibility, these limbs are particularly adept at such movements.

Received 22 January 1991; accepted 8 April 1991.

Introduction

Shrimps of the family Alpheidae are commonly referred to as snapping shrimp, or pistol shrimp, because of the audible popping sound they make when closing their major cheliped. The major or snapper cheliped is highly specialized both morphologically and physiologically, to produce this defensive response (Prizbram, 1901; Ritzmann, 1974). The opposite cheliped or claw, referred to as the minor or pincer claw, is smaller, less elaborate, and used primarily in burrowing behaviors. Although these paired claws have attracted much attention, because of their asymmetry and their capacity to reverse this asymmetry (Prizbram, 1901; Wilson, 1903), the next pair of thoracic limbs, which are also highly specialized in form and function, have been somewhat neglected.

The second thoracic limbs are bilaterally symmetrical and very thin compared to the chelipeds. The most striking morphological specialization is, however, the multisegmented carpus, which is made up of five separate segments rather than the single segment characteristic of all the other thoracic limbs in the shrimp and of crustacean limbs in general. The multisegmented carpus gives the second thoracic limb a high degree of flexibility. Indeed, in another snapping shrimp, *Alpheus pachychirus*, these second thoracic limbs are used as needles with which to stitch algal mats into a temporary retreat (Schmitt, 1975). Although this type of behavior is not seen in *Alpheus heterochelis*, the second thoracic limbs are, nevertheless, strikingly flexible in their movements. Moreover, these movements are not associated with walking, which is performed by the remaining three pairs of thoracic limbs, but with exploring the environment, feeding, and grooming. Thus the second thoracic limbs make almost constant searching movements, by which their distal ends delicately explore the surrounding substrate.

Another interesting point about these highly flexible second thoracic limbs is that their ganglion appears to be larger than that of any of the other thoracic ganglia. This would imply that the volume of neural tissue concerned with the behavior of the second thoracic limb is greater than that of any other thoracic limb. We have therefore investigated the morphology and behavior of these limbs.

Materials and Methods

Adult snapping shrimps, *Alpheus heterochelis* (Say), were collected from tidal pools around Beaufort, North Carolina, and shipped to our laboratory in Scarborough, Ontario. In the laboratory, the animals were held in 25 l glass aquaria equipped with a bottom gravel filter and partitioned into 12 compartments with fiberglass screens. The aquaria were filled with artificial seawater that was kept at room temperature (22°C). A specially prepared diet—a blended mash of chicken livers and hearts and commercial dog food—was fed to the animals daily. The shrimps were sexed on arrival in the laboratory, and their molt history during captivity was recorded. Behavioral and morphological observations were made on adult animals obtained from the wild, and a few juveniles reared in our laboratory were used to supplement the morphology.

Morphology

Scanning electron microscopy. The second thoracic limbs of adult shrimps were removed by a gentle pinch, which induces the animal to autotomize the limb at its base. These isolated limbs (or in the case of juvenile shrimps, whole animals) were fixed for 1–3 h in a 0.15 *M* sodium cacodylate buffer (pH 7.4) containing 2.5% glutaraldehyde, 0.2% formaldehyde, 2 m*M* $CaCl_2$, 0.06 *M* NaCl, and 0.3 *M* sucrose. Next, the tissue was washed in 0.15 *M* cacodylate buffer, containing 2 m*M* $CaCl_2$, 0.06 *M* NaCl, and 0.3 *M* sucrose for 1 h, with several changes. Following dehydration in a graded ethanol series, the tissue was transferred into acetone, before being critical point dried, and mounted with silver paste on Cambridge SEM stubs. The tissue was sputter-coated with gold-palladium and examined with a Hitachi S-530 scanning electron microscope.

Transmission electron microscopy. The focus of this study was the muscles and nerves within the 2nd thoracic limb. Isolated limbs were pinned out in a dish and superfused with the fixative described previously. When the nerves at the base of the ganglion were to be studied, the thoracic nervous system was exposed on its ventral side *in situ* and superfused with fixative. Following an initial fixation of 1 h, the tissues were further dissected, and selected pieces were removed and allowed to fix for an additional hour. A rinse in buffer solution for 0.5 h followed, and the pieces of tissue were then post fixed in 2% O_sO_4 for 1 h. Next, the tissue was briefly rinsed in buffer solution, dehydrated in a graded ethanol series, cleared in propylene oxide, and embedded in Epon-Araldite (Pearce *et al.*, 1986).

Thin (75–100 nm) cross-sections of the nerve were taken close to the ganglion to capture all the axons between the limb and its hemiganglion. These sections were mounted on Formvar-coated single-slot grids, stained with uranyl acetate and lead citrate, and examined with a Zeiss 9S and a Siemens 102 electron microscope.

Cross-sections of the ganglionic nerves were photographed in their entirety via a series of overlapping exposures at 1800×. The resulting negatives were printed to 6000× and assembled into a montage in which the smallest, usually unmyelinated, axons (0.2 μm diameter) were distinct, and could be easily counted. A similar procedure was followed for the ventral nerve cord connectives, except that the initial exposures were at 500× and the final prints were at 3500×. At this magnification, individual axon profiles were easily recognized, as the overwhelming majority were myelinated and therefore relatively large.

Behavior

Observations were carried out on animals acclimated to conditions in the laboratory (room temperature, 10:14 L:D photoperiod) for at least one month. Two small observation tanks (32 cm × 9 cm × 16 cm) were set up as follows: the sides and back were covered with opaque paper, and the inside was partially filled with sloped gravel or sand, and half-filled with artificial seawater. The animals to be observed were placed in the observation tanks and allowed to acclimate overnight. Observations were carried out in the morning and afternoon, under artificial lighting.

Time budget. The focus of our reconnaissance observation was the flexible limb, and our ethogram was constructed with this in mind. We then determined the percentage of time occupied by the cataloged behavioral states using instantaneous sampling (Lehner, 1979). Behavioral states were scored at 20-s interval points throughout an 11-min observation period.

Foraging experiments. An experiment was designed to test the importance of the flexible limb in foraging, specifically for concealed food; *i.e.*, the foraging behavior of shrimp with intact flexible limbs (control) was compared to that of shrimp with missing flexible limbs. Males ranging in length (rostrum to telson) from 28 to 34 mm were used. The flexible limbs were autotomized and the shrimp allowed at least a week to recover. The procedure appeared to cause little stress, as expected, because autotomy is a defensive adaptation and, indeed, shrimp are frequently found with missing limbs. Their general behavior appeared normal.

The trials for observing the foraging behavior were set up as follows: the individual to be tested was confined to one end of the tank with a piece of screen and, at the other end, a small piece of coral was partially buried. Into one of the corralites (approximately 5 mm deep × 2 mm wide) was placed a previously frozen brine shrimp, along with a generous squirt of "brine-shrimp water." The shrimp was released from confinement by removal of the dividing screen, and the time taken to locate the food and actually retrieve it were both recorded. In order for the trial to be valid, the animal had to demonstrate foraging behavior; *i.e.*, frantic crawling around with intense substrate probing. If the food was not located or found within 10 min, the trial was terminated. Each animal was tested twice daily, in the morning and afternoon.

Results

External morphology

Alpheus heterochelis bears five pairs of thoracic limbs: the first two pairs are chelated, and the remaining three pairs are not (Fig. 1A). The first pair of limbs is elaborated into chelipeds; they are bilaterally asymmetrical, one bearing a major (snapper) chela, and the other a minor (pincer) chela, both held in front of the animal. The remaining four pairs of thoracic limbs are not as elaborate, are much smaller, and are held to the side of the animal. The second pair of thoracic limbs differ from the others in that they are much thinner and have a multisegmented carpus. There are five carpal segments; the proximal two are much longer than the distal three, but the joint between each of the segments is in the same orientation as that between the most proximal segment and the merus (Fig. 1B). Consequently, at each joint the distal segment can lie in line with its proximal partner, or it can be bent to almost touch its proximal partner through an angle of 130–140°. This degree of bending at each of the four intercarpal joints makes this limb extremely flexible, allowing its chelated propus-dactyl segment to reach parts of the body otherwise inaccessible to a limb with a single segmented carpus.

The multisegmented nature of the carpus also makes it the longest segment of this limb, much longer than its counterpart in the other three posterior limbs. In contrast, the propus is much shorter in the second limb than in the remaining limbs.

Each of the carpal segments, as well as the more proximal merus, is smooth and bare (Fig. 1B) except for a few scattered short simple setae (Fig. 1C). The apical end of these simple setae are specialized into a sheath (Fig. 1D). The propus is also relatively free of cuticular projections (Fig. 1B) except for its most distal parts, the pollex and the dactyl (Fig. 1E). Situated at the distal end of the pollex and dactyl, on each of the medial and lateral aspects, are prominent clusters of long setae. Scattered more proximally are one or two smaller clusters. These long setae are serrulate in form and have an apical pore (Fig. 1F). Others have their tip elaborated into a sheath (Fig. 1G). A row of short setae occur along the closing edge of the dactyl (Fig. 1E) and these are serrulate and have an apical pore (Fig. 1H).

An opportunity to examine juvenile shrimps arose in our laboratory when a berried female hatched its eggs and we were able to rear these developing shrimps into juvenile forms. In the early juvenile stages, when the paired chelipeds have not yet differentiated into snapper and pincer types, the carpus in the second thoracic limb was fully differentiated with five segments on the one side but only four on the other (Fig. 2A). Of these four segments, the distal three were matched in shape, size, and location to their counterparts on the opposite limb, while the fourth, most proximal segment had not yet subdivided into two. Indeed, a short, shallow furrow on its ventral side (Fig. 2B, C) seemed to mark the formation of a new segment. This observation suggests that the segmentation of the carpus may occur in a distal to proximal direction; possibly the carpus arises as a single unit initially and subsequently becomes segmented.

No sensilla occur on the carpal segments at this juvenile stage; only a single cluster of long setae was present at the distal tip of the pollex and dactyl (Fig. 2A).

Internal morphology

Muscle elements. The musculature in the propus and carpus was examined in thick and thin cross-sections of these segments. The propus typically has two muscles, a small opener and a large closer muscle. Both originate on the exoskeleton and insert via apodemes to the dactyl, which opens and closes in response to contraction of the respective muscles. The fine structure of these muscles is typical of other crustacean striated muscles (Govind and Atwood, 1982) and of the snapping shrimp claw closer muscle (Mellon and Stephens, 1980); *viz.*, myofibrils composed of serially repeating sarcomeres, in which thick filaments are surrounded by thin filaments. We did not further characterize these muscles into fiber types. Mitochondria were found typically around the periphery of the fiber, where they formed a relatively thick rind. They also occurred occasionally interspersed within the fiber, usually in a single row separating myofibrils.

Both muscles also occasionally displayed nerve terminals that resembled those previously described in the

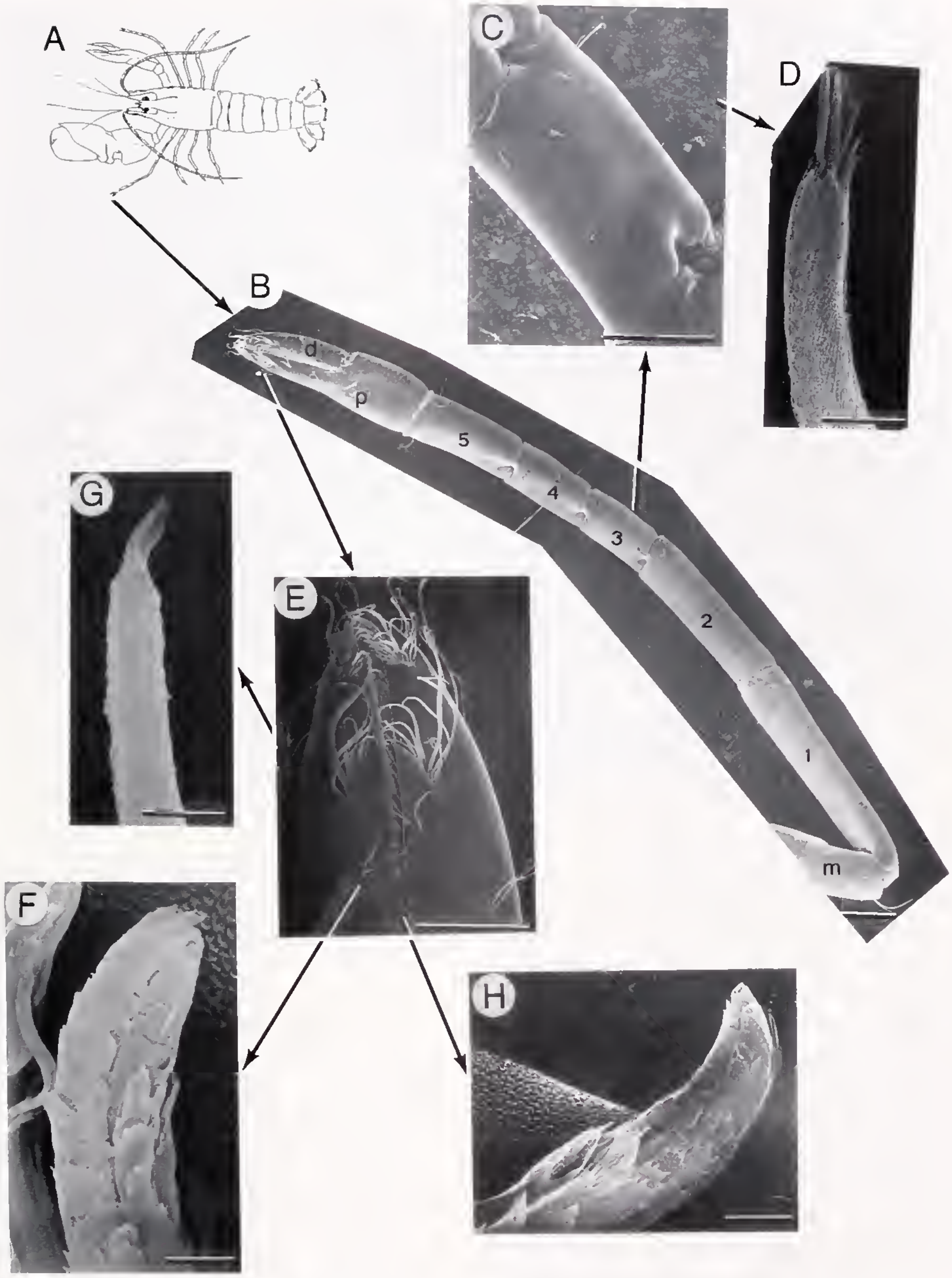

Figure 1. External morphology of the second thoracic limb of the snapping shrimp viewed with scanning electron microscopy. (A) Line drawing of the intact animal showing the five pairs of thoracic limbs, of which the first pair is the enlarged, bilaterally asymmetric chelipeds, and the second pair is the thin, elongated, chelated, and highly flexible limb. (B) The second thoracic limb with dactyl (d) and propus (p), 5-segmented (1 to 5) carpus and merus (m). Morphology and distribution of setae on this limb are shown in the accompanying figures. (C) A typical carpal segment with few sensilla which are of the setal type (D). (E) Distal end of the propus and dactyl with several clusters of long setae and a single row of short setae along the apposing edge of the dactyl. (F) Typical long setae showing serrulate nature and an apical pore. (G) Long setae with a sheath-like tip. (H) Typical short setae with serrulate form and apical pore. Scale bars: B, C, 500 μm; E, 250 μm; D, F, G, H, 2 μm.

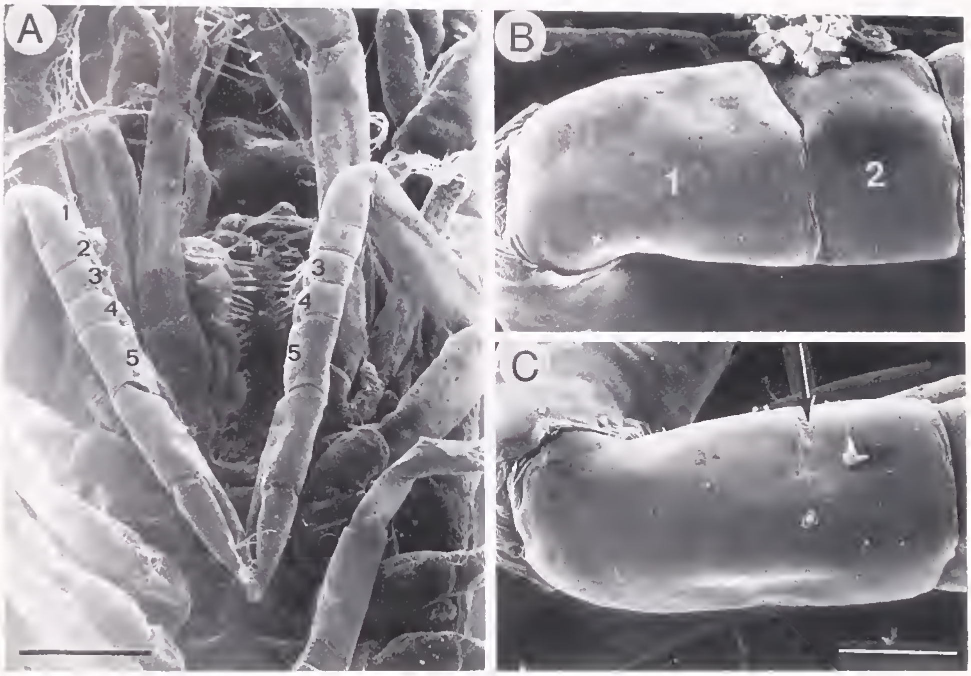

Figure 2. (A) External morphology of the paired second thoracic limbs in a juvenile shrimp. The carpus of the right limb is differentiated into five segments (1 to 5), while the left limb shows the most distal three segments (3 to 5) differentiated but not the most proximal two. (B) High power views of the most proximal segments (1, 2) of the right carpus while the corresponding region of the left carpus (C) is a single segment with a furrow (arrow) marking the beginning of segmentation into two. Scale bars: A, 200 μm; B, C, 50 μm.

closer muscle of the first thoracic limb (Phillips *et al.*, 1982). The nerve terminals were characterized by a population of clear synaptic vesicles that were spherical in most cases; occasionally, terminals with more irregularly shaped vesicles were encountered. The shape of these synaptic vesicles with aldehyde fixation—*i.e.*, spherical or irregular—effectively denotes excitatory or inhibitory nerve terminals (Atwood *et al.*, 1972).

The most distal carpal segment contains three muscles, a large stretcher muscle, a small bender muscle, and an even smaller rotator muscle (Fig. 3). The latter two muscles are closely juxtaposed and are situated in one compartment while the stretcher muscle lies by itself in the other compartment. The apodemes of these muscles attach to the next distal segment, although the muscles themselves do not traverse the full length of the segment but are restricted to the distal half. In fine structure these carpal muscles are similar to those in the propus, and they also display neuromuscular terminals indicative of innervation by both excitatory and inhibitory axons.

The musculature in each of the other segments of the carpus resembles that found in the most distal segment.

Neural elements. The second thoracic ganglion is consistently larger than the first (Fig. 4). In freshly dissected preparations from three adult shrimps, the surface area of the second ganglion was 25 to 30% larger than the first ganglion.

Differences in the input to the ganglia might account for the size differences between them. Hence we examined the nerves and connectives belonging to these ganglia.

A. Nerve. Each of the thoracic limbs is served by two separate nerves, the first and second nerve (Fig. 5A), which originate from the hemiganglion. Each nerve is mixed, composed of sensory and motor axons. The majority of axons within crustacean nerves are sensory, with their cell bodies located at the periphery (Bullock and Horridge, 1964). These sensory axons enter the ganglion and ramify in the neuropil, the integrative region of the ganglion. In crustaceans, relatively few (<60) motor axons innervate the limb musculature (Wiersma, 1961; Govind and Atwood, 1982).

The nerves of the snapping shrimp are unusual in that they have myelinated axons (Ritzmann, 1974), although peneid shrimp also have this feature (Heuser and Doggenweiler, 1966). Usually, however, crustacean nerves have only unmyelinated axons (Bullock and Horridge, 1964). Consequently in cross-sections, snapping shrimp nerves prominently display numerous, large Schwann cell nuclei characteristic of myelinated axons (Fig. 5A). At a higher magnification, myelinated axons are readily distinguishable from their unmyelinated counterparts, because the myelin forms a dense sheath around the axon (Fig. 5B). The unmyelinated axons are wrapped by glial sheaths to different degrees, depending on their size. The

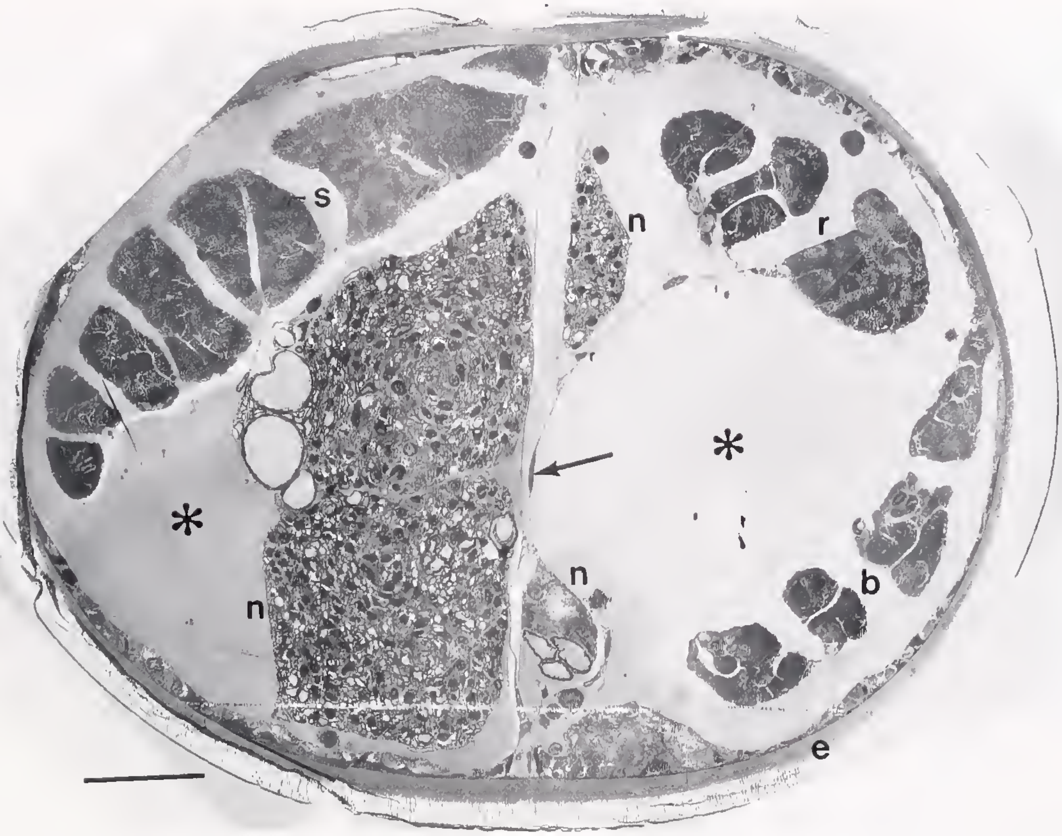

Figure 3. Cross-section through the first carpal segment with an exoskeleton (e) boundary and the interior separated into two compartments (asterisks) by a thin septum (arrow). One compartment has the stretcher (s) muscle and a large branch of the limb nerve (n) while the other compartment has the bender (b) and rotator (r) muscles and two smaller nerve (n) branches. Scale bar: 50 μm.

smaller axons are naked, whereas the larger axons have several layers of glial covering.

Because most of the axons in the nerves are sensory, we can estimate the sensory innervation from the limbs by counting the total number of axons close to the ganglion. Such counts were made in two animals, and the results were similar in both cases (Table I). The total numbers of axons on the right and left sides are almost equal. There is also an equal distribution between myelinated and unmyelinated axons on the right and left sides in each of the two animals.

To determine how the numbers of axons in the second limbs compare to those of the highly specialized and asymmetrical first thoracic limbs or chelipeds, counts were also made of the nerves to the pincer and snapper chelipeds (Table I). The present counts of numbers of axons to the snapper and pincer nerves confirms previous findings; the snapper side has more axons than the pincer side (Govind and Pearce, 1988).

Comparison between the first and second limbs reveals that the second limb has a much smaller number of axons than either the pincer or the snapper (Table I). In shrimp #1, for example, the second thoracic limb has 6000 axons, whereas the snapper on the first limb has over 13,000 axons and the pincer has 10,000 axons. In terms of total numbers of axons, the snapper has the largest number, followed by the pincer, and then the second thoracic limbs, which have the smallest number. The distribution of unmyelinated and myelinated axons is interesting; the first thoracic limbs (both the pincer and the snapper) have more (60–70%) unmyelinated than myelinated axons, whereas the second limbs have an equal number of myelinated and unmyelinated axons.

The above counts of axons taken close to the ganglion represented the total number to the limb, including those to the thorax at the base of the limb. Because we were interested largely in the multisegmented carpus, we counted the axons in the nerve running through the distal segments of a second thoracic limb. In all cases, counts were made from the most distal end of each segment. As anticipated, the axon number increased progressively, beginning at 1500 in the propus, to 1700 in the fourth carpal segment, to 2000 in the second carpal segment, to 2400 in the merus. The difference in number between the pro-

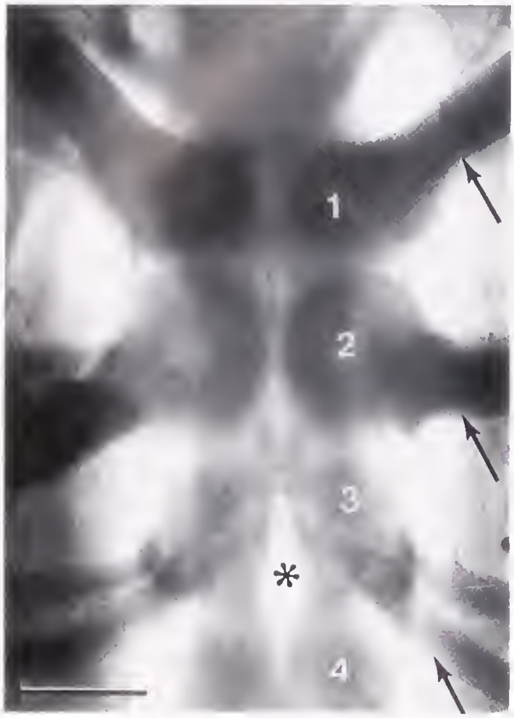

Figure 4. Photomicrograph of the thoracic nervous system in a freshly dissected shrimp, showing the paired hemiganglia to the first (1), second (2), third (3), and fourth (4) thoracic limbs, the nerves (arrows) from these hemiganglia and the opening (asterisk) for the dorsal artery in the connective between the third and fourth ganglia. Note the larger size of the second ganglia compared to the first or third. Scale bar: 250 μm.

pus and merus of 1000 represents the number of sensory axons originating in the multisegmented carpus.

B. Connectives. Apart from the nerves, the only other external source of neural input to the ganglia is via the connectives (Fig. 4). Therefore the number of axons that enter the ganglia via the connectives may be estimated by counting axon profiles in both the anterior and posterior connectives to the ganglion, as this would encompass both ascending and descending inputs. Consequently, counts were made in two animals, of the connectives anterior to the first, second, and third thoracic ganglia to estimate the anterior and posterior inputs to the first and second thoracic ganglia (Table II). The number of axons in the paired, left and right connectives at each of the three sampling stations were highly symmetrical. But the number in each of the three sampling stations was distinct, indicative of the relative degree of neural traffic to and from each of the first and second thoracic ganglia. Because the direction of the neural traffic—*i.e.,* whether it is ascending, descending or through-going—cannot be distinguished in these cross-sections of the connectives, the numbers from the anterior and posterior connectives were simply added as an estimate of the input into each of the first and second thoracic ganglia. The second thoracic ganglion had a higher number than the first, approximately 4000 *versus* 3000 axons, suggesting that the neural input is greater to the second thoracic ganglion than to the first.

Behavior

Both casual and formal observations of adult snapping shrimps in glass aquaria show the second thoracic limbs to be almost constantly active, primarily in probing the environment and, to a lesser degree, in grooming body parts. Probing is the rapid, jerky touching of the substrate or other objects by the chelae of the flexible limb. This is greatly facilitated by the multi-segmented carpus, which gives the limb enhanced flexibility, allowing it to probe deeply into the benthic crevices.

Probing occurs when the shrimp are crawling (backwards and forwards), burrowing (shovelling substrate with pereiopods, pleopod beating of substrate), or just standing still (including pleopod beating of the water).

Grooming involves picking at various parts of the body with the rapidly opening and closing chelae of the flexible limbs. Although virtually every part of the body is accessible, the most frequently groomed areas include the rostrum, gills, ventral thorax and abdomen (including pleopods), and the large chelae.

The flexible limb also retrieves and brings food to the mouth. Occasionally these limbs lifted and carried relatively heavy objects, such as large pebbles.

Time budget. As mentioned previously, one of the most striking aspects of the flexible limbs was their almost constant activity. This is reflected in the time budget analysis (Table III), which shows these limbs as being active 95% of the time and inactive only 5%. The majority (77%) of this activity was devoted to probing the substrate, be it sand or gravel. Moreover, immobilizing the carpal segments, by gluing them, had little effect on the probing activity. Probing occurred whether the shrimp was stationary, crawling, or burrowing, and the time devoted to this activity was approximately similar for each of the three states.

Grooming was the only other activity that occupied a significant amount of the time of the flexible limbs, although the time occupied (13%) was considerably smaller than that spent in probing. Grooming was confined principally to the head region.

Foraging experiments. The flexible limbs were actively engaged in foraging for food, the introduction of which caused very intense probing activity. When found, food was retrieved and brought to the mouthparts exclusively by the flexible limbs. Sometimes, the food was held by the pincer while bits were torn off by the flexible limb chelae, and the pincer was occasionally used to push the food into the sand. Rarely, jets of water produced by closure of the snapper were used to uncover food.

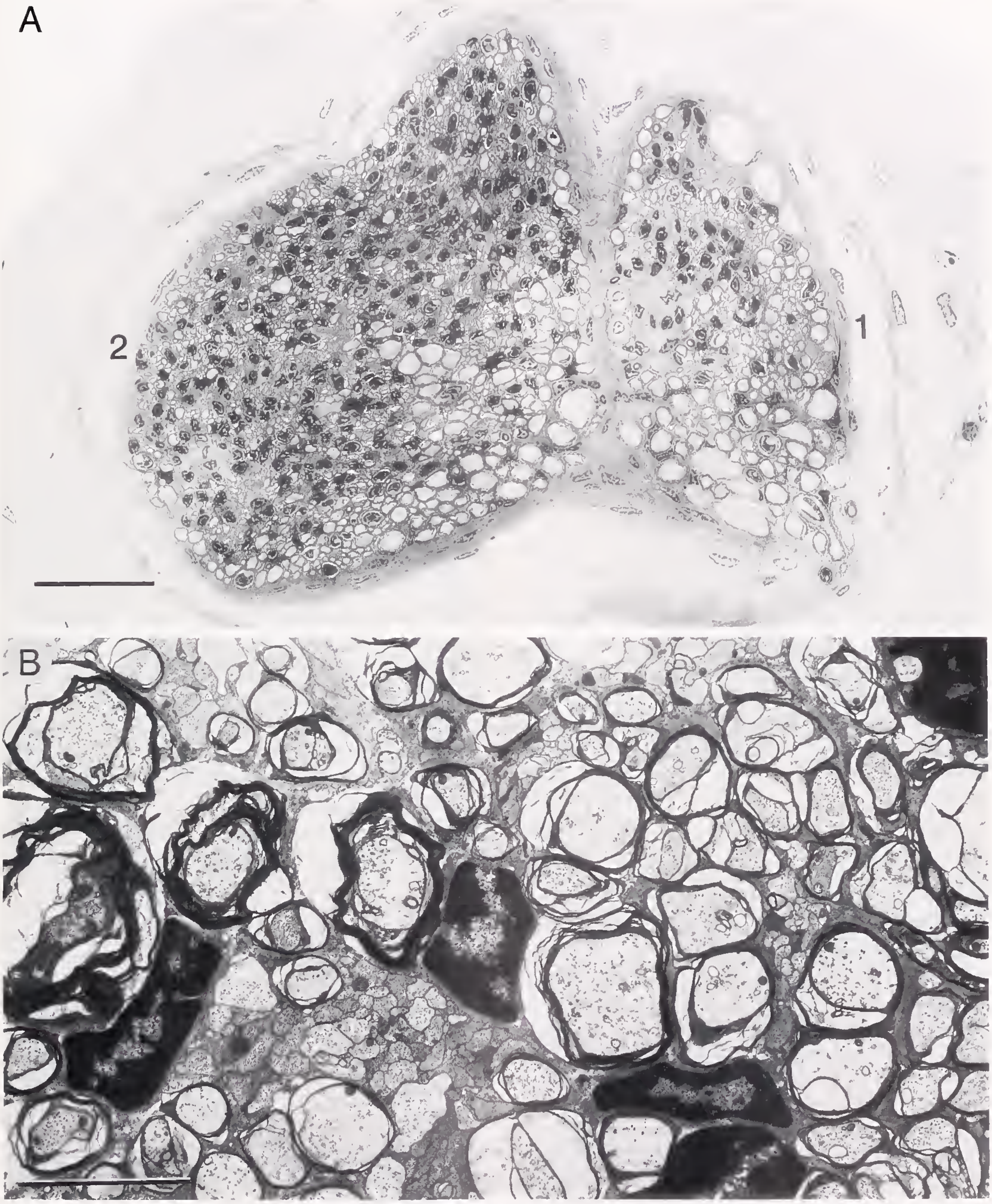

Figure 5. (A) Cross-section of the small first (1) and large second (2) nerves at the base of the hemiganglion to a second thoracic limb; each nerve has tightly packed axons and prominent nuclei of Schwann cells. (B) Representative area of the nerve cross-section showing clusters of small unmyelinated axons which are naked while myelinated axons have a densely stained sheath and scattered dense staining nuclei. Scale bars: A, 50 μm; B, 5 μm.

Table I

Number of axon profiles in the paired (right and left) nerves to the first and second thoracic limbs in two snapping shrimps

Thoracic limbs	Myelinated	Unmyelinated	Both
	Shrimp #1		
First thoracic limb			
right (pincer)	4071	6441	10512
left (snapper)	4286	8722	13008
Second thoracic limb			
right	3197	3072	6269
left	2885	3117	6002
	Shrimp #2		
First thoracic limb			
right (pincer)	3247	6214	9461
left (snapper)	4637	9232	13869
Second thoracic limb			
right	3451	3880	7331
left	3691	3791	7482

To evaluate the role of the second thoracic limbs in locating and retrieving food, these functions were compared in two groups of 10 shrimp each. The flexible limbs of the first group were intact; they were autotomized in the second group. In 21 separate trials, the intact shrimps were able to locate and retrieve the concealed food in all cases. The time taken to locate the food was 72 ± 18 s (SEM), and to retrieve it with the second thoracic limbs added only a few more seconds (80 ± 18 s SEM). Unexpectedly, the autotomized shrimps, in 17 out of 19 separate trials, successfully located the concealed food and the time taken was 115 ± 24 s (SEM) which was not significantly different (Students *t*-test) from the time for the intact group. The food location was done by frequent and direct contact of the substrate with the mouthpart region, *i.e.*, substrate pressing. However, once the food was located via such substrate pressing, the shrimps were unable to retrieve it because the second thoracic limbs were missing. Only in exceptional cases, and with the persistent use of other appendages, were the autotomized shrimps able to retrieve the food placed in the coral. Clearly, the second thoracic limbs were not required in locating concealed food, but were indispensable for retrieving it.

Conspecific interactions. To determine the role of the second thoracic limbs in conspecific interactions, observations were made of male/female and male/male pairs. The flexible limbs appeared to play little part in hetero- or homosexual interactions, and, in fact, during such encounters, the limbs were held reflexed posteriorly in a locked position, completely out of the way.

Table II

Number of axon profiles in the paired (left and right) connectives to the first and second thoracic ganglia in two snapping shrimps

Thoracic ganglia	Connectives		Total (right and left)	Total (anterior and posterior)
	left	right		
		Shrimp #1		
First thoracic	403	443	846	3293 to first ganglion
Second thoracic	1187	1260	2447	4169 to second ganglion
Third thoracic	876	846	1722	
		Shrimp #2		
First thoracic	486	454	940	3137 to first ganglion
Second thoracic	1087	1110	2197	4348 to second ganglion
Third thoracic	1120	1031	2151	

Discussion

The chitinized exoskeleton of crustaceans restricts flexibility within a limb to its segmental joints. Hence the unusual occurrence of a multisegmented carpus in the second thoracic limb of the snapping shrimp, *Alpheus heterochelis,* makes this limb particularly adept at exploratory behavior, food gathering, and grooming. Such behaviors occur constantly and are subserved by a ganglion which is larger than its neighbors. This size difference is related to the greater number of axon profiles in the longitudinal connectives to this ganglion than to the neighboring ganglia. The significance of these findings concerning the external and internal morphology of the second thoracic limbs and their behavior are discussed below.

Table III

Time budget for activities related to the second thoracic limbs in snapping shrimps

	% of time		
	Sand	Gravel	Overall
Probing:			
total	79.5	75.1	77.0
burrowing	16.8	32.3	24.6
crawling	34.1	20.5	27.3
stationary	28.6	22.2	25.2
Grooming:			
total	16.3	10.4	13.3
head	12.1	7.4	9.8
chelae	2.5	1.0	1.7
abdomen	1.7	2.0	1.9
Miscellaneous	3.0	6.7	4.8
Inactive	1.2	8.4	4.8
Number animals/observations	6/405	6/405	12/810

Morphology

The features of the second thoracic limb in the snapping shrimp, *Alpheus heterochelis*, that prompted this study were: its multisegmented carpus, its unusual flexibility, and its ganglion, which is larger than that of its neighbors. The first two are directly related, in that division of the carpus into five segments makes the limb highly flexible. The extent to which this specialization in the structure and function of the second thoracic limb regulates the size of its ganglion is somewhat more difficult to resolve. A simple possibility was that the input to the ganglion would regulate its size, and we tested this possibility by counting the number of axon in the limb nerve and the longitudinal connectives to this ganglion.

Numbers of axons in nerves. Cross-sections of nerves to the thoracic ganglia in several crustaceans reveal thousands of axon profiles of varying diameters, with the majority being small (<5 μ) (Sutherland and Nunnemacher, 1968; Govind and Pearce, 1985). Some of the large profiles are presumably motor axons, and these are comparatively few because crustacean limb muscles are innervated by only a few (1–5) motor axons (Govind and Atwood, 1982). For each of the distal segments of the limb—the merus, carpus, and propus—there are typically two antagonistic muscles, and each muscle is innervated by 2–5 axons; thus there are altogether about 30 axons. Another 30 motor axons would account for the more proximal muscles of the limb, making a total of 60 motor axons. This number is a very small percentage of the thousands of axons counted in the nerves.

The vast majority of axons in these nerves are presumably sensory. Consequently, counting axon profiles in these nerves provides an index of the sensory input to the ganglion. Furthermore, because the size of the ganglion will, in part, be governed by the sensory input, differences in the axonal counts between the first and second thoracic limbs may underlie the differences in size of the respective ganglia.

The correlation we find between axon numbers and size in the snapping shrimp hemiganglia is a negative one, however. The chelipeds, both of which have a substantially larger number of axons (9,000 and 13,000), are each associated with a smaller ganglion than that of the second thoracic limbs. Therefore, as a first approximation, the peripheral input to the ganglia cannot explain the size differences between the first and second ganglia.

Alternatively, the size differences between the ganglia might be attributed to the extra carpal segments in the second thoracic limb; there are five of these, compared to only one carpal segment in the chelipeds. Each of the five carpal segments in the second thoracic limb has at least three muscles, and they may receive their own motor axons. If this were the case, and assuming that each muscle receives a minimum of two axons, the extra segments would add an additional 24 motor axons. Because each motor axon extends a dendritic tree within the neuropil, it is likely that the addition of 24 motor axons would increase the size of the neuropil.

Numbers of axons in the connectives. Apart from peripheral nerves, the only other source of nerve input to the ganglia is via the connectives. The total input to each of the ganglia was estimated by simply adding the numbers of axons in the connectives anterior and posterior to each ganglion; ascending and descending input could not be distinguished. A positive correlation was seen between axon numbers and the size of the ganglia, as there were 4000 axons to the second thoracic ganglion, and 3000 axons to the first ganglion. This 25% difference is close to the 25–30% difference in the size of the hemiganglia.

In summary, the greater size of the second thoracic ganglion, relative to its first thoracic counterpart, is not simply due to differences in the number of sensory axons from the periphery to the ganglion. Consequently, it must be due to central factors. Finding a greater number of axons in the ventral connectives to the second thoracic ganglion, compared to the first, is consistent with this conclusion. The exact nature of these central features is unknown, but they may be related to the specialized nature of the second thoracic limb as a highly flexible mechanosensory "arm" capable of delicate movements. Consequently, we may anticipate additional motor axons, as in the extra carpal segments, a higher concentration of proprioceptors and, perhaps, a higher concentration of interneurons emanating from the ganglion. All of these features would contribute to increasing the size of the ganglion.

Behavior

Nolan and Salmon (1970) observed that *A. heterochelis* spent most of its active time grooming. In contrast, we found that the overwhelming majority of time was spent probing. Undoubtedly though, the flexible limbs are vitally important in both functions and are in almost constant motion, whether the shrimp is burrowing, crawling (walking), cleaning, feeding, or stationary. The ability to effectively "put them away" during agonistic encounters perhaps underscores their importance.

Food foraging. Animals that had autotomized their flexible limbs were at a great disadvantage in foraging for food. The ability to find concealed and hard-to-get-at food would obviously be beneficial in the coral reefs, oyster beds, and sponges frequently inhabited by *A. heterochelis* (Brooks and Herrick, 1892). Since alpheid shrimps spend much time actively browsing across the substrate, using their flexible limb chelae as probes and micromanipulators, this is likely an important means of foraging. In this respect they are similar to prawns (Hindley and Alexander, 1978). However, alpheid shrimps are reported to stun prey such as other shrimps (McLaughlin, 1982) or to crack open clam shells by means of their snap. This would be another means of foraging, although the availability of such large prey would likely be insufficient to support a dense population of shrimps (Dahl, 1968).

Autotomized shrimp easily located concealed food, suggesting that the limbs are not important for olfaction. Indeed, the flexible limb has relatively few external sensilla, even taking into account their small size. Those seen were similar to sensilla observed on the chelipeds (Read and Govind, 1990). Functions of the flexible limb sensilla, probably related to foraging, may include contact chemoreception (*i.e.*, taste as opposed to olfaction), contact mechanoreception, and perhaps texture sensitivity.

Grooming. Grooming reduces the incidence of epizoic and sediment fouling, which could seriously affect the health and sensory and locomotory abilities of individuals and increase the mortality of brooding embryos (Bauer, 1975, 1979). *A. heterochelis*, in particular, is parasitized by a conspicuous epicaridean isopod. Seen in about 2% of captured specimens, this parasite lodges in the ventral surface of the abdomen (pers. obs.), undoubtedly impairing the reproduction, if not the health and the molt cycle of affected animals. Obviously, grooming would be important in discouraging this parasite. In addition, *A. heterochelis* hosts another parasite which was a sac-like organism filled with eggs and which lodges beneath the carapace in the thoracic region, an area which is subject to very frequent grooming. Molting, which occurs every 18–25 days, does not rid the shrimp of either the abdominal or thoracic parasites, thereby underscoring the importance of grooming.

Acknowledgments

We thank Blair Feltmate for advice on the behavior experiments, Bill Kirby-Smith for collecting snapping shrimps, and Christine Gee and Joanne Pearce for animal rearing and maintenance and for criticism of the study. Financial support was provided by the Natural Sciences and Engineering Research Council of Canada.

Literature Cited

Atwood, H. L., F. Lang, and W. A. Morin. 1972. Synaptic vesicles: selective depletion in crayfish excitatory and inhibitory axons. *Science* **176:** 1353–1355.

Bauer, R. T. 1975. Grooming behavior and morphology of the caridean shrimp *Pandalus danae* Stimpson (Decopoda: Natantia: Pandalidae). *Zool. J. Linn. Soc.* **56:** 45–71.

Bauer, R. T. 1979. Anti fouling adaptations of marine shrimp (Decapoda: Caridea): gill cleaning mechanisms and grooming of brooded embryos. *Zool. J. Linn. Soc.* **65:** 281–303.

Brooks, W. K., and F. H. Herrick. 1892. The embryology and metamorphosis of the Macrura. *Mem. Nat. Acad. Sci.* **5:** 322–576.

Bullock, T. H., and G. A. Horridge. 1964. *Structure and Function in the Nervous System of Invertebrates.* W. H. Freeman & Co., San Francisco.

Dahl, W. 1968. Food and feeding of some Australian peneid shrimp. *F. A. O. Fish Rep.* **57:** 251–258.

Govind, C. K., and H. L. Atwood. 1982. Organization of Neuromuscular Systems. Pp. 63–103 in *The Biology of Crustacea,* Vol. 3, *Neurobiology: Structure and Function,* H. L. Atwood and D. C. Sandeman, eds. Academic Press, New York.

Govind, C. K., and J. Pearce. 1985. Lateralization in the number and size of sensory axons to the dimorphic chelipeds of crustaceans. *J. Neurobiol.* **16:** 111–125.

Govind, C. K., and J. Pearce. 1988. Remodelling of nerves during claw reversal in adult snapping shrimps. *J. Comp. Neurol.* **268:** 121–130.

Heuser, J. E., and C. F. Doggenweiler. 1966. The fine structural organization of nerve fibers, sheaths, and glial cells in the prawn *Palaemonetes vulgaris. J. Cell Biol.* **30:** 381–403.

Hindley, J. P. R., and C. G. Alexander. 1978. Structure and function of the chelate pereiopods of the banana prawn *Penaeus merguiensis. Mar. Biol.* **48:** 153–160.

Lehner, P. N. 1979. *Handbook of Ethological Methods.* Garland STPM Press, New York.

McLaughlin, P. A. 1982. Comparative morphology of crustacean appendages. Pp. 197–256 in *The Biology of Crustacea,* Vol. 2, *Embryology, Morphology and Genetics,* D. E. Bliss, ed. Academic Press, New York.

Mellon, DeF., Jr., and P. J. Stephens. 1980. Modification in the arrangement of thick and thin filaments in transforming shrimp muscle. *J. Exp. Zool.* **213:** 173–179.

Nolan, B. A., and M. Salmon. 1970. The behaviour and ecology of snapping shrimp (Crustacea: *Alpheus heterochelis* and *Alpheus normanni*). *Forma Functio* **2:** 289–335.

Pearce, J., C. K. Govind, and R. R. Shivers. 1986. Intramembranous organization of lobster excitatory neuromuscular synapses. *J. Neurocytol.* **15:** 241–252.

Prizbram, H. 1901. Experimentell Studien über Regeneration. *Arch. Entwick. Mech.* **11:** 321–345.

Phillips, C. E., J. A. Wilson, and DeF. Mellon, Jr. 1982. A comparative study by serial section electron microscopy of neuromuscular junctions in the dimorphic claws of the snapping shrimp, *Alpheus heterochelis. J. Neurobiol.* **13:** 495–505.

Read, A. T., and C. K. Govind. 1990. Composition of external setae during regeneration and transformation of the bilaterally asymmetric claws of the snapping shrimp, *Alpheus heterochelis. J. Morphol.* **207:** 1–9.

Ritzmann, R. 1974. Mechanisms for the snapping behavior of two Alpheid shrimps, *Alpheus californiensis* and *Alpheus heterochelis. J. Comp. Physiol.* **114:** 91–101.

Schmitt, W. L. 1975. *Crustaceans.* University of Michigan Press, Ann Arbor.

Sutherland, R. M., and R. F. Nunnemacher. 1968. Microanatomy of crayfish thoracic cord and roots. *J. Comp. Neurol.* **132:** 499–518.

Wiersma, C. A. G. 1961. The Neuromuscular System. Pp. 191–240 in *The Physiology of Crustacea,* T. H. Waterman, ed. Academic Press, New York.

Wilson, E. B. 1903. Notes on the reversal of asymmetry in the regeneration of chelae in *Alpheus heterochelis. Biol. Bull.* **4:** 197–210.

Reference: *Biol. Bull.* **181:** 169–174. (August, 1991)

Ecdysteroid Treatment Delays Ecdysis in the Lobster, *Homarus americanus*

JIN-HUA CHENG[1] AND ERNEST S. CHANG[2]

Bodega Marine Laboratory, University of California, P. O. Box 247, Bodega Bay, California 94923

Abstract. Premolt stage D_3 of juvenile lobsters, *Homarus americanus,* was further divided into five substages according to the degree of cuticle digestion along the dorsal midline of the carapace and on the dorsal surface of the merus of the chelipeds. The mean times to ecdysis for intact lobsters (5.5 ± 1.1 g) at each substage were 71.4, 57.7, 30.0, 16.1, and 6.6 h, respectively. The level of ecdysteroids dropped continuously during stage D_3, from 0.5 μg/ml at substage 1, to less than 0.1 μg/ml at substage 5. Injections of 20-hydroxyecdysone (20-HE) (1.0 or 5.0 μg/g) delayed ecdysis in animals receiving an injection at substages 3 or 4, but not 1, 2, or 5. The staging method can be applied to eyestalk-ablated (ESX) lobsters as well; but those animals complete stage D_3 and molt much more rapidly. In addition to the time of ecdysis, the rate of development (based on the degree of cuticle digestion) in both intact and ESX lobsters was decreased by injections of 20-HE. We conclude that decreased ecdysteroid titers in the hemolymph of lobsters is a prerequisite to the initiation of ecdysis, and that rates of development during stage D_3 are regulated negatively by ecdysteroids. We suggest that the time of ecdysis is controlled in lobsters through the regulation of the rate of decline of ecdysteroid titers.

Introduction

Like most other crustaceans, lobsters (*Homarus americanus*) increase their body size by molting. Before each molt, the inner layers of the old cuticle are reabsorbed, and the outer layers of the new cuticle are synthesized underneath the old one (Skinner, 1985, for review). Shedding the cuticle at ecdysis is accompanied by a sudden increase in body weight because of rapid water uptake (Mykles, 1980). This water occupies the space made available by the larger and more pliable new cuticle synthesized before molt. The enlarged space is needed for subsequent tissue growth prior to the next molt. This cyclic event, which is repeated throughout the life of many crustaceans, is under the control of ecdysteroids (molting hormones) (Chang, 1989, for review).

In lobsters, as in many other crustaceans, the ecdysteroid level rises during early premolt and reaches its peak at late stage D_2, or early D_3, then drops to a low level immediately before ecdysis (Chang and Bruce, 1980, 1981; Chang and O'Connor, 1988). A similar ecdysteroid profile has been found in insects (Steel and Vafopoulou, 1989, for review). In both insects and crustaceans, the rising titers of ecdysteroids initiate the cascade of events that culminate in ecdysis (Skinner, 1985; Chang, 1989). In addition, decreasing titers of ecdysteroids in late premolt are necessary for the initiation of ecdysial behavior in some insects (Sláma, 1980; Truman *et al.*, 1983; Reynolds, 1986; Zdarek and Denlinger, 1987).

Injections of ecdysteroids during late premolt inhibit ecdysis in some amphipods (Graf, 1972a, b). Similar results, though, have not been obtained in other crustacean species (Skinner, 1985, for review). One possible explanation for these negative results is that injections were not made at the right time. In an insect, *Manduca sexta*, injections made before or after the critical period have no effect on the time of ecdysis (Truman *et al.*, 1983). The lack of a precise staging method for crustaceans in late premolt may have prevented the discovery of an analogous critical period.

In insects, decreasing titers of ecdysteroids prior to molt not only regulate the time of ecdysis itself, but also modulate the rate of premolt development (Schwartz and Truman, 1983). Although crustaceans can regulate the

Received 20 December 1990; accepted 8 April 1991.

[1] Present address: Tungkang Marine Laboratory, Tungkang, Pingtung, Taiwan 928, Republic of China.

[2] To whom all correspondence should be addressed.

time of ecdysis to varying degrees (Skinner, 1985), a study comparable to that in insects has not yet been conducted.

During the last few days before ecdysis, certain regions of the cuticle are digested to a greater extent than others, enabling the lobster to shed its old exoskeleton. In our study, we developed precise staging criteria for stage D_3 lobsters. The time of ecdysis during the last three days of the molt cycle could be predicted on the basis of these criteria. In addition, the effect of injecting 20-hydroxyecdysone on the rate of cuticle digestion and the time of ecdysis was investigated.

Materials and Methods

Maintenance of animals

Two families of full-sibling juvenile *Homarus americanus* (5.5 ± 1.1 and 3.2 ± 0.7 g wet weight; mean ± S.D.) were used for these experiments. The lobsters were raised in a semi-recirculating system at 20.0 ± 0.5°C on a diet of live adult brine shrimp (Chang and Conklin, 1983; Conklin and Chang, 1983). The photoperiod was 16L:8D.

Molt prediction

Before stage D_3, intact and eyestalk-ablated (ESX) lobsters (5.5 g) were staged based on the setal development of the pleopods (Aiken, 1973). Stage D_3 lobsters, about three days before molt, were further subdivided into five substages, based on the degree of cuticle breakdown along the dorsal midline of the carapace, and on the dorsal surface of the merus of the chelipeds (Table I). These are areas where extensive cuticle digestion occurs prior to ecdysis. For staging, the lobster's dorsal carapace was wiped dry and evaluated with a dissecting microscope.

Exogenous ecdysteroid injection

Intact lobsters (5.5 g) at various substages of stage D_3 received a single injection (0.2, 1.0, or 5.0 μg/g wet weight) of 20-hydroxyecdysone (20-HE; Rohto Pharmaceutical; purity checked by high-performance liquid chromatography before use). Control animals received vehicle only (lobster saline; Mykles, 1981).

ESX lobsters (3.2 g) were used for one injection study. Both eyestalks were removed from stage B–C animals, with fine scissors, about 5–10 days after molting. When animals were approaching the first postoperative molt, they were staged by the same method described above and injected with lobster saline, either containing 20-HE or not. Only one dose of 20-HE (1.0 μg/g wet wt.) was used per animal in these experiments. The time between injection and ecdysis was recorded on time-lapse video with a time stamp.

Endogenous ecdysteroid determination

Before injection, a hemolymph sample (25 μl) was taken from each animal and the content of its endogenous ecdysteroids determined quantitatively by radioimmunoassay (Chang and O'Connor, 1979); the IB-4 antiserum from Dr. W. E. Bollenbacher was used (University of North Carolina, Chapel Hill).

Rate of development

The effect of ecdysteroid titers on the rate of progression through the D_3 substages was investigated. Lobsters (5.5 g for both intact and ESX animals) received an injection of 20-HE (1.0 μg/g), once per day, starting from substage 1 of stage D_3. The rates of development were recorded twice daily based on criteria described in detail below.

Results

Stage D_3 was divided into five substages according to the degree of the cuticular digestion in the regions shown in Figure 1. At substage 1, only the posterior region of the dorsal midline of the carapace shows signs of digestion. This is manifested as a narrow crack that starts at the posterior end of the midline and proceeds anteriorly about one-third of its total length.

At substage 2, another narrow crack appears in the dorsal midline of the carapace. It starts from the anterior of the carapace and proceeds posteriorly to about one-third of the total length of the dorsal line.

At substage 3, the narrow crack forms along the entire dorsal midline. At substage 4, the crack widens to occupy the entire width of the dorsal midline along the posterior two-thirds of its length. At substage 5, the crack widens along the entire length of the midline. Also, the dorsal surface of the merus of each cheliped becomes soft (Table I).

The times to ecdysis for animals in substages 1 to 5 are given in Table I. Although the molt-staging technique can be applied to ESX lobsters, these animals spend much less time in each substage (Table I). The levels of the ecdysteroids in the hemolymph of intact lobsters drop continuously during stage D_3, from 0.55 μg/ml at substage 1, to less than 0.1 μg/ml at substage 5 (Fig. 2).

The role of ecdysteroids in regulating the time of ecdysis was examined by injecting stage D_3 lobsters with various doses of 20-HE. Lobsters were divided into the five substages as described. Each animal received a single injection of lobster saline, with or without 20-HE. A low dose (0.2 μg/g) of 20-HE did not significantly delay ecdysis in animals receiving the 20-HE injection at any substage (Fig. 3). High doses (1.0 and 5.0 μg/g) delayed ecdysis in animals receiving an injection at substages 3 and 4, but not 1, 2, or 5 of stage D_3.

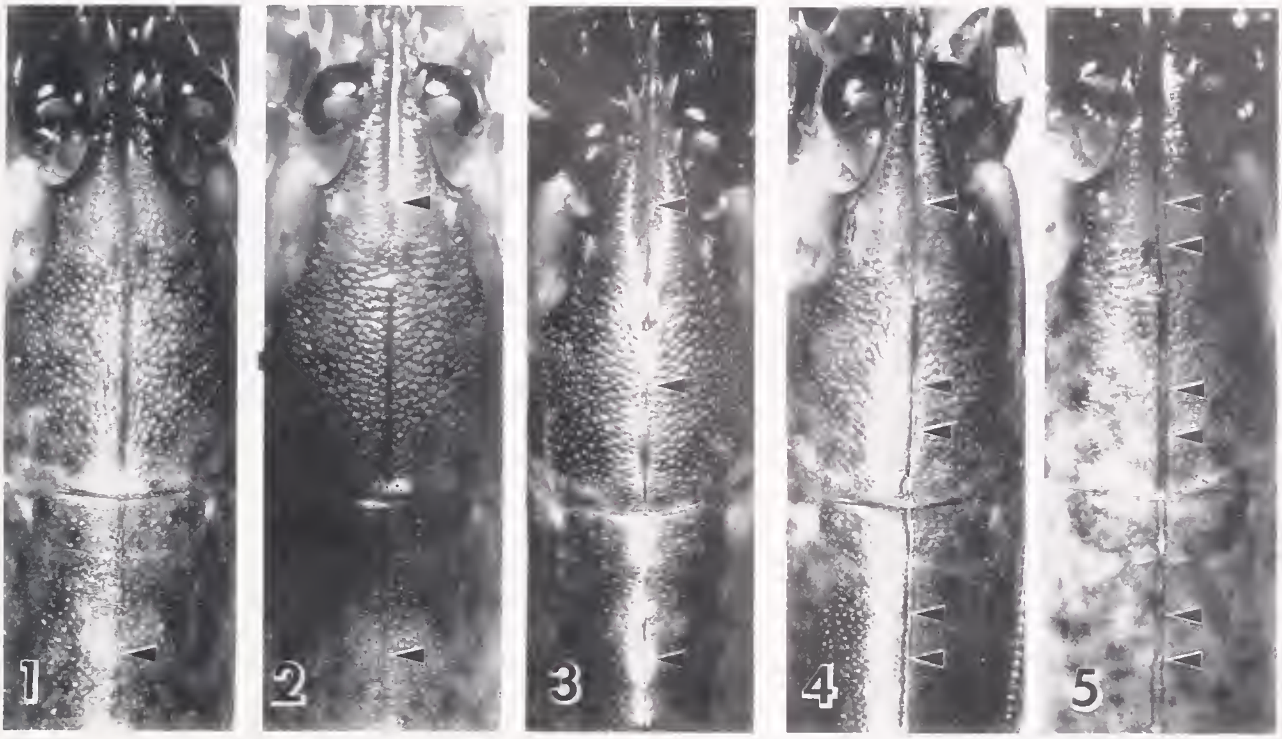

Figure 1. Carapace of juvenile lobsters, *Homarus americanus*, showing the progress of cuticular digestion along the dorsal midline. Single arrow indicates slight digestion. Double arrows indicate heavy digestion (see Table 1). The numbers indicate the substages of D_3. Field of view is approximately 7 × 20 mm.

Ecdysis of ESX lobsters receiving an injection of 20-HE was also delayed (Fig. 4). Ecdysis was delayed in all lobsters receiving a 20-HE injection at substages 1 or 2, and in seven of nine lobsters at substage 3, but in none of the lobsters at substages 4 and 5. The unresponsiveness of the two lobsters (at substage 3) to the 20-HE injections might have been due to lower ecdysteroid titers (0.18 and 0.28 μg/ml) than the other seven animals (range of 0.35 to 0.66 μg/ml). These two animals may have been approaching substage 4.

Injection of 20-HE not only delayed ecdysis, but also depressed the rate of development. This was assayed by the degree of cuticle digestion over time in both intact and ESX lobsters (Fig. 5).

Table I

Substages of D_3 based upon cuticle digestion in both intact and eyestalk-ablated juvenile Homarus americanus *(5.5 g) at 20°C*

	Cuticle digestion at				Hours before ecdysis (n) (mean ± S.E.)	
	Dorsal midline of carapace					
Substage of D_3	Anterior region	Central region	Posterior region	Dorsal surface of merus of cheliped	Intact	Ablated
1	–	–	+	hard	71.4 ± 9.5 (9)	32.4 ± 8.2 (8)
2	+	–	+	hard	57.7 ± 4.0 (9)	21.8 ± 5.4 (6)
3	+	+	+	hard	30.0 ± 6.0 (6)	10.8 ± 5.0 (6)
4	+	++	++	hard	16.1 ± 2.0 (7)	6.0 ± 1.0 (4)
5	++	++	++	soft	6.6 ± 0.7 (7)	4.2 ± 2.3 (5)

– Indicates digestion absent, + indicates slight digestion (width of the crack is less than the width of the dorsal line), ++ indicates heavy digestion (width of the crack is wider than the width of the dorsal line).

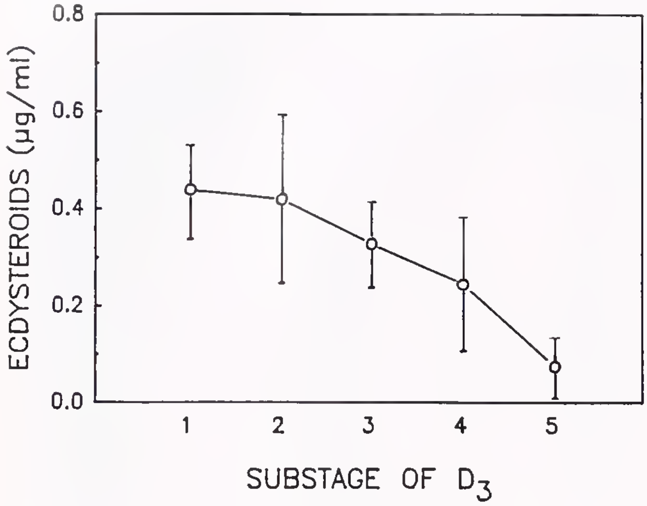

Figure 2. Ecdysteroid titers in the hemolymph of intact 5.5 g lobsters, plotted against substage of D_3 (means ± 1 S.D.). Each datum point represents 10–19 animals.

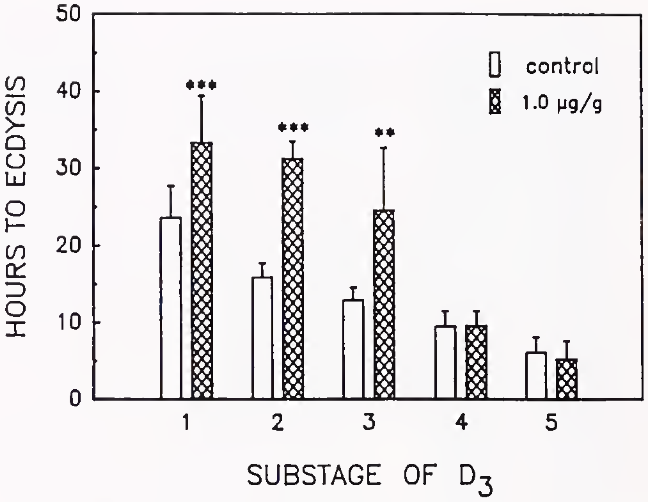

Figure 4. The effect of 20-HE injection (1.0 µg/g) on time of ecdysis in eyestalk-ablated 3.2 g lobsters (means ± 1 S.D.). Animals received a single injection of saline with or without 20-HE at the stage indicated. The time of ecdysis was recorded using time-lapse video. Asterisks (** and ***) indicate significant differences ($P < 0.01$ and 0.001, respectively). Each group contained 6–12 animals.

Discussion

Intensive cuticle digestion along the dorsal midline of the carapace starts about three days before ecdysis and permits lateral expansion of the carapace at ecdysis. The intensive cuticle digestion on the dorsal surface of the merus of the chelipeds permits lobsters to withdraw their large chelipeds through the narrow basiischial joints. Cheliped withdrawal is also facilitated by the differential degeneration of cheliped muscle tissue (Mykles and Skinner, 1981) and active water uptake (Mykles, 1980; Cheng, 1990).

Our molt-staging technique, based on cuticle digestion, reliably predicted the time of ecdysis, which was critical for this study. This technique should also be applicable to other species, for research and for the commercial production of soft-shell crustaceans.

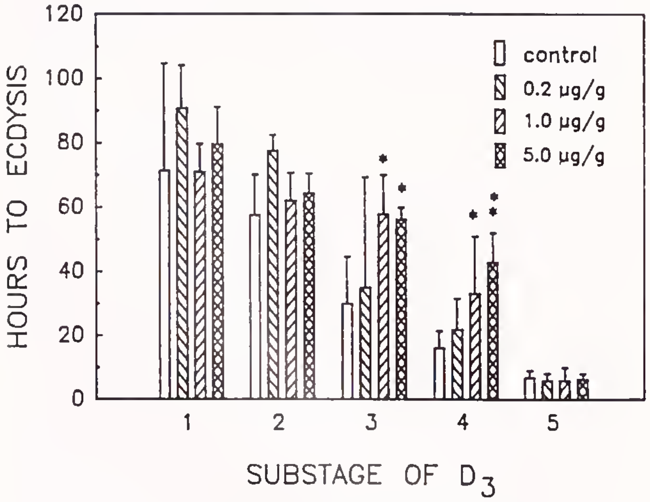

Figure 3. The effect of injection of various concentrations of 20-HE (0, 0.2, 1.0, or 5.0 µg/g) on time of ecdysis in intact 5.5 g lobsters (means ± 1 S.D.). Animals received a single injection of saline with or without 20-HE at the stage indicated. The time of ecdysis was recorded using time-lapse video. Asterisks (* and **) indicate significant differences ($P < 0.05$ and 0.01, respectively). Each group contained 7–9 animals.

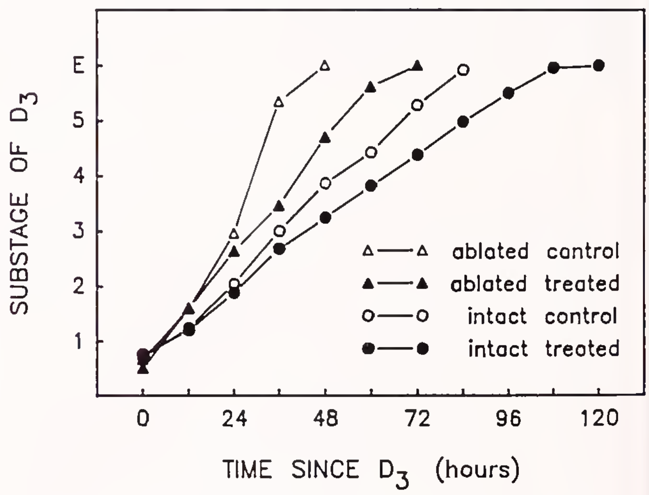

Figure 5. The effect of 20-HE injection on the rate of cuticle digestion in intact and eyestalk-ablated 5.5 g lobsters. Animals received an injection of saline with (treated) or without (control) 20-HE (1.0 µg/g) every 24 h, starting from substage 1. The stage of cuticle digestion was subsequently checked every 12 h. Each group contained 7–12 animals. E indicates ecdysis.

We observed that ecdysteroid titers continued to decline during the last three days of the molt cycle. Similar results have been reported for juvenile lobsters in our laboratory (Chang and Bruce, 1980, 1981). The mechanisms responsible for the decline are not clear, but a decrease in the rate of production of ecdysteroid by the Y-organ may be the predominant means of controlling the declining hormone titers. Evidence for this is the observation that the secretory rate of ecdysteroids by the Y-organs of *Pachygrapsus crassipes in vitro* was correlated with circulating ecdysteroid concentrations (Chang and O'Connor, 1978). Both negative and positive short-loop feedback mechanisms have been demonstrated in the prothoracic glands of *Manduca sexta* (Sakurai and Williams, 1989), and similar mechanisms may operate in Y-organs of crustaceans as well. In addition, increased rates of degradation of ecdysteroids in late premolt may play an important role in regulating the declining titers of ecdysteroids (Snyder and Chang, 1991).

High doses of 20-HE (1.0 or 5.0 μg/g) delayed molt in intact lobsters receiving injections at substages 3 or 4. This observation is consistent with the observation in insects that the decline in circulating ecdysteroids must precede the occurrence of ecdysis (Sláma, 1980; Truman *et al.*, 1983; Reynolds, 1986; Ždárek and Denlinger, 1987). In addition, the delay of ecdysis by exogenous ecdysteroid in lobsters is similar to observations in insects, where there is a critical period when animals are most sensitive to hormonal treatment (Truman *et al.*, 1983; Ždárek and Denlinger, 1987).

Intact lobsters become insensitive to exogenous 20-HE when they reach substage 5, as development nears completion (within 7 h before ecdysis), and as the circulating level of the hormone declines to its low level (less than 0.1 μg/ml). This insensitivity suggests that the ecdysial programs have already been triggered. In *M. sexta*, this trigger includes the acquisition of the sensitivity to and release of eclosion hormone (EH), which coordinate ecdysial behavior and related physiological events (Truman, 1985). Although Truman *et al.* (1981) found EH activity in insects from five non-lepidopteran orders, and quantified it with a *Manduca* bioassay, direct demonstration of the existence of an EH-like factor capable of initiating ecdysis has not been reported in any non-lepidopteran.

In crustaceans, an exuviation factor analogous to EH has been proposed, based on the observation that ecdysteroid injection blocked ecdysis in some amphipods (Graf, 1972a, b; Charmantier and Trilles, 1976). There is no direct evidence, however, for EH in crustaceans. Peptide extracts from brains and thoracic ganglions of pre- and postmolt crabs were assayed for EH activity, all with negative results (Cameron, 1989). Crustaceans and non-lepidopteran insects may not use an EH-like factor to initiate ecdysis, but instead directly rely on the declining titers of ecdysteroids to trigger ecdysial behavior.

The declining ecdysteroid titers at late premolt influence other aspects of development, in addition to the time of ecdysis. As shown in Figure 5, cuticular digestion was delayed by multiple injections of 20-HE. These results suggest that the events in late premolt are negatively modulated by ecdysteroids. This is consistent with observations in insects (Schwartz and Truman, 1983). In *M. sexta*, however, morphological development was completely suspended by continuous ecdysteroid infusion. The negative effect of ecdysteroids on late premolt events is in contrast to their positive effect on development at other molt stages in both insects and crustaceans.

Acknowledgments

We thank D. K. Aronstein, M. J. Bruce, and W. A. Hertz for technical assistance and Dr. M. Snyder for helpful discussions. The gifts of lobsters from M. Syslo (Massachusetts State Lobster Hatchery and Research Station) and ecdysteroid antisera from Dr. W. E. Bollenbacher (University of North Carolina, Chapel Hill) are gratefully acknowledged. The Aquaculture and Fisheries Program of the University of California, Davis, is acknowledged for financial support (to J.-H.C.). This work is a result of research sponsored in part by NOAA, National Sea Grant College Program, Department of Commerce, under Grant NA85AA-D-SG140, Project R/A-80, through the California Sea Grant College Program (to E.S.C.). The U.S. Government is authorized to reproduce and distribute copies for governmental purposes.

Literature Cited

Aiken, D. E. 1973. Proecdysis, setal development, and molt prediction in the American lobster (*Homarus americanus*). *J. Fish. Res. Board Can.* **30:** 1337–1344.

Cameron, J. N. 1989. Post-moult calcification in the blue crab, *Callinectes sapidus:* timing and mechanism. *J. Exp. Biol.* **143:** 285–304.

Chang, E. S. 1989. Endocrine regulation of molting in Crustacea. *Rev. Aquatic Sci.* **1:** 131–157.

Chang, E. S., and M. J. Bruce. 1980. Ecdysteroid titers of juvenile lobsters following molt induction. *J. Exp. Zool.* **214:** 157–160.

Chang, E. S., and M. J. Bruce. 1981. Ecdysteroid titers of larval lobsters. *Comp. Biochem. Physiol.* **70A:** 239–241.

Chang, E. S., and D. E. Conklin. 1983. Lobster (*Homarus*) hatchery techniques. Pp. 271–275 in *CRC Handbook of Mariculture*, Vol. 1, J. P. McVey, ed. CRC Press, Boca Raton, FL.

Chang, E. S., and J. D. O'Connor. 1978. *In vitro* secretion and hydroxylation of α-ecdysone as a function of the crustacean molt cycle. *Gen. Comp. Endocrinol.* **36:** 151–160.

Chang, E. S., and J. D. O'Connor. 1979. Arthropod molting hormones. Pp. 797–814 in *Methods of Hormone Radioimmunoassay*, 2nd ed., B. M. Jaffe and H. R. Behrman, eds. Academic Press, New York.

Chang, E. S., and J. D. O'Connor. 1988. Crustacea: molting. Pp. 259–278 in *Invertebrate Endocrinology*, Vol. 2, H. Laufer and R. G. H. Downer, eds. Alan R. Liss, New York.

Charmantier, G., and J. P. Trilles. 1976. Ecdystérone premue et exuviation chez *Sphaeroma serratum* (Fabricius, 1787) (Crustacea, Isopoda, Flabellifera). *Gen. Comp. Endocrinol.* **28:** 249–254.

Cheng, J.-H. 1990. Control of the time of ecdysis and postmolt size increase in the American lobster, *Homarus americanus.* Ph.D. Dissertation, University of California, Davis.

Conklin, D. E., and E. S. Chang. 1983. Grow-out techniques for the American lobster, *Homarus americanus.* Pp. 277–286 in *CRC Handbook of Mariculture,* Vol. 1, J. P. McVey, ed. CRC Press, Boca Raton, FL.

Graf, F. 1972a. Action de l'ecdystérone sur la mue, la cuticule et la métabolisme du calcium chez *Orchestia cavimana* Heller (Crustacé, Amphipode, Talitridé). *C. R. Acad. Sci. Paris* **274:** 1731–1733.

Graf, F. 1972b. Etude comparative de l'action de l'ecdystérone chez le Gammaridé hypogé Niphargus et le Talitridé épigé *Orchestia* (Crustacés, Amphipodes). *C. R. Acad. Sci. Paris* **275:** 2045–2048.

Mykles, D. L. 1980. The mechanism of fluid absorption at ecdysis in the American lobster *Homarus americanus. J. Exp. Biol.* **84:** 89–101.

Mykles, D. L. 1981. Ionic requirements of transepithelial potential difference and net water flux in the perfused midgut of the American lobster, *Homarus americanus. Comp. Biochem. Physiol.* **69A:** 317–320.

Mykles, D. L., and D. M. Skinner. 1981. Preferential loss of thin filaments during molt-induced atrophy in crab claw muscle. *J. Ultrastruct. Res.* **75:** 314–325.

Reynolds, S. E. 1986. Endocrine timing signals that direct ecdysial physiology and behavior. Pp. 53–77 in *Insect Neurochemistry and Neurophysiology,* A. A. Borkovec and D. B. Gelman, eds. Humana Press Inc., Clifton, NJ.

Sakurai, S., and C. M. Williams. 1989. Short-loop negative and positive feedback on ecdysone secretion by prothoracic gland in the tobacco hornworm, *Manduca sexta. Gen. Comp. Endocrinol.* **75:** 204–216.

Schwartz, L. M., and J. W. Truman. 1983. Hormonal control of rates of metamorphic development in the tobacco hornworm *Manduca sexta. Dev. Biol.* **99:** 103–114.

Skinner, D. M. 1985. Molting and regeneration. Pp. 43–146 in *The Biology of Crustacea,* Vol. 9, D. E. Bliss and L. H. Mantel, eds. Academic Press, New York.

Sláma, K. 1980. Homeostatic function of ecdysteroids in ecdysis and oviposition. *Acta Entomol. Bohemoslov.* **77:** 145–168.

Snyder, M. J., and E. S. Chang. 1991. Metabolism and excretion of injected [^{3}H]-ecdysone by female lobsters *Homarus americanus. Biol. Bull.* **180:** 475–484.

Steel, C. G. H., and X. Vafopoulou. 1989. Ecdysteroid titer profiles during growth and development of arthropods. Pp. 221–231 in *Ecdysone: From Chemistry to Mode of Action,* J. Koolman, ed. Georg Thieme Verlag, Stuttgart.

Truman, J. W. 1985. Hormonal control of ecdysis. Pp. 413–440 in *Comprehensive Insect Physiology, Biochemistry, and Pharmacology,* Vol. 8, G. A. Kerkut and L. I. Gilbert, eds. Pergamon Press, Oxford.

Truman, J. W., P. H. Taghert, P. F. Copenhaver, N. J. Tublitz, and L. M. Schwartz. 1981. Eclosion hormone may control all ecdyses in insects. *Nature* **291:** 70–71.

Truman, J. W., D. B. Rountree, S. E. Reiss, and L. M. Schwartz. 1983. Ecdysteroids regulate the release and action of eclosion hormone in the tobacco hornworm *Manduca sexta* (L.). *J. Insect Physiol.* **29:** 895–900.

Ždárek, J., and D. L. Denlinger. 1987. Pupal ecdysis in flies: the role of ecdysteroids in its regulation. *J. Insect Physiol.* **33:** 123–128.

Reference: *Biol. Bull.* **181:** 175–180. (August, 1991)

Long-Term Culture of Freshwater Mussel Gill Strips: Use of Serotonin to Affect Aseptic Conditions

D. B. GARDINER, F. S. TURNER, J. M. MYERS, T. H. DIETZ, AND H. SILVERMAN

Department of Zoology and Physiology, Louisiana State University, Baton Rouge, Louisiana 70803

Abstract. Serotonin relaxes the musculature and increases epithelial ciliary activity in freshwater mussel gills. This results in greater than normal water flow through the labyrinth of water canals and channels of the gill. These water spaces harbor significant microbial populations that make aseptic culture of freshwater mussel gills difficult. High concentrations of antibiotics can maintain short-term cultures, but are toxic to the tissue and reduce the lifespan of the culture. Moderate levels of antibiotics used in combination with 0.1 m*M* serotonin during a single, short pretreatment produces aseptic cultures. These cultures can now be established routinely and are viable for over a month as assayed by gill structural integrity, trypan blue exclusion, leucine incorporation into TCA precipitable protein, and normal physiological responsiveness to serotonin re-exposure.

Introduction

Attempts at establishing molluscan organ cultures have been made since the mid-1920's. Zweibaum (1925) tried to culture freshwater mussel gills in various diluted vertebrate Ringer's solutions enriched with peptone. Mantle tissue explants, from the land snail *Helix aspersa* (Gatenby, 1931; Gatenby *et al.*, 1934) and the marine bivalve *Pinctata* (Bevelander and Martin, 1949), were cultured. Cultured explants of the heart, lungs, and foot of various *Helix* species have also been reported (Konicek, 1933). Unfortunately, these organ cultures remained functional for only a few days.

More recently, certain cells and tissues, particularly of pulmonate gastropods and some marine organisms, have been successfully cultured. The cell lines cultured were derived from several tissues: ganglia, gills, heart, digestive tract, foot, mantle, oviduct, connective tissue, and gonad (Burch and Cuadros, 1965; Cheng and Arndt, 1973; Hansen, 1975; Kaczmarek *et al.*, 1979; Sengal, 1961a,b; Stephens and Hetrick, 1979; Vago and Chastang, 1958). Unfortunately, attempts at culturing freshwater mussel tissue have failed due to fungal and bacterial contamination (Sengel, 1964), and the lack of well-defined maintenance media.

The gills of freshwater mussels are complex organs that function in ion transport, respiration, food capture and sorting, storage and maintenance of embryos during reproduction, calcium storage, and water movement. Several different cell types are associated with the gill, but culturing gill explants or sub-culturing specific cell lines allows the study of tissue- and cell-specific responses of the gill in isolation from the rest of the organism. Previously we have studied gills excised from the animal immediately before use (Dietz and Findley, 1980; Dietz *et al.*, 1982; Dietz and Hagar, 1990; Silverman *et al.*, 1991). Having viable gill explants functioning in culture expands the range and duration of experiments that can be accomplished.

Here we report the successful long-term culture of freshwater mussel gills under aseptic conditions. A suitable medium, methods for reducing antibiotic exposure, and culture viability (as judged by normal appearance and physiological responses in gill tissue) are documented.

Materials and Methods

Animals and maintenance

Freshwater mussels *Anodonta grandis* and *Ligumia subrostrata* were collected from shallow ponds near Baton Rouge, Louisiana. The animals were maintained in aerated artificial pond water (Table 1) at 22–25°C, and were

Received 12 December 1990; accepted 1 April 1991.

Abbreviations: Penicillin (Pen); streptomycin (Strep); amphotericin B (Am-B); Artificial mussel hemolymph (AMH).

allowed to acclimate to laboratory conditions for a week before use.

Initial short-term culture methods

Gills were washed (3 × 20 min) in sterile pondwater or 30 mM Tris-HCl, pH 7.8, containing up to 1500 U ml^{-1} penicillin G (Pen) and 1.5 mg ml^{-1} streptomycin (Strep). The preliminary media we tested contained multiple components chosen for their presence in diluted vertebrate culture media, or in mussel hemolymph (Table I). As the major source of the defined nutrients, we selected either a medium based on vertebrate Ham's F-12 (Gibco) (dilution I), or artificial mussel hemolymph (AMH). All cultures contained 1 mg l^{-1} phenol red, which allowed us to monitor pH. Cultures in each medium appeared normal and were viable for 1–4 days, but microbial and fungal contamination remained a problem.

Antibiotic treatments

To reduce fungal contamination, we exposed gill strips to amphotericin B (Am-B) in concentrations ranging from 25 to 500 μg ml^{-1} and for exposure times of from 1 to 24 h. We also pretreated intact animals in solutions of antibiotics at concentrations patterned after those used by Stephens and Hetrick (1979) to decontaminate oyster tissues. For such whole animal treatment, the following antibiotics were added to mussel Ringer's or pondwater (Table I): 1000 U ml^{-1} penicillin G and 1 mg ml^{-1} streptomycin, 100 μg ml^{-1} neomycin, 50 μg ml^{-1} chlortetracycline, 125 μg ml^{-1} gentamicin, 500 μg ml^{-1} kanamycin sulfate, 500 μg ml^{-1} polymyxin B sulfate, 100 μg ml^{-1} erythromycin, 25 μg ml^{-1} amphotericin B, and 250 U ml^{-1} nystatin. The mussels were immersed in this solution for 3–4 days. Gills were removed from both pretreated and non-pretreated clams, cut into 3–5 mm strips, and cultured as described above.

Serotonin application

Serotonin enhances the ciliary activity and relaxes the muscles of the gills in freshwater mussels (Gardiner *et al.*, 1991), so we used it as an aid in decontamination. Gills were isolated and placed in sterile tubes containing 10^{-4} M serotonin in freshwater mussel Ringer's, pH 7.8. The solution was changed every 5 min for 20 min. The gills were removed and placed in sterile tubes containing freshwater mussel Ringer's with 500 U ml^{-1} penicillin G, 0.5 mg ml^{-1} streptomycin, 500 μg ml^{-1} colistin, 10 μg ml^{-1} chlortetracycline, 250 U ml^{-1} nystatin, and 10^{-4} M serotonin, pH 7.8. This solution was replaced every 15 min for a total incubation period of 45 min. Gills were cut into 3–5 mm strips that were distributed in 24-well Corning culture plates containing an enriched Ham's F-12 medium (Table I, Ham's F-12 dilution II) or artificial mussel hemolymph (AMH, Table I). Both media were fortified with 500 U ml^{-1} penicillin G, 0.5 mg ml^{-1} streptomycin, and 5 μg ml^{-1} chlortetracycline, pH 7.8. To some of these cultures, 250 U ml^{-1} nystatin also was added. The pH was adjusted to 7.8, and the osmolality adjusted to 60 mosm (Precision System Micro Osmometer), as needed. The explants were maintained at 20–23°C, and the explant was placed in a new well with fresh medium every two days.

Assessment of tissue viability

The initial assessment of viability was by observation, with an inverted microscope, of explant integrity, periodic muscular contractions, and ciliary activity. Trypan blue exclusion was used to determine cellular viability (Freshney, 1987). Cells detached from the explant were placed in a 0.2% trypan blue in mussel Ringer's for 5 min. Cells were viewed under a light microscope, and dying ones were identified by their uptake of trypan blue.

Serotonin (10^{-5} M) increases the gill ciliary activity and relaxes gill musculature. We used these responses to assay for the proper physiological response of the explants. The explants were placed into fresh medium containing serotonin and observed for 5 min for muscular reflex activity and changes in the pattern of ciliary motion (Gardiner *et al.*, 1991).

Several cultures were assayed for their ability to incorporate ^{3}H-leucine into a trichloroacetic acid (TCA) precipitable protein fraction. Approximately 1 μCi ml^{-1} ^{3}H-leucine (specific activity 1 mCi μM^{-1} leucine) was added to AMH culture medium in which the leucine concentration had been reduced to 1 μM. After a 1-h exposure, the gills were denatured with 10% TCA, rinsed in pondwater, blotted, and their wet tissue weights recorded. The gills were homogenized in 1 ml 10% TCA and centrifuged at 5000 × g for 5 min. The pellet was twice resuspended and centrifuged in 10% TCA. The pellet was dissolved in 1 M NaOH, and the radioactivity was determined in a liquid scintillation counter. Protein concentration was determined by the method of Bradford (1976).

Analysis of microbial contaminants

Fungi growing in the cultures were identified only by the appearance of structural hyphae; no attempt was made to identify the species. The bacterial contaminants surviving antibiotic treatment were cultured in antibiotic-free Ham's F-12 dilution II (Table I) and sent to Louisiana State Veterinary Medical Diagnostic Laboratory for identification.

Results

Our initial attempts to establish sterile gill explants in culture, using a variety of antibiotics, were unsuccessful.

Table 1

Composition of media used for culturing freshwater mussel gills

	Pond water	FW mussel Ringer's	Ham's F-12 dilution I	Ham's F-12 dilution II	Art. mussel hemolymph	FW mussel hemolymph
Inorganic salts (mM)						
$CaCl_2$	0.40	5.0	0.04	0.03	4.79	a, b, c
$CuSO_4 \cdot 5H_2O$	0	0	1.4×10^{-7}	1.0×10^{-7}	0	—
$FeSO_4 \cdot 7H_2O$	0	0	4.2×10^{-4}	2.99×10^{-4}	0.028	d
KCl	0.05	0.5	0.438	0.313	0	a, b, c
K_2HPO_4	0	0	0	0	0.197	a, b, c
$MgCl_2 \cdot 6H_2O$	0	0	0.09	0.061	0.187	b
$MnCl_2 \cdot 4H_2O$	0	0	0	0	0.12	d
NaCl	0.50	5.0	18.2	13.0	16.18	a, b, c
$NaHCO_3$	0.20	5.0	0	0	4.59	a, b, c
Na_2HPO_4	0	0	0.190	0.142	0	a, b, c
Na_2SO_4	0	5.0	0	0	0	b
$ZnSO_4 \cdot 7H_2O$	0	0	4.2×10^{-4}	3.0×10^{-4}	0.0048	d
Amino acids (μM)						
L-Alanine	0	0	14.0	10.0	55.0	55 ± 7 (4) e
L-Arginine	0	0	140.0	100.0	14.0	14 ± 4 (4) e
L-Asparagine	0	0	14.0	10.0	0	—
L-Aspartate	0	0	14.0	10.0	27.0	27 ± 10 (4) e
L-Cysteine	0	0	28.0	20.0	0	—
L-Glutamate	0	0	14.0	10.0	54.0	54 ± 16 (4) e
L-Glutamine	0	0	140.0	100.0	0	—
Glycine	0	0	14.0	10.0	12.0	12 ± 4 (4) e
L-Histidine	0	0	14.0	10.0	26.0	26 ± 4 (4) e
L-Isoleucine	0	0	4.2	3.0	8.0	8 ± 1 (4) e
L-Leucine	0	0	14.0	10.0	13.0	13 ± 1 (4) e
L-Lysine	0	0	28.0	20.0	15.0	15 ± 4 (4) e
L-Methionine	0	0	4.2	3.0	0	—
L-Phenylalanine	0	0	4.2	3.0	8.0	8 ± 1 (3) e
L-Proline	0	0	42.0	30.0	14.0	14 ± 1 (4) e
L-Serine	0	0	14.0	10.0	83.0	83 ± 7 (4) e
L-Threonine	0	0	14.0	10.0	134.0	59; 134 e
L-Tryptophan	0	0	1.4	1.0	0	—
L-Tyrosine	0	0	4.2	3.0	3.0	3.0 e
L-Valine	0	0	14.0	10.0	14.0	14 ± 2 (4) e
Vitamins (mM)						
Biotin	0	0	4.2×10^{-6}	3.0×10^{-6}	4.09×10^{-3}	—
Choline chloride	0	0	0.02	0.01	7.16×10^{-3}	—
Folic acid	0	0	4.2×10^{-4}	3.0×10^{-4}	2.26×10^{-3}	—
myo-inositol	0	0	0.014	0.01	0.011	—
Niacinamide	0	0	4.2×10^{-5}	3.0×10^{-5}	8.19×10^{-3}	—
Pantothenate (Ca)	0	0	1.4×10^{-4}	1.0×10^{-4}	2.09×10^{-3}	—
Pyridoxine	0	0	4.2×10^{-5}	3.0×10^{-5}	4.86×10^{-3}	—
Riboflavin	0	0	1.4×10^{-5}	1.0×10^{-5}	2.70×10^{-4}	—
Thiamine	0	0	1.4×10^{-4}	1.0×10^{-4}	2.96×10^{-3}	—
Vitamin B-12	0	0	1.4×10^{-4}	1.0×10^{-4}	0	—
Other (mM)						
Glucose	0	0	1.4	5.55	5.55	—
Fetal serum (v/v)	0	0	8.7%	5%	5%	—
Hemolymph (v/v)	0	0	8.7%	0	0	100%
Hypoxanthine	0	0	0.0042	0.003	0	—
Insulin (U ml^{-1})	0	0	0.25	0	0	—
Linoleic acid	0	0	4.2×10^{-5}	3.0×10^{-5}	0	—
Lipoic acid	0	0	1.4×10^{-4}	0	0	—
pH	7.0	7.8	7.8	7.8	7.8	7.8
Phenol red (mg l^{-1})	0	1.0	1.0	1.0	1.0	0
Putrescine	0	0	1.4×10^{-4}	1.0×10^{-4}	0	—
Pyruvic acid	0	0	0.15	0.1	0	—
TES buffer	0	0	2.0	0	0	—
Thioctic acid	0	0	0	1.0×10^{-4}	0	—
Thymidine	0	0	1.4×10^{-4}	3.0×10^{-4}	0	—

Refer to (a) Dietz (1979), (b) Potts (1954), (c) Silverman *et al.*, (1983), (d) Silverman *et al.*, (1987) for ionic composition and (e) Hanson and Dietz (1976) for amino acids in freshwater mussel hemolymph. Art. = artificial, FW = freshwater.

All of the explants remained functional for several days, but were contaminated by predominantly gram-negative bacteria of the genus *Leukothrix*, commonly associated with freshwater mussels and shrimp (Louisiana State Veterinary Medical Diagnostic Laboratory). In addition, the gill cultures treated with Am-B at concentrations up to 500 μg ml^{-1} for 12 h had fungi within a few days. High doses of Am-B caused copious mucus secretion and inhibition of ciliary activity. With the growth of fungi and bacteria, the culture medium rapidly acidified in spite of frequent (1–2 days) medium changes.

Treatment with high concentrations of antibiotics was ineffective; 75% of the cultures still contained fungal contamination, and all contained 2–3 strains of bacteria. Explants not contaminated with fungus remained viable for 10–14 days, but all had bacterial contamination. Pretreatment of the intact animal with antibiotics did not reduce microbial contamination. The microorganisms were unlikely to be resistant to the wide spectrum of antibiotics we used; we conclude rather that the gill was harboring the microorganisms in the extensive branchial canals and channels, isolating them from the antibiotics in the medium.

Serotonin pretreatment of gill explants

Explants treated with serotonin rarely exhibited bacterial or fungal contamination. When nystatin was only present in the initial wash, 15–25% of the explants had fungi. If nystatin were present continuously in the medium, only 4–8% of the cultures were infected. The serotonin pretreatment, in combination with moderate levels of antimicrobial agents, resulted in cultures that were visibly free of bacterial and fungal contamination. After 38 days in culture, 96% of the explants remained free of bacteria.

Once pretreated with serotonin, gill explants remained viable and free of bacteria for over a month. Neither the cells in the explant nor detached cells showed any uptake of trypan blue. The gill explant is lined with a ciliated epithelium organized into filaments. Filament organization remained unchanged (Fig. 1), and ciliary and muscular activity continued throughout the life of the explant. Both muscular and ciliary activity were altered by re-in-

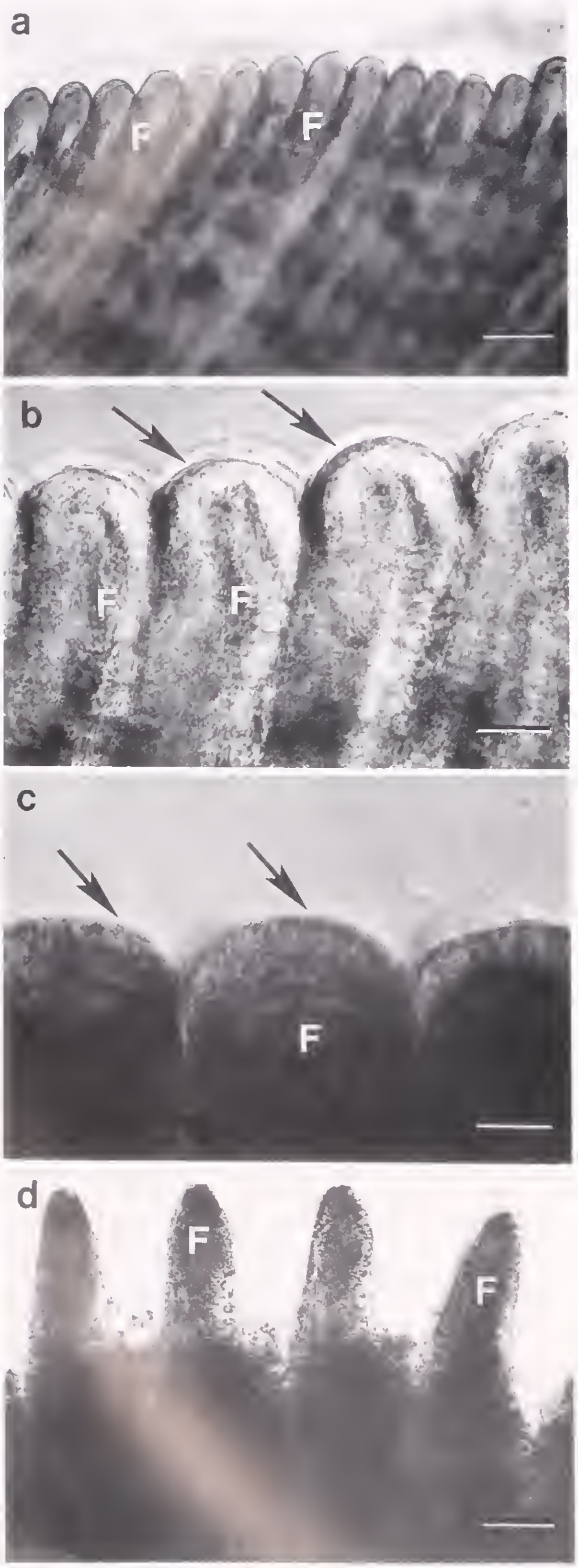

Figure 1. (a) Light micrograph of *Ligumia subrostrata* gill explant, in culture less than 24 h, showing normal filament (F) organization. (b) Higher magnification micrograph of (a) showing filaments (F) and active cilia (arrows) indicated by the refractile halo pattern. (c) Light micrograph of *Anodonta grandis* gill explant cultured for 30 days, showing filaments (F) and active cilia (arrows) as indicated by the halo pattern. (d) Light micrograph of *Anodonta grandis* gill explant maintained in culture for 40 days. Gill integrity has been compromised and cells have detached from explant. This detachment is mostly observable at the filaments (F). Bars (a) = 137 μm; (b) = 35 μm; (c) = 37 μm; (d) = 77 μm.

troducing serotonin into the culture medium, and the effects were the same as those seen in freshly isolated gills. That is, ciliary activity increased and was more coordinated, and the gill musculature was relaxed by serotonin treatment. Such treatment dilates the openings to the water canals in the gills (Gardiner *et al.*, 1991). Thus, physiological responses to a known effector of gill activity still occur in long-term explant culture.

Media development

Various media and supplements to those media have been examined for their ability to improve short-term gill culture (Table I). Osmolarity, mussel blood, vitamin solutions, and insulin are important factors in such considerations. For maintenance of gill explants for a week or less, both diluted Ham's F-12 and AMH were acceptable. At 10 days, some explants in Ham's F-12 showed increased cellular detachment, and at two weeks, ciliary activity was reduced or non-existent. AMH medium maintained explants for over 30 days in culture, and explants exhibited coordinated ciliary activity and periodic muscular contractions. In addition, few cells detached from the explants cultured in AMH. Those explants continuously cultured with nystatin in the AMH could not be distinguished from those exposed only initially to nystatin. After 40 days in AMH culture, some explants lost their integrity; epithelial cells began to detach from explants (Fig. 1).

Metabolic viability of the cultured explants

The ability of the cultures to incorporate ^{3}H-leucine into TCA-precipitable protein was maintained at stable levels for 30 days in culture. In a representative series of *A. grandis* gill tissues cultured for 10, 24, or 31 days, incorporation of ^{3}H leucine was 5.73 ± 0.41 ($n = 17$) CPM $(\mu g \text{ protein} \cdot h)^{-1}$, and there was no significant difference between the three groups of gills (ANOVA, $P > 0.05$). Beyond 30 days, the viability of the gill explants declined in both *A. grandis* and *L. subrostrata*, as indicated by reduced leucine incorporation. In another study of *A. grandis* gills, leucine incorporation remained essentially constant through 44 days of culture, but declined 50% in gills cultured for 54 days.

Discussion

Explants of freshwater mussel gill can be cultured under aseptic conditions, with minimal exposure to antimicrobial agents, by treating the gill in the initial decontamination stage with serotonin in combination with antibiotic and antifungal agents. Serotonin relaxes musculature in a number of molluscan systems (Twarog, 1954; Cambridge *et al.*, 1959; Kobayashi and Hasimoto, 1982). When applied to freshwater mussel gill, exogenous serotonin relaxes the branchial musculature, dilating the water canals leading into the central water channels. This effect, combined with an increased and more synchronous ciliary beat, maximizes fluid flow through the gill. These physiological effects of serotonin on gill explants occur within seconds (Gardiner *et al.*, 1991). Incubating gills in a combination of serotonin and moderate concentrations of an antibiotic mixture for 45 min virtually eliminates all microbial and fungal contamination. This suggests that many microbes are normally sheltered within the water spaces of the gill. One of the advantages of the serotonin treatment is that aseptic cultures can be established at lower concentrations of antibiotic and antifungal agents. These cultures can be maintained in an aseptic state with low levels of antibiotics, or even none. Freedom from the confounding results of antibiotics makes gill cultures far more suitable for physiological study.

Our initial attempts to achieve aseptic cultures of freshwater mussel gills were mainly directed at elimination of the microorganisms by increasing the variety of antibiotics and elevating their concentrations. The assumption in this approach is that microorganisms are "resistant" to the antibiotics being used. This is not the case. As observed in this study, our initial failure to establish sterile cultures was due to the tissue harboring microorganisms and fungal spores in compartments that were partially isolated from the antibiotics. Perhaps a principal reason for difficulty in establishing any aseptic organ culture is the complex architecture of the organ, which provides microenvironments relatively free of antibiotics.

Elevating the concentration of antibiotics may actually be detrimental to the tissue explant. Amphotericin B proved ineffective in controlling fungal contamination, and higher concentrations were toxic to the gill explants. High concentrations of Am-B resulted in abnormally high mucous secretion and cessation of ciliary activity. Thus, while fungal contamination is an important consideration in establishing long-term explants of freshwater mussel gill, Am-B should be avoided.

We can now routinely culture viable gills for over a month. Freshwater mussel gills will survive in a variety of media for short periods. Several functions, including explant structural integrity, ciliary beat, muscular reflex activity, and a continued ability to respond to re-addition of serotonin, all indicate that the explants are functioning in organ culture. Trypan blue is excluded from the majority of cells associated with the explant whether in place or detached. However, longer-term gill culture is apparently affected by medium composition and, as yet, unknown deficiencies. The established explant cultures are useful for the study of many events associated with gill cellular activity (*e.g.*, calcium concretion synthesis, cell membrane ion channel characteristics).

Acknowledgments

The Cell and Tissue Culture Facilities, Department of Veterinary Microbiology and Parasitology, Louisiana State University, offered facilities and helpful suggestions throughout this study. We thank Ms. Beckey Demler of the Basic Science Microscopy Center and Ron Bouchard for photographic assistance. Dr. A. H. Cincotta provided insight as we developed our culture media. We thank J. Cherry and J. Horohov for technical assistance. This work was supported by NSF-8802320 and 9017461.

Literature Cited

Bevelander, G., and J. Martin. 1949. Culture of mantle tissue of marine molluscs. *Anat. Rec.* **105:** 614.

Bradford, M. M. 1976. A rapid and sensitive method for the quantitation of microgram quantities of proteins utilizing the principle of protein-dye binding. *Anal. Biochem.* **72:** 248–254.

Burch, J., and V. Cuadros. 1965. A culture medium for snail cells and tissues. *Nature* **206:** 637–638.

Cambridge, G. W., J. A. Holgate, and J. A. Sharp. 1959. A pharmacological analysis of the contractile mechanism of *Mytilus* muscle. *J. Physiol.* **148:** 451–464.

Cheng, T., and R. Arndt. 1973. Maintenance of cells of *Biomphalaria glabrata* (mollusca) *in vitro. J. Invert. Pathol.* **22:** 308–310.

Dietz, T. H. 1979. Uptake of sodium and chloride by freshwater mussels. *Can. J. Zool.* **57:** 156–160.

Dietz, T. H., and A. M. Findley. 1980. Ion-stimulated ATPase activity and NaCl uptake in the gills of freshwater mussels. *Can. J. Zool.* **58:** 917–923.

Dietz, T. H., and A. F. Hagar. 1990. Chloride uptake in isolated gills of the freshwater mussel *Ligumia subrostrata. Can. J. Zool.* **68:** 6–9.

Dietz, T. H., J. I. Scheide, and D. G. Saintsing. 1982. Monoamine transmitters and cAMP stimulation of Na transport in freshwater mussels. *Can. J. Zool.* **60:** 1408–1411.

Freshney, R. I. 1987. *Culture of Animal Cells: A Manual of Basic Technique.* 2nd ed. Alan R. Liss, Inc. New York. pp. 246.

Gardiner, D. B., H. Silverman, and T. H. Dietz. 1991. Musculature associated with the water canals in freshwater mussels and response to monoamines *in vitro. Biol. Bull.* **180:** 453–465.

Gatenby, J. B. 1931. Outgrowths from pieces of *Helix aspersa*, the common snail. *Nature* **128:** 1002–1003.

Gatenby, J., J. Hill, and T. MacDougald. 1934. On the behavior and structure of cells of *Helix aspersa* in aseptic and non-aseptic tissue culture. *Q. J. Microsc. Sci.* **77:** 129–159.

Hansen, E. L. 1975. Secondary daughter sporocysts of *Schistosoma mansoni:* their occurrence and culture. *Ann. N.Y. Acad. Sci.* **266:** 426–436.

Hanson, J. A., and T. H. Dietz. 1976. The role of free amino acids in cellular osmoregulation in the freshwater bivalve *Ligumia subrostrata* (Say). *Can. J. Zool.* **54:** 1927–1931.

Kaczmarek, L. K., M. Finbow, J. P. Revel, and F. Strumwasser. 1979. The morphology and coupling of *Aplysia* bag cells within abdominal ganglion and in cell culture. *J. Neurobiol.* **10:** 535–550.

Kobayashi, M., and T. Hasimoto. 1982. Antagonistic responses of the radular protractor and retractor to the same putative neurotransmitters. *Comp. Biochem. Physiol.* **72C:** 343–348.

Konicek, H. 1933. Über die Kultivation des lungenbentel und herzgewebes bei *Helix pomatia Arch. Exp. Zellforsch.* **13:** 709–716.

Potts, W. T. W. 1954. The inorganic composition of the blood of *Mytilus edulis* and *Anodonta cygnea. J. Exp. Biol.* **31:** 376–385.

Sengel, P. 1961a. Survie en culture *in vitro* de divers organes d'invertébrés marins adultes. *C. R. Acad. Sci., Paris* **252:** 3666–3668.

Sengel, P. 1961b. Explantation *in vitro* de quelques organes d'invertébrés marins adultes. *Bull. Soc. Zool. Fr.* **86:** 301–302.

Sengel, P. 1964. Utilisation de la culture organotypique pour l'etude de la morphogenèse et de l'endocrinologie chez les invertébrés. *Bull. Soc. Zool. Fr.* **89:** 10–41.

Silverman, H., J. W. McNeil, and T. H. Dietz. 1987. Interaction of trace metals Zn, Cd, and Mn, with Ca concretions in the gills of freshwater unionid mussels. *Can. J. Zool.* **65:** 828–832.

Silverman, H., J. M. Myers, and T. H. Dietz. 1991. Invertebrate calcium concretions: novel biomineralization system. Pp. 125–138 in *Surface Reactive Peptides and Polymers*, C. S. Sikes and A. P. Wheeler, eds. American Chemical Society, Washington, DC.

Silverman, H., W. L. Steffens, and T. H. Dietz. 1983. Calcium concretions in the gills of a freshwater mussel serve as a calcium reservoir during periods of hypoxia. *J. Exp. Zool.* **227:** 177–189.

Stephens, E. B., and F. M. Hetrick. 1979. Decontamination of the American oyster tissues for cell and organ culture. Procedure 70676 *TCA Manual* **5:** 1029–1031.

Twarog, B. M. 1954. Responses of a molluscan smooth muscle to acetylcholine and 5-hydroxytryptamine. *J. Cell. Comp. Physiol.* **44:** 141–163.

Vago, C., and S. Chastang. 1958. Obtention de lignées cellulaires en culture de tissus d'invertébrés. *Experientia* **14:** 110–111.

Zweibaum, J. 1925. Analyse histophysiologique de l'epithelium vibratile en état de survie *in vitro. C. R. Soc. Biol.* **93:** 785–787.

Reference: *Biol. Bull.* **181:** 181–188. (August, 1991)

Bioluminescence Maintenance in Juvenile *Porichthys notatus*

ALLEN F. MENSINGER AND JAMES F. CASE

Department of Biological Sciences and Marine Science Institute,
University of California, Santa Barbara, California 93106

Abstract. Bioluminescence in the midshipman fish, *Porichthys notatus* from the Santa Barbara coastal region, was quantified from onset through the first two years of life. Maximum light emission was 2.5×10^9 photons s^{-1} upon leaving the nest and reached 2.0×10^{10} photons s^{-1} within the first year. These intensities may be sufficient for counterillumination in moon or starlight over most of the depth range of the fish. The bioluminescence of juveniles recently detached from the nest was depleted by multiple topical applications of a dilute noradrenalin solution. A luciferin-free diet also exhausted luminescence in 10–18 months. Bioluminescence was restored within 24 h after feeding depleted fish with dried specimens of the bioluminescent marine ostracod *Vargula hilgendorfii*, and light emission capacity was correlated with the amount consumed. Predation by second year fish (18 months) upon juvenile *P. notatus* (3 months) or upon live *V. tsujii* also restored luminescence. After restoration, luminescence gradually disappeared within several months. Consumption of luciferin-containing organisms by already competent fish did not increase light intensity. Juvenile *P. notatus* from the Santa Barbara coastal region require exogenous luciferin to remain luminescent.

Introduction

The midshipman fish, *Porichthys notatus*, has been the subject of many investigations since Greene (1899) first noted its bioluminescence originating from hundreds of dermal photophores, primarily confined to the ventral surface. Its natural history has been reviewed by Hubbs (1920), Arora (1948) and Ibara (1967). A nocturnal predator, it remains buried in the sand during the day and ascends at night to feed. The habitat is moderately deep waters to 400 m on the coastal shelf except during the breeding season. Then, during late spring and early summer, sexually mature adults migrate inshore to spawn in the intertidal to 80 m depths (Feder *et al.*, 1974). Males establish sheltered nesting sites and acoustically attract females. Females deposit up to 400 eggs, and multiple matings may result in the male guarding nests containing more than 1000 eggs.

P. notatus ranges from southeastern Alaskan waters to Baja California (Wilimovski, 1954) with a discontinuity along the coast of Oregon dividing the group into northern and southern divisions (Warner and Case, 1980). Although the photophores of both groups are ultrastructurally indistinguishable, the northern fish are non-luminescent (Strum, 1969). Both populations contain luciferase, but the northern population lacks luciferin (Tsuji *et al.*, 1972; Barnes *et al.*, 1973). Administration of the bioluminescent marine ostracod *Vargula hilgendorfii*, induces luminescence in Puget Sound fish (Tsuji *et al.*, 1972; Barnes *et al.*, 1973).

Fish of the southern division, south of Monterey Bay, are uniformly luminescent, while the central population, north of Monterey to Cape Mendocino, includes luminescent and non-luminescent fish (Warner and Case, 1980; Thompson and Tsuji, 1989). The analog of *V. hilgendorfii* along the western North American coast is *V. tsujii*, whose distribution coincides with the southern midshipman population (Kornicker and Baker, 1977). Its absence from northern waters led to speculation that *V. tsujii* is the luciferin source for the southern population (Warner and Case, 1980).

The inability to experimentally deplete luminescence in luminous adults despite long periods of captivity and repeated challenges with noradrenalin suggested that adult *P. notatus* have already acquired large luciferin reserves from the diet or that there is a luciferin recycling or syn-

Received 17 December 1990; accepted 21 March 1991.

thesis mechanism (Barnes *et al.*, 1973). Ingestion of small numbers of luminescent ostracods rendered northern adults capable of luminescence for up to two years, with light yield greater than was considered theoretically possible for the amount of luciferin consumed, suggesting that *de novo* synthesis is triggered by exogenous luciferin or that there is a recycling mechanism (Thompson *et al.*, 1988a). A preferential mechanism for rapid uptake of luciferin from the digestive system has also been reported in *P. notatus* (Thompson *et al.*, 1988b).

The purpose of our study was to observe the effects of a luciferin-free diet on the development of bioluminescence in *P. notatus* juveniles of the southern population and to ascertain whether the fish of this population need exogenous sources of luciferin to remain luminescent. To this end, light emission was quantified from its onset in larval fish through the first two years in laboratory-reared and in locally collected individuals of *P. notatus*. The effects of multiple challenges with noradrenalin on the depletion of luminescence in the fish are described as are experiments that contributed to the evaluation of the luciferin recycling hypothesis.

Materials, Methods and Results

Collection

Breeding pairs of *P. notatus* were collected intertidally along the Pacific Coast, just north of Santa Barbara, California. They were maintained in large aquaria with sand filtered, running seawater (16–20°C). Masonry and large, inverted abalone shells provided nesting sites. Mating usually ensued during the first night in captivity and produced between 100–400 eggs. Females were removed after spawning and males were retained to maintain the nests. Additional nests with guardian males were obtained by divers. After larval detachment (35–50 days post-fertilization), juveniles were placed in aquaria with sand-covered bottoms sufficient for burrowing.

Free-living juveniles were collected with a twenty-five foot, semi-balloon otter trawl from October to May. Minimum depth of capture of first year fish ranged from 30 m in the fall to 80 m in late spring. All fish were maintained on a luciferin-free diet consisting of living *Artemia* and kelp mysids and frozen squid.

Laboratory reared and trawled fish of the same year class had similar growth rates (Fig. 1A). Photophore diameter increased directly with standard length (Fig. 1B).

Light measurement

Bioluminescence was quantified with an integrating sphere quantum counting photometer (Latz *et al.*, 1987). Small fish, less than 4 cm sl (standard length) were placed individually in a head down position in a clear plastic test tube (10 × 75 mm or 15 × 75 mm) inside the 0.25 m diameter integrating sphere. Approximately 6 ml of free volume remained in the test tube after the introduction of the fish. A translucent stopper, containing delivery and output intramedic tubing, sealed the tube. Twelve milliliters of freshly prepared 0.005 *M* (±)-noradrenalin (Sigma) in filtered seawater was then administered by means of a syringe attached to the input tubing externally to the sphere. The fish was completely immersed in the solution. Two minutes later, a second dose of 6 ml was administered and the overflow collected outside the

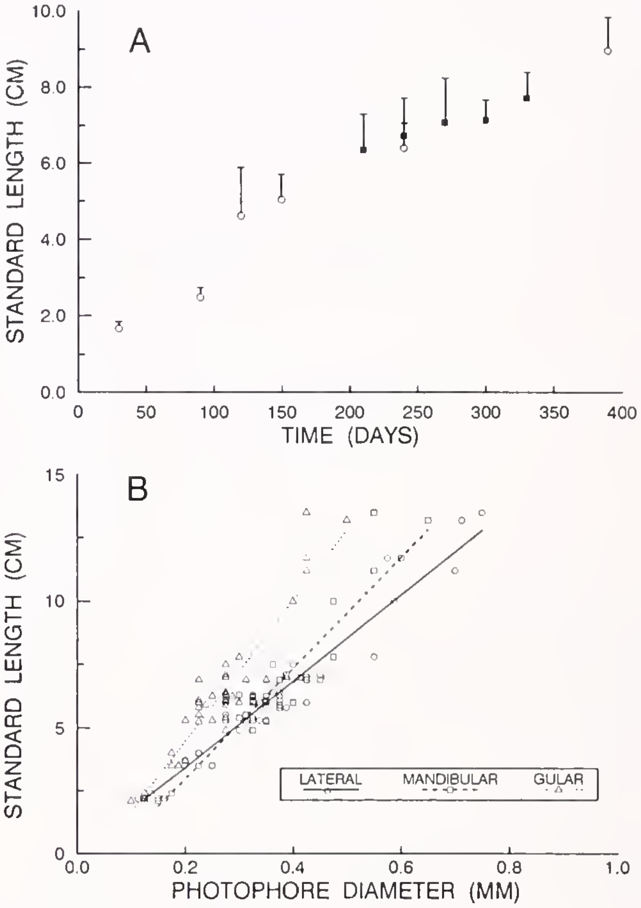

Figure 1. *Porichthys notatus* growth and photophore development. (A) Standard length (cm) *versus* time (days) post-fertilization. For each group tested, mean values are shown; error bars represent one SD of mean. Data represent laboratory raised (circles) and captured (squares) fish. For wild fish, age was determined from average time when fish left nest at capture site. Sample size ranged from 20 to 150. (B) Standard length (cm) *versus* photophore diameter (mm). The fifth anteriormost photophore of each series from the right side of the fish was measured. One specimen contributed one point for each series. Data for lateral (circles), mandibular (squares), and gular (triangles) series are presented together with calculated least-squares linear regressions of length on time according to the equations: $y = 0.31 + 17x$, $r^2 = 0.93$ (solid) for lateral; $y = -1.38 + 21.8x$, $r^2 = 0.90$ (dashed) for mandibular; $y = -1.08 + 27.8x$, $r^2 = 0.88$ (dotted) for gular.

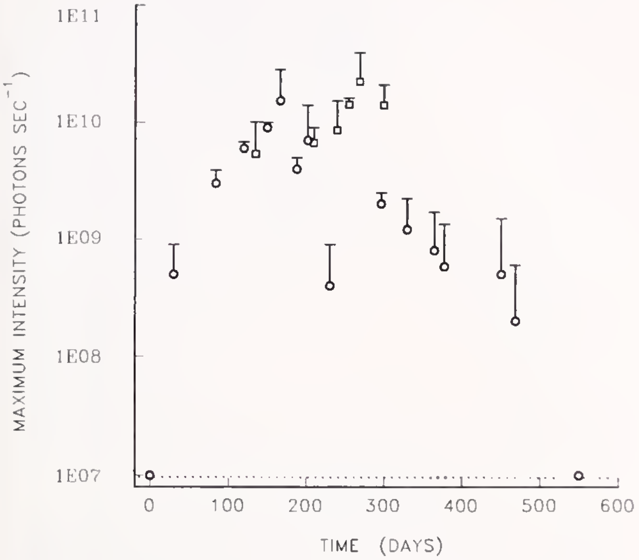

Figure 2. Bioluminescence induction and depletion. Maximum intensity (photons s^{-1}) *versus* time (days) after fertilization. Data represent laboratory raised (circles) and captured (squares) fish. Laboratory raised fish received no exogenous luciferin in the diet. Trawled fish were tested two weeks after capture. For each group tested, mean values are shown; error bars represent one SD of mean. Sample size ranged from 10 to 25. Dotted line represents noise background of integrating sphere and points on line are to be considered nonluminescent.

sphere. Larger fish were placed in a 7.0 cm diameter circular plexiglass chamber, 3.5 cm high, containing 40 ml of 0.005 *M* noradrenalin.

Bioluminescence was recorded for 5 min with a RCA 8850 photomultiplier tube operated at −1700 V and baffled so that only light reflected from the sphere internal surface was measured. This procedure is essential to accurately measure total emission from large organisms containing many non-isotrophically radiating photophores. The detector signal was processed through a discriminator calibrated at −0.315 V and the resulting frequency signal was counted with an Ortec No. 776 counter/timer and displayed on a Norland No. 5400 multichannel analyzer (MCA). Radiometric calibration of the detection system involved determination of the combined spectral responsitivity of the integrating sphere and photomultiplier tube using an Optronic Laboratory Model 310 calibration source. Light absorbance by fish within the sphere was checked against a C^{14} activated phosphore and found to be negligible. The MCA trace was stored on film or floppy disk.

Immersion in noradrenalin solution elicited bioluminescence within 20 s by transcutaneous absorption as shown by the effectiveness of topical application in air, thus avoiding mouth and gills. Luminescence was not observed prior noradrenalin application.

Maximum light emission was usually attained within 5 min and gradually declined until exhaustion approximately 40 min later. Exposure to fresh noradrenalin solutions during the trial did not appreciably raise intensity levels.

A 365 nm emitting ultraviolet (UV) lamp (UVSL 25, Ultraviolet Products Inc.) was used to qualitatively test for luciferin in photophores by observing fluorescence visually (Barnes *et al.*, 1973).

Bioluminescence depletion and induction

Luminescence was initially detected about 30 days after spawning in 1.7 cm sl larval fish still attached to the nest. Bioluminescence capacity in the laboratory population maintained on a luciferin-free diet increased for 6 months, before gradually declining (Fig. 2). Loss of luminescence capacity occurred from 10 to 18 months after spawning. Laboratory reared and trawled fish showed indistinguishable luminescence levels up to approximately 300 days.

Recently detached juvenile fish (2.5–3.5 cm sl) were exhausted of luminescence capacity by immersing them in 0.005 *M* noradrenalin for approximately 5 min every other day until no luminescent response was elicited (Fig. 3). Depleted animals remained nonluminescent unless their diet was supplemented with luciferin as described below. The remaining untreated population was tested bimonthly for luminescence with noradrenalin. For each sample of the latter group, the tests represented the first exposure to noradrenalin.

Noradrenalin-depleted fish invariably could be restored to luminescence competence by the administration of

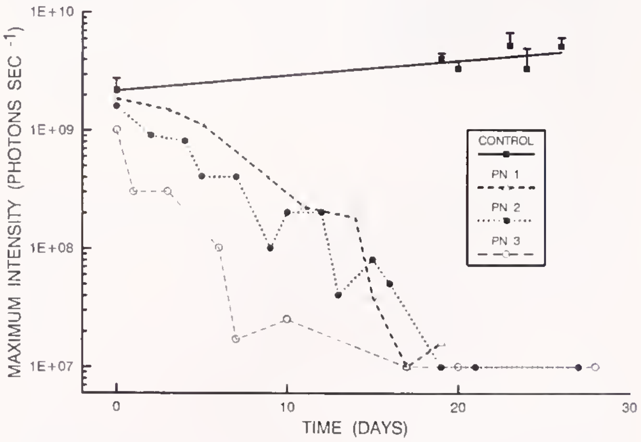

Figure 3. Noradrenalin induced depletion of bioluminescence. Maximum intensity (photons s^{-1}) *versus* time (days) after first challenge with noradrenalin. For control group tested (squares), mean values are shown; error bars represent one SD of mean. Data points represent time of first challenge with noradrenalin. Control fish received only one challenge. For the three experimental fish (circles and triangles), each point represents a challenge. Sample size of each control group was 10. Solid line represents calculated least-squares logarithmic regression of intensity on time according to equation $y = 2.3 \times 10^9 + 0.02x$, $r^2 = 0.61$.

dried *Vargula hilgendorfii* (0.7 to 4.0 mg). Depleted fish were anesthetized in tricaine methane sulfonate (MS 222, ICN-K&K Laboratories), 100 mg/l filtered seawater, and fed 6–12 whole, dried *Vargula hilgendorfii* via intramedic tubing (PE 190) slipped into the anterior gut. Controls were anesthetized but not fed. To guard against regurgitation, fish were monitored for 15 min after regaining their ability to swim. The few ostracods expelled were dried and their weight subtracted from the total.

Restored luminescence neared but never exceeded previous maximum output. Restoration was evident within 24 h, but maximal light output was usually not attained for several weeks. Total light emission was related to the amount of *Vargula* administered (Fig. 4).

Naturally depleted, second year *P. notatus* (9.0 cm sl) also had luminescence capacity restored by ingestion of dried *Vargula hilgendorfii* (5.0–9.0 mg), live *V. tsujii* (n = 3) and recently detached juvenile *P. notatus* (n = 3 to 5) (Fig. 5). For the live feedings, fish were placed in small aquaria containing either three live *V. tsujii*, or five recently detached juvenile *P. notatus* (2.5 cm sl) and monitored until prey were consumed. Restored luminescence neared but never exceeded previous maximum output. Living *Vargula* produced the most rapid onset and greatest intensities. Reinduction was not permanent, and luminescence capacity gradually disappeared with time (Fig. 5). The rise indicated after day 90 in Figure 5 for juvenile *P. notatus* feeding on other *P. notatus* is an aberration representing one fish that had been gradually losing its capacity for luminescence. The other three fish were depleted, but died before testing on day 120. Ingestion of live *V. tsujii* by already competent juveniles did not result in increased light output.

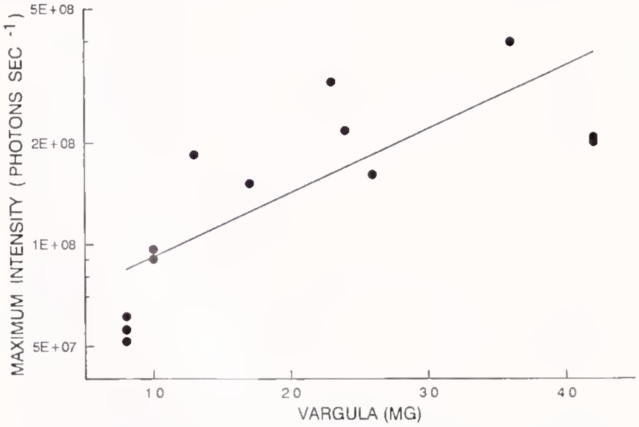

Figure 4. Maximum intensity (photons s^{-1}) *versus* weight of *Vargula* (mg) fed to depleted fish. Points represent individual fish tested 48 h after administration. Line represents calculated least-squares linear regression of light on weight of *Vargula* according to equation $y = 0.43x + 5.9 \times 10^7$, $r^2 = 0.62$.

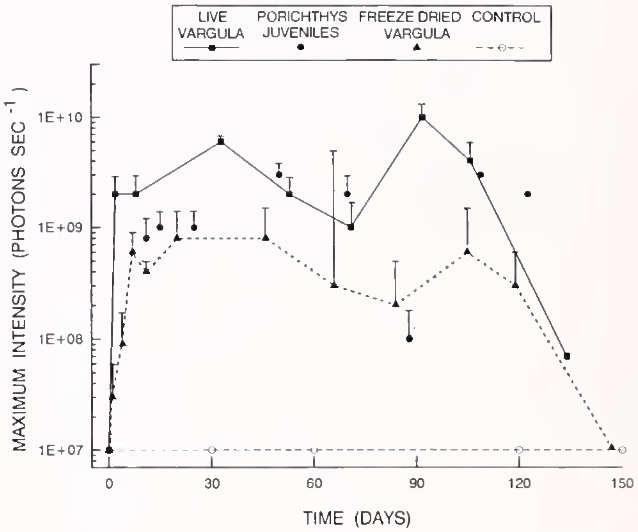

Figure 5. Maximum intensity (photons s^{-1}) *versus* time (days) after feeding with luciferin sources at day 0. Prey included live *Vargula tsujii* (squares), freeze dried *V. hilgendorfii* (triangles), and recently detached *P. notatus* (circles, dotted line). Controls are represented by circles, dashed line. Sample size ranged from 4 to 8 prior to day 90, and 1 to 4 for the rest of the experiment. Dashed line represents background of integrating sphere and points on line are to be considered nonluminescent.

Trawling also reduced or depleted luminescence. The effect was more pronounced in younger (4.2 cm sl) fish captured in November than in older fish of the same year class (6.9 cm sl) trawled the following spring (Fig. 6). Two weeks were needed for captured animals to attain maximum light levels.

Individual photophore responses

Light from individual photophores was also quantified. Thirty microliters of 0.001 *M* noradrenalin was injected under the branchiostegal photophores of a fish anesthetized with tricaine methane sulfonate MS 222 as outlined by Thompson *et al.* (1987). After a 10-min delay to insure that the fish was luminescing, 5–10 photophores of a specific anatomical series were removed surgically as a strip, and immediately placed in filtered seawater in a small, clear plexiglass chamber (4 × 2 × 0.3 cm) in the integrating sphere. Luminescence was measured for 5 min. To insure that preparation time did not bias the measurements, the test order was reversed for every other fish in the test series. All photophore series were tested within 1 h of injection.

The average light intensity of single photophores varied with location on the fish. Photophores from the gular series were significantly brighter (ANOVA: $P < 0.01$) than all other photophores except those from the branchiostegal series (Table I).

Discussion

Larval *P. notatus* from the southern population are initially luminescent. However, these experiments demon-

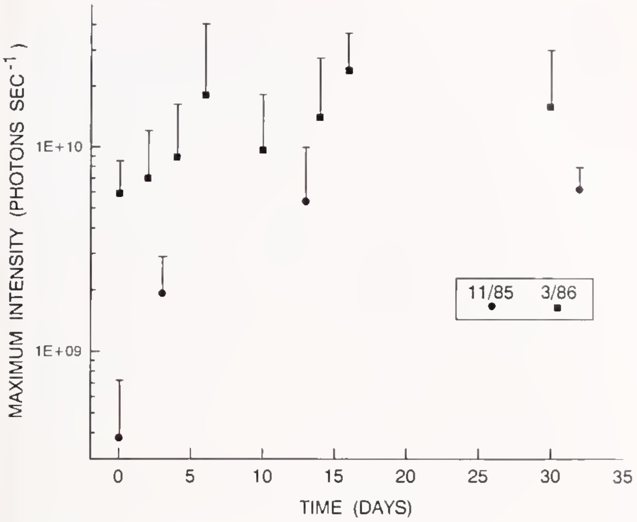

Figure 6. Bioluminescence recovery after collection by trawling. Maximum intensity (photons s^{-1}) *versus* time (days) after trawl. For each group tested, mean values are shown; error bars represent one SD of mean. All fish are from first year class. Points indicate average intensity from *Porichthys notatus* captured off Santa Barbara during 11/85 (circles) or 4/86 (squares). Average standard lengths were 4.2 cm (November) and 6.9 cm (April). The initial two points in each graph represent fish receiving first challenge with noradrenalin. Remaining points represent fish with at least one previous challenge. Sample size ranged from 12 to 25.

strate that exogenous sources of luciferin must be acquired during at least the first two years of life if luminescent capacity is to be retained. Bioluminescence was detected in smaller (1.7 cm sl) fish than has been previously reported, owing perhaps to the increased sensitivity of the integrating sphere photometer over previously used detectors, and to the fact that this photometer allows accurate quantification of luminescence for entire animals rather than only for groups of photophores as in previous studies (Tsuji *et al.*, 1972; Anctil, 1977).

The increase in bioluminescence capacity during the initial six months in laboratory animals shows the importance of maternally provided luciferin reserves. Luminescent capacity did not increase with added exogenous luciferin during this period, indicating emission capacity was not initially substrate limited. The rise in light output during juvenile life is positively correlated with increasing photophore area. Other contributing factors might be increased emission per unit area or increased efficiency of use of luciferin reserves. A comparison of light emission and standard length of laboratory and trawled fish of the same age indicated that our laboratory maintenance procedures had no detrimental effect on bioluminescence capacity or growth during the first half year.

Trawling resulted in an average 60–90% temporary reduction of light capacity with a much greater effect noted in smaller than in larger fish of the same year class. Approximately 25% of trawled fish tested negative for both fluorescence and bioluminescence within 24 h of retrieval. As even dip netting can stimulate luminescence in captive fish, it is highly likely that the stress of trawling invokes luminescence. Although trawl stress may have depressed neurological pathways controlling luminescence, the absence of fluorescence and subsequent return of luminescence indicates that the cause is luciferin depletion in the light organs and that time is required to replenish the substrate from reserves. Larger fish exhibited less reduction perhaps due to greater luciferin concentration in their larger photophores and reserves or better resistance to stress. These results strongly indicate that care should be taken in interpreting luminescence capacity of recently trawled fish, especially smaller ones, because our tests with UV and noradrenalin indicate that 25–50% of a particular trawl would be non-luminescent immediately after capture, even though all regained luminescence within a week. Our results indicate that Thompson and Tsuji (1989) may have overestimated the number of nonluminescent fish in their trawls as fish were not given time to recover.

The adaptive significance of bioluminescence in the midshipman has long been obscure. It has been speculated that the photophores attract prey by mimicking euphausiid swarms (Tsuji *et al.*, 1971). Displays have been observed during mating and in response to predators (Crane, 1965; Lane, 1967). A role in mating is unclear because females are acoustically attracted to mate and the nesting environment does not optimize the effect of bioluminescent displays. We have observed numerous successful matings in laboratory tanks and only once was luminescence briefly noted. Furthermore, the northern population reproduces without luminescence capability.

The dominantly ventral photophore position and the intensity range of light emission seems ideal for counter-

Table I

Average intensity (photons s^{-1}) of individual photophores from various anatomical series

Individual Photophore Response		
Photophore location[1]	n	Average intensity ± 1 S.D. photons s^{-1} per photophore
Mandibular	36	$1.7 \times 10^6 \pm 1.1 \times 10^6$
Branchiostegal	32	$4.3 \times 10^7 \pm 1.6 \times 10^7$
Gular	29	$7.6 \times 10^7 \pm 4.5 \times 10^7$
Ventral	36	$2.7 \times 10^6 \pm 2.6 \times 10^6$
Pleural	33	$4.0 \times 10^6 \pm 2.9 \times 10^6$
Scapular	23	$4.4 \times 10^5 \pm 8.1 \times 10^4$

[1] According to Greene (1899).

Light was quantified for five minutes. Five to ten photophores were tested in each fish and n represents total number of photophores tested. Photophores were taken from four adult fish.

illumination. Although the *P. notatus* emission spectrum (Tsuji *et al.*, 1975) does not exactly match nocturnal astronomic light (Munz and MacFarland, 1977), this may be unimportant because many of the California nearshore fishes that feed primarily at night lack the visual pigments necessary to detect hue differences (Hobson *et al.*, 1981). Additionally, the variability in water quality of nearshore waters can alter the apparent emission spectrum. Luminescence intensity is sufficient to counterilluminate moon or starlight throughout most of the normal depth range. Upon leaving the nest, fish emit at 2.0×10^4 photons s^{-1} cm^{-2}, which is sufficient to counterilluminate starlight at approximately 30 m depth and full moonlight at 70 m depth in Class 1A oceanic water (Jerlov, 1976) on cloudless nights. The fish probably could match intensities at somewhat shallower depths because the nests are found in water usually less clear than class IA and the effects of kelp canopies or clouds are considerable.

Although counterillumination in fish has not been demonstrated in captivity, its presumed importance may explain the early onset of luminescence in larval fish that become competent to luminesce weeks before detachment. Given the inverted position of the larvae, low reflectivity of the substrate and presence of a guardian male, it is doubtful that luminescence has much functional significance on the nest. However, it may be vital to counterilluminate immediately after detachment.

This study shows, for the first time, depletion of luminescence in previously competent fish. Other investigators had been unable to deplete naturally luminous adult fish or ostracod-induced northern fish despite long periods of captivity or multiple challenges with noradrenalin (Tsuji *et al.*, 1972; Barnes *et al.*, 1973; Thompson *et al.*, 1987). In our study, luminescence was depleted by frequent challenges with topically applied noradrenalin or by maintenance on a luciferin-free diet. Noradrenalin treatment depleted luminescence within three weeks in recently detached fish, thus leading to the conclusions that frequent stimulation expends maternally acquired reserves and that a regeneration process is not present. In juvenile southern fish, lack of exogenous luciferin also depleted luciferin reserves within 10–18 months. The depletion may have been the result of spontaneous luminescence or metabolic elimination of luciferin. Loss of luminescent capacity by whatever means was not detrimental to the photophores as luminescence could be restored by luciferin administration.

The three luciferin sources used in our experiments all induced luminescence between 20 and 48 h, more than twice as quickly as reported in previous studies (Tsuji *et al.*, 1972; Barnes *et al.*, 1973). This is attributed to the smaller body size of the fish, which presumably allowed quicker substrate transport to the photophores, and improved instrumentation.

Although it has long been speculated that *V. tsujii* is the source of *P. notatus* luminescence, this is the first study in which fish were found to actively prey on *V. tsujii*, albeit in laboratory tanks. Cannibalism was also observed for the first time in *P. notatus*. First year fish are easy prey of older fish, and small conspecifics have been noted in the stomach of the closely related species, *P. myriaster* (Allen, 1982). Previously it had been thought that young fish must accumulate adequate life-time luciferin reserves before reaching maturity (Warner and Case, 1980), because it seemed unlikely that larger fish would consume small ostracods and would, at any rate, occupy deeper water outside the range of *Vargula*. Clearly, such is not the case and the overlapping ranges of first and second year fish off Santa Barbara make it possible for younger fish to be an additional exogenous source of luciferin for older conspecifics, thus establishing a link which would allow the larger fish effective indirect access to *Vargula* luciferin.

It was calculated using the methods of Thompson *et al.*, (1987) that the fish should theoretically yield approximately 2×10^{15} photons s^{-1} for the amount of dried *Vargula* ingested. Although light emission was only quantified for 5 min, none of the induced fish emitted light for over 40 min and many displays lasted less than 20 min towards the end of the study. Even using the extremely liberal calculation of multiplying the maximum intensity attained during the run by 40 min to derive photon yield, and then summing the trials for each fish, the brightest fish only produced 2×10^{13} photons s^{-1} (range 2×10^{12} to 2×10^{13} photons s^{-1}), a value two orders of magnitude below the theoretical yield. Thompson *et al.* (1988) report that the fish retain approximately 1% of the luciferin ingested. Even after estimating the luciferin retention rate at two orders of magnitude less than actually ingested, the majority of the induced fish fall short of attaining theoretical values.

These experiments do not support either a luciferin synthesis or recycling mechanism for juveniles of the southern population. Luminescence could be depleted by continual challenges with noradrenalin or maintenance on a luciferin-free diet. Although luminescence could be restored with exogenous sources of luciferin, the effect was not prolonged and emission values fell short of theoretical values.

These results contrast with the reports of Thompson *et al.* (1987; 1988a,b) who found that the persistence of *V. hilgendorfii* [^{14}C]luciferin in the photophores and long lasting luminescence after feeding small amounts of luciferin suggested an active recycling mechanism in Puget Sound adults (Thompson *et al.*, 1988b). Furthermore, they reported *Vargula* feeding to previously non-luminescent fish, yielded more light than was theoretically possible for amount of luciferin ingested.

A major difference between our investigations and those of Thompson *et al.* (1987; 1988a,b) was our use of southern juveniles instead of northern adults. These populations may have evolved different luciferin pathways in response to availability of exogenous luciferin in the diet of adults. The southern habitat includes two luciferin sources, *V. tsujii* and young *P. notatus*. Perhaps owing to this, they have lost or have never evolved an alternative mechanism, or possibly it does not function until their later, deep water stage when they are out of range of exogenous sources. If *Vargula* disappeared gradually from the northern range, the northern fish might have evolved mechanisms to maximize the effects of increasingly rare encounters with luciferin sources. Another possibility is that the pathways require minimal amounts of luciferin to function. Once levels drop below a critical concentration, enzymes needed for synthesis or recycling are no longer produced.

A second difference in these investigations is that the use of the integrating sphere photometer allowed us to quantify more accurately the total light emission per fish and avoid the assumptions concerning total light emitted, average intensity, and differential photophore emission made in previous reports (Thompson *et al.*, 1987). For example, Thompson *et al.* (1987) multiplied the directly measured intensity of 127 photophores mostly from the branchiostegal and gular series (Greene, 1899) by 4.3 to determine light emission from the whole fish, with the underlying assumption that all photophores emit equal intensities. However, we find that the branchiostegal and gular series contain the most intensely emitting photophores of the entire fish (Table I). We calculated emission based on photophore average intensity by dividing the fish into three areas: ventral photophores inside the light capture geometry of the Thompson *et al.* (1987) photomultiplier (branchiostegal and gular series; n = 127), remaining ventral and lateral photophores (mandibular, ventral, and lateral series; n = 397) and head and dorsal photophores (scapular series; n = 150). We determined total light output by taking the average intensity of the photophores contained within representative series (listed above for each area) and multiplying the average photophore intensity by the approximate number of photophores contained within each area. Our values indicate that quantification of light intensity for the whole animal by extrapolating from only the branchiostegal and gular photophores overestimates light emission by at least a factor of 3.5.

Another factor not considered by Thompson *et al.*, (1987) in arguing for luciferin recycling is that, in the course of losing luminescence capability, fish initially lose luminescence capacity in posterior photophores. Fish low in luminescence capacity were noted by dark adapted observers to have many posterior photophores unresponsive to noradrenalin application (Mensinger and Case, unpub.). Whether this is due to smaller reserves in posterior photophores or a transport mechanism that gives the anterior sites higher priority remains unknown. A mechanism favoring supply of luciferin to anterior ventral photophores during luciferin limitation would have adaptive value in preserving counterillumination capability for the larger and therefore more conspicuous, anterior regions. If the latter is true, however, the localized anterior noradrenalin injection sites used in Thompson *et al.* (1987) may have disproportionately depleted luciferin reserves from the anterior series, thus resulting in the transport of luciferin from the more distal sites. Whatever the mechanism, extrapolating intensities from anterior photophores would, therefore, result in erroneously higher emission estimates and thereby induce error into calculations of luciferin use.

We found no evidence of a mechanism for long-term maintenance of luminescence capacity in southern fish. Eventual loss of luminescence in animals without previous noradrenalin exposure rules out the possible deleterious effects of repeated noradrenalin challenges in the fish used in our investigation. The loss of luminescence capacity after induction with luciferin showed that there was no synthesis mechanism dependent on priming with non-maternal sources of luciferin. The loss of maternally or naturally acquired reserves through spontaneous luminescence, diffusion, or autoxidation may have decreased luciferin below recyclable levels. However, the relatively short reinduction periods (3–6 months) and low photon yields cast doubt on the presence of a recycling mechanism in second year southern fish.

We conclude that fish of the southern population must continually acquire exogenous sources of luciferin, at least during their early life history, to remain luminescent.

Acknowledgments

J. Warner contributed to the early phases of this study. J. G. Morin and A. Huvard kindly provided living *Vargula*. J. G. Morin also most helpfully reviewed the manuscript and provided other useful comments. A. Uriu and L. Trebasky helped with animal maintenance. Research was supported in part by Office of Naval Research Contracts N00014-84-K-0314 and N00014-89-J-1736.

Literature Cited

Allen, M. J. 1982. Functional structure of soft-bottom communities of the southern California shelf. Ph. D. thesis, University of California, San Diego, La Jolla, California.

Anctil, M. 1977. Development of bioluminescence and photophores in the Midshipman fish, *Porichthys notatus*. *J. Morphol.* **151:** 363–396.

Arora, H. L. 1948. Observations on the habits and early life history of the batrachoid fish, *Porichthys notatus* Girard. *Copeia* **1948:** 89–93.

Barnes, A. T., J. F. Case, and F. I. Tsuji. 1973. Induction of bioluminescence in a luciferin deficient form of the marine teleost *Porich-*

thys, in response to exogenous luciferin. *Comp. Biochem. Physiol.* **46A:** 709–723.

Crane, J. M. 1965. Bioluminescent courtship display in the teleost *Porichthys notatus. Copeia* **1965:** 239–241.

Feder, H. M., C. H. Turner, and C. Limbaugh. 1974. Observations on fishes associated with kelp beds in Southern California. *Calif. Dept. Fish and Game, Fish Bull.* **160.** 144 pp.

Greene, C. W. 1899. The phosphorescent organs in the toadfish, *Porichthys notatus* Girard. *J. Morphol.* **15:** 667–696.

Hobson, E. S., W. N. McFarland, and J. R. Chess. 1981. Crepuscular and nocturnal activities of Californian nearshore fishes, with consideration of their scotopic visual pigments and the photic environment. *Fish. Bull.* **79:** 1–30.

Hubbs, C. L. 1920. The bionomics of *Porichthys notatus* Girard. *Am. Nat.* **54:** 380–384.

Ibara, R. M. 1967. Biology of the midshipman fish, *Porichthys notatus* Girard. M. A. thesis, University of California, Santa Barbara, California.

Jerlov, N. G. 1976. *Marine Optics,* Elsevier, Amsterdam, 231 pp.

Kornicker, L. S., and J. H. Baker. 1977. *Vargula tsujii,* a new species of luminescent ostracoda from lower and southern California (Myodocopa: Cypridininae). *Proc. Biol. Soc. Wash.* **90:** 218–231.

Lane, E. D. 1967. A study of the Atlantic midshipman *Porichthys porosissimus* in the vicinity of Port Aransas, Texas. *Contri. Mar. Sci* **12:** 1–53.

Latz, M. I., T. M. Frank, M. R. Bowlby, E. A. Widder, and J. F. Case. 1987. Variability in flash characteristics of a bioluminescent copepod. *Biol. Bull.* **173:** 489–503.

Munz, F. W., and W. N. McFarland. 1977. Evolutionary adaptation of fishes to the photic environment. Pp. 193–274 in *Handbook of Sensory Physiology,* Vol. VII/5, F. Crescitelli, ed. Springer, Berlin, Heidelberg, New York.

Strum, J. 1969. Fine structure of the dermal luminescent organs, photophores, in the fish *Porichthys notatus. Anat. Rec.* **164:** 433–461.

Thompson, E. M., B. G. Nafpaktitis, and F. I. Tsuji. 1987. Induction of bioluminescence in the marine fish *Porichthys* by *Vargula* (crustacean) luciferin. Evidence for *de novo* synthesis or recycling of luciferin. *Photochem. Photobiol.* **45:** 529–533.

Thompson, E. M., Y. Toya, B. G. Nafpaktitis, T. Goto, and F. I. Tsuji. 1988a. Induction of bioluminescence capability in the marine fish, *Porichthys notatus,* by *Vargula* (crustacean) [^{14}C]luciferin and unlabeled analogues. *J. Exp. Biol.* **137:** 39–51.

Thompson, E. M., B. G. Nafpaktitis, and F. I. Tsuji. 1988b. Dietary uptake and blood transport of *Vargula* (crustacean) luciferin in the bioluminescent fish, *Porichthys notatus. Comp. Biochem. Physiol.* **89A:** 203–209.

Thompson, E. M., and F. I. Tsuji. 1989. Two populations of the marine fish *Porichthys notatus,* one lacking in luciferin essential for bioluminescence. *Mar. Biol.* **102:** 161–165.

Tsuji, F. I., Y. Haneda, R. V. Lynch III, and N. Sugiyama. 1971. Luminescence cross-reactions of *Porichthys* luciferin and theories on the origin of luciferin in some shallow-water fishes. *Comp. Biochem. Physiol.* **40A:** 163–179.

Tsuji, F. I., A. T. Barnes, and J. F. Case. 1972. Bioluminescence in the marine teleost, *Porichthys notatus,* and its induction in a nonluminous form by *Cypridina* (ostracod) luciferin. *Nature* **237:** 515–516.

Tsuji, F. I., B. G. Nafpaktitis, T. Goto, M. J. Cormier, J. E. Wampler, and J. M. Anderson. 1975. Spectral characteristics of the bioluminescence induced in the marine fish, *Porichthys notatus,* by *Cypridina* (ostracod) luciferin. *Molec. Cell. Biochem.* **9:** 3–8.

Warner, J. A., and J. F. Case. 1980. The zoogeography and dietary induction of bioluminescence in the midshipman fish, *Porichthys notatus. Biol. Bull.* **159:** 231–246.

Wilimovski, N. J. 1954. List of the fishes of Alaska. *Stanford Ichthyol. Bull.* **4:** 279–294.

Reference: *Biol. Bull.* **181:** 189–194. (August, 1991)

Vanadobin, a Vanadium-Binding Substance, Extracted from the Blood Cells of an Ascidian, Can Reduce Vanadate(V) to Vanadyl(IV)

HITOSHI MICHIBATA[1,*], AKEMI MORITA[1], AND KAN KANAMORI[2]

[1]*Biological Institute and* [2]*Department of Chemistry, Faculty of Science,*
Toyama University, Gofuku 3190, Toyama 930 Japan

Abstract. Ascidians specifically accumulate high levels of vanadium from seawater in their blood cells. Almost all of the vanadium is present in a reduced form in the blood cells, although the metal exists in a +5 oxidation state in seawater. It has, therefore, been assumed that agents that cause the reduction of vanadate(V) to vanadyl(IV) must be present within ascidian blood cells. In this regard, we have extracted a vanadium-binding substance, which we have called vanadobin, from the vanadocytes of ascidians. We examined whether vanadobin is involved in the reduction of vanadate(V) accumulated from seawater. Data obtained by spectrophotometry and ESR spectrometry revealed that not only a crude homogenate of vanadium-rich blood cells but also a purer form of vanadobin eluted from a column of Sephadex G-15 could reduce vanadate(V). Our experiments demonstrate that vanadobin, a vanadium-binding substance extracted from ascidian blood cells, can reduce vanadate(V) to vanadyl(IV) and maintain it in the reduced form.

Introduction

Vanadium, a multivalent metal, is generally present in the biosphere in the +5, +4, and +3 oxidation states (Chasteen, 1983; Kustin *et al.*, 1983). Among all organisms examined, ascidians appear to be the only ones that contain high levels of vanadium. High levels of specifically accumulated vanadium in the blood cells of ascidians are reduced predominantly to the +3 oxidation state, with a small amount of vanadium also present in the +4 oxidation state (Tullius *et al.*, 1980; Dingley *et al.*, 1981; Frank *et al.*, 1986; Lee *et al.*, 1988; Hirata and Michibata, 1990), even though the vanadium dissolved in seawater seems to be present as vanadate(V) anions in the +5 oxidation state (McLeod *et al.*, 1975). Therefore, it has been assumed that some agent that causes the reduction of vanadate(V) to vanadyl(IV) must be present in ascidian blood cells because they accumulate the metal from seawater.

We have already reported the extraction of a vanadium-binding substance, which we have called vanadobin, from the vanadocytes of ascidians (Michibata *et al.*, 1986; Michibata and Uyama, 1990; Michibata *et al.*, 1990a). Vanadium incorporated into vanadobin is maintained in the reduced form and, therefore, vanadobin seems to be able to reduce vanadate(V) to vanadyl(IV). In the present experiments, the metal-reducing ability of vanadobin was examined by spectrophotometry and ESR (electron spin resonance) spectrometry, after we demonstrated that the supernatant of a homogenate of the blood cells could reduce the vanadate(V).

Materials and Methods

Homogenates of blood cells

Specimens of *Ascidia gemmata* were collected at the Asamushi Marine Biological Station of Tohoku University in Asamushi, Aomori, Japan. The animals were transported to our laboratory and maintained in an aerated aquarium at 12°C until use. Blood was collected by cardiac puncture under an anaerobic atmosphere of nitrogen gas to preclude oxidation by air; subsequent manipulations were also carried out under the same conditions. The blood cells were separated from the blood plasma by centrifugation at 3000 × *g* for 10 min at 4°C. About

---

Received 16 January 1991; accepted 18 March 1991.

* Present address: Mukaishima Marine Biological Laboratory, Hiroshima University, Mukaishima-cho, Hiroshima 722, Japan.

10 g wet weight of the pellet of blood cells were resuspended in 3 ml of acidified, deionized, and distilled water (acidic DDW) that had been degassed, bubbled with nitrogen gas, and adjusted to pH 2.3 with 2 *M* HCl. We feared that the buffer solution, such as HCl-glycine buffer, might interfere with ESR spectrometry; therefore, no buffer solution was used in these experiments. The suspension was then ground in a glass-Teflon homogenizer at 4°C. After adding 12 ml of acidic DDW, the homogenate obtained was centrifuged at 11,500 × *g* for 10 min, to remove the cell debris. An aliquot of the supernatant of the homogenate was examined for its ability to reduce vanadate(V) to vanadyl(IV).

Extraction of vanadobin (vanadium-binding substance)

The extraction of vanadobin was carried out as described previously using 7 ml of supernatant obtained as described above (Michibata *et al.*, 1990a). The supernatant was loaded onto a column (3.6 cm $\phi \times 56$ cm long) of Sephadex G-15 (Pharmacia Fine Chemicals, Uppsala, Sweden) and eluted with acidic DDW in 5 ml.

The peak fractions, monitored at 254 nm, were separately pooled and lyophilized, and then were redissolved in 10 ml of acidic DDW and kept in anaerobic atmosphere before use.

Spectrophotometric measurements of the reduction of vanadate(V)

Aqueous solutions of vanadium(III) sulfate [$V_2(SO_4)_3$] and vanadium(IV) oxide sulfate ($VOSO_4$) at low pH exhibit absorption maxima at 420 nm and 620 nm, and at 760 nm with a shoulder around 625 nm, respectively, whereas an aqueous solution of sodium vanadium(V) (Na_3VO_4) exhibits no absorption maximum in the visible range. We have already demonstrated that the ratio of vanadium ions in the +3 state to those in the +4 oxidation state, which are associated with vanadobin, can be calculated from the respective molar absorption coefficients (ϵ) (Michibata *et al.*, 1990a), using the following formulae:

$$D_{620} = A[M] \times \epsilon^{III}_{620} + B[M] \times \epsilon^{IV}_{620}$$

$$D_{760} = A[M] \times \epsilon^{III}_{760} + B[M] \times \epsilon^{IV}_{760}$$

Here, D_{620} and D_{760} are the observed absorbance of vanadobin at 620 nm and 760 nm, respectively and ϵ^{III}_{620}, ϵ^{III}_{760}, ϵ^{IV}_{620}, and ϵ^{IV}_{760} are the molar absorption coefficients of inorganic vanadium(III) and vanadium(IV) in water at each wavelength. Molar concentrations of vanadium(III) and vanadium(IV) associated with vanadobin, A[M] and B[M], can be calculated from the observed absorbance at 620 nm and 760 nm.

Electron spin resonance (ESR) measurements of the reduction of vanadate(V)

ESR spectrometry was carried out as described previously (Hirata and Michibata, 1990). Briefly, 100 μl of a mixture of two volumes of sample and one volume of 4 *M* H_2SO_4 were put into a quartz tube. We used a JES-RE1X ESR spectrometer (JEOL Ltd., Tokyo) for ESR spectrometry. The instrument conditions were adjusted as follows: microwave frequency, 9.2 GHz; magnetic field, 330 ± 100 mT; microwave power, 5 mW; field modulation frequency, 100 kHz; field modulation width, 0.63 mT; and sweep time for recording, 4 min.

Chemicals

All chemicals used were obtained from commercial sources and were of special grade, except for $V_2(SO_4)_3$, which was prepared according to the literature (Claunch and Jones, 1963).

Results

Reduction of vanadate(V) by a homogenate of blood cells

As shown in Figure 1, the supernatant of the homogenate of blood cells exhibits two absorption maxima at

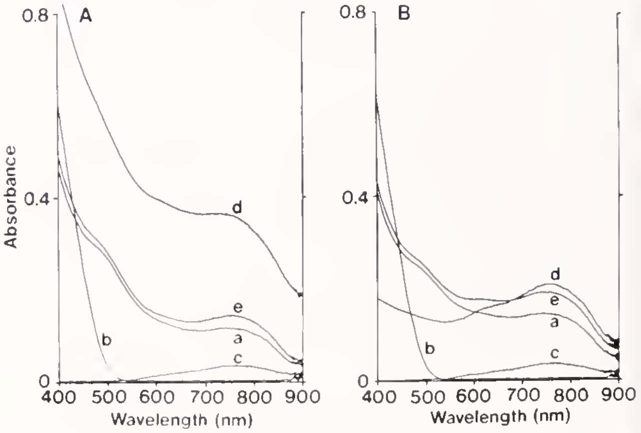

Figure 1. Reduction of vanadate(V) by the supernatant of a homogenate of blood cells from *Ascidia gemmata*, as monitored by spectrophotometry. A. Immediately after the start of the reaction. B. Thirty-one hours after the start of the reaction. Absorption spectrum of the supernatant of the homogenate of blood cells (a), of 8 m*M* vanadate(V) (b), and of 8 m*M* vanadyl(IV) (c). When an 8 m*M* solution of vanadate(V) was added to the supernatant, absorbance in the vicinity of 760 nm due to vanadyl(IV) increased (d). Thirty-one hours after the reaction, absorbance at the shorter wavelength than 530 nm due to vanadate(V) decreased and that at 760 nm became clear (d), suggesting that the added vanadate(V) was reduced to vanadyl(IV) by the supernatant. By contrast, addition of an 8 m*M* solution of vanadyl(IV) to the supernatant resulted in little change in the absorption spectrum (e) both immediately after and 31 hours after the start of the reaction. The higher base line in the absorption spectrum of (d) than the others caused turbidity appeared when vanadate(V) solution was added to the sample.

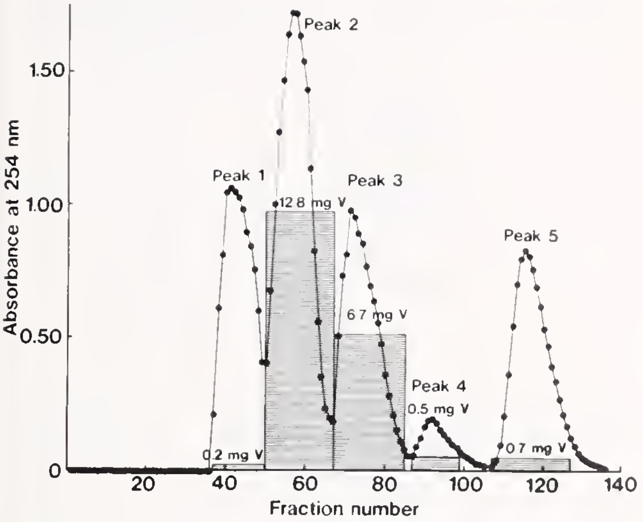

Figure 2. Elution profile of the supernatant of a homogenate of blood cells from *Ascidia gemmata* from a column of Sephadex G-15. The supernatant (7 ml) was loaded onto a column (3.6 cm ϕ × 56 cm long) of Sephadex G-15 (Pharmacia Fine Chemicals) and eluted with DDW (see text) at pH 2.3 in 5 ml. Fractions composing each peak were separately pooled, and amounts of vanadium in individual aliquots were measured by ESR spectrometry. Then, the material under each peak was lyophilized and kept under anaerobic conditions. The material in the second peak contained the highest amount of vanadium. V_t: 570 ml, V_o: 226 ml, and V_e: 280 ml.

620 nm and 760 nm, which are assignable to vanadium(III) and vanadyl(IV), respectively. Comparing the corresponding spectra observed in inorganic vanadium complexes, as demonstrated previously (Michibata *et al.*, 1990a), we calculated that the supernatant of the homogenate of the blood cells intrinsically contained 25 m*M* vanadium in the +3 and +4 oxidation states at a ratio of 30:70.

After adding 1.2 ml of an 8 m*M* solution of vanadate(V) to an equal volume of the supernatant, spectral changes were recorded. Figures 1A and 1B show the spectra immediately after mixing and after 31 h. The absorbance at 760 nm due to vanadyl(IV) became conspicuous, accompanying the decrease of the absorbance at the wavelength shorter than 530 nm due to vanadate(V) with time, suggesting that the added vanadate(V) was reduced to vanadyl(IV) by the supernatant. By contrast, the addition of the same amount of an 8 m*M* solution of vanadyl(IV) resulted in little change. These observations indicate clearly that some reducing agent is present in the supernatant of homogenate of blood cells from *Ascidia gemmata*, which can reduce vanadate(V) to vanadyl(IV). As shown in Figure 1B, the spectral change with time reveals that reduction of vanadate(V) to vanadyl(IV) occurred very slowly over the course of 31 h after the onset of the reaction.

Reduction of vanadate(V) by vanadobin; observations by spectrophotometry

When the supernatant of the homogenate of blood cells was eluted from Sephadex G-15, five peaks were obtained (Fig. 2). Amounts of vanadium contained in each peak of material are illustrated as shaded squares in Figure 2.

Reduction experiments were performed with samples of elutant that had been lyophilized and redissolved in 10 ml of acidic DDW. From the ratio of absorbance at 620 nm to that at 760 nm, it was calculated that the material in peak 2 contained vanadium in the +3 and +4 oxidation states at a ratio of 1:25. When 0.8 ml of a solution of vanadyl(IV) or vanadate(V) at concentrations from 4 m*M* to 16 m*M* was added to each peak fraction, reduction of vanadate(V) to vanadyl(IV) was significant in the case of the material in peak 2, when monitored by spectropho-

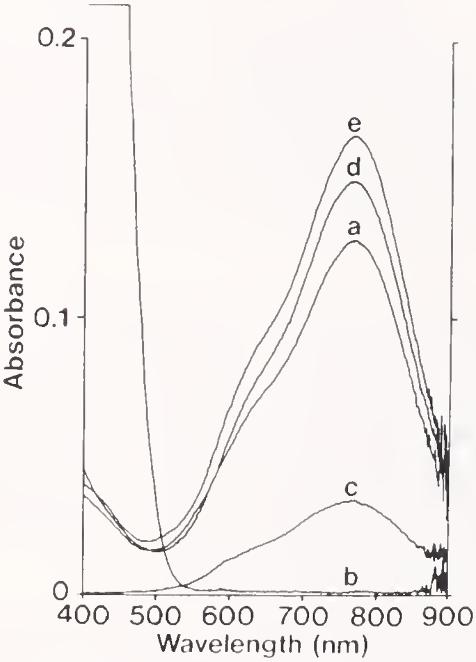

Figure 3. Reduction of vanadate(V) by vanadobin from *Ascidia gemmata* as monitored by spectrophotometry. The samples of lyophilized material (described in the legend to Fig. 2) were redissolved in 10 ml of acidic DDW and reacted with an equal volume of either vanadate(IV) or vanadyl(V), both solutions were at 8 m*M* to examine their ability to reduce vanadium. Absorption spectra of: (a) vanadobin; (b) an 8 m*M* solution of vanadate(V); and (c) an 8 m*M* solution of vanadyl(IV). (d) When vanadate(V) (8 m*M*) was reacted with vanadobin, a marked increased in absorbance at about 760 nm due to vanadyl(IV) was observed, indicating that vanadate(V) was reduced to vanadyl(IV) by vanadobin. (e) By contrast, addition of vanadyl(IV) (8 m*M*) to vanadobin resulted in little change in the absorption spectrum, indicating that no further reduction of vanadyl(IV) to vanadium(III) had occurred. Unlike the results obtained with the supernatant of the homogenate of blood cells depicted in Figure 1, the above changes in absorbance were observed immediately after the start of the reaction, and the reduction was maintained for at least 24 h.

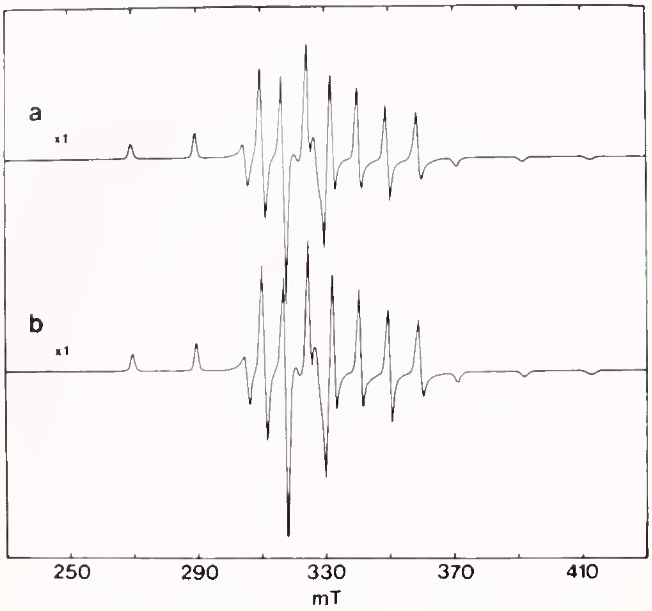

Figure 4. ESR spectra of vanadobin and of a mixture of vanadobin with an 8 m*M* solution of vanadate(V) at 77 K under anaerobic atmosphere of nitrogen gas. (a) Vanadobin, (b) a mixture of vanadobin and 8 m*M* vanadate(V). Oxovanadium [VO^{2+}(IV)] that was intrinsically present in the vanadobin gave typical ESR signals (a). The addition of an 8 m*M* solution of vanadate(V), which alone gave no ESR signal, to an equal volume of vanadobin increased the signal intensity to about 1.2 times that generated by vanadobin alone.

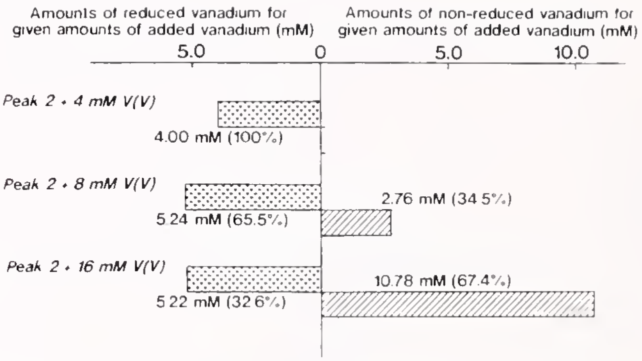

Figure 5. Reduction of vanadate(V) at different concentrations by material from peak 2 contained vanadobin, as measured by ESR spectrometry. All vanadate(V) was reduced to vanadyl(IV) at a concentration of 4 m*M* vanadate(V). However, at 8 m*M* and 16 m*M*, a part of the vanadate(V) added was reduced by vanadobin. Thus, 0.8 ml of solution of vanadobin could completely reduce about 5.2 m*M* of vanadate. In 0.8 ml of the solution of vanadobin, the concentration of vanadium was intrinsically 25 m*M*. If 1 mole of vanadobin contains 1 mole of vanadium ions, then 5 moles of vanadobin readily reduce 1 mole of vanadate(V) to vanadyl(IV).

tometry. Figure 3 shows the rapid reduction of vanadate(V) to vanadyl(IV) that followed the addition of the material in peak 2 (vanadobin). Although vanadate(V) in solution exhibits no absorption in the vicinity of 760 nm, the addition of vanadobin induced a drastic increase in absorbance at 760 nm, which indicates the reduction of vanadate(V) to vanadyl(IV). This spectral change was observed immediately after the start of the reaction, and the reduction was maintained for at least 24 h.

Reduction of vanadate(V) by vanadobin: observation by ESR spectrometry

ESR spectrometry was used to confirm the above results. The oxovanadyl chemical species [VO^{2+}(IV)] is the only species of vanadium that is detectable with an ESR spectrometer. Because the intensity of the ESR signal due to VO^{2+}(IV) depends on the pH, the pH of samples was adjusted to 0.21 (the pH at which the highest intensity of signals was obtained) by the adding one half volume of 4 *M* H_2SO_4. Figure 4 shows the ESR spectra derived from (a) vanadobin and (b) from a mixture of vanadobin and 8 m*M* vanadate(V). The signal intensity of the latter was about 1.2 times as strong as that of the former solution, suggesting that a portion of the added vanadate(V) was reduced to the vanadyl(IV) species by vanadobin. The results obtained are summarized in Figure 5; all of the vanadium in 4 m*M* vanadate(V), 65.5% of that in 8 m*M* vanadate(V) and 32.6% of that in 16 m*M* vanadate(V) was reduced, respectively, after adding vanadobin. It is clear that 0.8 ml of vanadobin prepared by us can reduce 5.2 m*M* vanadate(V) to vanadyl(IV). An aliquot of 0.8 ml of vanadobin contained 25 m*M* intrinsic vanadium. If 1 mole of vanadobin contains 1 mole of vanadium, 5 moles of vanadobin readily reduce 1 mole of vanadate(V) to vanadyl(IV). This assumption, however, needs further investigation.

When the same experiments were carried out with the material in peak 1, a decrease in reducing ability was detected, as shown in Figure 6. The material in peak 1 re-

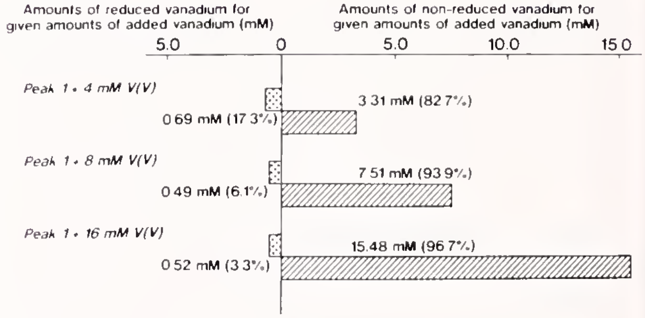

Figure 6. Reduction of vanadate(V) at different concentrations by material in peak 1 which contained no vanadobin, measured by ESR spectrometry as described in the legend to Figure 5. Less reducing ability was observed in this case, unlike that shown in Figure 5. The material in peak 1 reduced a solution of about 0.5 m*M* vanadate(V) which corresponded to between 17.3% and 3.3% of the added metal.

duced about 0.5 m*M* vanadate(V), which corresponded to 17.3% to 3.3% of the added metal. The material in the other peaks eluted from the column showed little reducing ability. Among the rest, the material in peak 3 did not show a reducing ability, although it contained the second highest level of vanadium.

Discussion

Because almost all the vanadium contained in vanadobin is kept in a reduced chemical form (Michibata *et al.*, 1990a), it seems clear that vanadobin cannot only reduce the metal but also maintain in the reduced form. The present results have demonstrated that vanadobin, extracted from the vanadium-rich blood cells of *Ascidia gemmata* by elution from a column of Sephadex G-15, can reduce vanadate(V) to vanadyl(IV), as shown both by spectrophotometry and ESR spectrometry. We have confirmed that no reduction of vanadate(V) occurred when inorganic vanadate(V) and vanadyl(IV) (8 m*M*) were mixed together under the same conditions as those used in the experiments described here (data not shown). It is therefore clear that vanadobin reduces vanadate(V) to vanadyl(IV).

Except for the vanadobin eluted in peak 2 (Fig. 2), the materials in the other peaks showed little ability to reduce the metal. Unexpectedly, the material in peak 3, which contained the second highest amount of vanadium (Fig. 2), did not show a reducing ability. Although its absorption spectrum was different from that of peak 2, which was the typical spectrum of vanadobin, it closely resembled that of the inorganic vanadium complex in the +4 oxidation state, as reported previously (Michibata *et al.*, 1990a). In other words, it may be that peak 3 did not contain vanadobin but inorganic vanadium released from vanadobin; therefore, no reducing ability would be observed.

A crude supernatant, obtained from a homogenate of the blood cells of *A. gemmata*, was also able to reduce vanadate(V). This result is not surprising. In living blood cells, various reducing agents, such as ascorbic acid, glutathione, and cysteine, are generally present. In fact, the supernatant reduced vanadate(V) slowly—for over 31 h after mixing of the supernatant with vanadate(V)—while the extracted vanadobin rapidly reduced the metal after mixing vanadobin with vanadate(V). These phenomena suggest that the crude supernatant contains not only several reducing agents but also several oxidizing agents and, therefore, the reduction of vanadate(V) to vanadyl(IV) may compete against a re-oxidation of vanadium(IV) by some intrinsic oxidizing agents. This may require much more time than that required for purer vanadobin.

Nakanishi's group isolated a tunichrome, composed of three pyrogallol subunits, from ascidian blood cells, and they proposed that it was involved in both the accumulation and the reduction of vanadium in the blood cells (Macara *et al.*, 1979a, b; Bruening *et al.*, 1985). However, in addition to the fact that no fluorescence due to the tunichrome was observed from the vanadocytes (Michibata *et al.*, 1988; 1990b), Bulls *et al.* (1990) pointed out that analogues of the tunichrome were barely able to reduce vanadium(V) to vanadium(IV). Moreover, specific binding of vanadium has not yet been observed within the tunichrome. Therefore, it is noteworthy that the agent that combines with vanadium can reduce vanadate(V), as shown in the present experiments.

We have already demonstrated that the vanadium-containing blood cells—the vanadocytes—are the signet ring cells, and not the morula cells as previously thought (Michibata *et al.*, 1987); we have also shown that vanadobin is contained in the signet ring cells (Michibata and Uyama, 1990) and we have demonstrated that vanadobin may well be a universal complex in ascidians, playing a prominent role in the accumulation of vanadium in blood cells and in the maintenance of its concentration (Michibata *et al.*, 1990a). Therefore, we conclude that vanadate(V) is reduced by vanadobin in the vanadocytes of vanadium-containing ascidians, even though details of the mechanism remain unresolved. The physiological ability, observed uniquely in ascidian blood cells, to reduce and maintain vanadium in the low-oxidation state attracts many investigators in a variety of fields.

Acknowledgments

We would like to express our heartfelt thanks to Dr. T. Numakunai and all other members of the staff of the Asamushi Marine Biological Station of Tohoku University in Asamushi, Aomori, Japan, for supplying the materials and facilitating parts of our work. Thanks are also due to Dr. A. Takeuchi of Toyama University for kindly making his ESR spectrometer available to us. This work was supported in part by Grants-in-Aid from the Ministry of Education, Science and Culture, Japan (#01480026 and #01304007) and was also supported financially from the Institute for Marine Biotechnology.

Literature Cited

Bruening, R. C., E. M. Oltz, J. Furukawa, K. Nakanishi, and K. Kustin. 1985. Isolation and structure of tunichrome B-1, a reducing blood pigment from the tunicate *Ascidia nigra* L. *J. Am. Chem. Soc.* **107:** 5298–5300.

Bulls, A. R., C. G. Pippin, F. E. Hahn, and K. N. Raymond. 1990. Synthesis and characterization of a series of vanadium-tunichrome B 1 analogues. Crystal structure of a tris(catecholamide) complex of vanadium. *J. Am. Chem. Soc.* **112:** 2627–2632.

Chasteen, N. D. 1983. The biochemistry of vanadium. *Structure and Bonding* **53:** 105–138.

Claunch, R. T., and M. M. Jones. 1963. Vanadium(III) sulfate. *Inorg. Synthesis* **7:** 92–94.

Dingley, A. L., K. Kustin, I. G. Macara, and G. C. McLeod. 1981. Accumulation of vanadium by tunicate blood cells occurs via a specific anion transport system. *Biochim. Biophys. Acta* **649:** 493–502.

Frank, P., R. M. K. Carlson, and K. O. Hodgson. 1986. Vanadyl ion EPR as a noninvasive probe of pH in intact vanadocytes from *Ascidia ceratodes Inorg. Chem.* **25:** 470–478.

Hirata, J., and H. Michibata. 1990. Valency of vanadium in the vanadocytes of *Ascidia gemmata* separated by density-gradient centrifugation. *J Exp. Zool.* **257:** 160–165.

Kustin, K., G. C. McLeod, T. R. Gilbert, and L. B. R. Briggs. 1983. Vanadium and other metal ions in the physiological ecology of marine organisms. *Structure and Bonding* **53:** 139–160.

Lee, S., K. Kustin, W. E. Robinson, R. B. Frankel, and K. Spartalian. 1988. Magnetic properties of tunicate blood cells. I. *Ascidia nigra. J. Inorg. Biochem.* **33:** 183–192.

Macara, I. G., G. C. McLeod, and K. Kustin. 1979a. Isolation, properties and structural studies on a compound from tunicate blood cells that may be involved in vanadium accumulation. *Biochem. J.* **181:** 457–465.

Macara, I. G., G. C. McLeod, and K. Kustin. 1979b. Tunichromes and metal ion accumulation in tunicate blood cells. *Comp. Biochem Physiol.* **63B:** 299–302.

McLeod, G. C., K. V. Ladd, K. Kustin, and D. L. Toppen. 1975. Extraction of vanadium(V) from seawater by tunicates: a revision of concepts. *Limnol. Oceanogr* **20:** 491–493.

Michibata, H., T. Miyamoto, and H. Sakurai. 1986. Purification of vanadium binding substance from the blood cells of the tunicate, *Ascidia sydneiensis samea Biochem. Biophys. Res. Commun.* **141:** 251–257.

Michibata, H., J. Hirata, M. Uesaka, T. Numakunai, and H. Sakurai. 1987. Separation of vanadocytes: determination and characterization of vanadium ion in the separated blood cells of the ascidian, *Ascidia ahodori. J. Exp. Zool.* **244:** 33–38.

Michibata, H., J. Hirata, T. Terada, and H. Sakurai. 1988. Autonomous fluorescence of ascidian blood cells with special reference to identification of vanadocytes. *Experientia* **44:** 906–907.

Michibata, H., H. Hirose, K. Sugiyama, Y. Ookubo, and K. Kanamori. 1990a. Extraction of a vanadium-binding substance (vanadobin) from the blood cells of several ascidian species. *Biol. Bull.* **179:** 140–147.

Michibata, H., and T. Uyama. 1990. Extraction of vanadium-binding substance (vanadobin) from a subpopulation of signet ring cells newly identified as vanadocytes in ascidians. *J. Exp. Zool.* **254:** 132–137.

Michibata, H., T. Uyama, and J. Hirata. 1990b. Vanadium-containing blood cells (vanadocytes) show no fluorescence due to the tunichrome in the ascidian, *Ascidia sydneiensis samea. Zool. Sci.* **7:** 55–61.

Tullius, T. D., W. O. Gillum, R. M. K. Carlson, and K. O. Hodgson. 1980. Structural study of the vanadium complex in living ascidian blood cells by X-ray absorption spectrometry. *J Am. Chem. Soc.* **102:** 5670–5676.

(1)

Reference: *Biol. Bull.* **181:** 195–198. (August, 1991)

A Breeding Population of the Western Pacific Crab *Hemigrapsus sanguineus* (Crustacea: Decapoda: Grapsidae) Established on the Atlantic Coast of North America

JOHN J. McDERMOTT

Department of Biology, Franklin and Marshall College, Lancaster, Pennsylvania 17604

The west Pacific grapsid crab Hemigrapsus sanguineus *was found in the United States for the first time in 1988. Additional crabs were recovered in 1990 from Townsends Inlet and Cape May Harbor, New Jersey (22 males, 16 females), and four of the females collected from June through September were ovigerous. Thus,* H. sanguineus *has now established itself in southern New Jersey, the first well-documented case of an exotic brachyuran becoming established along the east coast of the United States.*

The marine grapsid crab *Hemigrapsus sanguineus* (de Haan, 1853), native to the western Pacific Ocean, was first recovered in the eastern United States in September 1988; a single ovigerous female was found in a rocky intertidal zone under a bridge at Townsends Inlet, Cape May County, New Jersey (1) (Fig. 1). The site was not reinvestigated until 20 months later (28 May 1990), and at that time an immature female *H. sanguineus* was recovered [carapace width (CW) × carapace length (CL) = 12.8 × 10.8 mm]. This second finding suggested that the original record of the crab in New Jersey was not simply fortuitous, but that this Pacific brachyuran was established in Atlantic waters. The discovery also provided a rare opportunity to document a potentially major introduction.

Subsequently, 36 additional mature and immature crabs (22 males and 14 females) (Fig. 2) were collected (26 June, 3 and 6 July, 22 August, 21 September, 15 and 28 October 1990) at the same site. Crabs were usually located in the mid to upper intertidal zone under rocks covered with *Fucus vesiculosus,* but at low tide some moved below the mid intertidal. As with many intertidal grapsid crabs that live among rocks, individuals of *H. sanguineus* are secretive and swift, and one must turn rocks over rapidly and snatch them quickly in order to catch them; otherwise, they retreat among the lower inaccessible rocks. All crabs were transported to the Franklin and Marshall laboratory where they were easily maintained individually in 2 cm of unaerated seawater (temperature 19°C, salinity ~30‰); they subsisted on pieces of the macroscopic algae *Enteromorpha* sp. and *Ulva lactuca,* and otherwise required minimal care, except for a daily water change. Crabs were measured with a dial calipers to the nearest 0.1 mm. The 22 males ranged from 8.3 to 24.1 mm CW (mean 17.2 ± 4.6), and from 7.3 to 21.0 mm CL (mean 15.2 ± 4.1); 15 females ranged from 3.6 to 24.4 mm CW (mean 17.6 ± 5.1), and from 3.3 to 21.3 mm CL (mean 15.3 ± 4.4). The greater range in females was due to one juvenile (3.6 mm), resulting from the 1990 spawning season, collected 15 October. The next smallest female was the 12.8 mm specimen collected 28 May; the smallest male (8.3 mm) was collected 26 June. These and other juveniles were probably from the 1989 spawning season.

Ovigerous females (n = 4) were found from June through September (not in July collections). One ovigerous crab, obtained on 26 June (CW × CL = 24.4 × 21.3 mm), carried embryos half filled with yolk but with no apparent pigment or eye development. The crab was preserved three days later, and the embryos were counted (n = 28,702). Two ovigerous crabs (CW × CL = 15.2 × 13.2 mm, 23.2 × 19.8 mm) were collected on 22 August. The smaller of them released its zoeae (n = 6328) two days later, and on 27 August it had another brood. Although the crab aborted many undeveloped eggs from this brood,

Received 15 November 1990; accepted 30 April 1991.

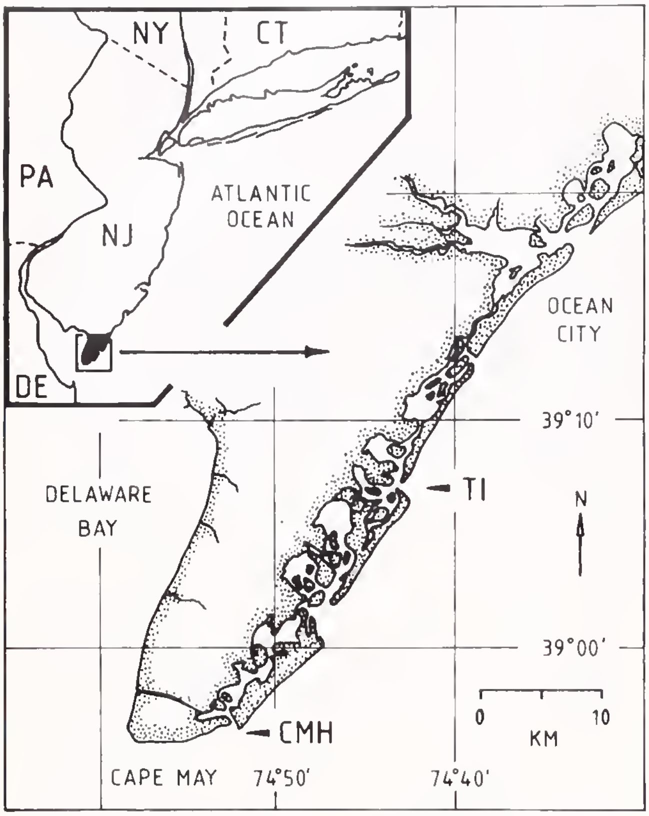

Figure 1. Sites on the Atlantic coast of the Cape May peninsula, New Jersey, where *Hemigrapsus sanguineus* has been discovered. TI = Townsends Inlet (the main study location; CMH = Cape May Harbor, which is inside of Cape May Inlet (indicated).

the zoeae (n = 3360) hatched from the remaining eggs 25 days later. The larger of the two crabs had nearly the full complement of yolk in its embryos, and released its zoeae after 17 days. Many zoeae were eaten by the crab, so the brood was not counted. One of the two females collected on 21 September (CW × CL = 19.3 × 16.8 mm) was ovigerous, and it released its zoeae the next day (n = 13,090). The first female *H. sanguineus* collected 24 September 1988 (1) was also ovigerous. Thus the egg-bearing period extends from at least June through September.

A non-ovigerous female *H. sanguineus* (CW × CL = 18.5 × 16.2 mm) was collected by Lisa Wargo sometime during January or February 1990, in Cape May Harbor (38° 57′ 12″ N, 74° 53′ 20″ W), 23.4 km south of the Townsends Inlet site (Fig. 1). This crab was one of at least three specimens, of apparently the same species; they were recovered from small clumps of mussels (*Mytilus edulis* L.) obtained in the Harbor and were maintained in an aquarium, with fish and other invertebrates, at the Cape May Point State Park. The crabs must have been very small when collected, because they were only noticed later when they were ~10 mm CW. The crab delivered to me was maintained in the aquarium until it was preserved on 18 June 1990.

H. sanguineus has become established on the ocean side of Cape May County, New Jersey, and likely will be found in environmentally suitable locations elsewhere in the state (*i.e.*, in the upper intertidal levels of rocky areas or possibly on artificial substrates suspended near the water line). This crab was probably introduced into the United States before 1988, because its presence could have been easily overlooked. New Jersey may not be *the* focal point or the *only* focal point of its introduction, and perhaps it is already established in adjoining mid-Atlantic states.

H. sanguineus is now the only other member of the genus found in the Atlantic Ocean (2,3,4), except for *H. affinis* Dana, 1851, which ranges from Cape St. Roque, Brazil, to the Gulf of San Matias, Patagonia (5). The genus is represented in the northern hemisphere of the eastern Pacific by *H. nudus* (Dana, 1851) and *H. oregonensis* (Dana, 1851) (5,6), and by *H. crenulatus* (H. Milne Edwards, 1837) in the southern hemisphere (5).

A brief résumé of its life history characteristics may give insight into the potential impact that this grapsid might have on the intertidal environment along the Atlantic seaboard. In Japan, at about the same latitude as New Jersey, *H. sanguineus* is one of the largest and most common grapsid crabs living in rocky intertidal habitats (7). It is sympatric there with at least one other abundant grapsid, *H. penicillatus* (de Haan, 1835). In the rocky intertidal of New Jersey, it may be competitive with the native brachyurans found in the same habitat; *i.e.*, three xanthids, *Eurypanopeus depressus* (Smith, 1869), *Neopanope sayi* (Smith, 1869), and *Panopeus herbstii* H. Milne Edwards, 1834; juveniles of the portunid, *Carcinus maenas* (Linnaeus, 1758); and juveniles of the cancrid, *Cancer irroratus* Say, 1817.

Fukui's studies (8) on the fecundity of *H. sanguineus* in Japan, along with my observations in New Jersey, indicate the potential for its rapid increase in Atlantic waters. Fukui determined that females may live for at least three years, the largest capable of producing more than 5 broods/year, with as many as 56,000 eggs/brood. Using Fukui's regression equation for the correlation between the number of eggs/brood and carapace width, the 35.8 mm ovigerous crab collected in 1988 (1) may have carried more than 52,000 embryos. My preliminary data, however, on brood size *versus* carapace width from the other New Jersey specimens give values somewhat greater than those predicted by Fukui's equation. In Japan, the crab's breeding season is from March to October, with the main peak in May–June (8), a period longer than the four-month season suggested by my preliminary information from New Jersey. The 25-day developmental period at 19°C, recorded for the second brood of the 15.2 mm *H.*

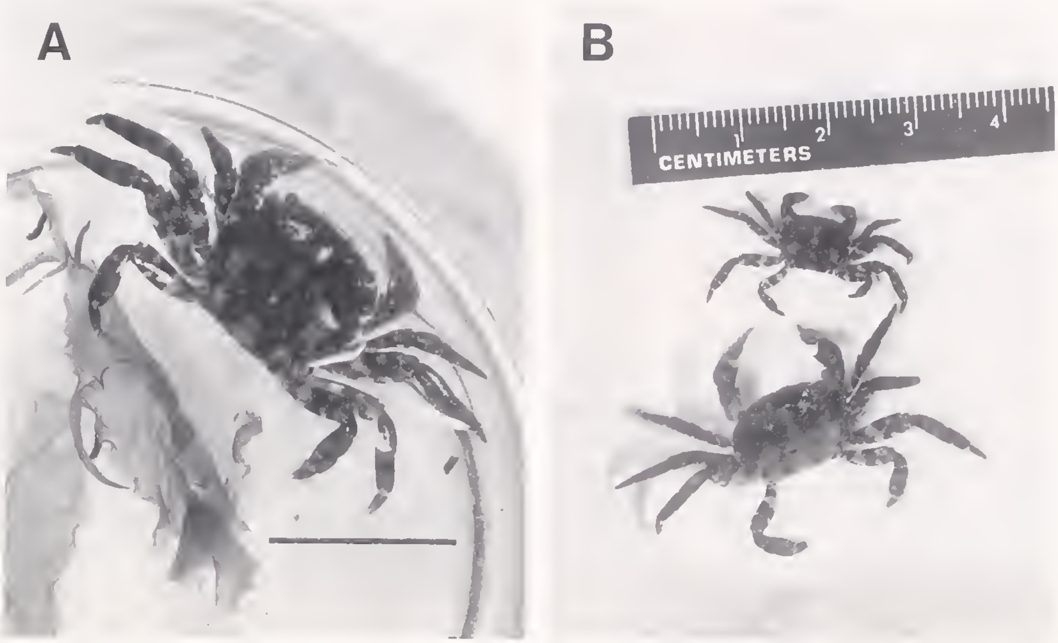

Figure 2. Three living *Hemigrapsus sanguineus* collected 26 June 1990 at Townsends Inlet, New Jersey: A. mature female, 18.5 mm CW, scale = 20 mm; B. mature male, 14.2 mm CW and immature female, 8.3 mm CW.

sanguineus mentioned above, is predicted by Fukui's regression equation for the relationship between incubation period and water temperature for embryos raised in Japan. Water temperatures in New Jersey from June through September would be conducive to the production of about four broods during this period. Fukui found that females reach maturity at 14.0 mm CW, and have a maximum CW of 39.0 mm. Thus, the 35.8 mm ovigerous female collected in New Jersey in 1988 is near the maximum size recorded for Japan, and the smallest mature crab found at Townsends Inlet (CW = 15.2 mm) is close to Fukui's value.

H. sanguineus has not been recorded from the west coast of the United States (6,9,10,11), where the only exotic brachyuran is *Rhithropanopeus harrisii* (Gould, 1841), a xanthid introduced from the Atlantic east coast. There may have been numerous attempts at colonization of the Atlantic coast of the United States and Canada by species of exotic brachyurans, but most seem to have failed prior to *H. sanguineus*. Several authors, cited by Williams (4), agree that the green crab, *C. maenas*, was probably introduced into North America from the eastern Atlantic; it now ranges from Nova Scotia to Virginia (greatest abundance in New England). The timing of such an introduction is not known, and because it could have been prehistoric, its establishment has never been documented. *Carcinus* has had considerable impact in the United States because it prefers bivalves (some commercial) as prey (12,13). The notorious Chinese mitten crab, *Eriocheir sinesis* H. Milne Edwards, 1853, has been reported in Lake Erie, but seems never to have established a breeding population in the Great Lakes (14). A single specimen of *Eriocheir* was reported from Louisiana's Mississippi River Delta region in 1987 (15,16), but has not been found again since.

H. sanguineus could have a great impact on the normal rocky intertidal environment. Therefore, the latitudinal extent of the species must be determined, its spread monitored, and its community interactions studied. Research on its further distribution in New Jersey and other mid-Atlantic states is now underway.

Acknowledgments

I thank L. Wargo, formerly of the Cape May Point State Park, New Jersey, for sending me a specimen of *H. sanguineus* from Cape May Harbor and supplying pertinent information on its collection. I am grateful to J. N. Kraeuter and R. Wargo of the Rutgers University Shellfish Research Laboratory for their assistance, to J. L. Richardson of Franklin and Marshall College and A. B. Williams of the NMFS Systematics Laboratory, Smithsonian Institution, for reviewing the manuscript, and to C. R. Shearer, Jr. and R. A. Fluck of Franklin and Marshall College for providing photographs and for help in the maintenance of crabs, respectively.

Literature Cited

1. **Williams, A. B., and J. J. McDermott. 1990.** An eastern United States record for the western Indo-Pacific crab, *Hemigrapsus san-*

guineus (Crustacea: Decapoda: Grapsidae). *Proc. Biol. Soc. Wash.* **103:** 108–109.

2. **Monod, Th. 1956.** Hippidea et Brachyura ouest-africains. *Mémoires de l'Institut Français d'Afrique Noire,* No. 45, 674 pp.
3. **Manning, R. B., and L. B. Holthuis. 1981.** West African brachyuran crabs (Crustacea: Decapoda). *Smithson. Contrib. Zool.* No. 306, 379 pp.
4. **Williams, A. B. 1984.** *Shrimps, Lobsters, and Crabs of the Atlantic Coast of the Eastern United States, Maine to Florida.* Smithsonian Institution Press, Washington, DC. 550 pp.
5. **Rathbun, M. J. 1918.** The grapsoid crabs of America. *U. S. Natl. Mus. Bull.* No. 97: 461 pp., 161 plates.
6. **Morris, R. H., D. P. Abbott, and E. C. Haderlie. 1980.** *Intertidal Invertebrates of California.* Stanford University Press, Stanford, CA. 690 pp.
7. **Sakai, T. 1976.** *Crabs of Japan and the Adjacent Seas.* Kodansha Ltd. Tokyo, 773 pp. (English text), 251 plates (many colored), 461 pp. (Japanese text), as 3 separate volumes.
8. **Fukui, Y. 1988.** Comparative studies on the life history of the grapsid crabs (Crustacea, Brachyura) inhabiting intertidal cobble and boulder shores. *Pub. Seto Mar. Biol. Lab.* **33:** 121–162.
9. **Carlton, J. T. 1979.** Introduced invertebrates of San Francisco Bay. Pp. 427–444 in *San Francisco Bay the Urbanized Estuary,* T. J. Conomos, ed. Pacific Division, American Association for the Advancement of Science, San Francisco, CA.
10. **Carlton, J. T. 1985.** Transoceanic and interoceanic dispersal of coastal marine organisms: the biology of ballast water. *Oceanog. Mar. Biol. Ann. Rev.* **23:** 313–371.
11. **Carlton, J. T. 1989.** Man's role in changing the face of the ocean: biological invasions and implications for conservation of near-shore environments. *Conserv. Biol.* **3:** 265–273.
12. **Glude, J. B. 1955.** The effects of temperature and predators on the abundance of the soft-shell clam, *Mya arenaria,* in New England. *Trans. Am. Fish. Soc.* **84:** 13–26.
13. **Ropes, J. W. 1968.** The feeding habits of the green crab, *Carcinus maenas* (L.). *Fish. Bull.* **67:** 183–203.
14. **Nepszy, S. J., and J. H. Leach. 1973.** First records of the Chinese mitten crab, *Eriocheir sinensis,* (Crustacea: Brachyura) from North America. *J. Fish. Res Bd. Can.* **30:** 1909–1910.
15. **Horwath, J. L. 1988.** Injurious wildlife: mitten crabs. Proposed rule. *Federal Register* **53**(219): 45784–45788.
16. **Horwath, J. L. 1989.** Importation or shipment of injurious wildlife: mitten crabs. Rules and regulations. *Federal Register* **54**(96): 22286–22289.

CONTENTS

Annual Report of the Marine Biological Laboratory . . . 1

Lenhoff, Howard M.
Ethel Browne, Hans Spemann, and the discovery of the Organizer Phenomenon 72

BEHAVIOR

Painter, Sherry D., Maria G. Chong, Mary A. Wong, Ann Gray, Jeffry G. Cormier, and Gregg T. Nagle
Relative contributions of the egg layer and egg cordon to pheromonal attraction and the induction of mating and egg-laying behavior in *Aplysia* 81

DEVELOPMENT AND REPRODUCTION

Ikegami, Susumu, Tomoko Mitsuno, Masanori Kataoka, Satoshi Yajima, and Miéko Komatsu
Immunological survey of planktonic embryos and larvae of the starfish *Asterina pectinifera*, obtained from the sea, using a monoclonal antibody directed against egg polypeptides 95

Morse, Daniel E., and Aileen N. C. Morse
Enzymatic characterization of the morphogen recognized by *Agaricia humilis* (scleractinian coral) larvae 104

ECOLOGY AND EVOLUTION

Brown, Alice F.
Outbreeding depression as a cost of dispersal in the harpacticoid copepod, *Tigriopus californicus* 123

Salter-Cid, Luisa, and Charles H. Bigger
Alloimmunity in the gorgonian coral *Swiftia exserta* 127

Wolfe, Connie J., and Margo G. Haygood
Restriction fragment length polymorphism analysis reveals high levels of genetic divergence among the light organ symbionts of flashlight fish 135

GENERAL BIOLOGY

Copeland, D. Eugene
Fine structure of photophores in *Gonostoma elongatum:* detail of a dual gland complex 144

Read, A. T., J. A. McTeague, and C. K. Govind
Morphology and behavior of an unusually flexible thoracic limb in the snapping shrimp, *Alpheus heterochelis* 158

PHYSIOLOGY

Cheng, Jin-Hua, and Ernest S. Chang
Ecdysteroid treatment delays ecdysis in the lobster, *Homarus americanus* 169

Gardiner, D. B., F. S. Turner, J. M. Myers, T. H. Dietz, and H. Silverman
Long-term culture of freshwater mussel gill strips: use of serotonin to affect aseptic conditions 175

Mensinger, Allen F., and James F. Case
Bioluminescence maintenance in juvenile *Porichthys notatus* 181

Michibata, Hitoshi, Akemi Morita, and Kan Kanamori
Vanadobin, a vanadium-binding substance, extracted from the blood cells of an ascidian, can reduce vanadate(V) to vanadyl(IV) 189

RESEARCH NOTE

McDermott, John J.
A breeding population of the Western Pacific crab *Hemigrapsus sanguineus* (Crustacea: Decapoda: Grapsidae) established on the Atlantic coast of North America 195

Volume 181 Number 2

THE BIOLOGICAL BULLETIN

Marine Biological Laboratory
LIBRARY
NOV 4 1991
Woods Hole, Mass.

OCTOBER, 1991

Published by the Marine Biological Laboratory

THE
BIOLOGICAL BULLETIN

Marine Biological Laboratory
LIBRARY

NOV 4 1991

Woods Hole, Mass.

PUBLISHED BY
THE MARINE BIOLOGICAL LABORATORY

Associate Editors

PETER A. V. ANDERSON, The Whitney Laboratory, University of Florida
DAVID EPEL, Hopkins Marine Station, Stanford University
J. MALCOLM SHICK, University of Maine, Orono

Editorial Board

GEORGE J. AUGUSTINE, University of Southern California
LOUIS LEIBOVITZ, Marine Biological Laboratory
RUDOLF A. RAFF, Indiana University
KENSAL VAN HOLDE, Oregon State University
STEVEN VOGEL, Duke University

Editor: MICHAEL J. GREENBERG, The Whitney Laboratory, University of Florida
Managing Editor: PAMELA L. CLAPP, Marine Biological Laboratory

OCTOBER, 1991

Printed and Issued by
LANCASTER PRESS, Inc.
PRINCE & LEMON STS.
LANCASTER, PA

THE BIOLOGICAL BULLETIN

THE BIOLOGICAL BULLETIN is published six times a year by the Marine Biological Laboratory, MBL Street, Woods Hole, Massachusetts 02543.

Subscriptions and similar matter should be addressed to Subscription Manager, THE BIOLOGICAL BULLETIN, Marine Biological Laboratory, Woods Hole, Massachusetts 02543. Single numbers, $25.00. Subscription per volume (three issues), $72.50 ($145.00 per year for six issues).

Communications relative to manuscripts should be sent to Michael J. Greenberg, Editor-in-Chief, or Pamela L. Clapp, Managing Editor, at the Marine Biological Laboratory, Woods Hole, Massachusetts 02543. Telephone: (508) 548-3705, ext. 428. FAX: 508-540-6902.

POSTMASTER: Send address changes to THE BIOLOGICAL BULLETIN, Marine Biological Laboratory, Woods Hole, MA 02543.

Copyright © 1991, by the Marine Biological Laboratory

Second-class postage paid at Woods Hole, MA, and additional mailing offices.
ISSN 0006-3185

INSTRUCTIONS TO AUTHORS

The Biological Bulletin accepts outstanding original research reports of general interest to biologists throughout the world. Papers are usually of intermediate length (10–40 manuscript pages). A limited number of solicited review papers may be accepted after formal review. A paper will usually appear within four months after its acceptance.

Very short, especially topical papers (less than 9 manuscript pages including tables, figures, and bibliography) will be published in a separate section entitled "Research Notes." A Research Note in *The Biological Bulletin* follows the format of similar notes in *Nature*. It should open with a summary paragraph of 150 to 200 words comprising the introduction and the conclusions. The rest of the text should continue on without subheadings, and there should be no more than 30 references. References should be referred to in the text by number, and listed in the Literature Cited section in the order that they appear in the text. Unlike references in *Nature*, references in the Research Notes section should conform in punctuation and arrangement to the style of recent issues of *The Biological Bulletin*. Materials and Methods should be incorporated into appropriate figure legends. See the article by Lohmann *et al.* (October 1990, Vol. **179:** 214–218) for sample style. A Research Note will usually appear within two months after its acceptance.

The Editorial Board requests that regular manuscripts conform to the requirements set below; those manuscripts that do not conform will be returned to authors for correction before review.

1. ***Manuscripts.*** Manuscripts, including figures, should be submitted in triplicate. (Xerox copies of photographs are not acceptable for review purposes.) The original manuscript must be typed in no smaller than 12 pitch, using double spacing (*including* figure legends, footnotes, bibliography, etc.) on one side of 16- or 20-lb. bond paper, 8½ by 11 inches. Please, no right justification. Manuscripts should be proofread carefully and errors corrected legibly in black ink. Pages should be numbered consecutively. Margins on all sides should be at least 1 inch (2.5 cm). Manuscripts should conform to the *Council of Biology Editors Style Manual*, 4th Edition (Council of Biology Editors, 1978) and to American spelling. Unusual abbreviations should be kept to a minimum and should be spelled out on first reference as well as defined in a footnote on the title page. Manuscripts should be divided into the following components: Title page, Abstract (of no more than 200 words), Introduction, Materials and Methods, Results, Discussion, Acknowledgments, Literature Cited, Tables, and Figure Legends. In addition, authors should supply a list of words and phrases under which the article should be indexed.

2. ***Title page.*** The title page consists of: a condensed title or running head of no more than 35 letters and spaces, the manuscript title, authors' names and appropriate addresses, and footnotes listing present addresses, acknowledgments or contribution numbers, and explanation of unusual abbreviations.

3. ***Figures.*** The dimensions of the printed page, 7 by 9 inches, should be kept in mind in preparing figures for publication. We recommend that figures be about 1½ times the linear dimensions of the final printing desired, and that the ratio of the largest to the smallest letter or number and of the thickest to the thinnest line not exceed 1:1.5. Explanatory matter generally should be included in legends, although axes should always be identified on the illustration itself. Figures should be prepared for reproduction as either line cuts or halftones. Figures to be reproduced as line cuts should be unmounted glossy photographic reproductions or drawn in black ink on white paper, good-quality tracing cloth or plastic, or blue-lined coordinate paper. Those to be reproduced as halftones should be mounted on board, with both designating numbers or letters and scale bars affixed directly to the figures. All figures should be numbered in consecutive order, with no distinction between text and plate figures. The author's name and an arrow indicating orientation should appear on the reverse side of all figures.

4. ***Tables, footnotes, figure legends, etc.*** Authors should follow the style in a recent issue of *The Biological Bulletin* in preparing table headings, figure legends, and the like. Because of the high cost of setting tabular material in type, authors are asked to limit such material as much as possible. Tables, with their headings and footnotes, should be typed on separate sheets, numbered with consecutive Roman numerals, and placed after

the Literature Cited. Figure legends should contain enough information to make the figure intelligible separate from the text. Legends should be typed double spaced, with consecutive Arabic numbers, on a separate sheet at the end of the paper. Footnotes should be limited to authors' current addresses, acknowledgments or contribution numbers, and explanation of unusual abbreviations. All such footnotes should appear on the title page. Footnotes are not normally permitted in the body of the text.

5. ***Literature cited.*** In the text, literature should be cited by the Harvard system, with papers by more than two authors cited as Jones *et al.*, 1980. Personal communications and material in preparation or in press should be cited in the text only, with author's initials and institutions, unless the material has been formally accepted and a volume number can be supplied. The list of references following the text should be headed Literature Cited, and must be typed double spaced on separate pages, conforming in punctuation and arrangement to the style of recent issues of *The Biological Bulletin*. Citations should include complete titles and inclusive pagination. Journal abbreviations should normally follow those of the U. S. A. Standards Institute (USASI), as adopted by BIOLOGICAL ABSTRACTS and CHEMICAL ABSTRACTS, with the minor differences set out below. The most generally useful list of biological journal titles is that published each year by BIOLOGICAL ABSTRACTS (BIOSIS List of Serials; the most recent issue). Foreign authors, and others who are accustomed to using THE WORLD LIST OF SCIENTIFIC PERIODICALS, may find a booklet published by the Biological Council of the U.K. (obtainable from the Institute of Biology, 41 Queen's Gate, London, S.W.7, England, U.K.) useful, since it sets out the WORLD LIST abbreviations for most biological journals with notes of the USASI abbreviations where these differ. CHEMICAL ABSTRACTS publishes quarterly supplements of additional abbreviations. The following points of reference style for THE BIOLOGICAL BULLETIN differ from USASI (or modified WORLD LIST) usage:

A. Journal abbreviations, and book titles, all underlined (for *italics*)

B. All components of abbreviations with initial capitals (not as European usage in WORLD LIST *e.g. J. Cell. Comp. Physiol.* NOT *J. cell. comp. Physiol.*)

C. *All* abbreviated components must be followed by a period, whole word components *must not* (*i.e. J. Cancer Res.*)

D. Space between all components (*e.g. J. Cell. Comp. Physiol.*, not *J.Cell.Comp.Physiol.*)

E. Unusual words in journal titles should be spelled out in full, rather than employing new abbreviations invented by the author. For example, use *Rit Vísindafjélags Islendinga* without abbreviation.

F. All single word journal titles in full (*e.g. Veliger, Ecology, Brain*).

G. The order of abbreviated components should be the same as the word order of the complete title (*i.e. Proc.* and *Trans.* placed where they appear, not transposed as in some BIOLOGICAL ABSTRACTS listings).

H. A few well-known international journals in their preferred forms rather than WORLD LIST or USASI usage (*e.g. Nature, Science, Evolution* NOT *Nature, Lond., Science, N.Y.; Evolution, Lancaster, Pa.*)

6. ***Reprints, page proofs, and charges.*** Authors receive their first 100 reprints (without covers) free of charge. Additional reprints may be ordered at time of publication and normally will be delivered about two to three months after the issue date. Authors (or delegates for foreign authors) will receive page proofs of articles shortly before publication. They will be charged the current cost of printers' time for corrections to these (other than corrections of printers' or editors' errors). Other than these charges for authors' alterations, *The Biological Bulletin* does not have page charges.

Reference: *Biol. Bull.* **181**: 199–204. (October, 1991)

Social Control of Sex Change in the Bluehead Wrasse, *Thalassoma bifasciatum* (Pisces: Labridae)

ROBERT R. WARNER* AND STEPHEN E. SWEARER†

**Department of Biological Sciences and Marine Science Institute, University of California, Santa Barbara, California 93106, and †Division of Biology and Medicine, Box G, Brown University, Providence, Rhode Island 02912*

Abstract. While the bluehead wrasse has long been used as a test species in sex allocation theory, there is no published evidence that sex change in this species is socially controlled. Here we show that removal of large terminal color phase (TP) males from local populations leads to sex and color change in the largest initial color phase (IP) females. In contrast, no sex changes occurred in control populations in which the TP males were handled but replaced, and in which only the IP males were removed. The response to removals was quite precise, resulting in a nearly one-to-one replacement of TP males.

Large individuals that had been seen spawning as females on the day prior to the manipulation, initiated male behaviors within minutes of the removal of the TP males and spawned in the male role the same day. Color changes were noted within a day and were distinct within four days. Sex change was verified by histological examination of the gonads of the changing individuals. All had functional testes, and all showed evidence of recent transition from the ovarian condition. Mature sperm can be produced in as little as eight days after the initiation of sex change.

Introduction

The bluehead wrasse, *Thalassoma bifasciatum*, has been the subject of intensive study in behavior and ecology for nearly 60 years (*e.g.*, Tee-Van, 1932; Stoll, 1955; Feddern, 1965; Roede, 1972; Reinboth, 1973; Warner *et al.*, 1975; Victor, 1986, and references therein; Warner, 1988a, 1990, and references therein). The majority of individuals in this species are protogynous hermaphrodites (Warner and Robertson, 1978), and the species has served as a model against which the sex allocation theory has been tested (Warner *et al.*, 1975; Warner and Hoffman, 1980; Charnov, 1982a,b; Warner, 1984; Hoffman *et al.*, 1985; Shapiro, 1989). An assumption made in many of these studies is that the bluehead wrasse changes sex in response to local social conditions. Here we show that *T. bifasciatum* does indeed demonstrate rather precise social control of sex change and give data as well on the time course of sex and color change.

Background and Methods

Adult bluehead wrasses occur in two major color phases (Warner and Robertson, 1978). Smaller males and all females are in the initial color (IP) phase: a yellow dorsal stripe surmounts a lateral series of green blotches separated by white bars. The largest individuals are in the terminal color phase (TP): a bright blue head is separated from a green body by three vertical bars, two of which are black and the other white. As an individual changes from the IP to the TP phase, the head becomes suffused with blue, the two most anterior green blotches intensify, darken, and lengthen vertically, while the other blotches fade. Individuals with blue heads and green bodies, but still retaining remnants of the posterior blotches, are termed intermediate (INT). The change to TP coloration is permanent: individuals cannot temporarily revert to the IP pattern (Warner and Robertson, 1978). Both IP males and females can become TP males, the latter through sex change. Gonad anatomy can be used to distinguish TP males that are the result of sex change (termed secondary males) from those that originated as IP males (primary males; see Reinboth, 1967).

All fieldwork was carried out on patch reefs in Tague Bay, St. Croix, U. S. Virgin Islands, near the West Indies Laboratory. Manipulations of population structure on small reefs were carried out in June–August, 1989, while

Received 29 May 1991; accepted 9 July 1991.

the larger reef experiments were performed during the same period in 1990.

For the small reef manipulations, we chose five isolated reefs (all less than 100 m^2 in area) ranging in adult population size from 24 to 57 individuals. After three days of observation of mating on these reefs, all individuals were captured, sexed through examination of their genital papillae, and measured to the nearest 0.1 mm (S.L.). Females have a blunt genital papilla that protrudes over the broad genital opening, while males have a pointed papilla that terminates in a small genital aperture. In addition, sperm can always be expressed from functional males. All IP males were removed from the reefs, and on the randomly chosen experimental reefs ($n = 3$) all TP and INT individuals were removed as well. On all reefs, females larger than 60 mm S.L. were tatooed with unique combinations of spots of a vital stain (Alcian Blue) before they were returned to the reef. On the control reefs ($n = 2$), we removed the TP and INT males and then replaced them after 30 min. We then monitored the reproductive activity and coloration of the females on all reefs, intensively for two days after the removal, and on a weekly basis for a month thereafter. The identity of individuals showing male courtship behavior and transition to TP coloration was confirmed by noting the markings that had been applied.

Reproductive behavior was monitored during the daily mating period, which begins in the early afternoon and lasts for an average of 110 min (Warner and Hoffman, 1980). Male reproductive behavior consists primarily of aggression and courtship. Males vigorously chase all conspecifics away from the mating site, except females arriving to spawn. When a ripe female arrives, the male positions himself in the water column over the female, swimming in tight circles while rapidly vibrating his pectoral fins. He may then descend to the female and touch her dorsal area, or may swim rapidly upwards and back down in a movement reminiscent of the actual spawning rush. Females are never seen to perform these behaviors. To indicate their readiness to spawn, females will turn their head upwards, and soon after will dash upwards about a meter toward the surface, accompanied by the male. At the apex of the spawning rush, the female will flip upside down, release her eggs, and then rapidly descend.

Individuals showing evidence of sex change (that is, prior females who had initiated male behavior and coloration) were later collected. The markings and length were rechecked, and the individuals were dissected to determine gonadal state. The gonads of ten of these individuals were preserved in Bouin's solution and prepared for histological examination. Cross-sections cut at 12 μm were stained with hematoxylin and eosin. Testicular function was verified by the presence of crypts of developing sperm. Secondary male status was indicated by the presence of a central lumen (the previously functional ovarian cavity) into which the gonadal lamellae protrude (Reinboth, 1967; Sadovy and Shapiro, 1987). Recently sex-changed labrid fishes also have large amounts of degenerating oocytes scattered throughout the lamellae (see Warner, 1975). In contrast, primary males have a solid testis, with no evidence of either a central cavity or degenerating oocytes (Reinboth, 1967).

When the sex-changed individuals were removed from the experimental reefs, we continued to monitor the remaining residents. In addition, the TP and INT males were removed from the control reefs once the initial two-week observation period was over; subsequent monitoring ensured that the initial lack of response seen on these reefs was not due to some inherent quality of the reef itself. After the initial two-week period, we also verified sexual function of the remaining IP individuals on all reefs by capturing them before the spawning period began and holding them in nets until after spawning on nearby reefs had ended. Females who were to spawn that day could then be stripped of ripe eggs with gentle pressure applied in the dorsal area of the body cavity; on average, females spawn on two out of every three days (Warner, 1985; Schultz and Warner, 1989). Functional males express sperm under the same treatment.

Most populations of the bluehead wrasse are much larger than those present on the small patch reefs used in the experiment. To determine the precision of TP male replacement in larger populations, in 1990 we removed all TP and INT individuals from four larger reefs (300–2600 m^2; total population sizes ranging between 256 and 422 individuals), and returned two weeks later to monitor the number of individuals in the remaining population that had undertaken the shift toward TP male status. Past tagging studies have shown that adults do not move from reef to reef (Warner and Hoffman, 1980; Warner, 1984, 1987), so that new TP and INT individuals could be reliably assumed to have arisen from the resident population.

Results

Responses to removals of large males

Removals were performed in the morning. On the experimental reefs, several (2–4) of the largest females present began to exhibit aggression towards other large females and to court smaller females within minutes of the removal of the large males. During the mating period that day, these same largest IP individuals (who had been observed to mate as females with a TP male on the previous day) courted and spawned in the male role with the remaining females on the reef. In contrast, on the two control reefs, the largest females spawned in normal fashion as females with the resident TP males, and continued to do so for the two-week experimental period.

Overall, there was a very strong response to the removal of TP and INT males on the experimental reefs (Table 1). Eleven such males were removed from the three experimental reefs, and nine females changed to male roles within two weeks. In contrast, no changes were noted on the control reefs over the same period, even though IP males had been removed in the same fashion as on the experimental reefs.

In every case, the individuals that undertook the shift to male function were the largest remaining individuals on the reef. Figure 1 gives an example from one of the experimental reefs. It is worth noting that the IP males tended to be located in the larger end of the IP size range, which might be expected because on small reefs they grow faster than females (Warner, 1984).

Of the 18 large IP individuals that continued to display female coloration during the initial observation period (6 on the experimental reefs and 12 on the controls), none showed evidence of male function; all continued to spawn in the female role. Fifteen of the 18 produced normal clutches of eggs on the day of capture. The remaining three had normal female genital papillae, and sperm could not be expressed from any of them.

The pattern of sex changes in response to the removal of TP and INT males continued after the initial observation period on both the experimental and control reefs (Table 1). For six subsequent removals on the experimental reefs, five females changed to the male role. The removal of 12 TP and INT individuals from the former control reefs resulted in 8 females changing to male roles, whereas none had behaved as males before. This indicates that the control reefs contained individuals that were capable of sex change, so that the initial lack of response on these reefs was likely due to the fact that the larger males were left in residence.

The overall pattern of response for both small and larger reefs was quite precise (Fig. 2). The slope of the regression relating number changing to number removed was 0.89, which was not significantly different from a one-to-one

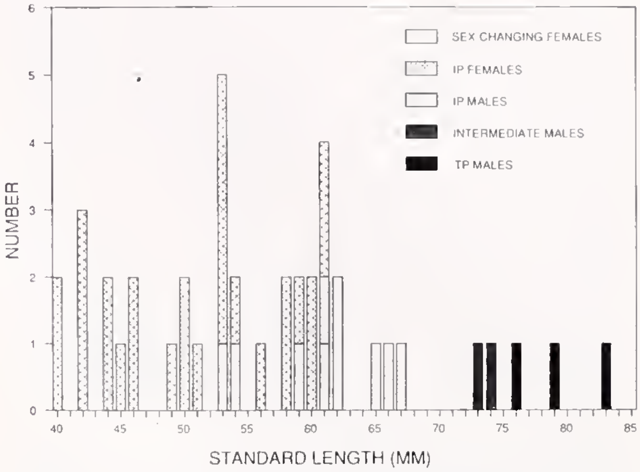

Figure 1. Beginning size, sex, and color distribution and outcome of removal of large males of *Thalassoma bifasciatum* from Reef 9A, Tague Bay, St. Croix. All males were removed, and the four largest females on the reef changed sex.

Table 1

Outcomes of two sets of experiments removing Thalassoma bifasciatum *from small patch reefs in Tague Bay, St. Croix*

A. TP and INT removed at outset:

	No. males removed			No. females remaining		No. changing sex	No. subsequent removals	No. subsequent sex changes
Reef	TP	INT	IP	<60mm	≥60mm			
9A	3	2	6	21	6	4	2	1
9B	1	4	4	14	4	3	2	2
10	0	1	1	23	5	2	2	2

B. TP and INT remain at outset, subsequently removed:

	No. males							
	Remaining		Removed	No. females remaining		No. changing sex	No. subsequent removals	No. subsequent sex changes
Reef	TP	INT	IP	<60mm	≥60mm			
12	4	5	7	38	5	0	9	6
14	3	0	4	24	7	0	3	2

TP = Terminal Phase coloration; INT = Intermediate coloration (early Terminal Phase); IP = Initial Phase coloration. In the first set (A), all males (TP, INT, and IP) were removed at the outset. In the second set (B), only IP males were removed. The seventh column shows the number of individuals having changed sex two weeks after the experiment began. At that point, in both sets of experiments, some TP and INT individuals were subsequently removed, and the responses of the remaining individuals were noted, again after a two-week interval.

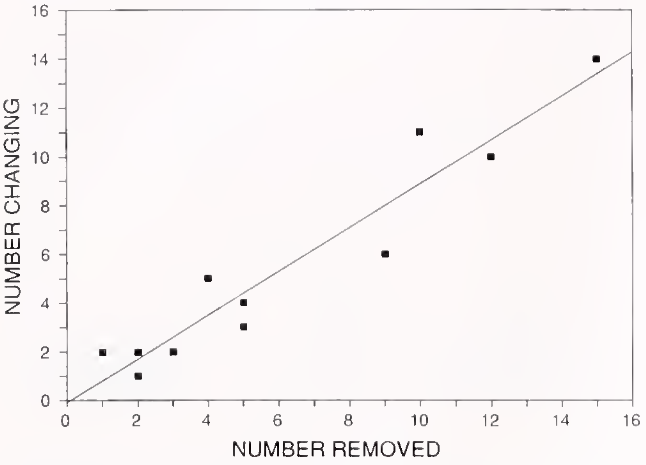

Figure 2. Responses of remaining individuals to removals of INT and TP males of *Thalassoma bifasciatum* on patch reefs in Tague Bay, St. Croix. Shown are the results from the removals from reefs shown in Table II (initial and subsequent removals shown separately) and four larger reefs. On the vertical axis are the total number of individuals changing from IP coloration to INT coloration during a two-week period. The dotted line represents a one-for-one response. The solid line is a regression of the number changing (NC) against the number removed (NR). The regression equation is $NC = .894NR - 0.049$; $r^2 = .91$, $P < 0.001$.

response. It should be noted, however, that not all of the responses on larger reefs were necessarily sex changes, because IP males were not removed along with the TP and INT males.

Changes in coloration

As early as the first day of the manipulation, IP individuals sometimes slightly darkened their heads while courting and mating. These coloration differences were not detectable outside of the mating period. By day 3, however, the largest individuals had begun the transition to TP coloration. Over the course of the observations (a maximum of 28 days), only the two or three largest individuals on each reef proceeded to develop full INT coloration, and this was apparent within five days. In the rest of the changing individuals, the head region had a permanent bluish tinge, and the two anterior lateral blotches had darkened and enlarged, but the body was not yet green. No individuals attained full TP status over the course of the experiment. None of the IP fishes on the control reefs initiated color change during the initial experimental period.

Sex change verified

No individual identified as a potential sex-changer had functional ovaries. All 10 gonads examined histologically were testes engaged in active sperm production (Table II). Furthermore, all of these testes were secondary (derived from previously functional ovaries), with varying amounts of degenerating oocytic material still in the gonadal lamellae.

Sex change apparently can proceed quite rapidly. Even individual 10A3, observed spawning as a female before the manipulation and captured 8 days later, was already producing tailed sperm. Of the 10 individuals investigated histologically, in only three had spermatogenesis not yet proceeded to the production of mature sperm. All of these had been first observed to display early intermediate coloration 8 to 9 days before capture.

Discussion

It is clear that female bluehead wrasses change sex when larger brightly colored males are removed from the local population. Social control of sex change in reef fishes was first documented two decades ago (Fishelson, 1970; Rob-

Table II

Size, coloration, two estimates of time since initiation of sex change, and gonadal state for ten individuals observed to change from initial phase coloration and female behavior to male coloration and behavior over the course of the experiments

Fish ID	Length at capture (mm S.L.)	Coloration	Days since beginning of experiment	Days since individual began to display male coloration	Histological condition of gonad
9A2	67.0	INT	19	19	Act 2°, t.s.
9A6	65.8	early INT	28	9	Act 2°, t.s.
9B1	65.2	INT	28	28	Act 2°, t.s.
9BX	63.9	early INT	28	8	Recent 2°, t.s.
9BY	55.0	early INT	28	8	Act 2°, t.s.
9BZ	55.2	early INT	28	8	Recent 2°, no t.s.
10A1	64.6	early INT	17	9	Act 2°, no t.s.
10A3	69.3	early INT	8	8	Act 2°, t.s.
10A4	65.3	early INT	17	9	Act 2°, no t.s.
T41	64.5	early INT	17	9	Act 2°, t.s.

INT = Intermediate coloration; Act 2° = active secondary male, with most of the gonad occupied by spermatogenic crypts; Recent 2° = transitional gonad, with much of the gonad still containing degenerating oocytic material, some spermatogenic crypts present; t.s. = tailed sperm present.

ertson, 1972), and its precision has been described on several occasions (*e.g.*, Fricke and Fricke, 1977; Moyer and Nakazono, 1978; Shapiro, 1979, 1980; Ross *et al.*, 1983, 1990; comprehensively reviewed by Ross, 1990). Within the genus *Thalassoma*, social control has been shown in captive groups of *T. lucasanum* (Warner, 1982), and *T. duperrey* (Ross *et al.*, 1983, 1990), but never before under field conditions. In *T. duperrey* it was further shown that it was the relative size of the individual within the local social group that was the cue for sex change; neither the sex nor the coloration of the other individuals in the group appeared to have any additional stimulatory or inhibitive effect. While this is likely to be true for *Thalassoma bifasciatum* as well, it cannot be conclusively shown, given our experimental design.

Shapiro (1980) obtained a remarkably precise response to multiple removals of males in the serranid *Anthias squamipinnis*, and also observed that not all individuals responded immediately to the removal. Instead, sex changes (as indicated by coloration changes) tended to be separated by an interval of about two days. Shapiro hypothesized that the subsequent development of sex change in subordinate females was slowed by the initial development of male characters in higher-ranked females. While our monitoring was not conducted often enough to detect the exact sequence of successive sex changes, some individuals did not initiate the process immediately. Of the 22 individuals that changed sex on the small reefs, 4 were known to have delayed changing at least 7 days after the removal of the males. The aggression directed by large sex-changing females toward other large individuals may have contributed to this delay.

While the removal of TP males in *Thalassoma bifasciatum* results in a precise sex-change response (Fig. 2), it is unclear how this precision is attained. Particularly on bigger reefs with large populations, it seems unlikely that the mechanism is a direct response by one individual to the loss of a particular male. On the basis of their experiments with small groups of fishes, Ross *et al.* (1990) suggested that sex change in *T. duperrey* was mediated by a critical size-ratio mechanism: individuals would change sex when there were sufficiently few larger individuals as well as enough smaller individuals present in the local population. In our study, it is difficult to distinguish direct responses to removal from reactions to changes in the size, sex, or color ratios because removals changed these ratios as well. The proportions of color types in the pre-manipulation populations in our study was variable: from 81 to 96% of the total population was in the IP color phase (Table I). The mean percentage of the total population within the IP size range was 88%, a ratio of IP to TP of 7.3:1. Of the 147 females remaining on all reefs after the initial removals, the 17 largest (11.6%) changed sex, resulting in a color ratio of 7.6:1. One can also investigate the possibility of a critical ratio by monitoring the minimum sex- or size-ratio at which individuals were seen to change sex. In other words, what percent of the population was smaller than the smallest individual seen changing sex on each reef? This varied from 83 to 94%, with a mean of 88.2% (n = 5), suggesting a critical ratio of 7.5 smaller individuals to larger. However, we stress that these various ratio measures would be very similar even if a simple one-for-one replacement sex-change mechanism was in operation. To resolve this issue, one would need to vary the number of smaller individuals left on the reef after the male removals, similar to the experiments of Ross *et al.* (1990) for captive populations of *T. duperry.*

In any event, there is certainly no fixed critical ratio for *T. bifasciatum* as a whole, because the sex and coloration ratios change radically with reef size (Warner and Hoffman, 1980). It may be, however, that individuals respond to a ratio appropriate to the reef on which they find themselves (termed the behavioral-scaling model in Ross, 1990). Sex change of a number of large females also reduces the pool of potential mates for the newly dominant males. If the critical-ratio hypothesis is correct, there should be slightly fewer individuals changing sex than were removed on the experimental reefs. There does exist such a trend in our removal experiments (Fig. 2), but it will take much larger sample sizes to distinguish this trend from random variation.

The behavioral, coloration, and gonadal responses to male removals among the females on the experimental reefs were very rapid, as were seen in other sex-changing species (Robertson, 1972; Shapiro, 1979, 1985). Behavioral responses occurred almost instantaneously, suggesting that the initiation of mating and aggressive behaviors characteristic of males in this species are not dependent on hormone levels (see Crews and Moore, 1986, for a discussion of the various possible relationships between hormones and mating behavior). While we did not collect gametes from matings, it is extremely unlikely that sex-changing individuals could produce sperm in the first few days after the manipulations. Thus these individuals appear capable of spawning in the male role without release of sperm.

Ross (1990) suggested that gametocytes of the heterologous sex are maintained in the gonads of some species to facilitate rapid sex change. While *T. bifasciatum* shows no sign of such heterologous gametocytes in the ovary, this does not appear to inhibit the ability of females to rapidly assume functional male status.

In this study, we could not determine the relative timing of changes in coloration and gonadal condition; all individuals that were collected had initiated changes toward TP coloration, and all were well advanced in sperm production. Stoll (1955) induced both color change and sex change in 13 females with injections of methyl testosterone; the color change began four days after treatment, and all individuals were producing sperm when they were examined 20 days after the injection. However, other studies on this species have shown that under normal circumstances, sex change can precede color change, because larger IP individuals can be secondary males (Warner and Robertson, 1978).

Individuals should change sex when the reproductive prospects of functioning as the opposite sex exceed the expectations of the current sex (the size-advantage model; see Ghiselin, 1969; Warner *et al.*, 1975; Charnov, 1982a; Warner, 1988b). If mate monopolization depends on the ability to dominate other individuals, and if dominance depends on relative size, then it is the largest individuals in a local population that should change sex in response to large male removals. Relative size does convey dominance in the bluehead wrasse (Warner and Schultz, in prep.), and the largest males are most reproductively successful (Warner, 1984). Accordingly, it is only the largest females that change sex when the TP and INT males are removed (Fig. 1), as predicted by the size-advantage model.

Acknowledgments

We thank J. Caselle, C. Gabor, and B. L. Rogers for assistance in the field, and E. T. Schultz and two anonymous reviewers for helpful comments. This research was supported by the National Science Foundation (BSR 8704351 to R.R.W.).

Literature Cited

Charnov, E. 1982a. *The Theory of Sex Allocation.* Monographs in Pop. Biol. 18. Princeton University Press, Princeton, NJ.

Charnov, E. 1982b. Alternative life-histories in protogynous fishes: a general evolutionary theory. *Mar. Ecol. Prog. Ser.* **9:** 305–307.

Crews, D., and M. C. Moore. 1986. Evolution of mechanisms controlling mating behavior. *Science* **231:** 121–125.

Feddern, H. A. 1965. The spawning, growth, and general behavior of the bluehead wrasse, *Thalassoma bifasciatum* (Pisces: Labridae). *Bull. Mar. Sci.* **15:** 896–941.

Fishelson, L. 1970. Protogynous sex reversal in the fish *Anthias squamipinnis* (Teleostei, Anthiidae) regulated by the presence or absence of male fish. *Nature* **227:** 90–91.

Fricke, H. W., and S. Fricke. 1977. Monogamy and sex change by aggressive dominance in a coral reef fish. *Nature* **266:** 830–832.

Ghiselin, M. T. 1969. The evolution of hermaphroditism among animals. *Q. Rev. Biol.* **44:** 189–208.

Hoffman, S. G., M. P. Schildhauer, and R. R. Warner. 1985. The costs of changing sex and the ontogeny of males under contest competition for mates. *Evolution* **39:** 915–927.

Moyer, J. T., and A. Nakazono. 1978. Protandrous hermaphroditism in six species of the anemonefish genus *Amphiprion* in Japan. *Japan J. Ichthyol.* **25:** 101–106.

Reinboth, R. 1967. Biandric teleost species. *Gen. Comp. Endocrinol., Abstracts* **9:** 46.

Reinboth, R. 1973. Dualistic reproductive behavior in the protogynous wrasse *Thalassoma bifasciatum* and some observations on its day-night changeover. *Helgol. Wiss. Meeresunters.* **24:** 174–191.

Robertson, D. R. 1972. Social control of sex reversal in a coral reef fish. *Science* **177:** 1007–1009.

Roede, M. J. 1972. Color as related to size, sex, and behavior in seven labrid fish species (Genera *Thalassoma, Halichoeres,* and *Hemipteronotus*). Studies on the fauna of Curacao and other Caribbean islands **138:** 1–264.

Ross, R. M. 1990. The evolution of sex-change mechanisms in fishes. *Environ. Biol. Fish.* **29:** 81–93.

Ross, R. M., T. F. Hourigan, M. M. F. Lutnesky, and I. Singh. 1990. Multiple simultaneous sex changes in social groups of a coral-reef fish. *Copeia* **1990:** 427–433.

Ross, R. M., G. S. Losey, and M. Diamond. 1983. Sex change in a coral reef fish: dependence on stimulation and inhibition on relative size. *Science* **221:** 574–575.

Sadovy, Y., and D. Y. Shapiro. 1987. Criteria for the diagnosis of hermaphroditism in fishes. *Copeia* **1987:** 136–156.

Schultz, E. T., and R. R. Warner. 1989. Phenotypic plasticity in life-history traits of female *Thalassoma bifasciatum* (Pisces: Labridae). 1. Manipulations of social structure in tests for adaptive shifts of life-history allocations. *Evolution* **43:** 1497–1506.

Shapiro, D. Y. 1979. Social behavior, group structure, and the control of sex reversal in hermaphroditic fish. *Adv. Studies Behav.* **10:** 43–102.

Shapiro, D. Y. 1980. Serial female sex changes after simultaneous removal of males from social groups of a coral reef fish. *Science* **209:** 1136–1137.

Shapiro, D. Y. 1985. Behavioral influences on the initiation of adult sex change in coral reef fishes. Pp. 583–585 in *Current Trends in Comparative Endocrinology,* B. Lofts and W. N. Holmes, eds. University of Hong Kong Press, Hong Kong.

Shapiro, D. Y. 1989. Sex change as an alternative life-history style. Pp. 177–195 in *Alternative Life-History Styles in Animals.* M. N. Burton, ed. Kluwer Publishers, Dordrecht, Netherlands.

Stoll, L. M. 1955. Hormonal control of the sexually dimorphic pigmentation of *Thalassoma bifasciatum. Zoologica* **40:** 125–132.

Tee-Van, J. 1932. Color changes in the bluehead wrasse, *Thalassoma bifasciatum* (Bloch). *Bull. N. Y. Zool. Soc.* **35:** 43–47.

Victor, B. C. 1986. Larval settlement and juvenile mortality in a recruitment-limited coral reef fish population. *Ecol. Monogr.* **56:** 145–166.

Warner, R. R. 1975. The reproductive biology of the protogynous hermaphrodite *Pimelometopon pulchrum* (Pisces: Labridae). *Fish. Bull.* **73:** 262–283.

Warner, R. R. 1982. Mating systems, sex change, and sexual demography in the rainbow wrasse, *Thalassoma lucasanum. Copeia* **1982:** 653–661.

Warner, R. R. 1984. Deferred reproduction as a response to sexual selection in a coral reef fish: a test of the life historical consequences. *Evolution* **38:** 148–162.

Warner, R. R. 1985. Alternative mating behaviors in a coral reef fish: a life-history analysis. *Proc. Fifth International Coral Reef Congress, Tahiti* **4:** 145–150.

Warner, R. R. 1987. Female choice of sites versus males in a coral reef fish, *Thalassoma bifasciatum. Anim. Behav.* **35:** 1470–1478.

Warner, R. R. 1988a. Traditionality of mating-site preferences in a coral-reef fish. *Nature* **335:** 719–721.

Warner, R. R. 1988b. Sex change in fishes: hypotheses, evidence, and objections. *Environ. Biol. Fishes* **22:** 81–90.

Warner, R. R. 1990. Male *versus* female influences on mating-site determination in a coral reef fish. *Anim. Behav.* **39:** 540–548.

Warner, R. R., and S. G. Hoffman. 1980. Local population size as a determinant of mating system and sexual composition in two tropical reef fishes (*Thalassoma* spp.). *Evolution* **34:** 508–518.

Warner, R. R., and D. R. Robertson. 1978. Sexual patterns in the labroid fishes of the western Caribbean, 1: The wrasses (Labridae). *Smithsonian Contrib. Zool.* **254:** 1–27.

Warner, R. R., D. R. Robertson, and E. G. Leigh, Jr. 1975. Sex change and sexual selection. *Science* **190:** 633–638.

Reference: *Biol. Bull.* **181:** 205–215. (October, 1991)

Ontogeny *Versus* Phylogeny in Determining Patterns of Chemoreception: Initial Studies with Fiddler Crabs

MARC J. WEISSBURG[1,*] AND RICHARD K. ZIMMER-FAUST[1,2,*]

[1]*Marine Environmental Sciences Consortium and* [2]*Department of Biology, University of Alabama, P.O. Box 369-370, Dauphin Island, Alabama, 36528*

Abstract. Fiddler crab (*Uca longisignalis*) first stage zoea and adults were assayed for behavioral responses to 16 amino acids and sugars. Larval chemosensitivity was examined using computer–video motion analysis of swimming behavior. Adult sensitivity was assayed by determining the substances that elicit feeding. The pattern of chemoreception expressed by *U. longisignalis* adults is strongly correlated with that measured previously in adult sand fiddler crabs, *Uca pugilator.* This concordance among abilities probably reflects shared trophic ecologies of the two species. In contrast, a quantitative analysis shows no significant correlation between the sets of compounds inducing chemoreceptive behavior by larval and adult *U. longisignalis.* The strongest responses (by both stages) are elicited by substances found in potential prey, and differences in prey types among larvae and adults appear responsible for the lack of correlation. Larvae do, however, respond to substances abundant in prey consumed by adults, even though these substances are absent, or occur at low levels, in larval prey. Adults, on the other hand, appear insensitive to compounds that cue only larval food, but which are maximally stimulatory to larvae. Consequently, our results indicate that the abilities of one life-history stage may be constrained, through development, by the requirements of later stages. The patterns of correlation among adults of different species, and among life-history stages within a species, indicate that both ecological context and developmental factors influence patterns of chemosensitivity.

Introduction

Studies on marine invertebrates have engendered a large body of literature on chemosensory properties and their ecological implications. Several broad scale patterns are apparent, based on current work. In general, the particular spectrum of substances eliciting a response is correlated with diet. Flesh eaters tend to respond strongly to amino acids, sometimes to organic acids and nucleotides, and are generally unresponsive to sugars (see reviews of Ache, 1982; Carr, 1988; Laverack, 1988; Zimmer-Faust, 1989). The particular substances generating large responses are often dominant organic components in prey tissues. In contrast to flesh eaters, herbivorous organisms are highly responsive to carbohydrates (Zimmer *et al.,* 1979; Robertson *et al.,* 1981; Trott and Robertson, 1984; Rittschof and Buswell, 1989), which occur as algal storage products and components of extracellular mucous sheaths (Fogg, 1966; Fogg *et al.,* 1973; Craigie, 1974; Darley, 1977; Paulsen *et al.,* 1978) and sometimes to amino acids that are characteristic of algal material.

In spite of broad scale associations between diet and the response spectrum of organisms, related or ecologically similar species can display quite dissimilar fine scale patterns of chemosensitivity. The spiny lobsters *Panulirus argus* and *P. interruptus* each respond to a wide array of amino and organic acids, and exhibit a broad overlap in the substances eliciting a response. However, within the overlapping subset of stimulatory substances, these two species are differentially responsive to the same compounds. For example, *P. argus* is most responsive to citric acid, ascorbic acid, succinic acid, taurine, and glycine (Ache *et al.,* 1978), whereas *P. interruptus* responds mostly to glycine, alanine, serine, succinic acid, oxalic acid, and adenosine triphosphate (Zimmer-Faust *et al.,* 1984; Zimmer-Faust, 1987). Similarly, the coexisting copepods *Acartia hudsonica* and *Eurytemora herdmani* both respond to amino acids, although *Acartia* is stimulated mostly by aliphatic amino acids (*e.g.,* leucine and valine) whereas *Eurytemora* is most responsive to the dicarboxylic

Received 26 April 1991; accepted 23 July 1991.

* Present address: Department of Biology and Marine Sciences Program, University of South Carolina, Columbia, South Carolina, 29208.

amino acids (*i.e.*, glutamic and aspartic acid). When responses to the same compounds are observed, each species reacts to them in different ways (Poulet and Ouellet, 1982). *Acartia*, for instance, is repelled by aspartic acid, while *Eurytemora* is attracted to it.

To date, explanations of chemosensory abilities have focussed largely on adaptive hypotheses. It is implicitly assumed that the response magnitude varies directly with the relative concentration of substances in prey, thus allowing animals to locate potential food items more efficiently. Other explanations exist, especially where organisms progress through a series of life-history stages requiring different chemosensory abilities. At any one stage, abilities (1) may be functionally important, (2) may represent incipient abilities required at a later stage, or (3) may be relictual abilities that were required by previous life-history stages. Developmental explanations for patterns of chemosensitivity may be especially important for marine organisms where differences in the habitats occupied by larval and adult stages can be large.

Fiddler crabs (genus *Uca*) provide an excellent system with which to quantitatively investigate correlations of abilities among species, and life-history stages. All adult fiddler crabs are deposit feeders, foraging on intertidal sediments (Crane, 1975). Trophic habits are quite uniform (Teal, 1958; Miller, 1961; Crane, 1975; Robertson *et al.*, 1980; Weissburg, 1990), and several species often coexist within a limited geographic area (Crane, 1975). Further, adult and larval habitats are markedly different in terms of abundance levels, and specific components of the chemical environment (*e.g.*, Degens *et al.*, 1964; Andrews *et al.*, 1971; Clark *et al.*, 1972; Mopper *et al.*, 1980; Mopper and Lindroth, 1982).

The investigation reported here was designed to explore the potential influence of both ecological and developmental processes on adult and larval chemosensitivity. The logical starting point for detecting developmental constraints on chemoreception is to determine patterns of chemosensitivity at the endpoints of the ontogenetic series. Similarly, the concordance of chemosensory abilities in at least one pair of species with similar trophic habits should be established before a detailed survey of ecologically and taxonomically related species is attempted. Therefore, we have examined, quantitatively, the chemosensory abilities of first stage zoea and adult stages of the crab, *Uca longisignalis*, and have compared the properties of different life-history stages in the same species, and among adults of *U. longisignalis* and *U. pugilator*.

Materials and Methods

Preparation of test solutions

Metabolites released by Artemia salina *in culture.* An initial experiment was performed to explore larval swimming behavior in response to substances released by a documented prey species. The solution was prepared from a culture of young brine shrimp (*Artemia salina*)—a standard food source used in rearing carnivorous larvae of marine invertebrates, including fiddler crabs (*e.g.*, Herrnkind, 1968; Rabalais and Cameron, 1983; Christy, 1989). *Artemia* nauplii were hatched from cultures incubated in 20 ppt artificial seawater media (ASW) (Forty Fathoms Marinemix) prepared with HPLC grade deionized water. When nauplii were 1–3 h old, 100 ml of the batch culture were spun down in a Beckman (Model J2-21) centrifuge at 10,400 × g and 2°C for 30 min. The resulting supernatant was decanted, filtered through a 0.45 μm membrane filter, diluted to a concentration of 15 ppt, then stored at −87°C.

Amino acids and sugars. Chemicals were prepared in ASW media at a concentration of 15.0 ppt, using HPLC grade deionized water. The following amino acids were used as test compounds: β-alanine (ALA), arginine (ARG), cysteine (CYS), glutamic acid (GAD), glycine (GLY), proline (PRO), taurine (TAU), and valine (VAL). The following sugars were used: galactose (GAL), glucose (GLU), maltose (MAL), sorbose (SOR), sucrose (SUC), and trehalose (TRE). These compounds were selected because they are important chemical constituents in either plant or animal components of the diet of marine zooplankters (*e.g.*, Jeffries, 1969), or have been found stimulatory to other deposit feeding crustaceans (*e.g.*, Robertson *et al.*, 1981; Rittschof and Buswell, 1989). Except where noted, all amino acids were L-isomers, and all sugars D-isomers. Chemicals were all reagent grade, obtained from the Sigma Chemical Company. Test solutions were prepared in single batches at a concentration of 10^{-4} M for experiments performed using larvae, or 10^{-1} M for experiments performed using adults, divided into 20 ml aliquots, and stored at −87°C until needed. Where necessary, solutions were adjusted to pH 8.0 using 1 M NaOH or HCl.

Experiments testing larval chemosensory abilities

Gravid *Uca longisignalis* females, collected from Airport Marsh, Dauphin Island, Alabama, were held until their broods hatched. Females were placed in finger bowls containing a small amount of filtered 15 ppt seawater, and kept in incubators at 26°C under a 14:10 light-dark cycle. Females were checked for brood release twice per day, and water was changed daily. Usually several females simultaneously released larvae, and these broods were combined, and held in filtered seawater at densities of about 10 larvae/ml prior to assaying chemosensory behavior.

Experiments on larval chemosensory abilities began 24–36 h after hatching and ran for 24 h. We specifically restricted our experiments to these early stages because larvae are only competent to settle on substrates and metamorphose to the adult form later in the developmental series, after they have reached the megalopa stage (*e.g.*, Epifanio *et al.*, 1988). Therefore, behavior in response to test compounds cannot be ascribed to substrate selection and settlement processes. Twenty larvae were transferred in 5 ml of ASW into plexiglass microcosms (3 cm long × 3 cm wide × 5 cm high), and 20 ml of the 10^{-4} *M* test solution was gently added. After about 30 s of gentle stirring to disperse the test compound, the microcosm was placed into a darkened chamber, and larval swimming behavior was recorded. Each trial was video-recorded for a 10-min period. Order of the test solutions was determined by a random numbers table, subject to the constraints that: a specific compound was not presented twice in succession; and that seawater treatments were performed after every block of five test solutions. Five to eight replicate trials of each test compound were performed. Individual larvae were tested in only one trial and then discarded.

Larval swimming behavior in the horizontal plane was filmed using a Sony infrared-sensitive CCD camera (model HVM-200) equipped with a Tamron 180 mm lens, mounted beneath the microcosm, and focused 1.0 cm (25 to 35 larval body lengths) above the bottom. Similarly sized chambers and techniques have been successfully used for video recording locomotory behavior of small zooplankters, including copepods (Buskey, 1984), tintinnids (Buskey and Stoecker, 1989), and polychaete (Butman *et al.*, 1988) and molluscan larvae (Zimmer-Faust and Tamburri, in prep.). The chamber was illuminated with an infrared light source (>830 nm) oriented 90° to the axis of the video camera. The field of view was 6.9 × 6.8 mm, about 6.4% of the total cross-sectional area of the microcosm. Depth of field was determined by mounting a pipette (tip diameter = 300 μm) on a micromanipulator calibrated in 10 μm increments. Using the computer-video motion analyzer (see below) with gray scale threshold set for discriminating larvae, the pipette tip was moved vertically to determine the limits at which the analyzer would 'recognize' the tip as an object. The recognition distance was 1.5 mm in the vertical dimension.

Quantification of swimming speed and turning behavior was accomplished by replaying each video tape through a computer—video motion analysis system (Motion Analysis Corp. Model VP 110 and ExpertVision software package) interfaced with an Amdek 386 microcomputer. The system constructs a digitized record of the raw video data, using a gray scale detector to enhance the contrast between objects in the video field and background. The outlines of the objects are defined, and the x,y coordinates of the centroid (geometric center) are calculated. The path of an object is reconstructed, on a frame-by-frame basis, as the translational movement through space of an object's centroid (see Buskey and Stoecker, 1989; Zimmer-Faust and Tamburri, in prep.). The video sampling rate of the motion analysis hardware was set at 10 frames/s, and, based on preliminary results, only the first 5 min of each trial were used in the analysis.

Analysis of larval behavior consisted of determining swimming speed and net-to-gross displacement ratio (NGDR) for each larval swimming path. The NGDR is the ratio of the linear distance between the starting and ending points (net distance) and the total distance traversed by the path (gross distance). The NGDR measures the tendency of paths to be circular or twisted, and reaches a maximum value of 1.0 for paths that are completely straight. An NGDR of zero implies a looped or circular path, with the origin and endpoint occurring at the same spatial coordinates. For each test substance, data for all paths were pooled across trials, and means compared to swimming behavior observed in seawater using a Student's *t*-test. Experiments exposing larvae to *Artemia* culture water and test compounds indicated mean speeds, and NGDRs did not differ significantly among paths during the 5-min analysis period.

Based on initial findings, glucose, valine, and trehalose were selected for dose-response trials because they were among the compounds producing the largest changes in larval swimming behavior. Using the above protocol, larval swimming behavior was determined for larvae exposed to a series of half log-step dilutions from 10^{-4} to 10^{-6} *M*. Three replicate trials were run at each concentration, and within each dilution series the order of presentation was randomly determined. Seawater controls were run every fifth trial, as before. Solutions were prepared by serial dilutions of the primary stock used in the initial assays. Individual larvae were tested once, then discarded. Swimming speed and NGDR were regressed on concentration using SAS regression procedures (SAS Institute, Carey, North Carolina).

Experiments testing adult chemosensory abilities

Adult *Uca longisignalis*, also collected from Airport Marsh, were held in a 1 × 2 m sea table equipped with a continuous flow of filtered, UV sterilized seawater, and a sandy substrate allowing animals to construct burrows. Animals had continuous access to both shallow water (5 cm depth) and exposed sandy regions. Air temperature varied between 27–32°C, water temperature was 24–27°C at a salinity of 18–20 ppt. Animals were fed a diet of commercial fish food pellets, and the benthic diatom *Cylindrotheca closterium*. Forty-eight hours prior to experimentation, animals were removed from sea tables, and in small groups, isolated in bowls containing clean azoic substrate and 15 ppt ASW held at 26°C.

Chemosensory assays were conducted on individual adult crabs (mean carapace width: 18.4 ± 1.8 mm SD) exposed to one of the 16 amino acids or sugars used previously in tests with larvae. A 40-l aquarium was subdivided into three sections using opaque partitions, and the bottom lined with a layer of clean beach sand. The sand was sloped so that when approximately 200 ml of ASW was added, the back third of each section contained about 1 cm of standing water. This arrangement allows crabs access to water required in feeding (Miller, 1961), and crabs forage readily in this type of arena (Weissburg, 1990). A glass cover maintained humidity.

Each crab was presented with a food patch embedded in the sand at the front of the test section. The patch was a 2.3 cm diameter culture dish, containing 4.0 g substrate mixed with 3 ml of the test solution. Based on the work of Robertson *et al.* (1981), test solutions were prepared at 10^{-1} *M*, because this concentration proved maximally stimulatory to adult *U. pugilator.* The parallel methodology employed by Robertson *et al.* (1981) and by us facilitates a quantitative comparison between the two studies. The substrate was mud, collected from a location at Airport Marsh where crabs were observed feeding. Sediment was washed through a 1 mm sieve, ashed overnight at 600°C, treated in hot 10 *M* HCl for 8 h, then washed repeatedly with HPLC-grade distilled water to remove all traces of acid. Feeding experiments took place at 26°C.

Crabs were allowed to feed for 2 h while their behavior was recorded on video tape, using a NEC black and white CCD video camera (Model Ti 22AII) equipped with a Tokina 35–70 mm macrofocal lens and 2× multiplier, connected to a JVC (Model BR 3200U) tape recorder and a Panasonic TR-124-MA video monitor. All three animals in the aquarium were visible, and at the front of the tank (where the patches were embedded), the image of the animals was magnified by approximately 25%, facilitating accurate analysis of feeding behavior. Each chemical was tested on 15 individuals of each sex.

The tapes were reviewed and the frequency of feeding induction was determined, where feeding was defined as more than three successive lifts of the chelae to the mouth in any 5-s interval. We chose this criterion to be conservative in distinguishing a feeding response from patch sampling behavior. We observed that 75–80% of the animals, including those tested on seawater controls, lifted a chelae to their mouth at least once during a trial, although none of the animals lifted its chelae more than three consecutive times in sediments containing only seawater. Fiddler crabs possess chemosensitive organs on the minor chelae (Robertson *et al.*, 1981), and probing is a mechanism to allow animals to determine the contents of each patch. Three consecutive lifts seems to discriminate feeding from sampling. Any animal that was not scored as sampling the patch was excluded from analysis. Approximately 75% of the animals met the criterion of exhibiting sampling behavior, and additional animals were tested as needed to produce sample sizes of 15 animals of each sex per compound. Thus, results cannot be considered artifacts of differences in sampling frequency among compounds. The total time spent feeding was also measured to indicate the intensity of the response, and was recorded to the nearest 1 s with the time counter on the video tape recorder.

Preliminary results indicated that males and females were similar in their responses, so the data from both sexes were pooled. A William's corrected *G*-test was used to determine whether the percentage of animals responding to a substance was greater than that of seawater controls. Time spent feeding was analyzed using a Student's *t*-test. Animals did not feed on the seawater controls, giving feeding times of 0.00 (see Results). Because feeding times on other compounds cannot be less than zero, this was a one-tailed *t*-test to determine whether feeding times were significantly greater than zero.

Comparing larval and adult chemosensory responses

Responses of larval and adult *Uca longisignalis* were quantitatively compared using a non-parametric correlation analysis. Kendal's Tau was computed based on the rankings of the significance tests of larvae and adults. Each stimulatory compound (for either life history stage) was ranked by the *t*-value (larvae) or *G*-value (adults). For larvae, the highest *t*-value from measurement of either NGDR or swimming speed was used (see Results). We ranked the *G*-scores for the adults, because, unlike the *t*-test, they are less affected by variation in the time at which an animal commenced feeding. If, for instance, an animal began feeding near the end of a trial, feeding times could be truncated as an artifact of the experimental trial length, whereas estimates of the percentage of animals feeding are immune to the timing of the response. In any case, results obtained using *t*-test scores differ little from an analysis done using the *G*-test scores (see Results). Because we are interested in comparing the subsets of chemicals stimulatory to each life-history stage, compounds producing no response in both larvae and adults were excluded from the correlation analysis.

Responses of adult *Uca longisignalis* and adult *Uca pugilator* were also quantitatively compared using Kendal's Tau. Rankings for *Uca pugilator* were taken from Robertson *et al.* (1981), giving the number of foodballs/animal produced by crabs foraging on a particular substrate and compound. The rankings for the stimulus intensity of each compound on *U. pugilator* were computed by averaging results from all trials performed presenting a particular compound. Several compounds were tested in only one experiment, and the confidence limits for the

Table I

Sample sizes and t*-values for* Uca longisignalis *larval swimming responses to chemical test solutions, relative to seawater controls*

Compound	Number of paths analyzed	*t*-value	
		Speed	NGDR
Artemia culture water	66	2.48**	2.97**
Amino acids			
β-alanine	108	2.86**	0.76
arginine	65	1.18	0.58
asparagine	120	1.14	1.77
cysteine	141	0.30	0.72
glutamic acid	40	0.77	0.76
glycine	145	0.68	1.19
proline	119	0.25	0.16
serine	109	0.41	0.23
taurine	150	0.49	1.77
valine	98	7.60***	3.76***
Sugars			
galactose	124	2.99**	0.37
glucose	114	3.72**	0.01
maltose	106	0.71	2.18*
sorbose	109	3.36**	0.16
sucrose	134	2.54**	0.61
trehalose	140	0.01	4.37***
Seawater	259	—	—

* = $P < 0.05$, ** = $P < 0.01$, *** = $P < 0.001$.

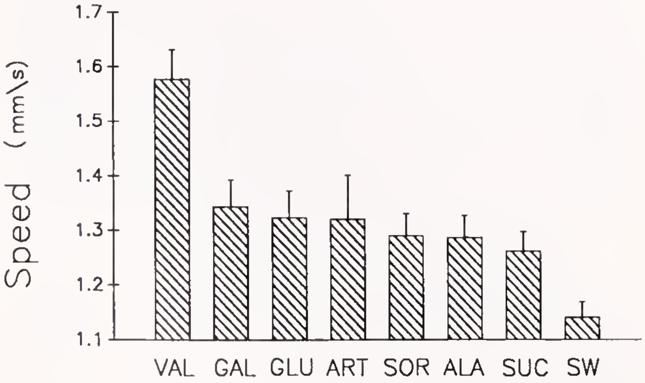

Figure 1. Mean swimming speeds (±1 SEM) of larvae exposed to test compounds at 10^{-4} *M*, metabolites released by *Artemia salina* (ART), and seawater. Data appear only for those compounds producing a significant change in larval swimming speed relative to seawater controls ($P < 0.05$; see Table I).

number of foodballs produced in response to these compounds overlapped. In this case, the rankings were considered ties.

Results

Experiments testing larval chemosensory abilities

Responses to metabolites released by Artemia *in culture.* Larvae responded to solutions derived from *Artemia* cultures by changing both swimming speed and turning behavior. Larval swimming speeds and NGDR's were significantly higher, relative to behavior in seawater (Table 1; Figs. 1, 2). We measured ammonia-N and dissolved organic carbon (DOC) in ASW and in culture water to assay for the presence of *Artemia* metabolites. The concentration of ammonia in culture water was 8.5 μ*M*, and in ASW was 0.8 μ*M*, as determined with an Alpkem nutrient autoanalyzer (Model RFA/2). Dissolved organic carbon occurred at 3.21 mg/l in culture water and at 0.75 mg/l in ASW, determined with a Shimadzu organic carbon analyzer (Model TOC-5000). The values obtained in culture water were typical for estuarine waters (Dame *et al.*, 1989; J. R. Pennock, pers. comm.) and clearly indicated the presence of *Artemia* metabolites.

Responses to amino acids and sugars. All of the sugars tested, as well as the amino acids valine and β-alanine, were stimulatory. Each substance, except for trehalose, caused changes in larval swimming behavior consistent with larval responses to *Artemia* culture water. Swimming speeds were increased in the presence of most sugars, and the two amino acids (Table 1; Fig. 1). The response to valine was the most dramatic, while responses to the other compounds were weaker. Galactose, glucose, sucrose, and β-alanine constituted a group producing roughly equal increases in swimming speed. Path trajectories were also changed in response to valine, maltose, and trehalose, as shown by the changes in NGDR (Table 1; Figs. 2, 3). Valine and maltose resulted in straighter paths, while larvae in trehalose solutions produced paths that were more circuitous (Fig. 3). For each of the other compounds listed in Table 1, but not appearing in Figures 1 or 2, mean swimming speeds were within ± 0.02 mm/s of that in

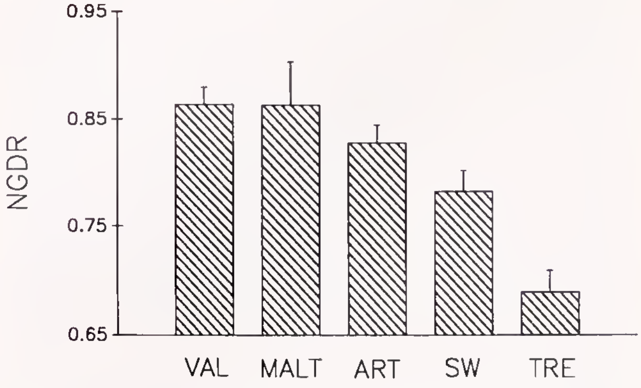

Figure 2. Mean NGDR (± 1 SEM) of larvae exposed to test compounds at 10^{-4} *M*, metabolites released by *Artemia salina* (ART), and seawater. Data appear only for those compounds producing a significant change in larval turning behavior relative to seawater controls ($P < 0.05$; see Table I).

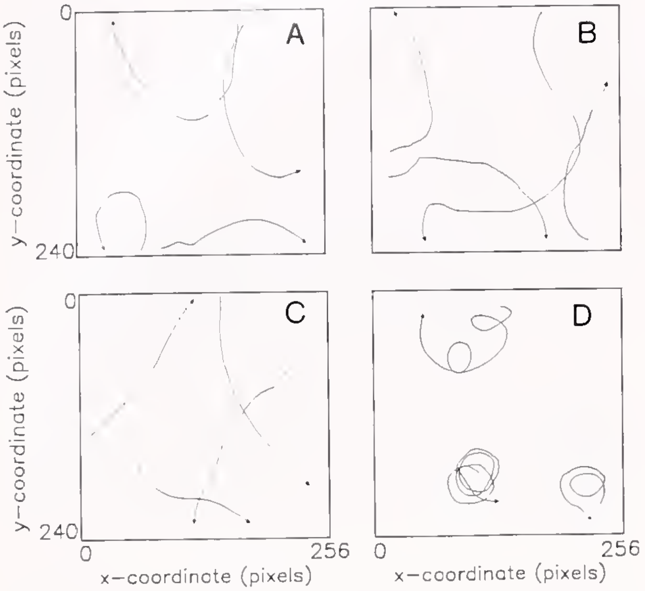

Figure 3. Typical swimming paths in the horizontal plane by larvae exposed to seawater and to test substances causing maximal responses. The x,y coordinates are in units of picture elements (pixels), where 1 pixel = 0.028 mm. All substances were tested at 10^{-4} *M*: A. seawater, B. glucose, C. valine, and D. trehalose. Relative to seawater, larvae swim faster in glucose, faster and straighter in valine, and turn more frequently in trehalose.

seawater, and *t*-tests yielded values of 0.0022–1.183 ($P > 0.20$, Table I). Mean NGDR values for non-stimulatory compounds were all within ± 0.02 of the NGDR in seawater, and *t*-values ranged from 0.020 to 1.77 ($P > 0.05$, Table I).

The dose-response curves for glucose, valine, and trehalose generally display a log-linear form (Fig. 4), allowing analysis by linear regression. There is a significant relationship between solution strength and response magnitude for all compounds. Responses to valine display the most sensitivity to dosage (slope = 0.097), followed by glucose (slope = 0.062), with responses to trehalose being least sensitive to dosage (slope = −0.048). The y-intercept of each curve is significantly different from seawater controls, according to a *t*-test (Fig. 4, $t \geq 8.94$, d.f. ≥ 229, $P < 0.01$, all comparisons). Larvae therefore respond to micromolar concentrations, and can probably respond to sub-micromolar stimulus concentrations as well. None of the regressions explain a great deal of the observed variance ($r^2 < 0.05$ in all cases), either due to the small slopes, or because additional factors may be important in determining larval swimming responses.

Experiments testing adult chemosensory abilities

Adult *Uca longisignalis* were induced to feed by a limited subset of the amino acids and sugars (Table II). The monosaccharide glucose, and the glucose-containing disaccharides, maltose and sucrose, induced the greatest percentage of animals to feed. Feeding was also elicited by the sugars, trehalose and sorbose, but to a much smaller degree, and the amino acids serine, glutamic acid, and β-alanine also provoked minor responses. Except for valine, which generated a non-significant increase in feeding, none of the other compounds elicited any behavioral response at all—*G*-values were 0.00 (Table II).

The feeding intensity elicited by each of the test compounds is also given in Table II, which lists foraging time for each treatment. All of the compounds that caused crabs to feed generated feeding times significantly greater than zero (one-tailed *t*-test) and, in general, the magnitude of response initiation and intensity was correlated. A Kendal's Tau, based on the rankings of feeding percent

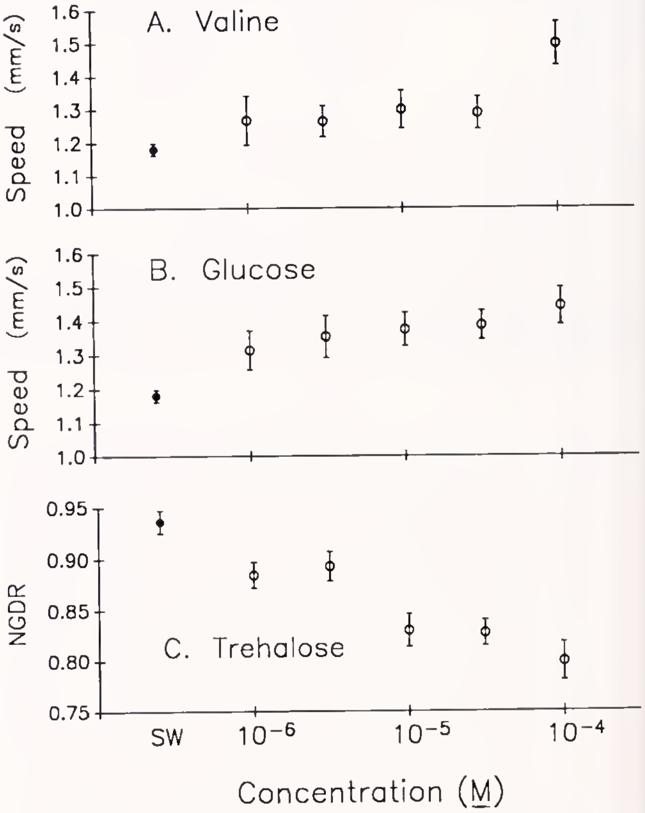

Figure 4. Dose-response curves for larvae exposed to test substances causing maximal responses. Each point gives the mean ± 1 SEM. Values for seawater controls (SW) at extreme left are shown for comparison, *n* for seawater = 79. A. Swimming speed in valine as a function of concentration, $F_{1,264} = 5.932$, $P < 0.025$; *t*-score testing for intercept different from seawater = 8.937, $n = 131$, $P < 0.001$. B. Speed in glucose as a function of concentration, $F_{1,295} = 3.65$, $P < 0.05$; *t*-score testing for intercept different than seawater = 45.881, $n = 155$, $P < 0.001$. C. NGDR in trehalose as a function of concentration, $F_{1,538} = 22.897$, $P < 0.001$; *t*-score testing for intercept different than seawater = 12.204, $n = 181$, $P < 0.001$.

Table II

Feeding responses by adult Uca longisignalis *to chemical test solutions and seawater controls*

	Proportion feeding		Feeding time	
Compound	Proportion	G-value	Time (s)	t-value
Amino acids				
β-alanine	0.17	7.33**	11 ± 2	4.59***
arginine	0.00	0.00		
asparagine	0.00	0.00		
cysteine	0.00	0.00		
glutamic acid	0.13	5.98*	28 ± 5	4.92***
glycine	0.00	0.00		
proline	0.00	0.00		
serine	0.17	7.33*	57 ± 23	2.51*
taurine	0.00	0.00		
valine	0.07	2.83		
Sugars				
galactose	0.00	0.00		
glucose	0.60	36.61***	841 ± 164	5.12***
maltose	0.80	43.71***	367 ± 63	6.91***
sorbose	0.20	8.22**	269 ± 108	2.48*
sucrose	0.60	36.61***	437 ± 86	5.91***
trehalose	0.33	10.97**	535 ± 81	6.63***
Seawater	0.00	—		

Thirty different crabs were tested with each compound and with seawater. Mean feeding time is given ±1 SEM. When there was no significant feeding as judged by a G-test, t-tests of feeding times were not performed. * = $P < 0.05$, ** = $P < 0.01$, *** = $P < 0.001$.

versus feeding time, yields a value of 0.58 ($0.03 < P < 0.06$). In spite of this association, the patterns of feeding induction (frequency or proportion) and feeding intensity (time) show qualitative differences. Trehalose, for instance, produced a feeding frequency little different from serine or glutamic acid, yet feeding times for animals exposed to trehalose rank second only to glucose (Table II). Maltose treatments exhibited the greatest ability to induce feeding, yet rank fourth in the intensity of the response (Table II).

Correlations among life-history stages, and among species

The correlations among adult and larval responses of *U. longisignalis* are based on the data given in Table III. Responses of the two life-history stages are similar at a very coarse scale, where a binomial test indicates that adults and larvae mutually respond either positively or negatively to the same substances more often than predicted by chance alone (binomial test: $n = 16$, $x = 12$, $P < 0.04$). However, the fine scale pattern of response exhibited by each life history stage differs substantially. A Kendall's Tau performed on ranks based on the magnitudes of larval and adult responses to the same compounds yields a value of −0.0227, indicating no significant correlation ($P > 0.50$). Behavior of larvae in trehalose is quite different than responses to the other compounds, making the functional significance of the response to trehalose unclear. Therefore, the correlation analysis was repeated with the larval response to trehalose ranked last, and also with this compound deleted from the analysis entirely. In both cases, the results are unchanged; Kendall's Tau,

Table III

Analysis of chemosensory responses between life-history stages in Uca longisignalis, *and between adults of* U. longisignalis *and* U. pugilator

	Larvae		Adults			
	U. longisignalis		*U. longisignalis*		*U. pugilator*	
Compound	Score	Rank	Score	Rank	No.	Rank
Valine	7.60	1	2.84	9[a]	—	—
Trehalose	4.31	2	10.97	4	20.3	5
Glucose	3.75	3	36.61	2.5	60.0	3
Sorbose	3.36	4	8.24	5[a]	—	—
Galactose	2.99	5	0.00	10[a]	—	—
β-alanine	2.86	6	7.33	6.5[b]	10.0	7
Sucrose	2.54	7	36.61	2.5	133.7	1
Maltose	2.14	8	43.71	1	85.5	2
Serine	0.79	9	7.33	6.5[b]	51.1	4
Glutamic acid	0.77	10	5.98	8[c]	10.0	7
Asparagine	—	—	0.00	8[d]	10.0	7

Score refers to the results of a t-test (larvae) or G-test (adults) for significant behavioral responses to the test compound. For *U. pugilator*, No. refers to the mean number of foodballs produced by individual crabs foraging on the test compound, with the data taken from Robertson *et al.* (1981). [a] Ranking for adult-larval comparison only, not used in adult-adult comparison. [b] Ranking for adult-larval comparison only, rank for adult-adult comparison is 5.5; [c] Ranking for adult-larval comparison only, ranking for adult-adult comparison is 7; [d] Ranking for adult-adult comparison only, compound not used in adult-larval comparison. See text for details.

computed with trehalose ranked last, is −0.3423, and is −0.2319 with trehalose removed ($P > 0.25$ in both cases).

The difference in fine *versus* coarse scale patterns reflects changes in the stimulatory capacity of substances excitatory to both life history stages. Only four compounds were significantly stimulatory exclusively to larvae or to adults (valine and galactose were highly excitatory solely to larvae, while glutamic acid and serine induced only adults to feed); the majority of the remaining compounds tended to be more highly excitatory to one stage or the other. Maltose and sucrose, for instance, were highly stimulatory to adults, but less stimulatory to larvae, while trehalose was more stimulatory to larvae than to adults.

In contrast to the within species comparison, the responses of adult *U. pugilator* and *U. longisignalis* are highly correlated at both coarse and fine scales. A binomial test indicates that adults from both species mutually respond either positively or negatively to the same compounds more frequently than expected by chance (binomial test: $n = 14, x = 13, P < 0.001$). Similarly, a Kendall's Tau, computed on the rankings in Table III, gives a value of 0.78 ($P < 0.03$), indicating a quantitatively similar response pattern to individual compounds among adults of each species. Although we present our tabulation using rankings of the proportion feeding for *Uca longisignalis*, the results using feeding time are not substantially different (Tau = 0.57, $0.03 < P < 0.06$). The monosaccharide glucose, its disaccharide isomers, and the amino acid serine were the most stimulatory, while the remaining amino acids were weakly stimulatory to both species.

Discussion

This is the first examination of patterns of chemoreception in zoea stage larvae. We have shown that brachyuran crab larvae possess chemosensory abilities, and that these abilities are present, although perhaps not fully developed, at a very early stage. Larvae respond to various amino acids and sugars with a change in swimming behavior. Such changes have previously been demonstrated as reliable indicators of chemosensitivity in a variety of zooplankters, such as copepods (Poulet and Ouellet, 1982; Buskey, 1984), tintinnids (Buskey and Stoecker, 1989), oyster larvae (Zimmer-Faust and Tamburri, in prep.), and ciliates (Levandowsky *et al.*, 1984).

Workers have interpreted the changes in swimming behavior as indicating that waterborne substances act to cue resource acquisition behavior, since changes often involve decreases in swimming speed and in NGDR, and an increased rate of turning (Buskey, 1984; Buskey and Stoecker, 1989; Zimmer-Faust and Tamburri, in prep.). Together, these changes have been viewed as 'adaptive' responses, allowing predators to remain in aggregations of potential prey, or enabling larval settlers to conduct site-restricted searches for microhabitats favorable to substrate colonization. Clearly, the increased turning behavior displayed by fiddler crab larvae in trehalose solutions might facilitate location of prey within patches, because the turning causes animals to loop back, focusing locomotory activity within a small area (*e.g.*, Koopman, 1980).

Paradoxically, increases in swimming speed and NGDR also seem to be associated with prey detection. In this study, *Uca* zoea responded to metabolites from *Artemia*, a known zooplankton prey species, with an increase in both speed and NGDR. Buskey (1984) determined that, when copepods are given diatom suspensions, swimming speed and NGDR decrease, whereas copepods exposed to diatom exudates alone, increase both speed and NGDR. In the absence of mechanical stimuli, these behaviors might allow animals to cover large areas in search of prey patches, whereupon encountering prey, paired mechanical and chemical stimuli would result in site-restricted behavior. Additional experiments are necessary to determine the functional roles of chemoreception and mechanoreception in mediating prey search by *Uca* zoea.

To some degree, substances stimulatory to larvae are those that signal the presence of potential food items. Zooplankton are the primary prey species of *Uca* larvae, which have been successfully reared only using various motile zooplankton (*e.g.*, Herrnkind, 1968; Christiansen and Yang, 1976; Rabalais and Cameron, 1983; Christy, 1989). The larvae lack setae necessary for capturing phytoplankton, instead pinning prey between the telson and anteroventral spine (Herrnkind, 1968). *Uca longisignalis* larvae respond to the amino acids valine and β-alanine. Although the response spectrum is narrower than that observed in other (adult) crustaceans (see reviews of Ache, 1982; Carr, 1988; Laverack, 1988), these two amino acids strongly signal the presence of fleshy prey. Beta-alanine constitutes as much as 12% of the free-amino acids released into the water by zooplankton, with both valine and β-alanine being consistently among the most abundant amino acids released into the surrounding environment by potential zooplankton prey (Webb and Johannes, 1967). Beta-alanine is generally one of the most abundant free amino acids present in flesh, and valine is quite often abundant, averaging over 5% of the free-amino acid pool (Cowey and Corner, 1964; Srinivasagam *et al.*, 1971). Zooplankton assemblages have 2–3 times the free amino acid concentration of valine and β-alanine as phytoplankton-dominated communities (Jeffries, 1969).

Some of the stimulatory sugars may also signal the presence of prey. Glucose is the major blood sugar present in animals, while trehalose is found in the hemolymph of some crustaceans (Telford, 1968). Both of these compounds evoke filter feeding responses in the planktivorous porcelain crab *Petrolisthes cinctipes* (Hartman and Hartman, 1977). There is little work done on the distributions of other sugars in seawater or in tissues of marine animals, although galactose and galactose derivatives found in seawater may originate from flagellates (Sakugawa *et al.*, 1985).

Adult *U. longisignalis* respond to a rather limited suite of the compounds tested, primarily carbohydrates, and stimuli that are more effective at inducing feeding also produce more intense feeding responses (Table II). Glucose and glucose dissacharide moieties are particularly potent stimuli. Contrary to what has been found in other studies, there is little evidence that disaccharides are more stimulatory than constituent monosaccharides (*e.g.*, Zimmer *et al.*, 1979; Robertson *et al.*, 1981; Trott and Robertson, 1984). Judging by both the induction as well as the intensity of the response, crabs respond more highly to glucose compounds than to other substances. Some additional sugars produce appreciable responses of one type or the other (*i.e.*, induction or intensity), but the joint function of the two components is not as great as for glucose and its dissacharides. Although a few amino acids, particularly serine, provoke responses, they have small effects both as inducers, and in terms of the response intensity.

The pattern of chemosensitivity suggests adult *U. longisignalis* are well constructed to allow efficient foraging in their natural habitat. Diatoms, bacteria, and, occasionally, blue-green algae are dominant flora of the mud-flats preferred by crabs. The primary storage product in diatoms is a glucan, and carbohydrates are primary constituents of the extracellular mucose sheaths of diatoms and blue-green algae (*e.g.*, Fogg, 1966). These sugars are often released into the environment by algal species (Fogg, 1966; Fogg *et al.*, 1973; Craigie, 1974; Darley, 1977; Paulsen *et al.*, 1978). Serine is the dominant amino acid of the free amino acid pool of diatoms (Parsons *et al.*, 1961), and it appears that adult fiddler crabs are unique in responding primarily to this amino acid (*i.e.*, Robertson *et al.*, 1981). Strong responses to carbohydrates and serine may be expected in light of their specificity as a cue to microalgal food resources.

The methodology of this study and that of Robertson *et al.* (1981) on the sand fiddler crab, *Uca pugilator*, are parallel enough to quantify the correlation among chemosensory abilities of the two species. The analysis indicates that, in at least this species pair, similar trophic ecologies have produced a broad concordance among patterns of adult chemosensitivity, even on a fine scale. The high correlation among the abilities of *Uca* species may be a function of the habitat occupied by adult fiddler crabs. For the semi-terrestrial *Uca*, molecules present in sediments where crabs forage are derived from a variety of sources, including microbial breakdown processes (Rittschof, 1980), and leakage from dead cells and decaying material (Kennish, 1986). High background levels of substances in sediments, and the large number of potential non-prey sources of stimulatory molecules, may make intertidal mudflats particularly "noisy" environments. Under these conditions, only a few substances most closely associated with the presence of food (*i.e.*, serine and carbohydrates) may be good signal carriers, forcing convergence among the properties of organisms occupying these habitats. Future studies on animals in subtidal, intertidal, and semi-terrestrial habitats are needed to fully discern the influence of habitat type on patterns of correlation among chemosensory abilities of related crustacean species.

In contrast to the between-species comparison, larval and adult *Uca longisignalis* express different patterns of chemosensory ability at the fine scale. It appears that differences in the chemical environment of the pelagic and benthic habitats, or differences in diet, may require that varying life-history stages respond disparately to similar suites of chemicals. A number of compounds stimulatory to one life-history stage of *U. longisignalis* are either non-stimulatory or only slightly stimulatory to the other stage. For instance, valine and galactose are excitatory only to larvae; serine and glutamic acid only to adults. Valine and serine are cues that are well-defined markers for prey types favored by a particular form, so it is perhaps not surprising that each substance is strongly stimulatory to only one life-history stage. The significance of glutamic acid and galactose to certain stages is less clear. Glutamic acid is not readily released into seawater by zooplankton (Webb and Johannes, 1967), but is an abundant constituent of the amino acids found in diatoms (Cheucas and Riley, 1969). Glucose appears to be unique in its ability to function as a cue for both larval and adult food sources, and is highly stimulatory to both life-history stages.

Patterns of larval and adult abilities must be cautiously interpreted, because it appears that some stimulants may produce responses that do not enhance the ability of the organism to detect prey. There is no evidence that the sugars sorbose, maltose, and sucrose are present in zooplankton, but they are intimately associated with adult food sources. It may be that detection of these substances by larvae has some function. However, in view of the close association of these substances with adult food, we tentatively hypothesize that the chemosensory responses of larvae to these sugars are incipient abilities. That is, sensitivity to these compounds by larvae may be the result of developmental processes required in providing sensitivity by adults.

While larval abilities appear partially a consequence of adult requirements, adult abilities do not seem to reflect larval needs. Substances which act as potential cues to larval, but not adult prey items (*e.g.*, valine), do not elicit adult feeding behaviors, while still evoking strong larval responses. Central neural processing is known to attenuate chemical signals, thereby reducing or eliminating behavioral responses, even though substances may evoke strong electrophysiological activity from receptor cells (Dethier, 1980; Derby *et al.*, 1985). It is sometimes observed that substances that produce action potentials from sensory cells do not always have detectable effects on behavior. Shepheard (1974) compared results of his electrophysiological study on responses by olfactory cells of *Homarus americanus*, to behavioral studies of McLeese (1970), and concluded that a variety of compounds with strong electrophysiological activity elicited little or no behavioral reactions. Working with *U. pugilator*, Vermeer (1981) has documented that valine and β-alanine are both extremely potent substances in electrophysiological assays, although valine is not an adult feeding stimulant, and β-alanine is only weakly so (Robertson *et al.*, 1981). We suggest this type of discordance between electrophysiological and behavioral responses in adults may be adaptive, serving to reduce or eliminate adult feeding reactions to substances that cue only larval food resources.

The conclusions reached as a result of our study must be regarded as working hypotheses, primarily because we did not assay the changes in chemosensory-mediated behavior continuously through ontogeny from zoea and megalopa stages, to the adult stage. Our aim is to call attention to the patterns we have observed, to help investigators interpret chemosensory abilities of other organisms. Additional studies on the development of chemoreceptive behavior in fiddler crabs and in other organisms will be needed to confirm the patterns we have detected. Further investigations also will be required to determine the conditions under which chemosensory abilities of early life-history stages are constrained by developmental processes and ecological requirements of later forms. While the ecological context of organisms may produce concordance among chemosensory abilities, it nonetheless appears that constraints arising from developmental processes may sometimes complement ecological pressures in determining the expression of chemosensory-mediated behavior.

Acknowledgments

The authors thank M. N. Tamburri for assistance in performing video recording and motion analysis and Dr. S. G. Morgan for guidance in raising larvae. Research was sponsored, in part, by grants from the National Science Foundation (R11-8996152, DIR-8954231, and DIR-9013187), by a faculty development award from the Marine Environmental Sciences Consortium, and by an award from the Research Grants Committee, University of Alabama.

Literature Cited

Ache, B. W. 1982. Chemoreception and thermoreception. Pp. 369–398 in *The Biology of Crustacea Vol. 3*, L. Atwood and D. C. Sandeman, eds. Academic Press, New York.

Ache, B. W., B. J. Johnson, and E. Clark. 1978. Chemical attractants of the Florida spiny lobster *Panulirus argus*. *Florida Sea Grant Technical Paper No. 10.* 28 pp.

Andrews, P., P. J. Williams, and B. Lee. 1971. Heterotrophic utilization of organic compounds in the sea III. Measurement of the oxidation rates and concentration of glucose and amino acids in sea water. *J. Mar. Biol. Assoc. U. K.* **51:** 111–125.

Buskey, E. J. 1984. Swimming pattern as an indicator of copepod sensory systems in the recognition of food. *Mar. Biol.* **79:** 165–175.

Buskey, E. J., and D. K. Stoecker. 1989. Behavioral responses of the marine tintinnid *Favella* sp. to phytoplankton: influence of chemical, mechanical and photic stimuli. *J. Exp. Mar. Biol. Ecol.* **132:** 1–16.

Butman, C. A., J. P. Grassle, and E. J. Buskey. 1988. Horizontal swimming and gravitational sinking of *Capitella* sp. I larvae: implications for settlement. *Ophelia* **29:** 43–57.

Carr, W. E. S. 1988. The molecular nature of chemical stimuli in the aquatic environment. Pp. 3–28 in *Sensory Biology of Aquatic Animals*, J. Atema, R. R. Fay, A. N. Popper, and W. N. Tavolga, eds. Springer-Verlag, New York.

Chuecas, L., and J. P. Riley. 1969. The component amino acids of some marine diatoms. *J. Mar. Biol. Assoc. U. K.* **49:** 117–120.

Christiansen, M. E., and W. T. Yang. 1976. Feeding experiments on the larvae of fiddler crabs reared in the laboratory. *Aquaculture* **8:** 91–98.

Christy, J. H. 1989. Rapid development of megalopae of the fiddler crab *Uca pugilator* reared over sediment: implications for models of larval recruitment. *Mar. Ecol. Prog. Ser.* **57:** 259–265.

Clark, M. E., G. A. Jackson, and W. J. North. 1972. Dissolved free amino acids in southern California coastal waters. *Limnol. Oceanogr.* **17:** 749–758.

Cowey, C. B., and E. D. S. Corner. 1966. Amino acids and other nitrogenous compounds in *Calanus finmarchicus*. *J. Mar. Biol. Assoc. U. K.* **43:** 485–493.

Crane, J. 1975. *Fiddler Crabs of the World.* Princeton University Press, Princeton, NJ. 737 pp.

Craigie, J. S. 1974. Storage products. Pp. 206–235 in *Algal Physiology and Biochemistry*, W. D. P. Stewart, ed. Blackwell Scientific Publications, Oxford.

Crisp, D. J. 1967. Chemoreception in cirripedes. *Biol. Bull.* **133:** 128–140.

Dame, R. F., J. D. Spurrier, and T. G. Wolaver. 1989. Carbon, nitrogen and phosphorus processing by an oyster reef. *Mar. Ecol. Prog. Ser.* **54:** 249–256.

Darley, W. M. 1977. Biochemical composition of diatoms. Pp. 198–223 in *Biology of Diatoms*, D. Werner, ed. Blackwell Scientific Publications, Oxford.

Degens, E. T., J. H. Reuter, and N. F. Shaw. 1964. Biochemical compounds in offshore California sediments and sea waters. *Geochim. Cosmochem. Acta* **28:** 45–66.

Derby, C. D., B. W. Ache, and E. W. Kennel. 1985. Mixture suppression in olfaction: electrophysiological evaluation of the contribution of peripheral and central neural components. *Chem. Senses* **10:** 301–316.

Dethier, V. G. 1980. Evolution of receptor sensitivity to secondary plant substances with special reference to deterrents. *Am. Nat.* **115:** 45–66.

Epifanio, C. E., K. T. Little, and P. M. Rowe. 1988. Dispersal and recruitment of fiddler crab larvae in the Delaware River Estuary. *Mar. Ecol. Prog. Ser.* **43:** 181–188.

Fogg, G. E. 1966. The extracellular products of marine algae. *Oceanogr. Mar. Biol. Ann. Rev.* **4:** 195–212.

Fogg, G. E., W. D. P. Stewart, P. Fay, and A. E. Walsby. 1973. *The Blue-green Algae.* Academic Press, New York. 459 pp.

Fuzessery, Z. M., and J. J. Childress. 1975. Comparative sensitivity to amino acids and their role in the feeding activity of bathypelagic and littoral crustaceans. *Biol. Bull.* **149:** 522–538.

Hartman, B. H., and M. S. Hartman. 1977. The stimulation of filter feeding in the porcelain crab *Petrolithes cinctipes* Randall by amino acids and sugars. *Comp. Biochem. Physiol.* **56A:** 19–22.

Herrnkind, W. F. 1968. The breeding of *Uca pugilator* (Bosc) and mass rearing of the larvae with comments on the behavior of larval and early crab stages (Brachyura: Ocypodidae). *Crustaceana Suppl.* **II:** 214–224.

Jeffries, H. P. 1969. Seasonal composition of temperate plankton communities: free amino acids. *Limnol. Oceanogr.* **14:** 41–52.

Kennish, M. J. 1986. *Ecology of Estuaries, Vol. I. Physical and Chemical Aspects.* CRC Press, Miami, FL 254 pp.

Koopman, B. O. 1980. *Search and Screening.* Pergamon Press, Elmsford, NY. 368 pp.

Laverack, M. S. 1988. The diversity of chemoreceptors. Pp. 3–28 in *Sensory Biology of Aquatic Animals,* J. Atema, R. R. Fay, A. N. Popper, and W. N. Tavolga, eds. Springer-Verlag, New York.

Levandowsky, M., T. Cheng, A. Kehr, J. Kim, L. Gardser, L. Silvern, L. Tsang, G. Lai, C. Chung, and E. Prakash. 1984. Chemosensory responses to amino acids and certain amines by the ciliate *Tetrahymena:* a flat capillary assay. *Biol. Bull.* **167:** 322–330.

McLeese, D. W. 1970. Detection of dissolved substances by the American lobster (*Homarus americanus*) and olfactory attraction between lobsters. *J. Fish. Res. Board Can.* **27:** 1371–1378.

Miller, D. C. 1961. The feeding mechanism of fiddler crabs, with ecological considerations of feeding adaptations. *Zoologica* **46:** 86–101.

Mopper, K., R. Dawson, and V. Ittekkot. 1980. The monosaccharide spectra of natural waters. *Mar. Chem.* **10:** 55–66.

Mopper, K., and P. Lindroth. 1982. Diel and depth variations in dissolved free amino acids and ammonium in the Baltic Sea determined by shipboard HPLC analysis. *Limnol. Oceanogr.* **27:** 336–347.

Parsons, T. R., K. Stephens, and J. D. H. Strickland. 1961. On the chemical composition of eleven species of marine phytoplankton. *J. Fish. Res. Board Can.* **18:** 1001–1016.

Paulsen, B. E., A. Haug, and B. Larsen. 1978. Structural studies of a carbohydrate-containing polymer present in the mucilage tubes of the diatom *Berkeley rutilans* (Trent.) Grun. *Carbohydrate Res.* **66:** 103–111.

Poulet, S. A., and G. Ouellet. 1982. The role of amino acids in the chemosensory swarming and feeding of marine copepods. *J. Plankton Res.* **4:** 341–361.

Rabalais, N. N., and J. N. Cameron. 1983. Abbreviated development of *Uca subcylindrica* (Stimpson, 1859) (Crustacea, Decapoda, Ocypodidae) reared in the laboratory. *J. Crust. Biol.* **3:** 519–541.

Rittschof, D. 1980. Enzymatic production of small molecules attracting hermit crabs to simulated gastropod predation sites. *J. Chem. Ecol.* **6:** 665–675.

Rittschof, D., and C. U. Buswell. 1989. Stimulation of feeding behavior in three species of fiddler crabs by hexose sugars. *Chem. Senses* **14:** 121–130.

Robertson, J. R., K. Bancroft, G. Vermeer, and K. Plaisier. 1980. Experimental studies on the foraging behavior of the sand fiddler crab *Uca pugilator* (Bosc 1802). *J. Exp. Mar. Biol. Ecol.* **44:** 67–83.

Robertson, J. R., J. A. Fudge, and G. K. Vermeer. 1981. Chemical and live feeding stimulants of the sand fiddler crab *Uca pugilator* (Bosc). *J. Exp. Mar. Biol. Ecol.* **53:** 47–64.

Sakugawa, H., N. Handa, and K. Ohta. 1985. Isolation and characterization of low molecular weight carbohydrates dissolved in seawater. *Mar. Chem.* **17:** 341–362.

Shepheard, P. 1974. Chemoreception in the antennule of the lobster, *Homarus americanus. Mar. Behav. Physiol.* **2:** 261–274.

Srinivasagam, R. T., J. E. G. Raymont, C. F. Moodie, and J. K. B. Raymont. 1971. Biochemical studies on marine zooplankton X. The amino acid composition of *Euphausia superba, Meganyctiphanes norvgica* and *Neomysis integer. J. Mar. Biol. Assoc. U. K.* **51:** 917–925.

Teal, J. M. 1958. Distribution of fiddler crabs in Georgia salt marshes. *Ecology* **39:** 185–193.

Telford, M. 1968. The identification and measurement of sugars in the blood of three species of Atlantic crabs. *Biol. Bull.* **135:** 574–584.

Trott, T. J., and J. R. Robertson. 1984. Chemical stimulants of cheliped flexation behavior by the Atlantic ghost crab *Ocypode quadrata* (Fabricus). *J. Exp. Mar. Biol. Ecol.* **78:** 237–252.

Vermeer, G. K. 1981. Chemoreception in the sand fiddler crab *Uca pugilator* (Bosc): an electrophysiological and behavioral approach. Masters thesis, University of Georgia, Athens, GA.

Webb, K. L., and R. E. Johannes. 1967. Studies on the release of dissolved free amino acids by marine zooplankton. *Limnol. Oceanogr.* **12:** 376–382.

Weissburg, M. 1990. The foraging biology of *Uca pugnax:* mechanics, functional morphology, and feeding strategies. PhD. Dissertation, SUNY at Stony Brook, Stony Brook, NY.

Zimmer, R. K., D. P. Cook, and J. F. Case. 1979. Chemosensory induced brachycardia in the kelp crab, *Pugietta producta* (Randall). *J. Exp. Mar. Biol. Ecol.* **38:** 135–150.

Zimmer-Faust, R. K. 1987. Crustacean chemical perception: towards a theory on optimal chemoreception. *Biol. Bull.* **172:** 10–29.

Zimmer-Faust, R. K. 1989. The relationship between chemoreception and foraging behavior in crustaceans. *Limnol. Oceanogr.* **34:** 1367–1374.

Zimmer-Faust, R. K., J. E. Tyre, W. M. Michel, and J. F. Case. 1984. Chemical mediation of appetitive feeding in a marine decapod crustacean: the importance of suppression and synergism. *Biol. Bull.* **167:** 339–353.

Reference: *Biol. Bull.* **181**: 216–221. (October, 1991)

Genetic Variation in the Timing of Gonadal Maturation and Spawning of the Eastern Oyster, *Crassostrea virginica* (Gmelin)

BRUCE J. BARBER[1], SUSAN E. FORD[2], AND ROBERT N. WARGO[2,*]

[1]*Virginia Institute of Marine Science, College of William and Mary, Gloucester Point, Virginia 23062, and* [2]*Shellfish Research Laboratory, Rutgers University, New Jersey Agricultural Experiment Station, Institute of Marine and Coastal Sciences, Port Norris, New Jersey 08349*

Abstract. The gonadal cycles of four groups of eastern oysters, *Crassostrea virginica* (Gmelin), including native stocks collected that year and inbred strains (reared in Delaware Bay for 5–6 generations) from both Long Island Sound and Delaware Bay, were compared in Delaware Bay in 1987. Inbred strains resembled their respective native stocks; both Long Island groups initiated gonadal development and spawning about one month earlier and spawned over a shorter duration than both Delaware Bay groups. Analysis of covariance revealed that the effect of time on gonadal development was statistically different ($P \leq 0.05$) for all between-location group comparisons, but not for the two within-location comparisons. Thus, after six generations of inbreeding in Delaware Bay, Long Island oysters maintained their characteristic pattern of gonadal development and spawning, indicating the existence of genetically different environmental requirements for gonadal maturation between the two locations.

Introduction

Intraspecific variation in various aspects of reproduction has been noted for several species of marine bivalves, and can be either genetic or non-genetic (adaptive) in nature (see Sastry, 1979; Barber and Blake, 1991). The suggestion that there are genetically distinct populations or "races" of eastern oysters, *Crassostrea virginica* (Gmelin), was first made by Loosanoff and Engle (1942). Stauber (1950) concluded that there were three physiological races of oysters, based on differences in temperatures at which spawning was initiated in Long Island, New Jersey, and Texas populations. Because transplant experiments were not conducted, the relative contribution of genetic *versus* non-genetic factors to the observed differences was not determined. Loosanoff and Nomejko (1951) and Loosanoff (1969) transplanted stocks from various locations along the eastern and Gulf coasts of the U.S. to Milford, Connecticut, and histologically compared gonadal development. Differences in the timing and extent of gonadal development and spawning between some of these stocks **in the common environment** suggested the existence of genetic differences in the environmental factors regulating gonadal maturation. The possibility of acclimatization after transfer to the new environment, however, was not precluded. As stated by Loosanoff (1969), the best way to separate the genetic and environmental aspects of oyster reproduction would be to use "successive generations of laboratory-reared oysters originating from parents of different geographical areas."

The oyster (*C. virginica*) selective breeding program of the Rutgers University Shellfish Research Laboratory includes a variety of wild (imported) stocks and laboratory-reared strains that originated from several locations (Haskin and Ford, 1979; Ford and Haskin, 1987). Initial examination of some of these strains (originating from Long Island Sound, Delaware Bay, and James River, Virginia, stocks) indicated that after several generations of inbreeding and maintenance in Delaware Bay, the timing of specific reproductive events remained characteristic of the site of geographic origin (Ford *et al.*, 1990). The object of the present study was to establish whether these observed differences are attributible to intraspecific genetic variation. This was accomplished by simultaneously

Received 25 February 1991; accepted 24 May 1991.

Present address: AT&T, 412 Mt. Kemble Ave., Morristown, New Jersey 07960.

comparing cycles of gonadal maturation and spawning in both wild stocks and inbred strains originating from two locations: Long Island Sound and Delaware Bay.

Materials and Methods

Native oysters from Long Island Sound (LIN), native oysters from Delaware Bay (DBN), a 6th generation, 1985 year class, inbred strain originally imported from Long Island Sound to Delaware Bay in 1964 (LII), and a 5th generation, 1985 year class, inbred strain originating from Delaware Bay (DBI) were obtained in March 1987. Because the endoparasite *Haplosporidium nelsoni* (MSX) alters gonad development and relative fecundity (Barber *et al.*, 1988; Ford and Figueras, 1988), all oysters used in this study were first "purged" of MSX (Ford and Haskin, 1988a, b) by being suspended in wire trays from the laboratory dock (Bivalve, New Jersey) in the Maurice River (salinity < 5 ppt) for several weeks. On 1 May 1987, all experimental groups were moved to the tidal flats of lower Delaware Bay, Cape May County (salinity 18–24 ppt), for the remainder of the study.

Each group of oysters was sampled periodically between 17 March and 5 October 1987; ten individuals were shucked and fixed in Davidson's solution. A standard transverse (anterior) section across gill, stomach, intestine, and digestive diverticula was dehydrated, cleared, and embedded in paraplast. Six-μm sections were stained with iron hematoxylin, acid fuchsin, and aniline blue. Slides were examined for MSX prevalence (% of sample infected) and intensity (Ford, 1985; Barber *et al.*, 1988). Gonadal development was assessed from the histological sections using the Bioquant Image Analysis System (R&M Biometrics, Inc., Nashville, Tennessee) to obtain a Gonadal Area Index, defined as the ratio of gonadal area to the entire visceral mass area × 100. The gonadal area technique is a sensitive indicator of gametogenic events in oysters (Mori, 1979; Barber *et al.*, 1988) and is more precise than measuring the thickness of the gonadal layer alone, as performed by Loosanoff and Nomejko (1951).

Cycles of gonadal development of the four groups of oysters, based on mean gonadal area indices, were compared using analysis of covariance after correcting for heteroscedasticity with the least squares method of White (1980). Analysis of covariance was accomplished using the dummy variable regression procedure of Wonnacott and Wonnacott (1970). Gonadal area index was regressed on a quadratic function of time (elapsed days from the date of the first sample) as:

$$\text{Gonadal Area Index} = \alpha_i \text{ Days} + \alpha_j D_j \text{ Days} + \beta_i \text{ Days}^2 + \beta_j D_j \text{ Days}^2,$$

using the Tobit estimation to overcome the problem of zeros in the data set (Goldberger, 1964). The t statistic was then used to test the null hypothesis that $\alpha_i = \alpha_j$ and $\beta_i = \beta_j$, for each pair-wise group comparison. Conventional analysis of variance was not applied because of the presence of zero-valued observations, which invalidated the required normality assumption. Moreover, conventional analysis of variance compares only means, while the procedure used here allowed a global comparison.

Water temperature data from the experimental site were collected only sporadically during 1987. Weekly averages of "calculated" daily water temperatures were therefore obtained from the regression of daily air temperatures (Cape May, New Jersey) on actual water temperatures collected at the experimental site from 1978–80 and 1985–88 ($n = 358$; $r = 0.77$). These are presented in Figure 1.

Results

The haplosporidan parasite *H. nelsoni* had little effect on gonadal development in any of the groups in this study. Prevalence and intensity of the parasite remained relatively low throughout the first four months of the study period because of the exposure of oysters to low salinity prior to initial sampling (Table I). Prevalence of *H. nelsoni* did not exceed 50% until 15 July, and systemic infections exceeded 50% only in the LIN group, after 15 July and the completion of spawning in that group. Gonadal development in *C. virginica* is most affected in individuals having systemic *H. nelsoni* infections (Barber *et al.*, 1988; Ford and Figueras, 1988; Ford *et al.*, 1990).

Cycles of gonadal maturation and spawning for the four groups of oysters are represented as mean gonadal area indices in Figure 2. Both Long Island groups (LIN and LII) initiated gonadal development in April and had maximal gonadal areas in late May (Figs. 2A, B). Some spawning occurred in both Long Island groups in late May and June, but greatest spawning activity occurred in July. Long Island oysters (both LIN and LII) were spent by August. Although some gonadal development was apparent in the DBI group in late April, most gonadal growth in both Delaware Bay groups (DBN and DBI) occurred in May (Figs. 2C, D). Maximal gonadal areas were found for both Delaware Bay groups in June, which was followed by a period (from June to August) of what appeared to be partial spawning and redevelopment. Final spawning and the cessation of gonadal activity in the Delaware Bay groups occurred in September. Thus there were similarities between inbred strains and native stocks within each site of origin but differences between sites of origin.

The null hypothesis of similarity of coefficients was rejected in all four pair-wise comparisons between strains having different geographic origins (Table II), indicating that the timing of gonadal growth and spawning of both native stocks and inbred strains from Delaware Bay were statistically different ($P \leq 0.05$) from those of oysters (both

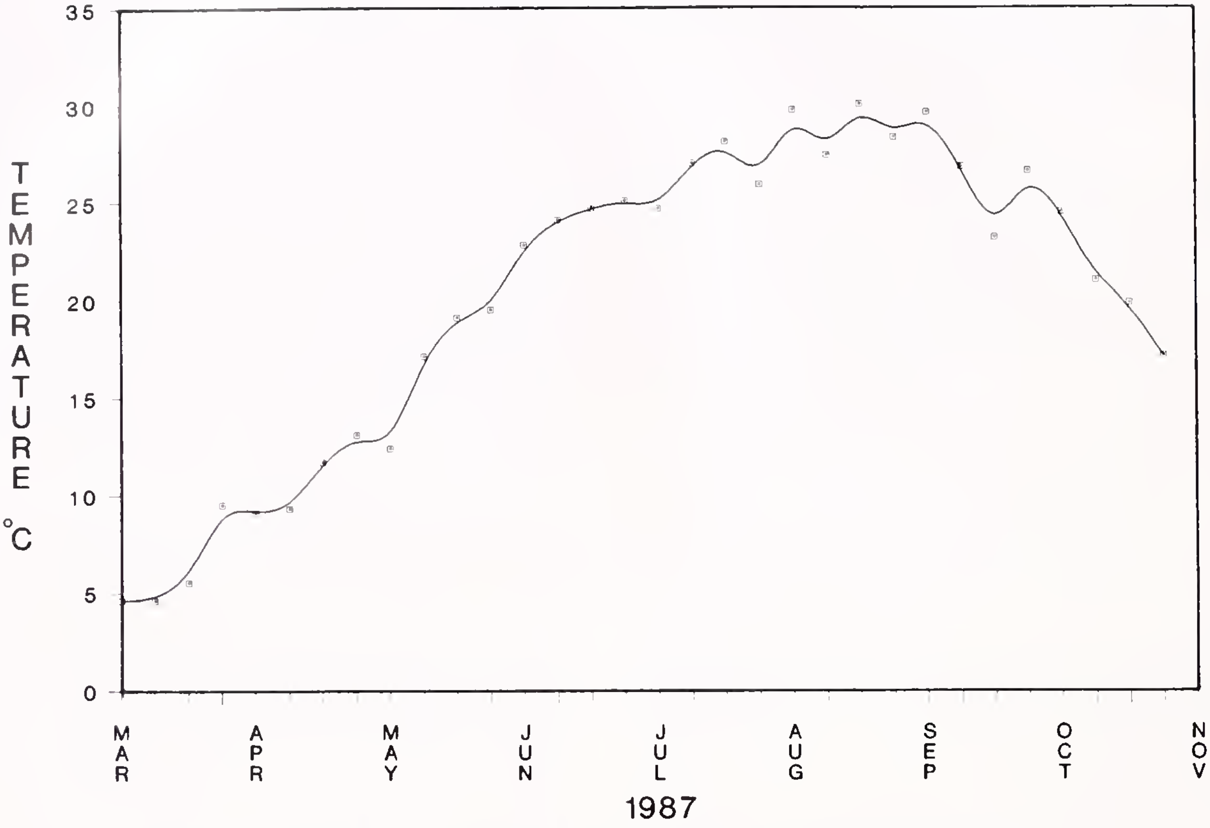

Figure 1. Weekly mean water temperature at the experimental site, lower Delaware Bay, as calculated from the regression of daily air temperature at Cape May, New Jersey, on water temperature readings from 1978 to 1980 and 1985 to 1988.

native and inbred) from Long Island Sound. On the other hand, the null hypothesis was accepted in the two comparisons involving inbred and native groups having the same site of origin (LIN-LII and DBN-DBI), indicating that the timing of gonadal maturation cycles was similar for native stocks and inbred strains within each site of origin.

Discussion

There were distinct differences in the timing of gonadal development and spawning of both native stocks and inbred strains between the Long Island and Delaware Bay sites of origin. Oysters in the Long Island groups initiated gonadal growth, achieved maximal gonadal development, and began spawning about one month earlier than oysters in the Delaware Bay groups. Additionally, both Delaware Bay groups exhibited a protracted period (about three months) of partial spawning and redevelopment. The statistical comparison of gonadal area indices reinforced the observations reported in this study and those of Ford *et al.* (1990). Time (elapsed days) had the same effect on gonadal area index for the LIN and LII groups and for the DBN and DBI groups, but not for any between-location comparison. Thus, the timing of gonadal development differed significantly between the Long Island and Delaware Bay locations. These differences were maintained in the Long Island inbred strain, even after six generations (23 years) in Delaware Bay, demonstrating that there are genetically determined differences in environmental criteria necessary for the initiation or completion of a particular gametogenic event at these two locations.

Several potential environmental regulators of bivalve reproduction have been identified, with the foremost of these being temperature (Sastry, 1979; Barber and Blake, 1991). Scallops (*Argopecten irradians*) from Woods Hole, Massachusetts, and Beaufort, North Carolina, acclimated to similar laboratory conditions prior to the initiation of gonadal development, exhibited maximal gonadal growth at 15 and 23°C, respectively, indicating a non-adaptive (genetic) difference in temperature requirements for gonadal development between these two populations (Sastry, 1966). One of the original criteria upon which the determination of physiological races of oysters was based was the temperature at which spawning began. According to

Table I

Prevalence (P, %) and intensity (I, expressed as % systemic infections) of Haplosporidium nelsoni *in experimental groups of oysters,* Crassostrea virginica, *on the various sampling dates*

Date (1987)	LIN %P/%I	LII %P/%I	DBN %P/%I	DBI %P/%I
17 March	—	20/0	50/20	0/0
29 April	0/0	10/10	20/0	0/0
7 May	0/0	0/0	—	—
13 May	0/0	0/0	0/0	0/0
21 May	0/0	0/0	0/0	0/0
27 May	0/0	20/10	0/0	0/0
3 June	0/0	20/10	20/10	10/10
12 June	0/0	40/20	40/10	0/0
18 June	0/0	20/20	20/20	30/10
24 June	40/10	10/0	40/20	10/0
2 July	—	—	20/0	0/0
15 July	90/0	60/10	50/0	0/0
29 July	100/60	10/0	60/20	30/0
12 August	—	—	70/20	10/0
26 August	90/70	0/0	40/0	20/0
19 September	—	—	40/30	10/0
5 October	0/0	10/0	60/20	40/30

LIN = Long Island Native.
LII = Long Island Inbred.
DBN = Delaware Bay Native.
DBI = Delaware Bay Inbred.

Stauber (1950), the Long Island Sound population was distinct because it began spawning when temperature reached 16.4°C, while other populations spawned at higher temperatures. In this study, both Long Island groups began spawning when water temperature was between 15 and 20°C, while spawning in the Delaware Bay groups began when water temperature was about 25–28°C (Fig. 1). Thus there is little difference in the temperature at which Long Island oysters spawn in their native setting or in Delaware Bay, even after six generations of inbreeding in Delaware Bay.

Gonadal development is an energy demanding process, with necessary nutrients coming either from stored reserves, recently ingested food, or both (Sastry, 1979; Barber and Blake, 1991). Site-specific variation in gonadal development of *Mytilus edulis, A. irradians,* and *Placopecten magellanicus* has been reported to be due to adaption (non-genetic) to local variations in environmental factors, most notably food availability (Newell *et al.*, 1982; Bricelj *et al.*, 1987; MacDonald and Thompson, 1988). The fact that at the same site in Delaware Bay, both inbred and native Long Island oysters have distinctly different gonadal cycles than Delaware Bay oysters, effectively eliminates food abundance as the sole regulator of gonadal development in *C. virginica.* Perhaps gonadal development in oysters is initiated in the presence of adequate food supplies, at a genetically determined temperature.

The results of this study and previous studies establish the existence of populations of *C. virginica* along the east coast of the United States that are genetically distinct based on differences in the timing of cycles of gonadal development and spawning. These intraspecific differences occur between populations located north and south of Long Island, New York. Loosanoff and Nomejko (1951) found that oysters from Massachusetts and Long Island Sound spawned successfully in Milford, Connecticut, while oysters from New Jersey and Virginia did not spawn or only partially spawned. Similarly, Loosanoff (1969) saw a difference in the temperature at which gonadal development was initiated between oysters from north of Long Island and south of Long Island. Oysters transplanted from Chesapeake Bay (Maryland) to Florida conformed to local spawning conditions after one year (Butler, 1955), indicating that observed differences in spawning temperatures between these locations were non-genetic.

Genetic discontinuities along the distributional range of *C. virginica* have been reported at Brownsville, Texas, based on electrophoretic variation in proteins encoded by nuclear genes (Buroker, 1983) and along the mid-Atlantic coast of Florida based on restriction site variation in mitochondrial DNA (Reeb and Avise, 1990). It is noteworthy that populations of oysters exist that have genetically distinct gonadal maturation cycles and yet are indistinguishable based on both allozyme frequencies and mtDNA restriction site variation. The fact that discrepancies exist between allozyme frequencies, mtDNA patterns, and physiological processes such as reproduction, point out that there is no simple means of delineating genetic boundaries among oyster populations (see review by Gaffney, 1991).

The existence of stocks of oysters having genetically distinct reproductive cycles has implications for the oyster fishery. Oysters transplanted from a northern location (north of Long Island) to a southern location (south of Long Island), requiring lower temperatures to initiate gonadal development, would spawn earlier than the local population. In the case of Long Island oysters in Delaware Bay, there is a potential one month overlap in spawning periods during which inter-breeding could occur. For the most part, however, the spawning periods would remain distinct. Oysters transplanted from southern to northern locations might not experience temperatures high enough to initiate gonadal development or spawning. In this case, oysters with unspawned or partially spawned and resorbing gametes would have little reproductive value and would be of poorer quality and lower commercial value. Hatchery production of oysters would be enhanced by the ability to obtain naturally conditioned broodstock over a wider time interval than what is available with local stocks alone.

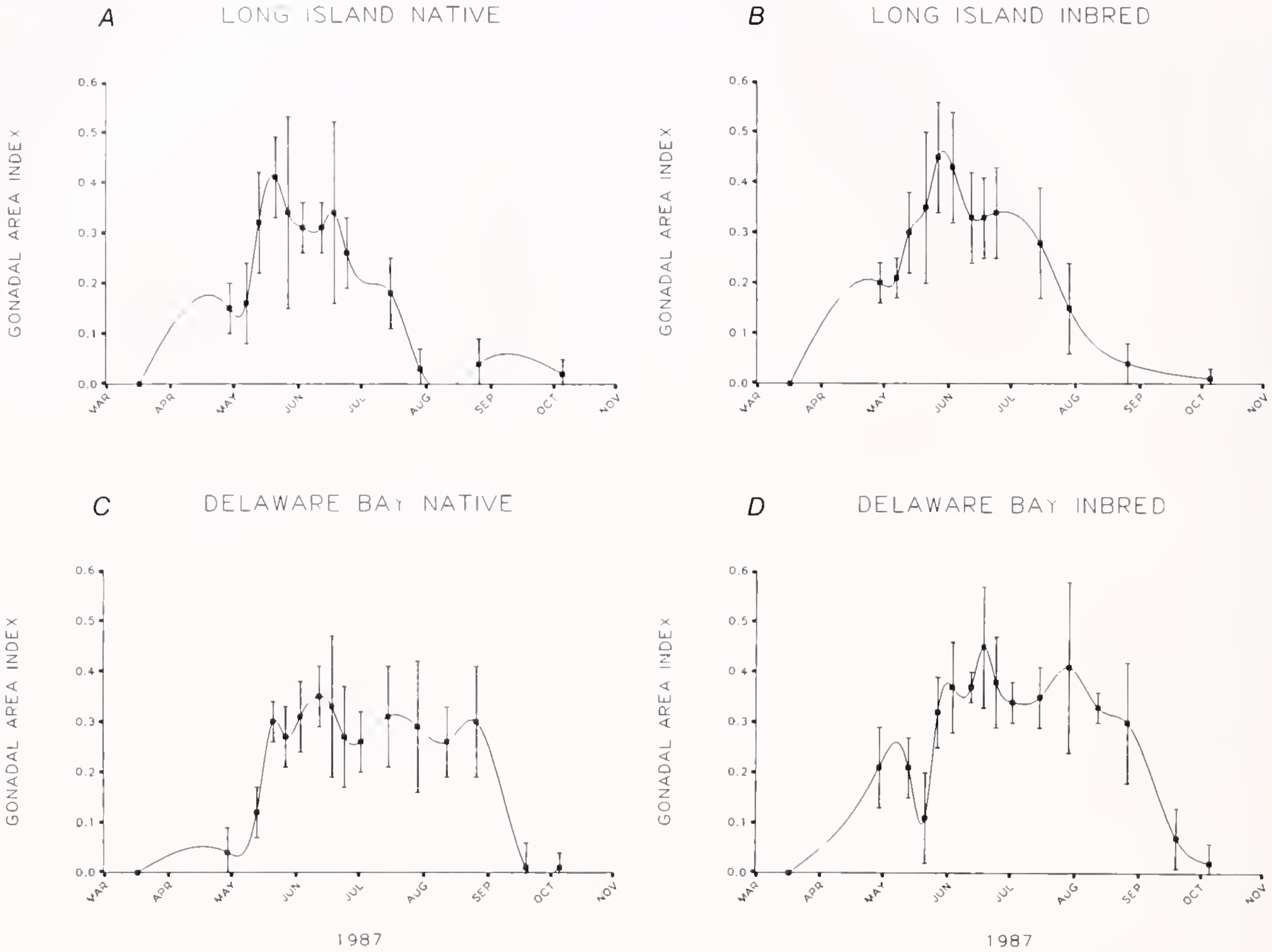

Figure 2. Mean gonadal area index (±1 SD) for four groups of *Crassostrea virginica*: A = Long Island Native (LIN); B = Long Island Inbred (LII); C = Delaware Bay Native (DBN); D = Delaware Bay Inbred (DBI). Fitted lines are spline interpolations.

Table II

Statistical comparison (t-test) of coefficients α *and* β *from the quadratic model for each possible combination of oyster,* Crassostrea virginica, *groups* H_0: $\alpha_i = \alpha_j$ *and* $\beta_i = \beta_j$, *where i and j are different groups of oysters*

Groups i j	t $(\alpha_i = \alpha_j)$	t $(\beta_i = \beta_j)$	P*
LIN—DBN	6.17	7.72	$P \leq 0.002$
LIN—LII	1.39	0.44	
LIN—DBI	4.01	6.33	$P \leq 0.02$
DBN—LII	5.50	6.66	$P \leq 0.005$
DBN—DBI	2.62	1.59	
LII—DBI	2.89	4.36	$P \leq 0.05$

* If comparisons of both α and β are rejected.
LIN = Long Island Native.
LII = Long Island Inbred.
DBN = Delaware Bay Native.
DBI = Delaware Bay Inbred.

Acknowledgments

We thank J. Kirkley for generous assistance with the statistical analysis and D. O'Connor and R. Barber for histological preparation and disease analysis. Comments by R. Mann, J. Graves, and P. Gaffney improved the manuscript. This work is the result of research sponsored by NOAA, Office of Sea Grant, Department of Commerce, under grant No. NA89AA-D-SG057 (Project No. R/F-23). The U.S. Government is authorized to produce and distribute reprints for governmental purpose notwithstanding any copyright notation that may appear hereon. This is New Jersey Sea Grant Publication No. NJSG-90-238 and New Jersey Agricultural Experiment Station Publication No. D 32405-3-90, supported by state funds. This is contribution No. 1673 from the Virginia Institute of Marine Science, College of William and Mary, and No. 91-22 from the Institute of Marine and Coastal Sciences, Rutgers University.

Literature Cited

Barber, B. J., S. E. Ford, and H. H. Haskin. 1988. Effects of the parasite MSX (*Haplosporidium nelsoni*) on oyster (*Crassostrea virginica*) energy metabolism. I. Condition index and relative fecundity. *J. Shellfish Res.* **7:** 25–31.

Barber, B. J., and N. J. Blake. 1991. Reproductive physiology. Pp. 377–428 in *Scallops: Biology, Ecology and Aquaculture*, S. Shumway, ed. Elsevier Science Publishers B. V., Amsterdam.

Bricelj, V. M., J. Epp, and R. E. Malouf. 1987. Intraspecific variation in reproductive and somatic growth cycles of bay scallops *Argopecten irradians*. *Mar. Ecol. Prog. Ser.* **36:** 123–137.

Buroker, N. E. 1983. Population genetics of the American oyster *Crassostrea virginica* along the Atlantic coast and the Gulf of Mexico. *Mar. Biol.* **75:** 99–112.

Butler, P. A. 1955. Reproductive cycle in native and transplanted oysters. *Proc. Natl. Shellfish Assoc.* **46:** 75.

Ford, S. E. 1985. Chronic infections of *Haplosporidium nelsoni* (MSX) in the oyster *Crassostrea virginica*. *J. Invertebr. Pathol.* **45:** 94–107.

Ford, S. E., and A. J. Figueras. 1988. Effects of sublethal infection by the parasite *Haplosporidium nelsoni* (MSX) on gametogenesis, spawning, and sex ratios of oysters in Delaware Bay, USA. *Diseases Aquat. Org.* **4:** 121–133.

Ford, S. E., and H. H. Haskin. 1987. Infection and mortality patterns in strains of oysters *Crassostrea virginica* selected for resistance to the parasite *Haplosporidium nelsoni* (MSX). *J. Parasitol.* **73:** 368–376.

Ford, S. E., and H. H. Haskin. 1988a. Management strategies for MSX (*Haplosporidium nelsoni*) disease in Eastern oysters. *Am. Fish. Soc. Spec. Publ.* **18:** 249–256.

Ford, S. E., and H. H. Haskin. 1988b. Comparison of *in vitro* salinity tolerance of the oyster parasite *Haplosporidium nelsoni* (MSX) and hemocytes from the host, *Crassostrea virginica*. *Comp. Biochem. Physiol.* **90A:** 183–187.

Ford, S. E., A. J. Figueras, and H. H. Haskin. 1990. Influence of selective breeding, geographic origin, and disease on gametogenesis and sex ratios of oysters, *Crassostrea virginica*, exposed to the parasite *Haplosporidium nelsoni* (MSX). *Aquaculture* **87:** 285–301.

Gaffney, P. M. 1991. Biochemical and population genetics. In *Biology, Culture and Management of the American Oyster*, V. L. Kennedy, A. F. Eble, and A. Rosenfield, eds. Maryland Sea Grant, College Park. In Press.

Goldberger, A. S. 1964. *Econometric Theory.* John Wiley and Sons, Inc., New York.

Haskin, H. H., and S. E. Ford. 1979. Development of resistance to *Minchinia nelsoni* (MSX) mortality in laboratory-reared and native oyster stocks in Delaware Bay. *Mar. Fish. Rev.* **41:** 54–63.

Loosanoff, V. L. 1969. Maturation of gonads of oysters, *Crassostrea virginica*, of different geographical areas subjected to relatively low temperatures. *Veliger* **11:** 153–163.

Loosanoff, V. L., and J. B. Engle. 1942. Accumulation and discharge of spawn by oysters living at different depths. *Biol. Bull.* **82:** 413–422.

Loosanoff, V. L., and C. A. Nomejko. 1951. Existence of physiologically-different races of oysters, *Crassostrea virginica*. *Biol. Bull.* **101:** 151–156.

MacDonald, B. A., and R. J. Thompson. 1988. Intraspecific variation in growth and reproduction in latitudinally differentiated populations of the giant scallop *Placopecten magellanicus* (Gmelin). *Biol. Bull.* **175:** 361–371.

Mori, K. 1979. Effects of artificial eutrophication on the metabolism of the Japanese oyster *Crassostrea gigas*. *Mar. Biol.* **53:** 361–369.

Newell, R. I. E., T. J. Hilbish, R. K. Koehn, and C. J. Newell. 1982. Temporal variation in the reproductive cycle of *Mytilus edulis* L. (Bivalvia, Mytilidae) from localities on the east coast of the United States. *Biol. Bull.* **162:** 299–310.

Reeb, C. A., and J. C. Avise. 1990. A genetic discontinuity in a continuously distributed species: mitochondrial DNA in the American oyster, *Crassostrea virginica*. *Genetics* **124:** 397–406.

Sastry, A. N. 1966. Variation in reproduction of latitudinally separated populations of two marine invertebrates. *Am. Zool.* **6:** 149.

Sastry, A. N. 1979. Pelecypoda (excluding Ostreidae). Pp. 113–292 in *Reproduction of Marine Invertebrates*, Vol. V, A. C. Giese and J. S. Pearse, eds. Academic Press, New York.

Stauber, L. A. 1950. The problem of physiological species with special reference to oysters and oyster drills. *Ecology* **31:** 109–118.

White, H. 1980. A heteroskedasticity-consistent covariance-matrix estimator and a direct test for heteroskedasticity. *Econometrica* **48:** 817–838.

Wonnacott, R. J., and T. H. Wonnacott. 1970. *Econometrics.* John Wiley and Sons, Inc., New York.

Reference: *Biol Bull* **181**: 222–231. (October, 1991)

Ploidy and Pronuclear Interaction in Northeastern Pacific *Lasaea* Clones (Mollusca: Bivalvia)

DIARMAID Ó FOIGHIL[1] AND CATHERINE THIRIOT-QUIÉVREUX[2]

[1]*Department of Biological Sciences, Simon Fraser University, Burnaby, British Columbia, Canada V5A 1S6 and* [2]*Université P. et M. Curie, Observatoire Océanologique, B. P. 28, 06230 Villefranche-sur-mer, France*

Abstract. A natural population of the bivalve genus *Lasaea* from Victoria, British Columbia, Canada was karyologically characterized, and pronuclear interaction was studied in newly spawned eggs. Mitotic metaphases from 95 cells were enumerated, and chromosome numbers ranged from 58 to 108, with 90 to 100 being most frequent. Ten well-spread metaphases were karyotyped, and the chromosomes were classified into 32 triplet subgroupings on the basis of shared morphology and size, together with a variable number of supernumerary chromosomes. Northeastern Pacific *Lasaea* clones share broad karyological features with direct developing congeners, but detailed comparisons reveal that they have experienced different evolutionary mechanisms of polyploidy. The pronuclear interaction study generated two key pieces of evidence that establish that northeastern Pacific *Lasaea* clones do not reproduce by self-fertilization, but that parthenogenetic development is triggered by autosperm. The incorporated sperm nucleus disintegrates in the egg cortex and does not fuse with the egg "pronucleus," *i.e.*, syngamy does not occur. Both polar bodies have a diploid chromosome number, a result inconsistent with meiosis, implying that they are products of mitotic divisions. Non-hybridizing lineages of northeastern Pacific *Lasaea* therefore represent true asexual clones, not inbred lines. *Lasaea* is the first bivalve genus in which asexual reproduction has been confirmed and is also the first molluscan genus in which pseudogamy (gynogenesis) has been detected.

Introduction

Lasaea is a near-cosmopolitan genus of minute, hermaphroditic, brooding clams that inhabit crevices in rocky intertidal shores (Keen, 1938; Ponder, 1971; Beauchamp, 1986). We are interested in these organisms because they allow valuable insights into the genetic and evolutionary consequences of alternate life history trait combinations in marine benthic invertebrates. A major reproductive and developmental dichotomy exists within *Lasaea*. One species, *L. australis* (Lamarck, 1818), reproduces by cross-fertilization, releases its progeny as planktotrophic larvae (Ó Foighil, 1988; Tyler-Walters and Crisp, 1989) and is restricted in its distribution to the western Pacific (Ó Foighil, 1989). In contrast, the congeners of *L. australis* all release their young as crawl-away juveniles and form a complex grouping of poorly defined systematic status (Ó Foighil, 1989).

Although lacking pelagic larvae, this group of organisms have attained—possibly by rafting—a remarkably extensive collective geographic range, which includes all continents apart from Antartica and a large number of oceanic islands (Ó Foighil, 1989). Population genetic studies of *Lasaea* with this developmental mode have revealed that natural populations are composed of non-hybridizing, frequently sympatric, genetic strains (Crisp *et al.*, 1983; Crisp and Standen, 1988; Ó Foighil and Eernisse, 1988; Tyler-Walters and Crisp, 1989; Tyler-Walters and Davenport, 1990). There is currently no evidence for cross-fertilization in this grouping. Individuals can reproduce in isolation for at least two generations (Crisp *et al.*, 1983), and progeny from pair mating experiments (Ó Foighil and Eernisse, 1988) and from field brooding specimens (Ó Foighil and Eernisse, 1988; Tyler-Walters and Davenport, 1990) preserve maternal protein phenotypes. *Lasaea* strains studied to date in Europe and Kerguelen Island are highly, and variably, polyploid; indeed, they produce a record number of chromosomes for the Class Bivalvia (Thiriot-Quiévreux *et al.*, 1988, 1989). It is not

Received 5 March 1991; accepted 8 July 1991.

clear, however, if polyploidy is linked to this developmental mode, and the evolutionary mechanism of polyploidy in these organisms is obscure.

The general biology of *Lasaea* is known in considerable detail, but one important question still remains to be resolved: what is the reproductive mode of *Lasaea* strains that lack pelagic larvae? This has proven to be surprisingly difficult to answer, and there are lines of evidence for both self-fertile (Ó Foighil, 1987) and asexual reproductive modes (Crisp and Standen, 1988; Thiriot-Quiévreux *et al.*, 1988, 1989; Tyler-Walters and Crisp, 1989). All studied populations of *Lasaea* that lack pelagic larvae are now known to be simultaneous hermaphrodites with a minute male allocation (Ó Foighil and Eernisse, 1988). Preliminary data on sperm-egg interaction are consistent with self-fertilization: both gamete types are spawned simultaneously into the brood chamber: sperm bind to eggs via an acrosomal reaction, penetrate the egg, and two polar bodies are extruded prior to first cleavage (Ó Foighil, 1987). A variety of other data, however, suggests an asexual reproductive mode in which the sperm merely trigger parthenogenetic development (pseudogamy). Individual *Lasaea* frequently express putative heterozygote electromorphs at multiple loci (Crisp and Standen, 1988; Ó Foighil and Eernisse, 1988; Tyler-Walters and Crisp, 1989). These electromorphs, if real, are inconsistent with a self-fertile reproductive mode. Karyological analyses of *Lasaea* strains have failed to find meiotic metaphases, and the presence of odd ploidy numbers and of supernumary chromosomes may render accurate meiosis impossible (Thiriot-Quiévreux *et al.*, 1988, 1989).

The aims of this study were twofold. First, we karyologically characterized northeastern Pacific populations, an approach to understanding how the exceptionally high chromosome assemblages in *Lasaea* strains evolved. Second, we studied pronuclear interaction in newly spawned eggs to distinguish between the two competing hypotheses about the reproductive mode in *Lasaea* strains.

Materials and Methods

Karyology

Specimens of *Lasaea* were sampled at McNeill Bay, Victoria, British Columbia, Canada in October 1989 and air-mailed live to Villefranche-sur-mer for karyotyping. The McNeill Bay population is composed of at least five non-hybridizing genetic strains that can be reliably distinguished only by electrophoretic analyses (Ó Foighil and Eernisse, 1988). Air-mailed specimens were maintained on arrival in aquaria for 10 days and fed cultured microalgae (*Isochrysis galbana*) to stimulate cell divisions.

Specimens were incubated for 12 h in seawater containing 0.005% colchicine, following which the valves of each clam were gently half-opened to allow effective hypotonic treatment (45 min in 0.9% sodium citrate). Subsequent processing involved fixation in freshly mixed absolute alcohol and acetic acid (3:1) with three changes of 20 min duration. During the second fixation step, the bodies were dissected from the valves. Slide preparations were made from 1 to 4 bodies using an air-drying technique (detailed in Thiriot-Quiévreux and Ayraud, 1982). The preparations were stained for 10 min with 4% Giemsa (pH 6.8), and photographs of well-spread metaphases were taken with a Zeiss III photomicroscope.

For karyotyping, chromosomes were cut out of the photomicrographs and were paired on the basis of size and centromere position. Measurement of chromosomes from the best karyotypes were made with a Digitizer (BIT PAD 10, Summa Graphic) interfaced with a microcomputer (ATV 286). Statistical interpretations were made using a CHROMOS program (Thiriot-Quiévreux, 1984; Thiriot-Quiévreux *et al.*, 1988). Terminology relating to centromere position follows that of Levan *et al.* (1964). When a centromere position was borderline between two categories, the mean was calculated with 95% confidence limits, and both categories were listed.

Pronuclear interaction

Additional animals were sampled from the McNeill Bay in February 1990 for the pronuclear interaction study. Gravid individuals were cultured in petri dishes containing seawater at room temperature and checked daily using a dissecting stereomicroscope for evidence of spawning activity. Newly spawned individuals were detected by the presence of eggs in the brood chamber, an event visible through the semi-transparent valves of most adults. Fifty-four early broods (uncleaved eggs—4 cell stage) were dissected from the parents and individ-

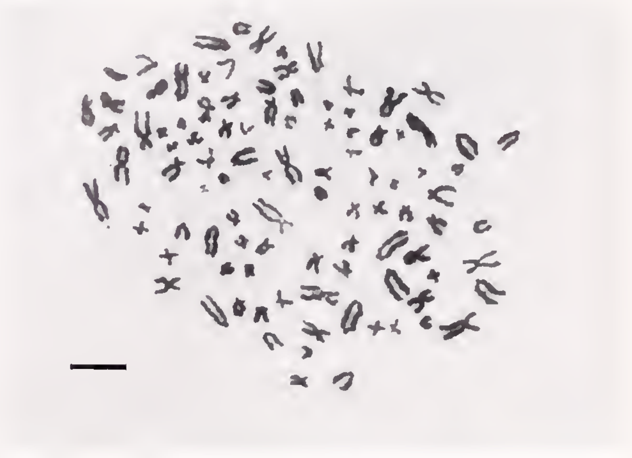

Figure 1. Mitotic metaphase with 100 chromosomes in northeastern Pacific *Lasaea*. Scale bar = 10 μm.

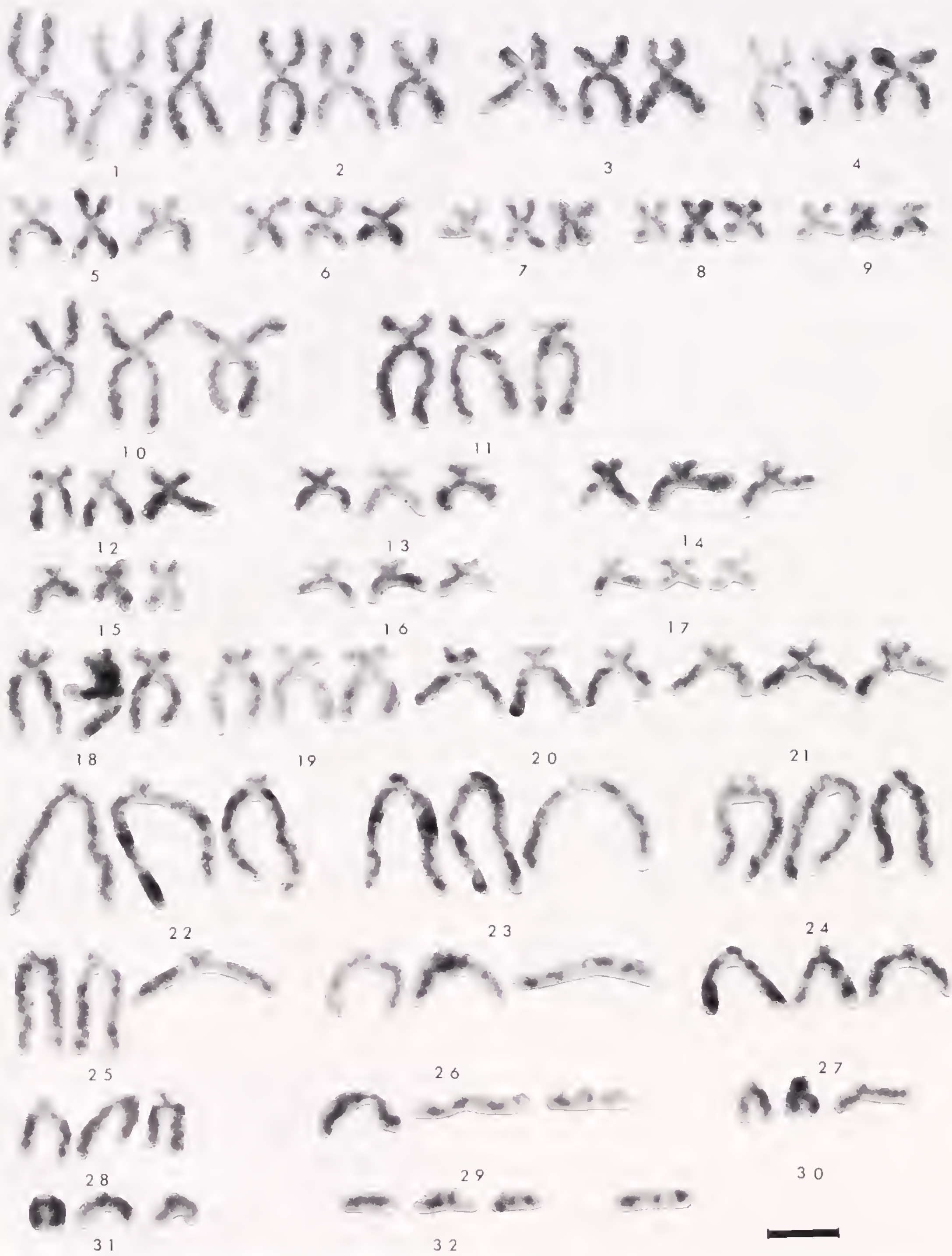
1
2
3
4
5
6
7
8
9
10
11
12
13
14
15
16
17
18
19
20
21
22
23
24
25
26
27
28
29
30
31
32

Figure 2. Karyotype taken from a northeastern Pacific *Lasaea* metaphase with 97 chromosomes. Scale bar = 5 μm.

ually fixed in three changes of freshly made Carnoy's fixitive (3:1 methanol, glacial acetic acid). Fixed broods were cleared in 45% glacial acetic acid and were gently pipetted into Vaseline-sealed wells on microscope slides. The cleared cells were viewed under phase-contrast or darkfield optics using a compound Zeiss photomicroscope and photographed with Kodak Tech Pan film. Cytological events following spawning were reconstructed

Table I

Chromosome measurements and classification in seven metaphases of northeastern Pacific Lasaea

Chromosome pair no.	Relative length		Arm ratio		Centromeric index		Classification
	Mean	SD	Mean	SD	Mean	SD	
1	5.75	0.16	0.864	0.037	46.18	1.06	m
2	4.69	0.28	0.757	0.066	42.85	2.05	m
3	3.98	0.21	0.733	0.056	42.07	1.77	m
4	3.51	0.33	0.777	0.078	43.92	2.42	m
5	2.63	0.33	0.811	0.075	44.43	2.30	m
6	2.38	0.31	0.842	0.069	45.46	1.97	m
7	2.11	0.39	0.873	0.056	46.37	1.54	m
8	1.92	0.33	0.821	0.087	44.75	2.64	m
9	1.62	0.26	0.842	0.082	45.45	2.52	m
10	5.89	0.55	0.436	0.063	29.91	3.00	m
11	4.50	0.37	0.423	0.056	29.42	2.86	sm
12	2.66	0.15	0.355	0.039	26.02	2.15	sm-st
13	2.47	0.20	0.353	0.079	25.70	4.14	sm-st
14	2.27	0.12	0.352	0.063	25.68	3.56	sm-st
15	2.16	0.22	0.366	0.067	26.41	3.43	sm-st
16	2.03	0.21	0.366	0.056	26.46	2.99	sm-st
17	1.80	0.22	0.346	0.075	25.27	4.05	sm-st
18	3.67	0.31	0.306	0.094	22.87	5.36	st-sm
19	3.28	0.22	0.328	0.038	24.32	1.98	st-sm
20	3.01	0.15	0.306	0.023	23.28	1.33	st
21	2.84	0.12	0.314	0.046	23.68	2.66	st
22	5.33	0.42	0.089	0.022	8.05	1.75	t
23	4.84	0.30	0.071	0.013	6.58	1.10	t
24	4.50	0.14	0.088	0.022	8.04	1.82	t
25	4.03	0.22	0.081	0.014	7.46	1.22	t
26	3.32	0.26	0.099	0.013	8.96	1.02	t
27	2.84	0.23	0.108	0.036	9.61	2.91	t
28	2.68	0.14	0.099	0.017	8.93	1.34	t
29	2.31	0.20	0.116	0.044	10.23	3.44	t
30	1.87	0.28	0.137	0.029	11.88	2.22	t-st
31	1.66	0.24	0.115	0.010	10.26	0.75	t
32	1.31	0.16	0.134	0.038	11.57	2.94	t-st

by examining broods that were fixed at different developmental stages.

Results

Karyology

The 85 slide preparations examined in this study contained large interphase nuclei (approximately 35 μm in diameter) and mitotic metaphase spreads. Meiotic divisions were not encountered. The mitotic metaphases were remarkable due to their large sizes and their high chromosome numbers (Fig. 1). Ninety-five metaphase spreads were photographed, and chromosome counts were scored, although the latter process was frequently complicated by the presence of overlapping chromosomes. Chromosome numbers ranged from 58 to 108; the majority of metaphases (76 out of 95) contained more than 80 chromosomes, and 32 spreads had 90–100 chromosomes.

Ten well-spread metaphases were karyotyped. Figure 2 shows the karyotype taken from one metaphase spread containing 97 chromosomes. The chromosomes have been arranged into 32 triplet subgroupings on the basis of shared morphology and size. Triplets can be further classified into groups of similar morphology: metacentrics, submetacentrics, subtelocentrics, and telocentrics. The identification of homologous chromosomes is relatively unambiguous for the largest chromosomes. But the smallest chromosomes have less distinctive morphologies, so ambiguities remain. One minichromosome within this metaphase (Fig. 2) could not be classified. The chromosomes of other karyotyped metaphases could similarly be arranged into triplets. Variation in chromosome number between metaphases resulted from the absence of single chromosomes from individual triplet subgroupings or from the occurrence of supernumerary chromosomes among the smaller members of each morphological group.

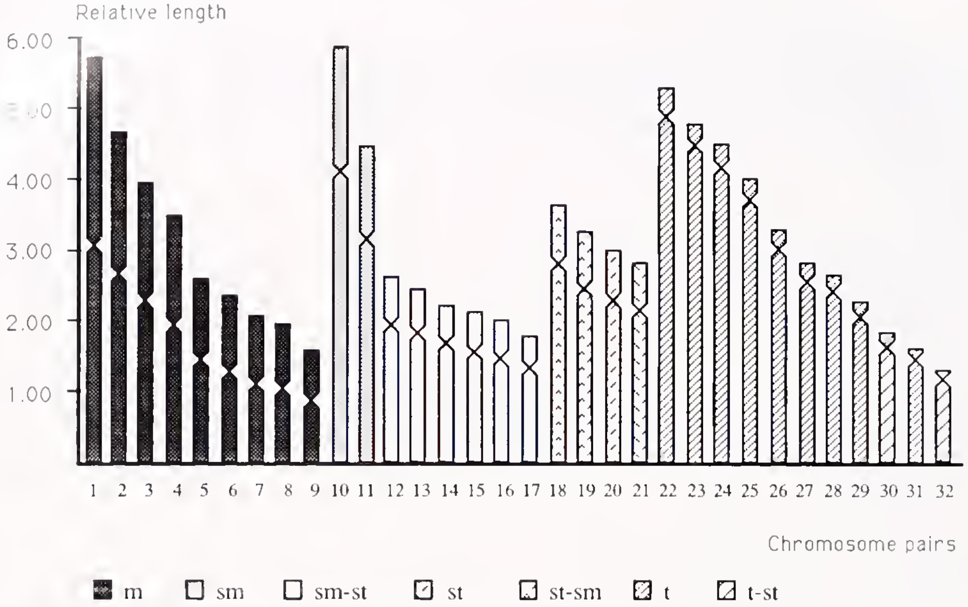

Figure 3. Ideogram of northeastern Pacific *Lasaea* chromosomes constructed from relative length and centromeric index values. Lengths are in μm. m, metacentric; sm, submetacentric; sm-st, submetacentric-subtelocentric; st, subtelocentric; st-sm, subtelocentric-submetacentric; t, telocentric; t-st, telocentric-subtelocentric.

Chromosomes were measured from seven well-spread metaphases (3 with 95 chromosomes, 3 with 97, and 1 with 100). Table I gives the mean and standard deviations of the relative lengths, arm ratios, and centromere indices of 32 chromosome triplets and their classification. An ideogram (Fig. 3) was constructed from the relative length and centromere index values so that the different morphological types of chromosomes could be better visualized.

The karyotype of northeastern Pacific *Lasaea* consists of 8 metacentrics, 8 submetacentrics (including 6 submetacentric-subtelocentrics), 4 subtelocentrics (including 2 subtelocentric-submetacentrics), and 11 telocentrics (including 2 telocentric-subtelocentrics). Within each morphological grouping of chromosomes, some triplets were difficult to distinguish because of their similar lengths: *e.g.*, metacentrics no. 7–8, submetacentric-subtelocentrics no. 12–13 and 15–16, subtelocentrics no. 20–21, and telocentrics no. 27–28 and 30–31. In these cases, the loss of individual chromosomes or the occurrence of supernumary chromosomes could not be assigned with accuracy.

Pronuclear interaction

A single sperm penetrates the cell membrane of each egg shortly after spawning. The egg germinal vesicle breaks down, and the egg chromosomes condense and become aligned for first metaphase (Fig. 4a). The incorporated sperm nucleus remains in the egg cortex in a condensed

Figure 4a. Phase contrast light micrograph (PCLM) of an uncleaved northeastern Pacific *Lasaea* egg showing the incorporated, condensed sperm nucleus (arrow) in the cortex and the egg chromosomes arranged for first metaphase (on left). Scale bar = 20 μm.

Figure 4b. PCLM showing detail of sperm nucleus from Figure 4a. Scale bar = 6 μm.

Figure 5. PCLM of decondensing sperm nucleus (N) located in the cortex of an northeastern Pacific *Lasaea* egg. Scale bar = 10 μm.

Figure 6. Darkfield light micrograph (DFLM) of an uncleaved northeastern Pacific *Lasaea* egg with a decondensing sperm nucleus situated in its cortex (large arrow). This egg has extruded two polar bodies and the egg chromosomes are arranged for first cleavage metaphase (small arrow). Scale bar = 50 μm.

Figure 7. DFLM of a northeastern Pacific *Lasaea* first cleavage telophase. Note presence of aggregated sperm chromatin (n) in one of the daughter cells and of daughter chromosomes (large arrows) in both daughter cells. The cleavage furrow (c) is also apparent, as are the first (lower small arrow) and second (upper small arrow) polar bodies. Scale bar = 40 μm.

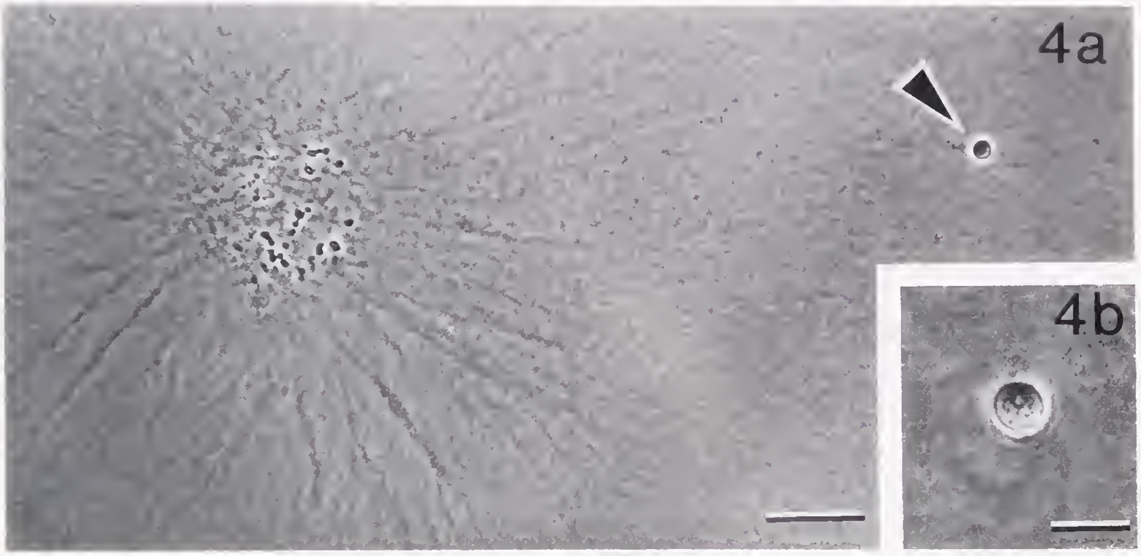
4a
4b

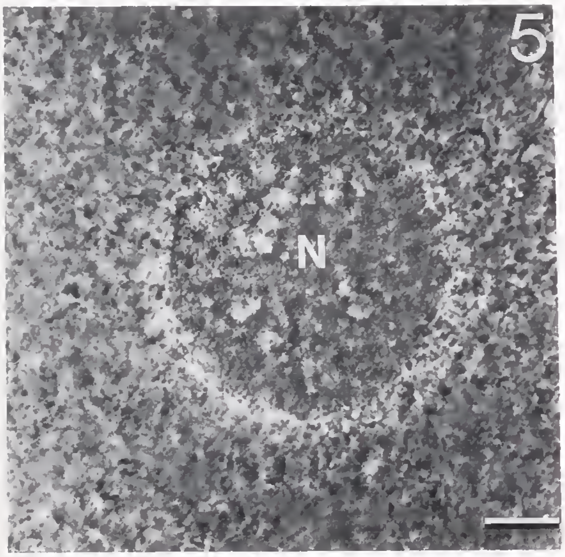
5
N

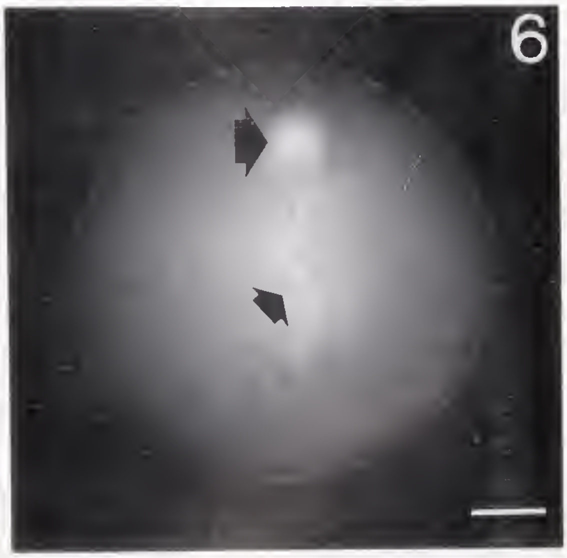
6

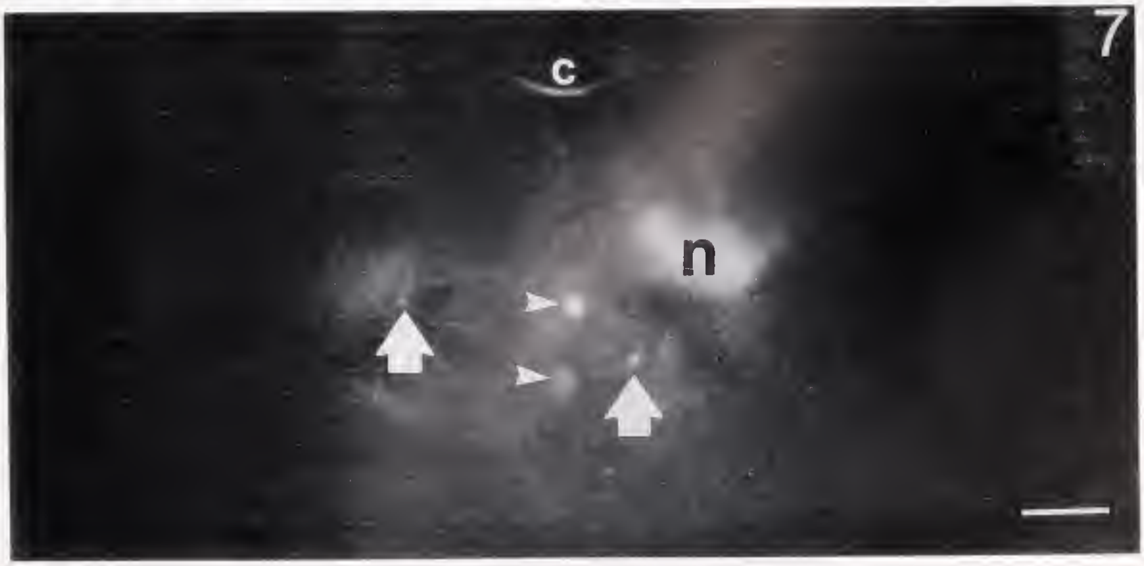
7
c
n

state (Figs. 4a, b), until after the production of the two polar bodies. The sperm nucleus then slowly decondenses and can be distinctly visualized in the egg cortex with phase contrast (Fig. 5) and, especially, darkfield optics (Fig. 6). However, the sperm nucleus does not recondense to form chromosomes or to associate with the egg chromosomes. During first cleavage, the sperm chromatin remains aggregated and typically ends up in the cortex of one of the two daughter cells (Fig. 7).

Prior to first cleavage, the egg extrudes two polar bodies, each involving the formation of a spindle at the animal pole and the division of chromosomes. The first division (Fig. 8) results in the formation of a polar body containing an average of 48 (±5.2 S.E.; n = 17) well defined chromosomes (Fig. 9). After formation of an additional spindle, a second polar body is extruded adjacent to the first (Fig. 10). Unlike those of the first polar body, the chromosomes of the second are tightly aggregated and are very difficult to distinguish microscopically (Fig. 10). In a preliminary study, Ó Foighil (1987) assumed that the second polar body of northeastern Pacific *Lasaea* strains is haploid. During the present work, however, the second polar body chromatin was sufficiently dispersed in a few cases, and we could determine that each chromosome is composed of two homologous interphase chromatids (Fig. 11), *i.e.*, is diploid. In 2 eggs out of the 123 examined, the number of chromosomes in the second polar body could be established accurately and were in each case (49, 45) equal to that of the adjoining first polar body. The egg chromosomes that remain within the egg (female "pronucleus") migrate to the center of the cell and become arranged in homologous pairs for first cleavage (Fig. 12), without associating with the sperm nucleus. A mean of 95.9 (±12 S.E.; n = 9) chromosomes were arranged at the first cleavage metaphase. This is consistent with the results obtained in metaphase spreads of adult tissue. During first cleavage, the homologous chromosome pairs separate (Fig. 13) and migrate into the forming daughter cells.

Discussion

Northeastern Pacific *Lasaea* strains have high chromosome numbers, ploidy grouping of the chromosomes by three, and variable numbers of supernumerary chromosomes. Congeners that lack pelagic larvae have also been characterized karyologically from European (Thiriot-Quiévreux *et al.*, 1989) and from Kerguelen Island populations (Thiriot-Quiévreux *et al.*, 1988). These congeners share with northeastern Pacific strains the karyological features of high chromosome numbers and the presence of supernumerary chromosomes, but show varying degrees of polyploidy. In Kerguelen strains, a chromosome number of 100–120 was found, but ploidy levels could not be determined (Thiriot-Quiévreux *et al.*, 1988). Chromosome numbers in European strains range greatly (63–340) and can be grouped into different ploidy levels of 3, 5, and 6, in addition to variable supernumeraries (Thiriot-Quiévreux *et al.*, 1989).

A meaningful comparison of karyotypes among these different *Lasaea* populations is complicated because we cannot precisely distinguish homologous chromosome sets from the large and variable number of supernumaries. However, we can compare the first 17 chromosome pairs identified in the karyotype of Kerguelen strains (Thiriot-Quiévreux *et al.*, 1988) with the first 17 sets of homologous chromosomes ordered in decreasing size in the karyotypes of European (Thiriot-Quiévreux *et al.*, 1989) and of northeastern Pacific strains (this study). The karyotypes of the three populations differ in their relative numbers of metacentric, submetacentric, subtelocentric, and telocentric chromosome sets (8m, 3sm, 2st and 4t in Kerguelen strains; 6m, 1sm, 6st and 4t in European strains; 4m, 2sm, 4st and 7t in northeastern Pacific strains). These karyological distinctions not only imply that the three geographically isolated populations are reproductively incompatible, but also that they have experienced different evolutionary mechanisms of polyploidy.

Polyploidy in mollusks has been reported in several hermaphroditic pulmonate snails that are capable of self-fertilization or asexual reproduction (Jacob, 1957; Burch and Huber, 1966; Patterson and Burch, 1978; Goldman *et al.*, 1984). But among the Bivalvia, this phenomenon is exceptional, and beside the polyploid *Lasaea* strains, only one species, *Corbicula leana*, with a triploid chro-

Figure 8. PCLM showing a lateral view of the first metaphase spindle in a northeastern Pacific *Lasaea* egg. Scale bar = 8 μm.

Figure 9. PCLM of the first polar body extruded by a northeastern Pacific *Lasaea* egg. Scale bar = 10 μm.

Figure 10. PCLM of both first (P) and second (arrow) northeastern Pacific *Lasaea* polar bodies. Scale bar = 20 μm.

Figure 11. PCLM showing details of northeastern Pacific *Lasaea* second polar body chromosomes. Arrows point to homologous chromatids. Scale bar = 7 μm.

Figure 12. PCLM of northeastern Pacific *Lasaea* egg chromosomes arranged at first cleavage metaphase. Arrows point to pairs of homologous chromosomes. Scale bar = 6 μm.

Figure 13. PCLM of first cleavage anaphase. Arrows indicate daughter chromosomes. Scale bar = 35 μm.

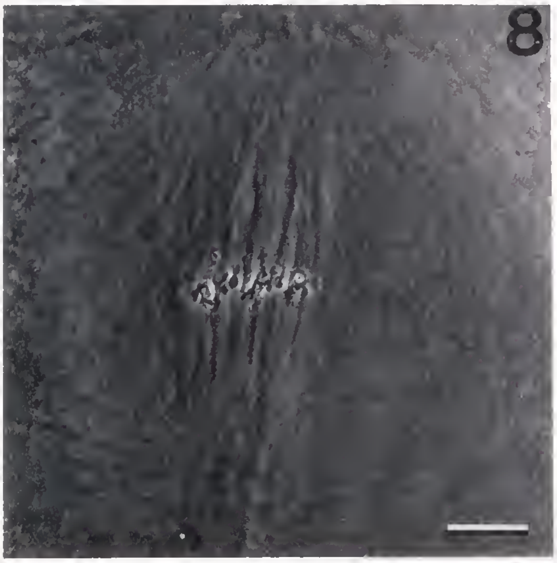
8

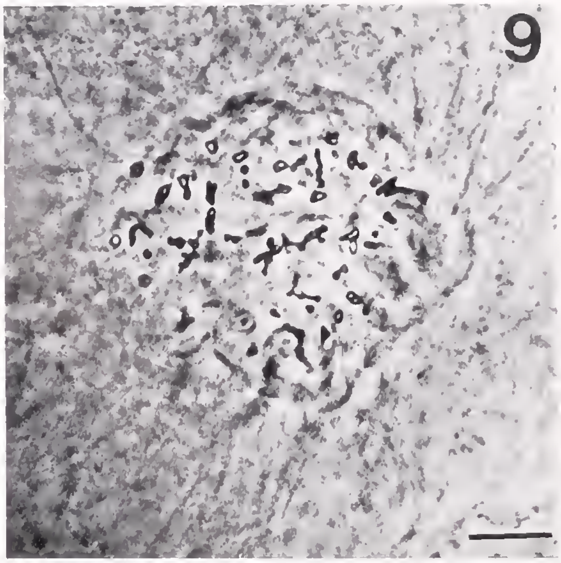
9

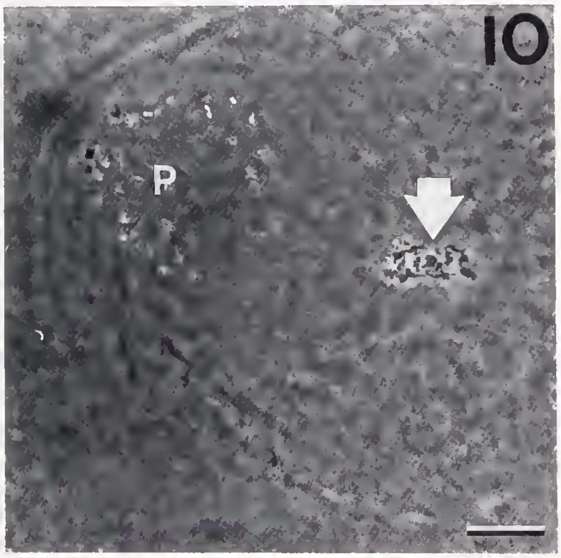
10
P

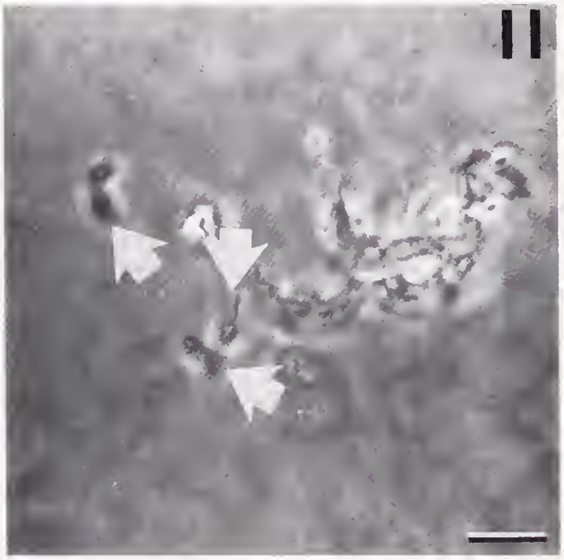
11

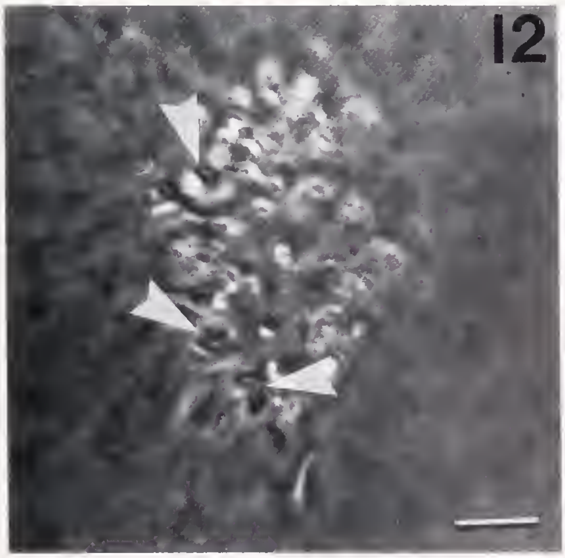
12

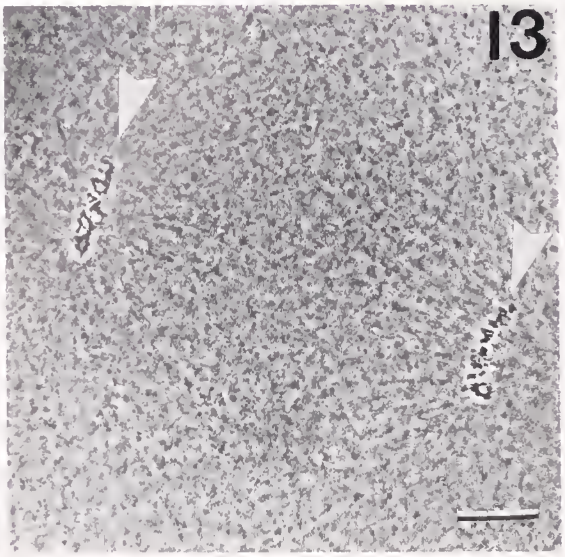
13

mosome number of 54, has been recorded (Okamoto and Arimoto, 1986).

The genus *Lasaea* contains one sexual species, *L. australis*, that undergoes a planktotrophic larval development (Ó Foighil, 1988; Tyler-Walters and Crisp, 1989). Ó Foighil (1988) proposed that this reproductive and developmental combination represented the primitive condition in the genus. Tyler-Walters and Crisp (1989) provided a preliminary estimate of chromosome number in two *L. australis* eggs (one with n = 21–22, the other with 2n = 42–44). A more detailed karyological analysis currently underway has yielded a diploid number of 2n = 36 for this species (C. Thiriot-Quiévreux, unpubl.). Work in progress on the karyotype of *L. australis* may help to clarify chromosomal evolutionary mechanisms within the genus *Lasaea*.

Karyological analyses of *Lasaea* strains in both present and previous studies (Thiriot-Quiévreux *et al.*, 1988, 1989) have failed to find meiotic metaphases and the presence of odd ploidy numbers and of supernumary chromosomes presumably renders accurate meiosis impossible. Although not all aspects of egg maturation have been revealed in this present study, two key pieces of evidence establish that northeastern Pacific *Lasaea* strains are parthenogens, not self-fertilizers. The incorporated sperm nucleus disintegrates in the egg cortex and does not fuse with the egg "pronucleus"; *i.e.*, syngamy does not occur. Both polar bodies have a diploid chromosome number, a result inconsistent with meiosis, implying that they are products of mitotic divisions. Our data confirm Crisp and Standen's (1988) proposal that parthenogenetic development is triggered by auto sperm in *Lasaea* strains lacking dispersive larvae. Non-hybridizing lineages of northeastern Pacific *Lasaea* therefore represent true asexual clones, not inbred lines. *Lasaea* is the first bivalve genus in which asexual reproduction has been confirmed and is also the first molluscan genus in which pseudogamy (gynogenesis) has been detected.

Egg maturation in northeastern Pacific *Lasaea* differs from that of the great majority of other apomictic (ameiotic) organisms in that two polar bodies are extruded rather than one (Hughes, 1989). Two polar bodies are also mitotically produced in the gastropods *Thiara* (*Melanoides*) *tuberculatus* and *T. lineatus*, which avoid a reduction in chromosome number by arresting an oogonial division (Jacob, 1957). More detailed analyses of *Lasaea* egg maturation divisions are needed to determine if these organisms restitute chromosome numbers in a similar manner prior to first cleavage.

We have no direct data on the chromosome complement of the northeastern Pacific *Lasaea* sperm cells, but meiotic metaphases have not been discovered in *Lasaea* clones despite intensive karyological study of populations from British Columbia, Kerguelen Island, and Europe (present study, Thiriot-Quiévreux *et al.*, 1988, 1989). Reliance on sperm activation leaves open the possibility of occasional leakage of sperm chromosomes and may be the origin of the supernumary chromosomes that are characteristic of asexual *Lasaea* karyotypes.

Pseudogamy (gynogenesis) occurs in a wide variety of taxa (Kiester *et al.*, 1981; Stenseth *et al.*, 1985; Hughes, 1989) and pseudogamous individuals are typically sexual parasites of closely related cross-fertilizing species. *Lasaea* clones, however, are exceptional in that each individual is reproductively independent, using its own sperm to trigger asexual development. *Lasaea* clones, therefore, have much greater evolutionary potential than most gynogenetic forms.

Gynogens typically originate from hybridization events between related species, *e.g.*, the *Ambyostoma jeffersonianum* complex (Uzzell, 1964), *Rana esculenta* (Uzzel and Berger, 1975; Turner and Nopp, 1979), and possibly the freshwater bivalve *Corbicula leana* (Okamoto and Arimoto, 1986). Hybrid, gynogenetic F1 progeny are frequently triploid, incapable of meiosis, and reproduce by sexually parasitizing males of the parental species (Hughes, 1989). Northeastern Pacific *Lasaea* clones are triploid and may have arisen from rare hybridization events between ancestral lineages. Hybrid, triploid *Lasaea* F1 progeny that produced a small amount of phenotypically normal sperm cells (Ó Foighil, 1985, 1987) may then have reproduced by autogynogenesis. This evolutionary scenario is, however, speculative and needs to be verified by independent phylogenetic reconstruction.

It is now apparent that the genus *Lasaea* includes some very unusual marine mollusks. Direct developing members are collectively much more successful than sexual congeners, which retain pelagic larval development (Ó Foighil, 1989). In the present study, we have confirmed that direct development in this genus is linked to polyploidy and to the presence of supernumary chromosomes (Thiriot-Quiévreux *et al.*, 1988, 1989). Direct development is also linked to minute male allocation (Pelseneer, 1903; Oldfield, 1964; Ó Foighil, 1985; McGrath and Ó Foighil, 1986; Ó Foighil and Eernisse, 1988) and to a clonal population genetic structure (Crisp *et al.*, 1983; Crisp and Standen, 1988; Ó Foighil and Eernisse, 1988; Tyler-Walters and Crisp, 1989). Autogynogenesis, which we have documented in northeastern Pacific *Lasaea* populations, may also be a persistent theme in other members of the genus that share this developmental mode, but see Tyler-Walters and Davenport (1990) for a potential exception. The genus *Lasaea* promises to become a valuable model system for exploring the long-term evolutionary and genetic consequences of contrasting reproductive modes in benthic marine metazoans.

Acknowledgments

Thanks are due to A. Insua and G. Quélart for assistance in karyotyping. This work was supported by an NSERC postdoctoral fellowship to D. Ó Foighil. We thank Stephen Palumbi and an anonymous reviewer for their constructive comments.

Literature Cited

Beauchamp, K. A. 1986. Reproductive ecology of the brooding, hermaphroditic clam *Lasaea subviridis*. *Mar. Biol.* **93:** 225–235.

Burch, J. B., and J. M. Huber. 1966. Polyploidy in mollusks. *Malacologia* **5:** 41–43.

Crisp, D. J., A. Burfitt, K. Rodrigues, and M. D. Budd. 1983. *Lasaea rubra:* an apomictic bivalve. *Mar. Biol. Lett.* **4:** 127–136.

Crisp, D. J., and A. Standen. 1988. *Lasaea rubra* (Montagu) (Bivalvia: Erycinacea), an apomictic crevice-living bivalve with clones separated by tidal level preference. *J. Exp. Mar. Biol. Ecol.* **117:** 27–45.

Goldman, M. A., P. T. LoVerde, C. L. Chrisman, and D. E. Franklin. 1984. Chromosomal evolution in planorbid snails of the genera *Bulinus* and *Biomphalaria*. *Malacologia* **25:** 427–446.

Hughes, R. N. 1989. *A Functional Biology of Clonal Animals*. Chapman and Hall, London. 331 pp.

Jacob, J. 1957. Cytological studies of Melaniidae (Mollusca) with special reference to parthenogenesis and polyploidy. I. Oögenesis of the parthenogenetic species of *Melanoides* (Prosobranchia—Gastropoda). *Trans. R. Soc. Edinb.* **63:** 341–355.

Keen, A. M. 1938. New pelecypod species of the genera *Lasaea* and *Crassinella*. *Proc. Malacol. Soc. Lond.* **23:** 18–32.

Kiester, A. R., T. Nagylaki, and B. Shaffer. 1981. Population dynamics of species with gynogenetic sibling species. *Theoret. Pop. Biol.* **19:** 358–369.

Levan, A., K. Fredga, and A. A. Sandberg. 1964. Nomenclature for centromere position in chromosomes. *Hereditas* **52:** 101–220.

McGrath, D., and D. Ó Foighil. 1986. Population dynamics and reproduction of hermaphroditic *Lasaea rubra*. *Ophelia* **25:** 209–219.

Ó Foighil, D. 1985. Fine structure of *Lasaea subviridis* and *Mysella tumida* sperm (Bivalvia: Galeommatacea). *Zoomorphology* **105:** 125–135.

Ó Foighil, D. 1986. Prodissoconch morphology is environmentally modified in the brooding bivalve *Lasaea subviridis*. *Mar. Biol.* **92:** 517–524.

Ó Foighil, D. 1987. Cytological evidence for self-fertilization in the brooding bivalve *Lasaea subviridis*. *Int. J. Invertebr. Reprod. Dev.* **12:** 83–90.

Ó Foighil, D. 1988. Random mating and planktotrophic larval development in the brooding hermaphroditic clam *Lasaea australis* (Lamarck, 1818). *Veliger* **31:** 214–221.

Ó Foighil, D. 1989. Planktotrophic larval development is associated with a restricted geographic range in *Lasaea*, a genus of brooding, hermaphroditic bivalves. *Mar. Biol.* **103:** 349–358.

Ó Foighil, D., and D. J. Eernisse. 1988. Geographically widespread, non-hybridizing, sympatric strains of the hermaphroditic, brooding clam *Lasaea* in the northeastern Pacific Ocean. *Biol. Bull.* **175:** 218–229.

Okamoto, A., and B. Arimoto. 1986. Chromosomes of *Corbicula japonica, C. sandai* and *C. (Corbiculina) leana* (Bivalvia: Corbiculidae). *Venus* **45:** 194–202.

Oldfield, E. 1964. The reproduction and development of some members of the Erycinidae and Montacutidae (Mollusca, Eulamellibranchiata). *Proc. Malacol. Soc. Lond.* **36:** 79–120.

Patterson, C. M., and J. B. Burch. 1978. Chromosomes of pulmonate molluscs. Pp. 171–217 in *Pulmonates: Systematics, Evolution and Ecology.* Vol. 2A, V. Fretter and J. Peake, eds. Academic Press, New York.

Pelseneer, P. 1903. Mollusques (amphineures, gastropodes et lamellibranches). *Res. Voy. S. Y. Belgica Zool.*, Buschmann, Anvers, 1–85.

Ponder, W. F. 1971. Some New Zealand and Subantarctic bivalves of the Cyamiacea and Leptonacea with descriptions of new taxa. *Rec. Dom. Mus. (Wellington)* **7:** 119–141.

Stenseth, N. C., L. R. Kirkendall, and N. Morgan. 1985. On the evolution of pseudogamy. *Evolution* **39:** 294–307.

Thiriot-Quiévreux, C. 1984. Chromosome analysis of three species of *Mytilus* (Bivalvia: Mytilidae). *Mar. Biol. Lett.* **5:** 265–273.

Thiriot-Quiévreux, C., J. Soyer, F. de Bovée, and P. Albert. 1988. Unusual chromosome complement in the brooding bivalve *Lasaea consanguinea*. *Genetica* **76:** 143–151.

Thiriot-Quiévreux, C., A. M. Insua Pombo, and P. Albert. 1989. Polyploïdie chez un bivalve incubant *Lasaea rubra* (Montagu). *C. R. Acad. Sci. Paris.* **308:** 115–120.

Thiriot-Quiévreux, C., and N. Ayraud. 1982. Les caryotypes de quelques espéces de Bivalves et de Gastéropodes marins. *Mar. Biol.* **70:** 165–172.

Tyler-Walters, H., and D. J. Crisp. 1989. The modes of reproduction in *Lasaea rubra* (Montagu) and *L. australis* (Lamarck): (Erycinidae; Bivalvia). Pp. 299–308 in *Proceedings of the 23rd European Marine Biological Symposium, Swansea*, J. S. Ryland and P. A. Tyler, eds. Olsen and Olsen, Denmark.

Tyler-Walters, H., and J. Davenport. 1990. The relationship between the distribution of genetically distinct inbred lines and upper lethal temperature in *Lasaea rubra*. *J. Mar. Biol. Assoc. U. K.* **70:** 557–570.

Turner, H. G., and H. Nopp. 1979. Heterosis in the common European water frog. *Naturwissenschaften* **66:** 268–269.

Uzzell, T. M. 1964. Relations of the diploid and triploid species of the *Ambyostoma jeffersonium* complex (Amphibia, Caudata). *Copeia* **2:** 257–300.

Uzzell, T. M., and L. Berger. 1975. Electrophoretic phenotypes of *Rana ridibunda, Rana lessonae* and their hybridogenetic associate *Rana esculenta*. *Proc. Nat. Acad. Sci.* **127:** 13–24.

Reference: *Biol. Bull.* **181**: 232–237. (October, 1991)

Variation in Fertilization Rate in the Tropical Reef Fish, *Halichoeres bivattatus*: Correlates and Implications

CHRISTOPHER W. PETERSEN

Smithsonian Tropical Research Institute, Box 2072, Balboa, Panama

Abstract. Fertilization rates were estimated for natural spawns in the tropical wrasse, *Halichoeres bivattatus*. Fertilization rate averaged 88%, but varied with both sea conditions and with the addition of males (streakers) to pair spawns. As sea conditions became rougher, the mean fertilization rate for a day decreased. This effect was due to the two days with the roughest sea conditions and the lowest mean fertilization rates; there was no obvious trend when these two days were excluded from the analysis. On a given day, pair spawns, with a single male and female, had fertilization rates approximately 7% lower than spawns where 1–2 streakers joined the pair spawn. These results suggest that variation in fertilization rate must be considered as a potential selective force in shaping reproductive behavior in fishes with external fertilization of pelagic eggs.

Introduction

The social and mating systems of tropical reef fishes, especially the more colorful and abundant species like the wrasses (Pisces: Labridae), have been the focus of a large body of research (Robertson, 1972, 1981; Robertson and Choat, 1974; Robertson and Hoffman, 1977; Warner and Robertson, 1978; Thresher, 1979; Warner and Hoffman, 1980a, b; Moyer and Yogo, 1982; Tribble, 1982; Kuwamura, 1984; Warner, 1984a, b, 1987, 1988; Nemtzov, 1985; Hoffman, 1985; Ross, 1986; Lejeune, 1987; Victor, 1987; Baird, 1988). Much of this work has involved documenting spawning behavior, quantifying the reproductive success of various mating tactics, and speculating on the adaptive significance of morphological and behavioral differences between and within the sexes.

The wrasses have reproductive behaviors typical of free-spawning tropical reef fishes, with spawning occurring at downcurrent sites of reefs. Spawning consists of one to over ten males and a female rushing upward 0.2 to several meters toward the surface and releasing gametes into the water column at the apex of the spawning rush. Although past workers have proposed many alternative mechanisms for the evolution of reproductive behaviors in tropical reef fishes, one fundamental factor has been almost completely ignored: the effect of fertilization rate on individual reproductive success and spawning behavior (for exceptions see Shapiro, 1989; Petersen, 1991). In this paper, I provide measurements for fertilization rate in the tropical wrasse, *Halichoeres bivattatus,* examine patterns and the potential causes of variation in fertilization rate, and discuss the role that fertilization rate may play in the evolution of reproductive behavior in this species.

Selection on males has been generally thought to act such that individuals produce enough sperm to fertilize all of the eggs of a female, implying that investigations of variation in fertilization rate would be uninteresting. However, as the amount of sperm released in a spawn increases, the number of additional fertilizations for a given number of sperm released should decrease, reducing the benefit for producing more sperm (Petersen, 1991). There is no reason to expect that the benefits to males for producing additional sperm will outweigh the costs of sperm production until all eggs are fertilized. Under these circumstances, the selected level of sperm production may not be enough to fertilize all available eggs, and the fertilization rate should be less than 100% (Petersen, 1991).

The extent to which fertilization rate is important in discussions of mating-system evolution depends on how

Received 1 April 1991; accepted 24 May 1991.

Present address: College of the Atlantic, 105 Eden St., Bar Harbor, Maine 04609-1198.

much variance exists in fertilization rate and how much of that variance is predictable. Given that fertilization rate may not always be 100%, it is still not clear whether fertilization rate plays a significant role in determining male and female mating strategies in organisms that have external fertilization of pelagic eggs.

In many tropical reef fishes, there is more than one male mating behavior within a population (*e.g.*, Warner *et al.*, 1975; Robertson and Warner, 1978; Warner and Robertson, 1978; Thresher, 1984; Petersen, 1990). Spawning sites may be occupied by either a large territorial male who mates singly with the female (pair spawning) or by a group of smaller males who mate together with the female (group spawning). In addition, small non-territorial males are known to rush in and join pair spawns at the moment of gamete release, a mating behavior called streaking (Warner *et al.*, 1975; Thresher, 1984). In many species, there may be several active spawning locations within the range of an individual female, providing females with a choice of conditions for spawning. The extent that males choose or compete for spawning locations and females choose either spawning locations or the identity of the male-role spawners based on fertilization rate is unknown.

Reproductive Biology of *Halichoeres bivattatus*

The slippery dick, *Halichoeres bivattatus*, is the most common Caribbean wrasse found over shallow reefs and seagrass communities. Smaller males and females have an initial-phase (IP) drab coloration; large terminal-phase (TP) individuals are more brightly colored and are invariably male (Warner and Robertson, 1978). TP males may be the result of sex change, or merely a coloration change from IP males (Warner and Robertson, 1978). Sex ratio is only slightly biased towards females (1:1.2), and IP males outnumber TP males approximately 2.3:1 (Warner and Robertson, 1978).

Spawning occurs daily in the mid-afternoon over the lee edges of reefs and over turtle grass (Warner and Robertson, 1978). In pair spawning, gravid females enter the territories of TP males, are approached by the TP male, and after one to several rushes by the male toward the female both rise quickly 0.3 to over 1 m in the water column in a fast spawning rush. Gametes are released at the apex of this spawning rush, after which both fish dart back to their normal positions closer to the bottom. The eggs are fertilized externally as they begin to float away from the location of the spawn. The TP male continues to court additional females, and may spawn over 20 times in a day (pers. obs.). Streaking occurs when an IP male joins the spawning pair at the apex of their spawning rush and presumably releases sperm. Only TP males were observed pair spawning in this study; IP males were observed streaking pair spawns and, on one occasion, approximately 10 IP males took part in a group spawn. Both pair and group spawning appear to be common in this species (Warner and Robertson, 1978). All data reported here are from pair spawns with or without streakers.

Materials and Methods

Data were collected during February 1990 along the northeast coast of St. Croix, Virgin Islands, and during March 1990 in the San Blas Islands of Panama. At St. Croix, collections of eggs were made in shallow water (1–4 m depth) while snorkeling behind the barrier reef approximately 1 km west of Tague Bay. In the San Blas, collections were made while snorkeling at 1–3 m depth at Smithsoniantupo reef adjacent to the Smithsonian Tropical Research Institute San Blas Field Station.

To collect eggs from natural spawnings, observers positioned themselves within 2–4 m of a spawning site near the beginning of the daily spawning period. When a spawn was observed, the gamete cloud was marked by a small amount of fluorescein dye released by the observer near the spawn. After waiting for at least 30 s, the observer swept the area around and including the expanded fluorescein cloud for 30 s with a 6-inch brine-shrimp net (maximum mesh size approximately 100×300 μm). Collections of eggs from another wrasse (*Thalassoma bifasciatum*, Petersen *et al.*, 1992) indicated that harsher-textured nylon nets, such as plankton netting, severly reduced the fertilization rates while the brine-shrimp net had no effect. At the end of the sweep, the net was drawn away from the fluorescein cloud, the contents of the net were transferred to a small plastic bag, and the bag was sealed. For each spawn, the location of the spawn was recorded, and the number of streakers that joined the spawn (0–2) was noted.

The next morning the contents of each bag were filtered through 100 μm nylon mesh to collect the eggs, which were then examined under a dissecting microscope and scored as fertilized or unfertilized. By counting eggs 16–20 h post-spawning, fertilized, developing eggs could be unambiguously distinguished from undeveloped eggs. Developing eggs contain nearly fully developed larvae, because hatching is completed within 24 h. Undeveloped eggs were scored as unfertilized. Estimates of fertilization rate for spawns relied on collections with at least 20 eggs.

To test whether the 30-s delay before collection was adequate to allow fertilization to occur, on three days collections were alternated between 30-s delays and 60-s delays. A significant increase in fertilization rate in the 60-s sample would suggest that the 30-s samples underestimate fertilization rate. In addition, collections were made at spawning locations during the spawning period but not immediately after a spawn to verify that eggs collected

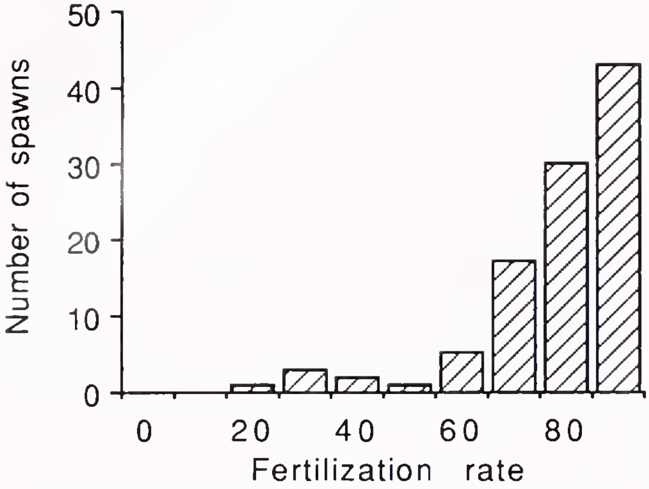

Figure 1. Frequency distribution of fertilization rates for all spawns with $\geq$20 eggs. The lower bound for the 10% categories is given, the last category included two spawns with 100% fertilization of collected eggs.

after spawns were not in the water column from spawns elsewhere.

On each date, a qualitative score of sea conditions was made during the spawning period. This score varied from 1 for the calmest conditions to 5 for the roughest conditions experienced during the study. These data were used to test for decreased fertilization rate on days with higher water velocities and increased water mixing. Based on theoretical studies of water turbulence and fertilization rate, increased water mixing was predicted to reduce sperm concentrations and reduce fertilization rates (Denny and Shibata, 1989).

The possibility that sperm depletion in males during the daily spawning period causes lower fertilization rates was examined by testing for a negative correlation between fertilization rate and the order of collection of spawns for a specific male during a spawning period. Only sequences with at least seven samples were used for this purpose.

For statistical analysis, fertilization rate data were angularly transformed before applying parametric statistical techniques. In cases where the sea-condition ranking or the spawning-order ranking was used, non-parametric statistics were employed.

Results

A total of 180 collections of eggs were taken over 19 days. Of the 180 collections, 102 (57%) had the minimum of 20 eggs and were used in the analysis of fertilization rate. The mean fertilization rate of these collections was 88.1% (median = 87.3%) (Fig. 1). The number of eggs collected from a spawn varied from 0 to 536 (median = 26.5; for collections with at least 20 eggs, median = 65.5). The three control collections had 0–4 eggs, implying that eggs in collections do come largely from the spawn that was observed immediately prior to sampling.

There was no evidence that collecting eggs after 30 s detrimentally affected the estimate of fertilization rate. Eggs collected from spawns after 60 s had virtually identical fertilization rates to spawns collected after 30 s ($F_{1,15} = 0.001$, $P = 0.98$).

Spawning date had a significant effect on fertilization rate. Over the 18 dates with at least two collections with 20 eggs, fertilization rate varied significantly among dates (ANOVA, $F_{17,84} = 8.31$, $P < 0.001$).

One of the causes of variation in fertilization rate among days appeared to be sea conditions. There was a negative correlation between the qualitative score of sea condition and the mean fertilization rate for a day, with rougher days having lower fertilization rates (Fig. 2, $r_s = -0.44$, $P_{[1\text{-tailed}]} < 0.05$, $n = 18$ days). This analysis used only spawns without streaking; an identical trend existed for the spawns with streakers ($r_s = -0.48$, $P_{[1\text{-tailed}]} < 0.05$, $n = 16$). Much of the variation in fertilization rates among dates was due to the two dates that had the roughest sea conditions and also had the lowest mean fertilization rates. Excluding these two days, there was no significant effect of sea conditions on fertilization rate (both types of spawns, $P_{[1\text{-tailed}]} > 0.25$).

Spawns with streakers had significantly higher fertilization rates than pair spawns without streakers collected on the same day. To test for changes in fertilization rate with the presence of streakers, date of collection and the presence of streakers were examined simultaneously in a two-way ANOVA for the subset of days with collections from pair spawns both with and without streakers ($n = 16$ dates). Using this database, both the presence of a streaker joining the pair spawn and the day a spawn was collected

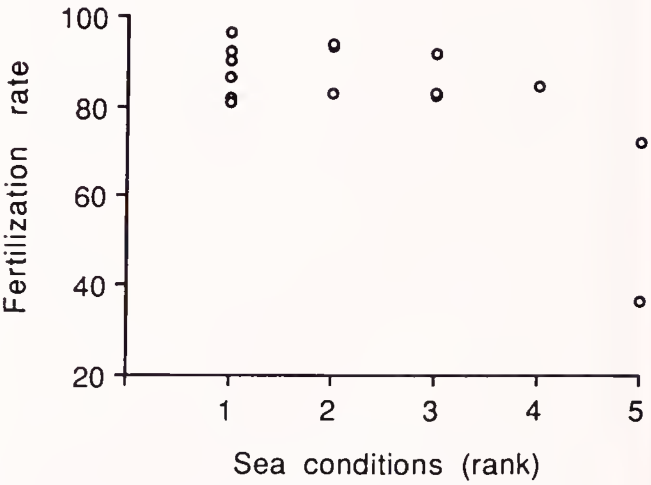

Figure 2. The relationship between sea conditions (rank score) and mean fertilization rate on a day for all spawns without streakers with $\geq$20 eggs.

had a significant effect on fertilization rate (Table 1). Spawns with streakers had an average of 6.6% higher fertilization rate on a day (range = −4 to 18%) compared with pair spawns without streakers.

The identity of the male did not appear to affect fertilization rate. On two days collections were made simultaneously from three males on the same back reef area within 30 meters of one another. There was a significant effect of date ($F_{1,19}$ = 6.41, P = 0.02), but no significant effect of male identity ($F_{2,19}$ = 0.56, P = 0.58).

There was also no evidence that fertilization rate for spawns by a male changed in any systematic way during the spawning period. Over the course of the study, there were three sequences of 7–10 spawns successfully collected from a male. These sequences occurred over a period of 33–48 min. The order in the spawning sequence was not significantly correlated with fertilization rate (r_s = −0.25 to 0.64, $P_{[1\text{-tailed}]} > 0.1$ in all cases). Thus, the fertilization rate data does not provide evidence for sperm depletion by TP male *H. bivattatus.*

Table 1

Two-way mixed-model ANOVA of the effect of presence of streakers and collection day on fertilization rate

Dependent variable—Fertilization rate (angular transformation)

Independent variable	df	MS	F	*P*
Day of collection	15	0.10	6.62	<0.001
Presence of streakers	1	0.12	6.77	<0.05
Interaction	15	0.02	1.1	>0.25
Error	65	0.016		

$R^2 = 0.74$.

Discussion

Fertilization rate has been a previously ignored aspect of the reproductive biology of tropical reef fishes. The result that lower fertilization rates occur on days of rougher water conditions and higher current velocity is consistent with a theoretical treatment of the effect of turbulence on fertilization rate (Denny and Shibata, 1989) and with empirical data for marine invertebrates (Pennington, 1985; Levitan, 1989) and another marine fish (Petersen *et al.*, 1992).

A difference in fertilization rate was also observed between pair spawns and pair spawns joined by streaking males. The most likely cause of the increase in fertilization rate in spawns with streakers is a higher total amount of sperm released with the addition of another male. However, this result could also be caused by some other factor associated with streaking. For example, a slower spawning ascent or a lower spawning rush height might be associated both with increased fertilization rates and with a higher probability of additional males joining the spawn. Although these alternatives are possible, I will assume that the most straightforward interpretation is correct, that streakers directly increase fertilization rate in *Halichoeres bivattatus.* If so, the result that streaking increases fertilization rate indicates that some of the assumptions that have been made about reproduction in reef fishes have been violated and that fertilization rate must be considered as a potential selective force in shaping spawning behavior.

If females attempt to maximize fertilization rates in their spawns, irrespective of the identity of the male that fertilizes the eggs, then these data provide evidence for a conflict of interests between the TP territorial male and the spawning female. Females gain fertilizations by having a streaking male join the spawn, while the TP male will almost certainly lose fertilizations due to sperm competition with the streaking IP male. Territorial males chase IP individuals away from the spawning site during the spawning period, and many, if not all, of these are presumably males and potential streakers. In addition, immediately before spawning, males sometimes exhibit a behavior called "looping" (see Thresher, 1984, for a description and drawing). Looping consists of the TP male going through a series of quick rushes upward near the spawning site. Looping has traditionally been thought of as a courtship behavior, but appears to have a second function of exposing potential streakers in *H. bivattatus.* In several instances, IP individuals streaked while the male was looping, and were immediately chased by the male. Thus, looping appears to be a tactic by territorial males to expose potential streakers before spawns.

Although there is convincing evidence that males attempt to exclude streakers, there is no convincing evidence that females alter their behavior to increase their fertilization rate by increasing the probability of successful streaking. In the Mediterranean wrasse, *Symphodus tinca,* females avoid nesting males with large numbers of peripheral males (van den Berge *et al.*, 1989). Fertilization rates of the demersal eggs were near 100% and did not differ for nests with and without frequent spawning by peripheral males, so spawning site selection did not appear to be based on differences in fertilization rate (van den Berge *et al.*, 1989).

In the seabass, *Serranus fasciatus,* Petersen (1987) interpreted hesitation by female-role spawners before beginning the spawning rush as a behavioral tactic to reduce streaking. When the spawning partner hesitated, males often broke off spawning and patrolled the spawning area, chasing any individuals that were close enough to the spawning location potentially to streak. However, the increased fertilization rate for spawns with streakers in *H. bivattatus* suggests a different interpretation for this behavior. Hesitations by females before beginning the spawning rush in tropical reef fishes could be a female mating tactic to increase streaking rate, and not a female response to imperfect positioning by the TP male prior to spawning or a tactic to reduce streaking rate. This hypothesis needs to be tested with comparative data, including species with and without streaking males. Females in *H. bivattatus* often hesitate several times before ultimately spawning with a TP male (pers. obs.).

Despite the possible advantages of female spawning behavior that increases fertilization rate, these modifications may be highly constrained by predation pressure during spawning. Behaviors that may increase the chance of a nearby male seeing and joining the spawn, such as slowing down the spawning rush, may also increase the vulnerability of the female to predators. In two instances during this study, a lizardfish (*Synodus* sp.) struck at the fish in a pair spawn at the apex of the spawning rush. Although neither attempt was successful, predators may limit the advantages of female behaviors that could increase their visibility to streakers but at the same time make them more vulnerable to predators. Thresher (1984) has noted that many of the observations of reef-fish being preyed upon have occurred during spawning.

In another Caribbean wrasse, *Thalassoma bifasciatum*, fertilization rates do not differ between pair spawns and group spawns (Petersen *et al.*, 1992), despite an estimated 80-fold increase in sperm released in group spawns relative to pair spawns. Group spawns typically involve at least five males, and may produce higher levels of turbulence and water mixing, reducing the concentration of gametes faster than in pair spawns. Group spawns may also lack the close juxtaposition of a male and female during gamete release that exists between the pair-spawning male and female with or without streaking (Petersen *et al.*, 1992). Thus, fertilization rate comparisons between different types of spawns may depend both on the number of males in the spawn and the type of spawn. This difference for spawns with streaking and group spawns compared with pair spawns should be tested for other species to determine its generality.

In transforming male mating success into reproductive success, researchers have had to rely on approximations of how fertilizations are divided among males in cases of sperm competition. The approach has varied from assigning all of the reproductive success to the male using the alternative reproductive pathway due to his higher sperm production and proximity to the female (Gross and Charnov, 1980) to dividing the fertilization evenly among all males in the spawn (Warner and Hoffman 1980a, b; Petersen 1987, 1990). In all of these studies, fertilization rate was assumed constant. This study shows that additional males alter the fertilization rate, and, although it is not clear how fertilizations are divided among the two types of males, it is clear that our assumptions of how mating success is translated into reproductive success in these fishes needs to be reappraised.

These results suggest two avenues for future research in the reproductive biology of tropical reef fishes. First, variation in female mate choice, spawning site selection, and temporal patterns of spawning may be at least in part a response to variation in fertilization rate. Second, the spawning behavior of both males and females needs to be reconsidered as a potential tactic to increase individual fertilization rates.

Acknowledgments

This study was supported by NOAA grant NURC 90-1 and a Smithsonian Tropical Research Institute postdoctoral fellowship to the author. I would like to thank Sarah Cohen, Helen Hess, and Amy Sewell for help with data collection and Helen Hess and two anonymous reviewers for making helpful comments on the manuscript.

Literature Cited

Baird, T. A. 1988. Abdominal windows in straight-tailed razorfish, *Xyrichthys martinicensis*: an unusual female sex character in a polygynous fish. *Copeia* **1988:** 496–499.

van den Berge, E. P., F. Wernerus, and R. R. Warner. 1989. Female choice and the mating costs of peripheral males. *Anim. Behav.* **38:** 875–884.

Denny, M. W., and M. F. Shibata. 1989. Consequences of surf-zone turbulence for settlement and external fertilization. *Am. Nat.* **134:** 859–889.

Gross, M. R., and E. L. Charnov. 1980. Alternative male life histories in bluegill sunfishes. *Proc. Nat. Acad. Sci. U.S.A* **76:** 6937–6940.

Hoffman, S. G. 1985. Effects of size and sex on the social organization of reef-associated hogfishes, *Bodianus* sp. *Environ. Biol. Fish.* **14:** 185–197.

Kuwamura, T. 1984. Social structure of the protoynous fish *Labroides dimidiatus*. *Publ. Seto Mar. Biol. Lab.* **29:** 117–177.

Lejeune, P. 1987. The effect of local stock density on social behavior and sex change in the Mediterranean labrid *Coris julis*. *Environ. Biol. Fish.* **18:** 135–141.

Levitan, D. R. 1989. Life history and population consequences of body size regulation in the sea urchin *Diadema antillarum* Phillipi. *Ph.D. Dissertation* University of Delaware, Newark.

Moyer, J. T., and Y. Yogo. 1982. The lek-like mating system of *Halichoeres melanochir* (Pisces: Labridae) at Miyake-jima, Japan. *Z. Tierpsychol.* **60:** 209–226.

Nemtzov, S. C. 1985. Social control of sex change in the Red Sea razorfish *Xyrichtys pentadactylus* (Teleostei, Labridae). *Environ. Biol. Fish.* **14:** 199–211.

Pennington, J. T. 1985. The ecology of fertilization of echinoid eggs: the consequences of sperm dilution, adult aggregation, and synchronous spawning. *Biol. Bull* **169:** 417–430.

Petersen, C. W. 1987. Reproductive behaviour and gender allocation in *Serranus fasciatus*, a hermaphroditic reef fish. *Anim. Behav.* **35:** 1601–1614.

Petersen, C. W. 1990. The relationships among population density, individual size, mating tactics, and reproductive success in a hermaphroditic fish, *Serranus fasciatus*. *Behaviour* **113:** 57–80.

Petersen, C. W. 1991. Sex allocation in hermaphroditic seabasses. *Am. Nat.* (in press).

Petersen, C. W., R. R. Warner, S. Cohen, H. C. Hess, and A. T. Sewell. 1992. Variation in pelagic fertilization success: implications for production estimates, mate choice, and the spatial and temporal distribution of mating. *Ecology* (in press).

Robertson, D. R. 1972. Social control of sex reversal in coral-reef fish. *Science* **177:** 1007–1009.

Robertson, D. R. 1981. The social and mating systems of two labrid fishes, *Halichoeres maculipinna* and *H garnoti*, off the Caribbean coast of Panama. *Mar. Biol.* **64:** 327–340.

Robertson, D. R., and J. H. Choat. 1974. Protogynous hermaphroditism and social systems in labrid fishes. *Proceedings Second International Symposium Coral Reefs* **1:** 217–225.

Robertson, D. R., and S. G. Hoffman. 1977. The roles of female mate choice and predation in the mating systems of some tropical labroid fishes. *Z. Tierpsychol.* **45:** 298–320.

Robertson, D. R., and R. R. Warner. 1978. Sexual patterns in the labroid fishes of the western Caribbean. II: The parrotfishes (Scaridae). *Smith. Contrib. Zool.* **255:** 1–26.

Ross, R. M. 1986. Social organization and mating system of the Hawaiian reef fish *Thalassoma duperrey* (Labridae). Pp. 794–802 in *Indo-Pacific Fish Biology: Proceedings of the Second International Conference on Indo-Pacific Fishes*, T. Uyeno, R. Arai, T. Taniuchi, and K. Matsuura, eds. Ichthyological Society of Japan, Tokyo.

Shapiro, D. Y. 1989. Sex change as an alternative life-history style. Pp. 177–195 in *Alternative Life-history Styles in Animals*, M. N. Burton, ed. Kluwer Publishers, Dordrecht, The Netherlands.

Thresher, R. E. 1979. Social behavior and ecology of two sympatric wrasses (Labridae: *Halichoeres* spp.) off the coast of Florida. *Mar. Biol.* **53:** 161–172.

Thresher, R. E. 1984. *Reproduction in Reef Fishes.* T.F.H. Publications, Neptune City, NJ.

Tribble, G. W. 1982. Social organization, patterns of sexuality, and behavior of the wrasse *Coris dorsomaculata* at Miyake-jima, Japan. *Environ. Biol. Fish.* **7:** 29–38.

Victor, B. C. 1987. The mating system of the Caribbean rosy razorfish, *Xyrichthys martinicensis*. *Bull. Mar. Sci.* **40:** 152–160.

Warner, R. R. 1984a. Mating behavior and hermaphroditism in coral reef fishes. *Am. Sci.* **72:** 128–136.

Warner, R. R. 1984b. Deferred reproduction as a response to sexual selection in a coral reef fish: a test of the life historical consequences. *Evolution* **38:** 148–162.

Warner, R. R. 1987. Female choice of sites versus mates in a coral reef fish, *Thalassoma bifasciatum*. *Anim. Behav.* **35:** 1470–1478.

Warner, R. R. 1988. Traditionality of mating-site preferences in a coral-reef fish. *Nature* **335:** 719–721.

Warner, R. R., and S. G. Hoffman. 1980a. Local population size as a determinant of mating system and sexual composition in two tropical reef fishes (*Thalassoma* spp.) *Evolution* **34:** 508–518.

Warner, R. R., and S. G. Hoffman. 1980b. Population density and the economics of territorial defense in a coral reef fish. *Ecology* **61:** 772–780.

Warner, R. R., and D. R. Robertson. 1978. Sexual patterns in the labroid fishes of the western Caribbean, I: The wrasses (Labridae). *Smith. Contrib. Zool.* **254:** 1–27.

Warner, R. R., D. R. Robertson, and E. G. Leigh, Jr. 1975. Sex change and sexual selection. *Science* **190:** 633–638.

Reference: *Biol Bull.* **181**: 238–247. (October, 1991)

Spermatophore Diversity Within and Among the Hermit Crab Families, Coenobitidae, Diogenidae, and Paguridae (Paguroidea, Anomura, Decapoda)

C. C. TUDGE

Zoology Department, University of Queensland, Queensland, 4072, Australia

Abstract. The spermatophore morphology of 13 species of hermit crab from the families Coenobitidae, Diogenidae and Paguridae is described and illustrated, and comparisons are made with existing descriptions to show that spermatophore form, at the light microscope level, can be used to separate three families of the Paguroidea. Spermatophores from members of the family Coenobitidae are robust in nature with large, ovoid-spherical ampullae mounted on short, thick stalks. Members of the family Diogenidae have more fragile spermatophores with small spherical ampullae mounted on long, slender stalks. The spermatophores of members of the family Paguridae are distinctive in possessing large, elongate, ampullae, an accessory ampulla at the base of the main ampulla and a pseudo-stalk analogous with the true stalk of the Coenobitidae and Diogenidae. The occurrence of double-headed spermatophores (two ampullae on a single stalk) is recorded for the first time, in a *Dardanus* species. The ultrastructure of the lateral ridge, which divides the ampulla of the paguroidean spermatophore into two halves, is described using both scanning and transmission electron microscopy. A simple, branching key for classifying the investigated hermit crabs (from the families Coenobitidae, Diogenidae and Paguridae only) into their respective family, based on the gross morphology of their spermatophore, is presented.

Introduction

The infraorder Anomura consists of 13 families of which only 6 have been investigated for spermatophore morphology. Representatives of three hermit crab families in the superfamily Paguroidea (*sensu* McLaughlin, 1983) have been investigated for spermatophore morphology. These are listed below. Coenobitidae: *Birgus latro* (Linnaeus), Matthews, 1956; Tudge and Jamieson, 1991. *Coenobita rugosus* H. Milne Edwards, Matthews, 1956. Diogenidae: *Clibanarius misanthropus* (Risso), Mouchet, 1930, 1931. *Dardanus arrosor* (Herbst), Mouchet, 1931 (as *Pagurus arrosor*). *Dardanus asper* (De Haan), Matthews, 1953. *Dardanus punctulatus* (Olivier), Matthews, 1956. *Diogenes pugilator* (Roux), Mouchet, 1930, 1931. *Paguristes oculatus* (Fabricius), Mouchet, 1931. *Aniculus maximus* Edmondson, *Trizopagurus maximus* (Herbst) and *T. strigatus* (Herbst), Matthews, 1957 (as *Aniculus strigatus*). Paguridae: *Anapagurus hyndmanni* (Thompson), Mouchet, 1930, 1931. *Anapagurus brevicarpus* A. Milne Edwards and Bouvier and *A. laevis* (Bell), Mouchet, 1931. *Cestopagurus timidus* (Roux), *Pagurus anachoretus* Risso, *P. cuanensis* (Thompson), *P. excavatus* (Herbst) and *P. sculptimanus* (Lucas), Mouchet, 1931 (all as *Eupagurus*). *Pagurus prideaux* Leach, Mouchet, 1931; Hamon, 1937 (both as *Eupagurus prideauxi*). *Pagurus bernhardus* (Linnaeus), Mouchet, 1931; Chevaillier, 1970 (both as *Eupagurus bernhardus*). *Pagurus novizealandiae* (Dana), Greenwood, 1972 (as *P. novae-zealandiae*). *Pagurus excavatus* (Herbst), Schaller, 1979 (as *P. meticulosus*). All of these previous studies of spermatophore structure have been at the light microscope level.

Except for *Trizopagurus maximus* and *T. strigatus* (Matthews 1957), the hermit crabs previously studied have a typically pedunculate spermatophore that can be divided into three major regions: a sperm-filled ampulla, a columnar stalk of variable length, and a foot or pedestal. The ampulla has a partition or line of division that runs around the lateral edge and separates the ampulla into two halves. This suture line is the point of weakness where the ampulla breaks to release the spermatozoa prior to fertilization.

Received 12 April 1991; accepted 17 July 1991.

Earlier pioneers in hermit crab spermatophore morphology include Mouchet (1930, 1931) and Matthews (1953, 1956, 1957), whose important contributions to this field also covered other decapods. These references, along with many other papers on decapod spermatophores, are adequately tabulated in Dudenhausen and Talbot (1983). Some additional, more recent, references to anomuran and brachyuran spermatophore studies can be found in Mann's (1984) book on spermatophores. Studies on hermit crab spermatophores have been neglected for the past 10 years, except for a recent review by Hinsch (1991); although some important works on brachyuran (Jeyalectumie and Subramoniam, 1989; Subramoniam, 1991) and caridean shrimp (Chow *et al.*, 1989) spermatophores have been published. Comparisons of the functional morphology of genitalia and subsequent sperm transfer and storage mechanisms among taxa can provide useful information on phylogenetic relationships and evolutionary divergence; especially in the Decapoda (Bauer, 1986, 1991). The present paper describes and illustrates the spermatophore structure of 13 species of hermit crab, from 3 families in the Paguroidea, and introduces a simple key to classify these hermit crabs to family, based on light microscope observations of their spermatophores.

Materials and Methods

Collection sites and dates for the species in this paper are as follows:

Family Coenobitidae

Birgus latro (Linnaeus 1767), Malaita Island, Solomon Islands, SW Pacific, October, 1988; *Coenobita brevimanus* Dana 1852, *Coenobita perlatus* H. Milne Edwards 1837 and *Coenobita rugosus* H. Milne Edwards 1837, Suwarrow Atoll National Park, Cook Islands, SW Pacific, August, 1990; *Coenobita spinosus* H. Milne Edwards 1837, Darwin, Northern Territory, Australia, May, 1990.

Family Diogenidae

Calcinus latens (Randall 1839), *Calcinus minutus* Buitendijk 1937 and *Clibanarius corallinus* (H. Milne Edwards 1848), Heron Island, Queensland, Australia, December, 1990; *Clibanarius virescens* (Krauss 1843), Dunwich, North Stradbroke Island, Queensland, Australia, April, 1990; *Dardanus lagopodes* (Forskål 1775) and *Dardanus megistos* (Herbst 1804), Heron Island, Queensland, Australia, December, 1990; *Diogenes gardineri* Alcock 1905, Mooloolaba, Queensland, Australia, October, 1990.

Family Paguridae

Pagurus hirtimanus Miers 1880, Heron Island, Queensland, Australia, December, 1990.

The male reproductive system was dissected from fresh specimens, 10% buffered formalin-fixed or 3% glutaraldehyde-fixed specimens. The spermatophores were teased out of the distal part of the vas deferens onto microscope slides. Spermatophores were viewed and photographed with an Olympus BH2 microscope equipped with Nomarski interference contrast optics. After the initial glutaraldehyde fixation and first phosphate buffer wash, the fixation procedure for transmission electron microscopy was carried out in a Lynx-el. Microscopy Tissue Processor. Portions of the vas deferens were fixed in 3% glutaraldehyde in 0.2 M phosphate buffer (pH 7.2) for 1 h at 4°C. They were washed in phosphate buffer (3 washes in 15 min), postfixed in phosphate buffered 1% osmium tetroxide for 80 min; similarly washed in buffer and dehydrated through ascending concentrations of ethanol (40–100%). After being infiltrated and embedded in Spurr's epoxy resin (Spurr, 1969), thin sections (50–80 nm thick) were cut on a LKB 2128 UM IV microtome with a diamond knife. Sections were placed on carbon-stabilized colloidin-coated 200 μm mesh copper grids and stained in 6% aqueous uranyl acetate for 40 min; rinsed in distilled water; stained with Reynold's lead citrate (Reynolds, 1963) for 20 min; and further rinsed in distilled water. Micrographs were taken on a Hitachi 300 transmission electron microscope at 80 kV.

For scanning electron microscopy, 3% glutaraldehyde-fixed spermatophores were dehydrated through a graded series of ethanol (80–100%) at 10 min intervals. They were then dried after being placed in a drop of ether and sputter coated with gold; micrographs were taken on a Philips 505 scanning electron microscope at 20–30kV.

Results

Family Coenobitidae

The tripartite, pedunculate spermatophores of *Birgus latro* are approximately 650 μm in length from pedestal to apex of the ampulla. The sperm-filled ampulla is 440 μm long and 450 μm wide and forms an inverted heart-shape (Fig. 1A). The stalk of the spermatophore is approximately 100 μm in length. The spermatophore is laterally wider than deep, and therefore is slightly spatulate and is composed of two halves, which meet at the lateral edge as a raised ridge (Fig. 3A). This ridge is 20 μm thick while the remaining spermatophore wall is only 10 μm thick. Under a double Mallory's staining procedure (Mallory, 1936) the spermatophore wall is shown to be composed of two layers: an inner, darker staining layer, which is discontinuous at the ridge, and an outer, lighter staining layer, which covers the entire ampulla and increases in thickness at the ridge.

The pedunculate spermatophores of *Coenobita spinosus* are similar in shape to those of *Birgus latro* but much

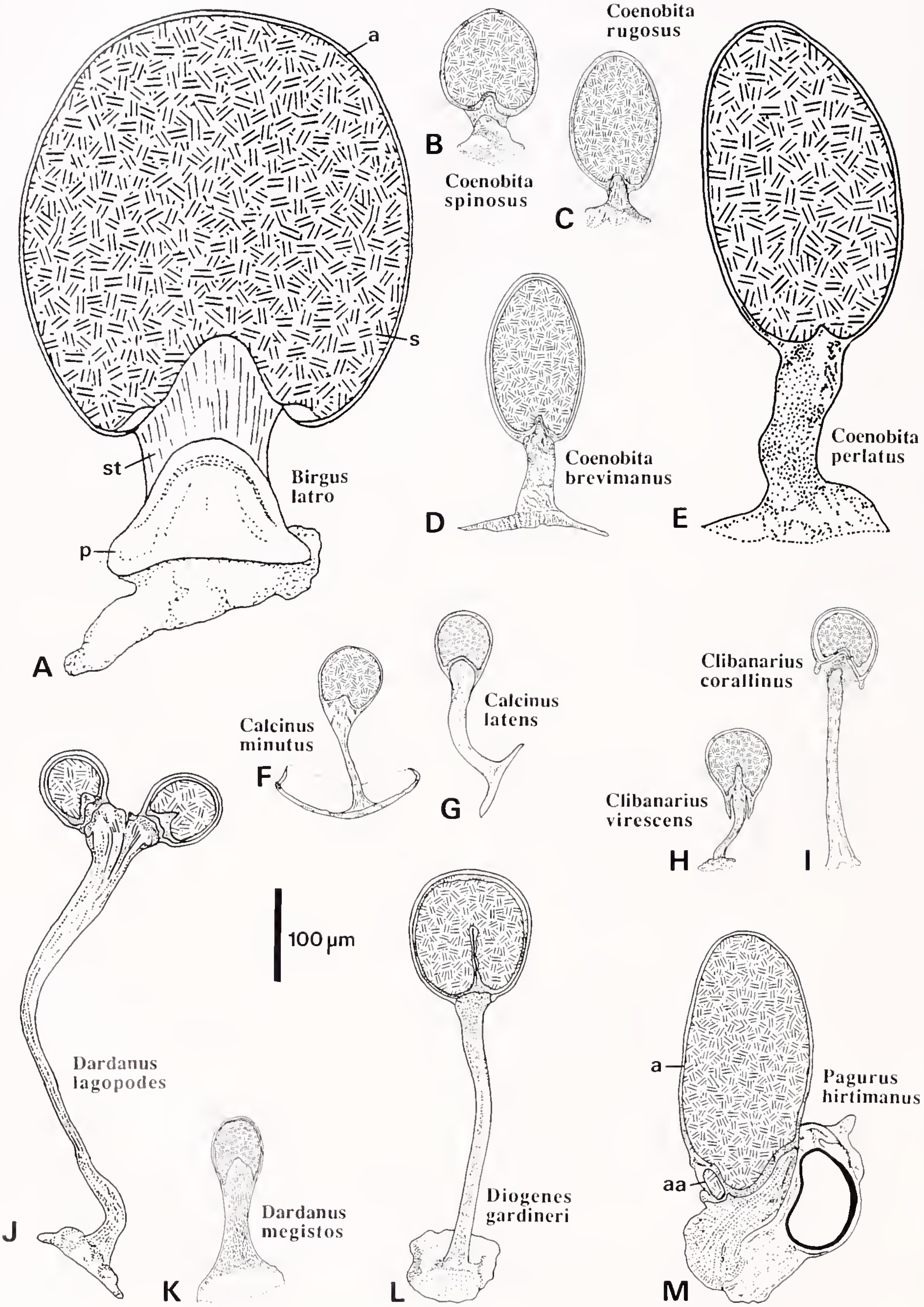
a
s
st
p
Birgus latro
A
B
Coenobita spinosus
Coenobita rugosus
C
Coenobita brevimanus
D
Coenobita perlatus
E
Calcinus minutus
F
Calcinus latens
G
Clibanarius corallinus
Clibanarius virescens
H
I
Dardanus lagopodes
J
100 μm
Dardanus megistos
K
Diogenes gardineri
L
a
aa
Pagurus hirtimanus
M

smaller (Fig. 1B). Each individual spermatophore is approximately 170 μm in length from base of the pedestal to the top of the ampulla. The ampulla, which is approximately 110 μm long, is composed of two halves that join at a conspicuous lateral ridge. The stalk of the spermatophore is only 20 μm long. The width of the ampulla from ridge to ridge is approximately 110 μm, while the depth of the ampulla is only 100 μm. This gives the ampulla a slightly spatulate shape, with the ridge running around the lateral edge. The ampulla is surrounded by a spermatophore wall 2 μm in thickness, which increases to 3 μm at the ridge, and is filled with many closely packed spermatozoa, separated by an extracellular matrix. Ultrastructural studies show the ridge to be a break in the fibrillar structure of this wall (Fig. 3C).

The spermatophores of *Coenobita rugosus* are larger than those of *Coenobita spinosus*, being 190 μm long, with an ampullar length and width of 150 and 100 μm, respectively. The ampulla, which is slightly more elongate than either *Birgus latro* or *Coenobita spinosus*, sits on a stalk 32 μm high (Fig. 1C).

Coenobita brevimanus has a spermatophore 290 μm in length which is composed of a stalk that is 90 μm long and an ampulla that is 180 μm long and 110 μm wide. Although the ampulla is larger than that of *Coenobita rugosus*, its shape is very similar (Figs. 1D, 2A).

The spermatophore of *Coenobita perlatus* is the largest of the four species of *Coenobita* studied. At 600 μm in length, it is only slightly smaller than the spermatophore of *Birgus latro* (Fig. 1A). The ampulla, 400 μm long and 230 μm wide, is similar in shape to those of *Coenobita rugosus* and *Coenobita brevimanus* and is situated on top of a stalk that is 180 μm long (Fig. 1E).

Family Diogenidae

The spermatophores of *Calcinus minutus* are 180 μm long, composed of a stalk that is 110 μm long and an ampulla 60 μm long and 70 μm wide. The stalk is very slender, only 10 μm wide, and gradually thickens distally to envelop the spherical ampulla (Figs. 1F, 3D). This shape is also found in *Calcinus latens*, but the entire spermatophore is smaller in the latter. The over-all length of the spermatophore of *Calcinus latens* is 150 μm, the thin stalk being 110 μm long and 15 μm wide, and the ampulla dimensions are 50 by 50 μm (Figs. 1G, 2C).

The spermatophore morphology of the two species of *Clibanarius* is similar to that of the *Calcinus* species. *Clibanarius virescens* has a small spermatophore, only 150 μm long with a short, thin stalk 70 μm long and 10 μm wide. The ampulla is 75 μm in length and width and has ventrally directed projections (25 μm long) which appear to be extensions of the lateral ridge (Fig. 1H). The distal end of the stalk penetrates into the ampulla as a dorsally directed projection.

The spermatophore of *Clibanarius corallinus* is twice the length (300 μm) of that of *Clibanarius virescens*, but otherwise it is morphologically similar (Fig. 1I). The 220 μm stalk is slightly wider at 15 μm. The ampulla is 60 μm long and 75 μm wide and possesses the same extensions of the lateral ridge, although the extensions in this species are only 12 μm in length. The ampulla is only slightly penetrated by a broad dorsal projection at the distal end of the stalk (Figs. 1I, 2E).

Dardanus lagopodes has a distinctive spermatophore, in comparison to the rest of the Paguroidea studied, in that some have two ampullae at the apex of a single stalk (Figs. 1J, 2D). Of the observed spermatophores, approximately 20% were double-headed. Both single and double-headed spermatophores were the same length, and each had similar ampullae. The spermatophores were 600 μm long with a 530 μm stalk, that had a mean width of 20 μm. Each ampulla was 70 μm long and 80 μm wide. In the spermatophores with two ampullae the stalk forked only at the most distal 50–70 μm (Fig. 2D).

The spermatophores of *Dardanus megistos* are very different from that of *Dardanus lagopodes* in both size and morphology (Figs. 1K, 2B). They appear more similar to the spermatophores of the two *Calcinus* species. *Dardanus megistos* has a spermatophore that is only 160 μm long, a stalk that is 90 μm long and 20 μm wide and an ampulla that is 60 μm long and 45 μm wide. As in *Calcinus minutus* and *Calcinus latens* (Figs. 1F, G), the stalk gradually widens distally so as to appear to envelop the ampulla, but unlike these species, the broad end of the stalk projects considerably into the ventral aspect of the ampulla (Fig. 1K).

The spermatophore of *Diogenes gardineri* is different from those of any of the other diogenid genera in this paper. The entire spermatophore is 430 μm in length, with 300 μm of that being the thin (15 μm) stalk. The ampulla is approximately square in outline with length and width dimensions both being 130 μm. The ampulla

Figure 1. Semidiagrammatic representations of spermatophores of hermit crabs from three families of the Paguroidea. (A–E) Coenobitidae. A. *Birgus latro*, B. *Coenobita spinosus*, C. *Coenobita rugosus*, D. *Coenobita brevimanus*, E. *Coenobita perlatus*. (F–L) Diogenidae. F. *Calcinus minutus*, G. *Calcinus latens*, H. *Clibanarius virescens*, I. *Clibanarius corallinus*, J. *Dardanus lagopodes*, K. *Dardanus megistos*, L. *Diogenes gardineri*. (M) Paguridae. M. *Pagurus hirtimanus*. Drawn from light micrographs. All to the same scale. a; ampulla, aa; accessory ampulla, p; pedestal, s; spermatozoa, st; stalk.

is penetrated ventrally by a thin projection, which originates at the distal end of the stalk, to a depth of 60 μm (Figs. 1L, 2G–I).

Family Paguridae

The spermatophores of the single representative collected from this family, *Pagurus hirtimanus*, are morphologically very different from any other Paguroidea in this paper. The spermatophores, although considered to be stalked (pedunculate), do not appear to have a definite stalk lifting the ampulla above the pedestal. Another important difference is the presence of a secondary or accessory ampulla, at the base of the main ampulla but much smaller than the latter (Figs. 1M, 2F). This accessory ampulla has only been described in representatives from this family. The entire spermatophore of *Pagurus hirtimanus* is 400 μm in length and the attached stalk is 100 μm long by 50 μm wide. The main ampulla is 280 μm long and 150 μm wide while the accessory ampulla is only 36 μm long and 12 μm wide (Fig. 1M). The accessory ampulla is often devoid of spermatozoa but may contain one or two sperm cells (Fig. 2F).

Discussion

Coenobitidae

The spermatophores of the five representatives in the Coenobitidae (Fig. 1A–E) all show a similar over-all morphology and only size differences distinguish them. The spermatophores in this family are characterized by large spherical to ovoid ampullae with short thick stalks, giving them a generally robust appearance. I consider the genera in the Coenobitidae to be either semi-terrestrial, *Coenobita* spp., or terrestrial, *Birgus latro*, based on their differing abilities to withstand desiccation and their subsequent dependence on the marine environment.

In the Paguroidea, spermatophores are attached to the exoskeleton of the female hermit crab or on the surface of the temporarily inhabited gastropod shell, by the sticky base or pedestal (Matthews, 1956; Greenwood, 1972), and generally are embedded in a gelatinous mass. In an aquatic habitat, the spermatophoric mass does not dry out and thus can be carried around for long periods; but for terrestrial species or species that venture from the water for periods of time, desiccation of the spermatophoric mass is a problem. Matthews (1956) assumed that copulation, spermatophore deposition, and fertilization in the semi-terrestrial species, *Coenobita rugosus*, and the terrestrial coconut crab, *Birgus latro*, occurred in water, mainly because the remainder of the reproductive cycle is aquatic and also because no one had observed a terrestrial mating in this family.

One instance of terrestrial copulation between two individuals of *Birgus latro* was later observed and reported by Helfman (1977). He also observed several terrestrial matings in the semi-terrestrial hermit crab, *Coenobita perlatus*. These observations indicate that, in the Coenobitidae, spermatophore transfer and fertilization can occur on land. The robust nature of the spermatophores in this family may be an adaptation to facilitate spermatophore survival on the external surface of the female while she is on land. Large spermatophores with short, thick stalks would be harder to damage or dislodge from the gelatinous spermatophoric mass attached to the female than slender stalked spermatophores.

Diogenidae

The Diogenidae is a large hermit crab family encompassing many genera including *Calcinus*, *Clibanarius*, *Dardanus*, and *Diogenes*. The representatives in this study, from the above genera, show a great diversity of spermatophore form (Figs. 1F–L), but within the limits of a characteristic familial morphology. The spermatophores generally have long, thin stalks (less than 20 μm in diameter) and small spherical ampullae approximately 50–70 μm in size. The investigated *Diogenes gardineri* is an exception to the latter case, as it has larger ampullar dimensions (Figs. 1L, 2G–I).

Each of the genera can be distinguished by its possession of specific structural features. These distinctive generic forms can be complicated by unusual morphologies, such as the double-headed spermatophores of *Dardanus lagopodes* (Figs. 1J, 2D). The 20% occurrence rate of this form among the majority of single-headed spermatophores suggests that they might not be aberrant. This is the first record of double-headed spermatophores in the Diogenidae (also for the Paguroidea), and further study may reveal whether this is more common among other genera.

All the representatives in the Diogenidae are aquatic; mating and fertilization occur in water. Spermatophores are placed externally on either the carapace of the female or the gastropod shell she inhabits. The fact that desiccation of the spermatophoric mass is not a problem in an aquatic habitat may be reflected in the fragile structure of the slender-stalked spermatophores of these species. The long slender stalks in *Clibanarius corallinus*, *Dardanus lagopodes*, and *Diogenes gardineri* (Figs. 1I, J, L) may reflect the need to use the water for the extra support of the sperm-filled ampullae.

Paguridae

The 12 species within the family Paguridae have been studied for spermatophore morphology (see Introduction), making it the most studied family of the Paguroidea. The single species for which the spermatophore is illustrated

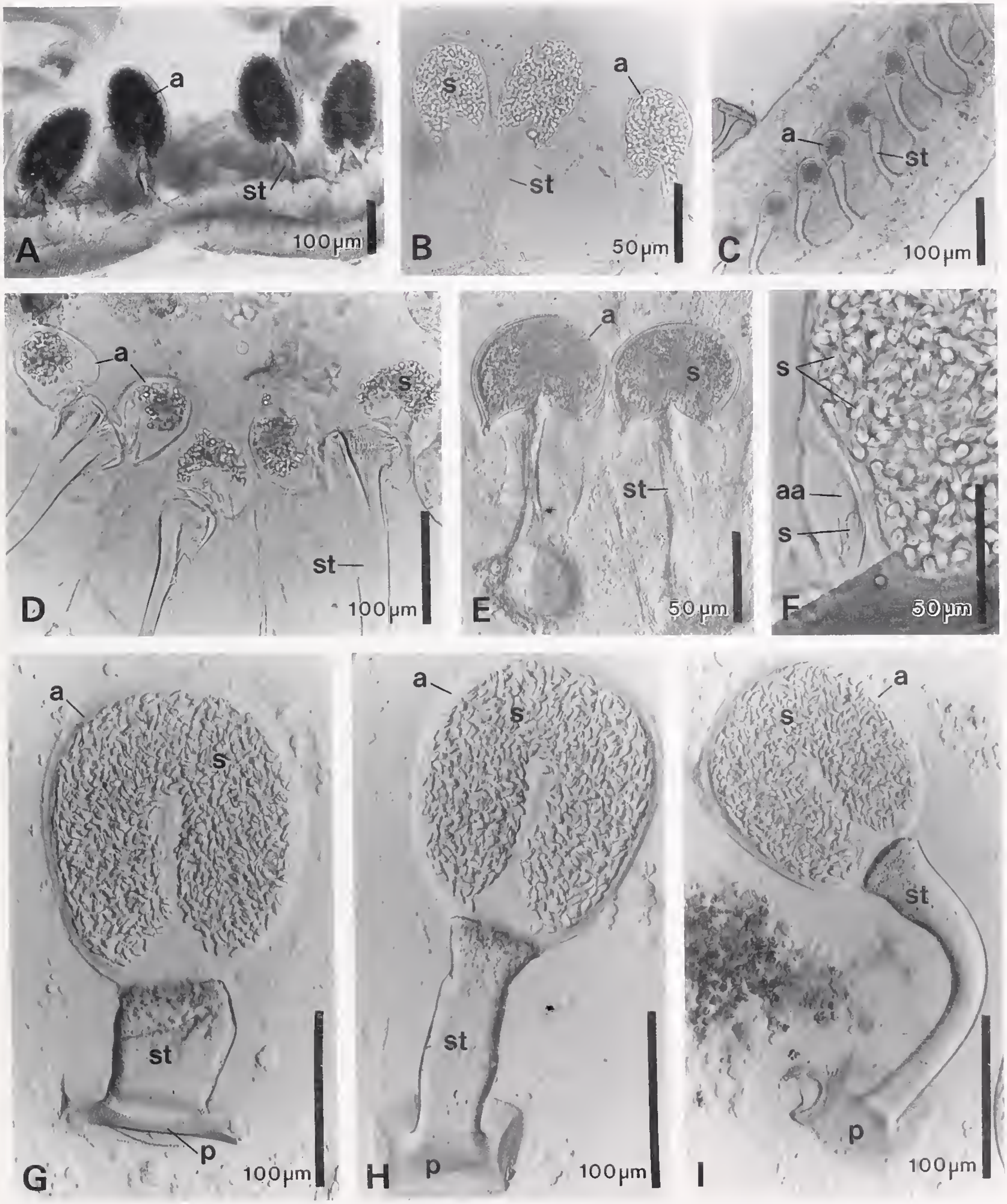
a
st
100µm
A
s
a
st
50µm
B
a
st
100µm
C
a
s
st
100µm
D
a
s
st
50µm
E
s
aa
s
50µm
F
a
s
st
p
100µm
G
a
s
st
p
100µm
H
a
s
st
p
100µm
I

Figure 2. Light micrographs of spermatophores of hermit crabs. (A) *Coenobita brevimanus* (Coenobitidae). (B) *Dardanus megistos* (Diogenidae). (C) *Calcinus latens* (Diogenidae). (D) *Dardanus lagopodes* (Diogenidae). Note the double-headed spermatophores. (E) *Clibanarius corallinus* (Diogenidae). (F) *Pagurus hirtimanus* (Paguridae). Detail of the accessory ampulla containing a single spermatozoa. (G–I) *Diogenes gardineri* (Diogenidae). Series of three micrographs from the proximal to the distal end of the vas deferens showing the progressive lengthening of the spermatophore stalk. a; ampulla, aa; accessory ampulla, p; pedestal, s; spermatozoa, st; stalk.

and described in this paper conforms with the general familial morphology (Fig. 1M). Pagurid spermatophores differ from those of the Coenobitidae and Diogenidae in three important ways:

1. Although considered pedunculate (Greenwood, 1972), the spermatophores of the Paguridae tend to have only a short stalk, which is often incorporated into the pedestal and gives the appearance of being non-pedunculate (Matthews, 1957). Greenwood (1972), following the terminology of Mouchet (1931), divided the vas deferens of the hermit crab, *Pagurus novizealandiae*, into nine discrete regions. The different musculature in each of the nine regions is responsible for fragmentation of the continuous sperm ribbon into spermatophores. The presence or absence of each of the nine regions dictates the form of the spermatophore in the Paguroidea. In the Paguridae, regions four and six (areas of stalk secretion and elongation respectively) are absent. This led Matthews (1957) to state that the spermatophores of members of the Paguridae were non-pedunculate. However, Greenwood (1972) found that there was a stalk in *Pagurus novizealandiae* but that is is moulded from the capsule sheath. He suggested that, in accordance with Mouchet's (1931) description of the spermatophores of other members of the Paguridae, a "pseudo-pedicule" forms the stalk in this family, which is analogous to the true stalk in the Coenobitidae and Diogenidae.
2. The ampullae are often elongate or cylindrical in nature and fairly large.
3. Most importantly, the spermatophores have a secondary, smaller ampulla, which is termed the accessory ampulla. This accessory ampulla is found at the base of the main ampulla and generally contains no spermatozoa, although one or two individual spermatozoa may be present (Fig. 3D). This accessory ampulla is formed by the vesiculation of the empty sperm column sheath that separates each of the developing main ampullae (Mouchet, 1931; Matthews, 1957). The rhythmic muscle contractions of the reproductive tract fold the continuous sperm column into partially closed arches filled with developing spermatozoa, with the compressed empty sperm column in between. In the Coenobitidae and Diogenidae the elongation of the stalk is sufficient to stretch this empty sperm column sheath and obscure it. Mouchet (1931) illustrated an accessory ampulla in the developing spermatophore of the diogenid *Paguristes oculatus*, but it is absent from the mature spermatophore. Because regions four and six are absent in the Paguridae, stalk elongation is not significant. The sperm column sheath is, therefore, not stretched, leaving an empty vesicle at the base of each main ampulla. Some spermatozoa may be sealed in this vesicle but their release, upon dehiscence of the main ampulla, is doubtful.

This process of stalk lengthening, whether there is a pseudo-stalk or a true stalk, occurs during maturation of all spermatophores of the Paguroidea, with the exception of *Trizopagurus maximus* and *Trizopagurus strigatus* (Matthews, 1957). If spermatophore morphology is to be compared between species, care must be taken to obtain only mature spermatophores from the most distal portion of the vas deferens or to use extruded spermatophores. Immature spermatophore morphology of one family may be consistent with the mature spermatophore form of another family. An example of this can be seen in Figure 2G–I, where the short stalked, immature spermatophore of *Diogenes gardineri* is reminiscent of a coenobitid type spermatophore, while the mature spermatophore from the distal vas deferens shows clearly its diogenid origins (Fig. 1L).

Spermatophore lateral ridge

The conspicuous lateral partition seen by Mouchet (1930) on the ampulla of the spermatophore of *Diogenes pugilator* and later by Hamon (1937) in a similar position for *Pagurus prideaux* (as *Eupagurus prideauxi*) was correctly identified by both workers as the joining line of the two halves of the ampulla. Hamon (1937) called this partition the "*ligne de suture*" and showed that it ran around the elongate spermatophore of *Pagurus prideaux* and was where the two halves of the ampulla separated to release the contained spermatozoa. Hamon also suggested two main mechanisms of spermatophore dehiscence: one being changes in internal pressure due to mechanical or osmotic forces and the other being the chemical dissolution of the suture that unites the two halves of the ampulla.

This suture line, or lateral ridge, has now been recorded in species from three paguroidean families, the Coenobitidae [*Birgus latro*, Tudge and Jamieson, 1991; present study (Fig. 3A); *Coenobita spinosus*, present study (Fig. 3C)], the Diogenidae [*Calcinus minutus*, *Clibanarius virescens*, present study (Figs. 3B, D); *Diogenes pugilator*, Mouchet, 1930], and the Paguridae (*Pagurus prideaux*, Hamon, 1937).

Light microscope studies using Mallory's staining techniques, scanning electron microscope studies (Fig. 3A), and transmission electron microscope studies (Fig. 3B, C) show that the lateral ridge is a thickening of the ampullar spermatophore wall. The spermatophore wall of *Coenobita spinosus* is fibrillar in nature, and at the lateral ridge there is a break in this structure (Fig. 3C). Although the ridge is structurally thicker than the remainder of the spermatophore wall, this gap in the fibrous matrix is a weakness where splitting of the two ampullar halves occurs. A similar break in the spermatophore wall structure is seen in *Clibanarius virescens* (Fig. 3B), but an external

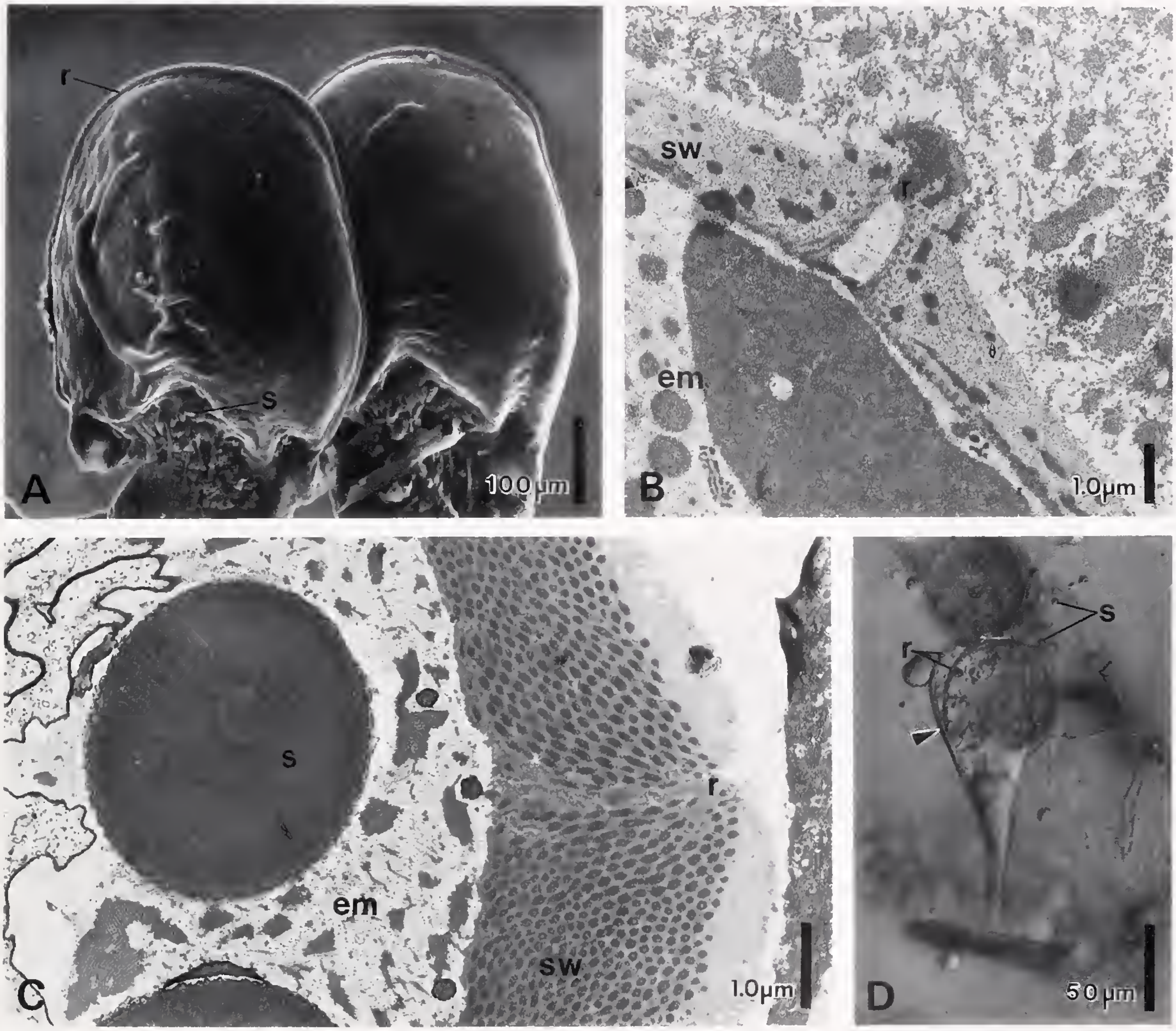

Figure 3. (A) *Birgus latro* (Coenobitidae). Scanning electron micrograph of two spermatophores showing conspicuous lateral ridge. (B and C) Transmission electron micrographs showing detail of the lateral ridge. (B) *Clibanarius virescens* (Diogenidae). Note the apparent plug of material in the lateral ridge. (C) *Coenobita spinosus* (Coenobitidae). (D) *Calcinus minutus* (Diogenidae). Light micrograph showing splitting of the spermatophore ampulla at the lateral ridge to release spermatozoa. (Arrow indicates the point of separation of the two ampullar halves). a: ampulla, em: extracellular matrix, r: lateral ridge, s: spermatozoa, sw: spermatophore wall.

plug appears to cement the two halves of the ampulla together in this species. Release of spermatozoa from the splitting lateral ridge of a spermatophore of *Calcinus minutus* is seen in Figure 3D.

Spermatophore morphology and modes of sperm transfer provide some clarification of systematic problems at familial and generic levels (Schaller, 1979; Bauer, 1986) and sometimes even at the specific level (Matthews, 1953, 1956). The phylogenetic value of spermatophore form and sperm transfer mode has been demonstrated in pseudoscorpions by Weygoldt (1966). One has to be cautious, however, in drawing homologies between species based on spermatophore form and modes of sperm transfer before the modes of formation, chemical nature, and ultrastructural morphology of the spermatophores in question have been studied in depth. Similarly, caution has to be exercised when phylogenetic hypotheses are formulated on limited data sets and small numbers of representatives from the selected taxa. Both Clark (1981) and Mann (1984) state that particular modes of sperm transfer used by organisms may be more directly influenced by the habitat of those organisms than the phy-

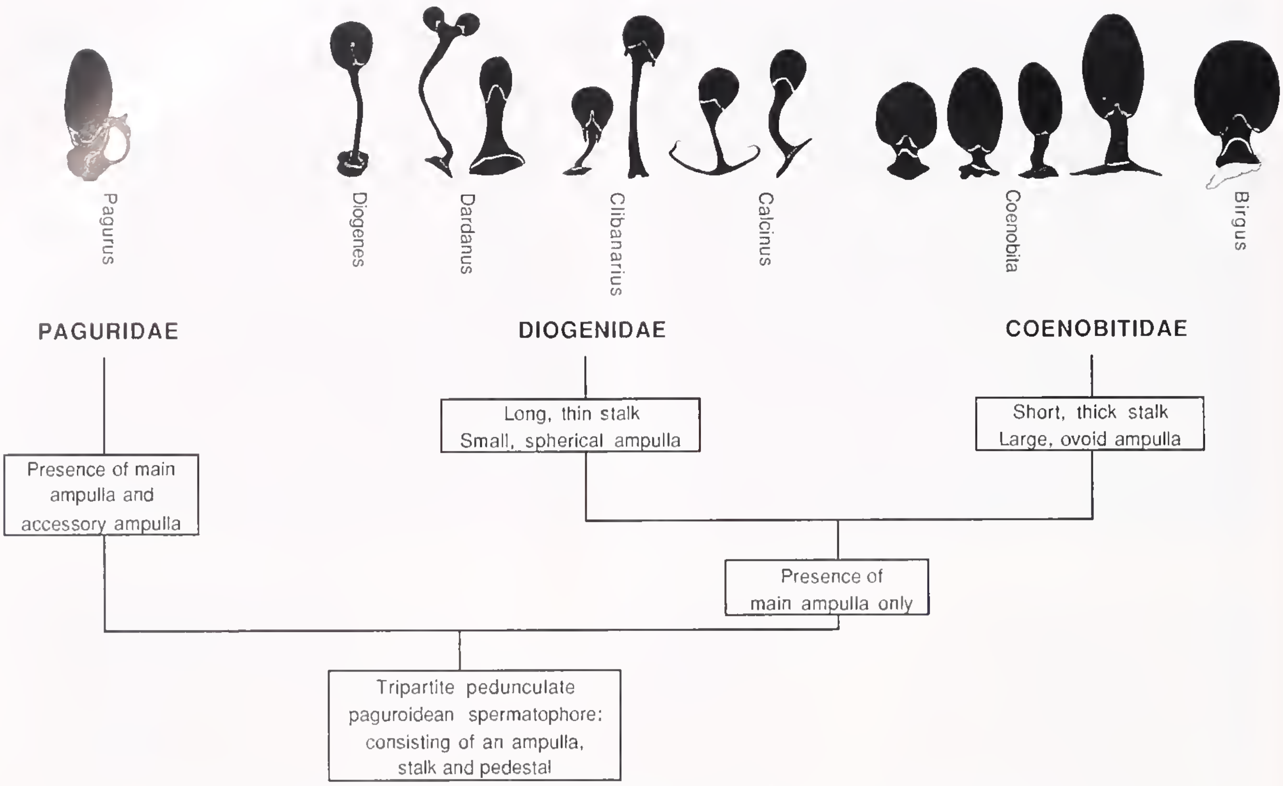
Pagurus
Diogenes
Dardanus
Clibanarius
Calcinus
Coenobita
Birgus
PAGURIDAE
DIOGENIDAE
COENOBITIDAE
Long, thin stalk
Small, spherical ampulla
Short, thick stalk
Large, ovoid ampulla
Presence of main ampulla and accessory ampulla
Presence of main ampulla only
Tripartite pedunculate paguroidean spermatophore: consisting of an ampulla, stalk and pedestal

Figure 4. A branching key to classify the investigated hermit crabs into their respective family based on the structure of their spermatophores. Spermatophores not to scale.

logenetic relationships. It seems very likely that both habitat and phylogeny influence spermatophore morphology of any particular taxa. For example, in the Coenobitidae, the move to a semi-terrestrial or terrestrial lifestyle from a marine one may have influenced the shape of the spermatophores of the species concerned, but the over-all tripartite, pedunculate spermatophore plan is phylogenetically set.

In the Paguroidea, light microscope observations of spermatophores can be used successfully to distinguish the three separate families and possibly even apply at the generic level, but more species will have to be studied to be confident at a specific level. Some exceptions have been recorded, as in the case of *Cestopagurus timidus* (Mouchet, 1931, as *Eupagurus timidus*), in which a pagurid was recorded as possessing a diogenid type spermatophore morphology. As spermatophore studies widen to include more species and even other families, further confirmation or contradiction to this system will undoubtedly occur. A simple key (not intended as a phylogeny), in branching form (Fig. 4), is presented here and can be used to classify the currently investigated hermit crabs to the family level based on gross spermatophore morphology.

Acknowledgments

I wish to acknowledge the assistance of Mr. S. Lavery for supplying the SW Pacific specimens and Mr. S. Fitzsimmons for helping to collect on Heron Island. Many thanks to Mr. S. Cook (Queensland Museum) and Dr. G. Morgan (Western Australian Museum) for identifying many of the species, and to Mrs. L. Daddow (Zoology Department, University of Queensland) and Mr. D. Waddell (Electron Microscope Centre, University of Queensland) for valuable technical assistance. I also wish to acknowledge the help of the staff at Heron Island Research Station, Great Barrier Reef, Queensland. The helpful and constructive suggestions of the reviewers were also greatly appreciated.

Literature Cited

Bauer, R. T. 1986. Phylogenetic trends in sperm transfer and storage complexity in decapod crustaceans. *J. Crust. Biol.* **6:** 313–325.

Bauer, R. T. 1991. Sperm transfer and storage structures in penaeoid shrimps. A functional and phylogenetic perspective. Pp. 183–207 in *Crustacean Sexual Biology*, R. T. Bauer and J. W. Martin, eds. Columbia University Press, New York.

Chevaillier, P. 1970. Recherches sur la structure et les constituants chimiques des cellules germinales mâles des Crustacés Décapodes. Doctor of Science Thesis, University of Rennes, Rennes, France.

Chow, S., Y. Taki, and Y. Ogasawara. 1989. Homologous functional structure and origin of the spermatophores in six palaemonid shrimps (Decapoda, Caridea). *Crustaceana* **57:** 247–252.

Clark, W. C. 1981. Sperm transfer mechanisms: some correlates and consequences. *N. Z. J. Zool.* **8:** 49–65.

Dudenhausen, E. E., and P. Talbot. 1983. An ultrastructural comparison of soft and hardened spermatophores from the crayfish *Pacifastacus leniusculus* Dana. *Can. J. Zool.* **61:** 182–194.

Greenwood, J. G. 1972. The male reproductive system and spermatophore formation in *Pagurus novae-zealandiae* (Dana) (Anomura: Paguridea). *J. Nat. Hist.* **6:** 561–574.

Hamon, M. 1937. Les mécanismes produisant la déhiscence des spermatophores d' *Eupagurus prideauxi* Leach. *C. R. Acad. Sci. (Paris)* **204:** 1504–1506.

Helfman, G. S. 1977. Copulatory behaviour of the coconut or robber crab *Birgus latro* (L.) (Decapoda, Anomura, Paguridea, Coenobitidae). *Crustaceana* **33:** 198–202.

Hinsch, G. W. 1991. Structure and chemical content of the spermatophores and seminal fluid of reptantian decapods. Pp. 290–307 in *Crustacean Sexual Biology,* R. T. Bauer and J. W. Martin, eds. Columbia University Press, New York.

Jeyalectumie, C., and T. Subramoniam. 1989. Cryopreservation of spermatophores and seminal plasma of the edible crab *Scylla serrata. Biol. Bull.* **177:** 247–253.

Mallory, F. B. 1936. The anilin blue collagen stain. *Stain Technol.* **11:** 101–102.

Mann, T. 1984. *Spermatophores: Development, Structure, Biochemical Attributes and Role in the Transfer of Spermatozoa.* Springer-Verlag, Berlin

Matthews, D. C. 1953. The development of the pedunculate spermatophore of a hermit crab, *Dardanus asper* (De Haan). *Pac. Sci.* **7:** 255–266.

Matthews, D. C. 1956. The probable method of fertilization in terrestrial hermit crabs based on a comparative study of spermatophores. *Pac. Sci.* **10:** 303–309.

Matthews, D. C. 1957. Further evidences of anomuran non-pedunculate spermatophores. *Pac. Sci.* **11:** 380–385.

McLaughlin, P. A. 1983. Hermit crabs—are they really polyphyletic? *J. Crust. Biol.* **3:** 608–621.

Mouchet, S. 1930. Mode de formation des spermatophores chez quelques Pagures. *C. R. Acad. Sci. (Paris)* **190:** 691–692.

Mouchet, S. 1931. Spermatophores des Crustacés Décapodes Anomoures et Brachyoures et castration parasitaire chez quelques Pagures. *Annal. Stat. Océanogr. Salammbô* **6:** 1–203.

Reynolds, E. S. 1963. The use of lead citrate at high pH as an electron opaque stain in electron microscopy. *J. Cell Biol.* **17:** 208–212.

Schaller, F. 1979. Significance of sperm transfer and formation of spermatophores in arthropod phylogeny. Pp. 587–608 in *Arthropod Phylogeny,* A. P. Gupta, ed. Van Nostrand Reinhold Company, New York.

Spurr, A. R. 1969. A low viscosity epoxy-resin embedding medium for electron microscopy. *J. Ultrastruct. Res.* **26:** 31–43.

Subramoniam, T. 1991. Chemical composition of spermatophores in decapod crustaceans. Pp. 308–321 in *Crustacean Sexual Biology,* R. T. Bauer and J. W. Martin, eds. Columbia University Press, New York.

Tudge, C. C., and B. G. M. Jamieson. 1991. Ultrastructure of the mature spermatozoa of the coconut crab *Birgus latro* (L.) (Coenobitidae, Paguroidea, Decapoda). *Mar. Biol.* **108:** 395–402.

Weygoldt, P. 1966. Vergleichende Untersuchungen zur Fortpflanzungsbiologie der Pseudoskorpione. Beobachtungen über das Verhalten, die Samenübertragungsweisen und die Spermatophoren einiger einheimischer Arten. *Z. Morphol. Oekol. Tiere* **56:** 39–92.

Reference: *Biol. Bull.* **181:** 248–260. (October, 1991)

Coexistence of Hydroid Eating Nudibranchs: Do Feeding Biology and Habitat Use Matter?

WALTER J. LAMBERT

Department of Zoology, University of New Hampshire, Durham, New Hampshire 03824

Abstract. The feeding biologies and habitats of four nudibranchs in colonies of the hydroid *Obelia geniculata* were investigated to determine whether these factors contribute to the coexistence of the nudibranchs. The radulae and feeding behaviors showed species-specific traits. *Dendronotus frondosus* has a multi-seriate radula; when small (<5 mm), individuals are suctorial feeders, whereas larger nudibranchs (>5 mm), bite whole polyps. *Doto coronata* uses a flat, uniseriate radula to penetrate stolons. *Eubranchus exiguus* penetrates hydrothecae with a triseriate radula. *Tergipes tergipes* has a curved, uniseriate radula and rakes naked tissue.

Each species of nudibranch occupied a distinct area within the hydroid colony, suggesting that the micro-habitats are dictated by feeding biology. *D. frondosus* occupies hydrocauli towards the center of the colony, *D. coronata* occurs along the edge of the colony on the kelp surface, *E. exiguus* is found on hydrocauli at the edge of the colony, and *T. tergipes* sits atop tall hydrocauli in the center of the colony.

Separation in the hydroid food resource exists among these nudibranchs and equilibrial coexistence could have operated, but equilibrial conditions necessary for exclusion are unlikely to occur or persist significantly long. Thus, this assemblage of nudibranchs appears structured by non-equilibrial processes perhaps similar to populations of phytophagous insects.

Introduction

In aquatic environments, the coexistence of sessile species has received much attention (Osman, 1978; Jackson, 1984; Keough, 1984; McGuinness and Underwood, 1986; Ojeda and Dearborn, 1989) where most studies are examples of pre-emptive or overgrowth competition of clonal invertebrates (Schoener, 1983). The co-occurrence of motile invertebrates in epifaunal and algal communities is well documented (Edgar, 1983; Coyer, 1984; Virnstein and Howard, 1987; Hall and Bell, 1988), but the mechanisms allowing their coexistence are generally unknown (Seed, 1986). Although variability in diet (Nybakken and Eastman, 1977; Shonman and Nybakken, 1978; Fernandez *et al.*, 1988), radular structure (Bloom, 1976; Blinn *et al.*, 1989), feeding behavior (Hawkins *et al.*, 1989), habitat preference (Bloom, 1981) and temporal appearance on the food resource (Yoshioka, 1986) provides explanations for the coexistence of epifaunal gastropod predators, little is known of the relationship of co-occurring nudibranchs in hydroid colonies (Todd, 1981).

The majority of nudibranchs in the Gulf of Maine prey on hydroids (Meyer, 1971; Clark, 1975; Lambert, 1985). Often nudibranchs demonstrate considerable overlap in their distribution with many nudibranch species feeding in the same hydroid colony (Kuzirian, 1979). Coexistence in these hydroid colonies may be mediated by differences in habitat or food, but the underlying mechanisms are unknown.

The hydroid *Obelia geniculata* grows epiphytically on laminarian kelps, often covering the entire blade surface. Four species of nudibranchs (*Dendronotus frondosus, Doto coronata, Eubranchus exiguus,* and *Tergipes tergipes*) inhabit these colonies sympatrically. Their spatial distribution within the colony suggests a separation in their use of the hydroid as food and micro-habitat. This study focuses on the feeding biology and micro-habitat use of those nudibranchs inhabiting colonies of *O. geniculata.* For each nudibranch species the following parameters are described: morphology of the radula, feeding behavior, and location within the hydroid colony. Skeletal morphology of the hydroid prey is also described. Differences

Received 29 October 1990; accepted 13 May 1991.

in trophic morphology and feeding mechanisms among predators may reflect the diets of these predators within hydroid colonies. The possibility that differences in feeding biology and habitat use help facilitate coexistence among these nudibranchs is considered.

Materials and Methods

Collection of animals

Nudibranchs and colonies of *Obelia geniculata* were collected from a shallow (4–10 m), kelp bed at Cape Neddick, York, Maine, (43° 10′ N, 70° 36′ W) from September, 1988, to September, 1989. Kelp blades (*Laminaria saccharina* and *L. digitata*) were examined underwater for nudibranchs, individually placed in plastic bags, and brought to the lab. In the lab, four species of nudibranchs (*Dendronotus frondosus, Doto coronata, Eubranchus exiguus,* and *Tergipes tergipes*) were isolated from the hydroid colonies, sized to the nearest mm with a dissecting microscope, and separated for different parts of the study.

Analysis of radulae

Radulae from four individuals each of *D. frondosus, D. coronata,* and *E. exiguus* and seven individuals of *T. tergipes* were examined. Entire animals were dissolved in 10% NaOH for 10–12 h. The radulae were then teased free and placed into 70% ethanol until they were mounted for scanning electron microscopy (SEM). Clean radulae were mounted onto glass coverslips in a drop of distilled water and allowed to air-dry. They were sputter coated with a 200–300 Å coating of Au/Pd and viewed with an AMR 1000 Scanning Electron Microscope at 20 kV.

Six parameters from three tooth rows from the center of each radula were quantified for each species; the aim was to characterize the morphology of the radula from each nudibranch species. From a dorsal perspective, the width (μm) of the radula and the length (μm) and width (μm) of the rachidian tooth were measured and the denticles on one side of the rachidian tooth were counted (Fig. 1A). The rake angle and curvature of the radula were measured from a lateral view (Fig. 1B). The rake angle (defined as the angle of the radula to the feeding surface when protruded from the mouth) was measured as the angle made from the tip of the rachidian tooth to the base of the tooth row. Curvature is the degree of hook or the amount of concavity along the inner margin of the radula (Bloom, 1976). Curvature was measured as the ratio between the height of the concavity along the inner margin of the rachidian tooth and the length of the rachidian tooth. All length measurements and angles were obtained from the SEM photos with a digitizing tablet.

A multivariate analysis of variance (MANOVA) was used to test the null hypothesis that no morphological differences in radular structure existed among the nudibranchs (Harris, 1985). Data were ln (x + 1) and square root (x + 0.5) transformed to correct for non-normality and heteroscedastic variances (Zar, 1984).

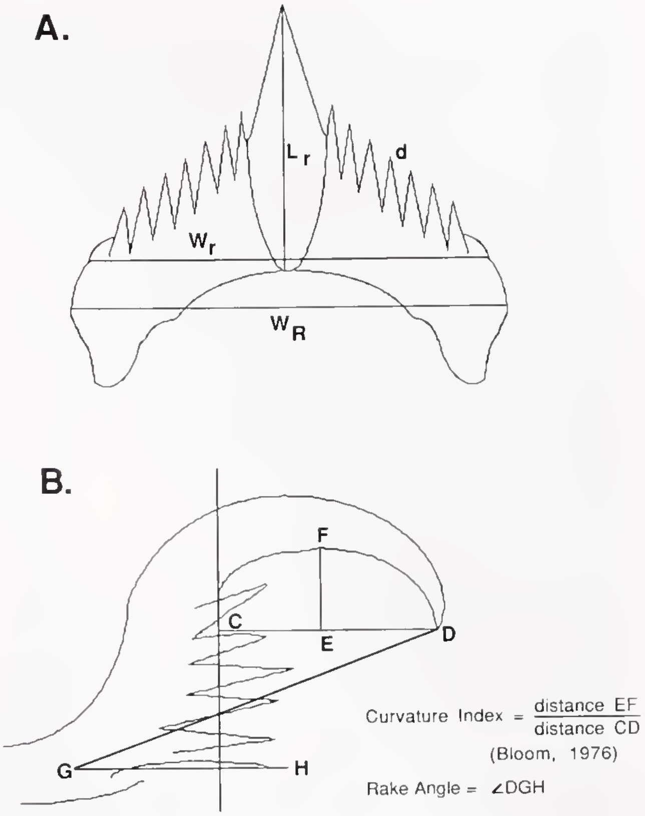
A.
L_r
d
W_r
W_R
B.
F
C
E
D
G
H
Curvature Index = $\frac{\text{distance EF}}{\text{distance CD}}$
(Bloom, 1976)
Rake Angle = ∠DGH

Figure 1. Drawings of a radula tooth from a (A.) dorsal and (B.) lateral perspective. Schematics show the measurements made to quantify radular structure. (W_R = width of radula, W_r = width of rachidian tooth, L_r = length of rachidian tooth, d = denticles.)

Feeding behavior and feeding damage

Feeding mechanisms were identified for each species of nudibranch. Nudibranchs were starved overnight and were then placed in 10 cm (diameter) stacking dishes containing kelp blades covered with *O. geniculata.* The feeding behaviors of each nudibranch were observed with a stereo microscope during a minimum of six feeding sessions. A feeding session consisted of approach, attack, manipulation, and consumption of the hydroid prey, and a session was considered complete when the nudibranch retreated from the polyp or stolon it had been eating.

Portions of hydroids that had been manipulated were collected from the colony as the nudibranchs were feeding. Where possible, the pieces of stolon were cut 0.5 cm from a site of feeding and lifted from the kelp surface. If the stolon could not be easily removed, the kelp itself was cut so that the feeding area could be obtained. Uprights were also removed from the colony after having been fed upon by nudibranchs. Hydroid skeletal pieces that had been fed upon were taken from each nudibranch species except *T. tergipes*, which feeds on naked tissue. All hydroid pieces were preserved in 2.5% phosphate buffered glutaraldehyde for 1–2 h and then stored in 70% ethanol. For SEM, the tissues were dehydrated through a graded ethanol series and placed in hexamethyldisilizane (HMDS) for final drying (Nation, 1983). Skeletons were mounted on stainless steel stubs with double-stick tape and coated as described for the radulae. The dimensions of the holes produced by the nudibranchs were measured on SEM photos with a digitizing tablet.

Nudibranch habitats

Hydroids with their nudibranchs were placed in flowing seawater and examined within 24 h. The location of each nudibranch within its colony was determined and quantified by four habitat parameters: (a) height of the nudibranch above the kelp surface (mm), (b) density of hydrocauli around the nudibranch (number/2.25 cm^2), (c) mean height (mm) of hydrocauli ($n = 5$) within a 2.25 cm^2 area around the nudibranch, and (d) the distance (cm) between the nudibranch and the closest edge of its colony.

Habitat parameters were analyzed with a MANOVA (H_0: nudibranch habitats do not differ within colonies of *Obelia geniculata*). Habitat data were ln $(x + 1)$ and reciprocal $(x + 1)$ transformed (Zar, 1984; Krebs, 1989) to meet the assumptions of analysis of variance.

Perisarc analysis

Five stolons and hydrocauli were isolated from the central and peripheral (outer 2 cm) portions of five colonies of *O. geniculata* and fixed overnight in Bouin's solution. After being washed in 50% ethanol, the pieces were dehydrated, stained with acid fuchsin, embedded in paraffin, and sectioned. The perisarc was stained with Lugol's solution (Lillie, 1954) according to procedures adapted from Drury and Wallington (1980). Thickness (μm) of the perisarc of stolons, hydrocauli, and theca from each area of the colony were measured with an ocular micrometer.

A two-way analysis of variance was used to compare the thickness of perisarcs from the center and the periphery of the hydroid colony. Data were log transformed to stabilize variances. A Tukey-Kramer HSD multiple comparison test was used to test comparisons of interest among structures within and between areas of the colony (Zar, 1984; Day and Quinn, 1989).

Results

Structure of the radulae

The radulae of the four nudibranch species differed statistically in the six parameters measured (Table I). Only the radula of *Tergipes tergipes* was curved; the others had no hook. The radula is an important taxonomic character for opisthobranchs (Thompson and Brown, 1984) and varied little among the individuals of a species.

Dendronotus frondosus had a wide (X ± SE = 157.70 ± 4.51 μm), multiseriate radula with 5–9 lateral teeth flanking the rachidian tooth (Fig. 2a). The rachidian tooth (width = 39.36 ± 1.01 μm, length = 29.93 ± 1.33 μm) was triangular with 9–11 small, lateral denticles. Each lateral tooth had a single cusp and 3–5 denticles. The rake angle was wide (58.2° ± 2.8) (Fig. 2b).

The uniseriate radula of *Doto coronata* was narrow (17.80 ± 0.25 μm) (Fig. 2c). The rachidian tooth was short and stubby (width = 17.73 ± 0.26 μm, length = 7.78 ± 0.36 μm) with 3–4 large lateral denticles on each side. The central denticle of the rachidian tooth was depressed, making the dorsal surface of the radula concave. The rake angle was narrow (21.6° ± 1.0) (Fig. 2d).

Eubranchus exiguus had a wide (103.70 ± 3.87 μm), triseriate radula (Fig. 3a). A single lateral tooth flanked the rachidian tooth. The rachidian tooth was long and thin (width = 28.62 ± 2.80 μm, length = 22.71 ± 0.60 μm) with 3–7 large denticles on each side; it appeared rake-like. The lateral teeth were wide at their base and tapered sharply to a thin, narrow, single cusp. The rake angle was moderately wide (36.5° ± 1.9) (Fig. 3b).

Tergipes tergipes had a narrow (34.99 ± 2.29 μm), uniseriate radula (Fig. 3c) with a short, wide rachidian tooth (width = 30.84 ± 2.19 μm, length = 19.50 ± 1.09 μm) that bore a prominent central denticle and 5–10 large, lateral denticles. The central denticle was approximately two times longer than the lateral denticles and had a nar-

Table I

*Analyses of variance of parameters of radular structure for the four species of nudibranchs (*Dendronotus frondosus, Doto coronata, Eubranchus exiguus *and* Tergipes tergipes*)*

Variable	df	F	*P*
ln W_R	3, 53	397.356	<0.001
ln W_r	3, 53	56.743	<0.001
ln L_r	3, 53	83.263	<0.001
Sqr(denticles)	3, 53	94.119	<0.001
Angle	3, 53	3882.190	<0.001

Model: ln W_R, ln W_r, ln L_r, sqr denticles, angle = constant + species of nudibranch. (MANOVA: Pillai Trace = 2.328, $P < 0.001$) (sqr = square root).

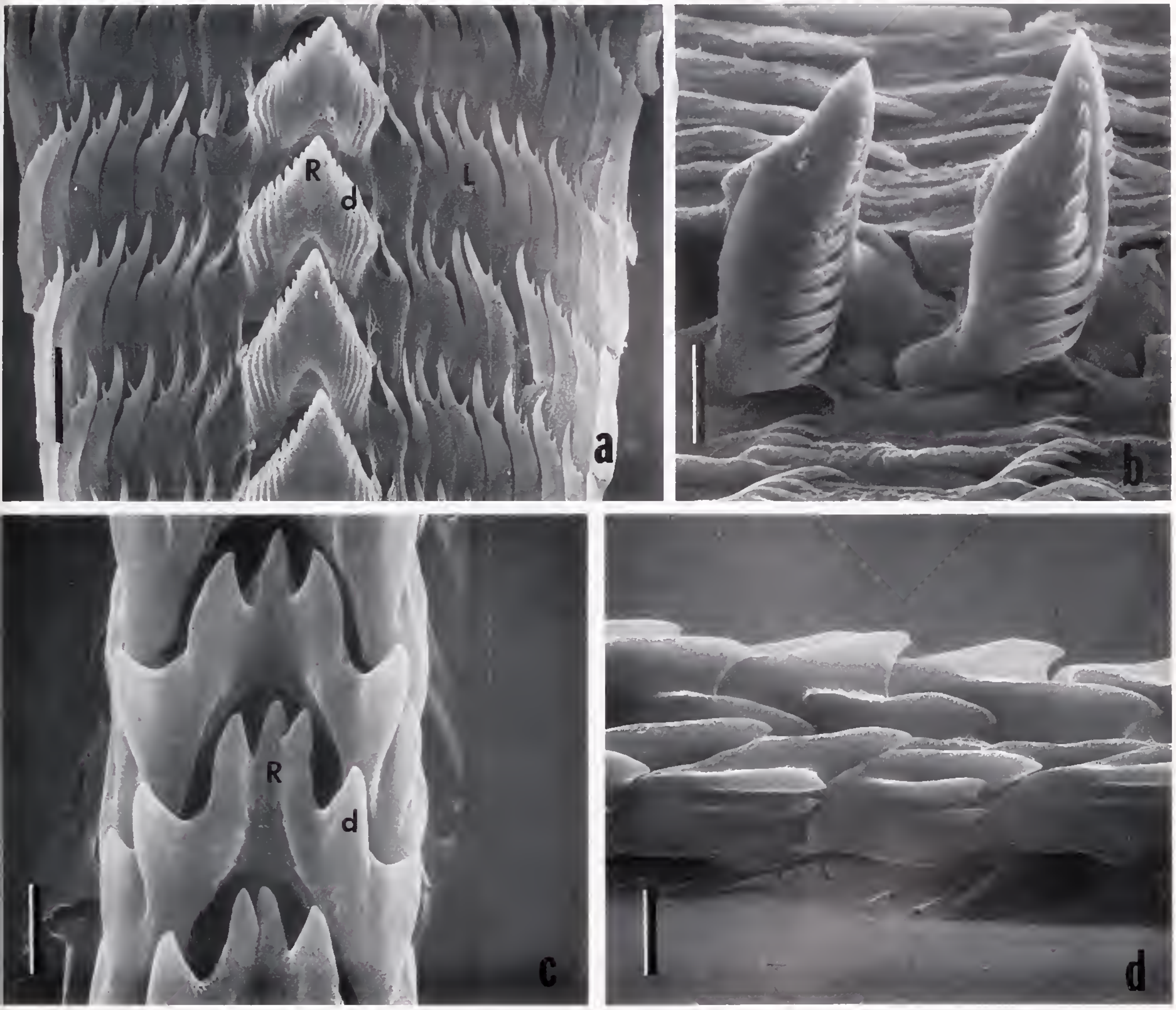

Figure 2. Scanning electron micrographs of radulae from *Dendronotus frondosus* (size = 4 mm) (a, b) and *Doto coronata* (size = 5 mm) (c, d) from a dorsal (a, c) and lateral (b, d) view. Scale bars: a = 20 μm, b = 15 μm, c, d = 5 μm. (d = denticles, L = lateral teeth, R = rachidian tooth.)

row rake angle (22.5° ± 1.9) (Fig. 3d, e). The radula of *T. tergipes* was the only one with a hook. The curvature index for all 21 tooth rows examined was 0.293, but there was considerable variation (SE = 0.04). Some of this variability could have occurred when the radulae were dried for viewing with the SEM.

Feeding behavior

Species specific behaviors for handling and consuming hydroid prey were observed in feeding nudibranchs; feeding behaviors among conspecifics varied little.

Depending upon their size, *D. frondosus* showed one of two feeding mechanisms; small individuals were suctorial feeders, whereas large individuals were polyp biters. Individuals less than 5 mm long (n = 7) penetrated the perisarc of thecae and stolons by scraping with the radula; they then grasped the hydroid with the anterior portion of their foot and sucked the tissue out. The average time required to penetrate a theca was 4.2 min (SE = 2.9). Once a hole had been made, suction created by the buccal apparatus served to draw out either the hydranth from a hydrotheca, or the juvenile medusae from a gonotheca.

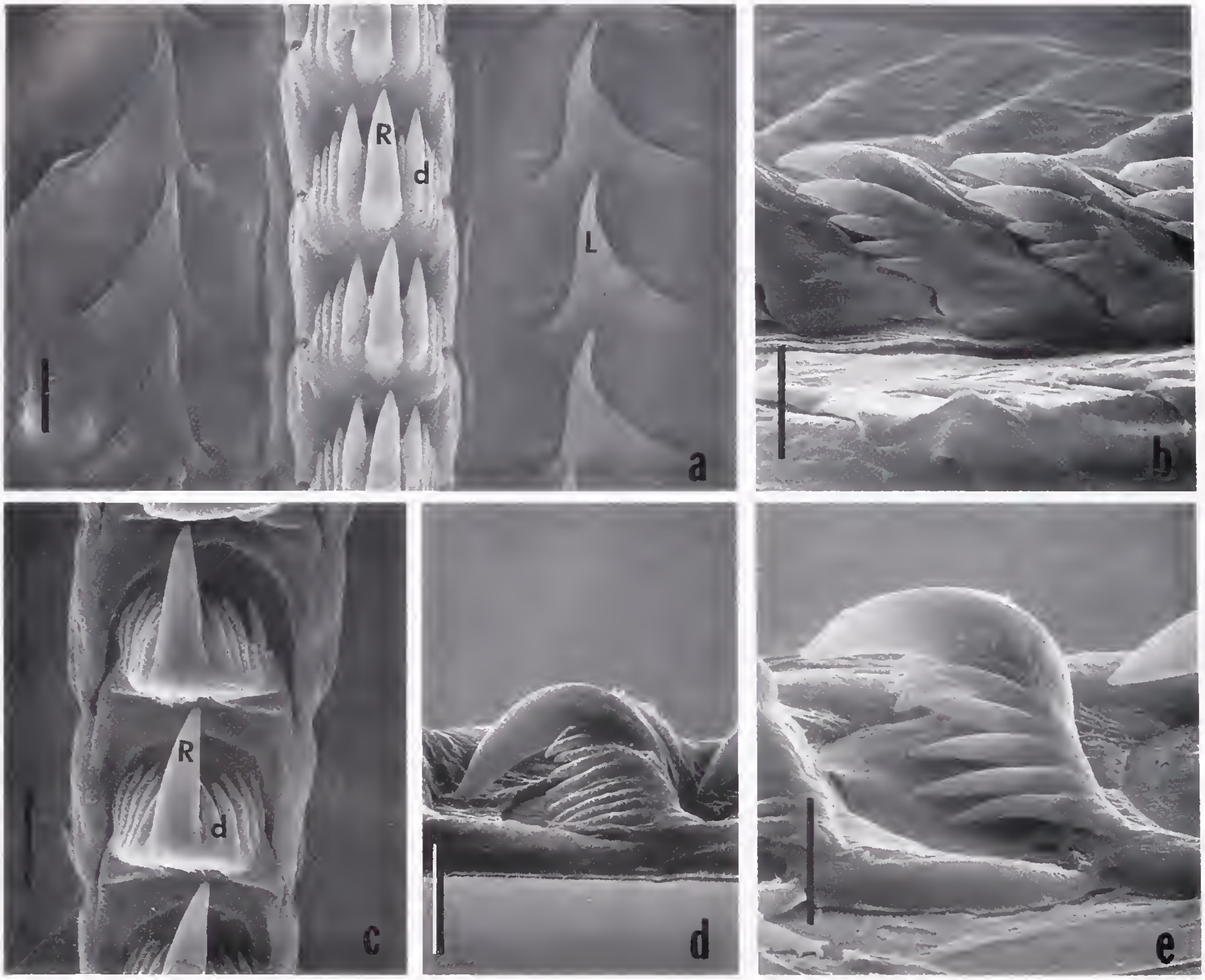

Figure 3. Scanning electron micrographs of radulae from *Eubranchus exiguus* (size = 4 mm) (a, b) and *Tergipes tergipes* (size = 4 mm) (c, d, e) from a dorsal (a, c) and lateral (b, d, e) view. Scale bars: a, b, c, d = 10 μm, e = 15 μm. (d = denticles, L = lateral teeth, R = rachidian tooth.)

When feeding on gonangia, the nudibranchs plucked individual, juvenile medusae from the bottom of the gonotheca. On stolons, tissue was extracted by a few, quick pulses of the buccal apparatus.

Dendronotus frondosus individuals greater than 5 mm were polyp biters or grabbers. The nudibranchs would crawl up a hydrocaulus and lightly contact the tentacles of an exposed hydranth with the anterior portion of the foot and mouth. Both suctorial and grasping mechanisms were used to consume polyps. Although the radula was everted from the mouth, it did not contact a polyp (n = 14). As buccal activity created a suction that pulled the polyp towards the nudibranch's mouth, the jaws were protruded, and the polyp was clipped off at its base leaving only the annuli. A nudibranch would continue in this manner along a hydrocaulus following the alternating pattern of polyp branching, feeding at a rate of 1–2 polyps per minute over a 5-min observation period (n = 6).

Doto coronata was a suctorial feeder preying predominantly on the stolons of *Obelia geniculata.* The nudibranch clutched a stolon with the anterior portion of the foot to bring the mouth against the stolon. The anterior portion of the foot flattened against the stolon during buccal activity, suggesting that the nudibranch was exerting additional pressure to assist in penetration. When a hole was produced through the perisarc, coenosarc was drawn into the animal's mouth. Tissue moved unidirectionally toward the mouth of the nudibranch in pulses that coincided with pulses of the buccal apparatus. Perisarc was penetrated by rasping with the radula. Drill holes produced by *D. coronata* of 4–5 mm were round, with a diameter of 35.7 μm (SE = 4.8) (Fig. 4). The holes had beveled sides with grooves corresponding to the denticles of the rachidian tooth. A raised lip around the perimeter of the holes was distinct from the perisarc and is either coenosarc of the hydroid or mucous produced by glands in the foot of the nudibranch. Incomplete holes (Fig. 4c, d) had a jagged or deteriorated perisarc at their center.

The time to penetrate a stolon by *D. coronata* was difficult to determine. A hole was considered complete when the coenosarc was drawn toward the nudibranch. It was common for an individual nudibranch to position itself atop a portion of stolon for 4–6 h. During any single hour, several periods of buccal activity alternated with longer periods of apparent inactivity. The periods of buccal activity were short, usually 1–3 min with up to 15 min between sets of buccal pulses. Penetration took a minimum of 1 h, but averaged 3.3 h (SE = 1.2, n = 6).

Eubranchus exiguus was also a suctorial feeder, but fed only through the perisarc of hydrothecae. Nudibranchs grasped the base of a theca with the anterior portion of the foot, thus bringing their mouths against the perisarc. The radula scraped the thecal surface creating a hole in 15–30 s, and the entire hydranth was drawn out through the base. The nudibranch left when all tissue was removed. Penetration and consumption of the first polyp took 1–2 min (SE = 10.6 s), but each successive polyp eaten took longer to consume.

The penetration hole produced by *E. exiguus* was elliptical (Fig. 5). The sides of the holes were jagged and the perisarc appeared ripped, rather than worn or scraped as in holes in stolons produced by *D. coronata* (Fig. 4). The width of the hole at its center and widest point (X ± SE = 8.00 ± 1.07 μm) was similar to the width of the top three denticles on the rachidian tooth (6.46 ± 0.48 μm). The lateral teeth on radulae of *E. exiguus* were not observed contacting the thecal perisarc during the feeding process.

Tergipes tergipes did not penetrate the perisarc, but attacked naked tissue. Small individuals (<4 mm) placed their mouths atop a polyp and rasped tissue directly from the area around the hypostome. If the hydranth was re-

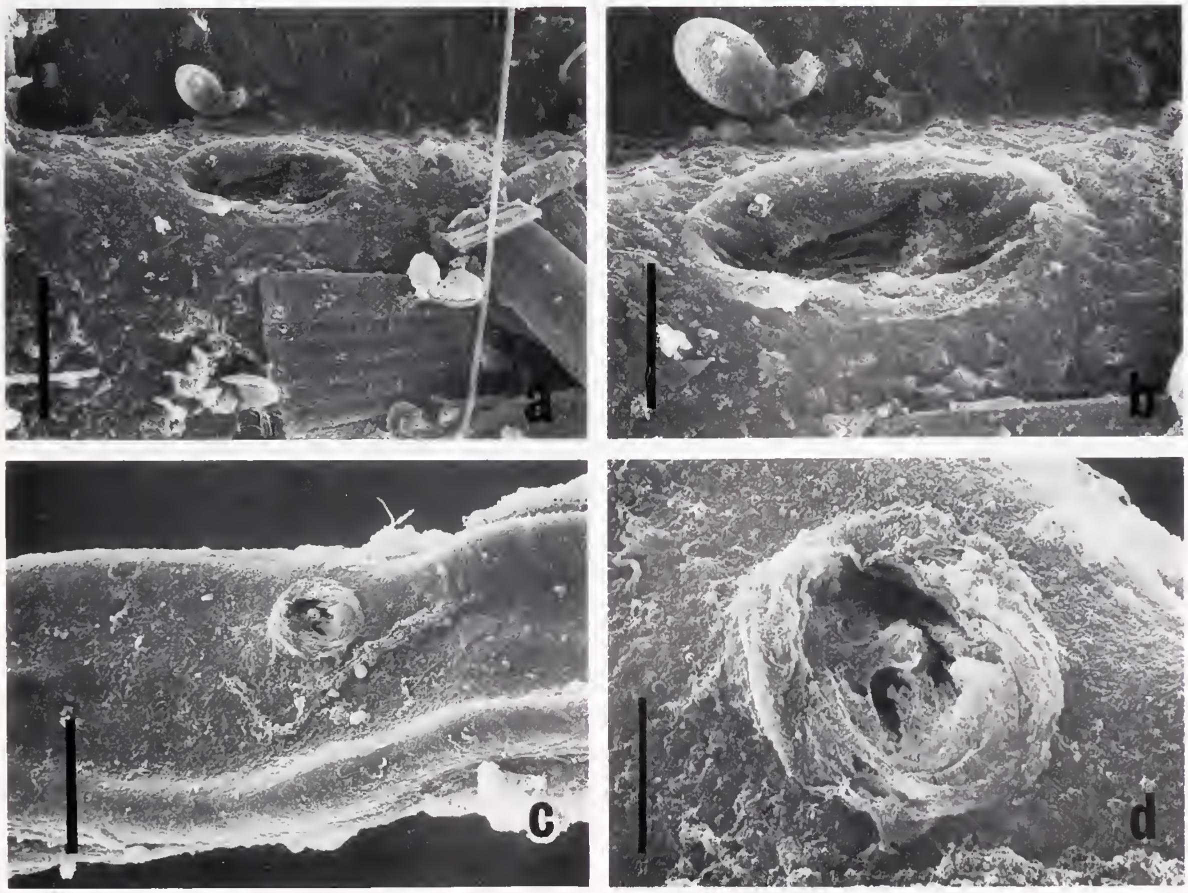

Figure 4. Scanning electron micrographs of stolons of *Obelia geniculata* showing drill holes produced by *Doto coronata* during feeding. Scale bars: a, c = 50 μm, b, d = 20 μm.

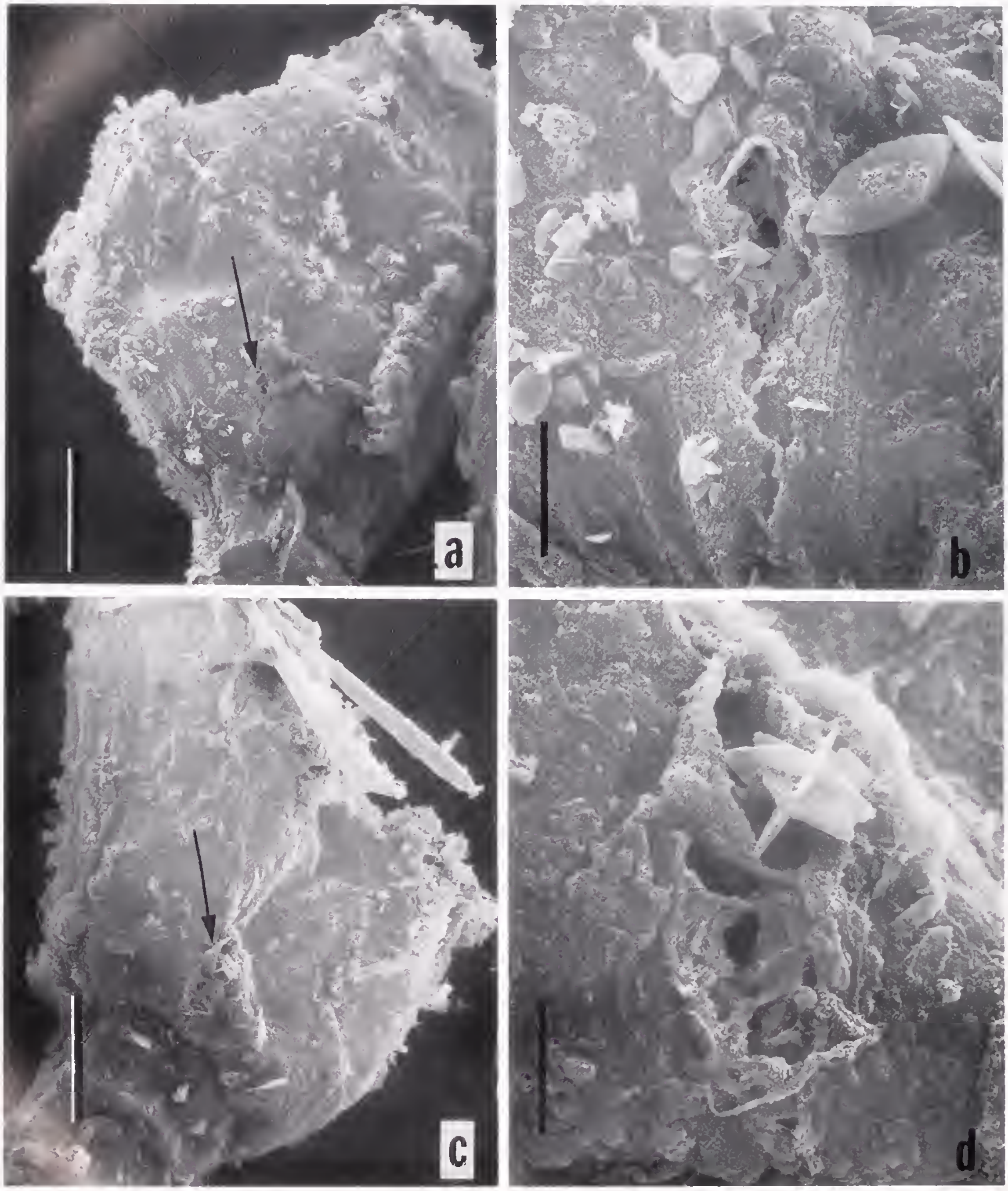

Figure 5. Scanning electron micrographs of hydrothecae of *Obelia geniculata* showing penetration holes produced by *Eubranchus exiguus* during feeding. In a and c the arrow points to the area of damage; b, d are magnifications of these areas. Scale bars: a, c = 50 μm, b, d = 10 μm.

tracted into the theca, the nudibranch curled its body over the thecal rim to reach the polyp tissue. Very small individuals (<1 mm) crawled into hydrothecae to feed upon polyps. While direct observations clarified the use of the radula in raking tissue from the polyp, it was not determined whether the jaws were also used. Small individuals (n = 5) of *T. tergipes* required up to 2 h to consume an entire polyp (75 ± 45 min).

Larger individuals (>3 mm) of *T. tergipes* (n = 8) either ripped the entire polyp from a hydrotheca or cropped tentacles. Each process was very rapid compared to the slow rasping of smaller *T. tergipes*. The approach to a

Table II

Analysis of variance table testing the relationship between habitat parameters of nudibranchs in colonies of Obelia geniculata *and species of nudibranch (MANOVA: Pillai Trace = 0.510, $P < 0.001$)*

Variable	df	F	*P*
Inverse height	3, 358	51.983	<0.001
Mean height	3, 358	11.115	<0.001
ln density	3, 358	8.827	<0.001
ln distance from edge	3, 358	13.981	<0.001

Model: Inverse (height on an hydrocaulus + 1), Mean height of hydrocauli, ln (density of hydrocauli around a nudibranch + 1), ln (distance from the edge of the colony + 1) = constant + species.

polyp, consumption of the polyp, and departure from the branch took as little as 60 s (150 ± 75 s), and one individual ate 60–80% of a whorl of tentacles on a polyp in 25–30 s.

Habitats of nudibranchs

Sizes of *D. frondosus*, *D. coronata*, and *E. exiguus* were not significantly related to the four habitat parameters measured. However, height and density of hydrocauli around a nudibranch were related to size of *T. tergipes* ($P < 0.001$, $P = 0.10$, respectively). Large nudibranchs of *T. tergipes* were in areas with taller, more numerous hydrocauli.

Each nudibranch species occupied a particular area within the hydroid colony. Each of the four habitat parameters measured was important in distinguishing where a particular nudibranch species occurred in a hydroid colony (Table II). A Tukey-Kramer HSD test was performed to determine differences between species within each habitat parameter (Table III).

Nudibranch species occupied different heights on hydrocauli (Table III). *T. tergipes* was consistently on hydrocauli well above the bottom of the hydroid colony and was seen crawling at the bottom of the colony in only 6% of all observations (n = 193). It also positioned itself higher on hydrocauli (6.0 ± 0.3 mm) than *D. frondosus* and *D. coronata* ($P < 0.001$), but its position was not significantly different from *E. exiguus* (5.6 ± 0.1 mm). *E. exiguus* was on hydrocauli 69% (n = 16) of the time and its position differed from *D. frondosus* and *D. coronata* ($P < 0.001$). *D. frondosus* maintained an intermediate position within the vertical component of the colony with individuals 3.0 mm (SE = 0.5) above the kelp surface, but in 56% (n = 77) of the observations *D. frondosus* was on stolons or crawling on the kelp surface. *D. coronata* was at the bottom of the colony on stolons or on the kelp surface (0.6 ± 0.3 mm) in 90% (n = 76) of all observations.

Mean height and density of hydrocauli were quantified to describe the immediate area (2.25 cm^2) around each species of nudibranch. The hydrocauli around *D. frondosus* (15.7 ± 0.6 mm) were significantly taller than those around all other nudibranchs ($P < 0.001$). The height of hydrocauli around *T. tergipes* (13.3 ± 0.3 mm), *E. exiguus* (12.3 ± 0.3 mm) and *D. coronata* (11. ± 0.5) were not significantly different from each other (Table III). The density of hydrocauli around individuals of each species of nudibranch showed the same general pattern (Table III). The areas around *D. frondosus* (14.6 ± 0.6 hydrocauli/2.25 cm^2) and *T. tergipes* (13.4 ± 0.5 hydrocauli/2.25 cm^2) contained a similar and higher density of hydrocauli and both were significantly different ($P < 0.001$) from the areas around *E. exiguus* (10.7 ± 0.4 hydrocauli/2.25 cm^2) and *D. coronata* (10.3 ± 0.5 hydrocauli/2.25 cm^2). *E. exiguus* and *D. coronata* occupied areas that were not significantly different from each other.

T. tergipes tended to occupy a more central area of the colony. Nudibranchs were 4.05 cm (SE = 0.2) from the edge of the colony. *T. tergipes* was further from the edge of the colony than *D. coronata* and *E. exiguus* ($P < 0.001$), but not significantly different from *D. frondosus*. *D. frondosus* was 2.65 cm (SE = 0.2) from the edge of the colony. *D. coronata* and *E. exiguus* occupied similar areas of the

Table III

Summary of habitats of nudibranchs inhabiting colonies of Obelia geniculata. *Vertical lines within a habitat parameter indicate significant differences (Tukey's, $P < 0.05$) between species of nudibranchs for each parameter*

	Height on upright	Height of uprights around nudibranch	Density of uprights around nudibranch	Distance from edge of colony
High	*Tergipes* *Eubranchus*	*Dendronotus*	*Dendronotus* *Tergipes*	*Tergipes*
Mid	*Dendronotus*	*Tergipes* *Eubranchus*	*Eubranchus*	*Dendronotus*
Low	*Doto*	*Doto*	*Doto*	*Doto* *Eubranchus*

colony as *D. frondosus* (Table III). *D. coronata* was 2.62 cm (SE = 0.2) from the edge of the colony while *E. exiguus* was 2.28 cm (SE = 0.3) from the edge of the colony.

Perisarc analysis

The thickness of the perisarc of colonies of *O. geniculata* differed among structures (stolons, hydrocauli, thecae) within an area of the hydroid colony (F = 186.73, $P < 0.001$) (Fig. 6). Along the edge of the colony, the thickness of perisarcs of each structure differed, while in the center of the colony the perisarcs surrounding stolons and hydrocauli were similar, but both were significantly thicker than the perisarc covering the hydrothecae. Between areas of the hydroid colony, the perisarcs surrounding stolons and hydrocauli were thicker in the center than at the edge of the colony ($P < 0.001$), while they were not significantly different on hydrocauli.

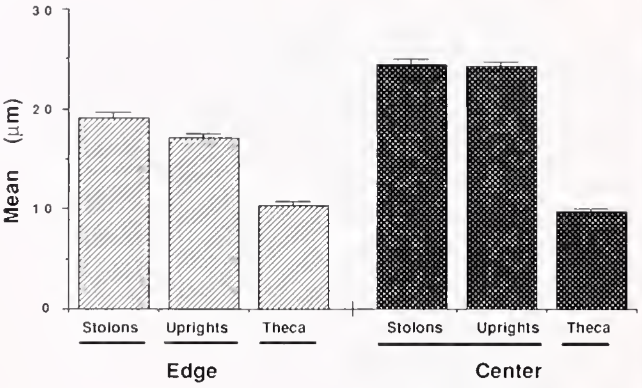

Figure 6. Mean thickness (±SE) of the perisarc of *Obelia geniculata* from stolons, hydrocauli, and thecae from central and peripheral areas of the hydroid colony. Horizontal lines indicate significant differences ($P < 0.001$) for structures within an area of the hydroid colony.

Discussion

Radular structures, feeding mechanisms and microhabitats vary in nudibranchs co-occurring within colonies of *Obelia geniculata*. Each nudibranch species used a distinct method to ingest hydroid tissue; little overlap existed between species. Individuals within a species showed some variation with respect to the hydroid structure they fed upon, but small nudibranchs (<6 mm) appeared to be restricted mostly by the structure of their radula (Hinde, 1958; Nybakken, 1970; Mills, 1977). Nudibranchs occupy areas of *O. geniculata* colonies in which they can feed, suggesting that feeding biology dictates habitat use for this suite of nudibranchs.

Feeding biology

Nybakken and McDonald (1981) predicted that nudibranchs with wide, triseriate radulae should feed upon naked hydranths and gonophores. *Dendronotus frondosus* has a wide, multiseriate radula (Fig. 2a), and Robilliard (1970) described the general feeding behavior of *D. frondosus* as biting whole polyps and sucking coenosarc. My findings support Robilliard, but I found that the mechanisms used by *D. frondosus* changed from piercing and sucking to biting with increase in size. Christensen (1977) described a mechanism of coordinating jaws and radula for feeding by *Precuthona peachi* on *Hydractinia echinata* similar to that for *D. frondosus*. Because *P. peachi* has a uniseriate radula (Thompson and Brown, 1984) in contrast to *D. frondosus*, nudibranch size relative to hydroid prey may be a better indicator of feeding mode than is radular structure.

Eubranchus exiguus with a triseriate radula penetrated the base of hydrothecae, contrary to the predictions of Nybakken and McDonald (1981). The jaws may assist penetration of a hydrotheca by pinching the thin perisarc. The lateral teeth are very thin, delicate structures that may have little functional utility and may be vestigial. The Eubranchidae are one of only two families within the superfamily Acleioprocta that have retained a triseriate radula (Schmekel and Portmann, 1982) and Schmekel (1985) suggested that a reduction from broad radulae to narrow radulae has occurred in the evolution of opisthobranch radulae. Two mechanisms for removing tissue after penetrating the hydrotheca are feasible: (1) the rachidian tooth pulls the polyp out from the bottom of the cup or (2) the buccal apparatus assists by creating a vacuum for suction (Kohn, 1983). The second mechanism is more probable because polyps are rapidly extracted through the base of a theca rather than incremently drawn out as would occur if rasped.

According to Nybakken and McDonald (1981), nudibranchs with uniseriate radulae should feed upon stolons that are covered with perisarc. They suggested that a uniseriate radula is better adapted for drilling holes than radulae with three teeth per row, but *Doto coronata* and *Tergipes tergipes* both have narrow, uniseriate radulae. *D. coronata* feeds by rasping a hole through stolons, whereas *T. tergipes* rakes naked tissue of hydranths.

The radula of *D. coronata* is flat with the central denticle of the rachidian tooth depressed below the lateral denticles (Fig. 2c, d). The penetration holes are circular (Fig. 4) and similar to those produced by muricid snails (Carriker, 1969), octopods (Nixon and Maconnachie, 1988) and by the dorid nudibranch *Okadaia elegans* (Young, 1969). Each of these predators preys upon organisms that have a calcareous exoskeleton (mollusks) or live in calcareous tubes (serpulid polychaetes) and use chemicals to assist the penetration process. Muricid and naticid snails use secretions from an accessory boring organ (Carriker, 1969, 1981), octopods use saliva from the posterior salivary glands (Nixon, 1979a, b; Nixon and Maconnachie, 1988) and Young (1969) suggests that *O. elegans* uses secretions from glandular cells around the lumen of the mouth, which he considers are part of the stomodeal gland. The etched pattern along the sides as well as the deteriorated top of the penetration hole produced by *D. coronata* suggest the presence of a caustic agent (Fig. 4b, d). The behavior of *D. coronata,* which sits atop stolons for long periods of time with short pulses of the buccal apparatus alternating with longer periods of inactivity, is similar to the drilling-related behavior of the snail *Urosalpinx* (Carriker, 1969), and suggests *D. coronata* may use chemicals to assist in the penetration of chitinous perisarc of *O. geniculata.* No reports show that dotoids possess glands capable of secreting substances for dissolution of prey skeleton. The salivary glands are unlikely candidates because they do not produce secretions containing lytic enzymes (Hyman, 1967; Welsch and Storch, 1973); however, histochemical work is needed to elucidate this mechanism.

Nybakken and Eastman (1977) showed that the curved radula of *Triopha carpenteri* is better for ripping flesh from erect bryozoa than the flat radula of *Triopha maculata,* which is used to scoop polypides from colonies of *Membranipora membranacea,* an encrusting bryozoan. The feeding mechanism observed for *T. tergipes* with a narrow, hooked radula is similar to the mechanism used by *T. carpenteri.* Feeding on polyp tentacles by slurping seems to be restricted to larger individuals (>3 mm) and may be a function of mouth size and ability to engulf whole strands of tissue.

Size

The nudibranchs inhabiting colonies of *Obelia geniculata* are all very small; nudibranchs greater than 5 mm are seldom found (Lambert, 1991). The mechanism each species uses to feed may in part be dictated by its size, in addition to the structure of its radula. Heavy jaws are used to break through relatively thin exoskeletons encasing zooecia of ectoproct colonies by the large dorids *Triopha carpenteri* and *T. maculata* (Nybakken and Eastman, 1977). *D. frondosus* may grow to 100 mm (Thompson and Brown, 1984), and animals larger than 5 mm use jaws to bite off whole polyps, a feeding mechanism similar to *Triopha* spp.

Newly metamorphosed juveniles may experience constraints due to size (Todd, 1991) when feeding upon *O. geniculata.* Because three of the four nudibranchs in colonies of *O. geniculata* feed by penetrating perisarc at some point during post-larval life, do any of these require an intermediate diet? *O. geniculata* may be considered an intermediate diet for juvenile *D. frondosus* because adults feed on larger tubularian hydroids. Both *D. coronata* and *E. exiguus* feed by penetrating the perisarc, but it is more likely that *D. coronata* is constrained by prey size because it feeds through the thicker stolon perisarc. Because long periods of time (2–4 h) are required for an adult *D. coronata* to penetrate a stolon, one could hypothesize that meiofaunal-sized juveniles are unable to efficiently drill through stolons. A microalgal diet would allow tiny nudibranchs to increase size before shifting to the adult prey. *T. tergipes* feeds on naked polyp tissue and is not constrained by its size; newly settled nudibranchs crawl into hydrothecae and rasp tissue directly (Lambert, 1990).

Habitats and feeding

Distribution within the hydroid colony and on hydrocauli demonstrated that nudibranchs segregate to areas in which they can feed. *D. frondosus* is a generalist predator within colonies of *O. geniculata.* Nudibranchs greater than 12 mm infrequently occupy colonies of *O. geniculata* (Lambert, 1991) and associate among athecate hydroids, particularly *Tubularia* spp. (Swennen, 1961; Thompson, 1964; Robilliard, 1970; Clark, 1975; Todd, 1981). Because large *D. frondosus* are very obvious in colonies of *O. geniculata* (pers. obs.), shifting to *Tubularia* colonies may provide a better refuge from fish predation as well as necessary calories.

Doto coronata occupied the edge of colonies, at the bases of hydrocauli or on the kelp surface and among few, short hydrocauli and fed predominantly on stolons. The perisarc of stolons is thinner along the perimeter of colonies than at the center and appears to be selected as a prey that is easier to handle (Pyke *et al.,* 1977). The preference to feed at the growing edge of colonies is similar to that in dorid nudibranchs, which feed at the edges of bryozoan colonies (Harvell, 1984; Todd and Havenhand, 1989). This behavior in dorids has been related to the lower calcification and strength of edge zooids (Best and Winston, 1984) and to differences in palatability of structures between zooids in a colony. Harvell (1984) suggested that colonies of *Dendrobeania lichenoides* have an ontogenetic gradient marked by morphological and physiological variation in tissue content of zooids. The gradient affects the grazing patterns of nudibranchs, which prefer to feed upon zooids at the perimeter, that are free of brown bodies and reproductive structures. In the case of *D. coronata,* the preference for stolons along the perimeter of colonies seems to be due to a greater mechanical ease of penetration. Composition of the coenosarc differs between the growing edge and the center of colonies of *O. geniculata* with respect to cellular activity (Crowell, 1957; Braverman, 1971), but no reports discuss differences in nutritional value between areas in hydroid colonies as were found in bryozoan colonies (Harvell, 1984).

Eubranchus exiguus was usually high on hydrocauli in areas where they were relatively numerous and tall. *E. exiguus* fed by penetrating hydrothecae and suctioning tissue and is thus found where the hydrothecae have the thinnest perisarc coverings (Fig. 6) and are more numerous (Crowell, 1957).

Tergipes tergipes feeds on exposed polyps and is found where food is most abundant, among many, relatively tall hydrocauli in the center of the colony. Crowell (1957) and Braverman (1963) showed that the centers of hydroid colonies are taller, denser, and have more polyps than the periphery.

Coexistence

The four species of nudibranchs found in colonies of *O. geniculata* differed in radular morphology, feeding behavior and micro-habitat. Thus, factors preventing competitive exclusion exist and traditional equilibrial coexistence could have operated (Connell, 1980), but large fluctuations and temporal shifts in abundances of populations are sufficient to explain species co-occurrences without competition (Birch, 1979; Chesson and Case, 1986; Hajek and Dahlsten, 1986). Relative abundances and age distributions of each population of nudibranch in the present study are temporally mediated (Lambert, 1991), and alternative food resources and habitats are present during the summer when nudibranch populations are highest (Lambert, 1985, 1991; Kuzirian, unpub. data). Also, because the majority of nudibranch larvae recruit to benthic habitats by the settlement of passively dispersed larvae (Todd, 1981), pre-settlement mortality could greatly contribute to variation in recruitment (Mileikovsky, 1974; Young and Chia, 1987). Thus, the apparent lack of a limiting resource and the absence of equilibrial population levels suggest that competition is unimportant among these nudibranchs (see Wiens, 1977; Strong *et al.*, 1984).

Behavioral interactions among organisms in a community can influence the use of resources by the species (Race, 1982; Brenchley and Carlton, 1983). Interspecific encounters among nudibranchs in *O. geniculata* occur frequently, but they do not influence the location of nudibranchs within the hydroid colony or where the nudibranchs feed (Lambert, 1990). These nudibranchs generally appear indifferent to the presence of others. Intraspecific encounters between pairs of nudibranchs result in non-aggressive responses (Lambert, 1990). The behavioral patterns of this assemblage of nudibranchs appear similar to some populations of phytophagous insects (Root, 1973; Simberloff, 1978; Strong, 1982; Hajek and Dahlsten, 1986), where non-equilibrial processes structure the community (Strong *et al.*, 1984).

Acknowledgments

This paper is part of a dissertation submitted in partial fulfillment of the requirements for a Ph.D. in Zoology at the University of New Hampshire. The manuscript was improved by comments from A. Marsh, M. Litvaitis, J. Berman, A. Kuzirian, L. Harris, J. Haney, R. Karlson, P. Levin, and three anonymous reviewers. I thank P. Martin, K. Verny, S. Truchon, N. Folino, L. Harris, G. Weisgarber, and P. Levin for diving assistance and J. Taylor for statistical advice. M. Litvaitis, C. Walker, and T. Gosliner provided technical assistance for histology and EM. Thanks also to H. Howell for providing space at the Coastal Marine Lab. Financial assistance was provided by a Central University Research Grant, a Summer Fellowship, and a Dissertation Fellowship from the University of New Hampshire.

Literature Cited

Best, B. A., and J. E. Winston. 1984. Skeletal strength of encrusting cheilostome bryozoans. *Biol. Bull.* **167:** 390–409.

Birch, L. C. 1979. The effect of species of animals which share common resources on one another's distribution and abundance. *Fortschr. Zool.* **25:** 197–221.

Blinn, D. W., R. E. Truitt, and A. Pickart. 1989. Feeding ecology and radular morphology of the freshwater limpet *Ferrissia fragilis. J. N. Am. Benthol. Soc.* **8:** 237–242.

Bloom, S. A. 1976. Morphological correlations between dorid nudibranch predators and sponge prey. *Veliger* **18:** 289–301.

Bloom, S. A. 1981. Specialization and noncompetitive resource partitioning among sponge-eating dorid nudibranchs. *Oecologia* **49:** 305–315.

Braverman, M. H. 1963. Studies on hydroid differentiation. II. Colony growth and the initiation of sexuality. *J. Embryol. Exp. Morphol.* **11:** 239–253.

Braverman, M. H. 1971. Studies on hydroid differentiation. VI. Regulation of hydroid formation in *Podocoryne carnea. J. Exp. Zool.* **176:** 361–382.

Brenchley, G. A., and J. T. Carlton. 1983. Competitive displacement of native mud snails by introduced periwinkles in the New England intertidal zone. *Biol. Bull.* **175:** 543–558.

Carriker, M. R. 1969. Excavation of boreholes by the gastropod, *Urosalpinx*: an analysis by light and scanning electron microscopes. *Am. Zool.* **9:** 917–933.

Carriker, M. R. 1981. Shell penetration and feeding by Naticacean and Muricacean predatory gastropods: a review. *Malacologia* **20:** 403–422.

Chesson, P. L., and T. J. Case. 1986. Overview: nonequilibrium community theories: chance, varibility, history and coexistence. Pp. 229–239 in *Community Ecology*, J. Diamond and T. J. Case, eds. Harper and Row Publ., Inc., New York.

Christensen, H. 1977. Feeding and reproduction in *Precuthona peachi* (Mollusca, Nudibranchia). *Ophelia* **16:** 131–142.

Clark, K. B. 1975. Nudibranch life cycles in the Northwest Atlantic and their relationship to the ecology of fouling communities. *Helgol. Meeresunters.* **27:** 28–69.

Connell, J. 1980. Diversity and the coevolution of competitors, or the ghost of competition past. *Oikos* **35:** 131–138.

Coyer, J. A. 1984. The invertebrate assemblage associated with the giant kelp, *Macrocystis pyrifera*, at Santa Catalina Island, California:

a general description with emphasis on amphipods, copepods, mysids and shrimps. *Fish. Bull. U. S.* **82:** 55–66.

Crowell, S. 1957. Differential responses of growth to nutritive level, age and temperature in the colonial hydroid *Campanularia. J. Exp. Zool.* **134:** 63–90.

Day, R. W., and G. P. Quinn. 1989. Comparisons of treatments after an analysis of variance in ecology. *Ecol. Monogr.* **59:** 433–463.

Drury, R. A. B., and E. A. Wallington. 1980. *Carleton's Histological Techniques.* Oxford Univ. Press, Oxford. 520 pp.

Edgar, G. J. 1983. The ecology of south-east Tasmanian phytal animal communities. II. Seasonal change in plant and animal populations. *J. Exp. Mar. Biol. Ecol.* **70:** 159–179.

Fernandez, E., R. Anadon, and C. Fernandez. 1988. Life histories and growth of the gastropods *Bittium reticulatum* and *Barleeia unifasciata* inhabiting the seaweed *Gelidium latifolium. J. Moll. Stud.* **54:** 119–129.

Hajek, A. E., and D. L. Dahlsten. 1986. Coexistence of three species of leaf-feeding aphids (Homoptera) on *Betula pendula. Oecologia* **68:** 380–386.

Hall, M. O., and S. S. Bell. 1988. Response of small motile epifauna to complexity of epiphytic algae on seagrass blades. *J. Mar. Res.* **46:** 613–630.

Harris, R. J. 1985. *A Primer of Multivariate Statistics, 2nd ed.* Academic Press, Orlando, FL. 576 pp.

Harvell, D. 1984. Why nudibranchs are partial predators: intracolonial variation in bryozoan palatability. *Ecology* **65:** 716–724.

Hawkins, S. J., D. L. Watson, A. S. Hill, S. P. Harding, M. A. Kyriakides, S. Hutchinson, and T. A. Norton. 1989. A comparison of feeding mechanisms in microphagous, herbivorous, intertidal prosobranchs in relation to resource partitioning. *J. Moll. Stud.* **55:** 151–165.

Hinde, R. 1958. Food and habitat selection in birds and lower vertebrates. *15th Internat. Congress Zool., Sect. 10.* **18:** 1–2.

Hyman, L. 1967. *The Invertebrates. Vol. VI, Mollusca I.* McGraw-Hill Book Co., New York. 792 pp.

Jackson, J. B. C. 1984. Ecology of cryptic coral reef communities. III. Abundance and aggregation of encrusting organisms with particular reference to cheilostome Bryozoa. *J. Exp. Mar. Biol. Ecol.* **75:** 37–57.

Keough, M. J. 1984. Effects of patch size on the abundance of sessile marine invertebrates. *Ecology* **65:** 423–437.

Krebs, C. J. 1989. *Ecological Methodology.* Harper and Row Publ., New York. 654 pp.

Kohn, A. J. 1983. Feeding biology of gastropods. Pp. 1–63 in *The Mollusca, Vol. 5, Physiology, Part 2.* K. M. Wilbur, ed. Academic Press, New York.

Kuzirian, A. M. 1979. Taxonomy and biology of four New England coryphellid nudibranchs (Gastropoda: Opisthobranchia). *J. Moll. Stud.* **45:** 239–261.

Lambert, W. J. 1985. The influence of predators on early colonists in a fouling community. MS Thesis, University of New Hampshire, Durham. 72 pp.

Lambert, W. J. 1990. Population ecology and feeding biology of nudibranchs in colonies of the hydroid *Obelia geniculata.* Ph.D. Dissertation, University of New Hampshire, Durham. 189 pp.

Lambert, W. J. 1991. Coexistence of hydroid eating nudibranchs: recruitment and non-equilibrial patterns of occurrence. *J. Moll. Stud.* **57:** in press.

Lillie, R. D. 1954. *Histopathologic Technic and Practical Histochemistry, 2nd edition.* Blakiston, New York. 692 pp.

McGuinness, K. A., and A. J. Underwood. 1986. Habitat structure and the nature of communities on intertidal boulders. *J. Exp. Mar. Biol. Ecol.* **104:** 97–123.

Meyer, K. B. 1971. Distribution and zoogeography of fourteen species of nudibranchs of northern New England and Nova Scotia. *Veliger* **14:** 137–152.

Mileikovsky, S. A. 1974. On predation of pelagic larvae and early juveniles of marine bottom invertebrates and their passing alive through their predators. *Mar. Biol.* **26:** 303–311.

Mills, P. M. 1977. Radular tooth structure in three species of Terebridae (Mollusca: Toxoglossa). *Veliger* **19:** 259–265.

Nation, J. L. 1983. Specialization in the alimentary canal of some mole crickets (Orthoptera: Gryllotalpidae). *Int. J. Insect. Morph. Embryol.* **12:** 201–210.

Nixon, M. 1979a. Hole boring in shells by *Octopus vulgaris* Cuvier in the Mediterranean. *Malacologia* **18:** 431–433.

Nixon, M. 1979b. Has *Octopus vulgaris* a second radula? *J. Zool.* **187:** 291–296.

Nixon, M., and E. Maconnachie. 1988. Drilling by *Octopus vulgaris* (Mollusca: Cephalopoda) in the Mediterranean. *J. Zool.* **216:** 687–716.

Nybakken, J. 1970. Correlation of radula tooth structure and food habits of three vermivorous species of *Conus. Veliger* **12:** 316–318.

Nybakken, J. W., and J. Eastman. 1977. Food preference, food availability and resource partitioning in *Triopha maculata* and *Triopha carpenteri* (Opisthobranchia, Nudibranchia). *Veliger* **19:** 279–289.

Nybakken, J., and G. McDonald. 1981. Feeding mechanisms of west American nudibranchs feeding on Bryozoa, Cnidaria and Ascidiacea, with special respect to the radula. *Malacologia* **20:** 439–449.

Ojeda, F. P., and J. H. Dearborn. 1989. Community structure of macroinvertebrates inhabiting the rocky subtidal zone in the Gulf of Maine: seasonal and bathymetric distribution. *Mar. Ecol. Prog. Ser.* **57:** 147–161.

Osman, R. W. 1978. The influence of seasonality and stability on the species equilibrium. *Ecology* **59:** 383–399.

Pyke, G., H. R. Pulliam, and E. L. Charnov. 1977. Optimal foraging: a selective review of theory and tests. *Q. Rev. Biol.* **52:** 137–154.

Race, M. S. 1982. Competitive displacement and predation between introduced and native mud snails. *Oecologia* **54:** 337–347.

Robilliard, G. A. 1970. The systematics and some aspects of the ecology of the genus *Dendronotus* (Gastropoda: Nudibranchia). *Veliger* **12:** 433–479.

Root, R. B. 1973. Organization of a plant-arthropod association in simple and diverse habitats: the fauna of collards (*Brassica oleracea*). *Ecol. Monogr.* **43:** 95–124.

Schmekel, L. 1985. Aspects of evolution within the Opisthobranchia. Pp. 221–267 in *The Mollusca, Vol. 10, Evolution,* E. R. Trueman and M. R. Clarke, eds. Academic Press, New York.

Schmekel, L., and A. Portmann. 1982. *Opisthobranchia des Mittelmeeres.* Springer-Verlag, Berlin and New York.

Schoener, T. W. 1983. Field experiments on interspecific competition. *Am. Nat.* **122:** 240–285.

Seed, R. 1986. Ecological patterns in the epifaunal communities of coastal macroalgae. Pp. 22–35 in *The Ecology of Rocky Coasts,* P. G. Moore and R. Seed, eds. Columbia University Press, New York.

Shonman, D., and J. W. Nybakken. 1978. Food preferences, food availability and food resource partitioning in two sympatric species of cephalispidean opisthobranchs. *Veliger* **21:** 120–126.

Simberloff, D. S. 1978. Using island biogeographic distributions to determine if colonization is stochastic. *Am. Nat.* **112:** 713–726.

Strong, D. R., J. H. Lawton, and T. R. E. Southwood. 1984. *Insects on Plants: Community Patterns and Mechanisms.* Blackwell Publ., Oxford. 313 pp.

Strong, D. R., Jr. 1982. Harmonious coexistence of hispine beetles on *Heliconia* in experimental and natural communities. *Ecology* **63:** 1039–1049.

Swennen, C. 1961. Data on distribution, reproduction and ecology of the nudibranchiate molluscs occurring in the Netherlands. *Netherlands J. Sea. Res.* **1:** 191–240.

Thompson, T. E. 1964. Grazing and the life cycles of British nudibranchs. Pp. 275–297 in *Grazing in Terrestrial and Marine Environments.* D. J. Crisp, ed. Blackwell, Oxford.

Thompson, T. E., and G. H. Brown. 1984. *Biology of Opisthobranch Molluscs, Vol. II.* The Ray Society, London. 229 pp.

Todd, C. D. 1981. The ecology of nudibranch molluscs. *Oceanog. Mar. Biol. Ann. Rev.* **19:** 141–234.

Todd, C. D. 1991. Larval strategies of nudibranch molluscs: similar means to the same end? *Malacologia* **32:** 273–289.

Todd, C. D., and J. N. Havenhand. 1989. Nudibranch-bryozoan associations: the quantification of ingestion and some observations on partial predation among Doridoidea. *J. Moll. Stud.* **55:** 245–259.

Virnstein, R. W., and R. K. Howard. 1987. Motile epifauna of marine epiphytes in the Indian River Lagoon, Florida. II. Comparisons between drift algae and three species of seagrasses. *Bull. Mar. Sci.* **41:** 13–26.

Wiens, J. A. 1977. On competition and variable environments. *Am. Sci.* **65:** 590–597.

Welsch, U., and V. Storch. 1973. *Comparative Animal Cytology and Histology.* University Washington Press, Seattle, WA. 343 pp.

Yoshioka, P. M. 1986. Competitive coexistence of the dorid nudibranchs *Doridella steinbergae* and *Corambe pacifica. Mar. Ecol. Prog. Ser.* **33:** 81–88.

Young, C. M., and F-S. Chia. 1987. Abundance and distribution of pelagic larvae as influenced by predation, behavior, and hydrographic factors. Pp. 385–464 in *Reproduction of Marine Invertebrates, Vol. IX,* A. C. Giese, J. S. Pearse, and V. B. Pearse, eds. Blackwell Scientific Publ., Palo Alto, CA.

Young, D. K. 1969. *Okadaia elegans,* a tube-boring nudibranch mollusc from the central and west Pacific. *Am. Zool.* **9:** 903–907.

Zar, J. H. 1984. *Biostatical Analysis, 2nd edition.* Prentice-Hall, Inc., New Jersey. 718 pp.

Reference: *Biol. Bull.* **181:** 261–268. (October, 1991)

Influence of Body Size and Population Density on Fertilization Success and Reproductive Output in a Free-Spawning Invertebrate

DON R. LEVITAN

Ecology Program, School of Life and Health Sciences, University of Delaware,
Newark, Delaware 19716

Abstract. Gamete production and fertilization influence zygote production. While gamete production is correlated positively with body size, individual fertilization success may be a function of population density. Usually it is assumed that when high population density leads to reduced body size and gamete production, per capita zygote production is diminished. This field study of the sea urchin *Diadema antillarum* Philippi provides a test of this assumption. Three experiments were conducted to determine the effect of male spawning on fertilization success. In the first experiment, unfertilized eggs were placed in Nitex bags at three distances up and downstream from a spawning male. In the second experiment, unfertilized eggs were released and captured at three distances downstream from a sperm source. In both experiments, fertilization decreased with distance from the sperm source. The final experiment tested the influences of male size and population density on fertilization success; the effect of density was significant, but size was not. A simple model estimates the average number of zygotes produced by females of average size under different density regimes: at high population density, increased fertilization success can compensate for decreased gamete production. Small individuals at high population density may have similar per capita zygote production as large individuals at low population density. Thus, estimates of reproductive output based on body size or gamete production alone can be misleading.

Introduction

One of the major generalizations in population biology is that, within a species, larger body size confers greater reproductive success (Williams, 1975). This generalization is based, in part, on evidence indicating that body size and gamete production are directly proportional (*e.g.*, Vertebrates: Bagenal, 1966; Invertebrates: Paris and Pitelka, 1962; Rinkevich and Loya, 1979; Suchanek, 1981; Angiosperms: Sarukhan, 1980; Algae: Vernet and Harper, 1980). However, estimating zygote production, or more generally reproductive success, from gamete production alone can be inappropriate and misleading. If gametes are shed into the surrounding medium, fertilization success, and thus zygote production, can be profoundly influenced by the abundance and behavior of conspecifics. While gamete production is correlated positively with body size, individual fertilization success may be a function of population density (discussed by Mortensen, 1938; Thorson, 1946; Denny and Shibata, 1989; Strathmann, 1990; empirical evidence provided by Pennington, 1985). An individual spawning a large number of gametes in isolation has poor reproductive success; yet estimates of fecundity (production of offspring) are generally based on gamete number or gonad size (*e.g.*, Paine, 1969; Sutherland, 1970, 1972; Branch, 1975; Wu, 1980; Suchanek, 1981; Jackson, 1985). The ecological and evolutionary interpretation of these data can be misleading if the significance of fertilization success is ignored.

Estimating fecundity from body size or gamete number can be particularly misleading when organisms exhibit an inverse relationship between body size and population density (*e.g.*, plants—Harper, 1977; animals—Paine, 1969; Sutherland, 1970, 1972; Branch, 1975; Wu, 1980; Suchanek, 1981; Lawrence and Lane, 1982; Sebens, 1983a). In such cases, there may be an important tradeoff between (a) large size with high individual gamete production at low population density, and (b) smaller size

Received 29 January 1991; accepted 20 June 1991.

Present address: Department of Zoology, University of California, Davis, California 95616-8755.

with lower gamete production at higher population density. An inverse relationship between size and density may be a result of resource limitation or other factors such as variation in recruitment and survivorship (Sebens, 1983b). Regardless of the mechanism, if body size is inversely related to population density, and density is important to fertilization success, then body size alone is a poor predictor of zygote production. If a gain in fertilization success balances the cost of reduced gamete production, then small organisms living at high population density may be just as fecund as large organisms living at low population density.

This study provides empirical evidence on the relative influence of male body size and population density on fertilization success and fecundity in the sea urchin *Diadema antillarum*. Because an inverse relationship between mean body size and population density has been documented for *Diadema* (St. Croix—Carpenter, 1981; Barbados—Hunte *et al.*, 1986; St. John—Levitan, 1988a), it is possible that small urchins at high density would have average per capita zygote production similar to large urchins at low density. I first determine an appropriate method for a field assay of fertilization success in free-spawning invertebrates, and then examine the relative influence of male body size and male population density on the fertilization of eggs. Finally, I present a model and its assumptions to calculate the average number of zygotes being produced by females at various population densities.

Materials and Methods

Determination of fertilization success

Fertilization success was assessed by two techniques during the summer of 1988 at Lameshur Bay, St. John, U.S. Virgin Islands. The first experiment investigated the effects of distance, flow, and current direction on fertilization success. A large male urchin (65–70 mm test diameter) was placed subtidally in 4–6 m of water. The direction and speed of the water flow was determined by releasing fluorescein dye 15 cm off the bottom with a syringe and recording the time taken for the center of the cloud to move 1 m. Nitex bags (35 micron mesh), 5 × 3 cm in size, were filled with 0.5 ml of unfertilized eggs (approximately 10^6 eggs) and placed upstream and downstream from the urchin at 1, 3, and 5 m distances (one bag at each distance). The bags, held between a weight and a float, were suspended 15 cm above the bottom. The mesh size of the bags was small enough to hold the 80–100 micron eggs, yet large enough to allow sperm (sperm head approximately 3 microns; Harvey and Anderson, 1943) to enter the bags. The male urchin was then injected with 0.5 *M* KCl to induce spawning. After 20 min, the egg bags were collected and rinsed in seawater. Two hours after the field work, 250 eggs from each bag were inspected in the laboratory for the presence of a fertilization membrane. The experiment was replicated ten times.

In the second experiment, I investigated fertilization success of free-drifting eggs. Sperm and eggs were collected less than 1 h before experiments were conducted by injecting urchins with KCl and then collecting the released gametes with a pipet held directly above the gonopores. Sperm were kept in concentrated form (dry) and the eggs were placed in a 300 ml jar filled with seawater to maximize viability. Samples of eggs were fertilized with sperm, just prior to and directly after the experiments, as a control for gamete viability. All controls with sperm were over 99% fertilized and without sperm were 0% fertilized. A syringe filled with 3.0 ml of dilute eggs (approximately 3 × 10^6) and another filled with 1.5 ml of concentrated sperm (approximately 3 × 10^{10}—Tyler *et al.*, 1956) were taken to a sandy bottom (4–6 m). The speed and direction of water flow were measured with fluorescein dye as described above. The syringe containing sperm was placed next to a syringe containing fluorescein dye; both were held 15 cm above the bottom. At either the 0.1, 1.0, or 3.0 m downstream interval, the syringe containing eggs was held 15 cm above the bottom. Directly downstream of the egg syringe was a 35 micron mesh plankton net (mouth opening diameter: 0.5 m, 300 ml glass jar at terminal end). The sperm and fluorescein dye were released simultaneously. When the edge of the dye cloud passed over the egg syringe, the eggs were released; 1 min later, the plankton net was brought to the surface. Within 30 s, the egg samples were poured over 35 micron mesh Nitex and rinsed with seawater to remove excess sperm. The eggs were re-suspended in seawater, fixed in formalin (after 2 h), and assayed for the presence of a fertilization membrane (250 eggs per sample). The experiment was replicated five times.

Population density and body size

A field experiment to test the effect of male size and population density on fertilization was conducted between February and August 1986, in Lameshur Bay. There was no apparent unidirectional current, and wave surge was minimal. Urchins from one of three size classes (40–50, 50–60, 60–70 mm test diameter) were haphazardly placed in subtidal arenas at one of three population densities (1, 4, 16 males/m^2). This size range represented 78% of the 1986 population structure (Levitan, 1988b). The range of population density was 6–20 urchins/m^2 before and 0.2–0.7/m^2 after the 1983 mass mortality of *Diadema* (Levitan, 1988a,b; Karlson and Levitan, 1990). Arenas were placed 15 m apart on a natural sand bottom at a depth of 4–6 m. An arena is simply an area of bottom defined by four egg-containing Nitex bags placed in a square. The urchins were injected with 0.5 *M* KCl to induce spawning. If an

Table I

Effect of distance, up and down stream position, and current velocity on the percentage (arcsine transformed) of eggs being fertilized

SV	DF	SS	MS	F
Distance	2	0.455	0.228	
Position	1	0.051	0.051	
Current	1	0.052	0.052	14.28***
Interaction	2	0.005	0.002	3.19 NS
Error	53	0.844	0.016	3.23 NS
Total	59	1.406		0.14 NS

*** = $P < .001$, NS = not significant.

Eggs were held in Nitex bags. Analysis of covariance with two main effects: distance between urchin and bags, and up-current or down-current position. The current velocity was the covariate.

urchin did not spawn or if it was female, it was replaced. All urchins, within an arena, were induced to spawn within 1 min. Control arenas with no males were used to check for ambient sperm in the water. Spawning lasted approximately 5 min. After 20 min, the egg bags were collected and rinsed in seawater. Within 2 h, 250 eggs per bag were assayed for the presence of a fertilization membrane. The 4 Nitex bags per arena were pooled to give 1000 eggs per replicate. There were 8 to 12 replicates for each level of male size and density. One set of replicates (3 male sizes × 3 male densities) was attempted each day.

Arenas, in the above experiment, were 1 m^2 at low density and 0.25 m^2 for medium and high density treatments (*i.e.*, 1 urchin per arena at low density, 1 and 4 urchins per arena at medium and high density). This was done because it was impossible to place ¼ of an urchin in the small arena and impractical to place (and spawn within the experimental time frame) 16 males in a large arena. Although both methods (varying urchin number and area) are true density manipulations, this design confounds the effect of number and distance between males and eggs at the low and medium densities. In another study (Levitan *et al.*, 1991), the relative influence of varying urchin number and distance was examined. The results suggest that both factors are important. When a few rare organisms clump, and spawn, the probability of fertilization increases slightly. When many organisms are at high density, and spawn, the probability of fertilization increases greatly. Thus, the use of a small number of spawning urchins underestimates the importance of any density effect noted.

Results and Discussion

Determination of fertilization success

At the low flow recorded in Lameshur Bay (0.009, SE = 0.003 m/s), current speed did not have a significant effect on fertilization success. Furthermore, fertilization success was not significantly different in up-current and down-current positions at the same distances (Table I). Diffusion and wave surge exposed the sperm to both up-current and down-current egg bags. Perhaps at higher current speeds these effects would be important. Yund (1990) also found no difference between up-current and down-current rates of fertilization in hydroids during periods of slack tide. Pennington's (1985) study indicated that current speeds greater than 0.2 m/s decreased fertilization success. An inverse relationship between flow and percent fertilization was also noted in *Strongylocentrotus franciscanus* (Levitan *et al.*, 1992). Recent models indicate that high turbulence quickly dilutes gametes below the concentration where fertilization is likely (Denny, 1988; Denny and Shibata, 1989).

The distance from the egg bags to the male urchin had a significant effect on fertilization success (Table I). This result, also seen in the work of Pennington (1985) and Yund (1990), reflects a dilution of sperm as it diffuses over larger volumes. It is not due to advection, because a similar fertilization profile occurred in both directions. This result was compared with the free-drifting egg experiment (Fig. 1) and indicates that this latter experiment also had a significant distance effect (Table II). Over comparable distances, the free-drifting eggs had 2.7 times the fertilization rate of eggs held in Nitex bags (2.75 and 2.62 times greater at 1 and 3 m, respectively). However, the amount of sperm released was 3.6 times greater in the drifting egg experiment (an average of 0.42 ml for 67.5 mm urchins *versus* 1.5 ml released by syringe).

Both the Nitex bag and the free-drifting egg experiments might have artifacts associated with the methods that affect fertilization success. With Nitex bags, the presence of the

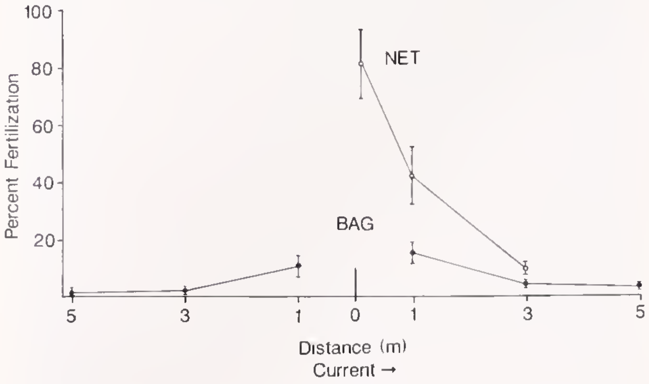

Figure 1. Relationship between percent fertilization and distance from a sperm source. Closed symbols represent eggs held in Nitex bags; open symbols represent free drifting eggs collected in a plankton net. On average, the plankton net experiment used 3.6 times the amount of sperm as the bag experiment. Water current flows left to right. Means and standard errors are plotted.

Table II

Percent (arcsine transformed) eggs fertilized in free-drifting eggs

SV	DF	SS	MS	F
Distance	3	2.081	1.041	13.60**
Current	1	0.020	0.020	0.26 NS
Error	11	0.842	0.076	
Total	14	2.975		

** = $P < .01$, NS = not significant.

Analysis of covariance with one main effect; distance between released eggs and sperm. The current velocity was the covariate.

Table III

Effect of population density and body size on the percentage of eggs being fertilized

SV	DF	SS	MS	F
Density	2	8389.82	4149.91	57.20***
Size	2	399.38	199.69	2.72 NS
Interaction	4	227.85	56.96	0.78 NS
Error	84	6160.52	73.34	

*** = $P < .001$, NS = not significant.

Two-way ANOVA of arcsine transformed data (percent fertilization). Factors were male density and male body size.

mesh impedes the flow through the containers, while holding the eggs stationary increases the amount of water and sperm sampled by eggs. With the free-drifting eggs, the release of gametes through syringes might increase estimates of fertilization because the sperm were extruded at a high rate (Denny and Shibata, 1989) and the eggs were released and captured in the center of the passing sperm plume. If, on balance, the Nitex method underestimates fertilization and the free-drifting method overestimates fertilization, then Figure 1 represents the upper and lower bounds of actual fertilization success at these current velocities. Most importantly, finding the same pattern of decreasing fertilization success with distance, using different techniques, provides the robust conclusion that relative fertilization rates can be assayed in the field. The Nitex bag method is convenient, and provides a clear relative measure of fertilization success.

Population density and body size

Over natural ranges of population density and body size, male population density had a highly significant effect on the percent of eggs fertilized, while male body size had no significant effect on the percent of eggs fertilized (Table III). The ranges of the two factors were 47-fold for size (measured as a function of gonad volume; see Levitan, 1989, for body and gonad size regression) and 16-fold for density. Thus, even though the experiment varied individual size more than density, male size did not significantly influence fertilization. The mean percent fertilization measurements (size classes pooled for each male density) were 0.1, 7.3, 18.0, and 45.0% for 0, 1, 4, and 16 males/m^2, respectively (Fig. 2). Density was manipulated in two ways, by varying area between low and medium density, and varying urchin number between medium and high density treatments. Both manipulations resulted in significant differences (all three densities were different from one another; 95% confidence interval test). This suggests that both the number and distribution of point sources of sperm release are important factors in fertilization success.

The finding that male size had no effect on fertilization can be related to the distribution of sperm sources. Sperm dilutes quickly over the two-dimensional area inhabited by urchins as it disperses through the three-dimensional volume of water. The number and position of sperm sources may be more important than the amount of sperm released from any given source. Another possibility involves the high variance associated with gamete production in male *Diadema* (Levitan, 1988c). In that study, KCl injections were made in the same manner but on a slightly larger size range of urchins (30–80 mm test diameter) than the present study. The results indicated a significant positive relationship of sperm release to body size with high variance (log gametes = log size 2.30–4.58, $R^2 = 0.10$, n = 134).

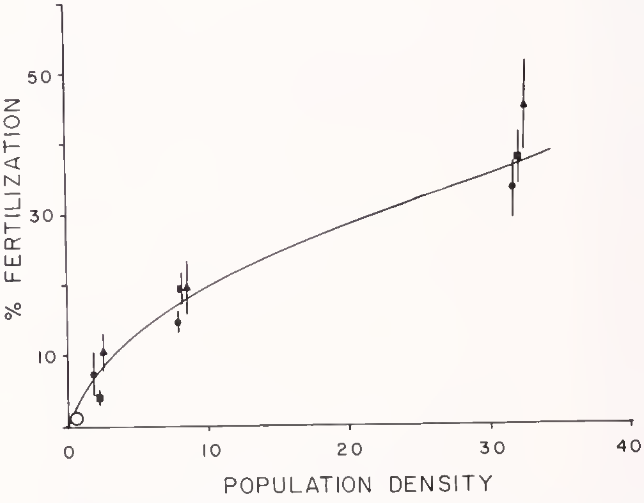

Figure 2. Relationship between population density of *Diadema* and percent fertilization of eggs. Population density is graphed as two times the male density, since the sex ratio of *Diadema* in Lameshur Bay was 1:1. The mean value and standard error are shown for each body size at each density (n = 8–12 for each value). Circles, squares, and triangles are 40–50, 50–60, and 60–70 mm test diameter urchins, respectively. The large circle is the control with no urchins. Regression calculated from individual data points: log percent fertilization = 0.72 log density $(m^{-2}) + 0.49$, $R^2 = 0.72$, $P < 0.0001$, n = 96.

Zygote production model

Percent fertilization was estimated rather than total number of fertilized eggs produced per individual. Below is a model that estimates average individual zygote production for average-size individuals at different population densities. This model provides information on the relative zygote production of individuals from different populations. It does not estimate differences between individuals within a spawning event.

Estimates of zygote production of average-size females at different densities were made from the following equations. Average female size at a specific density was estimated by:

log body size (mm)

$= -0.28$ log population density $(m^{-2}) + 1.87$,

$R^2 = 0.79$, $P < .001$, $n = 7$ sites,

(Lameshur Bay field distribution; Levitan, 1988a). (1)

The expected number of eggs released into the water by spawning females was estimated by:

log volume of eggs (ml) $= 3.56$ log size (mm) $- 6.59$,

$R^2 = 0.35$, $P < 0.001$, $n = 74$ (1 ml of eggs $= 2.1 \times 10^6$ eggs, from Levitan, 1988c). (2)

Average zygote production was estimated by calculating the percent of the released eggs fertilized at that specific density:

log percent fertilization $= 0.72$ log density (m^{-2})

$+ 0.49$, $R^2 = 0.72$, $P < 0.0001$, $n = 96$. (Fig. 2). (3)

This relationship and the variance associated with this calculation are plotted in Figure 3.

Figure 3 indicates a surprisingly even trade-off between gamete production and gamete fertilization with increasing density. Small individuals at high density, on average, produce a similar number of zygotes as larger individuals at low density. The model indicates that decreased fertilization success can offset increased individual gamete production of large individuals at low population density.

Model assumptions

Generalizing from this model to actual spawning events should be done with caution, and involves the following assumptions: (1) synchrony of spawning and the pattern of dispersion during spawning are independent of population density, (2) different size urchins at different densities spawn in the same manner and frequency, (3) there is no competition for sperm by eggs, and (4) survivorship of adult urchins is size-independent (to generalize beyond one spawning event).

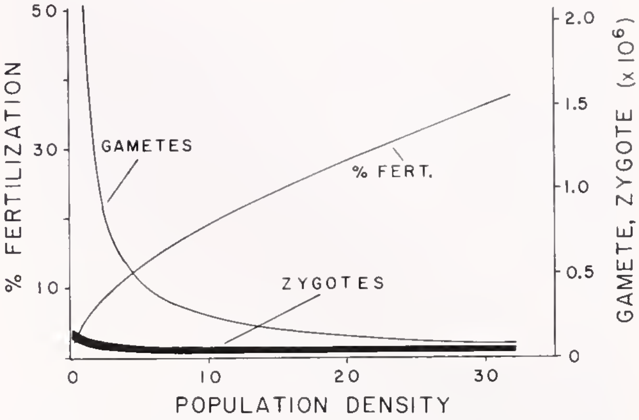

Figure 3. Trade-off between gamete production of average-size females (gametes) and gamete fertilization (% fert.). "Gametes" is calculated as the mean number of eggs being released into the water by a mean-size female urchin at that density (body size determined by equation 1, the amount of gametes released by that size female determined by equation 2). "% Fert." is calculated as the mean percent of eggs fertilized at that density (equation 3, Fig. 2). "Zygotes" is calculated as the product of "Gamete" and "% Fert.," and is plotted (by the thickness of the line) as the 95% CI calculated from the variance of the two regression lines [SE log zygotes = (variance [log gametes] + variance [log percent fertilized])$^{.5}$].

The first assumption involves the distribution and synchrony of spawning urchins and how this varies under different density regimes. Patterns of spawning synchrony and aggregation were investigated in Lameshur Bay following the mass mortality of *Diadema* (discussed below) when population density was relatively low (Levitan, 1988c). Spawning was weakly linked to the lunar cycle and occurred sporadically on all but the last five days of the lunar month. The degree of aggregation did not change over the lunar cycle and nearest neighbor distances (average of 75 cm) did not change as a function of reproductive readiness. Over 100 observations of *Diadema* spawnings indicate that individuals generally spawned alone [*i.e.*, no other urchins spawning within sight (5–10 m); Levitan, 1988c; pers. obs.]. On the one occasion, I observed two individuals spawning in contact with one another, they were both male. Thus, although a nearest neighbor distance of 75 cm is closer than expected by chance (random distribution would be 130 cm—Levitan, 1988c), the likelihood of two neighbors spawning at the same time was only 5% (Levitan, 1988c). Further, there is only a 50% chance that the nearest neighbor is of the opposite sex. This suggests that the model overestimates fertilization success at low density.

Published data also exists for *Diadema* in Lameshur Bay previous to the mass mortality, when density was 13/m^2 (Randall *et al.*, 1964). This is consistent with later estimates of 14/m^2 in Lameshur Bay the year before the mass mortality (Levitan, 1988a, b). Randall and his colleagues suggested that *Diadema* were aggregated independent of spawning activities (see also Pearse and Arch, 1969) and often had spines touching. They observed 13 spawning events: 10 were individuals spawning alone and 3 were small group spawnings (4–10 individuals with spines touching). The pattern of spawning was again weakly associated with the lunar cycle (significance test by Iliffe and Pearse, 1982). The evidence suggests that the pattern of spawning and aggregation does not change over a range of densities. If small group spawnings and occasional large spawning aggregations were more common at high density, this would only magnify the influence of density on fertilization success (*i.e.,* if spawning pheromones are effective only above a critical concentration), and increase the importance of a trade-off between gamete production and fertilization as suggested by the model. Low *Diadema* population density is not just an artifact induced by the mass mortality. Population density previous to the mass mortality varied widely and regionally ($0.04–25.8/m^2$: Bauer, 1980; $< 1–72/m^2$: Hay 1984).

The second assumption concerns size-dependent spawning. Experimental density manipulations indicated that body size is a good predictor of gonad volume and gamete release across densities (Levitan, 1989). There is also no influence of body size on the likelihood of spawning when injected with KCl (Levitan, 1988c). Whether this also holds true for natural spawning events is unknown and would be very difficult to establish. However, there is no evidence to date that suggests that these patterns vary with body size or population density.

The third assumption concerns the influence of egg number on fertilization success. Laboratory studies of *Strongylocentrotus franciscanus* conducted by placing eggs in small vials that would enhance sperm competition found no evidence of decreasing fertilization, at a constant sperm concentration, when egg number was increased 800% (Levitan *et al.,* 1991). Levitan *et al.,* using a fertilization kinetics model (Vogel *et al.,* 1982), also demonstrated that fertilization was insensitive to egg number at the concentrations likely to be found in the field.

The final assumption concerns relative survivorship patterns between large and small urchins across densities. These values are important for extending the results of one spawning to predicting lifetime reproductive output. Over the entire lifespan of an urchin, from egg to adult, an increasing survivorship pattern would be appropriate, due to high larval and post-larval mortality. However, the present model deals strictly with urchins after the age (and size) of first reproduction (approximately 25 mm for *Diadema*—Levitan, 1988c). Adult urchins in general (Ebert, 1982), and specifically *Diadema antillarum* (Karlson and Levitan, 1990), appear to exhibit size-independent survivorship. Further, experimental evidence indicates that *Diadema* does not exhibit density-dependent mortality induced by food limitation (Levitan, 1989).

Investigation of these assumptions indicates that the model may be quantitatively imprecise due to factors associated with spawning synchrony and aggregation. However, the evidence suggests that the conclusion of a trade-off between gamete production and gamete fertilization, associated with population density, is correct; individuals at low density are larger, but individuals at high density have a higher likelihood of fertilization. It is important to note that larger individuals, within a spawning event, would produce more zygotes than smaller individuals.

Example of the model

These experiments suggest that population density has a major influence on fertilization success and production of offspring in *Diadema.* An appraisal of fecundity (production of offspring) based on body size or gamete production in this species, without considering the compensatory effects of fertilization success, would be inappropriate. The following example demonstrates how misleading estimates of fecundity can be, when based solely on body size.

In 1983, *Diadema* population density declined 95–99% throughout the Caribbean (Lessios *et al.,* 1984). Since then, there has been a significant increase in mean body size (from 30 to 60 mm test diameter, at Lameshur Bay by June 1987) of the surviving *Diadema.* The median weight of individual *Diadema* has increased 10-fold since the mass-mortality (from 20 to 200 g live weight). During the same period, median gonad volume has increased 200-fold (from 0.05 to 10.0 ml; Levitan, 1988b). Predictions have been made that since growth rates and gamete production are high for this urchin, *Diadema* would rapidly return to former densities (Hughes *et al.,* 1985). However, recruitment since the mass-mortality continues to be at a low level (Hughes *et al.,* 1987; Lessios, 1988; Levitan, 1988b).

Individual zygote production can be estimated before and after the mortality event. In Lameshur Bay, 95% of the 1983 urchin population was between 20 and 40 mm in size and at a density of $15/m^2$. In 1987, at the same location, 70% of the population was between 60 and 80 mm in size and at a density of $0.2/m^2$ (Fig. 4). A 70 mm female releases an average of 2.0×10^6 eggs into the water, while a 30 mm female releases only 0.1×10^6 eggs (equation 2). However, fertilization success is estimated to be only 1% at a density of $0.2/m^2$ compared to 22% at $15/m^2$ (equation 3). Small females at high density are producing slightly more zygotes than the large females at low density (2.2×10^4 *versus* 2.0×10^4 zygotes per individual). Poor fertilization success at low population density might be contributing to the poor recruitment seen since the mass mortality.

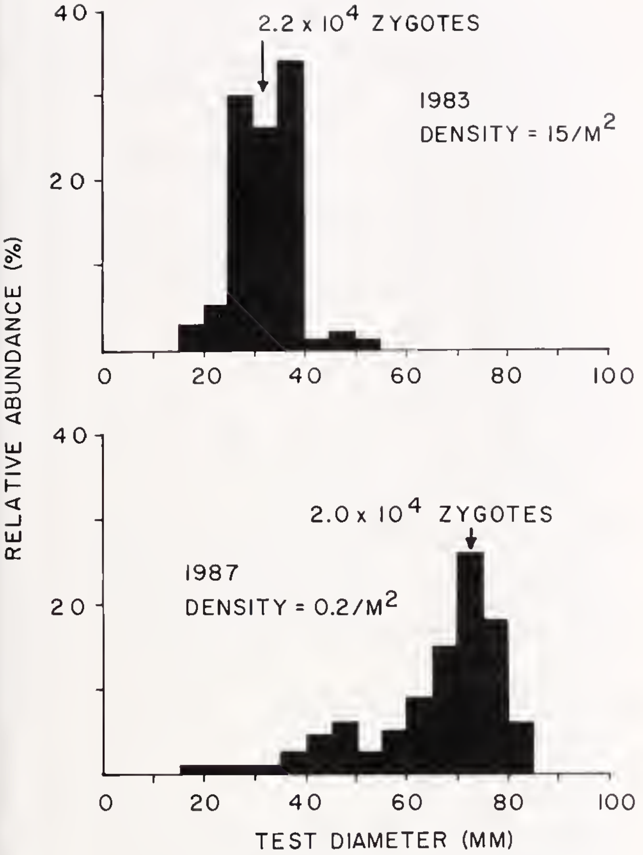

Figure 4. Size-frequency distribution and population density of *Diadema antillarum* before (1983) and after (1987) the mass mortality on a reef in Lameshur Bay, St. John, U. S. V. I.. Mean zygote production of the median size urchins are estimated from equations 2 and 3.

Conclusions

Many mobile invertebrates and fish aggregate or swarm during spawning (Levinton, 1982; Pennington, 1985). A temporary spawning aggregation would increase the likelihood of fertilization at low population density and reduce the nutritional costs of living at high density. Plants and sessile animals may suffer the consequences of isolation the most, and may be under high selection pressure to reproduce asexually, self-fertilize, or be hermaphroditic.

This study suggests that the influence of population density on fertilization success should be recognized and incorporated into an assessment of an organism's reproductive potential. This may change our perception of a "good" habitat and a "successful" organism. The assumption that large body size and high gamete production translate into high reproductive success may be incorrect when the importance of fertilization success is ignored.

Acknowledgments

S. Genovese, R. Haldeman, and C. Levitan assisted in the field. H. Cornell, R. Karlson, B. Ketcham, R. Eisenberg, M. Hay, T. Hughes, R. Olson, P. Petraitis, M. Sewell, P. Yund, and several anonymous reviewers made comments on an earlier draft of the manuscript. The University of the Virgin Islands, the National Park Service, and the Bamfield Marine Station provided facilities. This work was funded by the University of Delaware, The School For Field Studies, and the Lerner-Gray Fund for Marine Research from the American Museum of Natural History. This is contribution number 153 from the Ecology Program at the University of Delaware.

Literature Cited

Bagenal, T. B. 1966. The ecological and geographical aspects of the fecundity of the plaice. *J. Mar. Biol. Assoc. U. K.* **46:** 161–186.

Bauer, J. C. 1980. Observations on geographic variation in population density of the echinoid *Diadema antillarum* within the Western North Atlantic. *Bull. Mar. Sci.* **30:** 509–515.

Branch, G. M. 1975. Intraspecific competition in *Patella cochlear* Born. *J. Anim. Ecol.* **44:** 263–281.

Carpenter, R. C. 1981. Grazing by *Diadema antillarum* (Philippi) and its effect on the benthic algal community. *J. Mar. Res.* **39:** 749–765.

Denny, M. W. 1988. *Biology and Mechanics of the Wave-Swept Environment.* Princeton University Press, Princeton, New Jersey.

Denny, M. W., and M. F. Shibata. 1989. Consequences of surf-zone turbulence for settlement and external fertilization. *Am. Nat.* **134:** 859–889.

Ebert, T. A. 1982. Longevity, life history, and relative body wall size in sea urchins. *Ecol. Monogr.* **52:** 353–394.

Harper, J. L. 1977. *Population Dynamics of Plants.* Academic Press, New York.

Harvey, E. B., and T. F. Anderson. 1943. The spermatozoon and fertilization membrane of *Arbacia punctulata* as shown by the electron microscope. *Biol. Bull.* **85:** 151–156.

Hay, M. E. 1984. Patterns of fish and urchin grazing on Caribbean coral reefs: are previous results typical? *Ecology* **65:** 446–454.

Hughes, T. P., B. D. Keller, J. B. C. Jackson, and M. J. Boyle. 1985. Mass mortalities of the echinoid *Diadema antillarum* Philippi in Jamaica. *Bull. Mar. Sci.* **36:** 377–384.

Hughes, T. P., D. C. Reed, and M. J. Boyle. 1987. Herbivory on coral reefs: community structure following mass-mortalities of sea urchins. *J Exp. Mar. Biol. Ecol.* **33:** 39–59.

Hunte, W., I. Cote, and T. Tomascik. 1986. On the dynamics of the mass mortality of *Diadema antillarum* in Barbados. *Coral Reefs* **4:** 135–139.

Iliffe, T. M., and J. S. Pearse. 1982. Annual and lunar reproductive rhythms of the sea urchin *Diadema antillarum* (Philippi) in Bermuda. *Int. J Invertebr. Reprod.* **5:** 139–148.

Jackson, J. B. C. 1985. Distribution and ecology of clonal and aclonal benthic invertebrates. Pp. 297–355 in *Population Biology and Evolution of Clonal Organisms,* J. B. C. Jackson, L. W. Buss, and R. E. Cook, eds. Yale University Press, New Haven.

Karlson, R. H., and D. R. Levitan. 1990. Recruitment-limitation in open populations of *Diadema antillarum:* an evaluation. *Oecologia* **82:** 40–44.

Lawrence, J. M., and J. M. Lane. 1982. The utilization of nutrients by postmetamorphic echinoderms. Pp. 331–371 in *Echinoderm Nutrition,* M. Jangoux and J. M. Lawrence, eds. A. A. Balkema Press, Rotterdam.

Lessios, H. A. 1988. Fate of *Diadema antillarum* populations in the four years following mass mortalities. P. 802 in *Echinoderm Biology,* R. Burke, ed., Proceedings of the Sixth International Echinoderm Conference, A. A. Balkema Press, Rotterdam.

Lessios, H. A., D. R. Robertson, and J. D. Cubit. 1984. Spread of *Diadema* mass mortalities through the Caribbean. *Science* **226:** 335–337.

Levinton, J. S. 1982. *Marine Ecology.* Prentice-Hall, Englewood Cliffs.

Levitan, D. R. 1988a. Density-dependent size regulation and negative growth in the sea urchin *Diadema antillarum* Philippi. *Oecologia* **76:** 627–629.

Levitan, D. R. 1988b. Algal-urchin biomass responses following the mass mortality of *Diadema antillarum* Philippi at Saint John, U. S. Virgin Islands. *J. Exp. Mar. Biol. Ecol.* **119:** 167–178.

Levitan, D. R. 1988c. Asynchronous spawning and aggregative behavior in the sea urchin *Diadema antillarum* Philippi. Pp. 181–186 in *Echinoderm Biology.* R. Burke, ed. Proceedings of the Sixth International Echinoderm Conference, A. A. Balkema Press, Rotterdam.

Levitan, D. R. 1989. Density-dependent size regulation in *Diadema antillarum:* effects on fecundity and survivorship. *Ecology* **70:** 1414–1424.

Levitan, D. R., M. A. Sewell, and F. S. Chia. 1991. Kinetics of fertilization in the sea urchin *Strongylocentrotus franciscanus:* interaction of gamete dilution, age, and contact time. *Biol. Bull.* **181.**

Levitan, D. R., M. A. Sewell, and F. S. Chia. 1992. How distribution and abundance influences fertilization success in the sea urchin *Strongylocentrotus franciscanus. Ecology.*

Mortensen, T. 1938. Contributions to the study of the development and larval form of echinoids. *Kong. Danske Vidensk. Selsk. Nat. Math. Afd. 9 raekke* **4:** 1 (1938).

Paine, R. T. 1969. The *Pisaster—Tegula* interaction: prey patches, predator preference, and intertidal community structure. *Ecology* **50:** 950–961.

Paris, O. H., and F. A. Pitelka. 1962. Population characteristics of the terrestrial isopod *Armadillidium vulgare* in California grassland. *Ecology* **43:** 229–248.

Pearse, J. S., and S. W. Arch. 1969. The aggregation of *Diadema* (Echinodermata: Echinoidea). *Micronesica* **5:** 165–171.

Pennington, J. T. 1985. The ecology of fertilization of echinoid eggs: the consequence of sperm dilution, adult aggregation, and synchronous spawning. *Biol. Bull.* **169:** 417–430.

Randall, J. E., R. E. Schroeder, and W. A. Stark, II. 1964. Notes on the biology of the echinoid *Diadema antillarum. Carib. J. Sci.* **4:** 421–433.

Rinkevich, B., and Y. Loya. 1979. The reproduction of the Red Sea coral *Stylophora pistillata* I. Gonads and planulae. *Mar. Ecol. Prog. Ser.* **1:** 133–144.

Sarukhan, J. 1980. Demographic problems in tropical systems. *J. Bot. Monogr.* **15:** 161–188.

Sebens, K. P. 1983a. Population dynamics and habitat suitability in the intertidal sea anemones *Anthopleura xanthogrammica* (Brandt) and *A. elegantissima* (Brandt). *Ecol. Monogr.* **53:** 405–433.

Sebens, K. P. 1983b. Size structure and growth rates in populations of colonial and solitary invertebrates. Pp. 9–15 in *The Ecology of Deep and Shallow Seas,* M. Reaka, ed. NOAA.

Strathmann, R. R. 1990. Why life histories evolve differently in the sea. *Am. Zool.* **30:** 197–207.

Suchanek, T. H. 1981. The role of disturbance in the evolution of life history strategies in the intertidal mussels *Mytilus edulis* and *Mytilus californianus. Oecologia* **50:** 143–152.

Sutherland, J. P. 1970. Dynamics of high and low populations of the limpet *Acmea scabra* (Gould). *Ecol. Monogr.* **40:** 169–188.

Sutherland, J. P. 1972. Energetics of high and low populations of the limpet *Acmaea scabra* (Gould). *Ecology* **53:** 430–437.

Thorson, G. 1946. Reproduction and larval development of Danish marine bottom invertebrates. *Medd. Komm. Havundersog. Kbh. Ser. Plankton.* **4:** 1–523.

Tyler, A., A. Monroy, and C. B. Metz. 1956. Fertilization of sea urchin eggs. *Biol. Bull.* **110:** 184–195.

Vernet, P., and J. L. Harper. 1980. The cost of sex in seaweeds. *Biol. J. Linn. Soc.* **13:** 129–138.

Vogel, H., G. Czihak, P. Chang, and W. Wolf. 1982. Fertilization kinetics of sea urchin eggs. *Math. Biosci.* **58:** 189–216.

Williams, G. C. 1975. *Sex and Evolution.* Princeton University Press.

Wu, R. S. S. 1980. Effects of crowding on the energetics of the barnacle *Balanus glandula* Darwin. *Can. J. Zool.* **58:** 559–566.

Yund, P. 1990. An *in situ* measurement of sperm dispersal in a colonial marine hydroid. *J. Exp. Zool.* **253:** 102–106.

Reference: *Biol. Bull.* **181**: 269–274. (October, 1991)

Planktonic Copepods in a Sub-Tropical Estuary: Seasonal Patterns in the Abundance of Adults, Copepodites, Nauplii, and Eggs in the Sea Bed

NANCY H. MARCUS

Department of Oceanography, Florida State University, Tallahassee, Florida 32306

Abstract. The seasonal abundance of copepod eggs in the bottom sediments of the Apalachicola estuary was documented at bimonthly intervals between November 1989 and August 1990. Concentrations as high as 10^6 m^{-2} were noted. In addition, when bottom sediments from the estuary were incubated in the laboratory at ambient environmental conditions, large numbers of nauplii hatched, indicating that the eggs in the sediments constituted a large pool of potential recruits for the planktonic population. The eggs in the sediments and the nauplii that hatched were identified as *Acartia tonsa*, based upon morphology and the dominance of this species in the estuary. Therefore, the occurrence of copepod eggs in bottom sediments is not a phenomenon limited to temperate-boreal coastal environments.

Introduction

Estuaries are among the most productive marine systems in the world (Lauff, 1967) and as such are important nursery grounds for a wide variety of fish and invertebrates (Haedrich, 1983). Among the more important food items in the diets of these animals are copepod nauplii (Houde and Lovdal, 1984). In temperate estuaries, the appearance of copepod nauplii in the water column has been attributed to the hatch of eggs that were recently spawned by females, as well as to the hatch of eggs that were resuspended from the sea bottom, having been spawned by females some time previously (*e.g.*, Uye, 1983). The contribution of eggs in the sea bed to the naupliar population may be substantial, as concentrations as high as 10^6 m^{-2} have been documented for these ecosystems. With the exception of a study on the occurrence of eggs of *Centropages hamatus* in the sea bed of Alligator Harbor, Florida (Marcus, 1989), there have been no studies of the distribution and abundance of copepod eggs in the sea bottom sediments of sub-tropical or tropical waters. The purpose of this study was to determine whether copepod eggs are as numerous in the bottom sediments of sub-tropical estuaries as they are in temperate systems, and to relate such patterns to the occurrence of naupliar, copepodite, and adult planktonic stages.

Materials and Methods

The Apalachicola estuarine system in northwest Florida (29° 35′N to 29° 55′N; 84° 20′W to 85° 20′W) (Fig. 1) is typical of many sub-tropical estuarine systems found throughout the world. A recent summary of the physical, chemical, and biological characteristics of the system was provided by Livingston (1984). The system consists of East Bay, Apalachicola Bay, St. Vincent Sound, and western portions of St. George Sound. Three barrier islands that run along the extreme southern edge of the system limit the exchange of low salinity estuarine waters with the Gulf of Mexico. The Apalachicola River is the major source of fresh water to the system, followed by rainfall. As a result, East Bay is oligohaline, and the other sections grade from mesohaline to polyhaline. There are strong seasonal trends in temperature, salinity, dissolved oxygen, and turbidity. Vertical gradients of salinity are typical and reflect river flow and tidal conditions. On the other hand, thermal stratification is minimal due to wind-mixing. The average depth at mean low tide ranges from 2 to 3 m (the depth of the Intracoastal Waterway is 3.6 m). The sea bottom of the system includes areas that are extremely silty in the central portions of Apalachicola Bay and ones that are mixtures of sand and shell along the southern edge of St. George Sound.

Received 18 January 1991; accepted 20 June 1991.

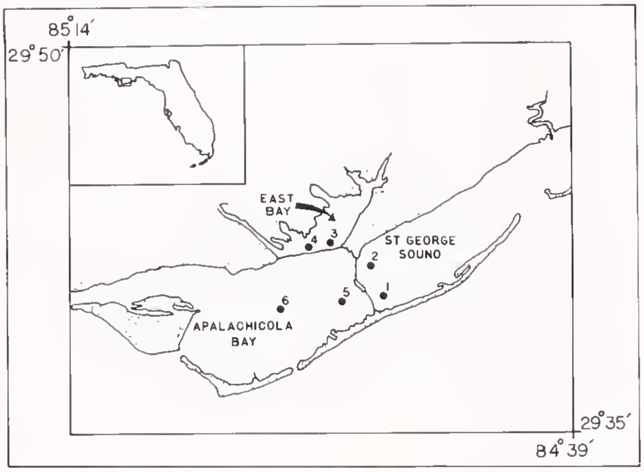

Figure 1. Location of sampling sites in the Apalachicola estuary.

The sampling program was initiated on 6 November 1989 and was continued at bimonthly intervals through 27 August 1990. Two sites were sampled in East Bay, Apalachicola Bay, and St. George Sound (Fig. 1). Their locations were chosen to represent the different salinity regimes occurring in the estuary. A complete sampling protocol involved the following: determination of surface temperature, surface and bottom salinity, and water depth; collection of two bottom cores (4.6D × 25L cm) with a pole corer; collection of two surface-to-bottom water column samples with an expandable (2–5 m in length, 4.6 cm diameter) plastic tube; collection of plankton with a .5 m 153 μm mesh net equipped with a General Oceanics digital flowmeter; and collection of additional surface water with a bucket. Exceptions to this scheme are the following: only one bottom core was taken at stations 3, 4, 5, and 6 in November; bottom salinity was not recorded in November; and flowmeter readings were not taken in November and January.

Surface temperature was determined with a thermometer placed in a bucket of surface water. Salinity of the same sample of water was determined with a Reichert-Jung hand-held refractometer. Bottom salinity was recorded for the top water above the sediments of one of the cores obtained from the sea bed. Depth was read off a meter scale on the pole of the coring device.

Immediately upon collection, the bottom cores were capped and stored in an insulated chest; the water column samples that were obtained with the plastic tube were filtered through a 35 μm mesh sieve, washed into small glass jars, and preserved in 5% formalin; the plankton net samples were washed into .5 or 1 liter jars and preserved in 5% formalin; the additional surface water obtained with a bucket was filtered through a 35 μm sieve and stored in large plastic jugs for transport.

The sediment cores were placed in a refrigerator at 5°C upon return to the laboratory. One day after collection, the upper 3 cm of each sediment core was extruded and divided at 1-cm intervals. Half of each layer was placed in a plastic screw cap test tube and preserved in 5% formalin. The eggs in these samples were extracted from the sediments and counted according to the methods of Marcus (1989). A quarter of each layer was placed in a dish with approximately 100 ml of the 35 μm filtered water and incubated at a temperature within 3°C of the temperature at the time of collection (with the exception of the July and August collections for which the incubations were conducted at a temperature 6–7°C lower than ambient). These dishes were monitored for two days, and the nauplii that hatched were counted and preserved in 5% formalin. The filtrates obtained with the plastic tube and preserved in the field were treated with Rose Bengal upon return to the laboratory. Subsequently, the number of nauplii in each sample was determined using a dissecting microscope. The samples obtained with the plankton net and preserved in the field were examined with a dissecting microscope for the presence of different copepod species. To reduce the concentration of animals to a number manageable for counting, the material was split several times with a Folsom Plankton splitter, according to the methods of Omori and Ikeda (1984). Plankton concentrations were then calculated based upon the number of splits and the volume of water filtered. The latter value was calculated from the flowmeter readings. For the samples collected in November and January for which there were no flowmeter readings, an average of all of the filtered volumes was used in the calculations.

Although the sample sizes were small, the non-parametric Kruskal-Wallis statistical test provided by Systat was used to determine if the concentration of eggs in the sediments, nauplii in the water column, adults and copepodites of *A. tonsa* in the water column, and emergence levels of nauplii from incubated sediments differed significantly between East Bay, Apalachicola Bay, and St. George Sound. For each of these regions and for the estuary as a whole, an average and standard deviation was calculated for each parameter for each collection date.

Results

Water depths at the times of sampling ranged from 1.5 to 4.0 m. Collections in November 1989, January 1990, and August 1990 were conducted during an outgoing tide. Collections in March, May, and July 1990 were conducted on an incoming tide. Extreme high and low tides occurred in March. For each collection date, the surface temperature varied little (less than 2°C) between the different regions of the estuary (Table I). The average surface temperature for the estuary varied seasonally from 12°C in

Table I

Average surface water temperatures, and surface and bottom salinities for the different regions of the Apalachicola estuary 1989–1990

	Nov-06	Jan-03	Mar-05	May-08	Jul-10	Aug-27
Surface temperature (°C)						
St. George Sound	22 (1)	12 (0)	17 (1)	24 (0)	33 (0)	31 (0)
East Bay	22 (1)	12 (0)	17 (0)	24 (0)	32 (0)	30 (0)
Apalachicola Bay	23 (1)	12 (1)	16 (0)	24 (0)	33 (0)	32 (0)
Surface salinity (ppt)						
St. George Sound	33 (1)	21 (1)	6 (2)	24 (0)	23 (1)	22 (0)
East Bay	5 (0)	0 (0)	0 (0)	15 (0)	7 (5)	5 (0)
Apalachicola Bay	18 (18)	14 (3)	2 (1)	23 (1)	22 (4)	19 (1)
Bottom salinity (ppt)						
St. George Sound	—	21 (1)	20 (0)	24 (0)	20 (0)	27 (2)
East Bay	—	5 (1)	0 (0)	17 (1)	9 (4)	11 (1)
Apalchicola Bay	—	18 (4)	13 (1)	24 (2)	21 (3)	23 (0)

Standard deviation in parenthesis; n = 2.

January to 33°C in July. Salinity varied spatially within the system (Table I). Values as low as 0 ppt characterized the surface and bottom waters in East Bay during March, and the surface waters in East Bay during January. High values (32–33 ppt) characterized the surface waters in St. George Sound during November. The average surface and bottom salinities for the estuary varied seasonally over a range of 19 and 10 ppt, respectively.

The number of copepod eggs isolated from the sediments varied spatially and temporally (Table II, Fig. 2a). In January, the concentrations of eggs in the sediments of East Bay were significantly ($P < .05$) different than in St. George Sound and Apalachicola Bay; in May, the concentrations in St. George Sound and East Bay were significantly different ($P < .05$) from Apalachicola Bay; and in August, concentrations were significantly different ($P < .05$) in St. George Sound than in the other areas. At the other times of the year there were no significant differences in the concentrations of eggs in the sediments in the different areas. The average concentration of eggs in the sediments of the system was highest (4.2×10^5 m^{-2}) in November; declined through March; increased in May; and declined to a low (7.8×10^4 m^{-2}) in August.

Table II

Concentration of eggs (mean and standard deviation × 10^5, n = number of samples) in the sediments of the different regions of the Apalachicola estuary 1989–1990

	Nov-06	Jan-03	Mar-05	May-08	Jul-10	Aug-27
St. George Sound						
Mean	7.07	2.31	1.05	2.45	1.40	1.23
SD	8.19	.89	.38	1.20	.41	.12
n	4	4	4	4	4	4
East Bay						
Mean	.32	5.03	.82	4.05	2.40	.53
SD	.25	1.46	.23	1.78	1.40	.22
n	2	4	4	4	4	3
Apalachicola Bay						
Mean	2.39	1.47	1.02	1.15	.75	.52
SD	1.30	.78	.38	.24	.32	.10
n	2	4	4	4	4	4

The number of nauplii that hatched from the sediments that were incubated in the laboratory varied spatially and temporally (Table III, Fig. 2b). In May, the concentrations of nauplii from the sediments of St. George Sound were significantly different ($P < .05$) than in Apalachicola Bay; and in March and July, the concentrations for East Bay were significantly different than in the other two portions of the system. The average concentrations for the system gradually declined from a maximum of 4.7×10^5 m^{-2} in November to a minimum of 2.4×10^4 m^{-2} in August.

Nauplii were always present in the water column, although their numbers varied temporally and, to a limited extent, spatially (Fig. 2c, Table IV). The average concentration for the system was high (7.1×10^4 m^{-3}) in November, low in January and March (1.2 to 2.0×10^4 m^{-3}), and high again in May, July, and August (7.4 to 9.6×10^4 m^{-3}). In November and May, the concentration of nauplii in the water column of East Bay was significantly different ($P < .05$) than in St. George Sound.

Acartia tonsa was the dominant planktonic copepod species in the estuary throughout the year, always exceeding 50% of the numerical copepod (adults and copepodites) density. *Oithona* (species not identified) accounted for 24%, 10%, and less than 5% of the numerical copepod density in March, May, and the remainder of the year, respectively; *Paracalanus* (species not identified) represented 41% of the numbers in November and less than 10% the remainder of the year. Together, these three genera accounted for 95 to 99% of copepods (adults and copepodites) throughout the year. The concentration of

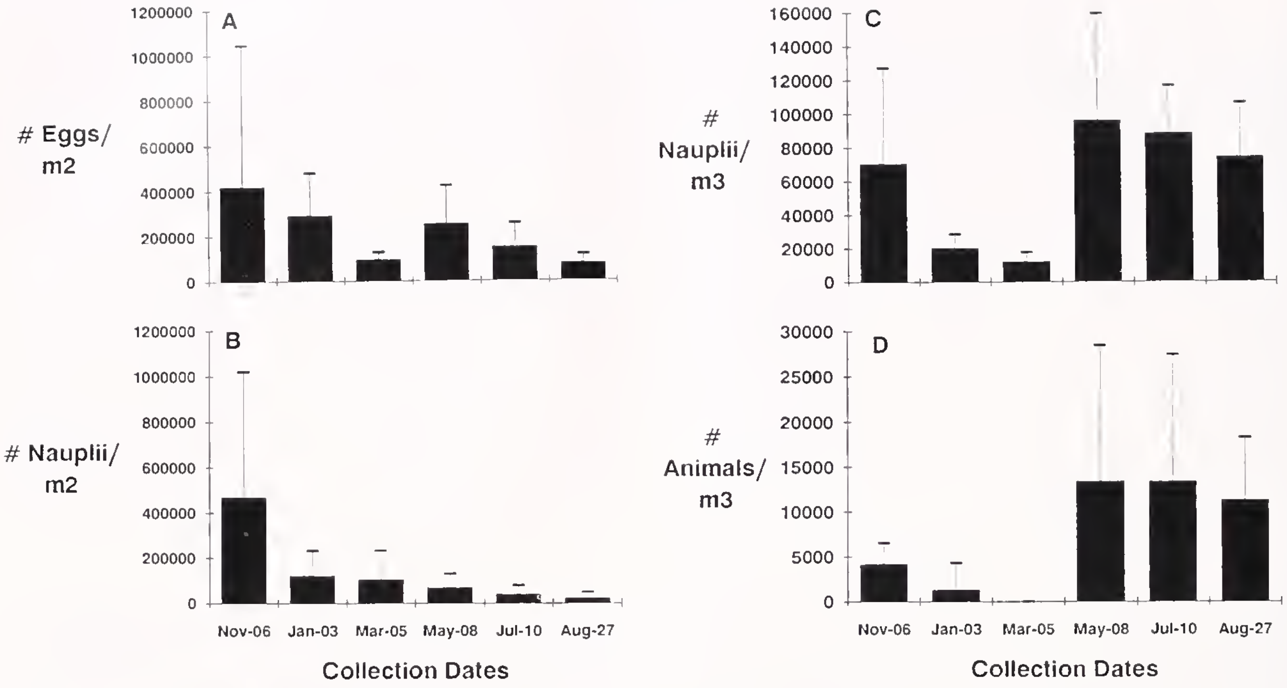

Figure 2. Seasonal trends of (A) resting egg concentrations in the sea bed, (B) numbers of nauplii emerging from sediments incubated in the laboratory, (C) nauplii concentrations in the water column, and (D) adult and copepodite concentrations in the Apalachicola estuary. Mean and standard deviation.

adults and copepodites of *A. tonsa* did not differ significantly between the three regions of the system. The average concentration of adults and copepodites of *A. tonsa* in the estuary varied seasonally, being moderately high (4.2×10^3 m^{-3}) in November, low (1.3×10^3 m^{-3}) in January, extremely low (13 m^{-3}) in March, and then high (1.1 to 1.3×10^4 m^{-3}) in May, July, and August (Fig. 2d).

Discussion

For most of the year, the average concentration of copepod eggs in the sea bed of the Apalachicola estuarine system was of the same order of magnitude (10^5 m^{-2}) as that reported for *Centropages hamatus* in Alligator Harbor, Florida (Marcus, 1989). These values for sub-tropical systems are equivalent in magnitude to the values reported for temperate bays and estuaries (*e.g.*, Kasahara *et al.*, 1975; Uye 1983). In the present study, the emergence of large numbers of nauplii (average 2.4×10^4–4.7×10^5 m^{-2}) from the sediments that were incubated in the laboratory at ambient field conditions indicated that large numbers of these eggs were viable. At such concentrations and levels of emergence, these eggs constitute a large potential source of naupliar recruits for the planktonic population and a large potential source of prey items for larval fish and invertebrates. Because the eggs isolated from the sediments of the Apalachicola system and those spawned by *Acartia tonsa* females in the laboratory are morphologically similar, and because *A. tonsa* is the numerically dominant copepod in the system, then most of the eggs isolated from the sediments, as well as the nauplii that emerged from the sediments, were probably *A. tonsa*. Eggs of *Oithona* and *Paracalanus*, the two other genera that were numerically prominent in the estuary, have never been reported from the sea bed of any system that has been studied. In the case of *Oithona*, the females carry their eggs in sacs attached to their bodies. Although females of *Paracalanus spp.* shed their eggs into the water column, the eggs may be too fragile to withstand mixing into the sediments. The salinity regimes of East Bay, St. George Sound, and Apalachicola Bay conformed to their designations as oligohaline, mesohaline, and polyhaline. However, a comparison of the concentration of eggs in the sediments, nauplii in the water column, adults and copepodites of *A. tonsa* in the water column, and emergence levels of nauplii from incubated sediments revealed no or only a few significant differences among the regions. These results may reflect the tolerance of *A. tonsa* to a wide range of salinities (Day *et al.*, 1989).

Since the initial discovery of calanoid copepod eggs in sea bottom sediments of temperate coastal waters (Kasahara *et al.*, 1974), eggs of planktonic copepods that have been isolated from the sea bed have typically been referred to as resting or dormant. Grice and Marcus (1981) dis-

Table III

Concentration of nauplii (mean and standard deviation × 10^5, n = number of samples) emerged from sediments incubated in the laboratory from the different regions of the Apalachicola estuary 1989–1990

	Nov-06	Jan-03	Mar-05	May-08	Jul-10	Aug-27
St. George Sound						
Mean	4.13	1.83	1.87	1.24	.20	.08
SD	4.28	1.24	1.36	.61	.12	.06
n	4	4	4	4	4	4
East Bay						
Mean	1.08	1.08	.01	.70	.80	.39
SD	.03	1.24	.01	.39	.43	.30
n	2	4	4	4	4	4
Apalachicola Bay						
Mean	9.44	.75	1.31	.15	.18	.23
SD	9.23	.72	1.26	.08	.14	.25
n	2	4	4	4	4	4

tinguished two types of resting or dormant eggs: diapause eggs and quiescent subitaneous eggs. Diapause eggs undergo a mandatory arrest of development, during which development does not resume even if conditions are suitable. Subitaneous eggs can develop without delay, but if they are exposed to unsuitable conditions (*e.g.*, low temperature or oxygen) development is delayed and they become quiescent. Unlike diapause eggs, quiescent subitaneous eggs resume development immediately upon reexposure to suitable conditions. Despite these differences, both types of resting eggs are functionally similar in terms of their impact on population growth, because both introduce a lag phase into the life cycle. In the present study, experiments were not conducted to determine whether the resting eggs that were isolated from the sea bed of the Apalachicola estuary were diapause or quiescent subitaneous eggs.

The seasonal trend observed in this study (Fig. 2d), in the abundance of adults and copepodites of *Acartia tonsa*, was similar to that previously reported for the Apalachicola system (Edmiston, 1979). Although the species was present throughout the year, the concentration of adults and copepodites cycled from high values in the spring and summer to low values in the fall and winter. On the other hand, the greatest concentration of eggs in the sediments occurred in the fall following the spring and summer peak of adults and copepodites. A similar phased relationship between the concentrations of eggs in the sediments and adult concentrations in the water column was reported for several species of copepods in the Inland Sea of Japan (Kasahara *et al.*, 1975). For these species, the hatch of resting eggs was crucial to their perpetuation in as much as the planktonic stages disappeared entirely from the water column for a portion of the year. Although the planktonic stages of *A. tonsa* did not disappear entirely from the Apalachicola estuary, they did undergo a marked seasonal cycle in abundance. The presence of eggs in the sediments suggests that these stages may provide an im-

Table IV

Concentration of nauplii (mean and standard deviation × 10^5, n = number of samples) in the water column of the different regions of the Apalachicola estuary 1989–1990

	Nov-06	Jan-03	Mar-05	May-08	Jul-10	Aug-27
St. George Sound						
Mean	.26	.22	.12	1.02	.81	.95
SD	.21	.08	.02	.33	.16	.42
n	4	4	4	4	4	4
East Bay						
Mean	1.23	.15	.14	.50	.78	.73
SD	.66	.05	.05	.20	.21	.13
n	2	4	4	4	4	4
Apalachicola Bay						
Mean	.64	.24	.09	1.36	1.07	.55
SD	.21	.10	.08	.91	.39	.27
n	2	4	4	4	4	4

portant source of recruits for the planktonic population especially during the Spring.

Although Reeve (1975) pointed out the potential importance of benthic resting stages in discussing the zooplankton of shallow sub-tropical lagoonal systems of southern Florida, and Tranter and Abraham (1971) suggested that a benthic diapause phase might be the basis of the seasonal replacement of several *Acartia* species in the Cochin backwater in India, the actual presence of such stages in sub-tropical systems had not been demonstrated. The results of Marcus (1989) on *Centropages hamatus* and this study on *Acartia tonsa* provide strong support for the hypotheses of Reeve and of Tranter and Abraham, for the existence of copepod resting eggs in the sea bed of sub-tropical estuaries is now evident.

Acknowledgments

I thank Teresa Donelan, Robert Lutz, Denise Miller, and Keith Taulbee for their assistance in the field and laboratory and two anonymous reviewers for their suggestions regarding the manuscript. Research supported by NOAA Grant NA89AA-D-CZ146 and NSF Grant OCE87-22922. Contribution Number 1062 of the Florida State University Marine Laboratory.

Literature Cited

Day, J. W., C. Hall, W. M. Kemp, and A. Yanez-Arancibia. 1989. *Estuarine Ecology.* John Wiley and Sons, New York. 558 pp.

Edmiston, L. 1979. *The Zooplankton of the Apalachicola Bay System.* M.S. Thesis, Florida State University. 104 pp.

Grice, G., and N. Marcus. 1981. Dormant eggs of marine copepods. *Oceanogr. Mar. Biol. Ann. Rev* **19:** 125–140.

Haedrich, R. 1983. Estuarine fishes. Pp. 183–208 in *Estuaries and Enclosed Seas,* B. H. Ketchum, ed. Elsevier, Amsterdam.

Houde, E. D., and J. A. Lovdal. 1984. Seasonality of occurrence, foods and food preferences of ichthyoplankton in Biscayne Bay, Florida. *Estuarine Coast. Shelf Sci.* **18:** 403–419.

Kasahara, S., S. Uye, and T. Onbé. 1974. Calanoid copepod eggs in sea-bottom muds. *Mar. Biol.* **26:** 167–171.

Kasahara, S., S. Uye, and T. Onbé. 1975. Calanoid copepod eggs in sea-bottom muds. II. Seasonal cycles of abundance in the populations of several species of copepods and their eggs in the Inland Sea of Japan. *Mar. Biol.* **31:** 25–29.

Lauff, G. H., ed. 1967. *Estuaries.* AAAS Publication # 83, Washington, DC.

Livingston, R. J. 1984. The ecology of the Apalachicola Bay system: an estuarine profile. *U. S. Fish. Wildl. Serv. FWS/OBS* 82/05. 148 pp.

Marcus, N. H. 1989. Abundance in bottom sediments and hatching requirements of eggs of *Centropages hamatus* (Copepoda:Calanoida) from the Alligator Harbor region, Florida. *Biol. Bull.* **176:** 142–146.

Omori, M., and T. Ikeda. 1984. *Methods in Marine Zooplankton Ecology.* John Wiley and Sons, New York. 322 pp.

Reeve, M. R. 1975. The ecological significance of the zooplankton in the shallow subtropical waters of south Florida. Pp. 352–371 in *Estuarine Research,* Vol. 1, L. E. Cronin, ed. Academic Press, New York.

Tranter, D. J., and S. Abraham. 1971. Coexistence of species of Acartiidae (Copepoda) in the Cochin Backwater, a monsoonal estuarine lagoon. *Mar. Biol.* **11:** 222–241.

Uye, S. 1983. Seasonal cycle in abundance of resting eggs of *Acartia steuri* Smirnov (Copepoda:Calanoida) in sea-bottom mud of Onagawa Bay, Japan. *Crustaceana* **44:** 103–105.

Reference: *Biol. Bull.* **181**: 275–288. (October, 1991)

The Function of Surface Sclerites in Gorgonians (Coelenterata, Octocorallia)

J. C. LEWIS AND E. VON WALLIS

Department of Biological Sciences, Brock University, St. Catharines, Ontario, Canada L2S 3A1

Abstract. Branches of a variety of species of gorgonians representing the common sclerite types were fixed in flexed (bent) positions and examined by scanning electron microscopy. To determine changes in position of sclerites associated with extension and compression, appropriate measures of sclerite density and angle were taken. From these and other data, probable function was hypothesized. Surface sclerites (spicules), called clubs, modify colony flexion by limiting compressibility of the outer cortex when they contact each other. Scaphoids progressively limit extension as their ventral tubercle belts engage similar tubercles on underlying spindles. Radiates limit both extension and compression by catching and locking up after a fixed, free-slide distance. Double-heads severely limit both extension and compression through random orientation of closely packed, spiny protruberences that preclude almost any freedom of movement. Unilaterally spinose spindles act as drawbridge-like, protective covers for polyps. They play no apparent role affecting whole colony mechanics. Possible roles of sclerites as mechanical systems are discussed briefly.

Introduction

The shapes of gorgonian surface sclerites (spicules) can often be used alone to identify specimens to the generic level. In most gorgonians, surface sclerites differ from those of deeper layers, and these combinations are used for identification to the specific level (Bayer, 1961). Because characteristic sclerite shapes are so highly conserved, we suspect that they are considerably and functionally significant to the organism. If they functioned solely as filler particles to stiffen the coenenchymal gel, the highly specific shapes, sizes, orientations, and positioning of sclerites such as is observed in gorgonians (Verrill, 1868; Kukenthal, 1901; Bayer, 1961) would probably be unnecessary. They undoubtedly perform this mechanical task (Koehl, 1982; Wainwright *et al.*, 1982; Currey 1984), but stiffening can be done by particles of almost any shape.

The principal support structure of a gorgonian colony is the core or axis composed of gorgonin, which contains a modified collagen (Goldberg, 1976) and which may be mineralized (Lowenstam, 1964; Leversee, 1969). Its stiffness roughly correlates with the broad water movement regimes within which various gorgonian species are found (Jeyasuria and Lewis, 1987; Yoshioka and Yoshioka, 1989). These mechanical properties however, are modified by the sclerite-containing coenenchymal material or cortex (Muzik and Wainwright, 1977; Esford and Lewis, 1990) that surrounds the axis and contains, in a series of cavities, the polyps and gastrovascular canals. In most instances, colonies are dependent on the polyps' ability to efficiently extract nutrients from the surrounding water. Water velocity and direction of movement can change rapidly in response to wave action, so the mechanical properties of the colonies must be specifically tuned to their environment (Koehl, 1982; Vogel, 1988). Polyps feed most effectively at an optimum ambient velocity (Leversee, 1984), and the velocity of food organisms flowing past polyps is kept within this range by the mechanical properties of the axis and coenenchyme (Vogel, 1981).

The coenenchyme is composed of two parts: mesogleal gel and calcareous sclerites. Mesoglea is an example of a compliant composite material composed of a series of discontinuous, randomly oriented, collagen-like fibrils in a hydrated polymer matrix (Chapman, 1953; Gosline, 1971a; Koehl, 1977; Wainwright *et al.*, 1982). Mechanical tests performed on mesoglea from *Metridium senile* reveal its ability to stretch three times its original length under small loads and yet exhibit complete elastic recovery (Gosline, 1971b). The results indicate that this is a time-dependent phenomenon in which quick extension of the material causes greater rigidity than slow extension (Alexander, 1983). This property of the mesoglea must be

Received 12 April 1990; accepted 7 June 1991.

considered in addition to the effect of the axial skeleton when considering the mechanical properties of the whole colony. The time-dependent rigidity of the mesoglea translates into resistance by stiffening to high velocity water movement that could flay the colony against the substratum. Compliance occurs at lower velocities, which are less detrimental to colony structural integrity.

Another major determinant of overall mechanical properties of an octocoral colony is the sclerite composition and content of the mesoglea. Sclerites, unlike mesoglea, exhibit little individual flexibility. They are crystalline (Kingsley, 1984) calcium carbonate (Kingsley and Watabe, 1984; Goldberg and Benayahu, 1987a, b; Majoran, 1987; Goldberg, 1988) and are, characteristically of gorgonians, densely packed in the mesoglea. With such characteristic dense packing, the sclerites must interact with any bending or twisting of the colony and consequently affect the mechanics of the whole colony.

In most gorgonians, sclerites are arranged in three distinct layers in the coenenchymal cortex. These layers are usually, though not invariably, distinguishable on the basis of sclerite type (Fig. 1). Immediately surrounding the axis is the axial sheath. Sclerites in this layer are usually short rods, spindles, radiates, or spheroids. These sclerites are densely packed, and are a major component of gastrodermal tube walls. Presumably, they function in support of gastrovascular cavity walls and prevent their collapse or kinking during torsion and flexion of the colony (Thibaudeau, 1983).

The middle cortex adjacent to the axial sheath contains the polyp cavities and branched gastrovascular canals. It is the thickest of all cortical layers. Major sclerite types are spindles, multiradiates, and double heads (Fig. 1), most of which are oriented with their longitudinal axes parallel to the axis of the colony (Bayer *et al.*, 1983). In the genera *Eunicea* and *Plexaura*, middle cortex sclerites can be quite large (up to 1.5 mm).

The outer cortex (the surface layer), usually the thinnest of all layers, is also interspecifically variable in sclerite composition. Generally, only one type of sclerite occurs on the surface of an individual species (Bayer, 1961). The nomenclature concerning the wide variety of sclerite morphs is confusing, but the five broad classes (Bayer *et al.*, 1983) into which surface sclerites of shallow water, Caribbean octocorals can be categorized are: clubs, scaphoids, spindles, radiates, and double heads (Fig. 1). The considerable variation within these basic categories is the basis for much of this confusion. Variants of clubs include sclerites named torches, leaf clubs, balloon clubs, thorn clubs, and wart clubs. Scaphoid variants include

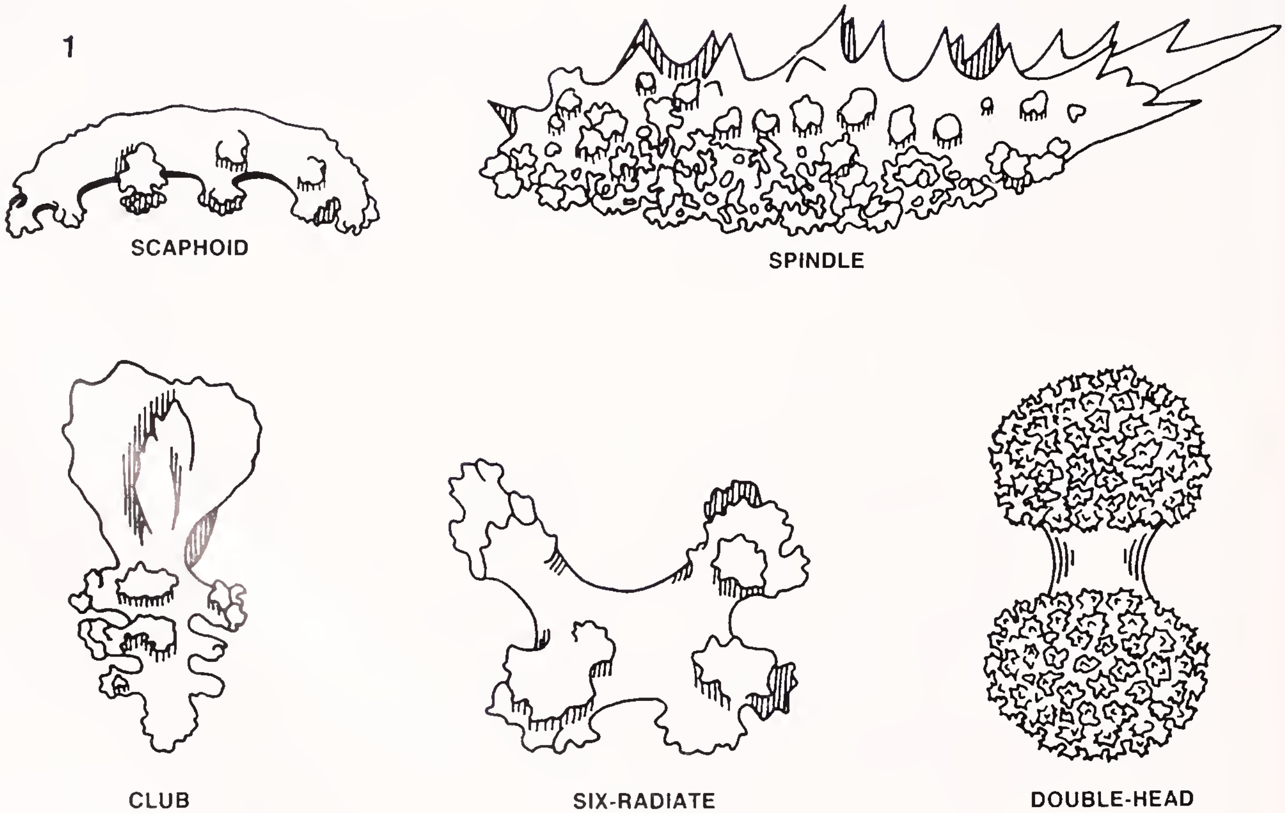

Figure 1. Line drawings of representatives of five of the most common types of outer cortex sclerites that occur in gorgonians. Figures not to scale.

crescents, smooth scaphoids (with crests), and scaphoids with transverse crests. Spindle is a general term for any sclerite of fusiform shape, small, medium, or large. Though found on the surfaces of some genera, they are more commonly the principal components of the middle cortex and the axial sheath. One variety of spindle that occurs as an outer cortex sclerite is the unilaterally spinose spindle. Names of radiate variants often correspond to numbers of rays; for instance, six-radiate, seven-radiate, and eight-radiate, but may also be known by such names as antleriform and butterfly. Double heads were formerly known as capstans (Bayer *et al.*, 1983).

Because mesogleal gel is hydrated and contains collagen fibrils (Wainwright *et al.*, 1982), a solid object embedded therein should be capable of motion. Movement under these conditions is described by any of six potential degrees of freedom: pitch, yaw, roll, lateral, vertical, and axial motion (Wainwright *et al.*, 1982; Alexander, 1983). Given this potential, flexion or torsion of the colony as a whole translates into forces that cause the displacement of the sclerites that can be described in terms of degrees of freedom. Limitations on movement are affected by sclerite architecture and orientation (Muzik and Wainwright, 1977).

Drag forces on a basally attached, erect structure will cause bending in the direction of the water flow when the force exceeds the inertial resistance of the material (Vogel, 1981). In general, when a solid bar is bent, it is compressed on the concave surface while being extended under tension on the convex surface. A line marking the midpoint between these two surfaces undergoes no transformation and is therefore named the neutral axis. Tissue on either side of the neutral axis will change in length. Rees (1972), Vogel (1981), and Sebens (1984) have documented a relationship between drag forces caused by waves, tides, and currents and distribution of coral species. Individuals of the same species display variation in growth forms that correlate with the intensity of water movement. Velimirov (1976) noted this phenomenon while studying *Eunicella cavolinii* and additionally noted concurrent sclerite variation. It has been pointed out by numerous investigators that axial mechanical properties are probably modified to varying degrees by the mechanical properties of the coenenchyme and that a major component of the coenenchyme responsible for this must be the sclerites. Scanning electron micrographs of gorgonian cortical layers (Thibaudeau, 1983) hint at complicated relationships between the sclerites in each layer. Somewhat surprisingly, no systematic investigations of the relationship of various different sclerite types with possible mechanical properties of colonies has been published. This examination of sclerite orientation on flexed branches of gorgonians is a preliminary attempt to relate shape to function, and, ultimately, to mechanical properties.

Materials and Methods

Specimens were obtained from the shallow (0–50 m) coastal waters of Tobago and Cay Sal Bank, Bahamas during field expeditions. Single colonies of *Ellisella barbadensis, E. elongata, Eunicea clavigera, E. calyculata, Muricea atlantica, M. elongata,* and *Lophogorgia punicea* were collected in Tobago. *Gorgonia ventalina, Pseudopterogorgia rigida, P. acerosa, Plexaurella grisea, Eunicea asperula, E. laciniata, E. knighti, Plexaura flexuosa, P. homomalla,* and *Pterogorgia anceps* were collected in the Bahamas. Several branches from each specimen were tied in a flexed (bent) position prior to fixation. Angles of flexion could not be kept consistent either inter- or intraspecifically because of large differences in stiffness, flexibility, and thickness between branches. Specimens from Tobago were dipped in 10% formalin, air dried, and transported to Brock University prior to preparation for scanning electron microscopy (SEM). Specimens from the Bahamas were fixed in 3% glutaraldehyde, transported in fixative, then air dried prior to preparation for SEM.

Fresh specimens were collected and examined in the field using a dissecting microscope. Surface sclerites, embedded in mesoglea and coated with mucus, were obscured to the extent that no meaningful analysis of sclerite orientation could be undertaken in the field. Fixation did not alleviate the problem. Only in the *Muricea* could surface sclerites be relatively clearly distinguished.

For SEM, cross and longitudinal sections were cut from various positions on each colony and dipped in sodium hypochlorite solution (Javex, T. M. Bristol Myers) to remove mesogleal gel from embedded sclerites. The time required to remove mesoglea without loosening sclerites varied from specimen to specimen, however, most required 10–40 s. Samples were immediately rinsed in distilled water and dried. Dried samples were mounted on aluminum specimen mounts with double-sided adhesive tape and coated with a thin layer of gold under vacuum in a Polaron PS-3 Sputter Coater. Specimens were examined with a Hitachi model S-570 scanning electron microscope.

We examined 17 species in 8 genera. Because a single analytical procedure could not be applied to all species, a number of measurements were used including sclerite density, space between sclerites, angles of sclerites with axes in the same plane as the colony axis, and angles of sclerites with axes tangential to the colony axis. Sclerite type determined the specific measurement technique used. In all cases, measurements were taken from compressed, neutral, and extended surfaces.

On specimens with surface clubs and double heads, sclerite density was determined. Density was measured directly from the Video Display Terminal (VDT) of the SEM by counting numbers of sclerites in the area bounded by the image edges of the VDT (6.67 mm^2). An image scale provided screen area. Sections from each surface (compressed, neutral, and tensed) were measured. Mean and standard deviation values of at least 50 separate locations per surface per sample were determined. To test nonparametrically for intergroup differences, a Kruskal-Wallis one-tailed analysis of variance by ranks was performed (Zar, 1984). The null hypothesis was that there were no differences between the means of the measurements from sclerites on compressed, neutral, and tensed surfaces. If Kruskal-Wallis test results were significant at the 0.05 level of significance or better, the method of multiple comparison (Siegel and Castellan, 1988) was used to determine which differences between medians of the groups were significant.

Because of the interdigitation of processes from adjacent radiates, it was usually not possible to discriminate individual sclerites. Relative density of radiates was obtained by a computer imaging process (MCID Image Analysis System, Imaging Research Inc., Brock University) calibrated to differentiate between areas occupied by sclerites and spaces between them. This was done from SEM photographs with results presented as the percentage of the area of the photographs occupied by sclerites or parts thereof. Data were analyzed using the one-tailed Kruskal-Wallis ANOVA by ranks.

Angles of scaphoids and spindles planar or tangential to the colony axis, respectively, were determined similarly. An acetate sheet, inscribed with a protractor, was affixed to the VDT screen. Using stage controls on the SEM, a sample was rotated to bring the long axis of the colony parallel to the base of the protractor. Compressed, neutral, and extended surfaces were each scanned while maintaining the axis in a constant position relative to the protractor. Measurements of sclerite angles were acquired directly from the VDT screen. Means and standard deviations were determined, again subjecting data to Kruskal-Wallis and multiple-comparison tests.

Results

Surface sclerites of the seventeen specimens examined were categorized into five main groups: clubs, scaphoids, double heads, radiates, and spindles (Bayer *et al.*, 1983).

Clubs

A single layer of clubs comprises the outer cortex of all *Eunicea* and *Plexaura* species. All are oriented perpendicular to the colony axis with the rectangular, spiny or rounded plates that form the club's "head" exposed to the surface of the colony while the "handle" projects toward the middle cortex. The bases of the club handles abutt middle cortex sclerites, which are usually large, closely grouped spindles oriented parallel to the colony axis. The results of measurements on one colony each of *Plexaura flexuosa, P. homomalla, Eunicea clavigera*, and *E. laciniata* are summarized in Table Ia. In all cases, densities were highest on compressed, intermediate on neutral, and lowest on tensed surfaces. Photomicrographs of compressed and extended surfaces appear in Figure 2a. Kruskal-Wallis tests were significant at the 0.05 level but multiple-comparison revealed no significance (Table Ia). When the *Eunicea* species that have much larger clubs than the others, were excluded from the analysis, a significant difference was found between the means of compressed and tensed surfaces. When a branch of a colony bends, clubs on the stretched surface separate; on the compressed surface, they move closer together.

Scaphoids

Scaphoids form the surface layer of *Pseudopterogorgia rigida, Pterogorgia anceps*, and *Gorgonia ventalina*. They are bent down at the tips and encircled with a series of tubercle belts (Fig. 1). In some genera, the tubercles may be reduced or absent from the convex surface. For these elongate sclerites, orientation with respect to colony axis was determined on the compressed, neutral, and tensed surfaces for the aforementioned species. On the neutral surface of *P. anceps* and *P. rigida*, mean angles of surface scaphoids are ±30–36° away from parallel with the longitudinal axis. On compression, mean sclerite angles are 5–12° above those of the neutral surface; on extension, 6–14° below (Table Ib). Sclerites on the surface of *G. ventalina* are 28–36° higher than the neutral on compression but only 9° lower on tension. Kruskal-Wallis tests were significant at the 0.01 level (Table Ib), though the multiple-comparison revealed significance only between the means of compressed and tensed surfaces. On stretched surfaces, sclerites rotate into an alignment closer to parallel with the longitudinal axis of the branch. On compression, they rotate into an orientation closer to perpendicular to the longitudinal axis (Fig. 2b).

Double heads

The double head, or dumb-bell, is characteristic of the genera *Ellisella* and *Lophogorgia*. As the name suggests, these sclerites are simple rods with whorls of tubercles at each end (Fig. 1). They are not organized in distinct layers in the coenenchyme, but appear randomly oriented. No changes in orientation or density can be discerned between compressed, neutral, and tensed surfaces. Kruskal-Wallis test results for intergroup differences between surfaces were not significant (Table Ic). Micrographs of surfaces compression and tension are shown in Figure 3a. Displacement of these small sclerites due to bending of a branch is slight.

Radiates

The sclerite type found on the surface layer of species of the genus *Plexaurella* is the radiate. In *Plexaurella*

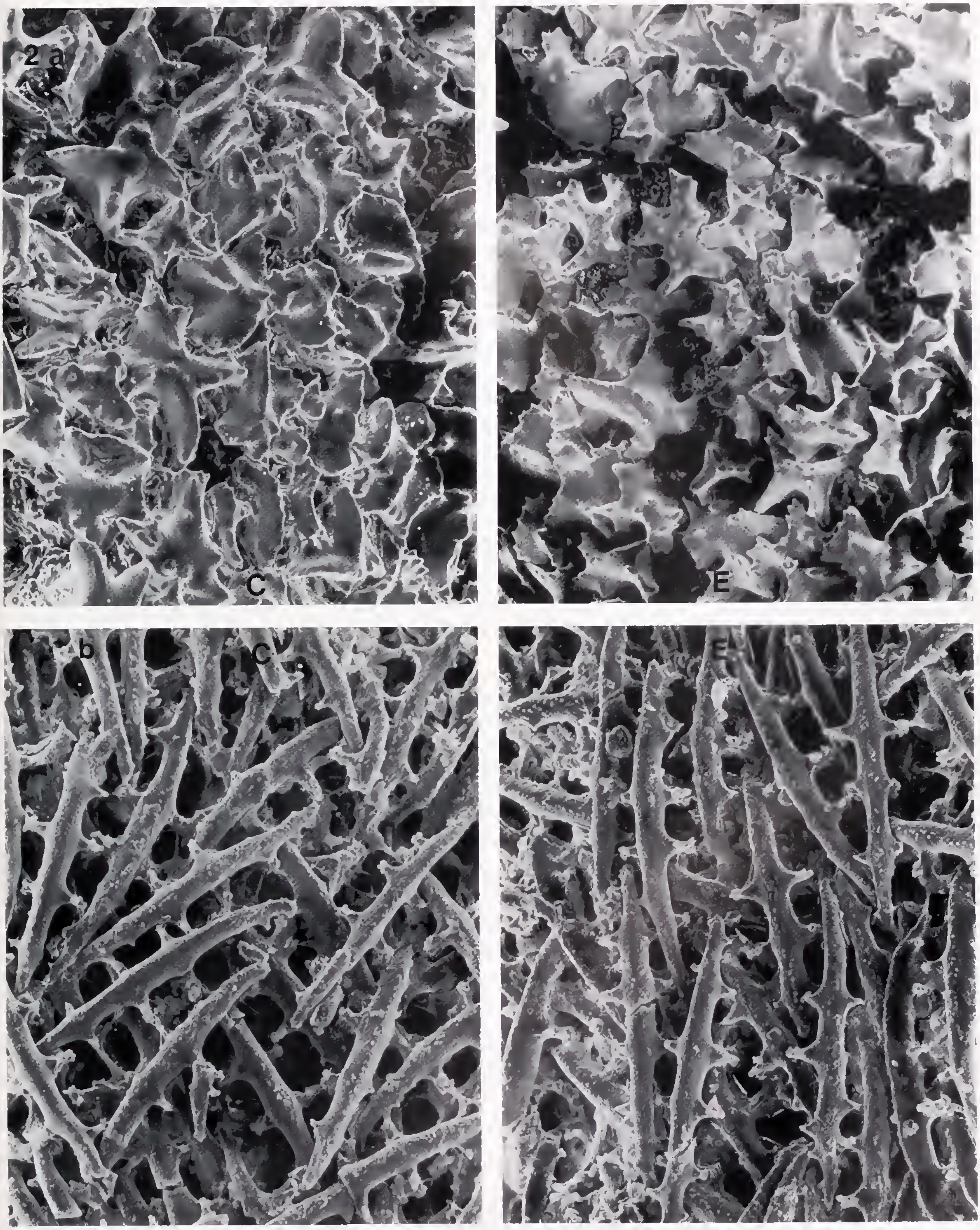

Figure 2. (a) Scanning electron micrographs of *Plexaura flexuosa* clubs in surface view under compression (C) where sclerite heads are closely fitted together and under tension (E) where club heads exhibit considerable separation. Mag. 165×. (b) Scaphoids of *Pseudopterogorgia acerosa* in surface view under compression (C) and extension (E). Longitudinal axis of the colony is vertical. Note the orientation of most scaphoids under compression at about 40° from the longitudinal axis, and under extension almost parallel to the longitudinal axis. Mag. 285×.

Table I

Measurements and statistics for surface sclerites on compressed (C), neutral (N), and tensed (T) surfaces of flexed specimens of several species of gorgonians

	Flexion	C			N			T						
Species	angle	(n)	X	S.D.	(n)	X	S.D.	(n)	X	S.D.	*P*	C-T	C-N	N-T
(a) Density of surface clubs per sample area of 6.67 mm^2. n = number of areas sampled.														
Plexaura homomalla	47°	50	33.4	4.7	51	29.7	2.7	50	24.7	2.7				
P. flexuosa A	12°	54	29.5	1.3	56	26.0	2.0	57	21.4	2.0				
P. flexuosa B	15°	57	31.4	2.7	57	26.7	1.3	56	24.0	2.0	0.05	ns	ns	ns
Eunicea laciniata	35°	59	7.4	0.6	56	4.7	0.6	51	3.4	0.6		(*)	(ns)	(ns)
E. clavigera	13°	61	22.0	2.0	57	19.3	2.0	60	18.0	4.0				
(b) Mean angles of surface scaphoids relative to the longitudinal colony axis.														
Gorgonia ventalina A	37°	150	56	19	159	20	15	138	11	7				
G. ventalina B	37°	167	52	17	191	24	12	181	15	10				
Pterogorgia anceps A	21°	167	44	11	159	36	12	170	22	14	0.01	*	ns	ns
P. anceps B	22°	191	40	11	217	30	9	189	18	12				
Pseudopterogorgia rigida A	39°	143	46	14	121	34	12	131	26	13				
P. rigida B	21°	157	40	9	141	35	10	165	29	10				
(c) Density of surface double heads per 0.33 mm^2 sample area. n = number of areas sampled.														
Lophogorgia punicea	17°	147	24	4	129	22	6	141	26	5	ns			
(d) Mean percentage of sectional area occupied by radiate sclerites.														
Plexaurella grisea	20°	5	87.1	4.3	5	74.6	3.1	5	71.1	2.1	ns			
P. grisea	16°	5	82.4	3.8	5	77.6	2.4	5	75.4	2.1				
(e) Mean angles of evaluation of spindles above the longitudinal colony axis.														
Muricea elongata	30°	413	46	7.5	391	37	6	370	33	3.5	0.10	*	ns	ns
M. atlantica	55°	322	58	11.5	299	39.5	12	319	28.5	11				

Degrees of freedom = 2. *P* values for Kruskal-Wallis one-way ANOVA. Significance (*) of multiple comparison tests between ranked medians; ( ) = exclusive of Eunicea species.

grisea, the six-radiate (Fig. 1) has a main axial rod with three branches on each end, one of which is upturned and longer than the other two, producing an antleriform appearance. The six-radiates are also located in the middle cortex and axial sheath layers; however, they lack the upturned branches and are randomly oriented. Compressed surfaces are comparatively uniform, with few cavities between sclerites, and give an impression of a solid wall of tubercle heads (Fig. 3b“C”). Tensed surfaces are more irregular and indented with more pits, cavities and patches of dark shadow (Fig. 3b“E”). The percentage of area occupied by sclerite as opposed to space was highest on compressed and lowest on extended surfaces (Table Id). The Kruskal-Wallis test for intergroup differences between surfaces was not significant (Table Id). These interdigitating sclerites compact on compression, but under tension spaces open up between the interdigitations.

Spindles

Large, unilaterally spinose spindles (Fig. 1) of the genus *Muricea* are oriented in tufts of approximately parallel sclerites (Fig. 4a). In some, but not all species of *Muricea,* these spindles form large, moveable lids for polyp calyces. In those species, which include *M. elongata* and *M. atlantica,* polyps are crowded together so the lids actually cover most of the surface of the colony and form the effective epidermis. One end of each group of 9–17 spindles is butted onto the middle cortex spindles. Butt end and undersurface tuberculation is extremely dense and irregular. The other, spiny end projects from the colony surface and accounts for its prickly texture. These structures form a trough-like, hinged, calycal lid reminiscent of a drawbridge (Fig. 4a). Between the tuft bases, the general surface is covered by smaller, normal spindles and mesoglea. Flexion of the branch results in a change in the angles of the tufts relative to the colony axis with tufts closer to parallel with the surface of the colony on the extended surface and more perpendicular to the surface on compression (Fig. 4a “E” + “C”). Angles of sclerites in tufts are shown in Table Ie for compressed, neutral, and extended surfaces. Kruskal-Wallis tests were significant

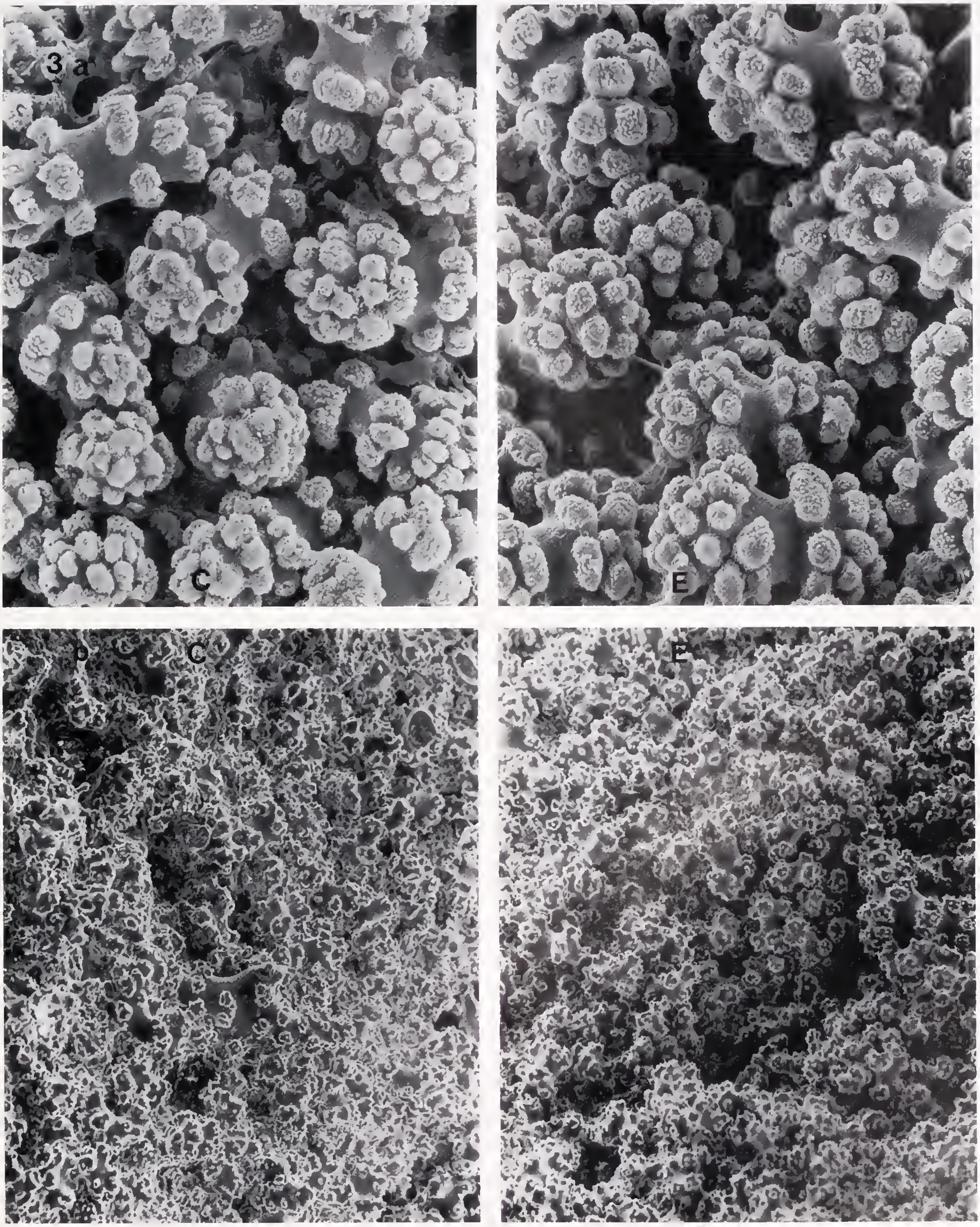

Figure 3. (a) Surface double-heads of *Ellisella barbadensis* under conditions of *compression* (C) and extension (E). No differences in density or orientation of the sclerites is discernable. Mag. 620×. (b) Six-radiate sclerites of *Plexaurella grisea* compressed (C), exhibiting few spaces between sclerites and extended (E), exhibiting more extensive spaces between sclerites. Mag. 105×.

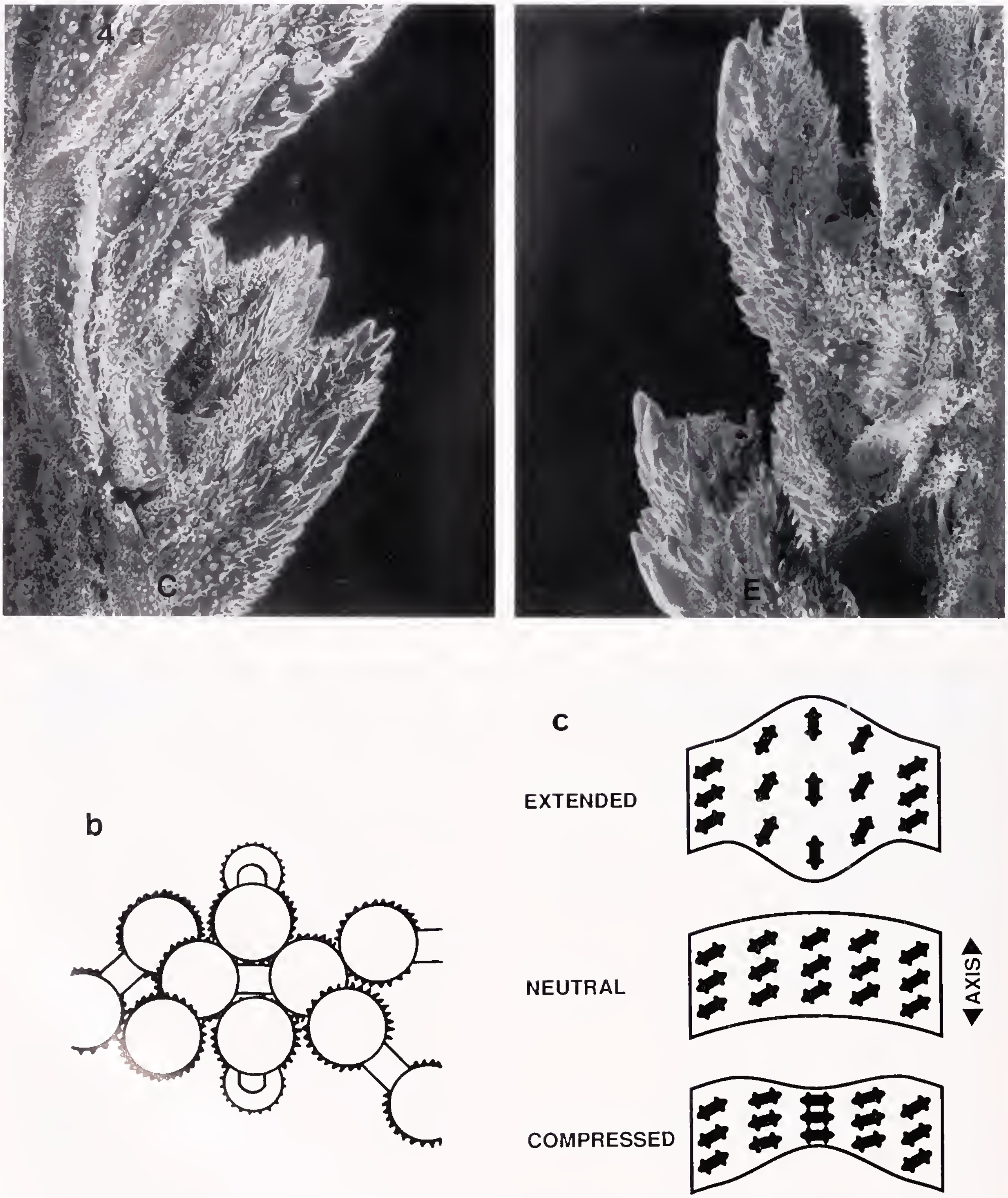

Figure 4. (a) Unilaterally spinose spindles of *Muricea elongata* under compression (C) and extension (E) to show that under compression, the tufts of spindles are deflected away from the longitudinal axis whereas on extension the spindles assume a position more nearly parallel with the axis of the colony. Longitudinal axis of the colony is vertical. Mag. 35×. (b) Diagramatic representation of possible function of double-heads. Random orientation of spine-covered double-head sclerites tends to preclude any but the slightest motion of sclerites relative to each other. These probably function primarily to increase coenenchymal stiffness. Approx. mag. 500×. (c) Diagramatic representation of translational and rotational movements of

at the 0.10 level, and multiple-comparison revealed a significant difference between the means of compressed and tensed surfaces.

When a plant stem is bent, thorns, bristles, and hairs on the outside of the curve tend to go erect, fan out over the outside of the curve, and project away from the surface. On an intuitive level, this would be expected of the *Muricea,* but the opposite happens. The bristle-like tufts almost lie down on the surface of the outer curvature. On the inside of a bend, spines or bristles fixed at an acute angle to the longitudinal axis tend to assume a more acute angle closer to the inside surface of the curve. Again, the opposite occurs with *Muricea.*

Discussion

The microscopic size of sclerites and the surrounding mesogleal matrix make it difficult to even visualize the relationships of sclerites to one another. Measurement and characterization of forces acting on individual sclerites when the colony is subjected to stresses of various kinds is truly daunting. Fixation and dehydration undoubtedly alter the properties of the mesoglea and cause some shrinkage of the highly hydrated gel if it is at all similar to other coelenterate mesoglea (Alexander, 1964; Gosline 1971a). The extent of shrinkage has not been measured for these species, but we estimate it to be less than 10%. On the one species we have measured on drying (a *Menella sp.* from the Indian Ocean), shrinkage was about 5% at seven different locations on the specimen. The volume fraction of sclerites in the coenenchyme of gorgonians is high, and it probably varies interspecifically although volume fraction, again, has not been recorded. For the aforementioned *Menella* species from the Maldives, it was 45% in the tips and 55% in primary branches. Because sclerites provide support for the mesoglea (Muzik and Wainwright, 1977; Koehl, 1982; Currey, 1984), their volume is probably responsible for the low shrinkage. We have assumed that all sclerites are relatively uniformly surrounded by mesoglea. In that event, shrinkage should affect all sclerites similarly so their relative positions should remain similar to that *in vivo.*

Removal of surrounding mesoglea with hypochlorite bleach loosens surface sclerites. In most species, examination with the dissecting microscope clearly reveals when the process has gone too far; *i.e.,* the surface layer is absent. If the process has not gone far enough, sclerites or large parts of them remain obscured by mesoglea. Care was taken to minimize dislocation, but mesoglea removal by hypochlorite is a rather imprecise procedure. The positions of individual sclerites may change during uncovering and subsequent processing and thus alter surface sclerite orientation. The degree of disturbance depends upon the extent to which sclerites loosen and interdigitate with neighboring sclerites.

The following ascribed functional relationships are postulated as those that can be reasonably implied from the rather crude manipulations to which the individual colonies were subjected.

Possible function of clubs (Fig. 5)

Clubs occur as outer cortex components in four of the *Plexaura* and *Eunicea* species examined. All exhibited a higher density of clubs on compressed surfaces than on either neutral or tensed ones. This illustrates vividly the contention of Wainwright *et al.* (1982) regarding the altered density of material on either side of the neutral axis of a bent bar. Compression on a colony surface causes the clubs to move laterally until they contact adjacent clubs. Resistance to compression increases substantially at this point.

Compression or tension of the colony surfaces would also cause a similar compression or tension of the mesogleal gel that surrounds each embedded sclerite. The mesoglea, an elastomer, responds to such forces like a rubber ball being compressed or stretched. Lateral compression of the ball causes its vertical diameter to increase, whereas stretching reduces this diameter (Wainwright, 1988). Clubs, held in the gel by the handle tubercles, move in a direction perpendicular to the colony axis and also separate from each other on extension. Immediately subjacent to the outer cortex is a layer of large, thick spindles in close contact with each other. On the surface under tension, the mesogleal gel stretches over the convex surface and pulls the surface clubs toward the middle cortex spindles. As the tubercles at the base of the club handles come in contact with the irregular tubercles covering the spindle surface, they catch. The first clubs to become engaged are those whose handles are nearest the spindle tubercles. As the clubs are carried along, they contact the clubs that have engaged spindle tubercles. This causes them to bunch up, leaving a series of cracks or spaces.

Compression of the colony surface compresses the mesoglea, which translates into a vertical force acting un-

---

elongate bodies (sclerites) embedded in an elastomer on one half of the surface of a cylinder. Conditions of compression, extension, and no stress (neutral) are illustrated. Inclusions (sclerites) are oriented at about 50° with respect to the longitudinal axis under all conditions of no stress. Maximal displacement occurs in the mid line of the bending plane of the cylinder. Intermediate displacement extends laterally each way from the center of the plane of bending, one quarter of the distance around the circumference, where no translation or rotation occurs.

derneath the surface clubs that lifts them off the spindle surface and disengages them (Wainwright, 1988).

Clubs can move in all six of the degrees of freedom of movement (Alexander, 1983). Pitch, yaw, lateral, and vertical movements of the clubs are all in the plane of the surface layer. Axial motion occurs during compression and tensing of the gel, which increases and decreases the distance between the base of the clubs and the middle cortex spindles. Roll, pitch, yaw, and lateral movement of the clubs are limited by the proximity of adjacent clubs and the degree to which they interdigitate with the plate tubercles on the heads of adjacent clubs. Colony torsion as a whole results in some degree of club rotation. Interdigitation of tubercles enables the rotational forces on a sclerite to be passed to adjacent sclerites.

Possible function of scaphoids (Fig. 5)

In unbent specimens, elongate scaphoids form a surface layer with all sclerites oriented in parallel, as in *G. ventalina*, or with sclerites in two parallel orientations as in *P. anceps* and *P. rigida*. Scaphoids are oriented at approximately 30° away from the longitudinal axis of the colony. Because the sclerites are in a sheet-like layer on the outside of a cylinder, the forces of tension and compression are applied asymmetrically to the sheet when the cylinder is bent (Koehl, 1982). The greatest displacement or distortion occurs in the center of the plane of flexion, with lesser displacement occurring out and around the sides of the cylinder toward neutral axes. On tension, translation will be toward the extremities of the longitudinal axis; rotation of the elongate sclerites will be toward the center of the plane of flexion, which is toward the longitudinal axis (Fig. 4c). Compression reverses both movements (Koehl, 1982).

Surface sclerites do not function completely independently of subjacent middle cortex sclerites. In the species examined, these are belted spindles oriented close to parallel with the longitudinal axis. We think the surface sclerites interact with middle cortex sclerites and modify the mechanical properties of the axial skeleton (Muzik and Wainwright, 1977). When a cylinder is bent, the outside undergoes further displacement than the inside (Wainwright, 1988). Therefore, sclerites on the outside will move more than those of inner layers. On a tensed surface, the mesogleal sheet containing the surface sclerites becomes thinner on being stretched (Wainwright, 1988) and pulls its sclerites down into contact with the middle cortex spindles. These spindles are nearer the center of the cylinder and will not be displaced toward the center as much as surface sclerites. It is unlikely that they will undergo as much translation or rotation even assuming complete freedom of movement. Consequently, the ventral tubercles of surface scaphoids will engage with dorsal tubercles on the underlying spindles and both their translational and rotational movement will be limited. The response will be graduated. As more tubercles engage, resistance to stretch will increase.

Compression thickens mesogleal gel and lifts scaphoids off the backs of underlying spindles. With tubercles disengaged, sclerites are free to undergo translation and rotation in directions opposite those of extension.

Possible function of double heads (Fig. 4)

No change in density of double heads was quantifiable on either compressed, neutral, or tensed colony surfaces. This could be an indication that either there is no difference between the three surfaces, or the techniques used were not sensitive enough to elucidate any differences. Close examination of double head terminal tubercles reveals a series of closely grouped tubercles covered with fine spines, almost like a Velcro ball surrounding each terminus of the central rod. The tuberculation suggests that any motion involving sliding of one tubercle over one of an adjacent sclerite would be inhibited by a high frictional force. The fine spines would limit freedom of motion of surface sclerites in pitch, yaw, lateral, vertical, and axial motion but would not completely inhibit roll. However, random sclerite orientation negates any overall effect that sclerite roll may have on colony flexibility. The main function of this type of sclerite, and its random orientation, is probably to increase coenenchyme stiffness. Because there is some mesoglea between sclerites, there is some slight freedom for movement of sclerites relative to each other that produces limited flexibility. Due to the small size of the sclerites (0.075 mm in length), even a small amount of movement could translate into considerable flexibility over a relatively short distance of a few centimeters.

Possible function of radiates (Fig. 5)

Six-radiate sclerites of the species *Plexaurella grisea* are found in both outer and middle cortex layers, but those in the middle cortex lack the extended rays of those on the surface. The orientation of the surface sclerites is irregular, and the long processes characteristic of them are deeply embedded in mesoglea. Individual sclerites could not be discriminated for counting, but results indicate a smaller sclerite area on sections under tension than under compression. Six-radiate sclerites have a series of smooth surfaces that terminate in large tubercles. The tubercles resemble cauliflower heads designed to catch on anything moving past them from any direction. When the smooth surfaces of two adjacent sclerites or their interlocked arms are in contact, they can slide across each other until the tubercles catch. Because the arms of these sclerites interdigitate, both compression and extension (and torsion for that matter) are limited by the same mechanism. By analogy, the model of a chain can be used to explain the mo-

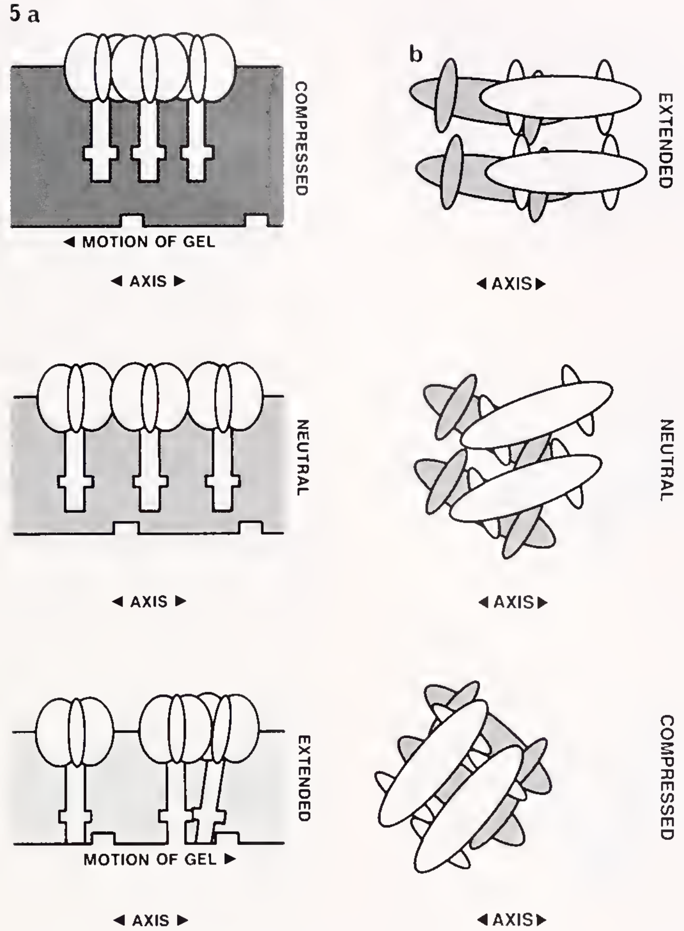

Figure 5. (a) Diagramatic representation of possible function of clubs from a lateral perspective. On compression of the coenenchyme, clubs are lifted by the compressed gel and moved into tighter contact and interdigitation with each other thereby increasing resistance to compression. On the neutral surface, club head processes interdigitate but are not in contact; their handles are not in contact with underlying spindles. On extension, clubs are pulled by elastic coenenchymal gel into contact with surfaces of large underlying spindles and spread apart. Some club handles catch tilt and jam on tubercles of underlying spindles. Approx. mag. 500×. (b) Diagramatic representation of possible function of scaphoids from a surface perspective. In a neutral state of compression, surface scaphoids are oriented at an angle of about 30° to underlying, tubercle-belted spindles. On extension, surface scaphoids are pulled by stretching coenenchymal gel down onto subsurface spindles. Because surface sclerites undergo greater translation (longitudinal movement) than underlying spindles, when their tubercles engage those on the backs of the spindles, they are rotated toward the longitudinal axis. On compression, surface scaphoids are lifted off the backs of spindles and disengage. They are free for both translation and rotation due to mesogleal compression. Because of their orientation in the neutral state, rotation is toward perpendicular *vis a vis* the longitudinal axis. Approx. mag. 200×. (c) Diagramatic representation of possible function of radiates. In neutral compression, radiates with spiny tubercles on the ends of smooth arms are loosely interdigitated. Upon compression, tuberculated arms slide over the smooth portions of the interdigitations until tubercles contact nearby tuberculated heads. On extension, the same process occurs in reverse. This mechanism defines the limits of both extension and compression. Approx. mag. 200×. (d) Diagramatic representation of possible function of unilaterally spinose spindles. Spindles form a pivotable cover attached to one side of the polyp. On compression, underlying cortical spindles and coenenchymal gel squeeze gastrovascular canals and force fluid into the polyp, which expands and forces the overlying lid of unilaterally spinose spindles to pivot and extend out from the longitudinal axis of the colony. Extension, which moves the cortical spindles in the opposite direction, pulls fluid from the polyp into the gastrovascular canals, deflating the polyp and pivoting the lid in toward the colony axis. Approx. mag. 50×.

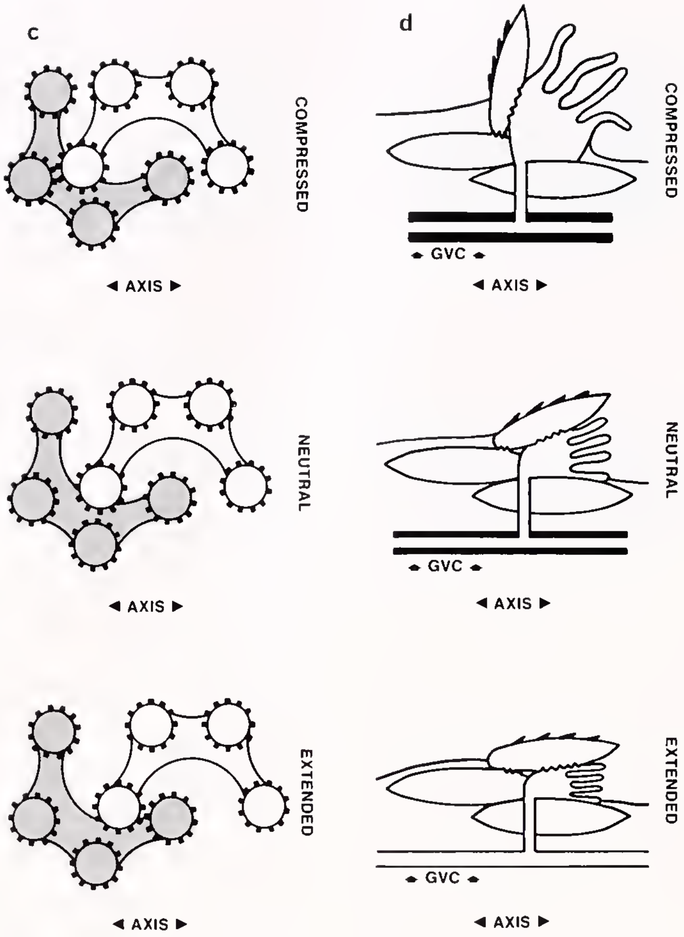

Figure 5. *(Continued)*

tion of a series of interacting six-radiates. Chain links have an extended smooth surface (smooth portion of the arms) on which interlocking links can slide, but which are terminated abruptly by the terminal cross piece (tubercles). Compression of the colony surface causes the smooth rays to slide along each other until the tubercles come into contact. When all radiates are compressed to the extent that they can no longer slide with respect to each other, the surface becomes rigid. Extension pulls the radiates apart along the smooth ray axes until terminal tubercles come in contact with the adjacent sclerite tubercles. This limits further extension of the coenenchyme.

Possible function of unilaterally spinose spindles (Fig. 5)

Compression or extension results in a change in angle of tufts relative to the colony axis with tufts closer to parallel with the colony on extension and more perpendicular to the colony on compression. A possible explanation for these results involves the interaction of the middle cortex spindles, mesogleal gel, and the gastrovascular system of the colony. The feeding polyps are located in the crevice between the calycal trough and the colony body. In a neutral state, the tufts extend out from the colony surface at an angle of approximately 40°, which allows the polyp tentacles to be extended from the crevice for food capture. Compression of the layer of mesogleal gel is translated into a lateral force that pushes the spindles away from the colony surface. Additionally, compression of the gastrodermal tubes that link the polyp cavities increases the internal pressure and forces water out into the only possible exit—the polyp cavities. Because the gastrodermal tubes are linked directly to the polyp gastrocoel, expulsion of water inflates the polyp bodies. Inflation of the polyps results in a force applied to the ventral surface of the surface tufts, pushing them away from the colony surface. There may be a muscle, tensor system associated with gastrovascular canals and the epidermis (Chapman, 1974) that acts on compression (Chapman, 1970; Esford and Lewis, 1990; and Lewis, unpubl. results). Contraction of myoepithelial cells on the back of the tuft will pull it into a more erect position away from the longitudinal axis of the colony. Contraction of the longitudinal muscles of the gastrovascular canals (Hyman, 1940) will shorten the canals, increase pressure, inflate the polyp, and push the tuft away from the surface.

On the extended surface, the gel stretches over the convex colony surface and pulls the tuft toward the colony axis. Extension of the surface results in negative or at least lower water pressure in the gastrodermal tube system. This pressure decrease causes the polyps to deflate and draws the tufts closer to the colony surface. Alternately or additionally, relaxation of the myoepithelial and gut muscle systems may permit the passive mesogleal stretch to pull the calycal tufts in toward the colony surface. There could also be a different set of muscles associated with the polyp that retracts the tufts.

Mechanisms

The foregoing are illustrations of simple and complex interactions of mechanical systems (sets of material objects) termed mechanisms. If a system is underconstrained and has one or more possible modes of motion, it is called a mechanism (Goodman and Warner, 1963); if it is completely constrained against motion, it is called a frame. The mechanism is therefore an assembly of bodies connected in such a way that movement of one causes a required movement of another (Alexander, 1983). The sclerites in gorgonians resemble links as opposed to joints (Alexander, 1983). Links are rigid bodies (Hunt, 1978). They act as passive devices for limiting the freedom of movement of the entire structure. In gorgonians, such passive mechanisms can be used because no muscle or tendon system is required for bending movements of the entire attached colony. The elastic properties of the axial skeleton in conjunction with wave action or current reversal, returns the colony to or through the upright (erect) position. The sclerites limit the extent of these movements.

Clubs form a simple mechanism that acts in one plane to limit compression. In addition, the interdigitation of vertical plates on the heads of clubs enables torsional forces to be transmitted, but this was not investigated.

Surface scaphoids only limit extension when their ventral tuberculations engage the dorsal tubercle belts of underlying sclerites.

At the limits of both extension and compression, six-radiates possibly produce a braced, three-dimensional framework. Though the system is a mechanism, at its limits it may approximate Maxwell's lemma (Parkes, 1965) a theorem for optimization of a space frame with all members in either tension or compression (Wainwright *et al.*, 1982).

The mechanism illustrated by the double heads, which restrict movement in any plane, may be an example that approaches a Michell structure (Wainwright *et al.*, 1982). In these orthogonal, space frameworks, some members are under compression, others under tension.

At their limits, all of these sclerite mechanisms may act as rigid space frames. Between those limits, the sclerite-collagen-gel system possibly functions as a tensegrity structure or what Vogel (1988) calls an unbraced framework. Verification of these suggestions awaits much more detailed observation and experimentation. This preliminary survey has revealed a hitherto unrecorded, compositionally novel, and complicated skeletal system that probably acts in conjunction with and modifies the more conventional axial support system of gorgonian colonial structures.

Acknowledgments

We thank Dr. Lorne Stobbs and Mr. Joe Van Schagen of the Agriculture Canada, Vineland Research Station, for the use of, and assistance with, the scanning electron microscope, and the governments of Trinidad-Tobago and the Bahamas for permission to collect gorgonians.

Literature Cited

Alexander, R. M. 1964. Visco-elastic properties of the mesogloea of jellyfish. *J. Exp. Biol.* **41:** 363–369.

Alexander, R. M. 1983. *Animal Mechanics*, Second Ed. Packyard Publ. Ltd., Oxford. 301 pp.

Bayer, F. M. 1961. *The Shallow-Water Octocorallia of the West Indian Region.* Martinus Nijoff, The Hague. 373 pp.

Bayer, F. M., M. Grasshoff, and J. Verseveldt. 1983. *Illustrated Trilingual Glossary of Morphological and Anatomical Terms Applied to Octocorallia.* E. J. Brill, Leiden. 75 pp.

Chapman, D. M. 1970. Reextension mechanism of a scyphistoma's tentacle. *Can. J. Zool.* **48:** 931–943.

Chapman, D. M. 1974. Cnidarian histology. Pp. 1–92 in *Coelenterate Biology.* L. Muscatine and H. M. Lenhoff, eds. Academic Press, New York.

Chapman, G. 1953. Studies on the mesoglea of coelenterates. I. Histology and chemical properties. *Q. J. Microsc. Sci.* **94:** 155–176.

Currey, J. 1984. *The Mechanical Adaptations of Bones.* Princeton University Press, Princeton, NJ. Pp. 8–40.

Esford, L. E., and J. C. Lewis. 1990. Mechanical properties of Caribbean gorgonians (Coelenterata, Octocorallia). *Mar. Ecol. Prog. Ser.* **67:** 189–200.

Goldberg, W. M. 1976. Comparative study of the chemistry and structure of gorgonian and antipatharian coral skeletons. *Mar. Biol.* **35:** 253–267.

Goldberg, W. M. 1988. Chemistry, histochemistry and microscopy of the organic matrix of spicules from a gorgonian coral. *Histochemistry* **89:** 163–170.

Goldberg, W. M., and Y. Benayahu. 1987a. Spicule formation in the gorgonian coral *Pseudoplexaura flagellosa* 1: Demonstration of intracellular and extracellular growth and the effect of ruthenium red during decalcification. *Bull. Mar. Sci.* **40**(2): 287–303.

Goldberg, W. M., and Y. Benayahu. 1987b. Spicule formation in the gorgonian coral *Pseudoplexaura flagellosa.* 2: Calcium localization by antimonate precipitation. *Bull Mar. Sci.* **40**(2): 304–310.

Goodman, L. E., and W. H. Warner. 1963. *Statics.* Wadsworth Publ. Co., Belmont, CA. 367 pp.

Gosline, J. M. 1971a. Connective tissue mechanics of *Metridium senile.* I. Structural and compositional aspects. *J. Exp Biol.* **55:** 763–774.

Gosline, J. M. 1971b. Connective tissue mechanics of *Metridium senile.* II. Viscoelastic properties and macromolecular model. *J. Exp. Biol.* **55:** 775–795.

Hunt, K. H. 1978. *Kinematic Geometry of Mechanisms.* Clarendon Press, Oxford. 465 pp.

Hyman, L. H. 1940. *The Invertebrates: Protozoa through Ctenophora.* McGraw-Hill, NY. 726 pp.

Jeyasuria, P., and J. C. Lewis. 1987. Mechanical properties of the axial skeleton in gorgonians. *Coral Reefs* **7:** 147–153.

Kingsley, R. J. 1984. Spicule formation in the invertebrates with special reference to the gorgonian *Leptogorgia virgulata. Am. Zool.* **24:** 883–891.

Kingsley, R. J., and N. Watabe. 1984. Synthesis and transport of the organic matrix of the spicules in the gorgonian *Leptogorgia virgulata* (Lamarch) (Coelenterata: Gorgonacea). *Cell Tissue Res.* **235:** 533–538.

Koehl, M. A. R. 1977. Mechanical diversity of the connective tissue of the body wall of sea anemones. *J. Exp. Biol.* **69:** 107–125.

Koehl, M. A. R. 1982. Mechanical design of spicule-reinforced connective tissue: stiffness. *J. Exp. Biol.* **98:** 239–287.

Kukenthal, W. 1901. Gorgonia. *Das Tierreich der Zoology.* **28:** 1–339.

Leversee, G. J. 1969. Composition and function of the axial skeleton in the gorgonian coral *Leptogorgia virgulata. Am. Zool.* **9:** 1115.

Leversee, G. J. 1984. Flow and feeding in fan-shaped colonies of the gorgonian coral *Leptogorgia. Biol. Bull.* **151:** 344–356.

Lowenstam, H. A. 1964. Coexisting calcites and aragonites from skeletal carbonates of marine organisms and their strontium and magnesium contents. In *Recent Researches in the Fields of Hydrosphere. Atmosphere and Nuclear Geochemistry,* Y. Miyake and T. Koyama, eds. Maruzen Co. Ltd., Tokyo.

Majoran, S. 1987. Structural investigation of ocotocoral sclerites. *Zool. Scr* **16**(4): 277–287.

Muzik, K., and S. A. Wainwright. 1977. Morphology and habitat of five Fijian sea fans. *Bull. Mar Sci.* **27**(2): 308–337.

Parkes, E. W. 1965. *Braced Frameworks.* Pergamon Press, Oxford. 198 pp.

Rees, J. T. 1972. The effect of current on growth form in an octocoral. *J Exp. Mar. Biol. Ecol.* **10:** 115–123.

Sebens, K. P. 1984. Water flow and coral colony size: interhabitat comparison of the octocoral *Alcyonium siderium. Proc. Nat. Acad. Sci. USA* **81:** 5473–5477.

Siegel, S., and N. J. Castellan. 1988. *Nonparametric Statistics for the Behavioral Sciences.* 2nd ed. McGraw-Hill, New York. 399 pp.

Thibaudeau, S. 1983. *The composition, form and function of spicules in octocorals.* B.Sc. Honours thesis. Brock University. 262 pp.

Velimirov, B. 1976. Variations in growth forms of *Eunicella cavolinii* Koch (Octocorallia) related to intensity of water movement. *Exp. Mar. Biol. Ecol.* **21:** 109–117.

Verill, A. E. 1868. Review of the corals and polyps of the West Coast of America. *Trans. Conn. Acad. Arts Sci.* **1:** 377–459.

Vogel, S. 1981. *Life in Moving Fluids, the Physical Biology of Flow.* Princeton University Press. New Jersey. 352 pp.

Vogel, S. 1988. *Life Devices.* Princeton University Press. New Jersey. 367 pp.

Wainwright, S. A. 1988. *Axis and Circumference.* Harvard University Press, Cambridge, MA. 132 pp.

Wainwright, S. A., W. D. Biggs, J. D. Currey, and J. M. Gosline. 1982. *Mechanical Design in Organisms.* Princeton University Press, Princeton, NJ. 423 pp.

Yoshioka, P. M., and B. B. Yoshioka. 1989. Effects of wave energy, topographic relief and sediment transport on the distribution of shallow-water gorgonians of Puerto Rico. *Coral Reefs* **8:** 145–152.

Zar, J. H. 1984. *Biostatistical Analysis.* Prentice-Hall, Englewood Cliffs, NJ. 718 pp.

Reference: *Biol. Bull.* **181:** 289–297. (October, 1991)

Acid-Base and Ionic Regulation, During and Following Emersion, in the Freshwater Bivalve, *Anodonta grandis simpsoniana* (Bivalvia: Unionidae)

ROGER A. BYRNE* AND BRIAN R. McMAHON

Department of Biological Sciences, The University of Calgary, 2500 University Dr. NW., Calgary, Alberta, Canada T2N 1N4

Abstract. Specimens of the boreal clam, *Anodonta grandis simpsoniana* were emersed at 10°C for 6 days and then reimmersed for 24 h. The clams lost water at a rate of 1.6% total water per day. After 144 h of emersion, water weight had declined by almost 15%, while extracellular fluid (ECF) osmolality had increased 30% to 52 mOsm kg^{-1}. Control levels were reattained after 6 h reimmersion. ECF P_{O_2} declined rapidly in the first 24 h of emersion, but remained near 20 Torr for the full 6-day exposure. After an initial rapid fall, pH declined at a slower rate, reaching 7.494 ± 0.037 (mean ± SEM) at 144 h. P_{CO_2} was elevated from 0.6 ± 0.6 to 12.4 ± 1.1 Torr after 96 h, but no further increase was noted. ECF [Ca] increased threefold to 13.1 ± 0.8 mmol l^{-1}, while [HCO_3app] rose from 5.4 ± 0.3 to a maximum of 12.9 ± 0.8 mmol l^{-1} after 144 h. ECF [Na] and [Cl] were not affected by emersion. On reimmersion, recovery was rapid, with pH, P_{O_2} and P_{CO_2} returning to control within 2 h, while [Ca] and [HCO_3app] remained elevated until 24 h after reimmersion. A 1:1 stoichiometry between [Ca] and [HCO_3app] existed throughout the emersion and reimmersion periods. In the absence of protein buffers, the fall in ECF pH was arrested by the mobilization of calcium carbonate, presumably from the shell. By 96 h emersion P_{CO_2} and P_{O_2} had stabilized, suggesting that diffusion gradients sufficient to allow limited gas exchange had been established.

Introduction

Marine intertidal bivalves experience cyclical episodes of emersion and reimmersion, and their physiological and behavioral responses have been documented (see reviews by McMahon, 1988; Shick *et al.*, 1988). In the freshwater environment, however, changes in water level and emersion events are unpredictable; their timing and duration is dependent on such factors as rainfall, temperature, and physical changes in the watershed. The responses to emersion of the freshwater bivalves that inhabit the shallower regions of such systems are less well known. As an adaptation to this stress, some species of freshwater bivalve can withstand emersion for up to a year (Hiscock, 1953).

An emersed clam is faced with opposing needs: water conservation, accomplished by valve closure, and respiration, requiring valve opening. In addition, the problems of acid-base balance, ion regulation, and excretion are all exacerbated by aerial exposure. Intertidal bivalves need only withstand approximately 12 h emersion before the next tidal inundation. Even so, many intertidal bivalves have evolved compensations, chiefly respiratory, that enable them to conserve energy during emersion. Examples include valve gaping and aerial gas exchange (Boyden, 1972; Widdows *et al.*, 1979) and the use of shell $CaCO_3$ for maintaining acid-base balance (Crenshaw and Neff, 1969; Crenshaw, 1972; Akberali *et al.*, 1977; Booth and Mangum, 1978; Jokumsen and Fyhn, 1982; Booth *et al.*, 1984).

The effects of emersion on freshwater clams are known primarily from studies of the responses of the corbiculid bivalve, *Corbicula fluminea* (Müller) (McMahon, 1979, 1983; McMahon and Williams, 1984; Byrne *et al.*, 1988, 1989, 1990, 1991a, b). *C. fluminea*, however, is a relatively recent invader of freshwater (Keen and Casey, 1969) and so displays many responses thought to be intermediate between those of estuarine clams and those of more an-

Received 2 February 1991; accepted 20 June 1991.

* Current address: Department of Biology, SUNY College at Fredonia, Fredonia, NY 14063.

cient freshwater species (McMahon, 1979; Byrne *et al.*, 1988). Dietz (1974) described aerial O_2 consumption and responses to dehydration in the unionid, *Ligumia subrostrata*, and Heming *et al.* (1988) examined acid-base changes in extrapallial (mantle cavity) fluid of *Margaritifera margaritifera* during emersion. These studies indicate that freshwater bivalves possess adaptations to emersion that may account for some of the observed tolerances to aerial exposure. But the respiratory, acid-base, and ion regulatory consequences of emersion and subsequent reimmersion have not been comprehensively examined in a unionid clam.

Here we report an examination of such events during an extended bout of aerial exposure and for 24 h after reimmersion in the unionid bivalve *Anodonta grandis simpsoniana*. Although this species inhabits the shallow, littoral region of lakes, and members of the population under study could become aerially exposed with minor changes in lake level, such occurrences would be rare. Therefore, any compensations to aerial exposure and subsequent reimmersion that may be noted in this species may be interpreted as an inherent ability of unionid clams to withstand periods of emersion and not any particular response of an often exposed species.

Materials and Methods

Animals

Anodonta grandis simpsoniana is a northern nearctic species inhabiting the littoral region of boreal lakes. Specimens were collected at depths of between 1–7 m by SCUBA divers from Narrow Lake in north-central Alberta. Clams were returned to the laboratory within 6 h and maintained, unfed, at 10°C in aerated aquaria containing artificial pondwater (APW; composition in mmol l^{-1}: 0.5 NaCl, 0.4 $CaCl_2$, 0.2 $NaHCO_3$, 0.05 KCl; Dietz and Branton, 1975) for at least 2 weeks prior to experimentation.

Emersion and reimmersion

Seventy animals were numbered, and groups of 14 individuals were placed on plastic mesh platforms suspended 3 cm above the bottom in each of 5 covered plastic basins (30 × 25 × 18 cm). The clams were submerged to a depth of 2 cm above the animal with aerated APW at 10°C.

A preliminary experiment indicated that a 144 h (6 days) period of emersion resulted in a significant response without mortality. Thus, after a 24 h acclimation period in the containers, the clams were emersed by emptying the container to a level of 2 cm from the bottom thereby retaining a water reservoir to maintain the humidity in the basin near saturation. The water in the five basins was lowered at 10-min intervals so that the subsequent samples could be taken at the same nominal exposure time. After an emersion period, at constant temperature, of 144 h, the clams were reimmersed by gently filling the basins with temperature-equilibrated APW. The reimmersion period lasted 24 h. No mortality resulted during either the emersion or reimmersion periods.

At intervals of 0, 1, 7, 25, 48, 96, and 144 h emersion, and at 2, 6, and 24 h reimmersion, five clams (one per basin) were removed and an extracellular fluid (ECF) sample taken anaerobically by pericardiac puncture using cooled glass syringes (after the method of Fyhn and Costlow, 1975). ECF P_{O_2}, P_{CO_2} and pH were measured immediately on 500 μl samples using a Radiometer BMS 3 Mk 2 Blood Microsystem maintained at experimental temperature and connected to a Radiometer PHM 73 pH/Blood gas monitor. P_{O_2} and P_{CO_2} were determined by means of a Radiometer P_{O_2} (E5047-0) and P_{CO_2} (E5037-0) electrode respectively; pH was measured using a Radiometer glass capillary pH electrode (G299A). Total CO_2 (C_{CO_2}) was also measured immediately on 45 μl samples by means of a Corning 965 CO_2 Analyzer calibrated with standard $NaHCO_3$ solution. The remaining ECF (500–800 μl) was stored at 4°C for subsequent ion analyses. Immediately following sampling, the soft tissue of the clams was removed from the shell and dried to constant weight (>96 h) at 80°C.

ECF [Na] and [K] were measured using a Perkin-Elmer model 5000 atomic absorption spectrophotometer on samples diluted with 1% CsCl, and ECF [Ca] was determined on samples diluted with 1% $LaCl_3$. ECF [Cl] was measured by means of a Radiometer CMT10 chloride titrator.

In another experiment, 60 specimens were individually numbered, blotted of excess water, and weighed to the nearest 0.1 mg. Animals were placed in containers filled with APW at 10°C for 24 h, emersed for 144 h, and reimmersed for 24 h, as described previously. At the same time intervals as in the previous experiment, a sample of five animals was removed, blotted of excess water, and reweighed to determine water loss or gain. An ECF sample was drawn from each animal and its osmolality determined on 50 μl aliquots using a freezing point depression osmometer (Precision Systems μOsmette). The soft tissue was excised, dried (80°C, >96 h), and weighed; the shell was blotted dry and weighed. Total body water [total weight at the beginning of the experiment − (shell weight + dry tissue weight)] was calculated. All weight changes were assumed to be due to water loss or gain. The change in body water content was calculated from the weight change at the experimental time and was expressed as a percentage of the initial body water content.

In vitro determinations of CO_2 combining curves were performed on ECF drawn from the pericardial cavities of six animals. The sample from each animal was centrifuged at 6000 × *g*, and the supernatants from all samples were then pooled and maintained on ice. Aliquots (100 μl) of pooled ECF were placed in equilibration tubes and tonometered at 10°C in a Radiometer BMS2 Mk 2 Blood Micro System with $CO_2/O_2/N_2$ mixtures of 0.05%, 0.1%, 0.4%, 1.0%, 2.0% and 3.0% CO_2 in 50% O_2 and balance N_2 supplied by Wösthoff precision gas mixing pumps. After equilibration, ECF pH and C_{CO_2} were determined as described previously.

Calculations

The pK_{app} (apparent pK of the CO_2/bicarbonate buffer system) of clam ECF was calculated from the P_{CO_2} equilibration tension (Torr) and the corresponding measurements of pH and C_{CO_2} (mmol l^{-1}) for each *in vitro* sample. The calculation was carried out by rearrangement of the Henderson-Hasselbalch equation as follows:

$$pK_{app} = pH - \log\left(\frac{C_{CO_2}}{\alpha CO_2 \cdot P_{CO_2}} - 1\right)$$

The solubility coefficient of CO_2 (αCO_2) at 10°C was calculated by interpolation from the table in Cameron (1986) as 0.069 mmol (l Torr)$^{-1}$. As there was no relationship between pK_{app} and pH ($r = 0.01$; $P > 0.05$), the average value of pK_{app} (6.436 ± 0.035) was used to calculate the P_{CO_2} isopleths for the plot of pH against apparent bicarbonate concentration (see Fig. 6). The apparent bicarbonate (HCO_3app mmol l^{-1}) is that portion of the C_{CO_2} remaining after the dissolved CO_2 is removed; it is predominantly HCO_3, but includes carbonate, carbamates, and other ion pairs (see Heisler, 1986). Concentrations of apparent bicarbonate were calculated from C_{CO_2} according to the equation:

$$HCO_3app = C_{CO_2} - \alpha CO_2 \cdot P_{CO_2}$$

The HCO_3app and pH data were used to estimate the *in vitro* buffer capacity of the ECF as the change in HCO_3app per unit change in pH (Slykes). Apparent '*in vivo*' buffering capacity was calculated from measured HCO_3app and pH values over the first 96 h of emersion.

Net ion flux on reimmersion

Ten clams were aerially exposed for 6 days at 10°C under conditions of about 100% relative humidity. The clams were then placed in individual baths containing 50 ml APW. Once the clams had opened their valves and had commenced siphoning (5–15 min), bathing medium samples were taken; two additional samples were taken after 1 h and 2 h incubation. The clams were then returned to an aquarium containing aerated pondwater. At 6, 12, 24, 36, and 48 h reimmersion, the same clams were again placed in 50 ml APW and samples of bathing medium taken initially and 1 h later. Handling and other disturbances were minimized throughout. Undiluted samples were assayed for Na and K by emission spectroscopy with a Perkin-Elmer model 5000 atomic absorption spectrophotometer. Calcium concentration was determined by atomic absorption spectroscopy on samples diluted with $LaCl_3$, while Cl content was measured by coulometric titration on a Radiometer CMT10 adjusted to assay low concentrations (± 0.05 mmol $\cdot$ l^{-1}). The soft tissues of each clam were excised and dried to constant weight at 80°C (96 h). The net ion flux (J_{net}) during each sampling period was calculated from the change in the ionic content of the bathing medium over time, and normalized to the dry weight of tissue. The net ion fluxes of a control group of ten continually immersed clams were also determined.

Statistics

All data are expressed as means ± SEM. For the changes in ECF ion and acid-base variables, a single classification ANOVA was performed with time of sample as the classificatory variable; emersion and reimmersion samples were both included. If the ANOVA proved to be significant ($P < 0.05$), sequential contrasts were performed in which the control value was compared with each experimental value to detect specific significant differences ($P < 0.05$). SYSTAT procedures were used for statistical analyses. The relationship between [Ca] and [HCO_3app] was tested by least squares linear regression. For the net ion flux experiment, a repeated measures ANOVA was performed on the flux of each ion over time. The mean fluxes were compared to the flux of the control group, and the difference and its significance were determined by post-hoc Neuman-Keul's tests ($\alpha = 0.05$) using the repeated measures ANOVA mean square error term and an "n" of 10.

Results

All experimental specimens of *Anodonta grandis simpsoniana* survived 6 days of aerial exposure at 10°C and a subsequent 24 h of reimmersion. While emersed, the clams lost about 1.6% of their total body water per day (Fig. 1). The weight loss was consistently significantly greater than pre-emersion controls by 48 h emersion. ECF osmolality increased from a control value of 42 ± 1 mOsm kg^{-1} to 54 ± 2 mOsm kg^{-1} by 144 h emersion (Fig. 1). This constituted a 28% increase in solute whereas water loss was only 13%. ECF osmolality was significantly related to emersion time:

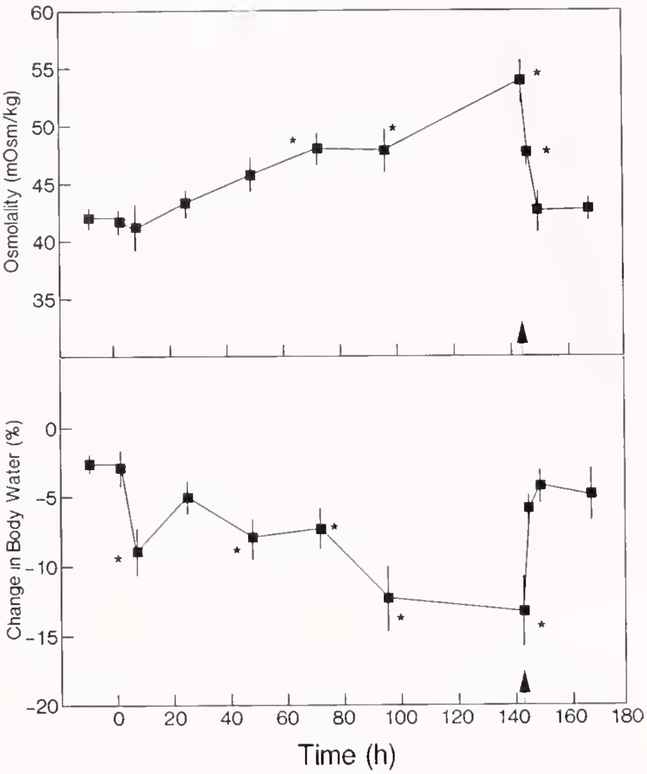

Figure 1. Time course of changes in ECF osmolality (upper panel) and body water content (lower panel) in *Anodonta grandis simpsoniana* during 144 h emersion and 24 h reimmersion in pondwater at 10°C. Symbols are mean values for five clams; bars are standard errors of the mean. Asterisks indicate values significantly different from control ($P < 0.05$). The arrows indicate the time of reimmersion in pondwater.

$$\text{Osmolality} = 41.4\ (\pm 3.2) + 0.082\ (\pm 0.010) \times \text{emersion time (h)}$$
$$(\pm\text{SE};\ R^2 = 0.63;\ df = 1, 38)$$

This translates to an increase in osmolality of approximately 2 mOsm kg^{-1} d^{-1}. Reimmersion resulted in return of water weight to control within 2 h. ECF osmolality declined to control within 6 h of resubmergence.

During the first hour of emersion the clams displayed a significant decline in ECF P_{O_2}; thereafter, a further, but slower decrease occurred over the course of the emersion period (Fig. 2). Values remained above 20 Torr throughout the time that the animals were exposed. During reimmersion, the ECF was rapidly reoxygenated, but not to pre-emersion controls values, even after 24 h of resubmergence.

ECF P_{CO_2} rose steadily during the first 24 h of emersion, reaching 7.7 ± 1.1 Torr (Fig. 2). Thereafter, P_{CO_2} continued to rise, but at a slower rate, and after 96 h of emersion values stabilized near 13 Torr. On reimmersion, ECF P_{CO_2} declined to pre-emersion values within 6 h of resubmergence.

Emersion resulted in an ECF acidosis, with pH falling significantly below pre-emersion values after the clams had been in air for 7 h (Fig. 2). Although the acidosis was progressive, the rate of pH decline slowed after 24 h and reached a seemingly stable level near 7.5; there it remained until the end of the emersion period. But the steady pH is misleading, as $[H^+]$ continued to rise until 96 h after the onset of emersion; then it remained unchanged. ECF pH returned to control values within 2 h of resubmergence.

Both ECF [Ca] and [HCO_3app] changed significantly with the duration of exposure and on return to water (Fig. 3). ECF [HCO_3app] increased rapidly to 8.8 ± 0.6 mmol l^{-1} during the first 24 h of exposure and then rose less rapidly to 12.9 ± 0.8 mmol l^{-1} by the end of the emersion period. ECF [Ca] had almost doubled from 5.5 ± 0.4 mmol·l^{-1} to 10.0 ± 0.5 mmol·l^{-1} after 48 h emersion and continued to rise, but at a slower rate, reaching 13.1 ± 0.8 mmol·l^{-1} after 144 h in air. When the clams were reimmersed, the ECF concentrations of both Ca and HCO_3app declined rapidly. [Ca] returned to pre-emersion

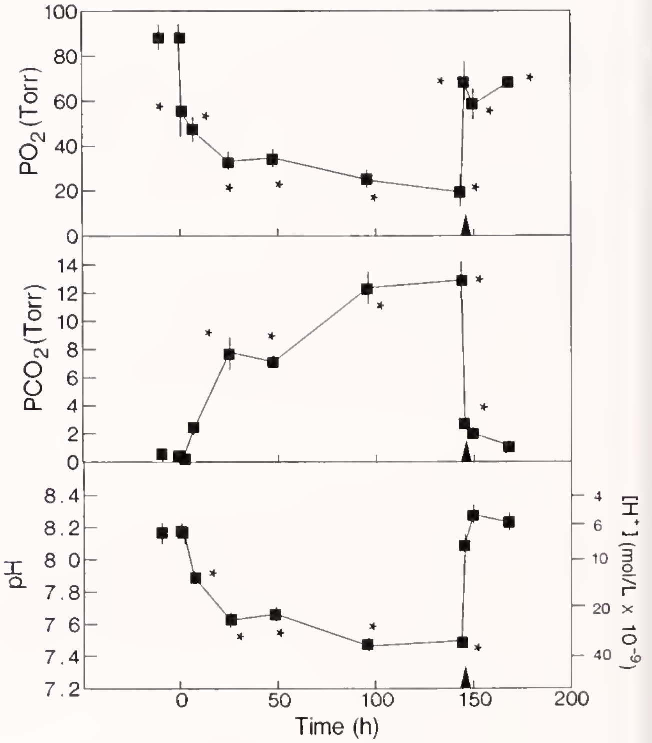

Figure 2. Time course of changes in ECF P_{O_2} (upper), P_{CO_2} (middle), and pH (lower) in *Anodonta grandis simpsoniana* during 144 h emersion and 24 h reimmersion in pondwater at 10°C. The control condition (time = 0) is repeated to the left for clarity. Symbols are mean values for five clams; bars are standard errors of the mean. Asterisks indicate values significantly different from control ($P < 0.05$). The arrows indicate the time of reimmersion in pondwater.

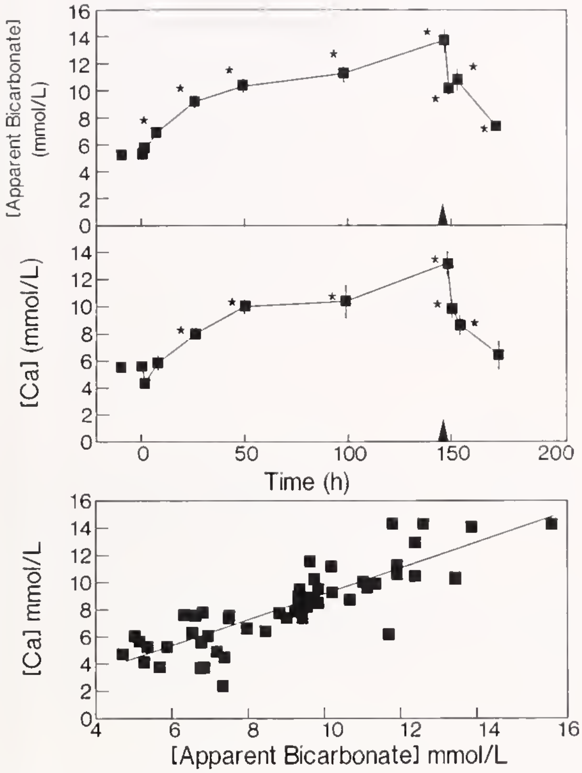

Figure 3. The upper two panels show the time course of changes in extracellular [HCO_3app] (upper), and [Ca] (middle) in *Anodonta grandis simpsoniana* during 144 h emersion and 24 h reimmersion in pondwater at 10°C. The control condition (time = 0) is repeated to the left for clarity. Symbols are mean values for five clams; bars are standard errors of the mean. Asterisks indicate values significantly different from control ($P < 0.05$). The arrows indicate the time of reimmersion in pondwater. The lower panel shows the relationship between [Ca] and [HCO_3app] in the extracellular fluid of both emersed and reimmersed specimens of *Anodonta grandis simpsoniana*. Note the 1:1 stoichiometry between these two ion species.

values by 24 h resubmergence whereas, after the same period of reimmersion, HCO_3app remained elevated over controls.

The pattern of increase and decline in ECF Ca and HCO_3app was strikingly similar. Indeed, there was a 1:1 stoichiometric relationship between ECF levels of Ca and HCO_3app (Fig. 3) measured throughout the emersion and reimmersion periods. The regression equation relating [Ca] to [HCO_3app] was:

$$[\mathrm{Ca}] = -0.6 + 0.99*[\mathrm{HCO_3app}] \qquad (R^2 = 0.72;\ \mathrm{df} = 1,\ 48)$$

The two other major ECF ions, Na and Cl, did not change significantly throughout either the emersion or reimmersion periods (Fig. 4). The slight decrease in concentrations of both these ions on reimmersion was not significant. ECF [K] constituted a small proportion of the total ionic strength but showed significant increases between 24 and 48 h emersion, and then declined to control levels for the balance of the emersion period and throughout the reimmersion period.

As the protein concentration in clam ECF is low (0.24 ± 0.03 $g \cdot l^{-1}$; R. A. Byrne and B. R. McMahon, unpub. data), the *in vitro* non-bicarbonate buffering capacity of the ECF was also low. The *in vitro* relationship between pH and HCO_3app was:

$$[\mathrm{HCO_3app}] = 13.64\ (\pm 0.30) - 0.68\ (\pm 0.20)*\mathrm{pH} \qquad (R^2 = 0.75,\ \mathrm{df} = 1,\ 4).$$

During the first 96 h of emersion, the relationship between ECF pH and apparent bicarbonate described a steeper linear association. This *in vivo* relationship yielded the following regression equation:

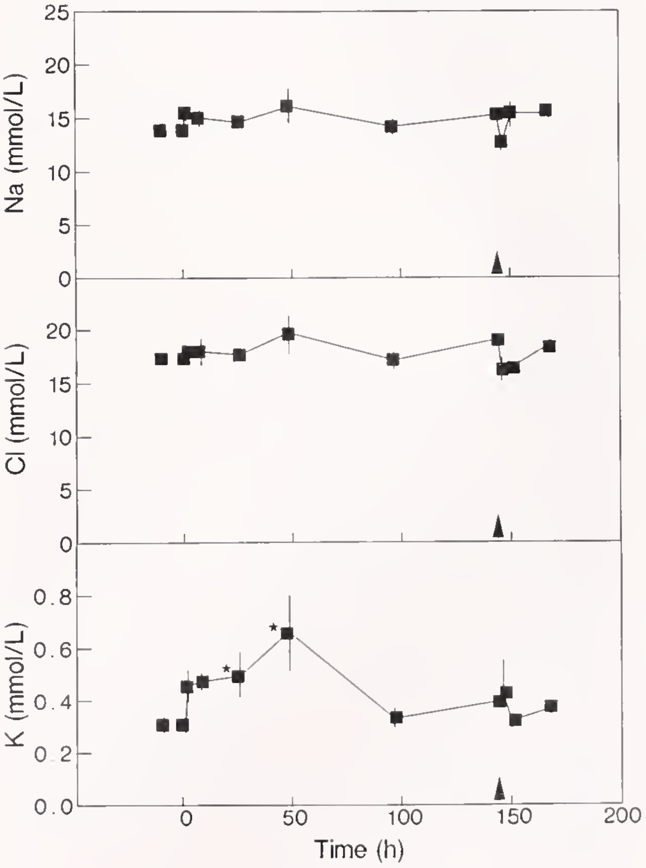

Figure 4. Time course of changes in extracellular [Na] (upper panel), [Cl] (middle panel), and [K] (lower panel) in *Anodonta grandis simpsoniana* during 144 h emersion and 24 h reimmersion in pondwater at 10°C. The control condition (time = 0) is repeated to the left for clarity. Symbols are mean values for five clams; bars are standard errors of the mean. Asterisks indicate values significantly different from control ($P < 0.05$). The arrows indicate the time of reimmersion in pondwater.

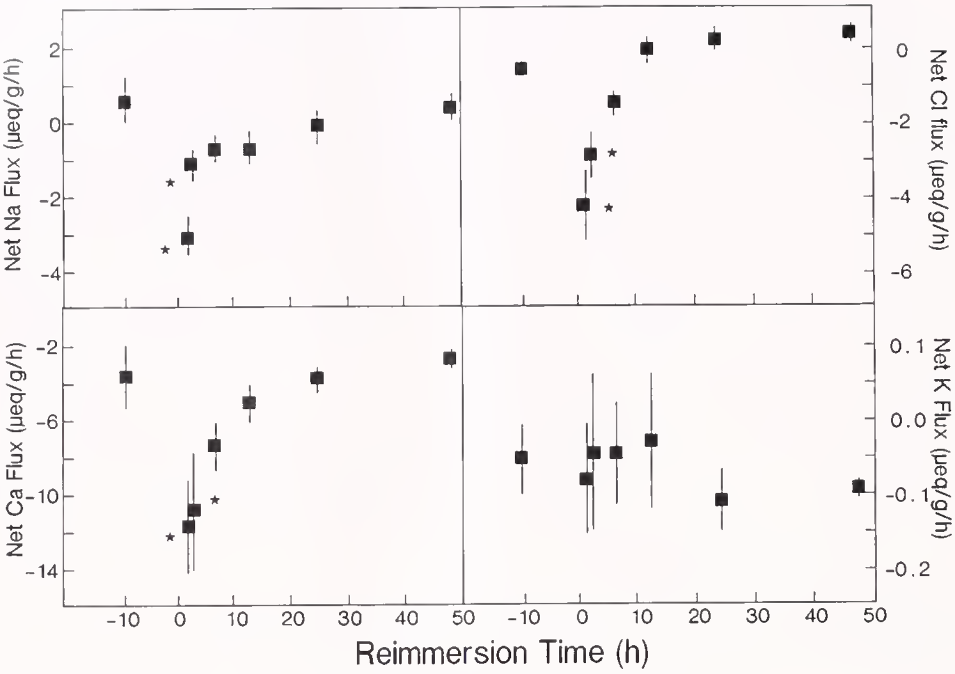

Figure 5. The time course of net ion flux ($\mu eq \cdot g^{-1} \cdot h^{-1}$) for specimens of *Anodonta grandis simpsoniana* over a 48 h reimmersion period following 144 h emersion at 10°C. Values are for Na, Cl, Ca, and K. Asterisks indicate significant differences when compared to the pre-emersion value ($P < 0.05$). Symbols are means of values for ten animals; bars are standard errors of the mean.

$$[HCO_3app] = 56.80 (\pm 1.32) - 6.24 (\pm 0.87)*pH \quad (R^2 = 0.65, df = 1, 28),$$

indicating an "*in vivo*" buffering capacity almost 10 fold higher than that suggested by the *in vitro* determination.

When clams were reimmersed after 6 days of aerial exposure, there were immediate and large losses of calcium, sodium, and chloride from the animals (Fig. 5), followed by a return to control flux levels over the reimmersion period. Initial (first hour) loss of calcium was the greatest, at −11.7 ± 2.5 $\mu eq \cdot g^{-1} \cdot h^{-1}$, whereas the value for sodium was −3.0 ± 0.5, and for chloride −4.3 ± 0.9 $\mu eq \cdot g^{-1} \cdot h^{-1}$. There was no significant change in potassium flux over the reimmersion period, but there was a large variation in initial flux (Fig. 6). Net fluxes for sodium, calcium, and chloride were not significantly different from control fluxes by 6 h reimmersion. Fluxes for sodium and chloride attained steady state ($J_{net} \sim 0$), whereas calcium net fluxes were always negative.

Discussion

Changes in ECF acid-base status during emersion and on reimmersion in *Anodonta grandis simpsoniana* are summarized in the pH-apparent bicarbonate diagram (Fig. 6). The clams experienced a respiratory acidosis during emersion that was partially compensated by increases in apparent bicarbonate concentration. After 96 h of emersion, the pH stabilized, and further increases in HCO₃app were not associated with an increase in P_{CO_2}. On reimmersion, a rapid rise in pH was accompanied by a fall in P_{CO_2} and bicarbonate. Although pH and P_{CO_2} returned to control levels rapidly, bicarbonate concentrations remained elevated even after 24 h reimmersion.

This pattern of acid-base response to emersion is similar to that reported for the freshwater corbiculid bivalve, *Corbicula fluminea* (Byrne *et al.*, 1991b) in that the acidosis is progressive, and the rise in HCO₃app keeps pace with the development of the respiratory component of the acidosis. The littoral crab *Pachygrapsus crassipes* also shows a qualitatively similar pattern when emersed (Burnett and McMahon, 1987).

Valve gaping, a behavior in which the shell valves open periodically and which may allow limited gas exchange, was observed in emersed *A. grandis simpsoniana*. ECF P_{O_2} never went below 20 Torr and P_{CO_2} stabilized at near 13 Torr, suggesting that clams were either not completely closed systems, *i.e.*, that O_2 and CO_2 could diffuse in and out, respectively, or that a reduction in aerobic metabolism had taken place. The 1:1 stoichiometry between calcium and apparent bicarbonate suggests an equilibrium resulting from

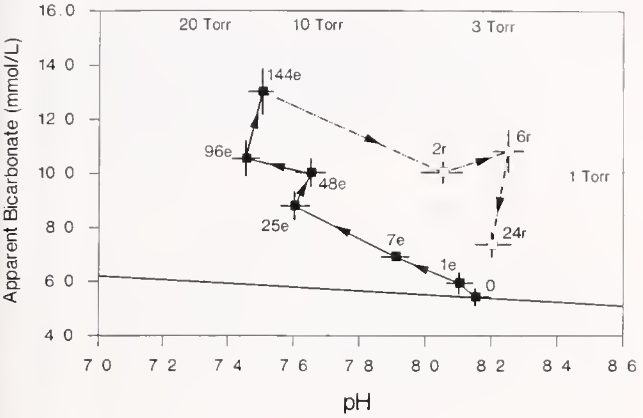

Figure 6. Diagram summarizing changes in extracellular pH, apparent bicarbonate and P_{CO_2} in *Anodonta grandis simpsoniana* during 144 h emersion and 24 h reimmersion in pondwater at 10°C. Closed symbols joined by solid lines are values for emersed clams while stippled symbols connected by dashed line are those of reimmersed clams. Values are means and vertical and horizontal bars are SEM's for HCO_3app and pH, respectively. The arrows indicate the time course while the numbers alongside the symbols indicate the length of time, in hours, emersed (e) or reimmersed (r). The solid straight line represents the *in vitro* non-bicarbonate buffer line for clam ECF at 10°C.

$$CaCO_3 + H^+ \rightarrow Ca^{2+} + HCO_3^-$$

In a completely closed system, the levels of HCO_3^- and Ca would rise as long as protons were being produced. In the emersed, incompletely closed clam, the levels of HCO_3^- that are accumulated are determined by the ability of the clam to offload CO_2 to the environment. The attainment of the new equilibrium between CO_2, HCO_3^-, and Ca^{2+} is achieved after a period in air, during which ECF P_{CO_2} rises to the "equilibrium" level. In *Anodonta grandis simpsoniana* at 10°C, this process takes 96 h. The continued production of Ca and HCO_3^- after this time suggests that the buffering of protons continues with the further dissolution of $CaCO_3$, but that an equilibrium has been established with CO_2 being released.

The effectiveness of the shell buffer system, presumably the major buffer system in operation, can be seen by the 10 fold increase in buffering capacity of the "*in vivo*" system over the *in vitro* determinations on isolated ECF. Mobilization of $CaCO_3$ from shell has been implicated in acid-base control in a number of bivalve species. During aerial exposure, calcium levels in the body fluids of *Mya arenaria* rose (Collip, 1920). Similarly, when the marine bivalve *Mercenaria mercenaria* was emersed, CO_2 and calcium levels in the ECF increased (Dugal, 1939). The source of calcium is from the shell as was reported by Crenshaw and Neff (1969) using ^{45}Ca labelling techniques. Later, it was shown that calcium appears in the extrapallial fluid before entering the extracellular compartment (Crenshaw, 1972), confirming that shell dissolution is the cause of increased calcium. A cyclical change in ECF calcium, presumably associated with HCO_3app production, was noted by Akberali *et al.* (1977). When the clam had closed valves and became hypoxic, calcium levels rose; during bouts of valve opening when ventilation would recommence, calcium levels declined. Additionally, Booth *et al.*, (1984) did not find any change in either ECF pH or [Ca] in *Mytilus edulis* during short-term emersion during which metabolism remained predominantly aerobic. However, under conditions of extended (6 days) aerial exposure, P_{CO_2} in the ECF of *Mytilus edulis* and *Modiolus modiolus* rose along with a decrease in pH (Jokumsen and Fyhn, 1982).

The very limited non-bicarbonate buffer system is balanced by the large store of readily mobilizable shell buffer. This is especially important for unionid clams, which have evolved a very dilute body fluid as an adaptation to life in freshwater. The low ionic strength of both the extracellular and intracellular compartments reduces the energy required to maintain homeostatic ionic levels by reducing the diffusive gradient. Nevertheless, emersion resulted in a large increase in extracellular solute. ECF osmolality of *Corbicula fluminea* during three days' aerial exposure at 25°C increased twofold (Byrne *et al.*, 1989), and a similar increase was noted for the unionid, *Ligumia subrostrata*, during a 5-day emersion period (Dietz, 1974). However, death from aerial exposure does not seem to result solely from a simple lethal increase in solute, as *C. fluminea* succumbed to aerial exposure after losing total body water ranging from 30 to 80% (Byrne *et al.*, 1988). Rather, death seems related to the inability of the clams to maintain acid-base balance or to avoid the production of toxic end-products (Byrne *et al.*, 1991a, b).

Extracellular sodium and chloride remain highly regulated both during emersion and during the reimmersion period. A similar situation was reported for *C. fluminea* during aerial exposure and subsequent resubmergence (Byrne *et al.*, 1989). Reports of changes in ECF contents of these ions in other bivalves undergoing emersion generally show a gradual increase in ECF ion concentrations related to the duration of aerial exposure. *Ligumia subrostrata* had an increased level of extracellular sodium and chloride proportional to the level of desiccation stress upon aerial exposure (Dietz, 1974). Similarly, chloride levels increased passively as body fluids became more concentrated during emersion in *Mytilus edulis* and *Modiolus modiolus* (Jokumsen and Fyhn, 1982). In severe hypoxic exposure, however, ECF sodium levels in *Scrobicularia plana* remained constant over time (Akberali *et al.*, 1977). The constant extracellular fluid [Na] and [Cl] in emersed *Anodonta grandis simpsoniana* suggests that these ions are moving into some other compartment, *e.g.*, intracellular space. This possibility is further evinced by the losses of these ions on reimmersion, even though ECF levels are not significantly altered. It has been postulated that, in *Corbicula fluminea,* these ions are shunted to the intracellular space to conserve cell volume (Byrne *et al.*, 1989), and a similar situation may be occurring in *A. grandis simpsoniana.* In any case, the tight regulation of these ions suggests that maintaining constant extracellular concentrations of sodium and chloride is a fundamental requirement and may be associated with maintenance of electrochemical balance.

On reimmersion, the accumulated extracellular calcium is removed over a 24 hour period, and ECF calcium levels return to control values. The loss is also evident by the high negative net fluxes for this ion during the initial stages of reimmersion. Other unionid clams recapture extracellular calcium in concretions made up primarily of calcium phosphate during and after periods of hypoxia (Silverman *et al.*, 1983). Although *A. grandis simpsoniana* possesses concretions (Byrne, McMahon, Silverman, and Dietz; unpubl. data), the capacity for extracellular calcium recapture is not known. As P_{CO_2} falls to control levels almost immediately on reimmersion, a sustained high calcium level in the ECF would result in an imbalance in the strong ion difference which would lead to an alkalosis. The loss of calcium on reimmersion (amounting to over 50 μeq for a 1 g dry weight animal in the first 6 h of reimmersion), however, must be regained at a later time, either from the diet or by epithelial transport mechanisms.

The lower ECF P_{O_2} on reimmersion perhaps was due to an enhanced ventilation and oxygen consumption, as valve gape seemed to be increased and ECF P_{CO_2} declined rapidly. This response is seen in intertidal bivalves, even those that remain fully aerobic during aerial exposure (Widdows *et al.*, 1979; Widdows and Shick, 1985).

In general, freshwater bivalves are more tolerant of extended periods of emersion than are estuarine or intertidal species (McMahon, 1979; Byrne *et al.*, 1988). As the freshwater bivalve, *Corbicula fluminea,* displayed intermediate responses to emersion and had the lowest reported tolerance to emersion for a freshwater species, it was thought that the greater capacity to survive aerial exposure of unionid species might be due to a more complete compensation for the consequences of emersion, in particular maintenance of acid-base and ion balance (Byrne *et al.*, 1991b). However, *Anodonta grandis simpsoniana* displays responses to emersion that seem to be similar to those of *C. fluminea.* The use of shell buffer to combat a predominantly respiratory acidosis; release of accumulated CO_2 and aerial O_2 consumption while minimizing water loss; redistribution of extracellular sodium and chloride; rapid recovery when reimmersed brought about by increased ventilation; and a loss of a large amount of ions may thus be general adaptations of freshwater bivalve species. Therefore, the extended tolerance of aerial exposure displayed by many unionid species may not be due to behavioral or physiological adaptations particularly unique to the group, but may simply reflect a wide latitude of capacity adaptation.

Acknowledgments

We wish to thank Dr. T. H. Dietz and two anonymous reviewers for comments on the manuscript. This study was supported by a University of Calgary Post-Doctoral Fellowship to RAB and NSERC operating grant A5762 to BRM.

Literature Cited

Akberali, H. B., K. R. M. Marriott, and E. R. Trueman. 1977. Calcium utilisation during anaerobiosis induced by osmotic shock in a bivalve mollusc. *Nature* **266:** 852–853.

Booth, C. E., and C. P. Mangum. 1978. Oxygen uptake and transport in the lamellibranch mollusc *Modiolus demissus. Physiol. Zool.* **51:** 17–32.

Booth, C. E., D. G. McDonald, and P. J. Walsh. 1984. Acid-base balance in the sea mussel, *Mytilus edulis.* I. Effects of hypoxia and air-exposure on hemolymph acid-base status. *Mar. Biol. Lett.* **5:** 347–358.

Boyden, C. R. 1972. Aerial respiration in the cockle *Cerastroderma edule* in relation to temperature. *Comp. Biochem. Physiol.* **43A:** 697–712.

Burnett, L. E., and B. R. McMahon. 1987. Gas exchange, hemolymph acid-base status, and the role of branchial water stored during air exposure in three littoral crab species. *Physiol. Zool.* **60:** 27–36.

Byrne, R. A., R. F. McMahon, and T. H. Dietz. 1988. Temperature and relative humidity effects on aerial exposure tolerance in the freshwater bivalve, *Corbicula fluminea. Biol. Bull.* **175:** 253–260.

Byrne, R. A., R. F. McMahon, and T. H. Dietz. 1989. The effects of aerial exposure and subsequent reimmersion on hemolymph osmolality, ion composition and ion flux in the freshwater bivalve, *Corbicula fluminea. Physiol. Zool.* **62(6):** 1187–1202.

Byrne, R. A., E. Gnaiger, R. F. McMahon, and T. H. Dietz. 1990. Behavioral and metabolic responses to emersion and subsequent reimmersion in the freshwater bivalve, *Corbicula fluminea. Biol. Bull* **178:** 251–259.

Byrne, R. A., T. H. Dietz, and R. F. McMahon. 1991a. Ammonia dynamics during and after prolonged emersion in the freshwater clam *Corbicula fluminea* (Müller) (Bivalvia: Corbiculacea). *Can. J. Zool.* **69:** 676–680.

Byrne, R. A., B. N. Shipman, N. J. Smatresk, T. H. Dietz, and R. F. McMahon. 1991b. Acid-base balance during prolonged emergence in the freshwater bivalve, *Corbicula fluminea. Physiol. Zool.* **64:** 748–766.

Cameron, J. N. 1986. *Principles of Physiological Measurement.* Academic Press, Orlando, FL. 278 pp.

Collip, J. B. 1920. Studies on molluscan coelomic fluid. Effect of change in environment in the carbon dioxide content of the coelomic fluid. Anaerobic respiration in *Mya arenaria. J. Biol. Chem.* **45:** 23–49.

Crenshaw, M. A. 1972. The inorganic composition of molluscan extrapallial fluid. *Biol. Bull.* **143:** 506–512.

Crenshaw, M. A., and J. M. Neff. 1969. Decalcification at the mantle-shell interface in molluscs. *Am. Zool.* **9:** 881–885.

Dietz, T. H. 1974. Body fluid composition and aerial oxygen consumption in the freshwater mussel, *Ligumia subrostrata* (Say): effects of dehydration and anoxic stress. *Biol. Bull.* **147:** 560–572.

Dietz, T. H., and W. D. Branton. 1975. Ionic regulation in the freshwater mussel, *Ligumia subrostrata* (Say). *J. Comp. Physiol.* **104:** 19–26.

Dugal, L.-P. 1939. The use of calcareous shell to buffer the product of anaerobic glycolysis in *Venus mercenaria*. *J. Cell. Comp. Physiol.* **13:** 235–251.

Fyhn, H. J., and J. D. Costlow. 1975. Anaerobic sampling of body fluids in bivalve molluscs. *Comp. Biochem. Physiol.* **52A:** 265–268.

Heisler, N. 1986. Buffering and transmembrane ion transfer processes. Pp. 3–47 in *Acid-Base Regulation in Animals*. N. Heisler, ed. Elsevier Science Publishers B. V. Amsterdam, Netherlands.

Heming, T. A., G. A. Vinogradov, A. K. Klerman, and V. T. Komov. 1988. Acid-base regulation in the freshwater pearl mussel *Margaritifera margaritifera:* effects of emersion and low water pH. *J. Exp. Biol.* **137:** 501–511.

Hiscock, I. D. 1953. Osmoregulation in Australian freshwater mussels (Lamellibranchiata). I. Water and chloride ion exchange in *Hyridella australis* (Lam.). *Aust. J. Mar. Freshwater Res.* **1:** 317–329.

Jokumsen, A., and H. J. Fyhn. 1982. The influence of aerial exposure upon respiratory and osmotic properties of haemolymph for two intertidal mussels, *Mytilus edulis* L. and *Modiolus demissus* L. *J. Exp. Mar. Biol. Ecol.* **61:** 189–203.

Keen, A. M., and R. Casey. 1969. Family Corbiculidae, Gray, 1847. Pp. 665–669 in *Treatise on Invertebrate Paleontology, part N*, N. R. C. Moore, ed. Geological Society of America, Boulder, CO.

McMahon, R. F. 1979. Tolerance of aerial exposure in the Asiatic freshwater clam, *Corbicula fluminea* (Müller). Pp. 227–241 in *Proceedings, First International Corbicula Symposium*, Joseph C. Britton, ed. Texas Christian University Research Foundation, Fort Worth, TX.

McMahon, R. F. 1988. Respiratory response to periodic emergence in intertidal molluscs. *Am. Zool.* **28:** 97–114.

McMahon, R. F., and C. J. Williams. 1984. A unique respiratory adaptation to emersion in the introduced Asian freshwater clam *Corbicula fluminea* (Müller) (Lamellibranchia: Corbiculacea). *Physiol. Zool.* **57:** 274–279.

Shick, J. M., J. Widdows, and E. Gnaiger. 1988. Calorimetric studies of behavior, metabolism and energetics of sessile intertidal animals. *Am. Zool.* **28:** 161–181.

Silverman, H., W. L. Steffens, and T. H. Dietz. 1983. Calcium concretions in the gills of a freshwater mussel serve as a calcium reservoir during periods of hypoxia. *J. Exp. Zool.* **227:** 177–189.

Widdows, J., B. L. Bayne, D. R. Livingstone, R. I. E. Newell, and P. Donkin. 1979. Physiological and biochemical responses of bivalve molluscs to exposure to air. *Comp. Biochem. Physiol.* **62A:** 301–308.

Widdows, J., and J. M. Shick. 1985. Physiological responses of *Mytilus edulis* and *Cardium edule* to aerial exposure. *Mar. Biol.* **85:** 217–232.

Reference: *Biol. Bull.* **181:** 298–306. (October, 1991)

The Physiological Effect of *Aureococcus anophagefferens* ("brown tide") on the Lateral Cilia of Bivalve Mollusks*

LOUIS F. GAINEY, JR.[1] AND SANDRA E. SHUMWAY[2,3]

[1]*Department of Biological Sciences, University of Southern Maine, Portland, Maine 04103 and*
[2]*Maine Department of Marine Resources,* [3]*Bigelow Laboratory for Ocean Sciences,*
W. Boothbay Harbor, Maine 04575

Abstract. The "brown tide" alga, *Aureococcus anophagefferens,* had no effect on the activity of the lateral cilia of isolated gills of the bivalve mollusks *Argopecten irradians, Geukensia demissa,* and *Mya arenaria. A. anophagefferens* caused a significant decrease in the activity of lateral cilia of five other bivalve mollusks, *Crassostrea virginica, Ostrea edulis, Mercenaria mercenaria, Modiolus modiolus,* and *Mytilus edulis.* Exposure of isolated gills of *M. edulis* to the water from which *A. anophagefferens* had been removed, or to polystyrene beads at the same concentration as *A. anophagefferens,* had no effect upon the activity of the lateral cilia. Thus, the inhibition of the lateral cilia is not caused by a compound excreted into the water, nor is it the result of the high density of cells. The response of lateral cilia to dopamine was identical to the response to *A. anophagefferens;* lateral cilia that were inhibited by dopamine were also inhibited by *A. anophagefferens.* Pretreatment of the gills of *M. edulis* with the dopamine antagonist ergometrine blocked the inhibition of the lateral cilia by both dopamine and *A. anophagefferens.* A water-soluble inhibitory compound was released from *A. anophagefferens* by exposing the cells to amylase, and then removing the cells by filtration. The effect of this inhibitory compound was also blocked by ergometrine. We propose that the isolated gills are digesting the extracellular coat of *A. anophagefferens* releasing a water soluble dopamine-mimetic compound that causes inhibition of lateral cilia.

Introduction

Monospecific blooms of a small, previously undescribed, coccoid chrysophycean alga (approximately 2 μm in diameter) began to plague coastal embayments of the northeastern United States during the summer of 1985, with recurrent blooms in some areas continuing through 1990. Concurrent blooms were reported in Gardiners Bay, Great South Bay, and Peconic Bay, Long Island, New York; Narragansett Bay, Rhode Island; and Barnegat Bay, New Jersey (Tracey, 1985; Olsen, 1986; Sieburth *et al.,* 1986; Cosper *et al.,* 1987). Concentrations as high as 10^6 cells ml^{-1} were recorded and resulted in discoloration of the waters and thus the term "brown tide" (Cosper *et al.,* 1987; Sieburth *et al.,* 1988). The organism has since been identified as *Aureococcus anophagefferens* (Seiburth *et al.,* 1986, 1988).

The effects of these "brown tides" on shellfish populations were immediately evident and, in some cases, catastrophic (Shumway, 1990). Bricelj *et al.* (1987) reported recruitment failure and starvation of post-reproductive adult bay scallops, *Argopecten irradians,* in eastern Long Island embayments. Mussels, *Mytilus edulis,* suffered reproductive failure and mortalities ranging from 30 to 100% of natural and transplanted animals in Narragansett Bay, Rhode Island (Tracey, 1988). The mechanisms responsible for these mortalities remain unclear (Tracey, 1985; Bricelj and Kuenstner, 1989). Bricelj and Kuenstner (1989) suggested that the adverse effects of *A. anophagefferens* on bivalve mollusks may be a result of small size, high density, poor digestibility, toxicity, or deficiency in essential micronutrients.

The efficiency with which bivalve mollusks can retain particles filtered from seawater varies between species of

---

Received 12 February 1991; accepted 2 July 1991.

* Publication No. 296 of the Tallahassee, Sopchoppy & Gulf Coast Marine Biological Association.

shellfish and is, in most cases, directly related to the size of the algal cells with small cells generally retained less efficiently than larger cells (Mohlenberg and Riisgard, 1978; Bayne and Newell, 1983). The very small size of *A. anophagefferens* led investigators to determine the effects of this alga on feeding rates in several species of bivalve mollusks. Scallops, *A. irradians,* and mussels, *M. edulis,* retained filtered cells with only 36 and 59% efficiency, respectively (Bricelj and Kuenstner, 1989), compared to 100% efficiency when fed cells with a diameter greater than 5 μm (Bayne and Newell, 1983). Furthermore, feeding rates in both species were significantly depressed when fed cultured *A. anophagefferens* at bloom densities. Reduced clearance rates have been observed in *M. edulis* and the quahog, *Mercenaria mercenaria,* in the presence of *A. anophagefferens;* reductions in clearance rates by the mussels were independent of particle size, and substances dissolved in bloom waters had no effect on clearance rates (Tracey, 1988; Tracey *et al.,* 1990). While specific cell toxins have not been identified from *A. anophagefferens,* there is morphological and physiological evidence to suggest that toxicity is related to a component of the cell surface. (Tracey *et al.,* 1988, 1990; Draper *et al.,* 1990).

Although the small size and high density of *A. anophagefferens* had detrimental effects on bay scallops, these effects were not enough to account for the starvation experienced by scallops in the field; these results might be ascribed to toxic effects following more prolonged exposure to bivalves to *Aureococcus* cells (Bricelj and Kuenstner, 1989). Other authors have also suggested that chronic toxicity of *A. anophagefferens* cells at high densities might be responsible for the detrimental effects observed in bivalve mollusks (Tracey *et al.,* 1988). There is strong evidence that chronic toxicity at high densities, rather than small size, indigestibility, or poor nutritional quality is responsible for the detrimental effects seen in bivalves (Tracey, 1988; Bricelj and Kuenstner, 1989; Bricelj *et al.,* 1989; Gallager *et al.,* 1989; Draper *et al.,* 1990). Recent studies indicate that direct contact with *Aureococcus* cells is necessary to inhibit grazing (Tracey, 1988; Gallager *et al.,* 1989; Ward and Targett, 1989; Draper *et al.,* 1990).

The control of lateral ciliary activity in bivalve mollusks, in particular *Mytilus edulis,* has been studied extensively during the last 70 years, and there is considerable evidence that dopamine is an inhibitory neurotransmitter involved in regulation of lateral cilia (for a review of early work, see Aiello, 1960). Exogenously applied dopamine inhibits the lateral cilia of *M. edulis* and *Crassostrea virginica* but not *Geukensia demissa* (Paparo and Aiello, 1970; Catapane, 1983; Paparo, 1985). In addition, high frequency stimulation of the cerebro-visceral nerve connective of *M. edulis* resulted in inhibition of the lateral cilia; this response was abolished by pretreating the gill or visceral ganglion with the antagonist ergometrine, which also blocked the effects of exogenously applied dopamine (Catapane *et al.,* 1978, 1979). Dopamine has been localized in the branchial nerve fibers of *M. edulis,* and these fibers appear to make synaptic contact with the lateral ciliary cells (Stefano and Aiello, 1975; Paparo, 1972). Paparo and Finch (1972) showed that isolated gills metabolized DOPA and tyrosine to dopamine.

Calcium has also been shown to regulate the activity of lateral cilia. For example, the lateral cilia of isolated gills and triton-extracted cells will beat in the absence of extracellular calcium, while an increase in the concentration of intracellular calcium will cause inhibition of the lateral cilia (Walter and Satir, 1978; Paparo, 1980; Murakami, 1983; Stommel and Stevens, 1985). Paparo and Murphy (1975) proposed that the inhibitory effects of dopamine on the lateral cilia are mediated by an influx of calcium, and studies on mammalian systems support this hypothesis (Ahlijanian and Cooper, 1988; Felder *et al.,* 1989; Mahan *et al.,* 1990).

In the present study, we examined the effects of *Aureococcus anophagefferens* and dopamine on the activity of the lateral cilia of eight species of bivalve mollusks. In addition, we examined the effects of polystyrene microspheres, the culture media from which *A. anophagefferens* had been removed by filtration, and the culture media from which *A. anophagefferens* treated with amylase had been removed by filtration on the activity of the lateral cilia of *Mytilus edulis.* Preliminary results of this study were presented at the Fourth International Conference on Toxic Marine Phytoplankton (Draper *et al.,* 1990) and to the American Society of Zoologists (Gainey and Shumway, 1989).

Materials and Methods

The original non-axenic culture of *Aureococcus anophagefferens* was supplied by E. M. Cosper (MSRC, State University of New York, Stony Brook). The culture was maintained at 18°C in an f/2 medium with .01 m*M* disodium glycero-phosphate added and sodium silicate omitted (Guillard, 1975). Cells were harvested during the late exponential growth phase as toxicity varies in relation to environmental growth conditions (Tracey *et al.,* 1990). Adult specimens of bivalves were collected at the following localities: *Mytilus edulis,* Falmouth; *Mya arenaria,* Boothbay Harbor; *Modiolus modiolus,* Damariscotta River; *Crassostrea virginica* and *Ostrea edulis,* Mook Sea Farms, Damariscotta (all in Maine); *Argopecten irradians,* Shinnecock Bay, Southhampton, New York; *Geukensia demissa,* Sakonnet River, Tiverton, Rhode Island; and *Mercenaria mercenaria,* Wachapreague, Virginia. With the exception of *Mytilus edulis,* all animals were maintained at the Maine Department of Marine Resources Laboratory, Boothbay Harbor, in running seawater at temperatures ranging from 9 to 12°C and a salinity of 33 ‰. Prior to use in experiments, animals were held at 10°C, 30 ‰ salinity on a 12 h light-dark cycle at the University of Southern Maine, Portland, for periods ranging from 1 week to a month.

Gills were dissected distal to the visceral ganglion and were then separated into demibranchs. The isolated demibranchs were pinned to strips of rubber band that had been glued to the bottom of petri dishes. The dishes were filled with 10 ml of artificial seawater with an ionic composition as follows: $CaCl_2$ = 10 m*M*, KCl = 9.8 m*M*, $MgCl_2$ = 53 m*M*, NaBr = .57 m*M*, NaCl = 400 m*M*, $NaHCO_3$ = 2.5 m*M*, Na_2SO_4 = 28 m*M* (ASW, Welsh *et al.*, 1968). The gills were used after the appearance of metachronal waves on the lateral cilia, usually within 1 to 12 h after dissection, depending upon the species.

The gills were observed at a magnification of 100× with a compound microscope with the substage illuminator replaced with a mirror. The rate of lateral ciliary beating was determined using a Pasco SF-9211 strobe driven by a Grass SD-9 stimulator. The gills were initially viewed at a flashing rate of 60 Hz, which was above the frequency of flicker fusion for our eyes; the flashing rate of the strobe was then decreased until the metachronal waves appeared motionless in the shape of a horseshoe. At harmonics above the actual ciliary rate, the wavelength of the metachronal waves appeared shorter than the true wavelength and the waves appeared to flicker (Catapane *et al.*, 1978, pers. obs.). Harmonics below the actual ciliary rate were avoided by always starting the strobe at a higher frequency than the actual rate.

Gills were first observed in artificial sea water; for the treatments, the artificial sea water was replaced with *A. anophagefferens* at concentrations of approximately 10^6 cells/ml. Readings were taken every hour for at least 5 h and again at 24 h for *Geukensia demissa, Mya arenaria, Mercenaria mercenaria,* and *Mytilus edulis.* Due to the fragility of the gills in *Argopecten irradians, Crassostrea virginica, Ostrea edulis,* and *Modiolus modiolus,* it was not possible to take readings at 24 h. All experiments were performed at 10°C.

Effects of dissolved exudates

Suspensions of *A. anophagefferens* were filtered through a 0.8 μm filter using the minimal vacuum possible to maintain flow through the filter; the filtered cells were viewed microscopically to insure that cell lysis did not occur. This filtrate was added to isolated gills of *Mytilus edulis* and ciliary rates were measured as described previously.

Effects of particulates

Isolated gills of *M. edulis* were exposed to 2.9 μm diameter polystyrene microspheres at a concentration of 7.85×10^6 spheres/ml. The microspheres were obtained from Polysciences, Inc., Warrington, Pennsylvania.

Effects of dopamine

The effects of dopamine on the lateral cilia of *Mytilus edulis, Geukensia demissa,* and *Crassostrea virginica* have been described previously (Paparo and Aiello, 1970; Catapane, 1983; Paparo, 1985). We tested the effects of dopamine on these bivalves as well as the others used in this study. Isolated gills were exposed to 10^{-4} *M* dopamine in ASW; this concentration is an order of magnitude greater than necessary to cause complete lateral ciliary arrest in *Mytilus edulis* (Catapane, 1983). The presence or absence of metachronal waves was noted immediately after the addition of dopamine and every 2 min thereafter for 20 min. If the lateral cilia ceased beating within this period, the response to dopamine was considered positive.

Effect of ergometrine

Catapane *et al.* (1978) demonstrated that application of 10^{-5} *M* ergometrine (ergonovine) to the isolated gills of *Mytilus edulis* had no effect on the rate of previously beating lateral cilia. Catapane *et al.* (1979) also demonstrated that application of 10^{-5} *M* ergometrine to the visceral ganglion blocked the lateral ciliary inhibition brought about by the addition of 10^{-4} *M* dopamine to the visceral ganglion if the ergometrine was added 10 min prior to the addition of dopamine. To determine if ergometrine would also block the lateral ciliary inhibition brought about by exposure of the isolated gills of *M. edulis* to 10^{-4} *M* dopamine, we exposed isolated gills to 10^{-5} *M* ergometrine. We then added fresh 10^{-4} *M* dopamine in ASW hourly for 4 h and again at 24 h. Both ergometrine and dopamine were purchased from Sigma Chemical Co.

Effects of amylase

Cultures of *A. anophagefferens* were exposed to a saturated solution of alpha amylase (Type I-A, Sigma Chemical Co, 4 mg/ml) for at least 16 h. The *Aureococcus* amylase mixture was then filtered through an 0.8 μm filter as described previously. Isolated gills of *M. edulis* were exposed to amylase at the same concentration to test the effects of amylase on lateral ciliary activity.

Ciliary rates were expressed as a percentage of the initial rate of each isolated gill preparation. The effects of various experimental treatments were evaluated using an F test, with the mean square for experimental treatment as a numerator and the mean square for animal nested within treatment, where animal was a class variable that represented repeated measures on the same piece of gill, as an error term. Superscripts and subscripts for F values represent degrees of freedom for the numerator and denominator. The Type III mean squares used for this test were generated using the model: percent initial rate = treatment time animal (treatment). The statistical procedures were performed using the general linear model program (Proc GLM) in version 5 of the Statistical Analysis System (SAS). Tests were considered significant at probabilities less than 0.05. Errors and error bars are ±1 standard error. Although readings were taken on experimental and control groups at the same time intervals, the groups have been offset by 15 min in all figures for the sake of clarity.

Results

Basal ciliary rates

The mean lateral ciliary rate of the eight species of bivalves prior to exposure to *Aureococcus anophagefferens* ranged from a low of 17 Hz in *Geukensia demissa* to a high of 25 Hz in *Crassostrea virginica* (Table I).

The response of bivalve gills to A. anophagefferens

Aureococcus anophagefferens had no significant effect on the activity of the lateral cilia of the following species of bivalve mollusks: *Argopecten irradians* (F^1_{20} = .07, *P* = .79), *Geukensia demissa* (F^1_{24} = .98, *P* = .33), and *Mya arenaria* (F^1_{16} = .00, *P* = .97, Fig. 1).

A. anophagefferens inhibited the lateral cilia in the following species of bivalves: *Crassostrea virginica* (F^1_{30}= 36.44, *P* = .0001), *Ostrea edulis* (F^1_{30} = 35.73, *P* = .0001), *Mercenaria mercenaria* (F^1_{21} = 7.30, *P* = .01), *Modiolus modiolus* (F^1_{22} = 36.44, *P* = .001), and *Mytilus edulis* (F^1_{22} = 13.91, *P* = .001, Fig. 1). All of these species exhibited depressed lateral ciliary activity within 1 h after exposure to *A. anophagefferens*, with the exception of *M. modiolus*, where the mean rate did not begin to decline until 3 h after exposure.

The time until maximal ciliary inhibition, and the magnitude of the inhibition, was species specific. For example, in *M. edulis* the mean rate declined to 48% (±10.2, n = 16) of the initial rate 3 h after exposure. In *C. virginica*, the mean rate declined to only 75% (±3.4, n = 24) of the initial rate 4 h after exposure, while in *M. modiolus* the mean rate declined to 89% (±0.86, n = 18) of the initial rate 5 h after exposure. In both *O. edulis* and *M. mercenaria*, the mean rates were 78% (±1.4, n = 24) and 32% (±15, n = 15) of the initial rates respectively, 6 h after exposure.

In *M. edulis* and *M. mercenaria*, the gills were hardy enough to carry out observations for longer periods of time than was possible for some of the other species. Twenty-four hours after exposure, the mean, ciliary rate of *M. mercenaria* had risen to 85% (±6.5, n = 15), while the controls had a mean rate of 96% (±3.7, n = 8) of the initial rate. Twenty-four hours after exposure, the mean rate of *M. edulis* had risen to 94% (±15, n = 16), while the controls had a mean rate of 108% (±7.3, n = 9) of the initial rate.

Table I

Mean lateral ciliary rates (beats/s), rounded to the nearest integer, of bivales used in this study

Species	Mean rate (beats/s)	Standard error	*n*
Argopecten irradians	24	1.6	22
Geukensia demissa	17	.47	26
Mya arenaria	20	1.42	18
Crassostrea virginica	25	.12	32
Ostrea edulis	24	.29	32
Mercenaria mercenaria	20	.45	23
Modiolus modiolus	20	.08	24
Mytilus edulis	19	.74	25

The nature of ciliary inhibition in Mytilus edulis

To determine if ciliary inhibition was caused by an exudate of *A. anophagefferens*, we exposed isolated gills of *M. edulis* to seawater from which *A. anophagefferens* had been removed by filtration. This water had no effect upon lateral ciliary activity (F^1_{16} = .56, *P* = .46, Fig. 2).

To determine if ciliary inhibition was caused by the presence of high concentrations of particulate matter, we exposed isolated gills of *M. edulis* to polystyrene microspheres. The microspheres had no effect upon lateral ciliary activity (F^1_{15} = .69, *P* = .42, Fig. 3).

All of the species tested that showed lateral ciliary inhibition upon exposure to *A. anophagefferens* also showed lateral ciliary inhibition upon exposure to 10^{-4} *M* dopamine; moreover, those species that did not have lateral ciliary inhibition upon exposure to *A. anophagefferens* were not inhibited by exposure to dopamine (Table II).

To determine if the inhibition of lateral cilia caused by exposure to *A. anophagefferens* was caused by dopamine, or a dopamine agonist, we first exposed isolated gills to 10^{-5} *M* ergometrine and then to fresh 10^{-4} *M* dopamine hourly for 4 h and again at 24 h to test whether ergometrine would block the inhibition brought about by dopamine. There was no difference in the rates of these gills after these treatments (F^4_{20} = .03, *P* = .99), *i.e.*, the single dose of ergometrine blocked the effects of dopamine for 24 h. We then exposed isolated gills of *M. edulis* to 10^{-5} *M* ergometrine for 10 min prior to exposure to *A. anophagefferens*. Gills pretreated with ergometrine showed no inhibition when exposed to *A. anophagefferens*, in

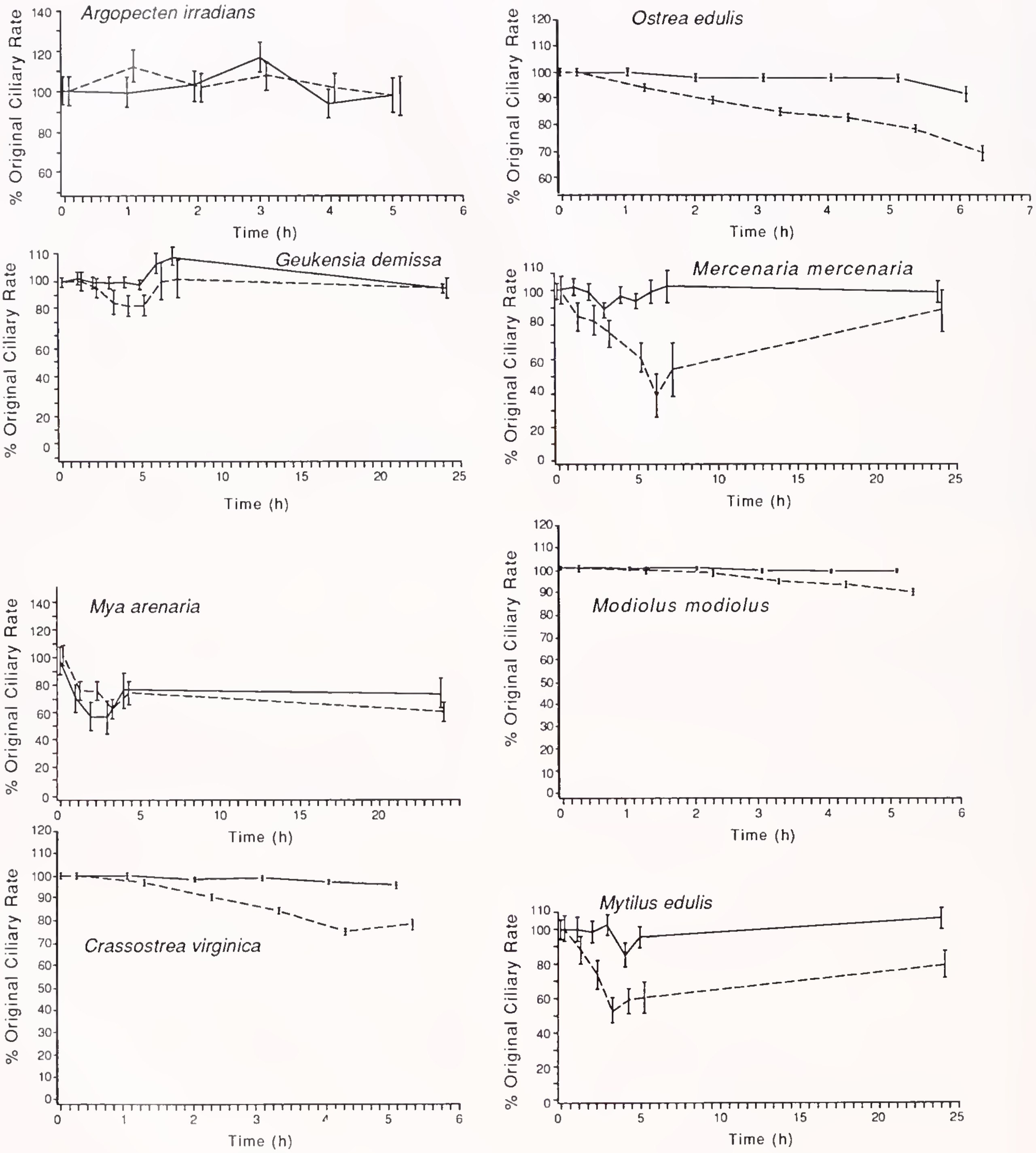

Figure 1. The effect of *Aureococcus anophagefferens* (brown tide) on the lateral cilia of eight species of bivalve mollusks. Solid line: control (c); dashed line: brown tide (BT). Number of gills: *Argopecten*, c = 9, BT = 13; *Geukensia*: c = 9, BT = 17; *Mya*: c = 6, BT = 12; *Crassostrea* and *Ostrea*: c = 8, BT = 24; *Mercenaria*: c = 8, BT = 15; *Modiolus*: c = 6, BT = 18; *Mytilus*: c = 9, BT = 16. Error bars are ± 1 standard error. Although readings were taken at the same times for both controls and treatments, they have been offset for the sake of clarity in this and subsequent figures.

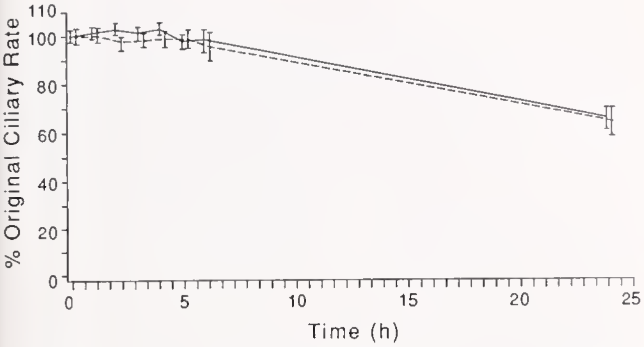

Figure 2. The effect of water, from which *Aureococcus anophagefferens* had been removed by filtration, on the lateral cilia of *Mytilus edulis.* Solid line: control (n = 6); dashed line: treatment (n = 12). Error bars are ± 1 standard error.

contrast to gills exposed to *A. anophagefferens* without a pretreatment of ergometrine ($F^{1}_{14} = 16.49$, $P = .001$, Fig. 4).

We tested the hypothesis that the isolated gills were digesting the extracellular polysaccharide coat of *A. anophagefferens,* which was described by Sieburth *et al.* (1988), by exposing cultures of *A. anophagefferens* to amylase. Exposure of isolated gills to seawater containing amylase had no effect upon lateral ciliary activity ($F^{1}_{15} = .12$, $P = .74$). Exposure of isolated gills of *M. edulis* to filtered seawater which had contained *A. anophagefferens* treated with amylase resulted in decreased lateral ciliary activity ($F^{1}_{16} = 7.19$, $P = .02$, Fig. 5). There was no difference in the activity of lateral cilia of isolated gills exposed to the enzymatically treated *A. anophagefferens* filtrate or to untreated *A. anophagefferens* ($F^{1}_{14} = .02$, $P = .88$).

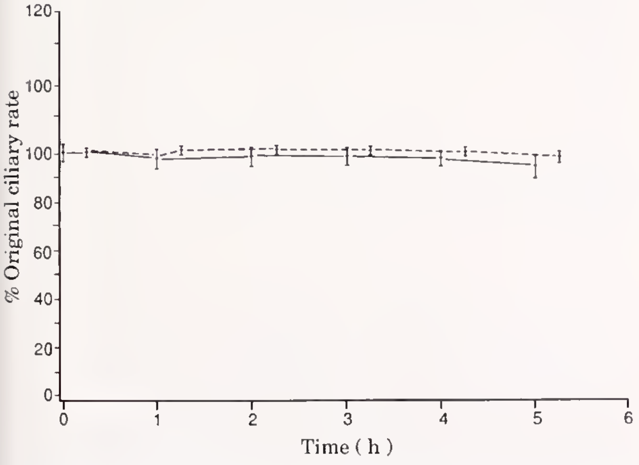

Figure 3. The effect of polystyrene microspheres on the lateral cilia of *Mytilus edulis.* Solid line: control (n = 8); dashed line: treatment (n = 11). Error bars are ± 1 standard error.

Table II

Summary of responses of lateral cilia to Aureococcus anophagefferens *and exogenously applied* 10^{-4} M *dopamine*

Species	Response to *Aureococcus*	Response to dopamine
Argopectin irradians	—	—
Geukensia demissa	—	—
Mya arenaria	—	—
Crassostrea virginica	inh	inh
Ostrea edulis	inh	inh
Mercenaria mercenaria	inh	inh
Modiolus modiolus	inh	inh
Mytilus edulis	inh	inh

— = no response, inh = inhibition.

To test if the inhibition was caused by the same type of compound in the experiment with the enzymatically treated *A. anophagefferens* filtrate and the experiments with intact *A. anophagefferens,* we exposed isolated gills to ergometrine, as described previously, then exposed the gills to the water from *A. anophagefferens* treated with amylase. The ergometrine blocked the inhibition of the lateral cilia brought about by the *A. anophagefferens* amylase filtrate ($F^{1}_{12} = 5.39$, $P = .04$, Fig. 6). In addition, there was no difference in the rates of untreated gills, gills exposed to ergometrine and the *A. anophagefferens* amylase filtrate, and gills exposed to ergometrine and intact *A. anophagefferens* ($F^{2}_{5} = 1.51$, $P = .31$).

Discussion

The bivalves whose lateral cilia were inhibited by *A. anophagefferens* were the same species whose lateral cilia were inhibited by dopamine. There are three possibilities

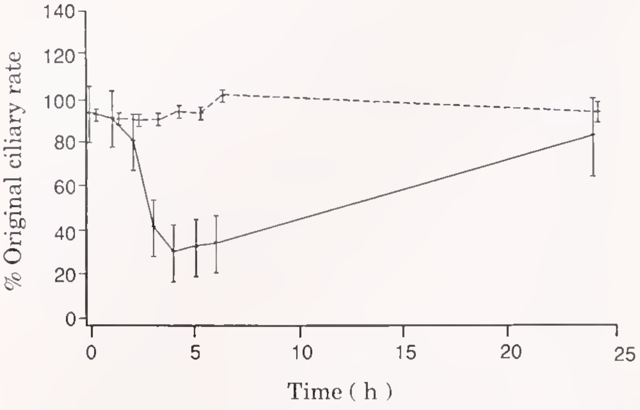

Figure 4. The effect of exposing the gills of *M. edulis* to 10^{-5} *M* ergometrine and then to *Aurecoccus anophagefferens.* Solid line: control (exposed to *A. anophagefferens,* n = 8); dashed line: treatment (n = 10). Error bars are ± 1 standard error.

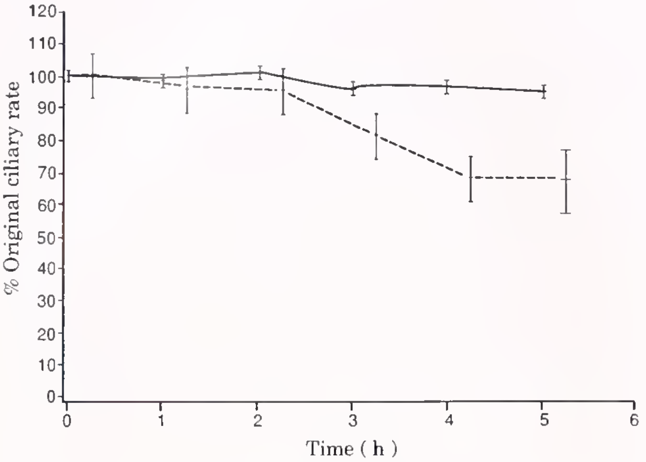

Figure 5. The effect of exposing *Aureococcus anophagefferens* to amylase, filtering the water, and exposing the gills of *Mytilus edulis* to the filtrate. Solid line: control (n = 9); dashed line: treatment (n = 10). Error bars are ± 1 standard error.

that could explain this correlation. First, *A. anophagefferens* could release dopamine upon contact with the bivalve gill. We think that this is unlikely because the oxidation products of dopamine are readily visible in seawater (pers. obs.) and we have not observed this characteristic discoloration in any of our experiments with either intact *A. anophagefferens*, or with the water from enzymatically treated *A. anophagefferens*. Moreover, the inhibitory effects of exogenously applied dopamine typically appear within 2 to 3 min and disappear within 20 to 30 min after application (Catapane *et al.*, 1978; pers. obs.), while the effects of the water from enzymatically treated *A. anophagefferens* did not appear for several hours and persisted for at least 5 h. Second, the inhibition could be caused by a dopamine-mimetic compound. Third, the inhibition could be the result of the stimulation of branchial nerve fibers in the gill. These fibers innervate the lateral ciliated cells and contain dopamine (Paparo, 1972; Stefano and Aiello, 1975). Our experiments cannot distinguish between these latter two possibilities because the dopamine antagonist ergometrine would block the inhibition of the lateral cilia brought about by exposure to *A. anophagefferens* in either case. We think that it is unlikely that the effects of *A. anophagefferens* are brought about by a direct influx of calcium into the lateral ciliated cells. If this were the case, inhibition of the lateral cilia would probably have occurred in all of the species tested, and the effects would not have been blocked by ergometrine.

Tracey (1988) found decreased clearance rates in both *Mytilus* and *Mercenaria* exposed to *A. anophagefferens*, and our results on isolated gills are parallel to his. Bricelj and Kuenstner (1989) found that *A. anophagefferens* inhibited clearance rates in juvenile *Argopecten irradians*; however, we found no inhibition of isolated gills of adult *A. irradians*. Several possibilities exist for this discrepancy. Sensitivity to *A. anophagefferens* could be age dependent, or the *A. anophagefferens* dopamine-mimetic could interact directly with the visceral ganglia in intact scallops to bring about lateral ciliary inhibition via nerves innervating the gills rather than acting directly on the gills, because the lateral cilia of isolated scallop gills are unaffected by dopamine.

Physical contact between a bivalve and *A. anophagefferens* is apparently necessary for inhibition. Tracey (1988) found no inhibition of clearance rates when *M. edulis* were exposed to Narragansett Bay water from which *A. anophagefferens* had been removed by filtration. Ward and Targett (1989) found similar results with *M. edulis* exposed to filtrates of cultured *A. anophagefferens*. We have found similar results with isolated gills. Taken together, these results indicate that *A. anophagefferens* is not excreting an inhibitory compound into the water. In addition, Ward and Targett (1989) found that exposing *M. edulis* to lysed cell filtrates of *A. anophagefferens* had no effect on clearance rates, indicating that the inhibitory compound is not intracellular in origin.

The inhibition of ciliary activity of isolated gills, and decreased clearance in whole animals, is not caused by the high density of small particulates present during a brown tide. Tracey (1988) found no inhibition of clearance in *M. edulis* exposed to high densities of kaolin clay particles, and we have found similar results with isolated gills exposed to polystyrene microspheres.

Pequignat (1973) found that the gills of *M. edulis* secrete amylase, and Sieburth *et al.* (1988) described *A. anophagefferens* as having ". . . a diffuse, sometimes copious layer of exocellular organic material which is probably

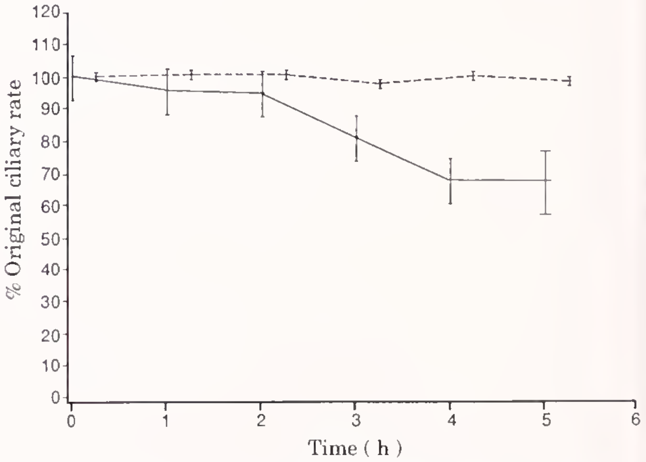

Figure 6. The effect of pretreating the gills of *Mytilus edulis* with 10^{-5} *M* ergometrine and then exposing the gills to the filtrate of *A. anophagefferens* treated with amylase. Solid line: filtrate of *A. anophagefferens* treated with amylase (n = 10); dashed line: treatment (n = 4). See text for further control comparisons.

polysaccharide. . . ." Our results demonstrate that the inhibitory compound is released upon exposure of *A. anophagefferens* to amylase. That this inhibitory compound is similar to that released upon exposure of intact *A. anophagefferens* to bivalve gills is indicated by the blockage of inhibition by pre-treatment of the gills with ergometrine in both instances.

The time for inhibition of clearance rates in bivalves exposed to *A. anophagefferens* is much faster than the time for inhibition of the lateral cilia of isolated gills. Tracey (1988) found inhibition of clearance rates after only 20 min of exposure to *A. anophagefferens,* whereas we found that the time for inhibition was much slower in isolated gills. These differences should, in fact, be expected for the following reason. The ingestion of *A. anophagefferens* by whole animals would result in the faster digestion of the extracellular coat in comparison to the digestion by isolated gills because digestion would occur not only on the gills but also in the digestive system of a whole animal.

In summary, we propose that the inhibition of clearance in bivalve mollusks exposed to *A. anophagefferens* is brought about by the digestion of the extracellular coat, releasing a dopamine-mimetic compound, which brings about the arrest of the lateral cilia in certain species.

Acknowledgments

We thank Jan Barter for assistance in culturing *A. anophagefferens;* Christy Draper, Karen Emery, and Christy Leigh for assistance in measuring ciliary rates; and Mike Castagna and Steve Tettlebach for providing bivalves.

This paper is funded, in part, by grant/cooperative agreement (NA-90-AA-H SK030) from the National Oceanic and Atmospheric Administration awarded to the New England Fisheries Development Association. The views expressed herein are those of the authors and do not necessarily reflect the views of NOAA or any of its subagencies.

Literature Cited

Ahlijanian, M. K., and D. M. Cooper. 1988. Distinct interactions between Ca^{2+}/calmondulin and neurotransmitter stimulation of adenylate cyclase in striatum and hippocampus. *Cell. Mol. Neurobiol.* **8:** 459–469.

Aiello, E. L. 1960. Factors affecting ciliary activity on the gill of the mussel *Mytilus edulis. Physiol. Zool.* **23:** 120–135.

Bayne, B. L., and R. C. Newell. 1983. Physiological energetics of marine molluscs. Pp. 407–515 in *The Mollusca,* V. 4, Physiology, Part I, A.S.M. Saleuddin and K. M. Wilbur, eds. Academic Press, New York.

Bricelj, V. M., J. Epp, and R. E. Malouf. 1987. Intraspecific variation in reproductive and somatic growth cycles of bay scallops *Argopecten irradians. Mar. Ecol. Prog. Ser.* **36:** 123–137.

Bricelj, V. M., N. S. Fisher, J. B. Guckert, and F. E. Chu. 1989. Lipid composition and nutritional value of the brown tide alga *Aureococcus anophagefferens.* Pp. 85–100 in *Novel Phytoplankton Blooms,* E. M. Cosper, V. M. Bricelj, and E. J. Carpenter, eds. Springer-Verlag, New York.

Bricelj, V. M., and S. H. Kuenstner. 1989. Effects of the "brown tide" on the feeding physiology and growth of bay scallops and mussels. Pp. 491–509 in *Novel Phytoplankton Blooms,* E. M. Cosper, V. M. Bricelj, and E. J. Carpenter, eds. Springer-Verlag, New York.

Catapane, E. J., G. B. Stefano, and E. Aiello. 1978. Pharmacological study of the reciprocal dual innervation of the lateral ciliated gill epithelium by the CNS of *Mytilus edulis* (Bivalvia). *J. Exp. Biol.* **74:** 101–113.

Catapane, E. J., G. B. Stefano, and E. Aiello. 1979. Neurophysiological correlates of the dopaminergic cilio-inhibitory mechanism of *Mytilus edulis J. Exp. Biol.* **83:** 315–323.

Catapane, E. J. 1983. Comparative study of the control of lateral ciliary activity in marine bivalves. *Comp. Biochem. Physiol.* **75C:** 403–405.

Cosper, E. M., W. C. Dennison, E. J. Carpenter, V. M. Bricelj, J. G. Mitchell, S. H. Kuenstner, D. Colefiesh, and M. Dewey. 1987. Recurrent and persistent brown tide blooms perturb coastal marine ecosystem. *Estuaries* **10:** 284–290.

Draper, C., L. Gainey, S. Shumway, and L. Shapiro. 1990. Effects of *Aureococcus anophagefferens* ("Brown Tide") on the lateral cilia of 5 species of bivalve molluscs. Pp. 128–131 in *Toxic Marine Phytoplankton,* E. Graneli, B. Sundstrom, L. Elder, and D. M. Anderson, eds. Elsevier, New York.

Felder, C. C., M. Belcher, and P. A. Jose. 1989. Dopamine-1-mediated stimulation of phospholipase C activity in rat renal cortical membranes. *J. Biol. Chem.* **264:** 8739–8745.

Gainey, L. F., Jr., and S. E. Shumway. 1989. Effects of *Aureococcus anophagefferens* ("brown tide") on the lateral ciliary activity of bivalve molluscs. *Am. Zool.* **29:** 72A.

Gallager, S. M., D. K. Stoecker, and V. M. Bricelj. 1989. Effects of the brown tide alga on growth, feeding physiology and locomotory behavior of scallop larvae (*Argopecten irradians*). Pp. 511–541 in *Novel Phytoplankton Blooms,* E. M. Cosper, V. M. Bricelj and M. J. Carpenter, eds. Springer-Verlag, New York.

Guillard, R. L. 1975. Culture of phytoplankton for feeding marine invertebrates. Pp. 29–60 in *Culture of Marine Invertebrates,* W. L. Smith and M. H. Chanley, eds. Plenum Press, New York.

Mahan, L. C., R. M. Burch, F. J. Monsma, Jr., and D. R. Sibley. 1990. Expression of striatal D1 dopamine receptors coupled to inositol phosphate production and Ca^{2+} mobilization in *Xenopus* oocytes. *Proc. Natl. Acad. Sci. U.S.A* **87:** 2196–2200.

Mohlenberg, F., and H. U. Riisgard. 1978. Efficiency of particle retention in 13 species of suspension feeding bivalves. *Ophelia* **17:** 239–246.

Murakami, A. 1983. Control of ciliary beat frequency in *Mytilus. J. Submicrosc. Cytol.* **15:** 313–316.

Olsen, P. 1986. Occurrence and distribution of brown tide in New Jersey. P. 10 in Proc. Emergency Conference on "Brown Tide," Oct. 23–24, 1986, Hauppauge, Long Island, State Dept. New York State, Albany, New York.

Paparo, A., and E. Aiello. 1970. Cilio-inhibitory effects of branchial nerve stimulation in the mussel, *Mytilus edulis. Comp. gen. Pharmacol.* **1:** 241–250.

Paparo, A., and C. E. Finch. 1972. Catecholamine localization, content, and metabolism in the gill of two lamellibranch molluscs. *Comp. Gen. Pharmacol.* **3:** 303–309.

Paparo, A. A., and J. A. Murphy. 1975. The effect of Ca on the rate of beating of lateral cilia in *Mytilus edulis*-II. a response to electrical stimulation of the branchial nerve. *Comp. Biochem. Physiol.* **50C:** 15–19.

Paparo, A. 1972. Innervation of the lateral cilia in the mussel *Mytilus edulis* L. *Biol. Bull.* **143:** 592–604.

Paparo, A. 1980. The regulation of intracellular calcium and the release of neurotransmitters in the mussel, *Mytilus edulis. Comp. Biochem. Physiol.* **66A:** 517–520.

Paparo, A. 1985. The relationship between lamellar-type cytosomes, DOPA decarboxylase, and lateral ciliary activity of the oyster *Crassostrea virginica* (Gmelin): response to salinity change. *J. Exp. Mar. Biol. Ecol.* **87:** 133–143.

Pequignat, E. 1973. A kinetic and autoradiographic study of the direct assimilation of amino acids and glucose by organs of the mussel *Mytilus edulis. Mar. Biol.* **19:** 227–244.

Shumway, S. E. 1990. A review of the effects of algal blooms on shellfish and aquaculture. *J. World Aquaculture Soc.* **21:** 65–104.

Sieburth, J. McN., P. W. Johnson, and P. E. H. Hargraves. 1986. *Pardococcus anorexus* nom. prov., a bloom-forming chrysophycean picoplankter inducing anorexia in filter-feeding animals in Narragansett Bay, R. I. during summer 1985: ultrastructure and predators. *ASLO Abstracts* June 1986, p. 119.

Sieburth, J. McN., P. W. Johnson, and P. E. Hargraves. 1988. Ultrastructure and ecology of *Aureococcus anophagefferens* gen. et sp. nov. (Chrysophyceae): the dominant picoplankter during a bloom in Narragansett Bay, Rhode Island, Summer 1985. *J. Phycol.* **24:** 416–425.

Stefano, G. B., and E. Aiello. 1975. Histofluorescent localization of serotonin and dopamine in the nervous system and gill of *Mytilus edulis* (Bivalvia). *Biol. Bull.* **148:** 141–156.

Stommel, E. W., and R. E. Stephens. 1985. Cyclic AMP and calcium in the differential control of *Mytilus edulis* cilia. *J. Comp. Physiol. A* **157:** 451–459.

Tracey, G. A. 1985. Picoplanktonic algal bloom causes catastrophic mussel kill in Narragansett Bay, Rhode Island. *Trans. Am. Geophys. Union* **66:** 1303.

Tracey, G. A. 1988. Feeding reduction, reproductive failure, and mortality in *Mytilus edulis* during the 1985 "brown tide" in Narragansett Bay, Rhode Island. *Mar. Ecol. Prog. Ser.* **50:** 73–81.

Tracey, G. A., P. W. Johnson, R. W. Steele, P. E. Hargraves and J. McN. Sieburth. 1988. A shift in photosynthetic picoplankton composition and its effect on bivalve mollusc nutrition: the 1985 "brown tide" in Narragansett Bay, Rhode Island. *J. Shellfish Res.* **7:** 671–675.

Tracey, G., R. Steele, and L. Wright. 1990. Variable toxicity of the brown tide organism, *Aureococcus anophagefferens,* in relation to environmental conditions for growth. Pp. 233–237 in *Toxic Marine Phytoplankton,* E. Graneli, B. Sundstrom, L. Edler, and D. M. Anderson, eds. Elsevier, New York.

Walter, M. F., and P. Satir. 1978. Calcium control of ciliary arrest in mussel gill cells. *J. Cell Biol.* **79:** 110–120.

Ward, J. E., and N. M. Targett. 1989. Are metabolites from the brown tide alga, *Aureococcus anophagefferens,* deleterious to mussel feeding behavior? Pp. 543–556 in *Novel Phytoplankton Blooms,* E. M. Cosper, V. M. Bricelj and M. J. Carpenter, eds. Springer-Verlag, New York.

Welsh, J. H., R. I. Smith, and A. E. Kammer. 1968. Laboratory Exercises in Invertebrate Physiology, 3rd. ed. Burgess, Minneapolis.

Reference: *Biol. Bull.* **181:** 307–311. (October, 1991)

Tidal and Seasonal Patterns in the Chondrophore of the Soft-Shell Clam *Mya arenaria*

ROBERT M. CERRATO[1], HEATHER V. E. WALLACE[1], AND KENT G. LIGHTFOOT[2]

[1]*Marine Sciences Research Center, State University of New York, Stony Brook, New York 11794-5000, and* [2]*Department of Anthropology, University of California at Berkeley, Berkeley, California 94720*

Thin sections of a compact, internal structure projecting from the hinge region of the bivalve Mya arenaria *reveal the presence of tidal and seasonal patterns. This is the first demonstration that microgrowth increments are formed in a structure not associated with the growing edge of the shell. The clarity and simple orientation of these extensive patterns, combined with the resilience of the hinge region to disturbance and damage, suggests that detailed examinations of internal shell structures will prove valuable in ecological, archaeological, and paleoecological studies.*

Ecologists, archaeologists, and paleoecologists share an interest in the calcified layers of animals, because such layers can be preserved and can record growth variations. The shells of bivalve mollusks consist of two or more calcified layers that can differ considerably in composition and structure. These layers are formed by the mantle tissue in different regions of the shell. The outer layer is deposited at the ventral or growing margin. The innermost layer forms in interior regions generally behind the pallial line (1), a region where the mantle tissue attaches to the shell. As one might expect, growth patterns within the shell are also preserved to a different degree in these layers. Several investigators have suggested that the finest, most detailed growth records are formed in the outer layer, while only major patterns in growth can be resolved in the innermost layer (2, 3). Experience to date has borne this out. Daily and tidally produced growth increments have been documented in the outer shell layer of a variety of species (2, 4–7). Only annual and seasonal patterns have been identified in the inner shell layer (3, 8–13).

Here we report, for the first time, the presence of tidally deposited growth increments within an inner shell layer and within a structure associated with the hinge region rather than the ventral margin of the shell. We also describe the occurrence of well-defined seasonal patterns in this species and suggest that, when present, detailed microgrowth records in the inner shell layer may more accurately reflect the physiological state of a bivalve than comparable patterns within the outer layer. The species studied is the soft-shell clam, *Mya arenaria,* which is widely distributed along the coastal areas of the North Atlantic and North Pacific Oceans.

Searching for growth patterns in the inner shell layer is not a common procedure, but tends to occur only after it has been determined that growth patterns are for some reason poorly preserved in the outer layer of the species being studied (13). This is the case for *Mya arenaria.* The shell of this species is thin and always shows signs of considerable damage, abrasion, and erosion. The ventral margin is usually chipped, irregular, and frequently repaired. Growth records are poorly preserved in cross-sections of the valve and are unreliable for estimating the age of individuals (8, 14). Instead, investigators have concentrated on examining the chondrophore, an internal, spoon-shaped shelf projecting from the hinge region of the left valve (Fig. 1a). Using thin sections or acetate peel replicas of the chondrophore, several prior studies established the presence of annual patterns (8, 14–16), and in one case (17), the presence of intra-annual features was noted.

Samples of *Mya arenaria* were collected bimonthly in 1986–87 and monthly during 1988–89 at an intertidal location in Stony Brook Harbor, Long Island, New York. Thin sections were produced according to the methods described in detail by Clark (18), and the shells were prepared as follows. First, the chondrophore, along with a portion of the left valve, was sectioned from the umbo to

Received 1 May 1991; accepted 3 July 1991.

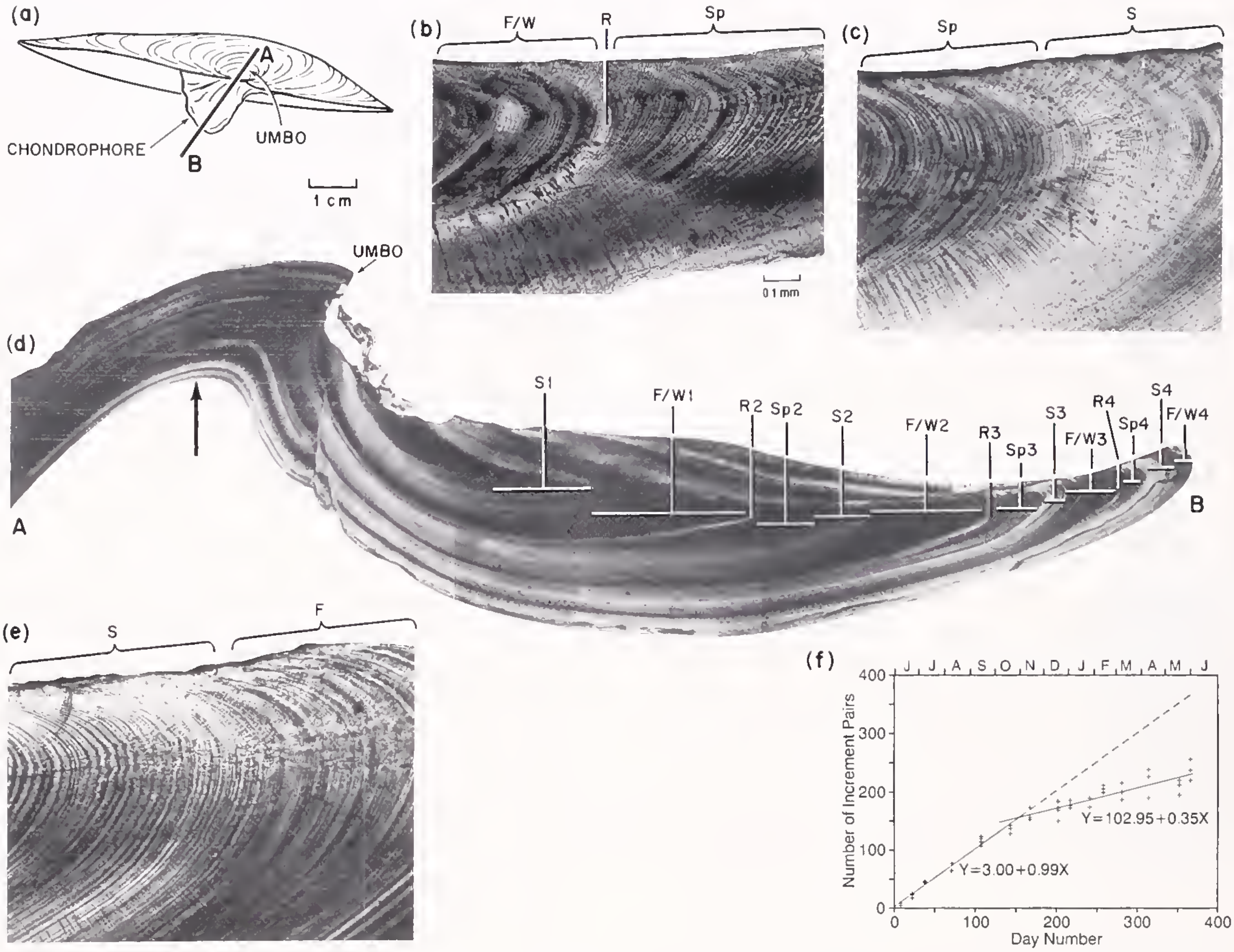

Figure 1. *Microgrowth patterns in the chondrophore of* Mya arenaria. *(a) View of left valve with associated chondrophore. Line A–B shows orientation of thin sections. (b), (c), and (e) Optical micrographs of thin sections illustrating the detailed microgrowth increment patterns. Note the seasonal variations in increment thickness and morphology. All three micrographs to same scale. (d) Composite optical micrograph of a thin section of the chondrophore and hinge region of a 4+ year old individual. Distinct summer (S) and spawning features (R) are evident. Spring (Sp) and fall/winter (F/W) appear as dark (opaque) regions in thin sections. Specimen collected in March 1989. (f) Counts of the number of microgrowth increment pairs occurring after the spawning band* versus *day number during 1988–89 ($n = 46$). Based on monthly sampling, the spawning band was produced in individuals after 13 May and prior to 8 June, the first date plotted in the figure. For the regression, 1 June is defined as the origin. The segmented or two-phase linear function was fit by least squares under the assumptions that the location of the join point was unknown and error variances in the two segments were unequal. Detailed methods for this regression may be found in Hudson (30). Slope of the first line segment verifies the semidiurnal rate of increment deposition (95% CI: $0.94 \leq b_1 \leq 1.04$ pairs of increments per day). Rate of increment production decreases in fall/winter as shown by the slope of the second line segment (95% CI: $0.28 \leq b_2 \leq 0.41$ pairs of increments per day).*

the chondrophore edge (Fig. 1a). Specimens were then mounted onto petrographic slides, sectioned a second time, ground, and polished by hand. Thin sections of 231 specimens were examined under transmitted light using a compound microscope at low magnification (12.5–100×). We analyzed growth patterns primarily by characterizing how features present at the edge of the chondrophore changed from one sampling date to the next. Unless otherwise noted, the specific features described below occurred in 90% or more of the specimens that were examined and that had been properly prepared.

The resolution of growth patterns in the chondrophore depends to a large extent on the thickness of the section (Fig. 2). Distinct variations in transparency are found in thin sections ground to 150–250 microns (Fig. 1d). At some time during May–June of each year, a thin translucent band is formed at the edge of the chondrophore (Fig. 2b); this event coincides with the spawning season, which was identified by Brousseau (19) for several nearby populations. This translucent band occurs infrequently in one-year-old individuals (32%). It is, however, readily apparent at all other ages up to the oldest individuals examined (91% of specimens 2–5 years old).

The translucent spawning band is followed by a seasonal cycle consisting of an opaque (optically dense) region formed in spring, a broad translucent region in summer, and a second opaque region in fall-winter (Fig. 2a–e). No discernible change differentiating fall from winter is apparent at the edge of the chondrophore, but an opaque layer does begin forming in January on the inner surface of the region where the chondrophore joins with the umbo (large arrow in Fig. 1d). This opaque layer is initially patchy and thin but increases in size and thickness during the winter.

When sections are ground thinner to 80–150 microns, extensive series of microgrowth increments become evident (Fig. 1b, c, e). These also vary seasonally with broad, regularly shaped increments in spring, grading into closely spaced, regular increments in summer. Regularly shaped increments also tend to be deposited during early fall, but by mid-fall, and throughout the winter, the increments appear irregular in form (*e.g.*, see transition in Fig. 1e). In addition, increment widths may be variable during early fall, but they gradually decrease in thickness during this season and remain thin throughout the winter.

The number of microgrowth increments in the interval between the most recent spawning band and the edge of the chondrophore can be related to the date of sample

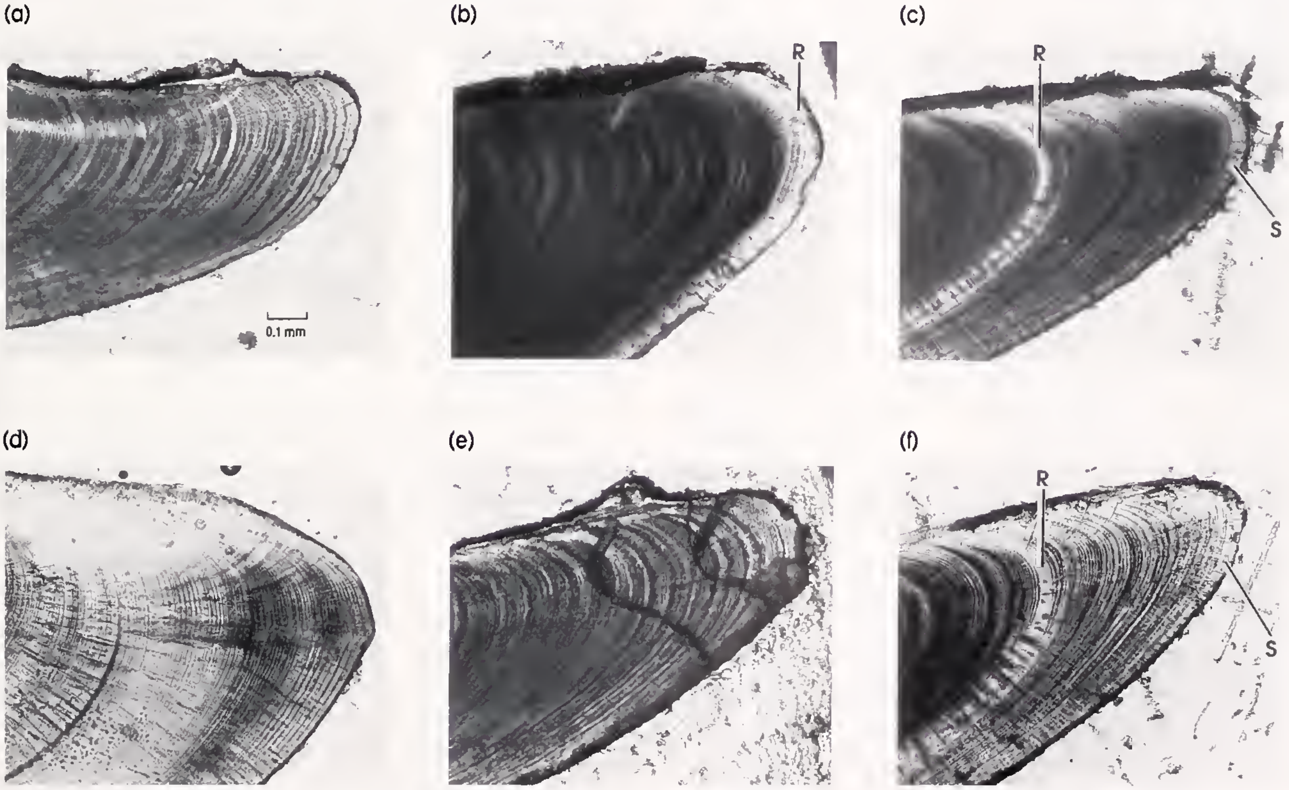

Figure 2. *Optical micrographs illustrating both seasonal changes at the edge of the chondrophore and the effect of section thickness on the resolution of microgrowth patterns. All micrographs to same scale. (a) Late winter collection. Opaque region with irregular microgrowth increments present at the edge of the chondrophore. Thin section is about 120 microns in thickness. (b) Spring collection. Newly formed spawning band (R) at the edge of the chondrophore. Opaque region in interior is previous winter; 180 micron thin section. (c) Early summer collection. Translucent region characteristic of summer growth (S) is just beginning to form at edge. Note spawning band (R) in interior and opaque spring region (between R and S); 180 micron thin section. (d) Early fall collection. Opaque region forming at edge. Note translucent summer region in interior; 100 micron thin section. (e) Early winter collection. Opaque region with irregular microgrowth increments occurs at edge. Interior region includes previous fall; 120 micron thin section. (f) Same individual as in (c) but with chondrophore ground to about 130 micron thickness. In general, microgrowth increments become evident but the contrast between opaque and translucent regions is lost as the section is ground thinner.*

collection (Fig. 1f). Increments are produced at a semidiurnal tidal frequency during the warmer months (*i.e.*, water temperatures above 15°), when a one-to-one correspondence is found between pairs of increments and day number. By mid-fall, the number of increment pairs produced per day falls below 1.0, but some increment production continues through the winter. We do not know whether this decline is due to a decrease in the rate of increment production, to periods of growth interruption, or to shell dissolution. The decline does, however, coincide with the formation of irregularly shaped microgrowth increments. We have also observed that older, slower growing individuals (4–5 years) tend to form irregular microgrowth increments, even during the warmer months, and increment production in these individuals no longer occurs at a semidiurnal tidal frequency.

Another common feature supports our semidiurnal tidal interpretation; *i.e.*, in portions of the chondrophore of almost every specimen examined, pairs of increments are separated by a diffuse, rather than a distinct boundary and appear coupled (*e.g.*, spring periods in Fig. 1b, c). This type of pattern has been observed in the outer shell layer of other species, and in each instance has been shown to be tidal in origin (2, 4, 7, 20, 21). In these prior studies, investigators have found that the alternating diffuse and sharp boundaries between increments are formed either when the semidiurnal tides are mixed (*i.e.*, unequal) (2, 7, 21) or when they are accompanied by large diurnal temperature variations (4, 20).

While we have demonstrated that detailed tidal patterns occur in the chondrophore, we do not generally expect that a direct correspondence will be found between microgrowth records produced in the inner and outer shell layers of bivalves. Increment deposition at the ventral margin is influenced by a wide variety of environmental conditions, including perturbations due to abrasion during movement, unsuccessful predator attacks, storms, and any other disturbances that may cause local injury or withdrawal of the mantle tissue (22). On the other hand, the inner shell layer, and the chondrophore in particular, is removed from direct contact with the external environment. The disturbance threshold required to affect increment deposition should be higher, and we expect that only environmental changes that cause a systemic physiological response will tend to be recorded. Thus, microgrowth patterns in the inner shell layer should contain less environmental noise due to minor disturbances and should be more integrated with, and more accurately reflect, the physiological processes of a bivalve than comparable patterns deposited in the outer shell layer.

Supporting this view is the sharp contrast between the distorted, highly disturbed form of the outer shell layer in *Mya arenaria* and the detailed, and at times very uniform, patterns preserved in the chondrophore. Another indication is the prominence of features in the chondrophore associated with the two periods of greatest physiological stress for *Mya arenaria*, *i.e.*, summer and spawning. The soft-shell clam is a boreal species, and summer represents an extended period of energetic stress due to high water temperatures and potentially low food supplies on Long Island's tidal flats. During July and August, water temperatures in protected, intertidal areas consistently reach 26–28° (23), and chlorophyll-a concentrations in both the water (24) and surficial sediments (23) can undergo mid-summer declines. Kennedy and Mihursky (25) have shown that the metabolic requirements of *Mya* continue to increase with temperature up to 30° and have suggested that high temperatures can lead to starvation if food supplies are scarce. Above 30°, *Mya* suffer significant mortalities (26). In *Mercenaria mercenaria*, the occurrence of a similar translucent region in the middle shell layer has been termed a "stress zone" by Clark (27) and has been observed to form when water temperatures exceed 25° (28), the upper limit for optimal shell growth in this species (29).

The second stress period, associated with spawning, appears as a prominent translucent band consisting of four or more closely spaced microgrowth increments (Fig. 1b, 2b, c, f). The morphology of this feature is very similar to the spawning band in the outer shell layer of *Mercenaria mercenaria* (22). However, in *Mercenaria mercenaria*, the spawning band is less prominent than growth interruptions produced by discrete environmental disturbances (22).

The hinge region in bivalves is the most resilient part of the shell, and it is also the only part containing a complete record of growth. These characteristics make the presence of detailed patterns in the hinge region particularly valuable in archaeological and paleoecological applications. For example, we are currently analyzing 1200-year-old, shell-bearing, archaeological deposits in which fully intact specimens of *Mya arenaria* are rare. However, complete chondrophores are commonly recovered, and both seasonal and microgrowth increment patterns are well preserved. These patterns are allowing us to reconstruct detailed aspects of growth in *Mya*, as well as to infer seasonal shellfish-harvesting practices for this species.

Chondrophores, cardinal platforms, and other internal structures associated with the hinge occur in many bivalve taxa but have been overlooked as potential sources of detailed microgrowth increment records. Our observations suggest that the microgrowth records preserved in these structures are not simply reflections of patterns found in other parts of the shell. As in the case of *Mya*, internal structures may contain the only usable growth patterns. At the very least, these patterns should have less environmental noise and should be more closely coupled to systemic physiological processes. Given the clarity and simple orientation of the microgrowth increments found in the chondrophore, these structures will also be quite amenable to microprobe and image analysis examination.

Acknowledgments

The 1986–87 samples were taken from a set of shells collected and archived by Bernice Malione. We would like to thank Jonathan Salerno, Richard Muller, and Mark Wiggins for their help in field collecting. We also thank David Conover, Valrie Gerard, and Robert Malouf for their comments on the manuscript.

Literature Cited

1. **Kennedy, W. J., J. D. Taylor, and A. Hall. 1969.** Environmental and biological controls on bivalve shell mineralogy. *Biol. Rev.* **44:** 499–530.
2. **Pannela, G., and C. MacClintock. 1968.** Biological and environmental rhythms reflected in molluscan shell growth. *J. Paleontol.* **42:** 64–80.
3. **Fritz, L. W., and R. A. Lutz. 1986.** Environmental perturbations reflected in internal shell growth patterns of *Corbicula fluminea. Veliger* **28:** 401–417.
4. **Richardson, C. A., D. J. Crisp, and N. W. Runham. 1979.** Tidally deposited growth bands in the shell of the common cockle, *Cerastoderma edule* (L.). *Malacologia* **18:** 277–290.
5. **Richardson, C. A. 1987.** Tidal bands in the shell of the clam *Tapes philippinarum. Proc. R. Soc. Lond. B.* **230:** 367–387.
6. **Richardson, C. A. 1989.** An analysis of the microgrowth bands in the shell of the common mussel *Mytilus edulis. J. Mar. Biol. Assoc. U.K.* **69:** 477–491.
7. **Evans, J. W. 1972.** Tidal growth increments in the cockle *Clinocardium nuttalli. Science* **176:** 416–417.
8. **MacDonald, B. A., and M. L. H. Thomas. 1980.** Age determination of the soft-shell clam *Mya arenaria* using internal growth lines. *Mar. Biol.* **58:** 105–109.
9. **Ropes, J. W., and L. O'Brien. 1979.** A unique method of aging surf clams. *Bull. Am. Malacol. Union* **1979:** 58–61.
10. **Ropes, J. W. 1984.** Procedures for preparing acetate peels and evidence validating the annual periodicity of growth lines formed in the shells of ocean quahogs, *Arctica islandica. Mar. Fish. Rev.* **46:** 27–35.
11. **Fritz, L. W., and D. S. Haven. 1983.** Hard clam, *Mercenaria mercenaria,* shell growth patterns in Chesapeake Bay. *Fish. Bull.* **81:** 697–708.
12. **Lutz, R. A., and D. C. Rhoads. 1978.** Shell structure of the Atlantic ribbed mussel, *Geukensia demissa* (Dillwyn): a reevaluation. *Bull. Am. Malacol. Union* **1978:** 13–17.
13. **Lutz, R. A. 1976.** Annual growth patterns in the inner shell layer of *Mytilus edulis* L. *J. Mar. Biol. Assoc. U.K.* **56:** 723–731.
14. **Malione, B. R. 1987.** Analysis of growth in *Mya arenaria* using internal growth lines. M.S. thesis, Marine Sciences Research Center, State University of New York, Stony Brook, NY.
15. **Newell, C. R. 1982.** The soft-shell clam *Mya arenaria* L.: growth rates, growth allometry, and annual growth line formation. M.S. thesis, University of Maine, Orono, Maine.
16. **Brousseau, D. J., and J. A. Baglivo. 1987.** A comparative study of age and growth in *Mya arenaria* (soft-shell clam) from three populations in Long Island Sound. *J. Shellfish Res.* **6:** 17–24.
17. **Barber, R. J. 1982.** The Wheeler's Site: a specialized shellfish processing station on the Merrimack River. *Peabody Museum Monographs 7,* Harvard University, Cambridge, MA.
18. **Clark, G. R. 1980.** Study of molluscan shell structure and growth lines using thin sections. Pp. 603–606 in *Skeletal Growth of Aquatic Organisms,* D. C. Rhoads and R. A. Lutz, eds. Plenum, New York.
19. **Brousseau, D. J. 1987.** A comparative study of the reproductive cycle of the soft-shell clam *Mya arenaria* in Long Island Sound. *J. Shellfish Res.* **6:** 7–15.
20. **Richardson, C. A., D. J. Crisp, and N. W. Runham. 1981.** Factors influencing shell deposition during a tidal cycle in the intertidal bivalve *Cerastoderma edule. J. Mar. Biol. Assoc. U.K.* **61:** 465–476.
21. **Richardson, C. A. 1987.** Microgrowth patterns in the shell of the Malaysian cockle *Anadara granosa* (L.) and their use in age determination. *J. Exp. Mar. Biol. Ecol.* **111:** 77–98.
22. **Kennish, M. J. 1980.** Shell microgrowth analysis: *Mercenaria mercenaria* as a type example for research in population dynamics. Pp. 255–294 in *Skeletal Growth of Aquatic Organisms,* D. C. Rhoads and R. A. Lutz, eds. Plenum, New York.
23. **Forbes, V. E. 1988.** Intraspecific variation among populations of the deposit-feeding gastropod, *Hydrobia truncata:* the effect of sediment particle size on physiological energetics. Ph.D. thesis, Marine Sciences Research Center, State University of New York, Stony Brook, NY.
24. **Bellantoni, D. C., and W. T. Peterson. 1987.** Temporal variability in egg production rates of *Acartia tonsa* Dana in Long Island Sound. *J. Exp. Mar. Biol. Ecol.* **107:** 199–208.
25. **Kennedy, V. S., and J. A. Mihursky. 1972.** Effects of temperature on the respiratory metabolism of three Chesapeake Bay bivalves. *Chesapeake Sci.* **13:** 1–22.
26. **Kennedy, V. S., and J. A. Mihursky. 1971.** Upper temperature tolerances of some estuarine bivalves. *Chesapeake Sci.* **12:** 193–204.
27. **Clark, G. R. 1979.** Seasonal growth variations in the shells of recent and prehistoric specimens of *Mercenaria mercenaria* from St. Catherines Island, Georgia. *Anthropol. Pap. Am. Mus. Nat. Hist.* **56:** 161–179.
28. **Fritz, L. W., and D. S. Haven. 1983.** Hard clam, *Mercenaria mercenaria,* shell growth patterns in Chesapeake Bay. *Fish. Bull.* **81:** 697–708.
29. **Ansel, A. D. 1968.** The rate of growth of the hard clam *Mercenaria mercenaria* (L) throughout its geographic range. *J. Cons. Perm. Int. Explor. Mer* **31:** 364–409.
30. **Hudson, D. J. 1966.** Fitting segmented curves whose join points have to be estimated. *J. Am. Stat. Assoc.* **61:** 1097–1129.

Reference: *Biol. Bull.* **181:** 312–314. (October, 1991)

Effects of Indomethacin on Active Ion Transport Across the Gills of the Shore Crab, *Carcinus maenas*

DIETRICH SIEBERS[1], TARIG MUSTAFA[2], AND KIRSTEN BÖTTCHER[1]

[1]*Biologische Anstalt Helgoland (Zentrale), Notkestr. 31, D-2000 Hamburg 52, Germany, and*
[2]*University of Odense, Department of Biology, Campusvej 55, DK-5230-Odense, M, Denmark*

Hyperosmoregulating brackish water crustaceans counteract continuous passive losses of inorganic salts along the internal/external concentration gradient by means of reductions of the permeabilities of their body surfaces to salts and water (1), increased rates of urination (2), and active absorption of ions across the gills (3).

Active uptake of Na^+ across the epithelial cell of the gill is considered to consist of an apical Na^+/H^+ exchange system (4) acting in combination with a basolateral Na-K-ATPase which drives Na^+ against the gradient from the epithelial cell into the hemolymph space (5). Transport of Cl^- consists of an apical Cl^-/HCO_3^- exchange (4) and a basolateral Cl^- channel (6) operating in combination with K^+ extrusion from cell to hemolymph along the electrochemical gradient via a basolateral K^+ channel (7).

Short-term modifications of ion transport capacities in shore crabs inhabiting a tidal estuary (8) imply a role for hormonal control mechanisms in ion uptake. In crab gills, cyclic AMP has been reported to activate both the Na-K-ATPase (9) and the basolateral Cl^--channel (10). Graves and Dietz (11) reported that, in the freshwater mussel *Ligumia subrostrata*, the injection of prostaglandin E_2 and indomethacin, an inhibitor of prostaglandin biosynthesis (12), affected Na^+ influx rates in intact mussels; they suggested that prostaglandins may be a component of the endocrine control of ion regulation in freshwater bivalves.

To analyze the potential role of prostaglandins in active ion uptake in crabs, we investigated the effects of indomethacin on transepithelial potential differences (PD) and ion fluxes across isolated perfused gills of the shore crab *Carcinus maenas*.

Shore crabs, *Carcinus maenas*, were collected in coastal waters of the Baltic Sea near Kiel and were maintained in the laboratory at a salinity of 10 ppm. The afferent and efferent vessels of isolated posterior gills were both cannulated with fine polyethylene tubing which was kept fixed in position with a small Plexiglas clamp covered on the internal side with a 3 mm layer of soft neoprene material (13). The gills were then perfused and bathed with DSW (dilute seawater, 200 m*M* Na^+, buffered to pH 7.8 with 10 m*M* HEPES/Tris). Transgill potential differences (PD) were measured with a millivolt meter in combination with two Ag/AgCl electrodes immersed in saturated KCl and connected with agar bridges (3 *M* KCl, 3% agar) to the external bath and the internal perfusate. Unidirectional ion fluxes, from bath to perfusate and vice versa, were measured using ^{36}Cl and ^{22}Na as tracers. Samples were counted in a liquid scintillation counter after the addition of 4 ml Instagel to 1 ml DSW samples. Indomethacin, $C_{19}H_{16}ClNO_4$ (1-[4-chlorobenzoyl]-5-methoxy-2-methyl-1H-indole-3-acetic acid) was purchased from Sigma (Munich). The substance was applied in the presence of 2% ethanol, a concentration without effects on PDs and ion fluxes (see Fig. 1).

When indomethacin at low concentrations of 2.5×10^{-4} *M* was dissolved in the external bath, the PDs measured under control conditions remained unaffected (Fig. 1). However, when IM was applied at the basolateral side of the gill cells, *i.e.*, in the internal perfusate, a fast depolarization of the epithelium resulted, an effect that was easily reversible upon omission of the inhibitor (Fig. 1). The lowest concentration of internally applied IM that significantly reduced the PDs of controls (by about 10%) was 10^{-4} *M*. At an IM concentration of 10^{-3} *M*, the gills were completely depolarized. In this concentration range (10^{-4} to 10^{-3} *M*), the drug—whether applied in the bath

Received 28 March 1991; accepted 8 July 1991.

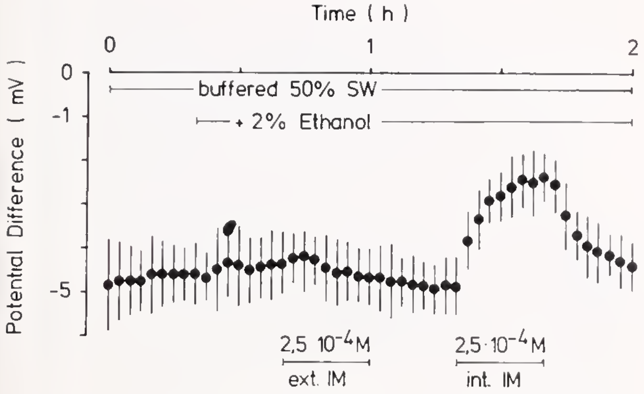

Figure 1. *Transbranchial potential differences across isolated perfused* Carcinus *gills bathed and perfused with 50% seawater (including 2% ethanol) in controls and in the presence of 2.5×10^{-4}* M *indomethacin applied to the external bath or the internal perfusion medium. Data represent means ± S.D. obtained from a sample size of n = 4 gills taken from four crabs.*

or in the perfusate—had no significant effect on the perfusion flow rates.

In controls, unidirectional influxes of Cl$^-$ (Fig. 2) greatly exceeded Cl$^-$ effluxes, a finding indicating net influx. Indomethacin had no effect on unidirectional in- or effluxes of Cl$^-$ when applied at 2.5×10^{-4} *M* in the external medium. Application of 2.5×10^{-4} *M* IM on the basolateral side resulted in a significant reduction (66%) of unidirectional Cl$^-$ influxes. Concomitantly, influxes of Cl$^-$ recovered quantitatively following IM removal. Unidirectional effluxes of Cl$^-$ were not changed significantly by 2.5×10^{-4} *M* internal IM. The lowest IM concentration that significantly inhibited unidirectional Cl$^-$ influxes was 10^{-4} *M* which reduced Cl$^-$ influx rates by 12%; complete inhibition was observed at 10^{-3} *M*. Comparable effects of IM were obtained on fluxes of Na$^+$ (data not shown).

It was reported earlier that depolarization of isolated perfused shore crab gills accompanies inhibition of unidirectional ion influxes (14). Accordingly, we demonstrate here depolarization of the epithelium and inhibition of transgill net influx of Cl$^-$ (Fig. 2) and Na$^+$ by IM. The effects on PDs and ion fluxes were only observed when IM was applied in the internal perfusate. Thus, we assume that the IM-sensitive transport step is located at the basolateral side of the epithelial cell.

The rapid and quantitative reversibility of depolarization and inhibition of Cl$^-$-influx upon IM removal indicates that the drug is not irreversibly bound in the crustacean gill, as it is in some mammalian tissues (12), and that it has no long-lasting cytotoxic effect on the branchial ion transport system.

The effects of IM in isolated perfused crab gills differ from those observed by Graves and Dietz (11) in intact mussels (*Ligumia subrostrata*). In individuals of this species, injection of IM caused a doubling of Na$^+$ influxes.

The results reported show that low doses of a commonly used drug for the inhibition of prostaglandin biosynthesis in mammalian systems (12) inhibited the process of active ion transport across the gill epithelium of a crab (Fig. 1). Indomethacin is a widely used anti-inflammatory agent with antipyretic and analgesic properties. It is orally applied in the treatment of several types of arthritis, including rheumatoid arthritis, osteoarthritis of the hip, and gouty arthritis (15). IM belongs to the NSAIDs (nonsteroidal anti-inflammatory drugs) which, to our knowledge, have not yet been shown to affect biological transport processes in mammals (15).

The findings communicated here may indicate the involvement of prostaglandins in ion transport in crustacean gills. However, the results on PDs presented in Figure 1 show that IM has a very rapid action when applied in the perfusate. The notion that this fast effect is due to a prostaglandin depletion caused by the inhibitory action of IM on prostaglandin biosynthesis is questionable. The rapid action of IM may rather be indicative of a direct drug effect on one of the ion transport systems present in the crustacean gill, an indication that would be of considerable biomedical relevance. Further experiments are thus being planned to clarify a potential role of prostaglandins in ion transport across crab gills, to test our hypothesis that the IM specifically inhibits the basolateral transport system, and to determine whether the respective transporters in mammalian tissues exhibit the same sensitivity.

Acknowledgments

This work was supported by the Deutsche Forschungsgemeinschaft (Si 295/1-5).

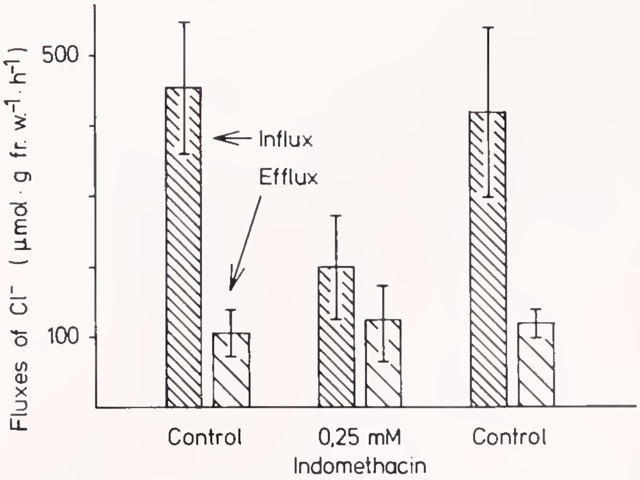

Figure 2. *Unidirectional in- and effluxes of Cl$^-$ across isolated posterior* Carcinus *gills bathed and perfused with 50% buffered seawater containing 2% ethanol in controls and in the presence of 2.5×10^{-4}* M *indomethacin applied in the internal perfusate. Data represent means ± S.D. obtained from a sample size of five gills taken from five crabs.*

Literature Cited

1. **Gross, W. J. 1957.** An analysis of response to osmotic stress in selected decapod crustacea. *Biol. Bull.* **112:** 43–62.
2. **Oglesby, L. C. 1981.** Volume regulation in aquatic invertebrates. *J. Exp. Zool.* **215:** 289–301.
3. **Gilles, R., and A. Péqueux. 1986.** Physiological and ultrastructural studies on NaCl transport in crustacean gills. *Boll. Zool.* **53:** 173–182.
4. **Kirschner, L. B. 1979.** Control mechanisms in crustaceans and fishes. Pp. 157–222 in *Mechanisms of Osmoregulation in Animals,* R. Gilles, ed. Wiley, Chichester.
5. **Towle, D. W. 1981.** Na^+-K^+-ATPase in ionic regulation by marine and estuarine animals. *Mar. Biol. Lett.* **2:** 107–121.
6. **Siebers, D., K. Böttcher, G. Petrausch, and A. Hamann. 1990.** Effects of some chloride channel blockers on potential differences and ion fluxes in isolated perfused gills of shore crabs *Carcinus maenas. Comp. Biochem. Physiol.* **27A:** 9–15.
7. **Drews, G., and K. Graszynski. 1987.** The transepithelial potential difference in the gills of the fiddler crab, *Uca tangeri.* Influence of some inhibitors. *J. Comp. Physiol. B* **157:** 345–353.
8. **Winkler, A., D. Siebers, and W. Becker. 1988.** Osmotic and ionic regulation in shore crabs *Carcinus maenas* inhabiting a tidal estuary. *Helgol. Meeresunters.* **42:** 99–111.
9. **Sommer, M. J., and L. H. Mantel. 1988.** Effect of dopamine, cyclic AMP, and pericardial organs on sodium uptake in the gills of the green crab *Carcinus maenas* (L.). *J. Exp. Zool.* **248:** 272–277.
10. **Bianchini, A., A. Péqueux, and R. Gilles. 1988.** Effects of TAP and DPC on the transepithelial potential difference of isolated perfused gills of the fresh water acclimated crab, *Eriocheir sinensis. Comp. Biochem. Physiol.* **90A:** 315–319.
11. **Graves, S. Y., and Dietz, T. H. 1979.** Prostaglandin E_2 inhibition of sodium transport in the freshwater mussel. *J. Exp. Zool.* **210:** 195–201.
12. **Mustafa, T., and K. C. Srivastava. 1989.** Prostaglandins (Eicosanoids) and their role in ectothermic organisms. Pp. 157–207 in *Advances in Comparative and Environmental Physiology,* Vol. 5, R. Gilles, ed. Springer, Berlin.
13. **Siebers, D., A. Winkler, C. Lucu, and G. Thedens. 1985.** Na-K-ATPase generates an active transport potential in the gills of the hyperregulating shore crab *Carcinus maenas. Mar. Biol.* **87:** 185–192.
14. **Siebers, D., C. Lucu, A. Winkler, L. Dalla Venezia, and H. Wille. 1986.** Active uptake of sodium in the gills of the hyperregulating shore crab *Carcinus maenas. Helgol. Meeresunters.* **40:** 151–160.
15. **Schlegel, S. I., and H. E. Paulus. 1987.** Update on NSAID use in rheumatic diseases. *Bull. Rheum. Dis.* **36:** 1–8.

Reference: *Biol. Bull.* **181**: 315–361. (October, 1991)

Reports of Papers Presented at the General Scientific Meetings of the Marine Biological Laboratory

August 12–14, 1991

Short Reports are arranged (after the first featured article by Llinas et al.*) alphabetically by first author within the following categories: Neurobiology and Biophysics (pp. 316–333); Cell and Molecular Biology (pp. 333–342); Fertilization and Development (pp. 342–350); Physiology (pp. 350–356); and Systems and Ecology (pp. 357–361).*

All Short Reports were reviewed by members of our Special Editorial Board. Board members include: George Augustine (University of Southern California); David Epel (Hopkins Marine Station); Judith Grassle (MBL); Ehud Kaplan (Rockefeller University); George Langford (University of North Carolina); Jack Levin (VA Medical Center, San Francisco); James Olds (NIH); Robert Palazzo (MBL); Darrell Stokes (Emory University); Ivan Valiela (Boston University Marine Program); and Steven Zottoli (Williams College).

In addition to the reports contained in this issue, the following papers were also presented, by title, at the meetings. The abstracts of these papers are available from the MBL Archives.

Du, Jun, and Raquel Sussman. "mRNA analysis of a DNA-damage-inducible operon involved in mutagenesis of *E. coli*."

van Egeraat, Jan M., Richard N. Friedman, and John P. Wikswo. "Magnetic measurement of the spatial distribution of action currents in injured squid giant axons and squid giant synapses."

Fox, S. H., A. B. DuBois, and C. S. Ogilvy. "The effect of carbon dioxide on blood pressure, heart rate, intracranial pressure, and the Cushing response in bluefish (*Pomatomus saltatrix*)."

Kaplan, Ilene M., Barbara C. Boyer, and Lesley Carmichael. "The impact of socio-economic trends in the New England Conch (*Busy Con*) fishery on environmental changes and seafood inspection."

Nelson, Leonard, and Lucio Cariello. "Enzymatic correlates of *Arbacia punctulata* gametes exposed to pesticides."

Reynolds, G. T., and D. A. Hajduk. "Luminescence from polymerization of acrylamide."

Sheetz, Michael P. "Expansion and linearization of nuclear material visualized by video microscopy."

Silver, R. B. "Temperature induced spawning in *Echinarachnius parma* experiments? Knot when they're hot."

Sweet, Hyla C., and Barbara C. Boyer. "Multiple first quartet micromere deletions in eight-cell stage embryos of *Ilyanassa obsoleta*."

Zhong, Nan, and Robert M. Gould. "Partial cDNA sequence of phosphatidylinositol-specific phospholipase C (PI-PLC) from squid and dogfish nervous tissues by RNA-PCR."

Zhou, Zhimin, Gordon L. Fain, and John E. Dowling. "Amino acid receptors in isolated horizontal cells from the white perch retina."

Imaging Preterminal Calcium Concentration Microdomains in the Squid Giant Synapse

R. Llinás[1], *M. Sugimori*[1] *and R. B. Silver*[2] *([1]Department of Physiology and Biophysics, New York University Medical Center, New York, New York; and [2]Section and Department of Physiology, Cornell University, Ithaca, New York 14853-6401)*

Intracellular calcium is the main trigger for transmitter release at most chemical synapses (1). The mechanisms by which calcium activates such release is presently unknown. The initial working hypothesis about the relationship between intracellular calcium concentration ($[Ca^{2+}]_i$) and transmitter release was based on results from the neuromuscular junction (2), and was proposed as a single-compartment release model. According to this model, vesicles are exocytosed following a fourth-order relation with respect to $[Ca^{2+}]_i$. This model, while useful, and clearly the best that could be made at the time, did not consider the many variables that regulate such parameters as $[Ca^{2+}]_i$ or vesicular availability. Moreover, calcium was thought to flow uniformly across the preterminal membrane, and the model of transmitter released did not adequately consider the ultrastructure of the presynaptic terminal. Present information regarding such parameters demand a more complete multi-compartment model.

Indeed, the possibility that calcium channels are localized at a discrete site in the preterminal was suggested in the late-70's (3). The suggestion came as a result of voltage-clamp experiments, which revealed the latency between the tail current calcium entry and transmitter release to be as short as 200 ms (3, 4). This morphological prerequisite of synaptic vesicles being directly apposed to the calcium channels was recently confirmed histologically (5). From voltage clamp data, the maximum $[Ca^{2+}]_i$ against the membrane was calculated to be about $10^{-4}M$ (4). These results shifted the focus from cytosolic residual calcium to the problem of what is now known as calcium microdomains (6–9). The term "calcium microdomains" refers to a very precise distribution of sites for $[Ca^{2+}]_i$ change. These microdomains were expected to occur against the inside of the presynaptic terminal at the active zone. In fact, each active calcium channel is thought to produce a rapid (*i.e.*, a few Ms) increase in $[Ca^{2+}]_i$, lasting for the duration of the average open time of the channel (8). This influx is thought to generate a $[Ca^{2+}]_i$ profile as high as 200–300 Mmoles in the proximity of the calcium channels. This being the case, transmitter release would be triggered by extraordinarily high transient calcium-concentration change in the immediate vicinity of the presynaptic release site where the vesicles are lodged (4, 8).

To test this hypothesis, a special type of signalling methodology was introduced. A hybrid synthetic n-aequorin/J (10), having a sensitivity to $[Ca^{2+}]_i$ in the order of 10^{-4}, was developed for this purpose by Dr. Shimomura. This aequorin was injected presynaptically at a concentration of 5%, in conjunction with "discharged" normal sensitivity aequorin made fluorescent to permit its intracellular localization. The distribution of the injected protein following impalement of the presynaptic terminal of the giant synapse of the squid *Loligo pealii* was visualized with a fluorescence microscope using a 40× water-immersion lens. Aequorin luminescence was then detected with a VIM camera operated in the photon counting mode; the images stored on videotape and characterized by digital image processing and analysis methods.

Results were obtained from eight different synapses bathed in artificial seawater (10 mM Ca^{2+}); one synapse was injected with normal aequorin, and the other seven injected with the n-aequorin/J. Upon tetanic stimulation, small points of light were detected over the preterminal region in the area of the "active zone" (Fig. 1).

These points had an average diameter of approximately 0.5 μm and were distributed over roughly 5–10% of the total area of the presynaptic membrane (with an average of 8.39 μ^2 per 100 μ^2) (Fig. 1). Results from all synapses were quite similar. They show that the portion of the presynaptic terminal forming the active zone emits light during presynaptic activation, indicating that the calcium concentration is elevated in the range of 10^{-4} M during this active period.

The location of these small light sources was determined by two methodologies. First, light-emission points were accumulated during several seconds of stimulation, and the spatial and temporal distribution of the blips was then studied. Second, to ensure that the location of the patches of blips were similar within repeating stimuli, sets of successive temporal image integrations of the recording were compared.

Both methods illustrated a similar distribution of microdomains and roughly the same size and intensity of light points. The results suggest that microdomains may belong to one of two varieties: (1) those frequently activated, and (2) those that, while repeating, activate less often. Finally, analysis of digitized sub-regions of the image field showed that the temporal and spatial distribution of microdomain action through time reflects the temporal cycling of active sites from one point of membrane to the next, during stimulation. This finding suggests that an even more complex modulation of activity may be present in these terminals. Indeed, in addition to calcium microdomains, compartmentalization of other parameters such as the degree of phosphorylation of synapsin I (11) may also show dynamic interaction, which would ensure a fine control of transmitter release from one impulse to the next. Of interest here is the possibility that a certain number of calcium channels may have to be active simultaneously in order to activate the aequorin signals observed here. In that case, the high level of $[Ca^{2+}]_i$ obtained at the microdomain may itself reduce, by a "lateral inhibition" type effect, the probability of further calcium channel activation in a given active site.

We extend our deep gratitude to Dr. Osamu Shimomura for his generous gifts of the custom aequorin preparations used in this study. The authors gratefully acknowledge research grant support from the NIH (NS 14014 to RL), the U. S. Air Force (OSRG85-0368 to RL), the NSF (DCB-9005343 to RBS) and the Cornell—U. S. Army Biotechnology Center of Excellence Program (24629-LS-UIR to RBS).

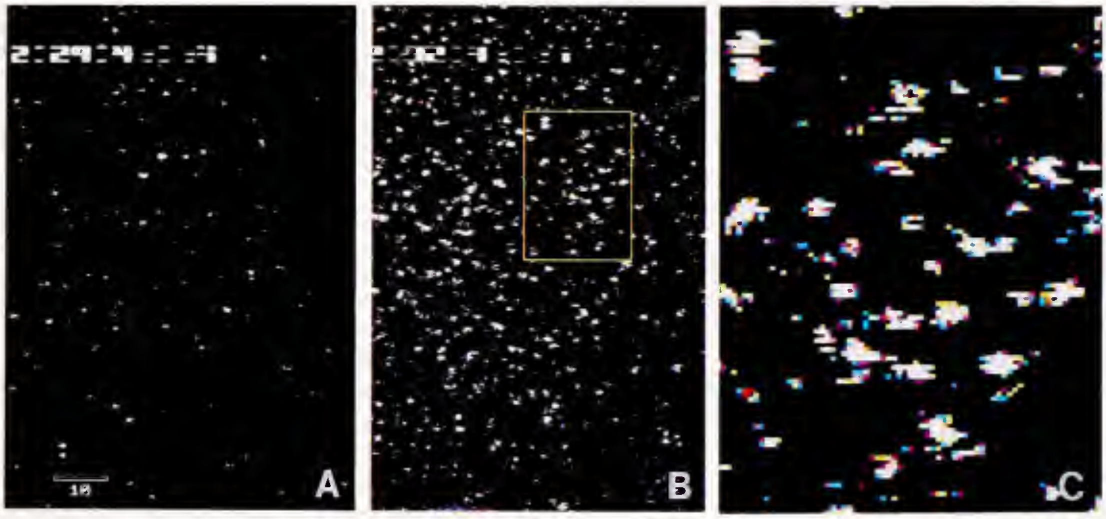

Figure 1. *Imagery of Ca^{2+}-dependent aequorin luminescence from pre-terminal of the squid giant synapse. Note the discrete sizes of individual blips. Pseudo-coloring is used to indicate brightness of each blip: white and red are the brightest blips, blue and violet blips are the least intense. Panel A. A 10-s integration of the pre-terminal 30 s prior to stimulation. Panel B. A 10-s integration of the same region of the pre-terminal shown in Panel A 60 s following the onset of tetanic stimulation. Note the increase in the number of blips compared to Panel A. Panel C. An enlarged image of calcium microdomains in the region indicated within the inset borders of Panel B. Bar = 10 μm.*

Literature Cited

1. **Katz, B. 1969.** *The Release of Neurotransmitter Substances.* The Sherrington Lectures X. Charles C. Thomas, Springfield, IL.
2. **Dodge, F. A., and R. Rachamimoff. 1967.** *J. Physiol. Lond.* **193:** 419–432.
3. **Llinás, R. 1977.** Pp. 139–160 in *Approaches to the Cell Biology of Neurons.* Soc. for Neurosciences, Bethesda, MD.
4. **Llinás, R., *et al.* 1981.** *Biophys. J.* **33:** 289–321.
5. **Robitaille, R., *et al.* 1990.** *Neuron* **5:** 773–779.
6. **Chad, J. E., and R. Ekert. 1984.** *Biophys. J.* **45:** 993–999.
7. **Simon, S. M., *et al.* 1984.** *Biophys. J.* **45:** 264a.
8. **Simon, S. M., and R. Llinás. 1985.** *Biophys. J.* **48:** 485–498.
9. **Fogelson, A. L., and R. S. Zucker. 1985.** *Biophys. J.* **48:** 1003–1007.
10. **Shimomura, O., *et al.* 1989.** *Biochem. J.* **261:** 913–920.
11. **Llinás, R., *et al.* 1985.** *Proc. Natl. Acad. Sci. U.S.A.* **82:** 3035–3039.

Synaptic Background Activity Influences Spatiotemporal Integration in Single Pyramidal Cells

Öjvind Bernander and Christof Koch (California Institute of Technology, 216-76, Pasadena, CA 91125)

Standard 1-D cable theory models the voltage behavior of spatially extended cable structures in response to synaptic inputs. These models usually assume R_m of 5–20,000 Ωcm^2 and a small number of activated synapses. Each synaptic input induces a transient increase in the membrane conductance, which is small relative to the total cell conductance. However, neurons do not exist in isolation, but are part of a heavily interconnected network of neurons that are spontaneously active: *e.g.*, in visual cortex at rates between 0.5–5 synaptic events per second [Hz] (1). Given that the average cortical pyramidal cell receives input from 10–20,000 synapses, this background activity can cause an added membrane conductance comparable to $G_m = 1/R_m$. In the light of recent evidence suggesting much higher values for R_m (2), this synaptic background activity may actually constitute the bulk of the effective membrane conductance. Here we study the overall effect of synaptic background activity on the spatial and temporal integrative properties of a single pyramidal cell.

A typical layer V pyramidal cell in the striate cortex was filled with HRP during *in vivo* experiments on anesthetized, adult cats; $R_{in} = 21$ MΩ and $\tau_m = 22$ ms (3). Lengths and diameters of all 163 dendritic branches were measured, and the data was fed into a modified version of NEURON, a single cell simulator developed by M. Hines and J. Moore (4). Passive properties were set to: $R_m = 100{,}000\ \Omega cm^2$, $C_m = 1\ \mu m^{-2}$, $R_i = 200\ \Omega cm$, and $E_{leak} = -66$ mV. Seven active Hodgkin-Huxley-like currents were located at the soma, including a calcium-dependent K current, giving such basic behavior as spike adaptation and primary slope of the curve relating injected current to the number of action potentials triggered. We modeled 4000 excitatory synapses using $g(t) = \text{const}\ te^{-t/t_{peak}}$ for the time-varying conductance in-

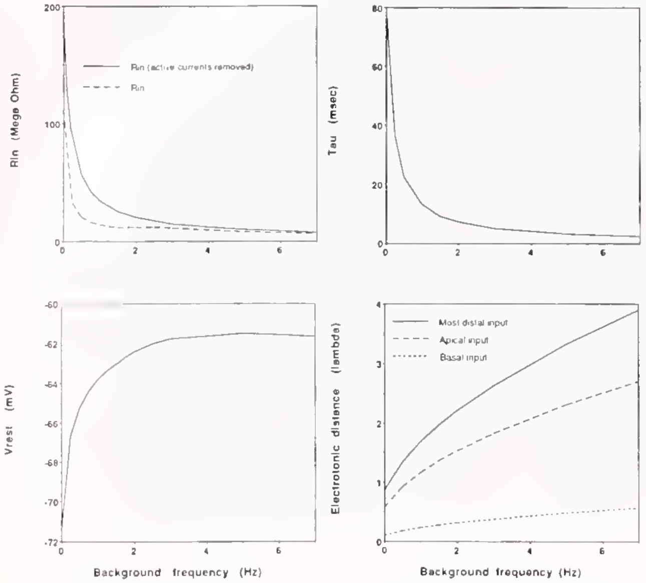

Figure 1. *Impact of synaptic background frequency (in synaptic events per second, Hz) on cellular parameters of the layer V cell described in the text. (a) Somatic input resistance, R_{in}, in the absence of any active currents (top curve; passive neuron) and in our standard model (bottom curve). Over this range, the somatic input conductance varies from 9.1 nS (at $f = 0$) to 151 nS (at $f = 7$ Hz). (b) Membrane time constant, τ_m measured at the cell body. (c) Somatic resting potential, V_{rest}. (d) Electrotonic distance, L, from the soma to three different locations (the distal end of a basal dendrite, a point halfway up the apical tree and the most distal point in layer I).*

crease (with $g_{peak} = 0.5$ nS and $t_{peak} = 1.5$ ms), 500 inhibitory synapses of the GABA$_A$ type (with $g_{peak} = 1.0$ nS and $t_{peak} = 10$ ms) and 500 of the GABA$_B$ type (with $g_{peak} = 0.1$ nS and $t_{peak} = 40$ ms). The density of inhibitory synapses was highest on, or close to, the soma, and vice versa for excitatory synapses.

Figure 1 illustrates what happens if the synaptic background activity, (f) is varied. In the absence of input (corresponding to slice conditions), $R_m = 153$ MΩ and $\tau_m = 80$ ms, while V_{rest} is pulled between E_{leak} and E_K (−95 mV). At 1 Hz background activity, 5 synaptic events are impinging on the cell every ms, contributing a total of 24 nS to the somatic input conductance G_{in} (corresponding to 34%). Along with R_m, τ_m drops with increasing f. This drop is most dramatic between 0 and 2 Hz. Because of the reversal potential of the excitatory synapses (0 mV), the membrane potential throughout the cell is pulled towards more depolarizing potentials. That the spatial integrative properties vary with f is demonstrated in Figure 1d. The electronic distance of three locations are plotted *vs.* f. As we go from 0 to 2 Hz, the distance increases almost by a factor 3, making the cell much less compact, effectively isolating distal parts of the apical tree.

We showed that the synaptic background activity can modify the temporal integration behavior of the cell, by computing the minimal number of excitatory synapses necessary to generate at least one action potential. We compare the case in which all synapses are activated simultaneously with the case in which the inputs arrive asynchronously, smeared out over 25 ms. If f = 0, 115 synapses must fire simultaneously to generate a single action potential, while 145 are needed if the input is desynchronized. This small difference is due to the long integration period of the cell. If the background activity increases to f = 1 Hz, 113 synchronized synaptic inputs—spread out all over the cell—are sufficient to fire the cell. If, however, the synaptic input is spread out over 25 ms, 202 synapses are now needed to trigger a response from the cell. This is mainly due to the much smaller value of τ_m relative to the period over which the synaptic input is spread out. The difference between synchronized and unsynchronized synaptic input in evoking action potentials becomes much larger if periodic, repetitive synaptic input is considered.

The principal phenomenon reported here is the dramatic effect that network activity can have on the spatiotemporal integration behavior of single neurons. Our results show that the large values of R_m and τ_m reported by several groups for pyramidal cells (2, 5, 6) may simply reflect the lack of general synaptic background activity typically observed in slice preparations. This would also explain the lower values of V_{rest} seen in slices as compared to *in vivo* intracellular recordings. Thus, the overall activity of the network can alter the properties and the behavior of single neurons. Our prediction can be simply tested by recording from one cell and varying the overall network activity with the help of sensory afferents.

Literature Cited

1. **Leventhal, A. G., and H. V. B. Hirsch. 1978.** *J. Neurophysiol.* **41:** 948–962.
2. **Major, G., *et al.* 1990.** *J. Physiol* **430:** 13P.
3. **Douglas, R. J., *et al.* 1991.** *J Physiol.* In press.
4. **Hines, M. 1989.** *Int. J. Biomed. Comput.* **24:** 55–68.
5. **Anderson, P., *et al.* 1990.** *Symp. Quant Biol.* **55:** 81–86.
6. **Spruston, N., and D. Johnston. 1991.** *J. Neurophysiol.* In press.

Responses of Horizontal Semicircular Canal Afferents to Rotatory and Mechanical Stimulation

Richard Boyle and Stephen M. Highstein (Marine Biological Laboratory)

Angular acceleration, the adequate stimulus for the vestibular semicircular canals, presumably exerts its effects by deflecting the cupula, thus beginning the stimulus cascade leading to the signaling of angular motion. However, considerable experimental advantage would be gained if cupular motion could be produced without rotating the preparation. Dickman *et al.* (1) have reported that controlled indentation of the membranous duct of the canal can mimic adequate stimulation. This method has therefore been adopted for stimulating the horizontal canal of the toadfish, both *in vivo* and *in vitro*.

Extracellular recordings employing rotary and mechanical stimuli were taken from horizontal semicircular canal afferents in intact, anesthetized, paralyzed toadfish (55 cells), and in an isolated toadfish skull preparation (12 cells). The horizontal canal was centered on the vertical axis of a rate table for rotation, and a piezoelectric micropusher, with a glass-ball probe approximately ⅓ the diameter of the canal, was positioned to just touch the membranous limb of the canal where it rests on the bony canal. Just touching the canal did not alter afferent spontaneous activity. The position of the pusher was measured with an in-line linear variable differential transducer (LVDT).

Afferents were characterized by their responses to rotation (Bode plots) and were sorted into the same three groups previously reported (2). The canal was then indented a variable amount (maximum 15 microns, 0.001–10 Hz) following a sinusoidal profile. Afferents responded to this indentation, just as they do to rotation, by modulating their responses about their resting rates (Fig. 1A). Afferent responses to indentation were analyzed, and mirrored those in response to rotation in individual afferents. High and low gain velocity-sensitive, and acceleration-sensitive afferents all responded to mechanical stimulation with characteristics that resembled their responses to rotation.

In many afferents, the two sinusoidal stimuli, rotation and indentation, were paired at slightly different frequencies, resulting in the stimuli beating, or moving relative to each other. Afferent responses interacted constructively and destructively to this beating (Fig. 1B). At certain stimulus phase relationships, afferent responses were enhanced over those to indentation or rotation alone (solid arrow). As the phase of the rotational stimulus advanced, relative to that of the mechanical stimulus, the responses began to decline (destructive interaction, open arrow). These constructive and destructive interactions were varied continuously, suggesting a similarity of mechanisms for modulating afferent discharges. Responses to rotation alone are illustrated for this cell (Fig. 1B, arrowhead). These results confirm that indentation of the semicircular canal limb is an alternative method of adequate stimulation for the toadfish. A factor can be calculated that equates microns of indentation to degrees/s of rotation for each afferent of each animal. Further, this method works well *in vitro*. By removing the requirement for rotating the preparation and the microscope, these results will simplify experiments designed to monitor cupular motion during adequate stimulation.

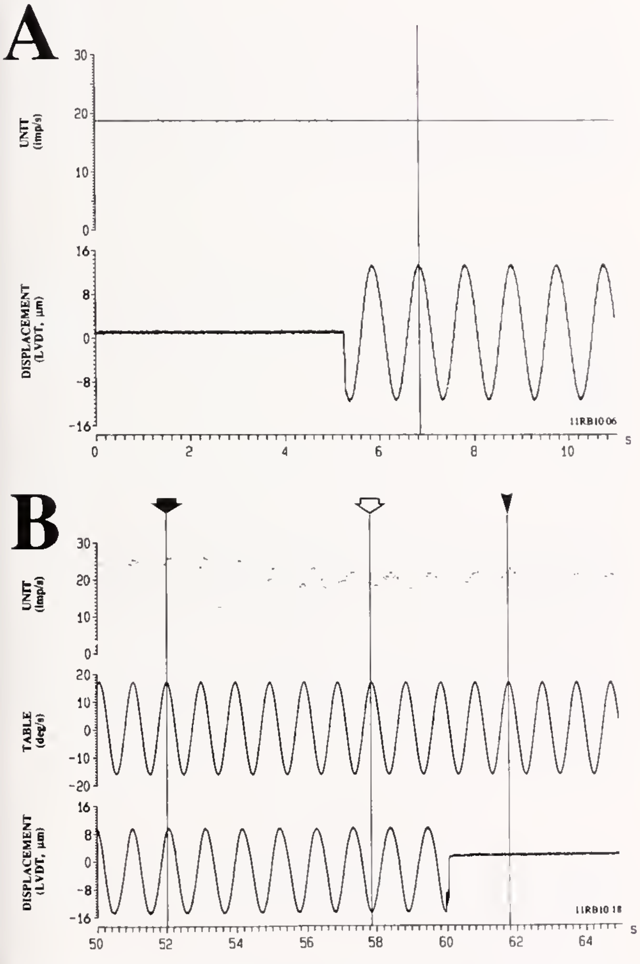

Figure 1. *In vitro responses of a horizontal semicircular canal afferent to mechanical and rotary stimulation of the canal. A. The top trace is the instantaneous frequency of the afferent. The lower trace is the readout of the LVDT in microns. Upward deflection is inward displacement. B. Top, same as A, middle traces are the tachometer of the rate table and lower trace, same as A. Afferent response is enhanced when inward micropusher displacements are in phase (vertical line, solid arrow) and reduced when out of phase (vertical line, open arrow). Responses to rotation are shown on the right.*

Literature Cited

1. **Dickman, J. D., *et al.* 1988.** A method for controlled mechanical stimulation of single semicircular canals. *J. Neurosci. Methods* **25:** 111–119.
2. **Boyle, R., and S. M. Highstein. 1990.** Resting discharge and response dynamics of horizontal semicircular canal afferents of the toadfish, *Opsanus tau*. *J. Neurosci.* **10:** 1557–1569.

Inhibitory Effects of Nonhydrolyzable Guanine Nucleotides on Neurotransmitter Release at the Squid Giant Synapse

Peter Doroshenko, Stephen Hess, and George Augustine (Duke University Medical Center)

We are examining the role of GTP-binding regulatory proteins in the control of neurotransmitter release. To this end, we injected two nonhydrolyzable guanine nucleotides into the giant presynaptic terminal of the most distal synapse of the stellate ganglion of the squid, *Loligo pealei*, and studied their effects on transmitter release evoked by action potentials. As an assay of release, the maximum rate of rise of postsynaptic potentials (PSPs) produced by intracellular stimulation of the presynaptic neuron was measured. The terminal was also pre-loaded with the Ca-sensitive dye Fura-2 to perform dual wavelength measurements of presynaptic free Ca^{2+} ion concentration, ($[Ca^{2+}]_i$).

Iontophoretic injection of GTPγS into the giant presynaptic terminal caused a marked depression of synaptic transmission. The rate of rise of PSPs began to decrease within a few minutes after the onset of injection and continued progressively for several tens of minutes after injection has been stopped. One hundred microCoulomb injections inhibited transmission by 60–80%. An upper estimate of the intraterminal concentration of injected nucleotide is in the high micromolar range. Additional injections did not seem to add to the inhibition. Inhibition of synaptic transmission was not accompanied by any significant changes in the electrical properties of the presynaptic terminal: neither presynaptic resting nor action potentials were affected by GTPγS injections. Further, the changes in the presynaptic $[Ca^{2+}]_i$ induced by a train of 250 action potentials (5s, 50 Hz) were not affected by injection of GTPγS. There was also no steady depolarization of the postsynaptic membrane potential, suggesting that GTPγS did not increase the tonic release of MPSPs. Therefore, GTPγS acts by altering the amount of transmitter release evoked by a given rise in intracellular calcium, rather than by regulating Ca^{2+} entry into the terminal.

We also evaluated the possibility that a low molecular weight GTP-binding protein is involved in this inhibition. A nonhydrolyzable analogue of GDP, GDPβS, was therefore injected into the terminal. GDPβS also inhibited evoked transmitter release, although the time course of its action was much slower than that of GTPγS; *i.e.*, visible inhibition of synaptic transmission required injections lasting about five-fold longer than those of GTPγS (about 30 min). This could be due to the lower electric charge of GDPβS (−3 as compared to −4 for GTPγS) causing a smaller quantity of the nucleotide being inotophoretically injected. Alternatively, GDPβS could be weaker or slower in inhibiting release. Like GTPγS, GDPβS had no significant effect on presynaptic potentials or $[Ca^{2+}]_i$ signals.

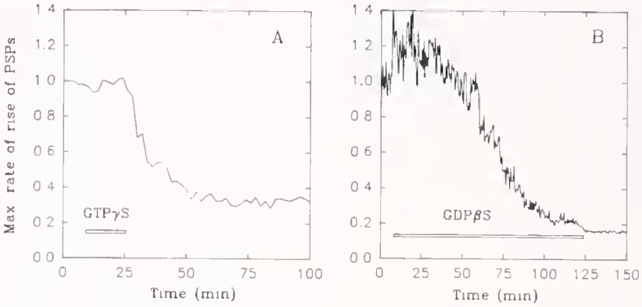

Figure 1. *Inhibition of synaptic transmission at the squid giant synapse by GTPγS (A) and GDPβS (B). The plots show changes in the maximum rate of rise of PSPs (normalized to their initial values) caused by iontophoretic injection of either nucleotide (shown by the horizontal bars) into the presynaptic terminal. Injection current: 100 nA, duration: 16 min in A and 120 min in B*

Control injections of either vehicle solution alone, or with GTP instead of GTPγS or GDPβS, did not inhibit synaptic transmission. On the contrary, injections of GTP appeared to maintain a stable transmission or, in some cases, to slightly enhance PSPs.

The two findings—that both GTPγS and GDPβS have inhibitory effects on synaptic transmission, and that neither nucleotide appears to change ion channel function—argue against the involvement of conventional, high molecular weight GTP-binding proteins (1). The similar actions of both nonhydrolyzable nucleotides is more consistent with the notion that they are interfering with synaptic vesicle trafficing, mediated by low molecular weight GTP-binding proteins (2). A likely candidate for such a target is rab3A, a low molecular weight GTP-binding protein that is associated specifically with synaptic vesicles (3), and that dissociates from vesicles during synaptic transmitter release (4).

Literature Cited

1. **Gilman, A. G. 1987.** *Annu. Rev. Biochem.* **56:** 615–649.
2. **Hall, A. 1990.** *Science* **249:** 635–640.
3. **Fischer v. Mollard, G., *et al.* 1990.** *Proc. Natl. Acad. Sci. USA* **87:** 1988–1992.
4. **Fischer v. Mollard, G., *et al.* 1991.** *Nature* **349:** 79–81.

Ultraviolet Light from the Nighttime Sky Enhances Retinal Sensitivity of *Limulus*

E. D. Herzog and R. B. Barlow, Jr. (Institute for Sensory Research, Syracuse, NY)

Ultraviolet light can be seen by a wide variety of animals. The impressive array of UV-sensitive organs includes the lateral eyes of birds (1) and shallow-living fishes (2); the dorsal ocelli of insects (3), arachnids (4), and horseshoe crabs (5); the parietal eye of lizards (6); and even the skin and pineal eye of frogs (7). Behavioral and electrophysiological studies have shown that these organs are most responsive to the short wavelength range (360–380 nm) of the sun's emission spectrum. Why have animals acquired sensitivity to such a minor component of natural light? What role does sensitivity to ambient UV light have in an animal's behavior?

Here we report that stimulation of the median ocelli of the horseshoe crab, *Limulus polyphemus*, by UV light from the nighttime sky enhances the sensitivity of the lateral eyes to visible light. At night a circadian clock in the brain of *Limulus* generates and transmits neural activity via efferent optic nerve fibers to the lateral eyes and median ocelli (8), significantly increasing their sensitivity (9,10). Experiments carried out in the laboratory show that illumination of the median ocelli at night with UV light enhances the clock's efferent output and thus further increases the sensitivity of the lateral eyes and median ocelli (11). We tested whether this occurs under natural conditions; that is, whether ocellar exposure to UV light from the nighttime sky increases visual sensitivity of the lateral eyes.

We carried out our experiments in an outdoor shed located in a remote area of Woods Hole, MA, where no artificial light was detectable at night. We mounted animals securely to a platform in an aquarium so that their gills were irrigated with recirculated seawater, but their lateral eyes and median ocelli remained above water. An opaque chamber was placed over the right lateral eye of each animal to occlude the eye from ambient light. A wick electrode and light emitting diode (LED) within the chamber allowed us to record electroretinograms (ERGs) from the eye in its dark-adapted state while the animal was exposed to normal diurnal changes in illumination. A computer-based system recorded ERGs every 30 min in response to a 10 ms light flash from the LED (12). Changes in the amplitude of the ERG of the occluded right eye provided a measure of the clock's effect on retinal sensitivity and the ocellar influence on the clock's action. Animals (n = 7) were maintained in this apparatus for approximately one month. During this period, ERGs were monitored while the median ocelli were either fully exposed, covered by a UV blocking filter (blocks $\gamma < 420$ nm), a UV bandpass filter ($\gamma_{max} = 360$ nm, 54 nm bandwidth at half maximum) or occluded to block all incident light.

Figure 1 shows the ERG data recorded from the lateral eye of an animal during five days of a month-long experiment (1990). The amplitude of the ERG increased at night and decreased during the day. The extent of the change depended, in part, on the light incident on the median ocelli.

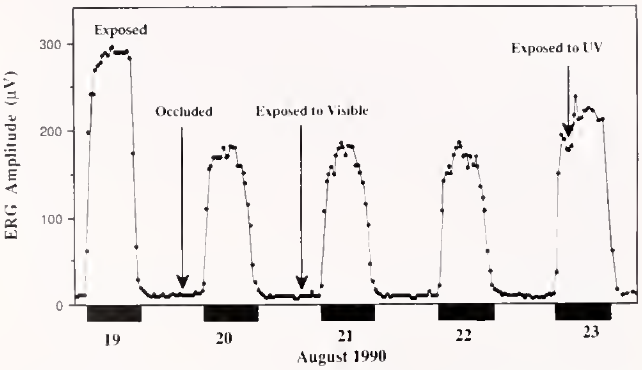

Figure 1. *Daily changes in lateral eye ERG of an animal exposed to natural diurnal lighting from 19–23 August 1990. Bars on the abscissa give the light cycle. Labels give the lighting condition on the median ocelli.*

Fully exposing the ocelli to the nighttime sky on 19 August produced the greatest ERG amplitudes (290 μV) and, consequently, the greatest sensitivity of the lateral eye. Measurements of the changes in ERG amplitude over a range of light intensities (12) indicate that the clock increased lateral-eye sensitivity by about 120 times on the night of 19 August. Occluding light to the median ocelli on the following night reduced the clock's effect; ERG amplitudes increased on 20 August to 170 μV, indicating only a 30-fold increase in sensitivity from day to night. Exposing the ocelli through the UV blocking filter to visible light from the nighttime sky on 21 August had no effect on lateral eye sensitivity. But exposing the ocelli through the UV bandpass filter on the night of 23 August increased the ERG amplitude to 220 μV, or a 60-fold increase in sensitivity, which is less than the level achieved when the ocelli were fully exposed. This difference was expected because the UV bandpass filter reduced the UV input to the ocelli relative to the fully exposed condition. Convolving the filter's transmission characteristics with the ocellar spectral sensitivity (11) indicates that the filter reduced by more than 50% the UV photons absorbed by the ocelli. In sum, exposure of the median ocelli in this experiment to UV light from the nighttime sky enhanced the sensitivity of the lateral eye by a factor of four.

The ocellar influence on lateral eye sensitivity via the circadian clock in the brain requires neural circuitry that involves all three structures. Anatomical studies show that the optic nerve fibers from the ocelli innervate loci deep within the brain (13). Anatomical (14) and physiological (8) studies also show that cell bodies deep within the brain transmit efferent activity to all major visual organs of the animal. However, we do not know enough about the circadian organization of the brain to understand how the ocelli modulate the sensitivity of the lateral eyes.

The ocellar enhancement of visual sensitivity may be related to the animal's mating behavior. In the spring, horseshoe crabs move in from deep water and build nests in shallow water (<1 m) at high tide near protected beaches along the eastern coast of North America (15). Numerous female-male pairs arrive together with an excess of males. Field observations carried out in Buzzard's Bay at Cape Cod, MA, indicate that males can use vision to find females at night (16,17) when mating activity is most pronounced. Coastal waters in Buzzard's Bay transmit more than 88% of moonlight per meter in the range of maximum lateral-eye sensitivity ($\gamma = 520$ nm) (18–21). Although such coastal waters significantly attenuate the transmission of UV light (<54% transmission per meter at $\gamma = 360$ nm) (16), the ocelli can detect the UV component of moonlight at depths of up to 10 m (threshold of 2.5×10^6 photons/s/cm^2 at $\gamma = 360$ nm) (18, 22). *Limulus* ocelli can therefore function as UV detectors in the animal's natural habitat at night during peak mating activity. By increasing the visual sensitivity of the crab, the ocelli may enhance the animal's ability to see mates at night. Given the rapid attenuation of UV light in coastal water, the ocelli may also provide information about depth, guiding the animals toward the beach (23).

Median ocelli and lateral eyes are major components of the circadian system of *Limulus*. By signaling the circadian clock, the ocelli rapidly increase the sensitivity of the lateral eyes to visible light and thus complement the known circadian rhythms in the visual system of noise (24), excitation (9, 10, 12), inhibition (25), and structure (26, 27, 28).

This work was supported by NIH grant EY-00667 and NSF grant BNS-8709059.

Literature Cited

1. **Wright, A. A. 1972.** *Vis. Res.* **12:** 1447–1464.
2. **Harosi, F. I., and Y. Hashimoto. 1980.** *Science* **222:** 1021–1023.
3. **Fent, K., and R. Wehner. 1985.** *Science* **228:** 192–194.
4. **Yamashita, S., and H. Tateda. 1978.** *J Exp. Biol.* **74:** 47–57.
5. **Nolte, J., and J. E. Brown. 1969.** *J. Gen Physiol.* **54:** 636–649.
6. **Jenison, G., and J. Nolte. 1980.** *Brain Res.* **194:** 506–510.
7. **Wald, G., and S. Rayport. 1975.** *Assoc. Res. Vis. Ophthal.* p. 5 (abs.).
8. **Eisele, L. E., *et al.* 1982.** *Biol. Bull.* **163:** 382.
9. **Barlow, R. B., Jr., *et al.* 1977.** *Science* **197:** 86–89.
10. **Barlow, R. B., Jr., *et al.* 1980.** *Science* **210:** 1037–1039.
11. **Westerman, L. A., and R. B. Barlow, Jr. 1981.** *Biol. Bull.* **161:** 352.
12. **Barlow, R. B., Jr. 1983.** *J. Neurosci.* **3:** 856–870.
13. **Chamberlain, S. C., and R. B. Barlow, Jr. 1980.** *J. Comp. Neurol.* **192:** 387–400.
14. **Calman, B. G., and B.-A. Battelle. 1991.** *Vis. Neurosci.* **6:** 481–495.
15. **Lockwood, S. 1870.** *Am. Zool.* **4:** 257–274.
16. **Barlow, R. B., Jr., *et al.* 1982.** *Nature* **296:** 65–66.
17. **Barlow, R. B., Jr., *et al.* 1991.** *Vis. Neurosci.* (in press).
18. **Jerlov, N. G. 1968.** P. 120 in *Optical Oceanography.* Elsevier Co., NY.
19. **Tyler, J. E., and R. C. Smith. 1970.** Pp. 10–13 in *Measurements of Spectral Irradiance Underwater* Gordon and Breach, NY.
20. **Graham, C. H., and H. K. J. Hartline. 1935.** *J. Gen. Physiol.* **18:** 917–931.
21. **Kaplan, E., and Barlow, R. B., Jr. 1975.** *J. Gen. Physiol.* **66:** 303–326.
22. **Stair, R., and R. Johnson. 1953.** *Res. Nat'l Bureal Stand.* **51:** 81–84.
23. **Lall, A. B., and R. M. Chapman. 1973.** *J. Exp. Biol.* **58:** 213–224.
24. **Kaplan, E., and R. B. Barlow, Jr. 1980.** *Nature* **286:** 393–395.
25. **Batra, R., and R. B. Barlow, Jr. 1982.** *Soc. Neurosci. Abstr.* **8:** 49.
26. **Chamberlain, S. C., and R. B. Barlow, Jr. 1979.** *Science* **206:** 361–363.
27. **Barlow, R. B., Jr., and S. C. Chamberlain. 1980.** Pp. 247–260 in *The Effects of Constant Light on Visual Processes.* Plenum Press, NY.
28. **Fahrenbach, W. H. 1971.** *Z. Zellforsch.* **114:** 532–545.

Change in Optical Activity Associated With Impulses in Squid Fin Nerves

David Landowne (Department of Physiology and Biophysics, University of Miami, Miami, FL)

Most biological material is optically active and will produce optical rotation on a beam of light passing through it. Some of this optical activity derives from the structure and arrangement of the proteins. Alpha-helices aligned with the beam are more rotatory than other orientations or β-sheets. In squid axons, changes in (linear) birefringence have been associated with activation and inactivation of sodium channels (1) indicating changes in protein conformation. Optical activity measurements have the potential of being more specific as to the nature of protein conformational changes. Recently, a change in optical activity of a lobster nerve associated with excitation has been reported (2). The squid fin nerve is more homogeneous in fiber diameters (3), and measurement of its optical rotation response could simplify the analysis of the optical changes.

Loligo pealii individuals were decapitated and the fin nerves isolated by the 'pulling out' method (3). The distal 3 cm of a nerve was mounted in a chamber (1) which permitted a light beam passing through a 4 mm length of the nerve, temperature control, stimulation at the proximal end, electrical recording with a KCl filled capillary near the surface of the bundle, and superfusion with Woods Hole seawater. Light from a 100 W tungsten iodide bulb passed sequentially through a collimator, a Glan Thompson polarizer (at an azimuth of −45°), a photoelastic modulator (at 0°), a cylindrical condensing lens, the nerve (at 0°) in seawater, a cover slip, a 10× microscope objective, a Glan Thompson analyzer (at +45°), and field stops at the image plane before striking a YAG-444 photodetector. The photoelastic modulator (Hinds PEM-80/FS5) was driven with a peak-to-peak retardation change of 500 nm. This is approximately quarter-wave modulation of the white light; that is, the light leaving the PEM alternated between right and left circular polarization at about 100 kHz. The electrical signal from the photodetector was led to a lock-in amplifier (E.G. & G. PAR 5210) with a 100 kHz reference signal from the PEM. The output of the lock-in amplifier phase-sensitive detector was filtered at 1 kHz, amplified, and led to a computer-based signal averager. The computer also sampled the voltage measured near the surface of the axon and provided stimuli at 4 Hz.

The system was calibrated by replacing the nerve and chamber with a 1 cm solution path containing 1 *M* sucrose and measuring the ratio of the lock-in 100 kHz signal to the dc light level. With the PEM off, the rotation of the same sucrose sample was measured in degrees by rotating the analyzer. Birefringence responses were measured by turning off the PEM and averaging the photodetector signal. Experiments were performed at 12–14°. Results are given as mean ± S.E.M. (n).

The figure shows the birefringence response (BRF), the change in lock-in amplifier output (ROT), and the voltage measured with an external electrode near the surface of the nerve. At the vertical line the nerve was stimulated about 1 cm away from the center of the light beam. About 2 ms later, birefringence decreased (plotted upward) and reached a peak of 1.1 ± 0.1 × 10^{-4} (10). Lock-in amplifier output began to decrease 1.0 ± 0.1 ms (6) later and reached a peak corresponding to 1.7 ± 0.5 × 10^{-4} degrees of optical rotation (6). The ROT signal reached a peak in 1.7 ± 0.1 ms (6) and returned to the baseline in 4.7 ± 0.4 ms (6). For the BRF signal, the corresponding values were 2.5 ± 0.2 (8) and 6.7 ± 0.3 (8) ms. Two additional measurements were made with a 650 ± 50 nm filter in front of the light source and the PEM set to 350 nm. The signal-to-noise ratio was lower, the amplitude of the ROT signal was about twice as large, and the timing was not significantly different. The increased amplitude may have been due to a better approximation of quarter wave operation of the PEM. Measurements with white light made with a 50 kHz reference to the lock-in amplifier gave responses with a time course similar to that of the BRF signal.

The amplitude of the ROT signal is about the same as that reported in lobster nerve (2). The time course relative to the BRF signal is different. In the lobster nerve, the peak ROT signal occurs during the rising phase of the BRF signal, but in the squid the peaks appear at the same time. Also, the delay between the start of the BRF signal and the ROT signal is not apparent in the lobster. Both nerves contain axons of different sizes, perhaps some differential contribution is made to the optical responses. Measurements on other nerve bundles should be made.

Because the ROT signal occurs during the BRF signal, it may be reporting some change associated with nerve excitation. The BRF signal can be shown by drug sensitivity to have more than one source. The differences in timing here could indicate that only some of the phenomena that produce the BRF response are seen in the ROT signal, or that the ROT signal has entirely different origins.

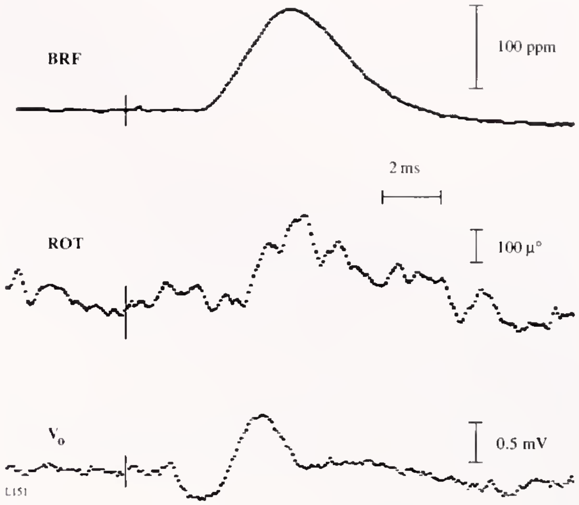

Figure 1. *The optical rotation response of a squid fin nerve. Upper trace shows the average of 64 birefringence measurements of light intensity made with the nerve between crossed polarizers. Middle trace is the average of 256 rotation measurements using the photoelastic modulator as described in the text. Lower trace is a single sweep electrical recording from a capillary electrode near the surface of the bundle. 12°C.*

This work was supported by NIH grant NS26651.

Literature Cited

1. **Landowne, D. 1985.** *J. Membrane Biol.* **88:** 173–185.
2. **Watanabe, A. 1987.** *J. Physiol.* **389:** 223–253.
3. **Gould, R. M., and M. Alberghini. 1990.** Pp. 323–368 in *Squid as Experimental Animals,* D. L. Gilbert *et al.,* eds. Plenum Press, NY.

Voltage- and Ligand-Gated Conductances of Bipolar Cells From the Skate Retina

Robert Paul Malchow (University of Illinois College of Medicine),
Richard L. Chappell, and Harris Ripps

The all-rod retina of the skate (*Raja ocellata* and *R. erinacea*) affords a unique opportunity to study, with electrophysiological methods, signal transmission and neuronal interactions devoted solely to the processing of rod-mediated signals, *i.e.,* uncomplicated by inputs from cone pathways such as occur in the 'duplex' retinae of other vertebrates. Indeed, a great deal is already known about the properties of skate rods (1) and about the responses generated by the large horizontal cells that mediate lateral interactions in the distal retina (2). In contrast, little is known about the characteristics of skate bipolar cells (3), second order neurons that receive direct input from the photoreceptors for transmission to neurons (amacrine and ganglion cells) of the inner retina. The purpose of the present project was to examine some of the basic membrane properties of these cells, and to begin to assess their responses to neurotransmitters. To accomplish this, we used the whole-cell version of the patch-clamp technique to study the voltage- and ligand-gated currents of single, dissociated bipolar cells in primary culture.

Isolated retinal cells were obtained according to the protocol described by Malchow *et al.* (2). Briefly, the retina was immersed for 1 h in an elasmobranch Ringer solution containing cysteine-activated papain. After extensive rinsing, the tissue was triturated through a large-bore pipette yielding suspensions of single cells, which were placed in Petri dishes filled with a modified L-15 solution, and stored at 14°C for periods of up to 2 weeks. An example of a cell that was isolated from the skate retina, and that bears a striking morphological resemblance to bipolar cells observed in the intact retina is shown in Figure 1A. The cell is characterized by a dendritic tuft at its apical portion, a small cell body located just beneath the dendrites, and a long, thin axon ending in a synaptic terminal. The terminal of this cell is characterized by fine processes radiating from the axon; in other cells, relatively large round synaptic terminals were observed.

Figure 1B illustrates an example of the electrical currents generated by voltage steps ranging from −130 mV to +30 mV from a holding potential of −70 mV; both inward and outward currents were produced in response to the voltage commands. We attempted to dissect pharmacologically the components of these voltage-gated conductances using chemicals known to block specific classes of ionic currents in other preparations. For example, we found that the classical potassium-channel blocker tetraethyl ammonium (TEA) at 20 m*M* suppressed a current activated by depolarization, which appeared similar in its voltage-activated profile to the delayed rectifier observed in many other preparations. The application of TEA also revealed a transient outward current activated by depolarization, which could be selectively blocked by the application of 10 m*M* 4-aminopyridine. In addition, an anomalous rectifying current activated by hyperpolarization was abolished by superfusion with 10 m*M* cesium chloride. We also obtained evidence for the presence of a calcium-dependent potassium conductance: superfusion with 4 m*M* cobalt chloride reduced an outward current that appeared when the cell was depolarized beyond −50 mV. Finally, in some of the cells, a small transient inward current was observed; the nature of this current remains to be established.

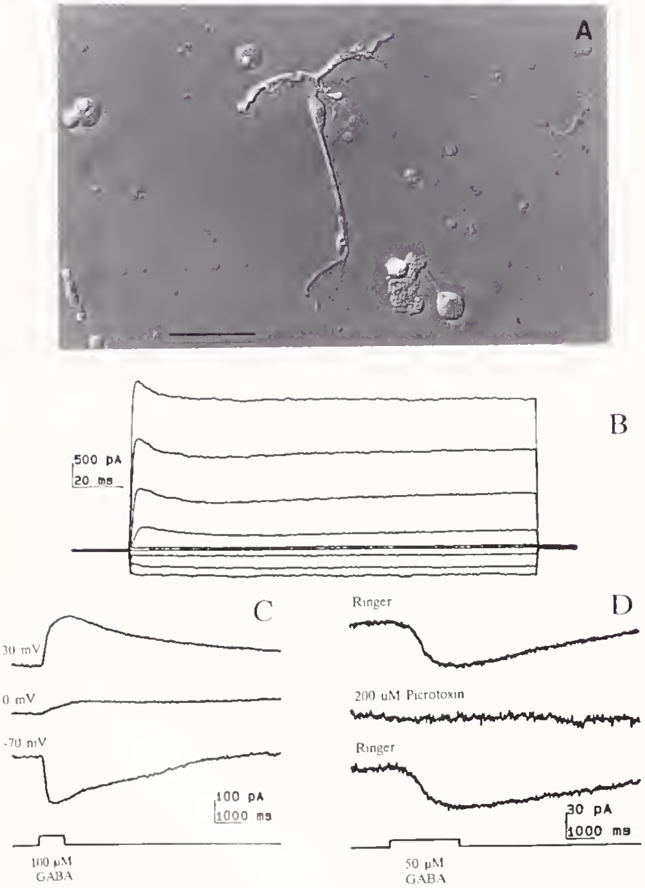

Figure 1. *A. A presumptive bipolar cell isolated from the skate retina Scale bar = 50 µm. B. Currents elicited by voltage steps ranging from −130 mV to +30 mV; the holding potential was −70 mV. C. Responses of one cell to puffs of 100 µM GABA. An inward current was observed with the cell held at −70 mV, a small outward current was detected with the cell held at 0 mV, and a large outward current seen with the cell held at +30 mV. D. Block of the GABA-induced current by picrotoxin.*

We also obtained preliminary data about the effects of the inhibitory neurotransmitter GABA, delivered by pressure ejection while the cell was superfused with Ringer. The bottom trace of Figure 1C shows a large GABA-induced inward current when the cell was held at −70 mV; this reversed into an outward current when the cell was depolarized beyond about −5 mV. Under our recording conditions, the value for the chloride equilibrium potential was approximately −5 mV, suggesting that the response to GABA might be mediated by the opening of chloride channels via the activation of $GABA_a$ receptors. This suspicion was confirmed by experiments examining the GABA response in the presence of bicuculline, a competitive antagonist of GABA at $GABA_a$ receptor sites, and of picrotoxin, a compound that blocks the chloride channels opened by $GABA_a$ receptors (Fig. 1D): both compounds markedly reduced the responses elicited by GABA.

These experiments demonstrate that individual cells bearing a morphological resemblance to bipolar cells can be readily identified in primary culture, and that voltage-clamp and ligand-gated conductances can be recorded and pharmacologically identified. The retina of the skate is likely to possess at least two distinct types of bipolar cells: one class of bipolar cells appears to stain selectively for protein kinase C, whereas another type can be identified based upon its ability to take up serotonin (4). Future experiments will be devoted to determining whether the different classes of bipolar cells exhibit distinct voltage- and ligand-gated properties.

This work was supported by a Doreen Grace Fellowship to RPM, Illinois Eye Fund awards to RPM and HR, and grants (EY-06516 to HR and EY-00777 to RLC) from the National Eye Institute. We are grateful to Renee Moran and the Burleigh Instrument Company for the loan of a piezoelectric micromanipulator.

Literature Cited

1. **Cornwall, M. C., *et al.* 1989.** *J. Gen. Physiol.* **94:** 633–647.
2. **Malchow, R. P., *et al.* 1990.** *J Gen. Physiol.* **95:** 177–198.
3. **Lasater, E. M., *et al.* 1984.** *J. Neurosci.* **4:** 1966–1975.
4. **Schlemermeyer, E., and R. L. Chappell. 1991.** *Invest. Ophthalmol. Vis. Sci.* **32:** 1264.

Imaging Free Calcium in Cultured *Aplysia* Bag Cell Neurons

Andrew L. Miller (Marine Biological Laboratory), Peter J. S. Smith, Carol A. Rainville, Osamu Shimomura, Felix Strumwasser, and Lionel F. Jaffe

Neurite differentiation in culture is not genetically predetermined, but requires that receptors in the plasma membrane interact with the environment and then with intracellular signal transduction mechanisms. This proposition has led us to consider the distribution of free cytosolic calcium as a regulator of signal transduction and growth control, a notion supported by the following recent reports: calcium has been implicated in the decision making processes of the neurite growth cone (1); substrate molecules can effect the phenotypic differentiation of neurite pattern and the distribution of calcium channels in the plasma membrane (2); calcium plays an important role in the stabilization and regulation of cytoskeletal elements (3); domains of high calcium have consistently been associated with other tip-growing structures (4).

Here we present a preliminary report on the cytosolic distribution of free calcium in cultured *Aplysia* bag cell neurons. We used the chemiluminescent protein aequorin to visualize calcium. This technique compliments purely fluorescent methods of imaging cytosolic calcium and may offer certain inherent and unique advantages. The latter have been greatly enhanced by two recent advances in aequorin chemistry (5). The first involves the conjugation of a fluorescein group to aequorin, which enables us to ratio between a luminescent signal of calcium activity and a fluorescent signal from aequorin distribution. Second, the attachment of synthetic chromophores to the cloned aequorin protein moiety has speeded up the luminescent reaction with calcium which results in the release of more photons per unit time. This equates to more signal, an important consideration where cell size is a limiting factor. Moreover, these new aequorins are non-toxic (5), a clear necessity if slow growing cells must be observed over several days. Both of these new aequorins were used.

Aplysia bag cells were cultured as described previously (6). Cells selected for injection had generated significant outgrowths. These were important in anchoring the cell to the substrate during the microinjection process. Cells were injected with bevelled silanized microelectrodes inserted in the soma. This minimized damage and facilitated removal of the microelectrode. Using a quantitative low pressure technique, cells were microinjected with ≈ 10 pl of a 1:1 cocktail of fluorescein-labeled recombinant and h-recombinant aequorin. The latter reacts with calcium ten times faster than recombinant aequorin (5). An ultra-sensitive imaging photon detector was used to record photon emission, from either the calcium-induced chemiluminescent reaction with h-recombinant aequorin, or the fluorescence of photoexcited fluorescein-labeled aequorin. Photon collection was interrupted at regular intervals so that we could acquire brightfield video images of the injected cells, and thus correlate photon images with cell morphology and growth.

Luminescence is clearly not evenly distributed throughout the soma, and several distinct domains of elevated luminescence were apparent. A ratio correction using fluorescence indicated these were indeed domains of high cytosolic free calcium. These domains emitted up to ten times more light than the background level in the soma. Calcium varies approximately as the cube-root of the luminescence. This would indicate an increase in free calcium of about two times background in the soma. In several cases, the regions of elevated calcium clearly coincided with the base of a neural outgrowth. In other instances, there was no obvious correlation with any outgrowth from the soma. We suggest that these might indicate sites of future outgrowth, or some other calcium dependent activity of these neurosecretory cells. Individual cells were imaged continuously for up to 20 hours, and the dimensions and intensity of the calcium domains varied throughout this period. The intermittent video sequences clearly showed that neural outgrowths were extending during the photon collection periods. We therefore conclude that our calcium images relate to functional cells and are not the result of pathological decline.

Supported by NSF grant DCB-8811198 (Amendment 01) to LFJ and NIH 21046 to FS.

Literature Cited

1. **Bentley, D., *et al.* 1991.** *J. Neurosci.* **11**(5): 1300–1308.
2. **Ross, W. N., *et al.* 1988.** *Proc. Natl. Acad. Sci. USA* **8**: 4075–4078.
3. *The Neural Cytoskeleton* 1991. R. D. Burgoyne, ed. Wiley-Liss & Son Inc.
4. **Jaffe, L. A., *et al.* 1975.** *J. Cell Biol.* **67**: 488–492.
5. **Shimomura, O., *et al.* 1989.** *Biochem. J.* **261**: 913–920.
6. **Strumwasser, F., *et al.* 1991.** *Biol. Bull.* **181**: 331.

Properties of Medullary Interneurons of the Skate Electrosense Provide Evidence for the Neural Circuitry Mediating Ventilatory Noise Suppression

John Montgomery and David Bodznick (Wesleyan University)

Afferent electrosensory fibers in elasmobranchs are strongly driven by electrical potentials produced by the animal's own ventilation (1,2). This reafference generated by movement can be considered a form of noise which ought to be removed at an early stage of sensory processing. The dorsal octavolateralis nucleus (DON) is the electrosensory center in the medulla, and the ascending efferent neurons (AENs) from this nucleus do indeed show a significant reduction in ventilatory modulation without sacrificing their response to extrinsic fields. The key to understanding the suppression of ventilatory noise is the observation that the ventilatory modulation of afferent activity is the same in all afferents, making it a "common mode" signal, which could be reduced by a subtraction of inputs from different parts of the body. Extrinsic signals are differentially represented within the afferent population and would not be suppressed by such a mechanism. The further observation, that an artificial common mode signal (produced by an electrode inserted into the gut) is also suppressed, is good evidence for the existence of a common mode suppression mechanism within the DON (3).

Several lines of evidence, but principally the lack of any central neurons responding to ventilation in *Platyrhinoidis* (1), led to the suggestion that common mode signals could be suppressed by a collateral feedback pathway between AENs (Fig. 1A), and the feasibility of such a mechanism was confirmed by modeling studies (4). Common mode suppression could also be achieved by an alternative and simpler mechanism: inhibitory interneurons onto AENs could be activated directly by afferent input (Fig. 1A). This study was designed to examine the circuitry responsible for the suppression of common mode signals in the DON of the little skate *Raja erinacea*.

The main finding of this study is that there is a common class of interneurons (INs) within the DON (20/28 cells) that have the characteristics suited to the suppression of common mode signals via the simpler mechanism postulated above. These interneurons are monosynaptically activated from the ipsilateral electrosensory afferents (and not disynaptic as required by the collateral model) (Fig. 1B); they respond vigorously to an artificial common mode signal (Fig. 1C); and they are not synaptically activated by antidromic activation of AENs, as would be predicted from the collateral model.

AENs are also monosynaptically activated from the ipsilateral nerve and then strongly inhibited. They typically show a discrete excitatory receptive field and a diffuse inhibitory surround, including contralateral input, which could mediate the common mode signal suppression. AENs almost universally show a clear inhibition following electrical shock to the contralateral electrosensory nerve, indicating input from inhibitory commissural neurons. INs show no evidence of commissural input, and have discrete, simple excitatory receptive fields. These results provide evidence that the convergence onto AENs to produce their diffuse inhibitory input occurs between the INs and the AENs.

In *Raja erinacea*, electrosensory relay neurons of the medulla have discrete excitatory receptive fields and a diffuse inhibitory surround mediated probably by interneurons in the DON that receive a direct afferent input from other parts of the body. The effect of this organization is to suppress electrosensory reafference generated by the animal's own bioelectric fields that might otherwise interfere with the detection and central processing of biologically important extrinsic fields.

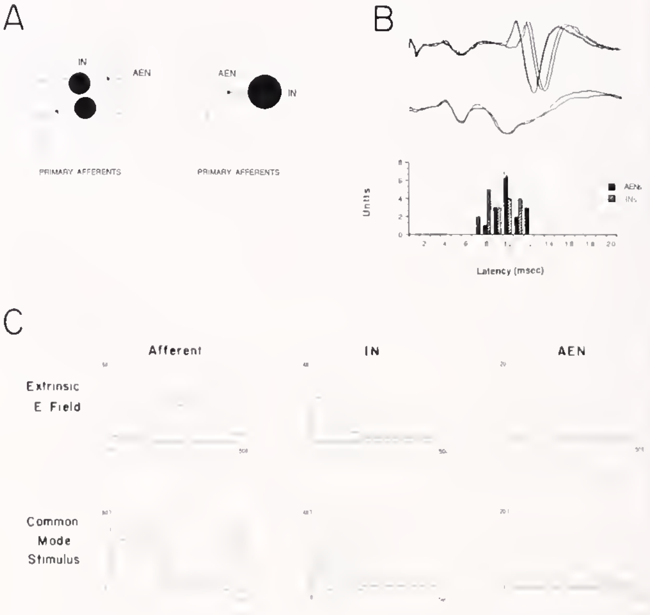

Figure 1. *(A) Simple circuit diagrams of the two alternate models for common mode suppression. In the first model, AENs are connected via reciprocal inhibitory feedback mediated via the INs. In the second model, INs receive direct afferent input and then inhibit AENs. (B) Evidence for monosynaptic activation of INs from the ipsilateral electrosensory afferents Top trace: 3 superimposed sweeps of an IN responding, at a latency of about 9–10 ms, to electrical stimulation of the hyomandibular ramus of the anterior lateral line nerve. Middle trace: field potential generated by nerve stimulation; the afferent fiber potential (onset latency 3.6 ms) is followed by a slow negative synaptic potential (onset latency 7.5 ms). Bottom panel: histogram of AEN and IN latencies to nerve stimulation. (C) Examples of a primary afferent, IN, and AEN responding to uniform extrinsic electrical field stimulation (top panel, 2 Hz, 2 μV/cm) and a common mode stimulus (lower panel, 2 Hz, delivered through a gut electrode, 20 μV measured between the interior of the animal and a distant electrode). Each panel is a histogram showing firing rate (1/s) as a function of time (ms).*

This work was supported by an NSF grant to DB and a Claude McCarthy Fellowship to JM.

Literature Cited

1. **Montgomery, J. C. 1984.** *J. Comp. Physiol.* **155A:** 103–111.
2. **New, J. G., and D. A. Bodznick. 1990.** *J. Comp. Physiol.* **167A:** 295–307.
3. **Bodznick, A. G., and J. C. Montgomery. 1988.** *Biol. Bull.* **175:** 303.
4. **Montgomery, J. C. 1987.** *Proc. Physiol. Soc. N.Z.* **7:** 68.

Serotonin-Like Immunoreactivity Reveals Evidence for Centrifugal Fibers and a Distinctive Class of Amacrine Cell in the Skate Retina

Etha Schlemermeyer and Richard L. Chappell (Hunter College of CUNY)

The retina of the skate (*Raja erinacea* and *R. oscellata*) has but one class of photoreceptors—the rods (1). It therefore provides a unique model system with which to study rod contributions to visual pathways in a vertebrate. Currently, we are particularly interested in understanding the organization of the inner retina of the skate.

Early studies of both autoradiography and immunocytochemistry in transverse sections of the skate retina provided evidence for serotonin (5-hydroxytryptamine) in amacrine (2,3) and bipolar (2) cells, as well as an occasional immunoreactive fiber in the optic fiber layer (3). It was suggested that the bipolar cells showing serotonin labelling were of the ON depolarizing type (2). Our recent double-labelling studies have indicated, however, that a class of skate bipolar cell showing protein kinase C-like immunoreactivity possesses the morphology typical of an ON depolarizing bipolar cell. Those showing serotonin-like immunoreactivity (SLI), on the other hand, have a morphology more typical of bipolar cells generally associated with OFF channels in having terminal branches in layers 1 and 4 of the inner plexiform layer (IPL) (4).

We have further examined SLI-stained processes in the IPL of this all-rod retina. SLI labelling was enhanced by incubating the eyecup preparation in Ringer containing 10 μM serotonin in the presence of 1 mM pargyline (5) prior to fixation in 6% paraformaldehyde. The fixed retina was isolated from the pigment epithelium and incubated in primary antibody (rabbit anti-serotonin, INCStar Corp., 1:1500 in PBS) containing 0.4% Triton X-100 (Sigma) for 3 days at 4°C. The retina was rinsed overnight in PBS. SLI was revealed using the indirect fluorescent method (FITC anti-rabbit, Sigma, 1:150, 24 h). After a final rinse in PBS, the tissue was mounted vitreal side up in glycerol and examined in whole mount.

Figure 1a shows the distinctive morphology of the SLI skate amacrine cells, with their short lengths of stout processes leaving the cell perikaryon and appearing to "dance" across the retina as they narrow down to a maze of finer varicose processes (Fig. 1b). The small, round cell bodies of the labelled bipolar cells can also be seen out of the focal plane in Figure 1a and b, providing information about the density distribution of SLI amacrine *vs.* bipolar cells.

An unexpected finding was the presence of a few fine immunoreactive fibers radiating from the optic disc. On close examination, we observed that these fibers branched centrifugally as they crossed the retina suggesting that they may represent a class of centrifugal fibers. As they cross the skate retina, these fibers turn distally toward the inner nuclear layer and appear to make *en passant* contacts with some, but not all, of the cell bodies of the SLI amacrine cells. Figure 1c shows such a fiber approaching the cell body of an amacrine cell from the left and branching at the cell body as it passes. These fibers may account for the immunoreactive processes observed by Brunken *et al.* (3) in the optic fiber layer. The possibility of serotonergic centrifugal fibers has also been suggested in the stingray retina (6) as well as in the retinas of rat (7), turtle (8), and *Xenopus* (9). The role of the centrifugal fibers is not yet known but is of considerable interest.

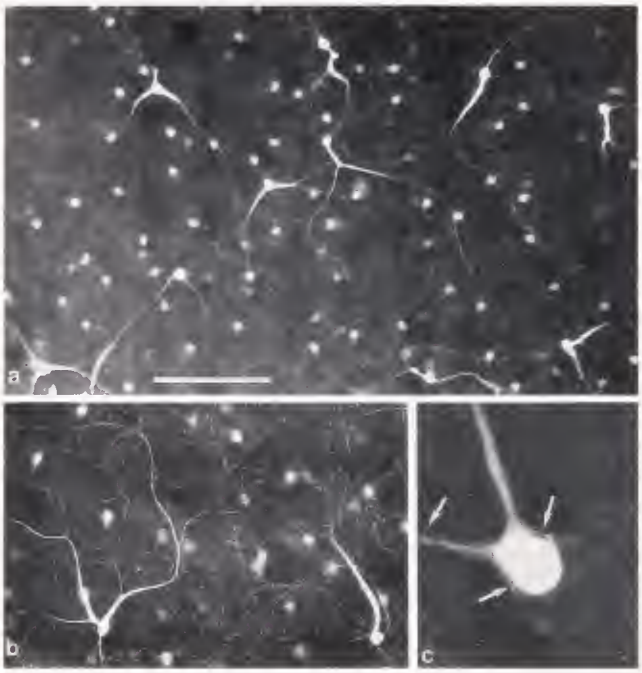

Figure 1. *(a) Whole-mounted skate retina processed for serotonin-like immunoreactivity (SLI) using an FITC-coupled secondary antiserum. The level of focus is in the inner nuclear layer between the somas of the amacrine and bipolar cells. Heavily labelled amacrine cells with thick primary processes are observed, as well as a more uniformly distributed matrix of bipolar cells with weaker immunoreactivity. (b) SLI in amacrine cells at the level of the distal IPL reveals a network of fine amacrine cell processes. Labelled bipolar cell somas are seen in the background. (c) An SLI presumed centrifugal fiber (arrows) wraps around and branches at an SLI amacrine cell soma. Scale bar: 150 µm (a), 100 µm (b), or 20 µm (c).*

It is intriguing to note that Bruun *et al.* (2) found that the levels of endogenous serotonin in this subset of amacrine cell were high enough to indicate that it may be their neurotransmitter and suggested that the skate SLI amacrine cells are likely to be connected to the OFF pathway. Our morphological data show that the SLI bipolar cells may also belong to the OFF pathway (4). While the physiological significance of serotonin in the skate retina has not yet been determined, these relationships of SLI bipolar cells, amacrine cells and centrifugal fibers suggest serotonin may prove to be important to visual processing in the skate, especially as it relates to OFF pathways.

This study of SLI-labelled cells in whole mounts of the skate retina has revealed a morphologically distinctive set of amacrine cells and the presence of a centrifugal fiber system. This knowledge provides a marker for identifying these cells and processes in order to examine their physiological role. A more detailed morphological analysis is currently underway.

Supported by NIH Grant EY00777.

Literature Cited

1. **Szamier, R. B., and H. Ripps. 1983.** *J. Comp. Neurol.* **215:** 51–62.
2. **Bruun, A., *et al.* 1984.** *Brain Res.* **295:** 233–248.
3. **Brunken, W. J., *et al.* 1986.** *J. Comp. Neurol.* **243:** 1–12.
4. **Schlemermeyer, E., and R. L. Chappell. 1991.** *Invest. Ophthalmol. and Visual Sci.* **32:** 1264.
5. **Weiler, R., and M. Schütte. 1985.** *Cell. Tiss. Res.* **241:** 373–382.
6. **Ritchie, T. C., and R. B. Leonard. 1983.** *Brain Res.* **267:** 352–356.
7. **Villar, M. J., *et al.* 1987.** *Neuroscience* **22:** 681–686.
8. **Schütte, M., and R. Weiler. 1988.** *Neurosci. Let.* **91:** 289–294.
9. **Schütte, M., and P. Witkovsky. 1990.** *J. Neurocytol.* **19:** 504–518.

Distribution of Synaptic Specializations in the Frog Cardiac Ganglion

Sally Schroeter (Emory University) and Milton P. Charlton

The development of the nervous system is a complex series of events including cell differentiation, process outgrowth, cell migration, axonal pathfinding, target selection, synaptogenesis, cell death, and synapse elimination. We have chosen to focus on one of these events—synaptogenesis—for two reasons. First, synaptic connections between nerve cells are arguably the major functional basis of the nervous system. Second, changes in synapses and synaptic connections are likely to be the basis for storing information and regulating behavior.

An ideal preparation in which to study the development of synapses is the frog cardiac ganglion. Its structural simplicity and optical clarity allow unparalleled visualization of nerve terminals even in living, unstained preparations (1). Most of the ganglion cells are clustered along the vagosympathetic nerve trunks in the interatrial septum. The nerve trunks contain the postganglionic axons, as well as the preganglionic axons that form synaptic boutons on the cell bodies of the ganglion cells.

A prerequisite for observing morphological changes during synaptogenesis is to identify markers for synaptic specializations. One such marker is provided by an antibody to a synaptic vesicle protein, 10H3 (2). Because synaptic vesicles are structurally and functionally characteristic of presynaptic terminals, their presence is one of the single most useful morphological criteria for recognizing a chemical synapse. Another marker is omega-conotoxin GVIA, which has been reported to block voltage-gated presynaptic calcium channels specifically and irreversibly (see 3 for review). Biotinylated and native forms of this toxin have been used, respectively, to localize calcium channels to active zones (4) and to block synaptic transmission at the frog neuromuscular junction (4,5). We have tested the ability of these two markers to reveal the spatial distribution of synaptic specializations in the adult frog cardiac ganglion. These studies are prerequisite to an analysis of synaptogenesis in tadpoles.

The pharmacological actions of omega-conotoxin GVIA were tested on interatrial septa that were isolated from the hearts of *Rana pipiens* and transferred to a recording setup similar to that previously described by McMahan and Kuffler (1). Intracellular recordings were made with conventional KCl microelectrodes (R_e = 50 megohms). The stability of impalements was greatly enhanced by the addition of 1 n*M* nifedipine to inhibit spontaneous rhythmic contractions. Synaptic transmission with nifedipine was not qualitatively different from that in control ganglia where muscle fibers were crushed to stop the contractions. Synaptic potentials were evoked by stimulation of the preganglionic nerve trunks at a rate of 0.5 Hz. Recordings were made in L-15 culture medium or in L-15 diluted to 80% with frog Ringer's solution. Native omega-conotoxin was applied at a concentration of 10 μg/ml.

The application of native omega-conotoxin dramatically decreased the amplitude of the evoked synaptic potentials and completely blocked synaptic transmission after about 15 min. The decrease in synaptic responsiveness was characterized by an increase in the number of synaptic failures after the addition of the toxin. The increase in the number of failures suggests that omega-conotoxin had the expected presynaptic effect.

Because the omega-conotoxin blocked synaptic activity in interatrial septa, we then attempted to localize the action by labeling ganglia with biotinylated omega-conotoxin. We also labeled preparations with 10H3 and double-labeled with both probes. Ganglia were incubated for 6 h in 100 μg/ml biotinylated omega-conotoxin and subsequently for 1 or 2 h in 250 μg/ml streptavidin-Texas Red (4). The toxin and the fluorescent label, or only the toxin, were omitted in the processing of control ganglia. Synaptic vesicles were labeled with an antibody to a synaptic vesicle protein (10H3; 1:300 dilution) and a fluorescein-conjugated goat-anti-mouse secondary antibody (1:100 dilution) (2). The primary antibody, or both primary and secondary antibodies, were omitted in the processing of control ganglia. Labeled preparations were viewed with an epifluorescence microscope and further examined with a confocal laser scanning microscope.

With biotinylated toxin, structures similar to those of the characteristic synaptic boutons near the base of the axon were labeled at an intensity similar to that of the underlying cell body. These structures were surrounded by areas devoid of staining. The characteristic morphology of the presynaptic terminals was not visible in ganglia labeled only with streptavidin-Texas Red. These results indicate that both presynaptic boutons and postsynaptic cell bodies have omega-conotoxin binding sites.

The synaptic vesicle antibody brightly labeled synaptic boutons of the presynaptic terminals. Intense, regularly spaced spots of 10H3 labeling also appeared along the length of individual axons and on small bundles of axons coursing through the septum, as well as on axons within the muscle of the atrial walls.

In addition to the diffuse labeling of cell bodies and axons, the biotinylated toxin produced bright spots of labeling over the surface of muscle cells within the septum. These bright spots of label did not appear in control ganglia stained only with streptavidin-Texas Red. One possible explanation is that the bright spots indicate presynaptic calcium channels in nerve terminals innervating muscle cells. To test this possibility, we double-labeled ganglia and observed whether the 10H3 labeling of axons crossing muscle fibers co-localized with the spots of toxin labeling in the muscle fibers. Since the two labels did not co-localize, it is not likely that omega-conotoxin is labeling presynaptic calcium channels here.

The synaptic vesicle antibody is a reliable synaptic marker that will, in the long term, prove useful in defining the environmental cues that lead to synaptogenesis. The experiments with omega-conotoxin revealed two unexpected findings. First, diffuse labeling at presynaptic terminals may indicate that calcium channels are not tightly clustered as at the frog neuromuscular junction (4). Alternatively, these results may be explained by a restricted access of the toxin or the fluorescent label. Second, and also unexpected, is the intense labeling seen on cardiac muscle cells. In fact, Horne and coworkers (6) have suggested that omega-conotoxin may not bind exclusively to calcium channels. Further optimization of the labeling procedure and experiments are needed to clarify these issues.

This work was supported by the Grass Foundation and the Muscular Dystrophy Association.

Literature Cited

1. **McMahan, U. J., and S. W. Kuffler. 1971.** *Proc. R Soc. Lond B* 177: 485–508.
2. **Matthew, W. D., *et al.* 1981.** *J. Cell Biol.* **91**: 257–269.
3. **Gray, W. R., *et al.* 1988.** *Ann. Rev. Biochem.* **57**: 665–700.
4. **Robitaille, R., *et al.* 1990.** *Neuron* **5**: 773–779.
5. **Kerr, L. M., and D. Yoshikami. 1984.** *Nature* **308**: 282–284.
6. **Horne, W. A., *et al.* 1991.** *J Biol. Chem.* **266**: 13719–13725.

Cyclic Nucleotide-Mediated Modulation of the Pyloric Motor Pattern in the Stomatogastric Ganglion of the Crab *Cancer borealis*

Nelson Spruston and Michael P. Nusbaum (Neurobiology Research Center, Dept. Physiol. & Biophys., University of Alabama, Birmingham, AL 35294)

The mechanisms responsible for controlling patterned motor behavior have been studied extensively in the stomatogastric ganglion (STG) of decapod crustaceans (1). This small ganglion of approximately 30 neurons generates the gastric mill and pyloric motor patterns, which underlie the chewing and subsequent movement of food from the stomach to the midgut, respectively.

Despite its apparent simplicity, the STG generates many variations of both motor patterns, due to the influence of modulatory substances released in the STG neuropil from inputs to the ganglion. These modulatory inputs alter the frequency of the motor pattern, phase relationships and activity levels of individual STG neurons, and can even cause the switching of individual neurons between functionally distinct STG networks (2). The STG motor patterns are dependent upon the presence of these inputs, and they cease when the ganglion is isolated from its input. From this quiescent state, the pyloric rhythm can be induced by bath application of any of the known STG modulators. Although many modulators have been identified in the STG and their effects on the pyloric rhythm characterized, little is known about the second messenger systems that presumably mediate these effects. We have therefore begun to examine the role of cyclic adenosine monophosphate (cAMP) and cyclic guanosine monophosphate (cGMP) in modulating the pyloric rhythm in the STG of the crab, *Cancer borealis*, by testing whether elevation of cAMP or cGMP levels can evoke a pyloric rhythm in the isolated STG.

All experiments were performed on the desheathed STG, which was pinned in a Sylgard-lined petri dish and superfused (5–10 ml/min) with *Cancer* saline at 10–14°C. The STG was isolated from all inputs by a sucrose block on the input nerve. Membrane-permeable analogs of cAMP or cGMP (1.0 m*M* 8-Br-cAMP or 8-Br-cGMP) were applied at a superfusion rate of 1–2 ml/min to a 1 ml well around the STG.

8-Br-cAMP and 8-Br-cGMP each elicited a distinct pyloric motor pattern. An example of the rhythm induced by 8-Br-cAMP is shown in Figure 1. In all nine preparations studied, application of 8-Br-cAMP (1.0 m*M*, 20–100 ml) induced a pyloric rhythm with maximal cycle frequencies of 0.8–1.9 Hz. The mean number of LP spikes per cycle at the maximal frequency ranged from 2–4 (n = 9).

8-Br-cGMP elicited a pyloric rhythm in 3 of the 4 preparations to which it was applied. In contrast to the results with 8-Br-cAMP, the pyloric rhythm induced by 8-Br-cGMP was slower and included more LP spikes per cycle. This rhythm had maximal cycle frequencies of 0.4–1.0 Hz and a mean number of LP spikes per cycle of 3–6 (n = 3).

The effects of both 8-Br-cAMP and 8-Br-cGMP developed slowly (peaking after 15–25 min of superfusion), presumably due to the time required for the membrane permeable analogs to reach effective intracellular concentrations. The effects were also slow to reverse, requiring a wash period of at least one h at an increased flow rate (5–10 ml/min).

Most STG modulators cause pyloric rhythms with cycle frequencies similar to those induced by the cyclic nucleotides. The relatively weak LP activity induced by 8-Br-cAMP and 8-Br-cGMP, however, is most consistent with the action of biogenic amines in this system. The effects of amines in the STG of the lobster, *Panulirus interruptus*, also appear to be mediated at least partially by cAMP because amines elevate cAMP levels in the ganglion (3), cAMP elevation induces a pyloric rhythm (3), and

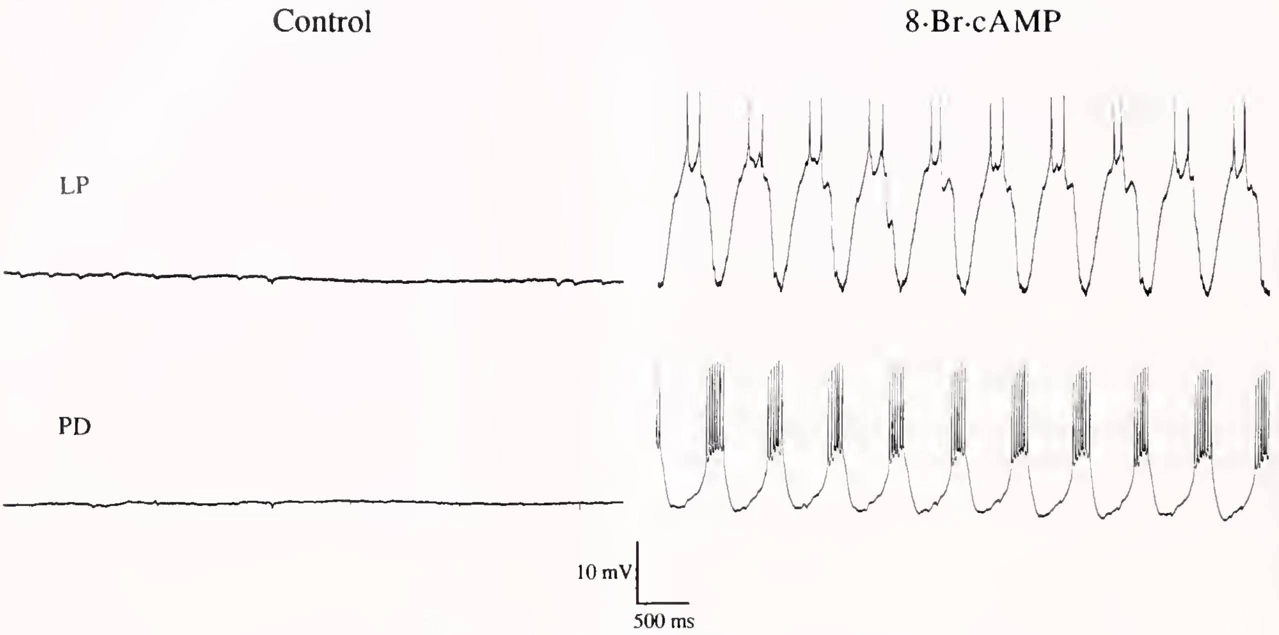

Figure 1. *Elevation of cAMP levels in the STG induces a pyloric rhythm with weak lateral pyloric constrictor (LP) neuron activity. Intracellular recordings of LP and the pyloric dilator (PD) neuron are shown before and during application of 1.0 mM 8-Br-cAMP to the crab STG. Baseline membrane potentials in control are identical to the trough of the oscillations induced by 8-Br-cAMP (LP, −72 mV; PD, −60 mV).*

the effect of dopamine is enhanced by phosphodiesterase inhibitors (4). These results from the lobster, and our results from the crab, strongly implicate a role for cAMP in the modulation of the pyloric motor pattern in the crustacean STG.

Because some modulators may act only partly through cAMP, or influence cAMP levels in only some pyloric neurons, we plan to examine the effects of cAMP (and cGMP) on individual neurons using intracellular injection. To identify the STG modulators that act through cAMP, we also plan to inject peptide inhibitors of the cAMP-dependent kinase. These experiments will help to elucidate the targets and mechanisms through which a large number of neuromodulators are capable of tailoring the rhythmic activity of the STG to an ever-changing environment.

We thank the Grass Instrument Co., Dan Johnston, and Ron Calabrese for the loan of valuable equipment. This work was supported by a Grass Fellowship to NS and BNS-8909613 (NSF) and NS29436 (NIH) to MPN.

Literature Cited

1. **Selverston, A. I., and M. Moulins. 1987.** *The Crustacean Stomatogastric System.* Springer-Verlag, Heidelberg.
2. **Marder, E., and J. M. Weimann. 1991.** In *Neurobiology of Motor Programme Selection: New Approaches to Mechanisms of Behavioral Choice.* J. Kein, C. McCrohan, and B. Winlow, eds. Manchester, University Press.
3. **Flamm, R. E., *et al.* 1987.** *J Neurophysiol.* **58:** 1370–1386.
4. **Ewald, D. A., and D. L. Barker. 1987.** Pp. 301–303 in *The Crustacean Stomatogastric System.* Springer-Verlag, Heidelberg.

Long-Term Monitoring of Ca^{2+} in Cultured *Aplysia* Neurons with Fluorescent Probes

Felix Strumwasser, Joseph McIntyre, and Carol A. Rainville (Marine Biological Laboratory)

Long-term monitoring and imaging of free Ca^{2+} in cultured neurons and other cells, would be useful for a variety of purposes, particularly in observing the role of the ion in slow events such as growth and circadian oscillations. Ca^{2+} is essential to the accomplishment of most cellular processes, including movement, secretion, early events of fertilization, and growth. We describe in this report some results of long-term Ca^{2+}-imaging in the bag cell (BC) neurons of *Aplysia*. The BC neurons synthesize and release egg-laying hormone, a peptide that controls egg laying (reviewed in 1). As neurons in primary culture, the neuropeptidergic BCs regenerate their neurites and maintain their electrophysiological properties, as observed in the intact preparation (2). We describe our methods and preliminary observations on loading of the fluorescent Ca^{2+} probes, the development of Ca^{2+} hot zones and spots in the soma during neurite extension, spontaneous oscillations of Ca^{2+} in the nucleus, and large spontaneous increases in Ca^{2+} in the cytoplasm and nucleus.

Primary cultures of BC neurons from *Aplysia californica* were prepared by treating the abdominal ganglion with up to 11 units/ml of neutral protease from *Bacillus polymyxa* (Sigma) for 3 h at 30°C, followed by rinses in the presence of BSA (24 mg/ml), and trituration onto 31 mm glass cover slips. Artificial seawater (ASW) was used with glucose and penicillin or streptomycin, instead of either MEM or L-15 media, which had been used in the past (2). We use either fura-2, AM or fluo-3, AM (Molecular Probes) as the calcium indicators (3,4). Neurons are loaded for 30 to 45 min in 1 ml ASW containing 3×10^{-6} *M* indicator at 21°C; the loading is followed by several rinses. Coverslips are mounted, with a silicone lubricant, onto a round cutout in a thin plastic plate. The plate is sealed into a teflon chamber with a silastic O-ring (Biophysica).

We have constructed a computer-controlled, fluorescence digital imaging system; it is built around a Leitz inverted microscope with a Ploem epifluorescence adapter and a high gain microchannel plate image intensifier (Videoscope, Model KS-1381). A relay lens couples the output of the luminescent screen of the intensifier to a high resolution, sensitive CCD TV camera (Videoscope CCD 200, 840 × 490 pixels). The computer is a DEC VaxStation II/GPX using Unix as its operating system. The interface between the CCD camera and the computer is a Datacube QVG AF-123 video acquisition and display system (768 × 480 pixels, 8 bit planes). Our acquisition, display, and analysis programs are written in the C language. The microscope focus and filter wheel are controlled by the computer through digital stepping motors. Two shutters, also computer-controlled, admit either white light or the exciting light from a 150 watt Xenon lamp. Appropriate narrow band interference filters are used.

BCs will commonly extend as many as 6 or 7 neurites in primary culture, even though they are maintained in a simple ASW medium with glucose. Neither an enriched medium, nor one containing *Aplysia* or other sera, are needed to maintain healthy growing BC neurons, as is the requirement with other *Aplysia* neurons (5). It is interesting that in another neurosecretory system, the X-organ-sinus gland of the crustacean eye stalk, neurite outgrowth of cultured peptidergic neurons can also occur in ASW supplemented with glucose, glutamine, and antibiotics (6).

Ca^{2+}-indicator loading, easily followed by intermittent imaging, reaches a steady level after three to four hours. We can perform experiments for a week or more on single isolated bag cells, provided that the exciting light is appropriately weak and exposure rates are kept low (≈ 1/h).

Many spontaneous, dynamic Ca^{2+} activities in the isolated BC neurons can be observed and have slow time courses (minutes to hours). Spontaneous Ca^{2+} hot zones and spots can be noticed developing in the cytoplasm, near the cell membrane, at the base of neuritic extensions. The Ca^{2+} levels in these hot spots and zones can be diminished by changing the normal ASW to a high Mg^{2+} (125 m*M*), low Ca^{2+} (1 m*M*) ASW (Fig. 1). The maximum reduction can take about 3 h to occur, but hot spots are re-established eventually, even in the presence of this medium. These results suggest that the hot spots depend, either directly or indirectly, on some trickle of external Ca^{2+} passing through the cell membrane, and that compensatory mechanisms are present to allow the Ca^{2+} hot spots to build up again when

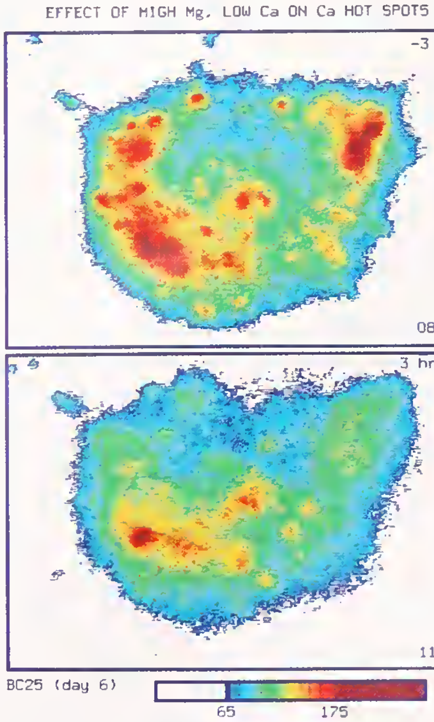

Figure 1. *Effect of high Mg^{2+} (125 mM), low Ca^{2+} (1 mM) ASW on Ca^{2+} hot spots in a cultured bag cell. The top frame was taken in 40 m*M* Li^{+}-ASW 3 min before the change to high Mg^{2+}, low Ca^{2+} ASW. The lower frame, taken 3 h and 14 min after the change of solution, was the maximum decrease observed in the hot spots.*

external Ca^{2+} is diminished. These latter results are similar to what Rehden *et al.* (7) have reported for calcium homeostasis in growth cones in the snail *Helisoma.* Once the neurites are fully extended, the hot zones and spots are relatively stable, over days, although hot spots can cycle in intensity. Thus, standing gradients of Ca^{2+} can be maintained in the cytoplasm of growing BCs over periods of days, suggesting some compartmentalization in the cytoplasm. The facts that extracellular high Mg^{2+}, low Ca^{2+} ASW can transiently diminish the levels of Ca^{2+} in these hot spots and zones, and that they can be re-established, indicate that Ca^{2+} can move in and out of these "compartments." The morphological correlates of these compartments remain to be observed at the electron microscope level but could include specialized endoplasmic reticulum or mitochondria. Preliminary experiments with simultaneous injection of h-recombinant and fluorescein-labeled aequorins (1:1) into bag cells indicate that aequorin is uniformly distributed in the cell, as measured by the fluorophore, but that hot spots can still be observed, as measured by chemiluminescence (8). The hot spots are still present when the ratio of light output from the two aequorins is taken (8).

Two other changes in Ca^{2+} can be observed during the early life of BCs in cell culture. A Ca^{2+} "explosion" can start in the cytoplasm and envelop the entire soma, including the nucleus. This event can take about 6 h to develop and then return to baseline. The nucleus of a BC can also show Ca^{2+} oscillations, having periods of a few hours, without any observable preceding Ca^{2+} events in the cytoplasm. The significance of these events to the bag cells and their relationship to neuritic outgrowth is unknown at this time. Our earlier electrophysiological studies on isolated bag cells indicated that they were electrically silent cells until depolarized or activated by cAMP (2). Thus, we think it is unlikely that the Ca^{2+} explosions are related to surface membrane activity.

This work was supported by an NIH grant (NS 21046) to FS.

Literature Cited

1. **Strumwasser, F. 1988.** In *Current Topics in Neuroendocrinology* **9:** 105–122.
2. **Kaczmarek, L. K., and F. Strumwasser. 1981.** *J. Neurosci.* **1:** 626–634.
3. **Grynkiewicz, G., *et al.* 1985.** *J. Biol. Chem.* **260:** 3440–3450.
4. **Minta, A., *et al.* 1989.** *J. Biol. Chem.* **264:** 8171–8178.
5. **Goldberg, D. J. 1991.** Pp. 155–176 in *Culturing Nerve Cells*, E. Banker and K. Goslin, eds.
6. **Cooke, I., *et al.* 1989.** *Proc. Natl. Acad. Sci. USA* **86:** 402–406.
7. **Rehden, V., *et al.* 1991.** *J. Neurobiol.* **22:** 499–511.
8. **Miller, A. L., *et al.* 1991.** *Biol. Bull.* **181:** 325.

Optical Recording of Membrane Potential Changes From Single Neurons Using Intracellular Voltage-Sensitive Dyes

Dejan Zecevic (Institute for Biological Research, Belgrade, Yugoslavia)

The significance of regional properties of neurons for signal integration in functional neuronal networks has been well established. But detailed analysis has been restricted by the difficulties of recording from fine neuronal processes with microelectrodes. Optical recording methods (1, 2) do allow simultaneous measurements of membrane potential changes from multiple sites on neuronal processes (3, 4). I have investigated the absorption optical signals from individual neurons from the suboesophageal ganglion of the terrestrial snail *Helix aspersa.* These neurons were selectively stained by intracellular application of voltage-sensitive dyes. The goal was to determine the most suitable potentiometric probe for intracellular application. We looked for optical signals that would be sufficiently large to allow the analyses of regional electrical properties of neurons in intact, isolated ganglia. Additional improvements in sensitivity will clearly be required before structure-function relationships in single nerve cells can be systematically analyzed. The presently available signal-to-noise ratio is the result of a relatively modest screening effort that was concentrated on fluorescent molecules (4).

Dyes were tested on individual neurons from the isolated suboesophageal ganglion complex of young (0.3–1 g) snails. The preparation was positioned at the stage of a microscope. Light from a tungsten-halogen lamp was passed through appropriate heat and interference filters and focused on the preparation. The image of the ganglion was formed by 25×, 0.4 NA objective. In the plane of the magnified image, we positioned a 12 × 12 array of photodiodes for multi-site recording of transmitted light intensity changes that correspond to changes in membrane potential. The output of each photodiode was converted to voltage, amplified, and filtered before digitizing. Optical signals were sampled at 2000/s, digitized to 16 bits, and stored in a Motorola VMEbus computer.

In this series of experiments, I concentrated on dyes that give large absorption signals in extracellular application and tested compounds with pyrazolone-oxonol, merocyanine-rhodanine, merocyanine-oxazolone, and barbituric-acid oxonol chromophores. Absorption dyes are significantly better in terms of photodynamic damage, as compared to fluorescence molecules. Out of 10 pyrazolone-oxonol molecules tested (RH155, RGA509, JPW1177, RH479, RH482, RGA565A, RGA574, RGA577, JPW1037, JPW1038), the largest signals were obtained with the positively charged dye JPW1177, while its closest negatively charged analog, RGA509, produced substantially smaller signals. Diffusion of JPW1177 inside the neuron was slow, and better results were obtained from neurons that were injected about 20–30 h before optical recording. With the oxonol dye JPW1177, optical signals corresponding to evoked action potentials could be recorded from areas in the ganglion that are some 500 microns away from the cell body (Fig. 1). Since intracellularly injected dyes stain only the selected cell, the source of the signal is known, and we conclude that it is a process of the injected cell. The dye did not degrade during a period of diffusion of some 20 or 30 h; it did not cause pharmacological effects when injected into

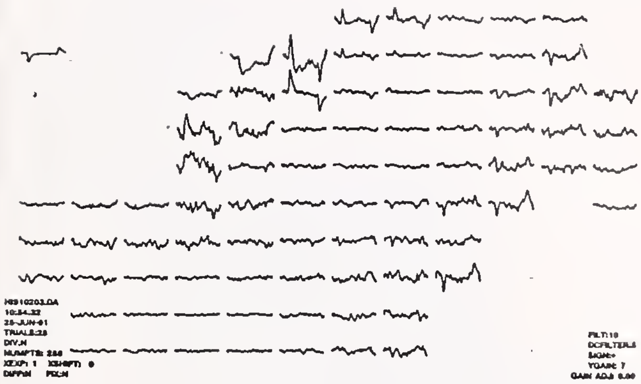

Figure 1. *Optical recording from 82 photodiodes. Optical signal corresponds to an action potential in single neuron. Average of 25 trials. Each trace is 147 ms. Each detector receives the light from a 60 × 60 micron area in the object plane.*

the neuron; it was not phototoxic; and bleaching of the dye was slow. However, the optical signals are still about 10 times smaller as compared to the most successful extracellular dyes, and averaging is required to detect signals from axons or dendrites.

Only three merocyanine dyes were tested (WW375, NK2367, JPW1124). All three merocyanines gave larger signals from the soma, as compared to oxonol JPW1177, if recording was done within 1 or 2 h after injection. However, the spread of these dyes through injected cells seems to require a longer period, and degradation of relatively unstable merocyanine molecules may become a problem. I do not yet know enough to decide upon the optimal conditions for the application of these merocyanine dyes; more experiments are needed.

One barbituric-acid dye (WW781) was tested, and further screening of dyes having similar structures seem justified. We did not record any pharmacological effects of the dye; photodynamic damage was not pronounced; the dye is chemically stable; and signal-to-noise ratio was comparable to one obtained with pyrazolone oxonols.

In several experiments, we recorded fluorescence optical signals using positively charged styryl dyes RH461 and RH437. The signal-to-noise ratio was 1 to 4 in different experiments in recording from cell soma. However, extensive averaging was not possible due to photodynamic damage.

Optimization of dye structures, staining protocols and measuring technology must be further improved before the resolution available when recording optically from dissociated neurons in culture can be achieved in experiments on individual cells in intact ganglia. We plan to look for more sensitive absorption dyes, as well as for sensitive fluorescence molecules that produce less pronounced photodynamic damage.

Valuable discussion with L. B. Cohen, B. Salzberg, and A. L. Obaid is appreciated. Supported by NIH grants NS-08437; NS-28443.

Literature Cited

1. **Cohen, L. B., and S. Lesher. 1986.** *Soc. Gen. Physiol. Ser.* **40:** 71–99.
2. **Zecevic, D., *et al.* 1989.** *J. Neurosci.* **9:** 3681–3689.
3. **Ross, W. N., and V. Krauthamer. 1984.** *J Neurosci.* **4:** 659–672.
4. **Grinvald, A., *et al.* 1987.** *Biophys. J.* **42:** 195–198.

Isolation and Protein Sequence Identification of *Aplysia californica* Lens Crystallins

Rachel L. Cox, David L. Glick, and Felix Strumwasser (Marine Biological Laboratory)

Lenses are a highly specialized tissue with several distinctive characteristics. They completely lack innervation or blood supply; the protein constituents do not turn over throughout the life of the organism; growth occurs only by the addition of new proteins; and they are continuously exposed to ultra-violet radiation. Crystallins comprise up to 95% of total soluble protein in the lens. Recent findings show that, in both vertebrates and invertebrates, these proteins are identical to enzymes found in other tissues (reviewed in 1 and 2). The present theory is that, during evolution, these enzymes were recruited as lens proteins because of their structural stability (2).

We have initiated a study of lens crystallins in the eye of *Aplysia*. Results from gel electrophoresis experiments and amino acid sequence analysis suggest that the *Aplysia* crystallins are unique. We report here on the biochemical and structural characterization of these novel proteins and on preliminary results from our protein data base search for amino acid sequence homology.

Aplysia californica and *Loligo pealii* eyes were dissected and trimmed of connective tissue. Complete lenses were removed, pooled, and homogenized in 124 m*M* Tris/20% glycerol/2% SDS, pH 6.75. The Pierce assay, with bovine serum albumin as a standard, was used to determine protein levels. Lens homogenates were run on a one-dimensional sodium dodecyl-sulfate polyacrylamide slab gel (SDS-PAGE) with a 5% stacking gel and 10% resolving gel (3). Protein bands were visualized with Pro-Blue stain (Integrated Separation Systems). Molecular weights of crystallin bands were determined by comparing the log Rf values to the following protein standards: myosin (205 kD), β-galactosidase (116 kD), phosphorylase b (97.4 kD), bovine serum albumin (66.2 kD), ovalbumin (45 kD), carbonic anhydrase (29 kD), and trypsinogen (24 kD). The percentage of each protein band within each pooled lens sample was quantified by densitometry.

For amino acid sequence analysis, lenses were prepared as above. Samples were run either by one-dimensional SDS-PAGE as above (24 μg per lane), but with the addition of sodium-thioglycolate (0.1 m*M*) and glutathione (50 μ*M*) to the running buffer, or by two-dimensional gel electrophoresis as previously described (4). Protein bands were transferred electrophoretically to Immobilon (Millipore) in 10 m*M* cyclohexylamino propane sulfonic acid/10% methanol. Transferred bands were visualized with Ponceau stain (0.5% Ponceau/1% acetic acid) for one-dimensional blots, and by Coomassie blue stain for two-dimensional blots. Spots or bands were cut from the membrane and subjected to sequence analysis by automatic Edman degradation on an ABI 477A protein sequencer.

The N-terminus of the 63 kD *Aplysia* crystallin was compared to other known protein sequences through the use of two separate protein data bases: European Molecular Biology Laboratory and Swiss Protein Data Base. It was compared also to a data base which contained 84 sequenced crystallins, 83 of which are vertebrate, with the majority from mammals.

Most of the mass (5), and at least 75% of the total soluble protein in the *Aplysia* eye is accounted for by the central acellular lens. Figure 1 compares the electrophoretic mobilities of *Aplysia* and *Loligo* crystallins. Three major crystallin bands are apparent in the *Aplysia* lens, as resolved by SDS-PAGE. Their molecular weights are 80 kD, 61–63 kD, and 28 kD. The series of low molecular weight bands were not always visible by Coomassie blue stain, and have therefore not been subjected to analysis. The percents of total stainable protein were calculated and are as follows: 80 kD band is 40%, the 61–63 kD doublet is 33%, and the 28 kD band is 22%. The squid lens exhibited a broad protein band between 23–28 kD that appears to consist of at least two bands. This finding is consistent with earlier reports on another squid species, *Nototodarus gouldi*, where subunits of the crystallins have been estimated at 30 and 27 kD (6).

N-terminal sequence was obtained, for the first 24 amino acids, of the *Aplysia* 63 kD band:

lys-THR-LYS-GLN-gln-PHE-VAL-ALA-ALA-ILE-LEU-arg-
gln-his-arg-MET-GLN-glu-GLN-ALA-GLN-GLN-ALA-ASP

The sequence is identical to that obtained for the 14 N-terminal amino acids of the *Aplysia* 80 kD band:

lys-THR-lys-GLN-GLN-PHE-VAL-
ALA-ALA-ILE-leu-x-gln-his

These bands represent either different, somewhat homologous, subunits of the same protein, or the 63 kD band is degraded, by proteolysis, from the 80 kD protein. Alternatively, the 80 kD protein may be post-translationally modified, compared with the 63 kD protein.

We were encouraged to search protein databases with these sequences because in squid the first 20 N-terminal amino acid residues of the two crystallin S_{III} subunits are 88% homologous (6, 7) and are strikingly similar to the N-terminus of glutathione S-transferase (2). The sequence of the *Aplysia* 63 kD band was subjected to a stringent protein data base search, using only exact matches (not conservative substitution) at the N-terminus. Preliminary results have revealed no striking similarities (8 alignments were at the 40% level) to any sequenced enzymes. (There are many 30–35% matches to sequenced enzymes and bacterial proteins). A more complete search will be carried out when we have determined some of the internal sequence.

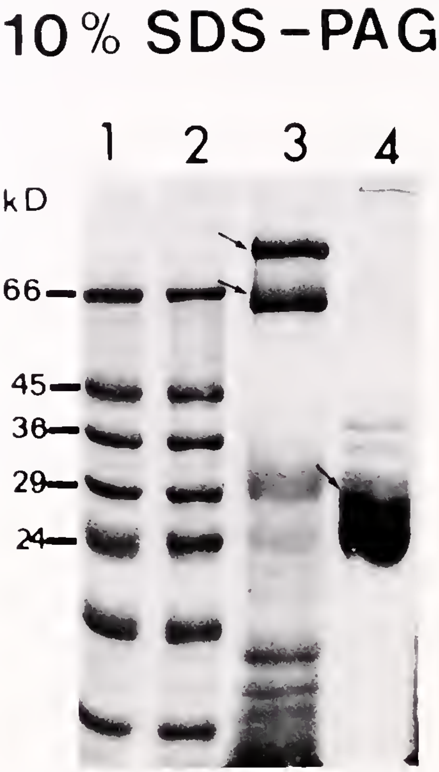

Figure 1. *SDS-PAGE of lens proteins: (lanes 1 and 2) molecular weight standards; (lane 3)* Aplysia *lens, arrows point to novel crystallins; (lane 4)* Loligo pealii *lens, arrow points to the S_{III}-crystallin.*

The squid crystallin, S_{III}, was the first example, in invertebrates, of enzymes being recruited to serve as structural proteins in the lens (8). The high molecular mass of the novel *Aplysia* crystallins presented here represents a striking departure from the squid S_{III}-crystallin. Furthermore, the N-terminal residues of the 63 kD *Aplysia* crystallin sequence share no homology with this squid crystallin.

Among invertebrates, there are few precedents for the existence of high molecular weight crystallins such as those described here for *Aplysia*. One interesting exception is the cellular lens of the hydromedusan *Cladonema radiatum* (Cnidaria). By SDS-PAGE, two high molecular weight crystallins have been identified with molecular masses of 70 and 40 kD (9). Sequences have not been obtained for these crystallins, but their similarly high molecular weights and some cross-immunoreactivity, suggest that they may be closely related to those of the amphibian *Rana catesbeiana* (8, 9).

During evolution, certain enzymes have been recruited, for use by the lens, to serve as structural proteins. Further analysis of the novel crystallins in the *Aplysia* lens may reveal yet another example of enzyme recruitment in the invertebrate eye and perhaps also shed some light on the ontogeny of the lens.

This work was supported by an NSF grant (BNS-9010115) to FS. We thank Dr. Richard Ridge for performing the sequence analysis.

Literature Cited

1. **Bloemendal, H., and W. W. de Jong. 1991.** *Prog Nucleic Acid Res.* **41:** 259–281.
2. **Wistow, G., and J. Piatigorsky. 1987.** *Science* **236:** 1554–1556.
3. **Laemmli, U. K. 1970.** *Nature* **227:** 680–685.
4. **Strumwasser, F. 1989.** *J. Physiol. Paris* **83:** 246–254.
5. **Strumwasser, F., *et al.* 1979.** In *Biological Rhythms and Their Central Mechanism.* Elsevier.
6. **Siezen, R. J., and D. C. Shaw. 1982.** *Biochim. Biophys. Acta* **704:** 304–320.
7. **Tomarev, S., and R. Zinovieva. 1988.** *Nature* **336:** 86–88.
8. **Wistow, G., and J. Piatigorsky. 1988.** *Ann. Rev. Biochem.* **57:** 479–504.
9. **Weber, C. 1981.** *J. Exp. Zool.* **217:** 15–21.

Mechanism of Paddle Cilia Formation in Molluscan Veligers

Michael Deiner and Sidney Tamm (Boston University Marine Program)

Cilia with a distal expansion of the membrane enclosing a curved or coiled end of the axoneme (paddle cilia or discocilia) have been described in a variety of marine invertebrates (1). Short and Tamm (1) showed that paddle cilia in veliger larvae of *Spisula solidissima* and *Lyrodes pedicellatus* are not genuine structures, but artifacts of osmotic stress caused by the hypotonic solutions used by previous workers (2). Short and Tamm (1) argued that most, if not all, examples of paddle cilia and discocilia are artifacts, and proposed a unifying mechanism to account for their formation in various animals under different conditions. According to this model, coiling of the axoneme is due to conformational changes of the doublet microtubules. Such alterations could be induced by a Ca^{++} influx or proton efflux (3, 4, 5), caused either by osmotic swelling and opening of cation channels in the ciliary membrane, or by membrane breakdown in isotonic or hypertonic fixatives. Alternatively, disruption of internal axonemal constraints by proteolysis during fixation or handling might allow spontaneous coiling of the doublet microtubules (6, 7).

Short and Tamm's model absolves membrane tension as the cause of axonemal coiling under hypotonic conditions. A simple test of the model is to remove the membrane from paddle cilia. If the end of the axoneme remains coiled, then membrane tension is not responsible; if, on the other hand, the axoneme uncoils and straightens, then membrane tension, not conformational changes of the axonemal microtubules, is the cause of paddle cilia formation.

We performed this test on compound preoral cilia of veliger larvae of *Crepidula fornicata*. Veligers were treated with the carbocyanine membrane probe DiI (C_{16}) in 1 *M* sorbitol for 20–25 min to label ciliary membranes. Larvae were washed in seawater (SW) and relaxed in 6.75% $MgCl_2$:SW (1:1) to prevent the velum from retracting. The formation of paddle cilia was induced by perfusion with a 35% or 40% dilution of the $MgCl_2$:SW solution in distilled water (hypotonic solution). The diameter of the flat side of the paddles in the hypotonic $MgCl_2$:SW solution was 1–3 μm. Ciliary length (60–75 μm in normal seawater, see Fig. 1A) decreased as paddles formed (Fig. 1B). Ciliary beat rate slowed and often stopped. The compound cilia tended to fray apart into individual cilia. Under phase contrast microscopy, the paddles appeared gray (distended membrane) with a black rim (coiled axoneme); under darkfield, they appeared as bright rings at the tips of bright shafts. Epifluorescence microscopy (TRITC filter set), with a DAGE SIT video camera, revealed the paddles as fluorescent disks atop brightly fluorescent shafts, confirming DiI as a useful marker for detecting ciliary membranes.

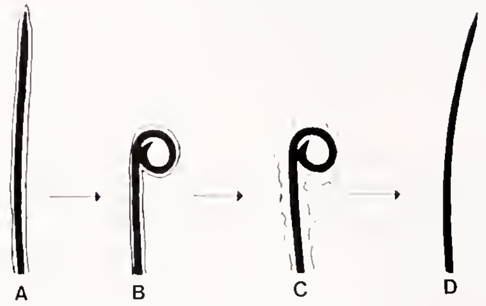

Figure 1. *The mechanism of paddle cilia formation by hypotonic solutions. Ciliary membrane is indicated by thin line, axoneme by heavy line. (A) Normal seawater. (B) Formation of a paddle cilium induced by hypotonic solution. (C) Disruption of ciliary membrane by detergent. (D) Uncoiling of axoneme after removal of membrane.*

Perfusion of different detergents in hypotonic $MgCl_2$:SW (0.1–1.0% Triton X-100, 0.1–1.0% Nonidet P-40, or 25–50 m*M* octyl glucopyranoside) typically removed all traces of ciliary membranes within several minutes, as judged by phase-contrast or fluorescence microscopy (Fig. 1C). Within 1 s after membrane loss, the axonemal tips uncoiled and straightened, increasing the length of the shafts (Fig. 1D).

To substantiate this finding, we repeated the above experiments using Ca^{++}-free ASW or 1 *M* sorbitol (pH 2.6) or 1 *M* sorbitol with 1 m*M* EGTA, 50 m*M* Tris, pH 7.0 in place of $MgCl_2$:SW. Thirty-five percent $MgCl_2$:Ca^{++}-free ASW hypotonic solution, or either of the 0.35 *M* sorbitol solutions induced paddle cilia to form. The 0.1% Triton X-100 in these solutions removed the membranes and uncoiled the axonemes. Therefore, neither external Ca^{++} nor other ions, nor proton efflux are necessary to induce paddle formation under hypotonic conditions, casting further doubt on the role of Ca^{++} or proton-dependent conformational changes in the axonemal microtubules in this process (1).

In addition, we tried to induce tip coiling of bare axonemes with Ca^{++} or Sr^{++} as reported for demembranated macrocilia

(5). Velar cilia were demembranated in 0.1% Triton X-100, 0.15 M KCl, 0.005 M $MgCl_2$, 0.001 M EGTA, 0.03 M PIPES, pH 6.9. After washing, Ca^{++} or Sr^{++} concentrations were raised to 0.1 M in wash solution. Nevertheless, the tips did not coil. High levels of Ca^{++} or Sr^{++} therefore are ineffective in producing detectable conformational changes of bare axonemes.

Our results indicate that axonemal coiling of paddle cilia induced by hypotonic conditions is due to membrane tension acting on elastic axonemes, not to proton or ionically induced conformational changes of axonemal microtubules as proposed previously (1). Cases of extensive coiling of the axonemes, accompanied by drastic decreases in ciliary length, may result from membrane forces arising during progressive, proximally directed breaking of membrane-axonemal connections (8). We cannot rule out the possibility that paddle cilia formation under other conditions (*i.e.*, fixation, isotonic conditions, etc.) is due to induced or intrinsic shape changes of doublet microtubules (3–7). Further experiments will be necessary to examine the mechanism of paddle formation in these cases.

This work was supported by NIH Grant GM45557 to SLT. We thank Ray Stephens, MBL, for the generous loan of the DAGE SIT camera, and for reagents and helpful discussions.

Literature Cited

1. **Short, G., and S. Tamm. 1991.** *Biol. Bull.* **180:** 466–474.
2. **Campos, B., and R. Mann. 1988.** *Biol. Bull.* **175:** 343–348.
3. **Miki-Noumura T., and R. Kamiya. 1976.** *Exp. Cell. Res.* **97:** 451–453.
4. **Miki-Noumura T., and R. Kamiya. 1979.** *J. Cell Biol.* **81:** 355–360.
5. **Tamm, S. L., and S. Tamm. 1990.** *Cell Motil. Cytoskel.* **17:** 187–196.
6. **Zobel, C. R. 1973.** *J. Cell Biol.* **59:** 573–594.
7. **Summers, K. E., and I. R. Gibbons. 1971.** *Proc. Natl. Acad. Sci. USA* **68:** 3092–3096.
8. **Dentler, W. L. 1981.** *Int. Rev. Cytol.* **72:** 1–47.

High-Resolution, 4-Dimensional Imaging of Early Development in *Lytechinus variegatus*

Shinya Inoué (Marine Biological Laboratory), Andreas Stemmer,
Theodore D. Inoué, and Robert A. Knudson

We have developed a video microscope system that allows time-lapsed, through-focal optical sectioning of live cells and developing embryos at high optical resolution. With the new system, we have examined developing *Lytechinus variegatus* zygotes, from pronuclear migration through the early cleavage stages.

Equipped with a high-numerical-aperture (NA) and a well-corrected objective lens coupled with a well-focused, high-NA condenser (whose aperture is uniformly filled with the illuminating beam), the light microscope, when combined with video contrast enhancement, can provide high-lateral resolution (within the focused image plane), as well as high-axial resolution (perpendicular to the image plane). In other words, the system provides good lateral resolution coupled with a very shallow depth of field (1). For studying structures in live cells and embryos, the use of such optical systems is at once a blessing and a bane. One gains a detailed image unencumbered by out-of-focus objects, but at the same time loses information in the third dimension.

To circumvent this last problem, and to capture images with a reasonably fast repeat rate, we developed a rapid and accurate, automated, through-focal recording system (Fig. 1A) that can scan the specimen axially at rates of 0.5 μm per video field time (1/60th s) and that has a cycle time under 5 s (Fig. 1B). The 0.5-μm-thick axial slice, thus obtained per video field, was appropriate for the 60×/1.4 NA plan apochromatic objective lens that we used in combination with a rectified condenser at NA of *ca.* 0.8.

When this new system was used with differential interference contrast (DIC, or Nomarski) optics, cellular features and their three-dimensional relationships were imaged with a clarity never before obtained. The results were played back at these General Meetings.

For example, for years we had been attempting in vain to visualize the microtubule-containing astral rays that were thought to draw the female pronucleus towards the male centrosome after fertilization. With the new system providing both the needed image resolution and the ability to track the slender, elongated astral rays through several optical sections, we can finally locate and follow those rays (which do not always run in a straight line) and make sense out of the deformation and tortuous movement of the large female pronucleus.

Also with the new system, the chromosomes (which had not been visible in the mitoses of early cleavage stages of live *L. variegatus* zygotes in the past) appeared clearly as sinuous thin threads, from metakinesis through the end of anaphase, starting with the first cleavage division. Likewise, slender mitochondria embedded in the centrosome and aligned along the astral microtubule bundles at the spindle poles were visible.

Among the fusing karyomeres that form around each chromosome in telophase, we could decipher a channel containing the spindle remnant. While we had observed this transient structure, which at any single focus gave the appearance of a double-walled septum at telophase in a variety of animal cells, through-focal imaging of the sea urchin cells finally clarified the topology of the late telophase nuclear envelope. Thus, in the late stages of karyomere envelope fusion, the envelope of each daughter nucleus takes on the shape of a toroid with a slender, elongated, central tunnel that is pierced by the polar region of the spindle remnant. This configuration, reminiscent of the telophase con-

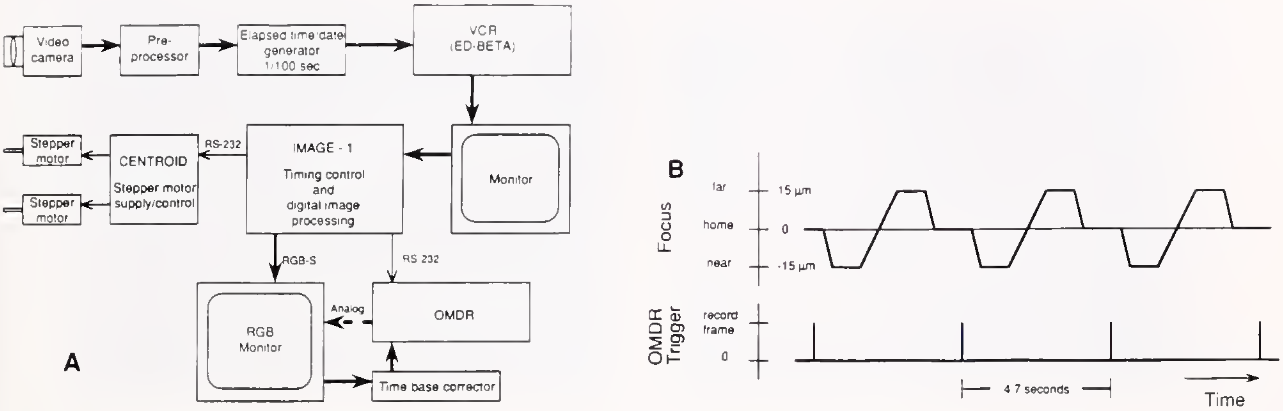

Figure 1. *A. Schematic of video and control systems for the 4-D image data acquisition system. The pre-processed video microscope image is recorded continuously onto an ED-Beta VCR (500-TV-line resolution). This signal, digitally processed, is then recorded one frame per cycle to the OMDR (optical memory disk recorder) according to the sync pulses (Fig. 1B) generated by the central processor—controller, Image-1. Image-1 also governs, through the Centroid unit, the movement of the stepper motors that drive the objective lens and condenser focus. B. Upper curve: focusing movement of objective and condenser lenses. Lower curve: recording pulses for the OMDR.*

figuration of the nuclear envelope in *Barbulanympha* (2), must therefore be a pattern widely distributed among animal cell nuclei at telophase.

Before long, we hope to be able to convert each stack of these through-focal images into stereo images, so that they can be observed as time-lapsed, stereoscopic images. When this is realized, we will have achieved true four-dimensional imaging. The spatial and functional relationships of cells, organelles, and macromolecular assemblies, and the dynamic changes in the three-dimensional structure of developing embryos and dividing cells at very high microscope resolution, should then become even clearer than with the system just presented.

We thank Universal Imaging Corporation for summer fellowship support at the MBL for AS, and research grants R37 GM31617-09 from NIH and DCB-8908169 from NSF.

Literature Cited

1. **Inoué, S. 1988.** *Cell Motility Cytoskel.* **10:** 13–17.
2. **Inoué, S., and H. Ritter, Jr. 1978.** *J. Cell Biol.* 77: 655–684.

Biochemical Changes Associated with Reduction of Cell Motility and Aggregation Following Sulfate Restriction in the Marine Sponge *Microciona prolifera*

William J. Kuhns[1], *Max M. Burger*[2], *and Gradimir Misevic*[3] *([1]Hospital for Sick Children Toronto, [2]Friedrich Miescher Institute, [3]University Hospital, Basel)*

Sulfation in vertebrate cells has been documented (1,2), but its precise role in growth, development, and disease is not well understood (3). Despite this, some studies demonstrate that abnormal patterns of sulfation occur, particularly in cell matrix proteoglycans and mucins, in a wide spectrum of diseases including cancers, cystic fibrosis, and connective tissue disorders (2, 4–6). In several non-vertebrate species, sulfate deprivation reduces cell migration and inhibits cell development (7, 8). Marine sponge cells are embedded in extracellular matrix—including sulfate containing glycans—to a much greater extent than are vertebrate cells. In addition, studies are simplified because controlled experiments can be carried out in artificial seawater (ASW), with or without added sulfate. For these reasons, the marine sponge is an appropriate model with which to study sulfation.

Earlier studies have shown that cells of the marine sponge secrete reduced amounts of macromolecules and become less motile when their medium is deprived of sulfate (9). Filopodia and pseudopodia become smaller, and this is associated with such functional disturbances as impairment of cellular aggregation and motility. The following experimental findings confirm and extend the original studies.

Detailed microscopic observations of chemically dissociated sponge cells were carried out, and the motility and aggregation of cell cohorts with 26 m*M* sulfate (SO_4^+) and without (SO_4^-) sulfate were compared. Time lapse photographs were taken of cell suspensions maintained for 4 h at room temperature in ASW either with or without sulfate. In sulfate-deprived cells, aggregation was minimal, although in individual cells, ruffling and some extrusions were noted. In contrast, SO_4^+ cells exhibited

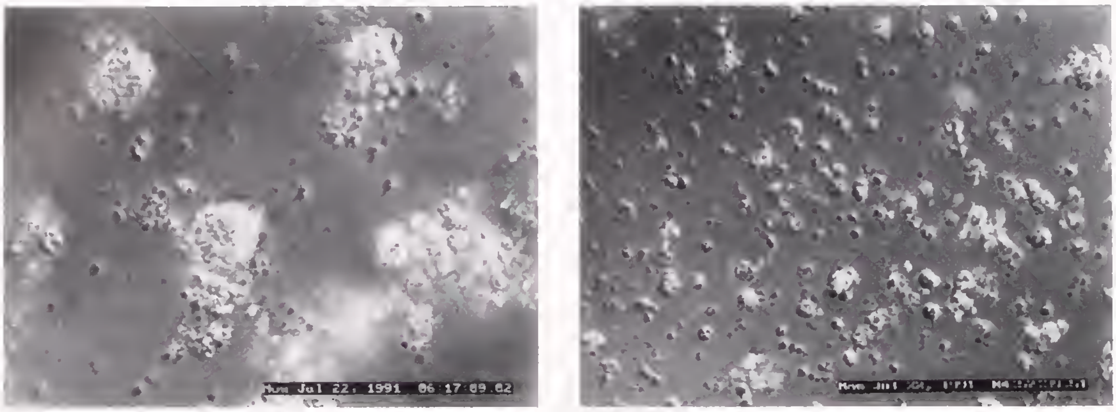

Figure 1. *Final frames of a motility and aggregation pattern of cells maintained in SO_4^+ (left) or SO_4^- ASW (right). Using a 20× objective focused on cells in a sealed chamber, photographs were taken at 15-s intervals over a 4-h period. Little or no alterations of cell patterns were observed in SO_4^- cells, while vigorous motility and formation of large aggregates occurred in SO_4^+ cells. Aggregation was graded as +++± and ±, respectively, in SO_4^+ and SO_4^- cell cohorts (10).*

good movement and tended to form progressively larger aggregates during the study so that very few single cells remained (Fig. 1).

To understand these changes and to define the role of aggregation factor (MAF), we carried out the following experiments. Carrier-free ^{35}S sulfate was introduced into rotated cells that had been previously treated by sequential low speed centrifugations and replacements of supernatants with fresh CMFASW to remove preformed secretions. The pellets were then distributed into ASW with or without 26 m*M* sulfate. Uptake of $^{35}SO_4$ in sulfate-deprived cells increased 3- to 10-fold over that in normal ASW over 2 to 5 days, while protein synthesis was similar in both cohorts (9).

Extracellular secretions produced by SO_4^- and SO_4^+ cells were collected, concentrated by ultrafiltration, and analyzed for protein and MAF, using specific monoclonal antiMAF (MoAb), and for radioactivity (9). Based on these criteria, MAF or macromolecule secretion was reduced from the normal when cells were maintained in sulfate free ASW. Furthermore, cell aggregation by SO_4^- MAF was greatly reduced when compared to the extent of aggregation in an equal amount of SO_4^+MAF. Thus, qualitative as well as quantitative defects are responsible for the impairment of MAF function. To study intracellular MAF or proteoglycans, Triton X-100 extracts derived from washed *Microciona* cells at different times following $^{35}SO_4$ were assayed for cellular MAF by mixing with MoAb, and then separating the complexes with Sepharose-staph-protein A beads. Washed test and control beads were examined for $^{35}SO_4$, and the results were related to total $^{35}SO_4$ macromolecules separated from the corresponding cell extracts by high voltage electrophoresis. MAF from SO_4^- Triton extracts was increased, compared to the SO_4^+ cellular MAF yield, on the basis of immunoprecipitation using anti MAF MoAb. In a typical experiment, retrieval of radioactivity on high voltage electrophoresis was as follows from 90 μg protein in SO_4^- and SO_4^+ extracts: 4120 dpm and 1181 dpm, respectively, in SO_4^- and SO_4^+ extracts. Specific activity derived from $^{35}SO_4$ MAF-anti MAF on Sepharose beads was 583 dpm and 360 dpm in SO_4^- and SO_4^+ extracts. Control values for SO_4^- and SO_4^+ cohorts were 34 dpm and 66 dpm, respectively. This result, coupled with the findings on secreted MAF, suggested that sulfate deprivation caused cell retention of undersulfated MAF and other cellular macromolecules.

A relationship between tyrosine-O-sulfation and the kinetics of secretion has been established by site directed mutagenesis experiments on vitellogenin, a secretory protein (11). To determine the possible role of tyrosine-O-sulfate in the sulfation or undersulfation of *Microciona* cell macromolecules, we carried out the following studies. SO_4^- and SO_4^+ cell extracts were spun at 12,000 rpm and the supernatants processed through SM Biobeads and then a Biogel PZ column to remove Triton and salts. The protein concentrations of both eluants were equalized, and the eluants were then subjected to base hydrolysis, and the amino acids characterized by HPLC using a tyrosine-O-sulfate reference standard. In duplicate sets of experiments, tyrosine-O-sulfate was found in SO_4^+ cells at levels two to three times greater than those present in SO_4^- cell extracts (8.9 nmol/mg compared to 3.0 nmol/mg protein). Although these early results have not been implemented by comparison with total tyrosine content on combined acid and base hydrolyzed protein, they suggest that reduced tyrosine sulfate ester may play a role in SO_4^- MAF retention and the undersulfated MAF secretion that follows withdrawal of ASW sulfate.

Together, these findings show that a decrease in tyrosine-O-sulfation is correlated with a decrease in secreted proteoglycan or mucopolysaccharide sulfation and increased cell retention and that they, in turn, are closely coupled to decreases in functional activity as measured by altered cell motility and aggregation. They also suggest that fine structure differences in MAF and possibly other macromolecules from sulfate-deprived *versus* normal *Microciona* cells may prove important in defining cellular regulatory proteins and extracellular prompting mechanisms that initiate or modulate functional changes.

Literature Cited

1. **Mulder, G. J. 1981.** Pp. 31–52 in *Sulfation of Drugs and Related Compounds* CRG Press, Boca Raton, FL.

2. **Hook, M., *et al.* 1984.** *Ann. Rev. Biochem.* **53:** 847–869.
3. **Humphries, D., *et al.* 1986.** *J. Biol. Chem.* **261:** 9122–9127.
4. **Stamatoglou, S., and J. Keller. 1983.** *J. Biol. Chem.* **96:** 1820–1823.
5. **Forstner, J., *et al.* 1991.** *Exp. Mol. Pathol.* **54:** 129–143.
6. **Fukui, S., *et al.* 1981.** *J. Biol. Chem.* **256:** 10310–10318.
7. **Katow, H., and M. Solursh. 1981.** *Exp. Cell Res.* **136:** 233–245.
8. **Wenzl, S., and M. Sumper. 1981.** *Proc. Natl. Acad Sci. USA* **78:** 3716–3720.
9. **Kuhns, W., *et al.* 1990.** *Biol. Bull.* **179:** 358–365.
10. **Jumblatt, J., *et al.* 1980.** *Biochemistry* **19:** 1038–1042.
11. **Huttner, W. B. 1988.** *Ann. Rev. Physiol.* **50:** 363–376.

Tektins from *Spisula solidissima* cilia

R. E. Stephens and G. Prior (Marine Biological Laboratory)

Described so far in only a limited number of organisms, the tektins are a unique class of highly insoluble proteins found in association with the junctional protofilaments of outer doublet microtubules in cilia and flagella (1, 2), and extending from base to tip (3, 4). To study ciliogenesis in embryos of the surf clam *Spisula solidissima* for comparison with sea urchins, we needed to identify specific *Spisula* ciliary tektins, because the limited or quantal synthesis of one particular tektin in sea urchin embryos (tektin-A) not only correlates with ciliogensis but limits the length of cilia as well (5, 6).

To define the tektins, we first extracted *Spisula* sperm flagellar axonemes with 0.5% sarkosyl to obtain tektin-tubulin protofilament ribbons (1), and then further fractionated these ribbons with increasing concentrations of urea to remove the tubulin (7). The pellet fractions were analyzed on 8T/2.5C discontinuous polyacrylamide gels containing 0.1% Sigma SDS (L-5750) and stained with Coomassie Blue. By electroblotting to nitrocellulose and staining with rabbit polyclonal antibodies prepared against purified sea urchin sperm flagellar tektins (8), we identified specific *Spisula* tektins. As illustrated in Figure 1A, the *Spisula* flagellar tektins fractionate in much the same manner as has been reported for other species (1, 7, 9), with the lowest molecular weight component (the presumptive tektin-C) being removed at urea concentrations above 2.0 *M*. The other two presumptive tektins solubilize together as the urea concentration is raised further.

The 2.0 *M* urea-insoluble fraction was used for antibody identification (Fig. 1B). The antibody to tektin-A (nominally 55 kDa in sea urchin) is the most specific, identifying one major tektin, but the position of this protein is reversed in *Spisula* relative to the presumptive tektin-B (nominally 51 kDa in sea urchin). Sea urchin anti-tektin-B cross-reacts more or less equally with both tektin-A and -B, whereas anti-tektin-C reacts with the lowest molecular weight *Spisula* tektin and also with tektin-A, as it does with authentic sea urchin tektins (8).

Lateral cilia were isolated from excised *Spisula* gills by hypertonic shock and serotonin stimulation (10). The cilia were demembranated and further fractionated by heating to produce ciliary remnants, nine-fold symmetrical structures containing tektin-tubulin protofilaments and associated proteins, but no microtubules (4). Such remnants were then subjected to the same sarkosyl-urea fractionation as sperm axonemes. Pellet and supernatant fractions were analyzed stoichiometrically by SDS-PAGE (Fig. 1C), and the tektin distribution was assessed both densitometrically and with the above antibodies. The relative solubility properties and positional identities of the three tektins in the pellet fraction from gill cilia remnants parallel those of

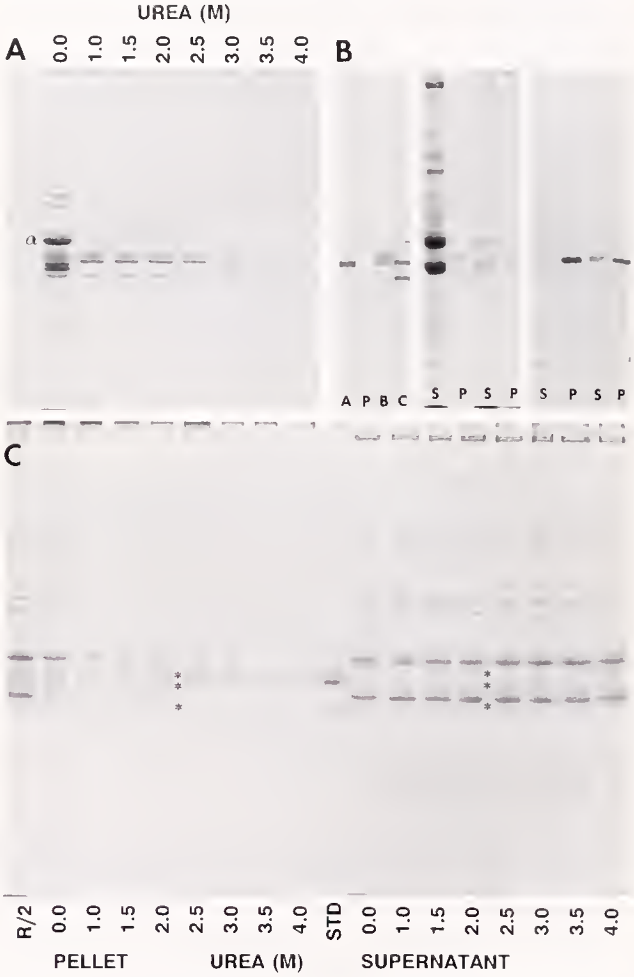

Figure 1. *Identification of tektins in* Spisula solidissima *cilia by sarkosyl-urea fractionation and antibodies. (A) Tektin-tubulin protofilament ribbons from flagella extracted with 0.5% sarkosyl containing the specified concentrations of urea. α = α-tubulin. (B) Left panel: immunoblots of the 2.0* M *urea pellet from (A) using rabbit antisera to sea urchin sperm flagellar tektins A, B, and C; P = preimmune serum, tektin-A. Center panel: Supernatant (S) and pellet (P) from 0.5% sarkosyl-2.0* M *urea extraction of sperm flagella (left pair) and ciliary remnants (right pair). Right panel: immunoblot of same, with antiserum to sea urchin tektin-A. (C) Stoichiometrically loaded pellets and supernatants of ciliary remnants extracted with 0.5% sarkosyl containing the specified concentrations of urea. R/2 = remnant starting material loaded at ½ stoichiometric ratio; STD = standard of flagellar tektins from 2.0* M *urea extraction. Asterisks designate the three tektins.*

flagella. But in contrast to flagellar tektins, which are resistant to sarkosyl solubilization in the presence of low concentrations of urea, substantial amounts of ciliary tektin-A (but not tektin-C) are found in the 0.5% sarkosyl-low urea supernatant (Fig. 1C). Similar results were reported earlier for cilia from sea urchin embryos (5) and scallop gills (11). The antibody to tektin-B detects little tektin-A (or tektin-B) in the supernatant, although it can detect tektin-A in the pellet fraction, suggesting two distinct isoforms of tektin-A.

Three basic conclusions can be drawn from this work. First, *Spisula* sperm flagella and gill cilia contain three tektins with general fractionation properties that parallel those of the sea urchin, so the same basic analytical methods can be used for both. Second, when analyzed by standard SDS-PAGE with Sigma SDS, the electrophoretic migration of the *Spisula* equivalent of sea urchin tektin-A is reversed with respect to tektin-B and this point is critical to the interpretation of possible quantal synthesis. Third, *Spisula* gill cilia, *unlike* sea urchin, scallop, and *Spisula* sperm flagella, but *like* sea urchin embryonic and scallop gill cilia, contain roughly equal amounts of a sarkosyl-soluble and a sarkosyl-insoluble fraction of tektin-A. Linck (9) observed that there are *two* tektin-tubulin protofilament equivalents per sea urchin flagellar outer doublet, a point confirmed in scallop and sea urchin ciliary remnants (4). Because flagella and cilia fractionate so differently, the former to individual outer doublet microtubules and the latter to cylinders of nine singlet A-tubules (12), these observations may reflect a difference in either the position or the chemistry of the tektin-containing protofilaments in these two otherwise morphologically identical organelles.

This work was supported by USPHS Grant GM 20,644. We thank Dr. Richard W. Linck of the University of Minnesota for providing antisera and affinity purified antibodies to sea urchin tektins.

Literature Cited

1. **Linck, R. W., and G. L. Langevin. 1982.** *J. Cell Sci.* **58:** 1–22.
2. **Amos, W. B., *et al.* 1986.** *J. Cell Sci. Suppl.* **5:** 55–68.
3. **Steffen, W., and R. W. Linck. 1988.** *Proc. Natl. Acad. Sci. USA* **85:** 2643–2647.
4. **Stephens, R. E., *et al.* 1989.** *J. Cell Sci.* **92:** 391–402.
5. **Stephens, R. E. 1977.** *Dev. Biol.* **61:** 311–329.
6. **Stephens, R. E. 1989.** *J. Cell Sci.* **92:** 403–413.
7. **Linck, R. W., and R. E. Stephens. 1987.** *J. Cell Biol.* **104:** 1069–1075.
8. **Linck, R. W., *et al.* 1987.** *J. Cell Sci.* **88:** 453–466.
9. **Linck, R. W. 1976.** *J Cell Sci.* **20:** 405–439.
10. **Stommel, E. W. 1984.** *J. Comp. Physiol.* **155A:** 457–469.
11. **Stephens, R. E. 1989.** *J Cell Biol.* **107:** 20a.
12. **Linck, R. W. 1973.** *J Cell Sci.* **12:** 951–981.

Identification of Unique Proteins in the Eye of *Aplysia californica*, a Circadian Organ

Jacalyn Vogel and Felix Strumwasser (Marine Biological Laboratory)

The eye of the marine mollusk *Aplysia californica* contains a circadian oscillator, demonstrated by changes in spontaneous action potential frequency in isolated eyes over time (1). The isolated eye synthesizes approximately 80 proteins for which the rate of ^{35}S-methionine incorporation changes over time. One of these proteins (42 kD, 5.5 pI) demonstrates a linear increase in rate of incorporation of ^{35}S-methionine over 24 h. This protein "resets" at the end of the 24-h cycle, and has been designated a circadian "sawtooth oscillator" protein (2). The presence of the sawtooth oscillator protein implies that proteins unique to the eye might be components in the circadian oscillator or photic functions of the eye. We have therefore attempted to identify eye-specific proteins by comparing the eye (lens removed) with other neuronal tissues, such as bag cell clusters (BC) and abdominal ganglia without BC (AGOBC), using two-dimensional (2D) gel electrophoresis. The bag cells are a homogeneous set of neurosecretory cells, and the output neurons of the eye appear to be homogeneous and neurosecretory by electron microscopic criteria (1).

Adults of *A. californica* were obtained from Alacrity Marine Supply and entrained to a light/dark cycle (12 h L:12 h D) for at least 4 days prior to experimentation. Eyes and ganglia (from light period animals) were delensed or desheathed in artificial seawater, then incubated in lysis buffer (0.3% Na-dodecylsulfate/0.6 *M* B-mercaptoethanol/50 m*M* tris, pH 8.8) at 95°C for 5 min. This incubation was repeated after a brief homogenization step. The resulting lysate was clarified by centrifugation (6000 × *g* for 5 min), treated with DNase and RNase (Worthington) to remove nucleic acids, and desalted by precipitation with acetone. The protein pellet was resuspended in urea sample buffer II (4:1 urea sample buffer I with lysis buffer) to a final concentration of >1 mg/ml. Urea buffer I consisted of 9.9 *M* urea/4% Nonidet P-40/10 m*M* (3-{(cholamidopropyl)dimethylammonio}-1-propanesulfate/100 m*M* dithiothreitol).

High resolution 2D gel electrophoresis was carried out on a Millipore Investigator 2D Electrophoresis system according to the method of O'Farrell (3, 4). For the isoelectric focusing (IEF) step, 15–20 μg of protein were used. The proteins were focused for 18,000 volt hours with 3–10 pH ampholytes (Millipore), then separated on 12.5% acrylamide gels, and stained with silver (4). Apparent molecular weights and isoelectric points were determined using internal standards and carbamylated carbonic anhydrase (Pharmacia).

Gel images were acquired with a Charge Coupled Display-based camera (Datacopy) provided with a MasterScan densitometer (CSPI), with an image resolution of 2240 × 1728 pixels. The images were corrected for background, and a file of the detected spots was generated. Composite spot files (databases) were created using one gel (eye) as a reference. Reference spots (actin, tubulin, etc.) were used to assure correct matching between gels, and the matches were further validated by extensive pattern comparison between synthetic images of the reference gel and additions to the database. Unmatched spots (tissue-specific) were validated in a similar fashion.

The number of spots detected by silver staining was ~300 (for all samples), compared to >1000 detected by ^{35}S-methionine labeling (6). Therefore, less abundant proteins, some of which may be tissue-specific, were not included in the analysis. The majority of proteins detected in whole cell lysates are common to most cell types (6). A control database for intra-tissue variation showed that about 85% of spots were matched between different eye samples (n = 4). The number of matches decreased to ~60% when eyes were compared to BC (n = 3), and ~75% when BC were compared to AGOBC (n = 3). Based on these comparisons, we expected that a greater number of eye-specific proteins than BC or AGOBC-specific proteins would be identified, and this was the case. The high degree of similarity in the spot profiles of BC and AGOBC may be due to the large number of glial cells found in both tissues (7).

Table I lists 15 proteins that are clearly unique to the eye, based on limits of detection with silver staining and present computer analysis. These proteins span a range of MW from 25 to 82 kD, and of pI from 5 to 6.6. A number of proteins (*e.g.*, dle14, dle17) may be isoforms based on charge differences, and other proteins (*e.g.*, dle33, dle199) may be post-translationally modified, based on differences in mass.

A partial protein database for the eye of *A. californica* has been generated, and we now aim to identify potential components in the circadian oscillator or photoreceptor functions of the eye. Future directions include: increasing the scope of the database by using a more sensitive detection method, purifying the cellular components of the eye, and obtaining partial amino acid sequence data for eye-specific proteins.

This work was supported by NSF grant (BNS-9010115) and NIH grant (NS-21046) to FS. The authors thank Mary Lopez (Millipore Corp.), Rachel Cox, and Karen A. Lewis for their assistance in this project as well as Mr. David Leighty and Mr. Charles Vecoli (CSPI, Billerica, MA) for providing access to the MasterScan system.

Table I

A partial list of eye-specific proteins of Aplysia californica

Spot name	pI	MW
dle14	5.15	82.0[1]
dle17	5.06	82.0
dle37	5.50	44.5
dle127	5.78	59.0
dle133	5.71	57.9
dle234	6.37	28.7
dle613	6.41	33.2[t]
dle618	6.49	31.0[t]
dle699	6.55	31.0[t]
dle23	5.26	25.5
dle25	5.33	27.5
dle33	5.42	25.7[1]
dle199	5.42	26.7
dle200	5.19	26.3
dle201	5.20	25.5

[1] Possible isoforms.

[t] Appears only in eyes taken in July (summer; n = 2).

Composition of eye-comparison database: eyes (delensed) n = 4, BC n = 3, AG0BC n = 3. Replicates (n) are pooled samples (2 to 4 animals in each preparation); duplicates of each sample were also included in the database to estimate variability between runs and introduced by silver staining.

Literature Cited

1. **Strumwasser, F. 1987.** Pp. 298–310 in *Neurobiology, Molluscan Models*, North-Holland Publishing Co., Amsterdam.
2. **Strumwasser, F. 1989.** *J. Physiol. Paris* **83:** 246–254.
3. **O'Farrell, P. H. 1975.** *J. Biol. Chem.* **250:** 4007–4021.
4. **Patton, W. F., *et al.* 1990.** *BioTechniques* **8:** 518–527.
5. **Morrisey, J. H. 1981.** *Anal. Biochem.* **117:** 307–310.
6. **Celis, J. E., *et al.* 1991.** *FASEB J.* **5:** 2200–2208.
7. **Kandel, E. R. 1979.** Pp. 149–185 in *Behavioral Biology of Aplysia* W. H. Freeman and Co., San Francisco.

Effects of Vitamin E and OH-TEMPO (Spin Label Trap) on UV-Induced Dogfish (*Mustelus canis*) Lens Opacification Relative to Cytoskeletal Actin

S. Zigman (University of Rochester School of Medicine), N. S. Rafferty, and R. B. Wheeler, Jr.

Near-UV radiation is known to be involved in cataract formation. The microanatomical and photochemical basis for this damage seems to be related to UV effects on the cytoskeletal actin in lens epithelial cells (1, 2). The purpose of this study is to determine whether the damage to lens actin could be related to the action of free radicals or oxidants produced by UV-A irradiation.

Lenses of smooth dogfish in elasmobranch Ringer's solutions were incubated with 5% CO_2 and 95% air to maintain the pH at about 7.0 and were exposed to 2–3 mW/cm^2 of UV-A (99%) radiation for 15 h. Micro-anatomical and cytochemical techniques (*e.g.*, rhodamine-phalloidin fluorescence binding to actin) were used to observe the state of the filamentous actin in these cells. ^{31}P-NMR was used to measure ATP content.

In parallel, rabbit muscle actin (obtained from Dr. T. Pollard, MBL) in polymerizing buffer was exposed to the same light source for 17 h and actin then determined by sucrose density ultracentrifugation, polyacrylamide gel electrophoresis, and high pressure liquid chromatography. The influence of a free radical scavenger (vitamin E) and a spin label trap (OH-TEMPO) on the above parameters were further investigated. Several reports have shown these agents to protect against oxidation (3).

UV-exposed lenses developed a distinct, anterior, superficial opacity not present in the controls (see Fig. 1a). ATP levels were

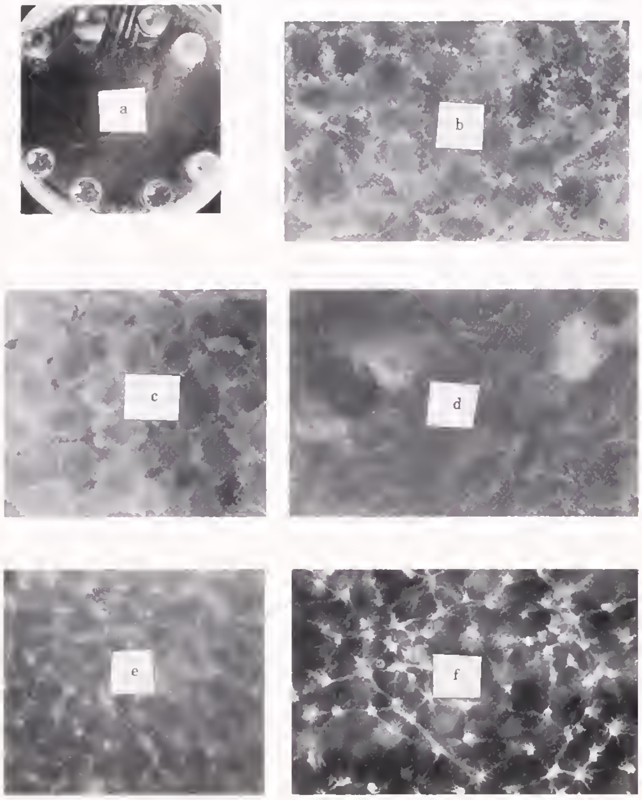

Figure 1. *Morphology and microanatomy of dogfish lenses exposed to UV-A radiation with or without modifiers. a) Opacities in whole lenses after 15 h of incubation: Lower row (left to right) dark control; with 0.1* mM *HT; with 1 mm HT, with 10* mM *HT; upper row (left to right) UV-exposed; with 0.1* mM *HT; with 1* mM *HT and with 10* mM *HT. (b–f) Rhodamine-phalloidin stained dogfish lens epithelial cells in whole mount (magnification 5250×) after 15 h incubation. b) Dark control; c) UV-exposed; d) UV-exposed plus α-tocopherol added at 25* μM*; e) dark control plus 10* mM *OH-TEMPO. f) UV-exposed plus 10* mM *OH-TEMPO added.*

depleted in the UV-exposed lenses by about 30–40% compared with dark controls. Thus, UV-A exposure lowered the ATP level concomitant with opacity formation.

UV-A-exposed lens epithelial cells contained few if any actin filaments, whereas in the dark controls filaments were prominent (see Fig. 1b, c). The degree of loss of these actin filaments due to UV-exposure was lessened when vitamin E was present in the medium (see Fig. 1d). However, OH-TEMPO caused a greater opacity and a greater degree of alteration of the actin filaments (Fig. 1e, f). When OH-TEMPO was added at 10 mM, a totally aberrant pattern of actin distribution was observed. The fluorescence due to phalloidin-rhodamine binding to actin was concentrated in intense spots near the lens cell membranes and interconnecting rays of filaments, forming star-like figures. Thus, opacification, ATP depletion, and F-actin breakdown all result from UV-A irradiation.

Purified rabbit muscle F-actin was also degraded by 5–20% into monomeric fragments due to UV-irradiation. HPLC data indicated that α-tocopherol (at 25 μM) neither protected nor enhanced UV-induced F-actin degradation.

We conclude that a photooxidative process degrades filamentous actin, and that α-tocopherol partially protects it in cells, whereas OH-TEMPO (the spin label trap) perhaps by acting as a photosensitizer, enhances this degradation. As α-tocopherol is known to be a free radical scavenger, its protective action may be related to quenching the UV-induced production of free radicals. The action of OH-TEMPO (a free radical) could be the result of a free radical attack on the actin polymer, leading to partial destabilization. The role of ATP diminution in this process is being investigated.

Supported by NIH (EY 00698 and EY 00459) and RPB, Inc.

Literature Cited

1. **Zigman, S. 1991.** *J Exp. Zool.* **5**(suppl): 29–40.
2. **Rafferty, N. S., *et al.* 1988.** *Biol. Bull.* **175**(abstr): 302.
3. **Reddan, J., *et al.* 1990.** *Int. Soc. Free Radical Res.* **9**: 171.

Towards the Development of a Technique for Introducing Aequorin into Amoebae of *Dictyostelium discoideum* Via Electroporation

Dawn M. Cishek (Marine Biological Laboratory), Richard H. Sanger, and Lionel F. Jaffe

Aequorin is a 22,000 molecular weight luminescent photoprotein that emits light at 470 nm when mixed with trace amounts of free calcium. It has been used extensively to image free calcium patterns, pulses, and waves as they occur in development (1). Ordinarily, aequorin is introduced into the cytosol of a single, large cell by microinjection. We are developing a technique by which aequorin can be mass-introduced to a great number of small animal cells at once, via electroporation. Electroporation is a relatively new technique in which a suspension of cells is subjected to one or a series of high voltage pulses. (Conventionally, 3–5 pulses of 2–5 kV/cm for 0.1–200 ms) The delivered pulse results in an electric field across each cell. When this field exceeds the dielectric strength of the cell membrane, the membrane breaks down in localized areas, forming "pores." If the field strength and pulse length are not excessive, then the pores will reseal after a brief time, leaving the cell intact and alive. If excessive, however, the cell membrane can be irreversibly damaged and the cells will lyse. While the pores are open, small molecules from the external medium can diffuse into the cytosol. Unfortunately, aequorin is not small enough to do this. Therefore, the conventional electroporation parameters must be modified. Instead of delivering a series of medium voltage, medium length pulses, we are going to electroporate in a two step process. First we will deliver a very high, very fast pulse. Then second, we will deliver a very long, very low voltage pulse. The theory is that the first will open pores and the second will not only keep the pores open, but also electro-osmotically drive the aequorin into the cytosol.

As a starting point, we repeated the work of Van Haastert *et al.* (1989), in which a 180 m.w. sugar was electroporated into amoebae of *D. discoideum*. We initially tried using a commercial device, but found that it could not deliver brief enough pulses for our purposes (control of pulse length is in the ms range.) The commercial equipment is intended to deliver long pulses through media several orders of magnitude less conductive than ours, therefore it is built with a very high capacitance and internal impedance. Because we were unable to modify the commercial device, we built our own. It is similar to the commercial one, but ours is able to deliver much faster pulses (*i.e.*, in the μs range as opposed to the ms range) at high voltages. (Fig. 1)

Once the equipment was built, we could begin to search for the electroporation conditions that would result in the greatest percentage of living, electroporated cells. Because aequorin is expensive and somewhat difficult to handle, we decided to begin our search using inexpensive fluorescent dyes, namely lucifer yellow CH (m.w. 487) and FITC-dextrans (m.w. 4400 and 10,000.)

Amoebae of *D. discoideum* are prepared for electroporation according to Van Haastert *et al.* (2). Cell suspensions, electroporation media, and the electroporation chamber are cooled to 0–4°C prior to electroporating. The cell suspension (0.75 ml) is mixed with the dye (0.25 ml) immediately prior to being placed in the electroporation chamber. The "chamber" is created by a 1.0 cm gap between two cylindrical aluminum electrodes, which are encased in plexiglass. The capacitors are charged to the desired voltage and the pulse is delivered through the cell suspension. The geometry of the chamber assures that a uniform field is delivered. After electroporation, the cell suspension is removed from the chamber and mixed with "healing medium" (2) and placed on ice for 10 min. Cells are washed by centrifugation three times in healing medium. The cells are examined for viability and uptake of dye, using both brightfield and fluorescence microscopy. Cell viability and dye uptake are the two criteria for judging the usefulness of each electroporation setting.

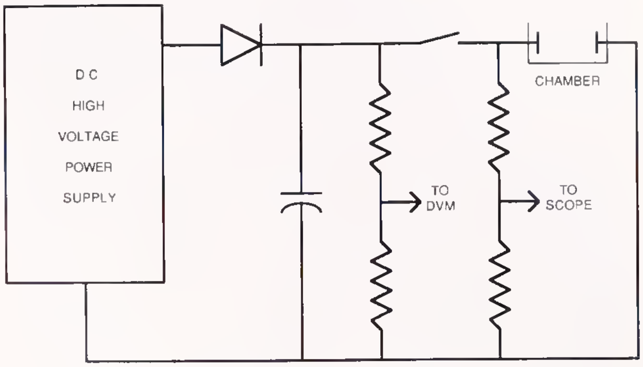

Figure 1. *Schematic of the electroporation device.*

Using lucifer yellow, we repeated the results of Van Haastert. Under the reported optimal conditions of two 7 kV pulses for 210 μs, we attained populations in which all living cells are stained, and the number of dead cells is not statistically attributable to electroporation.

Using FITC-dextran 4400, we attained populations in which 25% of the living cells are stained, and the number of dead cells is not statistically attributable to electroporation.

The next step in this research will be to use the larger dye, FITC-dextran 10,000. Once we have attained a high electroporation efficiency with this, we will begin using aequorin.

This work was supported by NSF and NIH grants to LFJ.

Literature Cited

1. **Blinks, J. 1982.** *Tech. Life Sci. Physiol.* V.P1/11.
2. **Van Haastert, P., *et al.* 1989.** *Biochem. J.* **258:** 577–586.

A Region of Steady High Calcium at the Vegetal Pole of Medaka Eggs

Lionel F. Jaffe (Marine Biological Laboratory), Andrew L. Miller, and Richard A. Fluck

Over a decade ago, it was conclusively demonstrated that a remarkable explosive wave of free cytosolic calcium travels from the animal pole to the vegetal pole following fertilization of the egg of the medaka fish (1). Since then it has been shown that such waves traverse a wide variety of, and perhaps all, deuterosome eggs, and may well be the explosive key that blasts the lock off the arrested development of unfertilized eggs. Such waves are propagated by calcium-induced calcium release and traverse a wide variety of eggs at a remarkably similar velocity of around 10 μm/s (2). In spite of the excitement at the confirmation of such a prominent and spectacular phenomenon, it was noted and recorded that the calcium wave lingered for some time at the vegetal pole of medaka. The significance of a domain of high calcium at the vegetal pole in early development, if indeed it was real, was subject to considerable speculation. However, such a phenomenon might be explained by two considerations that bear on the structure and early embryogenesis of the medaka egg. This large (1200 μm diameter) clear egg consists of a central membrane bound yolk mass with a thin (~40 μm thick) peripheral cytoplasm. Thus, the increased signal from the vegetal pole might be explained by the simple fact that there may be more cytoplasm at the vegetal pole or there might be an asymmetric distribution of the calcium recording molecule at this pole, perhaps explained by differential binding to some vegetal cytoskeletal element.

We have continued to use, as in the first report of calcium waves, the chemiluminescent photoprotein aequorin, as our method of choice for recording cytosolic free calcium. This technique has certain inherent and unique advantages that have been enhanced considerably by recent advances in aequorin chemistry (3). One of these, which was of great significance in addressing the question of the vegetal pole calcium hot spot, was the conjugation of fluorescein to aequorin. This enabled us to do a luminescence to fluorescence ratio correction, settling the question of unequal recorder molecule distribution. We also employed BAPTA type calcium shuttling buffers (4) to disperse any calcium hot spots at the pole.

Table I shows the results of a series of experiments where recombinant aequorin was microinjected into medaka eggs in combination with a fluorescein-labeled aequorin, dibromo-BAPTA, and a KCl blank. The injection technique was Hiramoto's quantitative low-pressure method (5). The procedures used to introduce a micropipette into the thin cytoplasmic layer of the medaka egg were those described by Gilkey (6). Apart from the eggs co-injected with dibromo-BAPTA, all of the others used in this study developed normally and hatched. The aequorin-generated luminescence was observed from eggs in their normal, blastodisc-down orientation with a Zeiss IM-35 inverted microscope, a Nikon Planapo 10/0.45 objective, and a 75 mm optical doublet, which together produced a 6× magnified image on the photocathode of an imaging photon detector or IPD (Imaging Technology Ltd., East Sussex, UK). This device consists of a microchannel plate intensifier with a resistive anode as the positional encoder (7). The raw data from the IPD consists of a sequential record of photon positions and times, measured one at a time. Our analysis involved counting photons in boxes placed at either the vegetal or animal poles, then dividing these numbers by those collected from similar sized boxes placed at the equator of the egg. The IPD was also used to acquire signal from the photoexcitation of fluorescein-labeled aequorin. A similar form of analysis was employed, and the true corrected luminescent ratios between the poles and the equator were calculated.

From Table I it is clear that even after the fluorescence correction, there is approximately three times more luminescence at the vegetal pole than at the equator of the egg. As calcium varies with the cube-root of the luminescence, this equates to a cytosolic free calcium level at the vegetal pole some 50% higher than the background level of the egg. This steady vegetal calcium hot spot persists up to 100 min after fertilization. The introduction of dibromo-BAPTA disperses the calcium in a manner explained by facilitated diffusion theory (4). This can be clearly seen by the reduction in pole to equator ratios. In addition to the confirmation of the vegetal calcium hot spot, it is also clear that the increase in signal at the animal pole cannot be explained simply by the accumulation of cytoplasm at the pole during embryogenesis. The fluorescent correction indicates that there is also an elevation in animal pole cytosolic free calcium during blastodisc segregation.

We conclude that domains of high free calcium do exist at both the vegetal and animal pole of the medaka egg for at least 100 min after fertilization, and therefore, that calcium gradients exist in the ooplasm of the egg during this time.

Supported by NSF DCB-8811198 (Amendment 01) to LFJ and DCB-9017210 to RAF.

Table I

Aequorin luminescence ratios (± SEM's) at the animal and vegetal poles of the medaka egg less than 100 min after fertilization

Injectate(s)	n	*Animal pole* Equator	*Vegetal pole* Equator
Aequorin	11	8.7 ± 3.4	3.0 ± 0.7
Aequorin + BAPTA	10	3.6 ± 0.8	1.6 ± 0.3
Aequorin + KCl	4	7.8 ± 1.9	3.0 ± 0.5
Aequorin + Fl-aequorin	9	4.9 ± 1.6	3.4 ± 1.4

Seven × seven pixel wide boxes were positioned at the animal pole or vegetal poles and divided by a similar sized box placed at the equator of the egg. In the case of the aequorin + fl-aequorin co-injection, the luminescence ratios between the poles and the equator were corrected for aequorin distribution.

Literature Cited

1. **Gilkey, J. C., *et al.* 1978.** *J. Cell Biol.* **76:** 448–466.
2. **Jaffe, L. F. 1991.** *Proc. Natl. Acad. Sci. USA* in press.
3. **Shimomura, O., *et al.* 1989.** *Biochem. J.* **261:** 913–920.
4. **Speksnijder, J. E., *et al.* 1989.** *Proc. Natl. Acad. Sci. USA* **86:** 6607–6611.
5. **Hiramoto, Y. 1962.** *Exp Cell Res.* **27:** 416–426.
6. **Gilkey, J. C. 1983.** *J. Cell Biol.* **112:** 711–718.
7. **Speksnijder, J. E., *et al.* 1990.** *J. Cell Biol.* **110:** 1589–1590.

Calcium Buffer Injections Block Cytokinesis in *Xenopus* Eggs

Jane A. McLaughlin (Marine Biological Laboratory), Andrew L. Miller,
Richard A. Fluck, and Lionel F. Jaffe

Vincent *et al.* (1) reported that injections of EGTA giving final cytosolic concentrations of about 8 mM had no detectable effects on cytokinesis; but final concentrations of about 30 mM delayed first division in half the eggs, while blocking second division in all injected eggs. [We have doubled the values given by Vincent *et al.* because they assume an accessible volume that is half that of the whole *Xenopus* egg; the true figure seems close to a quarter (2, 3)]. Inhibition at such extremely high buffer concentrations might well suggest that calcium is **not** involved in the natural control of cytokinesis in *Xenopus* eggs. However, the results of our study of buffer inhibition in fucoid eggs (4) suggested a reinvestigation with another buffer more closely matched to the calcium level in the cytosolic region responsible for initiating and driving the division process (5). Table I shows the results of injecting 5,5′-dibromo-BAPTA, a buffer with a cytosolic K_D of about 5 μM. The lower figure in each range corrects for total accessible volume, on the assumption that about 20% of the egg volume is accessible to the injected buffer; buffer accessibility was calculated, in turn by taking 70% of the egg volume as inaccessible yolk (2) and about 70% of the cytosol as water (3). The higher figure in each range takes into account the likelihood that, at the time of action, the buffer had diffused out through a sphere only about 800 μm in diameter instead of filling the whole 1200 μm diameter egg.

Table I

Inhibition of Xenopus *egg cleavage by the injection of 5,5′-dibromo-BAPTA calcium buffer*

Buffer conc. (mM)	n	Avg. first cleavage delay (minutes)	Death (hours)
2.0–0.6	40	180	≈6
0.76–3.3	69	100	≤24
0.23–1.4	40	25	None
0.10–0.45	120	7	None
0.007–0.24	50	No effect	None

Injection at 40 to 100 min after insemination. Done at 15°C, at which first cleavage begins in uninjected controls about 3 h after fertilization. Eggs were co-injected with 0.1 mol of Ca^{2+} per mol of buffer ($K_d = 3.6 \times 10^{-6}$ M).

This buffer is about one hundred times more effective than EGTA in delaying or blocking cytokinesis. Detectable delays occur in response to final cytosolic buffer concentrations as low as 0.1 mM. This finding supports both the hypothesis that calcium controls cytokinesis, and the validity of the following equation (4) in *Xenopus* eggs:

$$B = rC \cdot (D_{Ca}/D_B) \cdot [(1 + f)^2/f]$$

where: B is the total concentration of buffer within the cytosol needed to facilitate calcium diffusion r-fold; C is the concentration of free calcium within the biologically effective, dynamically maintained high calcium zone; D_{Ca} and D_B are rough values for the cytosolic diffusion constants (640 and 38 μ^2/s) of free calcium and of BAPTA-type calcium buffers respectively; $f = K_D/C$, where K_D is the calcium dissociation constant of the particular buffer employed.

Further support for these points emerges from two further quantitative tests. First, the total calcium found in *Xenopus* eggs during early cleavages is about 8 m-mole/liter egg (6), which about equals the 7.5 m-mole/liter egg of EGTA in the highest dose injected by Vincent *et al.* This rough equivalence is consistent with our assumption that a combination of release from internal reserves, plus some entry from the medium, provided enough calcium to neutralize the EGTA injected by Vincent *et al.* Second, the observed inhibitory buffer concentrations are consistent with the above equation if some quite reasonable assumptions are made. Specifically, if one assumes that doubling the effective diffusion constant of calcium will suffice to barely inhibit cytokinesis (*i.e.*, r = 1), that the calcium in the "target" zone or C is 5 μM, that D_{Ca}/D_B for dibromo-BAPTA is 17 (4), and for the smaller EGTA molecule about 10, and that K_D for EGTA is about 0.01 μM (7), then the equation predicts just inhibitory levels of dibromo-BAPTA and of EGTA of 0.4 and 30 mM, respectively.

In a second series of experiments, we delayed buffer injection until furrow initiation had clearly begun at the animal pole. The cytosolic concentration range of buffer (based on the same assumptions as above) was 1.5–5.1 mM. In 15 cases, we consistently arrested the first cleavage furrow as it progressed across the animal hemisphere. This suggests that the buffer may be delocalizing an elevated calcium region directly involved in the furrowing process, as opposed to indirectly inhibiting cytokinesis through some earlier calcium-dependent event occurring during the cell cycle.

Supported by NSF grants DCB-8811198 (Amendment 01) to LFJ and DCB-9017210 to RAF.

Literature Cited

1. **Vincent, J. -P., *et al.* 1987.** *Cell. Motil. Cytoskel.* **8:** 143–154.
2. **Kline, D. 1988.** *Dev. Biol.* **126:** 346–361.
3. **de Laat, S. W., *et al.* 1974.** *Exp. Cell Res.* **89:** 1–14.
4. **Speksnijder, J. E., *et al.* 1989.** *Proc. Natl. Acad. Sci. USA* **86:** 6607–6611.
5. **Fluck, R. A., *et al.* 1991.** *J Cell Biol.* In press.
6. **Slack, C., *et al.* 1973.** *J. Physiol. Lond.* **232:** 297–312.
7. **Rink, T. J., *et al.* 1980.** *Nature* **283:** 658–660.

Effect of Hydrogen Peroxide on Preventing or Contributing to Polyspermic Fertilization in Sea Urchin: Modification by Tamoxifen and Macroglobulin

Margalit Rosenkranz, Jong S. Lim, Krystyna Frenkel, and Walter Troll
(New York University Medical Center)

The sea urchin has been described recently as "the most facile experimental system for studying molecular mechanisms of fertilization" (1). A major contributor to successful fertilization is the induction of hydrogen peroxide (H_2O_2), which is produced, with the participation of protein kinase C, by the oxidative burst caused by the sperm's entry into the ovum. During the oxidative burst, NADPH reduces oxygen to superoxide anion radical ($\cdot O_2^-$) in a NADPH-oxidase catalyzed reaction, and H_2O_2 is formed by dismutation of $\cdot O_2^-$. H_2O_2 could prevent entry of other sperms in two ways: conversion by myeloperoxidase to hypochlorite, which would kill excess sperms (2) that are ready to enter and fertilize the ova; and by hardening the cell envelope by a cross-linking reaction catalyzed by a peroxidase that couples the tyrosyl residues between proteins (1). The oxidative burst induced by the sperm's entry has a mechanism similar to that induced by a tumor promoter, such as 12-0-tetradecanoyl-phorbol-13-acetate (TPA) in human neutrophils; *i.e.*, both involve the production of H_2O_2. In contrast, many chemopreventive agents, including protease inhibitors (that are capable of inhibiting chymotrypsin) and tamoxifen (an anti-cancer agent), suppress the formation of H_2O_2 in TPA-treated human neutrophils (3, 4).

We report four primary results of this year's work. 1) H_2O_2 induces the formation of a fertilization envelope in the absence of sperm. 2) H_2O_2 initiates an irregular division of the ovum. 3) Tamoxifen (a suppressor of H_2O_2 production in neutrophils), added before fertilization, prevents the formation of a hardened fertilization envelope. Moreover, if sperm are added, irregular division follows. In contrast, a pure antiestrogen (an activator of H_2O_2 formation in neutrophils) induces a hardened fertilization envelope, and the addition of sperm fails to lead to fertilization. 4) Finally, the addition of the protease inhibitor β-macroglobulin (purified from human plasma) before fertilization prevents the formation of the fertilization envelope, and irregular cleavage follows the addition of sperm.

Exogenous hydrogen peroxide added to sea urchins forms a hardened fertilization envelope as expected (1). In addition, it also causes uneven division mimicking the type of division produced by the entry of multiple sperms when a hardened fertilization envelope has not formed. We speculate that the entry of many sperms forms hydrogen peroxide by causing many oxidative bursts identical to that caused by the first sperm, and finally hardening the envelope. Hydrogen peroxide has been shown in many systems, including phorbol ester treated neutrophils, to cause oxidated modification of DNA bases—thymine glycol, 5-hydroxymethyl uracil and 8-hydroxyl guanine (5, 6). This type of modification may contribute to faulty division in sea urchins, as in tumor promotion.

Chemopreventive agents that are capable of interfering with tumor promotion also suppress the oxidative burst mediated by the tumor promoter, TPA, in human neutrophils. The same agents inhibit the oxidative burst initiated by the entry of the fertilizing sperm and cause fertilization envelope formation to fail; this, in turn, results in polyspermic fertilization.

For example, tamoxifen, the agent designed to interfere with estrogen-mediated breast cancer, suppresses the oxidative burst in human neutrophils and prevents formation of the hardened envelope in sea urchins as well. This activity is distinct from its ability to interfere with estradiol's effects, because we found that the specific antiestrogen ICI 164,384 has the opposite action. It mediates production of H_2O_2 in neutrophils, as well as the formation of a fertilization envelope, thus preventing fertilization. Estradiol slightly inhibits H_2O_2 production and causes polyspermy but at a concentration about ten times higher than that of tamoxifen.

β-Macroglobulin [the universally occurring inhibitor of virtually all proteases (7)] causes polyspermy in sea urchins at nanomolar concentrations. Perhaps its not as yet established function is to modulate the oxidative burst, which could cause multiple types of damage including tumor promotion.

We especially want to thank Dr. Catherine O'Brian for her advice and for providing samples, and ICI Pharmaceuticals (Cheshire, England) for their generous gift of antiestrogens. This report was supported in part by NIEHS grant numbers 1 P42 ES 04895 and ES 00260, and by grant numbers CA 53003 and CA 37858 from the National Cancer Institute. Its contents are solely the responsibility of the authors and do not necessarily represent the official views of the National Cancer Institute.

Literature Cited

1. **Shapiro, M. B. 1991.** *Science* **252:** 533–536.
2. **Frenkel, K., *et al.* 1986.** *J Cell. Biochem.* **30:** 181–193.
3. **Frenkel, K., *et al.* 1987.** *Carcinogenesis* **8(9):** 1207–1212.
4. **Troll, W., and J. S. Lim. 1991.** *Proc. Am. Assoc. Cancer Res.* **32:** 149.
5. **Frenkel, K. 1989.** *Environ. Health Perspect.* **81:** 45–54.
6. **Wei, H., and K. Frenkel. 1991.** *Cancer Res.* **51:** 4443–4449.
7. **Armstrong, P. B., *et al.* 1991.** *J Biol. Chem.* **266:** 2526–2530.

Evaluation of Spermatocidal Activity of Water Soluble Gossypol on the Sperms of *Arbacia punctulata* and *Spisula solidissima*

Hiroshi Ueno (Rockefeller University), Tatsuji Haneji, Yumiko Ueno,
Samuel S. Koide, and Sheldon J. Segal

Gossypol (GP), a phenolic aldehyde isolated from cotton seed, exhibits various biological activities. *In vitro* effects include inhibition of sperm motility (1), inactivation of some parasites (2), and inhibition of the infectivity of HIV (3). GP is lipophilic and has a maximum attainable concentration in aqueous media of about 100 μM. Although an effective dose for the *in vitro* activities is around 1–10 μM, 10-fold higher doses are required when 5% serum albumin is present in the medium. In some studies, high concentrations of GP are desired to establish dose-response relationships, and this proves difficult because of the limited aqueous solubility. This problem has hampered the development of potentially useful pharmaceutical preparations of GP, such as a protective vaginal cream (4).

Water soluble gossypol (GP-S) was prepared at the Institute of Bioorganic Chemistry, Uzbek Academy of Science (Tashkent, USSR). The content of gossypol in GP-S was determined by optical absorption spectrophotometry. The spectrum was analyzed for its shape by log-normal curve fitting analysis, as described by Metzler *et al.* (5). GP-S contains 7.5% gossypol (w/w), based upon its spectral analysis in 1 *N* NaOH and an apparent molar absorptivity of 22,000 $cm^{-1} M^{-1}$. We were able to prepare up to 6 mM GP-S solution in aqueous media (*i.e.*, 0.1 M potassium phosphate buffer, pH 8.0). Spectra at different pHs (2–11) showed the identical shift, as observed with the GP standard. *Arbacia* and *Spisula* sperms were used, as described before (6), to examine the potency of GP-S to inhibit sperm motility. Figure 1 shows the effect of GP-S on the fertilizability of *Arbacia* sperms. Fifty percent inhibition is observed at 10 μM of GP-S. Complete inhibition is observed at doses greater than 100 μM. Identical results were obtained with *Spisula* sperms (data not shown). The present results reveal that GP-S can inhibit sperm motility at concentrations equivalent to those of GP (7).

Kanwar *et al.* (8) previously reported that gossypol (10 μM) reduced the $^{45}Ca^{++}$ uptake (25%) of isolated human spermatozoal plasma membrane vesicles. This effect of GP-S upon calcium uptake was further examined with whole sperms from *Spisula*. Sperms were collected from clams, suspended, and washed in Ca^{++}-free artificial seawater (MBL). Time-dependent incorporation of $^{45}Ca^{++}$ into intact sperm was examined by: 1) incubating the sperm suspension with $^{45}Ca^{++}$ (10 μCi) at time zero, 2) taking aliquots at various time periods, 3) placing the aliquots on filter papers (Whatman GF-C) under the vacuum for repeated washing with the solution containing EGTA, then 4) counting the label incorporated into the filter paper with a Beckman scintillation counter. We observed an immediate incorporation of $^{45}Ca^{++}$ into intact sperm, which occurred within the first minute; a steady state was then maintained during the subsequent 40 min, followed by a slight reduction.

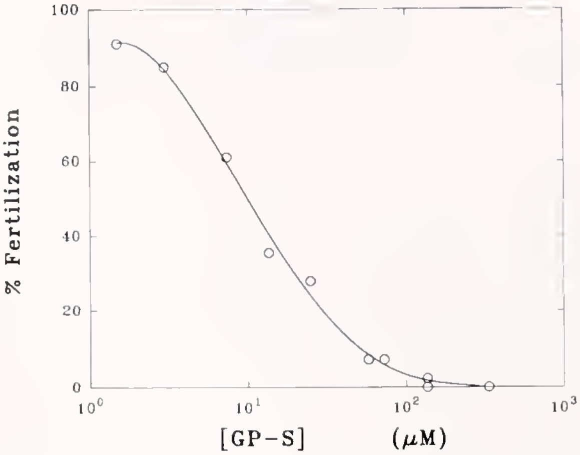

Figure 1. *Effect of water soluble gossypol (GP-S) upon the fertilizability of* Arbacia *sperm. The percent of fertilization of* Arbacia *oocytes was plotted against the concentration of GP-S in the incubation medium. A freshly prepared* Arbacia *sperm suspension in filtered seawater was incubated with the indicated amounts of GP-S for 5 min. Aliquots of sperm suspension were mixed with an oocyte suspension prepared in filtered seawater and maintained at room temperature for 2 h. Percent fertilization was derived by counting 50–200 eggs, in triplicate. Detailed procedure was described earlier (6).*

The effect of pre-treating intact sperm with GP-S was tested. Sperms were suspended in calcium-free seawater and preincubated with GP-S (0–100 μM) for 5 min prior to the addition of $^{45}Ca^{++}$ (10 μCi). After a 5-min incubation with $^{45}Ca^{++}$, aliquots of sperm suspension were placed on the filter paper, washed three times with water, and then counted for $^{45}Ca^{++}$ incorporation. The concentrations above 10 μM GP-S inhibited calcium uptake by about 30% compared with the control, which was similar to the results reported for isolated plasma membrane vesicles treated with GP (8). However, the concentrations below 10 μM, GP-S (1 and 0.1 μM) enhanced calcium uptake by more than 30%. A similar paradoxical effect was observed when studying the influence of GP on oxygen uptake of intact sperm (9). At high doses (above 10 μM), gossypol inhibited oxygen consumption, but at lower doses it increased oxygen consumption. This was probably due to GP acting to uncouple sperm respiration. The present results suggest that the respiration and calcium uptake mechanisms in sperm are tightly coupled.

In conclusion, water-soluble gossypol is an active spermatocidal agent that retains the spermatocidal activity and properties of GP. This water-soluble gossypol can be used to develop a vaginal cream with spermatocidal and virucidal activities.

The work was supported by a grant GAPS-9032 from the Rockefeller Foundation.

Literature Cited

1. **Segal, S. J. (ed.) 1984.** *Gossypol.* Plenum Publishing Co., NY.
2. **Eid, J. E., *et al.* 1988.** *Exp. Parasitol.* **66:** 140–142.
3. **Polsky, B., *et al.* 1989.** *Contraception* **39:** 579–587.

4. **Segal, S. J., and Ueno, H. 1989.** *Biol. Bull.* **177:** 316.
5. **Metzler, C. M., *et al.* 1980.** *J. Am. Chem. Soc.* **102:** 6075–6082.
6. **Segal, S. J., *et al.* 1985.** *Biol. Bull.* **169:** 543–544.
7. **Burgos, M. H., *et al.* 1980.** *Biol. Bull.* **159:** 467.
8. **Kanwar, U., *et al.* 1989.** *Contraception* **39:** 431–445.
9. **Ueno, H., *et al.* 1987.** *Biol. Bull.* **173:** 428.

KCl-Induced Calcium Rise in Squid Eggs: Measurement of Fura-2 Fluorescence

Rui Wang, Lingyun Wu, Andrew L. Miller, John M. Arnold,
and Lionel F. Jaffe (Marine Biological Laboratory)

Sperm break the block to development in unfertilized eggs by somehow inducing a large increase in intracellular free Ca^{2+} ($[Ca^{2+}]_i$). The mechanisms and sources for the increase in $[Ca^{2+}]_i$ have been hypothesized to be different in deuterostome and protostome eggs (1). A release of intracellular Ca^{2+} upon fertilization plays a major role in the regenerative and explosive increase in $[Ca^{2+}]_i$ in deuterostome eggs. By contrast, extracellular Ca^{2+} entry may be more important for the prolonged increase in $[Ca^{2+}]_i$ in protostome eggs. However, solid evidence substantiating this hypothesis in protostome eggs is limited. Squid eggs are unique in their size, mode of development, and phylogenetic position among protostomes (2). We have used these eggs to 1) investigate the existence of voltage-dependent calcium channels in unfertilized egg membranes, 2) establish the methodology of the fura-2 fluorescence measurement, and 3) correlate KCl-induced Ca^{2+} rise with egg activation.

Squid (*Loligo pealei*) were provided by the Marine Resources Department of the Marine Biological Laboratory during July and August. Clear, mature eggs were collected from the oviduct of female squid and washed several times with aerated millipore filtered artificial seawater (ASW). These eggs were put on coverslips, coated with poly-l-lysine, and maintained in ASW. A dual-excitation photometer (Deltascan; Photon Technology Inc.) was combined with the fura-2 technique (3) to measure $[Ca^{2+}]_i$. Eggs were loaded with 10 μM fura-2/AM [the membrane-permeable form, dissolved in dimethyl sulfoxide (DMSO)] for 3 h at room temperature, in the dark. Subsequently, the eggs were thoroughly washed with ASW and then mounted on the stage of an epifluorescence inverted microscope (Nikon diaphot). The fluorescence ratio obtained with two excitation wavelengths, *i.e.*, 350 nm and 380 nm, was used to monitor the relative $[Ca^{2+}]_i$. EGTA (1 m*M*) was added to nominally Ca^{2+}-free ASW to make Ca^{2+}-free artificial seawater (CaFASW). The appearance of polar bodies 1 h after the addition of either KCl or sperm was taken as indicating that the squid eggs had been activated or fertilized. All experiments were executed with batches of eggs exhibiting less than 6% spontaneous activation.

Intracellular fura-2 loading was reproducible in every batch of squid eggs. High concentration of extracellular K^+ applied to squid eggs maintained in ASW increased $[Ca^{2+}]_i$; two patterns of this effect were observed (Fig. 1). First, rapid increase in $[Ca^{2+}]_i$ induced by 15 m*M* KCl was seen in eight eggs (fast pattern). The increase in $[Ca^{2+}]_i$ was maximally developed within 1 min and was maintained at this enhanced level for more than 10 min after the addition of KCl. Moreover, this increased $[Ca^{2+}]_i$ did not tend to decay subsequently. In another group of eggs, 15 m*M* KCl only induced a slow increase in $[Ca^{2+}]_i$ (n = 5) (slow pattern). Here, $[Ca^{2+}]_i$ gradually rose over 30 min after the application of KCl. Only the slow pattern of increase in $[Ca^{2+}]_i$ could be induced by 15 m*M* KCl in eggs that were exposed to CaFASW. Furthermore, the amplitude of KCl-induced slow increase in $[Ca^{2+}]_i$ in eggs bathed in CaFASW was approximately 37% (n = 3) of that in eggs bathed in ASW. These results suggest that a high concentration of extracellular K^+ can increase $[Ca^{2+}]_i$ by acting on both extracellular and intracellular calcium pools with extracellular pool as the major source. In eggs exposed to ASW without a KCl challenge, neither pattern of $[Ca^{2+}]_i$ change could be observed.

After correcting for the spontaneous activation, we found that 26 ± 6% and 22 ± 6% of eggs, respectively loaded and not loaded with fura-2, were fertilized 60 min after the addition of squid sperm. DMSO alone did not affect the percentage of fertilization of eggs. Morphological observation also revealed that 15 m*M*

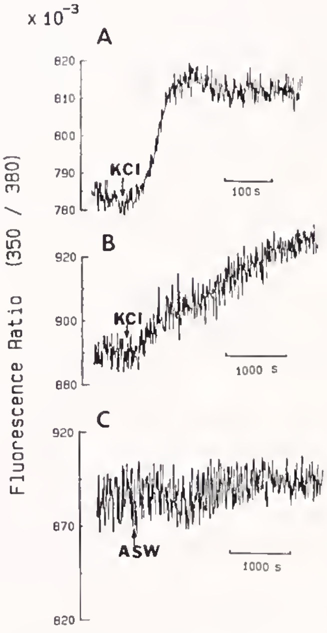

Figure 1. *KCl-induced increase in $[Ca^{2+}]_i$ in squid eggs. The eggs were bathed with 2 ml ASW in Petri dish. A. Addition of KCl at a final concentration of 15 mM induced a rapid increase in $[Ca^{2+}]_i$. B. Addition of KCl at a final concentration of 15 mM induced a slow increase in $[Ca^{2+}]_i$. C. Addition of 10 µl ASW (control) did not affect $[Ca^{2+}]_i$.*

KCl activated 15.5 ± 0.4% eggs bathed in ASW, which was significantly higher than the percentage of eggs that were activated spontaneously (5.6 ± 0.3%; $P < 0.05$).

While sperm-induced calcium entry has been demonstrated in other protostome eggs, such as those of Urechis, by use of a $^{45}Ca^{2+}$ uptake technique (4), our report is the first one, using the fura-2 technique, to provide the indirect evidence that a voltage-dependent pathway for the extracellular Ca^{2+} entry exists in unfertilized squid eggs. However, it is worth noting that KCl also induced a $[Ca^{2+}]_i$ rise via an extracellular-Ca^{2+} independent mechanism. Furthermore, because fura-2 loading did not interfere with the fertilization process, the methodology of using the fura-2 technique in squid eggs should greatly facilitate further efforts to correlate $[Ca^{2+}]_i$ change with fertilization in squid eggs.

This work was partly supported by the Grass Foundation. The insightful discussions with and sage advice from Drs. Worden and Moorman are acknowledged.

Literature Cited

1. **Jaffe, L. F. 1983.** *Dev. Biol.* **99:** 265–276.
2. **Arnold, J. M. 1974.** *A Guide to Laboratory Use of the Squid* Loligo pealei. Pp. 18–44. Marine Biological Laboratory, Woods Hole, Mass.
3. **Grynkiewicz, G., *et al.* 1985.** *J. Biol. Chem.* **260:** 3440–3450.
4. **Jaffe, L. A., *et al.* 1979.** *J Gen. Physiol.* **73:** 469–492.

Differences in Free Calcium Concentration Between Oocytes and Nurse Cells Revealed by Corrected Aequorin Luminescence

Richard I. Woodruff, Andrew L. Miller, and Lionel F. Jaffe (Marine Biological Laboratory)

In the ovarian follicles of the moth, *Hyalophora cecropia,* free Ca^{++} is not evenly distributed. Luminescence of microinjected aequorin suggests that internal Ca^{++} activity (Ca_i) is 50% higher in the oocytes than in the attached nurse cells. Each follicle consists of epithelium surrounding an oocyte and seven nurse cells; the latter cells supplying the oocyte with the RNA used in early development. The nurse cells communicate with the oocyte by >30 μm wide intercellular bridges, across which there is an electrical gradient of 2–10 mV. This gradient is such that nurse cells are more electronegative than the oocyte to which they are attached (1–3). The electrical gradient influences the movement of macromolecules through the bridges and thus brings about different equilibrium concentrations in each cell type, dependent on the charge on the molecules (2–5). It now appears that Ca^{++} may contribute either directly or indirectly to this electrical gradient.

Ovaries were dissected from female *Hyalophora cecropia* pupae in the 18th day of the pupal-adult molt. Follicles were maintained in physiological salt solution (PSS) to which 10% cell free blood was added (6). Following removal of the ovariole sheaths, the follicles were treated with collagenase (1 mg/ml PSS) to soften the basement membrane (3). Microinjections were performed using a Leitz micromanipulator and a Medical Systems Corp. PLI-100 microinjector system. Microinjected follicles were viewed with a Zeiss IM-35 microscope coupled to an ultra-sensitive imaging photon detector (7). To visualize the distribution of internal ionic Ca^{++}, 10 n l or less of a 0.62% recombinant aequorin solution, luminescence of which is dependent on free Ca^{++} (8), was injected into either the oocyte or one nurse cell of each follicle. Because the protein may not distribute evenly among the cells, it is essential to know the final distribution of the aequorin. Relative differences in virtual path length (thickness of tissue and relative opacity) through different parts of the follicle also must be considered. To accomplish this, aequorin to which fluorescein had been conjugated was mixed with unconjugated aequorin, and the two forms co-injected. The imaging photon detector was used to acquire signals either from the fluorescence of photoexcited conjugated aequorin, or from the Ca^{++}-induced luminescence of unconjugated aequorin. The acquired photon counts were stored on the Winchester drive of a Compuadd 200 computer.

Analyses of both the fluorescent and the luminescent images were performed by selecting representative 25 × 25-pixel blocks from the background, from the oocyte, and from the nurse cells and tabulating the number of photons/s recorded from each of these areas. After correction for background, oocyte luminescence ÷ nurse cell luminescence × nurse cell fluorescence ÷ oocyte fluorescence adjusts for differences in the concentration of aequorin between the two cell types and also for differences in

Table I

Corrected luminescent ratios between oocytes and nurse cells (N.C.)

Oocyte/N.C. complex number	Oocyte: N.C. corrected luminescent ratio	Oocyte injected	N.C. injected	Time after aequorin inject. (mins.)
July 302 (i)	1.7	+	−	40
July 302 (ii)	4.1	+	−	92
July 304 (i)	1.5	+	−	170
July 304 (ii)	2.3	+	−	180
July 305 (i)	3.8	+	−	206
July 305 (ii)	4.2	+	−	224
July 307*	2.1	+	−	272
July 308*	2.8	+	−	291
July 309*	1.9	+	−	306
July 311	2.4	−	+	250
July 312	6.5	−	+	270
July 313	2.4	−	+	292
July 315	2.2	−	+	335
Avg. Ratios	2.9 ± 0.4	2.7 ± 0.4	3.4 ± 1.1	

* *Unlike the other complexes, these did not undergo a collagenase treatment before microinjection of aequorin.*

their virtual path lengths. Thus, data were obtained, which gave the distribution of aequorin and also the relative Ca_i corrected for background, path length, and asymmetric aequorin distribution. Observation of follicles began within 40 min after microinjection, and continued either continuously or intermittently for several hours. By the following day, injected cells retained levels of photon emission comparable to those seen at the beginning of their incubation. This continued luminescence demonstrated that the membranes were still competent to exclude external Ca^{++}. Therefore, at least by this criterion, the follicles remained healthy even 24 h after aequorin was introduced into the cytoplasm.

Microinjected aequorin distribution was measured in nine oocyte injected follicles and four nurse cell injected follicles. In the oocyte injected follicles the electronegative aequorin remained more concentrated in the oocyte than in the nurse cells, in agreement with the pattern found previously for other electronegative microinjected proteins (1–3). An additional five follicles, into which only unconjugated aequorin had been microinjected, showed the same pattern. In addition to the four nurse cell injected follicles indicated in Table 1, two more follicles received their injections into nurse cell nuclei, where most of the microinjected aequorin remained. This nuclear-bound aequorin revealed a continuing high level of calcium activity. In each of the four nurse cell injected follicles, aequorin had already reached the ooplasm by the time the follicles were examined 40 min after the injection.

As the corrected luminescence of aequorin is around 3 times greater in the oocyte than in the attached nurse cells (Table 1), we estimate Ca_i to be 50% higher in the oocyte (9). Because oocytes are less negatively charged when compared to their nurse cells (3), higher Ca_i in the ooplasm can not be explained by Ca^{++} following its' electrochemical gradient. Indeed, the distribution of Ca_i between oocyte and nurse cells revealed by aequorin suggests that Ca^{++} may play a major role in the establishment of the transbridge potential between these two cell types.

This research was supported in part by a grant from the National Institutes of Health (AI28852) (RIW), and in part by a grant from the National Science Foundation (DCB-811198, amendment 01).

Literature Cited

1. **Woodruff, R. I., and W. H. Telfer. 1973.** *J. Cell Biol.* **58:** 172–188.
2. **Woodruff, R. I., and W. H. Telfer. 1980.** *Nature* **286:** 84–86.
3. **Woodruff, R. I., and W. H. Telfer. 1990.** *Dev. Biol.* **138:** 410–420.
4. **Woodruff, R. I., *et al.* 1988.** *Roux's Arch. Dev. Biol.* **197:** 231–238.
6. **Woodruff, R. I., *et al.* 1986.** *Dev. Biol.* **117:** 405–416.
7. **Speksnijder, J. E., *et al.* 1990.** *J. Cell Biol.* **110:** 1589–1590.
8. **Shimomura, O., *et al.* 1990.** *Biochem. J.* **270:** 309–312.
9. **Blinks, J. R. 1982.** *Tech. Cell Physiol.* **126:** 1–38.

Protease-Binding Activity of *Limulus* α_2-*Macroglobulin*

Peter B. Armstrong (Laboratory for Cell Biology, Department of Zoology, University of California, Davis, CA 95616-8755), Atsushi Ikai, and James P. Quigley

α_2-Macroglobulin (α_2M), a major protease-binding protein in the plasma of vertebrates and invertebrates, has been proposed to be the mediator of an evolutionarily conserved immune defense system (1). In vertebrates, binding of proteases by α_2M involves both non-covalent and covalent modes. Non-covalent binding involves a physical folding of α_2M around the protease molecule to "trap" it in the folds of an α_2M "cage" (2). The change in conformation of α_2-macroglobulin necessary for physical entrapment of proteases can be detected by its faster migration during non-denaturing polyacrylamide gel electrophoresis (3). Covalent binding involves the establishment of isopeptide bonds between nucleophilic residues on the protease and the γ-carbonyl of a unique reactive internal thiol ester that becomes activated following proteolysis of α_2M. The covalent binding can be shown by the presence of protease-containing high molecular mass complexes following SDS-polyacrylamide gel electrophoresis (4). It has been proposed that the high molecular mass complexes formed by this mode of covalent binding contain one or several fragments of α_2M linked by the protease molecule (4, 5). The involvement of the thiol ester in covalent binding can be demonstrated by the abolition of binding following pretreatment of α_2M with small amines, such as methylamine, that inactivate the thiol ester. Although tetrameric human α_2M can react successfully with proteases without forming covalent bonds, dimeric and monomeric forms of mammalian α_2M require isopeptide bond formation for binding (6, 7).

The form of α_2-macroglobulin in the blood of the American horseshoe crab (designated LAM for *L*imulus α_2-*m*acroglobulin) reacts with proteases of all major classes to inhibit activity against protein substrates (8, 9) and is organized as a homo-dimer (10). LAM binds one mole of protease per mole of dimer (data not shown). During reaction with proteases, LAM undergoes a major conformational compaction, as evidenced by more rapid mobility in non-denaturing polyacrylamide gel electrophoresis and slower migration during size exclusion chromatography. The extent of compaction is larger than that of human α_2M: human α_2M experienced a 28% increase in mobility in non-denaturing polyacrylamide gel electrophoresis, whereas LAM experienced a 38% increase.

LAM establishes isopeptide bonds following reaction with proteases (Fig. 1). As determined by reducing SDS-PAGE, the subunit of native LAM has a molecular mass of 185 kDa (lane 2). High molecular mass bands of apparent molecular masses 200, 250, and 300-350 kDa were present following reaction with

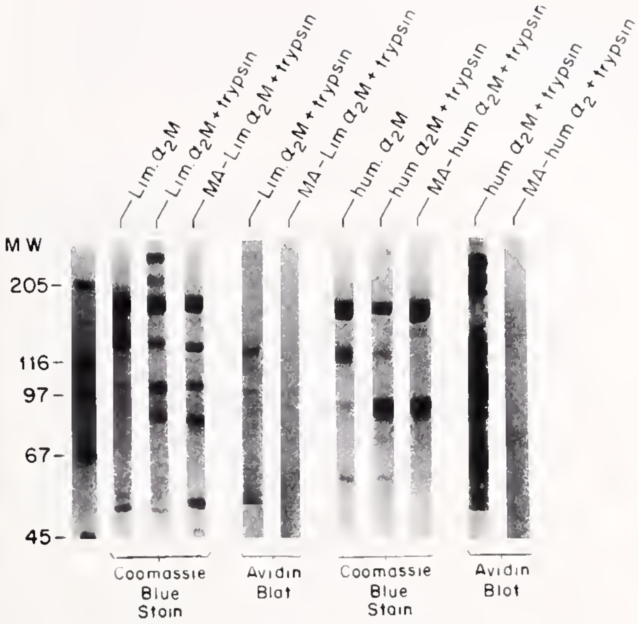

Figure 1. *LAM was purified as described previously (10). Methylamine (MA) treatment involved incubation with 0.2 M methylamine in 0.1 M Tris buffer, pH 8.4 for 12 h, at room T. LAM was reacted with biotin-conjugated trypsin (b-trypsin) for 2 min, then boiled in SDS-polyacrylamide gel electrophoresis sample buffer containing β-mercaptoethanol, and subjected to electrophoresis on a 6% polyacrylamide gel. Western blots were probed with horseradish peroxidase-conjugated avidin to reveal the presence of b-trypsin-containing products. Unreacted LAM (lane 2) had an apparent molecular mass of 185 kDa, similar to the molecular mass of the subunit of human α_2M (lane 7). The low molecular mass bands in lanes 2 and 7 are thermal breakdown products of α_2M formed when the samples were boiled in sample buffer just before SDS-polyacrylamide gel electrophoresis, and are thus an artifact of sample preparation and do not represent contaminants (11). Trypsin-reacted LAM showed high molecular mass products of apparent molecular masses of ca. 200 and 250 kDa (a 300–350 kDa product was also present in some samples) that migrated slower than the native polypeptide, plus uncomplexed proteolytic fragments with apparent molecular masses of 100 and 85 kDa that, based on our understanding of the reaction of human α_2M with proteases, are presumed to be the result of proteolytic cleavage of LAM at the "bait" region (lane 3). Pretreatment of LAM with methylamine abolished the formation of high molecular mass complexes during the subsequent reaction with trypsin (lane 4). Western blots probed with HRP-avidin to reveal the complexes with b-trypsin (lanes 5 and 6) showed faintly staining trypsin-containing products with molecular masses ca. 100 and 120 kDa (lane 5) that were absent when methylamine-treated LAM was reacted with trypsin (lane 6). Human α_2M formed high molecular mass complexes with trypsin that contained biotinylated trypsin (lane 10).*

proteases (lane 3). High molecular mass products were formed during reaction with all proteases tested (trypsin, chymotrypsin, plasmin, pancreatic elastase, thermolysin, and papain). Surprisingly, the major high molecular mass products did not contain protease (lane 5). Biotinylated trypsin formed covalent complexes with all of the high molecular mass products of human α_2M, as evidenced by probing Western blots with horseradish peroxidase (HRP)-conjugated avidin (lane 10), but trypsin was absent from the high molecular mass products of LAM. In this study, trypsin-reacted LAM was separated from unreacted trypsin by gel filtration chromatography, then subjected to SDS-polyacrylamide gel electrophoresis (reducing conditions), Western blotting, and the blots were probed with HRP-avidin to detect biotinylted trypsin. Faintly stained bands, which do contain covalently linked trypsin, were present at 100 and 120 kDa (lane 5), but most of the trypsin migrated at the position of free trypsin (*e.g.*, the biotinylated trypsin was present at the dye front of the reducing SDS polyacrylamide gel).

Thus, unlike mammalian α_2M, the α_2M-protease complexes formed by *Limulus* α_2M are predominately non-covalent in character, involving physical entrapment. The entrapped protease co-segregated with LAM during gel filtration chromatography and during non-denaturing polyacrylamide gel electrophoresis, but was released by denaturing conditions. The high molecular mass products revealed by SDS-polyacrylamide gel electrophoresis of proteolyzed LAM must involve direct covalent cross-linking of various proteolytic fragments of LAM, and do not include protease. The 200 kDa product may be the 100 and 85 kDa bait region fragments rejoined by a γ-glutamyl-ϵ-lysyl isopeptide bond and migrating anomalously slowly during electrophoresis, while the 250 kDa product may involve covalent linkage of one of the bait region fragments with an 185 kDa unproteolyzed chain. The ability of the dimeric form of α_2M found in *Limulus* to bind proteases without covalent bonding differs from dimeric and monomeric homologues of α_2M from mammals, which are incapable of binding proteases by non-covalent means (8, 9).

This research was supported by Grant No. GM 35185 from the National Institutes of Health. We thank Dr. Richard D. Feinman for the gift of purified human α_2M and Dr. Robert Goldman for the use of specialized equipment from his laboratory.

Literature Cited

1. **Sottrup-Jensen, L. 1987.** Pp. 191–291 in *The Plasma Proteins. Structure, Function, and Genetic Control*, vol 5, 2nd Edition, F. W. Putnam, ed. Academic Press, New York.
2. **Barrett, A. J., and P. M. Starkey. 1973.** *Biochem. J.* **133:** 709–724.
3. **Barrett, A. J., *et al.* 1979.** *Biochem. J.* **181:** 401–418.
4. **Wang, D., *et al.* 1984.** *Biochemistry* **23:** 2807–2811.
5. **Sottrup-Jensen, L., *et al.* 1990.** *J. Biol. Chem.* **265:** 17727–17737.
6. **Christensen, U., *et al.* 1989.** *Biochemistry* **28:** 9324–9331.
7. **Enghild, J. J., *et al.* 1989.** *J. Biol. Chem.* **264:** 11428–11435.
8. **Quigley, J. P., and P. B. Armstrong. 1983.** *J. Biol. Chem.* **258:** 7903–7906.
9. **Quigley, J. P., and P. B. Armstrong. 1985.** *J. Biol. Chem.* **260:** 12715–12719.
10. **Armstrong, P. B., *et al.* 1991.** *J. Biol. Chem.* **266:** 2526–2530.
11. **Armstrong, P. B., and J. P. Quigley, 1987.** *Biochem. J.* **248:** 703–707.

Calcium Waves Accompany Contraction Waves in the *Oryzias latipes* (Medaka) Blastoderm

Richard A. Fluck (Franklin and Marshall College), Andrew L. Miller, and Lionel F. Jaffe

Soon after the onset of epiboly in the medaka embryo, the blastoderm begins to contract rhythmically (1). Contraction waves, which propagate in a sub-epithelial (stellate) layer (2), arise in a pacemaker region and propagate across the blastoderm at about 15 μ/s at 20°C (1). The contractions continue even after the blastoderm is separated from the yolk, and the rhythmic contraction of such detached blastoderms is optimal in a balanced saline solution (BSS) containing ca. 1 m*M* Ca^{2+} and is inhibited in BSS containing higher (7.2 m*M*) or lower (0.18 m*M*) concentrations of Ca^{2+} (3).

To determine whether these contraction waves are accompanied by calcium waves, we microinjected recombinant aequorin into medaka eggs, fertilized them, and monitored their luminescence after about 24 h, by which time the embryos had begun to contract rhythmically. Photon emission was monitored with an ultrasensitive imaging photon detector, and the contraction waves were recorded by time-lapse video microscopy (4).

We examined 15 embryos and saw regular, periodic pulses of light in 9 of them. These pulses arose in the pacemaker region, spread across the blastoderm, and ended on the opposite side of the blastoderm, near the embryonic axis. We saw no pulses in two eggs that had not quite developed to the stage at which they begin to contract rhythmically. The interval between calcium pulses at the pacemaker (155 ± 11 s, $\bar{x}$ ± SEM, n = 9 embryos) was estimated by counting photons for 9–32 min in a 15-pixel-square box drawn over this region (Fig. 1); the interval between mechanical pulses at the pacemaker (146 ± 7 s, $\bar{x}$ ± SEM, n = 6 embryos) was estimated from an analysis of time-lapse video tape recordings. The velocity of the calcium wave (11.9 ± 1.1 μ/s, $\bar{x}$ ± SEM, n = 7 embryos) was estimated by comparing the timing of the pulses at the pacemaker with those near the embryonic axis. This velocity is in the range of the fast calcium waves that are propagated by calcium-induced calcium release or by some related reaction-diffusion process (5).

The calcium pulses and waves described herein are similar to the contraction waves in the following ways: 1) they both originate in the pacemaker region of the blastoderm, propagate across the blastodisc, and extinguish near the embryonic axis; 2) they have similar periods; and 3) they propagate at similar velocities.

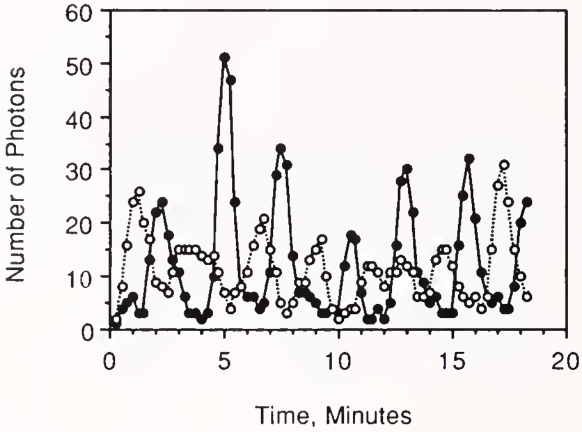

Figure 1. *Calcium pulses during rhythmic contractions of the medaka blastoderm. Photons were counted in 15-square-pixel boxes drawn over the pacemaker region (● —— ●) and near the embryonic axis (○ · · ·○), using a 45-s window and advancing it at 15-s steps for 18.25 min. These two regions represent the beginning and end, respectively, of the calcium (and contraction) wave; thus, for example, the calcium pulse in the pacemaker region at 2.25 min gave rise to a wave that reached the embryonic axis at about 3.75 min.*

Thus, we conclude that a wave of elevated Ca^{2+} accompanies the contraction wave.

We thank Dr. Osamu Shimomura for his generous gift of recombinant aequorin, Richard Sanger for engineering assistance, Eric Karplus for data analysis software, and Jane McLaughlin for technical assistance. Supported by NSF grant DCB-9017210 to RAF and by NSF DCB-8811198 (Amendment 01) and NIH RRO1395 to LFJ.

Literature Cited

1. **Barber, B., *et al.*, 1987.** *J. Exp. Zool.* **242:** 35–42.
2. **Cope, J., *et al.* 1990.** *J. Exp. Zool.* **254:** 270–275.
3. **Sguigna, C., *et al.* 1988.** *Comp. Biochem. Physiol.* **89C:** 369–374.
4. **Fluck, R. A., *et al.* 1991.** *J. Cell Biol.* In press.
5. **Jaffe, L. F. 1991.** *Proc. Natl. Acad. Sci. USA* In press.

Cardioregulatory Peptides in *Limulus:* Effects of F1, F2 and an Endogenous FMRFamide-like Peptide on the Neurogenic Heart

James R. Groome (Biology Department, Utah State University, Logan, UT 84322-5305) and Winsor H. Watson III

The neurogenic heart of the horseshoe crab, *Limulus polyphemus,* has been used as a model system with which to study the cellular and molecular mechanisms underlying specific actions of peptide and amine neuromodulators (1). The peptide Phe-Met-Arg-Phe-NH_2 (FMRFamide), or an analog, has been proposed as a candidate cardioregulator in *Limulus.* FMRFamide-like peptides have been detected in insects and crustaceans (2), and FMRFamide-like immunoreactivity has been detected in the *Limulus* CNS and cardiac ganglion (3). Although FMRFamide itself is cardioactive in the horseshoe crab only at high ($>10^{-5}$ *M*) doses, a potent endogenous cardioactive FMRFamide-like peptide has been reported to occur in *Limulus* (4). We have characterized the action of this native FMRFamide-like peptide on the neurogenic heart of the horseshoe crab, and have compared these effects with those of synthetic identified analogs.

A factor partially purified from the *Limulus* prosomal CNS produces characteristic excitatory chronotropic and inotropic effects when applied to the intact *Limulus* heart preparation (Fig. 1). This factor also produces FMRFamide-like contracture of the *Busycon* radula protractor muscle, a characterized bioassay for the peptide (5). The peptide character of this factor was determined by enzymatic degradation (loss of biological activity) with trypsin or pronase. A single peak of cardioactivity is detected by high performance liquid chromatography of the prosomal extract, eluting at 38% acetonitrile on a linear gradient of 66% to 48% in 70 min.

The chronotropic effect of this peptide factor on the intact heart is probably a result of actions on the cardiac ganglion, because it also increases the frequency of bursts recorded from the isolated ganglion. Moreover, the factor increases levels of cyclic AMP in the cardiac ganglion, and previous studies have shown that cyclic AMP mediates chronotropic excitation by amines (6). While the cellular site of inotropic action by this factor is uncertain, it does increase cardiac muscle cyclic AMP, which underlies the enhancement of contractility by amines (7).

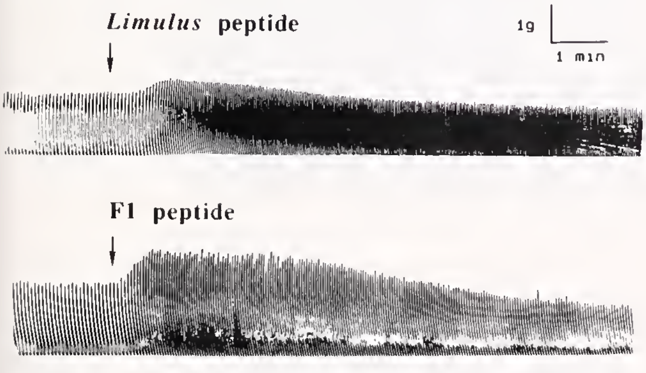

Figure 1. *An extract of five* Limulus *brains, partially purified with gel filtration, was added to the isolated* Limulus *heart preparation at the arrow. It produces chronotropic and inotropic excitation, as does application of 3×10^{-7} M F1 (arrow). Heart contractions were monitored with a Grass force transducer and polygraph.*

Two FMRFamide-like peptides isolated from the lobster *Homarus* (F1, Thr-Asn-Arg-Asn-Phe-Leu-Arg-Phe-NH_2, TNRNFLRFamide; F2, Ser-Asp-Arg-Asn-Phe-Leu-Arg-Phe-NH_2, SDRNFLRFamide; 8) produce actions on the isolated *Limulus* heart that are identical to those produced by the native FMRFamide-like cardioexcitatory peptide (Fig. 1). Both F1 (Bachem) and F2 (a gift from E. Marder, Brandeis University, Waltham, MA) elicit dose-dependent increases in heart rate, with a threshold dose of approximately 3×10^{-10} *M* for either peptide. At 10^{-8} *M,* F1 and F2 produce significant and long-lasting increases in the burst rate of isolated cardiac ganglia (F1, 64.4 ± 10.1%; F2, 64.0 ± 11.0% in 7 preparations).

The inotropic effects of F1 or F2 are dose-dependent, with a threshold of about 2×10^{-9} *M.* They are not as pronounced or long-lasting as the chronotropic effects, but the simultaneous increase in heart rate may reduce the force of contraction (1). To directly assess peptide effects on contractility, *Limulus* hearts were deganglionated and the motor roots of the cardiac ganglion removed. The myocardia were stimulated with current pulses of constant frequency to produce contractions in the absence of neuronal input. Contraction amplitude is increased by 68.1 ± 13.3% with 3×10^{-7} *M* F1 ($n = 9$), while the same dose of F2 produces a 65.1 ± 13.3% increase in 8 preparations. When deganglionated myocardia are not stimulated with current pulses, F1 and F2 occasionally produce rhythmic contractions and a slight contracture.

These data suggest that an endogenous FMRFamide-peptide has a role in the regulation of the heartbeat of the horseshoe crab *Limulus.* This peptide may bear some structural similarity to F1 or F2 because these peptides produce identical effects and are cardioactive at low doses. This hypothesis will be examined by determining the sequence of the native peptide.

This work was supported by a Grass Fellowship to JG and by NINCDS grant 19053-01 grant to WHW. We thank W. White for experimental assistance.

Literature Cited

1. **Watson, W. H. III, and J. R. Groome. 1989.** *Am. Zool.* **29:** 1287–1303.
2. **Price, D. A., and M. J. Greenberg. 1989.** *Biol Bull.* **177:** 198–205.
3. **Watson, W. H. III, *et al.* 1984.** *Peptides* **5:** 585–592.
4. **White, W., and Watson, W. H. 1984.** *Soc. Neurosci. Abstr.* **10:** 689.
5. **Nagle, G. T., and M. J. Greenberg. 1982.** *Comp. Biochem. Physiol.* **71C:** 101–105.
6. **Groome, J. R., and W. H. Watson, III. 1990.** *J. Exp. Biol.* **152:** 313–331.
7. **Groome, J. R., and W. H. Watson, III. 1989.** *J. Exp. Biol.* **145:** 419–437.
8. **Trimmer, B. A., *et al.* 1987.** *J. Comp. Neurol.* **266:** 16–26.

How *Beroë* Keeps Its Mouth Shut, or Its Lips Are Sealed

Sidney L. Tamm and Signhild Tamm (Boston University Marine Program, Marine Biological Laboratory)

We investigated how several species of the ctenophore *Beroë*, voracious predators in the marine zooplankton, keep their mouth shut to maintain a streamlined body shape during forward swimming in search of prey (1). In big-mouthed thin-walled beroids [*Beroë* sp. (Woods Hole), *B. forskali, B. mitrata*] we found that mouth closure requires neither muscular nor nervous activity, because the mouth remains firmly closed in 6.75% $MgCl_2$: seawater (1:1) which blocks muscular and nervous responses. Instead, mouth closure is due to paired strips of adhesive epithelial cells located on opposing stomodaeal walls. Sections through mouths that were fixed while closed show that the two joined epithelial layers make numerous close contacts interrupted by vacuolar intercellular spaces. Electron microscopy reveals that the plasma membranes are highly folded and interdigitated with each other at regions of apposition, and are separated by a uniform distance of about 15 nm. A dense cytoplasmic coat underlies the membranes only at such appositions. This morphology suggests that non-specific molecular attraction, such as London-van der Waals forces, may play a major role in cell-cell adhesion (2, 3).

Beroë sp. and *B. forskali* display mutually perpendicular orientations of the stomodaeal adhesive strips (circumoral *vs.* longitudinal), correlated with different distributions of feeding macrocilia in these species. In both cases, the adhesive strips coincide with macrocilia-free zones of the stomodaeal wall. The two different patterns of mouth closure and macrociliary arrangement may reflect differences in prey type or feeding behavior (4).

Contact of prey with sensory receptors on the lips triggers rapid opening of the mouth and engulfment of prey (5). The receptor cells bear actin pegs and onion-root cilia, and make synaptic contacts with the nerve net (6). Video analysis of egg white-induced feeding responses of *Beroë* sp. showed that mouth opening requires muscular contractions of the lips. However, the stomodaeal adhesive strips are not pulled apart all at once, but are peeled apart starting from a site of vigorous muscular tension. The mouth quickly re-seals after opening, showing that adhesion of the stomodaeal epithelia is readily reversible. Mouth opening may also require concomitant changes in the adhesive properties of the epithelial cells themselves. The adhesive cells are innervated by the nerve net, indicating that they make some kind of effector response. Food stimuli may thus signal both muscular contractions that pull the lips apart, and active de-adhesion processes in cells of the epithelial strips (*i.e.*, cytoskeletal rearrangements, surface modifications, etc.).

In conclusion, epithelial adhesion in several species of *Beroë* appears to be a low energy method for closing the mouth and streamlining the body of an active gelatinous predator that spends most of its time swimming mouth-forward in search of prey. Opening of the mouth is also an efficient process, because peeling apart of the adhesive strips requires much less force than separating them all at once (7). Tissue adhesion in these *Beroë* species shares many structural and functional properties with the transient adhesions formed between moving cells in embryos and culture (3), and may provide a useful experimental system for studying the mechanisms and regulation of dynamic cell adhesions.

Supported by NIH GM 27903 and GM 45557.

Literature Cited

1. **Vogel, S. 1981.** *Life in Moving Fluids.* Princeton University Press, Princeton, NJ.
2. **Nachtigall, W. 1974.** *Biological Mechanisms of Attachment.* Springer Verlag, Heidelberg.
3. **Trinkaus, J. P. 1984.** *Cells into Organs. The Forces that Shape the Embryo* 2nd ed. Prentice-Hall, Englewood Cliffs, NJ.
4. **Tamm, S. L., and S. Tamm. 1990.** *MBL Science* **4:** 28–29.
5. **Tamm, S. L. 1982.** Ctenophora. In *Electrical Conduction and Behaviour in 'Simple' Invertebrates.* G. A. B. Shelton, ed. Oxford University Press, Oxford, UK.
6. **Tamm, S., and S. L. Tamm. 1991.** *Cell Tissue Res.* **264:** 151–159.
7. **Vogel, S. 1988.** *Life's Devices.* Princeton University Press, Princeton, NJ.

Macrociliary Tooth Patterns in Beroid Ctenophores

Signhild Tamm and Sidney Tamm (Boston University Marine Program, Marine Biological Laboratory)

Macrocilia are compound ciliary organelles found inside the mouth of beroid ctenophores (1, 2). Macrocilia are used to ingest or bite through prey (other gelatinous zooplankton) (1, 2, 3). A single macrocilium contains hundreds or thousands of 9 + 2 axonemes surrounded by a common membrane (1, 4–6). A giant capping structure is present at the tip of the macrocilium. The

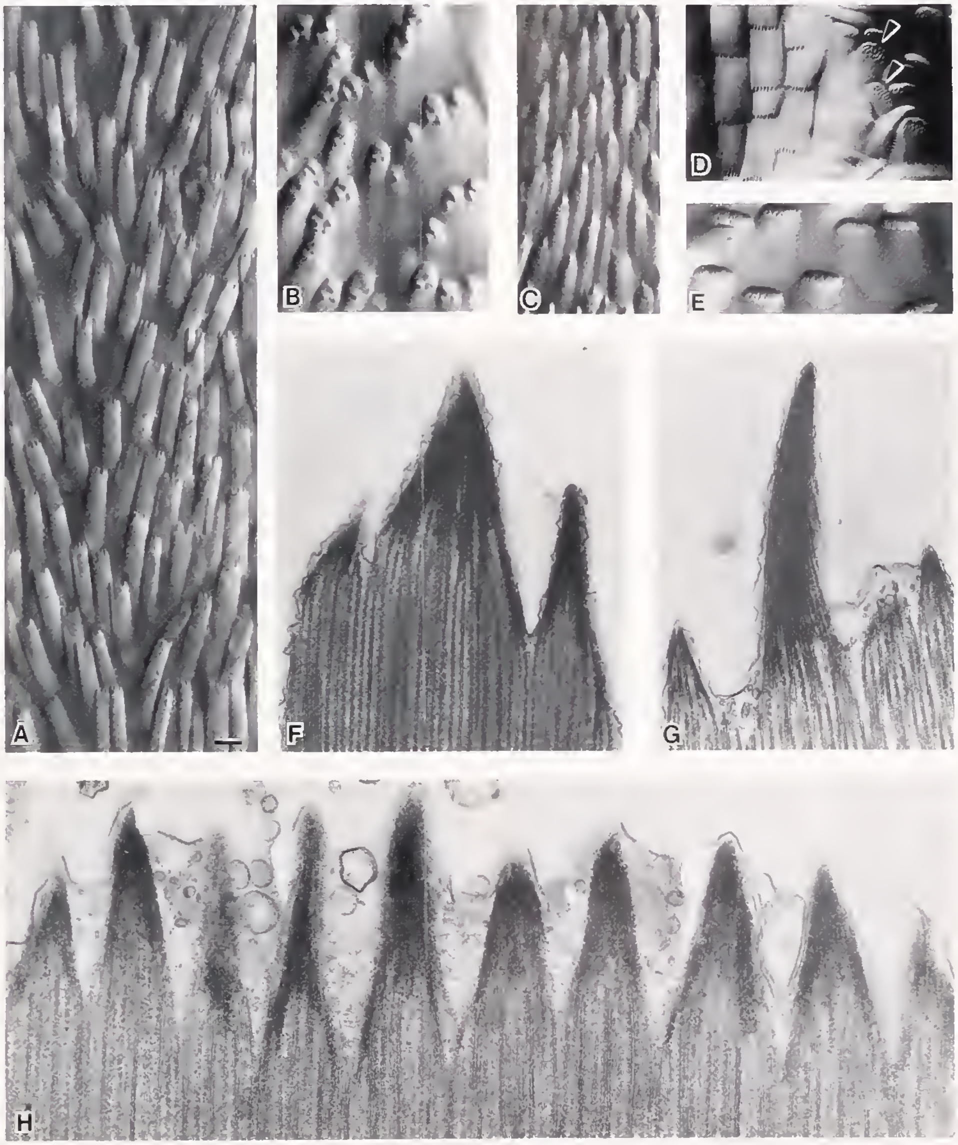

Figure 1. *A–E, DIC electronic flash photographs of living macrocilia from different species of Beroë. A, B. cucumis (Monterey, CA); 4 equally sized teeth at tips of effective-pointing macrocilia. B, B. cucumis (Friday Harbor, WA); 3-toothed claws of recovery-pointing macrocilia. C, B. gracilis (Monterey, CA); single long teeth of effective-pointing macrocilia. D, B. forskali (Monterey, CA); one of the 3 rows of fine teeth is visible on effective-pointing cilia (left). All 3 rows of teeth are revealed on recovery cilia (arrowheads, right). E, B. forskali (Monterey, CA); bottle cap-like profile of top row of teeth on recovery-pointing macrocilia. F-H, Longitudinal thin-section electron micrographs of macrociliary tips. F, B. cucumis (Woods Hole, MA); 3 teeth with larger middle tooth (from ref. 5). G, B. gracilis (Monterey, CA); long pointed central tooth with smaller lateral ones. H, B. mitrata (Villefranche-sur-Mer, France); 1 of the 3 rows of many fine teeth. Scale bar: A–C, 5 μm; D, E, 10 μm; F, G, 0.35 μm; H, 0.25 μm.*

cap is formed of extensions of the A and central-pair microtubules, which are firmly bound together by electron-dense material into rigid, pointed projections, or teeth (5) (Fig. 1F–H). To accommodate sliding displacement of the axonemal microtubules, the tip changes shape during the beat cycle. At the end of the effective stroke, the tip is straight, and at the end of the recovery stroke, the tip is hooked; these configurations are thought to facilitate the feeding function of macrocilia by acting as a "non-return" surface *vs.* grappling or tearing instruments, respectively (5).

We investigated the types of teeth and the sizes and arrangements of macrocilia in different species of *Beroë*. Motile macrocilia were examined by video light microscopy, and fixed organelles by thin-section electron microscopy. Beroids can be divided into two groups based on the relative sizes and distributions of their macrocilia. Large-mouthed species such as *B. forskali* and *B. mitrata* have bigger macrocilia (80–100 μm long, 12–15 μm diameter) that cover a large area of the stomodaeal cavity. In *B. mitrata,* the macrociliary field extends over the oral half of the stomodaeum, but in *B. forskali,* the macrocilia are arranged in tapering longitudinal stripes that run aborally from the lip edge. The distal ends of macrocilia in *B. forskali* and *B. mitrata* bear three rows of very short (1–1.5 μm long) pointed teeth, giving the tip a finely serrated appearance when viewed from above (Fig. 1D, E, H). There are about 12 teeth per row, or about 36 teeth on a single macrocilium. The rows of teeth run parallel to the rows of axonemes, *i.e.*, at right angles to the beat plane (Fig. 1D, E).

All other beroids examined to date possess smaller macrocilia (25–30 μm long, 4–5 μm diameter) that are restricted to a narrow band around the inner margin of the lips. Two main tooth patterns are found in this group. Macrocilia of *B. ovata, B.* sp. (Gloria), and *B. cucumis* (Monterey, CA, and Friday Harbor, WA) possess 3–10 teeth of equal length, depending on the species. Viewed at the end of the effective stroke, the upper side of the macrociliary tip appears notched into 3 or 4 equally sized teeth (Fig. 1A). At the end of the recovery stroke, the entire complement of teeth is visible. The teeth are arranged in an oval group, much like a paw or claw, in *B. ovata* and *B. cucumis* (Monterey and Friday Harbor) (Fig. 1B). However, in *B.* sp. (Gloria) the 6–8 teeth are arranged in a horseshoe pattern around the edge of the macrociliary tip, with the open side of the horseshoe facing proximally.

Macrocilia of *B. cucumis* (Woods Hole) and *B. gracilis* (Helgoland, Germany, and Monterey, CA) have only 3–4 teeth, but the middle tooth is longer and wider than the lateral ones (Fig. 1C, F, G). In *B. gracilis,* the central tooth is particularly long and pointed, like a single fang (Fig. 1C, G).

The above patterns are characteristic of a given species, and do not vary with developmental stage, body size, or feeding history. By analogy to dental patterns of vertebrate jaws, macrociliary tooth types, sizes, and distribution may provide a reliable morphological character for resolving unsettled problems of evolution, speciation, and classification of beroid ctenophores (7).

We imagine that the diversity of macrociliary patterns is related to the diet or feeding methods of particular species of *Beroë* (8). The different types of macrociliary teeth may be specializations for eating and processing different types of prey. For example, the finely serrated tips of macrocilia in *B. forskali* and *B. mitrata* may be adapted for rasping or scraping. The single long-fanged tooth of *B. gracilis* macrocilia suggests that it may serve to pierce or cut through prey. A search of published reports on prey selection and feeding behaviors of various beroids was not helpful in accounting for the various macrociliary patterns we found. A more complete investigation of the preferred menus and dining manners of different beroids is obviously necessary to understand the remarkable diversity of their eating utensils.

Literature Cited

1. **Horridge, G. A. 1965.** *Proc. R Soc. London B* **162:** 351–364.
2. **Tamm, S. L. 1983.** *Nature* **305:** 430–433.
3. **Swanberg, N. 1974.** *Mar. Biol.* **24:** 69–76.
4. **Tamm, S. L., and S. Tamm. 1984.** *J. Cell Biol.* **99:** 1364–1371.
5. **Tamm, S. L., and S. Tamm. 1985.** *J Cell Sci.* **79:** 161–179.
6. **Tamm, S. L., and S. Tamm. 1989.** *Proc. Natl. Acad. Sci. USA* **86:** 6987–6991.
7. **Harbison, G. R. 1985.** Pp. 78–100 in *The Origins and Relationships of Lower Invertebrates,* S. C. Morris *et al.,* eds. Clarendon Press, Oxford.
8. **Tamm, S. L., and S. Tamm. 1990.** *MBL Science* **4:** 28–29.

Mitochondrial DNA Variation of Copepods: Markers of Species Identity and Population Differentiation in *Calanus*

Ann Bucklin (Marine Biological Laboratory) and Lisa Kann (University of Rhode Island)

DNA amplification and restriction enzyme digestion of portions of two mitochondrial genes have provided molecular markers of species identity for three species of the copepod genus *Calanus: C. finmarchicus, C. pacificus,* and *C. marshallae.* These gene portions also demonstrated the genetic differentiation of conspecific populations of *C. pacificus,* based on comparison of a northern (Puget Sound, WA) and a southern (off San Diego, CA) population.

Samples of each species were collected by net tow and preserved in alcohol. The sample of *C. marshallae* and the northern sample of *C. pacificus* were collected from Dabob Bay, Puget Sound, WA, in April, 1990 and identified by Bruce Frost (University of Washington). The southern sample of *C. pacificus* was collected from the California Cooperative Fisheries Investigation survey in November, 1989 (station number 83.42) and identified by Michael Mullin (Scripps Institution of Oceanography). The *C. finmarchicus* sample was collected from the Gulf of Maine in April, 1991 by Ted Durbin (University of Rhode Island).

All DNA amplifications were done using genomic DNA extracted from alcohol-preserved copepods. (Identical results have been obtained using fresh, frozen, and buffered formalin-preserved samples.) DNA was extracted from individual copepods and from pools of 50 conspecific individuals. DNA extraction from individual copepods yielded amplification and restriction enzyme digestion patterns for both gene portions that were identical to those from pools of the 50 individuals. Since there was no variation among the individuals of any sample of any species or population we assayed, these results are based on the pooled DNA.

A 360 base pair (bp) portion of cytochrome b and a 650 bp portion of cytochrome oxidase I were amplified in a Coy Thermocycler. Vertebrate consensus primers were used to amplify cytochrome b (1); consensus primers from a variety of taxa amplified cytochrome oxidase I (2). The usual amplification program was: denaturing at 94°C for 1 min, annealing at 37°C for 2 min, and extension at 72°C for 3 min. Amplification was carried out for 30 cycles and was followed by a 9-min extension period. The amplification product was purified on a 1.4% agarose gel and reamplified at a higher annealing temperature (42°C). The second amplification tightened the cytochrome b product band. The reproducible artefactual bands that resulted from the first cytochrome oxidase I amplification of all samples were eliminated in the second amplification for the two *C. pacificus* samples, but not for the *C. finmarchicus* and *C. marshallae* samples. Attempts to purify the cytochrome oxidase I amplification product of *C. finmarchicus* and *C. marshallae* by filtration (Millipore Ultrafree-MC 30,000 NMWL filter units, Millipore Products Div., Bedford, MA) and by hot phenol extraction of excised bands were successful, but yields in both cases were too low to allow visualization of the digestion fragments.

The amplification products were digested with a suite of restriction enzymes to yield restriction fragment length polymorphism (RFLP) phenotypes. All results are based on four replicate amplifications and digestions from each sample. The cytochrome b product was digested with Taq I, Hinc II, Mbo I, and Ssp I. Taq I, Mbo I, and Ssp I cleaved the 360 bp amplification product into two fragments for samples of *C. finmarchicus,* the southern *C. pacificus* population, and *C. marshallae.* Sizes of the fragments (*i.e.,* placement of the restriction site) was unique to each sample for all three enzymes, except the Mbo I digestions of *C. marshallae* and the northern population of *C. pacificus* (Table I). The cytochrome b product for the southern population of *C. pacificus* was not cleaved by Taq I, Mbo I, or Ssp I. The amplification products of all samples were cleaved by Hinc II once; in each case the sizes of the two fragments were unique to that species or population (Table I).

Table I

Fragment sizes (in numbers of base pairs) resulting from restriction enzyme digestion of the 360 base pair cytochrome b amplification product for samples of Calanus finmarchicus, *a northern and southern population of* C. pacificus, *and* C. marshallae. *DNA was extracted from 50 pooled individuals for each sample; fragment sizes were determined on the basis of four replicate amplifications and digestions for each sample. DNC (did not cleave).*

Enzyme	*C finmarchicus*	*C pacificus*-N	*C pacificus*-S	*C marshallae*
Taq I	260, 110	200, 160	DNC	210, 150
Hinc II	280, 80	190, 170	210, 150	180
Mbo I	190, 170	180	DNC	180
Ssp I	210, 150	230, 130	DNC	250, 110

The cytochrome oxidase I products for samples of the two *C. pacificus* populations were digested by Taq I, Alu I, Hinc II, and Mbo I. The RFLP patterns for these latter three enzymes provided evidence of intraspecific variation in this gene also. Hinc II and Mbo I cleaved the northern population's gene portion into two fragments, but did not cut the southern population's. Alu I cleaved the products of both populations, but the fragment sizes differed between the northern (590 and 60 bp) and southern (400 and 250 bp) populations.

RFLP analysis of these and additional genes may allow us to estimate gene flow within planktonic species populations. Mitochondrial genes, which are clonally (matrilineally) inherited, may be useful descriptors of population genetic structure of plankton, since both ocean mixing and recombination during sexual reproduction may erase evidence of structure based on frequency differences of nuclear markers (3).

This work was supported by a National Science Foundation Research Fellowship in Biotechnology and Ocean Sciences to AB.

Literature Cited

1. **Kocher, T. D., *et al.* 1989.** *Proc. Natl. Acad. Sci.* **86:** 6196–6299.
2. **Kessing, B., *et al.* 1989.** The Simple Fool's Guide to PCR. (unpublished)
3. **Bucklin, A., *et al.* 1989.** *J. Geophys. Res.* **94:** 8277–8288.

Investigations into the Life Cycle of *Calliobothrium verticillatum*, a Tapeworm of *Mustelus canis*

Bryan Cherry[1], *Allison S. Neese*[2], *Robert A. Bullis*[3], *and Gerhard A. Schad*[3] *([1]Michigan State University, [2]University of Georgia, [3]University of Pennsylvania)*

Calliobothrium verticillatum, a tetraphyllidean cestode, is a common parasite in the spiral valve of the smooth dogfish, *Mustelus canis*. Until recently, nothing was known about the life cycle of this species; then Caira and Ruhnke (1) identified a plerocercoid larva from the hermit crab, *Pagurus pollicaris*, as *C. verticillatum*. The identification was based on the appearance of three suckers on the apical region of each bothridium, a characteristic known only in this species. Advanced plerocercoids differ from adults in the absence of bothridial hooks and the presence of a central apical sucker, which degenerates to a muscular pad in the adult. We hypothesize that this larval stage represents the immediate precursor to the adult tapeworm, but the intermediate stages have not been seen. Here we report the identification of an incompletely developed adult *C. verticillatum* that may represent one stage in the metamorphic process.

The intermediate stage was discovered as we were attempting to follow the metamorphosis of the plerocercoid to the adult. Predicting that dogfish stomach fluids would induce maturation, a smooth dogfish, which had not been fed for at least 48 h, was isolated and fed four *P. pollicaris*. We could assume that these crabs would be infected because plerocercoids infect more than 95% of hermit crabs from the Woods Hole area. Five days after being fed, the dogfish was sacrificed, and its gastro-intestinal contents analyzed. Four plerocercoids, found in association with hermit crab exoskeletal and tissue remnants in the stomach and spiral valve, were transferred to a culture medium used to simulate the spiral valve environment; they did not survive.

Also present in the spiral valve were several unique specimens. They were similar in size to the plerocercoids, but upon careful inspection, they differed from the typical plerocercoids of *C. verticillatum*: all showed two distinct pairs of hooks on each bothridium of the scolex, and none of these specimens possessed the distinct central apical sucker normally seen on the plerocercoid scolex (see Fig. 1). In fact, these are adult characteristics that we had seen in numerous adult *C. verticillatum* obtained from other smooth dogfish. However, typical adult *C. verticillatum* are several centimeters in length and possess a long, segmented strobila, whereas our new specimens were under 2 mm and lacked evidence of strobilization.

These immature adults could have developed from plerocercoids in the hermit crabs. Alternatively, they may have been present in the dogfish before the experiment began, a possibility we cannot exclude. However, no typical adult *C. verticillatum* were seen in the spiral valve, suggesting that no infection existed before the experiment. In either case, adult *C. verticillatum* like those seen in this experiment have not been reported previously. They probably represent one stage of development in the metamorphic change of plerocercoids into adults of this species.

We have also tried to induce metamorphosis in plerocercoids *in vitro*. High urea concentration in elasmobranch spiral valves is thought to be a starting signal for this metamorphic event, and culture media containing urea have induced metamorphosis in other species of tapeworms found in elasmobranchs (2, 3). However, we have yet to succeed with these techniques.

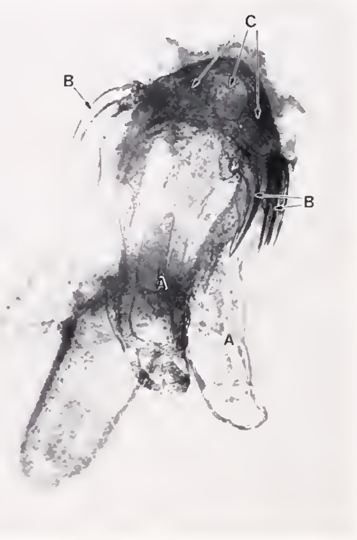

Figure 1. *Immature* Calliobothrium verticillatum *adult taken from a smooth dogfish fed hermit crabs infected with* C. verticillatum *plerocercoids. Bothridium (A), bothridial hooks (B), three suckers at apex of bothridium (C). Specimen length = 1 mm.*

The discovery of an immature adult, and the paucity of plerocercoids in the experimental dogfish, suggest a potentially useful time-frame for plerocercoid metamorphosis. Interrupting the experiment in under five days should reveal developmental stages between the plerocercoid and the newly discovered immature adult, while later interruption should yield adults with a greater degree of maturity. Continued efforts to culture plerocercoids of *C. verticillatum in vivo* and *in vitro* are needed to shed further light on the life cycle of this species.

This study has been supported in part by an Internship from the Woods Hole Marine Sciences Consortium (Cherry); an AQUAVET® Fellowship from the Madison Trust (Neese); and Grant No. P40-01333-11 from the National Center for Research Resources, NIH. The authors thank D. Abt, M. McCafferty, P. Moniz, R. Smolowitz, and L. Wadman for their contributions.

Literature Cited

1. **Caira, J. N., and T. R. Ruhnke. 1991.** *J. Can. Zool.* **69:** 1484–1488.
2. **Hamilton, K. A., and J. E. Byram. 1974.** *J. Parasitol.* **60:** 20–28.
3. **Carvajal, J., *et al.* 1982.** *Proc. Helminthol. Soc. Wash.* **49:** 226–230.

Role of Olfaction in Recognition of Dominance in the American Lobster (*Homarus americanus*)

Christy Karavanich and Jelle Atema (Boston University Marine Program,
Marine Biological Laboratory)

Dominance is important for the reproductive success of male American lobsters (*Homarus americanus*). Studies in semi-naturalistic environments have shown that only the dominant male in the tank will mate (1, 2). Communally held lobsters will engage in agonistic encounters upon initial introduction (3, 4, 2). Through such encounters, a dominant male will usually emerge. After establishing dominance, the relationship between dominants and subordinates remains stable with little overt aggression required. Dominance in lobsters has been correlated with size, sex, prior experience (5), and molt state (6). Because many of these factors are affected hormonally, we hypothesize that a dominant lobster has a different internal hormonal state than a subordinate, and that this aggressive state is broadcast to other lobsters as a unique dominance odor. Olfactory cues may therefore be involved in regulating stable dominance relationships.

Lobster antennules are a major site of odor reception and function in distance orientation and in social responses (7). Individual receptor cells of the lobster antennules respond to amino acids and other compounds that act as feeding cues. (8). Specific "pheromone" receptor cells have not been identified. Behavioral responses to urine and body odors have been demonstrated, however (9, 10). In this study, we investigated the importance of odor cues in male lobster dominance relationships.

When placed together in a small, enclosed tank, two lobsters will fight to establish dominance, as seen in the larger scale of communal tanks. These artificial "boxing matches" can be used to study the effect of olfaction on dominance relationships. Adult male intermolt lobsters (76–81 mm carapace length) were isolated visually and chemically for 48 h in individual holding tanks with separate water and air supplies. Pairs were formed by size, matching two lobsters that had no known prior knowledge of one another. Boxing matches between members of pairs were held for 20 min on four consecutive nights. The winner and loser of each match was determined by observing the stereotypical behaviors of dominants and subordinates (5). Dominants displayed aggressive behaviors such as pushing, boxing with their claws, rushing at their opponent and raising their claws high above their opponent's head in a behavior called a meral spread. Subordinates showed avoidance behaviors such as backing away, running away, or rapidly jumping backwards from the fight area, and generally avoiding the approach of the dominant. By observing these behaviors, we could determine the time required for a winner to be established. Before the 2nd, 3rd, and 4th fights, 7 pairs had their antennular chemoreceptors inactivated by a 5 min exposure to distilled water (treatment pairs). This treatment effectively eliminates their olfactory capabilities for at least 24 h (10). Eight pairs received seawater sham lesions (control pairs).

In all boxing matches, dominance was established during the first fight (mean latency: treatment: 435 s; control: 526 s). This dominance was maintained throughout all four fights, but for subsequent encounters, the time it took to determine a winner differed between control and treatment pairs. Control pairs showed a decrease in time needed to establish a winner during the 2nd (mean latency: 188 s), 3rd (94 s) and 4th (67 s) fights. Often no fight occurred when control pairs were placed together again. The loser from their first encounter would immediately back away and avoid the dominant. In the treatment pairs, however, the average latency until a winner was determined remained the same for all four boxing matches (2nd mean latency: 628 s; 3rd: 415 s; 4th: 458 s). The difference between treatment and control pairs in average fight duration of the 2nd encounter was highly significant; differences in third and fourth encounters continued to be significant (Fig. 1 Student's *t*-test; $P < 0.01$).

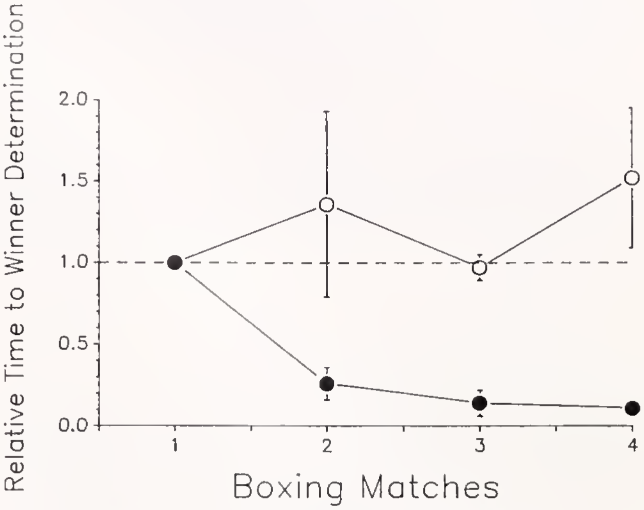

Figure 1. *Mean fight duration (±SEM) of 2nd, 3rd, and 4th fights relative to the duration of the 1st fight. This ratio decreases for the control pairs (solid circle) and remains at .97 or greater for the treatment pairs (open circle). The difference between the average ratios of control and treatment pairs is significant (Paired Student's t-test comparing control and treatment for 2nd, 3rd, and 4th encounters; $P < 0.001$ for 2nd and 3rd fights; $P < 0.01$ for 4th fights).*

The results suggest that olfactory communication occurs in recognition of dominance in male lobsters. Re-matched, anosmic animals continued to fight to re-establish dominance despite one member of the pair demonstrating clear dominance during the first fight. The dominance relationship of the control pairs remained well-established with a greatly decreased fight duration. From the subordinate's point of view, avoiding additional fights with an opponent he recognizes as dominant to himself is beneficial since re-fighting increases the chance for injury.

The olfactory cue in question may be based on dominance odor, but it may also involve individual odor. If lobsters recognize a specific individual, they may assign relative dominance status to that individual based on prior knowledge. The lobster can then adopt appropriate behavior when encountering familiar individuals. Experiments are in progress to separate out the possibilities of dominance relationships based on individual recognition *versus* dominance odor.

Literature Cited

1. **Stein, L., *et al.* 1975.** *Woods Hole Oceanogr. Inst. Tech. Rep.* 75-48, 1–192.
2. **Jacobson, S. 1977.** Ph.D. Thesis, Boston University.
3. **Karnofsky, E., and H. Price. 1989.** *Mar. Behav. Physiol.* **15:** 101–121.
4. **Cowan, D., and J. Atema. 1990.** *Anim. Behav.* **39:** 1199–1206.
5. **Scrivener, J. 1977.** *Fish. Res. Board Can. Tech. Rep.* **235:** 1–128.
6. **Cobb, J. S., and G. R. Tamm. 1975.** *Mar. Behav. Physiol.* **3:** 119–124.
7. **Phillips, B. F., *et al.* 1980.** *The Biology and Management of Lobsters.* pp. 2–72.
8. **Derby, C., and J. Atema. 1982.** *J. Exp. Biol.* **98:** 317–327.
9. **Cowan, D., and J. Atema. 1986.** *J. Chem. Ecol.* **12:** 2065–2080.
10. **Atema, J., and D. G. Engstrom. 1971.** *Nature* **232:** 261–263.

The Response of Oceanic Mixed Layer Depth to Physical Forcing: Modelled vs. Observed

M. M. O'Brien (Biology Department, University of Massachusetts, Dartmouth),
Al Plueddemann, and R. A. Weller

Mixing within the upper ocean is essential for resupplying nutrients to the depleted surface layer from the nutrient-rich, deeper water. Because productivity in the open ocean is often limited by nutrient availability, the dynamic features of the mixed layer may have a significant impact on such biological phenomena as planktonic patchiness and seasonal blooms. The goal of this report is to discuss the vertical structure of the upper ocean. It will concentrate on the physical mechanisms that contribute to fluctuations in the depth of the mixed layer.

The mechanisms of surface forcing at the air-sea interface include wind stress, heat flux, and surface waves. Traditionally, emphasis has been placed on the instabilities produced by wind stress and heat flux as the major causes of mixing. In most surface-forced upper ocean models (1) a high wind stress is accompanied by a negative heat flux, which results in an increase in the depth of the mixed layer. Conversely, if a low wind stress and a positive heat flux co-occur, then strong stratification is expected to develop and vertical mixing should be inhibited. Surface wave growth usually lags wind events, with maximum wave heights occurring after the maximum wind stress. Waves increase mixing either directly, through wave breaking, or indirectly through wave-related processes such as Langmuir circulation (LC) (2). LC is a flow pattern consisting of organized, counter-rotating helical vortices with the longitudinal axis aligned parallel to the direction of the wind (3).

To determine the effect of wind stress, heat flux, and surface waves on the vertical structure of the upper ocean data from the Surface WAve Processes Program (SWAPP) (3) was analyzed. Instruments were deployed from the Research Platform FLIP, moored off the coast of California, for a period of 22 consecutive days during February and March of 1990. The measurements used are averaged over 15-min time intervals, and include wind stress, surface wave height, heat flux, and the vertical profiles of temperature, salinity, density, and velocity of the upper 150 m.

A one-dimensional, surface forced model was used to simulate changes in the vertical structure, based on classical theories of mixed layer dynamics (4). Using the known wind stress and heat flux, the numerical model calculated velocity and density profiles as well as the penetration depth of mixing. The predicted vertical structure was compared to the observed density and velocity profiles to isolate time segments when the model, applying only wind stress and heat flux, failed to accurately predict and describe the recorded data. Specifically, the analysis focused on evidence that suggests that the surface wave driven LC may have occurred, and on what the impact of this three-dimensional flow on the vertical structure may be.

To illustrate the responses of the vertical structure to the forcing agents, the data from 4–7 March was evaluated (Fig. 1). There was an initial 24-h period of high wind from a steady direction. Waves were building continuously and reached a maximum height almost 2 h after maximum wind stress was

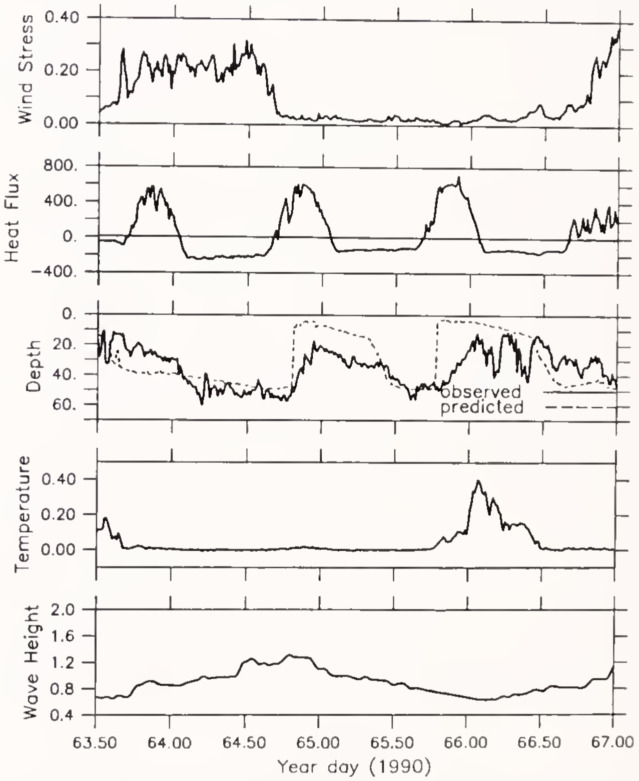

Figure 1. *SWAPP data (March 4–7, 1990). (a.) Wind Stress (N/m**2). (b.) Heat Flux (W/m**). (c.) Model simulation, dashed line, vs. Observed data, solid line. Rapid deepening occurs at day 64, inhibition of stratification occurs at day 65. (d.) Thermal Stratification, spikes indicate large temperature differences in upper 10 m. (e.) Wave Height (m).*

recorded. The model predicted a gradual increase in the depth of the mixed layer during the entire period of high wind stress. The recorded mixed layer depth shows that an initial brief, but rapid, deepening occurred. The depth of the well mixed layer was then maintained until the wind decayed (Fig. 1c). The implication is that a mixing mechanism, which is not accounted for in the model, plays a significant role in changing the vertical structure. Following the wind event was a 36-h period of low wind stress. Wave height was initially high but proceeds to decay. Stratification is expected because of the low wind stress and positive heat flux. The data shows only a slow shoaling of the mixed layer depth and never restratifies to the modelled depth (Fig. 1c, d). The heat flux becomes positive again at the onset of the next successive diurnal cycle and, because the wind stress has remained low, the model predicts nearly the same rate and depth of stratification. The observed data shows the restratification that the model predicted (Fig. 1d). The interesting difference is that during the first period of positive heat flux wave heights were still relatively high, because of the preceding high wind stress, but by the second period of positive heat flux the waves have decayed. A possible explanation for the lack of thermal restratification during the first period is that stratification rate and depth are inhibited by waves and LC.

Two trends were found in my evaluation of the data. First, rapid and unpredicted deepening was often observed during periods of high wind stress. And second, stratification did not occur at the rate, or to the depth, predicted if immediately following a period of high wind stress. This corresponded to when waves, a forcing agent not accounted for in the numerical model, were recorded at heights of greater than 1.2 m. In both cases, the model underestimates the depth and rate of mixing. Although further research must be completed, I contend that it is the activity of the surface waves that is largely responsible for the discrepancies between the modelled and observed mixed layer depth time series. Simple models of the response of the vertical structure of the upper ocean to surface forcing are not adequate because they do not account for the presence of waves or of mixing mechanisms such as Langmuir circulation. The possibility exists that after the decay of the wind, the waves still contain the energy to fuel mixing processes and inhibit the expected onset of stratification. Whether or not this is possible through LC merits further study.

This research project was supported by the Woods Hole Marine Science Consortium program for summer interns.

Literature Cited

1. **Pollard, R. T. 1977.** Pp. 102–117 in *Modelling and Prediction of the Upper Layers of the Ocean.* E. B. Kraus, ed. Pergamon Press, Oxford.
2. **Pollard, R. T. 1977.** Pp. 235–251 in *A Voyage of Discovery.* M. Angel, ed. Pergamon Press, New York.
3. **Weller, R. A., *et al.* 1991.** *Bull. A.M.S.* **72:** 163–183.
4. **Price, J. F., *et al.* 1986.** *J. Geophys. Res.* **91:** 8411–8427.

CONTENTS

BEHAVIOR

Warner, Robert R., and Stephen E. Swearer
Social control of sex change in the bluehead wrasse, *Thalassoma bifasciatum* (Pisces: Labridae) 199

Weissburg, Marc J., and Richard K. Zimmer-Faust
Ontogeny *versus* phylogeny in determining patterns of chemoreception: initial studies with fiddler crabs 205

DEVELOPMENT AND REPRODUCTION

Barber, Bruce J., Susan E. Ford, and Robert N. Wargo
Genetic variation in the timing of gonadal maturation and spawning of the eastern oyster, *Crassostrea virginica* (Gmelin) 216

Ó Foighil, Diarmaid, and Catherine Thiriot-Quiévreux
Ploidy and pronuclear interaction in northeastern Pacific *Lasaea* clones (Mollusca: Bivalvia) 222

Peterson, Christopher W.
Variation in fertilization rate in the tropical reef fish, *Halichoeres bivattatus:* correlates and implications 232

Tudge, C. C.
Spermatophore diversity within and among the hermit crab families, Coenobitidae, Diogenidae, and Paguridae (Paguroidea, Anomura, Decapoda) ... 238

ECOLOGY AND EVOLUTION

Lambert, Walter J.
Coexistence of hydroid eating nudibranchs: do feeding biology and habitat use matter? 248

Levitan, Don R.
Influence of body size and population density on fertilization success and reproductive output in a free-spawning invertebrate 261

Marcus, Nancy H.
Planktonic copepods in a sub-tropical estuary: seasonal patterns in the abundance of adults, copepodites, nauplii, and eggs in the sea bed 269

GENERAL BIOLOGY

Lewis, J. C., and E. von Wallis
The function of surface sclerites in gorgonians (Coelenterata, Octocorallia) 275

PHYSIOLOGY

Byrne, Roger A., and Brian R. McMahon
Acid-base and ionic regulation, during and following emersion, in the freshwater bivalve, *Anodonta grandis simpsoniana* (Bivalvia: Unionidae) 289

Gainey, Louis F., Jr., and Sandra E. Shumway
The physiological effect of *Aureococcus anophagefferens* ("brown tide") on the lateral cilia of bivalve mollusks 298

RESEARCH NOTES

Cerrato, Robert M., Heather V. E. Wallace, and Kent G. Lightfoot
Tidal and seasonal patterns in the chondrophore of the soft-shell clam *Mya arenaria* 307

Siebers, Dietrich, Tarig Mustafa, and Kirsten Böttcher
Effects of indomethacin on active ion transport across the gills of the shore crab, *Carcinus maenas* 312

SHORT REPORTS

Short Reports from the 1991 General Scientific Meetings of the Marine Biological Laboratory 315

Volume 181
Number 3

THE BIOLOGICAL BULLETIN

Marine Biological Laboratory
LIBRARY
DEC 3 0 1991
Woods Hole, Mass.

DECEMBER, 1991

Published by the Marine Biological Laboratory

Marine Biological Laboratory
LIBRARY

DEC 3 0 1991

Woods Hole, Mass.

THE
BIOLOGICAL BULLETIN

PUBLISHED BY
THE MARINE BIOLOGICAL LABORATORY

Associate Editors

PETER A. V. ANDERSON, The Whitney Laboratory, University of Florida
DAVID EPEL, Hopkins Marine Station, Stanford University
J. MALCOLM SHICK, University of Maine, Orono

Editorial Board

GEORGE J. AUGUSTINE, University of Southern California
LOUIS LEIBOVITZ, Marine Biological Laboratory
RUDOLF A. RAFF, Indiana University
KENSAL VAN HOLDE, Oregon State University
STEVEN VOGEL, Duke University

Editor: MICHAEL J. GREENBERG, The Whitney Laboratory, University of Florida
Managing Editor: PAMELA L. CLAPP, Marine Biological Laboratory

DECEMBER, 1991

Printed and Issued by
LANCASTER PRESS, Inc.
PRINCE & LEMON STS.
LANCASTER, PA

THE BIOLOGICAL BULLETIN

THE BIOLOGICAL BULLETIN is published six times a year by the Marine Biological Laboratory, MBL Street, Woods Hole, Massachusetts 02543.

Subscriptions and similar matter should be addressed to Subscription Manager, THE BIOLOGICAL BULLETIN, Marine Biological Laboratory, Woods Hole, Massachusetts 02543. Single numbers, $25.00. Subscription per volume (three issues), $72.50 ($145.00 per year for six issues).

Communications relative to manuscripts should be sent to Michael J. Greenberg, Editor-in-Chief, or Pamela L. Clapp, Managing Editor, at the Marine Biological Laboratory, Woods Hole, Massachusetts 02543. Telephone: (508) 548-3705, ext. 428. FAX: 508-540-6902.

POSTMASTER: Send address changes to THE BIOLOGICAL BULLETIN, Marine Biological Laboratory, Woods Hole, MA 02543.

Copyright © 1991, by the Marine Biological Laboratory

Second-class postage paid at Woods Hole, MA, and additional mailing offices.
ISSN 0006-3185

INSTRUCTIONS TO AUTHORS

The Biological Bulletin accepts outstanding original research reports of general interest to biologists throughout the world. Papers are usually of intermediate length (10–40 manuscript pages). A limited number of solicited review papers may be accepted after formal review. A paper will usually appear within four months after its acceptance.

Very short, especially topical papers (less than 9 manuscript pages including tables, figures, and bibliography) will be published in a separate section entitled "Research Notes." A Research Note in *The Biological Bulletin* follows the format of similar notes in *Nature*. It should open with a summary paragraph of 150 to 200 words comprising the introduction and the conclusions. The rest of the text should continue on without subheadings, and there should be no more than 30 references. References should be referred to in the text by number, and listed in the Literature Cited section in the order that they appear in the text. Unlike references in *Nature*, references in the Research Notes section should conform in punctuation and arrangement to the style of recent issues of *The Biological Bulletin*. Materials and Methods should be incorporated into appropriate figure legends. See the article by Lohmann *et al.* (October 1990, Vol. **179**: 214–218) for sample style. A Research Note will usually appear within two months after its acceptance.

The Editorial Board requests that regular manuscripts conform to the requirements set below; those manuscripts that do not conform will be returned to authors for correction before review.

1. ***Manuscripts.*** Manuscripts, including figures, should be submitted in triplicate. (Xerox copies of photographs are not acceptable for review purposes.) The original manuscript must be typed in no smaller than 12 pitch, using double spacing (*including* figure legends, footnotes, bibliography, etc.) on one side of 16- or 20-lb. bond paper, 8½ by 11 inches. Please, no right justification. Manuscripts should be proofread carefully and errors corrected legibly in black ink. Pages should be numbered consecutively. Margins on all sides should be at least 1 inch (2.5 cm). Manuscripts should conform to the *Council of Biology Editors Style Manual*, 4th Edition (Council of Biology Editors, 1978) and to American spelling. Unusual abbreviations should be kept to a minimum and should be spelled out on first reference as well as defined in a footnote on the title page. Manuscripts should be divided into the following components: Title page, Abstract (of no more than 200 words), Introduction, Materials and Methods, Results, Discussion, Acknowledgments, Literature Cited, Tables, and Figure Legends. In addition, authors should supply a list of words and phrases under which the article should be indexed.

2. ***Title page.*** The title page consists of: a condensed title or running head of no more than 35 letters and spaces, the manuscript title, authors' names and appropriate addresses, and footnotes listing present addresses, acknowledgments or contribution numbers, and explanation of unusual abbreviations.

3. ***Figures.*** The dimensions of the printed page, 7 by 9 inches, should be kept in mind in preparing figures for publication. We recommend that figures be about 1½ times the linear dimensions of the final printing desired, and that the ratio of the largest to the smallest letter or number and of the thickest to the thinnest line not exceed 1:1.5. Explanatory matter generally should be included in legends, although axes should always be identified on the illustration itself. Figures should be prepared for reproduction as either line cuts or halftones. Figures to be reproduced as line cuts should be unmounted glossy photographic reproductions or drawn in black ink on white paper, good-quality tracing cloth or plastic, or blue-lined coordinate paper. Those to be reproduced as halftones should be mounted on board, with both designating numbers or letters and scale bars affixed directly to the figures. All figures should be numbered in consecutive order, with no distinction between text and plate figures. The author's name and an arrow indicating orientation should appear on the reverse side of all figures.

4. ***Tables, footnotes, figure legends, etc.*** Authors should follow the style in a recent issue of *The Biological Bulletin* in preparing table headings, figure legends, and the like. Because of the high cost of setting tabular material in type, authors are asked to limit such material as much as possible. Tables, with their headings and footnotes, should be typed on separate sheets, numbered with consecutive Roman numerals, and placed after

the Literature Cited. Figure legends should contain enough information to make the figure intelligible separate from the text. Legends should be typed double spaced, with consecutive Arabic numbers, on a separate sheet at the end of the paper. Footnotes should be limited to authors' current addresses, acknowledgments or contribution numbers, and explanation of unusual abbreviations. All such footnotes should appear on the title page. Footnotes are not normally permitted in the body of the text.

5. ***Literature cited.*** In the text, literature should be cited by the Harvard system, with papers by more than two authors cited as Jones *et al.*, 1980. Personal communications and material in preparation or in press should be cited in the text only, with author's initials and institutions, unless the material has been formally accepted and a volume number can be supplied. The list of references following the text should be headed Literature Cited, and must be typed double spaced on separate pages, conforming in punctuation and arrangement to the style of recent issues of *The Biological Bulletin.* Citations should include complete titles and inclusive pagination. Journal abbreviations should normally follow those of the U. S. A. Standards Institute (USASI), as adopted by BIOLOGICAL ABSTRACTS and CHEMICAL ABSTRACTS, with the minor differences set out below. The most generally useful list of biological journal titles is that published each year by BIOLOGICAL ABSTRACTS (BIOSIS List of Serials; the most recent issue). Foreign authors, and others who are accustomed to using THE WORLD LIST OF SCIENTIFIC PERIODICALS, may find a booklet published by the Biological Council of the U.K. (obtainable from the Institute of Biology, 41 Queen's Gate, London, S.W.7, England, U.K.) useful, since it sets out the WORLD LIST abbreviations for most biological journals with notes of the USASI abbreviations where these differ. CHEMICAL ABSTRACTS publishes quarterly supplements of additional abbreviations. The following points of reference style for THE BIOLOGICAL BULLETIN differ from USASI (or modified WORLD LIST) usage:

A. Journal abbreviations, and book titles, all underlined (for *italics*)

B. All components of abbreviations with initial capitals (not as European usage in WORLD LIST *e.g. J. Cell. Comp. Physiol.* NOT *J. cell. comp. Physiol.*)

C. *All* abbreviated components must be followed by a period, whole word components *must not* (*i.e. J. Cancer Res.*)

D. Space between all components (*e.g. J. Cell. Comp. Physiol.*, not *J.Cell.Comp.Physiol.*)

E. Unusual words in journal titles should be spelled out in full, rather than employing new abbreviations invented by the author. For example, use *Rit Vísindafjélags Islendinga* without abbreviation.

F. All single word journal titles in full (*e.g. Veliger, Ecology, Brain*).

G. The order of abbreviated components should be the same as the word order of the complete title (*i.e. Proc.* and *Trans.* placed where they appear, not transposed as in some BIOLOGICAL ABSTRACTS listings).

H. A few well-known international journals in their preferred forms rather than WORLD LIST or USASI usage (*e.g. Nature, Science, Evolution* NOT *Nature, Lond., Science, N.Y.; Evolution, Lancaster, Pa.*)

6. ***Reprints, page proofs, and charges.*** Authors receive their first 100 reprints (without covers) free of charge. Additional reprints may be ordered at time of publication and normally will be delivered about two to three months after the issue date. Authors (or delegates for foreign authors) will receive page proofs of articles shortly before publication. They will be charged the current cost of printers' time for corrections to these (other than corrections of printers' or editors' errors). Other than these charges for authors' alterations, *The Biological Bulletin* does not have page charges.

CONTENTS

No. 1, August 1991

Annual Report of the Marine Biological Laboratory 1

Lenhoff, Howard M.
Ethel Browne, Hans Spemann, and the discovery of the Organizer Phenomenon 72

BEHAVIOR

Painter, Sherry D., Maria G. Chong, Mary A. Wong, Ann Gray, Jeffry G. Cormier, and Gregg T. Nagle
Relative contributions of the egg layer and egg cordon to pheromonal attraction and the induction of mating and egg-laying behavior in *Aplysia* 81

DEVELOPMENT AND REPRODUCTION

Ikegami, Susumu, Tomoko Mitsuno, Masanori Kataoka, Satoshi Yajima, and Miéko Komatsu
Immunological survey of planktonic embryos and larvae of the starfish *Asterina pectinifera*, obtained from the sea, using a monoclonal antibody directed against egg polypeptides 95

Morse, Daniel E., and Aileen N. C. Morse
Enzymatic characterization of the morphogen recognized by *Agaricia humilis* (scleractinian coral) larvae 104

ECOLOGY AND EVOLUTION

Brown, Alice F.
Outbreeding depression as a cost of dispersal in the harpacticoid copepod, *Tigriopus californicus* 123

Salter-Cid, Luisa, and Charles H. Bigger
Alloimmunity in the gorgonian coral *Swiftia exserta* 127

Wolfe, Connie J., and Margo G. Haygood
Restriction fragment length polymorphism analysis reveals high levels of genetic divergence among the light organ symbionts of flashlight fish 135

GENERAL BIOLOGY

Copeland, D. Eugene
Fine structure of photophores in *Gonostoma elongatum:* detail of a dual gland complex 144

Read, A. T., J. A. McTeague, and C. K. Govind
Morphology and behavior of an unusually flexible thoracic limb in the snapping shrimp, *Alpheus heterochelis* 158

PHYSIOLOGY

Cheng, Jin-Hua, and Ernest S. Chang
Ecdysteroid treatment delays ecdysis in the lobster, *Homarus americanus* 169

Gardiner, D. B., F. S. Turner, J. M. Myers, T. H. Dietz, and H. Silverman
Long-term culture of freshwater mussel gill strips: use of serotonin to affect aseptic conditions 175

Mensinger, Allen F., and James F. Case
Bioluminescence maintenance in juvenile *Porichthys notatus* 181

Michibata, Hitoshi, Akemi Morita, and Kan Kanamori
Vanadobin, a vanadium-binding substance, extracted from the blood cells of an ascidian, can reduce vanadate(V) to vanadyl(IV) 189

RESEARCH NOTE

McDermott, John J.
A breeding population of the Western Pacific crab *Hemigrapsus sanguineus* (Crustacea: Decapoda: Grapsidae) established on the Atlantic coast of North America 195

No. 2, October 1991

BEHAVIOR

Warner, Robert R., and Stephen E. Swearer
Social control of sex change in the bluehead wrasse, *Thalassoma bifasciatum* (Pisces: Labridae) 199
Weissburg, Marc J., and Richard K. Zimmer-Faust
Ontogeny *versus* phylogeny in determining patterns of chemoreception: initial studies with fiddler crabs 205

DEVELOPMENT AND REPRODUCTION

Barber, Bruce J., Susan E. Ford, and Robert N. Wargo
Genetic variation in the timing of gonadal maturation and spawning of the eastern oyster, *Crassostrea virginica* (Gmelin) 216
Ó Foighil, Diarmaid, and Catherine Thiriot-Quiévreux
Ploidy and pronuclear interaction in northeastern Pacific *Lasaea* clones (Mollusca: Bivalvia) 222
Peterson, Christopher W.
Variation in fertilization rate in the tropical reef fish, *Halichoeres bivattatus:* correlates and implications 232
Tudge, C. C.
Spermatophore diversity within and among the hermit crab families, Coenobitidae, Diogenidae, and Paguridae (Paguroidea, Anomura, Decapoda) ... 238

ECOLOGY AND EVOLUTION

Lambert, Walter J.
Coexistence of hydroid eating nudibranchs: do feeding biology and habitat use matter? 248
Levitan, Don R.
Influence of body size and population density on fertilization success and reproductive output in a free-spawning invertebrate 261
Marcus, Nancy H.
Planktonic copepods in a sub-tropical estuary: seasonal patterns in the abundance of adults, copepodites, nauplii, and eggs in the sea bed 269

GENERAL BIOLOGY

Lewis, J. C., and E. von Wallis
The function of surface sclerites in gorgonians (Coelenterata, Octocorallia) 275

PHYSIOLOGY

Byrne, Roger A., and Brian R. McMahon
Acid-base and ionic regulation, during and following emersion, in the freshwater bivalve, *Anodonta grandis simpsoniana* (Bivalvia: Unionidae) 289
Gainey, Louis F., Jr., and Sandra E. Shumway
The physiological effect of *Aureococcus anophagefferens* ("brown tide") on the lateral cilia of bivalve mollusks 298

RESEARCH NOTES

Cerrato, Robert M., Heather V. E. Wallace, and Kent G. Lightfoot
Tidal and seasonal patterns in the chondrophore of the soft-shell clam *Mya arenaria* 307
Siebers, Dietrich, Tarig Mustafa, and Kirsten Böttcher
Effects of indomethacin on active ion transport across the gills of the shore crab, *Carcinus maenas* 312

SHORT REPORTS

Short Reports from the 1991 General Scientific Meetings of the Marine Biological Laboratory 315

No. 3, December 1991

BEHAVIOR

Marko, Peter B., and A. Richard Palmer
Responses of a rocky shore gastropod to the effluents of predatory and non-predatory crabs: avoidance and attraction 363

DEVELOPMENT AND REPRODUCTION

Levitan, Don R., Mary A. Sewell, and Fu-Shiang Chia
Kinetics of fertilization in the sea urchin *Strongylocentrotus franciscanus:* interaction of gamete dilution, age, and contact time 371

ECOLOGY AND EVOLUTION

Ra'anan, Z., A. Sagi, Y. Wax, I. Karplus, G. Hulata, and A. Kuris
Growth, size rank, and maturation of the freshwater prawn, *Macrobrachium rosenbergii:* analysis of marked prawns in an experimental population 379
Zimmerman, Todd L., and Darryl L. Felder
Reproductive ecology of an intertidal brachyuran crab, *Sesarma* sp. (nr. *reticulatum*), from the Gulf of Mexico 387

GENERAL BIOLOGY

Cowan, Diane F.
The role of olfaction in courtship behavior of the American lobster *Homarus americanus* 402
Moore, Paul A., and Jelle Atema
Spatial information in the three-dimensional fine structure of an aquatic odor plume 408
Zimmer-Faust, Richard K.
Chemical signal-to-noise detection by spiny lobsters 419
O'Brien, Jack J., S. Sindhu Kumari, and Dorothy M. Skinner
Proteins of crustacean exoskeletons: I. Similarities and differences among proteins of the four exoskeletal layers of four brachyurans 427
Pullen, Julie, and Michael LaBarbera
Modes of feeding in aggregations of barnacles and the shape of aggregations 442

PHYSIOLOGY

Mangum, Charlotte P., John Greaves, and Julia S. Rainer
Oligomer composition and oxygen binding of the hemocyanin of the blue crab *Callinectes sapidus* . . 453
Paynter, Kennedy T., and Thomas T. Chen
Biological activity of biosynthetic rainbow trout growth hormone in the eastern oyster, *Crassostrea virginica* 459
Tamm, Sidney L., and Signhild Tamm
Reversible epithelial adhesion closes the mouth of *Beroë*, a carnivorous marine jelly 463

NEUROBIOLOGY

Scemes, Eliana, and John C. McNamara
The ultrastructure of the radial neuromuscular system of the jellyfish *Liriope tetraphylla* (Hydrozoa, Trachymedusae): implications in crumpling behavior 474
Soinila, Seppo, and George J. Mpitsos
Immunohistochemistry of diverging and converging neurotransmitter systems in mollusks 484

RESEARCH NOTE

Ohman, Mark D., Gail H. Theilacker, and Sandor E. Kaupp
Immunochemical detection of predation on ciliate protists by larvae of the northern anchovy (*Engraulis mordax*) 500

ABSTRACTS

Abstracts of papers presented at the Marine Biological Laboratory: 1991 Northeast Regional Developmental Biology Conference 505

Index to Volume 181 515

Reference: *Biol. Bull.* **181**: 363–370. (December, 1991)

Responses of a Rocky Shore Gastropod to the Effluents of Predatory and Non-predatory Crabs: Avoidance and Attraction

PETER B. MARKO[1] AND A. RICHARD PALMER[2]

Department of Zoology, University of Alberta, Edmonton, Alberta T6G 2E9 and
Bamfield Marine Station, Bamfield, British Columbia V0R 1B0 Canada

Abstract. Laboratory experiments revealed that the rocky shore gastropod, *Nucella lamellosa* (Gmelin), could discriminate between the effluents of predatory and non-predatory crabs. *N. lamellosa* turned away from seawater that had passed over the large predatory crab, *Cancer productus* Randall. This avoidance behavior was observed in snails from two localities that, based on differences in shell form, presumably experienced different levels of predation intensity. The scent of the non-predatory crabs *Pugettia producta* (Randall) and *Lopholithodes mandtii* Brandt had no effect on the turning behavior of snails from either site. Surprisingly, snails from both sites were attracted to the scent of a small shore crab, *Hemigrapsus nudus* (Dana), but moved at random in response to a common prey item *Balanus glandula* Darwin.

These results suggest that *N. lamellosa* can assess from a distance the relative risks posed by different species of crabs, and respond appropriately. The unexpected attraction to *H. nudus* suggests that *N. lamellosa* may use this effluent to home in from a distance on potential refugia, because *H. nudus* are often associated with crevices and the undersides of boulders where *N. lamellosa* would be less vulnerable to larger predators.

Introduction

Many marine invertebrates exhibit escape and avoidance behaviors (Bullock, 1953; Gore, 1966; Phillips, 1975; Lawn and Ross, 1982; Palmer *et al.*, 1982; Miller, 1986). An escape behavior is a response to direct contact with a predator and may be mediated by both physical and chemical stimuli, while an avoidance behavior is exclusively a response to substances diffused from a predator (Phillips, 1977). Hence, an avoidance behavior is a response to a distant threat, and may be adaptive for slow moving organisms that cannot otherwise escape from imminent attack by a faster moving predator.

Marine gastropods exhibit both escape and avoidance behaviors (for reviews see Kohn, 1961; Feder and Christensen, 1966; Ansell, 1969; Mackie, 1970; Snyder and Snyder, 1971; Feder, 1972). However, these responses are usually to slow-moving asteroid and gastropod predators (*e.g.*, Hoffman *et al.*, 1978; Fishlyn and Phillips, 1980; Schmitt, 1981), and few have involved predatory crabs [except see Geller (1982)]. Although predator-specificity of avoidance behaviors has been examined in some gastropods (Edwards, 1968; Phillips, 1976, 1977; Hoffman, 1980), the specificity of responses to highly mobile predators has not been investigated. In addition, few studies have tested for differences in responsiveness among populations experiencing different predation pressures.

The recent discovery that the scent from predatory crabs can influence the rates of feeding and growth, and the shell morphology of two thaidine gastropods, the northeastern Pacific *Nucella lamellosa* (Gmelin) (Appleton and Palmer, 1988) and the North Atlantic *N. lapillus* (L.) (Palmer, 1990), raises an important question. To what extent are these responses specific to predatory crabs rather than a more generalized response to crab effluents? A second question we addressed was whether snails from populations that had experienced different predation regimes exhibited different specificities or magnitudes of avoidance behaviors.

Received 18 June 1991; accepted 20 September 1991.

[1] Present address: Department of Zoology, University of California, Davis, CA 95616.

[2] Author to whom correspondence should be addressed.

Materials and Methods

Collection sites

Nucella lamellosa individuals were collected from two sites in the vicinity of Bamfield, Vancouver Island, British Columbia, during the summers of 1989 and 1990: (a) Grappler Inlet (48° 50′ 00″ N, 125° 06′ 49″ W), a quiet estuarine bay that receives little or no exposure to breaking waves; and (b) the Ross Islets (48° 52′ 24″ N, 125° 37′ 38″ W), a group of small islands in Barkley Sound that experiences intermediate wave action. With one exception, fresh snails were collected for each trial during low tide and held in air in the main aquarium room at the Bamfield Marine Station until used later the same day. However, one series of 100 snails from Grappler Inlet ('Grappler-lab') was acclimatized in running seawater for four days with *ad libitum* food (*Balanus glandula* Darwin on small stones). In all trials, snails were used only once and then returned to their site of origin. Care was taken not to collect again from the same area on the shore.

The effluent sources were acclimatized in the laboratory for four to five days after collection. In total, 4 *Cancer productus* Randall, 40 *Hemigrapsus nudus* (Dana), 9 *Pugettia producta* (Randall), 1 *Lopholithodes mandtii* Brandt, and approximately 600–900 *Balanus glandula* on small stones, were used as stimuli. Only male crabs were collected and were weighed wet in air. Because of large differences in body size, we could not precisely standardize the weights of crabs or barnacles in different trials. *C. productus* and *P. producta* individuals were collected from Grappler Inlet, *H. nudus* individuals from Dixon Island (48° 50′ N, 125° 06′ W), and the single *L. mandtii* from near Wizard Islet (48° 51′ N, 125° 09′ W). All crabs were offered frozen fish (sole and flounder) and blades of kelp (*Macrocystis* spp.) while held in the laboratory. *C. productus* and *H. nudus* consumed the fish; only *P. producta* ate kelp. The *L. mandtii* did not eat any food but was retained for only one week.

Experimental procedure and rationale

Nucella lamellosa specimens were exposed to effluents in a choice apparatus similar to that used by Pratt (1974). Two plastic holding tanks [Fig. 1a(i), 20 × 15 × 18 cm] supplied by a common seawater source each emptied into separate plastic header tanks [Fig. 1a(ii), 30 × 40 × 10 cm]. The header tanks overflowed onto inclined, textured glass plates that sloped toward each other [Fig. 1a(iii), 25 × 35 cm] and met at a central horizontal platform of plexiglass [Fig. 1a(iv)]. Seawater from the two sides only mixed on the center platform and drained from there via small holes (Fig. 1b). The flow rates into both holding tanks were adjusted to be equal (80 ml/s), and sufficient to produce a thin film of water (1–2 mm deep) flowing down each plate. The holding tanks were placed within header tanks to minimize the effect of crab movement on this thin film of flowing water. Two complete apparatuses were used in two separate seawater trays oriented perpendicular to each other. Experiments were conducted under ambient light levels during the late morning and early afternoon of the day snails were collected from the field.

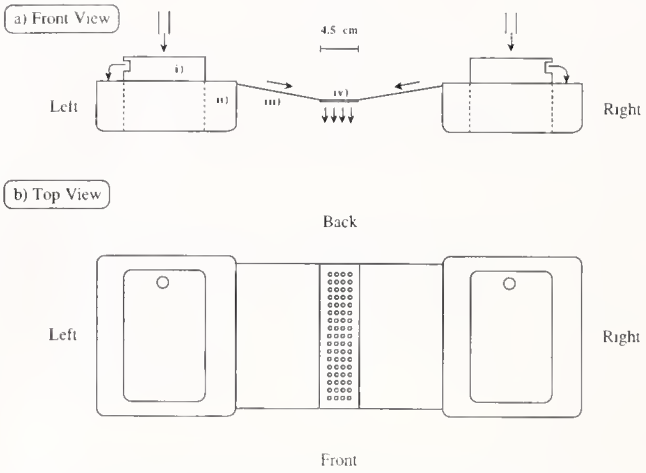

Figure 1. Schematic diagram of the choice apparatus used to assay behavioral responses of *Nucella lamellosa* individuals to various effluents: (a) front view, (b) top view. The effluent source was placed into one of the two holding tanks (i). The holding tanks emptied into header tanks (ii), which in turn emptied onto sloping, textured glass plates (iii). A thin film of water from each plate mixed on the central platform (iv) and was drained there by small holes (b). Snails were placed on the central platform with the coiling axis of their shells perpendicular to the flow of seawater.

A trial began by placing an effluent source, either one species of crab or stones covered with barnacles, into either the right or left holding tank and allowing it to acclimatize for 20 min. The opposite holding tank contained only running seawater. Four to six *Nucella lamellosa* were tested at a time, depending on their size. Snails were placed on the perforated center platform [Fig. 1a(iv)] with their axis of coiling perpendicular to the flow of water. Adjacent snails were placed in alternating orientations, with their siphonal canal pointing either to the front or back of the apparatus. They were placed 2–4 cm apart so they were free to move without contacting each other. If two did come in contact, they were removed from the experiment.

When approximately half the snails collected for a particular trial had been tested, the effluent source was removed, the apparatus rinsed out with seawater, and the same effluent source switched to the opposite holding tank. The remaining snails were then tested as before. This procedure allowed us to test for movement biases induced by the apparatus.

To determine whether behavioral responses varied with snail size, snails were scored as either shorter or longer than 30 mm in shell length (tip of siphonal canal to apex

Table I

Statistical tests of the effects of five factors on the direction of movement by Nucella lamellosa *relative to the choice apparatus*

	P-values for snails turning to right and left side of apparatus vs.:				
Effluent source	a) Year of experiment	b) Seawater tray	c) Snail size	d) Snail locality	e) Snail orientation at start
Cancer productus	0.9677	0.9055	0.8743	0.7958‡	0.0211
Hemigrapsus nudus	ND	ND	0.9893	0.4885	0.5084
Pugettia producta	0.5488	0.5488	0.7421	0.6806	0.5141
Lopholithodes mandtii	ND	ND	0.6158	0.9202	0.2404
Balanus glandula	ND	0.5354	0.6007	0.8877‡	0.0040

Data were pooled from all trials with a given effluent source. *P*-values, from 2 × 2 contingency tables, indicate the significance of the relationship between the listed variable's states and direction of movement (to right or to left). Variables and their states are as follows: year of experiment (1989, 1990), seawater tray (A, B; trays at right angles to each other), snail size (shell length < 30 mm, shell length > 30 mm), snail locality (Grappler Inlet, Ross Islets), snail orientation at start (siphon towards front, siphon towards back of apparatus). Note that stimuli were presented from the right and left sides in roughly equal frequencies. In the interest of economy, means from all these analyses are not presented but may be obtained from the authors on request.

‡ d.f. = 2 (*i.e.*, a third group from Grappler, acclimatized in lab, was included). ND = no data.

of shell). This length was chosen because most *N. lamellosa* shells less than 30 mm generally do not exhibit pronounced defensive traits, such as apertural teeth, which are typical of mature snails.

Since the initial orientation of each snail was known, the side of the snail exposed to the effluent source was known. The direction it turned with respect to itself (either toward the apertural lip or toward the columella) was thus also known, as well as the direction of its movement relative to the effluent source.

The direction a snail moved was scored only after its entire foot had moved off the perforated center platform and onto one of the glass plates. Snails that did not leave the platform after 45 min were noted but not included in the analyses. The average percent not responding was 12.4 ± 7.08% (n = 23) for large (>30 mm) and 5.1 ± 8.26% (n = 20) for small snails (<30 mm; mean ± SD).

Results

Tests for sources of experimental bias

Because each effluent was presented from both sides of the apparatus and from both sides of the snails at roughly equal frequencies, equal numbers should have moved to the right and left sides of the apparatus, regardless of the effluent. To determine whether the apparatus or other factors influenced turning direction, the effect of several factors on the direction moved relative to the apparatus was analyzed by 2 × 2 contingency tables.

With one exception, none of the potential sources of bias had a significant effect. Neither the year, the location within the laboratory, the size of snails, or source population had a significant effect on the direction of movement by snails *relative to the apparatus,* regardless of the effluent (Table I, columns a–d). The effect of snail locality was tested using data pooled from three effluent sources: *Hemigrapsus nudus, Pugettia producta,* and *Lopholithodes mandtii.* Lab-acclimatized snails from Grappler Inlet ('Grappler-lab') were treated as a third locality for the analyses where *Cancer products* and *Balanus glandula* were the effluent sources.

The only detectable source of bias we observed was the starting orientation of snails, and this effect was observed only for two effluent sources: *C. productus* and *B. glandula* (Table I, column e). For *C. productus,* snails turned to the left side of the apparatus more frequently than expected when the siphonal canal faced the front (58.0 *vs.* 50%). Similarly, more snails turned toward the right side of the apparatus than expected when the siphonal canal faced the back (54.1 *vs.* 50%). In other words, most snails turned toward the apertural lip, because the lip is on the left side when viewed from the siphonal canal. The same trend was observed with *B. glandula* effluent: 55.8% turned toward the left of the apparatus if started facing front, and 62.6% turned toward the right if started facing back.

Responses to stimuli

Specificity of behavioral responses. The behavioral responses of *N. lamellosa* depended on the stimulus (Table II; see also Fig. 3 below). Significant numbers moved away from the effluent in at least one trial for each of the five different *C. productus* individuals tested. Two individuals of *C. productus* were used twice, but exposed to different source populations of snails. In sharp contrast, significant numbers of snails were attracted to the effluent of *H. nu-*

Table II

Behavioral responses of Nucella lamellosa *to effluent from five crustaceans*

Effluent source			Source on right		Source on left		
Species	Wet weight (g)	Snail locality	Snails to right	Snails to left	Snails to right	Snails to left	χ^2
Cancer productus	325.5	Grappler	7	14	16	9	4.29*
	337.4	Grappler	6	13	15	7	5.46*
	337.4	Ross	9	19	25	20	3.80^{+}
	575.1	Grappler	7	7	7	7	0.00
	575.1	Grappler-lab§§	7	20	15	5	11.11***
	535.2	Grappler	12	25	24	14	7.09**
	339.3	Ross	5	18	16	6	11.75***
Hemigrapsus nudus	$206.4^{\dagger}$	Grappler	13	6	8	15	4.71*
	$206.4^{\dagger}$	Ross	21	15	13	24	3.95*
	$175.9^{\dagger}$	Grappler	23	11	14	22	5.80*
Pugettia producta	$148.8^{\ddagger}$	Grappler	11	10	11	12	0.09
	$125.1^{\ddagger}$	Grappler	10	11	11	9	0.22
	$125.1^{\ddagger}$	Ross	22	20	11	14	0.44
	$137.9^{\ddagger}$	Ross	8	14	8	6	1.50
Lopholithodes mandtii	440.5	Grappler	10	11	11	12	<0.01
	440.5	Ross	11	10	10	14	0.52
Balanus glandula	—§	Grappler	17	12	12	13	0.61
	—	Grappler	11	10	12	13	0.09
	—	Ross	14	12	15	9	0.38
	—	Ross	10	12	12	8	0.89
	—	Grappler-lab§§	9	3	7	8	2.22
	—	Grappler-lab§§	7	7	5	7	0.18

The effluent source was placed on either the right or the left of the snails in the choice apparatus, and each snail was scored according to the direction that it moved. Chi-square values resulted from comparing 'Source on right' and 'Source on left' data by means of a 2 × 2 contingency table (df = 1 for all tests).

$^{+}P < 0.1$, $*P < 0.05$, $**P < 0.01$, $***P < 0.001$.

† Combined weight of 20 crabs. ‡Combined weight of three crabs.

§ Weights of barnacles were not known for each experiment (100–150 individuals). §§Snails were acclimatized in the laboratory in running seawater with food for four days.

dus. Two different groups of *H. nudus* were used, and both attracted *N. lamellosa.* However, snails neither avoided nor were attracted to the effluent from three different groups of *P. producta,* six different groups of *B. glandula,* and the one *L. mandtii. L. mandtii* was thus the only stimulus for which we did not have more than one independent source.

Effects of manipulated variables on responses to effluent sources. Neither the year of experiment (Table III, column a), seawater tray (column b), nor snail size (column c) had a significant effect on patterns of movement relative to the effluent source. However, the direction that snails turned with respect to themselves depended significantly on the presence of effluent when *H. nudus* was the source (column e): among snails that turned away from *H. nudus,* 68.7% turned aperturally. That is, even though most snails turned toward *H. nudus,* those that turned away were more likely to do so if their apertural lip originally faced away from the stimulus.

To assess the extent of the apparent turning bias (column e, Tables I and III), the proportion of all snails that turned aperturally, regardless of the side of origin of the effluent, was tested against the proportion expected if turning was random. Out of 1026 snails, significantly more (54.9%) turned aperturally than expected (50%; $\chi^2 = 4.93$, df = 1, $P < 0.05$). This percentage (54.9%) was thus used as the percentage of snails expected to turn aperturally in the Chi-square tests of Figure 2.

When the effluent from *C. productus* arrived from the apertural side, significantly fewer snails than expected turned aperturally (Fig. 2, $P < 0.01$), whereas significantly more turned aperturally when the effluent came from the columellar side ($P < 0.01$). Conversely, more snails turned aperturally than expected when *H. nudus* effluent approached from the apertural side, though this was not quite significant statistically (Fig. 2, $P < 0.1$), and significantly fewer snails turned aperturally when effluent came from the columellar side ($P < 0.05$). The proportion of

Table III

Statistical tests of the effects of five factors on the response of Nucella lamellosa *to the effluent from five crustaceans*

	P-values for snails turning towards and away from effluent source vs.:				
Effluent source	(a) Year of experiment	(b) Seawater tray	(c) Snail size	(d) Snail locality	(e) Direction snail turned with respect to itself
Cancer productus	0.3029	0.9859	0.7333	0.3756‡	0.2760
Hemigrapsus nudus	ND	ND	0.3111	0.6249	0.0009
Pugettia producta	0.1580	0.1580	0.5570	0.9888	0.8507
Lopholithodes mandtii	ND	ND	0.4388	0.5996	0.8626
Balanus glandula	ND	0.9815	0.3437	0.2813‡	0.4106

Data were pooled from all trials with a given effluent source. P-values, from 2 × 2 contingency tables, indicate the significance of the relationship between the listed variable's states and *N. lamellosa* responses (towards or away from effluent source). See Table I for variable states except column e (to apertural lip, or to columella). See Figure 3 for sample sizes and means for snail locality. The remaining means from these many analyses are not presented in the interest of economy, but may be obtained from the authors on request.

‡ d.f. = 2 (as for Table I). ND = no data.

snails that turned aperturally when the effluent sources were *P. producta, L. mandtii,* and *B. glandula* were not significantly different from expected. Thus, incorporating the bias introduced by starting orientation had no effect on the results.

Differences between populations of snails

Nucella lamellosa from Grappler Inlet, the Ross Islets, and lab-acclimatized snails from Grappler Inlet, all exhibited a statistically significant avoidance of *C. productus* effluent (Fig. 3, Table II). Those from the Ross Islets exhibited as strong a response as those from Grappler Inlet. The proportion of lab-acclimatized snails that avoided *C. productus* was larger than that of freshly collected snails but was less significant statistically because of the smaller sample size.

N. lamellosa individuals from both localities were clearly attracted to the effluent from *Hemigrapsus nudus* (Fig. 3). Snails from the Ross Islets exhibited a stronger response ($P < 0.001$) than those from Grappler Inlet ($P < 0.05$). Neither of the two populations turned preferentially relative to the effluent from *P. producta, L. mandtii,* or *B. glandula.* Although lab-acclimatized snails from Grappler Inlet turned toward the effluent of *B. glandula* more frequently than freshly collected snails, this preference was not significantly different from 50.0%.

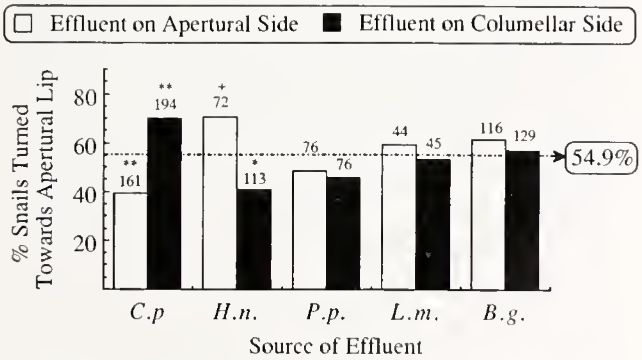

Figure 2. Behavioral responses of *Nucella lamellosa* individuals to the effluent from five different crustaceans. Snails received effluent in a choice apparatus from either the apertural or columellar side of their shells. Responses were pooled across all trials for each stimulus. The percent of snails that turned aperturally in response to a given effluent was compared by means of a Chi-square test to the percentage of all snails that turned aperturally (54.9%). *C.p.* = *Cancer productus, H.n.* = *Hemigrapsus nudus, P.p.* = *Pugettia producta, L.m.* = *Lopholithodes mandtii, B.g.* = *Balanus glandula.* $^{+}P < 0.1$, $^{*}P < 0.05$, $^{**}P < 0.01$, $^{***}P < 0.001$. Numbers above bars are sample sizes.

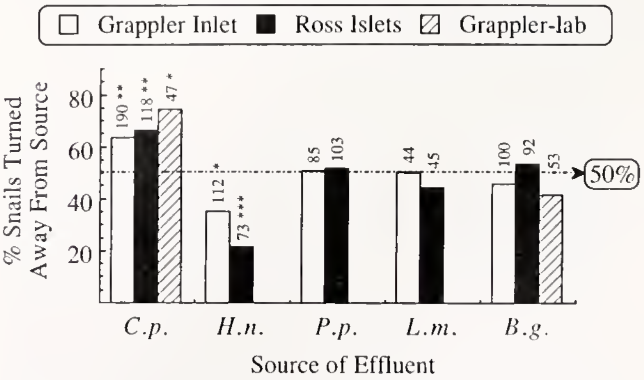

Figure 3. Avoidance responses of *Nucella lamellosa* individuals from two localities to various effluents. A third group of snails was acclimatized in the laboratory for one week with food ('Grappler-lab'). Snails were scored as moving either toward or away from each effluent source in a choice apparatus, and responses were pooled across all trials for each stimulus. The observed number of snails that turned away from each effluent source was compared by means of a Chi-square test to the number expected if they had turned at random (50.0%). Abbreviations and symbols as in Figure 2.

Discussion

Potential sources of experimental bias

Of the many possible sources of experimental bias we examined, only one had a statistically significant effect, and the effect was small. The preference of *Nucella lamellosa* to turn towards the apertural lip was slight, and appeared to have little effect on statistical inference whether incorporated in the analysis (Fig. 2) or ignored (Table II, Fig. 3). Although other explanations are possible, our handling protocol seems most likely to have been responsible for this turning bias. To standardize starting orientation, snails were placed with the coiling axis perpendicular to the flow of water. However, because the foot emerges from the apertural side, its long axis would generally have pointed toward one side of the apparatus, and snails thus may have been more likely to move in that direction.

Another possible source of bias in our experiments was the wet mass of stimulus used, because different responses to different species of crabs might have arisen as an artifact of differences in crab biomass. Biomass differences, however, seem unlikely to have influenced our results for two reasons. First, although the wet masses of *Pugettia producta*, for which no significant preference was detected, were the lowest of all crabs tested (125.1–148.8 g), the wet mass of *Lopholithodes mandtii* was the second highest (440.5 g), and no turning preference was observed for this stimulus either. Second, different sized *C. productus* individuals had no consistent effect on the magnitude of turning preference we observed: the largest crab (575.1 g) was associated with one highly significant response and one nonsignificant response, and the two most significant responses occurred with crabs of quite different size (575.1 and 339.3 g; Table II).

Responses to stimuli

Adaptive significance of a behavioral response to shell-breaking predators. The morphological responses of gastropods to shell-breaking predators have been well studied in both ecological and evolutionary time. The shell form of thaidine gastropods varies rather dramatically among local populations, and empirical evidence suggests that thick shells, characteristic of quiet-water shores, reduce vulnerability to predatory crabs (Kitching *et al.*, 1966; Hughes and Elner, 1979; Palmer, 1985). Defensive attributes of these shells can also be amplified by substances diffused from predatory crabs (Appleton and Palmer, 1988; Palmer, 1990). Geographic variation in shell morphology suggests that predation intensity increases toward tropical latitudes (Vermeij, 1978; Palmer, 1979; Bertness and Cunningham, 1981). Finally, shell-breaking predators appear to have been an important source of mortality as far back as the mid Palaeozoic (Signor and Brett, 1984) and appear to have increased in importance throughout the Mesozoic (Vermeij, 1977).

In contrast to the extensive studies of shell morphology, the behavioral responses of gastropods to highly mobile shell-breaking predators has received very little attention, presumably because the passive defense provided by the shell is usually considered the only option. Thicker shells, however, entail a greater cost (Palmer, 1981). Geller (1982) suggests that the lightly armored *Tegula funebralis* has evolved an avoidance response to a predatory crab as compensation for having a relatively thin shell. Our results indicate that *N. lamellosa*, a temperate species capable of secreting very thick shells, has also evolved a similar behavioral adaptation.

Although slow by comparison to the speed of their predators, the behavioral defenses of *N. lamellosa* may nonetheless still reduce their vulnerability. An avoidance response, if adaptive, functions to reduce the probability of encounter between predator and prey. Hence, it does not necessarily require quick movement. Its effectiveness would presumably increase as the distance to which the prey could detect the predator increased. Furthermore, in the heterogeneous environment of rocky shores, a refuge may be only a few centimeters away, also reducing the need for a dramatic response.

Adaptive significance of specificity. The avoidance of crabs by *N. lamellosa* appears to be specific to predatory species. Predator-specific defensive behaviors have been observed in other gastropods in response to both predatory asteroids and gastropods (Edwards, 1968; Phillips, 1976; Hoffman, 1980), and have also been observed in barnacles (Palmer *et al.*, 1982), anemones (Lawn and Ross, 1982), and echinoderms (Shaw and Fontaine, 1990). Such specificity presumably evolves because avoidance behaviors are costly in terms of time lost from foraging. Dogwhelks, for example, require from several hours to a day to handle a single barnacle (Dunkin and Hughes, 1984) or mussel (Hughes and Dunkin, 1984). Time spent retreating to and remaining in a refuge in response to a distant predator could otherwise be used for foraging. Avoidance behaviors should thus evolve to a level of specificity that minimizes inappropriate responses. Numerous studies suggest that invertebrates can weigh these tradeoffs between risk and reward while foraging (Sih, 1986; Burrows and Hughes, 1989).

The attraction of *N. lamellosa* to the scent of *Hemigrapsus nudus* was initially quite puzzling, because large *H. nudus* can break the shells of small *Nucella* in the laboratory (V. Ash and A. R. Palmer, unpub. obs.). This attraction was observed in three separate experiments with snails from two different populations (Table II) and hence was not a sampling artifact. On reflection, we feel this attraction may have a rather intriguing explanation. Because snails rely on olfaction as their primary sensory mechanism (Kohn, 1961), *N. lamellosa* may use the waterborne cues released by *H. nudus* to locate potential refugia, such as crevices or the undersides of boulders, from a distance. Without such distance chemoreception, snails would have to rely either on local cues encountered through random movement (*e.g.*, rapidly changing light levels or reduced water movement) or on their ability to retrace a path back to a refuge left earlier. Because *H. nudus* commonly occurs in crevices and under rocks on almost any rocky shore in the northeastern Pacific (Kozloff, 1987), they would consistently be associated with potential refugia. Although *N. lamellosa* might possibly have been attracted to what was perceived as a 'familiar' scent in the unfamiliar surroundings of the laboratory, the lack of an attraction to barnacles (Table II) would seem to rule this out.

The lack of a response to barnacles, common prey for *N. lamellosa,* was surprising. The experimental procedure was designed to minimize the effects of the laboratory on snail behavior by using animals as soon as they were brought back from the field. However, this procedure may have been mildly stressful, and may thus have suppressed normal foraging behaviors. Snails that experienced the slight 'trauma' of being detached and handled may have only been sensitive to risk-related stimuli rather than foraging-related stimuli.

Differences between populations

Nucella lamellosa individuals from the protected shores of Grappler Inlet have thick shells with pronounced apertural teeth, whereas those from the Ross Islets, a site of intermediate wave exposure, have much thinner shells and less pronounced apertural teeth (Appleton and Palmer, 1988). These large morphological differences imply very different predation regimes. Geller (1982) reported that *Tegula funebralis* from a site where crabs were absent did not show an avoidance behavior, while those sympatric with crabs did. Although we did not include a site where predatory crabs were totally absent, we found that snails from these two sites of presumably quite different predation intensity nonetheless responded similarly to the scent of *C. productus.* This result parallels others for *N. lamellosa* from the same two localities, where snails altered their morphology in an adaptive manner when exposed to the scent of *C. productus* over longer periods of time (Appleton and Palmer, 1988). Thus the ability of snails from both localities to distinguish between predatory and non-predatory crabs is not surprising.

Acknowledgments

We thank the director and staff of the Bamfield Marine Station for supplying research space and assistance, and Geerat Vermeij and an anonymous reviewer for comments on the MS. This research was supported by an NSERC undergraduate summer research award to PBM and NSERC operating grant A7245 to ARP, for which we are both grateful.

Literature Cited

Ansell, A. D. 1969. Defensive adaptations to predation in the Mollusca. *Proc. Symp. Mollusca* **2:** 487–512.

Appleton, R. D., and A. R. Palmer. 1988. Water-borne stimuli released by predatory crabs and damaged prey induce more predator resistant shells in a marine gastropod. *Proc. Natl. Acad. Sci. USA* **85:** 4387–4391.

Bertness, M. D., and C. Cunningham. 1981. Crab shell-crushing predation and gastropod architectural defense. *J. Exp. Mar. Biol. Ecol.* **50:** 213–230.

Bullock, T. H. 1953. Predator recognition and escape responses of some intertidal gastropods in the presence of starfish. *Behavior* **5:** 130–140.

Burrows, M. T., and R. N. Hughes. 1989. Natural foraging of the dogwhelk, *Nucella lapillus* (Linnaeus); the weather and whether to feed. *J. Moll. Stud.* **55:** 285–295.

Dunkin, S. d. B., and R. N. Hughes. 1984. Behavioral components of prey-selection by dogwhelks, *Nucella lapillus* (L.), feeding on barnacles, *Semibalanus balanoides* (L.) in the laboratory. *J. Exp. Mar. Biol. Ecol.* **79:** 91–103.

Edwards, C. D. 1968. Predators on *Olivella biplicata,* including a species-specific predator avoidance response. *Veliger* **11:** 326–333.

Feder, H. M. 1972. Escape responses in marine invertebrates. *Sci. Am.* **227:** 92–100.

Feder, H. M., and A. M. Christensen. 1966. Aspects of asteroid biology. Pp. 88–127 in *Physiology of Echinodermata,* R. A. Boolootian, ed. Wiley & Sons, New York.

Fishlyn, D. A., and D. A. Phillips. 1980. Chemical camouflaging and behavioral defenses against a predatory seastar by three species of gastropods from the surfgrass *Phyllospadix* community. *Biol. Bull.* **158:** 34–48.

Geller, J. B. 1982. Chemically mediated avoidance response of a gastropod, *Tegula funebralis* (A. Adams), to predatory crabs, *Cancer antennarius* (Stimpson). *J. Exp. Mar. Biol. Ecol.* **65:** 19–27.

Gore, R. H. 1966. Observations on the escape response in *Nassarius vibex* (Say), (Mollusca: Gastropoda). *Bull. Mar. Sci.* **16:** 423–434.

Hoffman, D. L. 1980. Defensive responses of marine gastropods to certain predatory sea stars and the dire whelk, *Searlesia dira. Pac. Sci.* **34:** 223–243.

Hoffman, D. L., W. C. Homan, J. Swanson, and P. J. Weldon. 1978. Flight responses of three congeneric species of intertidal gastropods (Prosobranchia: Neritidae) to sympatric predatory gastropods from Barbados. *Veliger* **21:** 293–296.

Hughes, R. N., and S. d. B. Dunkin. 1984. Behavioral components of prey selection by dogwhelks, *Nucella lapillus* (L.), feeding on mussels, *Mytilus edulis* L., in the laboratory. *J. Exp. Mar. Biol. Ecol.* **77:** 45–68.

Hughes, R. N., and R. W. Elner. 1979. Tactics of a predator, *Carcinus maenas,* and morphological responses of the prey, *Nucella lapillus. J. Anim. Ecol.* **48:** 65–78.

Kitching, J. A., L. Muntz, and F. J. Ebling. 1966. The ecology of Lough Ine XV. The ecological significance of shell and body forms in *Nucella. J. Anim. Ecol.* **35:** 113–126.

Kohn, A. J. 1961. Chemoreception in gastropod molluscs. *Am. Zool.* **1:** 291–308.

Kozloff, E. N. 1987. *Marine Invertebrates of the Pacific Northwest.* University of Washington Press, Seattle. 511 pp.

Lawn, I. D., and D. M. Ross. 1982. The release of the pedal disc in an undescribed species of *Tealia* (Anthozoa: Actinaria). *Biol. Bull.* **163:** 188–196.

Mackie, A. M. 1970. The escape reactions of marine invertebrates to predatory starfish. Pp. 269–274 in *Proceedings of the 5th European Marine Biology Symposium,* B. Battaglia, ed., Padova.

Miller, M. L. 1986. Avoidance and escape responses of the gastropod *Nucella emarginata* (Deshayes, 1839) to the predatory seastar *Pisaster ochraceus* (Brandt, 1835). *Veliger* **28:** 394–396.

Palmer, A. R. 1979. Fish predation and the evolution of gastropod shell sculpture: experimental and geographic evidence. *Evolution* **33:** 697–713.

Palmer, A. R. 1981. Do carbonate skeletons limit the rate of body growth? *Nature* **292:** 150–152.

Palmer, A. R. 1985. Adaptive value of shell variation in *Thais lamellosa:* effect of thick shells on vulnerability to and preference by crabs. *Veliger* **27:** 249–356.

Palmer, A. R. 1990. Effect of crab effluent and scent of damaged conspecifics on feeding, growth, and shell morphology of the Atlantic dogwhelk *Nucella lapillus* (L.). *Hydrobiologia* **193:** 155–182.

Palmer, A. R., J. Szymanska, and L. Thomas. 1982. Prolonged withdrawal: a possible predator evasion behavior in *Balanus glandula* (Crustacea: Cirripedia). *Mar. Biol.* **67:** 51–55.

Phillips, D. W. 1975. Distance chemoreception-triggered avoidance behavior of the limpets *Acmaea* (Collisella) *limatula* and *Acmaea* (Notoacmaea) *scutum* to the predatory starfish *Pisaster ochraceus. J. Exp. Zool.* **191:** 199–210.

Phillips, D. W. 1976. The effect of a species-specific avoidance response to predatory starfish on the intertidal distribution of two gastropods. *Oecologia* **23:** 83–94.

Phillips, D. W. 1977. Avoidance and escape responses of the gastropod mollusc *Olivella biplicata* (Sowerby) to predatory asteroids. *J. Exp. Mar. Biol. Ecol.* **28:** 77–86.

Pratt, D. M. 1974. Attraction to prey and stimulus to attack in the predatory gastropod *Urosalpinx cinerea. Mar. Biol.* **27:** 37–45.

Schmitt, R. J. 1981. Contrasting anti-predator defenses of sympatric marine gastropods (family Trochidae). *J. Exp. Mar. Biol. Ecol.* **54:** 251–263.

Shaw, G. D., and A. R. Fontaine. 1990. The locomotion of the comatulid *Florometra serratissima* (Echinodermata: Crinoidea) and its adaptive significance. *Can. J. Zool.* **68:** 942–950.

Signor, P. W. I., and C. E. Brett. 1984. The mid-Paleozoic precursor to the Mesozoic marine revolution. *Paleobiology* **10:** 229–245.

Sih, A. 1986. Predators and prey life-styles: an evolutionary and ecological overview. Pp. 203–224 in *Predation. Direct and Indirect Impacts on Aquatic Communities,* W. C. Kerfoot and A. Sih, eds. University Press of New England, Hanover, NH.

Snyder, N. F. R., and H. A. Snyder. 1971. Pheromone-mediated behavior of *Fasciolaria tulipa. Anim. Behav.* **19:** 257–268.

Vermeij, G. J. 1977. The Mesozoic faunal revolution: evidence from snails, predators and grazers. *Paleobiology* **3:** 245–258.

Vermeij, G. J. 1978. *Biogeography and Adaptation: Patterns of Marine Life.* Harvard University Press, Cambridge, MA. 332 pp.

Reference: *Biol. Bull.* **181:** 371–378. (December, 1991)

Kinetics of Fertilization in the Sea Urchin *Strongylocentrotus franciscanus:* Interaction of Gamete Dilution, Age, and Contact Time

DON R. LEVITAN[1,2,*], MARY A. SEWELL[1,2] AND FU-SHIANG CHIA[1]

[1] *Department of Zoology, University of Alberta, Edmonton, Alberta, Canada T6G 2E9; and*
[2] *Bamfield Marine Station, Bamfield, British Columbia, Canada V0R 1B0*

Abstract. Determining fertilization success of free spawning organisms in the field requires knowledge of how eggs and sperm interact under varying encounter frequencies and durations. In the laboratory, we investigated the relative influence of sperm concentration, egg concentration, sperm-egg contact time, and sperm age on fertilization in the sea urchin *Strongylocentrotus franciscanus.* Our results indicated that sperm concentration, sperm-egg contact time, sperm age, and individual variability were sequentially the most important factors influencing fertilization success. Egg concentration was not significant over the range tested. A theoretical model of fertilization (Vogel-Czihak-Chang-Wolf model) was used to estimate the two rate constants of fertilization kinetics: the rate constant of sperm-egg encounter and rate constant of fertilization. This model explained 91% of the variation in fertilization success, provided estimates of the rate constants involved in fertilization,.and indicated the proportion (3%) of sperm-egg contacts that result in fertilization. Estimates of sperm swimming velocity and egg diameter were used to independently calculate the rate of sperm-egg encounter and confirm the predictions of the model. This model also predicts the non-significant effect of egg concentration on fertilization success found empirically.

Introduction

At least two approaches can be used to resolve questions concerning the fertilization success of free spawning organisms. The first is to collect field data during spawning events, and the second is to construct models based on laboratory observations of fertilization and field observations of water flow conditions. Because of inherent problems with both approaches, a combination of methodologies would provide the best understanding of the processes involved in field fertilization success and the most powerful predictive abilities. Problems with *in situ* measures of fertilization include experimental artifacts that may influence estimates of fertilization (Pennington, 1985; Yund, 1990; Levitan, 1991; and Levitan *et al.*, in press) and the serendipitous nature of being able to collect relevant data during rare spawning events (Petersen, in press, Petersen *et al.*, in press). Problems with the construction of fertilization models include gathering accurate estimates of water flow and turbulence during periods of spawning (for a model of fertilization in wave-swept shores see Denny and Shibata, 1989) and knowledge of how gametes interact under various encounter frequencies and durations. Here we investigate, in the laboratory, the interaction of gamete concentration, age, and contact time in light of measures of sperm swimming velocity and egg size, and theoretical predictions of fertilization kinetics.

This is by no means the first attempt to describe fertilization success in the laboratory. There is a rich history of research on fertilization kinetics aimed at describing how the number of gametes, age of gametes, and other factors influence fertilization (*e.g.*, Lillie, 1915; Rothschild and Swann, 1951; Hultin and Hagstrom, 1956; Brown and Knouse, 1973; Vogel *et al.*, 1982; Pennington, 1985). These previous studies have documented that (1) fertilization is sensitive to sperm concentration and sperm age (references above), (2) fertilization is insensitive to egg concentration (Lillie, 1915), (3) fertilization is sensitive to the time of eggs spend in a sperm solution (Rothschild and Swann, 1951) and (4) fertilization kinetics should be

---

Received 13 May 1991; accepted 5 August 1991.

* Correspondence address: Department of Zoology, University of California, Davis, CA 95616-8755.

a function of gamete concentration, sperm age, sperm velocity, and egg size (however, the dependence of fertilization on egg size and sperm velocity was predicted and not tested empirically—Vogel *et al.*, 1982). These conclusions are crucial to our understanding of *in situ* fertilization (*e.g.*, Denny, 1988; Denny and Shibata, 1989). However, no study to date has addressed these factors simultaneously under the range of values normally encountered in nature, or has used estimates of sperm velocity and egg size to predict rates of fertilization.

In this study we first address four parameters of gamete kinetics and their interaction: sperm concentration, sperm age, sperm-egg contact time (the time an egg spends at a particular sperm concentration), and egg concentration. Second, we use a fertilization kinetics model (Vogel *et al.*, 1982—see below) to predict the rate constants of fertilization and sperm-egg encounter frequency. Third, we test the model's predictions of these rate constants against empirical measures of egg size and sperm velocity. Finally, we use the fertilization kinetics model to evaluate the relative sensitivity of fertilization to sperm and egg concentrations normally encountered in nature. This knowledge about the kinetics of fertilization will enhance the accuracy of future theoretical models, and provide insight into the interpretation of empirical field data.

The Vogel-Czihak-Chang-Wolf model

Vogel *et al.* (1982) proposed a fertilization kinetics model that predicts fertilization based on sperm and egg concentration, the half-life of sperm 'τ' and two rate constants β_0 (of sperm-egg contact, based on egg cross-sectional area and sperm swimming velocity) and β (of fertilization, based on sperm-egg contact and the fertilizability of the egg). This model assumes that sperm attach to the first egg they contact regardless of whether fertilization takes place.

The Vogel-Czihak-Chang-Wolf (VCCW) model is described by the following equation (Vogel *et al.*, 1982; p. 203):

$$\Phi\infty = 1 - \exp\left(-\frac{\beta S_0}{\beta_0 E_0}\left(1 - e^{-\beta_0 E_0 \tau}\right)\right) \qquad (1)$$

Where: S_0 = Sperm concentration (#/μl)
E_0 = Egg concentration (#/μl)

The ratio of β/β_0 is either the fertilizable area of the egg, the proportion of sperm able to fertilize an egg (Vogel *et al.*, 1982), or the number of sperm contacts needed to allow for the penetration of a single spermatozoan. Vogel *et al.* (1982) suggest the first explanation, although these alternate hypotheses have not been directly tested.

Vogel *et al.* (1982) estimated β and β_0 for the urchin *Paracentrotus lividus*. They observed 'τ' to be 1500 s (they did not account for changes in 'τ' as sperm concentration varied—see results) and using a nonlinear model determined the best fit of β and β_0 to be 3.8×10^{-6} and 3.3×10^{-4} mm^3/s, respectively. Vogel *et al.* suggest that because β/β_0 is approximately 0.01, only 1% of the egg surface is fertilizable. This value is critical to the low fertilization predicted by Denny and Shibata (1989) in their model of fertilization success on wave swept shores.

Materials and Methods

General

Experiments were conducted between 27 February and 8 May 1990 at the Bamfield Marine Station on the west coast of Vancouver Island, British Columbia, Canada. All urchins were gathered from the mouth of Bamfield Inlet (48° 50′ 30″ N, 125° 08′ W), at a depth of 9 m, from rock and cobble substrata. Animals were maintained in flowing seawater tables at 12°C prior to experiments. Gametes were collected by inducing urchins to spawn with a 5 ml injection of 0.55 *M* KCl. Sperm were obtained by inverting male urchins over a glass finger bowl. Sperm were kept "dry" and cool at 12°C until needed for experiments. Eggs were obtained by inverting female urchins over a large glass finger bowl filled with 1 μm filtered seawater. Eggs and all experiments were maintained at 12°C in a running seawater table.

Sperm concentration in each experiment was determined by fixing 5 ml of a 10^2 dilution of dry sperm with five drops of 100% formalin. At this dilution, sperm counts were made using a hemocytometer (8 replicate counts of 2.5×10^{-7} ml sub-samples). Eggs were collected with a 10 ml pipette and then diluted until there were between 6000 and 6500 eggs per ml in the stock egg suspension. For all experimental treatments, three replicates were conducted. In all but the preliminary sperm dilution experiment, each replicate used a different male and female. In the preliminary study, the replicates were from the same male and female. In all but the sperm-egg contact time experiments, eggs and sperm were placed into small vials, swirled for 15 s and the degree of fertilization assessed after 3 h. The percentage of eggs fertilized was estimated, using a compound microscope, by the presence of a fertilization membrane or later cleavage stages in 100 undamaged eggs randomly sampled from each experimental treatment.

For statistical analysis, an arcsine transformation was performed on all percent fertilization data. An analysis of covariance was used for differences in the percentage of eggs fertilized in the sperm age, sperm-egg contact time, and egg concentration experiments. Sperm concentration (log transformed) was the covariate. These initial experiments establish the range of responses used in the multifactorial experiment and most importantly provide data for the fertilization kinetics model. In the multifactorial experiment, we used a step-wise regression to analyze the contribution of each factor in explaining variation in fertilization success and an analysis of covariance to analyze the variation among urchins in gamete quality.

Sperm dilution experiment

To determine the range of sperm concentration over which fertilization success declines from 100 to 0%, we conducted a preliminary dilution experiment. A 1 ml aliquot of a diluted egg suspension (6000 to 6500 eggs per ml) was placed in a small vial with 8 ml of filtered seawater. Fresh "dry" sperm were diluted in a series of 10, 10-fold dilutions. A 1 ml aliquot from one of these sperm suspensions was then placed into the vial, to bring the final volumes to 10 ml (10 dilutions × 3 replicates = 30 vials).

Sperm age experiment

We assessed the influence of sperm age on fertilization using six levels of age (0, 10, 20, 40, 80, and 160 min) over six levels of dilution (10^2, 10^4, 10^5, 10^6, $10^{6.5}$, and 10^7). The range of dilutions was determined from the results of the previous experiment. A 1 ml aliquot of a dilute sperm suspension was placed in a vial with 8 ml of filtered seawater. A 1 ml aliquot of a dilute egg suspension was added to the vial at the appropriate time: at 0, 10, 20, 40, 80, and 160 min after the sperm were diluted (6 dilutions × 6 times × 3 replicates = 108 vials). Although both sperm and eggs were aged in this experiment, previous research (*e.g.*, Pennington, 1985) has shown that sperm are much more sensitive than eggs to age effects. Nevertheless, assuming synchronous spawning, sperm and eggs would age simultaneously in the field.

Sperm-egg contact time experiment

The influence of the duration of sperm contact on fertilization success was assessed by manipulating the time eggs were in contact with a diluted suspension of sperm. A 1 ml aliquot of a dilute egg suspension was pipetted into a plastic cylinder (66 mm in diameter and 30 mm deep with 35 μ mesh Nitex covering the base). The cylinder was then placed in a petri dish filled with filtered seawater. Sperm were diluted into six concentrations (dilutions of: 10^2, 10^3, 10^4, $10^{4.5}$, 10^5, and 10^6) each to a volume of 200 ml. The egg-filled cylinder was placed in a clean petri dish and then 40 ml of sperm (from one of the dilutions) were discharged from a syringe into the cylinder. The sperm remained in contact with the eggs for one of four time periods (0.5, 2, 8, and 32 min). The container was then rinsed with filtered seawater to remove excess sperm, and placed back into the petri dishes filled with filtered seawater (6 dilutions × 4 contact times × 3 replicates = 72 containers).

Egg concentration experiment

This experiment investigated how egg concentration influences fertilization over a range of sperm dilutions. We placed either a 1, 2, 4, or 8 ml aliquot of a dilute egg suspension (6000 to 6500 eggs per ml) into a vial and then added a 1 ml aliquot of a dilute sperm suspension (dilutions of either 10^3, 10^5, or 10^7) and filtered seawater to a final volume of 10 ml (3 sperm dilutions × 4 egg dilutions × 3 replicates = 36 vials).

Sperm-egg contact time, sperm age, and sperm dilution experiment

In this experiment, three factors were varied simultaneously. Egg concentration was not manipulated because it was not significant over the range tested (see results). This experiment had four levels of sperm age (5, 15, 25, and 35 min), four levels of sperm-egg contact time (7, 15, 30, and 60 s), and five dilutions (10^2, 10^3, 10^4, 10^5, and 10^6). The experimental protocol was identical to the sperm-egg contact time experiment, with the exception of the 7 s contact time trials. In these trials, the containers did not sit in the sperm solution since the time needed to discharge the 40 ml of sperm solution was 7 s (4 sperm ages × 4 contact times × 5 dilutions × 3 replicates = 240 containers).

Sperm velocity

We estimated sperm swimming velocity by analyzing slow motion videotapes of sperm at a concentration of 1.50×10^7/ml. Sperm were diluted and immediately placed in a depression slide on a cooled stage of a compound microscope and video taped at 400×. The video recorded time with an internal stop-watch. Sperm swimming was analyzed by tracing individual spermatozoa on acetate sheets attached to a video monitor. Distances were measured with a graphics tablet and velocities calculated by dividing distance moved by the elapsed time.

Results

Sperm dilution experiment

High percent fertilization was noted at the 10^2 dilution (4.7×10^7 sperm/ml) and showed a slight decline until the 10^6 (4.7×10^3 sperm/ml) dilution when fertilization decreased to 18% (Fig. 1). No fertilization was observed beyond the 10^8 dilution (47 sperm/ml).

For this, and in all other experiments, sperm in the 10^2 dilution were still actively swimming after 3 h and development was generally halted with a raised fertilization membrane. The halted development at this high sperm concentration was probably due to polyspermy. At other dilutions, sperm movement was not detected after 3 h,

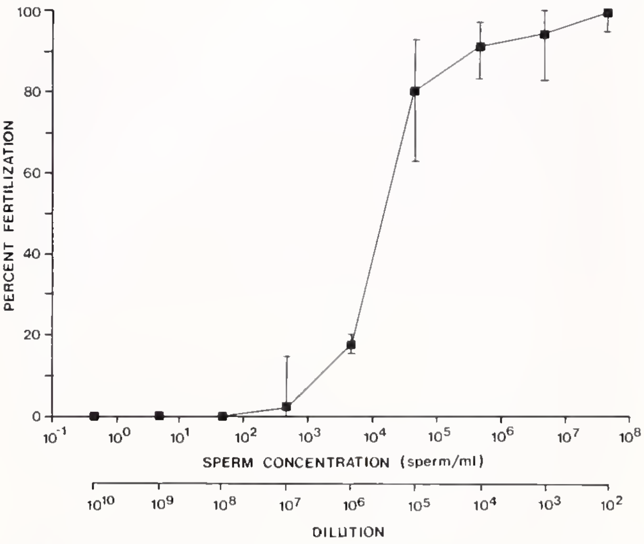

Figure 1. Fertilization as a function of sperm concentration (#/ml) in *Strongylocentrotus franciscanus.* Percent data were arcsine transformed, the mean and 95% CI are plotted after back transformation (n = 3). Sperm concentration estimated from hemocytometer counts at the 10^2 dilution (4.7×10^7 sperm/ml).

and development seemed to be progressing normally (*e.g.*, developmental times consistent with Strathmann, 1987).

Sperm age experiment

The results indicated a highly significant effect of sperm age and sperm concentration on fertilization success (ANCOVA, $P < 0.0001$ for both the covariate of sperm concentration and the main effect of sperm age). Figure 2 is a three-dimensional contour plot of fertilization as a function of sperm age and sperm dilution. Sperm age had little influence on fertilization at the highest sperm concentrations. In fact, sperm at the 10^2 (9.85×10^7 sperm/ml) dilution were still active after 7 h. A 10-fold dilution of this aged (7 h) concentration resulted in nearly 100% fertilization. Sperm age had the most influence on fertilization at the 10^5 dilution (9.85×10^7 sperm/ml). At greater sperm dilutions, the influence of sperm age lessened due to an overall decrease in fertilization.

Sperm-egg contact time

The results indicated a highly significant effect of sperm-egg contact time and sperm concentration on fertilization success (ANCOVA, $P < 0.0001$ for both covariate of sperm concentration and the main effect of sperm-egg contact time). Figure 3 is a three-dimensional contour plot of fertilization as a function of sperm-egg contact time and sperm dilution. Sperm-egg contact time had the greatest influence on fertilization at the intermediate dilution of $10^{4.5}$ (3.83×10^5 sperm/ml). At lesser or greater sperm dilutions, the influence of sperm contact time on fertilization decreased slightly.

Sperm-egg contact time influences fertilization most between the 0.5 and 2 min interval. This result suggests that sperm-egg contact time may be important at even finer time intervals. Thus, in the multi-factorial experiment we chose intervals of 7, 15, 30, and 60 s.

Egg concentration

The results indicated no significant effect of egg concentration, but a highly significant effect of sperm con-

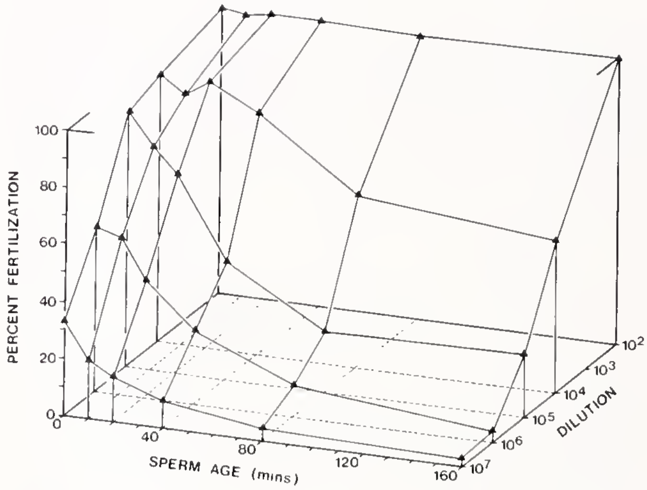

Figure 2. Fertilization as a function of sperm age and sperm dilution in *Strongylocentrotus franciscanus.* Mean percent fertilization plotted, error bars were omitted for clarity. Because sperm concentration varied slightly between replicates, sperm dilution was plotted for clarity.

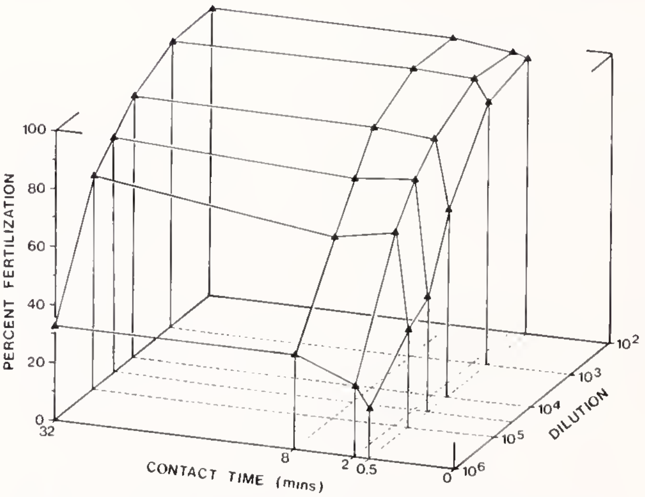

Figure 3. Fertilization as a function of sperm-egg contact time and sperm dilution in *Strongylocentrotus franciscanus.* Mean percent fertilization plotted, error bars were omitted for clarity. Because sperm concentration varied slightly between replicates, sperm dilution was plotted for clarity.

centration on fertilization success (ANCOVA, $P < 0.0001$ for covariate of sperm concentration and $P > 0.25$ for main effect of egg concentration). Figure 4 is a three-dimensional contour plot of fertilization as a function of egg concentration and sperm dilution.

Sperm-egg contact time, sperm age, sperm dilution

A forward step-wise regression analysis tested percent fertilization (arcsine transformed) with the following variables: sperm-egg contact time, sperm age, and sperm concentration (log transformed). All variables were highly significant ($P < 0.0001$) with sperm dilution (Fig. 5A), sperm-egg contact time (Fig. 5B) and sperm age (Fig. 5C) explaining cumulatively 61.8, 67.6, and 70.1% of the variation. The regression generated from these results is:

$$F = S(0.262) + T(0.006) + A(-0.007) - 0.846$$

Where: F = Percent fertilization (arcsine transformed)
S = Sperm concentration (sperm/ml, log transformed)
T = Sperm-egg contact time (s)
A = Sperm age (min)
With *ca.* 6250 eggs

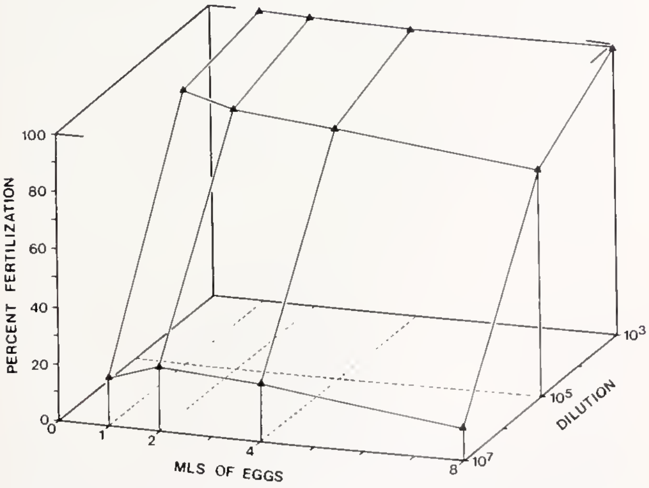

Figure 4. Fertilization as a function of mls of eggs (*ca* 6000–6500 eggs/ml) in 10 ml volume and sperm dilution in *Strongylocentrotus franciscanus*. Mean percent fertilization plotted, error bars were omitted for clarity. Because sperm concentration varied slightly between replicates, sperm dilution was plotted for clarity.

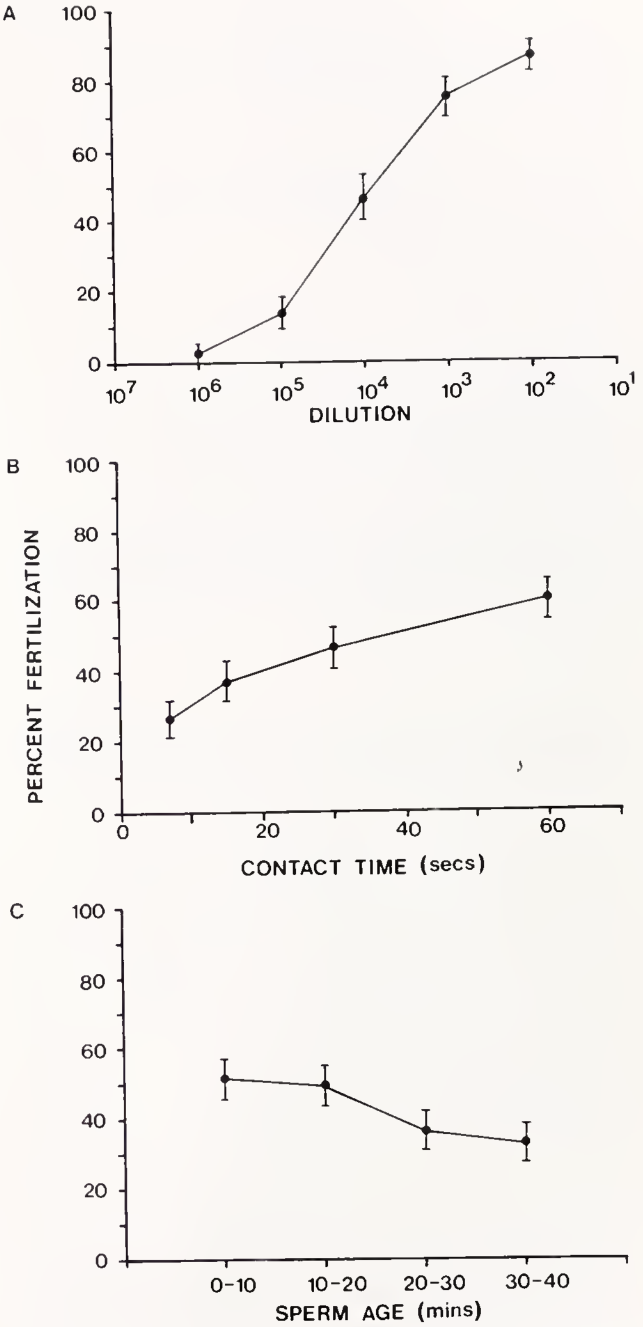

Figure 5. Fertilization in the multifactorial experiment; *Strongylocentrotus franciscanus*. Percent data were arcsine transformed, the mean and 95% CI are plotted after back transformation (3 replicates, 5 dilutions, 4 sperm-egg contact times, and 4 sperm ages). A) Sperm dilution, B) Sperm-egg contact time, C) Sperm age.

The remaining 30% of the variation can be attributed to three factors; within and between individual variation in gamete quality, and using linear or log transformed approximations for the relationships described above. The first two factors were addressed with an analysis of covariance used to compare the percentage of eggs fertilized (arcsine transformed), with gamete variability (individual male and female used for a series of experiments) as the main effect and sperm concentration (sperm/ml, log transformed), sperm-egg contact time (s) and sperm age (min) as covariates. All factors were significant; there were differences in the level of fertilization between gametes from individual urchins ($P < 0.0001$ for all covariates and

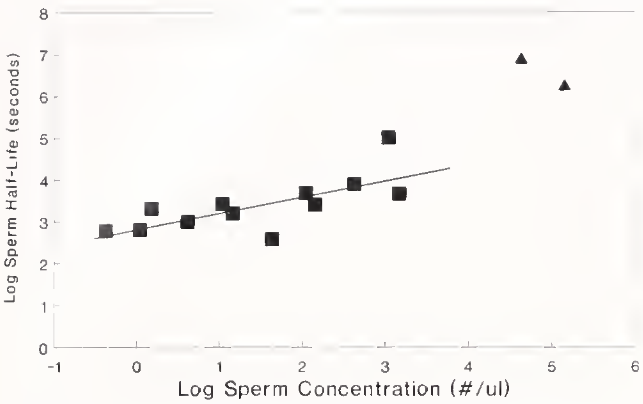

Figure 6. Sperm half-life ('τ'; log transformed) as a function of sperm concentration (log transformed) in *Strongylocentrotus franciscanus.* Each datum represents the sperm age when fertilization dropped to 50% of initial fertilization when sperm was freshly diluted. Triangle symbols represent sperm age trials where fertilization never dropped to 50% of initial fertilization. These points were calculated beyond the range of the experiment and were not included in the regression equation (Log sperm half-life (s) = [Log sperm concentration (#/μl) × 0.391] + 2.818, $R^2 = 0.51$, $n = 12$).

the main effect). The remaining problem of assuming linear or log-linear relations between the variables has been addressed theoretically by Vogel *et al.* (1982).

The Vogel-Czihak-Chang-Wolf model

We fitted a subset of our data, using only manipulations with fresh gametes ($n = 199$), to the VCCW model using their equation "14" (Vogel *et al.*, 1982; p. 203) which substitutes 't' (the sperm-egg contact time) with 'τ' (the sperm half-life). However, when 't' exceeded 'τ', we used the latter value, because higher values of 't' would overestimate the vitality of the sperm.

We calculated values of 'τ' by fitting the results of the sperm-age experiment at each dilution separately to an exponential regression equation. For each equation, the half-life was calculated from the predicted time when fertilization was half the initial value at time "0." These half-life values were then plotted as a function of sperm concentration (log transformed. Fig. 6) and a linear regression was performed to predict 'τ' values for the range of sperm concentrations used in the analysis.

To test the VCCW model we iterated the Marquardt method (the Gauss and Dud methods gave similar results) of non-linear regression (SAS statistical program) to find the best fitted values of β and β_0 for our values of sperm concentration (#/μl), egg concentration (#/μl), 't' or 'τ' (s), and the observed fertilization ratio.

The model of Vogel *et al.* (1982) appears to be quite robust as it explained 91% of the variation in fertilization in *Strongylocentrotus franciscanus* (in spite of the unexplained individual variation in gamete quality). The rate constant of fertilization (β) was estimated to be 6.044×10^{-5} mm³/s (SE = 1.072×10^{-5}) and the rate constant of sperm-egg encounter (β_0) was estimated to be 1.761×10^{-3} mm³/s (SE = 6.971×10^{-4}). Both these estimates are one order of magnitude larger than estimated for *Paracentrotus lividus* by Vogel *et al.* (1982). The ratio of β/β_0 is calculated to be 0.0343. This ratio is about three times higher than the ratio estimated by Vogel *et al.* (1982) and used by Denny and Shibata (1989) to predict fertilization in the field. Use of this ratio would therefore increase Denny and Shibata's predictions of *in situ* fertilization by a factor of three (from approximately 1 to 3% in highly turbulent water).

An independent estimate of β_0 can be made from the following equation (Vogel *et al.*, 1982; p. 208):

$$\beta_0 = \nu \times \sigma_0 \qquad (2)$$

Where: ν = Mean spermatozoan velocity (mm/s)
σ_0 = Egg cross-sectional area (mm²)

We analyzed a total of 116 spermatozoa from 4 urchins (Fig. 7). There were significant differences in swimming velocity between individual urchins (ANOVA, $P < 0.01$). These differences and perhaps similar differences in egg quality are possible reasons for individual variance in fertilization success. The mean sperm velocity was 0.149 mm/s (SE = 0.0113). Using this estimate of swimming velocity and egg cross-sectional area of 0.014314 mm² (egg diameter 0.135 mm; pers. obs., Strathmann, 1987), β_0 was calculated to be 2.13×10^{-3} (SE = 1.61×10^{-3}). There was no significant difference between this estimate of β_0 and our estimate from the VCCW model (Student's 't' = 0.075, $P > 0.9$).

Vogel *et al.* (1982) did not measure sperm swimming directly, they estimated velocity (ν) by solving equation (2) using their estimates of β_0 and egg diameter. Their estimate for *Paracentrotus lividus* was 0.040 mm/s. Gray (1955) measured sperm swimming velocity directly for *Psammechinus miliaris* and found rates of 0.190 mm/s. Gray also reviews studies of several other echinoid species

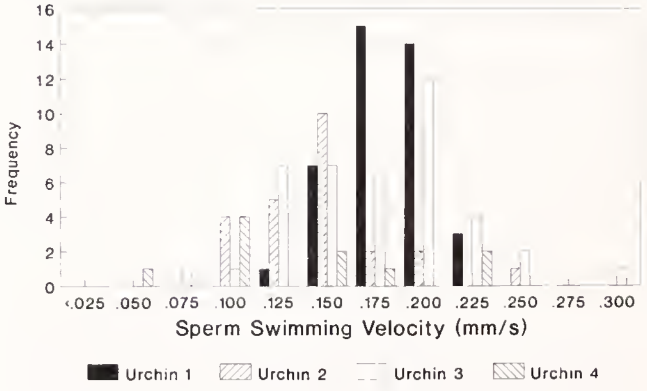

Figure 7. Frequency distribution of *Strongylocentrotus franciscanus* sperm swimming velocity.

and reports rates of between 0.120 and 0.190 mm/s (1955 and references within). Because we found significant differences between individuals, it should not be surprising to find differences between species.

Sensitivity of egg concentration to fertilization

Because fertilization is a result of sperm-egg encounters, it seems intuitive that egg concentration should be important to fertilization success, yet our empirical results suggest otherwise. To evaluate the sensitivity of fertilization success to egg concentration, we again iterated the Marquardt method of non-linear regression to find the best fitted values of β and β_0. This time we chose a subset of our data using only experiments with fresh gametes and constant egg concentrations (n = 40), to predict what fertilization should be in our egg concentration experiment. The empirical data indicated that the greatest effect of changes in egg concentration was a non-significant decrease of 4.9% between the lowest and highest egg concentration at the lowest sperm concentration. The VCCW model, using the subset of the data, predicted a decrease of only 6.3% over the same range of gamete concentration. There was no significant difference between the observed and predicted values (Student's 't' = 0.492, $P > 0.5$). Figure 8 is a three-dimensional contour graph of fertilization as a function of both sperm and egg concentration, using the original data set (n = 199) in the VCCW model. Clearly, it predicts the insensitivity of the fertilization process to egg concentration. Only when the concentration was over 100 eggs per μl was there a slight impact on fertilization. Because eggs of *S. franciscanus* are extruded at a concentration of 325/μl (range 169–499/μl, n = 5 urchins, subsample counts), and rapidly diluted in seawater, egg concentration would only be important to fertilization success within the first few seconds of release.

General discussion

Sperm concentration had the greatest effect on fertilization followed by sperm-egg contact time and sperm age. We found no significant effect of egg concentration on fertilization. Part of the reason for the order of importance was associated with the relative range of each factor examined (but, see above for egg concentration). Sperm concentration was varied over 100,000-fold, contact time was varied 64-fold in the first and 8-fold in the multi-factorial experiment, and sperm age was varied 160-fold in the first and 4-fold in the multifactorial experiment. Ranges were chosen based on results from the single factor results and our estimates on the probable interactions in the field (see below).

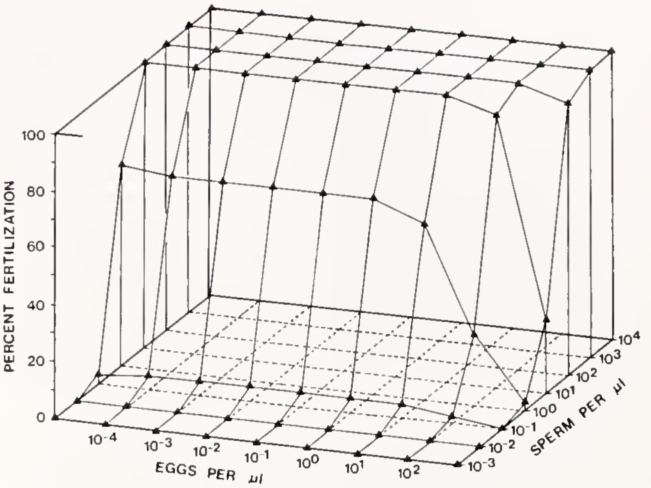

Figure 8. Predicted fertilization as estimated by the VCCW model for a range of sperm and egg concentrations. Sperm are extruded from the gonopore at a concentration of approximately $8.60 \times 10^6/\mu$l. Eggs are extruded at a concentration of approximately $3.25 \times 10^2/\mu$l.

Sperm dilutes rapidly within a few meters from a sperm source (modelled by Denny, 1988; Denny and Shibata, 1989; empirical evidence by Pennington, 1985; Yund, 1990; Levitan, 1991). Such a decline in sperm concentration has been shown to cause a profound decrease in fertilization success. Thus, only factors that change before sperm become too dilute to fertilize eggs are of relevance to estimates of fertilization success.

Factors influencing fertilization on the same time scale as sperm dilution are egg concentration and gamete contact time. An additional factor not examined is shear forces on gametes which might further decrease the chance of fertilization in turbulent water (Denny and Shibata, 1989; Denny, pers. comm.). Egg concentration did not significantly affect fertilization success within small containers that would enhance sperm competition. Lillie (1915) also found no significant effect of egg concentration on fertilization with *Arbacia*. The VCCW model confirms these empirical observations.

Sperm-egg contact time did have a significant effect on fertilization success, particularly within the small time intervals most likely to be important in the field (less than a minute). Rothschild and Swann (1951) came to a similar conclusion with *Psammechinus miliaris*. Hence it seems evident that in the future, this factor should be incorporated into fertilization models. As sperm and egg plumes expand into the water column, the rate of dilution influences both the concentration of sperm and eggs and the time spent at a particular concentration.

The finding that the lifespan of a spermatozoan is related to concentration has been termed the respiratory dilution effect (Chia and Bickell, 1983). The rate of spermatozoan oxygen consumption increases with dilution; the total amount of oxygen consumed by a spermatozoan over its lifetime, however, is independent of dilution. Thus, a spermatozoan in a concentrated medium can maintain a longer lifespan at a lower metabolic level compared to a spermatozoan in a dilute medium. This dilution effect has been attributed to carbon dioxide levels, pH, and possibly levels of cyclic AMP (Chia and Bickell, 1983).

In most cases, sperm longevity would not play a major role in fertilization (Pennington, 1985). However, the increased lifespan of concentrated sperm may be important when gametes are released in low flow conditions (*e.g.*, tide pools). In nature, released gametes have been observed to disperse into the water column (Pearse *et al.*, 1988; Levitan, 1988; pers. obs. MAS, DRL) as well as pooling around the gonopores (Pearse *et al.*, 1988; pers. obs. MAS, DRL). In addition, released sperm can stick together in strings or thin wisps as they travel downstream (pers. obs. MAS, DRL). The increased longevity of released but concentrated sperm might increase the likelihood of fertilization when spawning is not completely synchronous or if the distance between spawning individuals is great.

The above experiments provide information on fertilization kinetics in the laboratory. Estimating fertilization success in the field requires information at the gamete, individual, population, and environmental levels. Gamete level factors can best be studied in the laboratory. Knowledge of gamete kinetics along with estimates of flow conditions in the field allow for the construction of *in situ* fertilization models (*e.g.*, Denny and Shibata, 1989). These models can then be compared to field estimates of fertilization success (*e.g.*, Pennington, 1985; Yund, 1990; Grosberg, 1991; Levitan, 1991; Levitan *et al.*, in press). In addition, observations of natural spawning events are needed (*e.g.*, Randall *et al.*, 1964; Pennington, 1985; Giese and Kanatani, 1987; Levitan, 1988; Pearse *et al.*, 1988; Petersen *et al.*, in press), to determine under what demographic and environmental conditions organisms release gametes. A combination of these techniques will ultimately provide a robust understanding of patterns of fertilization success in nature.

Acknowledgments

We thank S. Lacasse, C. Levitan, and J. Watson for assistance in collecting urchins and the Bamfield Marine Station for providing facilities. Leif Bluck assisted us in the non-linear regression analysis. M. Denny, K. Durante, W. Jaeckle, and T. Rawlings made critical comments on an earlier version of this manuscript. This work was supported by a Bamfield Research Associate Fellowship to DRL, a graduate assistantship from the University of Alberta to MAS, and an NSERC grant to F-SC.

Literature Cited

Brown, G. G., and J. R. Knouse. 1973. Effects of sperm concentration, sperm aging, and other variables on fertilization in the horseshoe crab, *Limulus polyphemus* L. *Biol. Bull.* **144:** 462–470.

Chia, F. -S., and L. R. Bickell. 1983. Echinodermata. Pp. 545–620 in *Reproductive Biology of Invertebrates, Volume II: Spermatogenesis and Sperm Function*. K. G. Adiyodi and R. G. Adiyodi, eds. John Wiley and Sons, NY.

Denny, M. W. 1988. *Biology and the Mechanics of the Wave-swept Environment*. Princeton University Press, NJ. 329 pp.

Denny, M. W., and M. F. Shibata. 1989. Consequences of surf-zone turbulence for settlement and external fertilization. *Am. Nat* **134:** 859–889.

Giese, A. C., and H. Kanatani. 1987. Maturation and spawning. Pp. 252–329 in *Reproduction of Marine Invertebrates Vol. 9: General Aspects: Seeking Unity in Diversity*. A. C. Giese, J. S. Pearse, and V. B. Pearse, eds. Blackwell Scientific Publication and Boxwood Press, CA.

Gray, J. 1955. The movement of sea-urchin spermatozoa. *J. Exp. Biol.* **32:** 775–801.

Grosberg, R. K. 1991. Sperm-mediated gene flow and the genetic structure of a population of the colonial ascidian *Botryllus schlosseri*. *Evolution* **45:** 130–142.

Hultin, E., and B. E. Hagstrom. 1956. The variability in the fertilization rate. *Exp Cell Res.* **10:** 294–308.

Levitan, D. R. 1988. Asynchronous spawning and aggregative behavior in the sea urchin *Diadema antillarum* Philippi. Pp. 181–186 in *Echinoderm Biology: Proceedings of the Sixth International Echinoderm Conference*, R. D. Burke, P. V. Mladenov, P. Lambert, and R. Parsley, eds. A. A. Balkema Press, Rotterdam.

Levitan, D. R. 1991. Influence of body size and population density on fertilization success and reproductive output in a free-spawning invertebrate. *Biol. Bull.* **181:** 261–268.

Levitan, D. R., M. A. Sewell, and F. S. Chia. in press. How distribution and abundance influences fertilization success in the sea urchin *Strongylocentrotus franciscanus*. *Ecology*.

Lillie, F. R. 1915. Studies of fertilization. VII. Analysis of variations in the fertilization power of sperm suspensions of *Arbacia*. *Biol. Bull.* **28:** 229–251.

Pearse, J. S., D. J. McClary, M. A. Sewell, W. C. Austin, A. Perez-Ruzafa, and M. Byrne. 1988. Simultaneous spawning of six species of echinoderms in Barkley Sound, British Columbia. *Invert. Reprod. Dev.* **14:** 279–288.

Pennington, J. T. 1985. The ecology of fertilization of echinoid eggs: the consequence of sperm dilution, adult aggregation, and synchronous spawning. *Biol. Bull.* **169:** 417–430.

Petersen, C. W. 1991. Variation in fertilization rate in the tropical reef fish, *Halichoeres bivattatus*: correlates and implications. *Biol. Bull.* **181:** 232–237.

Petersen, C. W., R. R. Warner, S. Cohen, H. C. Hess, and A. T. Sewell. in press. Variation in pelagic fertilization rates: implications for production estimates, mate choice, and the spatial and temporal distribution of mating. *Ecology*.

Randall, J. E., R. E. Schroeder, and W. A. Stark, II. 1964. Notes on the biology of the echinoid *Diadema antillarum*. *Carib J. Sci.* **4:** 421–433.

Rothschild, L., and M. M. Swann. 1951. The fertilization reaction in the sea urchin. The probability of a successful sperm-egg collision. *J Exp. Biol* **28:** 403–416.

Strathmann, M. 1987. Phylum Echinodermata, Class Echinoidea. Pp. 511–534 in *Distribution and Development of Marine Invertebrates of the Northern Pacific Coast*, M. Strathmann, ed. University of Washington Press, Seattle.

Vogel, H., G. Czihak, P. Chang, and W. Wolf. 1982. Fertilization kinetics of sea urchin eggs. *Math. Biosci* **58:** 189–216.

Yund, P. 1990. An *in situ* measurement of sperm dispersal in a colonial marine hydroid. *J. Exp. Zool.* **253:** 102–106.

Reference: *Biol. Bull.* **181:** 379–386. (December, 1991)

Growth, Size Rank, and Maturation of the Freshwater Prawn, *Macrobrachium rosenbergii:* Analysis of Marked Prawns in an Experimental Population

Z. RA'ANAN, A. SAGI[1], Y. WAX[2], I. KARPLUS[3], G. HULATA[3], AND A. KURIS*[4]
Aquaculture Production Technology, P. O. Box 4330, Jerusalem, Israel 91042

Abstract. For four months we marked and followed through female maturation and adult male mophotypic differentiation, the growth of all 150 individuals in an experimental population of Malaysian giant freshwater prawns (*Macrobrachium rosenbergii*). Small immature female prawns had high growth rates. Growth of female prawns nearly ceased after maturation. This compensatory growth process produces adult females having a unimodal, symmetrical size distribution with a mean above the size threshold for maturation (about 18–26 g). The small male morphotype has a low growth rate, while the orange claw male morphotype has a high growth rate. As the orange claw males transform to the blue claw morphotype, growth ceases. Examination of changes in size rank during the maturation process supported the leapfrog phenomenon. The fastest growing, largest orange claw male is the first to metamorphose to the blue claw morphotype (at a size of 35 g). As other orange claw males exceed this size, they transform in a sequential process so that the most recent blue claw male is generally the largest blue claw male in the population. Thus, growth of males is depensatory throughout the process of morphotypic differentiation, leading to a wide size range of orange and blue claw males. The leapfrog phenomenon is discussed in terms of the reproductive success of the blue claw males and compared with related growth processes in male poeciliid fishes. Implications of this growth process for aquacultural productivity includes the stimulatory effect on the remaining prawns of selectively harvesting the largest blue claw and orange claw prawns and suggests that the inclusion of a small proportion of large "target" blue claw males might stimulate the rapid growth of orange claw males in a population of smaller prawns.

Introduction

Growth of individuals within a population is often highly variable. The causes vary, involving genetic, social, and environmental factors. Because body size often affects reproductive output and survivorship, variation in growth is a very important component of individual fitness. How intraspecific interactions cause variation in growth will be crucial to the evaluation of life history tactics. Variation in growth of aquatic animals is also of practical interest, as it influences the harvest of fisheries and aquaculture systems.

The giant freshwater prawn, *Macrobrachium rosenbergii,* is particularly interesting with respect to variation in growth and the role of size in the social structure of populations. Starting with a cohort of postlarvae having a normal size distribution (Sandifer and Smith, 1975; Ra'anan and Cohen, 1984), growth of juvenile prawns is depensatory (Malecha, 1980), the variance increasing more rapidly than mean size (Ricker, 1975). About half of the population grows rapidly and variably, while the other half grows slowly and relatively uniformly, leading to a markedly, positively skewed size distribution (Wickins, 1972; Forster and Beard, 1974; Ra'anan, 1983; Ra'anan and Cohen, 1985). Both sexes have similar size frequency distributions in populations of immature prawns (Ra'anan and Cohen, 1985). As the individuals mature, the size distribution becomes quite different for males and females. Mature females grow more slowly than males of similar size, and the size distribution of the fe-

---

Received 8 January 1991; accepted 8 August 1991.

[1] Present address: Department of Molecular & Cell Biology, The University of Connecticut, Storrs, CT 06269 and Marine Biological Laboratory, Woods Hole, MA 02543.

[2] Department of Statistics, Hebrew University, Jerusalem, Israel.

[3] Fish & Aquaculture Research Station, Dor 30820, Israel.

[4] Department of Biological Sciences and Marine Sciences Institute, University of California, Santa Barbara, CA 93106.

* To whom correspondence should be addressed.

males regains an approximately normal pattern (Cohen *et al.*, 1981). For the males, the skewed distribution is extended, even reinforced, upon maturation (Fujimura and Okamoto, 1972; Smith *et al.*, 1978; Brody *et al.*, 1980; Malecha *et al.*, 1984), and this is associated with the differentiation of three anatomically, physiologically, and behaviorally distinctive adult male morphotypes (Ra'anan, 1982; Ra'anan and Cohen, 1985; Ra'anan and Sagi, 1985; Kuris *et al.*, 1987; Sagi and Ra'anan, 1988; Sagi *et al.*, 1988). Small males include about 50% of the adult males and have small claws, grow slowly, and exhibit a normal size distribution. Orange claw males have relatively larger claws, grow rapidly, are highly variable in size, and include about 40% of the adult males. The remaining 10% are blue claw males. These are also highly variable in size, but grow slowly if at all. Blue claw males are behaviorally dominant over the other morphotypes, and orange claw males are dominant over the small males. Dominance is expressed in several ways, including retreat of subordinate males in the presence of a dominant male. An individual prawn may proceed from a small male to an orange claw and then to a blue claw male in a developmental sequence (Ra'anan and Cohen, 1985; Ra'anan and Sagi, 1985; Kuris *et al.*, 1987, Barki, 1989).

Blue claw males sequester females prior to mating, guard the females, and place spermatophores close to the female genital opening. Small males engage in "sneak" reproductive tactics, attempting to attach spermatophores in the vicinity of the vertical surface of the abdomen of females protected by blue claw males. The orange claw males do not show appropriate reproductive behavior, although they have mature sperm and can achieve mating when isolated with receptive females in aquaria (Ra'anan and Sagi, 1985). Karplus *et al.* (1986) have shown that the proportion of male morphotypes varies significantly with density. At densities as low as 1 prawn/m^2, the proportion of blue claw males may rise to 20%, while the proportion of small males decreases to 33%. Variable growth and differing reproductive tactics associated with morphologically distinctive types of males have also been recognized in many species of fishes (Parker, 1970; Moav and Wohlfarth, 1974; Gross and Charnov, 1980; Dominey, 1980; Warner, 1984; Gross, 1985), insects (Alcock *et al.*, 1977; Cade, 1981; Thornhill, 1981; Ward, 1983), and crustaceans (Shuster, 1987).

Ra'anan and Cohen (1985) proposed that the first male to attain blue claw status was one of the most rapidly growing orange claw males and that it would be subsequently surpassed by other orange claw males in a "leapfrogging" process such that the most recently metamorphosed blue claw male would generally be the largest blue claw male in the population. To test this hypothesis, we followed the growth of marked individuals in a population, paying close attention to their rank in size and their morphotypic status as operationally defined in Kuris *et al.* (1987).

The marking procedure also enabled us to define the relationship between growth rate and maturation of the female prawns. Little attention has been paid to growth of female prawns. Although individual juvenile female prawns show variation in size and growth rates comparable to juvenile male prawns, the adult female population has a normal size distribution with a small mean size. Tracking the growth of marked females enabled us to determine how such a size structure resulted during the process of maturation. Finally, we formulated a model for the relationship between growth, maturation, and morphotypic status of both male and female *Macrobrachium rosenbergii*.

Materials and Methods

Source of the animals

Juvenile prawns, averaging (±SD) 10.83 ± 8.55 g were selected haphazardly from a larger prawn population of the same age in a secondary nursery pond operated at the Nir David fish farm. The nursing period was 4 months. An experimental population of 150 individuals was established in a large, 4500-liter tank. All individuals were sexed and weighed. This population was composed of 80 males (average weight ±SD 10.6 ± 9.9 g) and 70 females (average weight ±SD 11.1 ± 6.1 g). All juveniles were individually marked by tattooing their uropods with a mounted insect pin, according to a method developed originally for crabs by Kuris (1971), and later successfully adapted to prawns (Kuris *et al.*, 1987).

Management procedures

The tank was connected to a biological filter in a closed recirculating system in a prawn hatchery at Ein Hamifratz. Water temperature was regulated between 26–28°C by a thermostat. Substrate, in the form of horizontal hanging nets composed of three layers of three-square-meters each, was provided to increase the submerged surface area and shelter subordinate and newly molted individuals. Prawns were fed once a day with ground fresh fish fillet, supplemented with carp pellets (25% protein). Food was offered in excess, and leftover food particles were removed daily by siphoning the tank bottom. The observation period was 142 days.

Routine measurements

Every two weeks, all prawns were removed from the tank, sexed, and individually weighed. The tattoo identification mark was renewed whenever necessary (mainly following ecdysis).

Females were classified into one of four groups. These were (a) pre-reproductive females, with narrow brood chambers and no visible gonads; and (b) ripening females, with narrow brood chambers but having visible gonads (Sagi and Ra'anan, 1985). These first groups were immature as males never placed spermatophores upon them. Mature females were either (c) ovigerous with enlarged brood chambers bearing eggs or (d) post-ovigerous, with enlarged brood chambers but no visible gonads. Thus, the appearance of an enlarged brood chamber operationally defined the onset of maturation.

Males were classified according to their morphotypic stage within the male social system (Ra'anan and Cohen, 1985; Kuris *et al.*, 1987).

Statistical analysis

Analysis of male growth characteristics. For each male, body weight was plotted over time. Males were separated into three categories: (1) individuals that were initially SM and remained in this morphotype until the end of the observation period; (2) SM individuals that transformed to the OC morphotype during the observation period; and (3) individuals, which were initially OC males, that transformed to the BC morphotype. On each sampling date, mean weight, standard deviation (SD), and the coefficient of variation, PCV, were calculated for each group of males. As the size distribution was skewed, the median body weights for each of these groups of males on each date were used to generate growth curves.

Daily growth rates (± standard error of the mean) were described using the instantaneous rate of growth (also called specific growth rate or relative growth rate), G, where $G = 100(\ln W_t - \ln W_o)/t$, with W_o and W_t being, respectively, the weights recorded initially and after t days (Fisher, 1946; Ricker, 1975; Kaufmann, 1981). This permitted the comparison of growth rates at different body sizes. The variance of the growth curve parameters was estimated for each morphotype according to Kaufmann (1981). The regression of G on lnW was calculated for each of the morphotypes, using simple linear regression analysis (Weisberg, 1980). In the case of the OC male category, it was concluded, after assessing the sensitivity of the regression analysis to outlying observations according to Cook and Weisberg (1982), that two (of the 67) observations were outliers. These were excluded from further analysis. The correlations between G and lnW for the different morphotypes were compared using the Zeller-Theil-Gupta statistic (Ali and Silver, 1985).

The relative size ranking of each individual within the male population was determined by scaling the total weight range at each measurement as 99, attributing to each male a rank according to its relative position between the smallest individual (1) and the largest (100). To examine whether individuals of a particular morphotype tended to gain or lose in relative rank within the male population, we plotted initial rank *versus* terminal rank of each individual while maintaining the same morphotypic characteristics. The direction of the changes in rank of all individuals within a given morphotype were evaluated using the sign test (Pratt and Gibbons, 1981).

Analysis of female growth characteristics. For each female, body weight was plotted over time. Females were grouped into two categories (immature and mature) and mean weights and PCV were calculated as for males. For each category, the median body weights at different times were used to generate growth curves. Individual growth rate was measured using G. The variance of growth rate and the linear relationship between G and lnW for each female category were established following similar routines described for analysis of the males.

Results

Evaluation of male growth characteristics

Median growth curves. Figure 1 shows growth curves obtained by plotting the medians of the lnW distributions of individual males for each morphotype against time. For the SM morphotype, growth rate was low compared with growth rates of animals that transformed to the OC morphotype. Following transformation to the BC morphotype, growth ceased, as reflected in the plateau in the growth curve after 12 weeks. Examination of individual growth curves revealed the same general pattern, although transformation from one morphotype to another occurred at different times (*i.e.*, different individuals spent different lengths of time in each morphotype). The growth rate during the OC phase (as measured by the slope of the growth curve) always remained higher than the growth

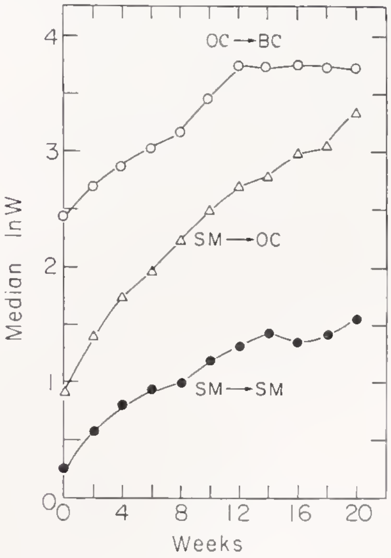

Figure 1. Median growth curves of small males (SM → SM), SM animals that transformed to OC males (SM → OC), and OC animals that transformed to BC males (OC → BC).

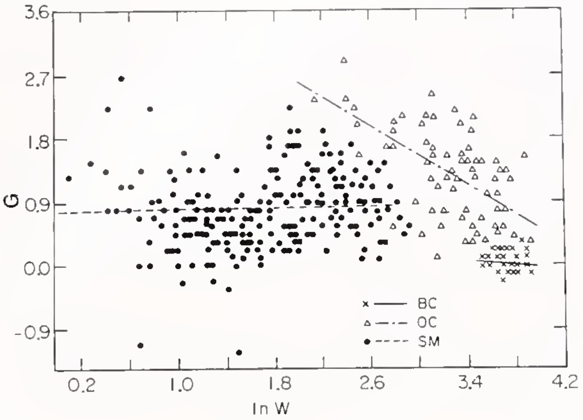

Figure 2. Scatter plots and regression lines for the association of instantaneous growth rate (G) and the natural logarithm of body weight (lnW) of individuals of the three male morphotypes.

rates of the same individual in either SM or BC morphotypic phases.

An examination of the male size distribution within the three morphotypic categories, over the entire observation period, revealed that the weight range of SM males was between 1–15 g (average weight 6.5 ± 4.0 g, PCV = 61.5%), that the weight range of OC males was 10–50 g (average weight 31.2 ± 7.9 g, PCV = 25.3%), while the weight range of BC males was relatively narrow, 35–50 g (average weight 45.0 ± 3.4 g, PCV = 7.5%). The smaller BC males were individuals that were the first to transform into the BC category.

Relationships between growth rate and morphotypic status. The OC males showed the highest growth rate ($G = 1.22 \pm 0.4$), while the BC males had the lowest growth rate ($G = 0.07 + 0.09$). Growth effectively ceased when a male transformed into the BC morphotype. The SM males had an intermediate growth rate ($G = 0.83 \pm 0.33$), indicating that this morphotype has a relatively slow growth rate compared to the OC morphotype. Differences in mean G-value between the three male morphotypes were significant (t-test, $P < .001$).

We examined the relationship between G and lnW for each morphotype (Fig. 2). The growth rate of males in the OC morphotype decreased with increase in lnW (t-test for significance of slope, two-tailed $P < .001$), while the growth rates of BC and SM males were relatively constant over size. When growth rates of SM and OC males were compared within the range where their lnW overlapped ($2 < \ln W < 3$), the OC males had a significantly higher G (95%) confidence band for the difference between the mean G of OC and SM males with the same lnW values. There was also a narrow overlap in the weight range of BC and OC males ($3.5 < \ln W < 3.8$), where G-values of the OC males were significantly higher than those of the BC males (t-test, two-tailed $P < .05$).

Relationship between size rank and morphotype. Figure 3 describes the relationship between the initial size rank of an individual, when first categorized into a specific morphotype, and its terminal ranking determined at the last measurement before its transformation into the next morphotype. All points that are located on the Initial rank = Terminal rank line represent individuals that did not change their size rank during the time they were in a particular morphotype. All points below the line represent a loss in rank, while those located above the line represent a gain in rank. The rank of all BC males decreased with time (sign-test, 1-tailed $P < .0005$) while ranks of all OC males increased (sign test, 1-tailed $P < .0003$). As for the SM males, 17 individuals lost in rank, while 28 individuals gained. There was a tendency to gain in rank while in the SM developmental stage, but this was not significant (sign test, 2-tailed $P = .072$).

Evaluation of female growth characteristics

Growth curve of M. rosenbergii *females.* Figure 4 shows a growth curve of the medians of the lnW distributions of individual females (both immature and mature). Prior to sexual maturation, females grew exponentially, as demonstrated by the linear increase of lnW. After sexual maturation, growth ceased. A comparison of individual growth curves of females revealed a similar pattern, although growth rate prior to sexual maturation, and the time of maturation, varied.

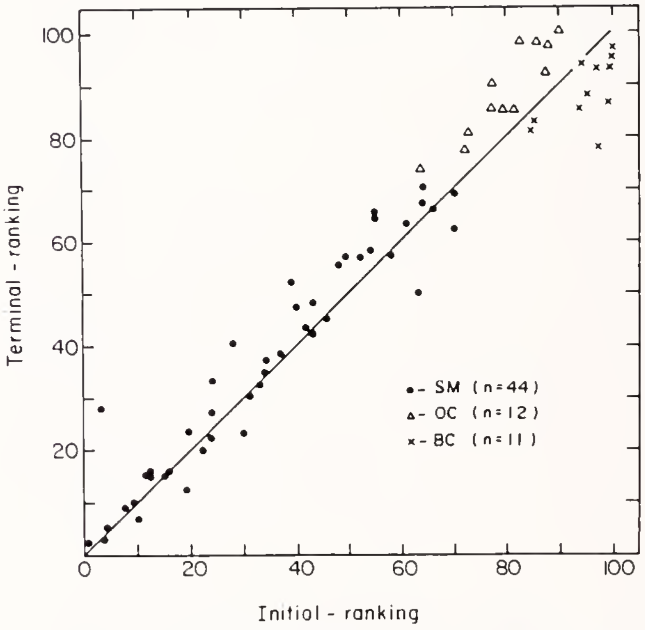

Figure 3. The relationship between initial and terminal size rank for the different morphotypes. Each point represents the rank of an individual when it entered the indicated morphotype (initial) and when it was last recorded in that morphotype (terminal). The diagonal line represents growth with no change in rank. Points above this line represent individuals that gained in rank when they were in a particular morphotype.

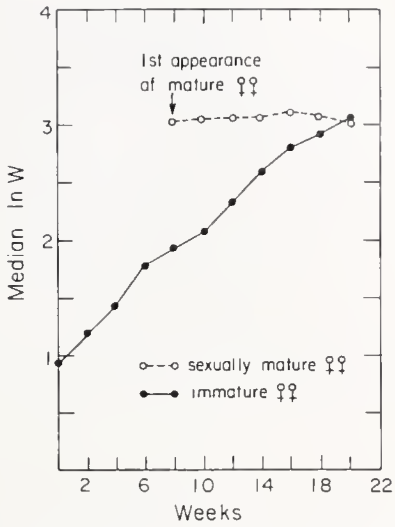

Figure 4. Median growth curves of females before and after sexual maturation.

A comparison of the size distribution of females before and after maturation revealed that the weight range of immature females was relatively wide, from 0.5 to 24.8 g (W = 6.12 ± 5.0 g, PCV = 81.7%), while that of the sexually mature females was relatively narrow, from 15.2 to 27.2 g (W = 21.35 ± 3.22 g, PCV = 15.1%). Part of the variation in weight of the sexually mature females may be attributed to the presence of eggs on ovigerous females. This comprised 10–15% of their weight (Ra'anan, pers. obs.). For the entire female population, it is notable that parallel to the increase in average weight with time, there was a continuous decrease in the coefficient of variation.

Relationship between female growth rate and sexual maturation. Figure 5 presents the relationship between G and lnW for all females that matured (n = 24), and all females that remained immature throughout the experiment (n = 24). Growth rate was inversely proportional to weight for all females. However, comparing animals of similar body weight, G-values for growth during the immature phase of females that ultimately matured were usually higher than those calculated for females that did not mature. G-values for females after becoming sexually mature were lowest, 0.2 ± .12, indicating that growth effectively ceased at maturation.

Relationship between female age, size, and initiation of maturation. Of 48 females, 24 became sexually mature during the observation period. The females began to mature between the sixth and eighth week (Fig. 6A). For the remainder of the period, a relatively constant proportion (range 9–21%) matured per two-week interval.

At maturity, ovigerous females exhibited an approximately normal weight distribution (Fig. 6B, W = 21.12 ± 5.20 g, PVC = 24.6%). The age of females when first ovigerous was negatively correlated with initial body weight (Fig. 7, r = −.712, $P < .002$). The females that were initially larger matured earlier than the smaller ones.

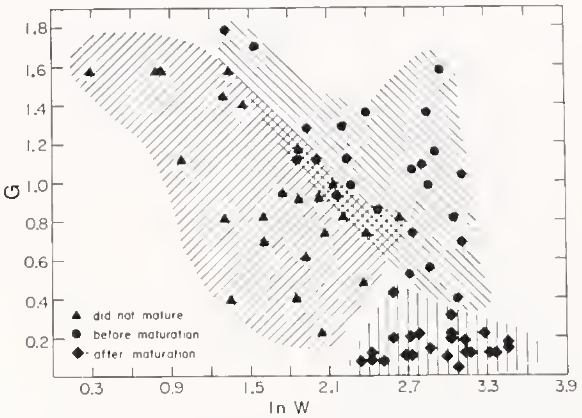

Figure 5. The relationship between female instantaneous growth rate (G) and the natural logarithm of body weight (lnW). Triangles represent growth of females that were immature throughout the experiment. Circles represent growth of females prior to maturation for females that did mature during the experiment. Diamonds represent growth of females after maturation.

The largest females at stocking usually remained the largest throughout the experiment, whether they matured or not (Fig. 8). Further, while both immature and mature females spanned a similar initial weight range, the weight of mature females was both higher and less variable than that of the immature females.

Discussion

These results confirm (Ra'anan and Cohen, 1985; Kuris *et al.*, 1987) that small males grow slowly, that orange claw males grow rapidly, and that blue claw males molt infrequently, if they molt at all. Regression analysis in-

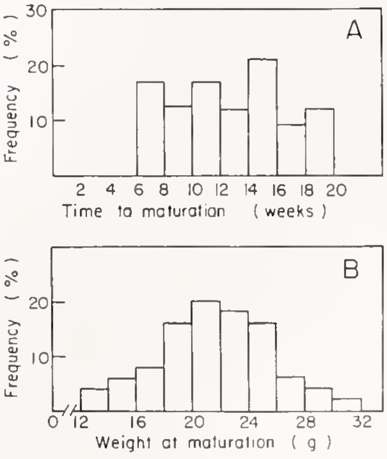

Figure 6. (A) Frequency distribution for the age (in weeks) at onset of maturation of females. (B) Frequency distribution of female body weight at onset of maturation.

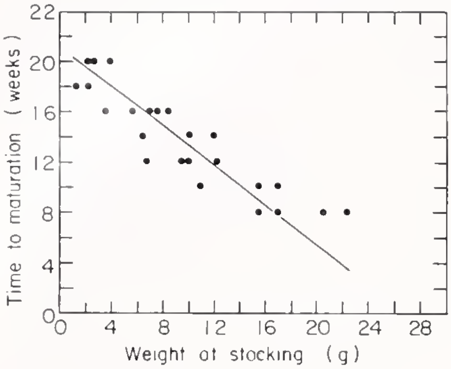

Figure 7. The correlation between age at maturation of females and their initial weight recorded at stocking.

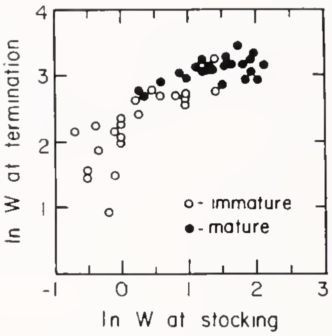

Figure 8. The relationship between weight of females at stocking and upon termination of the observation period.

dicated that growth rate of small males did not vary with size (Fig. 2). Thus, absolute size did not affect the relative size rank of these males throughout the observation period (Fig. 3). The significant tendency for small males to gain in rank is accounted for by the particularly poor growth performance of a few individuals. The high G for the smaller orange claw males indicates that the size disparity between small males and orange claw males increases with time, furthering the differentiation between these morphotypes. As the orange claw males increase in size and approach their metamorphosis to the blue claw morphotype (Kuris *et al.*, 1987), growth rate slows. Perhaps this decreased growth of the largest orange claw males is an energetic cost of morphotypic differentiation.

Ra'anan and Cohen (1985) observed that the size of blue claw males in a population was inversely proportional to the amount of algae adhering to their cuticles. Because coverage by epibionts is an indicator of time since the previous ecdysis (Smith *et al.*, 1979), this led to the hypothesis that the larger blue claw males were the more recently metamorphosed. Hence, Ra'anan and Cohen (1985) proposed the leapfrog hypothesis that orange claw males continue to grow and transform to the blue claw morphotype when they exceed the largest blue claw males in the population. Our size rank analysis provides direct support for the leapfrog growth phenomenon and permits a more explicit description of this unusual, socially mediated growth pattern.

Generally, the most rapidly growing, largest orange claw male becomes the first male to metamorphose into a blue claw male (Fig. 9). Other rapidly growing orange claw males soon exceed this first blue claw male and become the new, larger, blue claw males. Consistent with this model, the orange claw and blue claw males exhibit a similar range in sizes, and the largest male in pond populations may be either a blue claw or an orange claw male. The leapfrog growth pattern is probably due to social interactions among males, because males isolated in small cages did not follow this pattern (Karplus *et al.*, 1991).

A few orange claw males transformed to the blue claw morphotype while still somewhat smaller than the largest previous blue claw male. This variability may be due to variation in the time lag from the commitment to transform in molt stage D_1 (when new cuticular details are differentiated, Drach, 1939) to the time of ecdysis. If a male that committed early was slow to molt, it could be exceeded in size by a prawn that committed at a later time, but which passed through the proecdysial process more rapidly.

Recently, Barki (1989) showed that the largest blue claw male in a mixed population of blue claw and orange claw males is dominant over all orange claw and the smaller blue claw males. This dominance provides the α-male advantageous access to resources. Larger males presumably acquire larger or better territories and are more likely to sequester reproductive females for mating (Ra'anan and Cohen, 1985). Thus, the reproductive success of the early transforming, smaller, blue claw males probably declines over time as larger blue claw males enter the population.

The leapfrog model for male morphotypic differentiation is superficially similar to maturation of certain male poeciliid fishes (Borowsky, 1973a, b; 1987; Sohn, 1977; Campton and Gall, 1988). In small groups, the first

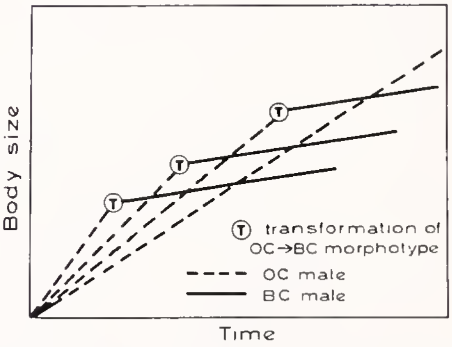

Figure 9. A model for the relationship between maturation and growth in males.

male fish to mature is usually the smallest. Males that mature later do so at larger sizes. In fishes this pattern is socially mediated. But the size variation exhibited by these male fishes is much less than that of *M. rosenbergii,* and in some experimental and natural circumstances, males frequently matured when smaller than other males in the population (Borowsky, 1978b, 1987). Behavioral dominance is associated with adult male size for *Xiphophorus maculatus* (Borowsky, 1973b) but not for *Girardinus metallicus* (Farr, 1980). In contrast, the presence of blue claw males suppresses neither growth nor metamorphosis of orange claw males [although the presence of either blue claw or orange claw males suppresses the growth but not the maturation of the small males (Ra'anan and Cohen, 1985)]. Experiments with poeciliid fishes have usually been conducted with a paired or small group (*e.g.,* 4) experimental design; thus the consistent replacement based on size rank that distinguishes the leapfrog model has not yet been shown in these fishes. The socially mediated leapfrog model of male morphotypic differentiation is a highly distinctive growth and maturation phenomenon, perhaps unique to *M. rosenbergii* and related prawns that may have a similar morphotypic system (Kuris *et al.,* 1987).

The growth rate of immature females was relatively high; approaching that of orange claw males (compare Fig. 1, 2 with 4, 5). After maturation, growth slowed considerably but did not cease (Fig. 5). Variation in size decreased with time because growth rate declined markedly with increasing size whether the prawns matured or not (Fig. 5). Thus, a model for female growth (Fig. 10) is quite different from the model for male growth (Fig. 9). The initially highly variable female size distribution [indistinguishable from juvenile males (Ra'anan and Cohen, 1984)] is ultimately replaced by a relatively normal distribution. Such a growth pattern is seen in many aquatic organisms (Ricker, 1975). Early in life there is depensatory growth; presumably because, among postlarvae, a size advantage, even though small in absolute terms, leads to a feeding advantage that exaggerates the size disparity in the population (Borowsky, 1978a). Later growth becomes compensatory because smaller animals have a higher growth rate, and growth slows as maturation approaches. Females then accumulate in a relatively narrow size range once they cross the size threshold (more realistically a size range) at which they mature (Fig. 10). The existence of the size threshold is the mechanism that produces a normal size distribution of adult females.

These findings have potential application to prawn aquaculture. Monosex growth experiments using females should yield a more homogenous product. Selective harvest of large blue and orange claw males is clearly beneficial as the growth rate of the remaining male prawns will increase due to the leapfrog mechanism. Population experiments with a small proportion of large blue claw males should prove interesting. The presence of such males might provide a "target" for rapid growth of orange claw males by preventing metamorphosis to the blue claw morphotype at sizes below that of the target males.

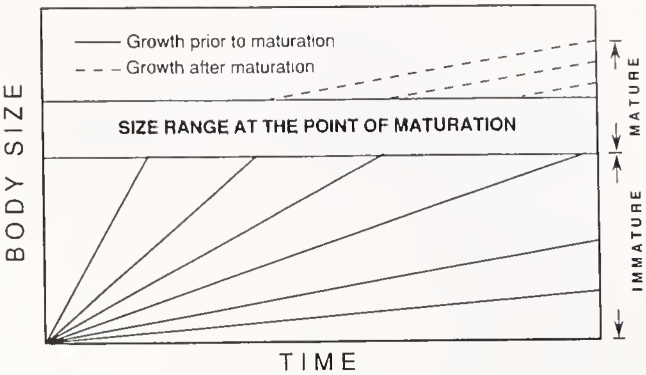
Growth prior to maturation
Growth after maturation
SIZE RANGE AT THE POINT OF MATURATION
BODY SIZE
TIME
MATURE
IMMATURE

Figure 10. A model for the relationship between maturation and growth in females. The shaded size range is the normally distributed size at maturation (see Fig. 6A).

Acknowledgments

We thank the hatchery management staffs of Kibbutzim Nir David and Ein Hamifratz for their cooperation and general assistance with this project. Aquaculture Production Technology, Ltd., Israel, provided financial and logistic support. The Life Sciences Institute and the Genetics Experimental Farm of the Hebrew University of Jerusalem provided facilities and support for AMK in Israel. We thank Kevin Lafferty and Eric Schultz for their helpful comments on the manuscript and Israel Einott for computer assistance.

Literature Cited

Alcock, J., E. Jones, and S. L. Buchmann. 1977. Male mating strategies in the bee *Centris pallida* Fox (Anthrophoridae: Hymenoptera). *Am. Nat.* **111:** 145–155.

Ali, M. M., and J. L. Silver. 1985. Tests for equality between sets of coefficients in two linear regressions under heteroscedasticity. *J. Am. Stat. Assoc.* **80:** 730–735.

Barki, A. 1989. The agonistic behaviour of the freshwater prawn *Macrobrachium rosenbergii.* M.Sc. thesis, Tel Aviv University. 113 pp. (Hebrew with English abstract).

Borowsky, R. L. 1973a. Social control of adult size in males of *Xiphophorus variatus. Nature* **245:** 332–335.

Borowsky, R. L. 1973b. Relative size and the development of fin color in *Xiphophorus variatus. Physiol. Zool.* **46:** 22–28.

Borowsky, R. L. 1978a. The tailspot polymorphism of *Xiphophorus* (Pisces: Poeciliidae). *Evolution* **32:** 886–893.

Borowsky, R. L. 1978b. Social inhibition of maturation in natural populations of *Xiphophorus variatus* (Pisces: Poeciliidae). *Science* **201:** 993–935.

Borowsky, R. L. 1987. Agonistic behavior and social inhibition of maturation in fishes of the genus *Xiphophorus* (Poeciliidae). *Copeia* **1987:** 792–796.

Brody, T., D. Cohen, and A. Barnes. 1980. Yield characters of *Macrobrachium rosenbergii* in monoculture. *Aquaculture* **21:** 375–385.

Cade, W. 1981. Alternative male strategies: genetic differences in crickets. *Science* **212:** 563–564.

Campton, D. E., and G. A. E. Gall. 1988. Effect of individual and group rearing on age and size at maturity of male mosquito fish, *Gambusia affinis. J. Fish. Biol.* **33:** 203–212.

Cohen, D., Z. Ra'anan, and T. Brody. 1981. Population profile development and morphotypic differentiation in the giant freshwater prawn *Macrobrachium rosenbergii* (de Man). *J. World Maricult. Soc.* **12:** 231–243.

Cook, D., and S. Weisberg. 1982. *Residuals and Influence in Regression.* Chapman and Hall, New York.

Dominey, J. W. 1980. Female mimicry in male bluegill sunfish—a genetic polymorphism? *Nature* **284:** 546–548.

Drach, P. 1939. Mue et cycle intermue chez les Crustacés Décapodes. *Ann. Inst. Océanogr. Monaco* **19:** 103–391.

Farr, J. A. 1980. The effect of juvenile social interactions on growth rate, size and age at maturity and adult social behavior in *Girardinus metallicus* Poey (Pisces, Poeciliidae). *Z. Tierpsychol.* **52:** 247–267.

Fisher, R. A. 1946. *Statistical Methods for Research Workers, 10th ed.* Oliver and Boyd, London.

Forster, J. R. M., and T. W. Beard. 1974. Experiments to assess the suitability of nine species of prawns for intensive cultivation. *Aquaculture* **3:** 355–368.

Fujimura, T., and H. Okamoto. 1972. Notes on progress in developing a mass culturing technique for *Macrobrachium rosenbergii* in Hawaii. Pp. 313–327 in *Coastal Aquaculture in the Indo-Pacific Region,* T. V. R. Pillay, ed. Fishing News (Books) Ltd., Surrey, England.

Gross, M. R. 1985. Disruptive selection for alternative life histories in salmon. *Nature* **313:** 47–48.

Gross, M. R., and E. L. Charnov. 1980. Alternative male life histories in bluegill sunfish. *Proc. Natl. Acad. Sci. USA* **77:** 6937–6948.

Karplus, I., A. Barki, Y. Israel, and S. Cohen. 1991. Social control of growth in *Macrobrachium rosenbergii.* II. The "leapfrog" growth pattern. *Aquaculture* **96:** 353–366.

Karplus, I., G. Hulata, G. W. Wohlsarth, and A. Halevy. 1986. The effect of density of *Macrobrachium rosenbergii* raised in earthen ponds on their population structure and weight distribution. *Aquaculture* **52:** 307–320.

Kaufmann, K. W. 1981. Fitting and using growth curves. *Oecologia* **49:** 293–299.

Kuris, A. M. 1971. Population interactions between a shore crab and two symbionts. Ph.D. Thesis. University of California, Berkeley, CA. 447 pp.

Kuris, A. M., Z. Ra'anan, A. Sagi, and D. Cohen. 1987. Morphotypic differentiation of male Malaysian giant prawns, *Macrobrachium rosenbergii. J. Crustacean Biol.* **7:** 219–237.

Malecha, S. 1980. Research and development in freshwater prawn, *Macrobrachium rosenbergii,* culture in the United States: current status and biological constraints with emphasis on breeding and domestication. Pp. 35–55 in *Proc. Ninth and Tenth U.S.-Japan Meetings on Aquaculture,* C. J. Sindermann, ed. NOAA Tech. Rep. NMFS 16.

Malecha, S. R., S. Masuno, and D. Onizuka. 1984. The feasibility of measuring the heritability of growth pattern variation in juvenile freshwater prawns, *Macrobrachium rosenbergii* (de Man). *Aquaculture* **38:** 347–363.

Moav, R., and G. W. Wohlfarth. 1974. Magnification through competition of genetic differences in yield capacity in carp. *Heredity* **33:** 181–202.

Parker, G. A. 1970. The reproductive behavior and the nature of sexual selection in *Scatophaga stercoraria.* II. The fertilization rate and the spatial and temporal relationships of each around the site of mating and oviposition. *J. Anim. Ecol.* **39:** 205–228.

Pratt, J. W., and J. D. Gibbons. 1981. *Concepts of Nonparametric Theory,* Springer-Verlag, New York.

Ra'anan, Z. 1982. The ontogeny of social structure in the freshwater prawn *Macrobrachium rosenbergii.* Ph.D. Thesis, Hebrew University of Jerusalem. 101 pp.

Ra'anan, Z. 1983. The effect of size ranking on the moulting cycle of juvenile stages of the freshwater prawn *Macrobrachium rosenbergii* (de Man) when reared individually and in pairs (Decapoda, Caridea). *Crustaceana* **45:** 131–138.

Ra'anan, Z., and D. Cohen. 1984. The effect of group interactions on the development of size distribution in *Macrobrachium rosenbergii* (de Man) juvenile populations. *Biol. Bull.* **166:** 22–31.

Ra'anan, Z., and D. Cohen. 1985. The ontogeny of social structure and population dynamics in the freshwater prawn *Macrobrachium rosenbergii* (de Man). Pp. 277–311 in *Crustacean Issues II: Crustacean Growth,* F. M. Schram and A. Wenner, eds. Balkema, Rotterdam.

Ra'anan, Z., and A. Sagi. 1985. Alternative mating strategies in males of the freshwater prawn *Macrobrachium rosenbergii* (de Man). *Biol. Bull.* **169:** 592–601.

Ricker, W. E. 1975. Computation and interpretation of biological statistics for fish populations. *Bull. Fish. Res. Bd. Canada* **191:** 1–382.

Sagi, A., Y. Milner, and D. Cohen. 1988. Spermatogenesis and sperm storage in the testes of behaviorly distinctive male morphotypes of *Macrobrachium rosenbergii* (Decapoda, Palaemonidae). *Biol. Bull.* **174:** 330–336.

Sagi, A., and Z. Ra'anan. 1985. Rapid identification of reproductive state and the receptive period of females in pond populations of *Macrobrachium rosenbergii*—a new technique. *Aquaculture* **48:** 361–367.

Sagi, A., and Z. Ra'anan. 1988. Morphotypic differentiation of males of the freshwater prawn, *Macrobrachium rosenbergii:* changes in the midgut glands and the reproductive system. *J. Crustacean Biol.* **8:** 43–47.

Sandifer, P. A., and T. I. J. Smith. 1975. Effect of population density on growth and survival of *Macrobrachium rosenbergii* reared in a recirculating water management system. *Proc. World Maricult. Soc.* **6:** 43–53.

Shuster, S. 1987. Alternative reproductive behaviors: three discrete male morphs in *Paracerceis sculpta,* an intertidal isopod from the northern Gulf of California. *J. Crustacean Biol.* **7:** 318–327.

Smith, T. I. J., P. A. Sandifer, and J. J. Manzi. 1979. Epibionts of pond reared adult *Macrobrachium rosenbergii* (de Man) in South Carolina. *Aquaculture* **16:** 299–308.

Smith, T. I. J., P. A. Sandifer, and M. H. Smith. 1978. Population structure of Malaysian prawns, *Macrobrachium rosenbergii* (de Man), reared in earthen ponds in South Carolina, 1974–1976. *Proc. World Maricult. Soc.* **9:** 21–38.

Sohn, J. J. 1977. Socially induced inhibition of genetically determined maturation in the platyfish *Xiphophorus maculatus. Science* **195:** 199–201.

Thornhill, R. 1981. *Panorpa* (Mecoptera: Panorpidae) scorpionflies: systems for understanding resource defense polygyny and alternative male reproductive efforts. *Ann. Rev. Ecol. Syst.* **12:** 355–386.

Ward, P. I. 1983. The effect of size on the mating behavior of the dung fly *Sepsis cynipsea. Behav. Ecol. Sociobiol.* **13:** 75–80.

Warner, R. R. 1984. Deferred reproduction as a response to sexual selection in a coral reef fish: a test of the life historical consequences. *Evolution* **38:** 148–162.

Weisberg, S. 1980. *Applied Linear Regression.* Wiley, New York.

Wickins, J. F. 1972. Experiments on the culture of the spot prawn *Pandalus platyceros* (Brandt) and the giant freshwater prawn *Macrobrachium rosenbergii* (de Man). *Fish. Invert. London Ser. 2* **27**(5): 1–23.

Reference: *Biol. Bull.* **181:** 387–401. (December, 1991)

Reproductive Ecology of an Intertidal Brachyuran Crab, *Sesarma* sp. (nr. *reticulatum*), from the Gulf of Mexico

TODD L. ZIMMERMAN AND DARRYL L. FELDER

University of Southwestern Louisiana, Department of Biology, and USL Center for Crustacean Research, Lafayette, Louisiana 70504-2451

Abstract. The natural history and reproductive ecology of a presently undescribed marsh crab endemic to the Gulf of Mexico were studied in both the laboratory and the field. Weekly sampling of populations in coastal Louisiana allowed us to determine the periodicity of molting and ovarian development, as well as the seasonal variation in egg laying and size of individual egg masses. Timing of molt, egg laying, and egg hatching were monitored in individual females under simulated tidal cycles in laboratory mesocosms. Peak periods of reproductive activity in Louisiana coincide with favorable temperatures and elevated primary productivity in coastal waters. Size cohort and fecundity differ between these periods. Egg-laying, larval release, and molting observed in individual females in the laboratory and extrapolated dates of egg-laying and larval release for those in field samples exhibit a semilunar influence throughout the season. Female receptivity to mating is tied to egg-laying. Rate of embryonic development was associated with decreases and increases in egg size. Behavior related to larval release is described. Adaptive significance in relation to the intertidal marsh habitat is discussed.

Introduction

Present distributional records for the burrowing grapsid crab, *Sesarma reticulatum* (Say, 1817), suggest a range from Woods Hole, Massachusetts to Volusia County, Florida along the East Coast of the United States, and from Sarasota County, Florida to Calhoun County, Texas within the Gulf of Mexico (see Williams, 1984). The original purpose of this study was to expand upon the ecological works concerning *S. reticulatum* (which have, to date, been carried out on the Atlantic Coast; Crichton, 1960, 1974; Mulstay, 1975; Seiple, 1979a, b, 1981; Seiple and Salmon, 1982, 1987) by closely examining the reproductive ecology of the Gulf populations. However, during other studies treating genetics (Felder and Staton, in prep.) and morphology (Felder and Zimmerman, in prep.), it became apparent that populations endemic to the Gulf are distinctly different from the east coast *S. reticulatum* and should be considered a distinct species. As its closest relative, *S. reticulatum* serves as the best source of background information to supplement what little is known about the Gulf crab.

Collections by one of us (D. L. Felder) indicate that the undescribed Gulf of Mexico form (hereafter referred to as *Sesarma* sp. (nr. *reticulatum*) ranges from Sarasota County, Florida, to Barra del Tordo, Tamaulipas, Mexico, while *Sesarma reticulatum* ranges from Woods Hole, Massachusetts, to Volusia County, Florida (Williams, 1984). *Sesarma reticulatum* inhabits estuarine environments with salinities ranging from less than 2 ppt to 35 ppt (Allen and Curran, 1974), prefers a mean of about 16 ppt (Seiple, 1979a, b), and is found commonly in intertidal areas along stream banks and in well-drained salt marsh habitats above mean tide level (Teal, 1958; Crichton, 1960, 1974; Allen and Curran, 1974; Mulstay, 1975; Seiple, 1979a, b). *Sesarma* sp. (nr. *reticulatum*) lives in similar habitats. It is generally found in areas of relatively low salinities (1–15 ppt) but may also occur in hypersaline habitats. Teal (1958) considered *S. reticulatum* to be an important member of the salt marsh community in Georgia, while *S.* sp. (nr. *reticulatum*) was found to rank as high as fifth among species in terms of both density and biomass in one Florida Gulf coast salt marsh (Subrah-

Received 16 May 1991; accepted 20 September 1991.

manyam *et al.*, 1976). In Gulf coast habitats, *S.* sp. (nr. *reticulatum*) is often found sympatrically with *Sesarma cinereum* (Bosc, 1802), *Eurytium limosum* (Say, 1818), *Panopeus obesus* Smith, 1869, *Rhithropanopeus harrisii* (Gould, 1841), and *Uca* spp. (Subrahmanyam *et al.*, 1976), especially *U. longisignalis* Salmon and Atsaides, 1968, *U. rapax* (Smith, 1870), and *U. spinicarpa* (Rathbun, 1900). The burrows of *S. reticulatum* are important in reworking the soil and often interconnect with those of other species (Crichton, 1960; Allen and Curran, 1974).

Sesarma reticulatum is primarily nocturnal (Crichton, 1960; Palmer, 1967; Mulstay, 1975; Seiple, 1981), and inhabits burrow networks (Crichton, 1960; Allen and Curran, 1974; Seiple and Salmon, 1982), in mean densities as high as 25 crabs/m^2 (Seiple, 1979a, b). Several females (Crichton, 1960; Seiple and Salmon, 1982) and juveniles (Mulstay, 1975) can be found in the network associated with a mature male. During the breeding season, males patrol and defend burrow entrances (Mulstay, 1975). Food reportedly consists primarily of live vegetation such as *Spartina alterniflora* Loisel (Crichton, 1960, 1974; Seiple and Salmon, 1982). *S. reticulatum* has also been observed to feed actively on the marsh surface during overcast days (Teal, 1959). The reproductive season varies depending on latitude (Mulstay, 1975; Seiple 1979a, b), and factors such as temperature and lunar phase influence reproduction (Seiple, 1979a, b).

Sesarma reticulatum, other *Sesarma* species, and many intertidal brachyurans exhibit reproductive periodicities corresponding to lunar and tidal phases (Saigusa and Hidaka, 1978; Seiple, 1979a, b; Saigusa, 1981, 1982, 1988; Christy, 1982; Christy and Stancyk, 1982; Forward, 1987; DeVries and Forward, 1989). Larval release rhythms for *Sesarma* species also coincide with solar day and tidal cycles (Saigusa, 1982; DeVries and Forward, 1989). The onset of the breeding seasons may be cued to temperature (Pillay and Ono, 1978; Seiple, 1979a, b). The synchrony of reproductive cycles is poorly developed in *S. reticulatum* at the beginning and end of the season (Seiple, 1979a, b). The spring asynchrony phenomenon has been recorded for other crabs as well (Wheeler, 1978; Dollard, 1980; Christy, 1982).

Semidiurnal tides have been shown to entrain biological rhythms in many intertidal crabs (Fingerman, 1957; Palmer, 1967; Saigusa, 1982; Decoursey, 1983; Christy, 1986; Forward, 1987), and latitudinal variations in breeding periodicities have been reported for populations of the intertidal grapsid crab *Helice crassa* Dana, 1851, in New Zealand (Jones and Simons, 1983). Also, larval release rhythms for fiddler crabs from the west coast of Florida, which are subject to diurnal tides, differ from those on the Atlantic coast (Christy, 1978). Thus, periodicities in Gulf of Mexico *Sesarma* populations may be expected to vary from those reported from the Atlantic Coast, both because of latitudinal differences and genetic divergence.

In the present study, we investigate aspects of reproductive ecology and life history in *S.* sp. (nr. *reticulatum*), an abundant and previously unstudied inhabitant of the most expansive intertidal estuarine and salt marsh habitats in the conterminous United States. We present information on annual female population changes in reproductive states, such as ovarian activity and growth, and factors that influence female reproductive cycles and molting throughout the year, such as lunar and tidal phases. We also describe details of events that take place during a single female reproductive cycle from mate receptivity, through egg laying and embryonic development, to larval release. The adaptive significance to a low salinity intertidal habitat is discussed.

Materials and Methods

Field samples

Mature-sized female specimens of *Sesarma* sp. (nr. *reticulatum*) were collected (n/collection = 17–44) periodically from 21 March 1989 to 21 March 1990 in coastal Louisiana habitats near Cocodrie, Cypremort Point, Redfish Point, Rockefeller Wildlife Refuge, and Cameron. These areas are all under similar tidal regimes and have salinities under 12 ppt. The majority of samples were collected from a fresh marsh dominated by bulltongue (*Sagittaria lancifolia* L.), *Iris* sp., and deer pea [*Vigna luteola* (Jacq.) Benth.]. Females brought to the lab were chilled on ice, examined, measured, and dissected. An impending molt was noted if a crab's exoskeleton was discolored and brittle with a thickened underlying integument, and a recent molt was noted if the exoskeleton was soft or abnormally thin and clean. Carapace width (CW) was measured ± 0.01 mm. When eggs were present, developmental stage (after Boolootian *et al.*, 1959; Brown and Loveland, 1985) was recorded. Wet weight of the egg mass (if present), body, and ovary were determined to the nearest 0.1 ± 0.03 mg. After weighing, egg masses were preserved in 7% formalin. An analysis of 18 egg masses was used to estimate the number of eggs per gram wet weight of egg mass. Calcification of the genital opercula (after Hartnoll, 1968), presence of spermatozoa in the spermatheca, and maturation stage of the ovary [as determined by color, (after Pillay and Ono, 1978)] were recorded. Spermatozoa were present in the spermatheca of all but the smallest females throughout the sampling period.

Voucher specimens from each field site were archived in the University of Southwestern Louisiana Zoological Collections, USLZ 3484–3493.

Laboratory mesocosms

Laboratory habitats consisted of two fiberglass tanks (0.3 × 1.12 × 2.3 m) each with a permeable partition separating the tanks into four equal mesocosms. A layer of gravel 5 cm thick was placed under 10 cm of topsoil separated by Weed-X® porous landscaping barrier and nylon window screening, to provide adequate drainage and enable a shallow layer of soil to be used. The area of the tank near the partition was free of soil and gravel and was a source of standing water at low tide periods. Soil was held back from the standing water area by a 10 cm high burlap covered board resting on the edge of the gravel. This enabled crabs to climb down to the water with ease. Topsoil was replaced with soil from the collection site on 6 June 1990, and this was replaced again, on 4 August, with soil from the same site. Four boards (approximately 30 × 40 cm) were placed on top of the soil in each section to provide cover under which crabs could take refuge. Water level was controlled by two (1/70 hp) pumps, one to pump water from storage tanks into the habitat tanks to simulate high tide and the second to reverse the process to simulate low tide. Each pump was controlled by a separate 24-h timer providing a high water period of 4 h per day. These were controlled by a third timer that advanced the high water period by 1 h each day. This tidal regime was for experimental purposes only, as the fluctuating natural tidal cycles could not be duplicated. Salinity was adjusted by mixing full strength seawater with dechlorinated water, and maintained at 5 ppt to represent a salinity value that is intermediate for the coastal Louisiana habitats sampled. Water was changed weekly.

Mesocosms were contained in a light proof room where fluorescent overhead lighting provided a 14 h light:10 h dark cycle. In addition, 1500 watt halogen lights (controlled to turn on and off 1 h after and before the overhead lights) were installed over each tank on 2 July 1990 to simulate the high temperatures characteristic of the natural summer habitat after sunrise. Light intensity reached a maximum of approximately 150 μE $s^{-1}m^{-2}$, while soil temperature ranged from 23–30°C during the day and dropped to 23°C at night. These temperatures approximated those in the field.

One hundred crabs (80 females and 20 males) of mature size were collected from Cypremort Point on 4 and 9 April 1990. Carapace width was measured, and a numbered plastic tag was glued to the carapace using cyanoacrylamide glue. Twenty-five (20 females and 5 males) crabs were placed in each mesocosm. This did not correspond to the ratio found in the field, but provided adequate breeding interactions and an increased sample size of females. Individual crabs were inspected every few days until crabs began laying eggs, at which time they were checked every 2–3 days for egg laying, developmental stage of the eggs, egg diameter (as an average of ten eggs), larval release, and molting. Crabs were initially fed Tetramin® flake food and Hartz® Shrimp-el-etts® supplemented periodically with lettuce and *Spartina* before the topsoil was replaced with marsh soil and the halogen lights were installed. After this time, the crabs did well without feeding but supplementary food in the form of commercial rabbit and guinea pig pellets was added and seemed to be much preferred over any of the previous foods. To maintain an optimal number of crabs in all of the mesocosms, this initial population of crabs was consolidated into two of the four mesocosms, and new crabs were collected from the same marsh on 7 June 1990, measured, marked, and placed into the empty mesocosms. This consolidation was repeated again on 5 August.

Video observation

To determine timing of genital operculum decalcification, egg laying, and larval release, 90 females were collected in early August, measured, marked, and whenever possible placed individually into 11 cm finger bowls with 1–2 cm of 5 ppt salinity water. Water was changed every day, and crabs were fed commercial rabbit pellets every other day. Crabs were checked daily for softening of the genital opercula by unfolding the abdomen and pressing on the opercula with the tip of a forceps. Very light pressure was needed to depress the opercula after the hinge had softened, and movement could be easily detected. Date and time of detection were recorded, and the crab was then monitored, with a time-lapse video system, for egg laying and subsequent egg hatching. Developmental stage of the eggs was recorded daily and these ovigerous crabs (along with those from the mesocosms with eggs approaching hatching) were placed under video observation. Video observation chambers consisted of four polystyrene boxes (30 × 15 × 8 cm), each spanned at mid-length by a 3 cm wide, 1 cm deep wax trough containing 5 ppt seawater in which larvae could be released and gill water replenished. A plate of glass was placed over the boxes to prevent escape, and an infrared light source was used for night observations. Activity was monitored using a video camera connected to a time-lapse video set to record for 72 h per 120 min VHS tape. The room was kept at a constant 28°C, and a 14:10 h light:dark photoperiod was maintained with overhead fluorescent lights in addition to the constant infrared light source. The larval release of a single crab was videotaped at close range and at real time speed to precisely record the event.

Larval rearing

Larvae from two females were reared in two sets of ten 11 cm finger bowls (initial densities = 20 larvae/bowl) in filtered seawater diluted with deionized water to 25 ppt salinity at 28°C. Larvae were fed newly hatched *Artemia* nauplii daily. These procedures were followed to ensure maximum survival and to yield results similar to those expected under optimal conditions in the field.

Results

Reproductive and molting peaks

Crabs with newly laid eggs were found in field collections as early as April 14 in 1989, and April 4 in 1990. Sampling throughout 1989 indicated a peak in the percentage of females carrying eggs from late April through late May, followed by another larger peak extending from mid-July through early September. Other ovigerous females were found in late July and from late September to mid-October, and the last egg carrying female of the collection period was taken on October 12. Egg carrying females ranged from a minimum of 11.1 mm to a maximum of 26.9 mm carapace width. A peak in molting for the population began in mid-May and extended to late June and was followed by another peak molt during mid-October. Some crabs also molted in late July and early August. Molting activity was not observed during the winter months, although collections were not made as frequently during this time (Fig. 1).

Size differences

Careful examination of peaks in molting and egg-carrying across all size classes sampled indicated that timing of crabs carrying eggs and crabs molting varied between two size cohorts. Crabs smaller than 17.5 mm CW were found carrying eggs only in the latter part of the season from July through September. Larger crabs were found with eggs throughout the reproductive season. Those crabs larger than 23.5 mm CW were found to molt only from late September through October while smaller crabs (≤23.5 mm CW) were found molting during the May–June peak, somewhat during mid-summer, and again in October (Fig. 2).

Reproductive effort

A mean of 20,400.8 (±2469.2 95% CI) eggs per gram wet weight of egg mass was determined from egg counts of 18 individuals. When multiplied by the wet weight of each individual egg mass, this estimated value resulted in average egg numbers ranging from 2,728 for the smallest egg bearing females (11–13 mm CW) to 18,087 for large females (25–27 mm CW). The maximum number of eggs estimated for a single brood was 27,847 found on a crab with a carapace width of 24.5 mm. Estimated numbers of eggs per crab increased with body size in all but the largest size grouping of crabs (Fig. 3).

Seasonal differences

Fecundity data (wet weight of egg mass/carapace width) for spring pre-molt and non-molting ovigerous females collected prior to 1 July (the end of the spring molting period) and summer ovigerous females collected after this date were fitted by linear regression ($y = -0.723 + 0.067X$, $r^2 = 0.454$ for spring crabs; $y = -0.999 + 0.074X$, $r^2 = 0.454$ for summer crabs). Weight of the egg mass increased together with female body size in both seasonal sets, and slopes were not significantly different from each other when compared by Student's *t*-test. However, there was a significant difference (Student's $t = 4.21$, $P \geq 0.001$) between the mean weights of egg masses (spring $\bar{X} = 0.719$ g, $n = 44$; summer $\bar{X} = 0.536$ g, $n = 63$) when the two sets were compared (Fig. 4).

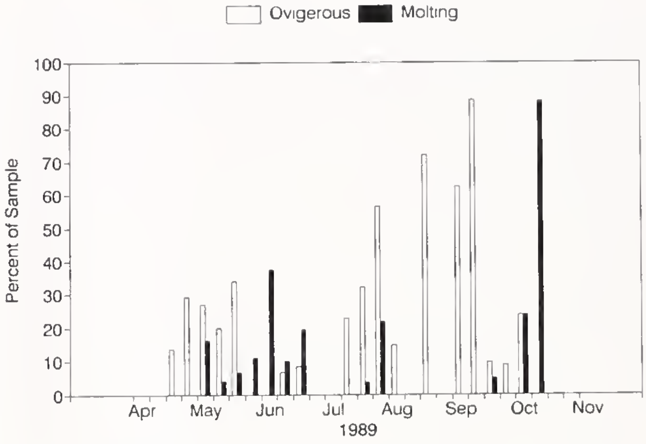

Figure 1. Percentages of ovigerous females (open bars) and females undergoing a molt (solid bars) found in periodic field samples of *Sesarma* sp. (nr. *reticulatum*) taken during 1989. All samples are represented by bars except for those collected during the third week of March, the first week of April, the third week of October and the third week of November, which contained no ovigerous or molting females.

Lunar periodicity

Date of egg laying and expected date of larval release for each ovigerous crab collected in the field were back calculated from data obtained by monitoring egg size and development in the laboratory. This was done to determine periodicity of reproductive events in field populations. The mean number of days required for a developmental stage to be reached in the laboratory was subtracted from the date that each ovigerous crab with eggs corresponding to that stage was collected. Expected dates of larval release were then determined by adding the mean number of days remaining from that stage in development to larval release. Extended developmental period caused by lower temperatures, if occurring, should have been reflected in distribution of developmental stages in relation to the dates of the new and full moons. Peak numbers of crabs laying eggs or releasing larvae should also then have been skewed away from the syzygies until increased temperature caused developmental rate in the field to equal

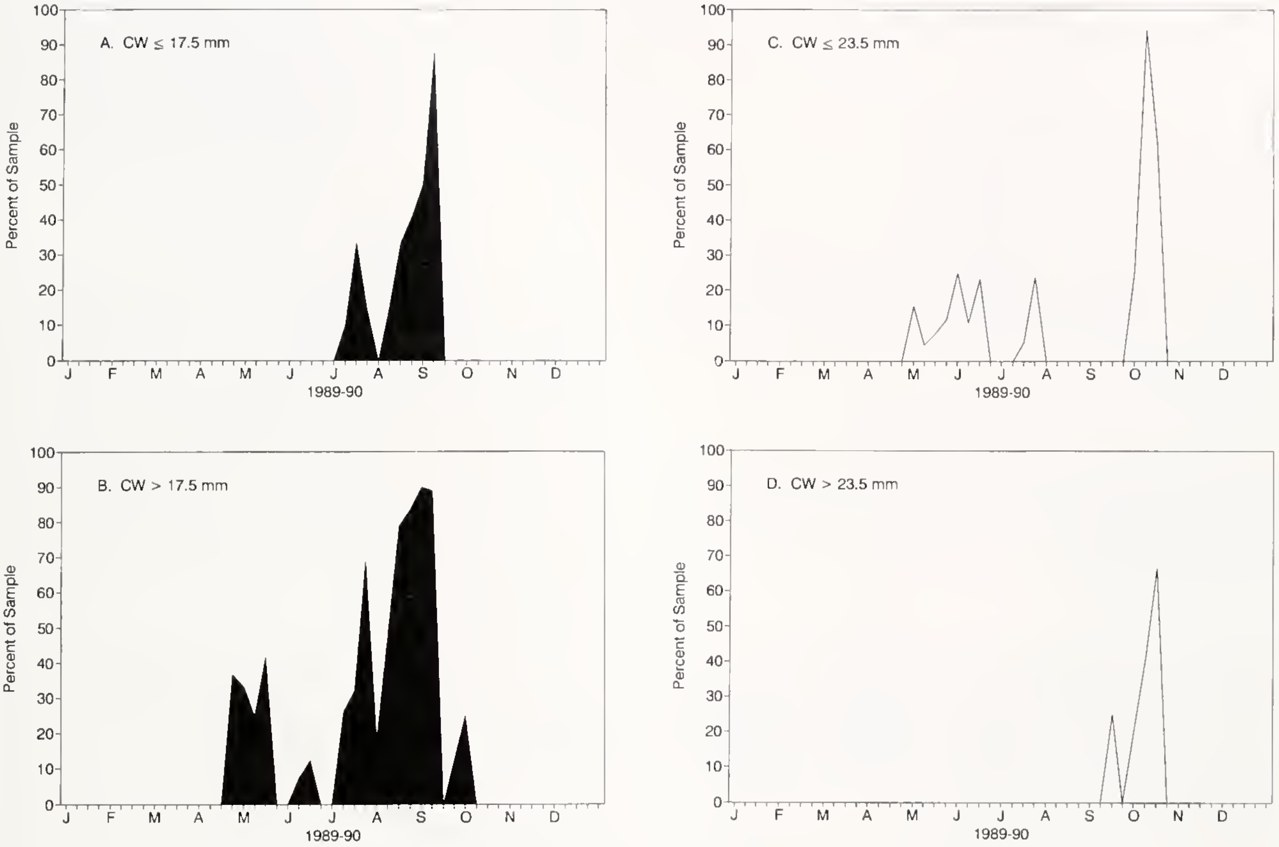

Figure 2. Reproductive and molting cohorts for female *Sesarma* sp. (nr. *reticulatum*) taken in field samples during 1989 and 1990. A. Ovigerous crabs ≤ 17.5 mm carapace width. B. Ovigerous crabs > 17.5 mm carapace width. C. Molting crabs ≤ 23.5 mm carapace width. D. Molting crabs > 23.5 mm carapace width.

that seen in the laboratory. Instead, peaks in egg laying and larval release occurred near dates of new and full moons throughout the reproductive season (Fig. 5).

Ovarian growth

Ovarian wet weights, expressed as an index of grams wet weight ovary per millimeter carapace width, were compared to ovary color; yellow ovaries were the lightest, which suggested inactivity, orange ovaries were slightly heavier, which suggested rebuilding or oogenesis, and red-black ovaries were the most massive because of vitellogenesis (Table 1). Vitellogenic ovaries were seen in 37.5% of the sample as early as mid-January, and the numbers of crabs possessing vitellogenic ovaries increased through the reproductive season until August when nearly all female crabs of mature size had reproductively active ovaries. This percentage dropped to near zero in September, after which a slight increase occurred in October before vitellogenesis ended for the season (Fig. 6). Inversely, the percentage of inactive yellow ovaries increased markedly in samples after the cessation of vitellogenesis in September and October. Ovarian rebuilding for the population quickly followed inactivity so that by 22 November 77.8% of the sample possessed orange ovaries.

When only vitellogenic ovaries were considered, intensity of yolk deposition began to increase in late March and April, and to peak in late April. Intensity of yolk deposition declined during the May-early June molting period, and increased to a high level throughout the summer reproductive peak. High values near 0.02 g/mm, which would indicate eggs are ready to be extruded, are absent during the two sampling dates (May 9 and June 1) that fell during peak molting periods (Fig. 7).

Rate of ovarian growth was measured for those crabs carrying eggs by plotting relative ovarian wet weight (g/mm) against developmental stage of the eggs. Early in the season, ovigerous crabs collected before, during, and just after the molting period showed little increase in ovary weight throughout the period that the eggs were carried. After the molt period, during peak reproductive activity, ovarian weight increased throughout the period that car-

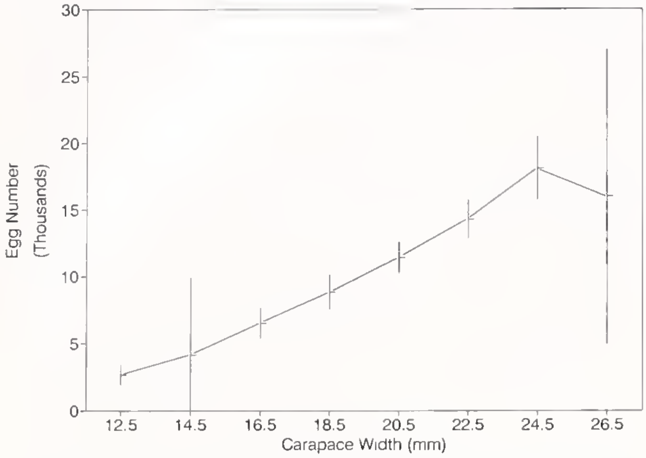

Figure 3. Estimated numbers of eggs per egg mass plotted against crab size as shown by 2-mm increments of carapace width (bars indicate 95% confidence levels) for female *Sesarma* sp. (nr. *reticulatum*) taken in field samples during 1989.

ried eggs were developing. Females bearing eggs (ovigerous) after 30 August possessed very light colored, inactive ovaries that showed no increase in weight while eggs were being carried (Fig. 8). Inferential statistical analyses were not performed on these data because of small and variable sample sizes.

Decalcified opercula

The only day (5 July 1989) in which softened genital opercula were found in a large percentage of the sample (37%) during the study was near full moon. While few ovigerous females (10.5% of females sampled) were found on this date, laboratory data suggested that the cohort with softened genital opercula should have laid eggs within 24 h. Indeed, 31% of the females collected on the following date (6 July 1989) were ovigerous, confirming the laboratory prediction. Because data were plotted at weekly intervals, collections made on these two dates were combined and a value of 23% appears on Figure 1.

Laboratory mesocosms

Crabs held in laboratory mesocosms did not produce a premolt spring brood of eggs possibly because of inadequate substrate or diet. This problem seemed to have been corrected with the substitution of substrate from the natural habitat and the installation of halogen lights. The molting period was also offset from that recorded from field samples by approximately one month. A first brood was produced a minimum of 21 days ($\bar{X}$ = 34 days) following the early season molt. This was followed by a second brood at $\bar{X}$ = 27.7 days later, and a third brood at $\bar{X}$ = 25 days later. A fourth brood was produced by three crabs collected in early April, at $\bar{X}$ = 21.7 days later, and the fall molt followed the last brood after a minimum of 34 days ($\bar{X}$ = 47.8) (Table II; Fig. 9). The brood number and date of egg laying for those crabs collected on 7 June and 5 August were estimated on the basis of field data and developmental stage of the eggs, respectively.

Semilunar periodicities in the laboratory

Dates of molting, egg laying, and larval release were plotted to determine whether there was an apparent lunar rhythm in events in the laboratory. The number of crabs molting increased during full moon periods. Molting usually occurred in the open water portion of the mesocosms, and when directly observed, it always occurred during periods of high water. Numbers of crabs both laying eggs and releasing larvae peaked on the syzygies, with egg laying slightly skewed (right) to the days preceding, and larval release slightly skewed (left) to the days following the new and full moon (Fig. 10).

Mating was observed during the day, both in the mesocosms (by inspecting under the refugia boards there provided) and in containers holding crabs as they were brought in from the field to be tagged or while they were periodically removed from the mesocosms and held together before and after examination and data recording. In all cases, mating females were found to have softened genital opercula, and in two cases the same female was observed mating with more than one male within a few hours time. Usually pairings were between similar sized individuals, but unequal size pairings of both kinds were also seen. In each instance, when tagged crabs from the mesocosms were observed mating (either in the mesocosms or in containers while they were held together dur-

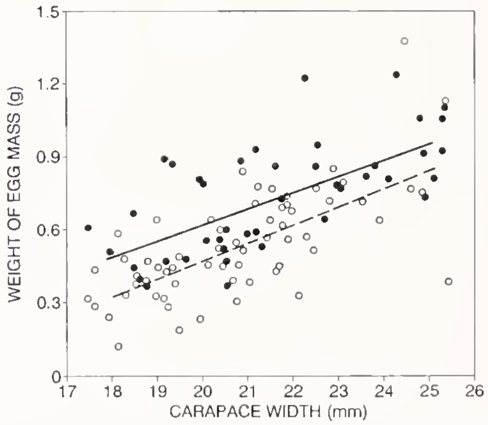

Figure 4. Regression of clutch size (wet wt egg mass) on carapace width (mm) for *Sesarma* sp. (nr. *reticulatum*). Open circles and broken line represent crabs collected before and during the spring molting period (1 July) 1989. Dots and solid line indicate crabs collected in 1989 after this date.

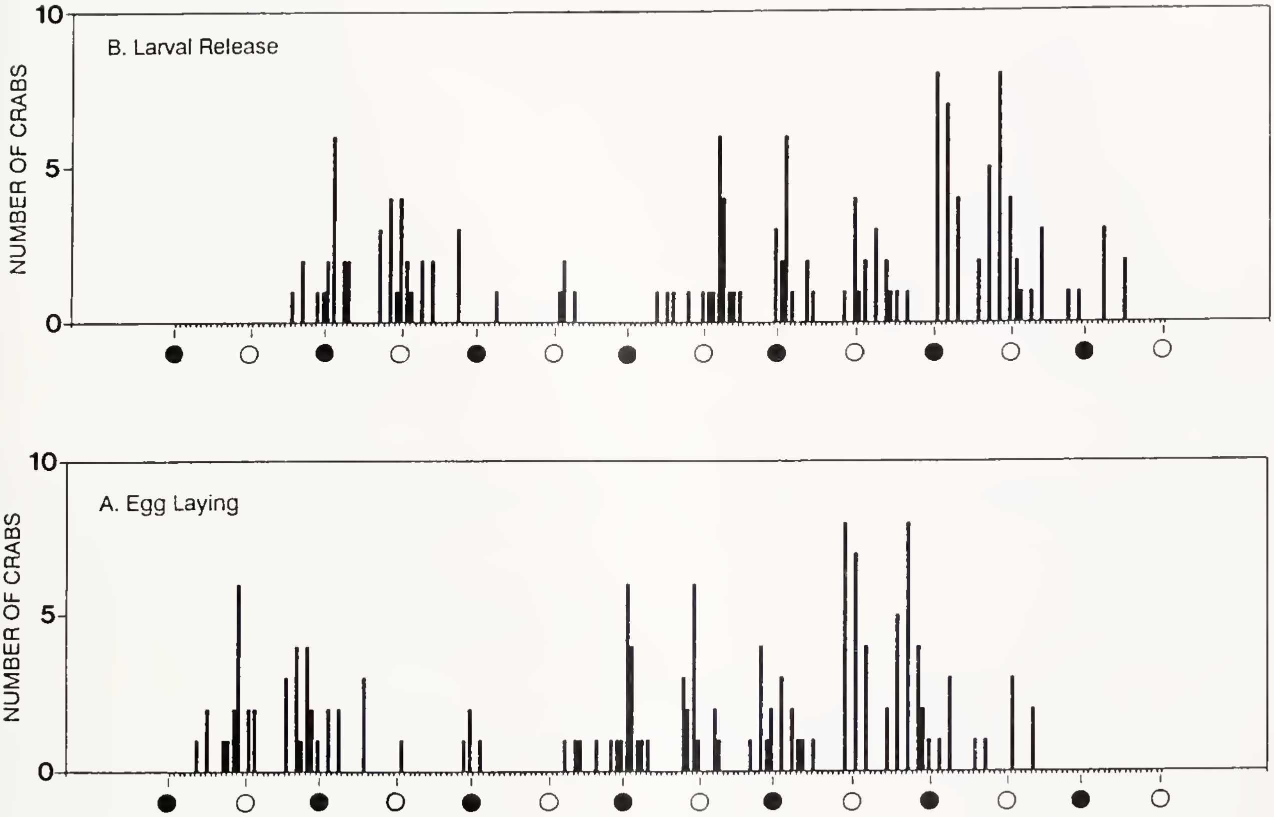

Figure 5. Relationship of lunar cycle to numbers of crabs laying eggs (A), and releasing larvae (B), for *Sesarma* sp. (nr. *reticulatum*) taken in field samples during the 1989 reproductive season. Dates are estimates based on developmental stage of eggs found on each crab. Lunar series begins on 6 April (first filled circle, new moon) and ends on 8 October (last open circle, full moon).

ing data recording), the females were found with eggs within 2–3 days when next captured. Females soft from a molt were never observed mating, and genital opercula, although soft, were not functionally hinged when manipulated under a dissecting scope.

Crabs held individually and checked periodically each day were found with decalcified opercula as early as 1045 h. Six of these crabs were videotaped as they laid eggs out of water between 2051 h of the same day and 0100 h of the following day. Visible light was removed at 2015 h, and the crabs laid eggs out of water after an activity period beginning shortly after darkness that day. Recalcification occurred soon after egg laying, and hard opercula were

Table I

Ovary color, mean wet weight (mg), 95% confidence interval, and number of individual female Sesarma *sp. (nr.* reticulatum*) taken in field collections during 1989 and 1990*

Ovarian color	Mean wet weight (mg)	95% CI	n
Red-black	7.05	0.54	320
Orange	1.98	0.24	126
Yellow	1.50	0.13	142

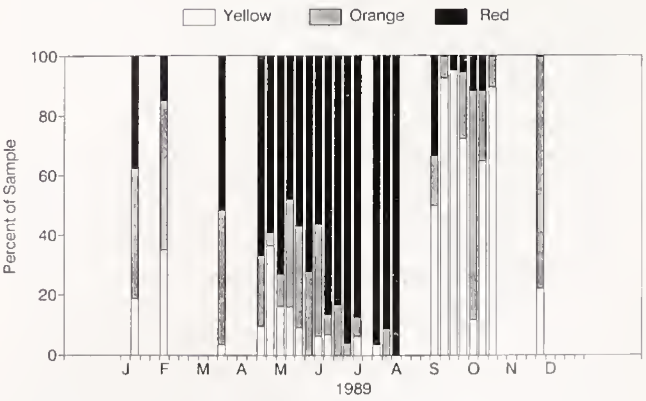

Figure 6. Ovarian activity of *Sesarma* sp. (nr. *reticulatum*) taken in field samples from 21 March 1989 to 21 March 1990 as determined by color. Percentages of crabs in each field sample with inactive (yellow, clear bar), rebuilding (orange, stippled bar), and vitellogenic (red-black, solid bar) ovaries.

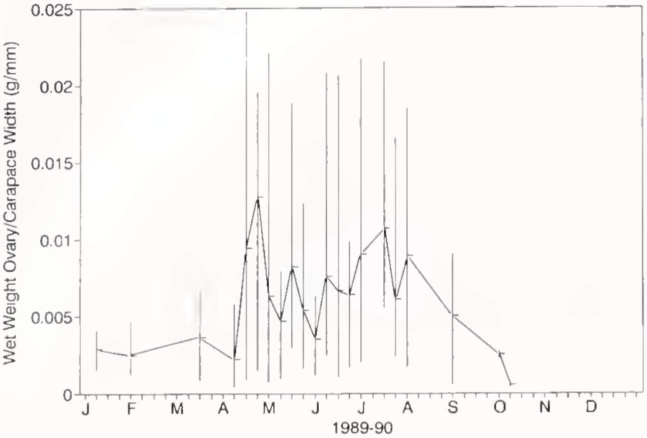

Figure 7. Relative vitellogenic ovary size (g wet wt ovary/mm carapace width) of *Sesarma* sp. (nr. *reticulatum*) taken in field samples from 21 March 1989 to 21 March 1990. Dashes and line represent mean values, and bars signify high and low values for each sample date.

found as early as 0800 h the following morning. One crab was videotaped entering water and laying eggs at 1057 h. Of the remaining five crabs found with soft opercula, two did not lay eggs and died shortly after, and three laid eggs at night but were not videotaped. In all instances, these eggs were fertilized with sperm stored from a previous mating.

Development of the embryo within the egg was divided into 10 distinct stages (Table III). The total period of embryo development, which began when the eggs were extruded onto the pleopods, and ended with release of the larvae, averaged 17.3 days (±0.3 95% CI; R = 15–19; n = 47). The first two embryonic stages (Table III; Fig. 11) persisted for approximately one third of the total developmental period. Egg diameter decreased 8% within two days of oviposition. After the fourth day, egg diameter began to increase, reaching 125.7% of the day 4 diameter at the time of hatching (Fig. 11). Neither an initial decrease nor any subsequent increase in egg diameter was seen over the 10-day period that an infertile brood was monitored.

Eighty-two crabs were videotaped releasing larvae. Seventy-nine crabs (96.3%) exhibited a characteristic period of constant increased locomotor activity (herein dubbed "hyperactivity") lasting from 5 to 47 min ($\bar{X}$ = 20.62 min) that ended with release of the larvae (usually in the water trough provided). Close-up video revealed that at the end of the "hyperactivity" period the female stopped and deflexed her abdomen, at that time her body shuddered and a cloud of larvae seemed to abruptly burst out of the egg mass. Not until this initial hatch had occurred and most of the larvae were free did the crab begin to pump her abdomen and pick at the empty egg casings with her chelipeds in an attempt to clear her pleopods.

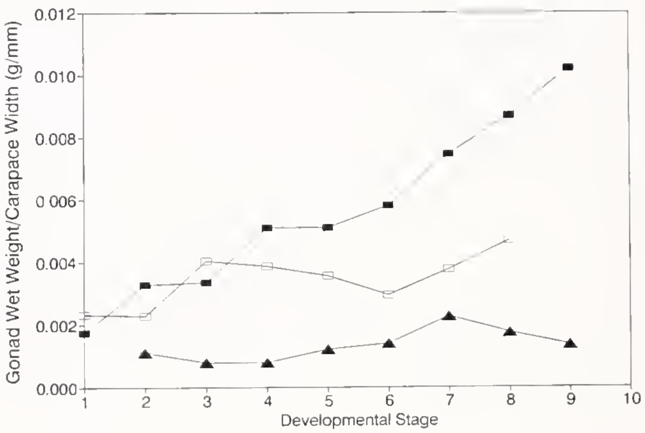

Figure 8. Mean ovarian growth (ovarian g wet wt/mm carapace width) of ovigerous *Sesarma* sp. (nr. *reticulatum*) taken in variably sized samples of each stage (n = 1–17) during the 1989 reproductive season plotted against developmental stage of the egg for (open squares) crabs collected between 14 April and 23 June (before and during the spring molt period), (solid squares) crabs collected between 7 July and 5 August (mid-season), and (solid triangles) crabs collected between 30 August and 3 October (end of season).

Within minutes, the crab's abdomen appeared to be free of most empty and inviable eggs. Sixty-five (79.3%) of the videotaped crabs released larvae at night. The majority of these released larvae within 1 h after dark (Fig. 12) on nights near or on the new and full moons (Fig. 13). During the latter part of this study, natural darkness fell up to 2 h before laboratory darkness, and increased locomotory activity was observed in the interim, but "hyperactivity" and larval release did not occur until cued by darkness. Seventeen crabs (20.62%) were observed releasing larvae during the day. These releases ranged from 0915 to 1907 h. Only two of these, 1907 h on 5 September and 1818 h on 20 September, occurred after natural sunset. None of the day releases corresponded to either natural or artificial high tide periods, although in the mesocosms, crabs did become more active, and larval release was recorded during periods of daytime high water.

Table II

Mean ($\bar{X}$) and minimum (Min.) number of days separating molting and egg laying events for individuals of Sesarma *sp. (nr* reticulatum*) held in laboratory mesocosms*

	M to B_1	B_1 to B_2	B_2 to B_3	B_3 to B_4	B_f to M
$\bar{X}$	34.1	27.7	25.0	21.7	47.8
95% CI	2.643	1.515	1.846	1.436	6.061
n	41	41	21	3	18
Min.	21	18	20	21	34

M is date of molt, $B_{1,2,3,4}$ are date of egg laying for the first, second, third, and fourth broods. B_f is the final brood produced by an individual.

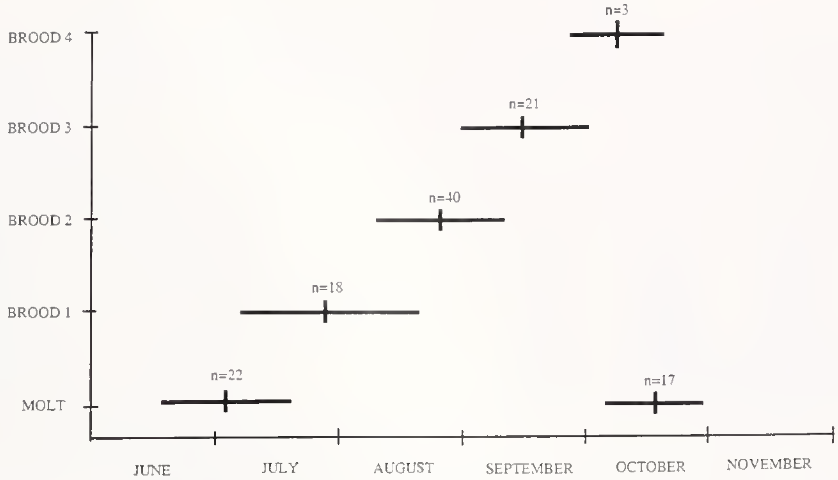

Figure 9. Mean dates and standard deviation of molts and egg laying for individuals of *Sesarma* sp. (nr. *reticulatum*) held in the laboratory in 1990.

The larvae reared in the laboratory passed through three zoeal stages and one megalopal stage before the first crab stage was reached. The minimum number of days from hatching required for a larva to reach second zoeal, third zoeal, megalopal, and first crab stages was 3, 5, 8, and 16 days, respectively.

Discussion

While a variety of factors may be responsible for the onset of the reproductive season for *Sesarma* sp. (nr. *reticulatum*), temperature is often considered to be the single most important factor in determining the beginning of the reproductive season in such temperate marine invertebrates (Geise, 1959). However, the effects of temperature may vary strikingly between populations and between closely related species that are adapted or acclimatized to differing latitudinal regimes (see Vernberg, 1962, for review). The onset of local reproductive seasons may coincide with increased larval food availability (zooplankton) by way of increased primary productivity in coastal waters (Thorson, 1950). Chemical stimulation in relation to diatom blooms has also been suggested as a link to spawning in laboratory-held barnacles (Barnes, 1957).

Populations of *Sesarma reticulatum* in North Carolina begin reproducing at a time when both temperatures and coastal primary productivity increase sharply (Seiple, 1979a, b). In Louisiana, coastal water temperatures are not limiting early in the year, but increases in coastal primary productivity lag behind because of light limitations caused by riverine-influenced turbidity levels (Sklar and Turner, 1981; Madden *et al.*, 1988). Vitellogenesis in *S.* sp. (nr. *reticulatum*) began early in the year with increasing temperatures, but maximum ovary growth, and subsequent egg production did not occur until slightly before the increase in coastal production. This would suggest that some factors other than temperature, such as day length, cue the onset of reproduction in the spring.

The end of the reproductive season occurred in late August to early September when ovaries became inactive after producing their final brood of eggs. At this time, water temperatures are high, but coastal productivity is beginning to decline (Sklar and Turner, 1981; Madden *et al.*, 1988). The majority of crabs held in the laboratory mesocosms produced their final brood of eggs and molted later than most in the field, but within the period recorded for natural populations. However, three crabs did produce a fourth brood of eggs after the end of the reproductive period recorded for field populations. This suggests that the natural seasonal rhythm had been offset.

Endogenous rhythms are cued to environmental events that synchronize free running physiological "clocks," which run either too fast or too slow (DeCoursey, 1983). The endogenous rhythms of some crabs from the mesocosms may have been affected by the lack of appropriate signals. If decreasing day length acts as a zeitgeber for the cessation of reproduction in natural populations, the constant photoperiod in the laboratory could have resulted in the extended reproductive season for these crabs. The length of time that some crabs (all of which were collected early the previous spring) were subjected to laboratory conditions may have contributed to their offset seasonal "clocks." Those crabs collected later in the season may also have been affected by the constant conditions, and their final brood may have been produced later in the season than it would have in the field.

In the field, molting occurred within a short period after release of the first brood of larvae in the spring, and the last brood in the summer. Both of these times were characterized by low or no ovarian growth. In the lab, the

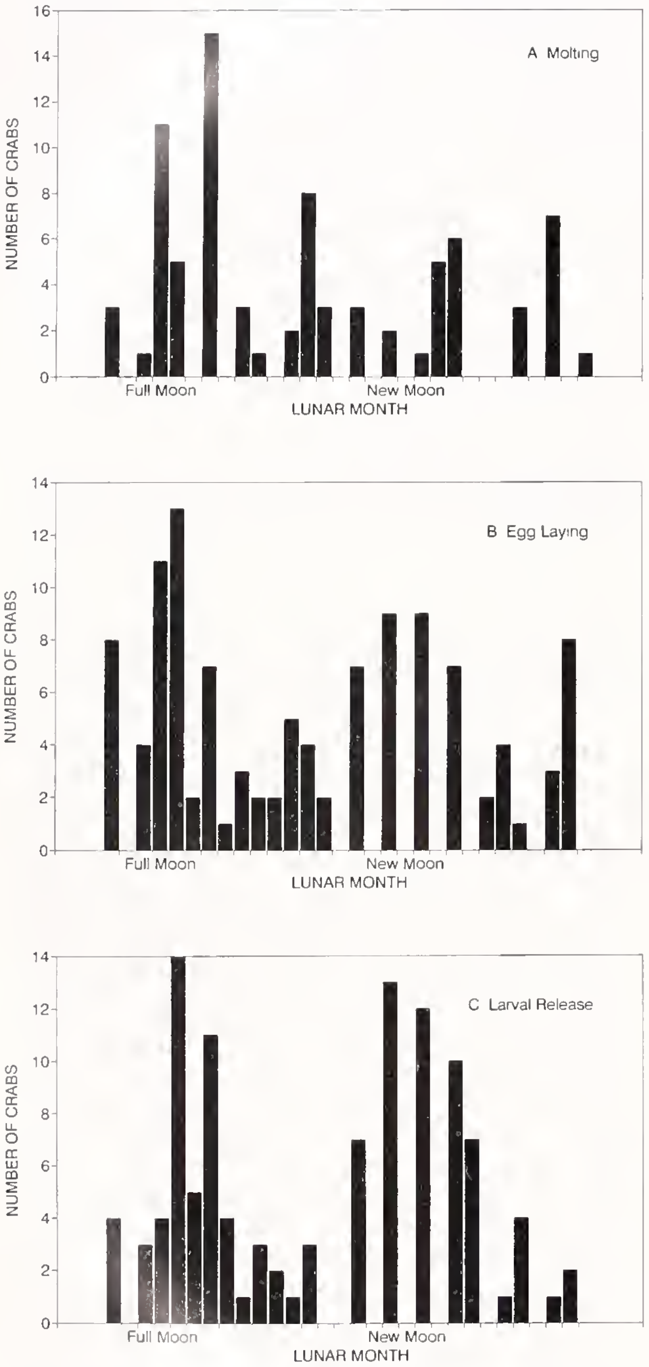

Figure 10. A. Molting, B. egg laying and C. larval release events for *Sesarma* sp. (nr. *reticulatum*) recorded in the laboratory during 1990, plotted by days of the lunar month.

constant regime of physical conditions probably affected the time of molting for those same crabs that had an extended reproductive season. It cannot be determined from this study whether the onset of molting is responsible for inactivation of the ovary in the fall, or whether molting and cessation of reproduction are independently controlled.

Table III

Criteria used for ranking the embryonic development of Sesarma *sp. (nr.* reticulatum*)*

Stage	Egg morphology
1	Egg completely filled with reddish purple yolk droplets.
2	Embryo visible as a small colorless plate of cells on one side of the yolk filled egg.
3	Approximately ⅓ of the egg consists of colorless embryo, yolk fills the remaining ⅔ of the egg.
4	Nearly ½ of the egg consists of colorless embryo, yolk fills the other ½.
5	Dark eye pigment and traces of dark chromatophores present, yolk fills approximately ½ of the egg.
6	Well-pigmented embryo comprises ⅔ of the egg the remainder being yolk.
7	Yolk forming distinctive "four leafed clover" lobed appearance, embryo fills ¾ of the egg.
8	Remaining yolk present as two connected lobes.
9	Traces of yolk remain as two separate patches, each containing a few droplets.
10	Embryo hatches as zoea.

Modified from Boolootian *et al.*, 1959, and Brown and Loveland, 1985.

Decrease in egg number per brood after the spring molting period could be caused by temporal constraints. The period of an individual reproductive cycle may not allow enough nutrients to be taken in or enough yolk to be produced for the maximum number of eggs allowed by body size. Crabs producing eggs in the spring have the advantage of an extended period for vitellogenesis; absence of somatic growth processes that follow a molt may avoid expending nutrients that are instead used to produce yolk. Another possible explanation for the lower fecundity might be an increase in egg mortality in the summer

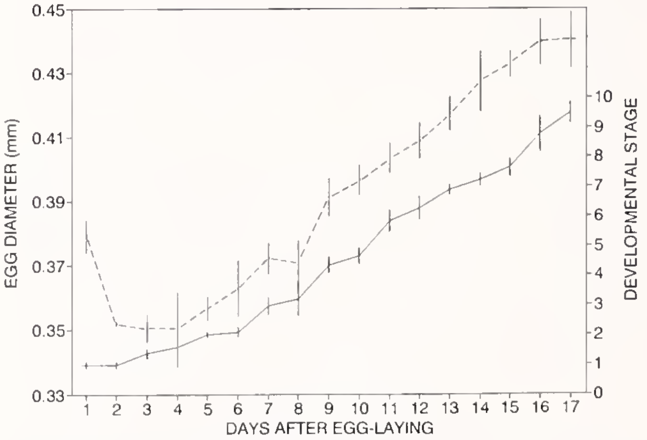

Figure 11. Mean change in egg diameter (broken line) and developmental stage (solid line) of *Sesarma* sp. (nr. *reticulatum*) plotted against the date from egg laying (bars are 95% CI).

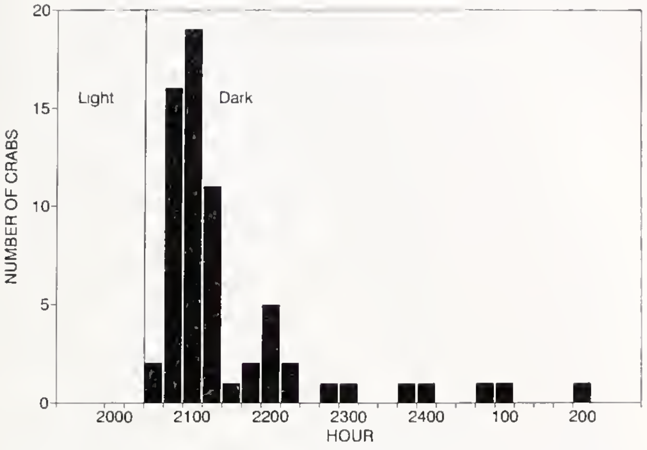

Figure 12. Number of individual *Sesarma* sp. (nr. *reticulatum*) videotaped releasing larvae versus time of release, in videomonitored experiment.

months. Dirty egg masses (often infested with peritrichous ciliates, nematode worms, and the harpacticoid copepod *Cancricola plumipes* Humes, 1941) seemed to be more prevalent in the warmer summer months. Many decapods groom their egg masses, but this behavior is relatively uncommon in brachyuran crabs (see review by Bauer, 1989) and seems to be particularly uncommon in the more terrestrial species such as grapsids and ocypodids.

Cycles within the reproductive season were correlated with the new and full periods (syzygies) of the lunar month. Such semilunar timing of larval release, so as to correspond to spring tides, is hypothesized to be an adaptation that facilitates export of larvae out of estuaries in *Uca* sp. (Sandifer, 1975; Christy and Stancyk, 1982). However, Sandifer (1975) found larvae of *Sesarma reticulatum* concentrated near the bottom, which would facilitate retention within an estuary. Larval release during spring tides in this species, and possibly *S.* sp. (nr. *reticulatum*), would enable females to release larvae under the protection of high tide in upstream areas not strongly affected by tides at other times, and may transport larvae out of marshes, ditches, and tidal creeks, and into deeper water.

For mature larvae to be released coincident with optimal conditions for their survival (*i.e.*, tides at new or full moons), eggs must be produced and laid in adequate advance of some developmental period, the duration of which itself varies according to exogenous factors (*i.e.*, temperature). Thus, selection would most likely favor egg-laying rhythms coincident with lunar phase but modulated to precede new and full moons by a time period that represents the mean period of embryonic development as would occur under typical environmental temperatures during the reproductive season. The period of embryonic development for *S.* sp. (nr. *reticulatum*) in laboratory mesocosms was very consistent (17.3 days, ± 0.3 95% CI, n = 47) for all broods monitored, slightly longer than the mean of 15.2 days (±2.6 SD, n = 10) reported for *S. reticulatum* by Seiple and Salmon (1987). The 17-day embryonic period positions larval release very near actual dates of new and full moons when it is used to project dates of larval release for field-captured ovigerous females (Fig. 5). To accommodate this 17-day developmental period, *S.* sp. (nr. *reticulatum*) populations may become entrained to lay eggs slightly before syzygies.

Species of crabs having reproductive periodicities that are strongly entrained to lunar or tidal cycles such as *S. cinereum*, *Uca pugnax* (Smith, 1870), and *U. pugilator* (Bosc, 1802) [studies by Seiple (1979a, b) and Dollard (1980), Christy (1978), and Wheeler (1978), respectively] may have periodic highs and lows in numbers of ovigerous females over the course of a reproductive season. These fluctuations could be used to estimate the number of days between each brood, or even the number of broods produced by a single crab each season. However, species such as *Sesarma haematochier* (de Haan, 1835) and *S. intermedium* (de Haan, 1835) studied by Saigusa and Hidaka (1978) and *S.* sp. (nr. *reticulatum*), which can be considered moderately entrained by lunar and tidal cycles, may have relatively constant numbers of ovigerous females in a population for long periods. Accurate estimations of time between broods cannot be made from periodic field samples when this situation exists. Long-term observation of some reproductive event such as larval release or mating in the field often yields valuable information about populations that can be used to infer conclusions about individual cycles, especially for *Uca* spp. Other species do not readily lend themselves to observation in nature, and use of an artificially reproduced habitat in the laboratory

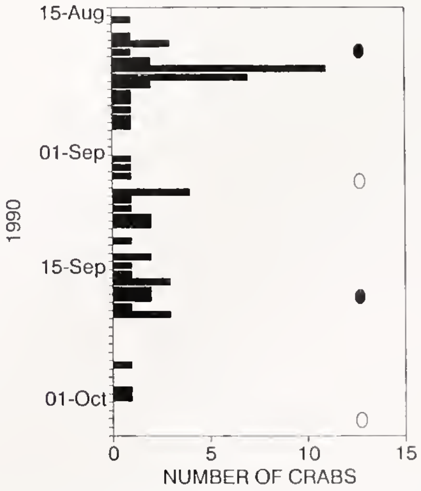

Figure 13. Number of individual *Sesarma* sp. (nr. *reticulatum*) releasing larvae versus date and lunar period, in videomonitored experiments. Solid ovals represent new moons, open ovals represent full moons.

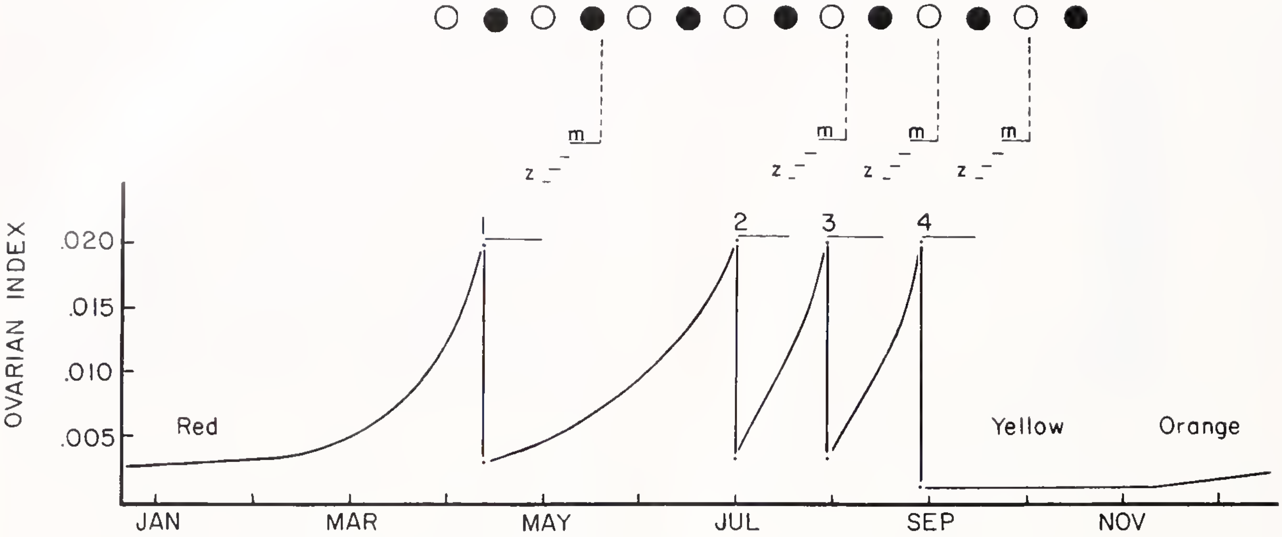

Figure 14. Hypothetical reproductive season for a fully mature female *Sesarma* sp. (nr. *reticulatum*). Base line represents ovarian growth (ovarian wet wt/mm carapace width) over time, peaks indicate egg laying, horizontal lines extending from peaks represent number of days required for embryonic development followed by date of larval release and duration of each larval instar (shorter lines). Vertical dashed lines represent metamorphosis to first crab stage. Molts are indicated, and lunar syzygies are represented by new (solid circles) and full (open circles) moons.

may be the best way to learn about reproduction in these organisms.

At the beginning of the reproductive season, larval release is often out of phase with the lunar cycle (Wheeler, 1978; Dollard, 1980; Christy, 1982). However, evidence of early season synchrony was seen when estimated dates of egg laying and larval release for field samples were compared to dates of new and full moons in the present study. Distinct semilunar peaks were found throughout the reproductive season, although more intensive collecting would have been required to test statistically for rhythmicity.

The previously reported asynchrony of reproductive phase for crabs sampled at higher latitudes (Wheeler, 1978; Dollard, 1980; Christy, 1982) may have been caused by relatively low winter temperatures just prior to the reproductive season. With a sharp increase in temperature cueing ovarian growth and maturation, crabs differentially weakened by winter may not all assimilate nutrients rapidly enough to lay eggs in time to hatch during full or new moons early in the season. Increased ovarian growth rates, together with other metabolic effects of increased temperatures, may be factors that later bring egg production into phase with the lunar cycle. Relatively mild winter temperatures in Louisiana, together with available food early in the year, may facilitate synchrony of reproductive activity even early in the reproductive season. During the latter part of the season, ovarian growth is constrained by the duration of each reproductive cycle, but in the spring ovaries have time to grow to their maximum size. It was at this time that the largest broods of the year were produced.

An overview of the reproductive season for a single crab, based on the evidence gathered in this study (Fig. 14), reveals how reproductive cycles might enable crabs to release larvae under the most favorable conditions for dispersal and survival. The slightly offset semilunar periodicity of egg laying, necessitated by a 17-day embryonic developmental period, would time larval release to take place on or near a full or new moon and thus to coincide with periods of highest tidal amplitude. A combined period of 25 days for oogenesis and vitellogenesis between broods would result in the hatch of a brood approximately one lunar month later. The 16-day larval period would enable a majority of early postlarvae, under optimal conditions, to colonize adult habitats within the marsh during flood tides on or near the dates of full and new moons. Ovarian maturation, decalcification of the genital opercula, and subsequent mating is probably under lunar-influenced hormonal control that corresponds to an offset semilunar rhythm. The minimum period seen between successive broods in the laboratory (21 days) may exemplify an accelerated ovarian maturation in an individual coming into phase synchrony with this rhythm.

Following ovarian maturation in these crabs, the short duration of opercular decalcification and mating receptivity might make it beneficial for females to mate as many times as possible, perhaps without much regard to mate choice. This might be especially advantageous if multiple broods must be fertilized from stored sperm. Delay of egg laying until the end of the population's early evening activity period would facilitate females encountering males if none had been encountered in burrows or on the surface during the day. Courtship for females appears to involve a mature male's construction of a burrow network in which females are found. While undocumented to date, it would appear advantageous for the male to inseminate as many females as possible and guard them within the burrow from other males. This would be especially true if, as has been found in some other brachyuran species (Diesel, 1991), the last male to copulate displaces and seals off predecessor sperm packets with a sperm gel ensuring fertilization by sperm from the final mating only.

Possible adaptations to a low salinity estuarine habitat in *S.* sp. (nr. *reticulatum*), when compared to *Sesarma cinereum* (a slightly higher salinity and more terrestrial sympatric crab), include an increased duration of embryonic development, increased size of the egg, decreased number of zoeal stages (development of the first zoeal stage within the egg), and decreased period of larval development (Costlow, 1960; Dollard, 1980; Seiple and Salmon, 1987). When compared to development in the majority of grapsid crabs reported in literature to date (most with five zoeal stages), both *S.* sp. (nr. *reticulatum*) and *S. reticulatum* (see Costlow and Bookhout, 1962) would be characterized as having advanced development (Rabalais and Gore, 1985). This adaptation may be advantageous under certain estuarine conditions where low salinity waters bathe the adult habitat and may, as in Louisiana, extend well offshore. Reduction in the number of larval instars from 5 to 2 in certain grapsid crabs has been postulated to serve as an adaptation for freshwater and terrestrial habitats by those species (Hartnoll, 1965), and larval instars may develop profound osmoregulatory ability (Foskett, 1977). Rabalais and Gore (1985), however, are quick to point out that many freshwater and terrestrial crabs, including some grapsids, do not have reduced numbers of larval stages, and they caution making any generalized conclusions about evolutionary trends and adaptive significance of abbreviated development.

Selection for larval release rhythms in *S.* sp. (nr. *reticulatum*) may have occurred because of different pressures than those resulting in rhythms in the more terrestrial *Sesarma* species or those that routinely experience large amplitude lunar tides. The findings of Saigusa and Hidaka (1978) for the Japanese land crabs *Sesarma intermedium* and *S. haematocheir* closely parallel many of the findings of the present study in that all three species were observed to release larvae shortly after dark on days surrounding new and full moons. Although *S. intermedium* and *S. haematocheir* are more terrestrial than *S.* sp. (nr. *reticulatum*), the areas in which these three species released larvae experienced tidal fluctuations in water level that were often greatly affected by other environmental conditions. In particular, the river in which *S. intermedium* and *S. haematocheir* released larvae was influenced by rainfall, and *S.* sp. (nr. *reticulatum*) habitats were influenced by wind. Saigusa (1981) found that *S. dehaani* H. Milne-Edwards, 1853, which lives in rice paddies and river bottoms near the sea, did not exhibit a clear semilunar rhythm of larval release, and the time of larval release was not correlated to times of high tides. The larvae of this species tolerated freshwater better than the larvae of *S. intermedium* and *S. haematocheir.* Saigusa (1982) found that time of larval release for a population of *S. haematocheir* subjected to high amplitude tides was entrained to local daily and tidal cycles; zoea were released during periods of nighttime high tides. But crabs from another population of the same species that experienced low amplitude tides were entrained to a daily rhythm only, and these crabs released larvae soon after dark. In both populations, a semilunar monthly rhythm was retained. Studies in the laboratory show that *S. haematocheir* will retain a natural semilunar rhythm in the absence of moon light, but this rhythm can be phase shifted with an artificial moon light regime (Saigusa, 1980), but not an artificial tidal regime (Saigusa, 1986). However, the time of day that larval release takes place can be entrained by artificial moon light (Saigusa, 1988).

During the present study of *S.* sp. (nr. *reticulatum*), a natural semilunar rhythm was maintained in the laboratory, and entrainment to an artificial tidal cycle was not observed. Entrainment to tidal cycles by moonlight was not addressed in the present study. The moderate and variable tides occurring in the habitat from which *S.* sp. (nr. *reticulatum*) was collected, the intertidal nature of the crab, and the observance of larval release during daytime tidal inundation, would support the hypothesis that *S.* sp. (nr. *reticulatum*) releases larvae whenever conditions insure it would be safest to be exposed, either in the early evening, like in the population of *S. haematocheir* from a low tidal amplitude area, or during tidal inundation. Both tidal inundation and darkness may provide protection for the crab and enable it to be active on the marsh, perhaps with reduced risk of predation during larval release. High tide periods also favor larval dispersal and survival as they are followed by ebbing tides, which carry larvae away. Additionally, high water tends to disperse small planktivorous fish, which may enter the flooded marshes and become less concentrated along shorelines or in tidal creeks during high water.

The control of the exact time of larval release appears to be modulated by behavior of the ovigerous female crab in *S.* sp. (nr. *reticulatum*). While this event may, in turn, be brought about by stimuli from larvae, the nature of such stimuli is unknown. Recent studies of *Sesarma cinereum* and *Uca pugilator* suggest that stereotypic larval release behaviors in these species are not directly mediated by chemical releases from hatching larvae, such as occurs in some less terrestrially adapted xanthid crabs (see De Vries and Forward, 1989, 1991; De Vries *et al.*, 1991). The period of "hyperactivity" observed to precede *S.* sp. (nr. *reticulatum*) larval release may be linked to this control mechanism, and is likely coupled to behavior in which crabs preparing to release larvae migrate to the marsh edge from burrows that range well into upper intertidal reaches of marshes, stream banks, and other wetland settings.

Acknowledgments

We thank R. T. Bauer, B. E. Felgenhauer, and R. R. Twilley for valuable advice during this study, as well as John Hook, Matt Draud, and Kevin Ray for technical assistance. Work was supported by small grants from the LUMCON Foundation Inc. and the Coypu Foundation, as well as supplemental funding from Louisiana NSF/EPSCOR Program grant R11-8820219, Cooperative Agreement No. 14-35-0001-30470 from the U.S. Minerals Management Service, U.S. Department of Commerce grant No. NA-88-AA-0-C2119 and Louisiana Education Quality Support Fund grants 86-LUM(1)-083-13 and (1987-88)-ENH-BS-10. This is contribution No. 25 of the USL Center for Crustacean Research.

Literature Cited

Allen, E. A., and H. A. Curran. 1974. Biogenic sedimentary structures produced by crabs in lagoon margin and salt marsh environments near Beaufort, North Carolina. *J. Sed. Petrol.* **44:** 538–548.

Barnes, H. 1957. Processes of restoration and synchronization in marine ecology. The spring diatom increase and the "spawning" of the common barnacle, *Balanus balanoides* (L.). *Annee Biol.* **33:** 67–85.

Bauer, R. T. 1989. Decapod crustacean grooming: functional morphology, adaptive value, and phylogenetic significance. Pp. 49–73 in *Crustacean Issues Vol. 6,* B. E. Felgenhauer, L. Watling, and A. B. Thistle, eds. A. A. Balkema, Rotterdam.

Boolootian, R. A., A. C. Giese, A. Farmanfarmaian, and A. J. Tucker. 1959. Reproductive cycles of five west coast crabs. *Physiol. Zool.* **32:** 213–220.

Brown, S. K., and R. E. Loveland. 1985. A calibration method to generate seasonal hatching profiles for the fiddler crabs *Uca pugnax* (Smith, 1870) and *Uca minax* (LeConte, 1885) (Decapoda: Brachyura). *J. Exp. Mar. Biol. Ecol.* **90:** 27–47.

Christy, J. H. 1978. Adaptive significance of reproductive cycles in the fiddler crab *Uca pugilator:* a hypothesis. *Science* **199:** 453–455.

Christy, J. H. 1982. Adaptive significance of semilunar cycles of larval release in fiddler crabs (Genus *Uca*): test of an hypothesis. *Biol. Bull.* **163:** 251–263.

Christy, J. H. 1986. Timing of larval release by intertidal crabs on an exposed shore. *Bull. Mar. Sci.* **39:** 176–191.

Christy, J. H., and S. E. Stancyk. 1982. Timing of larval production and flux of invertebrate larvae in a well mixed estuary. Pp. 489–503 in *Estuarine Comparisons,* V. S. Kennedy, ed. Academic Press, New York.

Costlow, J. D., Jr. 1960. The complete larval development of *Sesarma cinereum* (Bosc) reared in the laboratory. *Biol. Bull.* **118:** 203–214.

Costlow, J. D., Jr., and C. G. Bookhout. 1962. The larval development of *Sesarma reticulatum* Say reared in the laboratory. *Crustaceana* **4:** 281–294.

Crichton, O. W. 1960. Marsh crab, intertidal tunnel-maker and grass eater. *Est. Bull. Univ. Del.* **5:** 3–10.

Crichton, O. W. 1974. Caloric studies of *Spartina* and the marsh crab *Sesarma reticulatum* (Say). Pp. 142–144 in *Tidal Marshes of Delaware,* F. C. Daiber, ed. Pp. 99–149 in *Coastal ecological systems of the United States,* Vol. II, H. T. Odum, B. J. Copeland, and E. A. McMahan, eds. The Coastal Conservation Foundation, Washington, DC.

DeCoursey, P. J. 1983. Biological timing. Pp. 107–213 in *The Biology of Crustacea, Vol. 7,* J. F. Vernberg and W. B. Vernberg, eds. Academic Press, New York.

De Vries, M. C., and R. B. Forward Jr. 1989. Rhythms in larval release of the sublittoral crab *Neopanope sayi* and the superlittoral crab *Sesarma cinereum* (Decapoda: Brachyura). *Mar. Biol.* **100:** 241–248.

De Vries, M. C., and R. B. Forward Jr. 1991. Control of egg-hatching time in crabs from different tidal heights. *J. Crust. Biol.* **11:** 29–39.

De Vries, M. C., D. Rittschoff, and R. B. Forward Jr. 1991. Chemical mediation of larval release behaviors in the crab *Neopanope sayi. Biol. Bull.* **180:** 1–11.

Diesel, R. 1991. Sperm competition and the evolution of mating behavior in brachyura, with special reference to spider crabs (Decapoda, Majidae). Pp. 145–164 in *Crustacean Sexual Biology,* R. T. Bauer and J. W. Martin, eds. Columbia University Press, New York.

Dollard, H. A. 1980. Larval release patterns in the wharf crab, *Sesarma cinereum,* from North Inlet, South Carolina. Master of Science Thesis, University of South Carolina, Columbia. 34 pp.

Fingerman, M. 1957. Lunar rhythmicity in marine organisms. *Am. Nat.* **91:** 167–178.

Forward, R. B., Jr. 1987. Larval release rhythms of decapod crustaceans: an overview. *Bull. Mar. Sci.* **4:** 165–176.

Foskett, J. K. 1977. Osmoregulation in the larvae and adults of the grapsid crab *Sesarma reticulatum* Say. *Biol. Bull.* **153:** 505–526.

Geise, A. C. 1959. Comparative physiology: annual reproductive cycles of marine invertebrates. *Ann. Rev. Physiol.* **21:** 547–576.

Hartnoll, R. G. 1965. Notes on the marine grapsid crabs of Jamaica. *Proc. R. Soc.* **176:** 113–147.

Hartnoll, R. G. 1968. Morphology of the genital ducts in female crabs. *J. Linn. Soc. (Zool.)* **47:** 279–300.

Jones, M. B., and M. J. Simons. 1983. Latitudinal variation in reproductive characteristics of a mud crab, *Helice crassa* (Grapsidae). *Bull. Mar. Sci.* **33:** 656–670.

Madden, C. J., J. W. Day Jr., and J. M. Randall. 1988. Freshwater and marine coupling in estuaries of the Mississippi River deltaic plain. *Limnol. Oceanogr.* **33:** 982–1004.

Mulstay, R. 1975. Aspects of the life history and social behavior of the purple marsh crab *Sesarma reticulatum.* Ph.D. Dissertation, State University of New York, Stony Brook, 233 pp.

Palmer, J. D. 1967. Daily and tidal components in the persistent rhythmic activity of the crab, *Sesarma. Nature* **215:** 64–66.

Pillay, K. K., and Y. Ono. 1978. The breeding cycles of two species of grapsid crabs (Crustacea: Decapoda) from the north coast of Kyushu, Japan. *Mar. Biol.* **45:** 237–248.

Rabalais, N. N., and R. H. Gore. 1985. Abbreviated development in decapods. Pp. 67–126 in *Crustacean Issues Vol. 2,* A. M. Wenner, ed. A. A. Balkema, Rotterdam.

Saigusa, M. 1980. Entrainment of a semi-lunar rhythm by a simulated moon-light cycle in the terrestrial crab *Sesarma haematocheir. Oecologia* **46:** 38–44.

Saigusa, M. 1981. Adaptive significance of a semilunar rhythm in the terrestrial crab *Sesarma*. *Biol. Bull.* **160:** 311–321.

Saigusa, M. 1982. Larval release rhythm coinciding with solar day and tidal cycles in the terrestrial crab *Sesarma*—harmony with the semilunar timing and its adaptive significance. *Biol. Bull.* **162:** 371–386.

Saigusa, M. 1986. Tidal timing of larval release activity in the incubating crab *Sesarma*. *J. Comp. Physiol.* **159:** 21–31.

Saigusa, M. 1988. Entrainment of tidal and semilunar rhythms by artificial moonlight cycles. *Biol. Bull.* **174:** 126–138.

Saigusa, M., and T. Hidaka. 1978. Semi-lunar rhythm in zoeae-release activity of the land crab *Sesarma*. *Oecologia* **46:** 38–44.

Sandifer, P. A. 1975. The role of pelagic larvae in recruitment to populations of adult decapod crustaceans in the York River estuary and adjacent lower Chesapeake Bay, Virginia. *Est. Coastal Mar. Sci.* **3:** 269–279.

Seiple, W. 1979a. Distribution, habitat preferences and breeding periods in the crustaceans *Sesarma cinereum* and *S. reticulatum* (Brachyura: Decapoda: Grapsidae). *Mar. Biol.* **52:** 77–86.

Seiple, W. 1979b. The ecology and evolution of social behavior in the crabs *Sesarma reticulatum* and *S. cinereum*. Ph.D. Dissertation, University of Illinois at Urbana-Champaign, 170 pp.

Seiple, W. 1981. The ecological significance of the locomotor activity rhythms of *Sesarma cinereum* (Bosc) and *Sesarma reticulatum* (Say) (Decapoda, Grapsidae). *Crustaceana* **40:** 5–15.

Seiple, W., and M. Salmon. 1982. Comparative social behavior of two grapsid crabs, *Sesarma reticulatum* (Say) and *S. cinereum* (Bosc). *J. Exp. Mar. Biol. Ecol.* **62:** 1–24.

Seiple, W., and M. Salmon. 1987. Reproductive, growth and life-history contrasts between two species of grapsid crabs, *Sesarma cinereum* and *S. reticulatum*. *Mar. Biol.* **94:** 1–6.

Sklar, F. H., and R. E. Turner. 1981. Characteristics of phytoplankton production off Barataria Bay in an area influenced by the Mississippi River. *Contrib. Mar. Sci.* **24:** 93–106.

Subrahmanyam, C. B., W. L. Kruczynski, and S. H. Drake. 1976. Studies on the animal communities in two north Florida salt marshes: part two. Macroinvertebrate communities. *Bull. Mar. Sci.* **26:** 172–195.

Teal, J. M. 1958. Distribution of fiddler crabs in Georgia salt marshes. *Ecology* **39:** 185–193.

Teal, J. M. 1959. Respiration of crabs in Georgia salt marshes and its relation to their ecology. *Physiol. Zool.* **32:** 1–14.

Thorson, G. 1950. Reproductive and larval ecology of marine bottom invertebrates. *Biol. Rev. Cambr. Philos. Soc.* **25:** 1–45.

Vernberg, F. J. 1962. Comparative physiology: latitudinal effects on physiological properties of animal populations. *Ann. Rev. Physiol.* **24:** 517–546.

Wheeler, D. E. 1978. Semilunar hatching periodicity in the mud fiddler crab *Uca pugnax* (Smith). *Estuaries* **1:** 268–269.

Williams, A. B. 1984. *Shrimps, Lobsters and Crabs of the Atlantic Coast of the Eastern United States, Maine to Florida.* Smithsonian Institution Press, Washington DC.

Reference: *Biol. Bull.* **181**: 402–407. (December, 1991)

The Role of Olfaction in Courtship Behavior of the American Lobster *Homarus americanus*

DIANE F. COWAN

Boston University Marine Program, Marine Biological Laboratory,
Woods Hole, Massachusetts 02543

Abstract. Courtship behavior is well documented in captive lobsters. Sex pheromones contained in *female* urine and perceived by receptors on *male* antennules are thought to act as sex attractants or as signals necessary for pair formation. In this study, the lateral and medial antennules of male and female lobsters were removed. The result of these excisions were meant to indicate the gender-specific role of olfactory chemoreception in lobster courtship behavior. Removal of *male* antennules had little effect on pair bonding and mating. In contrast, removal of *female* antennules resulted in dramatic aberrations in behavior, including postmolt injuries and, in extreme cases, unsuccessful couplings and mortality. Therefore, *female* olfaction plays the more critical role in the normal reproductive behavior of *Homarus americanus.*

Introduction

Previous research on crustacean sex pheromones has focused on chemical signals found in female urine and detected by chemoreceptors on male antennules (see Dunham, 1978, 1988; Salmon, 1983, for reviews). For example, in courtship of the blue crab, *Callinectes sapidus,* females produce sex pheromones that are detected by receptors found on male antennules (Gleeson, 1980, 1982, 1984). In addition, many moth (and other insect) pheromones that act as sex attractants are produced by females and perceived by receptors on male antennae (Schneider, 1969; Conner *et al.*, 1980). Male pheromones play a role later in moth courtship, after the male has found the female, but before copulation (Eisner, 1980; Conner *et al.*, 1981). Because lobsters (*Homarus americanus*) are phylogenetically related to these organisms, they are assumed to have similar communication capabilities (Atema and Engstrom, 1971). To understand the role of animal signals, the behavioral context in which a signal is used should form the basis of experimental design. Before molting, mature female lobsters choose a dominant male and cohabit in his shelter for several days before and after female molting. Mating occurs shortly after the female completes ecdysis.

In this study, the behavior of normal lobsters was compared to the behavior of antennule-excised lobsters. Both females and males underwent antennule excisions; control groups for both were also studied. In the *female excision experiment,* the antennules of female lobsters were removed while those of males were left intact; the results should elucidate the role of female olfaction in lobster courtship and mating behavior. If males must recognize the scent of sexually mature premolt females before "allowing" the females to enter their shelters, then pair bonding should occur between normal males and antennule-excised females, provided that females continued to produce the proper signals. If, however, females must recognize the scent of a suitable mate (dominant male) before entering the shelter, then females without antennules should either fail to pair bond or pair indiscriminately with dominant or subordinate males. If no differences in behavior occurred, we could conclude either that female olfaction is not essential for normal courtship behavior or that other chemoreceptors compensate for the loss of olfaction.

In the *male excision experiment,* the antennules of male lobsters were removed while those of females were left intact, to answer the following questions. What role, if any, does male olfaction play in pair formation and courtship behavior? Will antennule-excised males "allow" premolt females to share their shelters? Finally, a comparison of the two types of experiments should indicate

Received 9 April 1991; accepted 25 September 1991.

whether antennule-excision operations cause similar aberrant behaviors regardless of sex.

Because it is the female lobster that selects a mate and moves into his shelter, my working hypothesis was that removing male antennules would have little or no effect on pair formation. If antennule-excised males behaved normally, "permitting" unexcised premolt females to enter and cohabit in their shelters, this result would not only serve as a control for the female excision experiments, but would challenge existing hypotheses concerning the role of female sex pheromones and the importance of pheromone detection by male antennules.

Materials and Methods

Male and female lobsters were captured in the wild and all were handled identically. They were removed from holding tanks, measured, sexed, given individual identification marks, and assigned to groups. Each group of lobsters was composed of five sexually mature females and two sexually mature males ($\bar{X} = 80.4 \pm 2.44$ SD mm in carapace length) held communally in one of three 5600-l aquaria. No individual was used more than once.

The *female excision experiment* consisted of three groups of lobsters each comprising five antennule-excised females and two unexcised males. In one of the antennule-excised female groups no females molted, but molting is a prerequisite for pairing and mating. Therefore, only 2 of the excised female groups, totalling 10 females and 4 males, were included in the data. The *male excision experiment* consisted of two groups of five normal females and two antennule-excised males. The *unexcised controls* consisted of three groups, totalling 15 females and 6 males.

The excision operation was straightforward: the antennules were snipped off at the base with a pair of sharp scissors. Other experimental conditions were similar to those described in an earlier study involving normal lobsters (Cowan and Atema, 1990). Aquaria were provided with ambient flow-through seawater and a seasonally adjusted light/dark cycle. Live prey items were available at all times, and diet was supplemented *ad libitum* with an excess of freshly killed or frozen squid, fish, and clams.

The control experiments were carried out during June–September 1983 and May–November 1987, and some of these data have been published elsewhere (Cowan and Atema, 1990). Data from antennule-excised lobsters were collected during July–November 1990 and May–July 1991.

During censuses (at approximately 0600, 1200, 1800, and 2400, daily) the following information for each lobster was recorded: time, date, time of feeding, position and activity, indications of molt stage or (in females) egg carrying, location and condition of pieces of molt shells. Activities recorded included social interactions, feeding, grooming, walking, resting, position of body and appendages, pushing gravel, digging, moving rocks, and building or repairing shelters.

Focal observations concentrated on each animal for 10 min twice a day, between 0700 and 0900, and between 1800 and 2100, whenever possible. At times, poor visibility made these observations impossible. Information was therefore quantified based on census rather than focal observations. Times of day for focal observations were chosen because female molting and mating usually occur in the morning (Cowan, pers. obs.), and the active period typically begins in the evening. In the aquaria, however, activity patterns are dependent on both the condition of the animal (*i.e.,* molt stage, egg bearing) and the time of day (Cowan, in prep.).

Long-term observations, focusing on pre-, post-, and molting females, were recorded in a notebook and on videotape. A light-sensitive video camera with a silicone intensifier tube was used to make video recordings at night. A color hand-held video camera was used during the day.

Duration of cohabitation for all molting females was determined during census observations. All cohabitation information is given as mean days ± SD. Cohabitations were divided into periods of intermittent and permanent, pre- and postmolt shelter sharing, where "intermittent" indicates that the female was inside of the male shelter during at least one, but not all, of the census observations, and "permanent" indicates that the female was never seen outside of the male shelter on a given day. The day of molting was considered as part of postmolt cohabitation, because females usually molt in the morning.

When the observations had been completed, the seminal receptacles of the postmolt antennule-excised females were dissected and examined for the presence of spermatophores. The lengths of any regenerating antennules were also measured at the end of each experiment.

Because females usually mate with dominant males, male dominance was measured by tallying all observed male-male agonistic encounters. The animal that avoided contact, retreated, fled, backed away, or tail flipped was considered the subordinate of the pair in each group.

Results

Control lobsters

Thirteen of the 15 females chose mates and cohabited with males. The average duration of cohabitation was 12.9 ± 5.0 days (Fig. 1). After a brief period of precopulatory shelter sharing ($\bar{X} = 6.3 \pm 3.2$ days), each female molted inside of a dominant male's shelter. Males did not touch females during ecdysis. When each female gained enough skeletal support to stand up (usually 30 min after molting), she approached and turned so that her abdomen faced the male. The male then mounted and the pair copulated.

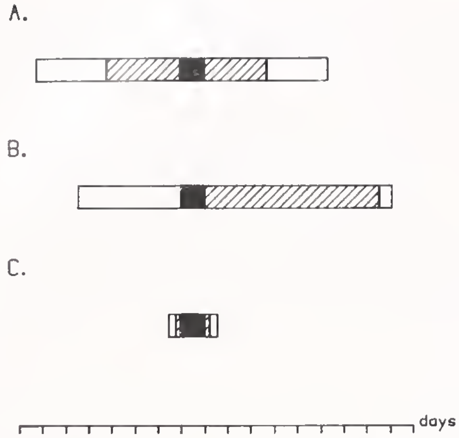

Figure 1. Mean duration of intermittent (open bars) and permanent (hatched bars) cohabitations between female and male lobsters *Homarus americanus*, relative to the day of female molting (filled bars). A, control (n = 15); B, normal females housed with antennule-excised males (n = 10); C, antennule-excised females housed with normal males (n = 10). In A, data are based on 13/15 females who molted and cohabited with males. In B, data are based on 3/10 females who molted and cohabited with males. In C, data are based on 6/10 females who molted, only two of which cohabited with males.

Each pair mated only once. After copulation, the females remained in the male shelter for 5.5 ± 3.2 days before leaving.

All thirteen females chose the dominant male as a mate; the remaining two females did not molt, cohabit, or mate.

Female antennule excisions

Antennule-excised females rarely pair bonded or cohabited. Six of ten antennule-excised females molted. Two of these six females cohabited briefly. The mean cohabitation duration for antennule-excised females was 1.0 ± 1.7 days (Fig. 1). Significantly fewer of the molting antennule-excised females cohabited as compared to controls (Fisher's exact test, $P = 0.02759$).

Post-treatment dissections revealed that five of the six molting females had mated (spermatophores present). Mating was observed in two cases. Both females were inseminated by the dominant male of their group.

The six females that molted showed a number of behavioral deviations never seen in controls. Four of these females molted outside their shelters and did not cohabit with males. One molted at night and without the protection of a male. She was killed after mating (spermatophore found in her spermathecum). A second did not mate. Two other females mated, but did not cohabit with males.

Of the two females that cohabited with males, one did so for two days after molting, and the other for two days before and two days after molting.

The deviations from normal behavior made copulation (which occurred at irregular times and places) difficult to observe. But the two matings that were observed (one in each group) were between the females and the dominant male.

Finally, five of six molting females suffered injuries as a consequence of molting; including one death. In contrast, only one injury was observed among the 13 control females that molted.

Male antennule excisions

Three females (of 10) molted. Antennule-excised males "permitted" all three premolt females to enter their shelters and to cohabit before, during, and after molting (Fig. 1). The duration of cohabitation was comparable to that of the unmanipulated lobsters ($\bar{X} = 13.3 \pm 3.2$ days *versus* $\bar{X} = 12.9 \pm 5.0$ days). Female behavior was similar to that seen in control females; *i.e.*, females pair-bonded, cohabited, and mated with antennule-excised males, in male shelters.

Subtle changes in male behavior were recorded. For example, antennule-excised males stood over females and touched them with pereopods and maxillipeds (chemoreceptor organs involved in taste), while the females were undergoing ecdysis. In no other instance did males touch females during ecdysis. In addition, two of the females were injured by their mate during premolt cohabitation. No other premolt injuries occurred in any males or females.

No agonistic encounters were seen between antennule-excised males. Therefore, the dominance status of the males could not be determined.

Discussion

A single sensory system—olfaction—plays an important role in pair formation in lobsters. In these experiments, antennule-excised females risked injury to themselves and, in two cases (one female did not mate, another was killed), missed an opportunity to reproduce. In contrast, normal premolt females paired, cohabited, molted, and mated with antennule-excised males. Antennule-excised males showed an insignificant deviation from the normal sequence of mating behavior. These findings contradict previous claims that olfactory detection of female sex pheromones by males is an essential part of lobster courtship behavior.

The possible existence of a female lobster sex pheromone was first suggested by Hughes and Matthiessen (1962) who wrote, "It appears as if the freshly molted female exerts a chemical attraction on the male." Their statement led to research designed to develop a behavioral bioassay that could be used to isolate and identify a female lobster sex phermone. In the early 1970's, two laboratories tested the responses of male lobsters to female odors. McLeese (1970) reported that male lobsters preferred the odor of freshly molted females to odors of other conspecifics. Atema and Engstrom (1971) concluded that ". . . a chemical compound (sex pheromone) is present in the water of a newly moulted female lobster that suppresses agonistic behavior and induces courtship."

Because mating follows female molting, attempts to identify a pheromone concentrated on physiological correlates of molting (McLeese *et al.*, 1977; Atema and Gagosian, 1973). However, efforts to isolate sex pheromones from female lobsters failed. To gain a better understanding of lobster courtship behavior, observations were made in large aquaria, where females initiated pair formation several days before molting and cohabited with a male before and after mating (Atema *et al.*, 1979; Cowan and Atema, 1990). Adult lobsters did not cohabit under any other circumstances. Contrary to the existing hypotheses requiring *males* to recognize *female* odors before mating, the excision experiments reported herein show that *female* olfactory perception is critical for the successful completion of courtship and mating behavior.

Cohabitations

Female lobsters apparently benefit from choosing a mate able to protect them from predation and cannibalism during the vulnerable molting period. In this study, only 1 of 13 control females suffered a postmolt injury, while all of the antennule-excised female lobsters suffered postmolt injuries. In a separate experiment, females held together in the same aquarium without males all incurred serious postmolt injuries (Cowan, in prep.). Therefore, females benefit from male protection during postmolt cohabitation. Wilber (1989) showed that postcopulatory guarding by male crabs of the genus *Menippe* serves to protect the female from predators and to prevent extrapair copulations. Shelter sharing in lobsters is analogous to mate guarding in many species of crabs that mate shortly after the female has molted (see Hartnoll, 1969).

The benefits of cohabitation appears to be greater for females than for males. Although males may benefit from cohabitations due to paternity assurance, males need not cohabit with females before inseminating them. Isolated females prevented from mating immediately after molting mated later when presented with males in communal tanks (Waddy and Aiken, 1990, 1991). The males discriminated between inseminated and uninseminated intermolt females and mated preferentially with uninseminated females (Waddy and Aiken, 1990, 1991). Female lobsters extruded fertilized eggs provided that insemination occurred at some time before egg extrusion, which often follows molting by many months (Waddy and Aiken, 1991; Cowan, in prep.).

Female antennule excisions

When deprived of their antennules, 4 of 6 females failed to cohabit. This failure to cohabit could be explained if males produce odors that females must detect before entering male shelters for cohabitation. Or the communication system may be more complex. For example, females may need to smell males before producing female odors that the male detects before allowing females to enter their shelters and cohabit. Because most females were inseminated, males were apparently able to recognize sexually receptive, postmolt females. If male recognition of sexually receptive females is based on female odor production, these findings do not support the hypothesis that antennule-excised females failed to produce pheromones. Rather, the aberrations in the behavior of antennule-excised females were apparently due to the failure of females to detect male odors.

Unoperated-control females moved into the shelter of a dominant male and cohabited for several days before and after molting (see also, Cowan and Atema, 1990). Reliable information about male suitability as a mate may be contained in male odors detected by receptors on female antennules. If females cohabit with males because they detect male odors, then a failure to perceive male odors may lead to female rejection of males. Because females investigate male shelters from the outside, waterborne odors emanating from within may be difficult for females to detect without their antennules. The use of contact chemoreceptors for this function seems unlikely, because females do not have the opportunity to touch males with other chemosensory appendages during courtship. This would explain why most antennule-excised females failed to cohabit, especially if specific receptors that detect male odors are located only on female antennules.

Regeneration of female antennules may explain some of the variability in behavior shown by different females in this group. At 90-mm carapace length, lobsters normally have antennule flagella that are 40–50 mm in length. After excision, females began to regenerate their antennules; the longest regenerated antennule was 10 mm. Few aesthetascs were present on the regenerates.

In general, antennule-excised females with the longest regenerated antennules presented the most normal behavior. The female that molted 10 days postexcision did not regenerate her antennules and showed the most aberrant behavior. She molted outside of her shelter at night without the protection of a male and was killed shortly thereafter. Another female molted 34 days postexcision, regenerated 8.5 mm of her antennules, mated successfully, and was unharmed. The female who molted 46 days postexcision, regenerated 10 mm of her antennules and cohabited for 4 days: 2 days pre- and 2 days postmolt.

In contrast to this general trend, one female molted five days postexcision and cohabited intermittently for two days in spite of not regenerating her antennules. Her ability to cohabit cannot be explained by antennule regeneration. Perhaps this female had begun courtship before her antennules were removed and was able to continue the sequence, although there was no premolt cohabitation. The effect of regeneration over a short time course is unclear.

Male antennule excisions

Unexcised females pair bonded, cohabited, molted, and mated with antennule-excised males. This indicates that male olfaction is not necessary for the normal sequence of lobster courtship behavior. How, then, is male signal detection or pheromone production involved in courtship?

Two pieces of evidence suggest that male signal detection was impaired by antennule excision. (1) There were no observed agonistic encounters between antennule-excised males. (2) An antennule-excised male wounded two mates during premolt cohabitation inside his shelter. The absence of male-male agonistic encounters suggests that male olfaction is involved in male dominance. The injuries inflicted on unexcised premolt females by antennule-excised males suggests that female odor may suppress male aggression toward females.

Atema and Engstrom (1971) hypothesized that females produce a pheromone that suppresses agonistic behavior and, therefore, protects soft-shelled females. Although two of the females were wounded during premolt, protection by the antennule-excised males during ecdysis suggests that other male chemosensory organs may have compensated for the loss of male antennules. Antennule-excised males touched the soft tissues of molting females with their pereopods and maxillipeds. These males may have been using gustatory chemoreceptors to compensate for the absence of olfaction. The same detection may not have been possible when antennule-excised males touched hard shelled females during premolt. This may explain why unexcised females who cohabited with antennule-excised males suffered pre- but not postmolt injuries.

Pheromone communication

Primer pheromones may function in the lobster mating systems by regulating the timing of female molting and subsequent mating (Cowan and Atema, 1990). In these experiments, fewer females molted when male antennules were excised and antennule-excised females molted with dominant males in sequence. However, the data reported here neither support nor contradict the primer pheromone hypothesis.

Odor communication appears to be very complex in this species. Successful courtship and mating probably involves the exchange of signals produced by both males and females. Perhaps the effects of antennule excisions were more dramatic in females than in males only because of the timing and method by which odors are transmitted. Chemical signal detection by females is important during pair formation, whereas odor detection by males may be important later, at the time of female molting and shortly afterward when the pair mate.

Because females cohabit with dominant males, they are apparently able to discriminate male dominance. Perhaps females detect a male dominance odor which may also be important in intermale agonistic encounters. Some evidence for male sex pheromones already exists in Crustacea. Teytaud (1971) described particular behavioral changes in premolt pubertal female blue crabs (*Callinectes sapidus*) in response to male odors coupled with a visual model. His results showed that females detect and respond to male blue crab odors. More recently, Gleeson (1991) conducted choice tests in which pubertal female blue crabs showed a preferential attraction to male blue crab odors. Given a choice between male and female odor, or male odor and blanks, females chose male odor. However, females did not show a preference when given a choice between different males.

It has long been accepted that female odors and male olfaction play important roles in the reproductive behavior of Crustacea. The results presented here indicate that female olfaction also plays a crucial role in lobster courtship and mating behavior. Together with previous observations of lobster courtship behavior (Atema *et al.*, 1979; Cowan and Atema, 1990) and studies showing that females detect male odors (Atema and Cowan, 1986), these data show that female perception of male odors are of extreme importance in lobster reproductive behavior.

Acknowledgments

Financial support was provided by Sigma Delta Epsilon Graduate Women in Science, the Lerner-Gray Fund for Marine Research, and two BUMP Alumni Awards. G. Cadwalader and L. Larson generously donated lobsters. I thank Drs. R. A. Gleeson and M. Salmon for comments that greatly improved this manuscript. I am grateful for the use of facilities and the help of B. Lancaster, D. Leavitt, and G. Hampson at the Woods Hole Oceanographic Institution.

Literature Cited

Atema, J., and D. F. Cowan. 1986. Sex-identifying urine and molt signals in lobster (*Homarus americanus*). *J. Chem. Ecol.* **12:** 2065–2080.

Atema, J., and D. G. Engstrom. 1971. Sex pheromone in the lobster, *Homarus americanus*. *Nature* **232:** 261–263.

Atema, J., and R. B. Gagosian. 1973. Behavioural responses of lobsters to ecdysones. *Mar. Behav. Physiol.* **2:** 15–20.

Atema, J., S. Jacobson, E. Karnofsky, S. Oleszko-Szuts, and L. Stein. 1979. Pair formation in the lobster, *Homarus americanus*: behavioral development, pheromones and mating. *Mar. Behav. Physiol.* **6:** 277–296.

Conner, W. E., T. Eisner, R. K. Vander Meer, A. Guerrero, D. Ghiringelli, and J. Meinwald. 1980. Sex attractant of an Arctiid moth (*Utetheisa ornatrix*): a pulsed chemical signal. *Behav. Ecol. Sociobiol* **7:** 55–63.

Conner, W. E., T. Eisner, R. K. Vander Meer, A. Guerrero, and J. Meinwald. 1981. Precopulatory sexual interaction in an arctiid moth (*Utetheisa ornatrix*): role of a pheromone derived from dietary alkaloids. *Behav. Ecol. Sociobiol.* **9:** 227–235.

Cowan, D. F., and J. Atema. 1990. Moult staggering and serial monogamy in American lobsters, *Homarus americanus. Anim. Behav.* **39:** 1199–1206.

Dunham, P. J. 1978. Sex pheromones in Crustacea. *Biol. Rev.* **53:** 555–583.

Dunham, P. J. 1988. Pheromones and behavior in Crustacea. Pp. 375–392 in *Endocrinology of Selected Invertebrate Types,* H. Laufer and G. H. Downer, eds. Alan R. Liss, Inc., New York.

Eisner, T. 1980. Chemistry, defense, and survival: case studies and selected topics. Pp. 847–878 in *Insect Biology in the Future,* M. Locke and D. S. Smith, eds. Academic Press, New York.

Gleeson, R. A. 1980. Pheromone communication in the reproductive behavior of the blue crab, *Callinectes sapidus. Mar. Behav. Physiol.* **7:** 119–134.

Gleeson, R. A. 1982. Morphological and behavioral identification of the sensory structures mediating pheromone reception in the blue crab, *Callinectes sapidus. Biol. Bull.* **163:** 162–171.

Gleeson, R. A. 1984. Characterization of a sex pheromone in the blue crab *Callinectes sapidus. J Chem. Ecol.* **10:** 913–921.

Gleeson, R. A. 1991. Intrinsic factors mediating pheromone communication in the blue crab, *Callinectes sapidus.* Pp. 17–32 in *Crustacean Sexual Biology,* R. T. Bauer and J. W. Martin, eds. Columbia University Press, New York.

Hartnoll, R. G. 1969. Mating in the Brachyura. *Crustaceana* **16:** 161–181.

Hughes, J. T., and G. C. Matthiessen. 1962. Observations on the biology of the American lobster, *Homarus americanus. Limnol. Oceanogr.* **7:** 414–421.

McLeese, D. W. 1970. Detection of dissolved substances by the American lobster (*Homarus americanus*) and olfactory attraction between lobsters. *J. Fish. Res. Board Can.* **27:** 1371–1378.

McLeese, D. W., R. L. Spraggins, A. K. Bose, and B. N. Pramanik. 1977. Chemical and behavioral studies of the sex attractant of the lobster (*Homarus americanus*). *Mar. Behav. Physiol.* **4:** 219–232.

Salmon, M. 1983. Courtship, mating systems, and sexual selection in Decapods. Pp. 143–169 in *Studies in Adaptation: The Behavior of Higher Crustaceans,* S. Rebach and D. Dunham, eds. John Wiley & Sons, New York.

Schneider, D. 1969. Insect olfaction: deciphering system for chemical messages. *Science* **163:** 1031–1036.

Teytaud, A. R. 1971. The laboratory studies of sex recognition in the blue crab *Callinectes sapidus* Rathbun. *Univ. Miami Sea Grant Prog. Sea Grant Tech. Bull.* **15:** i–vii, 1–63.

Waddy, S. L., and D. E. Aiken. 1990. Intermolt insemination, an alternative mating strategy for the American lobster, *Homarus americanus. Can. J. Fish. Aquat. Sci.* **47:** 2402–2406.

Waddy, S. L., and D. E. Aiken. 1991. Mating and insemination in the American lobster, *Homarus americanus.* Pp. 126–144 in *Crustacean Sexual Biology,* R. T. Bauer and J. W. Martin, eds. Columbia University Press, New York.

Wilber, D. H. 1989. The influence of sexual selection and predation on the mating and postcopulatory guarding behavior of stone crabs (Xanthidae, *Menippe*). *Behav. Ecol. Sociobiol.* **24:** 445–451.

Reference: *Biol. Bull.* **181:** 408–418. (December, 1991)

Spatial Information in the Three-Dimensional Fine Structure of an Aquatic Odor Plume

PAUL A. MOORE* AND JELLE ATEMA

Boston University Marine Program, Marine Biological Laboratory,
Woods Hole, Massachusetts 02543

Abstract. Turbulent odor plumes play an important role in many chemically mediated behaviors, yet the fine scale spatial structure of plumes has not been measured in detail. With the use of a newly introduced microelectrochemical recording technique, we have measured, in some detail, the fine structure of an aquatic odor plume in the laboratory. We sampled a turbulent odor plume at 10 Hz with a spatial sampling area of 0.02 mm^2, approximately that of a chemoreceptor sensillum of the lobster, *Homarus americanus.* A 3-min record was sampled at 63 different sites in 3 dimensions (x, y, z). As expected from time averaging models, the mean values of pulse parameters such as height and onset slope were greatest near the source. However, what cannot be described by time averaging models is the instantaneous distribution of pulses: periodically high peaks with steep concentration slopes (well above the local average and far above predictions from averaging models) can be found far away from the source. However, the probability of above-average pulse heights decreases with distance from the source in x, y, and z directions. The most intense odor fluctuations occurred along the x axis (the cross-sectional center of the plume). Odor profiles were analyzed with three different models of sensory filters; logarithmic, probability, and temporal filters. This analysis indicates that features contained within the plume structure could be used as directional cues for orienting animals. It remains to be demonstrated that animals use such sensory filters to extract biologically relevant spatial information from odor plumes.

Introduction

Many orientation studies have tried to elucidate the role of chemical signals in initiating and controlling orientation of an organism to an odor source. Authors have not only debated the behavioral mechanisms involved in chemically mediated orientation [Bell and Cardé, 1984 (preface); Bell, 1984; Kennedy, 1986], but also whether the odor signal plays a role in directional information (Preiss and Kramer, 1986; Sanders, 1986). Terms such as chemotaxis, klinokinesis, and menotaxis (Fraenkel and Gunn, 1961) have been tied to behavioral outputs of orienting animals, with a variety of underlying assumptions of the odor patterns and distributions as inputs. Yet in all of these studies, biologically relevant quantification of the stimulus signal either in the behavioral testing arena or arriving at the chemoreceptor organ has not been undertaken.

For years, orientation studies assumed that odor dispersion could be effectively described by time-averaged or Gaussian distribution models (Sutton, 1953; Bossert and Wilson, 1963). This model works for those organisms that operate either at small spatial scales *i.e.*, bacteria (Berg and Purcell, 1977), or sample over long time intervals *i.e.*, tsetse flies (Bursell, 1984). For animals that operate at other time and space scales, this model is a poor predictor of animal behavior (Elkinton *et al.*, 1984). Murlis and Jones (1981) and Atema (1985) have shown that odor distributions are quite heterogeneous as compared to the time-averaged models.

Still, quantification of odor signals at behaviorally relevant time and space scales remains rare (Murlis, 1986; Moore and Atema, 1988a). Present aerial studies use techniques such as smoke trails and bubble machines to try and quantify odor dispersal (David *et al.*, 1982; Brady *et al.*, 1989). These techniques only give qualitative de-

Received 14 December 1990; accepted 5 August 1991.

* Present address and correspondence: Department of Pharmacology, Campus box C236, University of Colorado Health Science Center, 4200 East Ninth Ave., Denver, CO 80262

scriptions of wind patterns. They do not give quantitative data on odor signals within or around the smoke patches or soap bubbles. The few studies that have quantified odor dispersal patterns have sampled relatively few sites (Murlis, 1986; Murlis and Jones, 1981), and the ion detectors used in these studies have a larger sampling volume than that of a biologically relevant sampling device, *e.g.*, an insect antenna. Aquatic studies have used sensors with greater spatial resolution than those used in aerial studies, but thus far, like terrestrial studies, these studies have only sampled a few points down current from the odor source (Atema, 1985; Moore and Atema, 1988a; Zimmer-Faust *et al.*, 1988). In addition, these studies involve techniques that may not sample at spatial scales relevant to animal chemosensory detectors (See Moore *et al.*, 1989, for discussion). Finally, to the best of our knowledge, we know of no study that has quantified odor signals outside the cross-sectional center of the plume.

Fluid dynamic principles apply equally in air and water; the difference can be bridged with a simple scaling factor (Vogel, 1981). The diffusion of a chemical tracer will be different in the two mediums, which will cause slight differences in the fine scale structure of odor plumes in air *versus* water. However, the aquatic environment provides an easier medium in which to measure and model odor distributions for a variety of reasons. The space scales in an aquatic environment are much smaller, which allows for easier physical modelling of plumes. With the introduction of microelectrochemical measurement techniques to chemoreception sciences (Moore *et al.*, 1989), quantification of stimulus concentrations under biologically relevant time and space scales and direct measurement of boundary layers are possible. Additionally, diffusion calculations and measurements are easier in water because there is no partitioning of stimulus molecules at air-water interfaces and there are no mucus layers surrounding the sensory surfaces of aquatic chemoreceptors. The compounds for which electrochemical techniques have been perfected (dopamine, serotonin, *etc.*) have approximately the same molecular weight as many of the stimulatory compounds for aquatic animals (*e.g.*, amino acids, amines). Thus, they have similar diffusion properties. Since the only difference between the physical dynamics of turbulent dispersal in water and air are time and space scale differences, the results obtained in an aquatic medium are directly applicable to terrestrial environments. Turbulence will vary depending on the environmental conditions. Different conditions will lead to different parameter values.

Our study was designed to describe quantitatively an aquatic odor plume at both the spatial and temporal sampling scales of the lobster, *Homarus americanus*. This animal samples chemical signals with a variety of receptor organs. For orientation behavior it depends largely upon sensory input from the lateral antennules (Devine and Atema, 1982). These antennules contain dense rows of cylindrical aesthetasc hairs, which hold the dendrites of primary chemoreceptor cells. Each hair is .03 mm in diameter at the tip and 1 mm in length. The distal 0.8 mm of cuticle surrounding the hair is thought to be completely permeable to odor molecules (Ghiradella *et al.*, 1968). Thus, it is likely that the aesthetasc hair can sample odor over the entire distal surface area of the cylinder. To measure at the space scales relevant to this lobster receptor organ, one needs a device with similar spatial dimensions as the aesthetasc sensillum, so that fluid boundary layers, and thus odor diffusion, will be similar. To accomplish this, electrochemical electrodes with 100–150 μm diameters were chosen to model the spatial scales and fluid dynamics of a single aesthetasc hair.

Just as important as matching the spatial resolution of receptor cells and electrodes is the matching of their temporal resolution. We define the temporal sampling rate of a chemoreceptor cell as the inverse of the integration period of the receptor. This is a specific period of time over which stimulus-generated cellular processes, including receptor-ligand binding, second messenger, and generator potentials events, are summed into a discrete receptor cell response. In realistic terms, there is probably no simple integration time of a receptor cell. Instead, it is a dynamic balance between the cell excitation and adaptation processes. However, for receptor modelling and signal analysis needs, an integration time must be estimated. Unfortunately, temporal sampling rates of chemoreceptor cells and organs are poorly understood. Consequently, estimates of receptor integration times must be drawn from the small amount of neurophysiological work involving flicker fusion frequency and receptor adaptation. Christensen and Hildebrand (1988) found CNS neurons and Kaissling *et al.* (1987) found peripheral receptors in two different moth species that give distinct responses to 10 Hz odor pulses. Similar studies in aquatic animals produced similar results (Marschall and Ache, 1989). Antennule receptor cells of *H. americanus* begin to adapt in 500 ms (Voigt and Atema, 1990) regardless of pulse length. Also, the downstroke of the antennule, when odor is sampled, takes about 100 ms (Moore and Atema, 1988a; unpubl. video analysis). Based on these results, we feel that an integration time is somewhere between 100 and 500 ms. Therefore, a temporal sampling of 10 Hz in an aquatic medium can give biologically relevant resolution of chemical signals.

Materials and Methods

Plume measurements

All measurements were taken in a flow-through flume (250 × 90 × 20 cm). Water depth varied from 19 cm at the front to 21 cm at the rear due to an intentional downward tilt of the flume. Unfiltered seawater entered through 15 holes at the head of the tank. Sheets of fluorescent light grating ("egg crates," 8 mm^2 holes) wrapped with plastic screens (1.5 mm^2 mesh) served as collimators (four upstream, one downstream). The carrier flow rate was 1.8 ± .1 l/s (S.D., n = 10). Average flow velocity in the tank was 1.00 ± .06 cm/s (n = 10). The test solution (described below) was gravity fed through a 1 mm pasteur pipette at a rate of 50 ± 2 ml/min (n = 10). The nozzle of the pipette was placed in the cross-sectional center of the tank 9 cm off the bottom, roughly at the odor sampling plane of a 0.5 kg lobster. As a frame of reference for further plume descriptions, the source is at x, y, z = 0. The x-axis is the main axis of the plume, and the y-axis is the other horizontal axis. Initial observations of the fluid flow with red dye did not indicate any large asymmetries in the general flow. Red dye was also used in the test solution, and observations showed that the plume was neutrally buoyant with respect to the carrier flow.

A total of 63 different sampling sites were chosen in three dimensions (Fig. 1). Sites along the x-axis were 25, 50, and 100 cm from the source. Sites along the y-axis were −10, −5, 0, +5, +10 cm at all x-axis locations. In addition, at x = 50 cm we added y = ±20 cm and at x = 100 cm, y = ±20 and ±30 cm. Sites along the z-axis were 3, 9, 15 cm from the flume bottom, *i.e.*, −6 cm (below) and +6 cm (above) all x, y sites in the z = 0 plane. All sites were sampled sequentially, each for a 3-min period.

Electrochemical microelectrodes

The electrochemical electrodes used in these experiments were scaled to be within the spatial sampling range of the olfactory sensilla of a macroscopic aquatic animal, specifically *Homarus americanus*. We used the graphite-epoxy capillary type of electrode (Gerhardt *et al.*, 1984) with a tip diameter of 100–150 μm. The sampling area is determined by the exposed carbon epoxy surface area. An electrode with a .15 mm diameter tip has an exposed surface area of .02 mm^2 (surface area of a circle = πr^2). A single aesthetasc hair has a sampling area of .06 mm^2 including the top and shaft (surface area of a cylinder plus circle = $2\pi rh + \pi r^2$). Thus, the sampling area of the electrodes used in this study is similar to that of a single aesthetasc hair. Recordings were made at a sampling rate of 10 Hz using the IVEC-5 (In Vivo Electrochemistry Computer System; Medical Systems Corp.). Each 100 ms epoch for the 10 Hz sampling rate is composed of a 50 ms epoch at 0.55 v (oxidation) followed by a 50 ms epoch at 0.0 v (reduction). The recording electrodes were sampled every 50 ms: analog-to-digital conversions of the samples occurred at 1 KHz, and data were averaged for the 50 ms time epoch. Further details of recording and digitizing are explained elsewhere (Moore *et al.*, 1989). All electrodes were calibrated in solutions of dopamine prepared in raw seawater and exhibited excellent linearity over a concentration range of 0.5 to 500 micromolar. To account for effects of molecular diffusion from odor patches, we chose source concentrations similar to those relevant to aquatic animals, such as the lobster. Amino acid levels found in the tissues of lobster prey range from .02 to 90 m*M* (Carr and Derby, 1986). Thus we chose a source concentration of 2 m*M* dopamine (and 0.5 m*M* ascorbic acid as an antioxidant).

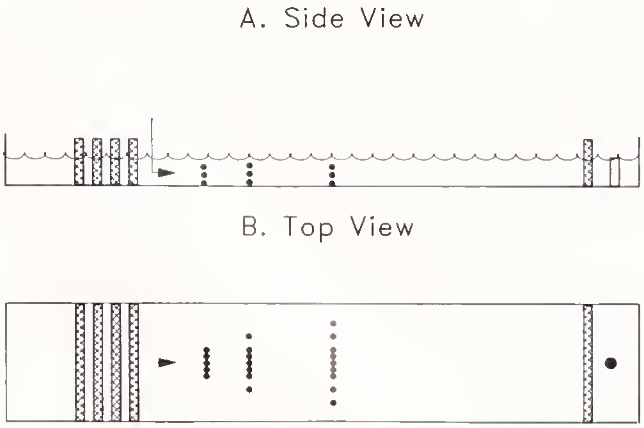
A. Side View

B. Top View

Figure 1. Diagram of flow-through flume used to create the turbulent odor plume. A: Side view, B: Top view. Flow from left to right. Arrow: odor tracer source. Dots: sampling sites. Hatched bars: collimators. Drain at far right. Scalloped water surface is merely symbolic and not reflecting degree of turbulence. See text for details.

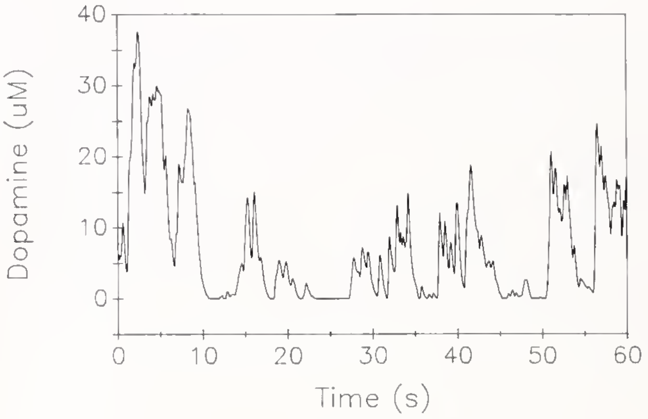

Figure 2. One-minute temporal profile of dopamine concentrations recorded at a 10 Hz sampling rate. This sampling site is at x = 25, y = z = 0. Source concentration is 2 m*M* dopamine.

Definition of terms

Odor signals can be dissected into various components and these components may be called by different names

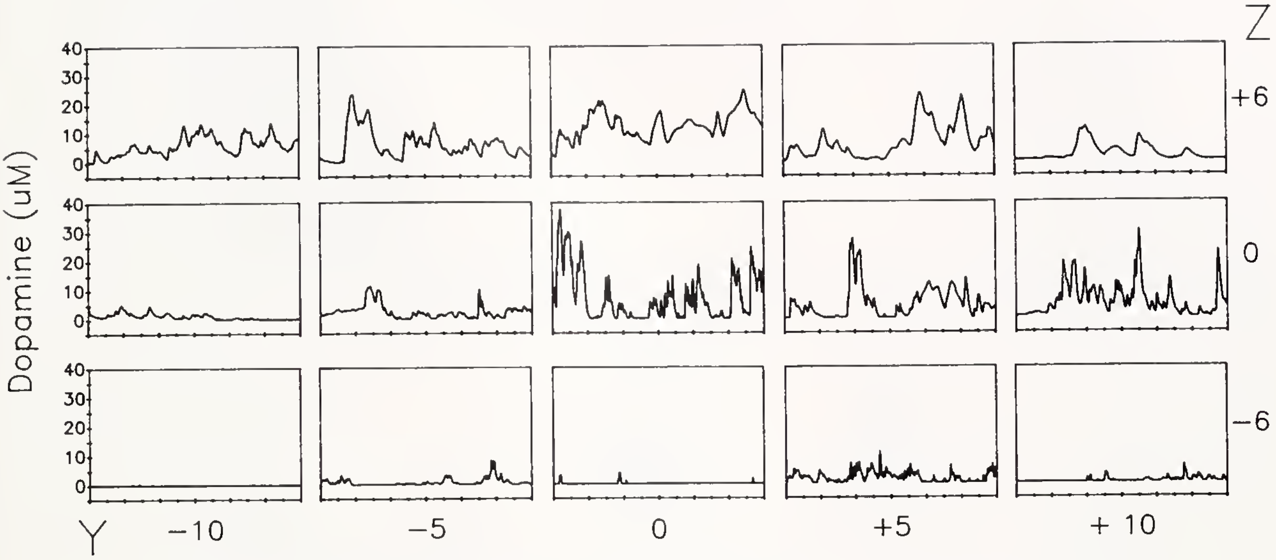

Figure 3. One-minute dopamine concentration profiles recorded at the x = 25 cm cross-sectional plane. One-minute segments were chosen to show the most intense period of odor fluctuations in the 3-min record. Numbers along bottom and right side indicate sampling site relative to source (x = y = z = 0). For example, the top left-hand graph labelled −10, +6 is 10 cm to the left and 6 cm up from the x-axis. Tick marks along the bottom indicate 5 s.

in the literature. Here we define the terms we will be using to describe an odor plume:

Odor profile: a concentration *versus* time plot that shows the concentration fluctuations at a single sampling site.

Odor burst: within an odor profile there are periods with and without odor. Periods during which the odor concentration is detectable by the sensor are called odor bursts. A burst ends when the concentration drops below detectable levels.

Off time: the period of time between two consecutive odor bursts.

Odor patch: the spatial equivalent of the odor burst. To a stationary sensor, a moving (spatial) patch of odor is measured as a (temporal) odor burst (Atema, 1987). With knowledge of the current speed, the size of the odor patch can be calculated from the length of the odor burst.

Odor pulse: within an odor burst, there may be multiple peaks and valleys of odor concentration. Each one of these peaks is considered a separate odor pulse only when the valley between the pulses falls to a value that is below 30% of the first pulse height. Odor pulses can be characterized by *pulse height,* highest concentration (measured against a background; see below) obtained during the pulse; *pulse length,* duration of pulse; *pulse onset slope,* maximum value of rising slope of pulse.

Data and statistical analysis

All measurements were converted from computer counts to micromolar concentrations of dopamine using the calibration factor determined for each electrode and set to a baseline of 0 dopamine (The theoretical detection limit of the system is below 10^{-9} *M* but due to electrical noise our limit is around 10^{-9} *M*). Concentration profiles plotted on a logarithmic scale had a baseline set at 10^{-8} *M*. This baseline roughly reflects both chemoreceptor cell thresholds commonly found in aquatic invertebrates (Ache, 1982) and amino acid background levels in seawater (Mopper and Lindroth, 1982; Carr, 1988). The natural chemical background of dopamine in seawater is not known, but unlikely to exceed 10^{-9} *M*.

Spectral analysis of the three-minute odor profiles were calculated via a Fast Fourier Transform method using a commercial signal processing program (DADiSP Worksheet). Fourier analysis breaks up a complex wave form into its component pure sine waves with different frequencies and amplitudes. This type of analysis gives a "power *versus* frequency" x, y plot, where frequency is expressed as cycles per second (as in a pure sine wave). In electrical terms, power is the integral of voltage squared over a given frequency range. Here, voltage reflects the pulse amplitude (*i.e.*, odor concentration) of a particular data point. Again in electrical terms, frequency is the inverse of the period of the different component sine waves of the signal being analyzed. In chemical terms, onset slopes are represented as frequencies: a steep slope with a short rise time is expressed in high frequency components. Thus, spectral analysis of an odor profile shows the mean value of pulse amplitudes within each frequency band. This is biologically relevant

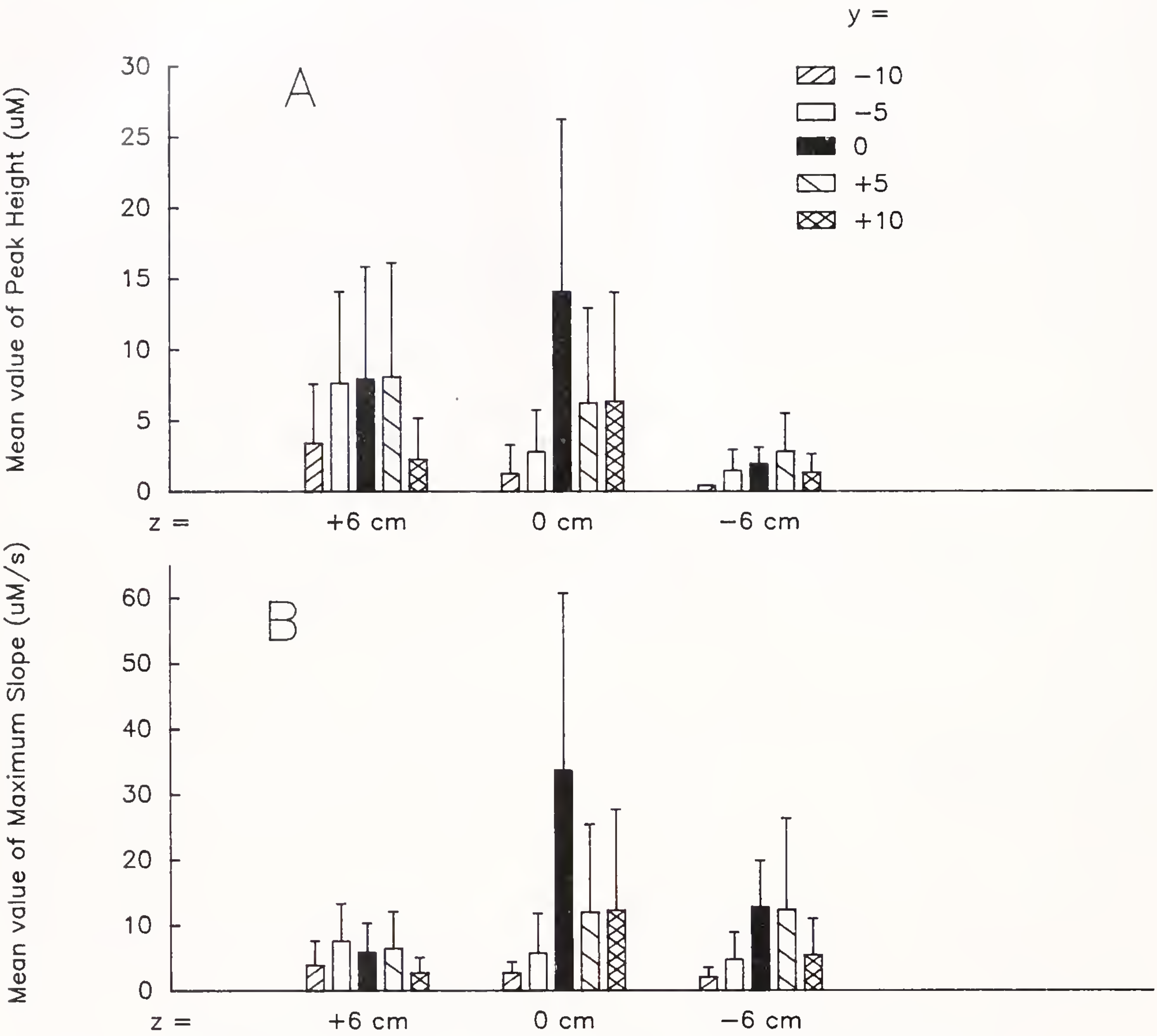

Figure 4. Mean (and standard deviation; T-bars) values of pulse height (A) and slope (B) for all pulses that occurred in the 3-min records at all x = 25 cm sites.

because it shows in which frequency band the strongest odor pulses lie.

Two odor profile characteristics, pulse height and maximum onset slope, were extracted from the calibrated odor plume signals based on the definitions above and the criteria set forth in Moore and Atema (1988a, b). The Tukey-Kramer multiple unplanned comparison method was used to compare the means for peak height and slope. These values, expressed in μM for pulse height and in μM/s for onset slope, were grouped into three log-step bins (.1–1, 1–10, 10–100). Although a small number of pulse height values were less than .1 μM, no pulse height values were higher than 100 μM. No slope values at any site were smaller than .1 μM/s or larger than 100 μM/s. For each site, probability distributions of height and slope for the three log-step bins were calculated from the number of occurrences within a log-step bin and the total number of pulses encountered at that site. The resulting values reflect the probability of encountering, at that site, a pulse having a height or slope value within a given bin.

Results

Odor profiles were characterized by bursts (Fig. 2). Bursts frequently lasted from 5 to 10 s, *e.g.*, Figure 2, 0–10 s or 38–45 s. Within a burst, pulses lasted between 0.5 and 6 s. Off times ranged from 0.2 to 3 s. The first odor burst in Figure 2 (0 to 10 s) shows four large (11, 38, 30,

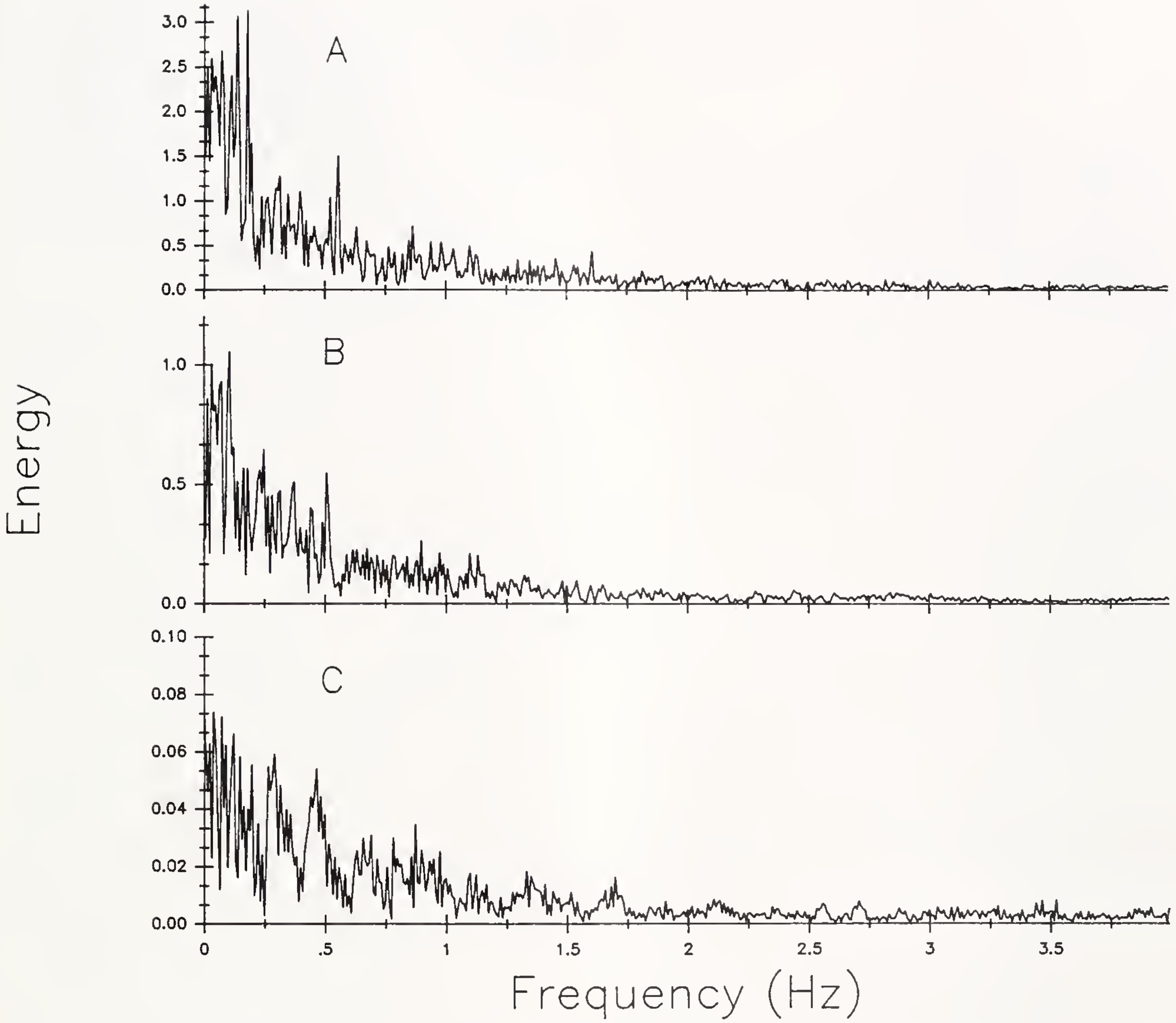

Figure 5. Frequency spectrum of concentration changes at three sites on the x-axis. A: x = 25, y = z = 0, B: x = 50, C: x = 100 cm. The ordinate is displayed as energy which corresponds to the number of pulses and pulse amplitude (See text). Note differences in Y-axis scaling. Based on 3-min records.

and 28 μM) and many smaller peaks. Using our definition, the first three peaks (11, 38 and 30 μM) are considered one pulse (because the value at valley is not less than 30% of the previous pulse amplitude, see Methods) and the last peak (28 μM) is considered a separate pulse. Note that peak concentrations are about 100 times diluted from source strength, *i.e.*, from 2 mM to 20 μM.

An initial qualitative picture of the spatial distribution of odor fluctuations is shown for the x = 25 plane in Figure 3. The most intense odor fluctuations occur in the center of the plume (site 25, 0, 0). At this site, large and rapid changes in concentration are more common than at other sites. Peak concentrations can exceed 25 μM dopamine. As areas further outside of this center point are sampled (y = ±5 and ±10 cm and z = ±6 cm), these large and sudden changes in concentration become less frequent. At one site (y = −10, z = −6), no odor could be detected. The z = +6 profiles (Fig. 3) contain large but considerably less steep steps in concentration but never exceed 25 μM dopamine. The z = −6 sites include small, but surprisingly steep, changes in concentration rarely exceeding 10 μM dopamine. Similar spatial distributions were seen in the x = 50 and x = 100 cm sampling planes (not shown for the sake of brevity).

Mean values of pulse height (Fig. 4a) and maximum slope (Fig. 4b) support the qualitative results seen in the 1-min profiles (Fig. 3). The highest values of both pulse height and slope are seen in the center of the odor plume,

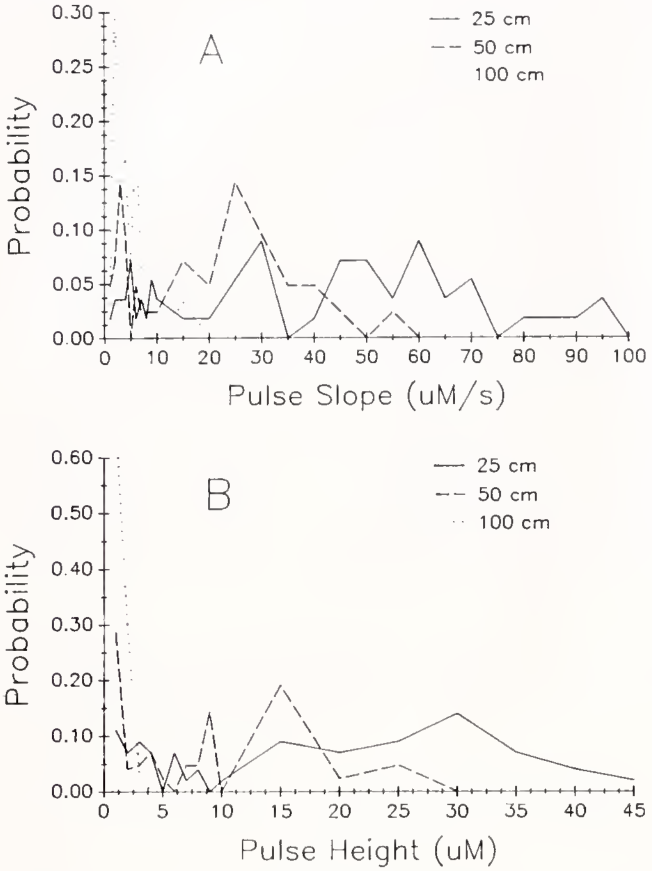

Figure 6. Probability distributions of pulse slope (A) and pulse height (B) at three sites on x-axis: $x = 25$ (Solid), $x = 50$ (Dashed), and $x = 100$ (Dotted). Based on 3-min records.

with values tapering off considerably to the sides. The ($x = 25$, $y = 0$) values were significantly different from the other means ($P < .01$). This tapering is asymmetrical: the differences in the left ($y = -5, -10$) and right ($y = +5, +10$) values within a z-plane are indicative of lateral meandering of the entire plume. The higher ($z = +6$) sampling sites had larger peak values (Fig. 4a) but slower-rising (Fig. 4b) odor pulses. The lower ($z = -6$) sampling sites had low intensity (Fig. 4a), but faster-rising (Fig. 4b) odor pulses; this will be discussed later. At the $x = 50$ and $x = 100$ cm sampling sites, the distributions of mean values were also centered around the cross-sectional middle of the plume with values tapering off (asymmetrically as above) away from the center. At all sites, the standard deviation of both pulse height and slope were approximately equal to the mean value at all sites. This is likely due to the chaotic nature of the turbulent odor plume and indicates that the mean value of any parameter is a poor indicator of the instantaneous value of that parameter.

Spectral analysis of the odor profiles (Fig. 5; note change in y-axis scale) from the three x-axis ($z = y = 0$) sampling sites shows the change in the temporal characteristics of odor signals with distance down-current (Fig. 4). Most pulses had slope values that translated into low frequency (<4 Hz) signals with the majority of the odor signal below 1 Hz at all sites. There is also a reduction in the total number and amplitude of odor bursts with distance, which is reflected in the decrease of the overall energy at the farther sites (compare ordinate scales): the odor becomes more widely and evenly distributed farther away from the source.

When considering animal behavior, the mean value of a sensory signal is often an inappropriate measure because this information is not available to an animal that has to make quick decisions. During orientation behavior, animals are forced by predation and competition pressures to make behavioral decisions based on relatively short sampling periods. Thus, we have selected probability distributions as a measure of information that may be available to the animal during short sampling intervals. Along the plume main axis, the probability distributions of pulse slopes shift to the left, *i.e.*, decrease in value, with increasing distance from the source (Fig. 6a). Pulse slope values larger than 15 μM/s are completely absent from the 100 cm site, and slope values above 55 μM/s are only present at the closest site. Thus, overall, there is a progressive change from predominantly shallow slopes at 100 cm to an intermediate range of slopes at 50 cm to a broad spectrum of predominantly steep slopes at 25 cm. The probability distributions of pulse height show a similar progressive change with distance (Fig. 6b).

To view the spatial distribution of a range of slope or height values, we calculated the probability distributions of slope or height values within 3 logarithmic bins (de-

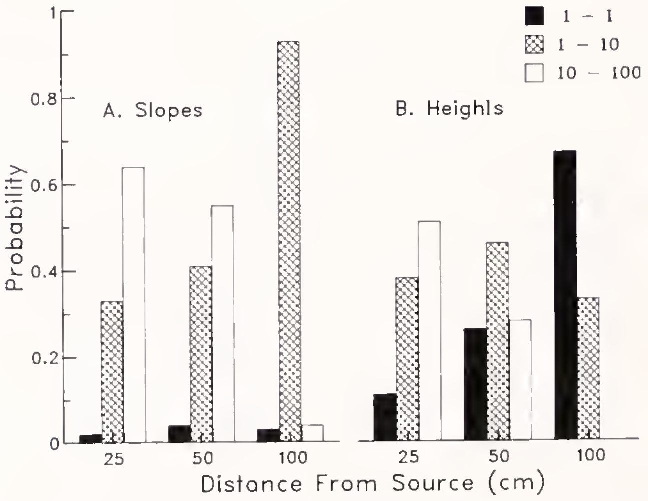

Figure 7. Probability distribution of pulse slope (A) and pulse height (B) at three sites on x-axis: $x = 25, 50, 100$. Probability values are calculated on the three bin sizes. .1–1, 1–10, 10–100.

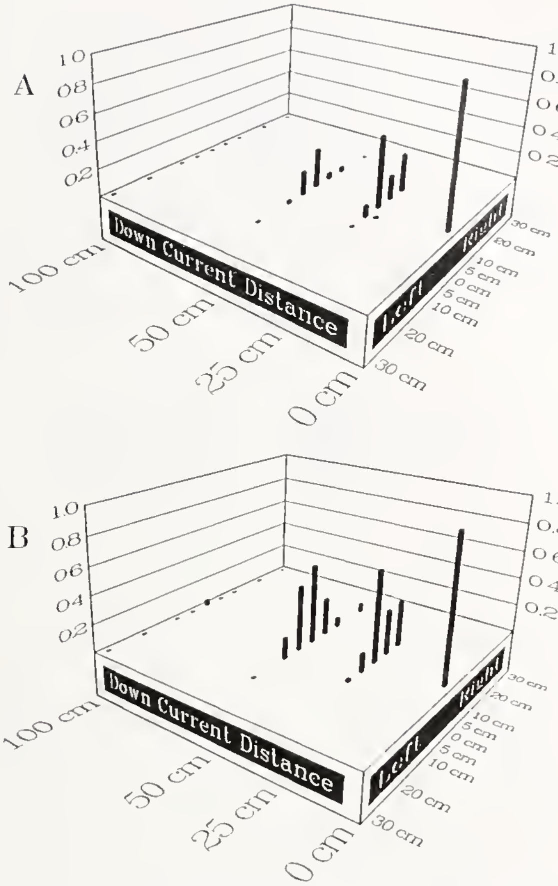

Figure 8. Spatial distribution of large (>10 μM) pulse heights (A) and large (>10 μM/s) pulse slopes (B) in the z = 0 plane. Source: P = 1.0 for reference.

scribed in Methods). The binned distribution of slope and height values at the x = 25, 50, and 100 sites (y = z = 0; Fig. 7) show a progressive change that was evident from continuous distributions in Figure 6. To illustrate how these probabilities are distributed in the x-y spatial plane, we plot one bin value at all of the sample points in this plane. The x-y spatial distribution of probabilities of large slopes (10–100 μM/s) in the z = 0 plane reveals that these values increase in the direction of the source (Fig. 8a). These values range from 0 (all x = 100 cm) to .64 (x = 25, y = 0 cm). At each x plane, the probabilities increase toward the middle of the plume with the largest values in the center. Similar distributions are seen in the z = +6 and z = −6 planes (not shown). The progressive changes seen in the slope distributions are also reflected in the pulse height distributions but with larger changes in the probabilities. The probabilities of large (10–100 μM) pulse heights in the z = 0 plane also increase toward the source and the center axis of the plume (Fig. 8b). The probabilities range from 0 at all but one of the x = 100 cm sites to .51 at the x = 25, y = 0 cm site. As with slopes, similar changes in probabilities are seen in the z = +6 and z = −6 planes (not shown).

Discussion

The structure of odor plumes is mainly due to turbulence produced by the mechanical forces within a moving fluid. These mechanical forces create large scale eddies (compared to the initial size of the odor plume) that transfer their energy to successively smaller eddies until the energy is dissipated as heat. This cascade of eddies is called the Kolmogoroff scale and has a lower size limit; molecular diffusion takes over below this limit. The lower size limit of eddies is determined by friction, viscous forces, and fluid velocity (Pedlosky, 1987).

The spatial range of eddies is important because it is the interaction between the size of the turbulent eddies and size of the odor plume that creates the size and length of concentration fluctuations within the odor plume (Aylor, 1976; Aylor *et al.*, 1976; Miksad and Kittredge, 1979). As the plume travels down-current, it expands relative to the size of eddies within the fluid medium. Initially, when the plume diameter is smaller than the smallest eddies, they cause the plume to meander as a whole. As the plume size expands to match the scale of eddies present, the plume is broken into separate patches of odor. This results in a fluctuating odor signal (Fig. 2). The final stage of plume growth occurs when the plume expands to sizes larger than the largest eddies. At this point, eddies begin to redistribute the odor within single patches and begin to homogenize the odor between patches. This results in signals that fluctuate less and have less off time (Fig. 3, top row).

Thus, as the plume as a whole and the patches within the plume increase in lifetime and size, there are changes taking place in the structure of the odor signal (Fig. 3).

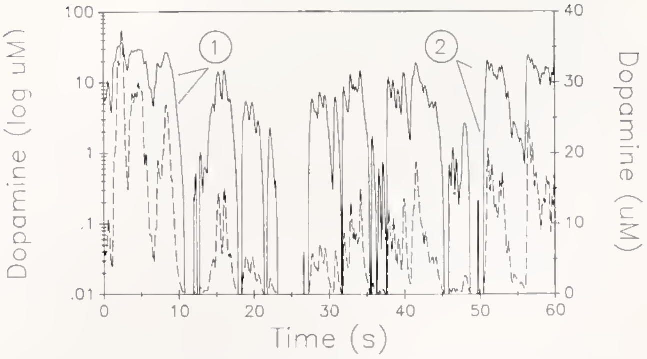

Figure 9. One-minute odor profiles from sample site at x = 25, y = z = 0 plotted on logarithmic (left hand, solid line) and linear (right hand, dashed line) scale. Dashed line is identical to profile in Figure 2. Baseline on logarithmic scale was set to 10^{-8} M (See text for explanation of 1 and 2).

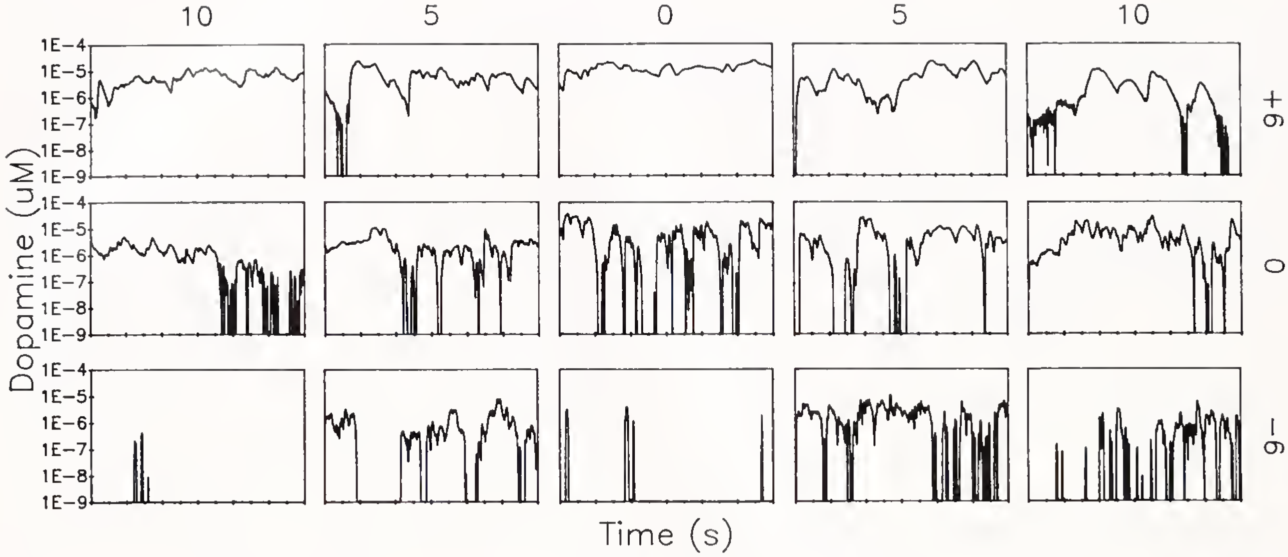

Figure 10. The same one-minute profiles shown in Figure 3 now plotted on logarithmic scale. Tick marks on bottom axis indicate 5 s.

The changes depend on the flow environment around the sampling point. The bottom row of profiles (Fig. 3) were sampled 3 cm from the bottom of the flume. The smooth, solid floor of the flume resulted in lower pulse heights but much faster rise times. Near the bottom of the flume, the eddies are confined to small and fast scales by the rigid, unmoving surface where fluid velocities must be zero. The top row of profiles (Fig. 3) were sampled 5 cm from the water surface. This moving surface allows larger and slower eddies, which acts as a "low pass" filter and dampens the faster rising slopes. This would result in an overall increased pulse height but slower rising slopes. These types of distributions are highly dependent upon the local substrate and fluid dynamic conditions.

These changes in the odor plume, with both distance and time can be seen as decreases in both mean pulse height and slope with distance (Fig. 5). Time-averaged plume dispersion models (Sutton, 1953; Bossert and Wilson, 1963) predict these decreases with distance and time, but they do not show the large variability of the values for pulse height and slope. This is evident from the large standard deviations at each site (Fig. 5, bars). While the long-term time-averaged pulse values may give a good prediction of the plume structure (and from that spatial position within a plume), the actual short-term (1–5 s) mean values of pulse height and slope may predict a different plume structure (and hence incorrect directional or positional information).

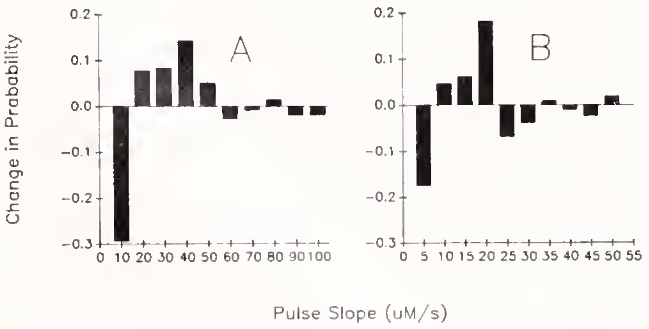

Figure 11. Probability distributions of pulse slope at the x = 25, y = z = 0 (A) and x = 50 (B) sampling sites. Solid bars represent change in distribution of same data as it is played through a model chemoreceptor filter (Moore and Atema, 1988; Model–Raw data). Positive values indicate enhancement from model, whereas negative values indicate reduction.

For an order of magnitude estimate, Atema (1988) reported that physiological responses of chemoreceptor cells may average over 0.01–1 s, and that behavioral responses may use sample intervals of 0.1–1000 s. Therefore, plume measurements averaging over periods longer than 1 s may be poor predictors of animal behavior within an odor plume. Ideally, one should measure an order of magnitude faster than the animal of study, *i.e.*, 1–100 ms resolution. For example, a behavioral assay with the gypsy moth produced quite different results than those that were predicted from time-averaged dispersion models (Elkinton *et al.*, 1984). Thus, it is not only important to consider both the spatial and temporal sampling scales of the chemoreceptor organ, but also the temporal scale of animal behavior analyzing odor concentrations. Probability distributions of parameters are a method to view the type of information available to the animal over a limited number of samples rather than the whole 3-min recordings. Animals may well base their behavioral decisions on sampling and encounter probabilities (Kamil, 1988). Therefore, probability analysis may be appropriate for assessing orientation cues within an odor plume.

It is also important to consider the filter properties of the chemoreceptor cells when analyzing odor signals. Physiological properties of receptor cells, such as integration time, adaptation, disadaptation, and dose-response curves, can filter the odor signal and alter its "perception" by the chemoreceptor cell (Moore and Atema, 1988a). Analyzing odor signals with biologically realistic filters will begin to give us insights into how the CNS views odor signals and may lead to how behavioral decisions within a plume are made.

For example, an animal with a chemoreceptor organ containing three types of receptor cells (A, B, and C) "tuned" to different ranges of pulse heights or intensities (range fractionation). As the animal moves within a turbulent odor plume, these three cells would respond differentially at the different intensities within the plume and could lead the animal to the source. At the most distant points in an odor plume, where only small peaks are found in highest probability and large peaks are rarely encountered (Figs. 6, 7, 8b), cell A would fire the most and cell B would have only occasional output. As the animal moves toward the source, a different pattern of firing would occur across a cell population. Directional information on the source can then be derived from different firing patterns (across fiber pattern).

Odor plume profiles are normally plotted on linear scales (Murlis, 1986; Moore and Atema, 1988a), but chemoreceptor cells often have linear responses to logarithmic changes in concentrations. Plotting the x = 25, y = z = 0 odor profile (Fig. 2) on a log scale produces a quite different view of the odor signal fluctuations (Fig. 9). This type of filter (logarithmic) enhances concentration changes *between* odor bursts, but diminishes changes *within* the bursts. The two marks (# 1 and 2; Fig. 9) indicate nearly identical concentration changes on a linear scale, but the initial concentration change (#2) of an odor burst is much more prominent on the log scale than the concentration change within the odor burst (#1). These same changes are also seen in the cross-sectional view at the x = 25 cm sampling site (Fig. 10). Thus, the initial onset of the odor burst seems (on a log scale) to have the most dramatic concentration changes.

Chemoreceptor cells also have the temporally dynamic properties of adaptation and disadaptation that cause changes in the receptor cell output, response threshold, and dose-response functions (Borroni and Atema, 1988, 1989; Voigt and Atema, 1990). These two properties can function together to filter turbulent odor signals (Moore and Atema, 1988a, b). To examine how adaptation and disadaptation affect plume structure, we analyzed the x = 25, y = z = 0 sampling site with the 10 s temporal filter introduced in Moore and Atema (1988a). The 3 log scale (.1–1, 1–10, 10–100 μM) probability grouping performed on the data in this study was repeated on the filtered data. Figure 11 shows the changes in the probability distributions of the onset slopes from the raw data as it is filtered through the model. At both the x = 25 (Fig. 11a) and x = 50 (Fig. 11b) sites, the model enhances the probability of detecting slopes in the middle range of values. This temporally dynamic filter seems to eliminate the smaller amplitude, slower rising peaks that are evident within the raw data.

Within all of these different filtering methods, one common theme appears. Although turbulent odor plumes produce odor signals that seem random and chaotic, there are biological and computational methods of analysis that can track changes occurring within the structure of odor plumes. Which structural features are detectable and used by the animal for orienting within a turbulent plume? To answer this question, we must measure different turbulent odor signals at biologically relevant time and space scales and then analysis those results with biologically relevant spatial and temporal filters; *i.e.*, logarithmic, adaptation, and sampling behavior of the chemosensory organ.

Acknowledgments

The authors would like to thank Nat Scholz and Lynne Lacomis for assistance during measurements and reviewing an earlier version of this manuscript; Dr. Greg A. Gerhardt and Medical Systems for the generous support of equipment and technology; and Drs. Greg Gerhardt, Ring Cardé, and Fred Wasserman for critically reviewing this manuscript as a chapter in P.M.'s Ph.D. thesis. We would especially like to thank Dr. Keith Stolenzbach for discussion and development of some ideas presented in the discussion. This work supported by a grant from NSF (BNS 90-12952) to J. A. and a BUMP Alumni research award to P.M.

Literature Cited

Ache, B. W. 1982. Chemoreception and thermoreception. Pp. 369–398 in *The Biology of Crustacea, Vol. 3. Neurobiology: Structure and Function,* H. L. Atwood and D. C. Sandeman, eds. Academic Press, NY.

Atema, J. 1988. Distribution of chemical stimuli. Pp. 29–56 in *Sensory Biology of Aquatic Animals,* J. Atema, A. N. Popper, R. R. Fay and W. N. Travolga, eds. Springer-Verlag, NY.

Atema, J. 1987. Chemoreceptor adaptation: a patch in space is a pulse in time. *Chem. Senses* **12:** 189–190.

Atema, J. 1985. Chemoreception in the sea: adaptation of chemoreceptors and behavior to aquatic stimulus conditions. *Soc. Exp. Biol. Symp.* **39:** 387–423.

Atema, J., K. Holland, and W. Ikehara. 1980. Olfactory responses of yellowfin tuna (*Thunnus albacares*) to prey odors: chemical search image. *J. Chem. Ecol.* **6:** 457–465.

Aylor, D., J-Y. Parlange, and J. Granett. 1976. Turbulent dispersion of disparlure in the forest and male gypsy moth response. *Env. Ent.* **10:** 211–218.

Aylor, D. E. 1976. Estimating peak concentrations of pheromones in the forest. Pp. 177–188 in *Perspectives in Forest Entomology*, J. E. Anderson and M. K. Kaya, eds. Academic Press, NY.

Bell, W. J. 1984. Chemo-orientation in walking insects. Pp. 93–106 in *Chemical Ecology of Insects*, W. J. Bell and R. T. Cardé, eds. Sinauer Associates, Inc., MA.

Bell, W. J., and R. T. Cardé (eds.). 1984. *Chemical Ecology of Insects*, Sinauer Associates, Inc., MA.

Berg, H. C., and E. M. Purcell. 1977. Physics of chemoreception. *Biophys. J.* **20:** 193–219.

Bossert, W. H., and E. O. Wilson. 1963. The analysis of olfactory communication among animals. *J. Theor. Biol.* **5:** 443–469.

Borroni, P. F., and J. Atema. 1989. Adaptation in chemoreceptor cells II. The effects of cross-adapting backgrounds depend on spectral tuning. *J. Comp. Physiol. A.* **165:** 669–677.

Borroni, P. F., and J. Atema. 1988. Adaptation in chemoreceptor cells I. Self-adapting backgrounds determine threshold and cause parallel shift of response function. *J. Comp. Physiol. A* **164:** 67–74.

Brady, J., G. Gabriella, and M. J. Packer. 1989. Odour movement, wind direction, and the problem of host-finding by tsetse flies. *Physiol. Entomol.* **14:** 369–380.

Bursell, E. 1984. Observations on the orientation of tsetse flies (Glossina pallidipes) to wind-borne odours. *Physiol. Entomol.* **9:** 133–137.

Carr, W. E. S. 1988. The molecular nature of chemical stimuli in the aquatic environment. Pp. 3–28 in *Sensory Biology of Aquatic Animals*, J. Atema, A. N. Popper, R. R. Fay, and W. N. Travolga, eds. Springer-Verlag, NY.

Carr, W. E. S., and C. D. Derby. 1986. Behavioral chemoattractants for the shrimp, *Palaemonetes pugio:* identification of active components in food extracts and evidence of synergistic mixture interactions. *Chem. Senses* **11:** 49–64.

Christensen, T. A., and J. G. Hildebrand. 1988. Frequency coding by central olfactory neurons in the Sphinx moth *Manduca sexta*. *Chem. Senses* **13:** 123–130.

David, C. T., J. S. Kennedy, A. R. Ludlow, J. N. Perry, and C. Wall. 1982. A reappraisal of insect flight towards a distant, point source of wind-bourne odor. *J. Chem. Ecol.* **8:** 1207–1215.

Devine, D. V., and J. Atema. 1982. Function of chemoreceptor organs in spatial orientation of the lobster, *Homarus americanus:* differences and overlap. *Biol. Bull.* **163:** 144–153.

Elkinton, J. S., R. T. Cardé, and C. J. Mason. 1984. Evaluation of time-average dispersion models for estimating pheromone concentration in a deciduous forest. *J. Chem. Ecol.* **10:** 1081–1108.

Fraenkel, G. S., and D. L. Gunn. 1961. The orientation of animals. 2nd edition, Dover Publishers Inc., N.Y.

Gerhardt, G. A., A. F. Oke, G. Nagy, B. Moghaddam, and R. N. Adams. 1984. Nafion-coated electrodes with high selectivity for CNS electrochemistry. *Brain Research* **290:** 390–395.

Ghiradella, H., J. F. Case, and J. Cronshaw. 1968. Structure of aesthetascs in selected marine and terrestrial decapods: chemoreceptor morphology and environment. *Am. Zool.* **8:** 603–621.

Kaissling, K. E., C. Zack-Straussfeld, and E. Rumbo. 1987. Adaptation processes in insect olfactory receptors: mechanisms and behavioral significance. Pp. 104–112 in *Olfaction and Taste IX*, S. Roper and J. Atema, eds. N.Y. Acad. Sci.

Kamil, A. C. 1989. Behavioral ecology and sensory biology. Pp. 189–202 in *Sensory Biology of Aquatic Animals*, J. Atema, A. N. Popper, R. R. Fay, and W. N. Travolga, eds. Springer-Verlag, NY.

Kennedy, J. S. 1986. Some current issues in orientation to odour sources. Pp. 11–25 in *Mechanisms in Insect Olfaction*, T. L. Payne, M. C. Birch, and C. E. J. Kennedy, eds. Clarendon Press, NJ.

Marschall, H-P., and B. W. Ache. 1989. Response dynamics of lobster olfactory neurons during simulated natural sampling. *Chem. Senses* **14:** 725.

Miksad, R. W., and J. Kittredge. 1979. Pheromone aerial dispersion: a filament model. *14th Conf. Agric. and For. Met. Am. Met. Soc.* **1:** 238–243.

Moore, P. A., G. A. Gerhardt, and J. Atema. 1989. High resolution spatio-temporal analysis of aquatic chemical signals using microelectrochemical electrodes. *Chem. Senses* **14:** 829–840.

Moore, P. A., and J. Atema. 1988a. A model of a temporal filter in chemoreception to extract directional information from a turbulent odor plume. *Biol. Bull.* **174:** 355–363.

Moore, P. A., and J. Atema. 1988b. A mathematical computer model of the temporal filtering characteristics of chemosensory adaptation. *Chem. Senses* **13:** 722.

Mopper, K., and P. Lindroth. 1982. Diel and depth variations in dissolved free amino acids and ammonium in the Baltic Sea determined by shipboard HPLC analysis. *Limnol. Oceanogr.* **27:** 336–347.

Murlis, J. 1986. The structure of odour plume. Pp. 27–38 in *Mechanisms in Insect Olfaction*, T. L. Payne, M. C. Birch, and C. E. J. Kennedy, eds. Clarendon Press, NJ.

Murlis, J., and C. D. Jones. 1981. Fine-scale structure of odour plumes in relation to insect orientation to distant pheromone and other attractant sources. *Physiol. Entomol.* **6:** 71–86.

Pedlosky, J. 1987. *Geophysical Fluid Dynamics*, Springer-Verlag, NY.

Preiss, R., and E. Kramer. 1986. Pheromone-induced anemotaxis in simulated free flight. Pp. 6–80 in *Mechanisms in Insect Olfaction*, T. L. Payne, M. C. Birch, and C. E. J. Kennedy, eds. Claredon Press.

Sanders, C. J. 1986. The role of pheromone concentration in male moth flight behavior. Pp. 117–122 in *Mechanisms in Insect Olfaction*, T. L. Payne, M. C. Birch, and C. E. J. Kennedy, eds. Clarendon Press, NJ.

Sutton, O. G. 1953. *Micrometeorology*, McGraw-Hill, NY.

Vogel, S. 1981. *Life in Moving Fluids: the Physical Biology of Flow*, Princeton University Press, Princeton, NJ. 352 pp.

Voigt, R., and J. Atema. 1990. Adaptation in chemoreceptor cells. III. Effects of cumulative adaptation. *J. Comp. Physiol. A.* **166:** 865–874.

Zimmer-Faust, R. K., J. M. Stanfill, S. B. Collard III. 1988. A fast, multichannel fluorometer for investigating aquatic chemoreception and odor trails. *Limnol. Oceanogr.* **33:** 1586–1595.

Reference: *Biol. Bull.* **181:** 419–426. (December, 1991)

Chemical Signal-to-Noise Detection by Spiny Lobsters

RICHARD K. ZIMMER-FAUST*

Marine Environmental Sciences Consortium and Department of Biology, University of Alabama,
P.O. Box 369-370, Dauphin Island, Alabama 36528

Abstract. The smallest difference in concentration detected between a chemical stimulus and background is called the threshold of "just noticeable difference" (*jnd*). Measurements of *jnd* thresholds have been made extensively in psychophysical research on olfactory and taste perception by terrestrial mammals, but not on chemoreception by marine organisms. Marine organisms live in a persistently noisy chemical environment, because stimulatory compounds are often components of the background in seawater. Measurements of *jnd* thresholds, therefore, should be especially appropriate in the marine environment and were the focus of this study. Laboratory assays were used in measuring the ability of spiny lobsters, *Panulirus interruptus,* to detect a glycine stimulus against a background concentration of glycine. Glycine was chosen as stimulant because it is a major component of dissolved organic matter (DOM) in seawater, is abundant in prey tissues, and is excitatory to the appetitive feeding phase of *P. interruptus.* Chemical determinations of glycine in seawater were made by reverse-phase, high-performance liquid chromatography. The *jnd* threshold that was estimated in this study for glycine detection by lobsters was about 2–8% above the background concentration of glycine in seawater. This threshold is slightly lower than ones demonstrated for odorant detection by humans and other terrestrial animals. Consequently, the olfactory sense of lobsters appears to be well constructed to detect subtle changes between concentrations of stimulus and background, a facility that may be important in the ecology of this animal.

Introduction

Chemical stimuli are important factors controlling the behavior of aquatic organisms. Chemical cues often mediate predator-prey interactions (Peckarsky, 1980; Croll, 1983; Zimmer-Faust, 1989; Sih and Moore, 1990), competition (Caldwell, 1982; Sammarco *et al.,* 1983; La Barre *et al.,* 1986), courtship and mating (Gleeson *et al.,* 1984; Miller, 1989), gregariousness and sociality (Zimmer-Faust and Spanier, 1987; Jensen, 1989), and habitat selection (Hadfield and Scheuer, 1985; Raimondi, 1988; Sweatman, 1988; Morse, 1990). Several properties of chemical cues, including molecular structure, concentration, and distribution in time and space, contribute to the stimulation of a behavioral response.

The ability to detect concentration differences is especially important, because instantaneous or time-averaged gradients in chemical concentration may provide animals with valuable information about their distance and direction from the odor source (Moore and Atema, 1988; Zimmer-Faust *et al.,* 1988). The source may be food or a mate, and chemical concentration might also provide information about the quantity or quality of the resource. Because many stimulatory molecules occur naturally as dissolved organic matter in seawater, marine organisms face the problem of resolving chemical signals from environmental background, or chemical "noise." In particular, free amino acids, nucleotides, sugars, and organic acids function as signals of food (see reviews of Carr, 1988; Laverack, 1988), but they also occur abundantly in seawater. The effects of chemical stimulus concentration have been considered in many studies on marine animal behavior (Ache, 1982; Carr, 1988; Zimmer-Faust, 1989), but in no investigation have response thresholds to applied stimuli been measured relative to background concentrations. Because many chemoreceptors function as detectors of relative changes in concentration, threshold determinations may be products both of animal sensitivity to tested compounds, and to background chemical levels in seawater.

The threshold of "just noticeable difference" (*jnd*) is the smallest difference detected between the concentration

Received 19 February 1991; accepted 26 September 1991.

* Present address: Department of Biology and Marine Sciences Program, University of South Carolina, Columbia, South Carolina 29208.

of the stimulus and that of the background. The *jnd* threshold has been used extensively in psychophysical research on olfactory and taste perception by vertebrates, especially humans (*sensu* McBurney *et al.*, 1967), but has not been applied to investigations of chemoreceptive behavior in marine organisms. Yet measurements of *jnd* thresholds should be especially appropriate to marine organisms, which live in a persistently noisy chemical environment. In fact, threshold determinations of *jnd* should be essential to understanding the environmental constraints imposed on chemical detection. For these reasons, during the present study, analytical procedures useful for measuring *jnd* thresholds of chemical detection by marine organisms were developed. The procedures were then applied in estimating the threshold of *jnd* for chemical detection by the spiny lobster, *Panulirus interruptus*.

Materials and Methods

Collection and maintenance of animals

Lobsters were captured by SCUBA divers and were brought immediately to the laboratory where small groups of individuals were placed in large, outdoor circular tanks (1.5 m diameter × 0.6 m height) having excess shelters (see Zimmer-Faust and Spanier, 1987). A continuous seawater flow (5 μm filtered) of 8 l/min maintained the aeration and temperature (15–16°C) of each holding tank. Incoming animals were tattooed on their ventral thoracic sternites, permitting individual recognition (Kuris, 1971), while gender and reproductive status were noted. Only hard-shelled animals, 60–69 mm carapace length, were used in the experiments. All animals were fed *ad libitum* on live mussels (*Mytilus californianus* and *M. edulis*), sea urchins (*Strongylocentrotus purpuratus*), and polychaete worms (*Phragmatopoma californica*), but were deprived of food for 24 h before testing.

Experimental chambers

Individual lobsters were tested for responses to chemical solutions presented in rectangular chambers, 30 × 30 × 15 cm, constructed so as to allow careful control of test stimulus flow characteristics. Opaque blinds around each chamber permitted us to observe the test animals without disturbing them. A diffuse red illumination, completely confined by the blinds, was provided, and the surrounding laboratory was maintained in darkness. Seawater (single-pass; 5 μm filtered) entered each chamber by a delivery system held under constant hydrostatic pressure. Polyethylene tubing carried a primary seawater flow (936 ml/min) from a head-tank to an adaptor positioned above each chamber; from the adaptor, the seawater was delivered to the center of the chamber, 0.5 cm below the water surface. A valve in each delivery line enabled fine adjustments of water flow. A secondary flow (122 ml/min) was carried by polyethylene tubing from a head-tank to a stimulus reservoir before it joined the primary flow at the adaptor. Test stimulant solution was introduced (10 ml/7 s) when a three-way valve that connected the stimulus reservoir to the secondary flow system was opened. A fitting in each adaptor eliminated back-flow, ensuring that seawater and test stimulants would pass from the secondary to primary flow before entering a chamber.

Choice of glycine as test stimulus

Glycine was used as test stimulant because it is excitatory to the appetitive phase of feeding by *P. interruptus* (Zimmer-Faust *et al.*, 1984; Zimmer-Faust, 1987). It is also abundant in the tissues of invertebrate prey consumed by lobsters (*e.g.*, Bowlus and Somero, 1979; Zurburg and DeZwaan, 1981; Yancey *et al.*, 1982) and is released by some prey as a metabolite (Zimmer-Faust, unpub. data). Because glycine is one of three most abundant amino acids in coastal seawater (Clark *et al.*, 1972; Dawson and Pritchard, 1978; Garrasi *et al.*, 1982; Mopper and Lindroth, 1982; Fuhrman and Bell, 1985), it is an ecologically relevant stimulus molecule that lobsters must naturally detect from background noise.

Experimental procedures

Lobsters were placed in experimental chambers 45 to 60 min before testing, and they usually acclimated within 30 min. Observations of behavior were initiated 1 min before the introduction of a test or control solution and were continued for 3 min afterwards; the observer was unaware of the solution being tested. In each trial, a lobster was presented with 10 ml of either 10^{-2}, 10^{-3}, 10^{-4}, 10^{-5}, 10^{-6}, 10^{-7}, 5×10^{-8}, or 10^{-8} M glycine added to the seawater as described above. Each concentration of glycine was tested 20 times, each time on a different animal. In 40 trials, lobsters were presented only with seawater (control). Each test and control solution was prepared fresh immediately prior to assay. Individual lobsters were tested only once in 48 h, for a maximum of three times during an 8-day period. Chemical solutions and their order of presentation were selected with a random-numbers table, except that identical solutions were never repetitively tested on the same animal.

Preparation of chemical solutions

Special care was taken in preparing test solutions. First, stocks were made by dissolving glycine in artificial seawater prepared with HPLC-grade DI water and analytical grade salts according to the Marine Biological Laboratory formula (Cavanaugh, 1975). The concentrations of the stock solutions were 100-times higher than those of the test solutions. Stocks were divided in 1 ml aliquots and frozen at −20°C until used. Test solutions were made by adding 100 μl of an appropriate stock to 9.9 ml seawater; control solutions were made by adding 100 μl of artificial seawater to 9.9 ml seawater. In fact, each solution was made with seawater drawn from the same experimental chamber that was to be used in the assay. Test concentrations, measured by high-performance liquid chromatography (HPLC) (n = 14 trials), were very accurate and deviated only 2–13% from values estimated volumetrically. Glycine concentrations that were maintained in chamber seawater did not measurably change during the 3–5 min required to prepare a solution (see Results). Consequently, the glycine added with each test solution was an accurate representation of the stimulus introduced above seawater background.

Behavioral assays

Antennule flicking, antennule wiping, leg probing, and mouthpart labiating were all used as behavioral assays. Both electrophysiological and behavioral investigations have shown that flicking is associated with the detection of chemical stimuli (Snow, 1973; Pearson and Olla, 1977; Price and Ache, 1977; Pearson *et al.*, 1979; Schmitt and Ache, 1979; Rebach *et al.*, 1990). Antennule wiping against the mouthparts is believed to function either in cleaning or resetting those antennule chemoreceptors that are important to feeding (Snow, 1973; Fuzessery and Childress, 1975). While leg probing is used in contacting food and passing it to the mouth (Derby and Atema, 1982; Zimmer-Faust and Case, 1982), mouthpart labiating in preparation for eating is carried out with the endopodites on the third maxillipeds. The following responses are defined: (1) "glycine detection" is an increase in the rate of flicking, over 15 s or longer, within the 3-min test period; whereas (2) "glycine-mediated appetitive feeding" is the co-occurrence of flicking, wiping, leg probing, and mouthpart labiating, all within the 3-min test period. Thus combined, the four acts constitute the initial phases of feeding (Zimmer-Faust *et al.*, 1984), and they differ markedly from the incipient phases of other behaviors, such as socializing and predator avoidance (Zimmer-Faust *et al.*, 1985; Zimmer-Faust and Spanier, 1987).

Chemical determinations

Concentrations of glycine, ammonium, and 13 other free-amino acids in the seawater sampled from test solutions and experimental chambers were determined. Each aliquot (1 ml) was collected with a polypropylene syringe and teflon tubing immediately prior to an experimental test. Samples were filtered gently (<10 psig) to 0.22 μm, then placed in cryogenic vials, put on liquid nitrogen, and stored at −76°C. All labwares and membrane filters were washed with 10% HCl (Baker Altrex grade), rinsed with HPLC-grade DI water, and then rinsed again with sample seawater before use. Chemical determinations were made by reverse-phase HPLC.

Chemical analytical procedures followed those described previously by Jones *et al.* (1981) and Manahan *et al.* (1983). Samples were reacted with ortho-phthaldialdehyde (OPA) in the presence of mercaptans to form fluorescent products. Sub-samples (100 μl) of OPA-derivatives were withdrawn and separated on an Altex ultrasphere ODS column (150 × 4.6 mm; particle size = 5 μm; length 15 cm). A gradient was created between two sodium acetate/methanol buffers (solvent A; 400 ml sodium acetate, 95 ml methanol; solvent B: 100 ml sodium acetate, 400 ml methanol) (see Jones *et al.*, 1981), held at pH 6.8 to improve separation of phenylalanine and ammonium. The eluant buffers were controlled by a Gilson (Model 42) gradient analytical system with dual pumps (Model 302) interfaced with a PC-based programming module (Gilson Model 704). Peaks in the eluant stream were monitored with a Gilson (Model 121) fluorometer and identified by elution time, relative to known standards. Reagents and solvents all were HPLC grade, degassed prior to use.

Determination of the ratiometric dilution associated with introduction of a test stimulus solution

The dilution associated with stimulus delivery was determined for a fluorescent dye (sodium fluorescein) introduced in place of the test or control solutions (n = 24 trials). Fluorescence was monitored with a fast, multichannel fluorometer sampling continuously at 10 ms intervals over 3-min trials (Zimmer-Faust *et al.*, 1988). The fluorometer was equipped with an optical fiber probe (500 μm diameter) placed about 1 cm below the point at which the stimulus entered the test chambers. Optical fibers, as light collecting devices, have a distinct advantage over other fluorometric and spectrophotometric methods; *i.e.*, because flow cells and pumping are eliminated, water flow is not disrupted. The placement of the probe ensured that the dye and seawater would be sampled as they entered the chambers and before contacting either the olfactory (antennules) or taste (mouthparts, leg tips) organs of *P. interruptus*. Because the dilution of the fluorescein dye was estimated from values determined for peak fluorescence, subsequent calculations of stimulus concentrations were conservative and probably over-estimated slightly those concentrations actually contacting the sensory appendages.

The dilution of fluorescein dye measured in each trial, then averaged over all trials, was 0.056 (±0.11 SD) times the initial concentration introduced. This value is only slightly lower than 0.074, which is the dilution, calculated volumetrically, from the point of stimulus (and dye) input to the point of entry into the experimental chamber, assuming uniform mixing during transport and delivery. Consequently, volumetric measurements, which are more easily obtained, also accurately estimate stimulus dilution.

Results

Chemical determinations

The glycine concentrations in the seawater of experimental chambers were sampled prior to 40 selected trials. Each of these trials was chosen at random from among all of those performed, except that determinations were distributed equally among days. The sources and magnitudes of within-day variation in glycine are difficult to assess. Duplicate seawater samples were occasionally taken at the same time from single chambers. The average range of glycine concentrations determined from the duplicate analyses is the mean ± 11%. While this range seems rather large, it is typical of those found by other investigators that have previously measured free amino acids in seawater (*e.g.*, Fuhrman and Bell, 1985). Sixty-five percent of the variance in glycine concentration is explained by differences occurring between days. The between-day variation does not differ significantly from the variation measured within each day (One-way ANOVA: d.f. = 7/32, $F = 1.93$, $P > 0.10$); thus the data justifiably can be pooled. Means and variances are given in Table I for concentrations of glycine, ammonium, and 13 other free amino acids in the seawater of experimental chambers.

Table I

Concentrations (nM) of dissolved glycine, ammonium, and 13 other free amino acids in the seawater of experimental chambers, immediately before stimulus introduction

Compound	Concentration
alanine	72.6 ± 36.5
ammonium	2512. ± 468.
arginine	18.2 ± 15.7
aspartic acid	81.0 ± 31.2
glutamic acid	49.4 ± 21.0
glycine	153.1 ± 52.2
histidine	17.9 ± 10.1
isoleucine	14.4 ± 6.5
leucine	18.3 ± 4.5
lysine	37.4 ± 12.6
methionine	3.9 ± 2.0
phenylalanine	11.3 ± 2.7
serine	20.5 ± 7.4
tyrosine	6.4 ± 3.5
valine	20.7 ± 11.3

Values are means (±1 standard deviation) determined for samples drawn before 40 randomly chosen trials.

Glycine also was measured for seawater drawn each day from a pair of experimental chambers randomly chosen, one tank holding a lobster and the other not. Mean concentrations in the seawater of paired tanks were found to be nearly equal before, and again 60 min after placing lobsters (Table II). These data suggest that the glycine concentrations in seawater were stable over intervals that were longer than the duration of the behavioral bioassay. Nevertheless, small, instantaneous fluctuations in glycine might well have occurred during trial intervals. The effect would have been to limit the detection of the glycine stimulus by the lobsters and to increase the threshold of *jnd* proportional to the magnitudes of the fluctuations (see arguments of Cain, 1977a). Because a very low *jnd* threshold was determined (see next section), it is unlikely that glycine fluctuated much, if at all, during the trials.

Ammonium in the seawater of experimental chambers increased significantly when lobsters were being held (Table II, and Student's *t*-test: $t = 3.96$, d.f. = 14, $P < 0.01$). Similarly, concentrations of alanine, aspartic acid, glutamic acid, histidine, and lysine all increased, but to a lesser extent. Sixty minutes after lobsters were placed in the seawater, the mean total concentration of free amino acids was 556 (±131 n*M* SD), as compared to 497 (±110 n*M* SD) before. This difference is not significant (*t*-test: $t = 0.98$, d.f. = 14, $P > 0.20$). Similarly, the mean total concentration of free amino acids in seawater without lobsters was 469 (±106 n*M* SD) after 60 min, as compared to 478 (±91 n*M* SD) before. This difference also is not significant ($t = 0.18$, d.f. = 14, $P > 0.50$).

Psychophysical research has shown that animals respond to changes in chemical stimulus concentrations. In fact, it is the *proportional* change in concentration, called the Weber fraction (W_f), that animals detect. The Weber fraction is the difference in concentration measured before (C_b) and after (C_a) the introduction of a stimulus, divided by the concentration before:

$$W_f = (C_a - C_b)/C_b \qquad (1)$$

In this study with lobsters, the peak difference in glycine, $C_a - C_b$, was accurately estimated by multiplying the concentration (C_s) of stimulus added to the test solution by the ratiometric dilution (x) associated with stimulus delivery. The Weber fraction is then:

$$W_f = xC_s/C_c \qquad (2)$$

where C_c is the concentration of glycine in the seawater of the experimental chamber immediately before stimulus entry. C_s can be treated as a constant, because it varied insignificantly (2–13%) from trial to trial for a given glycine addition (see Materials and Methods). Alternatively, both x and C_c varied significantly from trial to trial, and this associated variance can be used to derive the precision with which W_f is estimated. The distribution of W_f is sto-

Table II

Concentrations (nM) of dissolved glycine, ammonium, and 13 other free amino acids in the seawater of experimental chambers with lobsters present or absent

	Lobsters present		Lobsters absent	
Compound	Time = 0	Time = 60	Time = 0	Time = 60
alanine	72.9 ± 46.7	119.1 ± 125.9	57.3 ± 35.6	59.8 ± 38.1
ammonium	1416. ± 499.	2464. ± 349.	1386. ± 422.	1283. ± 368.
arginine	15.2 ± 8.1	14.8 ± 5.2	17.4 ± 11.7	18.7 ± 15.7
aspartic acid	74.0 ± 19.7	88.0 ± 28.8	77.7 ± 21.8	71.7 ± 41.1
glutamic acid	47.4 ± 14.0	57.5 ± 21.1	36.2 ± 17.3	35.6 ± 14.7
glycine	151.1 ± 40.4	138.7 ± 52.6	155.3 ± 23.0	150.8 ± 50.3
histidine	16.8 ± 2.9	18.4 ± 8.0	15.3 ± 8.1	14.0 ± 8.5
isoleucine	11.6 ± 1.7	11.3 ± 2.8	11.7 ± 2.1	12.0 ± 1.5
leucine	16.4 ± 2.9	16.3 ± 6.0	16.5 ± 4.6	16.6 ± 3.5
lysine	32.8 ± 10.1	35.3 ± 9.8	36.0 ± 8.2	34.7 ± 12.6
methionine	3.1 ± 2.3	3.4 ± 1.3	3.3 ± 0.8	3.3 ± 1.3
phenylalanine	10.7 ± 3.1	9.6 ± 2.3	10.5 ± 1.2	10.4 ± 2.5
serine	17.3 ± 3.4	16.4 ± 4.5	19.9 ± 6.3	20.5 ± 7.4
tyrosine	6.4 ± 1.6	5.8 ± 2.4	7.0 ± 2.1	7.7 ± 3.5
valine	21.2 ± 4.0	22.0 ± 8.5	14.6 ± 3.7	14.2 ± 2.5

Samples in each treatment were drawn from seawater of eight experimental chambers before (time = 0), and again after a 60 min holding period. Values are means (±1 standard deviation).

chastic and cauchy, because W_f is a quotient of two stochastic variables, x and C_c (see equation 2). Mean and variance of a cauchy distribution are theoretically undefined, but can be approximated (Hoel *et al.*, 1971). The steps used in this approximation are as follows. (1) Log transform all values of x (*i.e.*, $x_1, x_2, x_3 \ldots x_{24}$), C_c (*i.e.*, $C_{c1}, C_{c2}, C_{c3} \ldots C_{c40}$) and C_s (10^{-2}, 10^{-3}, 10^{-4}, 10^{-5}, 10^{-6}, 10^{-7}, 5×10^{-8} and 10^{-8} M). (2) Apply equation 2, repetitively, using all combinations of log transformed values, x and C_c, in deriving the distribution of W_f for each constant, C_s [note that each distribution of W_f had 960 values]. (3) Finally, calculate the mean and variance of W_f for each distribution, then back transform by taking the antilogs. Because the distributions of x and C_c were always the same and only C_s (a constant) changed between derivations, the coefficients of variation (SD/$\bar{x}$) were identical for each distribution of W_f. The coefficient of variation was 0.5-times the mean, providing some indication of the precision with which W_f was measured.

Table III

Detection and appetitive feeding by lobsters to applied glycine stimuli and seawater (control)

		Proportion responding[a]		
C_s	W_f	Detection	Feeding	Number tested
1×10^{-2}	$3.65\ (\pm 1.79) \times 10^{3}$	1.00***	0.75***	20
1×10^{-3}	$3.65\ (\pm 1.79) \times 10^{2}$	1.00***	0.60***	20
1×10^{-4}	$3.65\ (\pm 1.79) \times 10^{1}$	1.00***	0.55***	20
1×10^{-5}	$3.65\ (\pm 1.79) \times 10^{0}$	1.00***	0.20*	20
1×10^{-6}	$3.65\ (\pm 1.79) \times 10^{-1}$	0.95***	0.00	20
1×10^{-7}	$3.65\ (\pm 1.79) \times 10^{-2}$	0.80**	0.00	20
5×10^{-8}	$1.82\ (\pm 0.90) \times 10^{-2}$	0.70*	0.00	20
1×10^{-8}	$3.65\ (\pm 1.79) \times 10^{-2}$	0.55	0.00	20
(seawater control)				
0	0	0.38	0.00	40

[a] The proportion tested and responding to stimulus is significantly different from the proportion tested and responding to seawater (control). (*G*-test with Yates' correction for continuity: d.f. = 1, *$P < 0.05$, **$P < 0.01$, ***$P < 0.001$).

C_s is the molarity of glycine added to the stimulus solution, while W_f is the Weber fraction. The lowest W_f detected is the threshold of *jnd* Values of W_f are expressed as means ±1 standard deviation).

Lobster responses to applied glycine stimuli

An application of a glycine stimulus was considered excitatory if the proportion of lobsters tested and responding was significantly greater than the proportion tested and responding to seawater (control). On this criterion, the threshold of *jnd* determined for glycine detection by lobsters was 1.8% (±0.9% SD) above background (Table III). Lobsters were less sensitive in responding to glycine as a feeding cue. Behavioral induction required an applied dose, at least 3.65-times above background (Table III).

Although the threshold of *jnd* for glycine detection seems quite low, several lines of evidence suggest that the estimate is accurate. First, great care was taken in the measurement of glycine concentrations and ratiometric dilution. Ratiometric dilution was calculated from values of *peak* fluorescence recorded in trials in which dye was released. Consequently, dilution associated with stimulus delivery was the *minimum* observed. Second, the threshold of *jnd* is little affected by the method of estimating ratiometric dilution, whether fluorometric or volumetric. Substituting a value calculated volumetrically, 0.074, produces a threshold of *jnd* that is 2.4% above background. Third, values calculated for W_f are very robust. It follows from equation 2 that W_f increases as x increases, as C_c decreases, and as x increases, while C_c decreases. Substituting a value of x two standard deviations above the mean, while also substituting a value of C_c two standard deviations below the mean, yields a threshold of *jnd* that is 8.0% above background. Finally, the duration of increased antennule flicking was shortened in response to the lowest stimulus concentrations tested. For example, lobsters responded to glycine applied at 5×10^{-8} M by increasing flicking over only a 20–30 s interval, beginning about 10 s after the initial introduction of the stimulus solution. The onset of detection coincided with the timing of peak fluorescence as measured in trials in which dye was released. Therefore, the detection of glycine at low concentrations of this stimulus appears to be restricted to the period during which the level of introduced stimulus peaks.

Interestingly, 38% of all lobsters tested increased their antennular flicking in response to seawater (control); *i.e.*, in the absence of an applied glycine stimulus (Table III). Possibly, the lobsters were detecting substances introduced as contaminants during solution preparation, or issuing from other unspecified sources. Alternatively, antennule flicking may have been triggered by small changes in water flow, or by air bubbles produced when a valve was opened and closed during the introduction of solutions. To distinguish these possibilities, 20 trials were performed in which the valve was opened and then closed without stimulus or seawater being introduced. Six of the 20 lobsters tested responded with an increased rate of antennular flicking. The proportion responding (30%) is nearly identical to that when the seawater (control) was applied. Consequently, increased flicking in response to the seawater (control) is probably caused by the valve being opened and closed, not by the lobsters detecting some unidentified, stimulatory compound.

Discussion

To my knowledge, this is the first measurement ever of a threshold of "just noticeable difference" for chemoreception in an aquatic animal. The threshold concentration for glycine stimulus detection by the spiny lobster, *Panulirus interruptus*, is about 2–8% higher than the glycine background in seawater. Repeated measurements were made of the ratiometric dilution associated with the delivery of stimulus solutions to the experimental chambers, of the glycine concentrations in the stimulus solutions, and of the glycine concentrations in the seawater of the experimental chambers. The threshold determination was found to be very robust, changing little as a consequence of variation in stimulus dilution and glycine levels.

The threshold of *jnd* reported here for lobsters (2–8%) is slightly lower than those (4–33%) found for olfactory and gustatory detection by terrestrial animals, including humans (McBurney *et al.*, 1967; Shumake *et al.*, 1969; Pfaffman *et al.*, 1971; Cain, 1977a, b; Slotnick and Ptak, 1977). Direct chemical measurements of applied stimulus and background were made in only one of these studies (Cain, 1977a), and background concentrations fluctuated significantly. Because the applied stimulus was not always maintained above the mean background concentration, signal detection theory was used in estimating the likelihood of a given difference between stimulus and background (Green and Swets, 1974; Egan, 1975). Signal detection theory was not required in this study of lobsters because the applied stimulus was assumed always to be above background. The application of signal detection theory neither increases nor decreases estimates of *jnd* thresholds, but explains how variation in background stimuli influences threshold estimates.

An emerging theme in chemoreception research concerns mechanisms by which animals distinguish a stimulus from the background noise. Carr (1988) has hypothesized that compounds containing novel structural moieties provide the best chemical cues to marine animals. This hypothesis is appealing because it is advantageous for animals to detect signals that maximize the contrast between stimulus and background. Alternatively, substances occurring as DOM also serve as feeding cues to marine animals (Laverack, 1988). In such instances, the compounds providing the best cues may be those maintained at the lowest levels in seawater. Because glycine is abundant in seawater, yet is an effective stimulus detected by *P. interruptus* at concentrations only slightly above background, the results reported here suggest another alternative. It may be beneficial for animals to maximize differential sensitivity for signal molecules that otherwise lack unique structural moieties, but are strongly correlated with a valuable or limiting resource. Glycine, for example, is consistently one of three or four most abundant free amino acids in marine invertebrate flesh (Carr, 1988), occurring at 30–200 mM. Glycine, therefore, clearly signals the presence of potential prey, because marine invertebrates are the principal food resource exploited by lobsters (Lindberg, 1955).

The mechanism by which lobsters detect small differences between glycine stimulus and background is unknown, although sensory adaptation may be involved.

Adaptation is a change in sensitivity to an applied stimulus resulting from continuous prior exposure to a background stimulus. Stimulus backgrounds maintained for 2–3 min, or longer, are enough to influence the physiological response thresholds of chemoreceptors on the antennules of the Florida spiny lobster, *Panulirus argus* (Trapido-Rosenthal *et al.,* 1990), and on the walking legs of the American lobster, *Homarus americanus* (Borroni and Atema, 1988). In both cases, the effect is to mediate a parallel shift in dose-response functions corresponding to changes in the concentration of the adapting background. Insight may be gained by considering conclusions drawn from investigations on vision and hearing. Adaptation is thought to maintain the auditory and visual senses in working states that allow the detection of small, instantaneous changes in stimulus intensity; *i.e.,* <1% above background (*sensu* Keidel *et al.,* 1961). In this way, adaptation may act as an early filter, processing information and tuning animal responses to small differences between applied and background stimuli. Additional investigation will clearly be needed to more fully explore the interactions between sensory adaptation and chemical detection by *Panulirus interruptus.*

There is also an urgent need for future investigators of marine chemoreceptive behavior to measure background stimuli in seawater. Numerous studies have assayed responses by marine animals, representing nearly every major phylum, to a broad suite of stimuli, including amino acids, organic acids, sugars and nucleotides that also occur as DOM (see reviews of Linstedt, 1971; Carr, 1988; Laverack, 1988). In several previous studies, the relationship between applied dose and animal response has been examined, yet in none of them were the background levels of stimulant in the seawater of the experimental chambers measured. If the concentrations of stimulus in seawater had varied significantly between studies, then the differences in threshold response measured in these investigations may have been more apparent than real. Given that marine organisms live in a noisy chemical environment, measurements of the ability to distinguish between stimulus and background are required. Determinations of *jnd* thresholds, therefore, are critical to an understanding of chemically mediated behavior in the sea.

Acknowledgments

The author expresses his gratitude to J. Favuzzi and Dr. J. J. Childress for providing use of the HPLC. This research was performed at U. C. Santa Barbara in the laboratory of Dr. J. F. Case, who graciously gave both intellectual and material support. The final manuscript was prepared at University of Washington, Friday Harbor Laboratories, using computing and library facilities generously provided by Dr. A. O. D. Willows, Director. Special thanks go to Dr. M. J. Weissburg and Dr. W. E. S. Carr, whose constructive criticisms were essential in developing the manuscript. This project was sponsored by grants from the National Science Foundation (R11-8956672), Atlantic Richfield Corporation, and the Whitehall Foundation.

Literature Cited

Ache, B. W. 1982. Chemoreception and thermoreception. Pp. 369–398 in *The Biology of Crustacea, Vol. 3,* H. L. Atwood and D. C. Sandeman, eds. Academic Press, New York.

Borroni, P. F., and J. Atema. 1988. Adaptation in chemoreceptor cells: I. Self-adapting backgrounds determine threshold and cause parallel shift of dose-response function. *J. Comp. Physiol. A Sens. Neural Behav. Physiol.* **164:** 67–74.

Bowlus, R. D., and G. N. Somero. 1979. Solute compatibility with enzyme function and structure: rationales for the selection of osmotic agents and end-products of anaerobic metabolism in marine invertebrates. *J. Exp. Zool.* **208:** 137–153.

Cain, W. S. 1977a. Differential sensitivity for smell: "noise" at the nose. *Science* **195:** 796–798.

Cain, W. S. 1977b. Odor magnitude: coarse *vs.* fine grain. *Percep. Psychophys.* **22:** 545–549.

Caldwell, R. L. 1982. Interspecific chemically mediated recognition in two competing stomatopods. *Mar. Behav. Physiol.* **8:** 189–197.

Carr, W. E. S. 1988. The molecular nature of chemical stimuli in the aquatic environment. Pp. 3–27, in *Sensory Biology of Aquatic Animals,* J. Atema, R. R. Fay, A. N. Popper, and W. N. Tavolga, eds. Springer-Verlag, New York.

Cavanaugh, G. M. 1975. *Formulae and Methods VI of the Marine Biological Laboratory Chemical Room, 6th ed.* Marine Biological Laboratory, Woods Hole.

Clark, M. E., G. A. Jackson, and W. J. North. 1972. Dissolved free amino acids in southern California coastal waters. *Limnol. Oceanogr.* **17:** 749–758.

Croll, R. P. 1983. Gastropod chemoreception. *Biol. Rev.* **58:** 293–319.

Dawson, R., and R. G. Pritchard. 1978. The determination of alpha-amino acids in sea water using a fluorometric analyzer. *Mar. Chem.* **6:** 27–40.

Derby, C. D., and J. Atema. 1982. The function of chemo- and mechano-receptors in lobster (*Homarus americanus*) feeding behavior. *J. Exp. Biol.* **98:** 317–327.

Egan, J. P. 1975. *Signal Detection Theory and ROC Analysis.* Academic Press, New York.

Fuhrman, J. A., and T. M. Bell. 1985. Biological considerations in the measurements of dissolved free amino acids in seawater and implications for chemical and microbial studies. *Mar. Ecol. Prog. Ser.* **25:** 13–21.

Fuzessery, Z. M., and J. J. Childress. 1975. Comparative chemosensitivity to amino acids and their role in the feeding activity of bathypelagic and littoral crustaceans. *Biol. Bull.* **149:** 522–538.

Garrasi, C., E. T. Degens, and K. Mopper. 1979. The free amino acid composition of seawater obtained without desalting and concentration. *Mar. Chem.* **8:** 71–85.

Gleeson, R. A., M. A. Adams, and A. B. Smith, III. 1984. Characterization of a sex pheromone in the blue crab, *Callinectes sapidus:* crustecdysone studies. *J. Chem. Ecol.* **10:** 913–921.

Green, D. M., and J. A. Swets. 1974. *Signal Detection Theory and Psychophysics.* Krieger Publishing Company, New York.

Hadfield, M. G., and D. Scheuer. 1985. Evidence for a soluble metamorphic inducer in *Phestilla:* ecological and biological data. *Bull. Mar. Sci.* **37:** 556–566.

Hoel, P. G., S. C. Port, and C. J. Stone. 1971. *Probability Theory.* Houghton Mifflin Company, Boston.

Jensen, G. C. 1989. Gregarious settlement by megalopae of the porcelain crabs *Petrolisthes cinctipes* (Randall) and *P. eriomerus* Stimpson. *J. Exp. Mar. Biol. Ecol.* **131:** 223–231.

Jones, B. N., S. Paabo, and S. Stein. 1981. Amino acid analysis and enzymatic sequence determination of peptides by an improved σ-phthaldialdehyde precolumn labeling procedure. *J. Liq. Chromatogr.* **4:** 565–586.

Keidel, W. D., U. O. Keidel, and M. E. Wigand. 1961. Adaptation: loss or gain of information? Pp. 319–338 in *Sensory Communication: Contributions to the Symposium on Principles of Sensory Communication,* W. A. Rosenblith, ed. M.I.T. Press, Cambridge.

Kuris, A. M. 1971. Population interactions between a shore crab and two symbionts. Ph.D. Dissertation, University of California, Berkeley.

La Barre, S. C., J. C. Coll, and P. W. Sammarco. 1986. Competitive strategies of soft corals (Coelenterata: Octocorallia) III. Spacing and aggressive interactions between alcyonaceans. *Mar. Ecol. Prog. Ser.* **28:** 147–156.

Laverack, M. S. 1988. The diversity of chemoreceptors. Pp. 287–312 in *Sensory Biology of Aquatic Animals,* J. Atema, R. R. Fay, A. N. Popper, and W. N. Tavolga, eds. Springer-Verlag, New York.

Lindberg, R. G. 1955. Growth, population dynamics and field behavior of the spiny lobster, *Panulirus interruptus* (Randall). *Univ. Cal. Publ. Zool.* **59:** 157–248.

Lindstedt, K. J. 1971. Chemical control of feeding behavior. *Comp. Biochem. Physiol.* **39A:** 553–581.

Manahan, D. T., S. H. Wright, and G. C. Stephens. 1983. Simultaneous determinations of net uptake of 16 amino acids by a marine bivalve. *Am. J. Physiol.* **244:** R832–R838.

McBurney, D. H., R. A. Kasschau, and L. M. Bogart. 1967. The effect of adaptation on taste *jnds. Percep. Psychophys.* **2:** 175–178.

Miller, R. L. 1989. Evidence for the presence of sexual pheromones in free-spawning starfish. *J. Exp. Mar. Biol. Ecol.* **130:** 205–221.

Moore, P., and J. Atema. 1988. A model of a temporal filter in chemoreception to extract directional information from a turbulent odor plume. *Biol. Bull.* **174:** 355–363.

Mopper, K., and P. Lindroth. 1982. Diel and depth variations in dissolved free amino acids and ammonium in the Baltic Sea determined by shipboard HPLC analysis. *Limnol. Oceanogr.* **27:** 336–347.

Morse, D. E. 1990. Recent progress in larval settlement and metamorphosis: closing the gaps between molecular biology and ecology. *Bull. Mar. Sci.* **46:** 465–483.

Pearson, W. H., and B. L. Olla. 1977. Chemoreception in the blue crab (*Callinectes sapidus*). *Biol. Bull.* **152:** 46–54.

Pearson, W. H., P. C. Sugarman, D. L. Woodruff, and B. L. Olla. 1979. Thresholds for detection and feeding behavior in the Dungeness crab, *Cancer magister* (Dana). *J. Exp. Mar. Biol. Ecol.* **39:** 65–78.

Peckarsky, B. L. 1980. Predator-prey interactions between stoneflies and mayflies: behavioral observations. *Ecology* **61:** 932–943.

Pfaffman, C., L. M. Bartoshuk, and D. H. McBurney. 1971. Taste psychophysics. Pp. 75–101 in *Handbook of Sensory Perception, Vol. IV,* L. M. Beidler, ed. Springer-Verlag, New York.

Price, R. B., and B. W. Ache. 1977. Peripheral modification of chemosensory information in the spiny lobster. *Comp. Biochem. Physiol.* **57A:** 249–253.

Raimondi, P. T. 1988. Settlement cues and determination of the vertical limit of an intertidal barnacle. *Ecology* **69:** 400–407.

Rebach, S., D. P. French, F. C. von Staden, M. B. Eilber, and V. E. Byrd. 1990. Antennular sensitivity of the rock crab *Cancer irroratus* to food substances. *J. Crust. Biol.* **10:** 213–217.

Sammarco, P. W., J. C. Coll, S. La Barre, and B. Willis. 1983. Competitive strategies of soft corals (Coelenterata: Octocorallia): allelopathic effects on selected scleractinian corals. *Coral Reefs* **1:** 173–178.

Schmitt, B. C., and B. W. Ache. 1979. Olfaction: responses of a decapod crustacean are enhanced by flicking. *Science* **205:** 204–206.

Shumake, S. A., J. C. Smith, and J. C. Tucker. 1969. Olfactory intensity-difference thresholds in the pigeon. *J. Comp. Physiol. Psychol.* **67:** 64–69.

Sih, A., and R. D. Moore. 1990. Interacting effects of predator and prey behavior in determining diets. Pp. 771–796 in *Behavioural Mechanisms of Food Selection,* R. N. Hughes, ed. Springer-Verlag, London.

Slotnick, B. M., and J. E. Ptak. 1977. Olfactory intensity-difference thresholds in rats and humans. *Physiol. Behav.* **19:** 795–802.

Snow, P. J. 1973. The antennular activities of the hermit crab, *Pagurus alaskensis* (Benedict). *J. Exp. Biol.* **58:** 745–765.

Sweatman, H. 1988. Field evidence that settling coral reef fish larvae detect resident fishes using dissolved chemical cues. *J. Exp. Mar. Biol. Ecol.* **124:** 163–174.

Trapido-Rosenthal, H. G., R. A. Gleeson, and W. E. S. Carr. 1990. The efflux of amino acids from the olfactory organ of the spiny lobster: biochemical measurements and physiological effects. *Biol. Bull.* **179:** 374–382.

Yancey, P. H., M. E. Clark, S. C. Hand, B. D. Bowlus, and G. N. Somero. 1982. Living with water stress: evolution of osmolyte systems. *Science* **217:** 1214–1222.

Zimmer-Faust, R. K. 1987. Crustacean chemical perception: towards a theory on optimal chemoreception. *Biol. Bull.* **172:** 10–29.

Zimmer-Faust, R. K. 1989. The relationship between chemoreception and foraging behavior in crustaceans. *Limnol. Oceanogr.* **34:** 1364–1374.

Zimmer-Faust, R. K., and J. F. Case. 1982. Organization of food search in the kelp crab, *Pugettia producta* (Randall). *J. Exp. Mar. Biol. Ecol.* **57:** 237–255.

Zimmer-Faust, R. K., and E. Spanier. 1987. Gregariousness and sociality in spiny lobsters: implications for den habitation. *J. Exp. Mar. Biol. Ecol.* **105:** 57–71.

Zimmer-Faust, R. K., J. M. Stanfill, and S. B. Collard, III. 1988. A fast, multichannel fluorometer for investigating aquatic chemoreception and odor trails. *Limnol. Oceanogr.* **33:** 1586–1595.

Zimmer-Faust, R. K., J. E. Tyre, and J. F. Case. 1985. Chemical attraction causing aggregation in the spiny lobster, *Panulirus interruptus* (Randall), and its probable ecological significance. *Biol. Bull.* **169:** 106–118.

Zimmer-Faust, R. K., J. E. Tyre, W. C. Michel, and J. F. Case. 1984. Chemical mediation of appetitive feeding in a marine decapod crustacean: the importance of suppression and synergism. *Biol. Bull.* **167:** 339–353.

Zurburg, W., and A. DeZwaan. 1981. The role of amino acids in anaerobiosis and osmoregulation in bivalves. *J. Exp. Zool.* **215:** 315–325.

Reference: *Biol. Bull.* **181:** 427–441. (December, 1991)

Proteins of Crustacean Exoskeletons: I. Similarities and Differences among Proteins of the Four Exoskeletal Layers of Four Brachyurans

JACK J. O'BRIEN,[1] S. SINDHU KUMARI, AND DOROTHY M. SKINNER[2]

Biology Division, P. O. Box 2009, Oak Ridge National Laboratory, Oak Ridge, Tennessee 37831-8077 and East Tennessee State University, Johnson City, Tennessee 37614

Abstract. Most of the proteins extracted from exocuticle, endocuticle, and membranous layer of four species of anecdysial (intermolt) crabs (the Bermuda land crab *Gecarcinus lateralis,* the rock crab *Cancer antennarius,* the shield-backed kelp crab *Pugettia producta,* and the southern shield-backed kelp crab *Taliepus nuttalli*) were 31 kDa or smaller; proteins of similar M_r were common to all three layers. Proteins from the membranous layer were qualitatively indistinguishable in all four species. More proteins 31 kDa or smaller were similar in size and pI to proteins from other exoskeletal layers than were proteins larger than 31 kDa. Proteins extracted from the epicuticle of *G. lateralis* included a group of five ranging from 54 to 42 kDa that bound $^{45}Ca^{++}$ *in vitro.* The group was not seen in other layers of the exoskeleton of *G. lateralis* or, with the exception of 44 and 42 kDa protein bands that were in the epicuticle of *C. antennarius,* in any layers of the exoskeletons of the other three species. During proecdysis, the membranous layer is completely degraded, and proteins 31 kDa or smaller are preferentially degraded from the exocuticle and endocuticle of the old exoskeleton of *G. lateralis,* which is cast as an exuvia at ecdysis. The relative amounts of proteins in extracts of epicuticle from (1) anecdysial exoskeletons and (2) exuviae were very similar, suggesting that there was little degradation of epicuticle during proecdysis. Some of the proteins of the three inner layers of the exoskeleton of *G. lateralis* have characteristics similar to those of flexible cuticles of insects; they have acidic pIs and they form "charge trains," *i.e.,* proteins of the same size separated by differences in charge during isoelectric focusing.

Introduction

Arthropods grow by molting, a programmed process of developmental changes that occurs prior to ecdysis (proecdysis) and in the period immediately following ecdysis (metecdysis). After the events of metecdysis are completed, the molting process is considered to be finished and the animal enters anecdysis, the intermolt period during which there is no further increase in external dimensions. During each proecdysial period, the epidermis underlying the exoskeleton synthesizes a new epicuticle and exocuticle, the two outermost layers of the new exoskeleton. Concomitantly, the epidermis degrades about 75% of the old exoskeleton, the remainder of which is shed as an exuvia at ecdysis (reviewed in Skinner, 1985; Stevenson, 1985; Skinner *et al.,* 1991).

The exoskeleton of an anecdysial (intermolt) decapod crustacean consists of four layers. From the outside in they are epicuticle, exocuticle, endocuticle, and membranous layer. The epicuticle is thin [about 7 μm; thicknesses are given for the Bermuda land crab *Gecarcinus lateralis* (Skinner, 1962)] and composed of proteins, lipids and calcium salts, but no chitin (Travis, 1955; Welinder, 1975b; Stevenson, 1985). The epicuticle is thought to render the exoskeleton impermeable (Mary and Krishnan, 1974), preventing both water loss and solubilization of exoskeletal components in aqueous habitats (Dennell, 1960). The exocuticle (about 30 μm) is a calcified matrix of chitin and protein. The epicuticle and exocuticle form the soft shell of the newly exuviated crab. These layers are thought to harden during metecdysis by tanning (Vacca and Fingerman, 1975a,b) and calcification (Travis,

---

Received

[1] Present address: Department of Biological Sciences, University of South Alabama, Mobile, Alabama 36688.

[2] Corresponding author.

1960). The endocuticle (about 200–400 μm) is also a calcified matrix of chitin and protein. Its synthesis and calcification begin in metecdysis, several days after ecdysis (Stage B of Drach, 1939; see Skinner, 1962), and continue through Stage C_3. The membranous layer (about 20–30 μm) also contains chitin and protein but is not calcified; it is the innermost layer and abuts the epidermis at the apical cell membrane. The membranous layer is synthesized during Stage C_3 (Green and Neff, 1972), and its completion signals the onset of anecdysis, or intermolt (stage C_4; Skinner, 1962, 1985). A discrete membranous layer has not been described in reviews of insect cuticle (Neville, 1975; Filshie, 1982; Willis, 1987).

Compared to the exoskeletons or cuticles of many other arthropods, the greater size and thickness of the decapod crustacean exoskeleton present distinct advantages for isolating individual layers of the exoskeleton and of exuviae. These characteristics of the crab exoskeleton also permit the recovery of significant amounts of protein from individual layers. It is much more difficult to separate the individual layers of the cuticles of most insects (Hackman, 1974).

Despite the recoverability of the separate layers of crustacean exoskeletons, amino acid compositions have been determined only for entire exoskeletons of the crayfish *Astacus fluviatilis* (Welinder, 1974, 1975a; Herzog *et al.*, 1975); the crabs *Scylla serrata* (Hackman, 1974), *Cancer pagurus*, and *Carcinus maenus;* the Norway lobster *Nephrops norvegicus;* and the shrimp *Penaeus duorarum* (Welinder, 1974). Tyrosine, which is a rather rare component of most proteins, constitutes 3 to 7.5% of the total amino acids in most analyses. Such a result might be expected if tyrosine is involved in protein cross-linking in crustacean exoskeletons (Vacca and Fingerman, 1975a,b). In general, exoskeletal proteins are rich in glycine, which may play a role in covalent binding of protein to chitin (Herzog *et al.*, 1975). Acidic amino acids account for approximately 20% of the total.

Intact proteins of some exoskeletons have also been analyzed. Exoskeletons have either been extracted directly and their proteins displayed on polyacrylamide gels (*S. serrata;* Hackman, 1974), or prior to analyses, fractionated into three parts: epicuticle plus exocuticle, endocuticle, and membranous layer (*C. pagurus;* Welinder, 1975b). In both of these investigations, the positions of the extracted proteins in polyacrylamide gels after electrophoresis were diagrammed, but the actual gels were not shown. The amino acid compositions of mixtures of the extracted proteins have also been determined (Hackman, 1974; Welinder, 1975b). Exoskeletal proteins of the crayfish *Astacus leptodactylus* have been sized on one dimensional polyacrylamide gels (Vranckx and Durliat, 1980, 1986). With the exception of the latter analysis, in which some of the proteins were as large as 400 kDa (Vranckx and Durliat, 1986), most of the exoskeletal proteins from Crustacea had M_r smaller than 30 kDa.

Finally, different concentrations of 20-hydroxyecdysone, selected to mimic hemolymph concentrations throughout the intermolt cycle, have been tested on the synthesis of crustacean integumentary proteins, both exoskeletal and cellular. The effects have been monitored *in vitro* in *A. leptodactylus* (Bielefeld *et al.*, 1986; Traub *et al.*, 1987) and both *in vitro* (Paulson and Skinner, 1991) and *in vivo* (Stringfellow and Skinner, 1988) in *G. lateralis.* The most significant effects were on the synthesis of small M_r proteins.

We have been investigating some of the cellular and molecular events in the molting process. They occur during proecdysis, and include synthesis of muscle in regenerating limbs concomitant with atrophy of muscle in chelae (Skinner, 1966; Mykles and Skinner, 1982, 1985), and synthesis of the two outer layers of a new exoskeleton (epicuticle and exocuticle) concomitant with the partial degradation of the old exoskeleton. The mechanisms that control such events must be complex. We focus here on the composition, synthesis, and turnover of the exoskeleton.

In this report, we describe proteins present in the four layers of brachyuran exoskeletons, with an emphasis on *G. lateralis,* the exoskeleton of which has been analyzed during several different stages of the intermolt cycle. We show electrophoretic patterns of proteins and compare the proteins present in anecdysial, proecdysial, and metecdysial exoskeletons and exuviae of *G. lateralis.* The distribution of a number of the proteins in one or more layers of the exoskeleton (data shown here), as well as the patterns of their synthesis (Stringfellow and Skinner, 1988; Paulson and Skinner, 1991) and degradation (O'Brien and Skinner, 1987, 1988), make them favorable candidates for the investigation of genes specifically activated during the molting process.

The exuvia is much more friable than the anecdysial exoskeleton. The cuticular proteins that are degraded during proecdysis may be involved in the calcification and maintenance of rigidity, whereas those that are "protected" from degradation may be more important in determining the framework and shape of the exoskeleton.

Materials and Methods

Experimental animals and preparation of layers of their exoskeletons

G. lateralis specimens obtained from the Bermuda Biological Station were maintained at approximately 25°C and 12:12 h light:dark cycle. Precocious molts were induced in *G. lateralis* by autotomy of more than four limbs (Skinner and Graham, 1970, 1972). Specimens of the rock crab *Cancer antennarius,* the shield-backed kelp crab

Pugettia producta, and the southern shield-backed kelp crab *Taliepus nuttalli,* were collected near Santa Barbara, California.

Anecdysial animals were placed on ice for 0.5–2 h to separate integumentary tissues from the membranous layer (O'Brien *et al.,* 1986). Cell debris was removed from the membranous layer, and the external surface of the carapace was cleaned with moist Kimwipes. Epicuticles from anecdysial animals were removed from the dorsal carapace with a power rotor (Li'l Crafty, Sears) equipped with a steel pyramidal bit. Both exoskeleton and rotor were held inside a plastic bag, which collected airborne particles of epicuticle as they were scraped from the carapace. The procedure was repeated to collect exocuticle. In *G. lateralis,* epicuticle (dark purple in the dorsal carapace), exocuticle (orange), and endocuticle (white), can be distinguished easily on the basis of color. Following removal of the epicuticle and exocuticle, the endocuticle was cracked and the membranous layer (ML) peeled away from the inner surface of the endocuticle; this provided ML C (membranous layer adjacent to epidermal cells; Fig. 2, lane 5). The inner layer of the endocuticle was also scraped to remove any remnants of membranous layer; this provided ML E (adjacent to endocuticle; Fig. 2, lane 4).

The possibility that particular proteins are associated with pigmented regions of the exoskeleton was determined as follows. From the same animals, proteins were extracted from the pooled three outer layers (epicuticle plus exocuticle plus endocuticle) of the highly pigmented dorsal carapaces of anecdysial crabs, and from the unpigmented regions of the branchiostegites. The branchiostegites are lateral extensions of the thoracic exoskeleton, and cover the gill chambers; their underlying integumentary tissues comprise an inner and an outer sheet of epidermis separated by a layer of connective tissue containing storage cells, tegumental glands, and hemolymph sinuses (Skinner, 1962). Proteins were also extracted from the two newly synthesized outer layers (epicuticle plus exocuticle) of unpigmented regions of branchiostegites, moderately pigmented lateral branchiostegites, and the purple dorsal region of the carapaces of metecdysial animals within a few hours following ecdysis during Stage A (Drach, 1939; Skinner, 1962). Exuviae, remnants of the old exoskeleton from which the animal emerges at ecdysis, are lined by a transparent ecdysial membrane (Stevenson, 1985) which was removed. Epicuticles, exocuticles, and endocuticles were recovered from exuviae by careful chipping with a sharp scalpel. During vacuum desiccation, pieces of epicuticle separated spontaneously and cleanly from exuviae.

Extraction of proteins

Exoskeletal layers were dried at room temperature. The three outer calcified layers were pulverized separately in a mortar and pestle, and membranous layers were minced. Samples were extracted in 5 *M* guanidine thiocyanate, 0.4 *M* EDTA, 5 m*M* Pipes, pH 7, (1:10, w:v), with gentle shaking at room temperature for 2–5 h. Extracts were centrifuged at 16,000 × *g* for 5 min in an Eppendorf microfuge, and the supernatants were recovered. Samples to be stored or electrophoresed were dialyzed against Buffer A (10 m*M* ammonium bicarbonate, pH 7.8) overnight at 4°C. Samples to be iodinated were dialyzed overnight at 4°C against 0.4 *M* NaCl, 2.5 m*M* NaN_3, 5 m*M* Pipes, pH 7. Following iodination by the chloramine T method (McConahey and Dixon, 1980), the samples were dialyzed against Buffer A at 4°C overnight until radioactivity in the dialysate was reduced to background. Protein was measured by fluorescence (Avruch and Wallach, 1971); aliquots were then lyophilized and stored at −60°C. Lyophilized proteins were solubilized in appropriate buffers for 1 or 2D gel electrophoresis. Samples for ash-free dry weights were dried to constant weight at 55°C and then heated at 500°C for 4 to 24 h in pre-ashed aluminum boats.

Gel electrophoresis

A discontinuous gel system was used for 1D gels (Laemmli, 1970). Separating gels were gradients of 5–15% polyacrylamide (Stringfellow and Skinner, 1988) or 9–18% polyacrylamide, the latter contained 0–10% glycerol (O'Brien and Skinner, 1988); stacking gels were 4.5% acrylamide. In 2D analyses, proteins were separated in the first dimension by isoelectric focusing (IEF) using tube gels (0.8 mm × 11 cm) composed of 9 *M* urea, 3.8% acrylamide, 0.2% bis, and 5% ampholines (O'Farrell *et al.,* 1977). The ampholines were a 1:1:1 blend of pH = 3–5, 4–6, and 3–10 (Bio-Rad) that produced an approximate gradient of pH 5–7. Proteins were separated in the second dimension by size on SDS slab gels (O'Farrell, 1975). Gels were stained with silver (Wray *et al.,* 1981) or Coomassie blue. To compare the efficacy of the two stains, some gels were stained first with Coomassie blue, destained, and restained with silver. The relative intensities of bands in stained 1D gels were quantified with an LKB 2202 ULTROSCAN laser densitometer attached to an Apple II computer (scans not shown). Autoradiography was as described (Stringfellow and Skinner, 1988; Paulson and Skinner, 1991).

Detection of calcium-binding proteins

Calcium-binding by proteins in gels was detected according to the method of Maruyama *et al.* (1984). Proteins (75–100 μg/lane) extracted from specific layers of *G. lateralis* exoskeleton were separated by SDS-PAGE. Gels were equilibrated in transfer buffer (25 m*M* Tris, pH 8.5, 192 m*M* glycine, 20% methanol) with 3 (100 ml) × 20 min washes. Proteins were transferred to 0.1 μm (pore size) nitrocellulose membranes (Schleicher and Schuell) with a Trans-Blot Electrophoretic Transfer Cell (Bio-Rad) at 4°C for 16 h at 60 V. Membranes were washed with 10 m*M* imidazole-HCl, pH 6.8, 60 m*M* KCl, 5 m*M* $MgCl_2$ (Buffer B), 3 (100 ml) × 20 min then soaked 10 min in 50 ml Buffer B with 1 mCi/L $^{45}Ca^{++}$ (New England Nuclear), washed for 5 min in 500 ml 50% ethanol and dried at room temperature.

Results and Discussion

The intermolt cycle of a decapod crustacean is divided into an intermolt period (anecdysis), a premolt period (proecdysis), ecdysis, and a postmolt period (metecdysis). Two layers of the new exoskeleton, the epicuticle (outermost layer) and the exocuticle (the next inner layer) are synthesized during proecdysis. The animal emerges at ecdysis clad in these two layers only; the partially degraded old exoskeleton is shed as an exuvia. In metecdysis, synthesis of an endocuticle begins. In *G. lateralis,* formation of the endocuticle continues for a month or so after which synthesis of the innermost layer, the membranous layer, begins. The completion of the membranous layer signals the beginning of anecdysis.

Characteristics of the layers of the anecdysial (intermolt) exoskeleton

Some characteristics of the four layers of the anecdysial exoskeleton of *G. lateralis* are listed in Table I. Epicuticle constituted about 15%, exocuticle 8%, endocuticle 75%, and membranous layer only about 2% of the dry weight. The large contribution of the epicuticle may be related to its role in inhibiting water loss. Desiccation is a major influence affecting adaptation of crabs to a terrestrial environment (Wolcott, 1988) and *G. lateralis* has one of the lowest rates of evaporative water loss among brachyurans (Greenaway, 1988). Because epicuticle is only one quarter the thickness of exocuticle but has twice the dry weight, the water content of the native epicuticle must also be very low.

The concentration of extractable protein per unit mass of dry weight was lowest in the epicuticle and increased progressively with each deeper layer. Although the innermost membranous layer contributed the least to the relative weight of the exoskeleton, perhaps due to the lack of calcium salts, it yielded the most extractable protein per unit mass. Ash-free dry weights of the exoskeleton measure the relative composition of inorganic material, chiefly calcium salts in the form of calcite (Roer and Dillaman, 1984). The epicuticle and exocuticle of *G. lateralis* had slightly higher levels of inorganic material than the underlying endocuticle; the relative ash-free composition in the three outer layers of the exoskeleton ranged from 68 to 79% of their dry weights. These levels are only slightly less than levels of calcium salts found in the four layers combined of the carapaces of the marine crabs *C. pagurus* (85.0%) and *C. maenas* (84.1%; Welinder, 1974), and are very similar to the calcium content measured for the four layers combined of the carapace of the freshwater crayfish *A. fluviatilis* (78.8%; Welinder, 1975a).

Table I

Characteristics of layers of exoskeleton of Gecarcinus lateralis

Layer	Relative dry weight (% of total)	Protein concentration (μg protein/mg dry wt.)	Ash-free dry weight (% of pre-ash wt.)
Epicuticle	14.9	4.1	78.7
Exocuticle	8.2	8.3	76.1
Endocuticle	75.2	13.3	67.8
Membranous layer	1.7	69.3	1.9

Comments on methods used for detecting proteins on gels

Each of the three common methods for visualizing proteins in polyacrylamide gels, (1) staining with Coomassie blue (Fristrom *et al.*, 1978; Cox and Willis, 1985; Cox, 1987; Kimbrell *et al.,* 1988) or (2) silver staining (Wray *et al.,* 1981; Schleicher and Watterson, 1983; O'Brien and Skinner, 1987; Stringfellow and Skinner, 1988), or (3) autoradiography of iodinated proteins (O'Brien and Skinner, 1987; 1988), has some disadvantages. Differences in staining are observed when proteins extracted from the four layers of the exoskeleton of *G. lateralis* are electrophoresed in a single gel and then stained first with Coomassie, then, after destaining, restained with silver (Fig. 1). Two to three times as many protein bands stain intensely with silver (lanes 3, 5, 7, and 9) as with Coomassie blue (lanes 2, 4, 6, and 8). Silver staining is generally a more sensitive technique (Wray *et al.,* 1981). Nevertheless, silver stains certain proteins less intensely than Coomassie. For example, a pair of bands of about 14 and 13 kDa is clearly seen in Coomassie blue-stained lanes of epicuticle, exocuticle, and endocuticle, as is a 15 kDa band in epicuticle; only trace amounts of these three protein bands are seen in the silver-stained gel (Fig. 1). Iodination of proteins is the most sensitive method. With only 0.8 to 15.2 μg iodinated proteins in 2D gels (Fig. 4A–D), a number of novel spots were seen in charge trains forming a series of spots of the same M_r spanning a range of pH.

Two series of Coomassie blue-stained 2D gels of each of the four exoskeletal layers were analyzed. In one, 20 μg protein (slightly more than the maximum amount of iodinated protein used in any of the autoradiographs

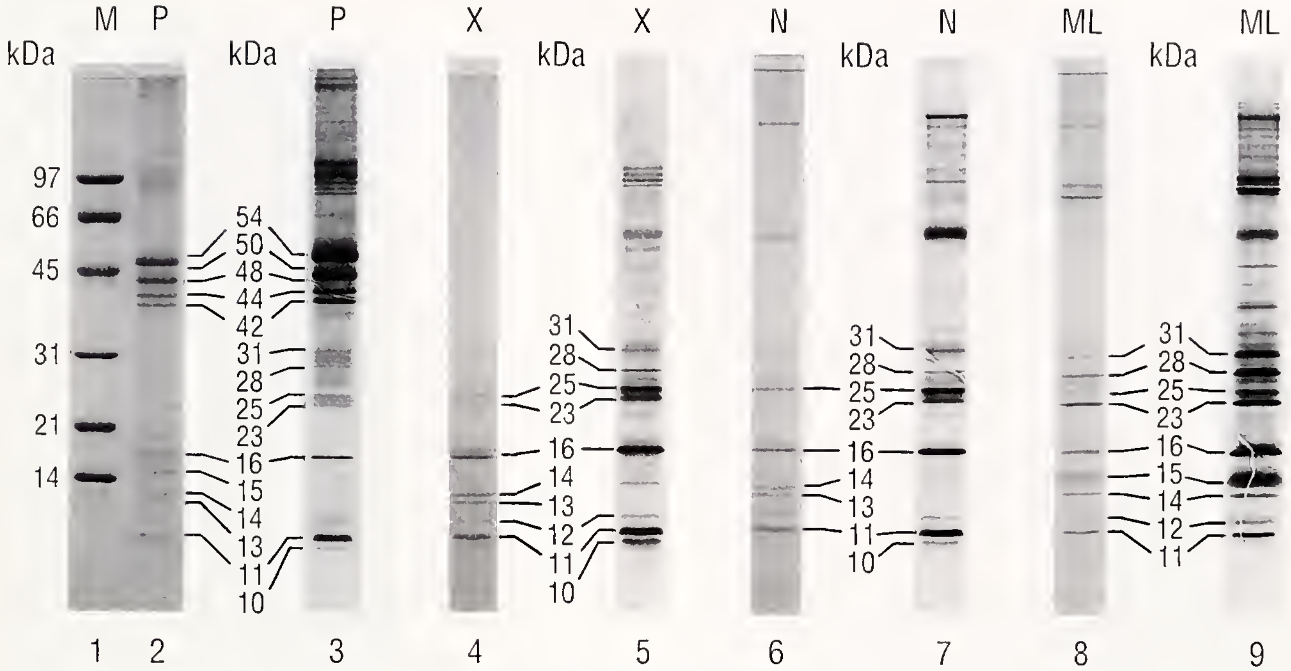

Figure 1. Comparison of *Gecarcinus lateralis* exoskeletal proteins stained with either Coomassie blue or silver. Lanes are from a 1D gel (9–18% acrylamide; 0–10% glycerol) on which was electrophoresed proteins (30 μg/lane) of each of the four exoskeletal layers of an anecdysial crab. After electrophoresis, the gel was stained with Coomassie blue, photographed, destained, then stained with silver and photographed again. The lanes from the two photographs were cut out and the two differently stained lanes of each of the four exoskeletal layers were placed adjacent to each other. Lane 1, low molecular weight standards (Bio-Rad), stained with Coomassie blue. Lanes 2–9, layers from exoskeleton; lanes 2, 3, epicuticle, P; lanes 4, 5, exocuticle, X; lanes 6, 7, endocuticle, N; lanes 8, 9, membranous layer, ML. Lanes 1, 2, 4, 6, and 8, stained with Coomassie blue; alternate lanes stained with silver. Approximate sizes of major protein bands equal or smaller than 55 kDa are indicated between the paired lanes; a dash indicates in which lane the band is present. Proteins larger than 55 kDa could not be accurately sized because a high concentration of acrylamide had been used and only low M_r standards had been run.

shown in Fig. 4) was loaded on each IEF tube gel and electrophoresed, after which the second dimension gels (9–18% acrylamide) were stained with Coomassie blue. In the gel of the epicuticle, only a group of five proteins, ranging in size from 54 to 42 kDa, referred to here as the epicuticular quintet, could be detected (data not shown). No bands were seen in the gels of the other layers even after attempts to maximally enhance visualization of the proteins.

In preparation for amino acid sequencing of individual protein spots, large amounts of protein (250 μg/gel), isolated from each of the four exoskeletal layers were electrophoresed on a second set of 2D gels. The gels were blotted on PVDF (polyvinylidene difluoride) membranes, which have a higher binding capacity than other types of membranes (Graddis, 1990). Fixation with 0.5% glutaraldehyde (Karey and Sirbasku, 1989) further increased the retention of the proteins to the filters. When such blots were stained with Coomassie blue, many spots were seen (Table III) that were not detected when smaller quantities of protein were analyzed.

Although radioiodination is the most sensitive method, the intensity of the bands observed depends on the amino acid composition of the proteins. Tyrosines, and to a lesser extent histidines, are the primary targets of iodination and proteins rich in these amino acids are the most readily visualized. In addition, iodination may cause structural modifications that may alter the electrophoretic mobilities on gels and, consequently, the banding patterns of proteins in comparison to the banding patterns of untreated proteins that are electrophoresed and then visualized by staining with either silver or Coomassie blue. Nevertheless, when populations of proteins are similarly treated, iodinated in this case, the same structural modifications should be sustained by the same proteins in each population. Thus, meaningful comparisons can be made among preparations analyzed by the same method.

Analysis of extractable proteins in anecdysial exoskeleton and exuvia by 1D gel electrophoresis

In the following, proteins of anecdysial (intermolt) animals are considered first, then proteins of proecdysial (prior to ecdysis) and metecdysial (after ecdysis) animals. In each category, layers of the exoskeleton are described from most external to most internal, *i.e.*, epicuticle, exocuticle, endocuticle, and membranous layer.

The members of the epicuticular quintet were prominent in both anecdysial epicuticle and epicuticle of exuviae (Fig. 2, lanes 1, 6, 7). Exuviae contain epicuticle and remnants of exocuticle and endocuticle, but little if any membranous layer, most or all of which is degraded during proecdysis. The presence of the epicuticular quintet was correlated with the extent of pigmentation (see Fig. 3). Other proteins ranging from 94 to 80 kDa that were prominent in anecdysial epicuticle, exocuticle, and endocuticle were missing from epicuticle of exuviae and markedly reduced in the other two layers (Fig. 2). Other than lacking the 94–80 kDa proteins, the profiles of epicuticle protein extracts were very similar before and after ecdysis.

Extracts from exocuticle, endocuticle, and membranous layer from anecdysial *G. lateralis* contained many protein bands 31 kDa or smaller (Fig. 2, lanes 2–5). Although protein bands of these sizes formed only traces in epicuticle, many were prominent in the other three layers. While this result points up a different composition for the epicuticle, the correspondence of M_rs of proteins in the other three layers does not necessarily imply their identity.

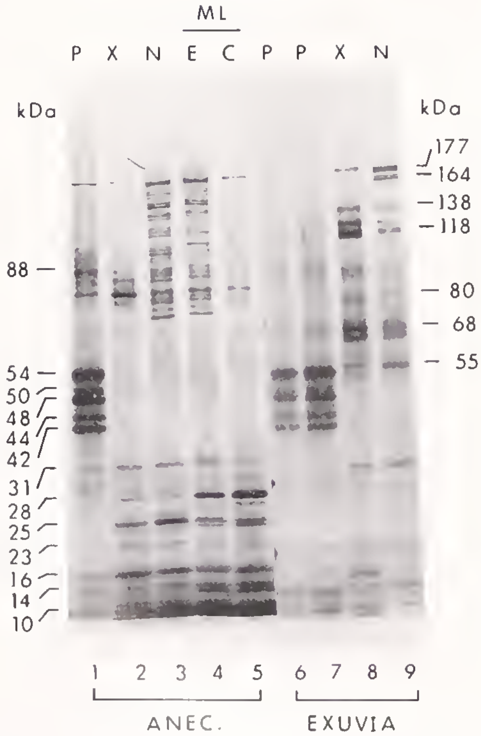

Figure 2. Proteins in anecdysial layers of the exoskeleton and layers of the exuvia of *Gecarcinus lateralis*. Silver-stained SDS gel (5–15% acrylamide), 7.5 μg protein/lane. Abbreviations as in Figure 1. Numbers to left and right of lanes indicate M_rs (kDa) of protein bands. Lanes 1–5, layers from exoskeleton of anecdysial animal. Lane 1, P; lane 2, X; lane 3, N; lane 4, membranous layer adjacent to endocuticle, ML E; lane 5, membranous layer adjacent to epidermal cells of integumentary tissues, ML C. Lanes 6–9, layers from exuvia. Lane 6, epicuticle isolated by vacuum desiccation, P; lane 7, epicuticle isolated by chipping with a scalpel, P; lane 8, X; lane 9, N.

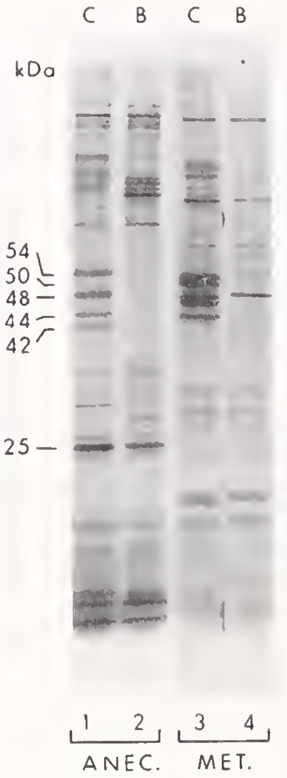

Figure 3. Epicuticular quintet occurs in pigmented regions of exoskeleton. Proteins extracted from P + X + N of the branchiostegite and dorsal carapace regions of *Gecarcinus lateralis*. SDS silver-stained gel (9–18% acrylamide, 0–10% glycerol); 7.5 μg protein/lane. C, dorsal carapace; B, branchiostegite. Numbers to left indicate M_rs (kDa) of protein bands. Lane 1, anecdysial purple dorsal carapace; lane 2, anecdysial unpigmented branchiostegite; lane 3, metecdysial purple dorsal carapace; lane 4, metecdysial unpigmented branchiostegite.

Protein bands of 16–10 kDa were very conspicuous in both fractions of the membranous layer (ML E, closer to endocuticle, and ML C, closer to epidermal cells); low M_r bands were also conspicuous in exocuticle and endocuticle. Most of these major low M_r protein bands as well as a prominent 25 kDa band in exocuticle, endocuticle, and ML C, were present only in trace amounts or missing in extracts from exuviae (Fig. 2, lanes 6–9). As a consequence of the preferential degradation of small M_r proteins *in vivo* during proecdysis, a number of other proteins 55 kDa or larger were relatively more prominent in extracts from exocuticle and endocuticle of exuviae than from the same layers from anecdysial animals.

Protein patterns in exocuticle extracts were highly reproducible. The gel shown in Figure 1 was 9–18% acrylamide and 0–10% in glycerol; the gel in Figure 2 was 5–15% acrylamide. The different concentrations of acrylamide in the two gels facilitate the clear display of proteins of low M_r in Figure 1 and those of high M_r in Figure 2. Comparison of the silver-stained lanes of all four layers including the membranous layer of Figure 1 (in which ML E and ML C were not separated) with the same lanes in Figure 2 (membranous layer operationally subdivided into ML E plus ML C) indicates the presence of many bands of similar M_r. As mentioned above, many of the protein bands that stained with silver did not stain with Coomassie blue; in particular, note those larger than 16 kDa seen only as traces or not seen at all in exocuticle and endocuticle, and those larger than 28 kDa also seen only as traces or not seen at all in the membranous layer. Evidence that the protein extractions are reproducible is also seen in Figure 2, lanes 6 and 7; arrays of proteins on 1D gels of extracts of epicuticle from *G. lateralis* that had been removed from exuviae by either a scalpel or vacuum desiccation were indistinguishable from one another. Epicuticle from highly pigmented regions of anecdysial exoskeletons (Fig. 1, lanes 2 and 3; Fig. 2, lane 1; Fig. 3, lane 1), exuviae (Fig. 2, lanes 6 and 7), and metecdysial exoskeleton (Fig. 3, lane 3) of *G. lateralis*, the latter extracted one day after ecdysis, contained the proteins of the epicuticular quintet.

As previously described (O'Brien and Skinner, 1987, 1988), we have isolated from integumentary tissues two alkaline cysteine proteinase activities (ACPs) and two proteinases with acidic pH optima (APs) that preferentially degraded membranous layer proteins 26 kDa or smaller. The absence of small M_r proteins from exuviae (Fig. 2, lanes 8 and 9) suggests that some (or all) of the ACPs and APs isolated from integumentary tissues participate in the degradation of the exoskeleton of the land crab during proecdysis. Other proteinases, as yet unidentified, may also contribute to the degradation.

Correlation of the epicuticular quintet with pigmentation

The epicuticular quintet, which was not seen in extracts of any other layer, was prominent in extracts of pigmented dorsal carapace of both anecdysial (epicuticle plus exocuticle plus endocuticle combined; Fig. 3) and metecdysial animals (epicuticle plus exocuticle combined), but much less prominent in extracts of unpigmented regions of branchiostegites of anecdysial and metecdysial animals. A 48 kDa protein band conspicuous in unpigmented regions of branchiostegites from metecdysial animals (Fig. 3, lane 4) is discussed in the section on proteins from metecdysial animals, below.

Two proteins of 54 and 42 kDa are major components in extracts of integumentary tissues maintained *in vitro*, labeled with ^{3}H-tyrosine, ^{3}H-leucine, or ^{35}S-methionine and electrophoresed on polyacrylamide gels (Stringfellow and Skinner, 1988). Both proteins are labeled with both leucine and methionine at relatively high rates throughout the intermolt cycle. During the stages of proecdysis when epicuticle and exocuticle are synthesized ($D_{2,early}$ and $D_{2,late}$), incorporation of methionine increases considerably, that of leucine more than doubles, and that of tyrosine, undetectable during anecdysis and early proecdysis, is almost as high as that of the other two radiolabeled amino acids (Stringfellow and Skinner, 1988). The absence of significant stainable quantities of the 54 and 42 kDa proteins from all layers of the exoskeleton of *G. lateralis* other than epicuticle may be due to a rapid turnover of these proteins as compared to longer-lived structural proteins of the exoskeleton. Alternatively, these may not be structural proteins of the exoskeletal matrix but may be metabolically active proteins in epidermal cells of the underlying integumentary tissues or in extensions of cells within pore canals that permeate the exoskeleton (Green and Neff, 1972; Halcrow, 1976; Roer, 1980).

In addition to the quintet, a major 25 kDa protein band is seen in samples of pooled epicuticle plus exocuticle plus endocuticle from both pigmented and unpigmented regions of anecdysial crabs (Fig. 3, lanes 1 and 2). The sources of the 25 kDa protein band are, in all likelihood, exocuticle and endocuticle; note the intense staining of the 25 kDa protein in those two layers relative to that in epicuticle (Fig. 2, compare lane 1 with lanes 2 and 3). The protein is not seen immediately after ecdysis (stage A of metecdysis) even though the newly synthesized exocuticle is present. Since the protein is extractable from anecdysial exocuticle, which should be considerably more rigid than metecdysial exocuticle, it seems unlikely that the protein is not extractable because the exocuticle has begun to harden (Fig. 3, lanes 3 and 4).

Distinguishing individual proteins by 2D gel electrophoresis: anecdysial exoskeleton

Analysis of 2D gels of radioiodinated (Fig. 4; Table II) exoskeletal proteins from each layer gave a somewhat different pattern of overlaps than the analysis of 2D gels of proteins stained with Coomassie blue (Table III). Nevertheless, the principal conclusion is the same in either case: proteins 31 kDa or smaller show extensive similarity (percentage of proteins of equivalent M_r and pI) among the layers, while proteins larger than 31 kDa show very much less similarity. In any case, whether the overlapping proteins are in fact identical awaits amino acid sequencing.

Epicuticular proteins (Fig. 4A), especially those 31 kDa or smaller, displayed the most distinct pattern when compared to proteins extracted from the other three layers. Epicuticle differs from the other three layers in: (1) the presence of the epicuticular quintet (Figs. 1–3); (2) having

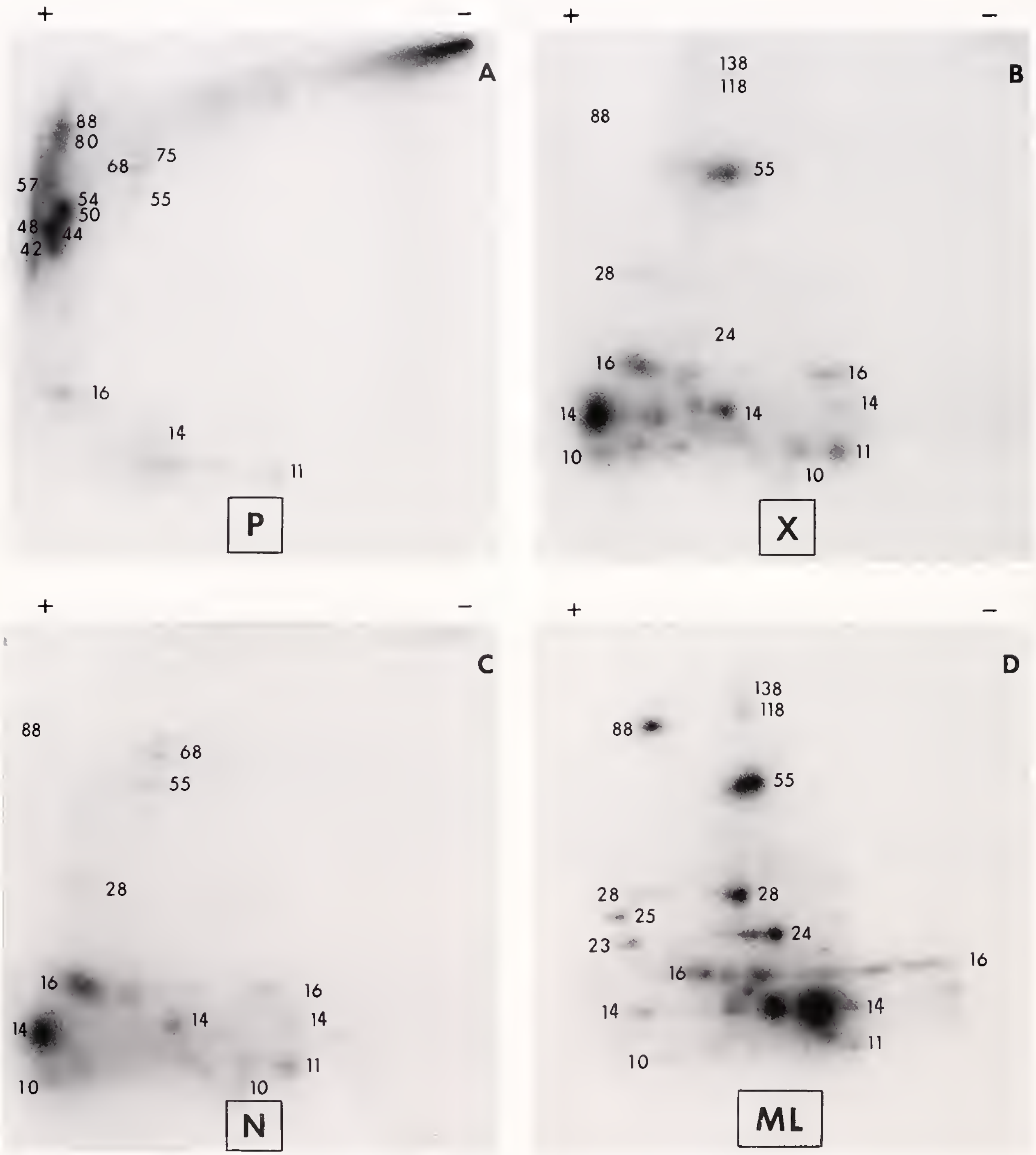
+
−
A
88
80
75
68
57
54
50
55
48
44
42
16
14
11
P
+
−
B
138
118
88
55
28
24
16
16
14
14
14
10
11
10
X
+
−
C
88
68
55
28
16
16
14
14
14
11
10
10
N
+
−
D
138
118
88
55
28
28
25
24
23
16
16
14
14
11
10
ML

Figure 4. Analyses on 2D gels of proteins from the four layers of the anecdysial exoskeleton of *Gecarcinus lateralis*. Autoradiographs of 2D gels. SDS gel for second dimension was 9–18% polyacrylamide, 0–10% glycerol. Approximate M_rs (kDa) of proteins are indicated adjacent to spots. (A) epicuticle; 3×10^6 cpm, 0.81 μg proteins. Streak in upper right corner is an artifact. (B) As (A) except 15.2 μg exocuticle proteins. (C) As (A) except 10.6 μg endocuticle proteins. (D) As (A) except 13.2 μg membranous layer proteins. Autoradiographs A–C exposed 48 h; D exposed 42 h.

Table II

Overlap on 2D gels (similar M_r and pI) of proteins isolated from the four different layers of anecdysial Gecarcinus lateralis *exoskeleton and labeled with* ^{125}I

	No. spots on gel	All Proteins P	All Proteins X	All Proteins N	All Proteins ML	No. spots on gel	>31 kDa P	>31 kDa X	>31 kDa N	>31 kDa ML	No. spots on gel	<31 kDa P	<31 kDa X	<31 kDa N	<31 kDa ML
		% (no.) of overlapping spots					% (no.) of overlapping spots					% (no.) of overlapping spots			
P	27	—	52 (14)	56 (15)	44 (12)	14	—	21 (3)	28 (4)	7 (1)	13	—	85 (11)	85 (11)	85 (11)
X	49	28 (14)	—	80 (39)	71 (35)	9	33 (3)	—	56 (5)	33 (3)	40	28 (11)	—	85 (34)	80 (32)
N	44	34 (15)	89 (39)	—	84 (37)	9	44 (4)	56 (5)	—	67 (6)	35	31 (11)	97 (34)	—	88 (31)
ML	54	22 (12)	65 (35)	68 (37)	—	9	11 (1)	33 (3)	67 (6)	—	45	24 (11)	71 (32)	69 (31)	—

A transparency of an autoradiograph or blot was laid over a transparency of the autoradiograph or blot of the exoskeletal layer to which it was to be compared. The number of spots in each category (total, >31 kDa, <31 kDa) on the 2D gel from each layer is listed in the left-hand column of each of the three sections of the table. In the other boxes in the table are given the percent (number in parentheses) of spots from each exoskeletal layer that matched the spots (same M_r and pI) from the exoskeletal layer listed on the left. P, epicuticle; X, exocuticle; N, endocuticle; ML, membranous layer. Fewer spots are numbered in the 2D gels in Figure 4A–D than are listed in Table II because some spots visible in autoradiographs were lost in reproduction. In addition, intense spots in some autoradiographs were composed of more than one protein; this was verified by inspection of other autoradiographs that had shorter exposure times.

fewer proteins 31 kDa or smaller in comparison to the other layers (Tables II and III); and (3) the absence of proteins that in other layers formed charge trains on 2D gels in the pH range of the IEF gradient (compare Fig. 4A with Fig. 4B–D). The charge trains can be seen as a series of spots of the same M_r spanning a range of pH. Note that only 0.8 μg epicuticular proteins were required to obtain 3×10^6 cpm for the autoradiograph as compared to 10- to 20-times as much protein for autoradiographs of the other layers. The proteins of the epicuticular quintet may be richer in tyrosine or histidine, and therefore more heavily iodinated, than proteins from other exoskeletal layers. Nevertheless, the epicuticular quintet proteins are also major components in gels stained with silver (Fig. 1, lane 3; Fig. 2, lanes 1, 6, 7) or Coomassie blue (Fig. 1, lane 2).

Similarities and differences of proteins in the four exoskeletal layers: anecdysial

For iodinated proteins 31 kDa or smaller (Table II), the degree of similarity was 69 to 97% among extracts from the exocuticle (Fig. 4B), endocuticle (Fig. 4C), and membranous layer (Fig. 4D). Thirty-nine of the 49 proteins in exocuticle matched 39 of the 44 proteins in endocuticle. The proteins (total) in extracts of membranous layer (Fig. 4D) were also similar in size and pI to those extracted from exocuticle and endocuticle. Of 54 membranous layer proteins, 71% were similar to proteins of exocuticle and 84% to those of endocuticle.

An 88 kDa protein was prominent in extracts of membranous layer (Fig. 4D); a similar sized protein was also present in extracts of the anecdysial epicuticle, but to a lesser extent. Only traces of an 88 kDa protein were seen in the other two anecdysial layers. The 88 kDa proteins stain only lightly with silver and are thus not seen in all layers in Figures 1 and 2; they label to a very high specific activity with ^{125}I, implying a richness in tyrosine or histidine (McConahey and Dixon, 1980). They may be identical with, or related to, the 89 kDa protein that incorporated ^{35}S-methionine, ^{3}H-leucine, or ^{3}H-tyrosine as much as twice as fast during proecdysis as compared to anecdysis (Stringfellow and Skinner, 1988). Several pro-

Table III

Overlap on 2D gels (similar M_r and pI) of proteins isolated from anecdysial Gecarcinus lateralis *exoskeleton and stained with Coomassie blue*

	No. spots on gel	All Proteins P	All Proteins X	All Proteins N	All Proteins ML	No. spots on gel	>31 kDa P	>31 kDa X	>31 kDa N	>31 kDa ML	No. spots on gel	<31 kDa P	<31 kDa X	<31 kDa N	<31 kDa ML
		% (no.) of overlapping spots					% (no.) of overlapping spots					% (no.) of overlapping spots			
P	40	—	55 (22)	38 (15)	25 (10)	12	—	25 (3)	8 (1)	0 (0)	28	—	68 (19)	50 (14)	36 (10)
X	49	49 (24)	—	39 (19)	41 (20)	16	19 (3)	—	31 (5)	38 (6)	33	64 (21)	—	42 (14)	42 (14)
N	45	27 (12)	51 (23)	—	44 (20)	16	13 (2)	44 (7)	—	25 (4)	29	34 (10)	55 (16)	—	55 (16)
ML	45	22 (10)	44 (20)	44 (20)	—	19	0 (0)	32 (6)	21 (4)	—	26	38 (10)	54 (14)	62 (16)	—

As Table II except data are from Coomassie blue stained PVDF filters.

teins of approximately 90 kDa (PCP-28) that are specific to pupal cuticles of *M. sexta* were also labeled by ^{3}H-leucine and focused at about the same pI (Kiely and Riddiford, 1985) as did the crab protein. The 88 kDa proteins were not degraded *in vivo* or *in vitro* by proteinases endogenous to the membranous layer (see Fig. 5 in O'Brien and Skinner, 1987) and were prominent in iodinated extracts of exuviae of *G. lateralis* (data not shown).

For Coomassie blue stained proteins smaller than 31 kDa (Table III), the degree of similarity was 36 to 68% among extracts from the exocuticle, endocuticle, and membranous layer. Twenty-three of the 49 proteins in exocuticle matched 23 of the 45 proteins in endocuticle. The proteins (total) in extracts of membranous layer were also quite similar in size and pI to those extracted from exocuticle and endocuticle. Of a total of 45 membranous layer proteins, 41% were similar to proteins of exocuticle and 44% to those of endocuticle.

Charge trains in proteins of anecdysial exoskeletal layers

Proteins that are approximately the same size, but that differ in net charge, form charge trains in isoelectric focusing gels. All four layers of the exoskeleton from anecdysial crabs had proteins with acidic pIs, and some of the proteins from the three internal layers formed charge trains between pH 5 and 7 (Fig. 4). These patterns are similar to those of proteins extracted from flexible insect cuticle (Andersen *et al.*, 1986; Cox and Willis, 1987a,b). There were more charge trains in membranous layer extracts than in extracts from other exoskeletal layers; these were at 28, 25, 24, 16, 14, 11, and 10 kDa (Fig. 4D). A 28 kDa protein band, minor in both exocuticle and endocuticle (Figs. 1, 2), focused in the acidic region of the gels (Fig. 4B, C). The major component of a 28 kDa charge train in the membranous layer focused in the neutral to basic region (Fig. 4D), similar to a 27 kDa charge train in the innermost layers of *M. sexta* endocuticle (Wolfgang and Riddiford, 1986), equivalent to the crustacean membranous layer. In 1D gels stained with silver, the 25 kDa protein band was very intense; the 24 kDa band barely detectable. The 24 kDa proteins may thus be expected to be very rich in tyrosine or histidine and consequently be more highly labeled *in vitro* with ^{125}I. In fact, in integumentary tissues removed from animals at the time that epicuticle and exocuticle are being synthesized ($D_{2,early}$ and $D_{2,late}$) and incubated with ^{3}H-tyrosine, a 24 kDa protein band is very heavily labeled (Stringfellow and Skinner, 1988). The 24 kDa charge train was specific to the exocuticle and membranous layer but was present in only trace amounts in the former (Fig. 4B, D).

Proteins extracted from the inner three exoskeletal layers also had 16 and 14 kDa charge trains. The most heavily ^{125}I-labeled protein in the 14 kDa charge train in the exocuticles and endocuticles focused in the acidic region of the gel, whereas the most heavily labeled 14 kDa protein in membranous layer focused in the neutral to basic region. It appears that proteins from the membranous layer are comprised more of neutral rather than acidic amino acids. These data agree with those of Welinder (1975b), who reported fewer acidic amino acids in proteins extracted from the membranous layer than from epicuticle plus exocuticle or endocuticle. Cox and Willis (1987a) described three groups of proteins from flexible insect cuticle: (1) those with acidic pIs, (2) those that formed charge trains, and (3) those that formed elongated vertical streaks. Crab exoskeletal proteins showed similarities to the first two groups of insect proteins, but not to the third. Such streaks are observed in gels that contain urea in the resolving gel, which ours did not.

Welinder (1975b) categorized the exoskeletons of arthropods as "soft" or "hardened"; soft cuticles had a high chitin content (63–72%) and proteins that were (1) rich in acidic amino acids, (2) poor in non-polar amino acids, and (3) highly soluble. The first characteristic is one found by Willis (1987) to be true of proteins of "flexible" cuticle of insects. By contrast, hardened crustacean exoskeleton had a low chitin content and proteins that were (1) rich in nonpolar amino acids and (2) less soluble (Welinder, 1975b). Welinder observed that the exoskeletons of all crustaceans he examined were "soft," even though they are physically hard due to calcification. Our data indicate that many crustacean exoskeletal proteins are acidic, similar to those of flexible insect cuticle; thus they support Welinder's observation that crustacean exoskeleton has some of the characteristics of "soft" cuticle.

Proteins of newly synthesized exoskeleton: metecdysial

Proteins were extracted from the newly synthesized epicuticle plus exocuticle which encase the animal as it emerges at ecdysis. Those proteins that became heavily iodinated had acidic pIs; all except members of the epicuticular quintet migrated to the bottom of the IEF tube gel (Fig. 5). Although three of the ^{125}I-labeled metecdysial proteins (Fig. 5; 57, 54, and 48 kDa) had similar mobilities to proteins present in extracts of anecdysial epicuticle (Fig. 4A), none was similar to those in anecdysial exocuticle (compare Fig. 5 with Fig. 4B). Perhaps the proteins missing from extracts of the anecdysial layers have been tanned and thereby rendered insoluble in guanidine thiocyanate as appears to have happened to a 48 kDa protein band. It was prominent in extracts from comparable regions of the exoskeleton, *i.e.*, unpigmented branchiostegites of metecdysial animals (Fig. 3, lane 4), but was absent from branchiostegites of anecdysial animals (Fig. 3, lane 2), suggesting that it had been altered during tanning of the

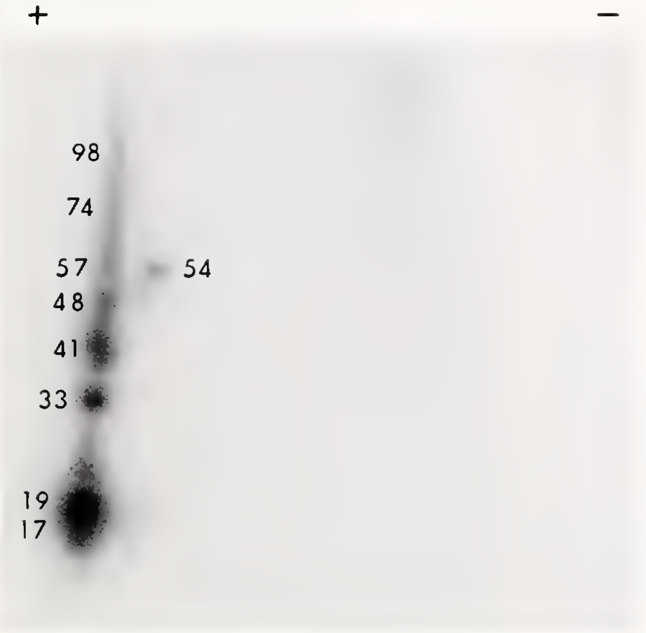

Figure 5. Proteins from newly synthesized metecdysial epicuticle + exocuticle of *Gecarcinus lateralis* have different charges from those in the same layers of anecdysial animals. Autoradiograph of 2D gel; SDS gel for second dimension as in Figure 4; 1 × 10^6 cpm, 1.1 μg proteins. Autoradiograph exposed 96 h. Approximate protein sizes are indicated (kDa).

exoskeleton and was no longer soluble. Similar changes in solubility have been reported for some cuticular proteins of the meal worm *Tenebrio molitor* (Roberts and Willis, 1980b). These proteins may play an important role during hardening of the exoskeleton. Gunthorpe *et al.* (1990) suggested that newly synthesized proecdysial crab exoskeleton contains unbound proteins that inhibit calcification, and that the cross-linking of these proteins to chitin following ecdysis creates a configuration that promotes calcification.

Prevalence of small proteins

The protein composition of the exocuticle, endocuticle and membranous layer of the anecdysial *G. lateralis* exoskeleton is dominated by small proteins (Figs. 1, 2, and 4; Table II), as are particular layers of some insect cuticles (Fristrom *et al.*, 1978; Roberts and Willis, 1980a; Cox and Willis, 1985; Silvert, 1985; Riddiford *et al.*, 1986; Wolfgang *et al.*, 1986; Horodyski and Riddiford, 1989). Except for the epicuticular quintet, the smallest proteins extracted from exoskeletons of anecdysial land crabs yielded the most intense protein bands on gels stained with either Coomassie blue or silver or were ^{125}I-labeled (Figs. 1, 2, and 4). Although the small proteins are seen as only a few very intense bands on 1D gels (Figs. 1 and 2), on 2D gels they separate into numerous proteins, differing from one another by net charge (charge trains; Fig. 4B–D). Gels of iodinated proteins are shown in Figure 4; similar results were obtained when gels were stained with Coomassie blue (data not shown). In part because the protein bands 28 kDa or smaller in 1D gels are seen to be composed of multiple components in 2D gels, the number of proteins 31 kDa or smaller exceeds those larger than 31 kDa for the three internal layers of the anecdysial exoskeleton (Tables II, III).

Interspecific similarities

Most of the proteins extracted from exocuticle, endocuticle, and membranous layer of the three crabs other than *G. lateralis* were also small. With few exceptions, the most intense bands on silver-stained 1D gels were 31 kDa or smaller (Fig. 6). Similarly sized protein bands (25, 23, 16, 14 and 10 kDa) were seen in extracts from a number of these layers; proteins 31 kDa or smaller showed very similar patterns in the membranous layer of all four species. Again, this similarity is only a suggestive preliminary observation; it does not necessarily imply their identity. Several of these small proteins, which appear as single bands on 1D gels, formed charge trains on 2D gels (data not shown) similar to those formed by some of the smaller proteins of *G. lateralis* (Fig. 4B, C). As was seen with *G. lateralis*, extracts of epicuticles were more likely to have unique proteins (Fig. 6).

Proteins that bind $^{45}Ca^{++}$ in vitro

In addition to M_r and pI, a third property that can be used to distinguish proteins is Ca^{++} binding *in vitro* (not implying Ca^{++} binding *in vivo*). Proteins rich in acidic amino acids may exhibit nonspecific affinity for calcium *in vitro* (Maruyama *et al.*, 1984). For example the 21 kDa size marker, soybean trypsin inhibitor, bound $^{45}Ca^{++}$ (Fig. 7, lane 1) even though its inhibitory activity is not Ca^{++}-dependent (Kunitz, 1947; Laskowski, 1955). We have used the *in vitro* binding of calcium by exoskeletal proteins as a characteristic to distinguish between similarly sized proteins found in extracts of several of the different exoskeletal layers.

The anecdysial epicuticle contained more than three times as many proteins that bound $^{45}Ca^{++}$ *in vitro* as exocuticle or endocuticle. In extracts of anecdysial layers, $^{45}Ca^{++}$ bound to 13 epicuticle protein bands, ranging in size from 141 to 14 kDa, to three exocuticle protein bands, five endocuticle protein bands, and to a 25 kDa protein band from membranous layer. Extracts of newly synthesized metecdysial epicuticle plus exocuticle had more proteins that bound $^{45}Ca^{++}$ in well defined bands than did layers from exoskeletons of anecdysial animals; proteins ranged in size from 71 to 15 kDa (Fig. 7). Six of these metecdysial protein bands (71, 66, 59, 57, 27, and

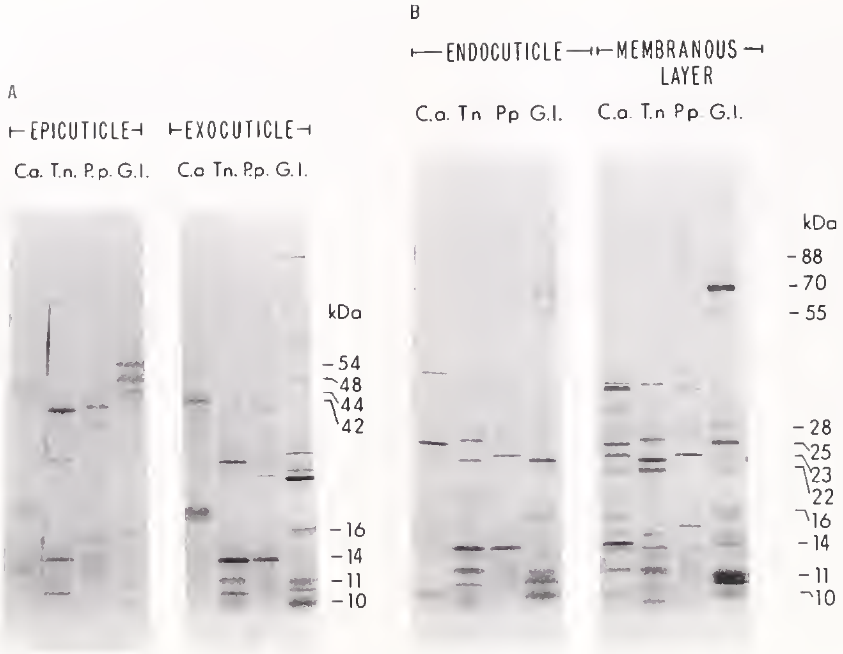

Figure 6. Proteins in the exoskeletal layers of four species of brachyurans. 9–18% 1D SDS-PAGE of proteins extracted from layers of exoskeletons of anecdysial crabs. Gels as in Figure 2; stained with silver. *Cancer antennarius*, C.a.; *Taliepus nuttalli*, T.n.; *Pugettia producta*, P.p.; *Gecarcinus lateralis*, G. l. (A) Epicuticle and exocuticle (B) endocuticle and membranous layer.

24 kDa; Fig. 7, lanes 2 and 3) were absent from extracts of anecdysial epicuticle and exocuticle. Conversely, a 14 kDa protein band in separate extracts of epicuticle, exocuticle, or endocuticle of anecdysial animals bound ^{45}Ca^{++}, while a similarly sized protein in metecdysial extracts did not (Fig. 7, compare lanes 2–4 with lane 6). Determination of a number of amino acids of the two 14 kDa proteins should indicate whether more than one protein is present (see Willis, 1989).

The presence of many more proteins that bind Ca^{++} *in vitro* in metecdysial extracts than in anecdysial extracts of comparable layers suggests that proteins are altered during the hardening of the exoskeleton, as discussed above. The biological significance of *in vitro* Ca^{++} binding requires further investigation.

Individuality of certain layers of the exoskeleton

Epicuticle has its own specific complement of proteins, while many of the proteins from the exocuticle and endocuticle are similar to each other and to proteins of the membranous layer in both M$_r$ and pI (Table II). Travis (1960) referred to the membranous layer as "the fourth major layer" of the crustacean exoskeleton and noted that it was distinguishable from endocuticle in: (1) staining properties, (2) thickness of its lamellae, and (3) absence of calcium. Babu *et al.* (1985) refer to the membranous layer as the "lower one-fourth region" of the endocuticle. Even though membranous layer appears to share a high fraction of its protein complement with endocuticle and a considerable number of proteins with exocuticle (Table II), it contains proteins not seen in other layers, *i.e.*, a 24 kDa charge train, large amounts of 88 and 28 kDa proteins, of which there are only traces in other layers, and a 25 kDa protein that binds Ca^{++} *in vitro* (Fig. 7). These differences suggest that it is more than simply an uncalcified endocuticle.

Significance of the similarity of proteins in the membranous layer of all four brachyuran species

P. producta, *T. nuttalli*, and *C. antennarius* are marine crabs, while *G. lateralis* is one of the few brachyurans to have adapted to a terrestrial habitat. Yet proteins of the same sizes (31 kDa or smaller) and similar pI's are found in the membranous layer of all four brachyurans examined despite the evolutionary distance of their taxa (Sections: Oxyrhyncha, Cancridea, and Brachyrhyncha). The protein patterns of all four exoskeletal layers of the two majids (*T. nuttalli* and *P. producta*) are much alike. However, except for the presence of several similarly sized small M$_r$ proteins in layers other than the membranous layer, in *G. lateralis* and *C. antennarius*, exoskeletal protein patterns are recognizably different; they are also different when compared to those of the two majids (Fig. 6). Relationships and homologies of the proteins in the exoskel-

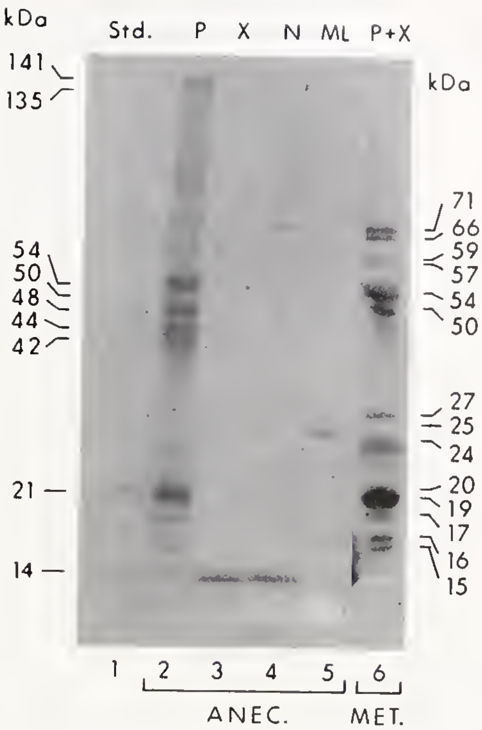

Figure 7. Ca^{++} binding by exoskeletal proteins of *Gecarcinus lateralis*. Autoradiograph of blot of exoskeletal proteins exposed to $^{45}Ca^{++}$. SDS gel as in Figure 2 except 75–100 μg proteins/lane. Abbreviations as in Figure 1. Lane 1, low molecular weight standards (Bio-Rad), Std. Lanes 2–5, proteins from anecdysial animal; lane 2, P; lane 3, X; lane 4, N; lane 5, ML; lane 6, proteins from P + X combined of metecdysial animal. Proteins had been electrotransferred to 0.1 μm (pore size) nitrocellulose. Autoradiograph exposed 15 days. The 21 kDa size marker that binds $^{45}Ca^{++}$ is soybean trypsin inhibitor.

etal layers in different crustacean species await at least partial amino acid analyses as have been performed for a number of insect cuticular proteins (Willis, 1987, 1989).

There is a possible reason for the evolutionary conservation of these small proteins. All arthropods undergo apolysis prior to forming a new exoskeleton and, in brachyurans, the membranous layer is the site at which apolysis occurs. As described above, a number of proteinases have evolved that appear to be active in the degradation of the exoskeleton that results in apolysis (O'Brien *et al.*, 1986; O'Brien and Skinner, 1987, 1988). These proteinases and possibly others degrade almost all of the proteins 31 kDa or smaller. As described above, some large M_r proteins such as the 94–80 kDa group prominent in exocuticle and endocuticle are degraded during proecdysis (Fig. 2). Data presented here show that, rather than being degraded during proecdysis, many of the large M_r proteins are shed with the exuvia (Fig. 2, lanes 6–9) in which they are greatly enriched in comparison with the proteins 31 kDa or smaller. Thus, these organisms appear to have evolved proteinases that degrade the major proteins of the membranous layer, but do not degrade as many or as much of the larger M_r proteins found in other layers.

Acknowledgments

We thank Adrian Wenner for laboratory space at the University of California, Santa Barbara, and Nette Crowe and Jim Hickey for preparing the figures. This research was supported by grants from the National Science Foundation and the Exploratory Studies Program of the Oak Ridge National Laboratory to DMS and by the Office of Health and Environmental Research, U. S. Department of Energy, under contract DE-ACO5-84OR21400 with Martin Marietta Energy Systems, Inc.

The submitted manuscript has been authored by a contractor of the U. S. Government under contract No. DE-ACO5-84OR21400. Accordingly, the U. S. Government retains a nonexclusive, royalty-free license to publish or reproduce the published form of this contribution, or allow others to do so, for U. S. Government purposes.

Literature Cited

Andersen, S. O., P. Hojrup, and P. Roepstorff. 1986. Characterization of cuticular proteins from the migratory locust, *Locusta migratoria*. *Insect Biochem.* **16:** 441–447.

Avruch, J., and D. F. H. Wallach. 1971. Preparation and properties of plasma membrane and endoplasmic reticulum fragments from isolated rat fat cells. *Biochim. Biophys. Acta* **233:** 334–337.

Babu, D. E., K. R. Rao, K. Shyamasundari, and D. V. U. Devi. 1985. Histochemistry of the cuticle of the crab *Menippe rumphii* (Fabricius) (Crustacea: Brachyura) in relation to moulting. *J. Exp. Mar. Biol. Ecol.* **88:** 129–144.

Bielefeld, M., G. Gellissen, and K.-D. Spindler. 1986. Protein production and the moulting cycle in the crayfish *Astacus leptodactylus*. I. Stage-specificity of polypeptide patterns in the hypodermis and hepatopancreas. *Insect Biochem.* **16:** 175–180.

Cox, D. L. 1987. Analysis of the cuticular proteins of *Hyalophora cecropia* with polyclonal antibodies. *Insect Biochem.* **17:** 485–492.

Cox, D. L., and J. H. Willis. 1985. The cuticular proteins of *Hyalophora cecropia* from different anatomical regions and metamorphic stages. *Insect Biochem.* **15:** 349–362.

Cox, D. L., and J. H. Willis. 1987a. Analysis of the cuticular proteins of *Hyalophora cecropia* with two dimensional electrophoresis. *Insect Biochem.* **17:** 457–468.

Cox, D. L., and J. H. Willis. 1987b. Post-translational modifications of the cuticular proteins of *Hyalophora cecropia* from different anatomical regions and metamorphic stages. *Insect Biochem.* **17:** 469–484.

Dennell, R. 1960. Integument and exoskeleton. Pp. 449–472 in *The Physiology of Crustacea*, T. H. Waterman, ed. Academic Press, New York.

Drach, P. 1939. Mue et cycle d'intermue chez les Crustaces decapodes. *Ann. Inst. Oceanogr. (Monaco)* **19:** 103–391.

Filshie, B. K. 1982. Fine structure of the cuticle of insects and other arthropods. Pp. 281–312 in *Insect Ultrastructure*, Vol. 1, R. C. King and H. Akai, eds. Plenum Press, New York.

Fristrom, J. W., R. J. Hill, and D. Watt. 1978. The procuticle of *Drosophila*: heterogeneity of urea-soluble proteins. *Biochemistry* **17:** 3917–3924.

Graddis, T. J. 1990. Application of polyvinylidene difluoride membrane in microsequence analysis of electrophoretically separated proteins. *DNA and Protein Engineering Techniques* **2:** 97–105.

Green, J. P., and M. R. Neff. 1972. A survey of the fine structure of the integument of the fiddler crab. *Tissue Cell* **4:** 137–171.

Greenaway, P. 1988. Ion and water balance. Pp. 211–248 in *Biology of the land crabs*. W. W. Burggren and B. R. McMahon, eds. Cambridge University Press, New York.

Gunthorpe, M. E., C. S. Sikes, and A. P. Wheeler. 1990. Promotion and inhibition of calcium carbonate crystallization *in vitro* by matrix protein from blue crab exoskeleton. *Biol. Bull.* **179:** 191–200.

Hackman, R. H. 1974. The soluble cuticular proteins from three arthropod species: *Scylla serrata* (Decapoda: Portunidae), *Boophilus microplus* (Acarina: Ixodidae) and *Agrianome spinicollis* (Coleoptera: Cerambycidae). *Comp. Biochem. Physiol.* **49B:** 457–464.

Halcrow, K. 1976. The fine structure of the carapace integument of *Daphnia magna* Straus (Crustacea Branchiopoda). *Cell Tiss. Res.* **169:** 267–276.

Herzog, K.-H., H. Grossmann, and M. Lieflander. 1975. Zur Chemie eines Chitin-Proteids aus Flusskrebs (*Astacus fluviatilis*). *Hoppe-Seyler's Z. Physiol. Chem.* **356:** 1067–1071.

Horodyski, F. M., and L. M. Riddiford. 1989. Expression and hormonal control of a new larval cuticular multigene family at the onset of metamorphosis of the tobacco hornworm. *Dev. Biol.* **132:** 292–303.

Karey, K. E., and D. A. Sirbasku. 1989. Glutaraldehyde fixation increases retention of low molecular weight proteins (growth factors) transferred to nylon membranes for Western blot analysis. *Anal. Biochem.* **178:** 255–259.

Kiely, M. L., and L. M. Riddiford. 1985. Temporal programming of epidermal cell protein synthesis during the larval-pupal transformations of *Manduca sexta*. *Roux's Arch. Dev. Biol.* **194:** 325–335.

Kimbrell, D. A., E. Berger, D. S. King, W. J. Wolfgang, and J. W. Fristrom. 1988. Cuticle protein gene expression during the third instar of *Drosophila melanogaster*. *Insect Biochem.* **18:** 229–235.

Kunitz, M. 1947. Crystalline soybean trypsin inhibitor II. General properties. *J Gen. Physiol.* **30:** 291–310.

Laemmli, U. K. 1970. Cleavage of structural proteins during the assembly of the head of bacteriophage T4. *Nature* **227:** 680–685.

Laskowski, M. 1955. Trypsinogen and trypsin. *Methods Enzymol.* **2:** 26–36.

Maruyama, K., T. Mikawa, and S. Ebashi. 1984. Detection of calcium binding proteins by ^{45}Ca autoradiography on nitrocellulose membrane after sodium dodecyl sulfate gel electrophoresis. *J. Biochem.* **95:** 511–519.

Mary, R. F., and G. Krishnan. 1974. On the nature and role of protein constituents of the cuticle of crustaceans in relation to permeability of the cuticle. *Mar. Biol.* **25:** 299–309.

McConahey, P. J., and F. J. Dixon. 1980. Radioiodination of proteins by the use of the chloramine-T method. *Methods Enzymol.* **70:** 210–213.

Mykles, D. L., and D. M. Skinner. 1982. Molt cycle-associated changes in calcium-dependent proteinase activity that degrades actin and myosin in crustacean muscle. *Dev. Biol.* **92:** 386–397.

Mykles, D. L., and D. M. Skinner. 1985. The role of calcium-dependent proteinase in molt-induced claw muscle atrophy. Pp. 141–150 in *Intracellular Protein Catabolism*, E. A. Khairallah, J. S. Bond, and J. W. C. Bird, eds. A. R. Liss, Inc., New York.

Neville, A. C. 1975. Biology of the arthropod cuticle. Pp. 1–448 in *Zoophysiology and Ecology*, Vol. 4/5, D. S. Farner, ed. Springer-Verlag, New York.

O'Brien, J. J., D. L. Mykles, and D. M. Skinner. 1986. Cold-induced apolysis in anecdysial brachyurans. *Biol. Bull.* **171:** 450–460.

O'Brien, J. J., and D. M. Skinner. 1987. Characterization of enzymes that degrade crab exoskeleton: I. Two alkaline cysteine proteinase activities. *J. Exp. Zool.* **243:** 389–400.

O'Brien, J. J., and D. M. Skinner. 1988. Characterization of enzymes that degrade crab exoskeleton: II. Two acid proteinase activities. *J. Exp. Zool.* **246:** 124–131.

O'Farrell, P. H. 1975. High resolution two-dimensional electrophoresis of proteins. *J. Biol. Chem.* **250:** 4007–4021.

O'Farrell, P. Z., H. M. Goodman, and P. H. O'Farrell. 1977. High resolution two-dimensional electrophoresis of basic as well as acidic proteins. *Cell* **12:** 1133–1142.

Paulson, C. R., and D. M. Skinner. 1991. Effects of 20-hydroxyecdysone on protein synthesis in tissues of the land crab *Gecarcinus lateralis*. *J. Exp. Zool.* **257:** 70–79.

Riddiford, L. M., A. Baeckmann, R. H. Hice, and J. Rebers. 1986. Developmental expression of three genes for larval cuticular proteins of the tobacco hornworm, *Manduca sexta*. *Dev. Biol.* **118:** 82–94.

Roberts, P. E., and J. H. Willis. 1980a. The cuticular proteins of *Tenebrio molitor* I. Electrophoretic banding patterns during postembryonic development. *Dev. Biol.* **75:** 59–69.

Roberts, P. E., and J. H. Willis. 1980b. The cuticular proteins of *Tenebrio molitor* II. Patterns of synthesis during postembryonic development. *Dev. Biol.* **75:** 70–77.

Roer, R. D. 1980. Mechanisms of resorption and deposition of calcium in the carapace of the crab *Carcinus maenas*. *J. Exp. Biol.* **88:** 205–218.

Roer, R., and R. Dillaman. 1984. The structure and calcification of the crustacean cuticle. *Am. Zool.* **24:** 893–909.

Schleicher, M., and D. M. Watterson. 1983. Analysis of differences between Coomassie blue stain and silver stain procedures in polyacrylamide gels: conditions for the detection of calmodulin and troponin C. *Anal. Biochem.* **131:** 312–317.

Silvert, D. J. 1985. Cuticular proteins during postembryonic development. *Comp. Insect Physiol., Biochem., Pharmacol.* **2:** 239–254.

Skinner, D. M. 1962. The structure and metabolism of a crustacean integumentary tissue during a molt cycle. *Biol. Bull.* **123:** 635–647.

Skinner, D. M. 1966. Breakdown and reformation of somatic muscle during the molt cycle of the land crab, *Gecarcinus lateralis*. *J. Exp. Biol.* **163:** 115–124.

Skinner, D. M. 1985. Molting and Regeneration. Pp. 43–146 in *The Biology of Crustacea*, Vol. 9, D. E. Bliss and L. H. Mantel, eds. Academic Press, New York.

Skinner, D. M., and D. E. Graham. 1970. Molting in land crabs: stimulation by leg removal. *Science* **169:** 383–385.

Skinner, D. M., and D. E. Graham. 1972. Loss of limbs as a stimulus to ecdysis in brachyura (true crabs). *Biol. Bull.* **143:** 222–233.

Skinner, D. M., S. S. Kumari, and J. J. O'Brien. 1991. Proteins of the crustacean exoskeleton. In *The Compleat Crab*, L. H. Mantel, ed. *Am. Zool.* in press.

Stevenson, J. R. 1985. Dynamics of the integument. Pp. 1–42 in *The Biology of Crustacea*, Vol. 9, D. E. Bliss and L. H. Mantel, eds. Academic Press, New York.

Stringfellow, L. A., and D. M. Skinner. 1988. Molt-cycle correlated patterns of synthesis of integumentary proteins in the land crab *Gecarcinus lateralis*. *Dev. Biol.* **128:** 97–110.

Traub, M., G. Gellissen, and K.-D. Spindler. 1987. 20(OH) ecdysone-induced transition from intermolt to premolt protein biosynthesis patterns in the hypodermis of the crayfish, *Astacus leptodactylus, in vitro*. *Gen. Comp. Endocrinol.* **65:** 469–477.

Travis, D. F. 1955. The molting cycle of the spiny lobster, *Panulirus argus* Latreille. II. Pre-ecdysial histological and histochemical changes in the hepatopancreas and integumental tissues. *Biol. Bull.* **108:** 88–112.

Travis, D. F. 1960. Matrix and mineral deposition in skeletal structures of the decapod Crustacea. Pp. 57–116 in *Calcification in Biological Systems*, R. F. Sognnaes, ed. AAAS, Washington, DC.

Vacca, L. L., and M. Fingerman. 1975a. The mechanism of tanning in the fiddler crab, *Uca pugilator*—I. Tanning agents and protein carriers in the blood during ecdysis. *Comp. Biochem. Physiol.* **51B:** 475–481.

Vacca, L. L., and M. Fingerman. 1975b. The mechanism of tanning in the fiddler crab, *Uca pugilator*—II. The cyclic appearance of tanning agents and attached carrier proteins in the blood during the molting cycle. *Comp. Biochem. Physiol.* **51B:** 483–487.

Vranckx, R., and M. Durliat. 1980. Cuticular protein analysis from *Astacus leptodactylus*—I. Electrophoretical studies of the soluble cuticular proteins. *Comp. Biochem. Physiol.* **65B:** 55–64.

Vranckx, R., and M. Durliat. 1986. Cuticular proteins in the crayfish *Astacus leptodactylus*—I. Main components. *Comp. Biochem. Physiol.* **85B:** 255–265.

Welinder, B. S. 1974. The crustacean cuticle. I. Studies on the composition of the cuticle. *Comp. Biochem. Physiol.* **47A:** 779–787.

Welinder, B. S. 1975a. The crustacean cuticle. II. Deposition of organic and inorganic material in the cuticle of *Astacus fluviatilis* in the period after moulting. *Comp. Biochem. Physiol.* **51B:** 409–416.

Welinder, B. S. 1975b. The crustacean cuticle. III. Composition of the individual layers in *Cancer pagurus* cuticle. *Comp. Biochem. Physiol.* **52A:** 659–663.

Willis, J. H. 1987. Cuticular proteins: the neglected component. *Arch. Insect Biochem. Physiol.* **6:** 203–215.

Willis, J. H. 1989. Partial amino acid sequences of cuticular proteins from *Hyalophora cecropia. Insect Biochem.* **19:** 41–46.

Wolcott, T. G. 1988. Ecology. Pp. 55–96 in *Biology of the Land Crabs,* W. W. Burggren and B. R. McMahon, eds. Cambridge University Press, New York.

Wolfgang, W. J., D. Fristrom, and J. W. Fristrom. 1986. The pupal cuticle of *Drosophila:* differential ultrastructural localization of cuticle proteins. *J. Cell Biol.* **102:** 306–311.

Wolfgang, W. J., and L. M. Riddiford. 1986. Larval cuticular morphogenesis in the tobacco hornworm, *Manduca sexta,* and its hormonal regulation. *Dev. Biol.* **113:** 305–316.

Wray, W., T. Boulikas, V. P. Wray, and P. Hancock. 1981. Silver staining of proteins in polyacrylamide gels. *Anal. Biochem.* **118:** 197–203.

Reference: *Biol. Bull.* **181:** 442–452. (December, 1991)

Modes of Feeding in Aggregations of Barnacles and the Shape of Aggregations

JULIE PULLEN[1,2] AND MICHAEL LABARBERA[2,*]

[1]*Macalester College, 1600 Grand Avenue, St. Paul, Minnesota 55105, and* [2]*Department of Organismal Biology and Anatomy, The University of Chicago, 1025 East 57th Street, Chicago, Illinois 60637*

Abstract. The interactions between the form of a barnacle aggregation, its flow environment, and the feeding behavior of each individual was determined in unidirectional flows; both models of barnacle aggregations and live barnacles were used. Hill-shaped aggregations of model barnacles captured significantly more particles than flat aggregations. In general, rows upstream of, and at the peak of, all hill-shaped profiles captured significantly more particles than downstream rows. Living barnacles located at, or upstream of, the peak of natural clusters captured significantly more food particles than did barnacles located downstream. Living barnacles located at, or upstream of, the highest point in a natural cluster fed passively, whereas barnacles downstream of the peak actively swept their cirral net against the flow. Flow was laminar up to the highest point in natural clusters, whereas flow was both reduced and turbulent over the downstream portions. Individual barnacles within a cluster differ in their feeding rates and net energy gains, and therefore differ in their growth such that, in unidirectional flow, the peak of a cluster will shift upstream over time; in oscillating flows, the clusters will develop a symmetrical profile.

Introduction

Acorn barnacles are sessile suspension-feeding animals. The feeding apparatus, the cirral basket, is a sieve-like net (LaBarbera, 1984) that typically is oriented perpendicular to the direction of ambient flow (Crisp and Bourget, 1985). Barnacles can draw upon a repertoire of feeding behaviors (Hazlett, 1988; Okamura, 1990). Changes in food concentration or flow rates elicit different feeding behaviors, largely expressed in the motion of the cirral basket. A feeding barnacle may use any of three patterns of cirral basket movement: normal beat, fast beat, and extension (Crisp and Southward, 1961). When flow velocity exceeds some threshold value, barnacles shift from fast beat to extension feeding (Crisp and Southward, 1961; Trager *et al.*, 1990), switching from sweeping their cirral baskets through the water, to simply holding their baskets against the flow. These two feeding behaviors are also known as active and passive, respectively (Jørgensen, 1966).

Both Crisp and Southward (1961) and Trager *et al.* (1990) focused on single barnacles in analyzing this flow-induced behavioral change. However, barnacle cyprids are gregarious settlers (Knight-Jones, 1953; Wethey, 1984), a behavior that often leads to aggregations of individuals (clusters) that generally display a hill-shaped contour. A common form consists "of a cluster of individuals enormously elongated at the centre of the hummock, and decreasing symmetrically towards the periphery" (Barnes and Powell, 1950).

Several explanations have been put forward for the origin of hill-shaped aggregations. Barnes and Powell (1950) suggested that pressure from neighbors caused growth of the central barnacles to be constrained to the upward direction; "barnacle shell growth is very plastic and . . . whenever forces are applied to the shell, its shape becomes modified" (Bourget and Crisp, 1975; also see Crisp, 1960). Crisp and Bourget (1985) suggested that food capture played a pivotal role in the development of hill-shaped aggregations. If some barnacles in a heavily settled area captured more food than their neighbors, they could only display their good feeding fortune by upward growth. Because taller barnacles feed higher in the flow boundary layer, they sample a higher flow velocity than their shorter neighbors (Crisp and Bourget, 1985). Faster flow implies

Received 5 April 1991; accepted 9 September 1991.

[*] To whom all correspondence should be addressed.

a larger volume of water sampled and hence more food particles encountered (Vogel, 1983); thus, if all else were equal, taller barnacles would tend to grow still more (Crisp and Bourget, 1985).

A combination of mechanisms probably underlies the origin of the hill-shaped form; constraints to lateral growth from the presence of neighbors, and differential food capture are probably both involved. To unravel the relative contributions of each of these factors is difficult because the interplay between them is probably highly species-dependent. We have chosen to focus on factors that underlie differential food capture among individual barnacles, on the assumption that differences in food capture will translate into differences in relative growth rate for all species of barnacles. Our primary emphasis was on the form of hill-shaped aggregations. Such aggregations can be viewed as either a transitory stage in the evolution of the shape of a cluster of barnacles, or as a stable assemblage which, once achieved, remains relatively constant despite the continued growth of its constituents and recruitment of new individuals. As we will show, these two perspectives are in fact compatible and converge to the same outcome.

To address this question, we have chosen to examine the distribution of food capture across hill-shaped arrays of "mock barnacles," using real clusters of barnacles to verify the relative particle capture rates observed with the models, and to determine the influence of different modes of feeding (active *vs.* passive). Our goal is to explore the correlation between local flow environment and location-dependent feeding rates in a barnacle cluster. This exploration is central to an understanding of food distribution patterns and the feeding behavior of individual barnacles in a cluster.

Materials and Methods

All statistical analyses were performed using StatView II (ver. 1.03; Abacus Concepts, Inc., Berkeley, California) run on a Macintosh SE/30 computer. All descriptive and test statistics of normalized capture values (NCV's; see below) were calculated after transforming the data as arcsin $\sqrt{NCV}$ (Sokal and Rohlf, 1981); the statistical values given below were back-transformed to normalized capture values. Unless otherwise specified, we have used a significance level of 5% in all statistical comparisons.

Mock barnacle arrays

Plastic cylinders of two heights (0.3 and 0.6 cm) were cut from commercial polybutylene tubing (0.97 cm diameter). The cylinders were filled with plastacene and positioned in direct contact with one another in 4 (wide) by 5 (long) arrays. Each row (line of cylinders perpendicular to the flow direction) consisted of cylinders or stacks of cylinders of the same height. Four mock barnacle clusters (Fig. 1) were constructed; the profiles produced were flat (all rows 0.6 cm tall), symmetrical (1.8 cm high peak in row 3), shifted upstream (peak in row 2), and shifted downstream (peak in row 4). We adopt the convention that row 1 is the extreme upstream row of a profile; row 5 is the extreme downstream row. To mimic barnacles engaged in passive suspension feeding, isosceles right triangles (base 1 cm) were cut from 250 μm (diagonal) mesh plankton netting and inserted into the plastacene on top of each cylinder so the plane of the triangle was perpendicular to the flow direction; the hypotenuse of the triangle was distal to the cylinder and horizontal.

The arrays were placed midway between the walls of a 15 × 15 cm cross section flow tank, designed following Vogel and LaBarbera (1978), that was filled with fresh water. The boundary layer at the leading edge of the array was approximately 0.5–0.8 cm thick, as estimated from the distortion of vertical dye fronts injected just upstream of the arrays. The tank was seeded with freshwater-soaked *Artemia salina* cysts stained with rhodamine dye. The number of *Artemia* cysts added was only roughly (±10%) standardized, but the nature of the comparisons made correct for variation in absolute particle concentration.

In the first series of measurements, each of the four mock barnacle arrays was placed singly in the tank and exposed to a unidirectional laminar flow of 4–5 cm/s for 10 min. The number of *Artemia* cysts captured by each mock barnacle was determined by removing the mesh net after each run and counting the stained cysts trapped on the net. Once attached to the net, the eggs were never observed to become detached either during removal from the tank or during counting; the cysts lodged in the mesh netting, and only after the mesh was dried could they be easily removed. Each profile was tested four times. Numbers of particles captured by each cylinder in a row were summed to give total row capture. Because the concentration of suspended particles varied between experimental runs, total capture by all rows in an array for each run was normalized to 100 particles and individual row totals appropriately scaled to yield normalized row capture values. Normalized row capture values are thus equivalent to percentage of total capture by the array.

In a second series of measurements, two arrays representing different profiles were tested simultaneously in the flow tank. These tests were conducted to allow comparison of absolute numbers of particles captured. The arrays were placed at equal distances from the flow collimator, symmetrically about the longitudinal midline of the tank, and exposed to a 4–5 cm/s flow for 10 min. Particle capture was quantified as described above. Symmetrical and flat profiles were simultaneously run in six trials, and the shifted downstream and flat profiles were simultaneously run in seven trials; the other potential combinations of profiles were not tested.

Living barnacles

Dome-shaped clusters of mixed *Balanus amphitrite* and *Balanus tintinabulum* were collected from rocks and buoys near Boca Raton, Florida on 7 August 1990. Flows in the environment where the barnacles were collected were primarily tidal; mainstream velocities in the vicinity of the clusters were approximately 5 cm/s as measured by timing movement of natural particles along a known distance. The clusters were shipped in Styrofoam containers to Chicago, where they were held in a 300-l aquarium filled with artificial seawater and fed every other day on newly hatched *Artemia* nauplii. Barnacles fed avidly on *Artemia* nauplii in the aquarium; molting was common, and the animals appeared to be healthy. Because *B. tintinabulum* was uncommon in these clusters, our observations were restricted to *B. amphitrite*.

Food capture was quantified for at least one barnacle in each of three positions (upstream, downstream, and peak) on the midlines of two clusters. For a third cluster, data were gathered only for barnacles in the peak and downstream positions. Clusters were placed individually in the flow tank (filled with artificial seawater) and subjected to a unidirectional flow of 4–5 cm/s carrying newly hatched *Artemia* nauplii. Individual barnacles were observed to switch from active beating to passive suspension feeding at local flow speeds of 2–3 cm/s. [Threshold velocity for switching from active to passive suspension feeding was determined by observing peak animals in natural clusters (which essentially see mainstream velocities; Fig. 2) while the mainstream flow speed in the tank was varied.] Feeding of individual barnacles was observed using a 3.5× binocular magnifier; data were restricted to continuous feeding bouts of at least 3-min duration. *Artemia* nauplii captured during a 3-min interval were recorded using a mechanical tally counter; a capture was scored when a brine shrimp was seen to contact the cirral basket of the barnacle and the cirral basket was subsequently retracted completely into the shell. Those barnacles for which food capture values were quantified were also videotaped while feeding, and the length of the extended cirral baskets were measured on a video monitor. Assuming that cirral basket growth was isometric, the relative areas of the cirral baskets of the barnacles observed was approximated by squaring their measured lengths.

The average frequency of cirral basket movement of individual barnacles was determined by measuring the duration of a sequence of either 10 or 20 retractions (for passive feeders) or beats (for active feeders). (Passively feeding barnacles frequently retract their cirral basket and then rapidly re-extend it. This behavior is distinct from the rhythmic beating of actively feeding barnacles.) A series of observations of 10 or 20 beats was recorded. Timing was begun either at the retraction (for passive feeders) or on the downstroke (for active feeders). Beat frequency of at least one barnacle in each of the three positions in a cluster (upstream, downstream, and peak) was determined. Beat frequency was measured only on animals whose particle capture rate had been determined; typically, we measured cirral basket beat frequency of a barnacle after we had measured particle capture in four feeding bouts of 3 min each.

To determine velocity distributions around the barnacle clusters, the midline of the cluster was illuminated from above with a 0.5 cm wide collimated light beam; the plane of the light beam was parallel to the flow direction. Photographs were taken using a 35 mm camera and macro lens; exposure durations were either 0.5 or 0.25 s. *Artemia* individuals illuminated by the light beam were imaged as streaks as they were carried with the flow; the streaks recorded on the negatives indicated both flow streamlines (by their path) and local velocities (by their length). The negatives were projected and the streaks superimposed by manual tracing. The length of the streaks were measured by digitizing the tracings on a Houston Instruments HiPad™ connected to an Apple IIc computer. These values, appropriately scaled to reflect true distances in the flow tank, were divided by the camera shutter speed to calculate the mean flow velocity along the streak. Accuracy of velocity measurements was approximately ±0.05 cm/s.

Results

Mock barnacle arrays

The mean normalized row capture values for the four profiles tested singly are given in Table I; the results are portrayed graphically in Figure 1. ANOVAs were performed on arcsine transformed normalized capture values for each profile (Table II), with the data grouped by row. As is apparent, patterns of particle capture across rows differ between the profiles. For the flat profile, the extreme upstream row (row 1) showed significantly higher nor-

Table I

Normalized row particle capture values for the four profiles of mock barnacle arrays (see Materials and Methods)

	Flat	Symmetrical	Shifted upstream	Shifted downstream
Row 1	95.0 (79–99)	24.1 (11–41)	35.8 (21–52)	29.8 (13–50)
Row 2	3.9 (0–16)	26.7 (21–33)	51.8 (27–76)	32.8 (19–49)
Row 3	0.2 (0–2.6)	41.9 (29–56)	1.3 (0–10)	4.9 (4.0–5.9)
Row 4	0.1 (0–1.9)	0.7 (0–5.8)	4.5 (0–21)	25.7 (13–41)
Row 5	0.1 (0–1.9)	2.3 (0–21)	2.3 (0–11)	3.7 (0–20)

Mean values were calculated from $\arcsin\sqrt{NCV}$ where NCV = the normalized capture values; the values given above were backtransformed to normalized capture values. Values given in parentheses are the 95% confidence intervals of the means calculated from the transformed values. In all cases, n = 4.

malized capture values than all rows downstream. The most downstream rows (rows 3–5) showed no significant differences in normalized capture values. The three hill-shaped profiles differed drastically from this pattern. For the symmetrical and shifted upstream profiles, the peak row and all rows upstream of peak showed significantly higher normalized capture values than did the rows downstream of the peak. The values for rows downstream of the peak were statistically indistinguishable. For the shifted downstream profile, the peak row and all rows upstream of peak (except row 3) showed significantly higher normalized capture values than did the row downstream of the peak.

Differences between normalized row capture values of the mock barnacle arrays were tested using two sample t-tests (Table III). Table III reveals significant differences in normalized particle capture between rows 1, 2, and 3 of the symmetrical and flat profiles; row 1 of the flat profile had a significantly higher normalized capture value than row 1 of the symmetrical profile, while rows 2 and 3 (the peak) of the symmetrical profile had significantly higher normalized capture values than the same rows of the flat profile. Downstream of row 3, there were no statistically significant differences between rows in the two profiles.

Table II

Analysis of variance of the differences in normalized particle capture between rows in the four profiles of mock barnacle arrays

	Flat				Symmetrical				Shifted upstream				Shifted downstream			
$F_{4,15}$	117.1				19.7				21.3				12.2			
Row	2	3	4	5	2	3	4	5	2	3	4	5	2	3	4	5
1	*	*	*	*	—	*	*	*	—	*	*	*	—	*	—	*
2		*	*	*		—	*	*		*	*	*		*	—	*
3			—	—			*	*			—	—			*	—
4				—				—				—				*

For each profile, the F value of the ANOVA is given; in all cases, the ANOVA's were highly significant ($P < 0.0001$). In the row matrix, significant differences are indicated by an asterisk (*); lack of statistical significance is indicated by a dash (—). Normalized particle capture values were arcsine transformed before analysis; differences between transformed normalized particle capture values were tested using the Fisher PLSD test.

Comparing the shifted upstream and flat profiles, rows 1 and 2 showed significant differences in normalized par-

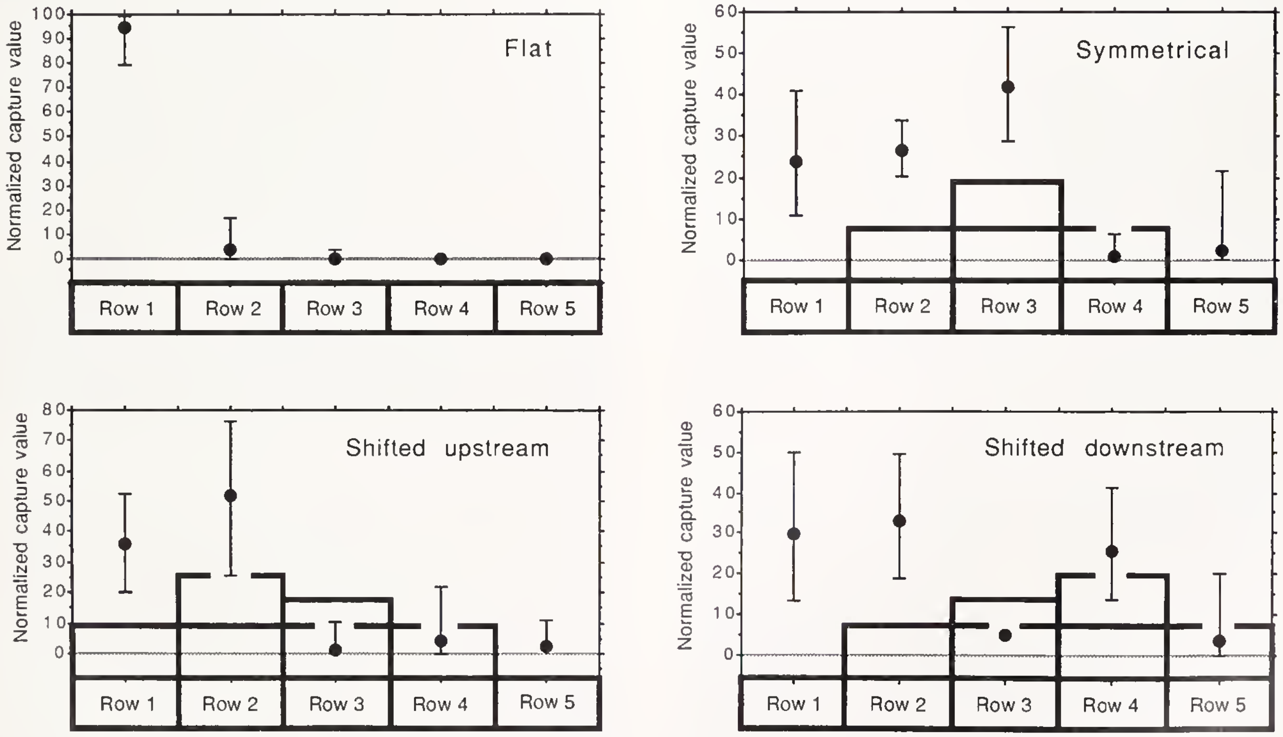

Figure 1. Mean normalized particle capture values (n = 4) for each row of various configurations of model barnacle arrays. Normalized particle capture = 100 ($C_r/\Sigma C_r$) where C_r = total number of particles captured per row. Ninety-five percent confidence intervals of the means are indicated by vertical lines; where no lines are visible, the confidence interval lies within the height of the point plotted. All arrays were tested individually in a unidirectional laminar flow of approximately 5 cm/s. The profile of each array is superimposed on the graphs; the upstream end (row 1) of each profile is on the left. Note that rows at or upstream of the peak of each array capture significantly more particles than rows downstream of the peak.

Table III

Two sample Student's unpaired t-tests of differences in arcsine-transformed normalized row capture values for the mock barnacle arrays tested singly in the flow tank

Row	Flat *vs.* Symm.	Flat *vs.* Shifted up	Flat *vs.* Shifted down	Symm. *vs.* Shifted up	Symm. *vs.* Shifted down	Shifted up *vs.* Shifted down
Row 1	8.53***	7.30***	7.59**	(−1.65)	(−0.76)	(0.73)
Row 2	−8.59***	−5.49**	−5.42**	(−3.07)	(−1.26)	(2.08)
Row 3	−9.20***	(−1.19)	−6.42**	8.37***	8.33***	(−1.44)
Row 4	(−1.09)	(−1.85)	−5.68**	(−1.50)	−5.39**	−3.61*
Row 5	(−1.11)	(−1.92)	(−1.47)	(0.43)	(−0.10)	(−0.65)

In all cases, n = 4 (df = 6 for each test). The values given are the t values. Values not significant at the $P = 0.05$ level are given in parentheses; asterisks indicate the level of significance (* = $P < 0.05$; ** = $P < 0.01$; *** = $P < 0.001$). In all cases, a two-tailed test was used; probabilities were adjusted for multiple comparisons using the Bonferroni method.

ticle capture; row 1 of the flat profile had higher normalized particle capture values than row 1 of the shifted upstream profile, whereas row 2 (the peak row) of the shifted upstream profile had higher values. Downstream of row 2, there were no statistically significant differences in normalized particle capture.

Comparison of normalized row capture values of the shifted downstream and flat profiles revealed significant differences between the two profiles for rows 1–4; row 1 of the flat profile had significantly higher normalized capture values than row 1 of the shifted downstream profile, while rows 2–4 of the shifted downstream profile had significantly higher normalized capture than the same rows of the flat profile. (Row 4 was the peak of the shifted downstream profile.) There was no statistically significant difference between the two profiles in normalized capture for row 5. Other comparisons (symmetrical *vs.* shifted upstream, symmetrical *vs.* shifted downstream, shifted upstream *vs.* shifted downstream) showed a common pattern—the rows located upstream of *both* peaks were indistinguishable in terms of normalized particle capture. Furthermore, rows located downstream of both peaks (rows 4 and 5 for symmetrical *vs.* shifted upstream; row 5 for the other two combinations) consistently showed no significant differences in normalized particle capture.

Cross-profile comparisons can be summarized as follows: (1) There were always significant differences in capture by peak and upstream rows between the flat *vs.* hill-shaped profiles. (2) In contrast, there were no significant differences in particle capture by those rows located upstream of the peaks of hill-shaped profiles. (3) *All* cross-profile comparisons confirm that there is no statistically significant difference in capture by rows downstream of the peak(s).

To compare absolute capture rates of the mock barnacle arrays, either the symmetrical or shifted downstream array and the flat array were placed in the flow tank simultaneously. Placing two arrays in the flow tank at the same time caused the arrays to be nearer the walls and hence a change in flow patterns would be expected; however, because the flow velocities in the tank are symmetric about the midline of the tank, these altered flow patterns are symmetric across the profiles and therefore do not invalidate comparison. The mean total row and array capture values are given in Table IV; the results of row-by-row and total capture paired Student's t-tests are given in Table V. These results mimic those described above. Most importantly, the rows located downstream of the peak showed no statistically significant difference in capture between the profiles. Both the symmetrical and the shifted downstream profiles captured about twice as many particles as the flat profile (Table IV); in both cases, the differences were statistically significant (Table V).

Clusters of living barnacles

Areas of the cirral baskets of the peak and downstream animals in Cluster I were comparable (within 20% of each other), as were the areas of the cirral baskets of the peak, upstream 1, and upstream 2 animals in Cluster II. The

Table IV

Mean particle capture of simultaneously tested mock barnacle arrays

	Symmetrical	Flat	Shifted downstream	Flat
Row 1	(29.3 ± 7.4)	(49.7 ± 17.5)	(21.9 ± 5.2)	(39.6 ± 8.7)
Row 2	32.3 ± 10.5	3.2 ± 1.5	33.4 ± 8.4	2.1 ± 0.7
Row 3	74.8 ± 22.2	4.0 ± 1.1	9.3 ± 2.4	1.6 ± 0.5
Row 4	(2.5 ± 0.8)	(4.7 ± 2.3)	32.4 ± 10.4	1.4 ± 0.6
Row 5	(2.8 ± 0.7)	(3.3 ± 1.7)	(0.4 ± 0.3)	(1.7 ± 0.7)
Total	142.2 ± 40.9	64.8 ± 23.0	97.4 ± 24.2	46.4 ± 9.7

The symmetrical array was tested against the flat array in six trials; the shifted downstream array was tested against the flat array in seven trials. Mean values of particles caught are given by row and for the total array. Paired values for the two arrays which are not significantly different from each other (see Table V) are given in parentheses.

Table V

Paired Student's t-tests of differences in particle capture for mock barnacle arrays tested simultaneously in the flow tank

	Symmetrical *vs.* Flat		Shifted down *vs.* Flat	
	t-value	*P*	t-value	*P*
Row 1	−1.920	0.113	−2.107	0.080
Row 2	3.206	0.024	3.887	0.008
Row 3	3.312	0.021	3.471	0.013
Row 4	−1.245	0.268	3.064	0.022
Row 5	−0.324	0.759	−1.486	0.188
Total	4.065	0.010	2.829	0.030

For the symmetrical *vs.* flat arrays, n = 6; for the shifted down *vs.* flat arrays, n = 7. In all cases, a two-tailed test was used.

cirral basket of the downstream animal of Cluster II was approximately half the size of those of the upstream 1, upstream 2, and peak animals. The peak and upstream animals of Cluster III were comparable in cirral basket area, but the cirral basket of the downstream animal was approximately two-thirds the size of those of the peak and upstream animals. For all three clusters, animals in the upstream and peak locations were clearly passively suspension feeding, while all animals downstream of the peak were clearly actively beating their cirral baskets.

For Cluster I, unpaired Student's t-tests (Table VI) indicated that both capture rates and cirral beat frequencies of the peak and downstream animals were significantly different ($t = 5.06$, $P = 0.002$ and $t = 54.159$, $P < 0.001$, respectively). For Cluster II (Table VI), ANOVA of relative capture rates was highly significant ($F_{3,12} = 15.377$, $P < 0.001$); using Fisher's protected least significant difference (PLSD) test, upstream 1, upstream 2, and peak animals were not significantly different in capture rates, but all three animals were significantly different from the downstream animal. ANOVA of cirral beat frequencies for Cluster II was also highly significant ($F_{3,25} = 44.065$, $P < 0.001$). Using Fisher's PLSD test, two animals (upstream 1 and upstream 2) were not significantly different in cirral beat frequencies; all other combinations of animals were significantly different from each other. ANOVA of relative capture rates for the animals in Cluster III (Table VI) was also highly significant ($F_{2,9} = 16.566$, $P = 0.001$). Using Fisher's PLSD test, the upstream, peak, and downstream animals were all significantly different from each other in capture rates. ANOVA of cirral beat frequencies was highly significant ($F_{2,18} = 298.69$, $P < 0.001$). Using Fisher's PLSD test, the upstream and peak animals were not significantly different from each other in cirral beat frequency, but both animals were significantly different from the downstream animal.

Figure 2 (A–C) presents the flow patterns and associated local velocities around the three live barnacle clusters. The qualitative flow environment of peak and upstream animals differed from that of downstream animals. Whereas the path lines upstream and over the peak of the clusters in Figure 2A–C were smooth, continuous, and long, those downstream were convoluted, discontinuous, and punctuated in length; a highly disordered, turbulent flow region (the wake) was present immediately downstream of all clusters. Local flow velocities also differed. The flow velocities in the upstream and peak areas of the clusters was approximately 2.0–5.5 cm/s; flow velocity in the turbulent region downstream of the clusters was approximately 0.3–1.5 cm/s.

Discussion

Hydrodynamic simulation

The flume used in this study was too narrow to accurately reproduce the essentially two dimensional flow typical of the ocean bottom; for such purposes, the width to depth ratio of the flow should be greater than 5:1 (Nowell and Jumars, 1987). However, because our interest was in the flow around a cluster rather than cluster-sediment interactions, and because the velocity profile was essentially flat across the center two thirds of the flume in both depth

Table VI

Artemia *nauplii capture rates and cirral basket beat frequencies for selected* Balanus amphitrite *individuals in three clusters*

	Mean capture/ 3 min	n	Feeding mode	Mean beats/s	n
Cluster I					
upstream	—	—	—	—	—
peak	6.75 ± 0.75	4	P	0.5 ± 0.03	6
downstream	2.75 ± 0.25	4	A	2.9 ± 0.03	7
Cluster II					
upstream 1	5.75 ± 0.85	4	P	1.3 ± 0.14	8
upstream 2	7.00 ± 1.29	4	P	1.7 ± 0.12	8
peak	6.50 ± 0.29	4	P	1.4 ± 0.11	6
downstream	0.25 ± 0.25	4	A	2.9 ± 0.02	7
Cluster III					
upstream	17.00 ± 2.27	4	P	1.3 ± 0.04	10
peak	9.00 ± 1.47	4	P	1.1 ± 0.08	6
downstream	3.75 ± 0.85	4	A	2.9 ± 0.02	5

Values given are means ± the standard errors of the means. Upstream and downstream animals were located on the leading and trailing edges of the clusters, respectively; peak animals were located on the highest points of the clusters (see Fig. 2). Feeding modes [active (A) or passive (P)] of each animal are indicated. Cirral basket areas of the peak and downstream animals in Cluster I were within 20% of each other, as were the cirral basket areas of the peak and upstream animals in Cluster II and Cluster III. The cirral basket of the downstream animal of Cluster II was approximately half the size of the other animals in the cluster; the cirral basket of the downstream animal in Cluster III was approximately two-thirds the size of the other animals.

and width, we believe that our laboratory experiments are representative of the field situation. Both a single mock barnacle array and a live barnacle cluster occupied about 25% of the width of the flow tank and 12–20% of the depth, but only about 4% of the total cross sectional area of the flow. Nowell and Jumars (1984, 1987) suggest that blockage effects will not be significant if the height of an obstacle to the flow is less than 35% of the depth of the flow and 25% of the width. For a flume of their recommended proportions, such an obstacle, semicircular in cross section, would block 4% of the area of the flume, the same value as both our models and live barnacle clusters.

When two mock barnacle arrays were placed simultaneously in the flow tank, they occupied at least 50% of the width of the tank and 8% of the cross section. Significant alteration of the flow patterns certainly occurred, and portions of each array were overlapped by the boundary layers on the side walls of the flume. Because both arrays were equally affected, these flow modifications do not compromise the comparisons we make between the arrays. The fact that the row-by-row relative capture patterns of profiles tested singly in the tank are in accordance with the results of two arrays tested simultaneously implies that the patterns of particle capture in these arrays are relatively immune to details of the flow regime, although absolute capture values will certainly be affected.

Barnacles apparently acclimate to the ambient flow regime; when exposed to altered flow velocities or flow cycles, they may refuse to feed until they become acclimated to the new conditions (Trager *et al.*, 1990). This would help explain the existence of a range of mainstream flow velocities below or above which the barnacles in our study were reluctant to feed. At mainstream velocities greater than around 7 cm/s, the barnacles in our study retracted into their test, while at mainstream velocities less than 1 cm/s, the barnacles would often beat and retract in a nonrhythmic fashion. We take this as indirect evidence that the clusters in our study had been exposed in the field to a mean mainstream flow velocity of 4–5 cm/s and believe that the single value we have for field flow velocity reflects typical conditions.

Mock barnacle arrays

In terms of particle capture, the mock barnacle arrays exhibited the following general features: (1) For hill-shaped profiles, the peak row and each row upstream of peak generally captured a significantly higher proportion of the total particles captured than did rows downstream of the peak, regardless of the particular profile of the array. For the flat profile, the extreme upstream row was functionally a "peak," capturing a significantly higher fraction of the particles available than did rows downstream. (2) Rows downstream of peaks showed no significant differences in proportional particle capture among themselves, regardless of the specific profile of the array. (3) Hill-shaped profiles captured significantly more particles as an entity than did flat profiles.

The triangular mesh used as a "cirral basket" mimic on the mock barnacles was an imperfect model of a barnacle cirral basket: (1) It was flat rather than concave upstream and thus is likely to be less efficient as a filter (Warner, 1977; Baumiller, 1988), and (2) the triangular shape we used was only a rough approximation of the outline of a barnacle's cirral basket (the distal edge of cirral baskets is an arc rather than a straight line). The mock barnacle arrays only mimicked barnacles passively suspension feeding; it was not possible to represent actively feeding barnacles. Because barnacles show plasticity in feeding behavior, the feeding behavior and feeding ability of live barnacles in a cluster must be considered before conclusions can be drawn from these modeling studies about the location-dependent feeding of barnacles.

Positional effects on feeding in living barnacles

It is clear that live barnacles in a cluster displayed differential feeding behavior that was correlated with location in the cluster. Those barnacles surveyed at upstream and peak locations displayed a significantly lower cirral basket beat frequency than did those barnacles situated downstream. No differences between upstream and peak locations in cirral beat frequency could be demonstrated. The mechanistic link between barnacle location and behavior is local flow environment; barnacles tend to be active feeders in slow flow environments (<2–3 cm/s) and passive feeders in higher velocity flows (>2–3 cm/s) (Crisp and Southward, 1961; Trager *et al.*, 1990). Figure 2A–C documents the linkage between barnacle location in clusters and local flow environment. The downstream turbulence apparent in the figure apparently arose from vortices shed from the cluster, a feature common to bluff bodies in flows at moderate to high Reynolds numbers

Figure 2. Streamlines and local flow velocities around the three *Balanus amphitrite* clusters observed. (A) Cluster I. (B) Cluster II. (C) Cluster III. All clusters were observed in a unidirectional, laminar flow of approximately 5 cm/s mainstream velocity. Note that flow is laminar and similar in speed to mainstream flow for regions of the clusters upstream or at the peak in height of each cluster, but that flow is turbulent and markedly reduced in speed in the wake of each cluster, downstream of the peaks. The locations of the barnacles whose feeding and beat frequency were quantified (Table VI) are indicated (U = upstream, P = peak, D = downstream). Direction of mainstream flow is indicated by arrows.

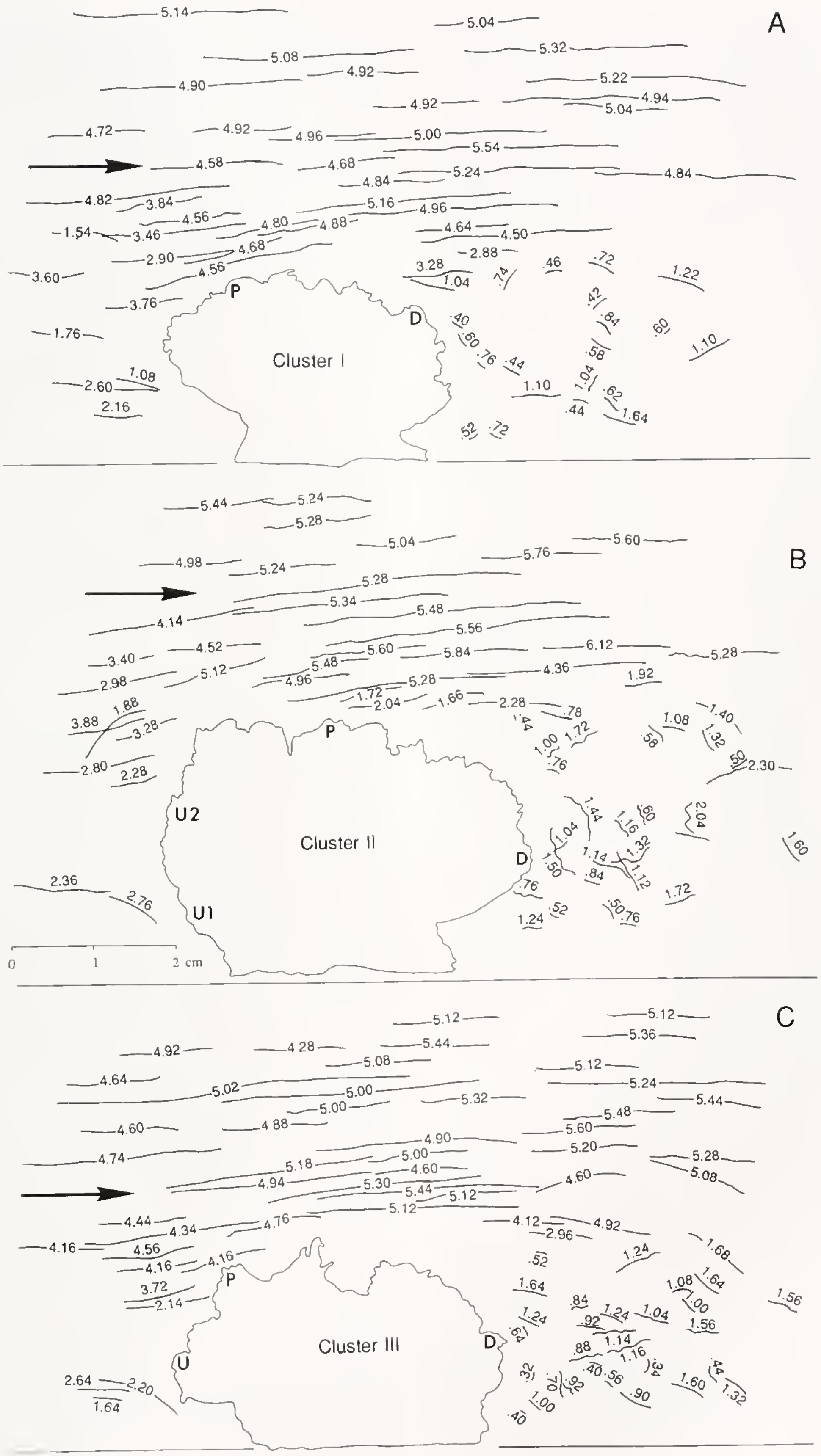
A
5.14
5.04
5.32
5.08
4.92
5.22
4.90
4.92
4.94
5.04
4.72
4.92
4.96
5.00
5.54
4.58
4.68
5.24
4.84
4.84
4.82
3.84
5.16
4.96
4.56
1.54
3.46
4.80
4.88
4.64
4.50
4.68
2.88
2.90
3.28
.74
.46
.72
4.56
1.04
1.22
3.60
P
3.76
D
.42
.84
1.76
.40
.60
.60
.76
.44
.58
1.10
Cluster I
1.04
.62
1.08
1.10
2.60
.44
1.64
2.16
.52
.72
B
5.44
5.24
5.28
5.04
5.60
4.98
5.76
5.24
5.28
5.34
5.48
4.14
5.56
4.52
6.12
3.40
5.60
5.84
5.28
5.12
5.48
2.98
4.96
4.36
1.92
5.28
1.72
2.04
1.66
2.28
.78
1.88
.44
1.08
1.40
3.88
3.28
P
1.00
1.72
.58
1.32
.76
.50
2.30
2.80
2.28
1.44
U2
.60
2.04
1.16
1.04
Cluster II
1.32
1.60
1.14
D
1.50
.84
1.12
2.36
.76
1.72
2.76
U1
.52
.50
.76
1.24
0
1
2 cm
C
5.12
5.12
5.36
4.92
4 28
5.44
5.08
5.12
4.64
5.24
5.02
5.00
5.44
5.00
5.32
5.48
4.60
4 88
5.60
4.90
5.20
4.74
5.00
5.28
5.18
4.60
5.08
4.94
5.30
4.60
5.44
5.12
5.12
4.44
4.12
4.92
4.34
4.76
2.96
4.16
4.56
1.68
.52
1.24
4.16
4.16
P
1.64
1.64
3.72
1.08
1.00
1.56
2.14
.84
1.24
1.04
1.24
.92
1.56
.64
D
Cluster III
.88
1.14
U
1.16
.34
.44
.32
.40
.56
2.64
2.20
.70
.92
1.60
.90
1.32
1.64
1.00
.40

(Vogel, 1983). The Reynolds number for a cluster of barnacles 2–3 cm in length exposed to a flow of 5 cm/s is on the order of 10^3. Although this study was carried out only at a mainstream flow velocity of 5 cm/s, the flow dynamics will obtain for velocities much higher than this. Absolute velocities at different sites on a cluster will, of course, be a function of mainstream velocity, but the qualitative differences in flow pattern upstream and downstream of the peak of a cluster and the strongly reduced velocities downstream of the peak should be present in a broad range of mainstream velocities.

The observed flow dynamics around clusters provides an explanation for the location-dependent food capture and feeding behavior differentials. Whereas barnacles located upstream and at the peak of a cluster will experience a high flux of particles due to the high flow velocity through their cirral baskets, barnacles located downstream in a cluster will see a lower flux of particles because of both the decrease in local flow velocity and the recirculation of fluid in the cluster's wake. Our data indicate that living barnacles in an upstream or peak position capture significantly more particles than those in a downstream position. No differences between upstream and peak locations in particle capture could be demonstrated. Barnacles located at upstream and peak locations need only hold their cirral nets against the flow to feed successfully. In contrast, barnacles located downstream must create their own feeding currents by actively beating their cirral baskets. The faster beat frequency and the qualitative difference in cirral motion implies a higher rate of metabolic activity on the part of downstream animals during feeding, but even given this increased activity, they exhibit significantly reduced feeding success.

Patterson (1984) studied the location-dependent feeding success of a passive suspension feeding colonial octocoral, *Alcyonium siderium*. His work demonstrated greater capture success by upstream polyps when the mainstream flow was slow (2.5 cm/s), equal capture by upstream and downstream polyps at an intermediate flow velocity (9.0 cm/s), and greater capture by downstream polyps when the flow was rapid (19 cm/s). The morphology of *Alcyonium* colonies modified the flow as it passed through the colony; flow was decelerated as it encountered the closely spaced polyps and feeding tentacles (Patterson, 1984). The flow experienced by most of the colony was both more complicated and substantially reduced in speed from the mainstream flow. Patterson (1984) suggested that these alterations in the pattern of feeding success as flow velocity increased might be due to changes in the contribution of turbulence to the eddy diffusion of food particles in the vicinity of downstream polyps. By contrast, many of the barnacles in a cluster experience quasi-mainstream flow, and our observations, although only conducted at a single flow speed, indicate that turbulence downstream of barnacle clusters does *not* increase food supply to downstream barnacles. We believe that the contrast between our results and Patterson's arises, in part, from the difference in mechanical compliance of octocoral polyps and individual barnacles. The plasticity of the octocoral colony due to polyp deflection in response to flow-induced forces may interact with the downstream turbulence to create particle transport conditions that are not present in the case of barnacle aggregations. Deflection in response to current-induced drag forces also seems to underlay differences between food capture rates of the hydroid *Obelia* in unidirectional and oscillating flows (Hunter, 1989). In unidirectional flow, hydroid colonies were bent over and pressed toward the substrate; in oscillating flow, the colonies remained relatively upright, bending from side to side (Hunter, 1989). Deformation resulting from flow-induced forces can have a profound influence on both local flow patterns (Harvell and LaBarbera, 1985) and feeding rates (Sponaugle and LaBarbera, 1991) of passive suspension feeders. However, because of their rigidity, on short (seconds) to medium (days to weeks) time scales where differential growth of individual barnacles can be ignored, the flow patterns around barnacle clusters are fixed.

The ontogeny of barnacle cluster shapes

Barnacles are sessile animals. Though barnacle cyprids typically have a prolonged competent period to sample settling sites, once a barnacle cyprid cements to the substrate, it is committed to remain with the aggregation it has joined or that develops around it (Buss, 1981). Because the extreme upstream row in a flat mock barnacle array captures significantly more "food" than downstream rows, upstream animals in an even-height cluster of living barnacles should grow taller than downstream animals. The peak and rows upstream of peak of hill-shaped clusters of either mock or living barnacles feed considerably better than rows downstream of peak; living barnacles in regions upstream of, or at the peak of, a cluster should show higher growth rates than animals in downstream regions, thus exaggerating height differences over time. This implies that, in a unidirectional flow, the shifted upstream profile is the stable configuration; *i.e.*, in unidirectional flow, all profiles should tend, over time, to grow into the shifted upstream profile. In nature, strictly unidirectional flow past barnacle aggregations is probably rare, but barnacles experience strictly unidirectional flow on ship hulls and in pipes through which water is pumped by human activities (*e.g.*, the seawater systems in marine laboratories, the cooling systems of power generating plants). We predict that shifted upstream profiles would be the dominant shape of groups of encrusting barnacles in these flow situations, but data are lacking to check this prediction.

All of our data was obtained in a unidirectional flow regime, but barnacles in nature experience various combinations of unidirectional and bidirectional flows. Caution must be used in extending data obtained in one flow regime to a different flow regime. At least two aspects of oscillating flows are potentially significant for suspension feeding animals—the alteration in flow direction *per se*, and the effects on flow patterns (Denny, 1988) of the forces that arise when fluids are accelerated. The influence of acceleration effects in oscillating flow on the flow patterns can be assessed via the period parameter, K (Denny, 1988), where $K = u_m T/L$ (u_m is the maximum velocity in each direction of flow, T is the period of oscillation and L is the characteristic length of the cluster). In a wave-swept subtidal or intertidal environment, the period parameter, K, for a barnacle cluster may be large. [For example, a cluster of *Balanus amphitrite* 3 cm in diameter in a (mainstream) flow of 5 cm/s oscillating with a period of 15 s would yield a K of 25.] This means that, in one oscillation, the flow travels a distance longer than the length of the cluster; that is, the flow can be considered to be essentially steady (Denny, 1988). The influence of waves of shorter periods, which tend to dominate in intertidal protected areas, could not be approximated by steady flow, but the flows in such protected environments are more likely to be dominated by tidal than wave-generated currents. Thus the flow patterns around a cluster in oscillating flow will probably not differ substantially from the flow patterns resulting from the unidirectional, steady flow we used in our investigations. At the level of the individual barnacle, the length scale is smaller and K is thus larger. In addition, the cirral basket of barnacles has distinct polarity (concave upstream) and is actively oriented into the flow. Barnacles must reorient the cirral basket when flow direction reverses; by the time a barnacle does so, the flow will be essentially steady and the effects of accelerated flows will be unimportant. Hence justification exists for extrapolating our data to predict the shape of barnacle cluster profiles in oscillating flow.

Even though the effects of fluid acceleration on flow patterns around individual barnacles and barnacle clusters are probably not large in most situations, the effects of change in flow direction *per se* will still be patent. Because upstream and downstream rows will be reversed every half period of oscillation, an end row of the cluster will only receive the benefits of being an upstream row half the time; the average food capture of an end row will be diminished relative to the peak row. In a unidirectional flow, the extreme upstream row of the symmetrical profile captures approximately 60% as many particles as the peak row (Table I). In oscillating flow, this value would be averaged with the value for the extreme downstream row; the end rows of a symmetrical profile would, on average, capture approximately 35% of the particles caught by the peak row. In oscillating flows, a shifted upstream profile is functionally transformed into a shifted downstream profile on flow reversal and *vice versa;* the two profiles actually represent alternative views of the same asymmetrical profile in an oscillating flow. From the data on our model arrays, the extreme row closest to the peak in such an asymmetrical profile should average 53% of the average particle capture of the peak row, while the extreme row furthest from the peak should average 43% of the average capture of the peak row. Similar logic can be applied to the live barnacle clusters. For example, if in Cluster II the two upstream animals switched positions with the downstream animal on flow reversal, these animals would capture, on average (correcting for differences in area of the cirral baskets), about 53% of the particles caught by the peak animal (Table VI). In Cluster III, if the upstream and downstream animals exchanged positions on flow reversal, these animals would, on average (again correcting for size differences), capture approximately the same number of particles as the peak animal; however, note that the peak animal would capture these particles exclusively by passive suspension feeding, while the other animals would spend half of their time actively beating with a concomitant increased cost. In an oscillating flow (whether of short period—from waves, or long period—from tides), all profiles should tend over time to grow into the symmetrical profile. Barnes and Powell (1950) encountered symmetrical barnacle hummocks near the shore in areas exposed to both tides and wave action. Their observations are consistent with our prediction that symmetrical hummocks should form from prolonged exposure of aggregations of barnacles to oscillating flow.

The data from both mock barnacle arrays and clusters of living *B. amphitrite* indicate that aggregations of barnacles will grow into hill-shaped clusters due to the interactions of cluster shape, flow, and feeding. Location in a cluster determines the local flow environment of a barnacle which, in turn, is the proximate cue determining the barnacle's feeding behavior (active or passive). Note the positive feedback present in this situation. Barnacles feed passively by virtue of the fact that their local flow environment is relatively rapid (*i.e.*, above threshold for passive feeding), and the local flow environment is relatively rapid because the barnacle is located at the peak or upstream end of the cluster. Passive suspension feeding is correlated with more successful feeding; successful feeders grow more rapidly and thus draw the cluster further towards one of the hill shaped profiles. Active suspension feeding is a metabolically more expensive (and apparently less successful) mode to which barnacles apparently resort only when ambient flows are too slow to deliver food particles at some minimal rate. The precise shape of a barnacle cluster will depend on the flow situation. A cluster with its peak shifted upstream will be the stable shape for an aggregation of barnacles in a unidirectional flow, while a symmetrical cluster will be the stable end point of the evolution of cluster shape for barnacles in an oscillating flow.

Barnes and Powell (1950) noted that barnacles in the center of hummocks become elongated to the point that they are often dislodged. Because barnacle cyprids preferentially settle in areas already populated by barnacles or barnacle remains (Knight-Jones, 1953; Wethey, 1984), the areas previously occupied by the dislodged barnacles would recruit a new settlement of barnacles and the growth of the aggregation form would be subject once again to the influence of feeding and flow.

Hill-shaped arrays do better at feeding as a unit than flat arrays. This indicates that there may be benefits to a barnacle in being in a hill-shaped aggregation even if that barnacle is not located at the peak. This will be true particularly for clusters in oscillating flow, for there will be a perpetual alternation of the barnacles favored by rapid flow, leading to a more balanced distribution of good feeding fortune across the whole cluster than in unidirectional flow.

A barnacle's position relative to flow is crucial in determining its relative and absolute feeding success in an aggregation. It is location-dependent differential food capture between individual barnacles in an aggregation that gives rise to the morphology of the whole aggregation. Although our data on living barnacles are limited to a single species, we believe that the patterns of flow and of feeding success we describe will be true for any aggregation of acorn barnacles in which some of the individuals in the aggregation are exposed to local flow speeds high enough to elicit passive suspension feeding. We suggest that the shape of barnacle aggregations will generally tend, via growth and recruitment of individuals, toward stable forms that are determined by the flow regime—shifted upstream for unidirectional flow, or symmetrical for oscillatory flow.

Acknowledgments

JP was supported by a Howard Hughes Medical Institute Summer Research Fellowship to the University of Chicago. We thank the College at the University of Chicago for making this support available and Jeanette Wyneken for collecting the barnacle clusters. Julie would like to thank her parents, Jeanie and Mike Pullen for their strong and consistent support.

Literature Cited

Barnes, H., and H. T. Powell. 1950. The development, general morphology and subsequent elimination of barnacle populations, *Balanus crenatus* and *B. balanoides*, after heavy initial settlement. *J. Animal Ecol.* **19:** 175–179.

Baumiller, T. K. 1988. Effects of filter porosity and shape on fluid flux: implications for the biology and the evolutionary history of stalked crinoids. P. 786 in *Echinoderm Biology*, R. D. Burke, P. V. Mladenov, P. Lambert, and R. L. Parsley, eds. A. A. Balkema, Rotterdam.

Bourget, E., and D. J. Crisp. 1975. Early changes in the shell form of *Balanus balanoides* (L.). *J. Exp. Mar. Biol. Ecol.* **17:** 221–237.

Buss, L. W. 1981. Group living, competition, and the evolution of cooperation in a sessile invertebrate. *Science* **213:** 1012–1014.

Crisp, D. J. 1960. Mobility of barnacles. *Nature* **188:** 1208–1209.

Crisp, D. J., and E. Bourget. 1985. Growth in barnacles. *Adv. Mar. Biol.* **22:** 199–244.

Crisp, D. J., and A. J. Southward. 1961. Different types of cirral activity of barnacles. *Phil. Trans. Royal Soc. B* **243:** 271–307.

Denny, M. W. 1988. *Biology and the Mechanics of the Wave-swept Environment.* Princeton University Press, Princeton, NJ.

Harvell, C. D., and M. LaBarbera. 1985. Flexibility: a mechanism for control of local velocities in hydroid colonies. *Biol. Bull.* **168:** 312–320.

Hazlett, B. A. 1988. Behavioral plasticity as an adaptation to a variable environment. Pp. 317–333 in *Behavioral Adaptation to Intertidal Life*, G. Chelazzi and M. Vannini, eds. Plenum Press, New York.

Hunter, T. 1989. Suspension feeding in oscillating flow: the effect of colony morphology and flow regime on plankton capture by the hydroid *Obelia longissima*. *Biol. Bull.* **176:** 41–49.

Jørgensen, C. B. 1966. *Biology of Suspension Feeding.* Pergamon Press, New York.

Knight-Jones, E. W. 1953. Laboratory experiments on gregariousness during setting in *Balanus balanoides* and other barnacles. *J. Exp. Biol.* **30:** 584–598.

LaBarbera, M. 1984. Feeding currents and particle capture mechanisms in suspension feeding animals. *Am. Zool.* **24:** 71–84.

Nowell, A. R. M., and P. A. Jumars. 1984. Flow environments of aquatic benthos. *Annu. Rev. Ecol. Syst.* **15:** 303–328.

Nowell, A. R. M., and P. A. Jumars. 1987. Flumes: theoretical and experimental considerations for simulation of benthic environments. *Oceanogr. Mar. Biol. Ann. Rev.* **25:** 91–112.

Okamura, B. 1990. Behavioral plasticity in the suspension feeding of benthic animals. Pp. 637–660 in *Behavioral Mechanisms of Food Selection*, R. N. Hughes, ed. Springer-Verlag, Berlin.

Patterson, M. R. 1984. Patterns of whole colony prey capture in the octocoral, *Alcyonium siderium*. *Biol. Bull.* **167:** 613–629.

Sokal, R. R., and F. J. Rohlf. 1981. *Biometry.* W. H. Freeman and Company, San Francisco, CA.

Sponaugle, S., and M. LaBarbera. 1991. Drag-induced deformation: a functional feeding strategy in two species of gorgonians. *J. Exp. Mar. Biol. Ecol.* **148:** 121–134.

Trager, G. C., J.-S. Hwang, and J. R. Strickler. 1990. Barnacle suspension-feeding in variable flow. *Mar. Biol.* **105:** 117–127.

Vogel, S. 1983. *Life in Moving Fluids.* Princeton University Press, Princeton, NJ.

Vogel, S., and M. LaBarbera. 1978. Simple flow tanks for research and teaching. *Bioscience* **28:** 638–643.

Wethey, D. S. 1984. Spatial pattern in barnacle settlement: day to day changes during the settlement season. *J. Mar. Biol. Assoc. U.K.* **64:** 687–698.

Warner, G. F. 1977. On the shapes of passive suspension feeders. Pp. 567–576 in *The Biology of Benthic Organisms*, B. F. Keegan, P. O. Ceidleigh, and P. J. S. Boaden, eds. Pergamon Press, New York.

Reference: *Biol. Bull.* **181**: 453–458. (December, 1991)

Oligomer Composition and Oxygen Binding of the Hemocyanin of the Blue Crab *Callinectes sapidus*

CHARLOTTE P. MANGUM[1], JOHN GREAVES[2], AND JULIA S. RAINER[2]

[1]*Department of Biology, College of William and Mary, Williamsburg, Virginia 23185*
and [2]*School of Marine Science, Virginia Institute of Marine Science,*
College of William and Mary, Gloucester Point, Virginia 23062

Abstract. In the blue crab, the ratio of hexamers to dodecamers of the O_2 carrier hemocyanin varies in natural populations. Isolated dodecamers have a lower O_2 affinity and greater cooperativity than isolated hexamers. The difference in O_2 binding can also be resolved in native mixtures that differ in polymer composition. A high content of dodecamers in native mixtures is, in fact, correlated with the presence of an invariant polypeptide chain that is believed to link two hexamers to form dodecamers. On the other hand, the content of a variable chain that has been postulated to play a role in hexamer pairing is correlated with a *low* content of dodecamers. The variable, but not the invariant, monomers can be present in levels so low that they must not be represented in all dodecamers in the blood.

Introduction

The hemocyanin (Hc) of the blue crab *Callinectes sapidus* Rathbun, like that of most crustaceans, exists in the blood as a mixture of hexamers (1 × 6) and dodecamers (2 × 6). The two oligomers are stable aggregates, not members of a chemical equilibrium. Oligomerization is important in optimizing the physical properties of the blood (Snyder and Mangum, 1982; Mangum, 1986) but its respiratory significance, if any, is not known. While both Brouwer *et al.* (1982) and Johnson *et al.* (1984) mentioned that hexamers and dodecamers do not differ in O_2 binding, neither reported the data. Brouwer (pers. comm.) has kindly communicated his opinion that the finding was not definitive because the two oligomers were poorly separated in their experiments by atmospheric pressure permeation gel chromatography.

In *C. sapidus,* the Hc oligomers are built of five to six different polypeptide chains, four of which (in our terminology, Nos. 1, 3, 5, and 6) exhibit considerable quantitative variability in natural populations. In the laboratory, changes in the concentrations of two to three of the four (Nos. 3, 5, and 6) can be induced by prolonged hypoxia or a change in acclimation salinity. Accompanying the alterations in monomeric subunit composition are highly adaptive changes in intrinsic O_2 affinity, which can be specifically attributed to the levels of chains 3 and 6 (Mason *et al.,* 1983; Mangum and Rainer, 1988; Rainer, 1989; deFur *et al.,* 1990).

The nature of the hexamers that do not form dodecamers, but remain as such in the blood, is unclear. Hamlin and Fish (1977) described them as comprising "as much as" 20% of the total material in their purified Hc preparations. Brouwer *et al.* (1982) and Johnson *et al.* (1984) mentioned similar figures. Herskovits *et al.* (1981), however, specified a range of 30–50% and raised the possibility of a seasonal change. Recently, we have found that the ratio does in fact vary in nature (Greaves *et al.,* 1991).

On the basis of a combination of electrophoretic and immunological properties, Markl (1986, for review) has classified the monomeric chains of the arthropod Hcs into four categories that differ in their interspecific variability and their putative role in the assembly of the native polymers. The chain (No. 4) that is believed to serve as the dodecamer-former in *C. sapidus* (Stöcker *et al.,* 1988) is one of the two essentially invariant ones in our ongoing sample, which presently totals about 1000 individuals (Rainer, 1989; Mangum, 1990). Densitometric scans shown by Johnson *et al.* (1984), however, indicate that

Received 20 June 1991; accepted 8 August 1991.

the concentration of chain 4 was at least as high in a hexameric fraction as in a dodecameric fraction. Moreover, their hexameric fraction lacked all but perhaps trace quantities of chains 5 and 6, two of the most variable ones in nature. They suggested that these chains, presumably instead of chain 4, play a role in dodecamer formation.

The way in which the variable chains influence O_2 binding is presently unclear. Those that do not play an important role in hexamer pairing (*e.g.*, No. 3) may have simple and direct effects on O_2 affinity. Chains that do participate in hexamer pairing, however, could exert their influence indirectly if O_2 binding of the two oligomers differs.

We attempted to circumvent the problem of poor separation at atmospheric pressure by developing a protocol for HPLC, which proved to achieve clean separation (Greaves *et al.*, 1992). In the present investigation we used the procedure 1) to examine the respiratory properties of the two fractions and 2) to correlate the ratio of 2 × 6:1 × 6 aggregates in native mixtures with their subunit composition and O_2 binding. We also tried, without success, to compare the respiratory properties of native hexamers with those of hexamers prepared as dissociation products of dodecamers.

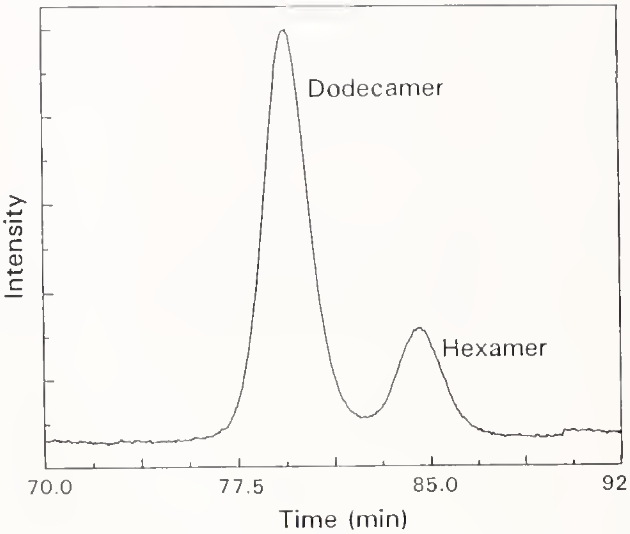

Figure 1. An example of the separation of oligomers obtained by HPLC. Absorbance was monitored at 337 nm.

Materials and Methods

Large adult males (≥80 g wet wt) were obtained from either the seaside (Eastern Shore of Virginia at Wachapreague) or estuarine (York R.) populations studied earlier (Mason *et al.*, 1983; Mangum and Rainer, 1988; Rainer, 1989). Blood samples were taken from the infrabranchial sinuses and declotted as previously described. In the present investigation the samples were also filtered at 0.22 μm for injection into the HPLC system.

HPLC

HPLC was carried out on a Perkin Elmer Series 4 system equipped with one or two (connected in series) Ultrahydrogel 1000 size exclusion columns (7.8 × 300 mm; Waters Associates). The mobile phase was a saline containing 300 mmol l^{-1} NaCl, 25 mmol l^{-1} $MgCl_2$, and 10 mmol l^{-1} $CaCl_2$; this saline was also filtered at 0.22 μm immediately prior to use. The Perkin Elmer Model LC-95 variable wavelength UV absorbance detector was set at 337 and 280 nm. Further details of the protocol were described by Greaves *et al.* (1992); an example of the separation is shown as Figure 1.

O_2 binding

These measurements were performed on the fractions separated by HPLC, after reconcentration by membrane centrifugation (Centricon 30), or on unfractionated aliquots of the same samples analyzed by HPLC, following dialysis against 0.05 mol l^{-1} Tris maleate buffered saline (specified above). Because reconcentration is a lengthy process, aliquots of the isolated oligomers were examined as soon as the Hc levels reached an absorbance at 337 nm of 0.25–0.58 (2–3 h centrifugation), using a tonometric procedure suitable for dilute samples. Precision mixed, humidified gases were passed across rapidly shaken samples at constant temperature and atmospheric pressure, and the changes in absorbance at 337 nm determined (procedure described in detail by Mason *et al.*, 1983) with a Mervyn Roy 501 spectrophotometer. Rather than dissociate the remainder of the available material for electrophoresis, we chose to use the cell respiration procedure (Mangum and Lykkeboe, 1979) to document more extensively the preliminary findings of the tonometry by performing repeated O_2 binding measurements on the two intact oligomers. The procedure required further reconcentration for a total of 7–8 h. Native mixtures of the two oligomers, aliquots of which were analysed by electrophoresis, were also examined using this procedure. These samples were dialyzed overnight against buffered saline.

Electrophoresis

Samples were dialyzed overnight against 50 mmol l^{-1} Tris HCl (pH 8.9) containing 10 mmol l^{-1} EDTA to dissociate the native oligomers into their monomeric subunits. Alkaline dissociation electrophoresis was carried out, as described by Mangum and Rainer (1988). The gels (12%) were scanned with a Shimadzu densitometer.

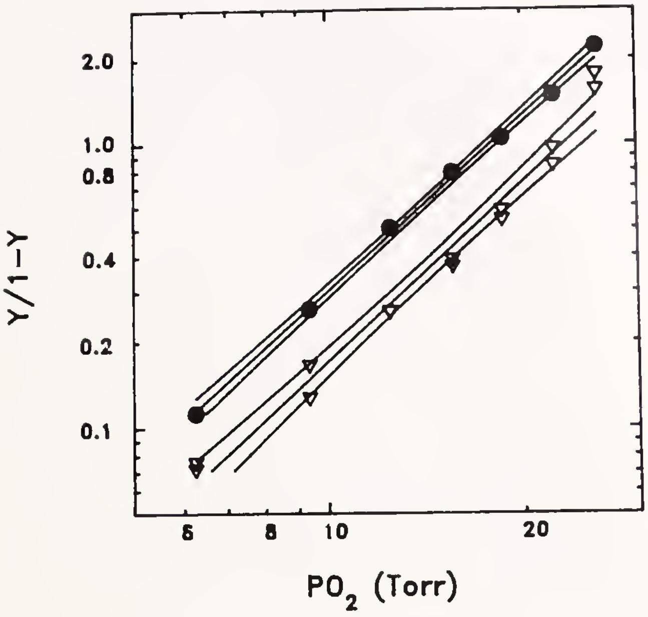

Figure 2. Hill plots of O_2 binding properties of isolated hexamers and dodecamers. 25°C, 0.05 mol l^{-1} Tris buffered saline containing 10 mmol l^{-1} $CaCl_2$, 25 mmol l^{-1} $MgCl_2$, and 300 mmol l^{-1} NaCl. Tonometric data for one aliquot of hexamers (circles, pH 7.49) and two of dodecamers (triangles, pH 7.52). Lines are regression lines and their 95% confidence intervals.

Results

HPLC

We did not observe the material larger than the about 900 kD dodecamers that had been reported by both Hamlin and Fish (1977) and Herskovits *et al.* (1981). Because this material (which has a sedimentation coefficient of 33S) should have a molecular weight in excess of the separation range of our gel, it should have appeared as a shoulder on the peak of the dodecameric fraction. Moreover, as pointed out earlier (Greaves *et al.*, 1992), the ratios of the 280:337 nm areas, obtained for the two oligomer fractions and for the samples from different individuals, were statistically indistinguishable, despite the variation in contents of the two oligomers described below. The optical evidence, then, indicates that no material other than Hc was present and that the condition of the active site of the two oligomers does not differ.

O_2 binding

The results obtained in three tonometric determinations suggest that isolated dodecamers have a significantly lower O_2 affinity than isolated hexamers (Fig. 2), despite a slightly higher experimental pH. The 95% confidence intervals do not overlap even though the fit of regression lines to the data for dodecamers is poor because, like many native mixtures of crustacean Hcs, they show an increase in cooperativity at higher oxygenation states. Because of the poor fit, cooperativity (n_{50}) was estimated in Figure 3 from regression analysis of only the points ($n = 6$) in Figure 2 that exceed 30% HcO_2; the available data in this region suggest that dodecamers have a significantly ($P < .015$) higher cooperativity than hexamers. The cell respiration procedure, with which a larger number of determinations was made (Fig. 3), yielded very similar results: the hexameric fraction has a significantly higher O_2 affinity ($P = .0325$ according to Student's t test) and lower cooperativity ($P = .0495$). Neither mean value for O_2 affinity of the isolated oligomers differs significantly from the intermediate value for the native, unfractionated mixture ($P = .25$ for the dodecamers and .12 for the hexamers) although, following the dilution, fractionation and reconcentration, cooperativity had clearly fallen in both cases ($P < .0005$). The value of n_{50} for the native mixture, which had not been diluted, fractionated, and reconcentrated, is typical of this species under the experimental conditions

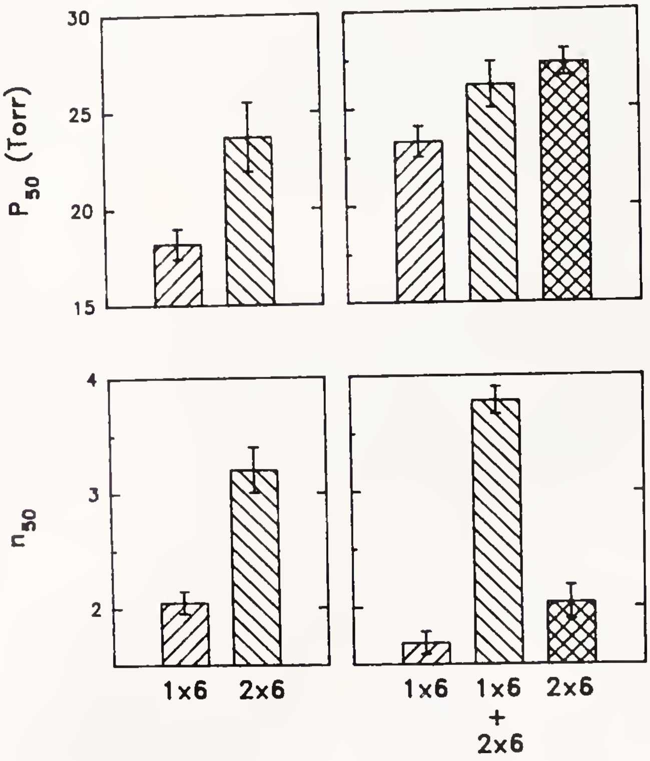

Figure 3. O_2 binding of isolated hexamers and dodecamers. 25°C. Panels at left show tonometric data (pH 7.49–7.52) from Figure 1, with error as 95% confidence intervals. Panels at right show cell respiration data for 6 replicate measurements of isolated hexamers (pH 7.40), dodecamers (pH 7.40), and the dialyzed but unfractionated (77% dodecamers) sample (pH 7.38) from which the two fractions were prepared. Buffered saline as in Figure 1. Mean values ± S.E.

employed here (*e.g.*, Mason *et al.*, 1983; Mangum and Rainer, 1988).

The O_2 binding properties of two undiluted and unfractionated samples with a high content of dodecamers (Fig. 4) are indistinguishable from one another (according to Student's *t* test, $P = .2$ for both P_{50} and n_{50}; $n = 6$); similarly, two with a low content of dodecamers had indistinguishable O_2 binding properties ($P > .4$; $n = 6$). The O_2 affinity of each pair differs significantly from that of the alternative pair ($P = .004$); specifically, a high content of dodecamers is accompanied by a lower affinity. The cooperativity values, which are well within the range usually observed in this species, are also significantly greater in the sample with the higher dodecamer content ($P = .005$).

We attempted to create artificial hexamers by freezing and thawing (11× over a two-day period) unreconcentrated dodecamers. Following membrane centrifugation, all O_2 binding activity had disappeared in this fraction, as well as that containing native hexamers. We then examined the polymer composition and O_2 binding of the remainder of the unfractionated and never diluted sample from which the two fractions had been prepared, which had also been frozen and thawed 11 times. Prior to freezing, 77% of this sample consisted of dodecamers, and it had the O_2 binding properties shown in Figure 2. Following freezing and thawing, 76% consisted of dodecamers, and it exhibited an indistinguishable O_2 affinity and cooperativity ($P = .63$).

Subunit composition

The monomer and oligomer compositions of samples from 13 individuals collected in the summer from the seaside population are shown in Table I. After first transforming the percentages to a normal distribution (arcsin), we examined the relationship between the quantities of each chain and the content of dodecamers by linear regression analysis. There is no indication of a correlation between the variation in levels of chains 1, 2, 3, or 6 and the content of dodecamers ($r = -.103$ to $.421$; $P > .10$). However, dodecamer content is highly and directly correlated with relative content of chain 4 ($r = .601$; $P = .02$) (Fig. 5). Both of the two invariant chains (2 and 4), unlike variable ones, are present in sufficient quantities to be represented in each hexamer of a 2 × 6 pair. The correlation with dodecamer content is not improved, however, by summing the relative contents of the chains 2 and 4 ($r = .341$; $P > .10$). Dodecamer content is highly but inversely correlated with the levels of chain 5 ($r = -.653$; $P = .01$).

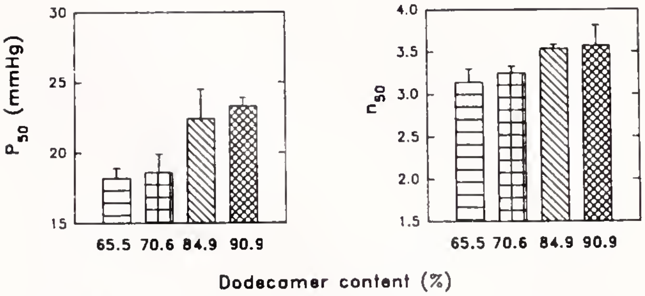

Figure 4. O_2 binding properties (cell respiration procedure) of native Hcs with different contents of dodecamers. 25°C, pH 7.50. Buffered saline as in Figure 1. Mean ± S.E. (n = 6).

Table I

Subunit and oligomer composition of hemocyanins from 13 individuals of Callinectes sapidus

	% Total peak area*						%
No.	1	2	3	4	5	6	2 × 6-mers
1	8.4	27.2	*5.4*	20.0	26.2	12.7	65.5
2	23.4	28.2	7.0	24.8	9.3	7.0	70.6
3	10.8	22.2	9.8	25.4	14.9	16.9	74.4
4	9.7	29.0	6.8	32.7	12.2	9.6	78.3
5	17.3	19.6	19.5	23.4	*5.3*	14.9	79.6
6	12.5	31.8	11.0	23.9	8.3	12.3	81.1
7	9.3	24.7	15.2	26.8	12.0	11.9	82.5
8	*5.8*	20.0	10.8	34.6	12.1	16.7	84.4
9	9.2	32.3	7.1	34.1	*4.0*	13.3	84.4
10	23.0	23.8	10.0	28.7	9.0	*5.8*	84.9
11	17.4	21.0	9.7	29.4	10.2	12.3	85.1
12	*5.1*	29.8	9.1	31.1	10.4	14.3	86.8
13	*5.4*	24.5	13.5	25.5	*6.1*	15.2	88.0

* Figures less than $^1/_{12}$th of the dodecameric fraction shown in italics.

The numerical relationship between the % composition values for the two parameters is also of interest. Any chain present in less than the figure [(its % composition)/(% dodecamers) = $^1/_{12}$th or] 8.3% must not be represented in all dodecamers. All four variable (but neither of the invariant) chains can fall into this category, some trivially and probably not outside of the error of densitometry, but some by a large margin (Table I).

Discussion

Morris (1988) systematically investigated the effects of freezing on crustacean Hcs. Repeated bouts of freezing and thawing resulted in progressive dissociation of dodecamers to hexamers, although to a different degree in the four species examined, and an attendant decrease in cooperativity. As noted by Morris (1988), much of our own experience concurs with his: thawed crustacean Hcs often show impaired cooperativity (see also Reese, 1989). Because freezing (at least using high concentrations and freezing for only a brief period) had no dis-

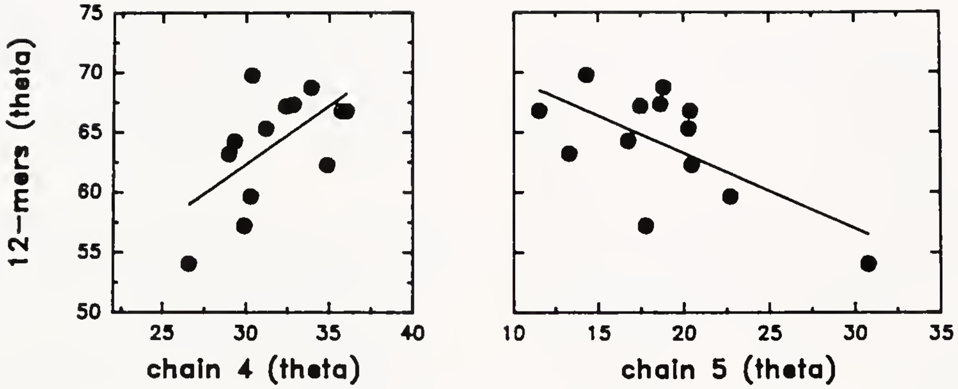

Figure 5. The relationship between the fractional composition of dodecamers and chains 4 and 5 of *Callinectes sapidus* Hc, expressed as arcsin transformed percentages. Lines are fitted regression lines.

cernible effect on *C. sapidus* Hc, we can only conclude that it is more stable than those examined by Morris (1988).

The present data provide further information on the natural variability of the two native oligomers in this species. They provide no evidence that chain 6 plays a role in the pairing of hexamers. However, our data strongly support the inference of Stöcker *et al.* (1988) that high levels of chain 4 promote dodecamer formation. Moreover, they do not support the conclusion reached by Johnson *et al.* (1984) that chain 5 promotes dodecamer formation.

We should note that, in the present sample, chain 1 appears to be more variable than 3 or 6 and almost as variable as 5. Although we have noticed the variability of this chain in much larger samples (Rainer, 1989), we have not previously found nearly as much variability, and we suggest that the present sample is misleading because of its small size. In addition, we have no evidence that chain 1 responds to an environmental stimulus or that it influences respiratory properties. The high and constant levels of chain 2 are intriguing because this monomer is not known to play a role in oligomerization. According to Markl's classification, it is an interspecifically conservative type of chain, but chain 3 (Stocker *et al.*, 1988), which is highly variable intraspecifically, is also classified as conservative interspecifically.

Our findings demonstrate different O_2 binding properties in the two native oligomers: dodecamers, the predominant aggregate in the blood, have a lower O_2 affinity and greater cooperativity than hexamers. The difference is detectable in both isolated fractions and native mixtures of different proportions of the two. The variable chain No. 5, which is not known to influence O_2 affinity directly, could have an indirect influence via inhibition of hexamer pairing. On the other hand, the variable chains 3 and 6, which influence O_2 affinity, are not correlated with dodecamer content. The most likely inference at present is that their respiratory effect is simple and direct.

Finally, Johnson *et al.* (1984) concluded that the levels of chains 5 and 6 indicate that they comprise $\frac{1}{6}$th of the dodecamers. The present data indicate that they (as well as chain 1) may occur in either considerably higher or lower levels, which suggests heterogeneity of the dodecamers in the blood. In fact, some heterogeneity would be expected if the changes in subunit composition that are responsible for the observed adaptability of respiratory properties of the Hc are physiologically labile.

Acknowledgments

Supported by NSF DCB 88-16172 (Physiological Processes) to CPM. We thank D. A. Scholnick for performing the tonometric measurements.

Literature Cited

Brouwer, M., C. Bonaventura, and J. Bonaventura. 1982. Heavy metal ion interactions with *Callinectes sapidus* hemocyanin: structural and functional changes induced by a variety of heavy metal ions. *Biochemistry* **21:** 2529–2538.

de Fur, P. L., C. P. Mangum, and J. E. Reese. 1990. Respiratory responses of the blue crab *Callinectes sapidus* to long-term hypoxia. *Biol. Bull.* **178:** 46–54.

Greaves, J., J. S. Rainer, and C. P. Mangum. 1992. Size-exclusion high performance liquid chromatography of the dodecameric and hexameric forms of hemocyanin from *Callinectes sapidus*. *Mar. Biol.* (in press).

Herskovits, T. T., L. J. Erhunmwunsee, R. C. San George, and A. Herp. 1981. Subunit structure and dissociation of *Callinectes sapidus* hemocyanin. *Biochim. Biophys. Acta* **667:** 44–58.

Hamlin, L. M., and W. W. Fish. 1977. The subunit characterization of *Callinectes sapidus* hemocyanin. *Biochim. Biophys. Acta* **491:** 46–52.

Johnson, B. A., C. Bonaventura, and J. Bonaventura. 1984. Allosteric modulation of *Callinectes sapidus* hemocyanin by binding of L-lactate. *Biochemistry* **23:** 872–878.

Mangum, C. P. 1986. Osmoregulation in marine and estuarine animals: the view of a respiratory physiologist. *Boll. Zool.* **53:** 1–8.

Mangum, C. P. 1990. Inducible O_2 carriers in the crustaceans. Pp. 92–103 in *Animal Nutrition and Transport Processes,* J-P. Truchot and B. Lahlou, eds. Karger, Basel.

Mangum, C. P., and G. Lykkeboe. 1979. The influence of inorganic ions and pH on the oxygenation properties of the blood in the gastropod mollusc *Busycon canaliculatum. J Exp. Zool.* **207:** 417–430.

Mangum, C. P., and J. Rainer. 1988. The relationship between subunit composition and O_2 binding of blue crab hemocyanin. *Biol. Bull.* **174:** 77–82.

Markl, J. 1986. Evolution of functionally and structurally diverse subunits in the respiratory protein hemocyanin from arthropods. *Biol. Bull.* **171:** 90–115.

Mason, R. P., C. P. Mangum, and G. Godette. 1983. The influence of inorganic ions and acclimation salinity on hemocyanin-oxygen binding in the blue crab *Callinectes sapidus. Biol. Bull.* **164:** 104–123.

Morris, S. 1988. Effects of freezing on the function and association state of crustacean haemocyanins. *J. Exp. Biol.* **138:** 535–539.

Rainer, J. S. 1989. Distribution of the heterogeneous hemocyanin subunits along a salinity gradient. M.A. Thesis, College of William and Mary, Williamsburg, Virginia. 62 pp.

Reese, J. E. 1989. Structure and function of crustacean hemocyanins. M.A. Thesis, College of William and Mary, Williamsburg, Virginia. 75 pp.

Snyder, G. K., and C. P. Mangum. 1982. The relationship between the size and shape of an extracellular oxygen carrier and the capacity for oxygen transport. Pp. 173–188 in *Physiology and Biology of Horseshoe Crabs,* J. Bonaventura, C. Bonaventura, and S. Tesh, eds. Alan R. Liss Inc., New York.

Stöcker, W., U. Raeder, M. M. C. Bijlholt, T. Wichertjes, E. F. J. van Bruggen, and J. Markl. 1988. The quaternary structure of four crustacean two-hexameric hemocyanins: immunocorrelation, stoichiometry, reassembly and topology of individual subunits. *J. Comp. Physiol.* **B158:** 271–289.

Reference: *Biol. Bull.* **181:** 459–462. (December, 1991)

Biological Activity of Biosynthetic Rainbow Trout Growth Hormone in the Eastern Oyster, *Crassostrea virginica*

KENNEDY T. PAYNTER[1]* AND THOMAS T. CHEN[2]

[1]*Department of Zoology, University of Maryland, College Park, Maryland 20742 and* [2]*Center of Marine Biotechnology, University of Maryland, 600 E. Lombard St., Baltimore, Maryland 21202*

Abstract. Juvenile oysters were exposed to seawater containing 10^{-9}, 10^{-8}, and 10^{-7} M biosynthetic rainbow trout growth hormone (rtGH); the treatment was applied for one five-hour period per week for five weeks. At the end of the five weeks, the animals treated with the two highest concentrations of hormone were significantly longer and had dry tissue weights 50% greater than did the lowest treatment group or the control group. Continuing *in vitro* experiments on isolated oyster tissue showed that the hormone treatment significantly increased oxygen consumption. Boiled hormone had no effect. In both sets of experiments (whole animals and isolated tissues), the % dry wt (dry wt/wet wt) was significantly higher in all animals and tissues that responded to rtGH. The results demonstrate that rtGH has biological activity in oyster tissues, and this activity may be directly associated with growth regulation in the whole animal. The results further show that bivalve growth is not directly limited by environmental parameters.

Introduction

The growth of many marine and estuarine pelecypods has long been thought to be determined by environmental conditions. Many studies have revealed specific correlations between bivalve growth rate and such environmental factors as water flow, salinity, temperature, oxygen, and food availability (Dame, 1975; Hall, 1984; MacDonald and Thompson, 1985a,b; Brown, 1988; Brown and Hartwick, 1988a,b). Yet endogenous control of growth by neural or hormonal systems has been investigated in only a few species. A significant body of knowledge indicates that mollusks possess complex endocrine systems (Joosse and Geraerts, 1983), and several recent findings suggest that bivalve growth may be regulated at least in part by an endocrine system.

In general, comparative endocrinological studies of mollusks have been limited to gastropods and cephalopods, and in many of those studies, endocrine control of reproduction has been a major focus. In the snail *Lymnaea stagnalis,* however, an endogenous growth-promoting hormone has been identified and well characterized. This hormone, called the molluscan insulin-like peptide (MIP), has been isolated from *Lymnaea* neuroendocrine cells and reported to affect various aspects of growth, metabolism, and shell formation in the snail (Geraerts, 1976; Dogterom *et al.*, 1979; Dogterom and Jentjens, 1980; Dogterom and Robles, 1980; Smit *et al.*, 1988).

While much is known about the physiology of the bivalves, little attention has been paid to the endocrine regulation of their metabolism and growth. In early, rather crude experiments, for example, the growth of oysters was arrested after their cerebral ganglia had been extirpated (Galtsoff, 1964), [and similar results were obtained with the gastropod, *Crepidula fornicata,* by Lubet (1971)]. More recently, Toullec *et al.* (1988) reported that extracts of cerebral ganglia prepared from *Mytilus edulis* stimulated the incorporation of leucine into the macromolecular fraction of mantle cells that had been isolated from several bivalve species. These studies suggest that bivalve growth, like that of snails, is controlled by endocrine mechanisms that are not species specific.

Conservation of sequence and function among vertebrate growth hormone polypeptides is also well established. Furthermore, bovine growth hormone (as well as insulin) has been shown to accelerate the growth of abalone larvae (Morse, 1981, 1984), and a growth hormone

---

Received 14 January 1991; accepted 20 September 1991.

* To whom correspondence should be addressed.

like polypeptide has been identified in the abalone (Moriyama *et al.*, 1989). Therefore, we have begun to investigate the effects of biosynthetic rainbow trout growth hormone (rtGH) on the growth and metabolism of the eastern oyster, *Crassostrea virginica*. Here we report that exogenously applied rtGH stimulates the growth of juvenile oysters and increases oxygen consumption in isolated oyster tissues.

Materials and Methods

Oyster larvae (*Crassostrea virginica*) were obtained from the Virginia Institute of Marine Science. The larvae were raised according to standard hatchery techniques. All competent larvae were induced to undergo cultchless metamorphosis (not attached to substrate) by treatment with epinephrine (10^{-6} *M*) in the seawater. The resulting juvenile oysters were raised in downwelling chambers in the hatchery at the Chesapeake Bay Institute (CBI) of the Johns Hopkins University.

Biosynthetic rtGH was prepared as previously described (Agellon *et al.*, 1988). The complementary DNA (cDNA) of rtGH (Agellon and Chen, 1986) was cloned and introduced into *E. coli* for large scale production of the polypeptide. GH inclusion bodies were isolated from *E. coli* cells, dissolved in a 5 *M* guanidine hydrochloride solution, and the denatured GH polypeptide was re-natured by differential dialysis against 50 m*M* ammonium bicarbonate buffer (pH 10.0). The lyophilized protein was resuspended in 10 m*M* ammonium bicarbonate buffer pH 10.0 at a concentration of 10 mg/ml and used in appropriate amounts to inoculate the experimental seawater.

Oyster growth

In September and October 1989, during the natural growing season of the oyster in the Chesapeake Bay region, an experimental hormone treatment was begun. Four groups of 25 juvenile oysters were constructed such that the initial mean heights of the groups were not different. One group (control group) was incubated in seawater inoculated with buffer; the other three groups were incubated in seawater containing 10^{-7} *M*, 10^{-8} *M*, or 10^{-9} *M* rtGH, respectively. Each group was incubated for 5 h, once per week, in Petri dishes containing 50 ml of 1 μ-filtered ambient seawater ($\approx 8‰$) at 23°C. Initially, and before each treatment thereafter, the shell height of each oyster was measured from the umbo to the ventral shell margin. The animals were maintained in an upwelling system with a continuous flow of 100 μ filtered seawater during the entire experiment. After five weeks the oysters were sacrificed, and the final height, total weight, shell weight, wet tissue weight, and dry tissue weight were determined for each individual. Whole oyster volume was calculated as the difference between total animal weight and shell weight.

Mean values of final height, total weight, shell weight, wet tissue weight, and dry tissue weight were calculated for each treatment group. Values were statistically compared using a t-test.

Oxygen consumption of isolated tissues

Respirometry was conducted according to standard manometric procedures. Oyster gills (two gill pairs per individual) were dissected and split into gill pairs. One pair from an individual was used as a control, the other was treated with boiled or native rtGH. Therefore, oxygen consumption was compared in gills that were taken from the same animal, but that were treated differently. The gill pairs were immediately placed in manometric flasks containing 2 ml filtered seawater inoculated with buffer, boiled rtGH, or native rtGH (10^{-6} *M*). Native and boiled insulin and bovine growth hormone (BST) were also tested. The flasks were affixed to a differential respirometer (Gilson), immersed in the water bath (25°C), and allowed to equilibrate for 30 min. After equilibration, the respirometer system was closed and initial readings on all manometers were recorded. At 15-min intervals thereafter, manometer readings were recorded. Incubations typically lasted for 2 h. Oxygen consumption was usually linear after the first 15-min reading. Any samples not showing linear decreases in oxygen concentration were discarded. After the respirometry had been completed, the tissues were removed from the flasks, weighed, dryed in a 60°C oven for 72 h, and reweighed.

Because oxygen consumption rates in gill pairs from a single individual were being compared, the oxygen consumption data were analyzed by means of a paired t-test to minimize the effects of between individual variation.

Results

After three weeks of treatment (Table I), the oysters treated with the highest concentrations of rtGH for five weeks (10^{-7} *M* and 10^{-8} *M*) were significantly larger with respect to shell height and dry tissue weight than either the control group or the lowest treatment group (10^{-9} *M*). But only the oysters treated with 10^{-7} *M* hormone had shell weights that were significantly larger than those of the control group. Increases in total weight and wet tissue weight were not significantly different from controls; variation was high in these categories due to the large contribution of water to the weights. Tissue hydration, as measured by the dry wt/wet wt ratio, was significantly higher in the highest treatment groups when compared to the control group. There was no mortality in any of the groups.

Trout GH induced significantly higher rates of oxygen consumption in isolated gill tissue (Fig. 1). The control oxygen consumption values for both boiled rtGH and native rtGH experiments were not different and were

Table I

Effect of exogenously applied trout growth hormone on oyster growth

Treatment	Initial ht	Final ht	Total wt	Shell wt	Dry wt	Dry wt/Wet wt
Control	8.14 (.25)	11.68 (.27)	206 (11)	136 (8)	6.10 (.66)	0.219 (.019)
10^{-9} *M*	8.04 (.27)	11.74 (.23)	199 (9)	131 (6)	6.87 (.66)	0.262 (.023)
10^{-8} *M*	8.72 (.18)	12.79 (.27)*†	244 (20)	171 (11)†	9.42 (.41)*†	0.273 (.010)*
10^{-7} *M*	8.65 (.32)	13.00 (.36)*†	252 (15)†	189 (13)*†	9.41 (.74)*†	0.287 (.026)*

* Significantly larger than the control group (t-test; $P < 0.05$).

† Significantly larger than 10^{-9} *M* treatment group (t-test; $P < 0.05$).

Initial height represents mean size at the beginning of the experiment and final height, total wt, shell wt, and dry wt are mean values determined after the five-week treatment cycle was concluded. See Materials and Methods section for details. Height (ht) was measured in mm from the umbo to the ventral shell margin; weight was measured in mg. Standard errors of the mean (SEM) are in parentheses.

combined for presentation in Figure 1. Oxygen consumption in tissues treated with rtGH was significantly higher than those in tissues treated with either buffer alone or with boiled rtGH. Although the magnitude of the response was variable between individuals, the rtGH treated tissues consumed more oxygen per unit time than either control group in every experiment performed. In other experiments, insulin and bovine somatotropin stimulated oxygen consumption as well (Table II).

Discussion

We have shown that exogenously applied rtGH stimulates growth in juvenile oysters and stimulates oxygen consumption in adult gill tissues. The two highest treatment concentrations (10^{-7} and 10^{-8} *M*), which are considered physiological concentrations in vertebrates, elicited positive responses of similar magnitude, however, final mean sizes in the lowest treatment (10^{-9} *M*) group were not different from those in the control group. Although these results do not establish a growth-regulating function for rtGH, they suggest that an endocrine growth-controlling system occurring in bivalves may be related to the growth regulating system in vertebrates.

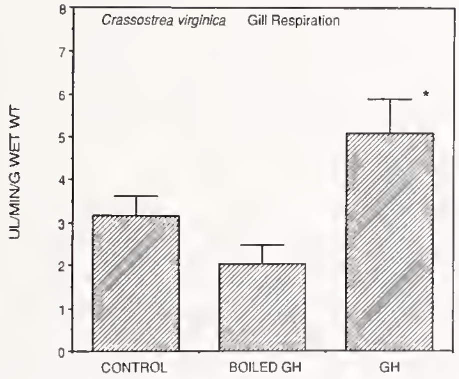

Figure 1. Oxygen consumption of isolated oyster gill tissues treated with trout growth hormone. Oxygen consumption in tissues treated with rtGH was significantly higher (paired t-test; $P < 0.05$) than in tissues treated with buffer alone or with boiled rtGH.

While bivalve growth has been widely studied, most experiments have focused on the relationship between growth and exogenous or environmental factors, such as water quality (seston level, chlorophyll content, temperature, and salinity). These factors have been shown to strongly influence growth rate, but recent studies have suggested that growth and the physiological functions associated with growth, such as digestion, feeding rate, and oxygen consumption, may be endogenously controlled with respect to the environment (see Bayne and Hawkins, 1990). Hawkins *et al.* (1985) concluded that feeding in mussels is time-optimized; not that nutrient gain is continuously maximized, but that feeding behavior is optimized over longer periods of time. They furthermore suggested that this feeding behavior is endogenously controlled to spare costly metabolic adjustments in response to an unstable environment, such as one typically found in the estuary.

But the growth of the juvenile oysters used in this study was much lower than that of sibling oyster groups placed in the field. Thus, the growth of the experimental oysters raised at CBI in the upwelling chambers may have been environmentally limited. Yet growth hormone treatment stimulated growth in the upwelling chambers. Therefore,

Table II

Mean increase in oxygen consumption in isolated oyster gill tissues produced by rtGH, insulin, or bovine somatotropin (BST) treatment

Treatment	Mean increase (μl/min/mg)	*P*
rtGH	3.1	.006
Insulin	2.4	.05
BST	4.2	.03

Mean increase values represent the mean increase in oxygen consumption over control gills. A paired t-test was employed to determine the significance (*P*) of the differences.

although sufficient nutrients must have been available for the enhanced growth to occur, the control oysters did not use them. We conclude that endogenous metabolic controls regulate growth rates with respect to, but not directly limited by, the environment, and that exogenously applied growth hormone causes a shift in that regulation. If the concentration of food in the upwellers was not limiting, the treated oysters may have fed at a greater rate to support their faster growth. On the other hand, if food levels were limiting, or nearly so, the treated oysters may have become more efficient and may have been able to assimilate and use a higher percentage of ration. These possibilities will be directly tested by performing feeding, assimilation, and utilization experiments and other scope-for-growth studies on treated and control oysters.

Our results also indicate that the effect of rtGH in oysters, like that of its evolutionary relative, prolactin, in fish (see Prosser, 1974), may be involved in osmoregulation, because it influenced tissue, and possibly cellular, hydration levels. Thus, the effect on growth could be even more indirect. Oysters grow faster at higher salinities where tissue hydration is normally slightly lower (Paynter and Mallonee, 1991; Paynter, pers. obs.). Changes in tissue hydration could affect numerous physiological functions, including feeding and digestion rates, which would ultimately lead to more rapid growth. Studies are currently underway to examine the *in vitro* effects of rtGH on various aspects of bivalve metabolism and growth.

Acknowledgments

The authors would like to thank Y. L. Tang for purifying the trout growth hormone and M. E. Mallonee for his assistance in conducting the growth experiments. The authors are deeply indebted to M. Castagna and K. Kirkowski, VIMS, for providing the oyster larvae. The bovine somatotropin was a generous gift of Dr. E. Popper, Lilly Research Lab, Greenfield, Indiana.

Literature Cited

Agellon, L. B., and T. T. Chen. 1986. Rainbow trout growth hormone: molecular cloning of cDNA and expression in *E. coli*. *DNA* **5:** 463–471.

Agellon, L. B., C. J. Emery, J. Jones, S. L. Davies, A. D. Dingle, and T. T. Chen. 1988. Growth enhancement by genetically engineered rainbow trout growth hormone. *Can. J. Fish. Aquat. Sci.* **45:** 146–151.

Bayne, B. L., and A. J. S. Hawkins. 1990. Filter feeding in bivalve molluscs: controls on energy balance. Pp. 253–297 in *Animal Nutrition and Transport Processes. Vol. 1. Nutrition in Wild and Domestic Animals*, J. Mellinger *et al.*, eds. Karger, Basel.

Bern, H. A. and C. S. Nicoll. 1968. Comparative endocrinology of prolactin. *Rec. Prog. Hormone Res.* **24:** 681–720.

Brown, J. R. 1988. Multivariate analyses of the role of environmental factors in the seasonal and site-related growth variation in the Pacific oyster, *Crassostrea gigas*. *Mar. Ecol. Prog. Ser.* **45:** 225–236.

Brown, J. R., and E. B. Hartwick. 1988a. Influences of temperature, salinity and available food upon suspended culture of the Pacific oyster, *Crassostrea gigas* I. Absolute and allometric growth. *Aquaculture* **70:** 231–251.

Brown, J. R., and E. B. Hartwick. 1988b. Influences of temperature, salinity and available food upon suspended culture of the Pacific oyster, *Crassostrea gigas* II. Condition index and survival. *Aquaculture* **70:** 253–267.

Dame, R. F. 1975. Day degree growth models for intertidal oysters. *Contrib. Mar. Sci.* **19:** 107–112.

Dogterom, A. A., and B. R. Robles. 1980. Stimulation of ornithine decarboxylase activity in *Lymnaea stagnalis* after a single injection with molluscan growth hormone. *Gen. Comp. Endocrinol.* **40:** 238–240.

Dogterom, A. A., and T. Jentjens. 1980. The effect of the growth hormone of the pond snail *Lymnaea stagnalis* on periostracum formation. *Comp. Biochem. Physiol. A* **66:** 687–690.

Dogterom, A. A., H. Van Loenhout, and R. Van der Schors. 1979. The effect of the growth hormone of *Lymnaea stagnalis* on shell calcification. *Gen. Comp. Endocrinol.* **39:** 63–68.

Galtsoff, P. S. 1964. The American oyster, *Crassostrea virginica* Gmelin. *U. S. Fish Wildl. Serv., Fish. Bull.* **64:** 480 pp.

Geraerts, W. P. M. 1976. Control of growth by neurosecretory hormone of the light green cells in the freshwater snail *Lymnaea stagnalis*. *Gen. Comp. Endocrinol.* **29:** 61–71.

Hall, S. 1984. A multiple regression model of oyster growth. *Fish. Res.* **2:** 167–175.

Hawkins, A. J. S., P. N. Salkeld, B. L. Bayne, E. Gnaiger, and D. M. Lowe. 1985. Feeding and resource allocation in the mussel *Mytilus edulis*: evidence for time-averaged optimization. *Mar. Ecol. Prog. Ser.* **20:** 273–287.

Joosse, J., and W. P. M. Garaerts. 1983. Endocrinology. Pp. 317–406 in *The Mollusca, Vol 4, Physiology, Part 1*, A. S. M. Saleuddin and K. M. Wilbur, eds. Academic Press, London.

Lubet, P. 1971. Influence des ganglions cerebroides sur la croissance de *Crepidula fornicata* Phil. (mollusque mesogasteropode). *C. R. Acad. Sci.* **273:** 2309–2311.

MacDonald, B. A., and R. J. Thompson. 1985a. Influence of temperature and food availability on the ecological energetics of the giant scallop *Placopecten magellanicus*. I. Growth rates of shell and somatic tissue. *Mar. Ecol. Prog. Ser.* **25:** 279–294.

MacDonald, B. A., and R. J. Thompson. 1985b. Influence of temperature and food availability on the ecological energetics of the giant scallop *Placopecten magellanicus*. II. Reproductive output and total production. *Mar. Ecol. Prog. Ser.* **25:** 295–303.

Moriyama, S., S. Atsuta, M. Kobayashi, and H. Kawauchi. 1989. Growth hormone-like substance of Abalone, *Haliotis discus hamai*. XI^th^ International Symposium on Comparative Endocrinology. Malaga, Spain. 14–20 May, 1989. Abstracts, p. 243.

Morse, D. E. 1981. Biochemical and genetic control of critical physiological processes in molluscan life-cycles: basic mechanisms, water quality requirements and sensitivities to pollutants. Biennial Report, University of California Sea Grant Program.

Morse, D. E. 1984. Biochemical and genetic engineering for improved production of abalones and other valuable molluscs. *Aquaculture* **39:** 263–282.

Paynter, K. T., and M. E. Mallonee. 1991. Site-specific growth rates of oysters in Chesapeake Bay and impact of disease. Proceedings of the 1990 Chesapeake Research Consortium meetings, Baltimore, MD Pub No. 137: 391–399.

Smit, A. B., E. Vreugdenhil, R. H. M. Ebberink, W. P. M. Geraerts, J. Klootwijk, and J. Joosse. 1988. Growth-controlling molluscan neurons produce the precursor of an insulin-related peptide. *Nature* **331:** 535–538.

Toullec, J., F. Lenoir, A. V. Wormhoudt, and M. Mathieu. 1988. Nonspecies-specific growth factor from cerebral ganglia of *Mytilus edulis*. *J. Exp. Mar. Biol. Ecol.* **119:** 111–117.

Reference: *Biol. Bull.* **181:** 463–473. (December, 1991)

Reversible Epithelial Adhesion Closes the Mouth of *Beroë*, a Carnivorous Marine Jelly

SIDNEY L. TAMM* AND SIGNHILD TAMM

Boston University Marine Program, Marine Biological Laboratory,
Woods Hole, Massachusetts 02543

Abstract. We investigated how the ctenophore *Beroë*, a carnivore of the marine zooplankton, keeps its mouth shut to maintain a streamlined body shape during forward swimming in search of prey. In big-mouthed, thin-walled beroids we found that mouth closure requires neither muscular nor nervous activity. Instead, mouth adhesion is due to paired strips of adhesive epithelial cells on opposing stomodaeal walls. The two joined epithelial layers make numerous close appositions interrupted by vacuolar intercellular spaces. At regions of apposition, the plasma membranes are highly folded and interdigitated with each other, and are separated by a uniform distance of about 15 nm. A dense cytoplasmic coat underlies the membranes at such appositions. Synapses of neurites are found on the basal ends of the adhesive cells. We found two orthogonally different orientations of the stomodaeal adhesive strips in *B.* sp. *vs. B. forskali*, correlated with different distributions of feeding macrocilia inside the stomodaeum.

Mouth opening in response to food requires muscular contractions of the lips. However, the stomodaeal adhesive strips are not pulled apart all at once, but are peeled apart starting from a site of vigorous muscular tension. The mouth re-seals after feeding, or after being experimentally pulled open, showing that tissue adhesion is functionally reversible.

Epithelial adhesion in *Beroë* appears to be a useful method for closing the mouth and streamlining the body of a gelatinous predator that spends most of its time swimming mouth-forward in search of prey. Opening of the mouth appears to be an efficient process as well, because peeling apart of the adhesive strips requires a smaller applied force than does separating them all at once. Tissue adhesion in *Beroë* shares many structural and functional properties with transient adhesions formed between moving cells in embryos and in culture, and may be a useful experimental system for studying the mechanisms and regulation of dynamic cell adhesions.

> "Loose lips
> Sink ships."
> —U. S. Navy slogan, WW II

Introduction

Ctenophores are important members of the gelatinous marine zooplankton and are significant predators in planktonic food chains (Thorson, 1971). Beroid ctenophores have a large mouth and a voluminous stomodaeum occupying most of the body, and are voracious predators of other ctenophores (Swanberg, 1974; Harbison *et al.*, 1978). *Beroë* actively seeks prey by swimming mouth forward, powered by the beating of giant ciliary comb plates. Yet the mouth remains closed, with the body shape streamlined, until prey is encountered. Then the mouth opens rapidly and the stomodaeum expands to suck in the prey (Horridge, 1965a; Tamm, 1982). Alternatively, the lips may spread over the prey, using the saber-shaped macrocilia lining the stomodaeum to bite off pieces (Horridge, 1965a; Swanberg, 1974; Tamm, 1983).

We have investigated the mechanism whereby a swimming *Beroë* keeps its mouth shut. We have found that mouth closure in certain beroids is due to a functionally reversible type of adhesion between paired strips of epithelial cells on the stomodaeal walls. Muscular activity is not required to keep the mouth shut, but is necessary to open the mouth in response to food. The adhesive seal is not separated all at once, but is peeled apart starting at a site of muscular tension. The mouth of *Beroë* may be a

Received 31 July 1991; accepted 24 September 1991.

* To whom correspondence should be addressed.

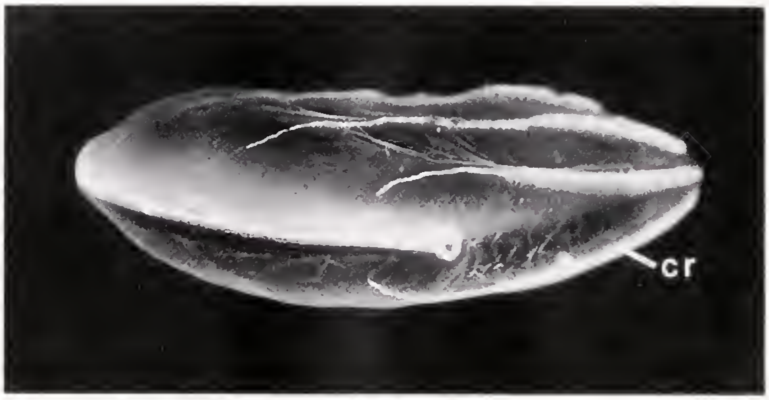

Figure 1. *Beroë mitrata* swimming mouth forward (to the left) with the lips closed into a wide curved slit. The body is flattened in the stomodaeal plane with a blunt front end and tapering rear. Longitudinal rows of ciliary swimming plates (cr, comb rows) extend from the aboral end toward the mouth. Photograph kindly provided by Dr. Claude Carré, Station Zoologique, Villefranche-sur-Mer, France. Natural size.

useful model for studying the mechanisms and control of reversible tissue adhesions, as well as the biomechanics of feeding behavior in soft-bodied marine animals.

Materials and Methods

Animals

Beroë sp. was collected at Woods Hole, Massachusetts, in fall, 1990. This unidentified species is similar to *B.* sp. collected at Woods Hole in fall, 1985, after Hurricane Gloria (Tamm and Tamm, 1988). The comb rows of this beroid run on high ridges that project from the flattened body surface.

B. forskali was collected at Monterey Bay, California, by Freya Sommer of Monterey Bay Aquarium, and shipped to the Marine Biological Laboratory in Woods Hole.

Observations on living material

An isotonic $MgCl_2$-seawater mixture (6.75% $MgCl_2$: seawater = 1:1) was used to block nervous and muscular responses in whole animals or in dissected preparations.

Experimental observations on the stomodaeal adhesive strips of *B.* sp. or *B. forskali* were made under a Wild dissecting microscope and recorded with a Panasonic CCD video camera and GYYR model 2051 video recorder allowing still-field playback and analysis. Still-fields were photographed from a Sony video monitor with an Olympus OM-2N camera on Kodak Tech Pan film.

Mouth opening responses of whole animals pinned to Sylgard were induced by a suspension of fresh egg white in seawater (A. Maselli, pers. comm). Responses were recorded with a Nikon macrolens on a Panasonic CCD video camera using the procedures described above. Tracings of selected video fields were made on matte acetate directly from a video monitor.

Differential interference contrast (DIC) images of living stomodaeal adhesive strips were made with Zeiss 16× or 40× objectives and recorded with an Olympus OM-2N camera on Kodak Tech Pan film by electronic flash.

Electron microscopy

Closed mouths of *B.* sp. and *B. forskali* were fixed as follows. The animals were first relaxed in $MgCl_2$-seawater. Simultaneous glutaraldehyde-paraformaldehyde-osmium fixation was then performed and tissue was processed for electron microscopy as described previously (Tamm and Tamm, 1985).

Results

Beroid ctenophores have a conical body flattened in the stomodaeal plane to varying degrees in different species. *Beroë* swims mouth forward at speeds of several cm/s or faster when seeking prey. In flattened thin-walled species such as *B.* sp., *B. forskali,* and *B. mitrata,* the front end is wide and blunt with the lips closed into a long curved slit, and the body tapers towards the rear (Fig. 1). This streamlined body shape depends on the mouth remaining closed during forward swimming.

We examined how beroids with flattened streamlined bodies and thin flexible body walls (*i.e.*, *B.* sp. and *B. forskali*) keep their mouth shut while swimming. *B.* sp. and *B. forskali* differ dramatically from each other in the size and arrangement of their feeding macrocilia; as we will show, this difference in macrociliary patterns is correlated with orthogonally different orientations of mouth closure.

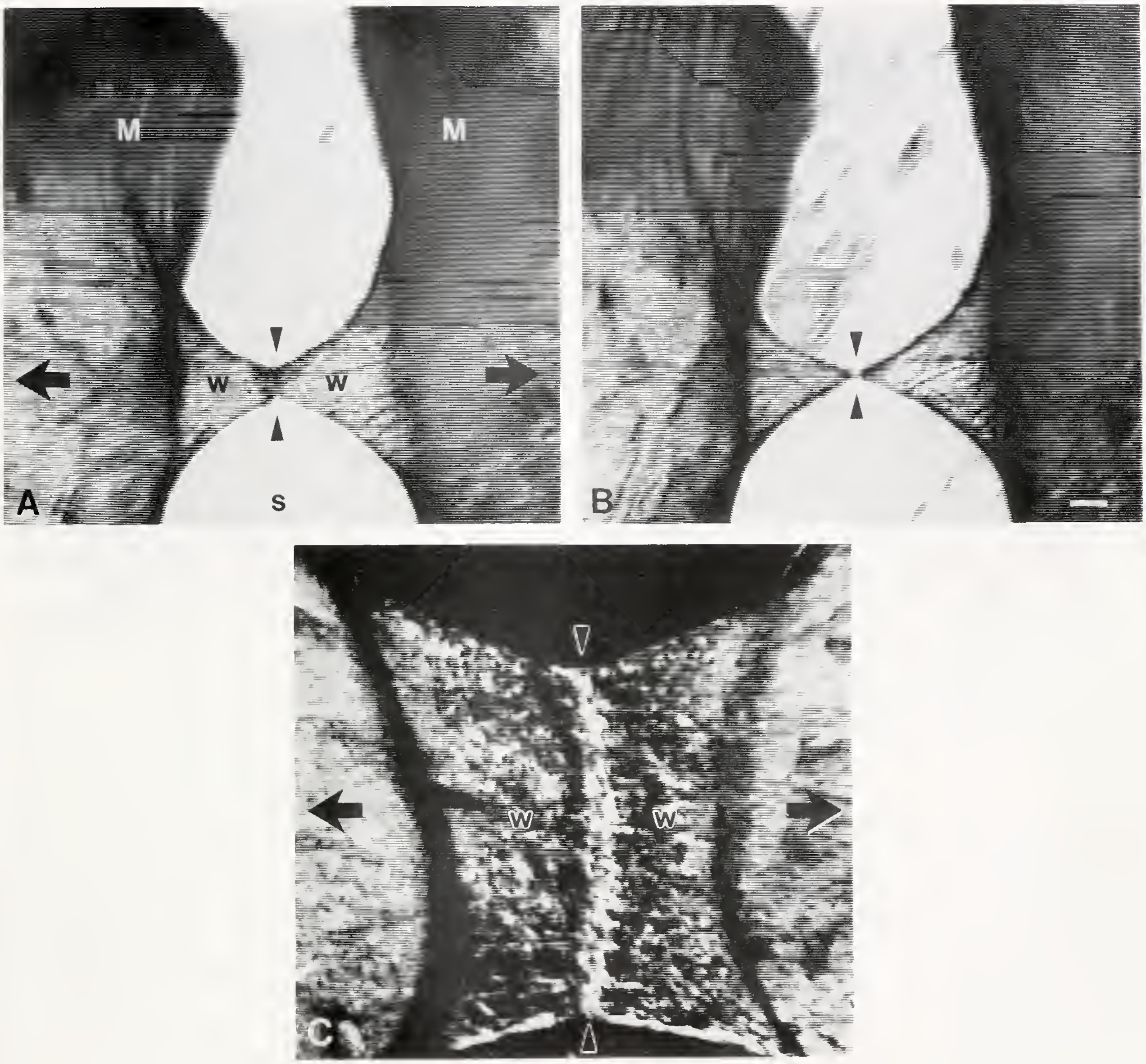

Figure 2. Zone of adhesion between Mg-relaxed lip segments of *Beroë* sp. under imposed tension (large arrows). A,B, The paired lip segments (left and right) are joined symmetrically along a zone (arrowheads) of stretched stomodaeal walls (w). The lip edges and furrowed macrociliary fields (M) are at the top; the stomodaeum (s) is down. Note that the attachment zone is located a short distance aboral to the macrociliary fields. B, Continued tension narrows the adhesive contact between the stretched lip surfaces (arrowheads). A short time later the lips snapped apart. C, Face view of the adhesion zone between stretched, separating stomodaeal walls (w) by darkfield microscopy. The adhesive contact runs medially (arrowheads) and scatters more light than the stretched surfaces. Scale bar: A,B, 165 μm; C, 110 μm.

First pattern of mouth adhesion: B. *sp.*

Treatment of *B.* sp. with excess $MgCl_2$ abolishes contraction of the body wall muscles and blocks neurally mediated ciliary responses (*i.e.*, ciliary inhibition). Mg-relaxed animals swim forward continuously with their mouth closed. The lips resist being pulled apart with forceps, as if they were stuck shut. After being forcibly opened, however, the stomodaeal walls and mouth of $MgCl_2$-anaesthetized animals gradually close, and the lips re-seal within 10–15 min. Similar observations were made on dissected oral ends. These findings show that mouth closure is functionally reversible and requires neither muscular nor nervous activity to maintain or re-establish adhesion.

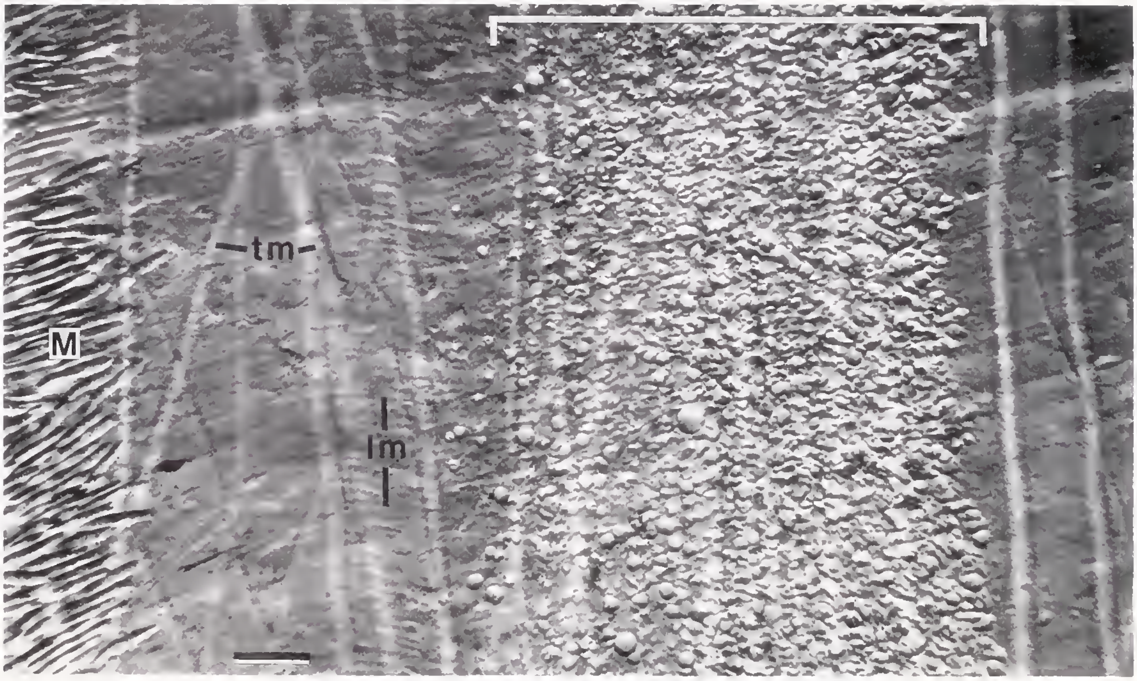

Figure 3. DIC view of the surface of a peeled apart lip of *Beroë* sp. in $MgCl_2$/seawater. The lip edge is to the left; the aboral direction is to the right. The adhesive strip (bracket) runs parallel to, and a short distance aboral to, the macrociliary field (M). The surface of the adhesive zone is covered with numerous small vesicles or craters. Subepithelial transverse muscle fibers (tm) run vertically and appear out-of-focus. The finer and more closely spaced longitudinal muscles (lm, cf. Fig. 5) run horizontally and are visible in the area between the adhesive strip and the macrocilia. Scale bar, 30 μm.

The adhesive region in the mouth was located by examining segments of adherent lips excised from Mg-relaxed animals. We found that lip segments are fastened together along a narrow zone of the apposing stomodaeal walls (Fig. 2). The belt of tissue adhesion runs around the inside of the mouth, a short distance aboral to the band of macrocilia encircling the lip edge (Fig. 2). Therefore, mouth closure is not due to Velcro-like attachment of macrocilia on apposing lips, a possibility that initially had seemed likely to us.

We next investigated the adhesive properties of closed lips. Adherent lip segments were pulled apart by forceps, starting at one end of the joined pair. Tension initially stretches the joined stomodaeal walls without separating the adhesive zone (Fig. 2A). Increased tension further draws out the two attached surfaces, which appear as mirror images of each other (Fig. 2B,C). Then the adhesive strips on either side separate at the site of greatest tension and the lips peel apart. This is followed by elastic recovery and flattening of the stretched stomodaeal walls.

Darkfield microscopy of joined, stretched lips under tension shows that the zone of stomodaeal contact scatters more light, and thus appears brighter than the adjacent walls (Fig. 2C). The increased light scattering is correlated with the greatly elaborated surface area of the adhesive cells (see below).

By DIC light microscopy the surface of mechanically peeled apart lips displays a well-defined tract of densely packed vesicles or vacuoles, that coincides with the location of the adhesive strips (Fig. 3). These vesicles or vacuoles are 2–10 μm in diameter, and appear to be modifications of the apical surfaces of stomodaeal epithelial cells. The tract is 200–300 μm wide and runs about 150 μm aboral to the band of macrocilia. The stomodaeal surface on either side of the adhesive tract is relatively smooth and featureless.

Toluidine blue-stained thick sections through fixed, closed mouths show that the stomodaeal epithelium is markedly thicker in the adhesive strips, due to the increased height of cells in this region (Fig. 4). Even by light microscopy, it is evident that the two epithelial layers make numerous close contacts, interrupted by many vacuolar intercellular spaces (Fig. 4B).

Corresponding electron micrographs through adherent epithelial strips show that apposed cell surfaces are folded and interdigitated with each other (Figs. 5, 6). In such appositions, the two plasma membranes conform to each other and run parallel, separated by a uniform space of about 15 nm (Fig. 6). The intercellular space frequently contains dense amorphous material, but there is no obvious structural continuity between the apposed cell surfaces (Fig. 6). The cytoplasmic sides of the membranes

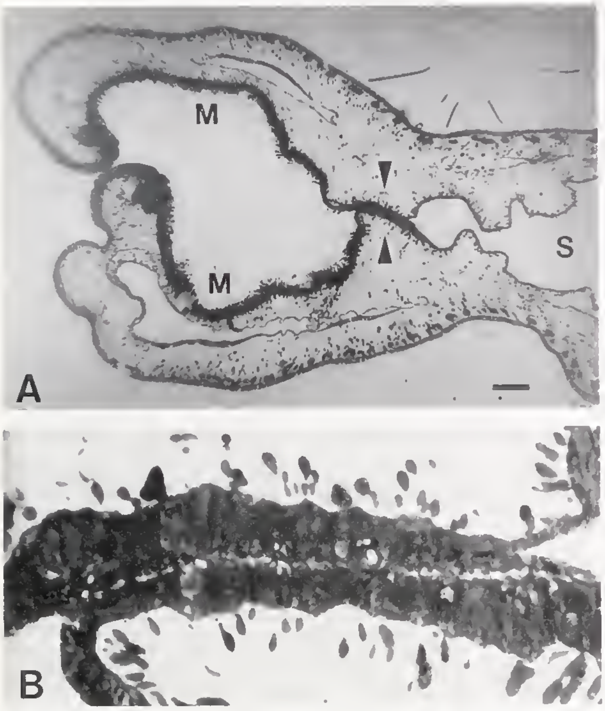

Figure 4. Toluidine blue-stained longitudinal thick sections (0.5 μm) through a closed mouth of *Beroë* sp. A, Survey view, lip edges at left. The stomodaeal walls are joined together by paired strips (here cut transversely) of thickened epithelia (arrowheads) located aboral to the macrociliary fields (M). S, Stomodaeum. B, Higher magnification of thickened joined epithelial strips. Apposing cell surfaces make numerous close contacts interrupted by vacuolar spaces. Scale bar, A, 100 μm; B, 17 μm.

are coated with dense material and wispy filaments that run parallel to the membrane. These close appositions are found almost exclusively between plasma membranes of adhesive cells, being rare or absent between cells within either epithelial layer.

The regions of close apposition alternate with widely separated, vacuolar spaces between the epithelial surfaces (Fig. 5). The plasma membranes in the widely spaced regions do not bear dense cytoplasmic coats, and so are readily distinguishable from closely apposed membranes. The widely spaced regions seen in sections may correspond to the edges or rims of the round vesicles or vacuoles, seen by DIC on the surfaces of adhesive strips pulled apart by forceps (Fig. 3).

Numerous thin muscle fibers run parallel to one another between the basal ends of the adhesive cells next to the mesoglea (Fig. 5). These muscles extend in the longitudinal direction of the body for long distances under the entire stomodaeal epithelium, and are not restricted to the adhesive strips. Neuromuscular junctions are common and show the characteristic presynaptic triad structure of ctenophore synapses described by Hernandez-Nicaise (1973).

Synapses of neurites are also found on the basal ends of the adhesive cells, indicating that some function of the adhesive cells must be under nervous control. The possibility that cell-cell appositions may be neurally regulated is discussed below.

The stomodaeal adhesive strips also contain cells bearing actin pegs and onion-root cilia. Such cells are found in the epidermis of many ctenophores (Horridge, 1965b; Hernandez-Nicaise, 1974; Tamm and Tamm, 1991), and are thought to function as chemo- and mechanoreceptors (see Tamm and Tamm, 1991). In closed mouths, the actin pegs project into the vacuolar intercellular spaces between apposed epithelial layers. The cells bearing actin pegs and onion-root cilia synapse directly onto underlying longitudinal muscle fibers, suggesting a pathway for sensory control of stomodaeal muscles in response to food (see also below).

Glandular cells are abundant throughout the stomodaeal epithelium, including the adhesive strips. Large membrane-bound secretory droplets are packed into oval groups, many of which are larger than the cell nucleus. The secretory granules contain finely granular material, or coalesce and appear electron-lucent with coarse dense deposits and fibrils. These gland cells are similar to the spumous gland cells described in the epidermis of various ctenophores by Hernandez-Nicaise and colleagues (Hernandez-Nicaise, 1991).

The adherent epithelial layers are structurally identical and have a mirror-image symmetry about the plane of apposition. This suggests that each epithelial strip of the pair makes an equal contribution to adhesion, and that both surfaces are necessary for adhesion. In fact, the epithelial strip of an excised lip segment will adhere to an unmodified region of the stomodeal wall, but such heterophilic attachments are weaker than adhesion between two lips.

Mouth opening

We investigated how *Beroë* separates its stomodaeal adhesive strips to open its mouth so widely and rapidly upon contact with food. Egg white pipetted onto the closed mouth of a *Beroë* pinned in seawater first triggers a series of brief, local muscular contractions of the lips perpendicular to the adhesive seal. These muscular twitches occur at various locations along the mouth edge, until one contraction pulls apart the adhesive strips at that site (Fig. 7A, B). The strips then rapidly peel apart from this point by coordinated muscular activity of the lips, leading to opening of the entire mouth (Fig. 7C–E). Without repeated stimulation, the mouth slowly relaxes and closes. Similar responses to egg white were observed in dissected oral ends. $MgCl_2$-relaxed animals cannot open their mouths due to inhibition of muscular and nervous activity.

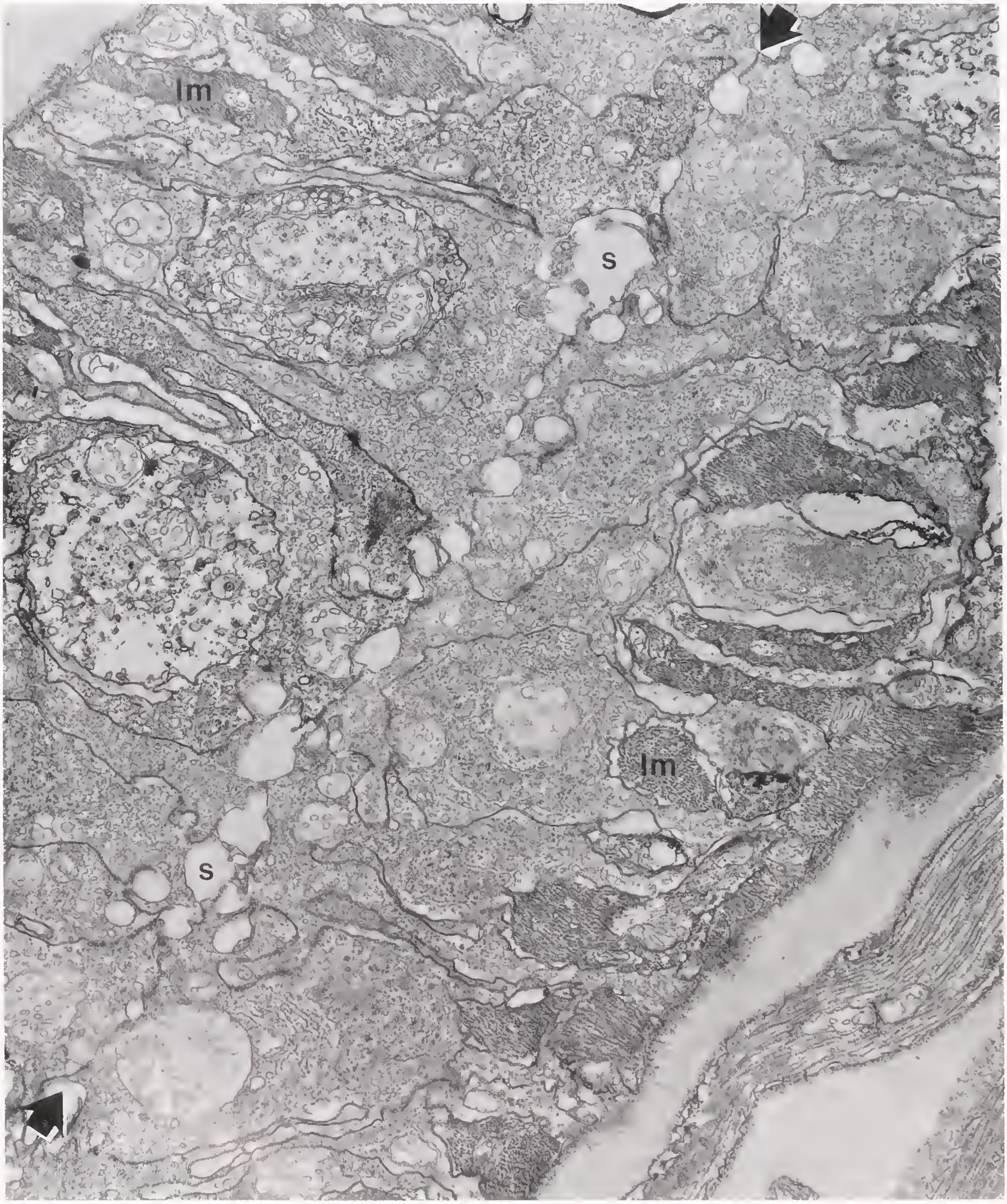

Figure 5. Survey electron micrograph of adherent epithelial layers in a closed mouth of *Beroë* sp. The zone of adhesion runs diagonally from lower left to upper right (arrows), and consists of numerous close appositions of the cell surfaces alternating with vacuolar intercellular spaces (s). The plasma membranes have a cytoplasmic coat and appear darker at the contact regions (see Fig. 6). Thin longitudinal muscle fibers (lm) abutting the mesoglea are cut transversely. ×9300.

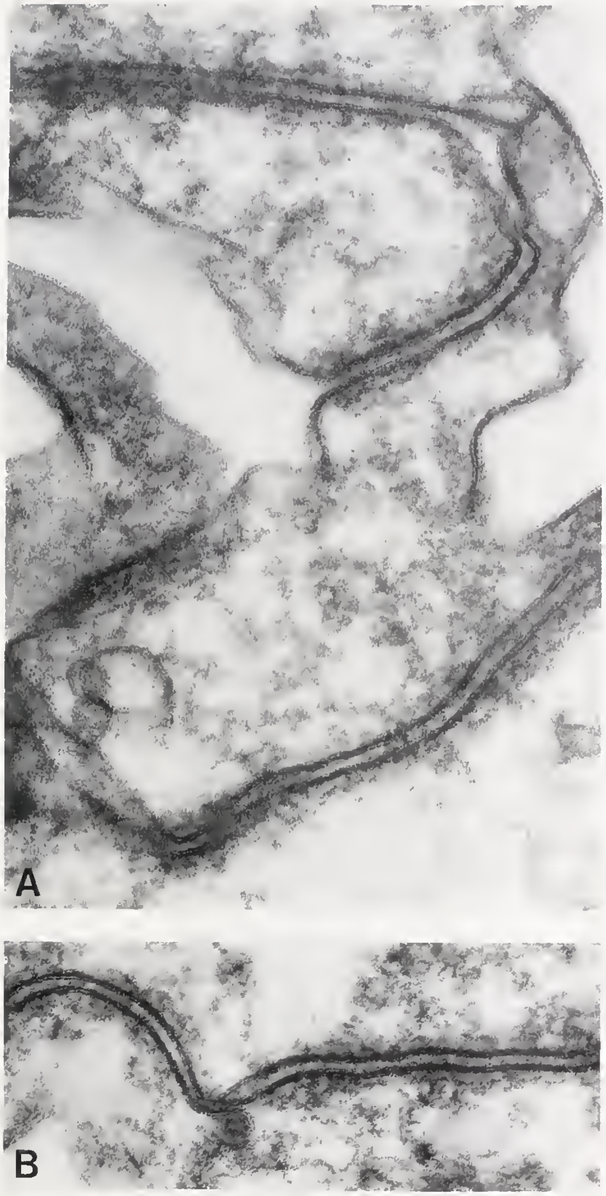

Figure 6. Appositions of plasma membranes of adherent stomodaeal epithelial cells in a closed mouth of *Beroë* sp. Although folded, the apposed plasma membranes run parallel to each other and are separated by a distance of about 15 mm. Note floculent material in the intercellular space. The cytoplasmic side of the membranes is coated with dense material. A, ×108,400; B, ×93,400.

Second pattern of mouth adhesion: B. forskali

B. forskali and *B. mitrata* differ from other beroids in that they possess considerably larger macrocilia; more importantly for this study, their macrocilia are not restricted to a band around the inside of the lips, but cover a large area of the stomodaeal cavity. In *B. forskali*, the macrociliary field comprises longitudinal stripes that extend almost half the length of the stomodaeum (Figs. 8, 10).

Using transverse segments of the body of $MgCl_2$-relaxed *B. forskali*, we found that the flattened stomodaeal walls are joined by paired macrocilium-free ridges that run longitudinally down the midline of the stomodaeum, effectively dividing the stomodaeal cavity into two lateral pockets (Fig. 9). These adhesive strips begin near the lip edge and extend ⅔–¾ the length of the stomodaeal cavity (Figs. 8, 10).

Pulling the flattened sides of the stomodaeum apart with forceps shows that the paired longitudinal ridges of *B. forskali* possess adhesive and tensile properties similar to those of the circumoral adhesive strips of *B.* sp. In addition, light and electron microscopy reveals no morphological differences between the adhesive strips of *B. forskali vs. B.* sp. We have not yet made observations on how *B. forskali* or *B. mitrata* open their mouths to feed.

In *B. mitrata*, the macrociliary field covers the entire oral half of the stomodaeal cavity, except for two bare zones that extend longitudinally and medially through the macrociliary fields on either wall of the stomodaeum. Although we have no data at present to show that these macrocilium-free zones are adhesive and keep the wide mouth closed, their location suggests that they do so in a manner similar to the longitudinal adhesive strips of *B. forskali*.

Discussion

Our curiosity about how a swimming *Beroë* keeps its mouth shut led to the discovery of a novel, reversible type of tissue adhesion. We found that the stomodaeum is fastened together by a matched pair of apposed epithelial strips. The remarkable, and obviously necessary feature of this tissue adhesion is its functional reversibility: tissue bonding is rapidly broken when *Beroë* opens its mouth to ingest prey, and is readily reformed after feeding.

Mechanism of adhesion

The reversible appositions of stomodaeal adhesive cells in *Beroë* are similar in several respects to the transient adhesions formed between moving cells in embryos and in culture (Trinkaus, 1984). In both cases, apposed plasma membranes typically (1) are highly folded and interdigitated, (2) conform to each other and run parallel over broad areas, (3) are separated by a distance of 10–20 nm, and (4) show no obvious structural continuity between them. These features are in marked contrast to the standard types of structurally differentiated localized contacts found between cells, such as tight junctions, gap junctions, desmosomes, etc.

Because the apposed cell membranes of *Beroë* adhesive cells and moving cells in embryos and culture are not structurally bound to one another, "bonds between the cell surfaces in such appositions would be more readily

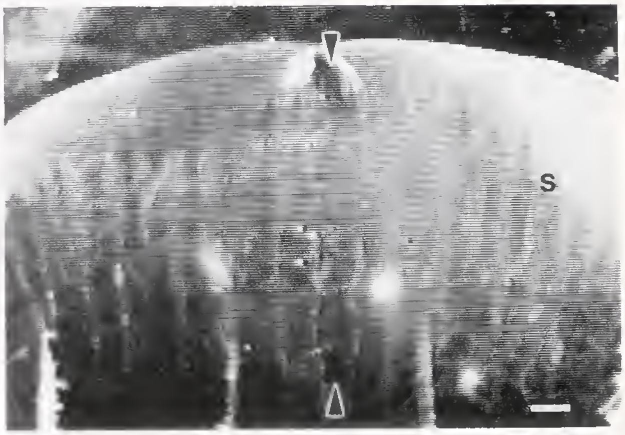

Figure 8. Surface at the oral end of one of the two stomodaeal walls of *B. forskali* (darkfield). The curved lip edge is at the top of the figure. Macrocilia appear brighter and extend downward from the lip edge as tapering longitudinal stripes (s). The adhesive strip runs longitudinally along the midline of the stomodaeal wall (arrowheads). Scale bar, 2.3 mm.

made and broken and remade again than in junctions" (Trinkaus, 1984, p 171). These cell-cell appositions in fibroblasts are believed to be "a prime candidate for the kind of adhesion that moving cells require" (Trinkaus, 1984, p 171). Similarly, such appositions would seem well-designed for the reversible type of tissue adhesion required to seal *Beroë*'s mouth.

The physical or chemical mechanisms of such cell-cell adhesions are not well understood in any system (Trinkaus, 1984). Suggested mechanisms range from non-specific molecular attraction, such as London-van der Waals forces (Nachtigall, 1974; Trinkaus, 1984), to chemical bonding by molecular "glues" or specific cell adhesion molecules (Takeichi, 1990, 1991; Edelman and Crossin, 1991).

Mouth opening and possible regulation of tissue adhesion

Using egg-white as a feeding stimulus to induce mouth opening, we found that the mouth does not open all at once, as assumed previously (Tamm, 1982), but is peeled apart starting at a site of vigorous muscular tension on

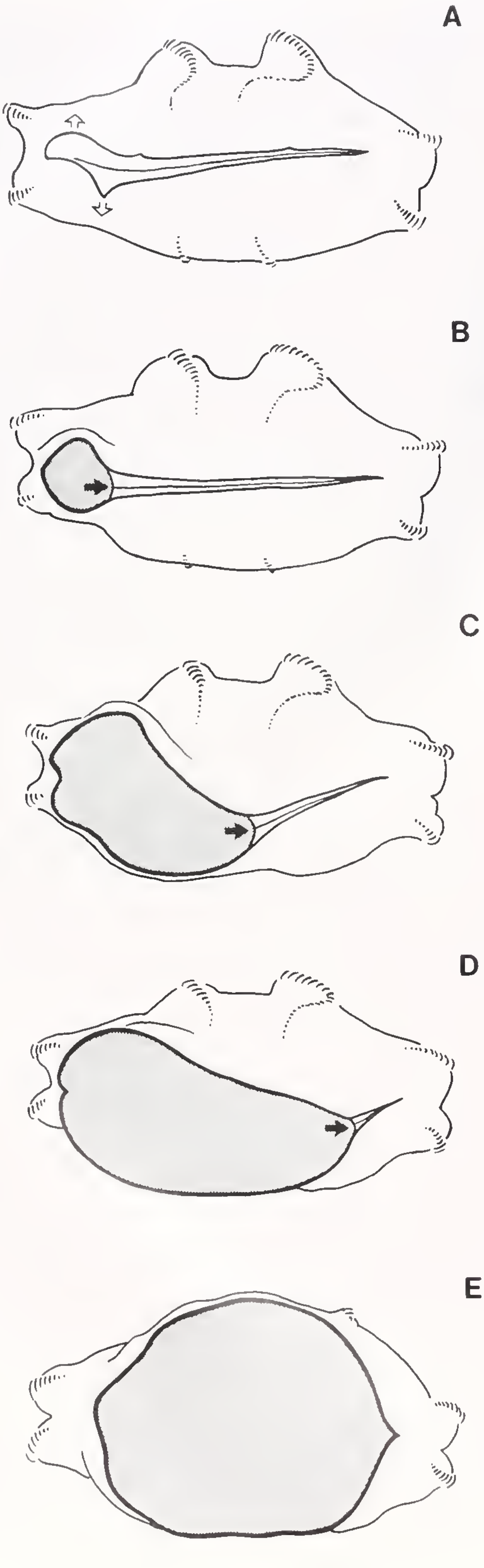

Figure 7. Mouth opening of *Beroë* sp. induced by egg white (viewed orally). A, Local muscular twitches pull the left sides of both lips away from the adhesion zone (line inside the lips). B, Muscular tension separates the adhesive zone (arrow) and pulls open the lips on the left side of the mouth. C, Continued muscular activity peels apart the adhesive seal from left to right (2 s later). D, Peeling apart of the adhesion zone and opening of the mouth has almost reached the right side (3.5 s later). E, The mouth is fully open and gaping (6.5 s later). 3× natural size. Tracings of video fields from monitor.

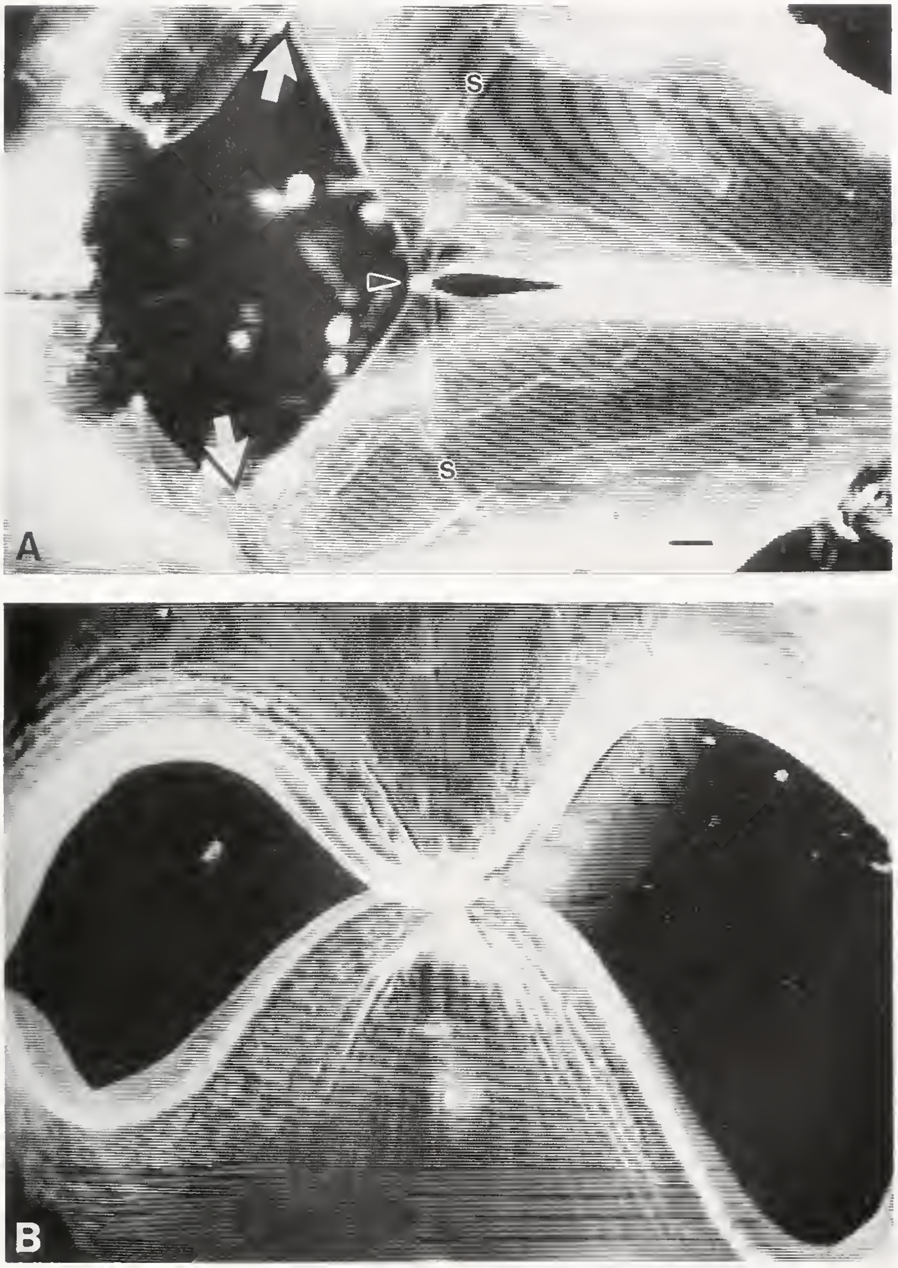

Figure 9. Stomodaeal walls of *Beroë forskali* are attached by paired longitudinal adhesive strips. A, The stomodaeal cavity of a transversely cut body segment is viewed along the oral-aboral axis from inside the animal. The stomodaeal walls on the left side have been cut and pulled apart (white arrows) to show the adhesive strips (s) running longitudinally on each wall. The strips are still joined like a spot weld at the arrowhead. The right side of the stomodaeum remains closed. B, Frontal view of a dissected mouth being pulled open with forceps. The middle of the mouth remains fastened by the longitudinal adhesive strips that divide the stomodaeal cavity into two lateral pockets. Scale bar: 1 mm.

the lips. Because peeling apart of two adherent surfaces requires a much smaller force, applied over a longer time, than pulling them apart all at once (Steinberg, 1964; Vogel, 1988), this method is likely to reduce the amount of muscular tension required to separate the stomodaeal adhesive strips of *Beroë*.

Mouth opening may also require concomitant changes in the adhesive properties of the epithelial cells themselves. The presence of synaptic contacts on the adhesive cells suggests that these cells make some kind of neuronally triggered effector response. Such responses may involve changes in the cortical cytoskeleton or cell

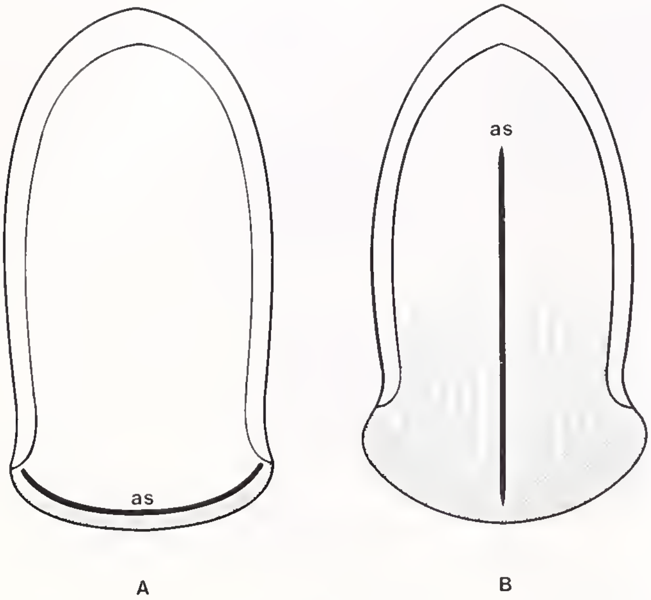

Figure 10. Diagram of mutually perpendicular orientations of stomodaeal adhesive strips (as, black bars) in *Beroë* sp. (A) *vs. B. forskali* (B). The inside of one wall of the flattened stomodaeum is shown. Macrociliary fields are indicated by stipple. The number of longitudinal macrociliary stripes in *B. forskali* (B) is reduced for clarity (see Fig. 8), and the relative width of the adhesive strips in both animals is exaggerated. Oral ends face down.

surface that modify the adhesive properties of the epithelial strips.

If so, mouth opening may require cellular de-adhesion processes as well as muscular activity. How might this be controlled? Mouth opening is triggered by contact of prey with sensory receptors on the lips. The presumed receptor cells bear actin pegs and onion-root cilia, and make synaptic contacts onto neurites of the nerve net (Hernandez-Nicaise, 1974; Tamm and Tamm, 1991). If this pathway is connected to muscles acting on the lips and also to cells of the adhesive strips, then food stimuli could signal both muscular contractions that pull the lips apart as well as de-adhesion of the epithelial cells themselves.

The gradual closure of the mouth after food-induced or experimentally forced opening does not require muscular activity. The voluminous extracellular matrix, or mesoglea, of ctenophores consists of a ground substance containing muscle fibers and other cells, as well as a felt-like meshwork of collagenous microfibrils linked to glycoproteins (Franc, 1985). Passive return of this fibrillar matrix to the resting state, following stress-evoked deformation, may be responsible for restoration of normal body shape that allows contact and adhesion of the epithelial strips on the two sides of the stomodaeum.

Patterns of stomodaeal adhesive strips

Beroids can be divided into two main groups based on differences in macrociliary size and distribution; these patterns are believed to reflect differences in feeding behavior and prey type (Tamm and Tamm, 1990). In *B.* sp. and most other species, macrocilia are relatively small and are restricted to a narrow band around the margin of the lips. The adhesive strips in *B.* sp. also run around the lips, just inside the band of macrocilia.

In contrast, *B. forskali* and *B. mitrata* have larger macrocilia that cover a much greater area of the stomodaeal cavity. The adhesive strips in *B. forskali* run longitudinally along the midline of the stomodaeum, between the stripes of macrocilia. The mutually perpendicular orientation of stomodaeal adhesive strips in *B.* sp. and *B. forskali* is probably due to the different arrangements of macrocilia in the two species, because adhesion between the stomodaeal walls seems to require macrocilium-free zones of contact. We therefore predict that the paired macrocilium-free zones that run longitudinally through the wide macrociliary fields of *B. mitrata* are also adhesive strips.

Mouth closure in other beroids

Do all beroids use epithelial adhesive strips to keep their mouths closed? Our preliminary observations on *B. cucumis* from Monterey Bay, California, suggest that this is not the case. *B. cucumis* differs from *B.* sp., *B. forskali,* and *B. mitrata* in several respects: it is not appreciably compressed in the tentacular plane, but is round or oval in cross-section. Moreover, the body wall is markedly thicker and firmer, and the mouth is considerably smaller than those of the species described in this report. *B. cucumis* swims with its mouth closed or slightly ajar, but we have found by direct observation and dissection of living animals that neither the lips nor the stomodaeal walls are fastened together in any manner.

Evidently, the small oral opening and the relatively thick, rigid body wall of *B. cucumis* provide sufficient resistance to maintain normal body shape during forward swimming without the necessity of mouth closure mechanisms. Other beroids with a similar body plan (*i.e., B. ovata*) are likely to use the same strategy.

Significance of stomodaeal adhesion

At the moderate Reynolds number of a swimming *Beroë,* the streamlined body shape should be effective in reducing drag (Vogel, 1981). In thin-walled beroids with stomodaeal adhesive strips, mouth closure does not require muscular or neural activity. Epithelial adhesion therefore seems to be a useful method for closing the mouth and streamlining the body of an active gelatinous predator that spends most of its time swimming mouth forward in search of prey. *Beroë* also appears to use an efficient method to open its mouth, because peeling apart the adhesive strips should require a smaller applied force than pulling them apart all at once (Steinberg, 1964; Vogel, 1988).

From a comparative viewpoint, it is interesting that many hydrozoan polyps (but not other classes of Cnidaria) lack a permanent mouth; a mouth is created by muscular stretching and rupturing of the tissue in the oral region (Campbell, 1987). Breaching of the epithelia involves breaking of intercellular attachments (septate junctions). *Beroë*'s adhesive strips allow effective joining of the stomodaeal epithelium without obliterating the mouth, and muscular contractions are required to open it. In the simplest to the most complex metazoans, then, mouth opening is usually a motile process, but only in the most primitive cases does the mouth completely disappear when closed.

Finally, the epithelial adhesive strips of *Beroë* share many structural and functional properties with reversible adhesions formed between moving cells in embryos and tissue culture. The ctenophore system may provide unique experimental advantages for studying the mechanisms and cellular control of dynamic adhesions between cells and tissues.

Acknowledgments

We are very grateful to Freya Sommer and Claudia Mills for kindly sending us *Beroë* from Monterey Bay Aquarium, CA, and Friday Harbor, WA, respectively. Andrew Maselli devised the egg white method for inducing feeding responses of *Beroë*, as part of his research project in the BUMP Physiology Course. Dorothy Hahn once again patiently and skillfully processed these words. This work was supported by NIH GM 27903 and GM 45557.

Literature Cited

Campbell, R. D. 1987. Structure of the mouth of *Hydra* spp. A breach in the epithelium that disappears when it closes. *Cell Tissue Res.* **249:** 189–197.

Edelman, G. M., and K. L. Crossin. 1991. Cell adhesion molecules: implications for a molecular histology. *Annu. Rev. Biochem.* **60:** 155–190.

Franc, J. M. 1985. La mésoglée des Cténaires. Doctoral dissertation no. 8534. Univ. Claude Bernard, Lyon, France.

Harbison, G. R., L. P. Madin, and N. R. Swanberg. 1978. On the natural history and distribution of oceanic ctenophores. *Deep-Sea Res.* **25:** 233–256.

Hernandez-Nicaise, M.-L. 1973. The nervous system of ctenophores. III. Ultrastructure of synapses. *J. Neurocytol.* **2:** 249–263.

Hernandez-Nicaise, M.-L. 1974. Ultrastructural evidence for a sensory-motor neuron in Ctenophora. *Tissue Cell* **6:** 43–47.

Hernandez-Nicaise, M.-L. 1991. Ctenophora. Pp. 359–418 in *Microscopic Anatomy of Invertebrates,* Vol. 2, F. W. Harrison and J. A. Westfall, eds. Wiley-Liss, New York.

Horridge, G. A. 1965a. Macrocilia with numerous shafts from the lips of the ctenophore *Beroë. Proc. R. Soc. Lond. B* **162:** 351–364.

Horridge, G. A. 1965b. Non-motile sensory cilia and neuromuscular junctions in a ctenophore independent effector organ. *Proc. R. Soc. Lond.* **162:** 333–350.

Nachtigall, W. 1974. *Biological Mechanisms of Attachment.* Springer-Verlag, Heidelberg.

Steinberg, M. 1964. The problem of adhesive selectivity in cellular interactions. Pp. 321–366 in *Cellular Membranes in Development,* M. Locke, ed. Academic Press, New York.

Swanberg, N. 1974. The feeding behavior of *Beroë ovata. Mar. Biol.* **24:** 69–76.

Takeichi, M. 1990. Cadherins: a molecular family important in selective cell-cell adhesion. *Annu. Rev. Biochem.* **59:** 237–252.

Takeichi, M. 1991. Cadherin cell adhesion receptors as a morphogenetic regulator. *Science* **251:** 1451–1455.

Tamm, S. L. 1982. Ctenophores. Pp. 266–358 in *Electrical Conduction and Behaviour in 'Simple' Invertebrates,* G. A. B. Shelton, ed. Oxford University Press, England.

Tamm, S. L. 1983. Motility and mechanosensitivity of macrocilia in the ctenophore *Beroë. Nature* **305:** 430–433.

Tamm, S. L. 1989. Control of reactivation and microtubule sliding by calcium, strontium, and barium in detergent-extracted macrocilia of *Beroë. Cell Motility* **12:** 104–112.

Tamm, S. L., and S. Tamm. 1985. Visualization of changes in ciliary tip configuration caused by sliding displacement of microtubules in macrocilia of the ctenophore *Beroë. J. Cell Sci.* **79:** 161–179.

Tamm, S., and S. L. Tamm. 1988. Development of macrociliary cells in *Beroë.* I. Actin bundles and centriole migration. *J. Cell Sci.* **89:** 67–80.

Tamm, S. L., and S. Tamm. 1990. Jellies with jaws. *MBL Sci.* **4:** 28–29.

Tamm, S., and S. L. Tamm. 1991. Actin pegs and ultrastructure of presumed sensory receptors of *Beroë* (Ctenophora). *Cell Tissue Res.* **264:** 151–159.

Thorson, G. 1971. *Life in the Sea.* McGraw-Hill, New York.

Trinkaus, J. P. 1984. *Cells Into Organs. The Forces that Shape the Embryo,* 2nd ed. Prentice-Hall, Englewood Cliffs, NJ.

Vogel, S. 1981. *Life in Moving Fluids.* Princeton University Press, Princeton, N. J.

Vogel, S. 1988. *Life's Devices.* Princeton University Press, Princeton, NJ.

Reference: *Biol. Bull.* **181:** 474–483. (December, 1991)

The Ultrastructure of the Radial Neuromuscular System of the Jellyfish *Liriope tetraphylla* (Hydrozoa, Trachymedusae): Implications in Crumpling Behavior

ELIANA SCEMES AND JOHN C. McNAMARA[1,*]

Departamento de Fisiologia Geral, Instituto de Biociências and [1]Departamento de Fisiologia e Biofísica, Instituto de Ciências Biomédicas, Universidade de São Paulo, 05508 SP, Brasil

Abstract. The ultrastructure of the radial neuromuscular system of the trachymedusa *Liriope tetraphylla* was examined to determine the morphological substrate underlying crumpling behavior—the folding of the margin into the subumbrellar cavity by radial muscle contraction. These contractions are produced by the four smooth muscle bands that run the length of the peduncle and extend over the subumbrellar surface to the margin, along the radii. Axons are present in the radial system and attain appreciable density at the base of insertion of the peduncle; contact between this radial nerve net and the inner nerve ring may occur at the margin. Gap junctions were not encountered within the ectodermal radial system. These various observations are discussed with respect to the control of crumpling in this and other species of hydromedusae.

Introduction

Structural differences apparent in the anatomy of the central nervous system of related species are often associated in a causal way with manifested behavioral differences.

The Cnidaria are among the first metazoans to possess identifiable neural elements. Members of all classes possess subepithelial networks of bipolar or multipolar neurons, which exhibit chemical or electrical synapses. In certain taxa, these elements are concentrated into well-defined tracts or ganglion-like structures (see Passano, 1982; Spencer and Schwab, 1982, for reviews and references).

The cnidarian nervous system may be considered structurally simple, but that does not necessarily mean that it is functionally simple, particularly given the sophisticated behavioral repertoire of many cnidarian species (see Donaldson *et al.*, 1980; Roberts and Mackie, 1980; Mackie and Meech, 1985).

Although not all species of hydromedusae exhibit precisely the same behaviors, recognizable individual components, such as swimming, feeding (pointing), crumpling, turning, righting, and tentacle posture have been defined (Hyman, 1940; Mackie, 1975; Mackie and Singla, 1975). The morphological substrate involved in these behaviors in different species, are not necessarily the same. For example, crumpling—a protective response involving contraction of the radial musculature and infolding of the margin into the subumbrellar cavity—is effected by one of at least three pathways: (1) through an entirely epithelial pathway (epithelial conduction), whereby excitation spreads from the ectoderm of the exumbrella into the endoderm, at the margin, and then to the effectors of the response (Mackie, 1975); (2) through the involvement of neurons, which presumably act as an intermediate link between epithelial conduction and radial muscle activation (Mackie and Passano, 1968; Spencer, 1975; King and Spencer, 1981); or (3) by a pathway composed entirely of neurons (von Carolsfeld, 1976).

In most hydromedusae so far investigated, the ability of the exumbrellar epithelium to propagate action potentials (epithelial conduction) has been attributed to the presence of gap junctions, which are abundant in their tissues (Mackie, 1975; Laat *et al.*, 1980; McDowall and Grimmelikhuijzen, 1980; Spencer and Satterlie, 1980; Westfall *et al.*, 1980; Dunlap *et al.*, 1987; Frazer *et al.*, 1987).

Liriope tetraphylla Chamisso and Eysenhardt, 1821, is a trachymedusa, the most conspicuous behavior of which is swimming. This occurs as irregular bursts of pulsations interrupted by periods of quiescence (Scemes and Freitas, 1989). Its other distinct behaviors are pointing and crum-

Received 14 September 1990; accepted 25 September 1991.

[*] Present address: Departamento de Biologia, FFCL-RP, Universidade de São Paulo, Ribeirão Preto, 14049 SP, Brasil.

pling. Pointing is produced by asymmetrical contractions of the radial muscles, and occurs frequently, even in the absence of a food stimulus. Crumpling is produced by simultaneous contraction of the four radial muscle bands and of the muscles in the peduncle, and is only infrequently observed. Attempts to induce crumpling through mechanical or electrical stimulation of the exumbrellar epithelium have not been successful (Scemes and Mendes, 1986, 1988; Scemes and Freitas, 1989), suggesting that *L. tetraphylla* lacks epithelial conduction, at least within the ectoderm (Scemes and Mendes, 1986; Scemes and Freitas, 1989). However, when this jellyfish is exposed to cholinergic agents, crumpling behavior does occur (Scemes and Mendes, 1986, 1988), and the involvement of a neuronal pathway in the crumpling behavior of *L. tetraphylla* thus has been surmised.

In the present paper, we describe the fine structure of the radial neuromuscular system of *Liriope tetraphylla* and provide ultrastructural support for the existence of the putative neuronal pathway involved in the control of crumpling behavior in this species.

Materials and Methods

Specimens of *Liriope tetraphylla* were collected by plankton net from the São Sebastião Channel, São Paulo State, Brazil.

The jellyfish were anesthetized with artificial seawater containing 200 m*M* $MgCl_2$. Body tissue was dissected in ice-cold fixative under a stereomicroscope, and fragments of the radial system were immersed (for 2.5 h at 4°C) in a primary fixative containing 0.25 *M* glutaraldehyde and 0.1 *M* paraformaldehyde, buffered with 0.2 *M* sodium cacodylate, in diluted artificial seawater (Pantin, 1948). The fragments were washed three times, for 5 min each, in 0.2 *M* cacodylate-buffered artificial seawater and postfixed in 0.2 *M* cacodylate-buffered artificial seawater containing 1% osmium tetroxide. After dehydration in a series of cold graded ethanols, the material was passed through propylene oxide, infiltrated overnight in a propylene oxide-Araldite mixture (1:1), and embedded in Araldite.

Thick sections (0.5 μm) were stained with equal parts of 1% methylene blue and 1% toluidine blue in 1% aqueous borax and analyzed and photographed with a Zeiss photomicroscope. Silver-gold, thin sections (50–80 nm) were contrasted with uranyl acetate and lead citrate and were examined in a JEOL 100C electron microscope at an accelerating voltage of 80 kV.

Results

Micro-anatomy of the neuromuscular system of Liriope tetraphylla

The anatomy of *Liriope tetraphylla* is summarized in Figure 1. The neuromuscular system of the subumbrellar surface consists of a radial system and a circular system. The radial muscular system is composed of four muscle bands. These run from the mouth, along the manubrium and peduncle, out over the subumbrellar surface, where they overlie the radial canals, to the margin.

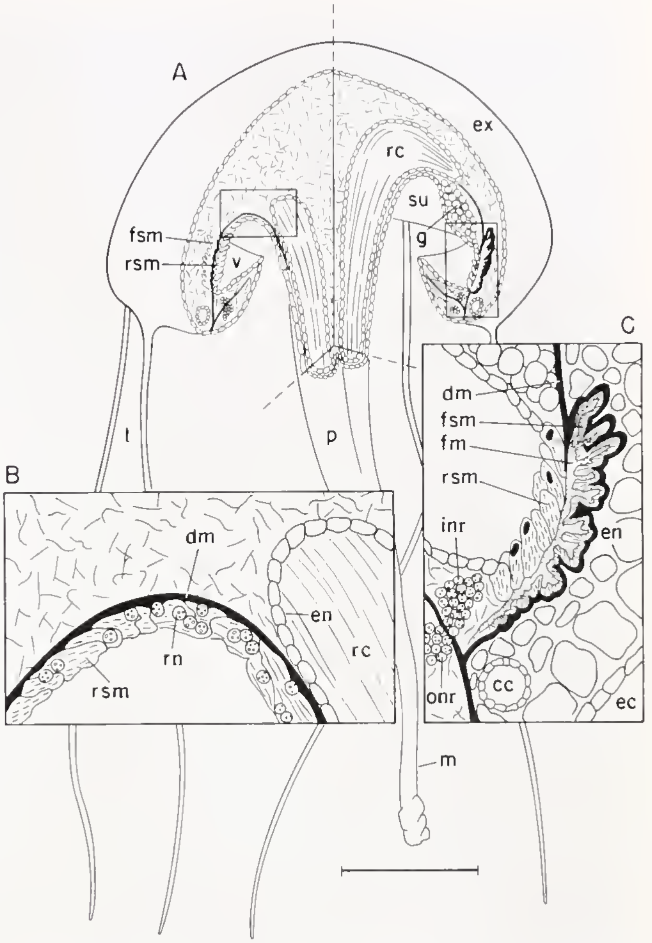

Figure 1. (A) Schematic transection through the body wall of the trachymedusa *Liriope tetraphylla* showing the disposition of the radial neuromuscular system and radial canals. (B) Detail of insertion of the peduncle into the subumbrella, showing radial smooth muscles, radial canal, and network of ectodermal neurons. (C) Detail of radial smooth muscles and folded, striated swimming muscles at the margin showing the relationship of the various structures to the mesoglea, inner and outer nerve rings, and circular canal. Circular canal (cc), dense mesoglea (dm), ectoderm (ec), endoderm (en), exumbrella (ex), fibrous mesoglea (fm), folded, striated swimming muscle (fsm), gonad (g), inner nerve ring (inr), manubrium (m), outer nerve ring (onr), peduncle (p), radial canal (rc), radial ectodermal neurons (rn), radial smooth muscle (rsm), subumbrella (su), tentacles (t), and velum (v). Scale bar: (A) = 0.5 cm, (B) and (C) = 0.5 mm.

In the manubrium (0.33 mm diameter) (Fig. 2), the four ectodermal muscle bands, which in cross section measure 24 μm high by 100 μm wide, are diametrically opposed and occupy almost the entire manubrium wall. The endoderm is reduced to a single cell layer in these regions, but thickens considerably in the areas between adjacent muscle bands. At the insertion of the peduncle into the subumbrella, the four muscle

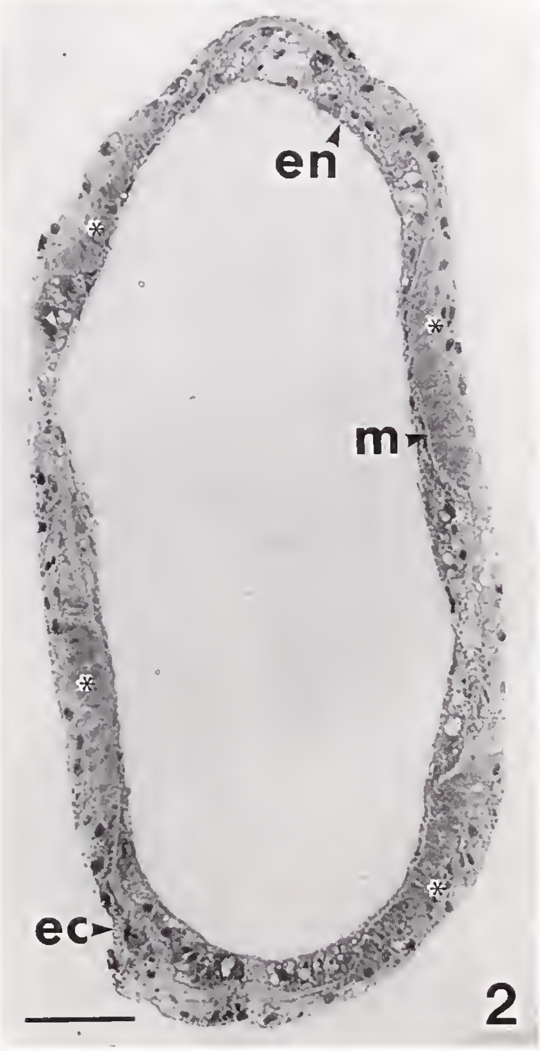

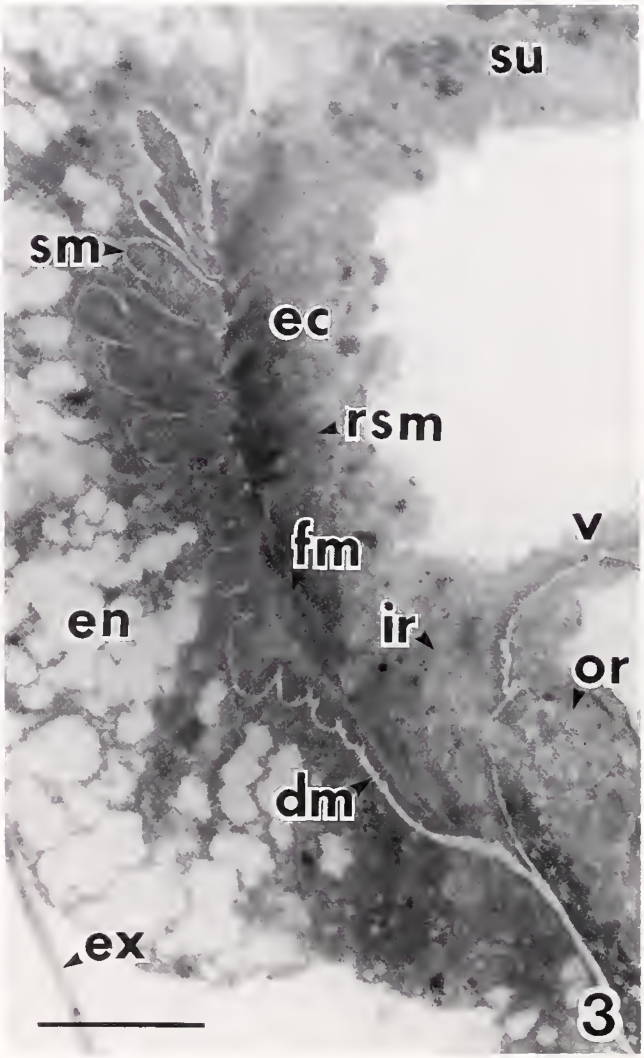

Figure 2. Light micrograph of a transverse section through the manubrium showing ectoderm (ec), endoderm (en), mesoglea (m), and four bands of ectodermal smooth muscle cells (*). Scale bar = 50 μm.

Figure 3. Light micrograph of a transverse section through the radial system at the margin showing ectodermal, radial smooth muscle cells (rsm), striated swimming muscle cells (sm), inner nerve ring (ir), outer nerve ring (or), dense mesoglea (dm), fibrous mesoglea (fm), exumbrella (ex), subumbrella (su), velum (v), and ectodermal (ec) and endodermal cells (en). Scale bar = 30 μm.

bands surround the peduncle, subsequently diverging to follow each of the four radial canals out to the umbrella margin.

The circular neuromuscular system consists of the striated, circular muscle layer which lines the subumbrellar surface, and the inner and outer nerve rings which lie at the margin. The striated muscle layer exhibits extensive infolding where it meets the radial neuromuscular system, from which it is separated by the mesoglea (Fig. 3).

Figure 4. Electron micrograph of a transverse section through the ectodermal smooth muscle layer in the manubrium. The filamentous mesoglea (m) and areas of desmosomal contact (d) between adjacent myofibrils are visible. Scale bar = 1 μm.

Figure 5. Area of synaptic contact (s) between two ectodermal neurons in the peduncle, showing a dense cored vesicle (dv) and a mitochondrion (m). Scale bar = 300 nm.

Figure 6. Transverse section of a neuron (n) juxtaposed to ectodermal smooth muscle cell (m). Scale bar = 0.8 μm. Insert: clear vesicles from ectodermal neuron. Scale bar = 140 nm.

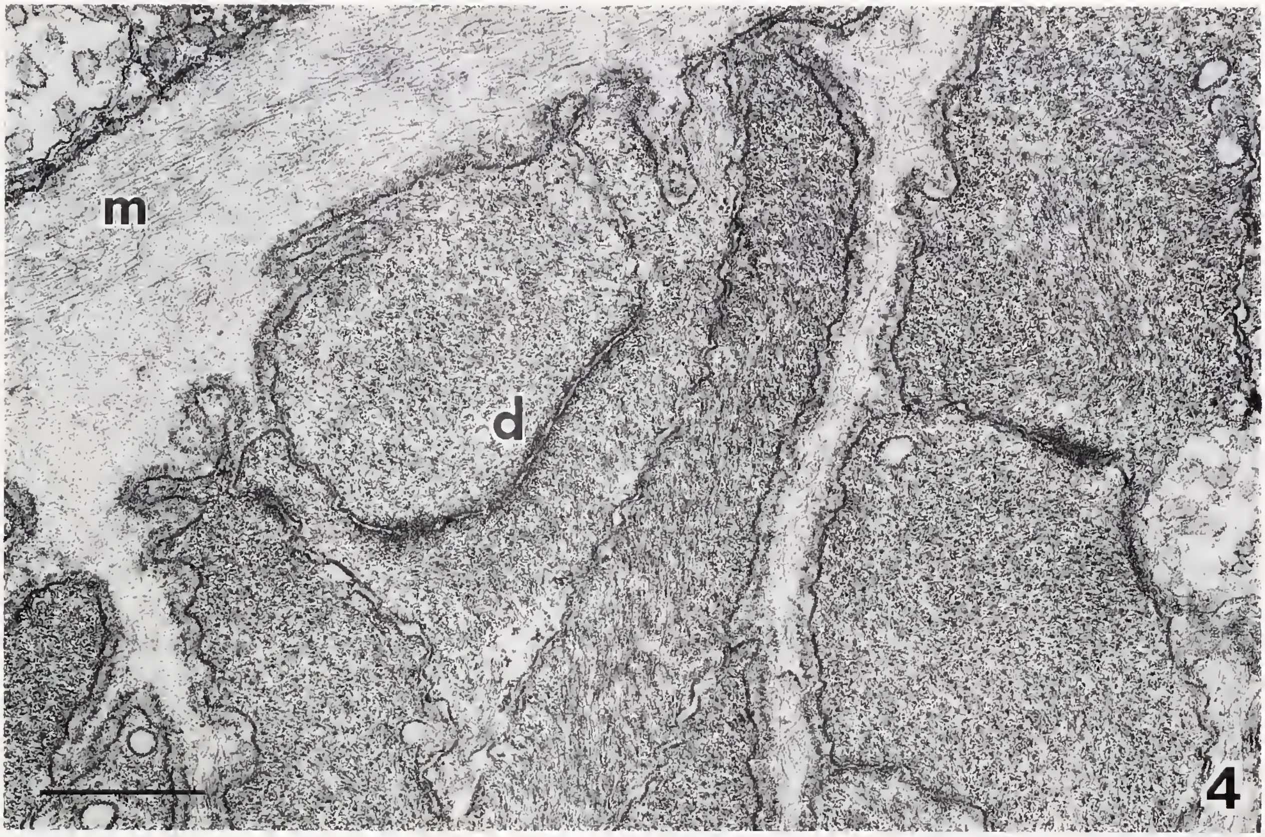
m
d
4

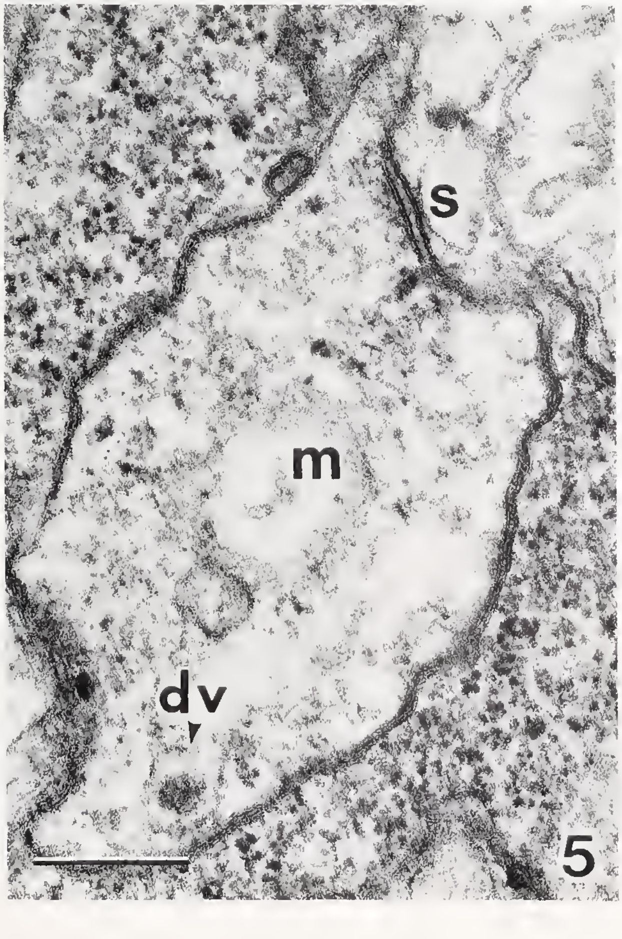
s
m
dv
5

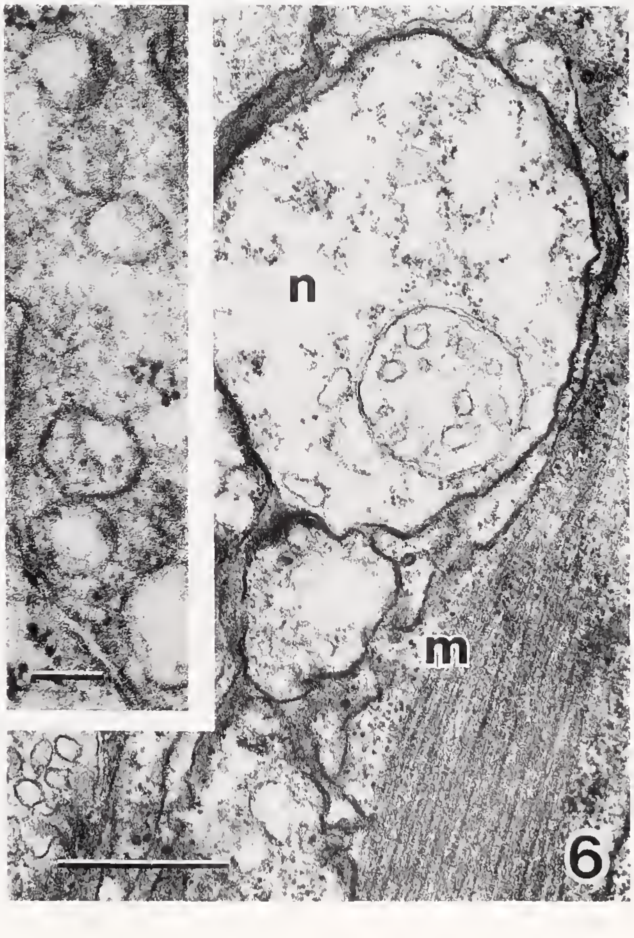
n
m
6

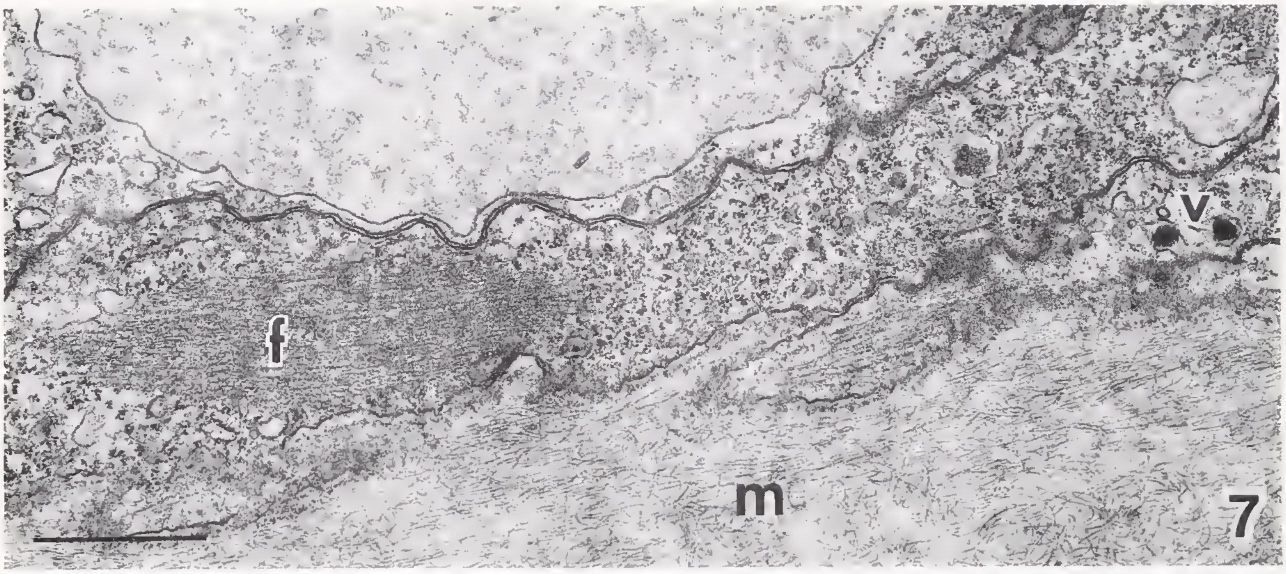

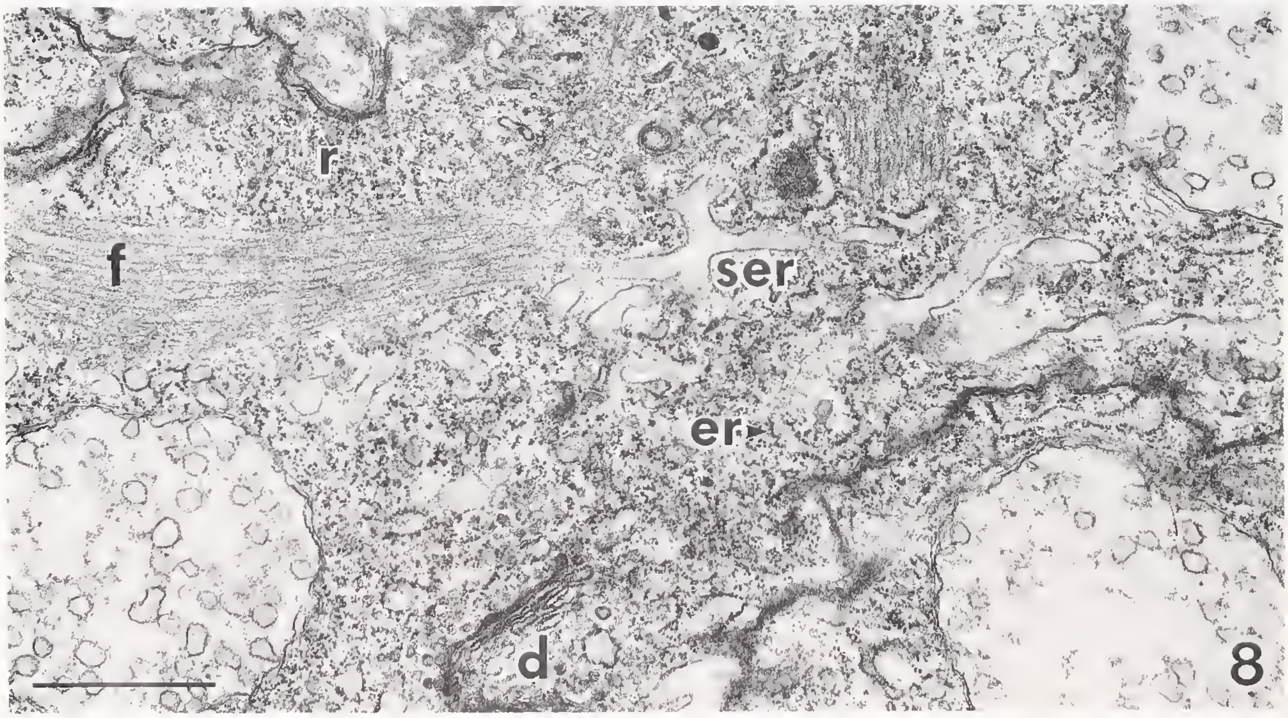

Figure 7. Endodermal myoepithelial cells showing myofilaments (f), vesicles (v) and the filamentous mesoglea (m). Scale bar = 1 μm.

Figure 8. Endodermal myoepithelial cell showing extensive myofilament bundles (f), areas of rough (er) and smooth (ser) endoplasmic reticulum, ribosomes (r) and a Golgi body (d). Scale bar = 1 μm.

Figure 9. Umbrella margin showing part of an ectodermal smooth muscle cell (ec), striated swimming muscle (sm), mesoglea (m), and radial neurons (n). Scale bar = 1.5 μm.

Figure 10. Dense, afilamentous mesoglea (m) separating the endodermal cell layer (en) from the swimming muscles (sm). Scale bar = 1.5 μm. Insert: gap junction between adjacent endodermal cells. Scale bar = 50 nm.

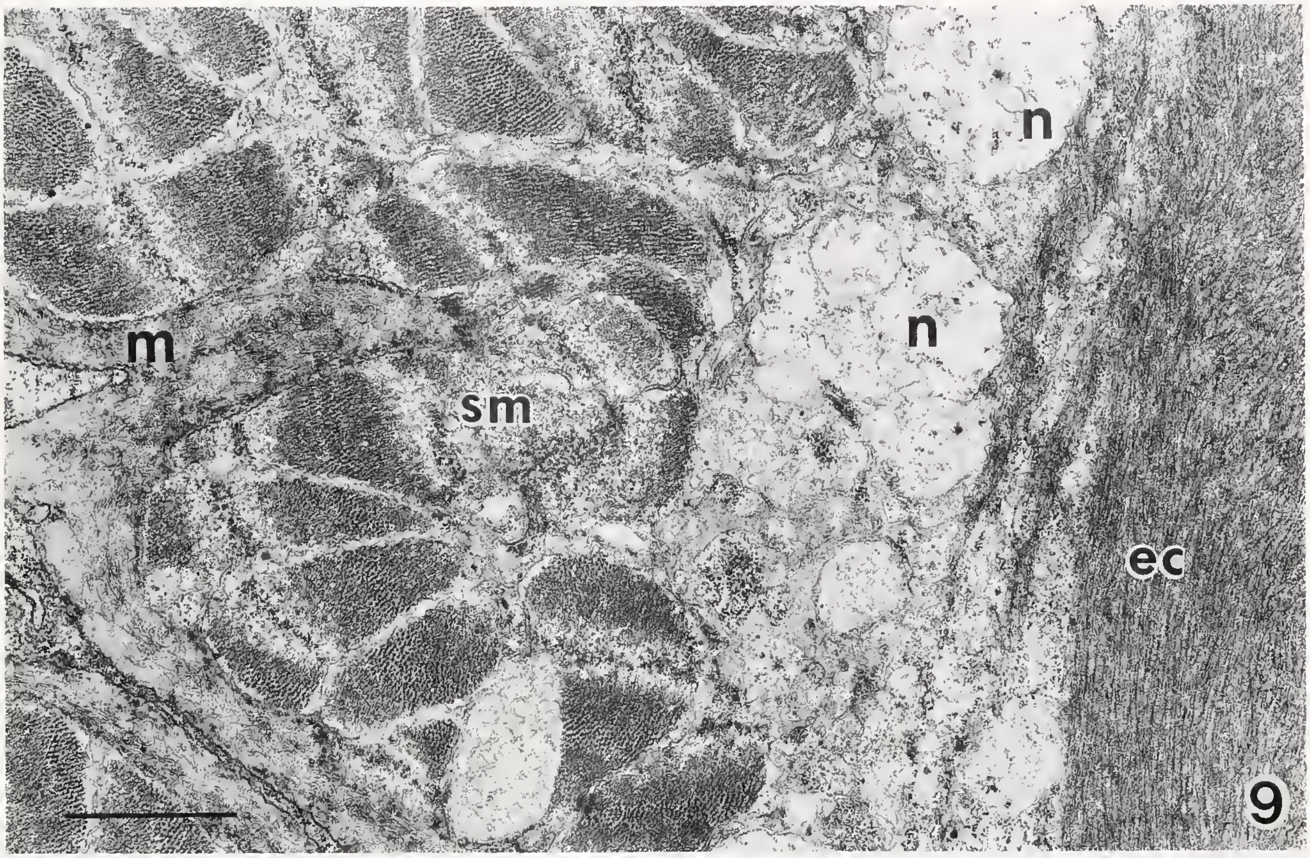
n
n
m
sm
ec
9

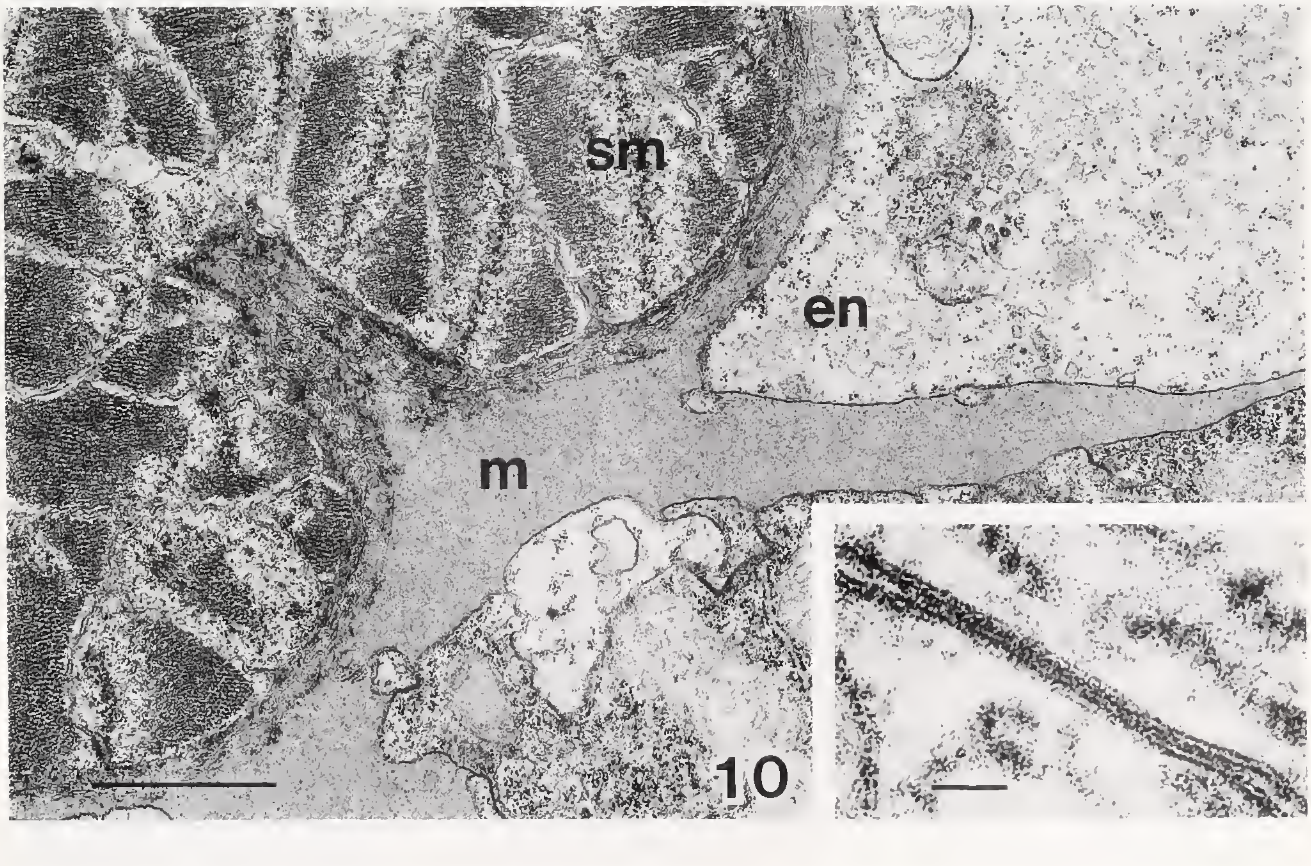
sm
en
m
10

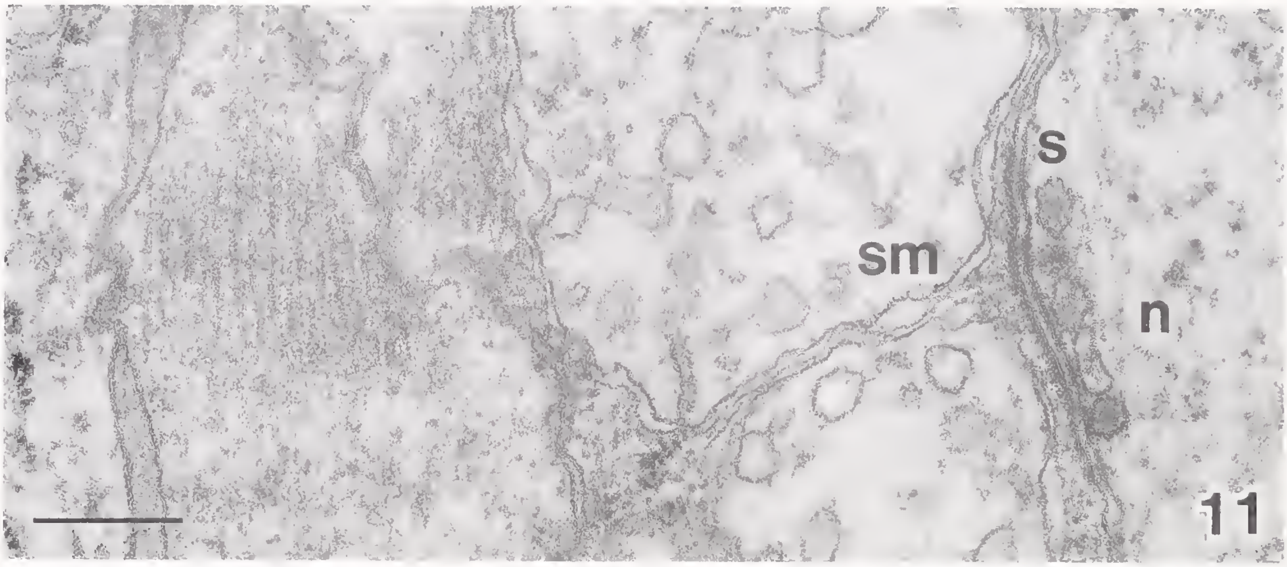
s
sm
n
11

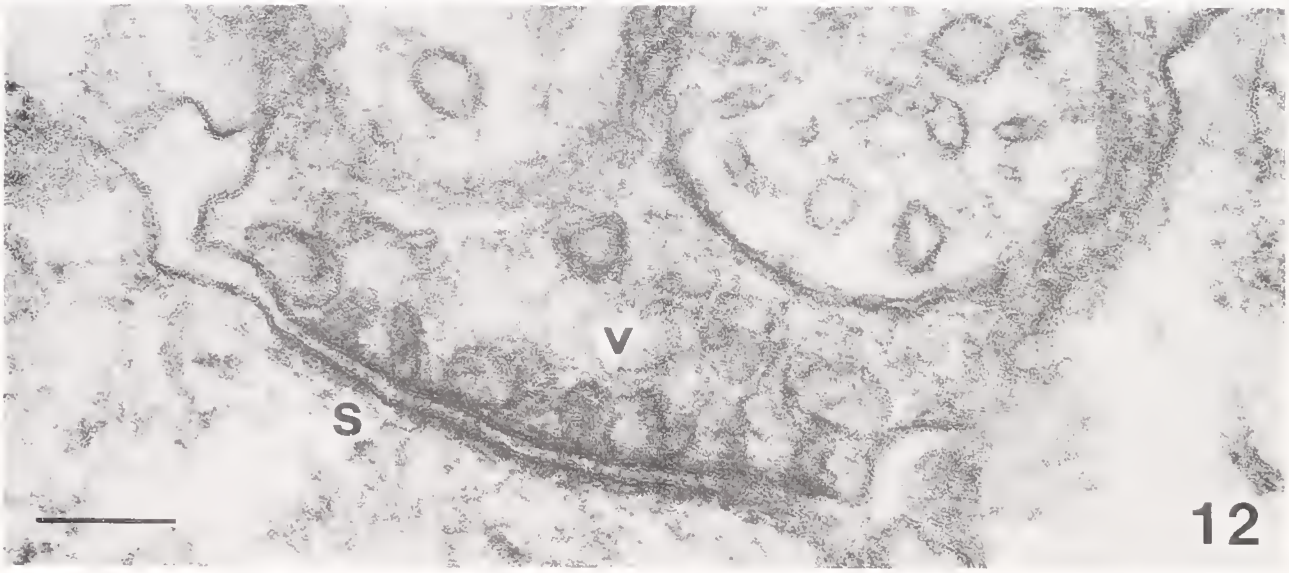
v
s
12

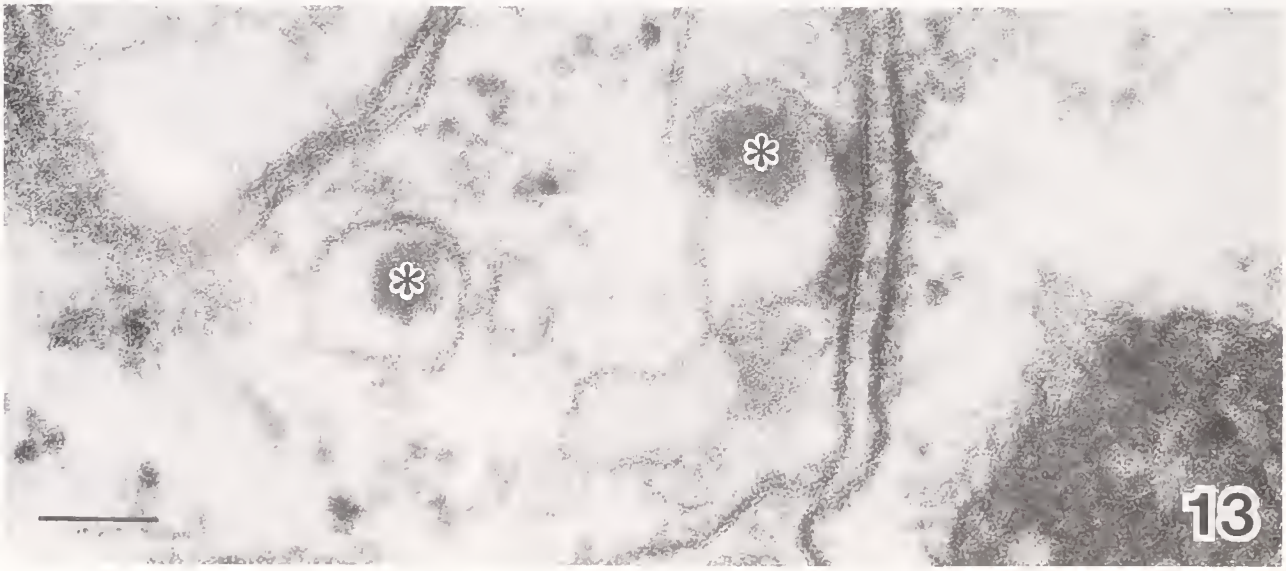
✻
✻
13

Ultrastructure

Three types of muscle cells are found in the manubrium and peduncle: two are located within the ectoderm, the third is restricted to the endoderm.

The predominant muscle type in the ectodermal muscle bands is a smooth muscle cell that measures 2 to 4 μm in width by at least 10 to 20 μm in length (Fig. 2). These cells are connected by desmosome-like structures and form a well developed layer (Fig. 4), the basal surface of which interdigitates extensively with the mesoglea. Their myofilaments are oriented parallel to the longitudinal axis of the manubrium and peduncle.

Axons, 0.4 to 1.5 μm in diameter, containing either dense cored vesicles of approximately 140 nm diameter (Fig. 5) or clear vesicles of about 200 nm diameter (Fig. 6), are interspersed between the muscle cells. While these axons are found throughout the manubrium and peduncle, presumably forming a diffuse nerve net, they are particularly dense at the base of the peduncle around which they appear to form a ring-like structure. Although interneuronal, chemical synapses (Fig. 5) are common, neuromuscular synapses were never observed between the neurons and smooth muscle cells.

The second type of ectodermal muscle cell was encountered only infrequently. It is distributed from the mouth throughout the manubrium and peduncle and is characterized by a spheroidal aggregation of myofilaments (3.5–5 μm diameter) surrounded by an electron-lucent cytoplasm. These myoepithelial cells lie close to the external surface of the ectoderm, their innermost surface being apposed to the underlying layer of ectodermal smooth muscle. The functional relevance of this cell type is not clear, but they could be myoblasts, or ectodermal smooth muscle cells undergoing lysis.

The endodermal myoepithelial cells are 1.3 μm in diameter and at least 17 μm long, and contain 6- to 8-nm diameter myofilaments that are oriented perpendicularly to the long axis of the manubrium. These cells also contain clear vesicles and dense cored vesicles of about 160 nm diameter, mitochondria, smooth and rough endoplasmic reticulum, ribosomes, and Golgi complexes (Figs. 7, 8). This endodermal muscle layer is well developed in those areas where the four ectodermal muscle bands do not predominate (Fig. 2). The existence of an endodermal nerve net is questionable, because any putative axon profiles may, in fact, represent transections of these endodermal myoepithelial cells.

The smooth muscle cells and neurons of the radial neuromuscular system of the manubrium and peduncle lie parallel to the radial canals that connect the manubrium to the circular canal (Fig. 1). Neuromuscular synapses were not observed within the radial system, but their existence cannot be refuted. No evidence was found for gap junctions, between either neurons or muscle cells, within the entire radial pathway. Where the radial and circular muscles overlap, they are separated by a fibrous layer, and the underlying, striated circular muscle is heavily infolded (Figs. 3, 9, 10). Axon profiles are very evident in the fibrous layer that separates the two muscle types (Fig. 9), and these axons, together with the muscle, come into close proximity with the inner nerve ring at the margin.

These ectodermal layers are separated from the endoderm by a layer of electron-dense mesoglea that apparently lacks filaments (Figs. 3, 10). Many gap junction-like structures (gap of 3 nm), and areas exhibiting an intercellular space of fixed width (10 nm), were observed between the endodermal cells (Fig. 10).

The striated muscle cell layer, which covers the entire subumbrellar surface of the bell, is innervated by neurons of the inner nerve ring (Fig. 11). These contacts are characterized by a synaptic cleft (15 nm) that separates plasmalemmae underlain by electron-dense plaques of finely filamentous material and by the presence of spherical to irregular, clear vesicles of about 75 nm diameter. Gap junction-like structures were not observed between the striated muscle cells. If such junctions do exist within this tissue layer, they are far less frequent than those seen within the endodermal layer (Fig. 10).

Synaptic contacts between the neurons within both the inner and outer nerve rings are characterized by a synaptic cleft of 20–23 nm and irregular to roughly spherical vesicles. In the inner nerve ring, these are clear and about 90 nm in diameter (Fig. 12); in the outer nerve ring, the vesicles are dense cored and about 140 nm in diameter (Fig. 13). Gap junctions were not observed within the nerve rings. In the inner nerve ring, single neurons were observed to make at least three neuro-neuronal synaptic contacts of the chemical type, all at the same locus.

Discussion

Crumpling behavior was originally defined as the infolding of the margin into the subumbrellar cavity and the subsequent cessation of swimming activity (Hyman,

---

Figure 11. Synaptic contact (s) between neuron (n) and striated muscle cell (sm) from subumbrellar surface. Scale bar = 300 nm.

Figure 12. Synaptic contact (s) between two neurons from the inner nerve ring showing irregular clear vesicles (cv). Scale bar = 200 nm.

Figure 13. Synaptic contact between two neurons from the outer nerve ring showing dense cored vesicles (*). Scale bar = 100 nm.

1940). In the species so far investigated, the main effectors of this behavior are the radial muscle systems of the peduncle and subumbrella and the longitudinal muscles of the tentacles. That the same effectors of crumpling act in *L. tetraphylla* is suggested by the high degree of development of the longitudinal, ectodermal muscle bands of the manubrium and peduncle and the radial muscle bands on the subumbrella.

Crumpling in hydromedusae appears to be coordinated by at least three pathways: one entirely dependent on epithelial conduction, one that employs both epithelial and neuronal substrates, and the third, an entirely neuronal pathway.

The purely epithelial pathway has been proposed for *Stomotoca atra* (Mackie, 1975). In this species, electrical stimulation of the exumbrella evokes action potentials that radiate over the exumbrella ectoderm and spread by way of the endodermal lamella to the subumbrella, where they elicit contraction of the radial muscles. Stimulation of the exumbrella also directly inhibits the animal's swimming rhythm. Significantly, gap junctions with a gap space of 3 to 4 nm, have been found within the exumbrella epithelium of *S. atra* (Mackie and Singla, 1975).

Crumpling in *S. atra* can also be induced by extracts of the predatory hydromedusa *Aequorea aequorea* (Schwab, 1977). But the response so evoked differs from that elicited by electrical or mechanical stimulation, in that the exumbrella ectoderm is not involved, and tetanic contractions of the peduncle are absent. These differences imply that crumpling in this species can be achieved by at least two pathways, one of which remains unknown.

In contrast, crumpling in *Sarsia tubulosa* (Mackie and Passano, 1968), *Proboscidactyla flavicirrata* (Spencer, 1975), and *Polyorchis penicillatus* (King and Spencer, 1981) involves neuronal elements that are thought to provide an intermediate link between epithelial conduction (sensory element) and radial muscle contraction (effector). Specifically, the absence of temporal correlation between radial muscle potentials and endodermal pulses in *Polyorchis penicillatus*, prompted King and Spencer (1981) to propose that epithelial pulses do not excite the radial muscles directly, but rather do so by way of the inner or outer nerve rings. In *P. penicillatus*, cells in the radial muscle bands, which are organized in the same way as those described here for *L. tetraphylla*, are connected laterally by desmosomes. Gap junctions are also present but rare (Spencer, 1979). While direct communication between the ectodermal epithelium and neurons might occur at the margin, specialized junctions have not been encountered (Spencer, 1979).

Conversely, the olindiad *Epiretmus typus* does not possess an excitable exumbrella or endodermal lamella (von Carolsfeld, 1976), and electrical or mechanical stimulation of these structures does not result in muscle contraction. Crumpling, however, can be triggered by electrical or mechanical stimulation of the tentacles; this behavior is entirely dependent on the integrity of the margin, where neuronal elements are present, and is prevented by high concentrations of magnesium.

Further, the olindiad *Gonionemus vertens* does not possess an excitable exumbrella and does not crumple, yet gap junctions are common in its exumbrellar epithelium, subumbrellar lamella, and endoderm of the radial canals, much as is found in other species in which epithelial conduction has been described (von Carolsfeld, 1976). Clearly, causal relationships between either the presence of an excitable epithelium and the manifestation of crumpling behavior, or the presence of gap junctions and excitability, cannot always be established.

In *L. tetraphylla*, the only specialized intercellular contacts observed between the radial muscle cells were desmosomes (Fig. 4); gap junctions are apparently absent. This observation suggests that excitation of these muscles is achieved exclusively by way of chemical synapses, although the possibility of limited electrical coupling through very small gap junctions cannot be excluded. The absence of identified neuromuscular synapses is problematic, but the abundance of neuronal profiles with either clear or dense cored vesicles suggests that such synapses must be present.

Epithelial conduction in the exumbrellar epithelium is probably not involved in the crumpling response of *L. tetraphylla*, because neither electrical nor mechanical stimulation of the exumbrella induces radial muscle contraction (Scemes, 1985; Scemes and Freitas, 1989). Furthermore, although the endodermal cells are connected by gap junctions, and so are presumably electrically coupled, any action potentials generated in this layer would be prevented from spreading to the ectodermal muscles and nerves by the presence of the dense mesoglea that separates the tissue layers. Transmesogleal, epithelial bridges (*cf.*, Mackie and Singla, 1975; Spencer, 1979) were not encountered. In general, gap junction-like structures were observed only in the endodermal cell layer and were not found between muscle and nerve cells. Symmetrical contraction of the radial muscles and retraction of the tentacles and manubrium (*i.e.*, crumpling) can, however, be induced in *L. tetraphylla* pharmacologically. Application of muscarinic antagonists (atropine) and nicotinic agonists (nicotine) to whole animal preparations induces the crumpling response (Scemes and Mendes, 1986, 1988), and under these conditions, with or without mechanical stimulation, exumbrellar potentials are not observable (Scemes, unpub. data).

As noted above, the exumbrellar epithelium in *Polyorchis penicillatus* has a sensory function, furnishing inputs to the neural elements that trigger the contraction of the crumpling effectors. Given that stimulation of the exumbrella elicits partial crumpling, while stimulation of the margin leads to a full crumpling response, King and

Spencer (1981) proposed that radial muscle contraction in *P. penicillatus* is achieved either through the nerve rings (the marginal pathway) or through the radial nerves in the peduncle (the apical pathway).

The marginal pathway, particularly the inner nerve ring, is probably involved in the crumpling behavior of *L. tetraphylla*, based on both morphological and physiological observations. The radial nerves and inner nerve ring are in close proximity at the margin, providing for possible interaction. Furthermore, electrophysiological studies have shown that crumpling in *L. tetraphylla* is associated initially with an increase in swimming activity and then, as crumpling persists, by inhibition (Scemes and Freitas, 1989). Whether the interactions between the radial and circular systems are uni- or bidirectional requires further investigation. The abundance of chemical synapses in both nerve rings, and specifically the presence of polysynaptic contacts within the inner nerve ring, suggest that highly complex neuronal interactions are possible.

An apical pathway, of the type suggested by King and Spencer (1981) for *Polyorchis penicillatus*, may also be present in *L. tetraphylla*, given the abundance of neurons in what may be a nerve ring at the base of the peduncle. Such a nerve ring may serve to effect the synchronous contraction of the four radial muscle bands that are necessary for crumpling.

Clearly, electrophysiological studies are required to elucidate the mechanisms underlying crumpling behavior in hydromedusae, and to reveal how the various conducting systems interact to modify observed behavioral output. The data obtained here, for *L. tetraphylla*, suggest that crumpling is effected by the nervous system through chemical synapses, implying the existence of a functionally complex nervous system despite the apparent morphological simplicity. Comparative studies will be valuable in establishing the degree of participation of the epithelial and neuronal elements involved in the behavioral repertoire of the Cnidaria, and will provide much needed insight into the means by which different mechanisms have evolved to bring about essentially similar behaviors.

Acknowledgments

The authors thank Professor Paulo A. Abrahamsohn of the Electron Microscopy Sector, Department of Histology and Embryology, University of São Paulo for access to electron microscopical facilities, and Moises Alexandre da Motta for collecting biological material at the Center for Marine Biology, University of São Paulo in São Sebastião. Photographic work by Francisco Abós Salvador, and particularly the line drawing by Dr. Lelio Favaretto, are gratefully acknowledged. This study was partially financed by the Conselho Nacional de Desenvolvimento Científico e Tecnológico (303982/86-8).

Literature Cited

Donaldson, S., G. O. Mackie, and A. Roberts. 1980. Preliminary observations on escape swimming and giant neurons in *Aglantha digitale* (Hydrozoa, Trachylina). *Can. J. Zool.* **58:** 549–552.

Dunlap, K., K. Takeda, and P. Brehm. 1987. Activation of a calcium-dependent photoprotein by chemical signaling through gap junctions. *Nature* **325:** 60–62.

Frazer, S. E., C. R. Green, H. R. Bode, and N. B. Gilula. 1987. Selective disruption of gap junctional communication interferes with a patterning process in *Hydra*. *Science* **237:** 49–55.

Hyman, L. H. 1940. Observations and experiments on the physiology of medusae. *Biol. Bull.* **79:** 282–296.

King, M. G., and A. N. Spencer. 1981. The involvement of nerves in the epithelial control of crumpling behaviour in a hydrozoan jellyfish. *J Exp. Biol.* **94:** 203–218.

Laat, S. W., L. G. Tertoolen, and C. J. Grimmelikhuijzen. 1980. No junctional communication between epithelial cells in *Hydra*. *Nature* **288:** 711–713.

Mackie, G. O. 1975. Neurobiology of *Stomotoca*. II. Pacemakers and conduction pathways. *J. Neurobiol.* **6:** 357–378.

Mackie, G. O., and R. W. Meech. 1985. Separate sodium and calcium spikes in the same axon. *Nature* **313:** 791–793.

Mackie, G. O., and L. M. Passano. 1968. Epithelial conduction in hydromedusae. *J. Gen. Physiol.* **52:** 600–621.

Mackie, G. O., and C. L. Singla. 1975. Neurobiology of *Stomotoca*. I. Action systems. *J. Neurobiol.* **6:** 339–356.

McDowall, A. W., and C. J. Grimmelikhuijzen. 1980. Intercellular junctions in nerve-free *Hydra*. *Cell Tiss. Res.* **209:** 217–224.

Pantin, C. A. F. 1948. *Notes on Microscopical Techniques for Zoologists*, Cambridge University Press, London. 79 pp.

Passano, L. M. 1982. Scyphozoa and Cubozoa. Pp. 149–202 in *Electrical Conduction and Behaviour in 'Simple' Invertebrates*, G. A. B. Shelton, ed. Clarendon Press, Oxford.

Roberts, A., and G. O. Mackie. 1980. The giant axon escape system of a hydrozoan medusa, *Aglantha digitale*. *J. Exp. Biol.* **84:** 303–318.

Scemes, E., and E. G. Mendes. 1986. Cholinergic mechanism in *Liriope tetraphylla* (Cnidaria, Trachymedusae). *Comp. Biochem. Physiol.* **83C:** 171–178.

Scemes, E., and E. G. Mendes. 1988. Pharmacology of the radial neuromuscular system of *Liriope tetraphylla* (Hydrozoa, Trachymedusae). *Comp. Biochem. Physiol.* **90C:** 385–389.

Scemes, E., and J. C. Freitas. 1989. Electrophysiology of the swimming system of hydromedusae and the effects of atropine-induced crumpling. *Braz. J. Med. Biol. Res.* **22:** 189–198.

Schwab, W. 1977. Electrical responses of *Stomotoca atra* induced by an extract of *Aequorea aequorea*. *Nature* **267:** 701–702.

Spencer, A. N. 1975. Behavior and electrical activity in the hydrozoan *Proboscidactyla flavicirrata*. II. The medusa. *Biol. Bull.* **149:** 236–250.

Spencer, A. N. 1979. Neurobiology of *Polyorchis*. II. Structure of effector systems. *J. Neurobiol.* **10:** 95–117.

Spencer, A. N., and R. A. Satterlie. 1980. Electrical and dye coupling in an identified group of neurons in a coelenterate. *J. Neurobiol.* **11:** 13–19.

Spencer, A. N., and W. E. Schwab. 1982. Hydrozoa. Pp. 73–148 in *Electrical Conduction and Behaviour in 'Simple' Invertebrates*, G. A. B. Shelton, ed. Clarendon Press, Oxford.

von Carolsfeld, J. S. 1976. Contributions to hydromedusan neuroethology from a study on two olindiads, *Gonionemus vertens* (Agassiz, 1885) and *Epiretmus typus* (Bigelow, 1915). M. Sc. Thesis University of Victoria, Canada. 283 pp.

Westfall, J. A., J. C. Kinnamon, and D. E. Sims. 1980. Neuro-epitheliomuscular cell and neuro-neuronal gap junctions in *Hydra*. *J Neurocytol.* **9:** 725–732.

Reference: *Biol. Bull.* **181:** 484–499. (December, 1991)

Immunohistochemistry of Diverging and Converging Neurotransmitter Systems in Mollusks

SEPPO SOINILA[1,2] AND GEORGE J. MPITSOS[1]

[1]*Oregon State University, Mark O. Hatfield Marine Science Center, Newport, Oregon 97365, and*
[2]*Department of Anatomy, Neurobiological Research Unit, University of Helsinki, Helsinki, Finland*

Abstract. This series of studies was undertaken to compare the distribution of several transmitter-specific neuron systems in the nervous systems of the marine mollusks, *Aplysia californica* and *Pleurobranchaea californica*. Several specimens of each of the major ganglia of both species were sectioned serially, and each series was stained immunohistochemically to reveal one of the neuron systems. The present paper reports the results of stainings for acetylcholine, histamine, serotonin, gamma-aminobutyric acid (GABA), vasoactive intestinal polypeptide (VIP), cholecystokinin (CCK), Phe-Met-Arg-Phe-NH_2 (FMRFamide), and small cardioactive peptide B (SCP_B). For all the transmitter-specific sets of neurons examined, relatively few neurons send diverging projections to large areas of the neuropil in one or more ganglia. Moreover, different transmitters converge onto similar areas, and several transmitters evidently project onto the same identified neuron. Many of these diverging and converging projections are sufficiently extensive and overlapping that they are unlikely to be specific for a particular motor-pattern. The overall findings are consistent with our previous neurophysiological data. These indicate that activity does not necessarily arise through circuit-specific, identifiable connections. Instead, appropriate response patterns, often containing mixtures of several behaviors, emerge variably through diffuse connections. These findings are also consistent with recent reports from other laboratories indicating that even light topical stimulation generates highly distributed neural activity, and that the responses of identifiable neurons are not constant. The anatomical data presented here should be combined with physiological experiments aimed at verifying the neurotransmitter action of the substances examined and elucidating the role of these agents in controlling the dynamics of neuronal responses.

Received 28 December 1990; accepted 25 September 1991.

Introduction

Adaptive systems, whether they be chemical, cellular, or organismal, are composed of many components that must communicate with one another if the systems are to generate coherent responses. The nervous system represents a special form of communication between cells characterized by the anatomical connection of the neurons with each other and with target cells. Communication occurs in two forms: electrical potentials are propagated along the neuronal membrane, and they are relayed to recipient cells through chemical neurotransmission. According to the classical view, nonspecific electric signals are prevented during conduction through mechanical isolation by glial cells, and chemical signalling is locally limited at the synapse through rapid breakdown of the transmitter substances. These arrangements allow individual neurons to be connected specifically with other neurons so that fixed circuits are formed. Many examples show that simple reflexes are produced by response-specific circuits. However, recent evidence suggests that even relatively simple reflexes, such as the *Aplysia* gill withdrawal reflex, may not necessarily be produced by stereotypically identified neurons (Leonard *et al.*, 1990). Furthermore, our analysis of molluscan feeding and other buccal-oral behaviors, and of the neuronal activity producing them, has suggested that such behaviors may not be based on behavior-specific circuits (Cohan, 1980; Cohan and Mpitsos, 1983a, b; Mpitsos and Cohan, 1986a, b; Mpitsos and Lukowiak, 1985).

More specifically, our findings on the *Pleurobranchaea* buccal and cerebral ganglia indicate that the neurons producing oral-buccal behaviors are multifunctional, so that the same set of connections generates many different behaviors. Our physiological and behavioral studies have shown that many mouth-related behaviors of *Pleurobranchaea* arise from a matrix of highly interconnected neurons showing the following characteristics: (1) extensive divergence occurs by which a single neuron connects with many others; (2) convergence occurs by which many neurons innervate the same neuron; (3) neurons feed back to neurons that drive them; (4) motor neurons are coupled to one another; (5) and the most important feature may be that the nervous activity and the corresponding behaviors are variable, noisy and chaotic (Mpitsos and Cohan, 1986a; Mpitsos *et al.*, 1988a, b). Variability expresses itself, for example, through the ability of neurons to drastically change their temporal firing order [*e.g.*, Fig. 5 in (Mpitsos and Cohan, 1986b], or the ability of a characterized set of neurons to reorganize into coherent action after a critically important neuron that controls the patterned activity has been functionally removed from the circuit [*e.g.*, Fig. 16 B and C in (Mpitsos and Cohan, 1986b]. Our simulation studies indicate that even random noise may have a controlling role in the ability of animals to learn or to generate activity patterns that are appropriate for a given environmental situation (Burton and Mpitsos, 1991).

The basic issue, therefore, in such parallel, distributed systems is to understand the implications of self-organizing action of groups of neurons that emerges from the underlying converging and diverging connections, and the role of variability in such processes (Mpitsos, 1989; Burton and Mpitsos, 1991). The traditional way to define neuroanatomical connectivity has largely been one based on characterization of individual neurons. This method has been valuable in revealing hierarchically different forms of neuronal activity. But it is bound to be incomplete because it only accounts for contributions by the identified elements of the system. The possibility that the unidentified elements may or may not affect the system is, by definition, neglected. This omission is critical, for evidence is accumulating that even simple reflexes may involve a significant proportion, if not most, of the neurons in a ganglion. Studies of *Aplysia* gill withdrawal movements elicited by light tactile stimulation of the siphon skin in *Aplysia* show that 300 to 400 of the 1000 neurons present in the ganglion become active (Zĕcević *et al.*, 1989). Moreover, as has also been observed in *Pleurobranchaea*, different subsets of these neurons in *Aplysia* become active in response to successive stimulations (Wu *et al.*, 1989). By contrast, the identified neurons constitute only a small fraction of the total neuron population (Kandel, 1979), and detailed analyses of variability in their responses are presently lacking.

The variability in neuronal responsiveness is, in our view, controlled by a variety of mechanisms. One may operate through neurotransmitters by adjusting the bifurcation dynamics of the system, as shown in computer simulations of neuronal membranes (Chay, 1985). Another mechanism may be to control the effects of noise (Burton and Mpitsos, 1991).

An understanding of the transmitter-specific connectivity, therefore, provides a necessary foundation for elucidating both the emergence of cooperative activity in distributed neural networks and the generation and control of variability. Toward this end, we have mapped classical and putative neurotransmitter systems in the major ganglia of the sea slugs *Aplysia californica* and *Pleurobranchaea californica*. Special emphasis has been paid to the buccal and cerebral ganglia, because they contain the neurons responsible for feeding behavior, and many forms of feeding behavior have been correlated with the activity patterns of particular neurons (Mpitsos and Cohan, 1986b; Mpitsos and Lukowiak, 1985). Although several transmitters have been mapped in these ganglia, most work has been performed on whole-mounts and, to our knowledge, no systematic study on complete serial sections is available. Furthermore, these ganglia have not been mapped for such important transmitters as GABA and ACh. Also, since most previous mapping studies have dealt with one substance at a time, we have made an attempt to gather the pieces together to allow for comparisons. In the present paper we summarize the results obtained on eight transmitters or neuropeptides: acetylcholine, histamine, serotonin, gamma-aminobutyric acid (GABA), vasoactive intestinal polypeptide (VIP), cholecystokinin (CCK), Phe-Met-Arg-Phe-NH_2 (FMRFamide), and small cardioactive peptide B (SCP_B).

In the experiments summarized here, we have asked whether the neurotransmitter-specific systems of each ganglion are distributed with high selectivity or whether they follow the same divergence and convergence strategies as those observed when these systems are examined neurophysiologically. For most substances studied, our observations are consistent with the latter possibility. Studies on invertebrates have demonstrated the neurobehavioral modulatory action of neurohumoral agents, and their ability to produce specific motor pattern changes (*e.g.*, Marder, 1984, 1988; Weiss *et al.*, 1986a, b; Dickenson and Marder, 1989; Rosen *et al.*, 1989; Dickenson *et al.*, 1990). The extensiveness of the divergence and convergence in our experimental systems favors the notion that the neurotransmitter systems collectively form another dimension of neurointegration, in addition to the neurophysiological variables. Many transmitters may act simultaneously, and the effect of a given substance depends on the context of all others present. This principle has been demonstrated recently for three interacting neuropeptides in the rat hypothalamus (Albers *et al.*, 1991). Much as behavior emerges from the melange of impinging sensations in whole animals, so it may be that the effect of interacting neurohumors may emerge nonlinearly from the aggregate dynamics rather than through the effects arising from the experimentally enforced action of single agents.

Materials and Methods

Experimental animals

The marine mollusks *Aplysia californica* and *Pleurobranchaea californica* were obtained from Dr. R. Fay (Pacific Biomarine, Venice, California) and maintained in an open seawater system held at 15°C for *Aplysia* and 11°C for *Pleurobranchaea*. The animals were anaesthetized by injecting approximately ⅓ of body weight 0.3 *M* $MgCl_2$ into the body cavity. The nervous system was dissected in seawater, the nerve roots were identified and the preparation was pinned out in a dish coated with Sylgard (Dow Corning).

Histological sections

One of the following fixatives was used. For serotonin, CCK, and VIP: Bouin's solution overnight at 4°C. For histamine and GABA: 4% carbodiimide for 1 h at room temperature, followed by Bouin's solution overnight at 4°C. For FMRFamide and SCPB: 0.5% p-benzoquinone for 1 h at room temperature, followed by Bouin's solution overnight at 4°C. For acetylcholine: Bouin's solution was supplemented with 0.1% glutaraldehyde overnight at 4°C. The specimens were rinsed and transferred into phosphate-buffered saline (PBS), pH 7.6 containing 20% sucrose. The ganglion was placed on a horizontal freezing plate so that the dorsal surface (caudal surface for *Aplysia* buccal ganglion) showed upwards and the left-right orientation corresponded to that *in situ*. The plane of sectioning was adjusted parallel to the freezing surface. Cryostat sections (16 μm) were cut and placed on chrome-alum-gelatin-coated glass slides and rinsed in PBS containing 0.25% Triton X-100. The slides were incubated with 10% normal swine serum for 20 min at room temperature, then with the primary antiserum diluted in PBS-Triton for 24 to 48 h at 4°C, and finally with fluorescein-(FITC)- or rhodamine-(TRITC)-labeled swine immunoglobulins specific for rabbit IgG (DAKO F205 and R156) diluted 1:100 in PBS-Triton for 1 h at room temperature. All incubations were performed in a humid chamber. After rinsing in PBS, the sections were covered with glycerol-PBS (50/50) and examined and photographed with a Zeiss Universal microscope incorporating an HBO mercury lamp and filter blocks 487712 for TRITC (excitation maximum 546 nm, emission barrier > 590 nm) and 487709 for FITC (excitation maximum 450–490 nm, emission barrier > 520 nm).

Antisera

Polyclonal histamine antiserum was obtained from Dr. P. Panula (Department of Anatomy, University of Helsinki, Finland). Its specificity has been characterized in a previous report (Panula *et al.*, 1988), and it has been shown to stain the previously reported histaminergic cell in both species studied (Soinila *et al.*, 1990). It was used at a dilution of 1:10,000. Immunoreactivity was completely inhibited by preabsorption with 1 μg/ml solution of histamine-protein conjugate.

Polyclonal serotonin antiserum was raised in rabbits against serotonin-albumin conjugates according to the method of Steinbusch *et al.* (1978). It was used in dilution 1:1,000 and it stained identifiable serotonergic neurons in molluscan ganglia and in rat sympathetic ganglia, but failed to stain cells containing catecholamines or histamine (Rathouz and Kirk, 1988, Soinila *et al.*, 1990). Immunoreactivity was completely inhibited by preabsorption with 10 μg/ml solution of serotonin-protein conjugate.

Polyclonal acetylcholine antiserum was raised in rabbits against choline-hemocyanin conjugates. The antiserum was used in dilution 1:500, and it stained previously identified cholinergic neurons in *Aplysia* ganglia and in rat brain and spinal cord. Immunoreactivity was inhibited by preabsorption of the antiserum with 1 μg/ml solution of choline-albumin conjugate or with 10 m*M* acetylcholine. Specificity was also checked by incubation of consecutive sections with antiserum raised against glutarylated hemocyanin, which did not stain any neurons indicating that the staining obtained with acetylcholine antiserum was not due to immunoglobulins directed against the carrier protein. Further indication of specificity was obtained from dot blotting experiments in which the antiserum readily recognized the choline-protein conjugate but not other related conjugates.

Polyclonal GABA antiserum was raised in rabbits against GABA-hemocyanin conjugates. It was used in dilution 1:500, and it stained known GABAergic structures in the rat cerebellum. Specificity was confirmed in dot blotting experiments in which the antiserum recognized GABA-protein conjugate but not the conjugates containing glutamate, glutamine, aspartate, or beta-alanine. Immunoreactivity was completely inhibited by preabsorption with 1 μg/ml GABA-hemocyanin solution.

Polyclonal antisera against VIP, FMRFamide, and CCK were purchased from Incstar (Stillwater, Minnesota), and they were used in dilution 1:250–1:500 for VIP, and 1:500 for FMRFamide and CCK. Specificity of these antisera has been characterized by the manufacturer.

Monoclonal antiserum against SCPB was obtained from the Monoclonal Laboratory, Department of Zoology, University of Washington (Seattle, WA) and it has been characterized in a previous study (Kempf *et al.*, 1987).

Electrophysiological identification of neurons

The abdominal ganglion was bathed in artificial seawater (Instant Ocean from Aquarium Systems, Inc.) containing 0.3 *M* sucrose, and its surface was desheathed mechanically. Neuron R15 was located in the right dorsal-caudal region and neuron L10 in the left ventral-caudal region, based on previously established maps (Kandel, 1979). Electrophysiological criteria of identification was confirmed by intracellular recordings using standard electrophysiological methods and micropipettes filled with potassium chloride (0.8 *M*) or Lucifer Yellow (Sigma; at 50% saturated solutions at 4°C). Physiological recordings were made in artificial seawater solutions maintained at 12°C. Following intracellular recording, some cells were iontophoretically injected with Lucifer Yellow by passing hyperpolarizing current from the recording micropipette for at least 2 h before being fixed and processed for serial sectioning and immunohistochemistry. Examination of several preparations under bright light optics indicated that R15 can be reliably identified based on morphological criteria alone, as ascertained by examination of the same sections under UV-light, which makes the Lucifer Yellow-injected neurons visible.

Cobalt back-injection technique

The cerebral or the buccal ganglion and approximately 5 mm stump of the cerebral-buccal connective were dissected out into seawater, and the connective was mechanically desheathed. The ganglion was pinned out on a Sylgard-coated dish and the distal end of the connective was immersed in an isolated compartment of the dish that contained 0.5 *M* cobalt chloride in seawater. After incubation for 12 h at 4°C, the preparation was rinsed in seawater and immersed in 1% ammonium sulfide for 15 min or until black cobalt precipitate appeared. The preparation was dehydrated and cleared in alcohol-xylene series.

Mapping of transmitter-specific neuron systems

Complete serial cryostat sections through each ganglion were obtained for immunostaining. Due to the large number of sections (70–120 per ganglion), the distribution of stained cells in individual sections was reconstructed on diagrams representing consecutive zones. Definition of the zones was based on identified structures in serially sectioned ganglia stained with Cresyl fast violet.

Buccal ganglion; three zones. In *Aplysia*, the ganglion is located on the caudal, sometimes the ventrocaudal, aspect of the buccal mass; in *Pleurobranchaea*, the ganglion is consistently on the dorsal surface of the buccal mass. The plane of sectioning was adjusted parallel to the buccal mass, so that the denotation caudal-rostral in *Aplysia* buccal ganglion corresponds to dorsal-ventral in the *Pleurobranchaea* buccal ganglion. For reconstruction, the ganglion was divided into three zones: the coelomic zone contains the sections from the caudal (*Aplysia*) or dorsal (*Pleurobranchaea*) surface to the level where the commissure first appears; the commissural zone consists of the sections showing the commissure; and the buccal zone consists of the rest of the ganglion.

Cerebral ganglion; four zones. The dorsal zone extends from the ganglion surface to the level where the neuropil first appears. The dorsal subsurface zone extends to the dorsal edge of the anterior (*Aplysia*) or the larger (*Pleurobranchaea*) tentacular nerve. The commissural zone contains all sections showing the commissure, and the sections ventral to that level form the ventral zone.

Abdominal ganglion; four zones. The dorsal zone extends from the surface to the level where the neuropil first appears. The dorsal and ventral subsurface zones contain the sections showing the commissure, divided equally between the two zones. The sections ventral to the commissure constitute the ventral zone. The *Pleurobranchaea* abdominal (visceral) ganglion is tiny and could not be subjected to the above division.

Pedal-pleural ganglion; three zones. The dorsal and ventral zones extend from the respective surfaces to the level of the neuropil, and the central zone contains the rest of the ganglion.

Results

Mapping of transmitters in Aplysia californica

Buccal ganglion. Histamine immunoreactivity was confined to a pair of 100 μm neurons located ventrally in the commissural zone in each hemiganglion and to a very dense plexus throughout the neuropil (Figs. 1A–2A). This plexus contained both fine varicose terminals and coarser nerve fibers which were confined to the neuropil region.

No *serotonin*-immunoreactive neurons were seen in the buccal ganglion, although the neuropil showed a dense serotonin-immunoreactive plexus throughout (Figs. 1B, 2B). Serotonin-immunoreactive varicose fibers were very thin and were closely associated with the somas of most buccal neurons.

Each hemiganglion contained eight *acetylcholine*-immunoreactive neurons, two on the coelomic (caudal) surface, three in the commissural zone, and three on the buccal (rostral) surface (Fig. 1C). Acetylcholine-immunoreactive nerve terminals formed a dense plexus, evenly distributed throughout the neuropil. A large proportion of buccal neurons showed Ach-immunoreactive varicosities around their soma (Fig. 2C).

GABA-immunoreactive neurons consisted of a paired cluster on the caudal surface containing less than 10 re-

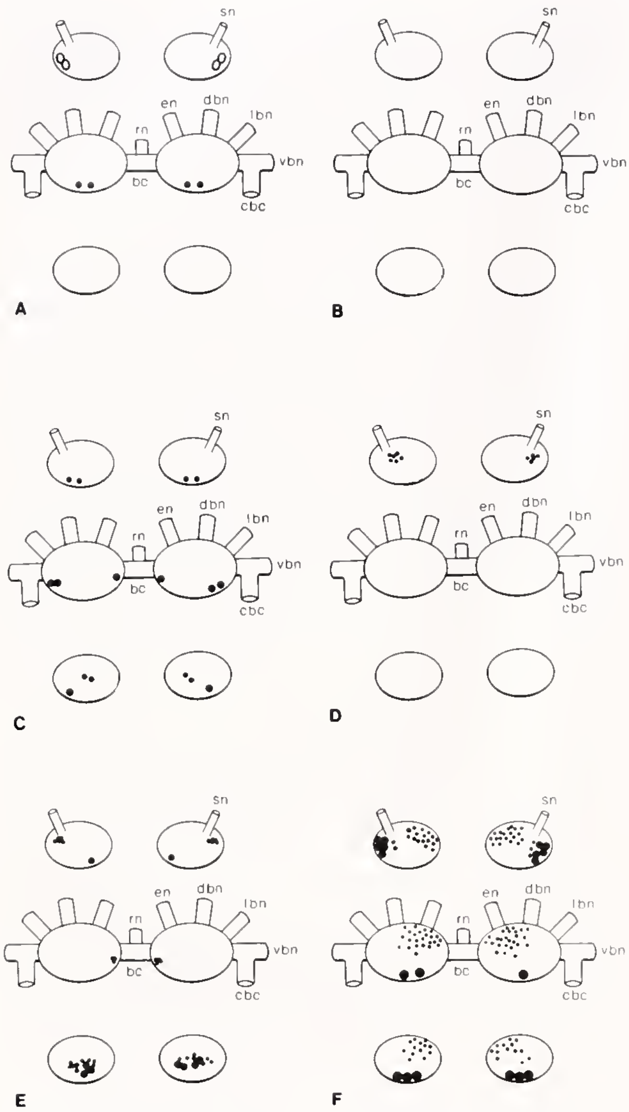

Figure 1. Schematic presentation of immunohistochemically identified neurons (black circles) in *Aplysia* buccal ganglion showing immunoreactivities for histamine (A), serotonin (B), acetylcholine (C), GABA (D), VIP (E), and FMRFamide (F). Open circles in A indicate the location of neurons B1 (lateral) and B2 (medial). Each set of three drawings summarizes the observations made in complete series through the ganglion. The top drawing represents the most caudal zone and the bottom drawing the most rostral zone. bc = buccal commissure, cbc = cerebral-buccal connective, dbn = dorsal buccal nerve, en = esophageal nerve, lbn = lateral buccal nerve, rn = radular nerve, sn = salivary nerve, vbn = ventral buccal nerve.

active cells per cluster (Fig. 1D). The GABA-immunoreactive neuropil consisted of fine, varicose fibers and terminals, and it was distributed throughout the neuropil region (Fig. 2D).

Each hemiganglion contained approximately 30 *VIP*-immunoreactive neurons (Fig. 1E). A single 100 μm cell and a cluster of small cells were located on the coelomic (caudal) surface. In the commissural zone, a group of a few small cells was located just ventral to the commissure. A larger group of VIP-immunoreactive cells was located on the buccal (rostral) surface. A VIP-immunoreactive fiber plexus was seen throughout the neuropil (Fig. 2E).

CCK-immunoreactivity was seen in 10–15 cells, most of which were located on the dorsal edge of the coelomic (caudal) surface. Two to three small cells were found on the rostral surface. A CCK-immunoreactive plexus was present throughout the neuropil (data not shown).

FMRFamide immunoreactivity was observed in a large number of cells throughout the ganglion, including most small neurons of the S-cluster and such identified neurons as B1 and B2 (Fig. 1F). FMRFamide-immunoreactive fibers formed a very dense plexus in all parts of the neuropil (Fig. 2F). This plexus was similar in appearance to, although considerably denser than, the histamine-immunoreactive plexus.

SCP_B-immunoreactive neurons were fewer in number than those showing reactivity for FMRFamide. Notably, neurons B1 and B2 were immunopositive. A dense $\mathrm{SCP_B}$-immunoreactive plexus extended throughout the neuropil (data not shown).

Cerebral ganglion. A total of 30–40 *histamine*-immunoreactive neurons were found in each hemiganglion. They consisted of a small cluster in the dorsal subsurface zone, a pair of 100 μm neurons and a cluster of small neurons in the frontal region, a large cluster including the neuron C2 in the lateral region in the commissural zone, and another large cluster on the ventral surface (Fig. 3A). Histamine-immunoreactive varicose fibers were distributed throughout the neuropil region.

Serotonin-immunoreactive neurons consisted of 20–30 cells in each hemiganglion (Fig. 3B). These include the neuron C1 and a cluster of smaller cells around it. Additional serotonin-immunoreactive neurons consisted of a large cluster in the central region of the dorsal surface and of 4–5 100 μm neurons in the posterior lobes. Serotonin-immunoreactive fibers were found in all parts of the neuropil.

Approximately 20 *acetylcholine*-immunoreactive neurons were found in each hemiganglion (Fig. 3C). They consisted mainly of two compact clusters: one in the lateral region, and the other in the rostral-medial region of the commissural zone. In addition, a few single cells were located on the ventral surface. The acetylcholine-immunoreactive fiber plexus was sparse, and it was located close to the two compact clusters.

The cerebral ganglion contained 15–20 *GABA*-immunoreactive neurons in each hemiganglion (Fig. 3D). These cells were small and formed two clusters, one in the lateral region and the other in the rostral region. The GABA-immunoreactive neuropil formed a dense plexus that extended from the lateral region around the neuron C2, to the frontal GABA-immunoreactive cluster and

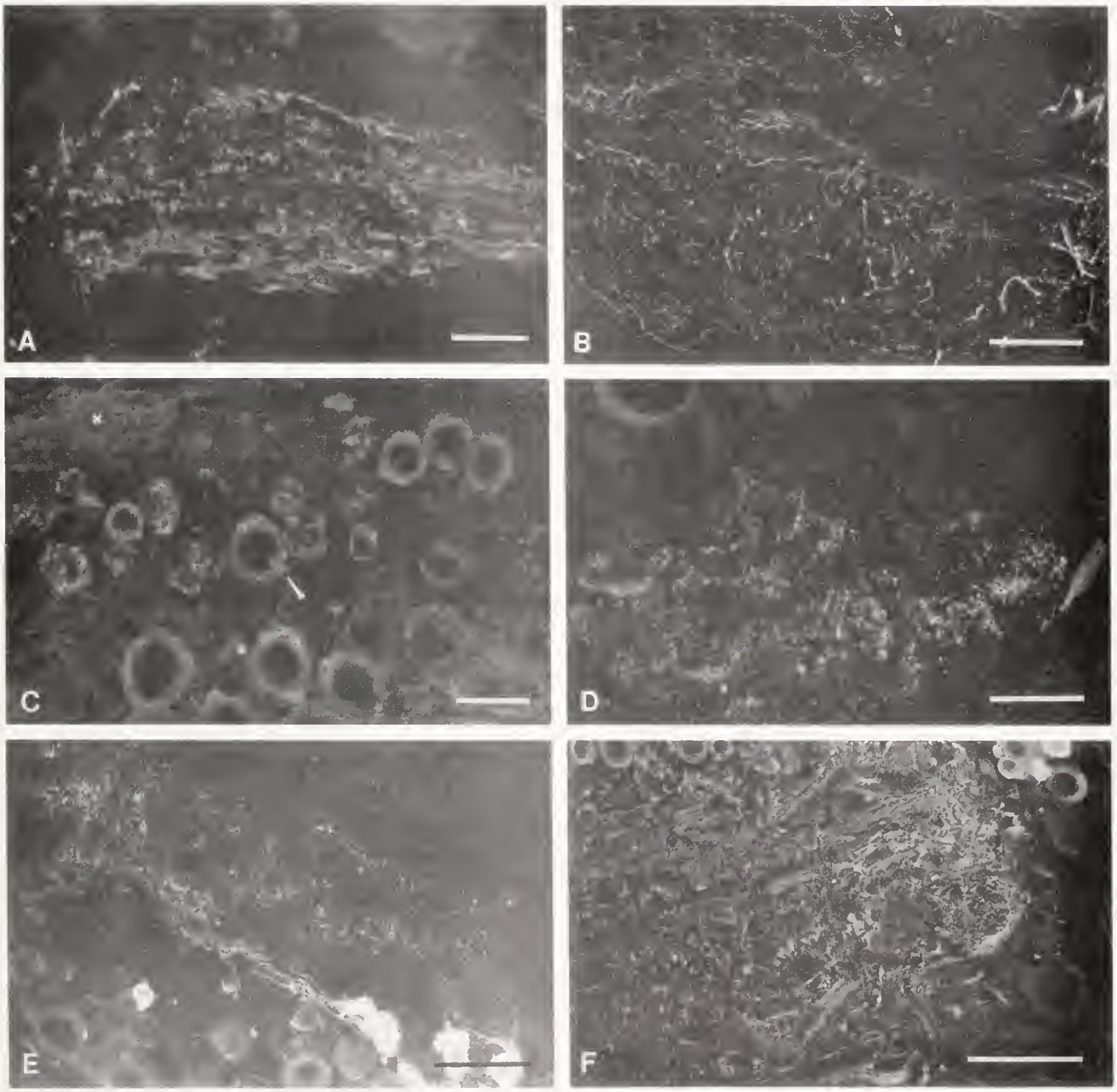

Figure 2. Photomicrographs of the neuropil region of *Aplysia* buccal ganglion showing immunoreactivity for histamine (A), serotonin (B), acetylcholine (C), GABA (D), VIP (E), and FMRFamide (F). Cross in C indicates immunoreactive neuropil and the arrowhead shows immunoreactive terminals around nonreactive neurons. Bar = 100 μm (A, D, E, F) or 50 μm (B, C).

further through the commissure to the same regions of the contralateral side. The other regions of the neuropil contained only few GABA-immunoreactive fibers.

Twenty to thirty neurons in each hemiganglion showed *VIP*-immunoreactivity (Fig. 3E): two large (200 μm) cells on the anterior edge, and some smaller solitary cells were found on the dorsal surface. The dorsal subsurface zone contained a large cell lateral to the outlet of the superior labial nerve and a few small cells on the medial and lateral edges. In the commissural zone, three large neurons were found in the anterior region, and small cells were scattered in the inner neuron rind. A cluster of four to seven neurons was located in the posterior region. The ventral surface contained several small VIP-reactive cells. A dense network of VIP-immunoreactive fibers was seen throughout the neuropil.

About 50 neurons showed immunoreactivity for *CCK*. Three large CCK-immunoreactive neurons were located along the dorsal edge of the ganglion. The other cells were small neurons along the inner neuronal rind. A dense CCK-immunoreactive plexus was present throughout the neuropil region (data not shown).

A large number of neurons showed immunoreactivity for *FMRFamide.* These cells were found in all parts of the ganglion and were especially numerous in the posterior region where several large neurons stained (Fig. 3F). The neuropil showed a dense FMRFamide-immunoreactive plexus.

Fewer neurons were immunoreactive for *SCP*$_B$ than for FMRFamide, but the staining revealed a dense plexus in all parts of the neuropil.

Abdominal ganglion. Histamine-immunoreactive neurons were found in three small clusters: one each on the lateral right and left margins of the dorsal subsurface zone, and a third one on the posterior edge of the ventral subsurface zone (Fig. 4A). A plexus of histamine-immunoreactive fibers was seen throughout the neuropil.

Serotonin-immunoreactivity was localized in several small neurons throughout the ganglion, but none of the large identified neurons showed immunoreactivity (Fig. 4B). All large neurons, including R2, R14, R15, L2-L7, and L10, received serotonin-immunoreactive innervation on their soma (Fig. 5A). Serotonin-immunoreactive fibers were diffusely distributed all over the neuropil region.

Of the large identified neurons, only L10 showed *acetylcholine* immunoreactivity; R2 was nonreactive (Fig. 4C). A cluster of relatively large (150 μm) neurons in the right caudal quadrant and several small neurons throughout the ganglion showed intense acetylcholine immunoreactivity. The neuropil showed an evenly distributed network of acetylcholine-immunoreactive fibers.

No *GABA*-immunoreactive neurons were seen in the abdominal ganglion, although the neuropil contained an extensive, widely distributed GABA-immunoreactive plexus (Fig. 4D).

Each hemiganglion contained 7–8 large *VIP*-immunoreactive neurons and four clusters of small cells (Fig. 4E). A VIP-immunoreactive plexus was found throughout the neuropil.

Several large *FMRFamide*-immunoreactive neurons were identified in the serial sections, such as R2, L2–L5

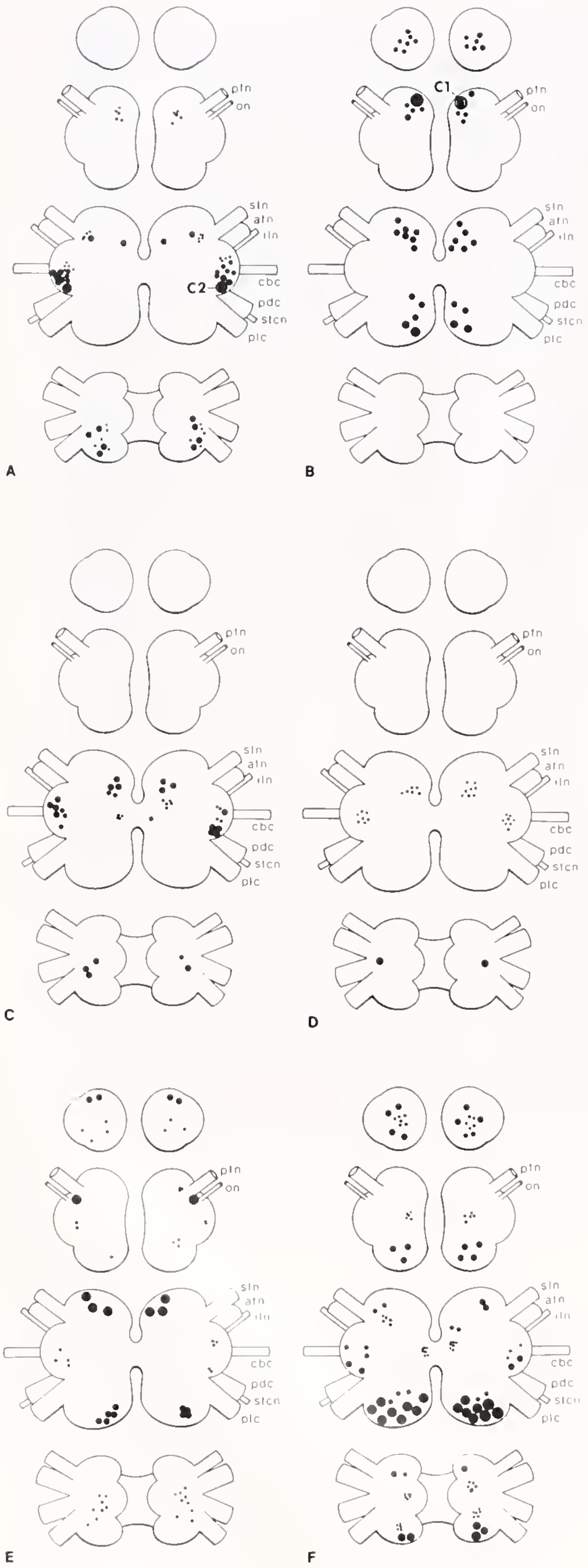

Figure 3. Schematic presentation of immunohistochemically identified neurons (black circles) in *Aplysia* cerebral ganglion showing immunoreactivities for histamine (A), serotonin (B), acetylcholine (C), GABA (D), VIP (E) and FMRFamide (F). Each set of four drawings summarizes the observations made of complete series through the ganglion. The top drawing represents the most dorsal zone, and the bottom drawing the most ventral zone. atn = anterior tentacular nerve, cbc = cerebral-buccal connective, iln = inferior labial nerve, on = optic nerve, pdc = cerebral-pedal connective, plc = cerebral-pleural connective, ptn = posterior tentacular nerve, sln = superior labial nerve, stcn = statocyst nerve.

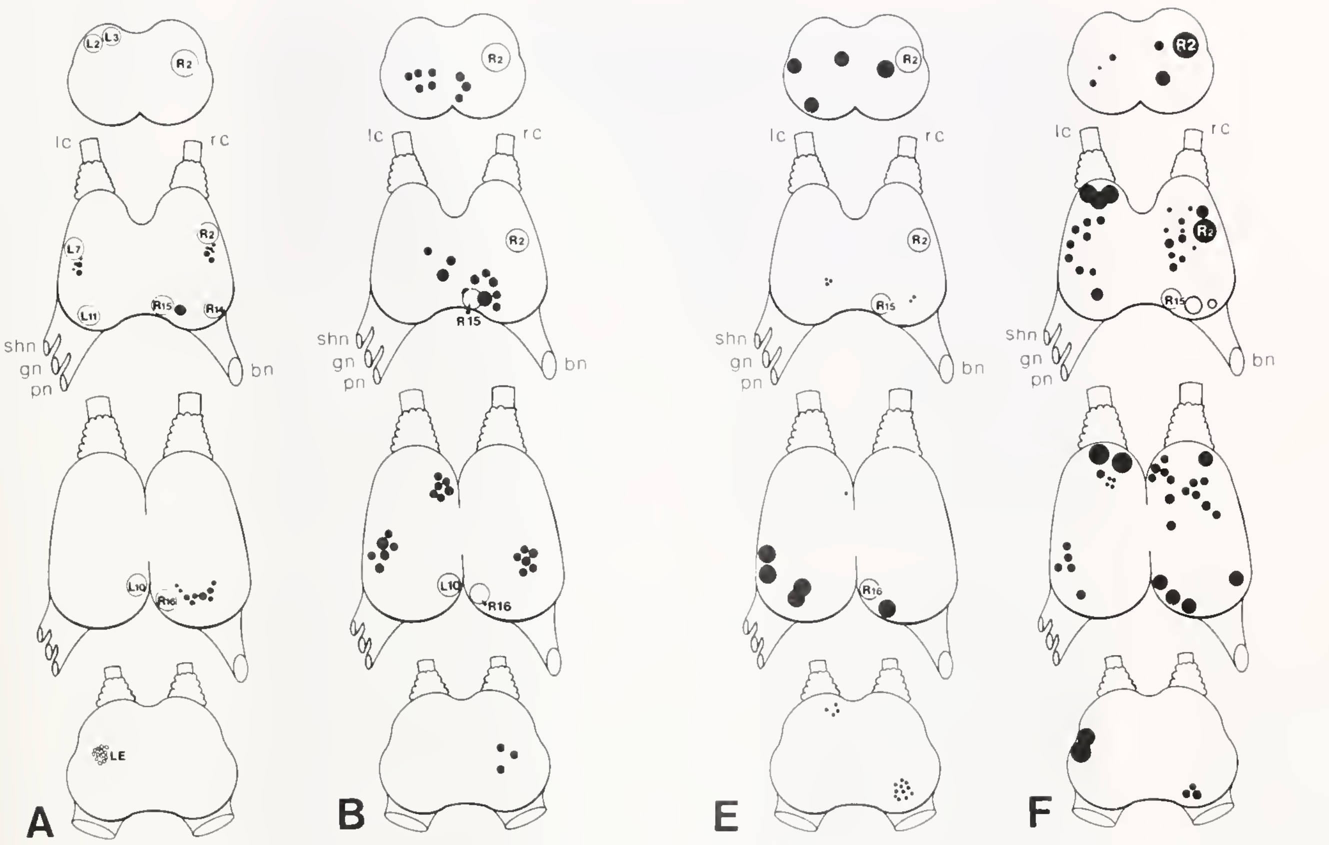

Figure 4. Schematic presentation of immunohistochemically identified neurons (black circles) in *Aplysia* abdominal ganglion showing immunoreactivities for histamine (A), serotonin (B), acetylcholine (C), GABA (D), VIP (E), and FMRFamide (F). Each set of four drawings summarizes the observations made of complete series through the ganglion. The top drawing represents the most dorsal zone, and the bottom drawing the most ventral zone. bn = branchial nerve, gn = genital nerve, lc = left connective, pn = pericardial nerve, rc = right connective, shn = siphon nerve.

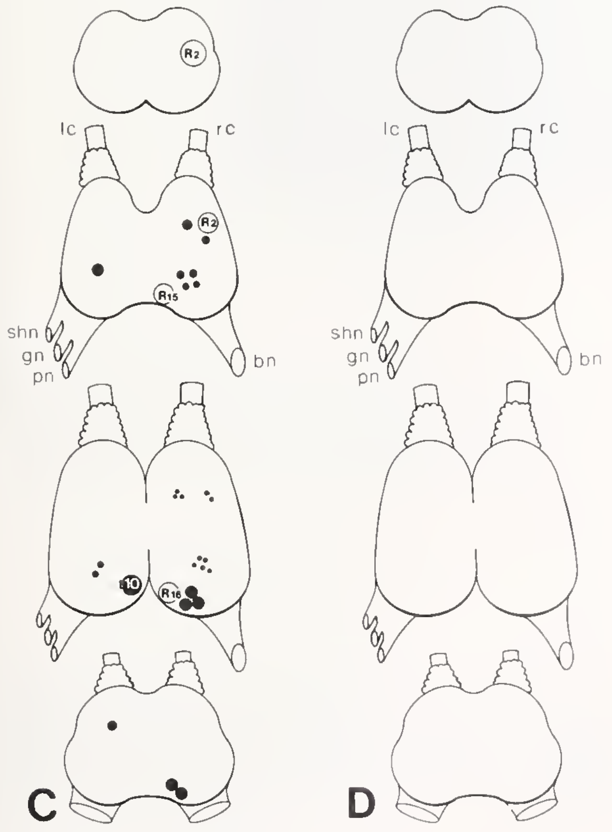

(Fig. 4F). R14 and R15, nonreactive themselves, received FMRFamide-immunoreactive innervation on their soma (Fig. 5B). In addition, a large number of unidentified neurons throughout the ganglion, and a very dense and extensive fiber network in the neuropil, showed FMRFamide-immunoreactivity.

SCP_B-immunoreactivity was distributed similarly to FMRFamide immunoreactivity. Thus, neurons R2 and L2–L5 were immunopositive, whereas R14 and R15 were nonreactive but received SCP_B-immunoreactive innervation on their soma.

Pedal and pleural ganglia. All antisera stained neurons and a uniformly distributed plexus of nerve fibers and terminals in the neuropil region of both ganglia. A few *histamine-, serotonin-, GABA-*, and *CCK*-immunoreactive neurons were dispersed throughout the neuronal rind of the pedal ganglion. The *acetylcholine*-immunoreactive neurons formed clusters on the rostral-medial and caudal-

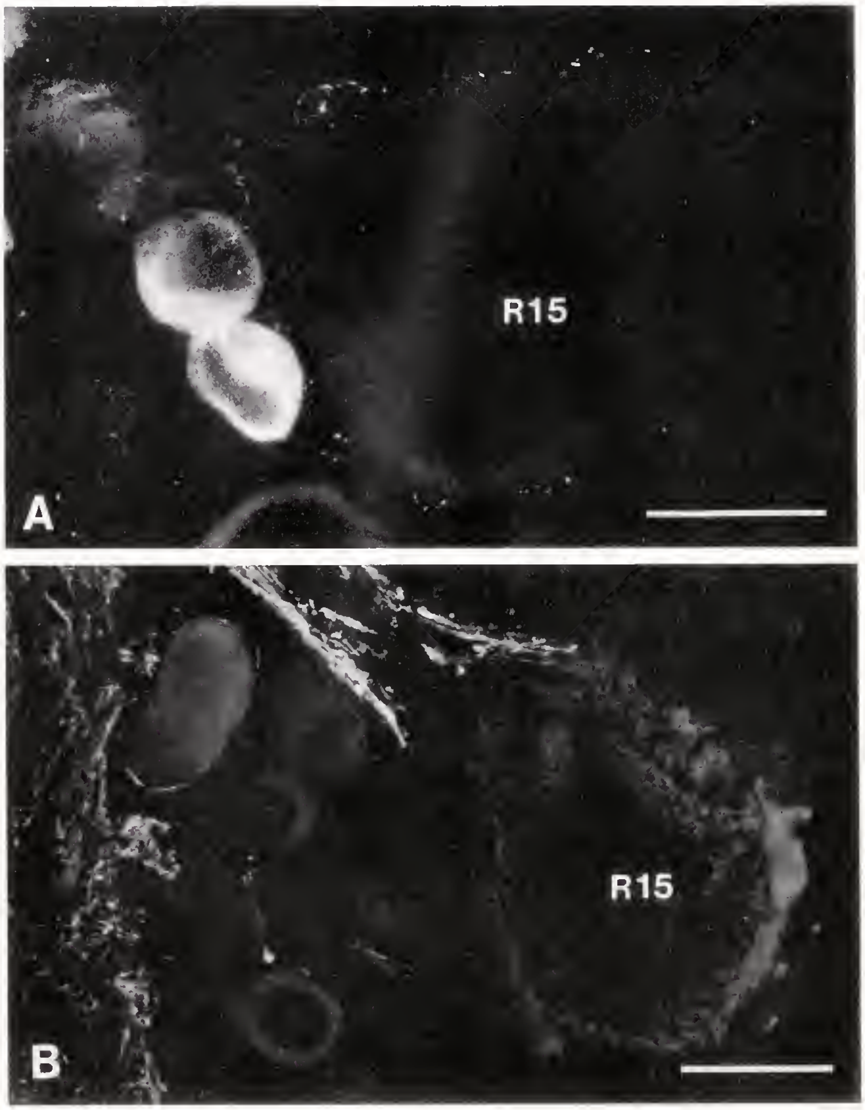

Figure 5. Neuron R15 of *Aplysia* abdominal ganglion. Serotonin- (A) and FMRFamide- (B) immunoreactive terminals surround intimately R15 soma (A) or its axon hillock region (B). Bar = 100 μm.

medial corners and on the caudal edge. The *VIP*-immunoreactive neurons were located mainly on the dorsomedial region. The number of FMRFamide- and SCP_B-immunoreactive neurons was greater than those for other stainings.

Back-injection of Aplysia *cerebral-buccal connective.* To examine the origin of the serotonin-containing innervation of the buccal neurons, the cerebral-buccal connective (CBC) was back-injected with cobalt chloride. Precipitation of cobalt-containing neurons in the cerebral ganglion revealed all cells that project into the CBC (Fig. 6). Distribution of the serotonin-immunoreactive neurons was obtained from serial sections (Fig. 3B). Comparison of the neuron populations revealed by the two techniques indicated that only one cell, the metacerebral giant cell (C1), stains with both methods. Serotonin immunoreactivity in cross-sections of the CBC was found in only one large axon profile. No serotonin-immunoreactive neurons were observed in the target tissues of the buccal ganglion, the esophagus, salivary gland, oral cavity mucosa, or the buccal muscles.

Mapping of neurotransmitters in Pleurobranchaea californica

Buccal ganglion. As in *Aplysia,* two large neurons on the dorsal surface showed *histamine* immunoreactivity. In addition, a cluster of about 10 small cells in each hemiganglion stained for histamine. All regions of the neuropil contained a very dense histamine-immunoreactive plexus

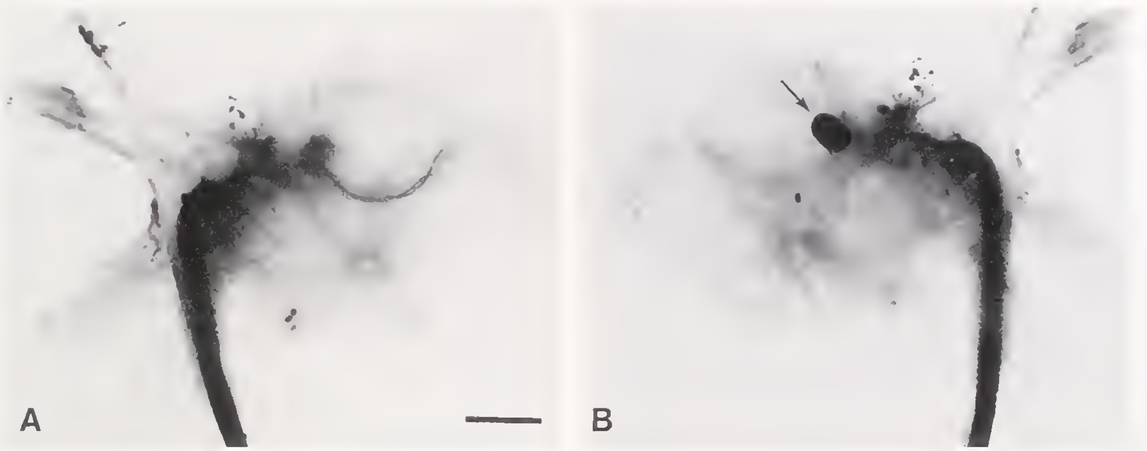

Figure 6. Whole *Aplysia* cerebral ganglion back-injected with cobalt chloride through the cerebral-buccal connective (black nerve trunk). A = ventral side, B = dorsal side. Arrow indicates neuron C1. Bar = 1 mm.

(Fig. 7A). In contrast to *Aplysia*, no *acetylcholine*-immunoreactivity was observed in this ganglion. A paired cell on the central coelomic (dorsal) surface and a cluster of small neurons on the buccal (ventral) surface showed immunoreactivity for *GABA* antiserum. A sparse GABA-immunoreactive plexus was present throughout the neuropil (Fig. 7B). Only two small clusters of *VIP*-immunoreactive cells were found in each hemiganglion. The ventral VIP-reactive cluster found in *Aplysia* was not present in *Pleurobranchaea*. VIP-immunoreactive plexus was present in the neuropil region. Several large (200–300 μm) *FMRFamide*- and *SCP$_B$*-immunoreactive neurons, including the neuron B1, were seen on the dorsal surface and on the posterior margin of the ganglion. The ventral surface contained a few immunoreactive neurons of varying size. Dense FMRFamide- and SCP$_B$-immunoreactive plexuses were present in all parts of the neuropil region (Fig. 7C).

Cerebral ganglion

Approximately 20 *histamine*-immunoreactive neurons were found in this ganglion, and they were distributed in all four zones. Histamine-immunoreactive fibers were seen in all parts of the neuropil. A few small *acetylcholine*-immunoreactive neurons were seen on the frontal lateral region of the dorsal surface. A distinct acetylcholine-immunoreactive plexus was present in a limited area close to the immunoreactive cells. Several small *GABA*-immunoreactive neurons were seen in the dorsal subsurface, commissural, and ventral surface zones located in a relatively narrow sector in the frontal part of the ganglion. A diffusely distributed GABA-immunoreactive fiber plexus was seen in the neuropil. Three clusters of small neurons, a pair of 50 μm neurons and a plexus in the neuropil showed *VIP* immunoreactivity. Many large (300 μm) and numerous smaller neurons scattered throughout the dorsal surface showed *FMRFamide*- and *SCPB*-immunoreactivity. On the ventral surface, several large neurons along the posterior margin, and two pairs of 150 μm cells in the frontal region, showed SCP$_B$ immunoreactivity. The neuropil contained a very dense plexus of both FMRFamide- and SCPB-immunoreactive fibers.

Pedal-pleural ganglion complex. Staining with antisera against *histamine, serotonin, acetylcholine, GABA*, and *VIP* revealed a few immunoreactive neurons and an immunoreactive plexus throughout the neuropil. *FMRFamide* antiserum stained a large number of neurons throughout the ganglion, whereas the *SCP$_B$* antiserum stained only two clusters. Both FMRFamide and SCP$_B$ antisera revealed a dense fiber plexus throughout the neuropil region.

Discussion

We report on the distribution of established neurotransmitters (histamine, serotonin, acetylcholine, GABA) and neuropeptides that are considered as putative neurotransmitters or -modulators (VIP, CCK, FMRFamide, SCP$_B$) in the nervous systems of *Aplysia* and *Pleurobranchaea*. We conclude, based on comparison of stained sets of cell bodies showing only little overlap, that the immunochemically identified neuronal populations represent largely separate pools. This conclusion is also supported by the observation that staining of the neuropil often exhibited a different pattern for different substances. Although examples of coexistence of a transmitter and neuropeptide have been described in individual *Aplysia* neurons (Brownstein *et al.*, 1974; Lloyd *et al.*, 1987; Ono, 1989; Cropper *et al.*, 1990), the present material indicates that there is no systematic colocalization of any two substances studied. With a few exceptions, we do not know

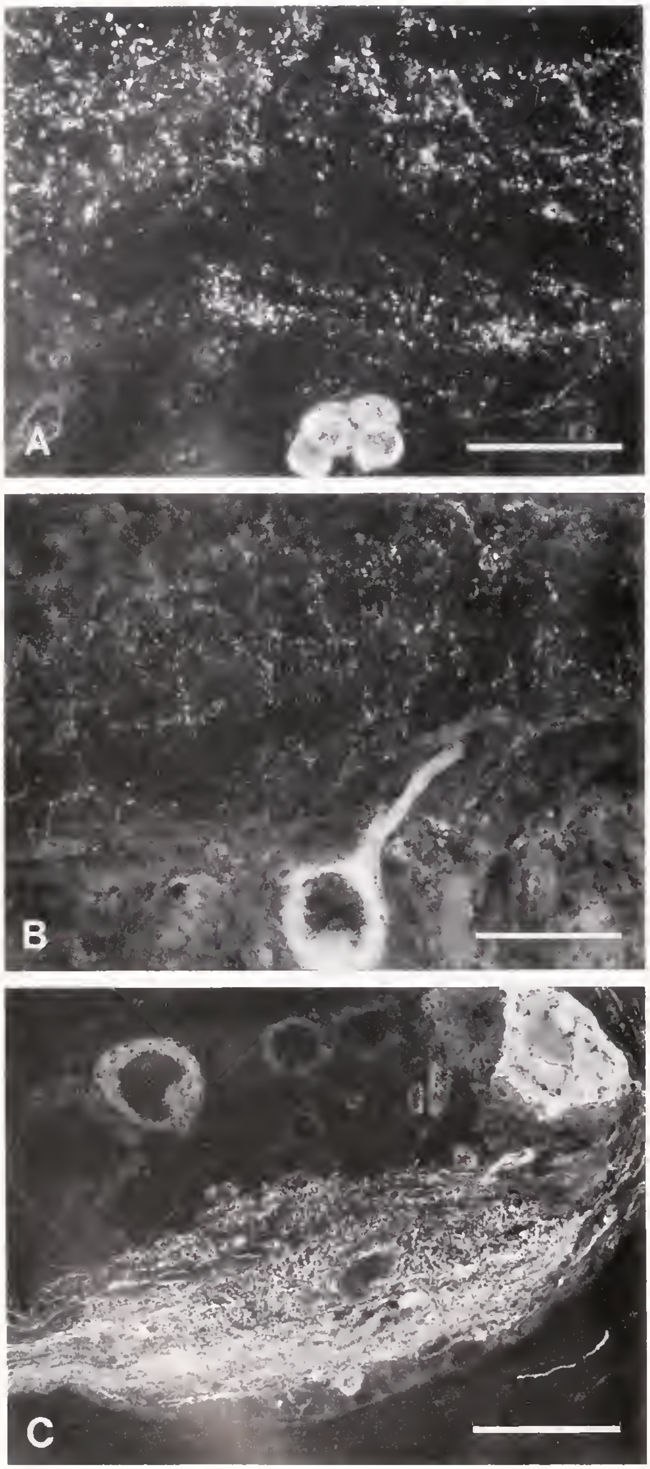

Figure 7. Photomicrographs of the neuropil region of *Pleurobranchaea* buccal ganglion showing immunoreactivity for histamine (A), GABA (B), and FMRFamide (C). Bar = 100 μm.

whether colocalization means corelease, or to what extent two colocalizing substances can be regulated independently. Consequently, the effect of transmitter colocalization on converging and diverging systems remains unknown.

Of the substances discussed here, histamine-, serotonin-, CCK-, FMRFamide- and SCP_B-immunoreactive neurons have been previously described in *Aplysia* ganglia (Ono and McCaman, 1984; Brown *et al.*, 1985; Kistler Jr. *et al.*, 1985; Longley and Longley, 1985; Ono, 1986; Lloyd *et al.*, 1987). In addition, identified molluscan neurons have been demonstrated to contain or use as transmitter histamine, acetylcholine, or GABA (*c.f.*, Leake and Walker, 1980). Our results, which are based on a complete series of sections, agree with the previous results largely obtained from whole ganglia. The use of serial sections has not only allowed us to study the distribution of stained nerve cell bodies, but also to examine transmitter-specific fiber systems both in the neuropil and around neuronal somata. Acetylcholine, which now has been localized immunohistochemically in a molluscan nervous system for the first time, is of particular importance in *Pleurobranchaea,* because the muscarinic cholinergic nervous system may be involved in associative learning in this species (Mpitsos *et al.*, 1988c).

Evaluation of the technique

The present study demonstrates that neurotransmitter systems in whole ganglia can be most effectively visualized and reconstructed through an examination of immunohistochemically stained, complete serial sections. In our study, reconstruction was performed manually and recorded on schematic drawings. For selected regions, this method can be supplemented by computer-assisted 3-dimensional analysis using commercially available programs. Serial sectioning offers the following advantages over whole-mount preparations: (1) uneven penetration of the reagents is largely avoided; (2) consecutive sections of the same ganglion can be used for double-staining or for controls with pre-immune serum; (3) better resolution of individual neurons and nerve terminals is obtained. In addition, the complete serial section technique allows regional analysis of the neuropil and visualization of somatic innervation of individual neurons, both features that have not been successfully revealed in whole-mounts. The main disadvantage of the current method is that it requires laborious reconstruction. Moreover, no single fixation method preserves the immunogenicity of all the substances studied, so staining of consecutive sections, each for a different transmitter, is often precluded. For example, histamine immunoreactivity is lost with formaldehyde fixation, serotonin immunoreactivity disappears even in low concentrations of glutaraldehyde, and peptide immunohistochemistry is superior in benzoquinone-fixed tissue. We have deliberately chosen the optimal fixation method for each substance. Another reason for staining complete series of sections for each substance is that some transmitter-specific cells or cell clusters are very small and might easily be missed if the series is not complete.

Although specificity of immunoreactions was confirmed by preabsorption with synthetic antigens, or in the case of small molecules (histamine, serotonin, acetylcholine, GABA), with corresponding conjugates, the reservation must be considered that immunoreactivity does not necessarily represent the presence of the substance against which the antiserum was raised. For example, closely related peptides and their precursor molecules, or totally unknown tissue components may cause false interpretations. This problem is inherent in all immunohistochemical techniques, and the findings should be confirmed with pharmacological and chemical techniques. However, the observed immunoreactivities are essential for directing further physiological tests of the proposed hypothesis.

Comparison with previously reported transmitter maps

We have described in detail the distribution of histamine-immunoreactive neurons of *Aplysia* and *Pleurobranchaea* in a previous study (Soinila *et al.*, 1989, 1990) which has recently been confirmed by others (Elste *et al.*, 1990). Both studies failed to detect histamine immunoreactivity in L32 neurons of the *Aplysia* abdominal ganglion. Lack of histamine uptake by L32 neurons (Elste *et al.*, 1990) supports our immunohistochemical finding. These cells have been considered to be histaminergic because the responses to their intracellular stimulation are mimicked by exogenous histamine and blocked by specific histamine antagonist (Kretz *et al.*, 1986). In explaining this discrepancy, the possibility must be considered that the target cells on L32 neurons also receive histaminergic innervation from other sources, the blocking of which would in some way inhibit the response to stimulation of L32 cells.

Our maps of serotonin-immunoreactive neurons are in accordance with those published previously (Ono and McCaman, 1984; Kistler *et al.*, 1985; Longley and Longley, 1985).

No previous mapping studies on ACh immunoreactivity in *Aplysia* or *Pleurobranchaea* ganglia have been published, although several individual cholinergic neurons have been described in *Aplysia* (Giller and Schwartz, 1971; McCaman and Dewhurst, 1970; Gardner, 1971; Cohen *et al.*, 1978; Ono, 1989). The current evidence supporting the cholinergic nature of certain identified *Aplysia* neurons comes along two lines (1) Choline acetyl-transferase activity and conversion of exogenous choline into acetylcholine have been reported in microdissected B2, B4, B5, B7, B13, R2, L10, L11, LP1 (McCaman and Dewhurst, 1970; Giller and Schwartz, 1970; Eisenstadt *et al.*, 1973; Lloyd *et al.*, 1985). Except for B2, these cells also contain endogenous ACh (McCaman *et al.*, 1973; Ono, 1986). In addition, evidence has been presented that L10 releases acetylcholine from its terminals (Koike *et al.*, 1974). (2) Electrophysiological responses of the target cells of B4, B5, B15, B16, and B13 of the *Aplysia* buccal ganglion can be simulated by exogenous ACh and reversibly inhibited by cholinergic blockers (Gardner, 1971; Cohen *et al.*, 1978; Ono, 1989).

We consistently found eight pairs of ACh-immunoreactive neurons in the buccal ganglion. One of the ACh-immunoreactive cells on the coelomic (caudal) surface (Fig. 1) locates identically to B13 (Ono, 1989). The location of the cell close to the commissure correlates closely to that of B4 (Gardner, 1971). Two cells were found on the buccal (rostral) surface at locations that correlate closely with those reported for B15 and B16 (Cohen *et al.*, 1978). In contrast, B2 did not stain, and no ACh immunoreactive cells were found in the region of B5 or B7. ACh immunoreactivity was also observed in several cells in the cerebral ganglion (Fig. 3). No cholinergic neurons have been physiologically characterized in this ganglion, although it contains choline acetyltransferase at levels comparable to those found in the buccal and abdominal ganglia (McCaman and Dewhurst, 1970). We found several small cholinergic neurons in the *Aplysia* abdominal ganglion (Fig. 4C), but only one of the three previously reported large neurons claimed to be cholinergic stained with our antiserum. ACh immunoreactivity of L10 was confirmed by electrophysiological recording and subsequent Lucifer Yellow injection. We also found a relatively large neuron in the dorsal-caudal region, possibly L11. In contrast, R2, which was readily identified in sections without Lucifer Yellow injection, was consistently nonreactive. Likewise, the left pleural giant neuron LP1, a proposed homologue of R2, did not stain for ACh antiserum.

The following factors must be considered in explaining the discrepancies described above. (1) Although exogenous choline injected into the cell is converted into ACh by L10 and R2 (Koike *et al.*, 1972, 1974), under physiological conditions most ACh synthesis in these and other cholinergic cells may occur in the terminals. Indeed, the cell bodies of R2, L10, and L11 synthesize only minute amounts of ACh when incubated in the presence of excess exogenous choline (Eisenstadt *et al.*, 1973). (2) Contamination of microdissected neurons by nearby unidentified cholinergic cells may affect ACh measurements from single cells, as discussed previously by Giller and Schwartz (1971). In fact, we often found small ACh-immunoreactive cells close to R2 (Fig. 4C). (3) Simulation and blocking of the electrophysiological responses to stimulated, identified neurons as a sole method of transmitter identification must be interpreted with caution, as demonstrated for L32 cluster (Elste *et al.*, 1990; Soinila *et al.*, 1990). Because systematic correlation of histochemistry to electrophysiology was not the aim of this study, the conclusion that, so far, only L10 identifies as cholinergic with chemical, histochemical, physiological, and pharmacological criteria is only preliminary and subject to extensive reinvestigation (Soinila and Mpitsos, in prep.). In conclusion, after confirming the specificity of our method by comparing the ACh staining with that produced by an antiserum against glutarylated carrier protein, we believe that the cells stained by our method are cholinergic, although the possibility cannot be excluded that the sensitivity of the method may limit visualization of neurons containing very low ACh concentrations. Notwithstanding this reservation, we consider the method useful for the purpose of the present study; *i.e.*, to map the distribution of ACh containing neurons and nerve fibers.

The distribution of GABA-immunoreactive neurons has not previously been studied in either *Aplysia* or *Pleurobranchaea*. Our findings, together with previous reports on the presence of GABA receptors in *Aplysia* neurons (Yarowsky and Carpenter, 1978; King and Carpenter, 1987), support the notion that GABA is a neurotransmitter in these species.

Although VIP-immunoreactive neurons have been described in other mollusks (Osborne, 1984), they had not previously been sought in either *Aplysia* or *Pleurobranchaea*.

Our results agree with those of other investigators on the distribution of immunoreactivities for CCK (Ono, 1986), FMRFamide, and SCP_B (Brown *et al.*, 1985; Lloyd *et al.*, 1987).

Evidence for diverging projection of transmitter systems in the buccal ganglia

In the buccal ganglia, immunostaining with each antiserum revealed a plexus of varicose fibers in the neuropil region. Although there were marked differences in the densities of the transmitter-specific plexuses, each plexus was observed throughout the depth of the neuropil. The diffuse, rather than regionally specific, distribution suggests that each system affects a large number of target neurons. In the case of histamine, serotonin, GABA, FMRFamide, and SCP_B, the immunostained plexus is so dense that most, or perhaps all, ganglionic neurons could be contacted by these plexuses.

On the other hand, our observations suggest that the source of each transmitter system is limited to a relatively small number of neurons. In both *Aplysia* and *Pleurobranchaea*, the potential sources of buccal neuropil include the buccal ganglion neurons themselves and those cerebral ganglion neurons that project into the buccal ganglia. Reconstruction of serial sections allowed us to estimate the number of stained neurons in both ganglia. Accordingly, the number of immunoreactive neurons in the *Aplysia* buccal ganglion was two for histamine, none for serotonin, eight for acetylcholine, less than 10 for GABA, about 10 for CCK, and about 30 for VIP. The cerebral ganglion contained 20–30 histamine-immunoreactive neurons, 20–30 serotonin-immunoreactive neurons, about 20 acetylcholine-immunoreactive neurons, 15–20 GABA-immunoreactive neurons, about 50 CCK-immunoreactive neurons, 20–30 VIP-immunoreactive neurons, and a large number of FMRFamide- and SCP_B-immunoreactive neurons. As revealed by cobalt back-injection technique, only about 40 cerebral neurons project into the buccal ganglion. In this study, however, the distribution of any immunostained set of neurons overlapped only partly with the distribution of cobalt-labeled neurons. Therefore, maybe fewer than 40 of any set of transmitter-specific cerebral neurons project into the buccal ganglion.

As for possible peripheral sources, *Aplysia* contains no ganglia between the buccal ganglion and its target tissues, and the stomatogastric ganglion of *Pleurobranchaea* is tiny and can therefore be neglected in the present discussion. In both species, some target tissues, such as the esophagus, contain a few intramural neurons. These neurons might send their axons to the buccal ganglion, but their number is small, and their possible contribution in the buccal neuropil is negligible.

Based on these estimations, we propose that, for each transmitter system, a set of relatively few neurons gives rise to a dense plexus of terminals distributed diffusely throughout the buccal neuropil. This implies that each neuron branches extensively and contacts many target neurons; *i.e.*, it shows anatomical divergence.

Cerebral neuron C1 as a source of diverging innervation

C1 is a known serotonergic neuron showing extensive divergence (Schwartz and Skolnik, 1981), so we examined how much of the serotonergic innervation in the buccal ganglion originates from this particular cell. The buccal neuropil contained an extensive serotonin-immunoreactive plexus and most buccal neurons received serotonin-immunoreactive terminals on their somas. Because the buccal ganglion contains no serotonin-immunoreactive neurons, the serotonin-immunoreactive terminals must originate in neurons outside the buccal ganglion. We did not observe any peripheral serotonin neurons, therefore we anticipated this innervation to come from the cerebral ganglion. A comparison of cerebral ganglia that had been back-injected through the cerebro-buccal connectives with ganglia that had been immunostained with serotonin antiserum and reconstructed allowed us to determine which of the cerebral serotonin-immunoreactive neurons could contribute to the buccal neuropil and, indeed, indicated that the neuron C1 is the only neuron revealed by both techniques. The possibility that C1 is the sole source of buccal serotonin innervation was substantiated by the observation that serotonin antiserum stains in cross-sections of the CBC only one, large axonal profile.

Evidence for converging innervation in the buccal ganglion

All of the antisera studied stained the buccal neuropil extensively and without regional specificity. We therefore propose that any given buccal neuron is innervated by many different transmitter systems; *i.e.*, innervation from many different sources converges on the same target neurons.

Some of the substances we studied, notably the neuropeptides FMRFamide, SCP_B, VIP, and CCK, may be colocalized in the same terminals with one of the classical transmitters: histamine, acetylcholine, serotonin, or GABA (Lloyd *et al.*, 1987; Ono, 1989). Although this may be the case for selected cells, the distributions of immunostained neurons on the whole showed distinct patterns, indicating that colocalization of any two substances in molluscan ganglia is not complete. This strongly suggests that the multiple immunoreactivities reported in this study represent truly multiple innervation.

Potential models of convergence in identified neurons

Several physiologically identified neurons can be recognized in histological sections due to their size and location, including C1 of the cerebral ganglion and R2 of the abdominal ganglion. Furthermore, our preliminary studies indicate that neurons R15 and R16 are identifiable on their morphological characteristics alone. Some previously physiologically identified neurons, such as the histaminergic neuron C2, can be identified in sections due to its transmitter content (Soinila *et al.*, 1990). Our survey suggests that R15 is a potentially useful model with which to study convergence of innervation at the level of a single neuron; *i.e.*, we observed somatic connections on R15 by serotonin-, FMRFamide-, and SCP_B-immunoreactive terminals. In addition, studies by other investigators indicate that R15 is innervated by acetylcholine-, GABA-, and dopamine-containing neurons (Leake and Walker, 1980). Other candidates for multi-innervated neurons include C1, which is innervated by FMRFamide-immunoreactive terminals, as well as by histamine-immunoreactive terminals (Ono and McCaman, 1980), and C2, which receives innervation by GABA- and FMRFamide-containing terminals.

Other ganglia

The distribution of transmitter-specific systems in all ganglia had as a common feature that a relatively small number of neurons seems to give rise to an extensive plexus of fibers. These plexuses (with the exception of GABA- and acetylcholine-immunoreactive ones in the cerebral ganglion) do not show regional specificity in their projection. Although our evidence on divergence and convergence of innervation was obtained mainly in the buccal ganglion, anatomical similarities in distribution patterns suggest that these properties will be common for other ganglia as well.

Conclusions

In the present study, divergence and convergence were anatomically demonstrated in individual identifiable neurons. For whole ganglia, the evidence for divergence is indirect and comes from the observation that the number of contributing neurons is small in comparison to the extent of contacts each system seems to make. Because our material consisted of complete serial sections, the number of immunoreactive neurons can be reliably estimated. We stipulate that additional neurons may contain these substances in levels too low to be detected immunohistochemically. In some systems, evidence has been reported that transmitter or neuropeptide concentration in the neuronal soma is considerably lower than that in the corresponding terminals (Storm-Mathiessen and Ottersen, 1986). However, our assumption on divergence seems reasonable because the stained neurons, except for FMRFamide-immunoreactive ones, represent only a fraction of the total ganglionic neuron population.

Our conclusion on divergence is based on two assumptions: (1) that the density of varicose terminals correlates with the extent of innervation; and (2) that lack of regional specificity in the distribution of terminals indicates that most, if not all, ganglionic neurons are targets of that particular system. The first assumption can be made because, in a wide variety of species, chemical synapses are located in terminal boutons that are visualized as varicosities at the light microscopic level. In the present material, the number of fibers is clearly correlated with the number of varicosities. The second assumption rests on the argument that, if diffusely distributed terminals contact only specific target neurons, there should be a precise recognition mechanism guiding the right innervation to the right targets during the ontogeny. Also, in such systems, the circuits must be strictly isolated electrically and protected against the diffusion of transmitters from nearby terminals. The ultrastructure of the molluscan neuropil is incompletely described, so such a possibility cannot be excluded.

Our conclusion about the convergence of innervation in whole ganglia is based on the deduction that the more extensively several systems diverge, the more probable that any given neuron receives multiple innervation. Although we have presented evidence that neurons receive innervation by several transmitter systems, we cannot be sure that all these contacts are functional. Previous studies suggest, however, that electrophysiological convergence and divergence occur commonly in the nervous systems of both *Aplysia* (Kandel and Tauc, 1968; Kandel and Wachtel, 1975; Shimara and Tauc, 1975) and *Pleurobranchaea* (Mpitsos and Cohan, 1986b). In future studies, transmitter histochemistry should be accompanied by corresponding receptor mapping, to determine whether a particular transmitter-specific neuron would be capable of responding to multiple inputs, and further by electrophysiological demonstration of the corresponding response. While selective projections might occur in extensively overlapping fields, as shown, for example, in Figure 2, we hypothesize that the tangle of fibers converging to the same area may not be motor specific. Thus, whereas specific, distributed convergence poses difficulties in genetic encoding or developmental expression, the possibility of nonspecific projection poses difficulties for demonstrating how behavior specific activity emerges appropriately.

Broader implications

The findings presented here are consistent with our previous studies indicating that neural systems, just as other adaptive systems, self-organize their activity by distributed, often error-prone action (Mpitsos and Cohan, 1986a, b; Burton and Mpitsos, 1991). "Neurocircuits" and the units that comprise them may have "fuzzy" functional characteristics (Zedah, 1965; Mpitsos, 1989) rather than exact, reliably identifiable ones. To be sure, one cannot deny the extensive evidence showing that relatively fixed action does occur, although we also believe that many instances of variability have been overlooked. From a broader analogy, as Newtonian physics has difficulty in growing into statistical mechanics, so classical definitions of response-specific neurocircuits have difficulty in accounting for flexible neural function. Nonetheless, theories that account for flexible action must also account for instances in which flexibility is not observed. This is to say that a general solution to the problem must also provide evidence for the more special case.

Acknowledgments

This work was supported by AFOSR 89-0262 to GJM, a grant from the Finnish Cultural Foundation to SS, and a grant from Markham Foundation, Oregon State University. The authors thank Prof. Lavern Weber for his encouragement and for making the Mark O. Hatfield Marine Science Center Facilities available to them.

Literature Cited

Albers, R. T., S.-Y. Liou, E. G. Stopa, and R. T. Zoeller. 1991. Interaction of colocalized neuropeptides: functional significance in circadian timing system. *J. Neurosci.* **11:** 846–851.

Brown, R. O., D. Gusman, A. Basbaum, and E. Mayeri. 1985. Identification of *Aplysia* neurons containing immunoreactive FMRFamide. *Neuropeptides* **6:** 517–526.

Brownstein, M. J., J. M. Saavedra, J. Axelrod, G. H. Zeman, and D. O. Carpenter. 1974. Coexistence of several putative neurotransmitters in single identified neurons in *Aplysia. Proc. Natl. Acad. Sci. USA* **71:** 4662–4665.

Burton, R. M., and G. J. Mpitsos. 1991. Event-dependent control of noise enhances learning in neural networks. *Neural Networks*, in press.

Chay, T. R. 1985. Chaos in a three-variable model of an excitable cell. *Physica* **16D:** 233–242.

Cohan, C. S. 1980. Centralized control of distributed motor networks in *Pleurobranchaea californica.* Ph.D. Dissertation, Case Western Reserve University.

Cohan, C. S., and G. J. Mpitsos. 1983a. The generation of rhythmic activity in a distributed motor system. *J. Exp. Biol.* **102:** 25–42.

Cohan, C. S., and G. J. Mpitsos. 1983b. Selective recruitment of interganglionic interneurons during different motor patterns in *Pleurobranchaea. J. Exp. Biol.* **102:** 43–58.

Cohen, J. L., K. R. Weiss, and I. Kupfermann. 1978. Motor control of buccal muscles in *Aplysia. J. Neurophysiol.* **41:** 157–179.

Cropper, E. C., M. W. Miller, F. S. Vilim, R. Tenenbaum, I. Kupfermann, and K. R. Weiss. 1990. Buccalin is present in the cholinergic neuron B16 of *Aplysia*, and it depresses ARC muscle contractions evoked by stimulation of B16. *Brain Res.* **512:** 175–179.

Dickenson, P. S., and E. Marder. 1989. Peptidergic modulation of a multioscillator system in the lobster. I. Activation of the cardiac sac motor pattern by neuropeptides and red pigment-concentrating hormone. *J. Neurophysiol.* **51:** 833–844.

Dickenson, P. S., C. Mecsas, and E. Marder. 1990. Neuropeptide fusion of 2 motor pattern generator circuits. *Nature* **344:** 155–158.

Eisenstadt, M., J. E. Goldman, E. R. Kandel, H. Koike, J. Koester, and J. H. Schwartz. 1973. Intrasomatic injection of radioactive precursors for studying transmitter synthesis in identified neurons of *Aplysia californica. Proc. Nat. Acad. Sci. USA* **70:** 3371–3375.

Elste, A., J. Koester, E. Shapiro, P. Panula, and J. H. Schwartz. 1990. Identification of histaminergic neurons in *Aplysia. J. Neurophysiol.* **64:** 736–744.

Gardner, D. 1971. Bilateral symmetry and interneuronal organization in the buccal ganglia of *Aplysia Science* **173:** 550–553.

Giller, E., and J. H. Schwartz. 1971. Choline acetyltransferase in identified neurons of abdominal ganglion of *Aplysia californica. J. Neurophysiol.* **34:** 93–107.

Kandel, E. R., and L. Tauc. 1965. Heterosynaptic facilitation in neurones of the abdominal ganglion of *Aplysia depilans. J Physiol.* **181:** 1–27.

Kandel, E. R., and H. Wachtel. 1968. The functional organization of neural aggregates in *Aplysia.* Pp. 17–65 in *Physiological and Biomedical Aspects of Nervous Integration*, F. D. Carlson, ed. Prentice Hall, Englewood Hills.

Kandel, E. R. 1979. *Behavioral Biology of Aplysia* Freeman and Co., San Francisco.

Kempf, S. C., B. Masinowsky, and A. O. D. Willows. 1987. A simple neuronal system characterized by a monoclonal antibody to SCP in embryos and larvae of *Tritonia diomedea* (Gastropoda, Nudibranchia). *J Neurobiol.* **18:** 217–236.

King, W. M., and D. O. Carpenter. 1987. Distinct GABA and glutamate receptors may share a common channel in *Aplysia* neurons. *Neurosci. Lett.* **82:** 343–348.

Kistler Jr., H. B., R. D. Hawkins, H. W. Koester, W. M. Steinbusch, E. R. Kandel, and J. H. Schwartz. 1985. Distribution of serotonin-immunoreactive cell bodies and processes in the abdominal ganglion of mature *Aplysia. J. Neurosci.* **5:** 72–80.

Koike, H., M. Eisenstadt, and J. H. Schwartz. 1972. Axonal transport of newly synthesized acetylcholine in an identified neuron of *Aplysia. Brain Res.* **37:** 152–159.

Koike, H., E. R. Kandel, and J. H. Schwartz. 1974. Synaptic release of radioactivity after intrasomatic injection of choline-^{3}H into an identified cholinergic interneuron in abdominal ganglion of *Aplysia californica. J. Neurophysiol.* **37:** 815–827.

Kretz, R., E. Shapiro, C. A. Bailey, M. Chen, and E. R. Kandel. 1986. Presynaptic inhibition produced by an identified presynaptic inhibitory neuron. II. Presynaptic conductance changes caused by histamine. *J. Neurophysiol.* **55:** 131–146.

Leake, L. D., and R. J. Walker, 1980. *Invertebrate Neuropharmacology.* John Wiley & Sons, New York.

Leonard, J. L., M. Martinez-Padron, J. P. Edstrom, and K. Lukowiak. 1990. Does altering identified gill motor neuron activity alter gill behavior in *Aplysia?* North Holland Publishing Co., Amsterdam.

Lloyd, P. E., A. C. Mahon, I. Kupfermann, J. L. Cohen, R. H. Scheller, and K. R. Weiss. 1985. Biochemical and immunocytological localization of molluscan small cardioactive peptides in the nervous system of *Aplysia californica. J. Neurosci.* **5:** 1851–1861.

Lloyd, P. E., M. Frankfurt, P. Stevens, I. Kupfermann, and K. R. Weiss. 1987. Biochemical and immunocytological localization of the neuropeptides FMRFamide SCP$_A$, SCP$_B$, to neurons involved in the regulation of feeding in *Aplysia. J. Neurosci.* **7:** 1123–1132.

Longley, R. D., and A. J. Longley, 1985. Serotonin immunoreactivity of neurons in the gastropod *Aplysia californica. J. Neurobiol.* **17:** 339–358.

Marder, E. 1984. Mechanisms underlying neurotransmitter modulation of a neuronal circuit. *Trends Neurosci.* **7:** 48–53.

Marder, E. 1988. Pattern generators: modulating a neuronal network. *Nature* **335:** 296–297.

McCaman, R. E., and S. A. Dewhurst. 1970. Choline acetyltransferase in individual neurons of *Aplysia californica. J. Neurochem.* **17:** 1421–1426.

McCaman, R. E., D. Weinreich, and H. Borys. 1973. Endogenous levels of acetylcholine and choline in individual neurons of *Aplysia. J Neurochem.* **21:** 473–476.

Mpitsos, G. J. 1989. Chaos in brain function and the problem of nonstationarity: a commentary. Pp. 521–535 in *Dynamics of Sensory and Cognitive Processing by the Brain,* E. Basar, and T. H. Bullock, eds. Springer-Verlag, New York.

Mpitsos, G. J., and C. S. Cohan. 1986a. Comparison of differential Pavlovian conditioning in whole animals and physiological preparations of *Pleurobranchaea:* implications of motor pattern variability. *J. Neurobiol.* **17:** 498–516.

Mpitsos, G. J., and C. S. Cohan. 1986b. Convergence in a distributed motor system: parallel processing and self-organization. *J. Neurobiol.* **17:** 517–545.

Mpitsos, G. J., and K. Lukowiak. 1985. Learning in gastropod mollusks. Pp. 95–267 in *The Mollusca,* A. O. D. Willows, ed. Academic Press, New York.

Mpitsos, G. J., R. M. Burton, H. C. Creech, and S. O. Soinila. 1988a. Evidence for chaos in spike trains of neurons that generate rhythmic motor patterns. *Brain Res. Bull.* **21:** 529–538.

Mpitsos, G. J., H. C. Creech, C. S. Cohan, and M. Mendleson. 1988b. Variability and chaos: neurointegrative principles in self-organization of motor patterns. Pp. 162–190 in *Dynamic Patterns in Complex Systems,* J. A. S. Kelso, A. J. Mandell, and M. F. Shlesinger, eds. World Scientific, Singapore.

Mpitsos, G. J., T. F. Murray, H. C. Creech, and D. L. Barker. 1988c. Muscarinic antagonist enhances one-trial food-aversion learning in *Pleurobranchaea. Brain Res. Bull.* **21:** 169–179.

Ono, J. K. 1986. Localization and identification of neurons with cholecystokinin and gastrin-like immunoreactivity in whole-mounts of *Aplysia* ganglia. *Neuroscience* **18:** 957–974.

Ono, J. K. 1989. Synaptic connections in the buccal ganglia of *Aplysia* mediated by an identified neuron containing a CCK/gastrin-like peptide co-localized with acetylcholine. *Brain Res.* **493:** 212–224.

Ono, J. K., and R. E. McCaman. 1980. Identification of additional histaminergic neurons in *Aplysia:* improvement of single cell isolation techniques for in tandem physiological and chemical studies. *Neuroscience* **5:** 835–840.

Ono, J. K., and R. E. McCaman. 1984. Immunocytochemical localization and direct assay of serotonin-containing neurons in *Aplysia. Neuroscience* **11:** 549–560.

Osborne, N. N. 1984. Putative neurotransmitters and their coexistence in gastropod mollusks. Pp. 395–409 in *Coexistence of Neuroactive Substances in Neurons,* Chan-Palay, V. and S. Palay, eds. John Wiley & Sons, New York.

Panula, P., O. Häppölä, M. S. Airaksinen, S. Auvinen, and A. Virkamäki. 1988. Carbodiimide as a tissue fixative in histamine immunohistochemistry and its application in developmental neurobiology. *J. Histochem. Cytochem.* **36:** 259–269.

Rathouz, M. M., and M. D. Kirk. 1988. Localization of catecholamines in the buccal ganglion of *Aplysia californica. Brain Res.* **458:** 170–175.

Rosen, S. C., K. R. Weiss, R. S. Goldstein, and I. Kupfermann. 1989. The role of a modulatory neuron in feeding and satiation in *Aplysia:* effects of lesioning of the serotonergic metacerebral cells. *J. Neurosci.* **9:** 1562–1578.

Schwartz, J. H., and L. J. Skolnik. 1981. The giant serotonergic neurons of *Aplysia:* a multi-targeted nerve cell. *J. Neurosci.* **1:** 606–619.

Shimara, T., and L. Tauc. 1975. Multiple interneuronal afferents to the giant cells in *Aplysia J. Physiol.* **247:** 299–319.

Soinila, S., G. J. Mpitsos, and P. Panula. 1989. Immunohistochemical and behavioral evidence for sensory function of histamine in molluscan nervous system. *Soc. Neurosci. Abstr* **15:** 235.

Soinila, S., G. J. Mpitsos, and P. Panula. 1990. Comparative study of histamine immunoreactivity in nervous systems of *Aplysia* and *Pleurobranchaea. J. Comp. Neurol.* **298:** 358–369.

Steinbusch, H. W. M., A. A. J. Verhofstad, and H. W. J. Joosten. 1978. Localization of serotonin in the central nervous system by immunohistochemistry: description of a specific and sensitive technique and some applications. *Neuroscience* **3:** 811–819.

Storm-Mathiessen, J., and O.-P. Ottersen, 1986. Antibodies against amino acid neurotransmitters. Pp. 107–136 in *Neurohistochemistry, Modern Methods and Applications,* P. Panula, H. Päivärinta, and S. Soinila, eds. Alan R. Liss, New York.

Weiss, K. R., H. J. Chiel, and I. Kupfermann. 1986a. Sensory function and gating of histaminergic neuron C" in *Aplysia. J. Neurosci.* **6:** 2416–2426.

Weiss, K. R., E. Shapiro, and I. Kupfermann. 1986b. Modulatory synaptic actions of an identified histaminergic neuron on the serotonergic metacerebral cell of *Aplysia. J Neurosci.* **6:** 2393–2402.

Wu, J.-Y., C. X. Falk, H.-P. Höpp, and L. B. Cohen. 1989. Trial-to-trial variability in the neuronal response to siphon touch in the *Aplysia* abdominal ganglion. *Soc. Neurosci. Abstr.* **15:** 1264.

Yarowsky, P. J., and D. O. Carpenter. 1978. Receptors for gamma-aminobutyric acid (GABA) on *Aplysia* neurons. *Brain Res.* **144:** 75–94.

Zecević, D., J.-Y. Wu, L. B. Cohen, J. A. London, H.-P. Höpp, and C. X. Falk. 1989. Hundreds of neurons in the *Aplysia* abdominal ganglion are active during the gill-withdrawal reflex. *J. Neurosci.* **9:** 3681–3689.

Zedah, L. A. 1965. Fuzzy sets. *Information and Control* **8:** 338–353.

Reference: *Biol. Bull.* **181**: 500–504. (December, 1991)

Immunochemical Detection of Predation on Ciliate Protists by Larvae of the Northern Anchovy (*Engraulis mordax*)

MARK D. OHMAN[1], GAIL H. THEILACKER[2], AND SANDOR E. KAUPP[1]
[1]*Scripps Institution of Oceanography, U.C. San Diego, La Jolla, California 92093-0227 and*
[2]*Alaska Fisheries Science Center FAKC1, National Marine Fisheries Service,*
7600 Sand Point Way, Seattle, Washington 98115

New approaches are needed for investigating planktonic prey-predator interactions *in situ,* free from enclosures and long term incubations. Lengthy incubations can lead to several artifacts, including selective mortality of planktonic organisms (1), lysis of some taxa upon fixation (2), alteration of prey-predator encounter rates through perturbations of the turbulent flow field (3), and modification of natural search and avoidance behaviors of predators and prey (4). Microscopic analysis of the gut contents of predators is a feasible alternative only if prey leave digestion-resistant hard parts. Here we describe a different approach involving immunochemical methods. We report the development and first application of an immunoassay that permits detection of predation on soft-bodied, nonloricate ciliates (*Strombidium* sp.). Polyclonal antibodies raised against *Strombidium* sp. recognize both intact ciliates and partially assimilated ciliate antigens occurring in a predator's gut. We demonstrate, by both immunochemical and conventional methods, unequivocal predation by first-feeding larvae of the northern anchovy (*Engraulis mordax*) on nonloricate ciliates. The intensity of the immunochemical reaction, quantified by enzyme-linked dot blots and reflection densitometry, is proportional to prey density and to the predator's ingestion rate.

Polyclonal antisera were produced in New Zealand white rabbits (5) against *Strombidium* sp. cultured on a diet of the bacterium *Vibrio natriegens* (6). Immunoglobulin G (anti-*Strombidium* IgG) was isolated from the antiserum by precipitation in 45% (w/v) ammonium sulfate, desalted by gel filtration, then fractionated by diethylaminoethyl ion exchange chromatography. Detailed protocols will be presented elsewhere. No significant cross-reaction was found between anti-*Strombidium* IgG and *V. natriegens* or 25 other species of planktonic algae, ciliates, and metazoans (cross-reactions were analyzed by dot blots, using at least 200 ng protein per spot). However, a significant cross-reaction was found with larval anchovy, *Engraulis mordax,* the predator of interest in this study. The reaction occurred with homogenates of isolated guts dissected from the larvae as well as with whole larvae. Pre-immune sera drawn from five rabbits and tested individually by dot blots also showed a strong cross-reaction with larval anchovy. We do not know the reason for this unexpected cross-reaction, but we successfully eliminated it by immunoadsorption against homogenates of larval anchovy bound to an affinity column.

We briefly present the method here; it is derived from the recommendations of the supplier of Sepharose 6MB (Sigma Chemical Co). A group of 100 unfed first-feeding larvae was homogenized in coupling buffer (0.1 *M* $NaHCO_3$, 0.5 *M* NaCl, pH 8.0), then sonicated in an ice water bath. This extract was mixed with cyanogen bromide-activated Sepharose 6MB overnight at 4°C. Unbound material was washed away with coupling buffer, then the remaining active groups reacted with 1 *M* ethanolamine (pH 8.0) for 2 h. Three washing cycles were then done, first with 0.1 *M* acetate buffer containing 0.5 *M* NaCl (pH 4.0), then with 0.1 *M* borate buffer containing 0.5 *M* NaCl (pH 8.0). The Sepharose beads were then packed into a capillary pipet to form a micro affinity column. Anti-*Strombidium* IgG was adsorbed against the affinity column-coupled larval extract after the procedure in reference (7) (section 10.3.1, substituting 0.1 *M* glycine HCl, pH 2.5, as elution buffer). The residence time of the

Received 7 June 1991; accepted 20 September 1991.

IgG solution in the column was 24 min. Dot blot immunoassays revealed remarkably effective elimination of the cross-reaction with anchovy larvae by this procedure. The optical density of the dot blot reaction with dissected anchovy guts decreased from a mean of 0.154 (maximum 0.225) prior to adsorption to a mean of 0.049 after adsorption.

Following immunoadsorption, the optical density of immunochemical dot blots varied with the quantity of *Strombidium* antigen (Fig. 1). Log-linear calibrations of this kind are not uncommon (*e.g.*, ref. 8) and may reflect quenching at high antigen concentrations. The antibody used for this calibration curve and for all other assays was affinity-purified anti-*Strombidium* IgG at a concentration of 0.4 μg IgG ml^{-1}.

In predation experiments, the quantity of ciliate remains detected in the gut contents of first-feeding anchovy larvae varied as a function of prey density (Fig. 2A). Even at the lowest prey concentration, 0.8 ciliates ml^{-1}, ingestion of ciliates occurred. The mass of *Strombidium* protein detected per larval gut was estimated from the calibration relation in Figure 1, and is illustrated in Figure 2B. A significant ($r^2 = 0.89$, $P < 0.05$) linear relation was found between the density of ciliate prey offered and the amount of ciliate protein in larval guts. (The values in Fig. 2A have been corrected for the blank.) Visual examination of larval gut contents at the end of the incubations confirmed that guts were at times packed full of amorphous, nearly transparent, and otherwise unidentifiable ciliate remains.

The time course of uptake of *Strombidium* sp. was evaluated in a separate experiment. The first sample of fed larvae was taken after 80 min, based on earlier results (9) suggesting that naive larvae take 1–2 h to learn to capture a new prey item. Indeed, the amount of *Strombidium* antigen in larval fish guts did not reach a maximum value until 2 h after the experiment began (Fig. 3). No significant variation ($P > 0.05$, ANOVA) in ciliate protein $larva^{-1}$ was found from 80 min onward, but the high variability among individuals could have masked a trend. The mean quantity of immunoreactive gut contents appeared to decrease after 2 h, perhaps due to the egestion of fecal matter, and then to attain the previous maximum after 6 h of feeding.

Prey disappearance experiments were carried out to describe the dependence of ingestion rate of first-feeding anchovy larvae on the density of the ciliate *Strombidium* sp. (Fig. 4). Again, even at the lowest prey concentration tested (4 ciliates ml^{-1}), ingestion of ciliates was detectable. The ingestion rates can be converted to daily carbon-specific rates, assuming 9 μg C $larva^{-1}$ and 12 h feeding per day. Accordingly, the carbon-specific ingestion rates reached 85–95% per day (right hand ordinate in Fig. 4).

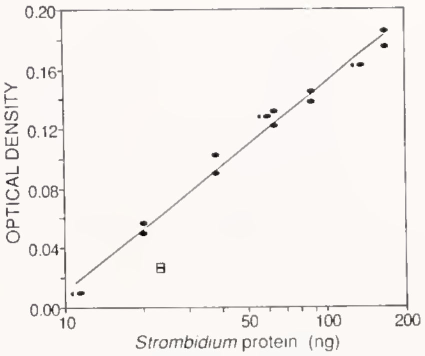

Figure 1. Calibration relation between the optical density of immunochemical dot blots and the quantity of *Strombidium* protein (OD = $-0.131 + 0.141$ [$\log_{10}$ protein], $r^2 = 0.987$, $P < 0.001$). The outliers indicated by open squares were excluded from the regression. Overlapping data points are offset. Dot blot assays were done on 0.45 μm nitrocellulose (Schleicher and Schuell) by a modification of the methods in refs. (17) and (27). Following incubation with the primary antibody (anti-*Strombidium* Ig), the blots were reacted with secondary antibody (goat anti-rabbit IgG conjugated to alkaline phosphatase), then with chromogenic substrate for alkaline phosphatase (8). Optical density was read at 530 nm with a calibrated reflection densitometer interfaced to a microcomputer.

There was a significant positive relation between immunochemical estimates of gut contents (G; ciliate protein $larva^{-1}$) and ingestion rates (I; ciliates $larva^{-1}$ h^{-1}) from prey disappearance experiments: $G = 9.53 + 0.22$ (I), $r^2 = 0.834$, $P < 0.05$. For this comparison, the ingestion rate was estimated from the curve illustrated in Figure 4, using the average prey density in each of the immunochemical treatments. Note that G is a static measure of gut contents, while I is a rate. This relation (and that in Fig. 2B) should not be extrapolated to $x = 0$, which would imply a positive y-intercept. There appears to be a threshold prey density below 0.8 ciliates ml^{-1} that elicits a rapid, nonlinear increase in capture rates of ciliates by anchovy larvae.

We have demonstrated the ability to detect soft-bodied nonloricate ciliates in the gut contents of predators using immunochemical methods. Unlike tintinnid ciliates, which leave loricae that can be identified by microscopy in predator guts (10), ingested nonloricate ciliates cannot be recognized by conventional means. Because nonloricate ciliates are more abundant and constitute greater biomass than tintinnids in most regions of the ocean (11), this technique permits a potentially significant food web linkage (12, 13) to be investigated *in situ*. Although we have initially used controlled laboratory experiments to establish the relationship between immunochemical measures and ingestion rates, the immunoassay presented here is suitable for analysis of field-collected predators.

Overviews of marine ecological applications of immunochemistry can be found in refs. (14) and (15). Feller *et al.* (16) identified unanticipated prey-predator links in

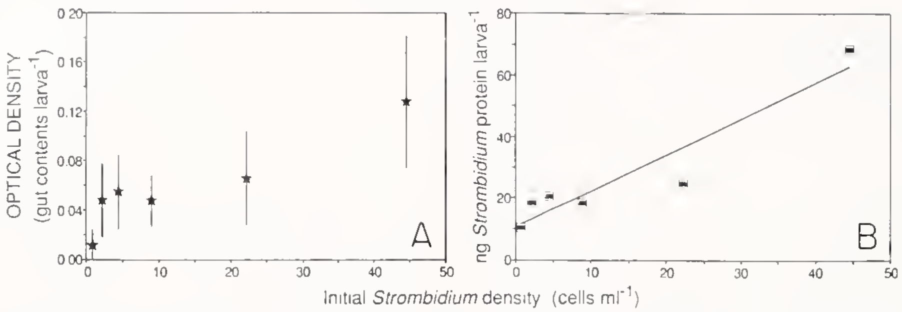

Figure 2. (A) Relation between the gut contents of first feeding anchovy larvae as determined from immunochemical dot blots ($\bar{x} \pm 95\%$) and the concentration of ciliate prey. Optical density readings have been corrected for the reaction blank from starved larvae. (B) As in part A, with gut contents expressed as ingested ciliate protein content larva^{-1} from the relation in Figure 1.

Anchovy larvae were raised from eggs collected in surface waters off La Jolla, California, and maintained in glass-fiber (GF/F) filtered seawater at 15°C under fluorescent lamps (12 μEin m^{-2} s^{-1}) on a 12:12 light: dark cycle. Containers for predation experiments were black polypropylene beakers containing 800 ml of filtered seawater, covered with Mylar lids. Only first-feeding larvae (3–4 days post-hatch, 4.0 mm standard length) were used. Ciliates (*Strombidium* sp. clone AH) were grown on a monoxenic diet of the bacterium *Vibrio natriegens* (6). The dimensions of stationary phase *Strombidium* sp. are 25 × 30 μm (width × height; preserved in 2% acid Lugols and thus reflecting cell shrinkage), cell biovolume 12,500 μm^3 (live volume), 1.4 ng protein ciliate^{-1}, and 1.6 ng C ciliate^{-1} (6). All *Strombidium* used in predation experiments were in stationary growth phase. Larvae were incubated for 6–8 h with *Strombidium* sp. Seven to 13 individual larvae were analyzed per treatment.

After predation experiments, larvae were quickly frozen in liquid N_2, then transferred to a −80°C freezer. Control first-feeding larvae (maintained continuously in filtered seawater) were treated in the same manner. For all immunoassays, guts of thawed larval anchovy were individually dissected onto a glass microscope slide. The gut contents were teased into 2–4 μl of PBS buffer, then blotted onto pre-washed nitrocellulose. A standard of known concentration of *Strombidium* sp. protein was blotted to ensure consistent reaction intensity.

a marine benthic assemblage using the precipitin reaction. Theilacker *et al.* (17) estimated the frequency of occurrence of euphausiid predation on larval anchovy using dot blots. Hentschel and Feller (18) established a quantitative relation between the intensity of the precipitin reaction (determined by rocket immunoelectrophoresis) and the mass of prey in the proventricular contents of a penaeid shrimp.

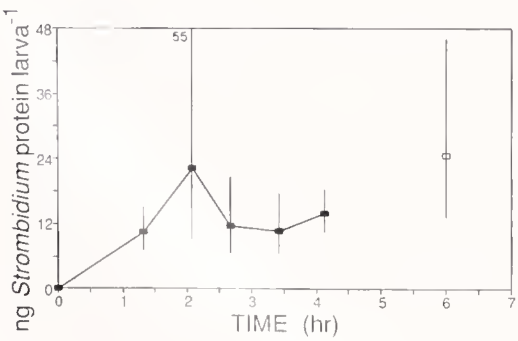

Figure 3. Time course of uptake of planktonic ciliates, as measured by immunochemical dot blots ($\bar{x} \pm 95\%$). The values at 6 h were obtained in a separate experiment. The initial prey concentration was 22 *Strombidium* ml^{-1} for all treatments. Five to eleven individual larvae were analyzed per treatment. Optical density readings were corrected for the reaction blank from starved larvae and converted to protein from the relation in Figure 1.

Our dot blot method, quantified by reflection densitometry, appears to be 10^4 times more sensitive than the immunoelectrophoretic methods employing the precipitin reaction (18, 19). Still greater sensitivity could be obtained by use of chemiluminescence to visualize the reaction, or perhaps with ELISA (enzyme-linked immunosorbent assays), provided the antigens of interest bind effectively to polystrene surfaces. The dot blot procedure has the additional advantages that it is relatively fast (about 4 h), is sparing of antibody, and provides a permanent record of the reaction.

Reflection densitometry makes it possible to quantify the amount of dye product formed from a known quantity of ciliate antigen, as exemplified by the calibration curve above (Fig. 1). However, quantification of the gut contents of predators requires the following additional assumptions: (1) a constant number of secondary antibody molecules bind to the primary antibody; (2) the antigenic fraction of ciliate protein bears a constant (or known) relationship to total ciliate protein; and (3) the gut residence time of antigens is known.

Assumption (1) appears to be reasonable over the range of antigen concentrations used here (Fig. 1). Assumption

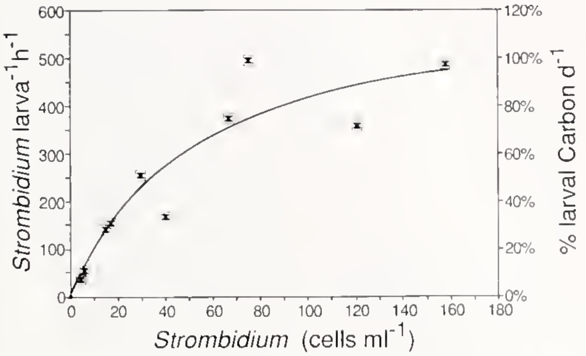

Figure 4. Ingestion rate (I) of first-feeding anchovy larvae as a function of concentration of the ciliate *Strombidium* sp. (C), determined by prey disappearance experiments. The right hand ordinate indicates daily carbon-specific ingestion rates, assuming feeding for 12 h each day. The ingestion rate is described by:

$$I = \frac{639.5 * C}{54.6 + C}$$

This curve was fitted by nonlinear least squares using the Simplex algorithm. Monte Carlo simulations (n = 1000) based on standard deviations of replicate cell counts indicated that the coefficient of variation about individual ingestion rates was approximately 15%.

Seven to twenty-five first-feeding larvae were incubated for 6–8 h with ciliates in illuminated 800-ml containers. Aliquots were preserved in 2% acid Lugols solution, then four subsamples settled overnight by the Utermöhl procedure and ciliates enumerated by inverted microscope. Control containers lacking larvae were run at each experimental density (average ciliate recovery 102%). Predation rates were calculated from the equations in (28).

(2) implies that if differential digestion of antigenic and non-antigenic protein occurs, the time course of this relationship must be determined. The antigenic properties of the prey ingested by a penaeid shrimp did not change over time during digestion (18), although this was not the case with a carid shrimp ingesting different prey (20). The immunochemical detectability of ingested prey varied with location in the intestinal tract of *Octopus vulgaris* (19). However, because first-feeding larval anchovy have a relatively simple tubular gut, we do not expect digestion to be compartmentalized. As an alternate solution to the issue of differential digestion, we have produced antibodies against partially assimilated ciliate protein, rather than against intact ciliates; these results will be reported elsewhere. Assumption (3), concerning gut residence time, requires considerable attention. Predation rate estimates are sensitive to both the speed of gut passage and to the theoretical model of digestion. The model of digestion is important because either ingestion or digestion may be discontinuous processes (Fig. 3).

Conventional prey disappearance experiments corroborated the ingestion of *Strombidium* sp. The maximum ingestion rate observed in these experiments would require 7–8 successful strikes min^{-1}. This compares with Hunter's (21) determination of 5–7 strikes min^{-1} for 4.5–4.9 mm anchovy larvae feeding on *Gymnodinium sanguineum* (=*splendens*, 40–50 μm), and implies that 25–35 μm ciliates are captured at rates comparable to those when larvae are fed an unarmored dinoflagellate that is thought to be an optimal prey item. The high rate of successful attacks on *Strombidium* sp. is somewhat surprising, given the relative transparency of these cells when in stationary growth phase and their size at the lower end of the range (22–100 μm) of prey previously documented from field-caught larvae (22). The distinctive swimming motions of these ciliates may enhance their detectability to visual planktivores.

Ingestion of ciliates by larval anchovy was detectable at prey concentrations as low as 0.8 ciliates ml^{-1}. An estimate of the ciliate density required to meet the daily metabolic requirements of first-feeding anchovy larvae can be obtained from Figure 4 combined with reported respiration rates (9, 23). *Strombidium* densities of 5–8 cells ml^{-1} are sufficient to meet basal metabolic requirements. Ambient densities of ciliates in the habitat of the northern anchovy range to at least 45 ciliates ml^{-1} (11). This is likely an underestimate due to difficulties in preserving some ciliates (2), combined with undersampling of microscale layers of organisms in the sea (24).

Among other evidence for the importance of ciliates in the diet of fish larvae, larval sea bream (*Lithognathus mormyrus*) appeared to grow faster, and with lower mortality, when ciliates were available as prey (25). Stoecker and Govoni (10) observed disproportionate consumption of the tintinnid *Favella* sp. by larval gulf menhaden (*Brevoortia patronus*), and noted that many ciliates and dinoflagellates lacking hard parts may have been overlooked in larval fish feeding studies.

Despite their small size and relative transparency, nonloricate ciliates are captured readily by first-feeding larval anchovy, at low prey concentrations and with high ingestion rates. Soft-bodied ciliates lacking hard parts may be significant links between microbial food webs and larger planktonic predators. Small scale "Lasker" patches of nonloricate ciliates, in addition to dinoflagellates (26), require attention as enriched sites of prey for teleost larvae and other planktonic predators in nature.

Acknowledgments

We thank J. R. Wilkinson for assistance with culturing ciliates, E. L. Venrick for the Monte Carlo simulations, and E. D. Gallagher for comments on the manuscript. Supported by NOAA Sea Grant NA89AA-D-SG138 and by NSF OCE-8812123.

Literature Cited

1. **Venrick, E. L., J. R. Beers, and J. F. Heinbokel. 1977.** Possible consequences of containing microplankton for physiological rate measurements. *J. Exp. Mar. Biol. Ecol.* **26:** 55–76.

2. **Snyder, R. A. and M. D. Ohman. 1991.** Description of a new species of Strombidinopsidae (Ciliophora: Choreotrichida) from coastal waters of southern California, U.S.A. *Trans. Am. Microsc. Soc.* **110:** 237–243.
3. **Yamazaki, H., T. R. Osborn, and K. D. Squires. 1991.** Direct numerical simulation of planktonic contact in turbulent flow. *J. Plank. Res.* **13:** 629–643.
4. **Ohman, M. D. 1988.** Behavioral responses of zooplankton to predation. *Bull. Mar. Sci.* **43:** 530–550.
5. **Vaitukaitis, J. L. 1981.** Production of antisera with small does of immunogen: multiple intradermal injections. *Meth. Enzymol.* **73:** 46–52.
6. **Ohman, M. D., and R. A. Snyder. 1991.** Growth kinetics of the omnivorous oligotrich ciliate *Strombidium* sp. *Limnol. Oceanogr* **36:** 922–935.
7. **Johnstone, A., and R. Thorpe. 1987.** *Immunochemistry in Practice*, 2nd ed. Blackwell Scientific, Oxford.
8. **Blake, M. S., K. H. Johnston, G. J. Russell-Jones, and E. C. Gotschlich. 1984.** A rapid, sensitive method for detection of alkaline phosphatase-conjugated anti-antibody on Western blots. *Analyt. Biochem.* **136:** 175–179.
9. **Theilacker, G. H. 1987.** Feeding ecology and growth energetics of larval northern anchovy, *Engraulis mordax*. *Fish. Bull.* **85:** 213–228.
10. **Stoecker, D. K., and J. J. Govoni. 1984.** Food selection by young larval gulf menhaden (*Brevoortia patronus*). *Mar. Biol.* **80:** 299–306.
11. **Beers, J. R., F. M. H. Reid, and G. L. Stewart. 1980.** Microplankton population structure in southern California nearshore waters in late spring. *Mar. Biol.* **60:** 209–226.
12. **Stoecker, D. K., and J. M. Capuzzo. 1990.** Predation on protozoa: its importance to zooplankton. *J. Plank. Res.* **12:** 891–908.
13. **Gifford, D. J. 1991.** The protozoan-metazoan trophic link in pelagic ecosystems. *J. Protozool.* **38:** 81–86.
14. **Yentsch, C. M., F. C. MaGue, and P. K. Horan (eds.). 1988.** *Immunochemical Approaches to Coastal, Estuarine and Oceanographic Questions.* Lecture notes on coastal and estuarine studies. v. 25, Springer-Verlag, New York.
15. **Ward, B. B. 1990.** Immunology in biological oceanography and marine biology. *Oceanography* **3:** 30–35.
16. **Feller, R. J., G. L. Taghon, E. D. Gallagher, G. E. Kenny, and P. A. Jumars. 1979.** Immunological methods for food web analysis in a soft-bottom benthic community. *Mar. Biol.* **54:** 61–74.
17. **Theilacker, G. H., A. S. Kimball, and J. S. Trimmer. 1986.** Use of an ELISPOT immunoassay to detect euphausiid predation on larval anchovy. *Mar. Ecol. Progr. Ser.* **30:** 127–131.
18. **Hentschel, B. T., and R. J. Feller. 1990.** Quantitative immunoassay of the proventricular contents of white shrimp *Penaeus setiferus* Linnaeus: a laboratory study. *J. Exp. Mar. Biol. Ecol.* **139:** 85–99.
19. **Grisley, M. S., and P. R. Boyle. 1988.** Recognition of food in *Octopus* digestive tract. *J. Exp. Mar. Biol. Ecol.* **118:** 7–32.
20. **Zagursky, G., and R. J. Feller. 1988.** Application of immunoblotting for dietary analysis. Pp. 117–129 in *Immunochemical Approaches to Coastal, Estuarine and Oceanographic Questions.* Lecture notes on coastal and estuarine studies. v. 25, C. M. Yentsch, F. C. MaGue and P. K. Horan. eds. Springer-Verlag, New York.
21. **Hunter, J. R. 1977.** Behavior and survival of northern anchovy *Engraulis mordax* larvae. *Calif. Coop. Oceanic Fish. Inv. Rep.* **19:** 138–146.
22. **Arthur, D. K. 1976.** Food and feeding of larvae of three fishes occurring in the California Current, *Sardinops sagax, Engraulis mordax*, and *Trachurus symmetricus*. *Fish. Bull.* **74:** 517–530.
23. **Hunter, J. R. 1972.** Swimming and feeding behavior of larval anchovy *Engraulis mordax*. *Fish. Bull.* **70:** 821–838.
24. **Owen, R. W. 1989.** Microscale and finescale variations of small plankton in coastal and pelagic environments. *J. Mar. Res.* **47:** 197–240.
25. **Kentouri, M., and P. Divanach. 1983.** Contribution à la connaissance du comportement et de la biologie des larves de marbré *Lithognathus mormyrus* (sparides) en élevage. *Ann. Zootech.* **32:** 135–152.
26. **Lasker, R. 1975.** Field criteria for survival of anchovy larvae: the relation between inshore chlorophyll maximum layers and successful first feeding. *Fish. Bull.* **73:** 453–462.
27. **Monroe, D. 1985.** The solid-phase enzyme-linked immunospot assay. Current and potential applications. *BioTechniques* **3:** 222–229.
28. **Frost, B. W. 1972.** Effects of size and concentration of food particles on the feeding behavior of the marine planktonic copepod *Calanus pacificus*. *Limnol. Oceanogr.* **17:** 805–815.

Reference: *Biol. Bull.* **181**: 505–514. (December, 1991)

Abstracts of Papers Presented at the Marine Biological Laboratory: 1991 Northeast Regional Developmental Biology Conference

19–21 April 1991

The conference was organized by Edward Bonder (Rutgers University) and Laura Grabel (Wesleyan University). Financial support for the meeting was provided by the Society for Developmental Biology and the National Science Foundation. The abstracts are listed alphabetically by first author under the session in which they were presented (see program outline below). All published abstracts have been reviewed by the conference organizers and by the editors.

Program

Keynote Address:

The mouse embryo: lineage pattern and genes. **Janet Rossant**, University of Toronto

Session I: Pattern Formation

Genes involved in cell signalling processes that control cell migration and cell fate determination in C. elegans. **Michael Stern**, MIT

Molecular analysis of the heterochronic gene lin-29 of C. elegans. **Anne Rougvie**, Harvard University

Non cell-autonomous control of morphogenesis in cotton. **Liam Dolan**, University of Pennsylvania

Genetic and molecular analysis of floral homeotic genes in Arabidopsis. **Vivian Irish**, Yale University

Dissection of ectopic function of the paired segmentation gene in Drosophila *embryos.* **David Morrissey**, Wesleyan University

Regulation of the bithorax complex along the anterior-posterior axis of Drosophila. **Jeff Simon**, Harvard Medical School

Session II: The Cytoskeleton and Extracellular Matrix in Development

Mutations in the Drosophila *myosin heavy chain gene disrupt morphogenetic movements during development.* **Paul Young**, Harvard University

The role of the Drosophila *gene* armadillo *in cell interactions and* wingless *signalling.* **Mark Peifer**, Princeton University

Voltage dependent-L-Type Ca^{2+} channels VDCCs participate in regulating neural crest development. **Denis Moran**, SUNY New Paltz

A dissection of the functions of PS integrins during Drosophila *development.* **Susan Zusman**, Harvard University

Notch-delta and Notch-cytoskeletal interactions in Drosophila *tissue culture cells.* **Ilaria Rebay**, Yale University

Integrin phosphorylation and focal contact assembly in dihydrocytochalasin B treated differentiating F9 cells. **Marc Lenburg**, Wesleyan University

Session III: Growth Factors and Signalling Molecules

Genetic analysis of hormonal regulation of seedling development in Arabidopsis thaliana. **Joe Kieber**, University of Pennsylvania

Role of inositol phospholipids in signal transduction in plants. **Richard Crain**, University of Connecticut

Calcium and the gravity response in plants. **Randy Wayne**, Cornell University

Embryonic induction and the TGF-β family in Xenopus. **Gerald Thomsen**, Harvard University

Intercellular signaling via gap junctions in the regulation of pattern formation during limb development. **Caroline Coelho**, University of Connecticut Health Center

Potential roles of a developmentally regulated cell surface proteoglycan. **Michael Hinkes**, Harvard Medical School

Identification in Drosophila *of a new member of the TGF-β family of cell signaling molecules.* **Kristi Wharton**, Harvard University

Regulation of a Drosophila *growth factor homolog,* Decapentaplegic (dpp). **Michele Sanicola**, Harvard University

Session IV: Development of the Nervous System

Regulation of mec-3, *a homeobox-containing gene that controls mechanoreceptor neuronal differentiation in* C. elegans. **Jeff Way**, Rutgers University

Neuronal and cell-lineage expression patterns of the C. elegans *gene, lin-11.* **Gwen Freyd**, MIT

Neuronal control of defecation in C. elegans. **Erik Jorgensen**, MIT

The role of the fizzy locus in the neuroectodermal differentiation in Drosophila. **Iain Dawson**, Yale University

Complex cellular and sub-cellular regulation of notch expression during embryonic and imaginal development of Drosophila: *implications for notch function.* **Richard Fehon**, Yale University

Laser inactivation of fasciclin I disrupts axon adhesion of embryonic pioneer neurons. **Haig Keshishian**, Yale University

Poster Session

Video Session

Pattern Formation

Non cell-autonomous control of leaf morphogenesis in cotton (Gossypium barbadense). LIAM DOLAN AND R. SCOTT POETHIG (Plant Science Institute, University of Pennsylvania, Philadelphia, PA 19104-6018).

The primordia of angiosperm leaves are derived from a large number of cells sequestered approximately one plastochron before the visible outgrowth from the meristem surface. In cotton, γ-ray induced sectors on plants homozygous for the v_7 mutation demonstrate that the leaf is derived from a population of over 100 cells, which gives rise to characteristic, though not invariable, regions of the mature leaf. Examination of sectors induced late in development of the lamina suggest that cell division ceases first at the tip of the leaf and subsequently at the leaf base. The frequency and the area of sectors induced at the leaf margin indicate that marginal cells contribute equally to the growth of the leaf.

The *Okra* (L_2^0) mutation increases the degree of leaf lobing by reducing the growth of the lamina and increasing the length of the wild type lobes. Allometric analysis suggests that this mutation acts early in development. Genetic mosaics comprised of *Okra* and wild type tissue indicate that the mutation acts in a non-cell-autonomous fashion. The presence of the mutation in different histogenic layers of the meristem results in distinctive mature leaf phenotypes. Periclinal chimeras containing a mutant epidermis and wild type internal tissue have a partial *Okra* phenotype. *Okra* tissue in the sub-epidermal (L2 derived) has an even more severe mutant phenotype, while the presence of *Okra* in the inner most tissue of the leaf (L3 derived) has no effect on the growth of the lamina but alters the length of the lobes. No distortion of leaf tissue is observed in mosaics, suggesting that there is compensation for differential growth of wild type and mutant tissue in the developing leaf. These results illustrate ways in which the histogenic layers of the meristem interact during morphogenesis in the leaf primordium and clearly show that the epidermis can play an important role in morphogenesis.

Dissection of ectopic function of the paired segmentation gene in Drosophila *embryos.* D. MORRISSEY, D. ASKEW, L. RAJ, AND M. WEIR (Department of Biology, Wesleyan University, Middleton, CT 06459).

An ectopic expression assay in *Drosophila* embryos was used to investigate the role of pair-rule segmentation genes in the spatial regulation of the segment-polarity gene, *engrailed* (*en*). It is hypothesized that the regions of overlap in expression of two genes, *paired* (*prd*) and *even-skipped* (*eve*), define the odd-numbered *en* expression stripes. Consistent with this combinatorial model, ectopic expression of *prd* caused these *en* stripes to be expanded posteriorly. Surprisingly however, ectopic expression of a *prd* gene with a deletion of the conserved paired box resulted in loss of these odd-numbered *en* stripes. This effect is a phenocopy of *en* expression in *prd*-mutant embryos, and suggests that the paired box is necessary for *prd* function at ectopic sites. A similar deletion of odd-numbered *en* stripes was also observed following ectopic expression of a chimeric *fushi tarazu* (*ftz*) gene containing a substituted *prd* gene homeobox; in addition, in these embryos the even-numbered *en* stripes were expanded anteriorly, as observed when the unaltered *ftz* gene is ectopically expressed. These effects suggest that the chimeric protein may have DNA or protein targets of both the normal Ftz and Prd proteins.

The Cytoskeleton and Extracellular Matrix in Development

Integrin phosphorylation and focal contact assembly in dihydrocytochalasin B treated differentiating F9 cells. M. E. LENBURG AND L. B. GRABEL (Department of Biology, Wesleyan University, Middletown, CT 06459).

Integrins are transmembrane mediators between specific extracellular matrix components and the cytoskeleton at points of close cell-substrate adhesion. A great deal of interest has therefore been focused on the process by which integrin-mediated adhesions are regulated during morphogenesis. F9 teratocarcinoma stem cells synthesize abundant amounts of the $\beta 1$ integrins but organize them into focal contact-like structures only upon the retinoic acid and cAMP induced differentiation into parietal endoderm. The assembly of focal contacts coincides with the accumulation of cell associated fibronectin fibers, the dephosphorylation of integrin, and the polymerization of actin microfilaments. We show here that preventing actin polymerization with the actin destabilizing agent dihydrocytochalasin B (DHCB) reversibly inhibits the organization of integrin and the accumulation of fibronectin fibers, although integrin continues to undergo the normal pattern of dephosphorylation and the cells continue to express other characteristics of the parietal endoderm phenotype. When DHCB is added to parietal endoderm cells that have already assembled focal contacts, although actin is disrupted, fibronectin and integrin remain organized. These results suggest that actin microfilaments are not necessary for the expression of the parietal endoderm phenotype, but do play a crucial role in the assembly of focal contacts, and are not required for focal contact maintenance. They also suggest that integrin dephosphorylation alone is not sufficient for focal contact assembly, and demonstrate that integrin dephosphorylation is developmentally regulated and not merely a result of integrin reorganization.

Voltage-dependent -L-type Ca^{2+} channels VDCCs participate in regulating neural crest development. DENIS MORAN (Developmental Biology Lab, SUNY, College at New Paltz, New Paltz, NY 12561).

Modulation of Ca^{2+} is important in the control of many morphogenetic processes. We investigated whether neural crest cells develop VDCCs and, if so, whether they function in regulating migration and establishing cytomorphology. Autoradiography with ^3H-verapamil, which binds VDCCs, indicates that *in vitro* migrating and differentiating neural crest cells develop VDCCs. Blockage of these channels by verapamil or nifedipine both *in vivo* and *in vitro,* leads to a dramatic and reversible inhibition of neural crest migration. Alterations are manifest *in vitro* in cell-to-cell and cell-to-substratum contact. Indirect immunofluorescence indicates a disrupted organization of the actin cytoskeleton. In whole embryos, verapamil or nifedipine inhibits pigment pattern formation. Moreover, blockage of the VDCCs in whole embryos or cultures, after cells have already migrated and differentiated, results in a significant change in individual cell shape and in the overall pigment cell pattern. Interactions that regulate the availability of Ca^{2+} through the VDCC may provide coordinate control of motile and adhesive interactions at the cell-substratum interface.

The role of the Drosophila *gene* armadillo *in cell interactions and* wingless *signaling.* M. PEIFER, E. WIESCHAUS, B. RIGGLEMAN, AND C. RAUSKOLB (Princeton University, Princeton, NJ 08544-1014).

Cell adhesion and cell interactions are thought to be important in regulating both the fate and the behavior of cells during development. In the past several years, the *Drosophila* system has provided connections between molecules known to be involved in cell interactions and genes known to be required for proper embryonic development. One of the best characterized processes in this context is the process of setting up an anterior or posterior pattern *within* each *Drosophila* segment. This process involves cell interactions, and is now thought to rely primarily on a graded extracellular signal, encoded by the *wingless* gene product. Cells, by reading the level of this signal, determine their position within the segment and decide on their fate. The *wingless/int-1* signaling pathway controls patterning not only in insects, but also in vertebrates.

We have been working on *armadillo*, a gene also involved in setting up patterns within each segment. We have shown that *armadillo* seems to be required by cells to perceive the *wingless* signal. This signaling pathway operates both in the embryo and in the imaginal discs which give rise to the adult cuticle (Peifer *et al.* 1991, *Development*, in press). We have further shown that *armadillo* is homologous to the human protein plakoglobin, a component of all adhesive cell-cell junctions (Peifer and Wieschaus 1990, *Cell* **63:** 1167). Both *armadillo* and plakoglobin share many features; they occur in soluble and membrane-associated forms, are polarized within cells, and co-localize with actin in some cell types but not in others. The *armadillo* protein is modular in function: severely truncated proteins retain activity. In response to the *wingless* signal, the intracellular distribution of the *armadillo* protein seems to be altered. Our results with *armadillo* suggest a role for adhesive cell junctions in both development and in signal transduction, and we are now trying to investigate this connection in greater detail.

A dissection of the functions of PS integrins during Drosophila *development.* SUSAN B. ZUSMAN[1], YEVGENYA GRINBLAT[2], GENE H. YEE[1], FOTIS KAFATOS[2] AND RICHARD O. HYNES[1] ([1]HHMI/M.I.T., Cambridge, MA, [2]Harvard University, Cambridge, MA 02139).

The vertebrate integrins are a family of transmembrane glycoproteins linking extracellular molecules (*i.e.*, fibronectin, laminin, collagen) that are involved in cell adhesion with the cytoskeleton. These molecules are thought to play an important role in the morphogenetic events associated with the formation of a multicellular organism. We have examined the *in vivo* functions of integrins in *Drosophila*, a system amenable to both genetic and molecular techniques. The β subunit of the *Drosophila* PS integrin family is encoded by the *lethal(1)myospheroid* gene (*l(1)mys*). An analysis of *lethal(1)myospheroid*$^-$ somatic clones induced during larval development has demonstrated postembryonic requirements for PS integrins in the development of the *Drosophila* wing and eye (Zusman *et al.*, 1990, *Development* **108:** 391–402). Mutant clones result in wing blisters, in which the dorsal and ventral epithelia of the wing blade have separated, and disorganized photoreceptor cells. Taking into account these phenotypes, the cell biological properties of integrins, morphological studies on various *l(1)mys* alleles, and temperature shift studies using transformed flies containing *Hsp70-l(1)myscDNA*, we have designed working models for the role of the PS integrins during *Drosophila* wing and eye development. Our models posit that integrins prevent the detachment of the dorsal and ventral epithelia of the pupal wing blade during the separation of these cell layers (Milner and Muir 1987, *Roux's Arch. Dev. Biol.* **195:** 63–73). In addition, they propose that the fenestrated membrane at the basal surface of the retina, thought to provide support for the photoreceptors (Cagan and Ready 1989, *Dev. Biol.* **136:** 346–362), requires integrins to remain attached to its underlying basement membrane. The integrin functions during embryogenesis are also under study.

To dissect further the mechanisms of β integrin function, *l(1)mys* constructs, transformed into flies, have been used to investigate the function of a region of the molecule that is derived from the alternative splicing of the 4th exon of the gene. Both forms of the integrin protein have the ability to rescue at least partially the mutant eye and wing phenotypes. *In vitro* mutagenesis in combination with P-element transformation is also being used to define functional domains within the cytoplasmic region of the integrin molecule.

This work is supported by the HHMI and The American Cancer Society.

Growth Factors and Signalling Molecules

Inositol phospholipid metabolism is involved in deflagellation of Chlamydomonas reinhardtii. RICHARD C. CRAIN, LYNNE M. QUARMBY, AND YIR G. YUEH (Department of Molecular and Cell Biology, The University of Connecticut, Storrs, CT 06269).

C. reinhardtii sheds its flagella when exposed to certain environmental stresses. We have previously shown that inositol phospholipid turnover is associated with deflagellation induced by pH shock or by mechanical shear. The deflagellation response of *C. reinhardtii* involves at least two signalling steps: the communication of stress to the molecular apparatus responsible for deflagellation and subsequently, or concurrently, the communication of the deflagellated condition to elements controlling gene expression and flagellar regeneration. To determine whether production of inositol 1,4,5-trisphosphate (IP_3) is involved in either of these signal pathways, we have used agents that perturb inositol phospholipid metabolism and have obtained evidence linking IP_3 formation to the deflagellation event. (1) Treatment of cells with mastoparan, an activator of G proteins, results in both accumulation of IP_3 and deflagellation. (2) Pretreatment of cells with levels of neomycin, an inhibitor of phospholipase C activity, that block accumulation of IP_3, prevents deflagellation in response to both pH shock and mastoparan. (3) Signals that cause deflagellation in wild type cells cause IP_3 production in the fa-1 mutant which does not deflagellate; these cells appear defective in the excision apparatus (Sanders and Salisbury 1989, *J. Cell Biol.* **108:** 1751–1760), not signal perception. (4) Preincubation of cells with 2 m*M* EGTA, a calcium chelator, blocks accumulation of IP_3 and inhibits deflagellation in response to mastoparan. These results suggest that extracellular calcium may be required for both deflagellation and IP_3 production.

Genetic analysis of hormone regulated seedling development in Arabidopsis thaliana. J. KIEBER, P. GUZMAN, G. ROMAN, A. WOLLENBERG, AND J. ECKER (Plant Science Institute, Department of Biology, University of Pennsylvania, Philadelphia, PA 19104).

The molecular mechanisms of plant hormone reception and signal transduction are poorly understood. We are studying the action of ethylene, a gaseous plant hormone, using the "triple response" of *Arabidopsis thaliana.* The "triple response" in *Arabidopsis* consists of three distinct morphological changes in seedlings upon exposure to ethylene: inhibition of hypocotyl and root elongation, radial swelling of the stem, and exaggeration of the apical hook. We have exploited the "triple response" to isolate a collection of mutants altered in their response to ethylene and auxin.

One class of mutants displays the triple response phenotype in the absence of exogenously added ethylene. These can be divided into two types, those revertible by silver and AVG (*eto*) and those non-revertible (*ctr*). Silver is a non-competitive inhibitor of ethylene binding and AVG is a potent inhibitor of ethylene production. *eto1* mutants were found to produce at least sixty-fold more ethylene than wild type plants. *eto1* is recessive and found to map to chromosome 5. Several independent EMS, x-ray, and DEB alleles of *eto1* have been isolated. A second eto mutant, *eto2*, has been identified; it is dominant and also maps to chromosome 5. The second type of constitutive mutant is represented by *ctr1-1* This mutant still displays the triple response in the presence of ethylene antagonists, and so is most likely affected at, or downstream of, the receptor.

A second class of mutants, which fails to display the triple response in the presence of ethylene, was identified. Two loci were identified; *ein1* (dominant) and *ein2* (recessive); they map to chromosome 1 and 4, respectively.

A final class of mutants, which is affected in only a subset of the ethylene responses, was also identified. These include *hls1*, a mutant which does not show an apical hook and *eir1*, a mutant in which only the root is insensitive to ethylene.

The epistatic relationship of the genes is being examined to begin to analyze the order of action of the gene products. Second site revertants are being isolated for the *eto1*, *ctr1*, and *ein1* mutants. Finally, we are beginning to isolate the genes that correspond to some of these mutations. This analysis will facilitate the understanding of regulatory mechanisms that govern ethylene action in plants.

Regulation of a Drosophila *growth factor homolog,* decapentaplegic (dpp) *in imaginal disks.* Michele Sanicola, Laurel A. Raftery, Ronald K. Blackman, and W. M. Gelbart (Harvard University, Cambridge, MA 02138).

The *dpp* gene of *Drosophila* encodes a TGF-β growth factor-like molecule that is needed for multiple developmental events including proximal-distal outgrowth of the adult appendages derived from imaginal disks. Previous work has demonstrated that a functional *dpp* gene is required on the anterior side of the anterior-posterior (A/P) compartment boundary for the formation of a complete wing and notum. *lacZ* reporter gene construct experiments that dissect the complex 3′ cis-regulatory region which governs *dpp's* expression along the A/P compartment boundary are presented. Using confocal microscopy to obtain single cell resolution, we examine the relationship of *dpp*-driven β-galactosidase expression to the posterior compartment marker, *engrailed* (*en*) in both wildtype and en^1 mutant disks. We have determined that in wildtype disks, the majority of cells expressing the *dpp*-driven reporter gene abut those cells expressing *en*. In en^1 mutant disks, where the A/P compartment boundary is disrupted, we observe ectopic expression of the *dpp*-driven reporter gene in the posterior compartment. These observations will be discussed with reference to the A/P compartment boundary.

The effect of gravity on cytoplasmic streaming in characean cells. Randy Wayne (Section of Plant Biology, Cornell University, Ithaca, NY 14853), Mark Staves, and A. Carl Leopold.

The velocity of cytoplasmic streaming in a horizontally oriented characean internodal cell is independent of the direction of streaming. However, when a cell is oriented vertically, the downwardly directed stream moves 10% faster than the upwardly directed stream. The polarity is eliminated if either or both of the cell ends are surgically removed or irradiated with a UV microbeam, indicating that a protein at the cell ends may be the gravireceptor. We propose that the protoplast falls within the rigid extracellular matrix, putting a tension or compression on the plasma membrane on the top of the cell and the bottom of the cell, respectively, as a consequence of gravitational pressure. This is supported by observations that a turgid membrane is required for the graviresponse, the graviresponse is reversed when cells are placed in solutions that are more dense than the protoplast, and that applying a differential pressure between the two ends hydrostatically emulates the gravity response. External Ca^{2+} contributes to the gravity-induced signal transduction chain. At concentrations above 1 μM, there is a normal response, otherwise it is reversed. Mathematical modelling shows that there is sufficient energy in the falling of the protoplast within the cell wall to open enough ion channels to realize the graviresponse. Furthermore, our model indicates that the gravitational pressure model can explain gravisensing in higher plant cells if the statoliths are considered to be ballast.

Identification in Drosophila *of a new member of the TGF-β superfamily of cell signalling molecules.* Kristi Wharton and William Gelbart (Cellular and Developmental Biology, Harvard University, Cambridge, MA 02138).

The transforming growth factor-β (TGF-β) superfamily of proteins have been implicated in the control of cell growth and differentiation in the developing organism. Approximately 16 members of the family have been identified in vertebrates and, until recently, only a single member, the *decapentaplegic (dpp)* locus, has been found in invertebrates. Using PCR to amplify *Drosophila* DNA, a second TGF-β-like gene was isolated. Based on its polytene chromosome localization, this gene is currently referred to as *60A*. The conceptual translation of sequence from cDNA clones identifies a single ORF with a signal sequence and multibasic residues preceding a clearly defined region showing TGF-β homology at the C-terminus. These results are consistent with the gene product being a secreted protein with proteolytic cleavage sites that would release a growth factor-like molecule. The *60A* sequence shows greatest sequence similarity within the TGF-β region to the human bone morphogenetic proteins BMP-5, BMP-6, and BMP-7, with small regions of similarity in the proposed "pro" region in the N-terminus. The fact that *60A* shows stronger homology to these mammalian proteins than it does to *dpp* suggests that the duplication of sequences leading to the existing multiple TGF-β-like proteins pre-dates the divergence of chordates and arthropods. The 1.7 kb mRNA transcribed from *60A* transcript is present in 4–10-h embryos, climbing third instar larvae, pupae, and adult males. The *60A* transcript is expressed throughout the germ band of embryos during which time the germband is forming and extensive movements associated with gastrulation take place. The expression is most intense in the mesoderm and ventral ectoderm, unlike the localization of *dpp*. The isolation of *60A* will now allow us to investigate molecularly and genetically the developmental relationship between two TGF-β-like proteins.

KW was a recipient of an NIH postdoctoral fellowship.

Neuronal and cell-lineage expression patterns of the C. elegans *cell lineage gene lin-11.* GWEN FREYD AND H. ROBERT HORVITZ (HHMI, Department of Biology, MIT, Cambridge, MA 02139).

Caenorhabditis elegans nematode worms that have mutations in the gene *lin-11* are slightly uncoordinated in their movement and are unable to lay eggs. These abnormalities are probably due to defects in their nervous system and in the division patterns of cells that form the hermaphrodite vulva and gonad. Molecular cloning and subsequent sequence analysis of *lin-11* cDNAs revealed that this gene encodes a protein that contains both a homeodomain and a highly conserved potential metal binding domain, called LIM (Freyd *et al.* 1990. *Nature* **344:** 876–879). The LIM domain contains tandem copies of a cysteine-rich motif that is found in several other proteins that also contain homeodomains.

To determine in which cells *lin-11* is expressed, we constructed a translational fusion between genomic DNA corresponding to the upstream regulatory regions and amino terminal end of *lin-11* and a reporter gene, *lacZ*. We injected the fusion plasmid into worms and obtained a strain in which the fusion was stably integrated on a chromosome. We find that the *lin-11-lacZ* fusion is expressed in the six VC neurons in the ventral nerve cord. The *lin-11-lacZ* fusion is also expressed in eight neurons in the head: two pairs of amphid sensory neurons and two pairs of interneurons. Some of these neurons are candidates for contributing to the behavioral defects in *lin-11* mutant animals. The *lin-11-lacZ* fusion is also expressed in a subset of cells that form the hermaphrodite vulva. These cells have altered division patterns in *lin-11* mutant animals. We have examined the affects of various mutations in neuronal and vulval development on *lin-11-lacZ* expression to confirm cell identities and analyze the regulation of *lin-11* expression by other genes.

Regulation of mec-3, *a homeobox-containing gene that controls mechanoreceptor neuronal differentiation in* C. elegans. JEFFREY C. WAY (Biology Department, Rutgers University, Piscataway, NJ 08855).

The *mec-3* gene promotes differentiation of the *Caenorhabditis elegans* touch receptors and two other sets of mechanoreceptors, probably by turning on structural genes necessary for mechanoreceptor function. In the touch receptors, *mec-3* is part of a sequentially activated set of genes: *unc-86->mec-3->mec-7*. *unc-86* is a member of the POU family of homeobox genes and is expressed in the parent of each *mec-3*-expressing cell and both daughters (Finney and Ruvkun 1990. *Cell* **63:** 895–905). *mec-3* is expressed only in the anterior daughter, which does not divide and differentiates into a neuron (Way and Chalfie 1989. *Genes Dev.* **3:** 1823–1833). *mec-7* is a touch receptor-specific β-tubulin subunit that is necessary for the function of this cell type. Our goal is to understand how *mec-3* is regulated in order to understand how a stereotyped cell lineage works.

We find that the *mec-3* promoter contains four non-coding regions that are conserved between two *Caenorhabditis* species. These regions contain presumptive binding sites for *unc-86* and *mec-3*. Maintenance of *mec-3* expression is mediated primarily by site II and partially by site III, which contain presumptive *mec-3* binding sites. Repression appears to be controlled by several regions; mutation of several different sites causes expression of a *mec-3-lacZ* fusion in the sisters of some cells that normally express *mec-3*. Thus, the *mec-3* promoter appears to mediate asymmetric cell division by mediating asymmetric expression of *mec-3*.

Posters and Video Session*

An analysis of abnormal oocyte, daughterless-abo-like, *and* wavoid-like *in* Drosophila melanogaster: *related genes that affect oocytes and embryos.* K. ALBRECHT, C. OSWALD, N. BROOKS, AND H. KRIDER (Department of Molecular and Cell Biology, University of Connecticut, Storrs, CT 06269).

Abnormal oocyte (*abo*, 2-44), *daughterless-abo-like* (*dal*, 2-44), and *wavoid-like* (*wdl*, 2-44) are related maternal effect defects which interact with heterochromatin. An external phenotype has not been reported for *abo*, *wavoid-like* displays a wing abnormality, and, recently, an embryonic phenotype was reported for *dal*. Embryos derived from homozygous *dal* females often cellularize at reduced nuclear density probably caused by a failure in centrosome formation during nuclear cycles 11–13. Our examination of DAPI stained early embryos from the above three mutants revealed defects similar to *dal*. The synchrony of the mitotic cycles is lost, and gaps in the otherwise uniform distribution of nuclei can be observed in preblastoderm embryos. In most cases, nuclei can be found just below the plane of the division figures. A new allele of *dal* which we have generated displays a more severe mutant morphology at all preblastoderm stages. All three mutants display a similar ovarian phenotype. In about 30% of the mutant derived ovaries examined, using Hoescht 33258, there are either too many or too few nurse cells, and the gametic nucleus may be absent. We have not seen any impact on follicle cells, but aberrant nurse cells may alter follicle cell distribution. In all cases, the aberrant number of nurse cells can be explained if divisions either ceased early or persisted too long in a cystoblast lineage. Two new alleles of *abo* (*abo*^{2} and *abo*^{3}) also display this phenotype. On occasion, a nuclear cluster or rosette is found in *wdl* oocyte cytoplasm. The embryonic defects may be the result of an imbalance of maternally derived products during oogenesis and not a separate zygotic defect. We conclude that *abo*, *dal*, *wdl* and other genes in close proximity may be part of a complex of related functions affecting early events that occur during oogenesis.

**Ionic changes at fertilization alter the orientation of pigment granule saltations in* Arbacia *eggs.* P. G. ALLEN, J. M. BALTZ, AND D. A. BEGG (Harvard Medical School, Boston, MA 02115).

Pigmented granules (PG) saltate throughout unfertilized *A. punctulata* eggs in a cytochalasin-sensitive process. After fertilization, PG are found strongly anchored to the cortex. Increased adhesion alone could account for the change in distribution observed. However, alterations in the paths followed by saltating PG could enhance this redistribution. Using time-lapse, DIC video microscopy, we have quantitatively analyzed the speed, distance, and direction of saltating PG, both before and after fertilization. We report that fertilization changes only the direction of these saltations. In the unfertilized egg, saltations follow paths that have no apparent polarity. After fertilization, the paths become radially aligned, and the majority of saltations become directed towards the cortex. Analysis of the signals regulating this transition indicate that both alterations in cytoplasmic calcium and pH are necessary to activate this process. These results suggest that the same ionic signals that trigger the reorganization of cortical actin at fertilization also induce the reorientation of PG saltations.

This work was supported by NIH RO1 HD20140 to DAB.

Localization of differentiation-specific mRNAs in differentiating F9 embryoid bodies. SANDY BECKER AND LAURA GRABEL (Biology Department, Wesleyan University, Middletown, CT 06457).

Primitive endoderm in the peri-implantation mouse embryo differentiates into two separate lineages: visceral and parietal endoderm

(VE and PE). F9 teratocarcinoma cells, when grown in suspension in the presence of retinoic acid, differentiate into embryoid bodies (EBs) consisting of a rind of VE, surrounding a core of stem cells. When dibutyryl cyclic AMP is also added to the culture medium, a rind of PE forms instead. These cells can therefore be used as a model system to study the role of cell interaction in the spatially appropriate induction of visceral- and parietal-specific gene expression. We have used a whole mount *in situ* hybridization technique, using digoxigenin labelled probes (BMB Genius) to visualize directly the localization of VE-specific AFP and PE-specific tPA mRNAs in EBs during their differentiation.

Results show that, whereas AFP and tPA mRNAs become localized to the endoderm layer in mature EBs, at earlier timepoints these endoderm-specific mRNAs are found in all cells of the EB. This suggests a two-step process wherein generalized up-regulation of expression of these transcripts throughout the EB precedes the restriction of expression to the outer differentiating layer. Results show also that AFP mRNA is localized to the apical edge of the VE in RA EBs, although other probes did not show such restriction. We also show that the low level of tPA previously reported in the VE of RA EBs (Sabbag *et al.* 1989. *Development* **106:** 195–201) is due not to a few aberrant cells among the VE, but to a low level of transcription of tPA by all the VE cells. We never see cells staining for endoderm-specific markers scattered randomly throughout the EB at early time points, then accumulating at the periphery as differentiation proceeds. This supports a model of embryogenesis in which lineage decisions are determined by cell position rather than sorting out of cells with distinct, predetermined lineage programs.

This work was supported by Grant #CD-314 from the American Cancer Society.

Gap junctional communication and homeobox genes in the regulation of pattern formation during chick limb development. Caroline N. D. Coelho, William B. Upholt, and Robert A. Kosher (Department of Anatomy, University of Connecticut Health Center, Farmington, CT 06030).

The zone of polarizing activity (ZPA) at the posterior margin of the limb bud appears to be the source of a diffusible morphogen, possibly retinoic acid (RA), that specifies the anterior-posterior (A-P) positional values of the skeletal elements of the limb according to its local concentration. We have found a gradient of gap junctional communication, as assayed by intercellular transfer of lucifer yellow dye, along the A-P axis of the limb bud, with extensive communication among posterior cells adjacent to the ZPA and progressively less communication among cells in more anterior regions of the limb bud. Such a gradient, possibly regulated by local RA concentrations, might generate a graded distribution of a low molecular weight intracellular regulatory molecule involved in specifying A-P positional values.

Homeobox containing genes have also been implicated in the regulation of pattern formation during limb development. We have studied, by *in situ* hybridization, the patterns of expression of the chicken homeobox genes GHox-7, -8, and -4.6 during chick limb development. Ghox-7 and -8 were localized to the anterior compartment of the limb, while Ghox-4.6 showed the opposite pattern and was restricted to the posterior ZPA containing region of the limb. These complementary patterns of expression along the A-P axis of the limb may suggest that interacting opposing gradients of expression of various molecules may be involved in determining positional values.

The apical ectodermal ridge (AER) is responsible for the outgrowth and formation of the various skeletal elements of the limb along the proximo-distal axis. We have found that the AER of the chick limb expresses GHox-8, while the cells directly subjacent to, and under the influence of, the AER express GHox-7. This observation suggests that GHox-7 and -8 may be involved in the function of the AER or in the ability of cells subjacent to the ridge to respond to its influence.

The shaping of the contours and digits of the developing limb is thought to occur through programmed cell death in localized regions of the limb, including the posterior necrotic zone (PNZ) and the interdigital mesenchyme (IDM). We have found that Ghox-8 and -7 are expressed in the PNZ and IDM, suggesting that these homeobox genes may also be involved in regulation of programmed cell death.

GABA function in locomotion and expulsion in Caenorhabditis elegans. Erik Jorgensen, Steve McIntire, and H. Robert Horvitz (HHMI, Department of Biology, MIT, Cambridge MA 02139).

GABA is the major inhibitory neurotransmitter of the central nervous system in mammals. We are studying GABA function in *C. elegans* and have identified genes required for GABA neurotransmission.

The neurotransmitter GABA inhibits muscle contraction in *C. elegans.* Muscimol, a GABA agonist, inhibits muscle contractions in wild-type animals. By contrast, *unc-25* mutants, which lack GABA immunoreactivity, display a hypercontracted (shrinker) phenotype. Killing the GABAergic VD and DD motorneurons also leads to the hypercontracted phenotype. These results suggest that GABA released from these motorneurons inhibits body muscle contractions.

The *unc-49* gene product mediates the inhibitory GABA input. *unc-49* mutants are similarly hypercontracted and are completely resistant to muscimol, which implies that *unc-49* encodes either a GABA receptor or a postsynaptic component required for receptor function.

GABA may provide a stimulatory function in defecation. *unc-25* animals *lack* contractions of the expulsion muscles during defecation and are constipated. Furthermore, killing two GABAergic neurons, AVL and DVB, phenocopies this expulsion defect. In the simplest model, GABA released from AVL and DVB directly stimulates muscle contraction; alternatively, AVL and DVB may act through an intervening neuron. Because *unc-49* mutants have normal expulsions, GABA cannot act through the *unc-49* product in expulsion muscle contraction, and a second receptor mechanism must exist.

A GABA agonist induces muscle contraction. More direct evidence that GABA can stimulate muscle contraction comes from experiments with muscimol. *unc-25 unc-49* double mutants lack expulsion muscle contractions and are resistant to inhibitory effects on muscle contraction by muscimol. Expulsions in such animals can be restored by muscimol or high concentrations of GABA. This rescue is not blocked by killing AVL and DVB, indicating that muscimol is acting postsynaptic to AVL and DVB, perhaps directly on the muscles.

AVL and DVB use exogenous GABA. Providing exogenous GABA at low concentrations to *unc-25* worms also rescues the expulsion defect. However, GABA rescue at these concentrations can be blocked by killing both AVL and DVB, or by adding nipecotic acid, a GABA reuptake blocker. We conclude that GABA at low concentrations is not acting directly on the muscle, but rather is taken up, presumably via a specific GABA transport protein, and then released by AVL and DVB. Thus, the only functional defect in *unc-25* appears to be a lack of GABA.

A number of mutants exist that display the shrinker phenotype or expulsion defects (S.M. and H.R.H., in prep.; Thomas 1990. *Genetics* **124:** 855–872). The pharmacological techniques described here will allow us to distinguish mutations causing presynaptic expulsion defects (affecting AVL and DVB or a preceding step) from those causing postsynaptic expulsion defects (presumably in the muscle).

*Cell motility and development in wild-type and mutant Dictyostelium *cells.*

DAVID KNECHT (University of Connecticut, Storrs, CT 06269), HEDI KERN, DIANE COX, JOHN CONDEELIS, DEB WESSELS, AND DAVID SOLL.

Dictyostelium amoebae undergo a variety of motile behaviors during their life cycle. These include random crawling, chemotactic migration toward bacteria during feeding, chemotactic migration towards endogenously produced cAMP to accomplish aggregation, and morphogenetic movements during development. In an effort to define the role of cytoskeletal components in driving and controlling these processes, we have begun to construct and analyze mutants that lack specific cytoskeletal proteins.

Dictyostelium cells have a single myosin II heavy chain gene. Mutants that do not express myosin II have been obtained by gene disruption and antisense RNA inhibition and have been described previously. During growth, some mutant cells become giant multinucleated syncytium due to incomplete cytokinesis, while during development, cells show severe alterations in chemotactic motility and are unable to perform morphogenetic movements. We have recently obtained new mutants by both antisense and insertional mutagenesis using a different parental cell line (AX3). These mutants share most of the phenotypes of the earlier cell lines, however, they are able to grow normally on a plastic substrate. The morphology and timing of cytokinesis appears similar to wild-type cells, indicating that these cells are able to accomplish cytokinesis in the absence of myosin II.

Mutants lacking the actin binding protein ABP-120 have also been constructed by insertional mutagenesis. This protein is believed to play a role in pseudopod formation or stability during chemotactic motility, since it is localized to newly formed pseudopods following a cAMP pulse and is capable of cross linking actin filaments into orthogonal arrays. Mutants that do not express ABP-120 are overtly normal in growth and development. However, high resolution computerized analysis of their motility reveals significant alterations in the rate, directionality, and mechanics of movement. In addition, synchronous biochemical analysis of the cAMP response reveals a significant reduction in F-actin incorporation into the cytoskeleton at the time when ABP-120 would normally be found in new pseudopods. Therefore, ABP-120 appears to play a role in pseudopodal motility, however, cells can overcome the loss of this protein and still accomplish development using other mechanisms.

Supported by GM 25813, 40599, HD 18577 and a training grant from NIH.

The use of PCR to identify novel mouse homeobox regions expressed during F9 embryoid body formation.

PATRICIA A. LABOSKY, MICHAEL P. WEIR, AND LAURA B. GRABEL (Department of Biology, Wesleyan University, Middletown, CT 06459).

We are interested in identifying genes involved in mediating early lineage decisions in the mouse embryo. F9 teratocarcinoma cells, when treated with retinoic acid in suspension culture, develop into embryoid bodies (EBs) with an inner core of stem cells and an outer layer of visceral endoderm. This mimics the early events seen in the peri-implantation mouse embryo and provides us with a model system. We are using PCR to identify novel homeobox containing genes that could be involved in establishing the visceral endoderm lineage. Degenerate primers most similar to the *zen* homeobox of *Drosophila* were used in PCR reactions with cDNAs from early EBs as template. The PCR product of the expected size was isolated, subcloned, and sequenced. Among the sub-cloned PCR products were representatives of previously identified mouse genes including Hox-1.3, -1.6, -1.7, -2.4, -2.8, and -3.1, as well as a clone representing a novel homeobox sequence. This novel homeobox appears to be most closely related to human HOX-3.6. This insert gives a single band on a Southern blot when the genomic DNA is cut with several different enzymes. Preliminary *in situ* hybridization analysis suggests that its expression is restricted to the outer edge in embryoid body differentiation. We are currently mapping this novel gene using the interspecies backcross technique, and constructing a cDNA library to obtain the entire coding sequence of the gene.

DC and AC field effects on early sea urchin development.

MICHAEL LEVIN, JORGE L. GONZÁLEZ, AND SUSAN G. ERNST (Department of Biology, Tufts University, Medford, MA 02155).

This study examined the effects of 300 Gauss DC magnetic fields and 60 Hz weak AC magnetic fields on the early development of two species of sea urchin: *Strongylocentrotus purpuratus* and *Lytechinus pictus*. Batches of developing eggs were exposed to the AC field (produced by a coil system) at different field strengths, or to the DC field of a permanent magnet starting at different times relative to fertilization. Samples of the continuous cultures were taken, fixed, and scored for cell division. It was demonstrated that AC fields between 17 and 88 Gauss in intensity produce a significant acceleration of early development (up to 90 min relative to controls, in the second cell division). The speed-up in the first two cell divisions is linearly dependent on the field strength. DC fields produced a significant delay in development; the effect is dependent on the time of initiation of exposure to the field. The optimum time of *L. pictus* is 30 min pre-fertilization, resulting in a delay of 22 min. The optimum time for *S. purpuratus* is 15 min pre-fertilization, resulting in a delay of 17 min. There is not a simple dose-effect relationship for exposure duration. The DC fields caused up to 8-fold increases in the incidence of exogastrulation in *L. pictus*, but not in *S. purpuratus*.

*The cytomechanics of growth cone-target interactions in Aplysia *bag cell neurons.*

CHI-HUNG LIN AND PAUL FORSCHER (Department of Biology, Yale University, New Haven, CT 06511).

Growth cones (GCs) of cultured *Aplysia* bag cell neurons are characterized by: a central cytoplasmic domain that exhibits directed microtubule-based organelle transport and a peripheral lamellar domain rich in F-actin. These actin networks are assembled along the leading GC margin and are translocated centripetally at rates of 3–6 μm/min. The resulting cortical actin flow is also capable of driving the movement of polycationic beads bound to the membrane surface (Forscher and Smith 1990, in *Optical Microscopy for Biology*, Wiley-Liss, Inc. pp. 459–471). In this study, GC-bead, GC-GC, and GC-neurite interactions were investigated using video-enhanced differential interference contrast microscopy and digital imaging techniques. When plated on poly-L-lysine substrates, isolated GCs migrated slowly (<0.5 μm/min). However, when two GCs encountered each other, ruffling in the peripheral domain became more intense at the contact site, followed by outward extension of the organelle enriched central domain at rates of 2–6 μm/min. The GC then turned and migrated along the neurite of the interacting GC at the rates of 1–3 μm/min. Using rhodamine-phalloidin and anti-β-tubulin double immunofluorescence staining at different time points during these interactions, F-actin was first observed to accumulate at the contact site, followed by microtubule extension, which correlated with preferential migration of the central domain toward the contact site. These interactions were reversibly inhibited by an actin poison, cytochalasin B. During the chronic exposure, the drug blocked both the GC-target interactions and neurite outgrowth.

This work was supported by National Institutes of Health grant NS28695 and The McKnight Endowment Fund for Neuroscience.

Distribution within dorsal root ganglia of horseradish peroxidase transported from the hindlimb bud of Rana pipiens. KAREN MONTGOMERY AND HAROLD D. BIBB (University of Rhode Island, Kingston, RI 02881).

The aim of this study was to determine, first, that time in development when the neural fibers extending to the hindlimb bud from ganglia 8, 9, and 10 are able to transport HRP and, second, the distribution of these transporting neurons in the spinal ganglia. Horseradish peroxidase was placed in the hindlimb rudiments of *Rana pipiens* of Taylor-Kollros stages III, IV, V, and X. The HRP pellets (0.15–0.33 mm) remained in the limb bud for 48 h, and the lumbar spinal cord and limb-associated ganglia were then fixed in 2.5% glutaraldehyde. The tissue was treated with diaminobenzidine, and 10 μm serial paraffin sections were cut. At stage III, when neural fibers are just entering the limb bud, fibers from all three ganglia demonstrate the capacity to transport HRP. The labelled neurons range in size, from the largest ones, to those with scant cytoplasm and with nuclear cross sectional areas as small as 40 μm^2. At stage X, when limb size permits a discrete placement of pellets, the 9th ganglia show labeled cells throughout their anterior-posterior extent, with the middle regions of each ganglion containing the largest number of labeled cell bodies. Similar numbers of labeled neurons are present dorsally and ventrally, and also laterally and medially. This distribution of labeled neurons suggests that fibers converging on a localized target area arise from cell bodies that are randomly distributed within the ganglia.

Developmental stage and contractile activity regulate expression of CAT transgene in skeletal muscle in vitro. JOHANNA L. PHILLIPS, OLIVERA JANJIC, AND JEANNE A. POWELL (Smith College, Northampton, MA 01063)

Transgenic mice from MLCCAT founder line 7 carry 45 copies (per haploid complement) of a transgene encoding the bacterial enzyme chloramphenicol acetyltransferase (CAT) integrated into the germline (Rosenthal *et al.* 1989. *PNAS* **86**: 7780–7784). The transgene is driven by the myosin light chain (MLC) 1 promoter–⅓ enhancer, so CAT expression is specific to skeletal muscle. The transgenic mice were bred to homozygosity (*cat/cat*) with respect to the transgene to achieve maximum CAT activity from individual transgenic nuclei. We were interested in the *in vitro* expression of CAT under the regulation of the MLC1 promoter–⅓ enhancer since expression of the two isoforms differs in developing (Periasamy *et al.* 1984. *J. Biol. Chem.* **259**: 13,595–13,604) and denervated muscle *in vivo* (Barton *et al.* 1989. *Development* **107**: 819–824). We examined three different stages of development: proliferating myoblasts/early fusion, early myotubes/late fusion, and mature myotubes that occasionally exhibited cross striations. We also examined three levels of contractile activity generated by maintaining cultures in media with different K^+ concentrations: quiescent myotubes (13 m*M* K^+), sporadically contractile myotubes (5 m*M* K^+), and highly contractile myotubes (3 m*M* K^+). CAT expression was detected biochemically by reacting culture cell extracts with a fluorescent derivative of chloramphenicol and acetyl CoA. The reaction products were separated by thin layer chromatography and visualized with UV illumination. In addition, CAT expression was detected immunocytologically, using an FITC-conjugated rabbit anti-CAT antibody. CAT expression was detected in some mononucleated myoblasts and in short myotubes at the onset of fusion, was strongest in myotubes at late fusion, and was weak in mature myotubes. Additionally, CAT was expressed at high levels in quiescent cultures, at intermediate levels in control cultures, and at low levels in cultures with enhanced contractile activity. The differential expression of CAT under these conditions may reflect preferential expression of MLC1.

Supported by grants from MDA and the Smith College Blakeslee Fund.

Identification of a cDNA encoding the cell recognition molecule, retina cognin. A. S. M. KRISHNA RAO AND R. E. HAUSMAN (Department of Biology, Boston University, Boston, MA 02215).

Cognin is a developmentally regulated 50 kDa cell surface glycoprotein that acts *in vitro* to enhance the reaggregation of embryonic retinal cells from chick and mouse, but not cells from other tissues. We report here the cloning of a cDNA encoding embryonic chick cognin. An embryonic chick retinal cDNA library was constructed in a λgt11 vector and screened with polyclonal antiserum to cognin. This screening yielded several immunoreactive clones. Antiserum was prepared to the fusion protein produced by one recombinant lysogen. This antiserum recognized a 50 kDa protein from retinal cell membranes, produced a developmental staining pattern in the chick retina similar to that seen with cognin antiserum and inhibited the *in vitro* aggregation of retinal cells. *In vitro* translation of RNAs from cDNA subclones yielded a 50 kDa protein that was recognized by cognin antiserum on Western blots. Using these criteria, we identify the cDNA clone as that encoding retina cognin. In addition, Northern blot analysis of embryonic chick retina with this cDNA probe detected two transcripts: a major 1.3 kb mRNA that, although present throughout embryogenesis, was most prominent in early embryonic retina, and a less abundant 1.9 kb mRNA.

Cloning of the chicken homologs of the human homeobox-containing genes Hox4F and 11 and analysis of their expression during chick limb development. BLANKA ROGINA, CAROLINE N. D. COELHO, ROBERT A. KOSHER, AND WILLIAM B. UPHOLT (Department of BioStructure and Function, University of Connecticut Health Center, Farmington, CT 06032).

Homeobox-containing genes are thought to be involved in the regulation of pattern formation and specification of positional information during vertebrate limb development on the basis of their regulated temporal and spatial expression during embryogenesis. To study the relationship between 5′ members of the Hox-4 gene cluster and the specification of positional identity, we have used polymerase chain reaction techniques to isolate the chicken cognates of mouse Hox-4.6 and human Hox-11 from a chick limb bud cDNA library. Published sequences for the human Hox-4F homeobox and its paralogs were compared and used to design oligonucleotides to be used as amplification primers in PCR reactions with aliquots of a limb cDNA library as template. The amplified DNA fragments were used to screen the cDNA library prepared from RNA isolated from 4–6 day embryonic chick limbs. Based on nucleotide and deduced amino acid sequences, six out of nine isolated cDNA clones have been identified as the chicken cognate of mouse Hox-4.6 (human Hox-4F), and three have been identified as the chicken cognate of human homeobox-containing gene Hox-11, a paralog of Hox-4.6. Our chicken cognate of the human Hox-11 differs in one amino acid from the human sequence, and our chicken cognate of human Hox-4.6 differs in two amino acids from human Hox-4F. The GHox-4.6 probe was hybridized to Northern blots of limb RNA from various stages and showed a band of 1.4 kb present at similar levels in stages 22–31. *In situ* hybridization analysis showed that at stage 24, high expression of GHox-4.6 is restricted to the ZPA (zone of polarizing activity)-containing posterior mesoderm of the limb bud with little or no expression detectable in the mesoderm in the middle or the anterior limb mesoderm. The ZPA is the putative source of diffusible morphogen, and this distribution of GHox-4.6 transcripts suggests that GHox-4.6 may be involved in the specification of pattern along the antero-posterior axis of the developing chick limb bud. Northern blots of GHox-11 mRNA showed a band at 2.7 kb. The intensity was similar in stages 22–28. GHox-4.6 and GHox-11 share considerable homology with each other over their entire lengths but do not contain the conserved amino terminus and conserved pentapeptide domains characteristic of the more 3′ homeobox genes of the major homeobox clusters.

Supported by NIH Grant HD22610.

Retina cognin mediates cholinergic differentiation in the embryonic chick retina. G. D. VIVEK SAGAR AND R. E. HAUSMAN (Department of Biology, Boston University, Boston, MA 02215).

Previous work showed that cholinergic differentiation in developing chick retina depends on insulin and cell-cell interactions. Here, we investigated the molecular nature of the dependence on cell interactions, specifically the role of retina cognin, a 50 kDa, retina-specific, cell recognition molecule. Cognin mediates cell adhesion *in vitro* and occurs during development on the same retinal neurons that exhibit cholinergic markers. We probed two markers of cholinergic differentiation: choline acetyltransferase (ChAT) activity and high affinity choline uptake. Both parameters show developmentally dependent increases during differentiation of retinal neurons in culture and can be measured by techniques published previously (Hausman *et al.* 1991. *Dev. Brain Res.* **59:** 31–38). Here, we blocked cognin-mediated cell interactions with antibodies specific to retina cognin and found a developmentally dependent reduction in ChAT activity but no reduction of high affinity choline uptake. Thus, the action of cognin-mediated cell interactions in cholinergic differentiation was by a pathway different than that of insulin, which stimulates both ChAT and choline uptake. This effect on the normal developmental increase in ChAT activity was seen only in retinal tissue, not in cerebrum or cerebellum, where ChAT activity increases normally with development. The effect of cognin antibodies was tissue specific and dose-dependent. Other molecules that bound to the surface of retinal neurons such as α-bungarotoxin or antibodies to the cell adhesion molecule Ng-CAM, did not inhibit ChAT activity. Thus, the effect was selective for cognin-mediated cell contact.

Supported by NIH grant EY04461.

**Germ plasm dynamics in* Xenopus *early development.* R. M. SAVAGE AND M. V. DANILCHIK (Biology Department, Wesleyan University, Middletown, CT 06459).

We have been studying the dynamic movements of germ plasm in early cleavage stage *Xenopus laevis* embryos. Components of the germ plasm can be selectively labeled with the fluorescent dye $DiOC_6$ (3), enabling us to track, using confocal laser-scanning microscopy and timelapse video, the movements of germ plasm in live embryos. We have defined three distinct phases of germ plasm movements during early cleavage. Approximately 500 islands of germ plasm are initially distributed throughout the vegetal subcortex in the unfertilized *Xenopus* egg. During the first cell cycle cortical cytoplasmic rotation, these islands move with the vegetal yolk mass. In early cleavage, the islands begin to aggregate into larger patches, eventually numbering usually less than 30. Concomitantly, these patches actively move towards the vegetal pole where they subsequently ingress into the embryo's interior along the cleavage furrows. The aggregation of germ plasm is microtubule dependent and microfilament independent, consistent with Ressom and Dixon's observations (1988. *Development* **103:** 507–518). However, experiments using pharmacological drugs, as well as parthogenetically activated egg data, show that ingression is cleavage dependent. We also discovered periodic cortical contractions that occur between cleavage divisions, which appear to drive the aggregated germ plasm towards the vegetal pole. Our efforts are presently focussed on understanding the mechanisms of these dynamic movements.

Modulation of programmed cell death and gene expression in mouse limb development. HARLEEN SINGH, MARCELLO CURTO, AJIT ALLES, AND ZAHRA ZAKERI (Department of Biology, Queens College of CUNY, Flushing, NY 11367)

Programmed cell death in interdigital areas strongly influences the correct morphogenesis of developing mouse limbs. This process shows the histomorphology of apoptosis (Kerr *et al.* 1972. *Br. J. Cancer* **26:** 239–257). Programmed cell death (PCD) requires RNA and protein synthesis, suggesting genetic control (Alles *et al.* 1991. *FASEB J.* **5:** 2127), with mechanisms still unknown. We used retinoic acid (RA), a gene expression regulator (Evans 1988. *Science* **240:** 889) and morphogen, to study interdigital cell death in embryonic limbs of Swiss Webster mice, where cell death normally reaches maximal levels at day 14 of gestation. We also analyzed the expression of the gene TRPM-2, which has been correlated with apoptosis in rat prostate involution (Buttyan 1989. *Mol. Cell Biol.* **9:** 3473–3481). RA 100 mg/kg was administered to 13 day pregnant females. The embryos were removed after 12 h. Dying cells were detected by Nile blue sulfate. RA expands areas of normal cell death, suggesting that it may play a role in normal PCD. Co-administration of actinomycin D (33 mg/kg) reduces this effect, indicating that the mode of cell death is by apoptosis. The effect of RA can also be seen in *in vitro* limb culture. Northern blot analysis of RNAs isolated from embryonic limbs and hybridized with a TRPM-2 cDNA radiolabeled probe showed progressively increasing levels of expression from day 12.5 (appearance of apoptosis) to day 16.5 (absence of apoptosis). The RA treatment also lowered TRPM-2 expression. The negative correlation between cell death and TRPM-2 expression suggests that in different tissues different sets of genes may be activated during apoptosis.

This work was supported by a grant from March of Dimes to ZZ and a fellowship from AIRC to MC.

Sea urchin Endo16 mRNA is potentially differentially processed, and its expression is sensitive to lithium chloride. MARGARET SOLTYSIK-ESPAÑOLA, CATHERINE NOCENTE-MCGRATH, ROBERT MCISAAC, AND SUSAN G. ERNST (Biology Department, Tufts University, Medford, MA 02155).

Northern blot and *in situ* hybridization analyses of spatial and temporal patterns of expression demonstrate that Endo16 encodes an endoderm-specific product and suggest that the Endo16 protein may play a role in gastrulation. Endo16 mRNA is first detected in the vegetal plate, a group of endodermal and mesenchymal precursor cells that will initiate gastrulation. As development proceeds, the transcript is expressed in cells of the invaginating archenteron, and becomes progressively restricted to the stomach as the archenteron differentiates into a three-part gut. Interestingly, the 6.8 kb message is not detected in the adult tissues, indicating that the function of the Endo16 gene product may be specific to embryogenesis. Indirect immunofluorescence studies reveal that the Endo16 protein appears to be localized on the surface of endodermal cells during gastrulation (Nocente-McGrath *et al.* 1989, *Dev. Biol.* **136:** 264–272). To determine the function of Endo16 in sea urchin development, we are using two approaches, (1) obtaining and analyzing the entire cDNA sequence of Endo16, and (2) examining the Endo16 expression when normal development is disrupted. The sequence analysis of three independent clones suggest the possibility of alternative splicing at the 3′ end of the message. Lithium chloride, a well known vegetalizing agent, causes overexpression of Endo16, as well as an increase of up to 1.7 fold in the proportion of endoderm tissue in the vegetal plate of LiCl-treated embryos. The increase of endoderm tissue as established by staining mesenchyme blastula embryos dissociated to single cells with both DAPI and Endo16 antibodies is proportional to the concentration of LiCl used. In addition, we observed a delay in development in lithium-treated embryos that is accompanied by a delay in the expression of a late class histone H2B gene.

Work supported by BRSG, the Betty Vernon & Charles Taylor Vernon Fund for Biological Research, and an NSF grant to SGE.

**Application of confocal laser scanning microscopy for spatial localization of actin, endoplasmic reticulum, and collagen mRNA in embryonic* Avian *corneal epithelia.* KATHY K. H. SVOBODA (Department of Anatomy and Neurobiology, Boston University School of Medicine, Boston, MA 02118).

Previous studies have shown that 6-day chick corneal epithelial cells produce types I, II, and IX collagen. In the current study, *in situ* hybridization, combined with confocal laser scanning analysis, was used to investigate the distribution of endoplasmic reticulum (ER) and collagen mRNA in whole mount preparations of freshly isolated corneal epithelia. cDNA probes specific for the C-propeptide region of $\alpha(1)$ and $\alpha(2)$ type I, and $\alpha(1)$ type II collagen were labeled with biotin-16-dUTP or digoxigenin-11-dUTP. The biotin labeled probes were visualized with avidin-FITC and digoxigenin-labeled probes identified with an antidigoxigenin Fab fragments conjugated to rhodamine. ER was localized with the lipophilic dye, DiOC6(3). Actin was labeled with FITC or rhodamine labeled phalloidin. $\alpha1$ and $\alpha2$ type I collagen mRNA colocalized, however, type I and II mRNA did not have the same distribution. There also appeared to be more type I than type II collagen mRNA in the corneal epithelial cells. Actin staining defined the cell borders and microvilli of the periderm cells and was prominent at the interface between the basal and periderm cells. The actin cortical mat in the basal compartment of the basal cells was visible in whole corneas and epithelia isolated +BL. ER was localized in both the periderm and basal cells. The basal cell staining was perinuclear in the center of the basal cells, then appeared as discrete spots in the individual optical section which were tubular in three-dimensional reconstructions. The *in situ* hybridization pattern for both type I and II collagen mRNA was similar to the ER staining pattern in the central region of the basal cells. Video recordings were made of the z-series images (Leica) and the double label *in situ* hybridization.

This work was supported by NIH grant, AR 38960, and the Whitaker Health Science Fund.

Construction of preimplantation mouse cDNA library by polymerase chain reaction. RUI YAN AND ANNA W. SEITZ (Department of Veterinary and Animal Sciences, University of Massachusetts at Amherst, Amherst, MA 01003).

Construction of cDNA libraries is a common approach for identification and characterization of differentially expressed gene products. The difficulty in obtaining a large number of mouse preimplantation embryos hampers this approach. We used polymerase chain reaction (PCR) to circumvent this problem. The cDNA synthesized from total RNA prepared from 200 morula-stage embryos was amplified to microgram quantities using PCR. The size of the amplified cDNA ranges from less than 0.5 kb to more than 4.0 kb. After fractionation cDNA larger than 0.4 kb was used for cloning and a library of 8.3×10^5 clones was obtained. The library is characterized for insert sizes and its representation of the poly(A)$^+$ RNA population in the morula embryo.

INDEX

A

A breeding population of the Western Pacific crab *Hemigrapsis sanguineus* (Crustacea: Decapoda: Grapsidae) established on the Atlantic coast of North America, 195
A dissection of the functions of PS integrins during *Drosophila* development, 507
A region of steady high calcium at the vegetal pole of *Medaka* eggs, 343
Acetylcholine, 484
Acid-base and ionic regulation, during and following emersion, in the freshwater bivalve, *Anodonta grandis simpsoniana* (Bivalvia: Unionidae), 289
Actin, 341
Aequorin, 325, 343
Agaricia, 104
Aggregation, 337
Albrecht, K., C. Oswald, N. Brooks, and H. Krider, An analysis of *abnormal* cell oocyte, *daughterless-abo-like,* and *wavoid-like* in *Drosophila melanogaster:* related genes that affect oocytes and embryos, 509
Allen, P. G., J. M. Baltz, and D. A. Begg, Ionic changes at fertilization alter the orientation of pigment granule saltations in *Arbacia* eggs, 509
Alles, Ajit, see Harleen Singh, 513
Alloimmunity in the gorgonian coral *Swiftia exserta,* 127
Alpha$_2$-macroglobulin, 350
Amacrine cell, 327
An analysis of *abnormal* cell oocyte, *daughterless-abo-like,* and *wavoid-like* in *Drosophila melanogaster:* related genes that affect oocytes and embryos, 509
Anodonta, 175, 289
Antibody, 500
Aplysia, 81, 325, 333, 340, 484
Aplysia neurons, 331
Application of confocal laser scanning microscopy for spatial localization of actin, endoplasmic reticulum, and collagen mRNA in embryonic *Avian* corneel epithelia, 513
Armstrong, Peter B., Atsushi Ikai, and James P. Quigley, Protease-binding activity of *Limulus* α_2-macroglobulin, 350
Arnold, John M., see Rui Wang, 348
Ascidian, 189
Asexual reproduction, 222
Askew, D., see D. Morrissey, 506
Asteriae, 95
Atema, Jelle, see Christy Karavanich, 359; and Paul A. Moore, 408
Atrial gland, 81
Augustine, George, see Peter Doroshenko, 320

B

Bacterial phylogeny, 135
Baltz, J. M., see P. G. Allen, 509
BAPTA buffers, 345
Barber, Bruce J., Susan E. Ford, and Robert N. Wargo, Genetic variation in the timing of gonadal maturation and spawning of the eastern oyster, *Crassostrea virginica* (Gmelin), 216
Barlow, R. B., Jr., see E. D. Herzog, 321
Barnacles, 442
Becker, Sandy, and Laura Grabel, Localization of differentiation-specific mRNAs in differentiating F9 embryoid bodies, 509
Begg, D. A., see P. G. Allen, 509
Behavior, 158, 402
Bernander, Öjvind, and Christof Koch, Synaptic background activity influences spatiotemporal integration of single pyramidal cells, 317
Beroë, 354, 355, 463
BFLP, 135
Bibb, Harold D., see Karen Montgomery, 511
Bigger, Charles, see Luisa Salter-Cid, 127
Biochemical changes associated with reduction of cell motility and aggregation following sulfate restriction in the marine sponge *Microciona prolifera,* 337
Biological activity of biosynthetic rainbow trout growth hormone in the eastern oyster, *Crassostrea virginica,* 459
Biological transport, 312
Bioluminescence, 135, 181
Bioluminescence maintenance in juvenile *Porichthys notatus,* 181
Bipolar cells, 323
Bivalve, 289, 298, 459
Blackman, Ronald K., see Michele Sanicola, 508
Blood cells, 189
Blue crab, 453
Body size, 261
Bodznick, David, see John Montgomery, 326
Böttcher, Kirsten, see Dietrich Siebers, 312
Boyle, Richard, and Stephen M. Highstein, Responses of horizontal semicircular canal afferents to rotary and mechanical stimulation, 319
Brachyuran crab, 195
Brooks, N., see K. Albrecht, 509
Brown, Alice F., Outbreeding depression as a cost of dispersal in the harpacticoid copepod, *Tigriopus californicus,* 123
Brown tide, 298
Browne (Harvey), Ethel, 72
Bucklin, Ann, and Lisa Kann, Mitochondrial DNA variation of copepods: markers of species identity and population differentiation in *Calanus,* 357
Bullis, Robert A., see Bryan Cherry, 358
Burger, Max M., see William J. Kuhns, 337
Byrne, Roger A., and Brian R. McMahon, Acid-base and ionic regulation, during and following emersion, in the freshwater bivalve, *Anodonta grandis simpsoniana* (Bivalvia: Unionidae), 289

C

Ca^{++}, 349
Ca uptake, 347
Calcium, 325, 331, 342, 343, 345, 348, 353
Calcium buffer injections block cytokinesis in *Xenopus* eggs, 345
Calcium in development, 342
Calcium waves accompany contraction waves in the *Oryzias latipes* (*Medaka*) blastoderm, 353
Calliobothrium verticillatum, 358
Cancer productus, 363
Carcinus maenas, 312
Cardioregulation, 353

Cardioregulatory peptides in *Limulus:* effects of F1, F2, and an endogenous FMRFamide-like peptide on the neurogenic heart, 353

Case, James F., see Allen F. Mensinger, 181

CCK, 484

Cell motility and development in wild-type and mutant *Dictyostelium* cells, 510

Cerrato, Robert M., Heather V. E. Wallace, and Kent G. Lightfoot, Tidal and seasonal patterns in the chondrophore of the soft-shell clam *Mya arenaria*, 307

Chang, Ernest S., see Jin-Hua Cheng, 169

Chappell, Richard L., see Robert Paul Malchow, 323; and Etha Schlemermeyer, 327

Charlton, Milton P., see Sally Schroeter, 328

Chelate limb, 158

Chemical
  detection, 419
  noise, 419
  signal, 359, 419

Chemical signal-to-noise detection by spiny lobsters, 419

Chemoreception, 205, 408, 419

Chen, Thomas T., see Kennedy T. Paynter, 459

Cheng, Jin-Hau, and Ernest S. Chang, Ecdysteroid treatment delays ecdysis in the lobster, *Homarus americanus*, 169

Cherry, Bryan, Allison S. Neese, Robert A. Bullis, and Gerhard A. Schad, Investigations into the life cycle of *Calliobothrium verticillatum*, a tapeworm of *Mustelus canis*, 358

Chia, Fu-Shiang, see Don R. Levitan, 371

Chondrophore, 307

Chong, Maria D., see Sherry D. Painter, 81

Cilia, 339

Ciliates, 500

Circadian rhythms, 321, 340

Cishek, Dawn M., Richard H. Sanger, and Lionel F. Jaffe, Towards the development of a technique for introducing aequorin into amoebae of *Dictyostelium discoideum* via electroporation, 342

Cloning of the chicken homologs of the human homeobox-containing genes Hox-4F and 11 and analysis of their expression during chick limb development, 512

Coelenterate, 127

Coelho, Caroline N. D., see Blanka Rogina, 512

Coelho, Caroline N. D., William B. Upholt, and Robert A. Kosher, Gap junctional communication and homeobox genes in the regulation of pattern formation during chick limb development, 510

Coenenchyme, 275

Coexistence of hydroid eating nudibranchs: do feeding biology and habitat use matter? 248

Comparative immunity, 127

Complex systems, 484

Condeelis, John, see David Knecht, 510

Construction of preimplantation mouse on cDNA library by polymerase chain reaction, 514

Copeland, D. Eugene, Fine structure of photophores in *Gonostoma elongatum*, detail of a dual gland complex, 144

Copepod, 123, 269, 357

Coral, 104

Coral reef fish, 199

Cormier, Jeffry, see Sherry D. Painter, 81

Courtship, 402

Cowan, Diane F., The role of olfaction in courtship behavior of the American lobster, *Homarus americanus*, 402

Cox, Diane, see David Knecht, 510

Cox, Rachel L., David L. Glick, and Felix Strumwasser, Isolation and protein sequence identificiation of *Aplysia californica* lens crystallins, 333

Crab, 312

Crab reproductive rhythms, 387

Crain, Richard C., Lynne M. Quarmby, and Yir G. Yueh, Inositol phospholipid metabolism is involved in deflagellation of *Chlamydomonas reinhardtii*, 507

Crassostrea virginica, 216

Crepidula veliger, 335

Crumpling behavior, 474

Crustacea, 158, 205, 402, 419

Crustacean reproduction, 387

Curto, Marcello, see Harleen Singh, 513

Cyclic nucleotide-mediated modulation of the pyloric motor pattern in the stomatogastric ganglion of the crab *Cancer borealis*, 329

Cytokinesis, 345

Cytomechanics of growth cone-target interactions in *Aplysia* bag cell neurons, The, 511

D

Danilchik, M. V., see R. M. Savage, 513

DC and AC field effects on early sea urchin development, 511

Defensive behavior, 363

Deiner, Michael, and Sidney Tamm, Mechanisms of paddle cilia formation in molluscan veligers, 335

Density dependence, 261

Developmental stage and contractile activity regulate expression of CAT transgene in skeletal muscle *in vitro*, 512

Diadema antillarum, 261

Dictyostelium, 342

Dietz, T. H., see D. B. Gardiner, 175

Differences in free calcium concentration between oocytes and nurse cells revealed by corrected aequorin luminescence, 349

Differential sensitivity, 419

Dioptric tissues, 144

Dispersal, 123

Dissection of ectopic function of the paired segmentation gene in *Drosophila* embryos, 506

Distance chemoreception, 363

Distribution of synaptic specialization in the frog cardiac ganglion, 328

Dolan, Liam, and R. Scott Poethig, Non cell-autonomous control of leaf morphogenesis in cotton (*Gossypium barbadense*), 506

Dominance, 359

Dormancy, 269

Doroshenko, Peter, Stephen Hess, and George Augustine, Inhibitory effects of nonhydrolyzable guanine nucleotides on neurotransmitter release at the squid giant synapse, 320

E

Ecdysteroid treatment delays ecdysis in the lobster, *Homarus americanus*, 169

Echinodermata, 371

Echinoid, 261

Ecker, J., see J. Kieber, 507

Effect of gravity on cytoplasmic streaming in characean cells, The, 508

Effect of hydrogen peroxide on preventing or contributing to polyspermic fertilization in sea urchin: modification by tamoxifen and macroglobulin, 346

Effects of indomethacin on active ion transport across the gills of the shore crab, *Carcinus maenas*, 312

Effects of vitamin E and OH-TEMPO (Spin Label Trap) on UV-induced dogfish (*Mustelus canis*) lens opacification relative to cytoskeletal actin, 341

Elasmobranch, 326

Electron microscopy, 144, 158

Electroporation, 342

Electrosense, 326

Emersion, 289

Enzymatic characterization of the morphogen recognized by *Agaricia humilis* (scleractinian coral) larvae, 104

Enzyme, 104

Epithelial adhesion, 463

ERG, 321

Ernst, Susan G., see Michael Levin, 511; and Margaret Soltysik-Española, 513

Ethel Browne, Hans Speman, and the discovery of the Organizer Phenomenon, 72

Evaluation of spermatocidal activity of water soluble gossypol on the sperms of *Arabacia punctulata* and *Spisula solidissima*, 347
External fertilization, 232

F

Feeding, 248, 419
Felder, Darryl L., see Todd L. Zimmerman, 387
Fertilization, 232, 336, 348
Fertilization success, 261, 371
Fine structure of photophores in *Gonostoma elongatum*: detail of a dual gland complex, 144
Fish, 232
Flagella, 339
Fluck, Richard A., Andrew L. Miller, and Lionel F. Jaffe, Calcium waves accompany contraction waves in the *Oryzias latipes* (*Medaka*) blastoderm, 353
Fluck, Richard A., see Lionel F. Jaffe, 343; and Jane A. McLaughlin, 345
Fluorescence, 348
FMRFamide, 484
FMRFamide-like peptides, 353
Ford, Susan E., see Bruce J. Barber, 216
Forscher, Paul, see Chi-Hung Lin, 511
Frenkel, Krystyna, see Margalit Rosenkranz, 346
Freyd, Gwen, and H. Robert Horvitz, Neuronal and cell-lineage expression patterns of the *C. elegans* cell lineage gene lin-11, 508
Function of surface sclerites in gorgonians (Coelenterata, Octocorallia), The, 275

G

GABA, 484, 510
GABA function in locomotion and expulsion in *C. elegans*, 510
Gainey, Louis F., Jr., and Sandra E. Shumway, The physiological effect of *Aureococcus anophagefferens* ("brown tide") on the lateral cilia of bivalve mollusks, 298
Gamete kinetics, 371
Gap junctional communication and homeobox genes in the regulation of pattern formation during chick limb development, 510
Gardiner, D. B., F. S. Turner, J. M. Myers, T. H. Dietz, and H. Silverman, Long-term culture of freshwater mussel gill strips: use of serotonin to affect aseptic conditions, 175
Gargonacea, 275
Gastropod ecology, 363
Gelbart, W. M., see Michele Sanicola, 508; and Kristi Wharton, 508
Genetic analysis of hormone regulated seedling development in *Arabidopsis thaliana*, 507
Genetic variation in the timing of gonadal maturation and spawning of the eastern oyster, *Crassostrea virginica* (Gmelin), 216
Germ plasm dynamics in *Xenopus* early development, 513
Gill, 312
Gill culture, 175
Gill musculature, 175
Glick, David L., see Rachel L. Cox, 333
Glycosaminoglycan, 104
Gonadal development, 216
González, Jorge, see Michael Levin, 511
Gossypol, 347
Govind, C. K., see A. T. Read, 158
Grabel, L. B., see M. E. Lenburg, 506; Sandy Becker, 509; and Patricia A. Labosky, 511
Gray, Ann, see Sherry D. Painter, 81
Greaves, John, see Charlotte P. Mangum, 453
Grinblat, Yevgenya, see Susan B. Zusman, 507
Groome, James R., Cardioregulatory peptides in *Limulus*: effects of F1, F2, and an endogenous FMRFamide-like peptide on the neurogenic heart, 353
Growth, 379, 459
Growth hormone, 459
Growth, rank, and maturation of the freshwater prawn, *Macrobrachium rosenbergii*: analysis of marked prawns in an experimental population, 379
GTP-binding proteins, 320
Guzman, P., see J. Kieber, 507
Gynogenesis, 222

H

Haneji, Tatsuji, see Hiroshi Ueno, 347
Hausman, R. E., see G. D. Vivek Sagar, 512; and A. S. M. Krishna Rao, 512
Haygood, Margo G., see Connie J. Wolfe, 135
Hemigrapsis sanguineus, 195
Hemocyanin, 453
Hermaphroditism, 199
Hermit crab, 238
Herzog, E. D., and R. B. Barlow, Jr., Ultraviolet light from the nighttime sky enhances retinal sensitivity of *Limulus*, 321
Hess, Stephen, see Peter Doroshenko, 320
High-resolution, 4-dimensional imaging of early development in *Lytechinus variegatus*, 336
Highstein, Stephen M., see Richard Boyle, 319
Histamine, 484
Histocompatibility, 127
History of science (biology), 72
Homarus americanus, 402
Horizontal canal, 319
Horseshoe crab, 353
Horvitz, H. Robert, see Gwen Freyd, 508; and Erik Jorgensen, 510
How *Beroë* keeps its mouth shut, or its lips are sealed, 354
Hulata, G., see Z. Ra'anan, 379
Hyalophora cecropia, 349
Hyara, 72
Hydrodynamics, 442
Hydrogen peroxide, 346
Hydroid, 248
Hydromedusa, 474
Hydrozoa, 474
Hynes, Richard O., see Susan B. Zusman, 507

I

Identification in *Drosophila* of a new member of the TGF-β superfamily of cell signalling molecules, 508
Identification of a cDNA encoding the cell recognition molecule, retina cognin, 512
Ikai, Atsushi, see Peter B. Armstrong, 350
Ikegami, Susumu, Tomoko Mitsuno, Masanori Kataika, Satoshi Yajima, and Miéko Komatsu, Immunological survey of planktonic embryos and larvae of the starfish, *Asterina pectinifera*, obtained from the sea, using a monoclonal antibody directed against egg polypeptides, 95
Imaging free calcium in cultured *Aplysia* bag cell neurons, 325
Imaging preterminal calcium concentration microdomains in the squid giant synapse, 316
Immunochemistry, 500
Immunodetection, 95
Immunohistochemistry of diverging and converging neurotransmitter systems in mollusks, 484
Immunological survey of planktonic embryos and larvae of the starfish, *Asterina pectinifera*, obtained from the sea, using a monoclonal antibody directed against egg polypeptides, 95
Inbreeding depression, 123
Indomethacin, 312
Inducer, 104
Influence of body size and population density on fertilization success and reproductive output in a free-spawning invertebrate, 261
Inhibitory effects of nonhydrolyzable guanine nucleotides on neurotransmitter release at the squid giant synapse, 320

Inositol phospholipid metabolism is involved in deflagellation of *Chlamydomonas reinhardtii*, 507

Inoué, Shinya, Andreas Stemmer, Theodore Inoué, and Robert A. Knudson, High-resolution, 4-dimensional imaging of early development in *Lytechinus variegatus*, 336

Inoué, Theodore, see Shinya Inoué, 336

Input resistance, 317

Integrin phosphorylation and focal contact assembly in dihydrocytochalasin B treated differentiating F9 cells, 506

Intracellular dyes, 332

Introduced marine species, 195

Invertebrate immunity, 350

Invertebrate tissue culture, 175

Investigations into the life cycle of *Calliobothrium verticillatum*, a tapeworm of *Mustelus canis*, 358

Ion regulation, 289

Ionic changes at fertilization alter the orientation of pigment granule saltations in *Arbacia* eggs, 509

Iridocyte (iridosome), 144

Isolation and protein sequence identification of *Aplysia californica* lens crystallins, 333

J

Jaffe, Lionel F., Andrew L. Miller, and Richard A. Fluck, A region of steady high calcium at the vegetal pole of *Medaka* eggs, 343

Jaffe, Lionel F., see Andrew L. Miller, 325; Dawn M. Chisek, 342; Jane A. McLaughlin, 345; Richard I. Woodruff, 349; Richard A. Fluck, 352; and Rui Wang, 348

Janjic, Olivera, see Johanna L. Phillips, 512

Jellyfish, 474

Jorgensen, Erik, Steve McIntire, and H. Robert Horvitz, GABA function in locomotion and expulsion in *C. elegans*, 510

K

Kafatos, Fotis, see Susan B. Zusman, 507

Kanamori, Kan, see Hitoshi Michibata, 189

Kann, Lisa, see Ann Bucklin, 357

Karavanich, Christy, and Jelle Atema, Role of olfaction in recognition of dominance in the American lobster (*Homarus americanus*), 359

Karplus, I., see Z. Ra'anan, 379

Karyology, 222

Kataoka, Masanori, see Susumu Ikegami, 95

Kaupp, Sandor E., see Mark D. Ohman, 500

KCl-induced calcium rise in squid eggs: measurement of fura-2 fluorescence, 348

Kern, Hedi, see David Knecht, 510

Kieber, J., P. Guzman, G. Roman, A. Wollenberg, and J. Ecker, Genetic analysis of hormone regulated seedling development in *Arabidopsis thaliana*, 507

Kinetics of fertilization in the sea urchin *Strongylocentrotus franciscanus:* interaction of gamete dilution, age, and contact time, 371

Knecht, David, Hedi Kern, Diane Cox, John Condeelis, Deb Wessels, and David Soll, Cell motility and development in wild-type and mutant *Dictyostelium* cells, 510

Knudson, Robert A., see Shinya Inoué, 336

Koch, Christof, see Öjvind Bernander, 317

Koide, Samuel S., see Hiroshi Ueno, 347

Komatsu, Miéko, see Susumu Ikegami, 95

Kosher, Robert A., see Caroline N. D. Coelho, 510; and Blanka Rogina, 512

Krider, H., see K. Albrecht, 509

Kuhns, William J., Max M. Burger, and Gradimir Misevic, Biochemical changes associated with reduction of cell motility and aggregation following sulfate restriction in the marine sponge *Microciona prolifera*, 337

Kumari, S. Sindhu, see Jack J. O'Brien, 427

Kuris, A., see Z. Ra'anan, 379

L

LaBarbara, Michael, see Julie Pullen, 442

Labosky, Patricia A., Michael P. Weir, and Laura B. Grabel, The use of PCR to identify novel mouse homeobox regions expressed during F9 embryoid body formation, 511

Lambert, Walter J., Coexistence of hydroid eating nudibranchs: do feeding biology and habitat use matter? 248

Landowne, David, Change in optical activity associated with impulses in squid fin nerves, 322

Langmuir circulation, 360

Larvae, 104, 205

Lateral cilia, 298

Leapfrog, 379

Lectin, 104

Lenburg, M. E., and L. B. Grabel, Integrin phosphorylation and focal contact assembly in dihydrocytochalasin B treated differentiating F9 cells, 506

Lenhoff, Howard M., Ethel Browne, Hans Speman, and the discovery of the Organizer Phenomenon, 72

Lens, 333

Lens epithelium, 341

Leopold, A. Carl, see Randy Wayne, 508

Levin, Michael, Jorge L. González, and Susan G. Ernst, DC and AC field effects on early sea urchin development, 511

Levitan, Don R., Influence of body size and population density on fertilization success and reproductive output in a free-spawning invertebrate, 261

Levitan, Don R., Mary A. Sewell, and Fu-Shiang Chia, Kinetics of fertilization in the sea urchin *Strongylocentrotus franciscanus:* interaction of gamete dilution, age, and contact time, 371

Lewis, J. C., and E. von Wallis, The function of surface sclerites in gorgonians (Coelenterata, Octocorallia), 275

Lightfoot, Kent G., see Robert M. Cerrato, 307

Ligumia, 175

Lim, Jong S., see Margalit Rosenkranz, 346

Lin, Shi-Hung, and Paul Forscher, The cytomechanics of growth cone-target interactions in *Aplysia* bag cell neurons, 511

Llinás, R., M. Sugimori, and Robert B. Silver, Imaging preterminal calcium concentration microdomains in the squid giant synapse, 316

Lobster, 402, 419

Localization of differentiation-specific mRNAs in differentiating F9 embryoid bodies, 509

Long-term monitoring of Ca^+ in cultured *Aplysia* neurons with fluorescent probes, 331

Luciferin, 181

Luminescent organs, 144

M

Macrobrachium rosenbergii, 379

Macrociliary tooth patterns in beroid ctenophores, 355

Macrogloblin, 346

Malchow, Robert Paul, Richard L. Chappell, and Harris Ripps, Voltage- and ligand-gated conductances of bipolar cells from the skate retina, 323

Mangum, Charlotte P., John Greaves, and Julia S. Rainer, Oligomer composition and oxygen binding of the hemocyanin of the blue crab *Callinectes sapidus*, 453

Marcus, Nancy H., Planktonic copepods in a sub-tropical estuary; seasonal patterns in the abundance of adults, copepodites, nauplii, and eggs in the sea bed, 269

Marko, Peter B., and A. Richard Palmer, Responses of a rocky shore gastropod to the effluents of predatory and non-predatory crabs: avoidance and attraction, 363

Maturation, 379

McDermott, John J., A breeding population of the Western Pacific crab *Hemigrapsis sanguineus* (Crustacea: Decapoda: Grapsidae) established on the Atlantic coast of North America, 195

McIntire, Steve, see Erik Jorgensen, 510

McIntyre, Joseph, see Felix Strumwasser, 331
McIsaac, Robert, see Margaret Soltysik-Española, 513
McLaughlin, Jane A., Andrew L. Miller, Richard A. Fluck, and Lionel F. Jaffe, Calcium buffer injections block cytokinesis in *Xenopus* eggs, 345
McMahon, Brian R., see Roger A. Byrne, 289
McNamara, John C., see Eliana Scemes, 474
McTeague, J. A., see A. T. Read, 158
Mechanisms of paddle cilia formation in molluscan veligers, 335
Mensinger, Allen F., and James F. Case, Bioluminescence maintenance in juvenile *Porichthys notatus,* 181
Mesopelagic fish, 144
Metabolism, 459
Metamorphosis, 104
Michibata, Hitoshi, Akemi Morita, and Kan Kanamori, Vanadobin, a vanadium-binding substance, extracted from the blood cells of an ascidian, can reduce vanadate (V) to vanadyl (IV), 189
Microgrowth patterns, 307
Midshipman fish, 181
Miller, Andrew L., Peter J. S. Smith, Carol A. Rainville, Osamu Shimomura, Felix Strumwasser, and Lionel F. Jaffe, Imaging free calcium in cultured *Aplysia* bag cell neurons, 325
Miller, Andrew L., see Jane A. McLaughlin, 345, Richard I. Woodruff, 349, Richard L. Fluck, 352, Rui Wang, 348, and Lionel F. Jaffe, 343
Misevic, Gradimir, see William J. Kuhns, 337
Mitochondrial DNA variation of copepods: markers of species identity and population differentiation in *Calanus,* 357
Mitosis, 336
Mitsuno, Tomoko, see Susumu Ikegami, 95
Mixed layer, 360
Modes of feeding in aggregations of barnacles and the shape of aggregations, 442
Modulation of programmed cell death and gene expression in mouse limb development, 513
Molluscan tissue culture, 175
Mollusk, 81, 222
Monoclonal antibody, 95
Monomeric subunit composition, 453
Montgomery, John, and David Bodznick, Properties of medullary interneurons of the skate electrosense provide evidence for the neural circuitry mediating ventilatory noise suppression, 326
Montgomery, Karen, and Harold D. Bibb, Distribution within dorsal root ganglia of horseradish peroxidase transported from the hindlimb bud of *Rana pipiens,* 511
Moore, Paul A., and Jelle Atema, Spatial information in the three-dimensional fine structure of an aquatic odor plume, 408
Moran, Denis, Voltage-dependent -L-type Ca^{2+} channels VDCCs participate in regulating neural crest development, 506
Morita, Akemi, see Hitoshi Michibata, 189
Morphogen, 104
Morphology and behavior of an unusually flexible thoracic limb in the snapping shrimp, *Alpheus heterochelis,* 158
Morrissey, D., D. Askew, L. Raj, and M. Weir, Dissection of ectopic function of the paired segmentation gene in *Drosophila* embryos, 506
Morse, Aileen N. C., see Daniel E. Morse, 104
Morse, Daniel E., and Aileen N. C. Morse, Enzymatic characterization of the morphogen recognized by *Agaricia humilis* (scleractinian coral) larvae, 104
Motility, 337
Mouth, 354
Mouth closure, 463
Mpitsos, George J., see Seppo Soinila, 484
Mustafa, Tarig, see Dietrich Siebers, 312
Mustelus canis, cestode parasite of, 358
Mya arenaria, 307
Myers, T. H., see D. B. Gardiner, 175

N

Nagle, Gregg T., see Sherry D. Painter, 81
Neese, Allison S., see Bryan Cherry, 358
Neural networks, 329
Neuromodulator, 329
Neuromuscular junctions, 474
Neuronal and cell-lineage expression patterns of the *C. elegans* cell lineage gene lin-11, 508
Neuronal growth, 331
Neurotransmitters, 484
New Jersey, 195
Nocente-McGrath, Catherine, see Margaret Soltysik-Española, 513
Noise suppression, 326
Non cell-autonomous control of leaf morphogenesis in cotton (*Gossypium barbadense*), 506
Northern anchovy larvae, 500
Nudibranch, 248
Nusbaum, Michael P., see Nelson Sprutson, 329

O

O'Brien, Jack J., S. Sindhu Kumari, and Dorothy M. Skinner, Proteins of crustacean exoskeletons: I. Similarities and differences among proteins of the four exoskeletal layers of four brachyurans, 427
O'Brien, M. M., Al Plueddemann, and R. A. Weller, The response of oceanic mixed layer depth to physical forcing: modelled vs. observed, 360
O'Foighil, Diarmaid, and Catherine Thiriot-Quiévreux, Ploidy and pronuclear interaction in northeastern Pacific *Lasaea* clones (Mollusca: Bivalvia), 222
Ocelli, 321
Octocorallia, 275
Odor plumes, 408
Ohman, Mark D., Gail H. Theilacker, and Sandor E. Kaupp, Immunochemical detection of predation on ciliate protists by larvae of the northern anchovy (*Engraulis mordax*), 500
Olfaction, 359, 402
Oligomer composition and oxygen binding of the hemocyanin of the blue crab *Callinectes sapidus,* 453
Ontogeny *versus* phylogeny in determining patterns of chemoreception: initial studies with fiddler crabs, 205
Optical recording of membrane potential changes from single neurons using intracellular voltage-sensitive dyes, 332
Organizer, 72
Orientation, 408
Ostracod, 181
Oswald, C., see K. Albrecht, 509
Outbreeding depression as a cost of dispersal in the harpacticoid copepod, *Tigriopus californicus,* 123
Ovarian follicle, 349
Oxygen binding, 453
Oysters, 216, 459

P

Paddle cilia, formation of, 335
Paguroidea, 238
Painter, Sherry D., Maria G. Chong, Mary A. Wong, Ann Gray, Jeffry G. Cormier, and Gregg T. Nagle, Relative contributions of the egg layer and egg cordon to pheromonal attraction and the induction of mating and egg-laying behavior in *Aplysia,* 71
Palmer, A. Richard, see Peter B. Marko, 363
Panulirus, 419
Paynter, Kennedy T., and Thomas T. Chen, Biological activity of biosynthetic rainbow trout growth hormone in the eastern oyster, *Crassostrea virginica,* 459
Peifer, M., E. Wieschaus, B. Riggleman, and C. Rauskolb, The role of *Drosophila* gene *armadillo* in cell interactions and *wingless* signaling, 507
Peterson, Christopher W., Variation in fertilization rate in the tropical reef fish, *Halichoeres bivattatus:* correlates and implications, 232
Pheromones, 81, 402

Phillips, Johanna L., Olivera Janjic, and Jeanne A. Powell, Developmental stage and contractile activity regulate expression of CAT transgene in skeletal muscle *in vitro*, 512

Photophores, 144

Physical forcing, 360

Physiological effect of *Aureococcus anophagefferens* ("brown tide") on the lateral cilia of bivalve mollusks, The, 298

Plankton, 95

Planktonic copepods in a sub-tropical estuary; seasonal patterns in the abundance of adults, copepodites, nauplii, and eggs in the sea bed, 269

Pleurobranchaea californica, 484

Ploidy and pronuclear interaction in northeastern Pacific *Lasaea* clones (Mollusca: Bivalvia), 222

Plueddemann, Al, see M. M. O'Brien, 360

Poethig, R. Scott, see Liam Dolan, 506

Polysaccharide, 104

Polyspermic fertilization, 346

Population genetics, 357

Porichthys notatus, 181

Powell, Jeanne A., see Johanna L. Phillips, 512

Prawn, 379

Predator avoidance, 363

Prey-predation interactions, 500

Prior, G., see R. E. Stephens, 339

Properties of medullary interneurons of the skate electrosense provide evidence for the neural circuitry mediating ventilatory noise suppression, 326

Protease inhibitor, 350

Protease-binding activity of *Limulus* α2-macroglobulin, 350

Protein sequence, 333

Proteins, 340, 427

Proteins of crustacean exoskeletons: I. Similarities and differences among proteins of the four exoskeletal layers of four brachyurans, 427

Protogyuy, 199

Pullen, Julie, and Michael LaBarbara, Modes of feeding in aggregations of barnacles and the shape of aggregations, 442

Pyramidal cells, 317

Q

Quarmby, Lynne M., see Richard C. Crain, 507

Quigley, James P., see Peter B. Armstrong, 350

R

Ra'anan, Z., A. Sagi, Y. Wax, I. Karplus, G. Hulata, and A. Kuris, Growth, rank, and maturation of the freshwater prawn, *Macrobrachium rosenbergii*; analysis of marked prawns in an experimental population, 379

Radial neuromuscular system, 474

Rafferty, N. S., see S. Zigman, 341

Raftery, Laurel A., see Michele Sanicola, 508

Rainer, Julia S., see Charlotte P. Mangum, 453

Rainville, Carol A., see Andrew L. Miller, 325; and Felix Strumwasser, 331

Raj, L., see D. Morrissey, 506

Rao, A. S. M. Krishna, and R. E. Hausman, Identification of a cDNA encoding the cell recognition molecule, retina cognin, 512

Rauskolb, C., see M. Peifer, 507

Read, A. T., J. A. McTeague, and C. K. Govind, Morphology and behavior of an unusually flexible thoracic limb in the snapping shrimp, *Alpheus heterochelis*, 158

Reduction, 189

Regulation of a *Drosophila* growth factor homolog, *decapentaplegic (dpp)* in imaginal disks, 508

Regulation of *mec-3*, a homeobox-containing gene that controls mechanoreceptor neuronal differentiation in *C. elegans*, 509

Relative contributions of the egg layer and egg cordon to pheromonal attraction and the induction of mating and egg-laying behavior in *Aplysia*, 71

Reproduction, 216, 232, 402

Reproductive
  behavior, 81
  ecology, 387
  success, 261

Reproductive ecology of an intertidal brachyuran crab, *Sesarma* sp. (nr. *reticulatum*), from the Gulf of Mexico, 387

Response of oceanic mixed layer depth to physical forcing: modelled vs. observed, The, 360

Responses of a rocky shore gastropod to the effluents of predatory and non-predatory crabs: avoidance and attraction, 363

Responses of horizontal semicircular canal afferents to rotary and mechanical stimulation, 319

Resting eggs, 269

Restriction fragment length polymorphism analysis reveals high levels of genetic divergence among the light organ symbionts of flashlight fish, 135

Retina, 323

Retina cognin mediates cholinergic differentiation in the embryonic chick retina, 512

Reversible epithelial adhesion closes the mouth of *Beroë*, a carnivorous marine jelly, 463

Riggleman, B., see M. Peifer, 507

Ripps, Harris, see Robert Paul Malchow, 323

Rogina, Blanka, Caroline N. D. Coelho, Robert A. Kosher, and William B. Upholt, Cloning of the chicken homologs of the human homeobox-containing genes Hox-4F and 11 and analysis of their expression during chick limb development, 512

Role of *Drosophila* gene *armadillo* in cell interactions and *wingless* signaling, The, 507

Role of olfaction in courtship behavior of the American lobster, *Homarus americanus*, The, 402

Role of olfaction in recognition of dominance in the American lobster (*Homarus americanus*), 359

Roman, G., see J. Kieber, 507

Rosenkranz, Margalit, Jong S. Lim, Krystyna Frenkel, and Walter Troll, Effect of hydrogen peroxide on preventing or contributing to polyspermic fertilization in sea urchin: modification by tamoxifen and macroglobulin, 346

S

Sagar, G. D. Vivek, and R. E. Hausman, Retina cognin mediates cholinergic differentiation in the embryonic chick retina, 512

Sagi, A., see Z. Ra'anan, 379

Salter-Cid, Luisa, and Charles H. Bigger, Alloimmunity in the gorgonian coral *Swiftia exserta*, 127

Sanger, Richard H., see Dawn M. Cishek, 342

Sanicola, Michele, Laurel A. Raftery, Ronald K. Blackman, and W. M. Gelbart, Regulation of a *Drosophila* growth factor homolog, *decapentaplegic (dpp)* in imaginal disks, 508

Savage, R. M., and M. V. Danilchik, Germ plasm dynamics in *Xenopus* early development, 513

Scemes, Eliana, and John C. McNamara, The ultrastructure of the radial neuromuscular system of the jellyfish *Liriope tetraphylla* (Hydrozoa, Trachymedusae): implications in crumpling behavior, 474

Schad, Gerhard A., see Bryan Cherry, 358

Schlemermeyer, Etha, and Richard L. Chappell, Serotonin-like immunoreactivity reveals evidence for centrifugal fibers and a distinctive class of amacrine cell in the skate retina, 327

Schoeter, Sally, and Milton P. Charlton, Distribution of synaptic specialization in the frog cardiac ganglion, 328

Sclerite function, 275

SCPb, 484

Sea urchin Endo 16 mRNA is potentially differentially processed, and its expression is sensitive to lithium chloride, 513

Second messengers, 329

Segal, Sheldon J., see Hiroshi Ueno, 347

Seitz, Anna W., see Rui Yan, 514

Self-organization, 484

Semicircular canal, 319
Sensory biology, 408
Serotonin, 175, 327
Serotonin-like immunoreactivity reveals evidence for centrifugal fibers and a distinctive class of amacrine cell in the skate retina, 327
Serotonins, 484
Sesarma, 387
Settlement, 104
Sewell, Mary A., see Don R. Levitan, 371
Sex change, 199
Shimomura, Osamu, see Andrew L. Miller, 325
Shumway, Sandra E., see Louis F. Gainey, Jr., 298
Siebers, Dietrich, Tarig Mustafa, and Kirsten Böttcher, Effects of indomethacin on active ion transport across the gills of the shore crab, *Carcinus maenas*, 312
Signal, 104
Signal integration, 332
Silver, Robert B., see R. Llinas, 316
Silverman, H., see D. B. Gardiner, 175
Singh, Harleen, Marcello Curto, Ajit Alles, and Zahra Zakeri, Modulation of programmed cell death and gene expression in mouse limb development, 513
Skate, 323
Skate retina, 327
Skinner, Dorothy M., see Jack J. O'Brien, 427
Smith, Peter J., see Andrew L. Miller, 325
Snapping shrimp, 158
Social control of sex change in the bluehead wrasse, *Thalassoma bifasciatum* (Pisces: Labridae), 199
Social organization, 379
Soinila, Seppo, and George J. Mpitsos, Immunohistochemistry of diverging and converging neurotransmitter systems in mollusks, 484
Soll, David, see David Knecht, 510
Soltysik-Española, Margaret, Catherine Nocente-McGrath, Robert McIsaac, and Susan G. Ernst, Sea urchin Endo 16 mRNA is potentially differentially processed, and its expression is sensitive to lithium chloride, 513
Spatial information in the three-dimensional fine structure of an aquatic odor plume, 408
Spawning, 232, 261
Speman, Hans, 72
Sperm motility, 347
Spermatophore diversity within and among the hermit crab families, Coenobitidae, Diogenidae, and Paguridae (Paguroidea, Anomura, Decapoda), 238
Spermatophores, 238
Sponge sulfate restriction, 337
Spruston, Nelson, and Michael Nusbaum, Cyclic nucleotide-mediated modulation of the pyloric motor pattern in the stomatogastric ganglion of the crab *Cancer borealis*, 329
Starfish embryo, 95
Staves, Mark, see Randy Wayne, 508
Stemmer, Andreas, see Shinya Inoué, 336
Stephens, R. E., and G. Prior, Tektins from *Spisula solidissima* cilia, 339
Strombidium, 500
Stronglyocentrotus franciscanus, 371
Strumwasser, Felix, Joseph McIntyre, and Carol A. Rainville, Long-term monitoring of Ca^+ in cultured *Aplysia* neurons with fluorescent probes, 331
Strumwasser, Felix, see Andrew L. Miller, 325; Jacalyn Vogel, 340; and Rachel L. Cox, 333
Sugimori, M., see R. Llinas, 316
Sulfated Polysaccharide, 104
Suspension feeding, 442
Svoboda, Kathy K. H., Application of confocal laser scanning microscopy for spatial localization of actin, endoplasmic reticulum, and collagen mRNA in embryonic *Avian* corneel epithelia, 513
Swearer, Stephen E., see Robert R. Warner, 199
Symbiosis, 135
Synapse, 320, 474
Synaptic background activity influences spatiotemporal integration of single pyramidal cells, 317

T

Tamm, Sidney L., and Signhild Tamm, How *Beroë* keeps its mouth shut, or its lips are sealed, 354
Tamm, Sidney L., and Signhild Tamm, Reversible epithelial adhesion closes the mouth of *Beroë*, a carnivorous marine jelly, 463
Tamm, Sidney, see Michael Deiner, 335, and Signhild Tamm, 355
Tamm, Signhild, and Sidney Tamm, Macrociliary tooth patterns in beroid ctenophores, 355
Tamm, Signhild, see Sidney L. Tamm, 354, 463
Tamoxifen, 346
Teeth, 355
Tektins from *Spisula solidissima* cilia, 339
Tettraphyllidean life cycle, 358
Thalassoma bifasciatum, 199
Theilacker, Gail H., see Mark D. Ohman, 500
Thiriot-Quiévreux, Catherine, see Diarmaid O'Foighil, 222
Threshold, 419
Tidal and seasonal patterns in the chondrophore of the soft-shell clam *Mya arenaria*, 307
Tigriopus californicus, 123
Tissue adhesion, 354
Tissue culture decontamination, 175
Towards the development of a technique for introducing aequorin into amoebae of *Dictyostelium discoideum* via electroporation, 342
Transmitter release, 320
Troll, Walter, see Margalit Rosenkranz, 346
Tudge, Christopher C., Spermatophore diversity within and among the hermit crab families, Coenobitidae, Diogenidae, and Paguridae (Paguroidea, Anomura, Decapoda), 238
Turbulent despersion, 408
Turner, F. S., see D. B. Gardiner, 175

U

Uca, 205
Ueno, Hiroshi, Tatsuji Haneji, Yumiko Ueno, Samuel S. Koide, and Sheldon J. Segal, Evaluation of spermatocidal activity of water soluble gossypol on the sperms of *Arabacia punctulata* and *Spisula solidissima*, 347
Ueno, Yumiko, see Hiroshi Ueno, 347
Ultrastructure, 144, 474
Ultrastructure of the radial neuromuscular system of the jellyfish *Liriope tetraphylla* (Hydrozoa, Trachymedusae): implications in crumpling behavior, The, 474
Ultraviolet light from the nighttime sky enhances retinal sensitivity of *Limulus*, 321
Unionid gills, 175
Upholt, William B., see Blanka Rogina, 512; and Caroline N. D. Coelho, 510
Use of PCR to identify novel mouse homeobox regions expressed during F9 embryoid body formation, The, 511
UV-induced damage, 341

V

Vanadate, 189
Vanadobin, a vanadium-binding substance, extracted from the blood cells of an ascidian, can reduce vanadate (V) to vanadyl (IV), 189
Vanadyl, 189
Vargula, 181
Variation in fertilization rate in the tropical reef fish, *Halichoeres bivattatus*: correlates and implications, 232
Vegetal pole, 343
Vestibular, 319
Video microscopy, 336
VIP, 484

Vogel, Jacalyn, and Felix Strumwasser, Identification of unique proteins in the eye of *Aplysia californica,* a circadian organ, 340

Voltage- and ligand-gated conductances of bipolar cells from the skate retina, 323

Voltage-dependent -L-type Ca^{2+} channels VDCCs participate in regulating neural crest development, 506

W

von Wallis, E., see J. C. Lewis, 275

Wallace, Heather V., see Robert M. Cerrato, 307

Wang, Rui, Lingyun Wu, Andrew L. Miller, John M. Arnold, and Lionel F. Jaffe, KCl-induced calcium rise in squid eggs: measurement of fura-2 fluorescence, 348

Wargo, Robert N., see Bruce J. Barber, 216

Warner, Robert R., and Stephen E. Swearer, Social control of sex change in the bluehead wrasse, *Thalassoma bifasciatum* (Pisces: Labridae), 199

Wax, Y., see Z. Ra'anan, 379

Way, Jeffrey C., Regulation of *mec-3,* a homeobox-containing gene that controls mechanoreceptor neuronal differentiation in *C. elegans,* 509

Wayne, Randy, Mark Staves, and A. Carl Leopold, The effect of gravity on cytoplasmic streaming in characean cells, 508

Weir, M., see D. Morrissey, 506; and Patricia A. Labosky, 511

Weissburg, Marc J., and Richard K. Zimmer-Faust, Ontogeny *versus* phylogeny in determining patterns of chemoreception: initial studies with fiddler crabs, 205

Weller, R. A., see M. M. O'Brien, 360

Wessels, Deb, see David Knecht, 510

Western Atlantic, 195

Wharton, Kristi, and William Gelbart, Identification in *Drosophila* of a new member of the TGF-β superfamily of cell signalling molecules, 508

Wheeler, R. B., Jr., see S. Zigman, 341

Wieschaus, E., see M. Peifer, 507

Wolfe, Connie J., and Margo G. Haygood, Restriction fragment length polymorphism analysis reveals high levels of genetic divergence among the light organ symbionts of flashlight fish, 135

Wollenberg, A., see J. Kieber, 507

Women in science (biology), 72

Wong, Mary A., see Sherry D. Painter, 81

Woodruff, Richard I., Andrew L. Miller, and Lionel F. Jaffe, Differences in free calcium concentration between oocytes and nurse cells revealed by corrected aequorin luminescence, 349

Wu, Lingyun, see Rui Wang, 348

Y

Yajima, Satoshi, see Susumu Ikegami, 95

Yan, Rui, and Anna W. Seitz, Construction of preimplantation mouse on cDNA library by polymerase chain reaction, 514

Yee, Gene H., see Susan B. Zusman, 507

Yueh, Yir G., see Richard C. Crain, 507

Z

Zakeri, Zahra, see Harleen Singh, 513

Zecevic, Dejan, Optical recording of membrane potential changes from single neurons using intracellular voltage-sensitive dyes, 332

Zigman, S., N. S. Rafferty, and R. B. Wheeler, Jr., Effects of vitamin E and OH-TEMPO (Spin Label Trap) on UV-induced dogfish (*Mustelus canis*) lens opacification relative to cytoskeletal actin, 341

Zimmer-Faust, Richard K., Chemical signal-to-noise detection by spiny lobsters, 419

Zimmer-Faust, Richard K., see Marc J. Weissburg, 205

Zimmerman, Todd L., and Darryl L. Felder, Reproductive ecology of an intertidal brachyuran crab, *Sesarma* sp. (nr. *reticulatum*), from the Gulf of Mexico, 387

Zooplankton, 500

Zusman, Susan B., Yevgenya Grinblat, Gene H. Yee, Fotis Kafatos, and Richard O. Hynes, A dissection of the functions of PS integrins during *Drosophila* development, 507

MARINE BIOLOGICAL LABORATORY COURSES 1992

ANALYTICAL AND QUANTITATIVE LIGHT MICROSCOPY IN BIOLOGY, MEDICINE, AND MATERIALS SCIENCE

COURSE: MAY 14 MAY 22, 1992
APPLICATION DEADLINE: MARCH 16, 1992

An in-depth examination of the theory of the microscope and application of video for exploring subtle interactions between light waves and the specimen is presented for 22 professional researchers and advanced graduate students who have considerable experience in microscopy; individuals well-grounded in the physical sciences, who wish to exploit microscopy techniques for analyzing dynamic fine-structural and chemical changes; and industrial scientists and engineers interested in advancing the design of equipment and techniques involving video microscopy. Extensive hands-on experience with state-of-the-art optical, electronic, and video equipment guided by an experienced staff from universities and industry is provided. *Directors: Edward D. Salmon, University of North Carolina, Chapel Hill; Greenfield Sluder and David Wolf, Worcester Foundation for Experimental Biology.*

ADVANCES IN MARICULTURE: TECHNIQUES AND FUTURE DIRECTIONS FOR PROVIDING MARINE ORGANISMS FOR BIOLOGICAL RESEARCH

COURSE: MAY 17 – MAY 29, 1992
APPLICATION DEADLINE: MARCH 20, 1992

This course is designed for 20 scientists, advanced technicians or students interested in any aspect of the biology of marine organisms requiring culture techniques. It combines intensive laboratory training with reviews of a wide range of basic principles relevant to the culture and maintenance of marine organisms. Visits are planned to research laboratories throughout Woods Hole as well as to local clam, scallop and lobster mariculture facilities. *Director: Roger T. Hanlon, Marine Biomedical Institute, Galveston, Texas.*

MICROINJECTION TECHNIQUES IN CELL BIOLOGY

COURSE: MAY 26 – JUNE 1, 1992
APPLICATION DEADLINE: MARCH 20, 1992

This research-oriented course is intended for 24 graduate students, postdoctoral researchers, and investigators. It will provide an opportunity to learn techniques of microinjection into a variety of living cells from leading practitioners. In addition, many of the latest methods of light microscopy, including the use of fluorescence and video techniques, will be used in conjunction with microinjection. *Director: Robert B. Silver, Cornell University*

MEDICAL INFORMATICS – [SPONSORED BY THE NATIONAL LIBRARY OF MEDICINE]

COURSE: MAY 31 – JUNE 6, 1992
APPLICATION DEADLINE: APRIL 1, 1992

This course is designed to train 30 individuals in the application of computer and information science in medicine. Participants will use computer – assisted learning tools, access computerized data bases, use communication networks, build and use a knowledge base for an expert system, and work with software for analysis of biologic sequence data. This is a National Library of Medicine fellowship program directed at medical educators, medical librarians, medical administrators and young faculty who are not currently knowledgeable but can become change agents in their institutions. *Director: Homer Warner, University of Utah School of Medicine*

PHYSIOLOGY: CELLULAR AND MOLECULAR BIOLOGY

COURSE: JUNE 13 – JULY 25, 1992
APPLICATION DEADLINE: MARCH 2, 1992

For a class of 36 graduate students, postdoctoral fellows, and established investigators who desire to learn the methods and research strategies used to study physiology at the cellular and molecular levels. Recent college graduates on their way to graduate school and physicians reentering laboratory research are also encouraged to apply. Interested students may apply for two weeks of postcourse research starting July 27. *Director: Thomas D. Pollard, Johns Hopkins University*

MARINE ECOLOGY: CONCEPTS, TECHNIQUES, AND APPLICATIONS OF MOLECULAR PROBES

COURSE: JUNE 14 – JULY 25, 1992
APPLICATION DEADLINE: MARCH 2, 1992

An intensive course for graduate students, postdoctoral fellows, and established investigators who wish to learn the techniques of molecular biology and their application to physiological and ecological investigations. Lectures and discussions will accompany the laboratories and will focus on the technologies being learned and applications to specific problems in marine ecology. Limited to 24 students. *Director: Kenneth H. Nealson, University of Wisconsin.*

MICROBIAL DIVERSITY

COURSE: JUNE 14 – JULY 30, 1992
APPLICATION DEADLINE: MARCH 2, 1992

An intensive course intended for graduate or postdoctoral students as well as established investigators who desire to become competent in microbiological techniques for isolating and working with a broad range of microbes. Limited to 20 students. *Directors. Martin Dworkin, University of Minnesota and John Breznak, Michigan State University.*

NEURAL SYSTEMS AND BEHAVIOR

COURSE: JUNE 14 – AUGUST 7, 1992
APPLICATION DEADLINE: MARCH 2, 1992

Intended for graduate and postdoctoral students as well as established investigators. The central theme of this course is the neural bases and ontogeny of behaviors. Twenty students participate in intensive laboratories/lectures which combine state-of-the-art neurobiological techniques with behavioral and developmental analyses. *Directors: Ronald Calabrese, Emory University and Martha Constantine-Paton, Yale University*

NEUROBIOLOGY

COURSE: JUNE 14 – AUGUST 15, 1992
APPLICATION DEADLINE: MARCH 2, 1992

For 12 pre- and postdoctoral fellows who intend to work in cellular and molecular neurobiology. Postdoctorals and students at an advanced stage of their graduate training are particularly encouraged to apply. The themes will be the functions of neural cells, the molecules involved in these functions, and the organization of molecular components required to generate cellular activity. *Directors: Leonard K. Kaczmarek, Yale University and Irwin Levitan, Brandeis University*

BIOLOGY OF PARASITISM: MODERN APPROACHES

COURSE: JUNE 14-AUGUST 15, 1992
APPLICATION DEADLINE: MARCH 2, 1992

This course, for students, postdocs, and faculty focuses on the molecular basis of parasite function and the host/parasite interaction, with special emphasis on the most recent and exciting developments in this area. The course has four sections: cell biology, immunology, molecular biology, and biochemistry. Each section includes daily lectures from course faculty and outside speakers, and intensive laboratory experimentation. Limited to 20 students. *Director: John C. Boothroyd, Stanford University.*

EMBRYOLOGY: CELL DIFFERENTIATION AND GENE EXPRESSION IN EARLY DEVELOPMENT

COURSE: JUNE 20-JULY 31, 1992
APPLICATION DEADLINE: MARCH 2, 1992

An advanced level course intended for graduate students, postdoctoral fellows, and other research scientists who wish a current treatment of major issues in the experimental analysis of developmental biology of the embryo, and the diverse intellectual approaches now useful in this field. Limited to 24 students. *Directors: Eric H. Davidson, California Institute of Technology; Michael Levine, University of California, San Diego; and David R. McClay, Duke University*

MOLECULAR EVOLUTION

COURSE: AUGUST 2 – AUGUST 14, 1992
APPLICATION DEADLINE: JUNE 1, 1992

A series of lectures and discussions exploring multiple approaches to molecular evolution, and a computer laboratory for phylogenetic and sequence analysis. This two week program is designed for a class of 60 established investigators, postdoctoral fellows, and advanced graduate students. *Director: Mitchell L. Sogin, Marine Biological Laboratory*

METHODS IN COMPUTATIONAL NEUROSCIENCE

COURSE: AUGUST 2 – AUGUST 29, 1992
APPLICATION DEADLINE: MAY 15, 1992

For 20 advanced graduate students and postdoctoral fellows in neurobiology, physics, electrical engineering, computer science, and psychology. A background in programming (preferably in C and UNIX) is highly desirable. This course presents the basic techniques necessary to study single cells and neural networks from a computational point of view and is organized around lectures, tutorials, and computer laboratories. *Directors: James M. Bower and Christof Koch, Computation and Neural System Program, California Institute of Technology*

FUNDAMENTAL ISSUES IN VISION RESEARCH: MOLECULAR AND CELL BIOLOGICAL APPROACHES [SPONSORED BY THE NATIONAL EYE INSTITUTE, NIH]

COURSE: AUGUST 16 – AUGUST 29, 1992
APPLICATION DEADLINE: MAY 1, 1992

This laboratory-lecture course is intended for 20 graduate students and postdoctoral fellows currently training in molecular biology, cell biology, and neurosciences who are not currently involved in vision research. The goal of the course is to present, in depth, the exciting theoretical and experimental approaches to fundamental research problems in vision so that the students can evaluate the potential for active research in this field. The faculty will describe and direct laboratories of on-going research in the tissues of the eye of invertebrates and vertebrates. Costs of attending the course, including travel, housing, and meals at MBL will be supported by a scholarship fund from NEI. *Directors: David S. Papermaster, University of Texas Health Science Center, San Antonio; and John E. Dowling, Harvard University*

RAPID MEASUREMENT OF NEUROTRANSMITTER SIGNALS IN THE CENTRAL NERVOUS SYSTEM USING IN VIVO ELECTROCHEMISTRY

COURSE: AUGUST 19 AUGUST 24, 1992
APPLICATION DEADLINE: JUNE 1, 1992

This course/workshop is intended for 16 graduate students, post-doctoral researchers, and investigators with interests in neuroscience, pharmacology, and chemoreception, who wish to learn the art and practice of in vivo electrochemistry as applied to studies of the CNS. The course will address the theory and practice of these techniques, and will encompass a combination of lectures, demonstrations, and hands-on use of these methods and technologies. *Directors. Greg A. Gerhardt and Paul A. Moore, Rocky Mountain Center for Sensor Technology, University of Colorado Health Sciences Center.*

OPTICAL MICROSCOPY AND IMAGING IN THE BIOMEDICAL SCIENCES

COURSE: SEPTEMBER 23 – 30, 1992
APPLICATION DEADLINE: JULY 1, 1992

Designed primarily for 22 research scientists, physicians, postdoctoral trainees, and advanced graduate students in animal, plant, and medical sciences as well as non-biologists with experience in microscopy and university faculty planning to develop courses on similar topics. The course covers the fundamental theory and practical use of modern optical microscopy. Special attention will be given to different optical techniques and the newest photographic and video methods used in biological and biomedical research. *Directors: Nina Strömgren Allen, Wake Forest University; and Colin S. Izzard, State University of New York at Albany*

For Further Information and Application Forms Contact:
Florence Dwane
Admissions Coordinator
Office of Sponsored Programs
Marine Biological Laboratory
Woods Hole, MA 02543
508 548-3705, ext 216

Financial Aid is available to Qualified Applicants
The MBL is an EEO Affirmative Action Institution

3711 089

~~4695 047~~

CONTENTS

BEHAVIOR

Marko, Peter B., and A. Richard Palmer
Responses of a rocky shore gastropod to the effluents of predatory and non-predatory crabs: avoidance and attraction 363

DEVELOPMENT AND REPRODUCTION

Levitan, Don R., Mary A. Sewell, and Fu-Shiang Chia
Kinetics of fertilization in the sea urchin *Strongylocentrotus franciscanus:* interaction of gamete dilution, age, and contact time 371

ECOLOGY AND EVOLUTION

Ra'anan, Z., A. Sagi, Y. Wax, I. Karplus, G. Hulata, and A. Kuris
Growth, size rank, and maturation of the freshwater prawn, *Macrobrachium rosenbergii:* analysis of marked prawns in an experimental population 379
Zimmerman, Todd L., and Darryl L. Felder
Reproductive ecology of an intertidal brachyuran crab, *Sesarma* sp. (nr. *reticulatum*), from the Gulf of Mexico 387

GENERAL BIOLOGY

Cowan, Diane F.
The role of olfaction in courtship behavior of the American lobster *Homarus americanus* 402
Moore, Paul A., and Jelle Atema
Spatial information in the three-dimensional fine structure of an aquatic odor plume 408
Zimmer-Faust, Richard K.
Chemical signal-to-noise detection by spiny lobsters 419
O'Brien, Jack J., S. Sindhu Kumari, and Dorothy M. Skinner
Proteins of crustacean exoskeletons: I. Similarities and differences among proteins of the four exoskeletal layers of four brachyurans 427
Pullen, Julie, and Michael LaBarbera
Modes of feeding in aggregations of barnacles and the shape of aggregations 442

PHYSIOLOGY

Mangum, Charlotte P., John Greaves, and Julia S. Rainer
Oligomer composition and oxygen binding of the hemocyanin of the blue crab *Callinectes sapidus* . . 453
Paynter, Kennedy T., and Thomas T. Chen
Biological activity of biosynthetic rainbow trout growth hormone in the eastern oyster, *Crassostrea virginica* 459
Tamm, Sidney L., and Signhild Tamm
Reversible epithelial adhesion closes the mouth of *Beroë*, a carnivorous marine jelly 463

NEUROBIOLOGY

Scemes, Eliana, and John C. McNamara
The ultrastructure of the radial neuromuscular system of the jellyfish *Liriope tetraphylla* (Hydrozoa, Trachymedusae): implications in crumpling behavior 474
Soinila, Seppo, and George J. Mpitsos
Immunohistochemistry of diverging and converging neurotransmitter systems in mollusks 484

RESEARCH NOTE

Ohman, Mark D., Gail H. Theilacker, and Sandor E. Kaupp
Immunochemical detection of predation on ciliate protists by larvae of the northern anchovy (*Engraulis mordax*) 500

ABSTRACTS

Abstracts of papers presented at the Marine Biological Laboratory: 1991 Northeast Regional Developmental Biology Conference 505

Index to Volume 181 515

MBL/WHOI LIBRARY
WH 1B2K /